

Spatially Resolved Strontium Isotope Micro-Analysis of Lower and Middle Palaeolithic Fauna from Archaeological Sites in Israel and Southern France

Ian Moffat BA, BSc. (Hons)

January 2013

A thesis submitted for the degree of Doctor of Philosophy of the Australian
National University.



Student Declaration

Unless otherwise acknowledged in the text, this thesis represents the original work of the author.

A handwritten signature in black ink, appearing to read "Ian Moffat".

Ian Moffat

22 January 2013

Acknowledgements

The process of writing this thesis has challenged me in ways I could never have imagined when I started. I could never have done it without a great deal of support and assistance from those below. Thank you!

Thank you to my principal supervisor, Professor Rainer Grün, whose unique approach of combining a very long supervisory leash, an exacting eye for editorial detail and a voracious appetite for analysis contributed greatly to this thesis. Professor Matthew Spriggs was a much-needed reader of drafts and a source of excellent advice. The remainder of my supervision committee—Dr John Magee, Dr Steve Eggins and Associate Professor Simon Haberle—were fantastic mentors and contributors of expertise to this research. A special thank you to Rainer, Matthew and my brother, Tom, for providing teeth for analysis. Thank you to the three anonymous examiners whose insightful comments contributed to the clarity and accuracy of this thesis.

The technical aspects of this research were entirely underpinned by generously offered advice from Les Kingsley, Dr Graham Mortimer and Linda McMorrow. Les tirelessly coached me in the operation of the MC-ICPMS, allocated highly sought after machine time and filled the laser on countless occasions. Graham was a very patient mentor from my earliest days of lab work and was a fantastic source of ideas on all matters geochemical. Linda McMorrow assisted on many occasions with ICP-AES work in this thesis, generously provided lab space in Building 47 at a critical time and was a source of much advice concerning general laboratory procedures.

The administrative team at the Research School of Earth Sciences at the Australian National University provided fantastic assistance which facilitated many aspects of this research. Unconditional support from Mike Avent was critical in the early days of this thesis and he was a good mate throughout, even if he opened the scotch too early. Eric Ward and Nigel Craddy provided essential practical support and in particular facilitated the many laboratory moves. Sussanne Hutchinson, Maree Coldrick and Robyn Petch made valiant attempts to keep my administrative affairs in order with Sussanne being particularly helpful during my fieldwork and Maree facilitating endless extensions of candidature. Shannon Avalos, Teresa Heyne, Nathalie Garrido and Rebecca Kelly also provided important support. Chris Harney helped me locate critical literature sources and renewed library loans on many occasions. Thank you to Professor Brian Kennett, Profesor Andrew Roberts and Professor Ian Jackson who, as directors of the Research School of Earth Sciences during my PhD candidature, have show a personal interest in and provided great assistance to this project. Thank you to the Research School of Earth Sciences student body for the generous award of the pink slippers as an encouragement to the submission of this thesis.

My colleagues in OHB-B provided great company, excellent advice and very useful technical assistance. Dr Maxime Aubert undertook sample collection in France in 2006 and was generous with his expertise on LA-MC-ICPMS, his secret camping spots and his home brew. Dr Renaud Joannes-Boyau was a fantastic source of advice, encouragement and tea. Tegan Kelly was a skilled camp-oven cook, a great source of strontium advice and graciously provided strontium offset data from her research. Ian McCulloch was a very welcome fellow late night prowler of the corridors.

Wendy Lees, Jess Hutchinson, Amergin Adair and Ceridwen Boyle generously assisted in the strontium laboratory and in Wendy's case, with its genesis. Malte Willmes was a fantastic sounding board and source of advice. Rebecca McMillan and Cameron Atkinson provided essential guidance with GIS.

Professor Avraham Ronen was a generous guide to the sites of Sefunim and Neve David, very kindly provided a bone point for analysis and was gracious about many delays. Dr Liora Horwitz was a gracious host, guide and provider of advice about Israeli archaeology, and facilitated my access to the Tel Safi material, which I unfortunately could not include in the final version of this thesis. Professor Chris Stringer provided, via Rainer, the samples from Skhul and Tabun used in this research.

Dr William Rendu and Cederic Beauval generously opened their project house to Rainer and me at La Chapelle-aux-Saints and provided samples for analysis. Magali Gerbe hosted us at the Les Fieux excavation and provided samples for analysis and a very nice lunch. Professor Bruno Maurellie was a kind host in Bordeaux and provided logistical support with the 2009 field work. Professor Jean-Philippe Brugal and Professor Jacques Jaubert provided the samples from Rescoundudou.

Thank you to Chantal Wright for allowing me to undertake the post-analysis photos at Flinders University. Karl Nissen graciously facilitated my access to Arc GIS to make the maps in this thesis. Brad Fergusson provided very useful advice about macro photography. Claire Wright from CSIRO Land and Water in Adelaide facilitated my access to a Neptune MC-ICPMS to perform a re-export of data contained within this thesis. Dr Michael Ellwood provided access to the G64 laboratory to undertake column chemistry. Dr Tim Barrows allowed me to take over the OHB-B 27 lab, which facilitated the processing of the mapping samples. Dr Steven Savage (Arizona State University) provided the Landsat image used as the background for the maps of Israel. Dr Richard Armstrong was an essential and generous source of advice about strontium isotopes. This thesis was edited by Elite Editing with editorial intervention being restricted to Standards D and E of the *Australian Standards for Editing Practice*, as per ANU policy 200912843-1297/2009. Thank you to Rhys Jones (1992) for bringing my attention to the Stockdale quotation that serves as the preface to this thesis.

This research was supported by Australian Research Council Discovery grants DP0664144 and DP110101415 and ARC Linkage grant LP0775058 to Grün et al. The Earth Environment group at the Research School of Earth Sciences provided support to attend the Australian Archaeology conference in 2009 and 2010 and the International Quaternary Association conference in 2011. The Vice Chancellor's Travel Grant scheme at the Australian National University supported my attendance at the International Quaternary Association conference in 2011. I was supported through the course of this thesis by a scholarship from the Australian National University and a top up scholarship from the Research School of Earth Sciences. The Research School of Earth Sciences also provided funding for analysis time for this research. The Environmental Futures Network provided funding for GIS training to support this research.

Ecophyte Technologies, Whistler Research, Spinifex Geology, Flinders University and a number of consulting projects kept me gainfully employed and financially solvent during periods of this thesis. My business partner in Precipice Training, Mark Reilly, was a constant source of encouragement, advice and distraction during this thesis and the fruits of our work were critical to me being able to finish this thesis after my scholarship ended. Thank you to Dug and Denise Smith and all of their helpers whose faultless organisation and superb catering made running the training courses so easy, allowing me to focus on finishing my thesis.

My mother, Anne, and her husband, Gary, staunchly supported me through this thesis in many ways and were even happy to be banished to the 'Donkey Express' when visiting so that I could get some writing done. Thank you, Mum, for all of the opportunities you have given me over the years, without which none of this would have been possible.

My father, Bruce, and his partner, Neva, were great sources of encouragement and assistance throughout the course of this thesis. Our Sri Lanka holiday is a great memory and provided a much-needed break before the final push to submit. Thank you, Dad, for all of the encouragement over the years and especially for the Sunday phone calls, which kept me on track during difficult times.

My grandmother, Jessie Glanfield, maintained constant optimism about the outcome of this thesis, even when I could not. It is a great regret for me that she passed away just before it was submitted and so could not see the fruits of all of her kind words over the years.

The Fisher family very kindly hosted me in their beautiful home during my time in Canberra. The Garnaut family were gracious hosts, supporters and providers of medicinal whisky during my many stays in Adelaide.

Dr Alice ‘Pottie’ Gorman convinced me that I needed a PhD in the first place and was a critical advisor and editor during all stages of the process. Dr Jenn McKinnon and (soon to be Dr) Jason Raupp were good friends, gracious hosts, thesis buddies and providers of Bundaberg rum (at least when Jenn was overseas).

Lastly, my partner, Julia Garnaut, unconditionally supported me through many late nights, missed occasions and bouts of grumpiness. She did everything possible to facilitate this thesis, including cooking meals, reading drafts, driving back and forth to Adelaide constantly and even disappearing to the Pilbara when I needed solitude to get writing done. I have treasured the time we have spent together writing, gardening and taking long walks on the SYP and cannot wait to spend the next 4 months going around the world together!

Dedication

For Nanna, who just missed out on another funny hat.

Abstract

The use of strontium isotope analysis to provenance biominerals such as bone and teeth has become a regularly applied component of archaeological research. This method works by comparing the isotopic composition of these materials with regional bioavailable soil values, allowing an estimation of the distance and vector of an individual's mobility. New advances in analytical equipment has facilitated the spatially resolved micro-analysis of strontium isotope composition using laser ablation sampling, allowing intra-sample heterogeneity to be quantified. This provides the opportunity to determine not only the overall provenance of a material, but also the degree of mobility during biomineral formation.

This research applies laser ablation multi-collector inductively coupled plasma mass spectroscopy (LA-MC-ICPMS) to 90 teeth of Lower and Middle Palaeolithic faunal prey from Lower and Middle Palaeolithic archaeological sites within Israel and France. These sites span a crucial period in human evolution, characterised by the radiation of multiple hominin species and by dynamic oscillations of climate with attendant changes in fauna and flora. The strontium isotope values from LA-MC-ICPMS analysis in this thesis show a high level of intra-sample variability, which would not have been captured by a traditional analytical methodology. This suggests that, despite some problems in obtaining accurate results due to offsets between solution and laser values, strontium isotope studies that do not utilise spatially resolved micro-analysis are unable to accurately determine mobility.

The results of this research demonstrate that fauna from the archaeological sites of interest—including Amud, Qafzeh, Tabun, Skhull, Holon, Bois Roche, Le Moustier, La Chapelle-aux-Saints, Les Fieux, Pech de l'Azé II and Rescoundudou—appear to have patterns of mobility that are controlled by

variables such as species, marine isotope stages (MIS) and regional physiography. Specifically, Persian fallow deer, bison, mountain goat/chamois and fox are frequently mobile between different geological environments during amelogenesis while wild boar and rhinoceros are sessile. The calculated range of distance for minimum possible mobility for each sample is large, ranging from 0 km to 350 km. The median values for minimum possible mobility for each species suggest that wild boar, bison and fox are mobile over the greatest distance while *Bos*, rhinoceros, Persian fallow deer and unidentified deer are mobile over the least. Furthermore, fauna in MIS 4 and 3 are significantly more mobile than in MIS 6 and 5. Fauna from France are more mobile than those from Israel, which is attributed to the location of the archaeological sites adjacent to significant river systems that could serve as conduits of mobility, even during inhospitable climate periods. Overall, these insights show that strontium isotope analysis can be usefully applied to quantifying mobility on a broad temporal and geographic scale, rather than simply being used, as is typical, for locating the source of material within a specific archaeological site.

Contents

Student Declaration	i
Acknowledgements	ii
Dedication	vii
Abstract	viii
Contents	x
List of Figures	xxiii
List of Tables.....	xli
List of Acronyms	li
Chapter One: Introduction	1
1.1. Introduction	1
1.2. Significance of the Thesis to the Field.....	4
1.3. Thesis Structure	6
Chapter Two: Strontium Geochemistry and Archaeology	7
2.1. Overview	7
2.2. Strontium Isotopes	8
2.2.1. Introduction.....	8
2.2.2. Notation of Strontium Isotope Values	9
2.3. Strontium Isotopes in Nature	10
2.3.1. Bedrock	10
2.3.1.1. Introduction	10
2.3.1.2. Igneous Rocks	11
2.3.1.3. Sedimentary Rocks	11
2.3.1.4. Metamorphic Rocks	12
2.3.2. Regolith	13
2.3.3. Plants.....	18
2.3.4. Water	19
2.3.4.1. Precipitation	19
2.3.4.2. Lake and River Water	20
2.3.4.3. Groundwater	21
2.3.4.4. Seawater.....	22
2.3.4.5. Bioavailable Strontium	23
2.3.4.6. Strontium in Vertebrates.....	24
2.3.4.7. Biopurification of Strontium	26
2.3.4.8. Post-burial Diagenesis	26
2.3.5. Biominerals	28
2.3.5.1. An Introduction to Dentogenesis	28
2.3.5.2. An Introduction to Bone.....	33

2.4. Applications of Strontium Concentration and Isotope Studies	34
2.4.1.1. Modern Ecological Studies	34
2.4.1.2. Modern Provenance Studies	35
2.4.1.3. Hydrogeological Studies	35
2.4.1.4. Dolomitisation Studies	36
2.4.1.5. Weathering Studies	37
2.4.1.6. Palaeo-Mobility Studies	37
2.4.1.7. Other Archaeological Applications	44
2.4.1.8. Palaeoecological Studies	44
2.4.1.9. Palaeodietary Studies	45
2.4.1.10. Palaeo-Occupation Intensity Studies	48
2.5. Summary	49
Chapter Three: Background to the Study Areas	50
3.1. Overview	50
3.2. Physiography	51
3.2.1. Topography	51
3.2.1.1. Israel	51
3.2.1.2. France	53
3.2.2. Sea Level	54
3.2.2.1. Israel	54
3.2.2.2. France	55
3.3. Climate, Vegetation and Fauna	56
3.3.1. Modern Climate, Vegetation and Fauna	56
3.3.1.1. Israel	56
3.3.1.2. France	59
3.3.2. Quaternary History	60
3.3.2.1. Israel	62
3.3.2.2. France	67
3.4. Geology	73
3.4.1. Geology of the Levant	73
3.4.1.1. Overview	73
3.4.2. Major Geological Provinces	74
3.4.2.1. Southern Igneous Province	74
3.4.2.2. Southern-Central Clastic Province	75
3.4.2.3. Central Carbonate Province	75
3.4.2.4. Northern Volcanic Province	77
3.4.2.5. Dead Sea Rift Sediments	80
3.4.2.6. Coastal Sediments	81
3.4.3. Quaternary Landscape Evolution	86
3.4.4. Soils in the Levant	86
3.4.5. Geology of Southern France	88
3.4.5.1. Overview	88
3.4.6. Major Geological Provinces	89
3.4.6.1. Massif Central	89
3.4.6.2. Aquitaine Basin	93
3.4.6.3. Rhône Valley	94
3.4.6.4. Coastal Sediments	95

3.4.7. Soils in Southern France	96
3.5. Previous Strontium Isotope Studies in Israel.....	97
3.6. Previous Strontium Isotope Studies in Southern France	101
3.7. Fauna	103
3.7.1. Fauna of the Levant.....	103
3.7.1. Fauna of the Southern France	104
3.8. Fauna Included in this Study	105
3.8.1. Order Artiodactyla.....	106
3.8.1.1. Family Suidae (Suborder Suiformes)	105
3.8.1.2. Family Cervidae (Suborder Ruminantia (Pecora))	109
3.8.1.3. Family Bovidae.....	112
3.8.1.4. Family Hippopotamidae	115
3.8.2. Order Perissodactyla	116
3.8.2.1. Family Equidae (Suborder Ruminantia/Pecora)	116
3.8.2.2. Family Rhinocerotidae	119
3.8.3. Order Carnivora.....	121
3.8.3.1. Family Hyaenidae	121
3.8.3.2. Family Canidae	123
3.9. Archaeology	125
3.9.1. Hominins Included in this Study.....	125
3.9.1.1. Overview	125
3.9.1.2. Homo Erectus	125
3.9.1.3. Homo Neanderthalensis.....	126
3.9.1.4. Anatomically Modern Humans	128
3.10. Palaeolithic Archaeology of the Levant	129
3.10.1. Overview.....	129
3.10.2. Key Periods in This Study.....	129
3.10.2.1. Lower Palaeolithic, 1.4 Ma to 200 Ka	129
3.10.2.2. Middle Palaeolithic, 200 to 48 Ka	131
3.10.3. Levantine Archaeological Sites in this Study	133
3.10.3.1. Skhul	133
3.10.3.2. Tabun	137
3.10.3.3. Amud.....	144
3.10.3.4. Qafzeh.....	147
3.10.3.5. Holon.....	151
3.11. Palaeolithic Archaeology of Southern France.....	151
3.11.1. Overview.....	151
3.11.2. Key Periods in This Study.....	152
3.11.2.1. Lower Palaeolithic, 2.6 Ma to 250 Ka	152
3.11.2.2. Middle Palaeolithic, ~250 to 48 Ka	152
3.12. French Archaeological Sites in this Study	153
3.12.1.1. La Chapelle-aux-Saints	153
3.12.1.2. Les Fieux.....	156
3.12.1.3. Le Moustier	159
3.12.1.4. Pech de l'Aze II	162
3.12.1.5. Bois Roche.....	166

3.12.1.6. Rescoundudou	168
3.13. Summary	171
Chapter Four: Methods	172
4.1. Overview	172
4.2. Mapping Samples.....	172
4.2.1. Israel 2008	172
4.2.2. France 2006.....	177
4.2.3. France 2009.....	179
4.3. Archaeological Samples	185
4.3.1. Israeli Archaeological Material	185
4.3.1.1. Skhul	185
4.3.1.2. Tabun	187
4.3.1.3. Amud.....	187
4.3.1.4. Qafzeh.....	188
4.3.1.5. Holon.....	188
4.3.2. French Archaeological Material	189
4.3.2.1. La Chapelle-aux-Saints	189
4.3.2.2. Les Fieux.....	189
4.3.2.3. Le Moustier	190
4.3.2.4. Pech de l'Azé II	190
4.3.2.5. Bois Roche	191
4.3.2.6. Rescoundudou	191
4.4. Sample Processing Procedures	192
4.4.1. Solution Samples	192
4.4.1.1. Preparation of Vessels for Analysis.....	192
4.4.1.2. Preparation of Samples for Dissolution	193
4.4.1.3. Dissolution of Samples	193
4.4.1.4. Analysis of Concentration.....	194
4.4.1.5. Ion Exchange Chromatography.....	194
4.4.2. Laser Ablation Samples	196
4.5. Instrumentation for Strontium Concentration Measurements	197
4.5.1. ICP-AES/ICP-OES.....	197
4.5.2. ICPMS	198
4.6. Instrumentation for Strontium Isotope Measurements	200
4.6.1. MC-ICPMS.....	200
4.6.1.1. Solution MC-ICPMS	200
4.6.1.2. LA-MC-ICPMS.....	201
4.7. MC-ICPMS Sample Analysis	203
4.7.1. Solution MC-ICPMS.....	203
4.7.2. LA-MC-ICPMS	204
4.8. Data Analysis	204
4.8.1. MC-ICPMS.....	204
4.8.2. LA-MC-ICPMS	205
4.8.2.1. Kr Correction	206
4.8.2.2. Mass Bias Correction	207

4.8.2.3. REE Interference Correction	207
4.8.2.4. Rb/Sr Correction	207
4.8.2.5. Ca Argide/Dimmer Correction	208
4.8.2.6. Other Corrections	208
4.8.2.7. Ca+P+O Offset Correction	208
4.9. Interpretation of Mobility	210
4.9. Overview	211
Chapter Five: Summarised Results	212
5.1. Overview	212
5.2. Regional Mapping Results	212
5.2.1. Israel.....	212
5.2.1.1. Israeli Soil Samples.....	212
5.2.1.2. Israeli Rock Samples	218
5.2.2. France	222
5.2.2.1. French Plant Samples.....	222
5.2.2.2. French Soil Samples	225
5.2.2.3. French Rock Samples	229
5.3. Israeli Archaeological Sites	231
5.3.1. Skhul.....	231
5.3.1.1. LA-ICPMS Results	231
5.3.1.2. MC-ICPMS Results	231
5.3.1.3. Regional Mapping Results	232
5.3.1.4. LA-MC-ICPMS Results.....	233
5.3.1.5. Mobility Interpretation.....	235
5.3.2. Tabun	238
5.3.2.1. LA-ICPMS Results	238
5.3.2.2. MC-ICPMS Results	238
5.3.2.3. Regional Mapping Results	239
5.3.2.4. LA-MC-ICPMS Results.....	240
5.3.2.5. Mobility Interpretation.....	242
5.3.3. Amud	243
5.3.3.1. MC-ICPMS Results	243
5.3.3.2. Regional Mapping Results	244
5.3.3.3. LA-MC-ICPMS Results.....	245
5.3.3.4. Mobility Interpretation.....	247
5.3.4. Qafzeh	248
5.3.4.1. LA-ICPMS Results	248
5.3.4.2. MC-ICPMS Results	248
5.3.4.3. Regional Mapping Results	249
5.3.4.4. LA-MC-ICPMS Results.....	250
5.3.4.5. Mobility Interpretation.....	251
5.3.5. Holon	254
5.3.5.1. LA-ICPMS Results	254
5.3.5.2. Regional Mapping Results	254
5.3.5.3. LA-MC-ICPMS Results.....	255
5.3.5.4. Mobility Interpretation.....	256
5.4. French Archaeological Sites.....	258

5.4.1.1. LA-ICPMS Results	258
5.4.1.2. MC-ICPMS Results	259
5.4.1.3. Regional Mapping Results	260
5.4.1.4. LA-MC-ICPMS Results.....	261
5.4.1.5. Mobility Results	263
5.4.2. Les Fieux	266
5.4.2.1. MC-ICPMS Results	266
5.4.2.2. Regional Mapping Samples	267
5.4.2.3. LA-MC-ICPMS Results.....	268
5.4.2.4. Mobility Interpretation	270
5.4.3. Le Moustier	273
5.4.3.1. Regional Mapping Results	273
5.4.3.2. LA-MC-ICPMS Results.....	273
5.4.3.3. Mobility Interpretation	275
5.4.4. Pech de l'Azé II	277
5.4.4.1. Regional Mapping Results	277
5.4.4.2. LA-MC-ICPMS Results.....	277
5.4.4.3. Mobility Interpretation	279
5.4.5. Bois Roche	282
5.4.5.1. LA-ICPMS Results	282
5.4.5.2. MC-ICPMS Results	282
5.4.5.3. Regional Mapping Results	283
5.4.5.4. LA-MC-ICPMS Results.....	284
5.4.5.5. Mobility Interpretation	286
5.4.6. Rescoundudou.....	288
5.4.6.1. MC-ICPMS Results	288
5.4.6.2. Regional Mapping Results	289
5.4.6.3. LA-MC-ICPMS Results.....	289
5.4.6.3. Mobility Interpretation	292
5.5. Standards	294
5.5.1. Durango Apatite	294
5.5.1.1. LA-MC-ICPMS Results.....	294
5.5.2. Tridacna	294
5.6. Summary	296
Chapter Six: Discussion.....	298
6.1. Overview	298
6.2. Mapping Studies.....	299
6.2.1. Israel.....	299
6.2.1.1. Comparison of Results to Local Geology	299
6.2.1.2. Comparison Between Soil and Rock Results	301
6.2.1.2. Comparison to Other Studies	306
6.2.1. France.....	307
6.2.2.1. Comparison of Results to Local Geology	307
6.2.2.2. Comparison to Other Studies	309
6.2. Geochemical Implications.....	310
6.2.1. Analysis of Standards	310

6.2.1.1. Durango Apatite	310
6.2.1.2. Tridacna	310
6.3.2. Laser Versus Solution Analysis	310
6.3.3. Intra-Tooth Variability.....	311
6.3.4. Establishing a ‘Local’ Signature	314
6.3.5. External Versus Internal LA-MC-ICPMS.....	315
6.4. Species-Specific Mobility.....	316
6.4.1. Wild Boar	318
6.4.2. Deer.....	318
6.4.2.1. Persian Fallow Deer (<i>Dama Mesopotamica</i>).....	318
6.4.2.2. Reindeer (<i>Rangifer Tarandus</i>).....	319
6.4.2.3. Unidentified Deer	320
6.4.3. Bovid.....	321
6.4.3.1. Unidentified Bovid	321
6.4.3.2. Bison	323
6.4.3.3. Bos	323
6.4.3.4. Mountain Goat/Chamois.....	324
6.4.3.5. Hippopotamus	324
6.4.4. Horse	325
6.4.5. Rhinoceros	326
6.4.6. Hyeana	327
6.4.7. Fox.....	327
6.5. Archaeological Implications.....	328
6.5.1. Comparison of Archaeological Sites	328
6.5.1. Effect of Climate	333
6.5.1.1. MIS 9, 8 and 7	335
6.5.1.2. MIS 6.....	335
6.5.1.3. MIS 5.....	336
6.5.1.4. MIS 4	337
6.5.1.5. MIS 3.....	338
6.5. Summary	339
Chapter Seven: Conclusions and Recommendations.....	340
7.1. Conclusions.....	340
7.2. Recommendations	342
Chapter Eight: References.....	344
Appendix One: Sample Collection Locations	440
A1.1. Israeli Sites	440
A1.1.1. IS001	441
A1.1.2. IS002.....	442
A1.1.3. IS003.....	443
A1.1.4. IS004.....	444
A1.1.5. IS005.....	445
A1.1.6. IS006.....	446
A1.1.7. IS007	447
A1.1.8. IS008	448
A1.1.9. IS009.....	449

A1.1.10. IS010	450
A1.1.11. IS011	451
A1.1.12. IS012	452
A1.1.13. IS013	453
A1.1.14. IS014	454
A1.1.15. IS015	455
A1.1.16. IS016	456
A1.1.17. IS017	457
A1.1.18. IS018	458
A1.1.19. IS019	459
A1.1.20. IS020	460
A1.1.21. IS021	461
A1.1.22. IS022	462
A1.1.23. IS023	463
A1.1.24. IS024	464
A1.1.25. IS025	465
A1.1.26. IS026	466
A1.1.27. IS027	467
A1.1.28. IS028	468
A1.1.29. IS029	469
A1.1.30. IS030	470
A1.1.31. IS031	471
A1.1.32. IS032	472
A1.1.33. IS033	473
A1.1.34. IS034	474
A1.1.35. IS035	475
A1.1.36. IS036	476
A1.1.37. IS037	477
A1.1.38. IS038	478
A1.1.39. IS039	479
A1.1.40. IS040	480
A1.1.41. IS041	481
A1.1.42. IS042	482
A1.1.43. IS043	483
A1.1.44. IS044	484
A1.1.45. IS045	485
A1.1.46. IS046	486
A1.1.47. IS047	487
A1.1.48. IS048	488
A1.1.49. IS049	489
A1.1.50. IS050	490
A1.1.51. IS051	491
A1.1.52. IS052	492
A1.1.53. IS053	493
A1.1.54. IS054	494
A1.1.55. IS055	495
A1.1.56. IS056	496
A1.1.57. IS057	497
A1.1.58. IS058	498
A1.1.59. IS060	499

A1.1.60. IS061	500
A1.1.61. IS062	501
A1.2. French Sites	502
A1.2.1. F01	503
A1.2.2. F02	504
A1.2.3. F04	505
A1.2.4. F06	506
A1.2.5. F08	507
A1.2.6. F12	508
A1.2.7. F16	509
A1.2.8. F19	510
A1.2.9. F21	511
A1.2.10. F23	512
A1.2.11. F24	513
A1.2.12. F25	514
A1.2.13. F27	515
A1.2.14. F33	516
A1.2.15. F34	517
A1.2.16. F35	518
A1.2.17. F36	519
A1.2.18. F37	520
A1.2.19. F38	521
A1.2.20. F40	522
A1.2.21. FS001	523
A1.2.22. FS006	524
A1.2.23. FS008	525
A1.2.24. FS010	526
A1.2.25. FS011	527
A1.2.26. FS016	528
A1.2.27. FS018	529
A1.2.28. FS021	530
A1.2.29. FS027	531
A1.2.30. FS029	532
A1.2.31. FS031	533
A1.2.32. FS033	534
A1.2.33. FS035	535
A1.2.34. FS036	536
A1.2.35. FS037	537
A1.2.36. FS041	538
A1.2.37. FS043	539
A1.2.38. FS044	540
A1.2.39. FS045	541
A1.2.40. FS046	542
A1.2.41. FS047	543
A1.2.42. FS049	544
A1.2.43. FS050	545
A1.2.44. FS051	546
A1.2.45. FS052	547
A1.2.46. FS053	548
A1.2.47. FS054	549

A1.2.48. FS055.....	550
A1.2.49. FS056.....	551
A1.2.50. FS057.....	552
A1.2.51. FS058.....	553
A1.2.52. FS059.....	554
A1.2.53. FS060.....	555
A1.2.54. FS061.....	556
A1.2.55. FS063.....	557
A1.2.56. FS065.....	558
A1.2.57. FS067.....	559
A1.2.58. FS070.....	560
A1.2.59. FS072.....	561
A1.2.60. FS074.....	562
A1.2.61. FS076.....	563
A1.2.62. FS078.....	564
A1.2.63. FS080.....	565
A1.2.64. FS081.....	566
A1.2.65. FS083.....	567
A1.2.66. FS084.....	568
A1.2.67. FS085.....	569
A1.2.68. FS086.....	570
A1.2.69. FS087.....	571
A1.2.70. FS088.....	572
A1.2.71. FS089.....	573
A1.2.72. FS090.....	574
A1.2.73. FS092.....	575
A1.2.74. FS093.....	576
A1.2.75. FS094.....	577
A1.2.76. FS096.....	578
A1.2.77. FS097.....	579
A1.2.78. FS099.....	580
A1.2.79. FS100.....	581
A1.2.80. FS102.....	582
A1.2.81. FS103.....	583
A1.2.82. FS104.....	584
A1.2.83. FS105.....	585
A1.2.84. FS107.....	586
A1.2.85. FS108.....	587
A1.2.86. FS111.....	588
A1.2.87. FS112.....	589
A1.2.88. FS113.....	590
A1.2.89. FS114.....	591
A1.2.90. FS115.....	592
A1.2.91. FS116.....	593
A1.2.92. FS118.....	594
A1.2.93. P2.....	595
A1.2.94. P3.....	596
A1.2.95. P4.....	597
A1.2.96. P5.....	598
A1.2.97. P6.....	599

A1.2.98. P7.....	600
A1.2.99. P8.....	601
A1.2.100. P9.....	602
A1.2.101. P10.....	603
A1.2.102. P11.....	604
A1.2.103. P12.....	605
A1.2.104. P13.....	606
A1.2.105. P14.....	607
A1.2.106. P15.....	608
A1.2.107. P16.....	609
A1.2.108. P17.....	610
A1.2.109. P18.....	611
A1.2.110. P19.....	612
A1.2.111. P20.....	613
A1.2.112. P23.....	614
A1.2.113. P24.....	615
A1.2.114. P25.....	616
A1.2.115. P26.....	617
A1.2.116. P27.....	618
A1.2.117. P28.....	619
A1.2.118. P29.....	620
A1.2.119. P30.....	621
A1.2.120. P31.....	622
A1.2.121. P32.....	623
A1.2.122. P33.....	624
A1.2.123. P34.....	625
A1.2.124. P35.....	626
A1.2.125. P36.....	627
A1.2.126. P37.....	628
A1.2.127. P38.....	629
A1.2.128. P39.....	630
A1.2.129. P40.....	631
A1.2.130. P42.....	632
A1.2.131. P43.....	633
A1.2.132. P44.....	634
A1.2.133. P45.....	635
A1.2.134. P46.....	636
A1.2.135. P47.....	637
A1.2.136. P48.....	638
A1.2.137. P49.....	639
A1.2.138. P50.....	640
A1.2.139. P51.....	641
A1.2.140. P52.....	642
A1.2.141. P53.....	643
A1.2.142. P54.....	644
A1.2.143. P55.....	645
A1.2.144. P56.....	646
A1.2.145. P57.....	647
A1.2.146. P58.....	648
A1.2.147. P59.....	649

A1.2.148. P60	650
A1.2.149. P61	651
A1.2.150. P62	652
Appendix Two: Fauna.....	653
A2.1. Israeli Archaeological Material	653
A2.1.1. Skhul	653
A2.1.2. Tabun	659
A2.1.3. Amud	665
A2.1.4. Qafzeh	667
A2.1.5. Holon	669
A2.2. French Archaeological Material.....	670
A2.2.1. La Chapelle-aux-Saints	670
A2.2.2. Les Fieux.....	681
A2.2.3. Le Moustier.....	689
A2.2.4. Pech de l'Azé II	692
A2.2.5. Bois Roche	698
A2.2.6. Rescoundudou	705
Appendix Three: Detailed Results.....	714
A3.1. LA-ICPMS Concentration Results	714
A3.1.1. Israeli Archaeological Samples	714
A3.1.1.1. Skhul.....	714
A3.1.1.2. Tabun.....	722
A3.1.1.3. Qafzeh	727
A3.1.1.4. Holon	728
A3.1.2. French Archaeological Samples.....	728
A3.1.2.1. La Chapelle-aux-Saints.....	728
A3.1.2.2. Bois Roche	733
A3.2. LA-MC-ICPMS Strontium Isotope Results	736
A3.2.1. Non-Archaeological Material	736
A3.2.1.1. Durango Apatite	736
A3.2.2. Israeli Archaeological Sites	738
A3.2.2.1. Skhul.....	738
A3.2.2.2. Tabun.....	778
A3.2.2.3. Amud	810
A3.2.2.4. Qafzeh	823
A3.2.3. French Archaeological Sites.....	840
A3.2.3.1. La Chapelle-aux-Saints.....	840
A3.2.3.2. Les Fieux	894
A3.2.3.3. Pech de l'Azé II	942
A3.2.3.4. Bois Roche	1004
A3.2.3.5. Rescoundudou.....	1048
Appendix Four: Tridacna Results.....	1105
A4.1. Overview	1105
A4.2. Tridacna Spots Collected 29/11/2010	1105
A4.3. Tridacna Spots Collected 30/11/2011	1106
A4.4. Tridacna Spots Collected 10/02/2011	1109
A4.5. Tridacna Spots Collected 11/02/2011	1111
A4.6. Tridacna Spots Collected 12/02/2011	1112

A4.7. Tridacna Spots Collected 7/04/2011	1113
A4.8. Tridacna Spots Collected 8/04/2011	1114
A4.9. Tridacna Spots Collected 9/04/2011	1115
A4.10. Tridacna Spots Collected 10/04/2011	1116
A4.11. Tridacna Spots Collected 13/05/2011	1117
A4.12. Tridacna Spots Collected 14/05/2011	1119
A4.13. Tridacna Spots Collected 15/05/2011	1120
A4.14. Tridacna Spots Collected 16/05/2011	1121
A4.15. Tridacna Spots Collected 20/06/2011	1121
A4.16. Tridacna Spots Collected 21/06/2011	1124
A4.17. Tridacna Spots Collected 22/06/2011	1125
A4.18. Tridacna Spots Collected 23/06/2011	1127
A4.19. Summary.....	1127

List of Figures

Figure 1.1 Archaeological Sites in Israel (left) and France (right) Included in this Study	2
Figure 1.2 A Comparison of the Oxygen Isotope Curve to Stratigraphic Units from France (left) and Israel (right) Included in this Study	3
Figure 2.1 Inputs and Outputs of Strontium for Regolith (Modified from Stewart et al. 1998:180).....	14
Figure 2.2 Strontium Fluxes in a Multi-Layered Soil System (Modified from Stewart et al. 1998).....	15
Figure 2.3 Strontium Isotope Composition of Soil, Vegetation and Source Material. Adirondack Mountains, New York (Miller et al. 1993:439)...	20
Figure 2.4: $^{87}\text{Sr}/^{86}\text{Sr}$ Ratio of Sea Water Through Phanerozoic Time (Elderfield 1986:77)	23
Figure 2.5 Generalised Structure of a Simple Mammalian Tooth (Hillson 2005:9)	29
Figure 3.1 Topography of Israel (Image: Modified from Sadalmelik 2007).....	52
Figure 3.2 Representation of the Topography of France using Shuttle Radar Topography (Modified Image: NASA)	54
Figure 3.3 Global Sea Level Curve for the Last 200 ka with MIS Noted (Galili et al. 2007).....	55
Figure 3.4 Annual Normal (1961 to 1990) Rainfall Map of Israel (Goldreich 1994:46)	58
Figure 3.5 Correlation Between MIS 3 to 5, Sea Surface Temperatures, Main Pollen Types on the Western French Margin and Dominant Fauna (Discamps et al. 2011:2770).....	69
Figure 3.6 Comparison of a) Greenland Temperature Curve to Data from Core MC04–2845 (Bay of Biscay), b) Pollen Percentage Curve for Atlantic Forest, c) Interpreted Sea Surface Temperatures, d) Percentage of Polar Planktic Foraminifera <i>Neogloboquadrina pachydemata</i> and e) Ice Rafted Debris (Sánchez Goñi et al. 2008:1144)	71
Figure 3.7 Comparison of Stages Identified from Velay Cores to the Oxygen Isotope Curve (Reille et al. 1998:1118)	72
Figure 3.8 Principal Structural Elements of the Eastern Mediterranean Basin (Garfunkel 1998).....	73
Figure 3.9 Geological Map of Southern Israel (Sneh, Bartov, Weissbrod and Rosensaft et al. 1998b).....	74
Figure 3.10 Geological Map of Southern-Central Israel (Sneh, Bartov, Weissbrod and Rosensaft et al. 1998a).....	75
Figure 3.11 Geological Map of Northern Central Israel (Sneh, Bartov and Rosensaft et al. 1998b).....	76
Figure 3.12 Geological Map of Northern Israel (Sneh, Bartov and Rosensaft et al. 1998a).....	78
Figure 3.13 Age of Basalts in Northern Israel (Weinstein et al. 2006).....	79

Figure 3.14 Generalised Stratigraphy of the Dead Sea Group (Stein 2001:272)	81
Figure 3.15 Key to Israeli Geological Maps (1) as Shown in Figure 3.10 to Figure 3.13	83
Figure 3.16 Key to Israeli Geological Maps (2) as shown in Figure 3.10 to Figure 3.13	84
Figure 3.17 Key to Israeli Geological Maps (3) as Shown in Figure 3.10 to Figure 3.13	85
Figure 3.18 Geological Provinces and Structural Elements of France (Blès and Gros 1991:266). 1 = Faults (Normal and Transcurrent), 2 = Principal Thrusts, 3 = Unfolded Post-Palaeozoic Terranes, 4 = Pyrenean and Alpine Folding, 5 = Internal Alps and Apennines, 6 = Old Massifs (Hercynian and Older), 7= Rhône Valley, PT = Pennine Thrust, B = Bordeaux, L = Lyon, P = Paris and M = Marseille	89
Figure 3.19 Geological Units Surrounding the French Archaeological Sites in this Study (Data: BRGM)	92
Figure 3.20 Bioavailable Strontium Map of Israel and Jordan (Perry et al. 2009)	98
Figure 3.21 Bioavailable Strontium Isotope Values from Western Jordan (Perry et al. 2008:539)	99
Figure 3.22: Chemical and Isotopic Composition of the Three Water Sources in the Jordan Valley (Rosenthal et al. 1989:243)	100
Figure 3.23 Presence/Absence Data for Different Taxon During Different periods of the Mousterian in South-west France (Discamps et al. 2011)	105
Figure 3.24 <i>Sus Scrofa</i> (Modified From Groves 2007:19).....	107
Figure 3.25 Male Bison (<i>Bison bison</i>) (Meagher 1986:3).....	113
Figure 3.26 Przewalski Horse (<i>Equus Caballus Prezwalskii</i>) (Bennett and Hoffman 1999:1).....	117
Figure 3. 27 Adult Male Indian Rhinoceros (<i>Rhinoceros Unicornis</i>) (Laurie et al. 1983:1).....	119
Figure 3.28 Striped Hyena (<i>Hyaena Hyaena</i>) (Rieger 1981:1)	122
Figure 3.29 Adult <i>Vulpes Vulpes</i> (Larivière and Pasitschniak-Arts 1996:2)	124
Figure 3.30 Plan of A) Skhul V Showing the Pig's Mandible (2) From Which Sample 1058 Derives and B) Skhul IX with the Bovid Skull (1) From Which Sample 1057 Derives (Garrod and Bates 1937).....	136
Figure 3.31 Garrod's Stratigraphy of Tabun (Bull and Goldberg 1985).....	138
Figure 3.32 Original ESR Chronology for Tabun (Grün et al. 1991:234)	141
Figure 3.33 North-South Stratigraphic Profile of Qafzeh Cave at Western Excavation Limit (Vandermeersch 1981:28)	148
Figure 3.34 Stratigraphic Section of La Chapelle-aux-Saints (Bouyssonie et al. 1908).....	155
Figure 3.35 The Archaeological Site of La Chapelle-aux-Saints During Sample Collection.....	155
Figure 3.36 The Archaeological Site of Les Fieux During Sample Collection .	157
Figure 3.37 Stratigraphy of the Archaeological Site of Les Fieux (Champagne et al. 1990:5)	158
Figure 3.38 Stratigraphic Section of the Secteur Central of the Archaeological Site of Les Fieux (Champagne et al. 1990:6)	159

Figure 3.39 Stratigraphic Section of Le Moustier (Mellars and Grün 1991)	162
Figure 3.40 Stratigraphic Section of Pech de l'Azé II (Goldberg 1979)	165
Figure 3.41 Plan View of the Excavation Squares at Bois Roche and a Cross-Section of the Cave.....	167
Figure 3.42 Stratigraphy of the Rescoundudou Archaeological Site (Jaubert 1983)	169
Figure 3.43 Archaeological Site of Rescoundudou During Sample Collection	169
Figure 4.1 Soil/Rock Sample Collection Locations in Israel (Landsat Data Provided by Dr Stephen Savage, Arizona State University 2010) ...	175
Figure 4.2 Israel Soil/Rock Sample Collection Locations Overlain on Regional Geological Maps (Sneh, Bartov and Rosensaft 1998a and 1998b, Sneh, Bartov, Weissbrod and Rosensaft 1998a and 1998b)	176
Figure 4.3 Location of all French Sample Collection Sites	182
Figure 4.4 Location of Sample Collection Sites Overlain on Geological Units of France	183
Figure 4.5 Location of Sample Collection Sites in Eastern France	183
Figure 4.6 Location of Sample Collection Sites in Central France	184
Figure 4.7 Location of Sample Collection Sites in Western France	184
Figure 4.8 Acid Dependency of Various Ions in Strontium Resin (Horwitz et al. 1992).....	196
Figure 4.9 Sample Mounted for LA-MC-ICPMS Analysis.....	197
Figure 4.10 Schematic Diagram of Neptune MC-ICPMS (Gäbler 2002:2)	200
Figure 4.11 Relationship Between Strontium Concentration and Laser/Solution Offset Used for Correction of LA-MC-ICPMS Data in this Study	209
Figure 5.1 Israeli Bioavailable Soil Strontium Results Overlain on Landsat Image (Provided by Dr Stephen Savage, Arizona State University 2010)	217
Figure 5.2 Israeli Bioavailable Rock Strontium Results Overlain on Landsat Image (Provided by Dr Stephen Savage, Arizona State University 2010)	221
Figure 5.3 French Bioavailable Strontium Results Overlain on Landsat Image.....	222
Figure 5.4 Bioavailable Soil Strontium Values Surrounding Tabun and Skhul	232
Figure 5.5 Summary Plot of Skhul Faunal Teeth LA-MC-ICPMS Sr Isotope Results.....	235
Figure 5.6 Bioavailable Soil Strontium Values Surrounding Tabun.....	240
Figure 5.7 Summary Plot of Tabun Faunal Teeth LA-MC-ICPMS Sr Isotope Results.....	242
Figure 5.8 Bioavailable Soil Strontium Values Surrounding Amud.....	245
Figure 5.9 Summary Plot of Amud Faunal Teeth LA-MC-ICPMS Sr Isotope Results.....	246
Figure 5.10 Bioavailable Soil Strontium Values Surrounding Qafzeh	250
Figure 5.11 Summary Plot of Qafzeh Faunal Teeth LA-MC-ICPMS Sr Isotope Results	251
Figure 5.12 Bioavailable Soil Strontium Values Surrounding Holon.....	254
Figure 5.13 LA-MC-ICPMS Track for Sample 1557	255
Figure 5.14 Sample 1557, Holon, Detailed LA-MC-ICPMS Sr Isotope Results.....	256

Figure 5.15 Bioavailable Soil Strontium Values Surrounding La Chapelle-aux-Saints.....	260
Figure 5.16 Summary Plot of La Chapelle-aux-Saints Faunal Teeth LA-MC-ICPMS Sr Isotope Results	263
Figure 5.17 Bioavailable Soil Strontium Values Surrounding Les Fieux	268
Figure 5.18 Summary Plot of Les Fieux Faunal Teeth LA-MC-ICPMS Sr Isotope Results	270
Figure 5.19 Bioavailable Soil Strontium Values Surrounding Le Moustier	273
Figure 5.20 Summary Plot of Le Moustier Faunal Teeth LA-MC-ICPMS Sr Isotope Results	275
Figure 5.21 Bioavailable Soil Strontium Values Surrounding Pech de l'Azé II	277
Figure 5.22 Summary Plot of Pech de l'Azé II Faunal Teeth LA-MC-ICPMS Sr Isotope Results	279
Figure 5.23 Bioavailable Soil Strontium Values Surrounding Bois Roche	284
Figure 5.24 Summary Plot of Bois Roche Faunal Teeth LA-MC-ICPMS Sr Isotope Results	286
Figure 5.25 Bioavailable Soil Strontium Values Surrounding Rescoundudou.....	289
Figure 5.26 Summary Plot of Rescoundudou Faunal Teeth LA-MC-ICPMS Sr Isotope Results	291
Figure 5.27 Summary Plot of Tridacna LA-MC-ICPMS Sr Isotope Results.....	296
Figure 6.1 Comparison of Israeli Bioavailable Soil Strontium Results to Lithology (Overall Range and Median Value Shown by Solid Lines, 25% and 75% Values Shown by Dotted Lines)	300
Figure 6.2 Comparison of Israeli Bioavailable Rock Strontium Isotope Results to Lithology (Overall Range and Median Value Shown by Solid Lines, 25% and 75% Values Shown by Dotted Lines)	301
Figure 6.3 Comparison of Bioavailable $^{87}\text{Sr}/^{86}\text{Sr}$ Results from Rock and Soil Samples from Sample Locations in Israel, Excepting Sample IS044	302
Figure 6.4 Comparison of French Bioavailable Strontium Isotope Results to Lithology (Overall Range and Median Value Shown by Solid Lines, 25% and 75% Values Shown by Dotted Lines)	308
Figure A2.1 Sample 851, Bovid, Unknown Stratigraphic Provenance, Skhul, Israel.....	653
Figure A2.2 Sample 852, Bovid, Unknown Stratigraphic Provenance, Skhul, Israel.....	654
Figure A2.3 Sample 853, Bovid, Unknown Stratigraphic Provenance, Skhul, Israel.....	654
Figure A2.4 Sample 1057A, Bovid, Unit B, Skhul, Israel	655
Figure A2.5 Sample 1057B, Bovid, Unit B, Skhul, Israel	656
Figure A2.6 Sample 1057C, Bovid, Unit B, Skhul, Israel	656
Figure A2.7 Sample 1058A, Wild Boar, Unit B, Skhul, Israel.....	657
Figure A2.8 Sample 1058B, Wild Boar, Unit B, Skhul, Israel.....	657
Figure A2.9 Sample 1058C, Wild Boar, Unit B, Skhul, Israel.....	658
Figure A2.10 Sample 554, <i>Bos</i> , Layer D, Tabun, Israel.....	659
Figure A2.11 Sample 556, <i>Bos</i> , Layer D, Tabun, Israel.....	659
Figure A2.12 Sample 557, <i>Bos</i> , Layer Ea, Tabun, Israel.....	660
Figure A2.13 Sample 557 (2), <i>Bos</i> , Layer Ea, Tabun, Israel.....	660
Figure A2.14 Sample 558, <i>Bos</i> , Layer Ea, Tabun, Israel.....	661
Figure A2.15 Sample 561, <i>Bos</i> , Layer Eb, Tabun, Israel.....	661

Figure A2.16 Sample 563, <i>Bos</i> , Layer Eb, Tabun, Israel	662
Figure A2.17 Sample 564, <i>Bos</i> , Layer Ec, Tabun, Israel	663
Figure A2.18 Sample 565, <i>Bos</i> , Layer Ec, Tabun, Israel	663
Figure A2.19 Sample 567, <i>Bos</i> , Layer Ed, Tabun, Israel	664
Figure A2.20 Sample 568, Rhinoceros, Layer Ed, Tabun, Israel	664
Figure A2.21 Sample 1024, <i>Dama mesopotamica</i> , Layer B1, Amud, Israel ...	665
Figure A2.22 Sample 1025, <i>Dama mesopotamica</i> , Layer B1, Amud, Israel ...	665
Figure A2.23 Sample 1026, <i>Dama mesopotamica</i> , Layer B1, Amud, Israel ...	666
Figure A2.24 Sample 371, Bovid, Layer XIX, Qafzeh, Israel	667
Figure A2.25 Sample 372, Bovid, Layer XVII, Qafzeh, Israel	667
Figure A2.26 Sample 373, Unidentified Species, Layer XV, Qafzeh, Israel....	668
Figure A2.27 Sample 1557, <i>Bos</i> , Layer C, Holon, Israel.....	669
Figure A2.28 Sample 592, Bovid, Bouffia Bonneval: Straum 1, La Chapelle-aux-Saints, France.....	670
Figure A2.29 Sample 593, Bovid, Bouffia Bonneval: Straum 1, La Chapelle-aux-Saints, France.....	671
Figure A2.30 Sample 595, Bovid, Bouffia Bonneval: Straum 1, La Chapelle-aux-Saints, France.....	672
Figure A2.31 Sample M001, Reindeer, Bouffia 118: Layer 2, La Chapelle-aux-Saints, France.....	673
Figure A2.32 Sample M002, Reindeer, Bouffia 118: Layer 2, La Chapelle-aux-Saints, France.....	674
Figure A2.33 Sample M003, Reindeer, Bouffia 118: Layer 2, La Chapelle-aux-Saints, France.....	675
Figure A2.34 Sample M004, Unknown Species, Bouffia 118: Unknown Layer, La Chapelle-aux-Saints, France	676
Figure A2.35 Sample M005, Bovid, Bouffia 118: Layer 1, La Chapelle-aux-Saints, France.....	677
Figure A2.36 Sample M006, Bovid, Bouffia 118: Layer 1, La Chapelle-aux-Saints, France.....	678
Figure A2.37 Sample M007, Bovid, Bouffia 118: Layer 1, La Chapelle-aux-Saints, France.....	678
Figure A2.38 Sample M008, Bovid, Bouffia 118: Layer 1, La Chapelle-aux-Saints, France.....	679
Figure A2.39 Sample M009, Bovid, Bouffia 118: Layer 1, La Chapelle-aux-Saints, France.....	679
Figure A2.40 Sample M010, Bovid, Bouffia 118: Layer 1, La Chapelle-aux-Saints, France.....	680
Figure A2.41 Sample M011, Horse, Layer G7, Les Fieux, France.....	681
Figure A2.42 Sample M012, Horse, Layer G7, Les Fieux, France.....	681
Figure A2.43 Sample M013, Wild Boar, Layer G7, Les Fieux, France.....	682
Figure A2.44 Sample M014, Fox, Layer G7, Les Fieux, France	682
Figure A2.45 Sample M015, Hyena, Layer G7, Les Fieux, France	683
Figure A2.46 Sample M016, Bison, Layer G7, Les Fieux, France	684
Figure A2.47 Sample M017, Bison, Layer G7, Les Fieux, France	684
Figure A2.48 Sample M018, Reindeer, Layer G7, Les Fieux, France.....	685
Figure A2.49 Sample M019, Reindeer, Layer G7, Les Fieux, France.....	686
Figure A2.50 Sample M020, Chamois, Layer G7, Les Fieux, France	687
Figure A2.51 Sample M021, Mountain Goat/Chamois, Layer G7, Les Fieux, France	688

Figure A2.52 Sample M022, Mountain Goat/Chamois, Layer G7, Les Fieux, France	688
Figure A2.53 Sample 845, Bovid, Layer G1, Le Moustier, France.....	689
Figure A2.54 Sample 846, Bovid, Layer G2, Le Moustier, France.....	689
Figure A2.55 Sample 847, Bovid, Layer G3, Le Moustier, France.....	690
Figure A2.56 Sample 848, Bovid, Layer G4, Le Moustier, France.....	690
Figure A2.57 Sample 849, Bovid, Layer G5, Le Moustier, France.....	691
Figure A2.58 Sample 850, Bovid, Layer G6, Le Moustier, France.....	691
Figure A2.59 Sample 614, Bovid, Layer 9, Pech de l'Azé II, France	692
Figure A2.60 Sample 615, Hippopotamus, Layer 9, Pech de l'Azé II, France	692
Figure A2.61 Sample 617, Horse, Layer 8, Pech de l'Azé II, France.....	693
Figure A2.62 Sample 618, Deer, Layer 8, Pech de l'Azé II, France.....	694
Figure A2.63 Sample 619, Horse, Layer 8, Pech de l'Azé II, France.....	694
Figure A2.64 Sample 620, Bovid, Layer 7, Pech de l'Azé II, France	695
Figure A2.65 Sample 622, Hippopotamus, Layer 7, Pech de l'Azé II, France	696
Figure A2.66 Sample 624, Deer, Layer 6, Pech de l'Azé II, France.....	697
Figure A2.67 Sample 625, Horse, Layer 6, Pech de l'Azé II, France	697
Figure A2.68 Sample 2417, Bovid, Layer 1C, Bois Roche, France	698
Figure A2.69 Sample 2418, Bovid, Layer 1C, Bois Roche, France	699
Figure A2.70 Sample 2419, Bovid, Layer 1C, Bois Roche, France	699
Figure A2.71 Sample 2420, Bovid, Layer 2, Bois Roche, France	700
Figure A2.72 Sample 2421, Bovid, Layer 2, Bois Roche, France	701
Figure A2.73 Sample 2422, Bovid, Layer 1C, Bois Roche, France	702
Figure A2.74 Sample 2423, Bovid, Layer 2, Bois Roche, France	702
Figure A2.75 Sample 2424, Bovid, Layer 2, Bois Roche, France	703
Figure A2.76 Sample 2425A, Bovid, Layer 2, Bois Roche, France.....	703
Figure A2.77 Sample 2425B, Bovid, Layer 2, Bois Roche, France.....	704
Figure A2.78 Sample 2425C, Bois Roche, France	704
Figure A2.79 Sample M033, Bovid, Layer 2, Rescoundudou, France	705
Figure A2.80 Sample M034, Bovid, Layer C1, Rescoundudou, France.....	705
Figure A2.81 Sample M035, Bovid, Layer C1, Rescoundudou, France.....	706
Figure A2.82 Sample M036, Horse, Layer C1, Rescoundudou, France	706
Figure A2.83 Sample M037, Horse, Layer C1, Rescoundudou, France	707
Figure A2.84 Sample M038, Horse, Layer C1, Rescoundudou, France	707
Figure A2.85 Sample M039, Bovid, Layer C1, Rescoundudou, France.....	708
Figure A2.86 Sample M040, Bovid, Layer C1, Rescoundudou, France.....	708
Figure A2.87 Sample M041, Bovid, Layer C1, Rescoundudou, France.....	709
Figure A2.88 Sample M042, Bovid, Layer C1, Rescoundudou, France.....	710
Figure A2.89 Sample M043, Deer, Layer C1, Rescoundudou, France	711
Figure A2.90 Sample M044, Deer, Layer C1, Rescoundudou, France	712
Figure A2.91 Sample M045, Deer, Layer C1, Rescoundudou, France	713
Figure A3.1 LA-MC-ICPMS Track for Durango Apatite.....	736
Figure A3.2 Durango Apatite LA-MC-ICPMS Uncorrected Sr Isotope Results.....	737
Figure A3.3 Durango Apatite LA-MC-ICPMS Uncorrected Sr Isotope Results.....	738
Figure A3.4 LA-MC-ICPMS Track for Sample 851, Bovid, Unknown Stratigraphic Provenance, Skhul	740
Figure A3.5 Detailed LA-MC-ICPMS Uncorrected Sr Isotope Results, Sample 851, Bovid, Unknown Stratigraphic Provenance, Skhul.....	743

Figure A3.6 Detailed LA-MC-ICPMS Corrected Sr Isotope Results, Sample 851, Bovid, Unknown Stratigraphic Provenance, Skhul.....	743
Figure A3.7 LA-MC-ICPMS Track for Sample 852, Bovid, Unknown Stratigraphic Provenance, Skhul.....	745
Figure A3.8 Detailed LA-MC-ICPMS Uncorrected Sr Isotope Results, Sample 852, Bovid, Unknown Stratigraphic Provenance, Skhul.....	749
Figure A3.9 Detailed LA-MC-ICPMS Corrected Sr Isotope Results, Sample 852, Bovid, Unknown Stratigraphic Provenance, Skhul.....	749
Figure A3.10 LA-MC-ICPMS Track for Sample 853 Bovid, Unknown Stratigraphic Provenance, Skhul.....	751
Figure A3.11 Detailed LA-MC-ICPMS Uncorrected Sr Isotope Results, Sample 853, Bovid, Unknown Stratigraphic Provenance, Skhul.....	754
Figure A3.12 Detailed LA-MC-ICPMS Corrected Sr Isotope Results, Sample 853, Bovid, Unknown Stratigraphic Provenance, Skhul.....	755
Figure A3.13 LA-MC-ICPMS Track for Sample 1057A, Bovid, Layer B, Skhul.....	757
Figure A3.14 Detailed LA-MC-ICPMS Uncorrected Sr Isotope Results, Sample 1057A, Bovid, Layer B, Skhul	759
Figure A3.15 Detailed LA-MC-ICPMS Corrected Sr Isotope Results, Sample 1057A, Bovid, Layer B, Skhul	759
Figure A3.16 LA-MC-ICPMS Track for Sample 1057B, Bovid, Layer B, Skhul.....	761
Figure A3.17 Detailed LA-MC-ICPMS Uncorrected Sr Isotope Results, Sample 1057B, Bovid, Layer B, Skhul	762
Figure A3.18 Detailed LA-MC-ICPMS Corrected Sr Isotope Results, Sample 1057B, Bovid, Layer B, Skhul	763
Figure A3.19 LA-MC-ICPMS Track for Sample 1057C, Bovid, Layer B, Skhul.....	765
Figure A3.20 Detailed LA-MC-ICPMS Uncorrected Sr Isotope Results, Sample 1057C, Bovid, Layer B, Skhul.....	767
Figure A3.21 Detailed LA-MC-ICPMS Corrected Sr Isotope Results, Sample 1057C, Bovid, Layer B, Skhul.....	767
Figure A3.22 LA-MC-ICPMS Track for Sample 1058A, Wild Boar, Layer B, Skhul.....	768
Figure A3.23 Detailed LA-MC-ICPMS Uncorrected Sr Isotope Results, Sample 1058A, Wild Boar, Layer B, Skhul	770
Figure A3.24 Detailed LA-MC-ICPMS Corrected Sr Isotope Results, Sample 1058A, Wild Boar, Layer B, Skhul.....	770
Figure A3.25 LA-MC-ICPMS Track for Sample 1058B, Wild Boar, Layer B, Skhul.....	772
Figure A3.26 Detailed LA-MC-ICPMS Uncorrected Sr Isotope Results, Sample 1058B, Wild Boar, Layer B, Skhul	774
Figure A3.27 Detailed LA-MC-ICPMS Corrected Sr Isotope Results, Sample 1058B, Wild Boar, Layer B, Skhul.....	774
Figure A3.28 LA-MC-ICPMS Track for Sample 1058C, Wild Boar, Layer B, Skhul.....	775
Figure A3.29 Detailed LA-MC-ICPMS Uncorrected Sr Isotope Results, Sample 1058A, Wild Boar, Layer B, Skhul	777
Figure A3.30 Detailed LA-MC-ICPMS Corrected Sr Isotope Results, Sample 1058A, Wild Boar, Layer B, Skhul.....	777

Figure A3.31 LA-MC-ICPMS Track for Sample 554, <i>Bos</i> , Layer D, Tabun.....	780
Figure A3.32 Detailed LA-MC-ICPMS Uncorrected Sr Isotope Results, Sample 554, <i>Bos</i> , Layer D, Tabun.....	781
Figure A3.33 Detailed LA-MC-ICPMS Corrected Sr Isotope Results, Sample 554, <i>Bos</i> , Layer D, Tabun.....	781
Figure A3.34 LA-MC-ICPMS Track for Sample 556, <i>Bos</i> , Layer D, Tabun.....	782
Figure A3.35 Detailed LA-MC-ICPMS Uncorrected Sr Isotope Results, Sample 556, <i>Bos</i> , Layer D, Tabun.....	783
Figure A3.36 Detailed LA-MC-ICPMS Corrected Sr Isotope Results, Sample 556, <i>Bos</i> , Layer D, Tabun.....	783
Figure A3.37 LA-MC-ICPMS Track for Sample 557, Track 1, <i>Bos</i> , Layer Ea, Tabun	786
Figure A3.38 LA-MC-ICPMS Track for Sample 557, Track 2, <i>Bos</i> , Layer Ea, Tabun	786
Figure A3.39 Detailed LA-MC-ICPMS Uncorrected Sr Isotope Results, Sample 557, <i>Bos</i> , Layer Ea, Tabun.....	787
Figure A3.40 Detailed LA-MC-ICPMS Corrected Sr Isotope Results, Sample 557, <i>Bos</i> , Layer Ea, Tabun	787
Figure A3.41 LA-MC-ICPMS Track for Sample 558, <i>Bos</i> , Layer Ea, Tabun... 788	
Figure A3.42 Detailed LA-MC-ICPMS Uncorrected Sr Isotope Results, Sample 558, <i>Bos</i> , Layer Ea, Tabun.....	789
Figure A3.43 Detailed LA-MC-ICPMS Corrected Sr Isotope Results, Sample 558, <i>Bos</i> , Layer Ea, Tabun	790
Figure A3.44 LA-MC-ICPMS Track for Sample 561, <i>Bos</i> , Layer Eb, Tabun... 792	
Figure A3.45 Detailed LA-MC-ICPMS Uncorrected Sr Isotope Results, <i>Bos</i> , Layer Eb, Tabun	793
Figure A3.46 Detailed LA-MC-ICPMS Corrected Sr Isotope Results, <i>Bos</i> , Layer Eb, Tabun	793
Figure A3.47 LA-MC-ICPMS Track for Sample 563, <i>Bos</i> , Layer Eb, Tabun... 795	
Figure A3.48 Detailed LA-MC-ICPMS Uncorrected Sr Isotope Results, Sample 563, <i>Bos</i> , Layer Eb, Tabun.....	796
Figure A3.49 Detailed LA-MC-ICPMS Corrected Sr Isotope Results, Sample 563, <i>Bos</i> , Layer Eb, Tabun	796
Figure A3.50 LA-MC-ICPMS Track for Sample 564, <i>Bos</i> , Layer Ec, Tabun ... 797	
Figure A3.51 Detailed LA-MC-ICPMS Uncorrected Sr Isotope Results, Sample 564, <i>Bos</i> , Layer Ec, Tabun	798
Figure A3.52 Detailed LA-MC-ICPMS Corrected Sr Isotope Results, Sample 564, <i>Bos</i> , Layer Ec, Tabun	798
Figure A3.53 LA-MC-ICPMS Track for Sample 565, <i>Bos</i> , Layer Ec, Tabun ... 800	
Figure A3.54 Detailed LA-MC-ICPMS Uncorrected Sr Isotope Results, Sample 565, <i>Bos</i> , Layer Ec, Tabun	801
Figure A3.55 Detailed LA-MC-ICPMS Corrected Sr Isotope Results, Sample 565, <i>Bos</i> , Layer Ec, Tabun	801
Figure A3.56 LA-MC-ICPMS Track for Sample 567, <i>Bos</i> , Layer Ed, Tabun... 803	
Figure A3.57 Detailed LA-MC-ICPMS Uncorrected Sr Isotope Results, Sample 567, <i>Bos</i> , Layer Eb, Tabun.....	804
Figure A3.58 Detailed LA-MC-ICPMS Uncorrected Sr Isotope Results, Sample 567, <i>Bos</i> , Layer Ed, Tabun.....	805
Figure A3.59 LA-MC-ICPMS Track for Sample 568, Rhinoceros, Layer Ed, Tabun	807

Figure A3.60 Detailed LA-MC-ICPMS Uncorrected Sr Isotope Results, Sample 568, Rhinoceros, Layer Ed, Tabun	809
Figure A3.61 Detailed LA-MC-ICPMS Corrected Sr Isotope Results, Sample 568, <i>Bos</i> , Layer Ed, Tabun	810
Figure A3.62 LA-MC-ICPMS Track for Sample 1024, <i>Dama mesopotamica</i> , Layer B1, Amud	812
Figure A3.63 Detailed LA-MC-ICPMS Uncorrected Sr Isotope Results, Sample 1024, <i>Dama mesopotamica</i> , Layer B1, Amud	814
Figure A3.64 Detailed LA-MC-ICPMS Corrected Sr Isotope Results, Sample 1024, <i>Dama mesopotamica</i> , Layer B1, Amud	814
Figure A3.65 LA-MC-ICPMS Track for Sample 1025, <i>Dama mesopotamica</i> , Layer B1, Amud	816
Figure A3.66 Detailed LA-MC-ICPMS Uncorrected Sr Isotope Results, Sample 1025, <i>Dama mesopotamica</i> , Layer B1, Amud	817
Figure A3.67 Detailed LA-MC-ICPMS Corrected Sr Isotope Results, Sample 1025, <i>Dama mesopotamica</i> , Layer B1, Amud	818
Figure A3.68 LA-MC-ICPMS Track for Sample 1026, <i>Dama mesopotamica</i> , Layer B1, Amud	820
Figure A3.69 Detailed LA-MC-ICPMS Uncorrected Sr Isotope Results, Sample 1026, <i>Dama mesopotamica</i> , Layer B1, Amud	822
Figure A3.70 Detailed LA-MC-ICPMS Corrected Sr Isotope Results, Sample 1026, <i>Dama mesopotamica</i> , Layer B1, Amud	822
Figure A3.71 Detailed LA-MC-ICPMS Uncorrected Sr Isotope Results, Sample 370, Bovid, Layer XV, Qafzeh	824
Figure A3.72 Detailed LA-MC-ICPMS Corrected Sr Isotope Results, Sample 370, Bovid, Layer XV, Qafzeh.....	825
Figure A3.73 LA-MC-ICPMS Track for Sample 371, Bovid, Layer XIX, Qafzeh	827
Figure A3.74 Detailed LA-MC-ICPMS Uncorrected Sr Isotope Results, Sample 371, Bovid, Layer XIX, Qafzeh	828
Figure A3.75 Detailed LA-MC-ICPMS Corrected Sr Isotope Results, Sample 371, Bovid, Layer XIX, Qafzeh.....	829
Figure A3.76 LA-MC-ICPMS Track for Sample 372, Bovid, Layer XVII, Qafzeh	831
Figure A3.77 Detailed LA-MC-ICPMS Uncorrected Sr Isotope Results, Sample 372, Bovid, Layer XVII, Qafzeh	833
Figure A3.78 Detailed LA-MC-ICPMS Corrected Sr Isotope Results, Sample 372, Bovid, Layer XVII, Qafzeh.....	833
Figure A3.79 LA-MC-ICPMS Track for Sample 373.....	835
Figure A3.80 Sample 373, Qafzeh, Detailed LA-MC-ICPMS Uncorrected Sr Isotope Results	836
Figure A3.81 Sample 373, Qafzeh, Detailed LA-MC-ICPMS Corrected Sr Isotope Results	836
Figure A3.82 LA-MC-ICPMS Track for Sample 374, Unidentified Species, Layer XV, Qafzeh	838
Figure A3.83 Detailed LA-MC-ICPMS Uncorrected Sr Isotope Results, Sample 374, Unidentified Species, Layer XV, Qafzeh.....	839
Figure A3.84 Detailed LA-MC-ICPMS Corrected Sr Isotope Results, Sample 374, Unidentified Species, Layer XV, Qafzeh.....	839

Figure A3.85 LA-MC-ICPMS Track for Sample 592, Bovid, Bouffia Bonneval: Stratum 1, La Chapelle-aux-Saints	842
Figure A3.86 Detailed LA-MC-ICPMS Uncorrected Sr Isotope Results, Sample 592, Bovid, Bouffia Bonneval: Stratum 1, La Chapelle-aux-Saints.....	844
Figure A3.87 Detailed LA-MC-ICPMS Corrected Sr Isotope Results, Sample 592, Bovid, Bouffia Bonneval: Stratum 1, La Chapelle-aux-Saints ..	844
Figure A3.88 LA-MC-ICPMS Track for Sample 593, Bovid, Bouffia Bonneval: Stratum 1, La Chapelle-aux-Saints	848
Figure A3.89 Detailed LA-MC-ICPMS Uncorrected Sr Isotope Results, Sample 593, Bovid, Bouffia Bonneval: Stratum 1, La Chapelle-aux-Saints.....	850
Figure A3.90 Detailed LA-MC-ICPMS Corrected Sr Isotope Results, Sample 593, Bovid, Bouffia Bonneval: Stratum 1, La Chapelle-aux-Saints ..	851
Figure A3.91 LA-MC-ICPMS Track for Sample 595, Bovid, Bouffia Bonneval: Stratum 1, La Chapelle-aux-Saints	853
Figure A3.92 Detailed LA-MC-ICPMS Uncorrected Sr Isotope Results, Sample 595, Bovid, Bouffia Bonneval: Stratum 1, La Chapelle-aux-Saints.....	855
Figure A3.93 Detailed LA-MC-ICPMS Corrected Sr Isotope Results, Sample 595, Bovid, Bouffia Bonneval: Stratum 1, La Chapelle-aux-Saints ..	856
Figure A3.94 LA-MC-ICPMS Track for Sample M001, Reindeer, Bouffia 118: Layer 2, La Chapelle-aux-Saints	858
Figure A3.95 Detailed LA-MC-ICPMS Uncorrected Sr Isotope Results, Sample M001, Reindeer, Bouffia 118: Layer 2, La Chapelle-aux-Saints.....	859
Figure A3.96 Detailed LA-MC-ICPMS Corrected Sr Isotope Results, Sample M001, Reindeer, Bouffia 118: Layer 2, La Chapelle-aux-Saints	859
Figure A3.97 LA-MC-ICPMS Track for Sample M002, Reindeer, Bouffia 118: Layer 2, La Chapelle-aux-Saints	861
Figure A3.98 Detailed LA-MC-ICPMS Uncorrected Sr Isotope Results, Sample M002, Reindeer, Bouffia 118: Layer 2, La Chapelle-aux-Saints.....	862
Figure A3.99 Detailed LA-MC-ICPMS Corrected Sr Isotope Results, Sample M002, Reindeer, Bouffia 118: Layer 2, La Chapelle-aux-Saints	862
Figure A3.100 LA-MC-ICPMS Track for Sample M003, Reindeer, Bouffia 118: Layer 2, La Chapelle-aux-Saints	864
Figure A3.101 Detailed LA-MC-ICPMS Uncorrected Sr Isotope Results, Reindeer, Bouffia 118: Layer 2, La Chapelle-aux-Saints	865
Figure A3.102 Detailed LA-MC-ICPMS Corrected Sr Isotope Results, Reindeer, Bouffia 118: Layer 2, La Chapelle-aux-Saints	866
Figure A3.103 LA-MC-ICPMS Track for Sample M004, Unknown Species, Bouffia 118: Unknown Layer, La Chapelle-aux-Saints	868
Figure A3.104 Detailed LA-MC-ICPMS Uncorrected Sr Isotope Results, Sample M004, Unknown Species, Bouffia 118: Unknown Layer, La Chapelle-aux-Saints	869
Figure A3.105 Detailed LA-MC-ICPMS Corrected Sr Isotope Results, Sample M004, Unknown Species, Bouffia 118: Unknown Layer, La Chapelle-aux-Saints	869

Figure A3.106 LA-MC-ICPMS Track for Sample M005, Bovid, Bouffia 118: Layer 1, La Chapelle-aux-Saints.....	871
Figure A3.107 Detailed LA-MC-ICPMS Uncorrected Sr Isotope Results, Sample M005, Bovid, Bouffia 118: Layer 1, La Chapelle-aux- Saints.....	872
Figure A3.108 Detailed LA-MC-ICPMS Corrected Sr Isotope Results, Sample M005, Bovid, Bouffia 118: Layer 1, La Chapelle-aux- Saints.....	872
Figure A3.109 LA-MC-ICPMS Track for Sample M006, Bovid, Bouffia 118: Layer 1, La Chapelle-aux-Saints.....	874
Figure A3.110 Detailed LA-MC-ICPMS Uncorrected Sr Isotope Results, Sample M006, Bovid, Bouffia 118: Layer 1, La Chapelle-aux- Saints.....	875
Figure A3.111 Detailed LA-MC-ICPMS Corrected Sr Isotope Results, Sample M006, Bovid, Bouffia 118: Layer 1, La Chapelle-aux- Saints.....	876
Figure A3.112 LA-MC-ICPMS Track for Sample M007, Bovid, Bouffia 118: Layer 1, La Chapelle-aux-Saints.....	878
Figure A3.113 Detailed LA-MC-ICPMS Uncorrected Sr Isotope Results, Sample M007, Bovid, Bouffia 118: Layer 1, La Chapelle-aux- Saints.....	879
Figure A3.114 Detailed LA-MC-ICPMS Corrected Sr Isotope Results, Sample M007, Bovid, Bouffia 118: Layer 1, La Chapelle-aux- Saints.....	879
Figure A3.115 LA-MC-ICPMS Track for Sample M008, Bovid, Bouffia 118: Layer 1, La Chapelle-aux-Saints.....	882
Figure A3.116 Detailed LA-MC-ICPMS Uncorrected Sr Isotope Results, Sample M008, Bovid, Bouffia 118: Layer 1, La Chapelle-aux- Saints.....	883
Figure A3.117 Detailed LA-MC-ICPMS Corrected Sr Isotope Results, Sample M008, Bovid, Bouffia 118: Layer 1, La Chapelle-aux- Saints.....	884
Figure A3.118 LA-MC-ICPMS Track for Sample M009, Bovid, Bouffia 118: Layer 1, La Chapelle-aux-Saints.....	887
Figure A3.119 Detailed LA-MC-ICPMS Uncorrected Sr Isotope Results, Sample M009, Bovid, Bouffia 118: Layer 1, La Chapelle-aux- Saints.....	889
Figure A3.120 Detailed LA-MC-ICPMS Corrected Sr Isotope Results, Sample M009, Bovid, Bouffia 118: Layer 1, La Chapelle-aux- Saints.....	889
Figure A3.121 LA-MC-ICPMS Track for Sample M010, Bovid, Bouffia 118: Layer 1, La Chapelle-aux-Saints.....	891
Figure A3.122 Detailed LA-MC-ICPMS Uncorrected Sr Isotope Results, Sample M010, Bovid, Bouffia 118: Layer 1, La Chapelle-aux- Saints.....	892
Figure A3.123 Detailed LA-MC-ICPMS Corrected Sr Isotope Results, Sample M010, Bovid, Bouffia 118: Layer 1, La Chapelle-aux- Saints.....	893
Figure A3.124 LA-MC-ICPMS Track for Sample M011, Horse, Layer G7, Les Fieux	895

Figure A3.125 Detailed LA-MC-ICPMS Uncorrected Sr Isotope Results, Sample M011, Horse, Layer G7, Les Fieux.....	897
Figure A3.126 Detailed LA-MC-ICPMS Corrected Sr Isotope Results, Sample M011, Horse, Layer G7, Les Fieux.....	897
Figure A3.127 LA-MC-ICPMS Track for Sample M012, Horse, Layer G7, Les Fieux	899
Figure A3.128 Detailed LA-MC-ICPMS Uncorrected Sr Isotope Results, Sample M012, Horse, Layer G7, Les Fieux.....	901
Figure A3.129 Detailed LA-MC-ICPMS Corrected Sr Isotope Results, Sample M012, Horse, Layer G7, Les Fieux.....	901
Figure A3.130 LA-MC-ICPMS Track for Sample M013, Wild Boar, Layer G7, Les Fieux	904
Figure A3.131 Detailed LA-MC-ICPMS Uncorrected Sr Isotope Results, Sample M013, Wild Boar, Layer G7, Les Fieux.....	906
Figure A3.132 Detailed LA-MC-ICPMS Corrected Sr Isotope Results, Sample M013, Wild Boar, Layer G7, Les Fieux.....	906
Figure A3.133 LA-MC-ICPMS Track for Sample M014, Fox, Layer G7, Les Fieux.....	908
Figure A3.134 Detailed LA-MC-ICPMS Uncorrected Sr Isotope Results, Sample M014, Fox, Layer G7, Les Fieux	909
Figure A3.135 Detailed LA-MC-ICPMS Corrected Sr Isotope Results, Sample M014, Fox, Layer G7, Les Fieux	910
Figure A3.136 LA-MC-ICPMS Track for Sample M015, Hyena, Layer G7, Les Fieux	912
Figure A3.137 Detailed LA-MC-ICPMS Uncorrected Sr Isotope Results, Sample M015, Hyena, Layer G7, Les Fieux	913
Figure A3.138 Detailed LA-MC-ICPMS Corrected Sr Isotope Results, Sample M015, Hyena, Layer G7, Les Fieux	913
Figure A3.139 LA-MC-ICPMS Track for Sample M016, Bison, Layer G7, Les Fieux.....	916
Figure A3.140 Detailed LA-MC-ICPMS Uncorrected Sr Isotope Results, Sample M016, Bison, Layer G7, Les Fieux	917
Figure A3.141 Detailed LA-MC-ICPMS Corrected Sr Isotope Results, Sample M016, Bison, Layer G7, Les Fieux	917
Figure A3.142 LA-MC-ICPMS Track for Sample M017, Bison, Layer G7, Les Fieux.....	920
Figure A3.143 Detailed LA-MC-ICPMS Uncorrected Sr Isotope Results, Sample M017, Bison, Layer G7, Les Fieux	922
Figure A3.144 Detailed LA-MC-ICPMS Corrected Sr Isotope Results, Sample M017, Bison, Layer G7, Les Fieux	922
Figure A3.145 LA-MC-ICPMS Track for Sample M018, Reindeer, Layer G7, Les Fieux	924
Figure A3.146 Detailed LA-MC-ICPMS Uncorrected Sr Isotope Results, Sample M018, Reindeer, Layer G7, Les Fieux.....	925
Figure A3.147 Detailed LA-MC-ICPMS Corrected Sr Isotope Results, Sample M018, Reindeer, Layer G7, Les Fieux.....	925
Figure A3.148 LA-MC-ICPMS Track for Sample M019, Reindeer, Layer G7, Les Fieux	928
Figure A3.149 Detailed LA-MC-ICPMS Uncorrected Sr Isotope Results, Sample M019, Reindeer, Layer G7, Les Fieux.....	929

Figure A3.150 Detailed LA-MC-ICPMS Corrected Sr Isotope Results, Sample M019, Reindeer, Layer G7, Les Fieux	929
Figure A3.151 LA-MC-ICPMS Track for Sample M020, Chamois, Layer G7, Les Fieux	931
Figure A3.152 Detailed LA-MC-ICPMS Uncorrected Sr Isotope Results, Sample M020, Chamois, Layer G7, Les Fieux	932
Figure A3.153 Detailed LA-MC-ICPMS Corrected Sr Isotope Results, Sample M020, Chamois, Layer G7, Les Fieux	933
Figure A3.154 LA-MC-ICPMS Track for Sample M021, Mountain Goat/Chamois, Layer G7, Les Fieux.....	936
Figure A3.155 Detailed LA-MC-ICPMS Uncorrected Sr Isotope Results, Sample M021, Mountain Goat/Chamois, Layer G7, Les Fieux	938
Figure A3.156 Detailed LA-MC-ICPMS Corrected Sr Isotope Results, Sample M021, Mountain Goat/Chamois, Layer G7, Les Fieux	938
Figure A3.157 LA-MC-ICPMS Track for Sample M022, Mountain Goat/Chamois, Layer G7, Les Fieux.....	939
Figure A3.158 Detailed LA-MC-ICPMS Uncorrected Sr Isotope Results, Sample M022, Mountain Goat/Chamois, Layer G7, Les Fieux	940
Figure A3.159 Detailed LA-MC-ICPMS Corrected Sr Isotope Results, Sample M022, Mountain Goat/Chamois, Layer G7, Les Fieux	941
Figure A3.160 LA-MC-ICPMS Track for Sample 845, Bovid, Layer G1, Le Moustier	944
Figure A3.161 Detailed LA-MC-ICPMS Uncorrected Sr Isotope Results, Sample 845, Bovid, Layer G1, Le Moustier	946
Figure A3.162 Detailed LA-MC-ICPMS Corrected Sr Isotope Results, Sample 845, Bovid, Layer G1, Le Moustier	946
Figure A3.163 LA-MC-ICPMS Track for Sample 846, Bovid, Layer G2, Le Moustier	948
Figure A3.164 Detailed LA-MC-ICPMS Uncorrected Sr Isotope Results, Sample 846, Bovid, Layer G2, Le Moustier	949
Figure A3.165 Detailed LA-MC-ICPMS Uncorrected Sr Isotope Results, Sample 846, Bovid, Layer G2, Le Moustier	949
Figure A3.166 LA-MC-ICPMS Track for Sample 847, Bovid, Layer G3, Le Moustier	952
Figure A3.167 Detailed LA-MC-ICPMS Uncorrected Sr Isotope Results, Sample 847, Bovid, Layer G3, Le Moustier	954
Figure A3.168 Detailed LA-MC-ICPMS Corrected Sr Isotope Results, Sample 847, Bovid, Layer G3, Le Moustier	954
Figure A3.169 LA-MC-ICPMS Track for Sample 848, Bovid, Layer G4, Le Moustier	957
Figure A3.170 Detailed LA-MC-ICPMS Uncorrected Sr Isotope Results, Sample 848, Bovid, Layer G4, Le Moustier	959
Figure A3.171 Detailed LA-MC-ICPMS Corrected Sr Isotope Results, Sample 848, Bovid, Layer G4, Le Moustier	959
Figure A3.172 LA-MC-ICPMS Track for Sample 849, Bovid, Layer G5, Le Moustier	961
Figure A3.173 Detailed LA-MC-ICPMS Uncorrected Sr Isotope Results, Sample 849, Bovid, Layer G5, Le Moustier	963
Figure A3.174 Detailed LA-MC-ICPMS Corrected Sr Isotope Results, Sample 849, Bovid, Layer G5, Le Moustier	963

Figure A3.175 LA-MC-ICPMS Track for Sample 850, Bovid, Layer G6, Le Moustier.....	966
Figure A3.176 Detailed LA-MC-ICPMS Uncorrected Sr Isotope Results, Sample 850, Bovid, Layer G6, Le Moustier	968
Figure A3.177 Detailed LA-MC-ICPMS Corrected Sr Isotope Results, Sample 850, Bovid, Layer G6, Le Moustier	968
Figure A3.178 LA-MC-ICPMS Track for Sample 614, Bovid, Layer 9, Pech de l'Azé II.....	971
Figure A3.179 A3.1 Detailed LA-MC-ICPMS Uncorrected Sr Isotope Results, Sample 614, Bovid, Layer 9, Pech de l'Azé II.....	972
Figure A3.180 Detailed LA-MC-ICPMS Corrected Sr Isotope Results, Sample 614, Bovid, Layer 9, Pech de l'Azé II.....	972
Figure A3.181 LA-MC-ICPMS Track for Sample 615, Hippotamus, Layer 9, Pech de l'Azé II.....	974
Figure A3.182 Detailed LA-MC-ICPMS Uncorrected Sr Isotope Results, Sample 615, Hippotamus, Layer 9, Pech de l'Azé II.....	975
Figure A3.183 Detailed LA-MC-ICPMS Corrected Sr Isotope Results, Sample 615, Hippotamus, Layer 9, Pech de l'Azé II.....	976
Figure A3.184 LA-MC-ICPMS Track for Sample 617, Horse, Layer 8, Pech de l'Azé II.....	978
Figure A3.185 Detailed LA-MC-ICPMS Uncorrected Sr Isotope Results, Sample 617, Horse, Layer 8, Pech de l'Azé II	980
Figure A3.186 Detailed LA-MC-ICPMS Corrected Sr Isotope Results, Sample 617, Horse, Layer 8, Pech de l'Azé II	980
Figure A3.187 LA-MC-ICPMS Track for Sample 618, Deer, Layer 8, Pech de l'Azé II.....	982
Figure A3.188 Detailed LA-MC-ICPMS Uncorrected Sr Isotope Results, Sample 618, Deer, Layer 8, Pech de l'Azé II	984
Figure A3.189 Detailed LA-MC-ICPMS Corrected Sr Isotope Results, Sample 618, Deer, Layer 8, Pech de l'Azé II	984
Figure A3.190 LA-MC-ICPMS Track for Sample 619, Horse, Layer 8, Pech de l'Azé II.....	986
Figure A3.191 Detailed LA-MC-ICPMS Uncorrected Sr Isotope Results, Sample 619, Horse, Layer 8, Pech de l'Azé II	987
Figure A3.192 Detailed LA-MC-ICPMS Corrected Sr Isotope Results, Sample 619, Horse, Layer 8, Pech de l'Azé II	988
Figure A3.193 LA-MC-ICPMS Track for Sample 620, Bovid, Layer 7, Pech de l'Azé II.....	990
Figure A3.194 Detailed LA-MC-ICPMS Uncorrected Sr Isotope Results, Sample 620, Bovid, Layer 7, Pech de l'Azé II.....	991
Figure A3.195 Detailed LA-MC-ICPMS Corrected Sr Isotope Results, Sample 620, Bovid, Layer 7, Pech de l'Azé II.....	991
Figure A3.196 LA-MC-ICPMS Track for Sample 622, Hippopotamus, Layer 7, Pech de l'Azé II.....	993
Figure A3.197 Detailed LA-MC-ICPMS Uncorrected Sr Isotope Results, Sample 622, Hippopotamus, Layer 7, Pech de l'Azé II.....	995
Figure A3.198 Detailed LA-MC-ICPMS Corrected Sr Isotope Results, Sample 622, Hippopotamus, Layer 7, Pech de l'Azé II.....	995
Figure A3.199 LA-MC-ICPMS Track for Sample 624, Deer, Layer 6, Pech de l'Azé II.....	997

Figure A3.200 Detailed LA-MC-ICPMS Uncorrected Sr Isotope Results, Sample 624, Deer, Layer 6, Pech de l'Azé II	998
Figure A3.201 Detailed LA-MC-ICPMS Corrected Sr Isotope Results, Sample 624, Deer, Layer 6, Pech de l'Azé II	998
Figure A3.202 LA-MC-ICPMS Track for Sample 625, Horse, Layer 6, Pech de l'Azé II	1000
Figure A3.203 Detailed LA-MC-ICPMS Uncorrected Sr Isotope Results, Sample 625, Horse, Layer 6, Pech de l'Azé II	1002
Figure A3.204 Detailed LA-MC-ICPMS Corrected Sr Isotope Results, Sample 625, Horse, Layer 6, Pech de l'Azé II	1003
Figure A3.205 LA-MC-ICPMS Track for Sample 2417, Bovid, Layer 1C, Bois Roche	1006
Figure A3.206 Detailed LA-MC-ICPMS Uncorrected Sr Isotope Results, Sample 2417, Bovid, Layer 1C, Bois Roche	1007
Figure A3.207 Detailed LA-MC-ICPMS Corrected Sr Isotope Results, Sample 2417, Bovid, Layer 1C, Bois Roche	1007
Figure A3.208 LA-MC-ICPMS Track for Sample 2418, Bovid, Layer 1C, Bois Roche	1009
Figure A3.209 Detailed LA-MC-ICPMS Uncorrected Sr Isotope Results, Sample 2418, Bovid, Layer 1C, Bois Roche	1010
Figure A3.210 Detailed LA-MC-ICPMS Corrected Sr Isotope Results, Sample 2418, Bovid, Layer 1C, Bois Roche	1011
Figure A3.211 LA-MC-ICPMS Track for Sample 2419, Bovid, Layer 1C, Bois Roche	1012
Figure A3.212 Detailed LA-MC-ICPMS Uncorrected Sr Isotope Results, Sample 2419, Bovid, Layer 1C, Bois Roche	1013
Figure A3.213 Detailed LA-MC-ICPMS Corrected Sr Isotope Results, Sample 2419, Bovid, Layer 1C, Bois Roche	1013
Figure A3.214 LA-MC-ICPMS Track for Sample 2420, Bovid, Layer 2, Bois Roche	1015
Figure A3.215 Detailed LA-MC-ICPMS Uncorrected Sr Isotope Results, Sample 2420, Bovid, Layer 2, Bois Roche	1016
Figure A3.216 Detailed LA-MC-ICPMS Corrected Sr Isotope Results, Sample 2420, Bovid, Layer 2, Bois Roche	1017
Figure A3.217 LA-MC-ICPMS Track for Sample 2421, Bovid, Layer 2, Bois Roche	1020
Figure A3.218 Detailed LA-MC-ICPMS Uncorrected Sr Isotope Results, Sample 2421, Bovid, Layer 2, Bois Roche	1022
Figure A3.219 Detailed LA-MC-ICPMS Corrected Sr Isotope Results, Sample 2421, Bovid, Layer 2, Bois Roche	1022
Figure A3.220 LA-MC-ICPMS Track for Sample 2422, Bovid, Layer 2, Bois Roche	1024
Figure A3.221 Detailed LA-MC-ICPMS Uncorrected Sr Isotope Results, Sample 2422, Bovid, Layer 2, Bois Roche	1025
Figure A3.222 Detailed LA-MC-ICPMS Corrected Sr Isotope Results, Sample 2422, Bovid, Layer 2, Bois Roche	1026
Figure A3.223 LA-MC-ICPMS Track for Sample 2423, Bovid, Layer 2, Bois Roche	1029
Figure A3.224 Detailed LA-MC-ICPMS Uncorrected Sr Isotope Results, Sample 2423, Bovid, Layer 2, Bois Roche	1031

Figure A3.225 Detailed LA-MC-ICPMS Corrected Sr Isotope Results, Sample 2423, Bovid, Layer 2, Bois Roche	1031
Figure A3.226 LA-MC-ICPMS Track for Sample 2424, Bovid, Layer 2, Bois Roche	1033
Figure A3.227 Detailed LA-MC-ICPMS Uncorrected Sr Isotope Results, Sample 2424, Bovid, Layer 2, Bois Roche	1035
Figure A3.228 Sample 2424, Detailed LA-MC-ICPMS Corrected Sr Isotope Results, Sample 2424, Bovid, Layer 2, Bois Roche	1035
Figure A3.229 LA-MC-ICPMS Track for Sample 2425A, Bovid, Layer 2, Bois Roche	1036
Figure A3.230 Detailed LA-MC-ICPMS Uncorrected Sr Isotope Results, Sample 2425A, Bovid, Layer 2, Bois Roche	1038
Figure A3.231 Detailed LA-MC-ICPMS Corrected Sr Isotope Results, Sample 2425A, Bovid, Layer 2, Bois Roche	1038
Figure A3.232 LA-MC-ICPMS Track for Sample 2425B, Bovid, Layer 2, Bois Roche	1040
Figure A3.233 Detailed LA-MC-ICPMS Sr Isotope Results for Dentine and Enamel, Sample 2425B, Bovid, Layer 2, Bois Roche	1042
Figure A3.234 Detailed LA-MC-ICPMS Corrected Sr Isotope Results, Sample 2425B, Bovid, Layer 2, Bois Roche	1042
Figure A3.235 LA-MC-ICPMS Track for Sample 2425C, Bovid, Layer 2, Bois Roche	1044
Figure A3.236 Detailed LA-MC-ICPMS Uncorrected Sr Isotope Results, Sample 2425C, Bovid, Layer 2, Bois Roche	1046
Figure A3.237 Detailed LA-MC-ICPMS Corrected Sr Isotope Results, Sample 2425C, Bovid, Layer 2, Bois Roche	1046
Figure A3.238 LA-MC-ICPMS Track for Sample M033, Bovid, Layer C1, Rescoundudou	1049
Figure A3.239 Detailed LA-MC-ICPMS Uncorrected Sr Isotope Results, Sample M033, Bovid, Layer C1, Rescoundudou	1051
Figure A3.240 Detailed LA-MC-ICPMS Corrected Sr Isotope Results, Sample M033, Bovid, Layer C1, Rescoundudou	1052
Figure A3.241 LA-MC-ICPMS Track for Sample M034, Bovid, Layer C1, Rescoundudou	1054
Figure A3.242 Detailed LA-MC-ICPMS Uncorrected Sr Isotope Results, Sample M034, Bovid, Layer C1, Rescoundudou	1055
Figure A3.243 Detailed LA-MC-ICPMS Corrected Sr Isotope Results, Sample M034, Bovid, Layer C1, Rescoundudou	1056
Figure A3.244 LA-MC-ICPMS Track for Sample M035, Horse, Layer C1, Rescoundudou	1058
Figure A3.245 Detailed LA-MC-ICPMS Uncorrected Sr Isotope Results, Sample M035, Horse, Layer C1, Rescoundudou	1060
Figure A3.246 Detailed LA-MC-ICPMS Corrected Sr Isotope Results, Sample M035, Horse, Layer C1, Rescoundudou	1060
Figure A3.247 LA-MC-ICPMS Track for Sample M036, Horse, Layer C1, Rescoundudou	1063
Figure A3.248 Detailed LA-MC-ICPMS Uncorrected Sr Isotope Results, Sample M036, Horse, Layer C1, Rescoundudou	1065
Figure A3.249 Detailed LA-MC-ICPMS Corrected Sr Isotope Results, Sample M036, Horse, Layer C1, Rescoundudou	1065

Figure A3.250 LA-MC-ICPMS Track for Sample M037, Horse, Layer C1, Rescoundudou.....	1067
Figure A3.251 Detailed LA-MC-ICPMS Uncorrected Sr Isotope Results, Sample M037, Horse, Layer C1, Rescoundudou.....	1070
Figure A3.252 Detailed LA-MC-ICPMS Corrected Sr Isotope Results, Sample M037, Horse, Layer C1, Rescoundudou.....	1070
Figure A3.253 LA-MC-ICPMS Track for Sample M038, Rhinoceros, Layer C1, Rescoundudou	1072
Figure A3.254 Detailed LA-MC-ICPMS Uncorrected Sr Isotope Results, Sample M038, Rhinoceros, Layer C1, Rescoundudou	1073
Figure A3.255 Detailed LA-MC-ICPMS Corrected Sr Isotope Results, Sample M038, Rhinoceros, Layer C1, Rescoundudou	1074
Figure A3.256 LA-MC-ICPMS Track for Sample M039, Bovid, Layer C1, Rescoundudou.....	1076
Figure A3.257 Detailed LA-MC-ICPMS Uncorrected Sr Isotope Results, Sample M039, Bovid, Layer C1, Rescoundudou	1077
Figure A3.258 Detailed LA-MC-ICPMS Corrected Sr Isotope Results, Sample M039, Bovid, Layer C1, Rescoundudou	1077
Figure A3.259 LA-MC-ICPMS Track for Sample M040, Bovid, Layer C1, Rescoundudou.....	1079
Figure A3.260 Detailed LA-MC-ICPMS Uncorrected Sr Isotope Results, Sample M040, Bovid, Layer C1, Rescoundudou	1080
Figure A3.261 Detailed LA-MC-ICPMS Corrected Sr Isotope Results, Sample M040, Bovid, Layer C1, Rescoundudou	1081
Figure A3.262 LA-MC-ICPMS Track for Sample M041, Bovid, Layer C1, Rescoundudou.....	1084
Figure A3.263 LA-MC-ICPMS Track for the External Enamel of Sample M041, Sample M041, Bovid, Layer C1, Rescoundudou	1084
Figure A3.264 Detailed LA-MC-ICPMS Uncorrected Sr Isotope Results, Sample M041, Bovid, Layer C1, Rescoundudou	1086
Figure A3.265 Detailed LA-MC-ICPMS Corrected Sr Isotope Results, Sample M041, Bovid, Layer C1, Rescoundudou	1086
Figure A3.266 LA-MC-ICPMS Track for Sample M042, Deer, Layer C1, Rescoundudou.....	1088
Figure A3.267 LA-MC-ICPMS Track for the External Enamel of Sample M042, Deer, Layer C1, Rescoundudou	1089
Figure A3.268 Detailed LA-MC-ICPMS Uncorrected Sr Isotope Results, Sample M042, Deer, Layer C1, Rescoundudou	1090
Figure A3.269 Detailed LA-MC-ICPMS Corrected Sr Isotope Results, Sample M042, Deer, Layer C1, Rescoundudou	1091
Figure A3.270 LA-MC-ICPMS Track for Sample M043, Deer, Layer C1, Rescoundudou.....	1094
Figure A3.271 Detailed LA-MC-ICPMS Uncorrected Sr Isotope Results, Sample M043, Deer, Layer C1, Rescoundudou	1096
Figure A3.272 Detailed LA-MC-ICPMS Corrected Sr Isotope Results, Sample M043, Deer, Layer C1, Rescoundudou	1096
Figure A3.273 LA-MC-ICPMS Track for Sample M044, Deer, Layer C1, Rescoundudou.....	1098
Figure A3.274 Detailed LA-MC-ICPMS Uncorrected Sr Isotope Results, Sample M044, Deer, Layer C1, Rescoundudou	1100

Figure A3.275 Detailed LA-MC-ICPMS Corrected Sr Isotope Results, Sample M044, Deer, Layer C1, Rescoundudou	1100
Figure A3.276 LA-MC-ICPMS Track for Sample M045, Deer, Layer C1, Rescoundudou	1102
Figure A3.277 Detailed LA-MC-ICPMS Uncorrected Sr Isotope Results, Sample M044, Deer, Layer C1, Rescoundudou	1103
Figure A3.278 Detailed LA-MC-ICPMS Corrected Sr Isotope Results, Sample M044, Deer, Layer C1, Rescoundudou	1104

List of Tables

Table 2.1 Average Concentrations of Strontium and other Elements in Common Materials (Modified from Capo et al. 1998:200)	8
Table 2.2 Average Strontium Isotope Composition of Some Common Geological Materials (Modified from Capo et al. 1998:204)	10
Table 2.3 Selected Strontium Isotope Studies of Palaeolithic or Older Archaeological Material	38
Table 2.4 Selected Strontium Isotope Studies of European Neolithic Archaeological Material	39
Table 2.5 Selected Strontium Isotope Studies of Other European Archaeology Material	40
Table 2.6 Selected Strontium Isotope Studies of Asian Archaeology Material..	41
Table 2.7 Selected Strontium Isotope Studies of Pacific Archaeology Material.....	41
Table 2.8 Selected Strontium Isotope Studies of American Archaeology Material.....	43
Table 2.9 Selected Strontium Isotope Studies of Middle Eastern Archaeology Material	43
Table 2.10 Selected Strontium Isotope Studies of Post-Palaeolithic African Archaeology Material	44
Table 3.1 Original MIS, Temperature Trends and Alpine Glaciations (Data From Gibbard and Van Kolfschoten 2004; Shackleton and Opdyke 1973; 1976)	61
Table 3.2 Correlation between Local Glacial Stages, MIS and Vegetation Based on the Palynology of Cores from Velay, Massif Central (Data: Reille et al. 1998; Reille and de Beaulieu 1990)	68
Table 3.3 Garrod's Stratigraphic Units for Tabun and Original Interpretation of Lithic Technology (Garrod 1934)	139
Table 3.4 Modified ESR Dates for Tabun (Grün and Stringer 2000:602).....	142
Table 4.1 Israeli Sample Collection Locations (All Locations WGS-84:36R-36S)	174
Table 4.2 Sample Collection Locations, France 2006 (All Locations in WGS84–31T).....	179
Table 4.3 Sample Collection Locations, France 2009 (All Positions WGS84: UTM/UPS)	184
Table 4.4 ESR Dates for Samples in this Study from Skhul (Data: Grün et al. 2005)	186
Table 4.5 Uranium Concentration of Samples in this Study from Skhul (Data: Grün et al. 2005)	186
Table 4.6 Uranium Concentration for Samples in this Study from Tabun (Data: Grun et al. 1991:242)	187
Table 4.7 MC-ICPMS Instrument Settings	203
Table 4.8 LA-MC-ICPMS Instrument Settings.....	204
Table 5.1 Israeli Bioavailable Soil Strontium Isotope Results	216

Table 5.2 Israeli Bioavailable Rock Strontium Isotope Results	220
Table 5.3 French Plant (Grass) Bioavailable Strontium Isotope Results	225
Table 5.4 French Soil Bioavailable Strontium Isotope Results.....	229
Table 5.5 French Rock Bioavailable Strontium Isotope Results	230
Table 5.6 Summary Table of LA-ICPMS Elemental Concentrations and Ratios for Faunal Teeth from Skhul	231
Table 5.7 $^{87}\text{Sr}/^{86}\text{Sr}$ Results from Archaeological Sediments from Skhul	232
Table 5.8 Summary Table of Skhul Faunal Teeth LA-MC-ICPMS Sr Isotope Results.....	234
Table 5.9 Summary of Mobility Results for Analysed Fauna from Skhul	237
Table 5.10 Summary Table of LA-ICPMS Elemental Concentrations and Ratios for Faunal Teeth from Tabun	238
Table 5.11 $^{87}\text{Sr}/^{86}\text{Sr}$ Results from Archaeological Sediments from Tabun.....	239
Table 5.12 Summary Table of Tabun LA-MC-ICPMS Sr Isotope Results.....	241
Table 5.13 Summary Table of Tabun Faunal Teeth LA-MC-ICPMS Sr Isotope Results.....	243
Table 5.14 $^{87}\text{Sr}/^{86}\text{Sr}$ Results from Archaeological Sediments from Amud.....	244
Table 5.15 Summary Table of Amud Faunal Teeth LA-MC-ICPMS Sr Isotope Results	246
Table 5.16 Summary of Mobility Results for Analysed Fauna from Amud	247
Table 5.17 Average Elemental Concentrations and Ratios for Sample 373, an unidentified tooth from layer XV of Qafzeh	248
Table 5.18 $^{87}\text{Sr}/^{86}\text{Sr}$ Results from Archaeological Sediments from Qafzeh	249
Table 5.19 Summary Table of Qafzeh Faunal Teeth LA-MC-ICPMS Sr Isotope Results	251
Table 5.20 Summary of Mobility Results for Analysed Fauna from Qafzeh....	253
Table 5.21 Average Elemental Concentrations and Ratios for Sample 1557, Bovid, Holon	254
Table 5.22 Summary Table of Holon Faunal Teeth LA-MC-ICPMS Sr Isotope Results	255
Table 5.23 Sample 1557, a Bovid from Holon, Detailed LA-MC-ICPMS Sr Isotope Results	256
Table 5.24 Summary of Mobility Results for Analysed Fauna from Holon	257
Table 5.25 Summary Table of LA-ICPMS Elemental Concentrations and Ratios for Faunal Teeth from La Chapelle-aux-Saints	259
Table 5.26 $^{87}\text{Sr}/^{86}\text{Sr}$ Results from Archaeological Sediments from La Chapelle-aux-Saints	260
Table 5.27 Summary Table of La Chapelle-aux-Saints Faunal Teeth LA-MC- ICPMS Sr Isotope Results	262
Table 5.28 Summary of Mobility Results for Analysed Fauna from La Chapelle-aux-Saints	266
Table 5.29 $^{87}\text{Sr}/^{86}\text{Sr}$ Results from Archaeological Sediments from Les Fieux	267
Table 5.30 Summary Table of Les Fieux Faunal Teeth LA-MC-ICPMS Sr Isotope Results	270
Table 5.31 Summary of Mobility Results for Analysed Fauna from Les Fieux	272
Table 5.32 Summary Table of Le Moustier Faunal Teeth LA-MC-ICPMS Sr Isotope Results	274
Table 5.33 Summary of Mobility Results for Analysed Fauna from Le Moustier.....	276

Table 5.34 Summary Table of Pech de l’Azé II Faunal Teeth LA-MC-ICPMS Sr Isotope Results	278
Table 5.35 Summary of Mobility Results for Analysed Fauna from Pech de l’Azé II.....	281
Table 5.36 Summary Table of LA-ICPMS Elemental Concentrations and Ratios from Bois Roche Faunal Teeth	282
Table 5.37 $^{87}\text{Sr}/^{86}\text{Sr}$ Results from Archaeological Sediments from Bois Roche	283
Table 5.38 Summary Table of Bois Roche Faunal Teeth LA-MC-ICPMS Sr Isotope Results	286
Table 5.39 Summary of Mobility Results for Analysed Fauna from Bois Roche	288
Table 5.40 $^{87}\text{Sr}/^{86}\text{Sr}$ Results from Archaeological Sediments from Rescoundudou.....	288
Table 5.41 Summary Table of Rescoundudou Faunal Teeth LA-MC-ICPMS Sr Isotope Results	291
Table 5.42 Summary of Mobility Results for Analysed Fauna from Rescoundudou.....	294
Table 5.43 Durango Apatite LA-MC-ICPMS Sr Isotope Results	294
Table 5.44 Summary Table of Tridacna LA-MC-ICPMS Sr Isotope Results ...	296
Table 6.1 Comparison of Matching Rock and Soil Bioavailable $^{87}\text{Sr}/^{86}\text{Sr}$ Results from Matched Sample Locations in Israel	305
Table 6.2 Summary of Faunal Mobility Patterns Based on Strontium Isotope Results.....	317
Table 6.3 Mobility Results for all Fauna and for Bovids from all Archaeological Sites in this Study	329
Table 6.4 Faunal Mobility of all Samples Compared to Marine Isotope Stages Based on Strontium Isotope Results	334
Table A3.1 Elemental Concentrations and Ratios for Enamel, Sample 851, Bovid, Unknown Layer, Skhul.....	715
Table A3.2 Elemental Concentrations and Ratios for Dentine, Sample 851, Bovid, Unknown Layer, Skhul.....	716
Table A3.3 Elemental Concentrations and Ratios for Enamel, Sample 852, Bovid, Unknown Layer, Skhul	718
Table A3.4 Elemental Concentrations and Ratios for Dentine, Sample 852, Bovid, Unknown Layer, Skhul	719
Table A3.5 Elemental Concentrations and Ratios for Enamel, Sample 853, Bovid, Unknown Layer, Skhul	721
Table A3.6 Elemental Concentrations and Ratios for Dentine, Sample 853, Bovid, Unknown Layer, Skhul	722
Table A3.7 Elemental Concentrations and Ratios for Enamel, Sample 554, <i>Bos</i> , Layer D, Tabun.....	722
Table A3.8 Elemental Concentrations and Ratios for Enamel, Sample 556, <i>Bos</i> , Layer D, Tabun	723
Table A3.9 Elemental Concentrations and Ratios for Enamel, Sample 557, <i>Bos</i> , Layer Ea, Tabun	723
Table A3.10 Elemental Concentrations and Ratios for Enamel, Sample 557 (2), <i>Bos</i> , Layer Ea, Tabun.....	724
Table A3.11 Elemental Concentrations and Ratios for Enamel, Sample 558, <i>Bos</i> , Layer Ea, Tabun	724

Table A3.12 Elemental Concentrations and Ratios for Enamel and Dentine, Sample 561, <i>Bos</i> , Layer Eb, Tabun.....	725
Table A3.13 Elemental Concentrations and Ratios for Enamel and Dentine, Sample 563, <i>Bos</i> , Layer Eb, Tabun.....	725
Table A3.14 Elemental Concentrations and Ratios for Dentine, Sample 564, <i>Bos</i> , Layer Ec, Tabun	726
Table A3.15 Elemental Concentrations and Ratios for Enamel and Dentine, Sample 565, <i>Bos</i> , Layer Ec, Tabun	726
Table A3.16 Elemental Concentrations and Ratios for Enamel and Dentine, Sample 567, <i>Bos</i> , Layer Ed, Tabun.....	727
Table A3.17 Elemental Concentrations and Ratios for Enamel, Sample 373, Unidentified Species, Layer XVII, Qafzeh.....	727
Table A3.18 Elemental Concentrations and Ratios for Enamel, Sample 1557, Bovid, Unit C, Holon	728
Table A3.19 Elemental Concentrations and Ratios for Enamel, Sample M001, Reindeer, Bouffia 118: Layer 2, La Chapelle-aux-Saints	729
Table A3.20 Elemental Concentrations and Ratios for Enamel, Sample M002, Reindeer, Bouffia 118: Layer 2, La Chapelle-aux-Saints	729
Table A3.21 Elemental Concentrations and Ratios for Enamel and Dentine, Sample M003, Reindeer, Bouffia 118: Layer 2, La Chapelle-aux-Saints.....	729
Table A3.22 Elemental Concentrations and Ratios for Enamel and Dentine, Sample M004, Unknown Species, Bouffia 118: Unknown Layer, La Chapelle-aux-Saints	730
Table A3.23 Elemental Concentrations and Ratios for Dentine, Sample M005, Bovid, Bouffia 118: Layer 1, La Chapelle-aux-Saints.....	730
Table A3.24 Elemental Concentrations and Ratios for Enamel Transect, Sample M006, Bovid, Bouffia 118: Layer 1, La Chapelle-aux-Saints.....	731
Table A3.25 Elemental Concentrations and Ratios for Enamel Transect, Sample M007, Bovid, Bouffia 118: Layer 1, La Chapelle-aux-Saints.....	731
Table A3.26 Elemental Concentrations and Ratios for Enamel and Dentine Transects, Sample M008, Bovid, Bouffia 118: Layer 1, La Chapelle-aux-Saints	732
Table A3.27 Elemental Concentrations and Ratios for Enamel and Dentine Transects, Sample M009, Bovid, Bouffia 118: Layer 1, La Chapelle-aux-Saints	732
Table A3.28 Elemental Concentrations and Ratios for Enamel and Dentine Transects, Sample M010, Bovid, Bouffia 118: Layer 1, La Chapelle-aux-Saints	733
Table A3.29 Elemental Concentrations and Ratios for Enamel and Dentine Transects, Sample 2417, Bovid, Layer 1C, Bois Roche	734
Table A3.30 Elemental Concentrations and Ratios for Enamel and Dentine Transects, Sample 2418, Bovid, Layer 1C, Bois Roche	734
Table A3.31 Elemental Concentrations and Ratios for Enamel and Dentine Transects, Sample 2421, Bovid, Layer 2, Bois Roche.....	735
Table A3.32 Elemental Concentrations and Ratios for Enamel and Dentine Transects, Sample 2422, Bovid, Layer 1C, Bois Roche	735
Table A3.33 Durango Apatite LA-MC-ICPMS Sr Isotope Results.....	737

Table A3.34 Detailed LA-MC-ICPMS Sr Isotope Results for Dentine, Sample 851, Bovid, Unknown Stratigraphic Provenance, Skhul.....	741
Table A3.35 Detailed LA-MC-ICPMS Sr Isotope Results for Enamel, Sample 851, Bovid, Unknown Stratigraphic Provenance, Skhul.....	742
Table A3.36 Detailed LA-MC-ICPMS Sr Isotope Results for Dentine, Sample 852 Dentine, Unknown Stratigraphic Provenance, Skhul, ..	747
Table A3.37 Detailed LA-MC-ICPMS Sr Isotope Results for Enamel, Sample 852, Unknown Stratigraphic Provenance, Skhul,.....	748
Table A3.38 Detailed LA-MC-ICPMS Sr Isotope Results for Dentine, Sample 853, Bovid, Unknown Stratigraphic Provenance, Skhul.....	752
Table A3.39 Detailed LA-MC-ICPMS Sr Isotope Results for Enamel, Sample 853, Bovid, Unknown Stratigraphic Provenance, Skhul.....	754
Table A3.40 Detailed LA-MC-ICPMS Sr Isotope Results for Dentine, Sample 1057A, Bovid, Layer B, Skhul	758
Table A3.41 Detailed LA-MC-ICPMS Sr Isotope Results for Enamel and Dentine, Sample 1057B, Bovid, Layer B, Skhul.....	762
Table A3.42 Detailed LA-MC-ICPMS Sr Isotope Results for Enamel and Dentine, Sample 1057C, Bovid, Layer B, Skhul.....	766
Table A3.43 Detailed LA-MC-ICPMS Sr Isotope Results for Enamel and Dentine, Wild Boar, Layer B, Skhul.....	769
Table A3.44 Detailed LA-MC-ICPMS Sr Isotope Results for Enamel and Dentine, Wild Boar, Layer B, Skhul.....	773
Table A3.45 Detailed LA-MC-ICPMS Sr Isotope Results for Enamel and Dentine, Sample 1058C, Wild Boar, Layer B, Skhul	776
Table A3.46 Detailed LA-MC-ICPMS Sr Isotope Results for Enamel, Sample 554, <i>Bos</i> , Layer D, Tabun	780
Table A3.47 Detailed LA-MC-ICPMS Sr Isotope Results for Enamel, Sample 556, <i>Bos</i> , Layer D, Tabun	783
Table A3.48 Detailed LA-MC-ICPMS Sr Isotope Results for Enamel, Sample 557, <i>Bos</i> , Layer Ea, Tabun	786
Table A3.49 Detailed LA-MC-ICPMS Sr Isotope Results for Enamel, Sample 558, <i>Bos</i> , Layer Ea, Tabun	789
Table A3.50 Detailed LA-MC-ICPMS Sr Isotope Results for Enamel and Dentine, Sample 561, <i>Bos</i> , Layer Eb, Tabun.....	792
Table A3.51 Detailed LA-MC-ICPMS Sr Isotope Results for Enamel and Dentine, Sample 563, <i>Bos</i> , Layer Eb, Tabun.....	795
Table A3.52 Detailed LA-MC-ICPMS Sr Isotope Results, Sample 564, <i>Bos</i> , Layer Ec, Tabun	798
Table A3.53 Detailed LA-MC-ICPMS Sr Isotope Results for Enamel and Dentine, Sample 565, <i>Bos</i> , Layer Eb, Tabun.....	800
Table A3.54 Detailed LA-MC-ICPMS Sr Isotope Results for Enamel and Dentine, <i>Bos</i> , Layer Ed, Tabun.....	804
Table A3.55 Detailed LA-MC-ICPMS Sr Isotope Results for Enamel and Dentine, Sample 568, Rhinoceros, Layer Ed, Tabun.....	809
Table A3.56 Detailed LA-MC-ICPMS Sr Isotope Results for Enamel and Dentine, Sample 1024, <i>Dama mesopotamica</i> , Layer B1, Amud.....	813
Table A3.57 Detailed LA-MC-ICPMS Sr Isotope Results for Enamel and Dentine, Sample 1025, <i>Dama mesopotamica</i> , Layer B1, Amud.....	817
Table A3.58 Detailed LA-MC-ICPMS Sr Isotope Results for Enamel and Dentine, Sample 1026, <i>Dama mesopotamica</i> , Layer B1, Amud.....	821

Table A3.59 Detailed LA-MC-ICPMS Sr Isotope Results for Enamel, Sample 370, Bovid, Layer XV, Qafzeh	824
Table A3.60 Detailed LA-MC-ICPMS Sr Isotope Results for Enamel, Sample 371, Bovid, Layer XIX, Qafzeh	828
Table A3.61 Detailed LA-MC-ICPMS Sr Isotope Results, Sample 372, Bovid, Layer XVII, Qafzeh	832
Table A3.62 Sample 373, Qafzeh, Detailed LA-MC-ICPMS Sr Isotope Results.....	835
Table A3.63 Detailed LA-MC-ICPMS Sr Isotope Results for Enamel, Sample 374, Unidentified Species, Layer XV, Qafzeh.....	838
Table A3.64 Detailed LA-MC-ICPMS Sr Isotope Results for Enamel and Dentine, Sample 592, Bovid, Bouffia Bonneval: Stratum 1, La Chapelle-aux-Saints	843
Table A3.65 Detailed LA-MC-ICPMS Sr Isotope Results for Enamel and Dentine, Sample 593, Bovid, Bouffia Bonneval: Stratum 1, La Chapelle-aux-Saints	850
Table A3.66 Detailed LA-MC-ICPMS Sr Isotope Results for Enamel and Dentine, Sample 595, Bovid, Bouffia Bonneval: Stratum 1, La Chapelle-aux-Saints	855
Table A3.67 Detailed LA-MC-ICPMS Sr Isotope Results for Dentine and Enamel, Sample M001, Reindeer, Bouffia 118: Layer 2, La Chapelle-aux-Saints	858
Table A3.68 Detailed LA-MC-ICPMS Sr Isotope Results for Enamel, Sample M002, Reindeer, Bouffia 118: Layer 2, La Chapelle-aux-Saints	862
Table A3.69 Detailed LA-MC-ICPMS Sr Isotope Results for Enamel and Dentine, Reindeer, Bouffia 118: Layer 2, La Chapelle-aux-Saints...	865
Table A3.70 Detailed LA-MC-ICPMS Sr Isotope Results for Enamel and Dentine, Sample M004, Unknown Species, Bouffia 118: Unknown Layer, La Chapelle-aux-Saints	868
Table A3.71 Detailed LA-MC-ICPMS Sr Isotope Results for Dentine and Enamel, Sample M005, Bovid, Bouffia 118: Layer 1, La Chapelle-aux-Saints.....	871
Table A3.72 Detailed LA-MC-ICPMS Sr Isotope Results for Dentine and Enamel, Sample M006, Bovid, Bouffia 118: Layer 1, La Chapelle-aux-Saints.....	875
Table A3.73 Detailed LA-MC-ICPMS Sr Isotope Results for Dentine and Enamel, Sample M007, Bovid, Bouffia 118: Layer 1, La Chapelle-aux-Saints.....	878
Table A3.74 Detailed LA-MC-ICPMS Sr Isotope Results for Dentine and Enamel, Sample M008, Bovid, Bouffia 118: Layer 1, La Chapelle-aux-Saints.....	882
Table A3.75 Detailed LA-MC-ICPMS Sr Isotope Results for Dentine and Enamel, Sample M009, Bovid, Bouffia 118: Layer 1, La Chapelle-aux-Saints.....	888
Table A3.76 Detailed LA-MC-ICPMS Sr Isotope Results for Dentine and Enamel, Sample M010, Bovid, Bouffia 118: Layer 1, La Chapelle-aux-Saints.....	892
Table A3.77 Detailed LA-MC-ICPMS Sr Isotope Results for Dentine and Enamel, Sample M011, Horse, Layer G7, Les Fieux.....	896

Table A3.78 Detailed LA-MC-ICPMS Sr Isotope Results for Dentine and Enamel, Sample M012, Horse, Layer G7, Les Fieux.....	900
Table A3.79 Detailed LA-MC-ICPMS Sr Isotope Results for Dentine and Enamel, Sample M013, Wild Boar, Layer G7, Les Fieux.....	905
Table A3.80 Detailed LA-MC-ICPMS Sr Isotope Results for Dentine and Enamel, Sample M014, Fox, Layer G7, Les Fieux	909
Table A3.81 Detailed LA-MC-ICPMS Sr Isotope Results for Dentine and Enamel, Sample M015, Hyena, Layer G7, Les Fieux	912
Table A3.82 Detailed LA-MC-ICPMS Sr Isotope Results for Dentine and Enamel, Sample M016, Bison, Layer G7, Les Fieux	916
Table A3.83 Detailed LA-MC-ICPMS Sr Isotope Results for Dentine and Enamel, Sample M017, Bison, Layer G7, Les Fieux	921
Table A3.84 Detailed LA-MC-ICPMS Sr Isotope Results, Sample M018, Reindeer, Layer G7, Les Fieux	924
Table A3.85 Detailed LA-MC-ICPMS Sr Isotope Results, Sample M019, Reindeer, Layer G7, Les Fieux	928
Table A3.86 Detailed LA-MC-ICPMS Sr Isotope Results, Sample M020, Chamois, Layer G7, Les Fieux	932
Table A3.87 Detailed LA-MC-ICPMS Sr Isotope Results for Dentine and Enamel, Sample M021, Mountain Goat/Chamois, Layer G7, Les Fieux.....	937
Table A3.88 Detailed LA-MC-ICPMS Sr Isotope Results, Sample M022, Mountain Goat/Chamois, Layer G7, Les Fieux.....	940
Table A3.89 Detailed LA-MC-ICPMS Sr Isotope Results for Dentine and Enamel, Sample 845, Bovid, Layer G1, Le Moustier	945
Table A3.90 Detailed LA-MC-ICPMS Sr Isotope Results, Sample 846, Bovid, Layer G2, Le Moustier	948
Table A3.91 Detailed LA-MC-ICPMS Sr Isotope Results for Dentine and Enamel, Sample 847, Bovid, Layer G3, Le Moustier	953
Table A3.92 Detailed LA-MC-ICPMS Sr Isotope Results for Dentine and Enamel, Sample 848, Bovid, Layer G4, Le Moustier	958
Table A3.93 Detailed LA-MC-ICPMS Sr Isotope Results for Dentine and Enamel, Sample 849, Bovid, Layer G5, Le Moustier	962
Table A3.94 Detailed LA-MC-ICPMS Sr Isotope Results for Dentine and Enamel, Sample 850, Bovid, Layer G6, Le Moustier	967
Table A3.95 Detailed LA-MC-ICPMS Sr Isotope Results for Dentine and Enamel, Sample 614, Bovid, Layer 9, Pech de l'Azé II.....	971
Table A3.96 Detailed LA-MC-ICPMS Sr Isotope Results for Dentine and Enamel, Sample 615, Hippotamus, Layer 9, Pech de l'Azé II.....	975
Table A3.97 Detailed LA-MC-ICPMS Sr Isotope Results, Sample 617, Horse, Layer 8, Pech de l'Azé II	979
Table A3.98 Detailed LA-MC-ICPMS Sr Isotope Results for Enamel and Dentine, Sample 618, Deer, Layer 8, Pech de l'Azé II.....	983
Table A3.99 Detailed LA-MC-ICPMS Sr Isotope Results, Sample 619, Horse, Layer 8, Pech de l'Azé II	987
Table A3.100 Detailed LA-MC-ICPMS Sr Isotope Results for Enamel and Dentine, Sample 620, Bovid, Layer 7, Pech de l'Azé II.....	990
Table A3.101 Detailed LA-MC-ICPMS Sr Isotope Results for Dentine and Enamel, Sample 622, Hippopotamus, Layer 7, Pech de l'Azé II.....	994

Table A3.102 Detailed LA-MC-ICPMS Sr Isotope Results, Sample 624, Deer, Layer 6, Pech de l'Azé II	997
Table A3.103 Detailed LA-MC-ICPMS Sr Isotope Results for Dentine and Enamel, Sample 625, Horse, Layer 6, Pech de l'Azé II	1002
Table A3.104 Detailed LA-MC-ICPMS Sr Isotope Results for Enamel and Dentine, Sample 2417, Bovid, Layer 1C, Bois Roche	1006
Table A3.105 Detailed LA-MC-ICPMS Sr Isotope Results for Enamel and Dentine, Sample 2418, Bovid, Layer 1C, Bois Roche	1010
Table A3.106 Detailed LA-MC-ICPMS Sr Isotope Results for Enamel, Sample 2419, Bovid, Layer 1C, Bois Roche	1012
Table A3.107 Detailed LA-MC-ICPMS Sr Isotope Results for Enamel, Sample 2420, Bovid, Layer 2, Bois Roche	1016
Table A3.108 LA-MC-ICPMS Sr Isotope Results for Enamel and Dentine, Sample 2421, Bovid, Layer 2, Bois Roche	1021
Table A3.109 Detailed LA-MC-ICPMS Sr Isotope Results, Sample 2422, Bovid, Layer 2, Bois Roche	1025
Table A3.110 Detailed LA-MC-ICPMS Sr Isotope Results for Enamel and Dentine, Sample 2423, Bovid, Layer 2, Bois Roche	1030
Table A3.111 Detailed LA-MC-ICPMS Sr Isotope Results for Enamel and Dentine, Sample 2424, Bovid, Layer 2, Bois Roche	1034
Table A3.112 Detailed LA-MC-ICPMS Sr Isotope Results for Enamel and Dentine, Sample 2425A, Bovid, Layer 2, Bois Roche	1037
Table A3.113 Detailed LA-MC-ICPMS Sr Isotope Results for Dentine and Enamel, Sample 2425B, Bovid, Layer 2, Bois Roche	1041
Table A3.114 Detailed LA-MC-ICPMS Sr Isotope Results for Dentine and Enamel, Sample 2425C, Bovid, Layer 2, Bois Roche	1045
Table A3.115 Detailed LA-MC-ICPMS Sr Isotope Results for Dentine and Enamel, Sample M033, Bovid, Layer C1, Rescoundudou	1051
Table A3.116 Detailed LA-MC-ICPMS Sr Isotope Results for Dentine and Enamel, Sample M034, Bovid, Layer C1, Rescoundudou	1055
Table A3.117 Detailed LA-MC-ICPMS Sr Isotope Results for Dentine and Enamel, Sample M035, Horse, Layer C1, Rescoundudou	1059
Table A3.118 Detailed LA-MC-ICPMS Sr Isotope Results for Dentine and Enamel, Sample M036, Horse, Layer C1, Rescoundudou	1064
Table A3.119 Detailed LA-MC-ICPMS Sr Isotope Results for Dentine and Enamel, Sample M037, Horse, Layer C1, Rescoundudou	1069
Table A3.120 Detailed LA-MC-ICPMS Sr Isotope Results, Sample M038, Rhinoceros, Layer C1, Rescoundudou	1073
Table A3.121 Detailed LA-MC-ICPMS Sr Isotope Results, Sample M039, Bovid, Layer C1, Rescoundudou	1076
Table A3.122 Detailed LA-MC-ICPMS Sr Isotope Results, Sample M040, Bovid, Layer C1, Rescoundudou	1080
Table A3.123 Detailed LA-MC-ICPMS Sr Isotope Results, Sample M041, Bovid, Layer C1, Rescoundudou	1085
Table A3.124 Detailed LA-MC-ICPMS Sr Isotope Results for Dentine and Enamel, Sample M042, Deer, Layer C1, Rescoundudou	1090
Table A3.125 Detailed LA-MC-ICPMS Sr Isotope Results for Dentine and Enamel, Sample M043, Deer, Layer C1, Rescoundudou	1095
Table A3.126 Detailed LA-MC-ICPMS Sr Isotope Results, Sample M044, Deer, Layer C1, Rescoundudou	1099

Table A3.127 Detailed LA-MC-ICPMS Sr Isotope Results, Sample M044, Deer, Layer C1, Rescoundudou	1103
Table A4.1 Detailed Tridacna Strontium Isotope Results Analysed 29/11/2010.....	1106
Table A4.2 Detailed Tridacna Strontium Isotope Results Analysed 30/11/2010.....	1109
Table A4.3 Detailed Tridacna Strontium Isotope Results Analysed 10/02/2011.....	1110
Table A4.4 Detailed Tridacna Strontium Isotope Results Analysed 11/02/2011.....	1111
Table A4.5 Detailed Tridacna Strontium Isotope Results Analysed 12/02/2011.....	1112
Table A4.6 Detailed Tridacna Strontium Isotope Results Analysed 07/04/2011.....	1113
Table A4.7 Detailed Tridacna Strontium Isotope Results Analysed 08/04/2011.....	1114
Table A4.8 Detailed Tridacna Strontium Isotope Results Analysed 09/04/2011.....	1115
Table A4.9 Detailed Tridacna Strontium Isotope Results Analysed 10/04/2011.....	1116
Table A4.10 Detailed Tridacna Strontium Isotope Results Analysed 13/05/2011.....	1118
Table A4.11 Detailed Tridacna Strontium Isotope Results Analysed 14/05/2011.....	1119
Table A4.12 Detailed Tridacna Strontium Isotope Results Analysed 15/05/2011.....	1121
Table A4.13 Detailed Tridacna Strontium Isotope Results Analysed 16/05/2011.....	1122
Table A4.14 Detailed Tridacna Strontium Isotope Results Analysed 20/06/2011.....	1123
Table A4.15 Detailed Tridacna Strontium Isotope Results Analysed 21/05/2011.....	1125
Table A4.16 Detailed Tridacna Strontium Isotope Results Analysed 22/06/2011.....	1126
Table A4.17 Detailed Tridacna Strontium Isotope Results Analysed 23/06/2011.....	1127

The Moral Philosopher who loves to trace the advances of his species through its various gradations from savage to civilized life, draws from voyages and travels, the facts from which he is to deduce his conclusions respecting the social, intellectual, and moral progress of Man.

Stockdale (1800:v)

List of Acronyms

AD	<i>Anno Domini</i>
BC	Before Christ
DNA	Deoxyribonucleic acid
EGNOS	European geostationary navigation overlay service
ESR	Electron spin resonance
G	Gram
GPS	Global positioning system
ICP	Inductively coupled plasma
ICP-AES/ICP-OES	Inductively coupled atomic emission spectroscopy/inductively coupled optical emission spectroscopy
ka	Thousand Years
kg	Kilogram
km	Kilometre
LA-ICPMS	Laser ablation inductively coupled mass spectrometry
LA-MC-ICPMS	Laser ablation multi collector inductively coupled mass spectrometry
M	Molar
m	Metre
ma	Million years
MC-ICPMS	Multi collector mass spectrometry
MIS	Marine isotope stages

mm	Millimetre
mM	Millimolar
Mpa	Megapascal
nm	Nanometre
OSL	Optically stimulated luminescence
ppm	Parts per million
REE	Rare earth element
SEM	Scanning electron microscope
TIMS	Thermal ionisation mass spectrometry
TL	Thermoluminescence
µg	Microgram
µm	Micrometre

Chapter One: Introduction

1.1. Introduction

The analysis of strontium isotopes in biological materials from archaeological sites can demonstrate the distance and vector of mobility of prehistoric fauna or human individuals. The $^{87}\text{Sr}/^{86}\text{Sr}$ ratio of bone and teeth reflects, prior to any post-burial diagenesis, the geological environment from which food and water were sourced while these biominerals were forming. Teeth are particularly amenable to tracing geographic origins of an individual's migration using strontium isotopes, as they generally mineralise early in life and do not change in composition once formed. As a result, if the strontium isotope composition found in an archaeological material is different from that of the local area, this individual is a migrant. Furthermore, if a biomineral has a heterogeneous intra-sample composition, it reflects movement during amelogenesis (enamel formation).

Strontium isotope analysis of biominerals has been commonly applied in the archaeological sciences since 1985 (Ericson 1985). The most common technique employed in analysing strontium isotopes in teeth is to dissolve dental material, process it through cation-exchange columns and measure an overall isotope value for this sample. New advances in instrumentation such as laser ablation multi collector inductively coupled mass spectrometry have, for the first time, allowed the rapid processing of samples and *in situ*, spatially resolved, minimally invasive analysis allowing consideration of intra-sample heterogeneity. This approach provides significantly more information about mobility as intra-sample enamel strontium isotope heterogeneity provides evidence of movement between different geological environments during

amelogenesis and variation between dentine and enamel may provide evidence of a specimen being non-local.

The faunal samples analysed in this study, from Lower and Middle Palaeolithic archaeological sites in Israel and France, including Amud, Qafzeh Tabun, Skhul, Holon, Bois Roche, Le Moustier, La Chapelle-aux-Saints, Les Fieux, Pech de l'Azé II and Rescoundudou (shown in Figure 1.1), span more than 300,000 years of the Lower and Middle Palaeolithic era and represent a tumultuous period in human history. *Homo erectus*, *Homo neanderthalensis* and *Homo sapiens* occupied the sites in this study at various times, leaving a rich material culture record, abundant faunal remains and some of the most important hominin material for understanding human evolution. The nature of the interactions between these various populations and their cultural responses to the rigorous conditions of the Pleistocene, in both desert and glacial environments, remains one of the major questions in understanding the emergence of behavioural modernity.

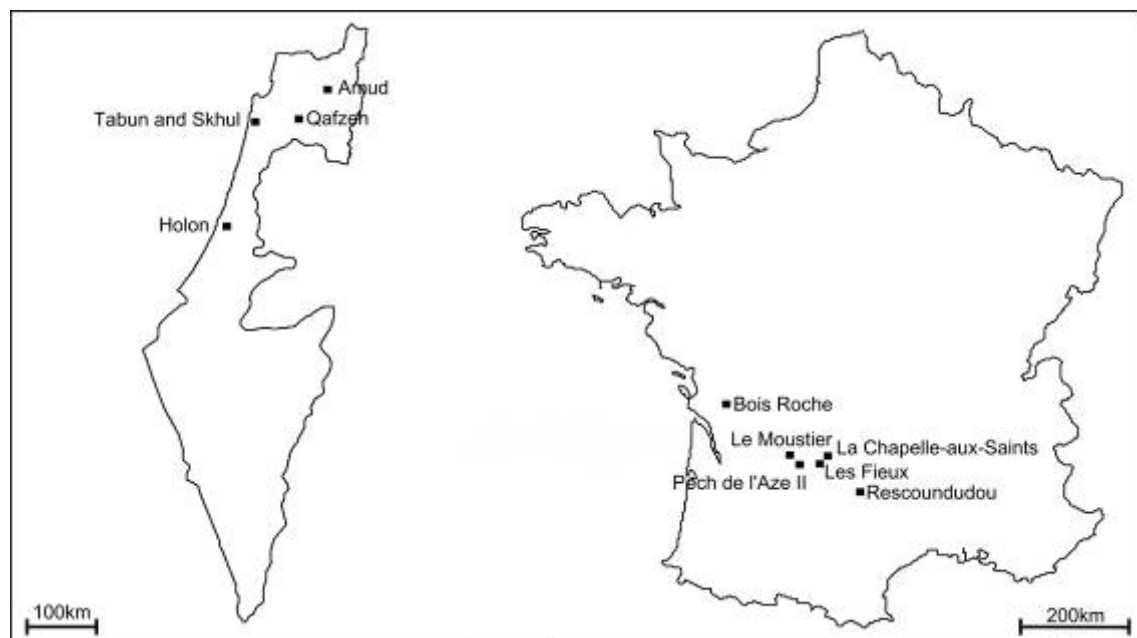


Figure 1.1 Archaeological Sites in Israel (left) and France (right) Included in this Study

The faunal material in this study was obtained from a variety of different species, each with their own distinctive diet, habitat and pattern of mobility. The large age range of samples allows the response of different species in different areas to be considered relative to climate change and, as these samples were most likely hominin prey, to consider how hunting has evolved during this period.

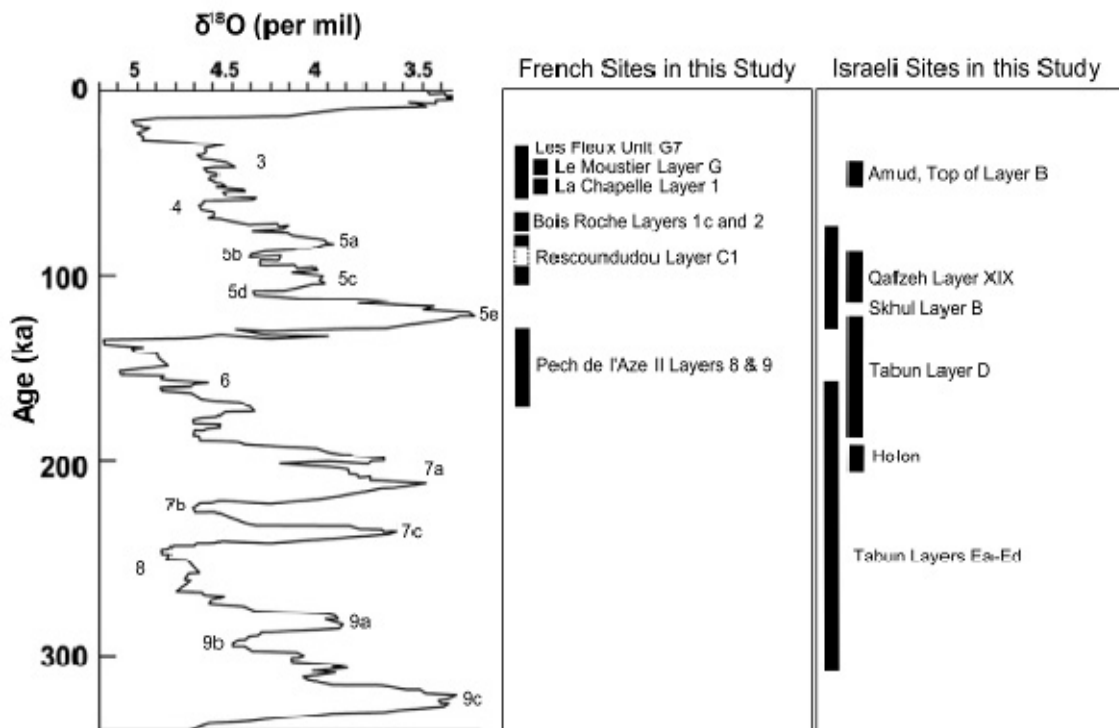


Figure 1.2 A Comparison of the Oxygen Isotope Curve (Shackleton and Pisias 1985) to Stratigraphic Units from France (left) and Israel (right) Included in this Study

During this period, climate changed abruptly and dramatically many times, leading to significant changes in vegetation and fauna. The climate in Israel was characterised by cold and humid glacial periods and warm and dry interglacial periods, while south-west France experienced cold and dry glacial periods and wet and warm interglacial periods. French sites in this study span marine isotope stages (MIS) 6 to 3, while Israeli sites span MIS 9 to 3, shown in Figure 1.2.

A comprehensive soil, rock and plant sampling programme was undertaken throughout Israel and in southern France, to map the bioavailable Sr⁸⁷/Sr⁸⁶ composition of the major geological provinces in these areas. This provided baseline data to compare to the results obtained from the spatially resolved LA-MC-ICPMS analysis of the strontium isotope composition of the enamel and dentine of 90 faunal teeth. This material was analysed to determine Sr⁸⁷/Sr⁸⁶ enamel heterogeneity, difference between enamel and dentine strontium isotope composition as well as the correlation between enamel domains and bioavailable soil/rock/plant values.

Overall, this thesis embraces the benefits available from improvements in the physical, chemical and social sciences to critically examine some of the assumptions underpinning other strontium isotope studies and answer new questions about human evolution.

1.2. Significance of the Thesis to the Field

This thesis aims to be significant to the field of archaeological science in 4 respects. Firstly, it demonstrates the utility of spatially resolved micro-analysis of teeth using laser ablation multi-collector inductively coupled mass spectrometry (LA-MC-ICPMS). Secondly, it provides a background for future research through large scale bioavailable strontium isotope mapping in Israel and southern France. Thirdly, it contributes important archaeological information through the analysis of material from the Israeli sites of Tabun, Holon, Skhul, Amud and Qafzeh and the French sites of Rescoundudou, La Chapelle-aux-Saints, Les Fieux, Bois Roche, Le Moustier and Pech de l'Azé II. Fourthly, strontium isotope results are compared to species, MIS and archaeological assemblage to determine if broad patterns in mobility vary based on these parameters.

The use of spatially resolved micro-analysis in this study allows the rapid determination of the isotope composition of enamel and dentine in multiple locations within each sample. This allows strontium isotope analysis to move beyond a simple determination of bulk isotope composition to determine the degree of $^{87}\text{Sr}/^{86}\text{Sr}$ heterogeneity within these materials. This heterogeneity reflects mobility during amelogenesis.

The mapping of bioavailable strontium isotope values of plant, rock and soil samples from Israel and southern France provides important baseline data that can be used for future studies in these regions. Most previous studies of strontium isotopes in these regions have failed to compare the archaeological isotope ratio to the background geology, impairing the utility of their results. The analysis of soil and rock samples from matched locations in Israel demonstrates that soil values are universally more radiogenic than rock values, probably due to the contribution of aeolian dust. This finding has significant implications for the design of future sampling programmes in these, and other locations.

The archaeological sites examined in this thesis contain important archaeological material, including several hominin specimens that are essential for understanding human evolution. Understanding the mobility of fauna from these locations contributes to developing a broader understanding of the archaeological history of each of these sites.

This study contains the largest collection of Palaeolithic teeth of archaeological fauna analysed to date for strontium isotope composition. This large sample provides a unique opportunity to compare variations in mobility (particularly given the advantages provided by LA-MC-ICPMS, discussed above) to patterns in climate, vegetation, archaeological assemblage and the species that the teeth derive from.

1.3. Thesis Structure

This thesis contains the following sections. Chapter One introduces the study, frames the research questions and summarises the significance of this research to the field. Chapter Two reviews the use of strontium isotope geochemistry within the earth and archaeological sciences. Chapter Three reviews the archaeology, geology, climate, physiography and previous strontium isotope investigations in the study areas. It also examines the biology of the species of interest in this study. Chapter Four discusses the methodology used in this thesis and Chapter Five reviews the results of the analyses undertaken. Chapter Six discusses the results and considers their geochemical and archaeological implications and Chapter Seven presents the conclusions of this research and make recommendations for future investigations. The appendices present the data from this research in more detail. Appendix One contains detailed information concerning each of the sample collection locations in Israel and France. Appendix Two displays detailed pre-analysis photographs of the fauna used in this study. Appendix Three contains the detailed results from all LA-ICPMS and LA-MC-ICPMS analyses in this thesis. Appendix Four includes all LA-MC-ICPMS analysis of Tridacna standards in this thesis.

Chapter Two: Strontium Geochemistry and Archaeology

2.1. Overview

Strontium isotope and concentration studies provide powerful tools for answering questions about mobility, diet, weathering and provenance. Strontium, an alkaline earth metal with 4 naturally occurring isotopes, is well suited to these applications because it is widely distributed within geological and biological materials. It can substitute easily for calcium in biominerals such as enamel, dentine and bone and is generally not fractionated by natural processes.

Central to mobility studies is the propensity of plants and animals to assimilate the bioavailable strontium component of local regolith and water into their biominerals without fractionation. Prehistoric human populations took up the local strontium composition through their own ingestion of plants and water, as well as through feeding on local animals. In teeth, the strontium isotope composition taken up during their formation during childhood is preserved for life and, potentially, survives post-burial diagenesis. In contrast, the strontium isotope composition of bone is continually changed due to bone remodelling so it reflects changes in inputs. The high porosity of bone also means it will be rapidly affected by post-burial diagenesis. Comparing the strontium isotope composition of archaeological teeth, particularly post-burial diagenesis resistant enamel, to regional mapping may allow an estimation of whether the individual was born locally and may provide a distance and vector of migration.

This chapter reviews the chemistry of strontium, its distribution in geological and biological systems and the literature on applying strontium isotopes to problems in earth, environmental and archaeological sciences.

2.2. Strontium Isotopes

2.2.1. Introduction

Strontium (Sr) is an alkaline earth metal (group 2A) element with the atomic number of 38 and an atomic mass of 87.62 (Zumdahl 1997). It was discovered by Crawford in 1790 in material from a mine near the Scottish village of Strontian and isolated as an element by Davy in 1808 (Murray 1993). It occurs in a range of concentrations throughout the earth (as shown in Table 2.1) and on average makes up 0.02 to 0.03% of the earth's crust (Pors Nielsen 2004). Sr²⁺ often substitutes the far more abundant Ca²⁺ based on the similarity between their ionic radii (Faure and Powell 1972:5). Hence, it can be easily incorporated into biominerals such as bone or teeth.

	Sr	Ca	Rb	K
<i>Geologic (ppm)</i>				
Average crust	370	41,000	90	21,000
Exposed upper crust	337		95	
Soil:				
Soil minerals	240	24,000	67	15,000
Soil (Jabile)	0.2–20			
Individual rock types:				
Ultramafic rock	1	25,000	0.2	40
Sandstone	20	39,100	60	10,700
Low-Ca granite	100	5,100	170	42,000
Deep-sea clay	180	29,000	110	25,000
Syenite	200	18,000	110	48,000
Shale	300	22,100	140	26,600
High-Ca granite	440	25,300	110	25,200
Basalt	465	76,000	30	8,300
Carbonate	610	302,300	3	2,700
Deep-sea carbonate	2,000	312,400	fs10	2,900
<i>Biologic (ppm)</i>				
Wood	8–2,500			
Roots (spruce)	19			
Conifer needles	2–20			
<i>Hydrologic ($\mu\text{g l}^{-1}$)</i>				
Seawater	7,620	414,000	110	425,000
Rivers	6–800	15,000	1.3	2,300
Rain	0.7–383	800–56,000		55–1,340
Snow ^b	0.01–0.76	8–75		5–20

Table 2.1 Average Concentrations of Strontium and other Elements in Common Materials (Modified from Capo et al. 1998:200)

Strontium has 4 naturally occurring isotopes— ^{84}Sr , ^{86}Sr , ^{87}Sr and ^{88}Sr —with an overall isotopic abundance of 0.56%, 9.87%, 7.04% and 82.53%, respectively (Faure 1986). The relative abundance of these isotopes are invariant and they are stable on geological time scales, except for ^{87}Sr . An additional 16 short-lived radioactive isotopes of strontium exist. Notable in this group is the ^{90}Sr isotope, which is a product of the nuclear fission of uranium and poses a serious risk to human health when present in bone (Kulp et al. 1957) and ^{89}Sr , which is used for the treatment of bone pain associated with cancer (Robinson et al. 1987).

^{87}Sr is formed by the decay of ^{87}Rb , which has a half-life of 48.8 billion years (Steiger and Jäger 1977). As a result, the abundance of ^{87}Sr relative to the other strontium isotopes is a function both of the age and the original Rb/Sr ratio of the source material (Faure 1986:118). Accordingly, the $^{87}\text{Sr}/^{86}\text{Sr}$ ratios are much higher in ancient, rubidium-rich rocks (Price et al. 2008). The Rb/Sr dating technique utilises this decay as a chronometer, which is suitable for the dating of meteorites, metamorphic rocks, ore deposits and sedimentary rocks, as summarised by Dicken (2005:42–57) and Faure and Powell (1972).

While there is evidence for the mass dependant fractionation of strontium isotopes (Knudson et al. 2010, Halica et al. 2008, Rüggeberg et al. 2008) over archaeological time scales, the $^{87}\text{Sr}/^{86}\text{Sr}$ ratio of a material can be considered static (Chadwick et al. 2009:64).

2.2.2. Notation of Strontium Isotope Values

Strontium isotope values are most often reported as the ratio of ^{87}Sr to ^{86}Sr , which for pure strontium metal has the ratio 0.7119 (Nier 1938:277). These isotopes are chosen in preference to ^{84}Sr and ^{88}Sr as their relative contribution to the total strontium concentration are similar and so produce the most analytically precise results (Beard and Johnson 2000).

Occasionally, strontium isotopes are reported as $\delta^{87}\text{Sr}$, defined as $((^{87}\text{Sr}/^{86}\text{Sr}_{\text{Sample}})/(^{87}\text{Sr}/^{86}\text{Sr}_{\text{Seawater}})-1)\times 1000$ (Capo et al. 1998; Stewart et al. 1998). Recent work by Knudson et al. (2010) has also introduced $\delta^{88}\text{Sr}$ as a measure of trophic level.

2.3. Strontium Isotopes in Nature

2.3.1. Bedrock

2.3.1.1. Introduction

Bedrock strontium is one of the principal inputs of the local bioavailable (see section 2.3.4.5) strontium isotope composition. Bedrock strontium isotope ratios are determined by the source composition of the material, its age and its geological history. Average strontium isotope compositions for common geological materials are summarised in Table 2.2.

Ranges and average $^{87}\text{Sr}/^{86}\text{Sr}$ ratios of some geologic materials

	$^{87}\text{Sr}/^{86}\text{Sr}$		$\delta^{87}\text{Sr}$	
	average	range	average	range
Continental crust	0.716		9.7	
Continental volcanics		0.702–0.714		–10.1 to +6.8
Oceanic island basalts	0.704	0.702–0.707	–7.3	–10.1 to –3.1
River water	0.712	0.704–0.922	4.0	–7.3 to 300
Modern seawater	0.7092		0	
Phanerozoic seawater		0.707–0.709		–3.1 to +0.2
Proterozoic seawater		0.702–0.709		–10.1 to +0.2

Table 2.2 Average Strontium Isotope Composition of Some Common Geological Materials (Modified from Capo et al. 1998:204)

2.3.1.2. Igneous Rocks

Igneous rocks have a wide range of strontium isotope compositions, dependent on their age, their mineralogy and whether they are derived from the crust or the mantle. The earth's original value of $^{87}\text{Sr}/^{86}\text{Sr}$ based on meteorite data is 0.699 (Raymond 1995). Mafic volcanic rocks have an average strontium isotope composition of approximately 0.704, which is considered close to the modern composition $^{87}\text{Sr}/^{86}\text{Sr}$ of the mantle (Faure and Hurley 1963). In general, mafic volcanics in continental areas have higher strontium isotope ratios than their oceanic counterparts, possibly due to contamination from crustal material (Pankhurst 1977). Continental crustal rocks have strontium isotope values over a very large range above 0.704 (Scott et al. 1971), with values for basic continental rocks reported of up to 0.7133 (Faure et al. 1974) and values for felsic granites reported of up to 1.981 (Couturié and Vachette-Caen 1980).

There is a marked variation in strontium isotope values between the crust and the mantle as a result of the enrichment of rubidium in the upper regions of the continental crust due to chemical differentiation (Faure and Hurley 1963). Additionally, the Rb/Sr ratio may reflect the relative degree of differentiation within a suite of igneous rocks due to fractional crystallisation of magma, as strontium tends to be concentrated in plagioclase, while rubidium stays in the liquid melt (Faure 1986). The elevated Rb levels from both fractional crystallisation and chemical differentiation will eventually lead to an increase in ^{87}Sr in some areas through Rb decay.

2.3.1.3. Sedimentary Rocks

The strontium isotope ratio of carbonate rocks, cements and concretions reflects the strontium isotope composition of the local seawater during the fluid phase of deposition. This ratio is preserved through geological time because rubidium is excluded by this process and due to the lack of fractionation

between ^{87}Sr and ^{86}Sr (Faure 1998). As a result, the age of carbonates can be estimated based on comparison to the interpreted strontium composition of the ocean through time. This has varied from approximately 0.707 to 0.709 during the Phanerozoic era (Elderfield 1986), as discussed in more detail in section 2.3.4.4.

Non-marine carbonates have a strontium isotope composition reflecting the local water body from which they have precipitated, which may be subject to local influences (Neat et al. 1979). Dolomites have a strontium isotope composition that reflects the local composition of dolomitising fluids (Mountjoy et al. 1992), despite the decrease in the Sr/Ca ratio of the rock during this process (e.g., Sass and Starinsky 1979). Clastic sedimentary rocks generally have a strontium isotope composition that reflects the lithology of their source material, tempered by the relative ease with which minerals containing strontium are removed by weathering processes. Weathering often leads to increased Rb/Sr ratios in the remnant material because Sr is preferentially removed and thus, eventually, elevates $^{87}\text{Sr}/^{86}\text{Sr}$ values (McDermott and Hawkesworth 1990). Some fine grained shales may suffer substantial strontium exchange during diagenesis, before subsequently behaving as a closed system (Dicken 2005), and so will have strontium compositions which vary markedly from their source material.

2.3.1.4. Metamorphic Rocks

The strontium isotope composition of metamorphic rocks often varies substantially from that of their parent lithology, regardless of whether their genesis is by regional or contact metamorphism (Faure and Powell 1972). Contact metamorphism often leads to the variable loss of ^{87}Sr from individual minerals. This is demonstrated through field (Hart 1964) and laboratory investigations (Misra and Venkatasubramanian 1977), although this change may not be homogeneous over large areas (Roddick and Compston 1977).

Regional metamorphism can lead to similar effects or, less commonly, can cause total rock samples to behave as an open system (Faure and Powell 1972).

A well-studied example of metamorphism leading to changes in the strontium isotope composition of a rock package is the action of hydrothermal metamorphism on the ocean floor through seawater/rock interaction, as evidenced from field sampling of ancient systems (Spooner et al. 1977), modern systems (Teagle et al. 1998) and through experimental studies (Menzies and Seyfried 1979).

2.3.2. Regolith

The strontium isotope composition of regolith (loose unconsolidated sediment and rock present on bedrock) is critical to mobility studies using strontium isotopes, as it provides (in combination with water) the principal source for bioavailable strontium to plants. The strontium isotope composition of regolith is derived principally from the local weathering of bedrock (Capo et al. 1998:203). This source, however, may be augmented by a number of additional inputs and be influenced by how effectively different components of the overall strontium composition are incorporated into biological systems (Evans et al. 2010:2). Complicating factors include windblown marine, mineral and anthropogenic aerosols (Frumkin and Stein 2004; Goede et al. 1998), differential mineral weathering rates, fertiliser use, transportation of regolith from a non-local source and pore water chemistry. Some of these inputs are summarised schematically in Figure 2.1. The difference is such that, in a study of marijuana from within the United States, the strontium values of the plants differed from the expected strontium isotope ratios based on bedrock in 80% of cases (West et al. 2009).

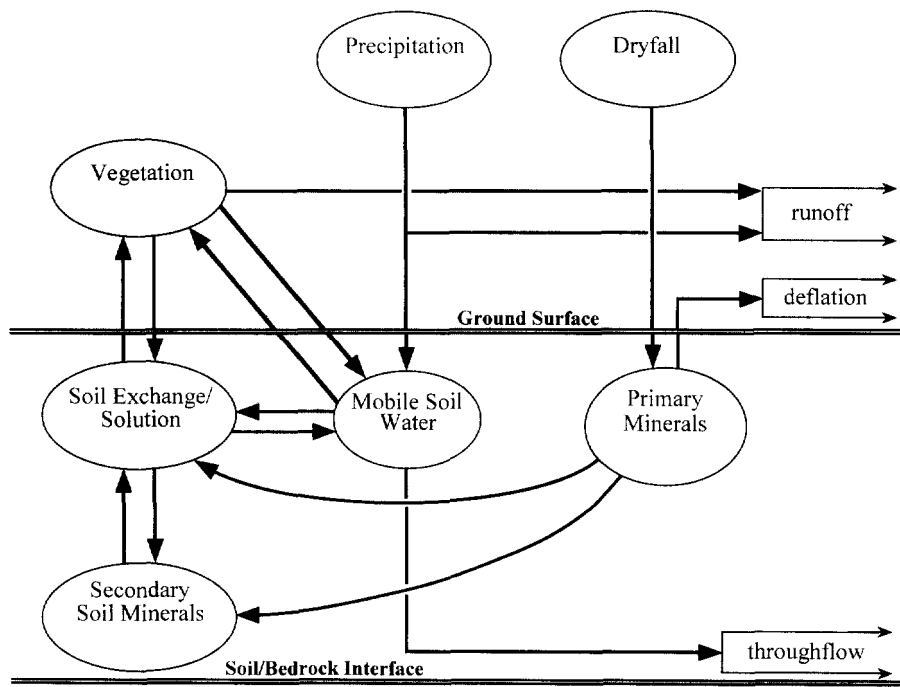


Figure 2.1 Inputs and Outputs of Strontium for Regolith (Modified from Stewart et al. 1998:180)

The quantum of different inputs is shown by Miller et al. (1993:438) from a study area at Whiteface Mountain in New York. In this study, new mineral weathering strontium derived from bedrock contributed 70% of strontium exported to stream water, but only 20% of strontium incorporated into vegetation. The processes may preferentially affect specific soil horizons, potentially leading to variations in the strontium isotope ratios within 1 regolith profile (Blum et al. 2008). This leads to a more complicated input model, shown in Figure 2.2.

Marine and mineral aerosols can make a significant contribution to the strontium composition of regolith. Marine aerosols are generated by the evaporation of sea spray salts, which may be found in various states of hydration and/or dissolution (Derry and Chadwick 2007). The composition of these aerosols is variable and dependant on their trajectory, which can be complex (Chadwick et al. 2009). This complexity is such that even in maritime regions they may differ from the marine value (Derry and Chadwick 2007). These aerosols can be deposited by wind, rain, snow or fog. They may lodge directly on the soil or be

deposited on foliage and subsequently remobilised into the soil profile by precipitation (Franzén 1990).

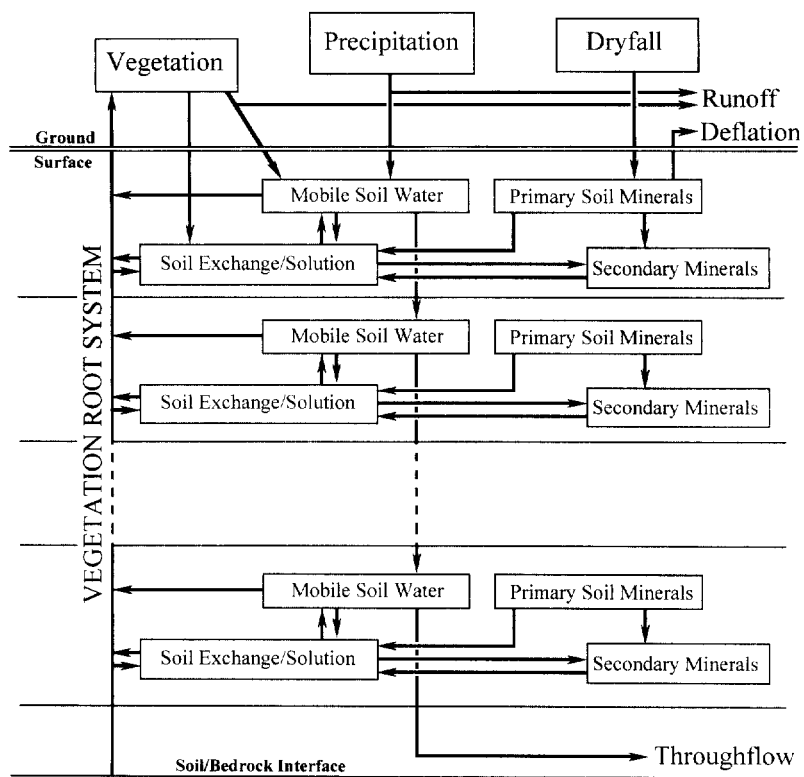


Figure 2.2 Strontium Fluxes in a Multi-Layered Soil System (Modified from Stewart et al. 1998)

Mineral aerosols are derived from the wind erosion of soil and sediment (Derry and Chadwick 2007). These particles are most common in desert areas (e.g., Frumkin and Stein 2004) but can also be found in more temperate environments (e.g., Goede et al. 1998). A critical factor in their presence is a suitable wind speed to entrain particles (Sterk 2003), the availability of suitable particles on the ground surface and a lack of vegetation cover to shield them from aeolian action. Strontium derived from aerosols has been measured at contributing between 17 to 59% of total strontium in cation-exchange pools in some soil horizons (Miller et al. 1993). Climate variations through time will strongly control the amount of aeolian material due to changes in vegetation cover (Pelletier 2007), although the effects can be complex (Leeder et al. 1998).

The contributions of these components can be sufficiently important that the strontium isotope composition of older soil profiles may be dominated by aerosol inputs rather than bedrock geology (Kurtz et al. 2001). A key variable for the contribution of aerosols to soil profiles is rainfall. An initial increase in rainfall leads to more bedrock-derived strontium in the soil profile as it weathers out of the bedrock. When this source is depleted, the contribution from aerosols becomes greater with increasing rainfall (Stewart et al. 2001). The contribution from aerosols has been shown to vary for a particular site through time (Whipkey et al. 2000). The relative contribution from marine aerosols diminishes with distance inland from the coast, while mineral aerosols become increasingly dominant (Raiber et al. 2009; Quade et al. 1995).

Soils in areas with rapid tectonic uplift may have a strontium isotope composition dominated by their bedrock-derived value, even when the aerosol flux is high. This effect is due to the increased weathering, which tends to overwhelm the contribution from marine and mineral aerosols (Bern et al. 2005; 2007). Topography may also control the contribution of bedrock to regolith strontium isotope values, as areas of elevated topography tend to shed weathered material to areas of low topography (Evans et al. 2009).

Different minerals within a bedrock unit may have variable strontium isotope compositions and up to several orders of magnitude difference (Lasaga 1984) in resistance to weathering (Capo et al. 1998). Additionally, some minerals may undergo mineralogical transformations, which lead to the release and retention of different cations (Nesbitt et al. 1980), which may affect the isotope ratio of the remaining material. In silicate rocks, individual minerals will have differing $^{87}\text{Sr}/^{86}\text{Sr}$ compositions due to varying Rb content (Evans et al. 2009). Brass (1975) observes that the weathering processes in soil profiles tend to remove ^{86}Sr . Capo et al. (1998:204) suggest that early weathering of high Rb/Sr such as biotite will deplete the amount of ^{87}Sr in the residual weathered material, while early weathering of Ca-plagioclase will have the opposite effect. Areas that have experienced continental glaciation may have elevated rates of biotite

weathering leading to significantly elevated riverine $^{87}\text{Sr}/^{86}\text{Sr}$ ratios compared to bedrock values (Blum et al. 1993). Weathering processes (particularly of igneous and metamorphic rocks, see Dasch 1969) tend to enhance the ^{87}Sr component (and the Rb/Sr ratio) of the resultant material by chemical processes (Fullagar and Ragland 1975). This is due to the relative resistance of rubidium bearing minerals (mica and K-feldspars) compared to strontium bearing minerals (plagioclase and calcite). Clay minerals will equilibrate with weathering solutions (Clauer et al. 1975), such that the strontium isotope composition of that solution is intermediated between that of the unweathered material and the initial composition of the solution (Daux et al. 1994).

An additional complexity is the strong relationship between grain size and strontium isotope composition in aeolian (Feng et al. 2009) and fluvial systems (Douglas et al. 1995). In aeolian systems, $^{87}\text{Sr}/^{86}\text{Sr}$ ratios tend to increase with decreasing grain size (Asahara et al. 1999; Grousset et al. 1992). This effect may be due to the extended weathering of finer particles relative to coarse ones, the more resistant nature of finer particles and the relative abundance of secondary minerals in the fine fraction (Feng et al. 2009).

Fertiliser may also contribute to the strontium isotope composition of both the soil and groundwater (Négrel 1999). This may affect the measured regolith strontium isotope composition. The extent is dependent on the type, source and amount of fertiliser added (Böhlke and Horan 2000) and may vary, at least in respect to groundwater composition, depending on the seasonal fertiliser application cycle (Kume et al. 2010). It is possible to correct for this effect by plotting $^{87}\text{Sr}/^{86}\text{Sr}$ compared to the Cl/Sr ratio (Petelet-Giraud et al. 2003). This method is effective because Cl is only introduced into the system from rainwater (the composition of which can be measured) and fertiliser and not from rock weathering (other than in the case of some evaporates) (Meybeck 1979).

The complexity of the inputs of strontium to regolith is exacerbated in areas where the soil is not derived from local bedrock, such as in areas with aeolian, alluvial, volcanic or glacial regolith. In these cases, the strontium isotope composition will reflect a mixing model between the mineralogical sources of these sediments and any other inputs, with the proportions controlled by the relative importance of each process (Widga et al. 2010).

Depth within the soil profile is also critical to the measured strontium isotope ratio of the regolith. Mineral and marine aerosols tend to accumulate near the ground surface, and so have a greater influence on the strontium isotope composition of the region (Chadwick et al. 2009). The pore water strontium isotope composition may vary with depth in the regolith, reflecting a varying degree of influence exerted by each input into the bioavailable strontium ratio (Pett-Ridge et al. 2009).

In summary, the strontium composition of regolith is dependent on a complex variety of processes, including mineral and marine aerosols, tectonics, topography, mineral resistance to weathering, grain size, fertiliser use, regolith transport and depth in soil profile. The relative contribution of these vary both spatially and temporally.

2.3.3. Plants

The strontium isotope composition of plants reflects the bioavailable component of the regolith and water strontium (see section 2.3.4.5 for a discussion of bioavailable strontium). Importantly, while fractionation may occur during the incorporation of strontium into plant tissue the $^{87}\text{Sr}/^{86}\text{Sr}$ is not affected (Hoppe et al. 1999). As vegetation extracts cations from soil water, the strontium composition of water in soil and plants should be identical (Négrel and Roy 1998). Despite this, the relative contribution of different sources of bioavailable strontium to each plant may vary, even in a discrete geographic area. This was

demonstrated by Gosz and Moore (1989), who showed that spruce in their study area derived approximately 70% of their strontium from precipitation, while aspen derived only 30%.

Plants should have a homogeneous isotope composition throughout their tissues, because they do not fractionate strontium. Some studies of spruce-firs contradicted this hypothesis by showing large variations between needles, bark and bole (Graustein and Armstrong 1983). This effect was attributed to a varying contribution of aerosol strontium to different parts of the plant based on their surface to volume ratio, rather than to processes within the plant itself (Graustein and Armstrong 1983). As discussed in section 2.3.2, strontium isotope ratios may vary between different components of a soil profile. This may affect the composition of the bioavailable strontium available to plants with different root depths. The difference may be substantial as roots can penetrate from less than 0.5 m to many tens of meters for woody and herbaceous species (Canadell et al. 1996).

2.3.4. Water

The strontium isotope composition of water varies substantially and is affected by different processes depending on its position in the water cycle, as discussed in more detail below.

2.3.4.1. Precipitation

The strontium isotope composition of rainfall reflects the local mix of marine, mineral and anthropogenic aerosols (Négrel and Roy 1998). Rainfall composition can vary spatially (Herut et al. 1993), temporally (Négrel et al. 2007) and even during a single rain event (Dupré et al. 1994). Primary strontium sources for rain include sea spray, anthropogenic contaminants and inland dust

(Raiber et al. 2009; Whipkey et al. 2000). Quantifying their relative contribution is difficult (Chadwick et al. 2009). The complexity of this system is such that even in maritime regions the strontium composition of precipitation may differ significantly from oceanic values (Derry and Chadwick 2007). The isotope composition of snow has also been shown to vary spatially (Andersson et al. 1990), suggesting a similar complexity.

2.3.4.2. Lake and River Water

In general, the strontium isotope composition of river or lake water reflects a balance between the composition of rain and local bedrock geology (Wickman and Åberg 1987), although other factors may be locally important. Miller et al. (1993) suggested that strontium derived from the local weathering of minerals makes a greater contribution to the local stream water composition than atmospheric strontium does (as shown in Figure 2.2).

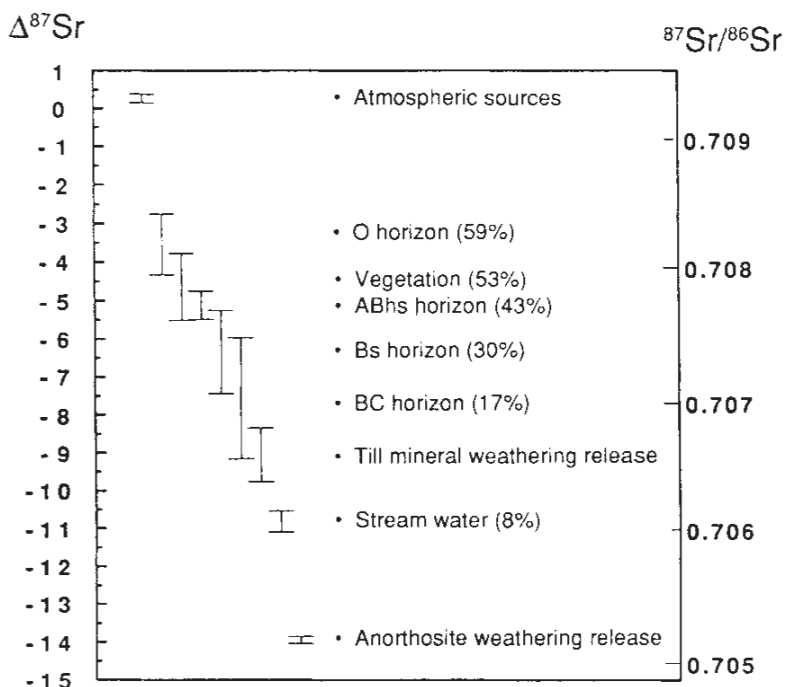


Figure 2.3 Strontium Isotope Composition of Soil, Vegetation and Source Material. Adirondack Mountains, New York (Miller et al. 1993:439)

It has been suggested that the discharge rate of rivers also influences their strontium isotope composition, with rainwater making a proportionally greater contribution at high flows (Åberg and Jacks 1987), although Bain et al. (1998) suggested that this affects only strontium concentration. Changes in discharge can also affect the $^{87}\text{Sr}/^{86}\text{Sr}$ due to variations in the depth at which water flow is leading to weathering of minerals within the soil profile (Nezat et al. 2010). The size of the catchment also affects the isotopic composition of the river water, as small catchments allow rock types with an unusual isotope composition, but limited geographic extent, to exert a much greater influence over the stream composition (Åberg and Wickham 1987). Important regional scale processes, which affect the strontium composition of river water, include glaciation and large scale regional metamorphism (Palmer and Edmond 1992).

The relative contribution from precipitation to the strontium isotope composition of rivers is variable, with measured contributions of $3.8\% \pm 1.1\%$ for the Loire River in France (Grosbois et al. 2000), 4 to 18% for different tributaries of the Congo in Africa (Négrel et al. 1993), 1 to 4% in the Amazon Basin in South America (Gaillardet et al. 1997) and 8 to 30% in the Maroni catchment in South America (Négrel and Lachassagne 2000).

2.3.4.3. Groundwater

The strontium isotope composition of groundwater reflects a balance between that of the water inputs to the system, water/rock interaction in the aquifer (Frost and Toner 2004) and additional inputs such as fertiliser (Böhlke and Horan 2000) or leachates (Vilomet et al. 2001). Groundwater may discharge into river systems, leading to changes in their isotope composition (Négrel and Petelet-Giraud 2005).

2.3.4.4. Seawater

The modern strontium isotope composition of seawater is 0.7092 (Veizer 1989) and its concentration is approximately 8 parts per million (ppm) (Åberg et al. 1990). The strontium isotope composition of seawater has varied through geological time, due to a number of process summarised by Dicken (2005:62–65) and discussed below.

This composition of seawater was originally thought to approximate the bulk composition of the earth's crust (Wickman 1948), the composition of the sedimentary material being deposited in the ocean basins (Hurley et al. 1960) or the composition of the weathering crust (Hedge and Walthall 1963). More refined interpretations suggest that a variety of processes control this value, including:

- changes in the balance between the erosion flux of non-radiogenic strontium from young volcanics
- radiogenic strontium from old crustal rocks and intermediate composition strontium from carbonates (Faure et al. 1965)
- the contribution of submarine hydrothermal exchange at mid ocean ridges (Spooner 1976)
- diagenetic recrystallisation of ocean floor carbonates (Elderfield and Gieskes 1982)
- sub-surface outflow of continental groundwater (Chaudhuri and Clauer 1986).

The strontium isotope composition of seawater is homogenous to the limits of modern analytical precision, due to the long residence time of strontium in the oceans compared to ocean mixing time (McArthur 1994).

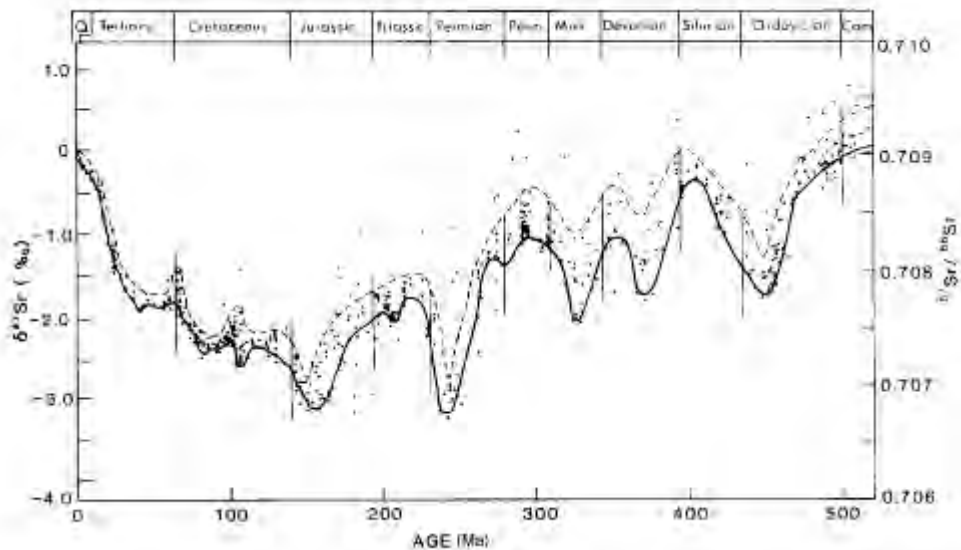


Figure 2.4: $^{87}\text{Sr}/^{86}\text{Sr}$ Ratio of Sea Water Through Phanerozoic Time (Elderfield 1986:77)

The strontium isotope curve through geological time has been reviewed by Veizer (1989). The implications of this curve for stratigraphic correlation and dating were reviewed by Elderfield (1986). Stoll and Schrag (1998) considered the effects of sea level lowstands in the Quaternary era on the strontium flux into ocean basins, and concluded that while these events significantly affected the Sr/Ca ratio in seawater, their effect on strontium isotope ratios would have been below detection limits.

2.3.4.5. Bioavailable Strontium

Bioavailable strontium is the component of strontium present in a particular environment available for incorporation into biological systems. Its $^{87}\text{Sr}/^{86}\text{Sr}$ composition may differ markedly from that of regolith or whole rock strontium. This bioavailable (or labile) strontium is that available to plants, which assimilate strontium from soil pore fluids (Evans et al. 2009). This represents only a proportion of the total strontium found in regolith or rock (Sillen et al. 1998). Indeed, whole rock or regolith strontium is considered a poor reflection of bioavailable strontium, particularly where the geological environment is variable (Budd et al. 2004). It should be noted that the regolith strontium composition

may also vary significantly from that of the underlying bedrock, as reviewed in section 2.3.2.

The extraction of bioavailable strontium can be replicated for rock or soil by the use of ammonium acetate or ammonium chloride, which remove cations from electrostatically bound pore water in addition to exchange sites on minerals and organic matter (Stewart et al. 1998). Chadwick et al. (2009) found that this method extracted between 0.1 to 62% of whole soil strontium.

Another approach to the mapping of bioavailable strontium isotope values is to use modern or fossil teeth from small vertebrates (Price et al. 2002). The strontium composition of this material is, by definition, bioavailable in its entirety and so no special leaching technique is required. Small herbivores are well suited to this task, as their feeding ranges are restricted (Bentley et al. 2004), although other species such as pigs can be used (Bentley and Knipper 2005a). If LA-MC-ICPMS techniques are used for this analysis, problems of offsets between solution and laser results (as discussed in section 4.6.1.2) may be avoided. This approach also allows the local strontium isotope signature to be ascertained under different geological and climatic conditions through time, providing a bioavailable value contemporary with archaeological material.

A more direct approach to determining the local signature is to analyse the enamel of people from archaeological sites that have died in childhood and thus have a limited opportunity to undertake migration (e.g., Montgomery 2002; Montgomery et al. 2005).

2.3.4.6. Strontium in Vertebrates

Strontium is found throughout the body, although 99% is held in bone mineral (Schroeder et al. 1972). The presence of strontium within the body appears to

serve no essential biological function. However, human consumption of high doses (greater than or equal to 4 mM Sr/kg/day) of strontium can induce rickets, defective bone mineralisation, alteration of the mineral profile of bone and can decrease the production of bioavailable vitamin D (Marie et al. 2001). Conversely, there is experimental evidence to suggest that the administration of strontium in conjunction with a normal calcium diet can increase bone formation, volume (Marie et al. 1985) and density (Grynpas et al. 1996).

Teeth are amenable to tracing geographic origins of an individual's migration using strontium isotopes, as they mineralise in the first 12 to 13 years of life (White and Folkens 2005) and do not subsequently change the strontium composition (Schweissing and Grupe 2003). However, the composition of teeth may undergo post-burial modification or mechanical disintegration in archaeological sites, as summarised in section 2.3.4.8. The concentration of strontium in human enamel is typically in the range of 50 to 300 ppm (Horstwood et al. 2008:5660), with a mean value in Britain of 105 ± 138 ppm (Evans et al. 2012). It may be elevated by industrial pollution (Oprea et al. 2009), in geological environments with high strontium concentration (Montgomery 2002:71) or when an individual's diet is high in seafood (Evans et al. 2012). The concentration of strontium in teeth is relatively homogeneous within a particular tooth (Lee et al. 1999:184) and controls the Sr/Ca ratio as a stoichiometric component and, therefore, is relatively constant (Horstwood et al. 2008).

The concentration of strontium in bone is 20 to 60 µg/g (Schroeder et al. 1972). The much higher remodelling rate of bone in the body compared to teeth provides a strontium isotope composition more contemporary with the time of the individual's death (Schweissing and Grupe 2003). A comparison between the strontium isotope composition of teeth and bone can provide a guide to the chronology of movement during a lifetime (Beard and Johnson 2000).

2.3.4.7. Biopurification of Strontium

Strontium is progressively removed (biopurified) by animals with increasing trophic levels. Plants do not discriminate between strontium and calcium and, hence, their Sr/Ca ratios are comparatively high (Vaughan 1967; Hutchin and Vaughan 1968; Vaughan et al. 1967), despite highly species dependent rates of strontium translocation from root to leaf (Russell and Sanderson 1967). When plant material enters the food chain, the strontium is incorporated into animals by substituting for Ca in bones and teeth without any significant fractionation (Blum et al. 2000). Mammals absorb 40 to 80% of ingested calcium and 20 to 40% of ingested strontium (Sips et al. 1996) and their kidneys excrete strontium around 3 times more efficiently than calcium. This may occur due to smaller reabsorption as a result of the larger size of the strontium atom (Pors Nielsen 2004:585). Once strontium has been metabolised and is incorporated in bone, it behaves in an almost identical fashion to calcium and thus is not removed preferentially.

This process of biopurification iterates with each level of the food chain, progressively removing more strontium material at each step. The quantum of this effect in bone, referred to as the ‘bone retention factor’ by Alexander et al. (1956:915), appears to vary between species. The result is that, for example, the concentration of strontium in human teeth is much lower than in herbivores (Evans et al. 2012).

2.3.4.8. Post-burial Diagenesis

Post-depositional changes to the strontium isotope composition of bones or teeth deposited in archaeological sites are of critical concern for mobility studies. Any variation to the strontium isotope composition of biological materials will provide a spurious signal and may defeat attempts to track

migration. The processes and effects of this relatively common phenomenon for bones and teeth were summarised by Lee-Thorp (2002).

Enamel has been shown to resist post-burial alteration of its strontium isotope composition far better than dentine, cementum or bone (Trickett et al. 2003). The resistance of enamel to chemical alteration is sufficient to preserve elemental and isotope composition in material of the Cretaceous age (Bocherens et al. 1994), although trace element studies suggest that it can occur.

Budd et al. (2000) showed that post-burial alteration of dentine was common but variable and appeared not to correlate to tooth type or burial conditions. Beeley and Lunt (1980) suggested that the collagen contained in cementum and dentine was subject to selective post-mortem attack, leading to physical softening but little change in concentration of calcium and phosphorus. One of the reasons for the integrity of enamel is its lower porosity compared to dentine or bone, leading to a lower diffusion coefficient (Pike and Hedges 2001). The formation of microbial diagenetic foci in dentine may also mediate this process (Bell et al. 1991). An elevation of strontium concentration may suggest post-burial diagenesis, as biogenic values rarely exceed 1000 ppm (Pellegrini et al. 2008).

Attempts have been made to develop a protocol for the removal of diagenetic strontium from enamel, dentine and bone through the ‘solubility profiling’ technique originally described by Sillen (1986). This technique involves multiple washes using weak acids, on the basis that differences exist between the solubility of biogenic (e.g., primary) and diagenetic apatite. However, more recent trials have cast doubts on the effectiveness of this technique (Trickett et al. 2003).

Buried bone will be subject to diagenesis through dissolution, precipitation, mineral replacement and recrystallisation (Pate and Brown 1985). In particular, bone apatite will quickly exchange with groundwater to alter the strontium concentration and isotopic composition, even when collagen is preserved (Nelson et al. 1986). Indeed, bone has been demonstrated to undergo extensive post-mortem alteration within a period of 1 to 40 years when exposed on the surface in a semi-arid environment (Trueman et al. 2004). Zapata et al. (2006:366) considered that post-burial diagenesis of bone was so common that ‘diagenetic masking of biogenic signals should be assumed for all bones unless evidence is proffered to the contrary’. Despite these difficulties, the rapid equilibration of bone strontium isotope composition to that of the local groundwater (e.g., Trueman et al. 2004) may actually be advantageous to archaeological studies, because (assuming early interaction) this provides a proxy for the groundwater composition at the time of burial (Evans et al. 2010:3) or may aid in determining how far along the diagenetic vector the samples have progressed (Montgomery et al. 2007).

2.3.5. Biominerals

2.3.5.1. An Introduction to Dentogenesis

Mammalian teeth are comprised of 3 different dental tissues: enamel, dentine and cementine (Driessens and Verbeeck 1990; see Figure 2.5), all of which consist of varying proportions of extracellular protein matrix, apatitic minerals and additional specialised cells (Skinner 2000:235). The apatitic minerals dominate as most dental tissues are comprised of 69 to 99% (by weight) calcium phosphate, mainly in the form of hydroxyapatite ($\text{Ca}_{10}(\text{PO}_4)_6(\text{OH})_2$), although substitutions of Na^+ or Sr^+ for Ca, HPO_4^{2-} , CO_3^{3-} or HCO_3^- and F^- , Cl^- or CO_3^{2-} for $(\text{OH})_2$ can occur (Hillson 2005:147). Non-apatitic minerals in dental tissues are most commonly compositionally variable and unstable amorphous calcium phosphates (Williams and Elliot 1989). Human deciduous teeth begin to form *in utero* and commonly emerge within 6 months of birth (Brescia 1961).

The permanent dentition begins forming with the first molar *in utero*—however, mostly from 3 to 4 months after birth until about 12 years of age (Millard et al. 2005)—and erupts from approximately 6 years of age (Brescia 1961).

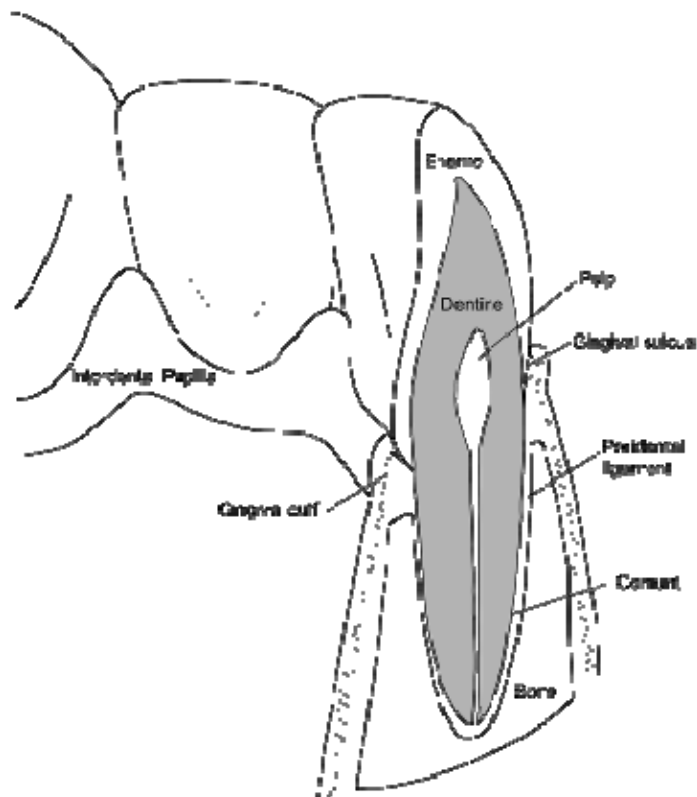


Figure 2.5 Generalised Structure of a Simple Mammalian Tooth (Modified from Hillson 2005:9)

Enamel is the most mineralised part of a mammalian tooth, containing over 99% apatite by weight (Skinner 2000), and is the hardest, most mineralised tissue in the vertebrate body (Fincham et al. 2000). In addition to apatite, an organic matrix exists comprised of amelogenin, ameloblastin and enamelin proteins (Simmer and Hu 2001:901). Enamel microstructure varies between species and through time, and often multiple structures can be present in the same species (von Koenigswald 2000). Enamel porosity is highest at the enamel-dentine junction and decreases towards the outer enamel surface (Shellis and Dibdin 2000). Crystallite size averages 160 nm in length and 20 nm in width for human enamel (Ronnlöf 1962), which is more than 200 times larger than for dentine

or bone (Sakae et al. 1997). Crystallite size is greatest and the degree of ionic substitution is less in the outer layer of enamel (Sakae et al. 1997).

Amelogenesis (the formation of enamel) is undertaken by ameloblasts in 2 stages: matrix production, in which an organic matrix forms, and enamel maturation, in which proteins and water are removed and an increase in crystal size occurs (Hillson 2005:155), changing the mineral component of the tooth from 10 to 20% to 80 to 90% as a percentage of volume (Robinson et al. 1981). This process, in human teeth, has 4 distinct phases in which: 1) partially mineralised matrix is secreted, 2) selective replacement of matrix proteins by tissue fluid begins, 3) almost all of the matrix protein is withdrawn and the resulting porosity is filled by tissue fluid, which is then replaced by calcium phosphate and 4) the enamel becomes almost fully mineralised, mature and hard (Robinson et al. 1981). This process is similar to that observed in rats (Hiller et al. 1975) and bovid (Robinson et al. 1980). This process differs in some creatures (such as pigs), in which enamel may not mature until it has erupted (Kirkham et al. 1988). Ameloblasts alter dramatically from the secretory to the maturational phase, with the loss of the Tomes' process (which controls the orientation of matrix production), a slight decrease in the height of the cell and the elimination of most protein synthesising organelles (Moss-Salentijn et al. 1997). Individual prisms formed by amelogenesis in humans extend from the enamel-dentine junction to the outer enamel surface without interruption (Sander 1997), although they rarely follow a straight path (Hillson 2005). Other species have their own characteristic prism structures, as summarised by Hillson (2005:176–184).

The structure of mature enamel suggests rhythmic amelogenesis during matrix secretion with alternating light and dark bands (known as cross-striations) resulting from small variations in apatite mineralisation. A combined light and dark package of prism cross-striations perpendicular to the main prism direction represents a 24-hour period (Antoine et al. 2009), suggesting these features may provide a robust chronology of matrix secretion for humans (Dean 1987).

These features may be formed by either shifts in the acid/base balance (Shinoda 1984) or changes in carbonate concentration (Boyde 1979). Other features—such as striae of Retzius, which present as oblique bands running from the enamel-dentine junction to the outer surface of the enamel where they form troughs known as perikymata (Lacruz et al. 2006)—are not formed in a regular periodicity, but instead represent occasional markers of disturbances in tooth formation (Dean 2000). Enamel mineralisation follows a pattern very different from matrix formation (Suga 1989), including 4 waves of maturation in different directions (Suga 1982). The timing of enamel maturation remains poorly understood (Montgomery 2002). Once enamel forms, it does not remodel or even stay in contact with the ameloblasts (Fincham et al. 2000).

Occlusal enamel thickness is a function of the rate and duration of matrix secretion. There is a clear gradient of increasing cuspal and lateral enamel thickness from the front of the mouth to the back in humans in both deciduous and permanent dentition (Macho 1994). Enamel extension rates vary from about 20 µm per day in the cuspal region to about 4 µm per day in the cervical region of human permanent teeth (Shellis 1984). Human deciduous teeth show higher secretion rates than permanent teeth. Enamel can contain defects, dental enamel hypoplasia, which record periods of physiological stress. They may be used as an aid to interpret palaeo-environmental conditions (Niven et al. 2004).

The sequence of the enamel formation of modern humans appears to be common to *Homo erectus* (Smith 1994), *Homo antecessor* (Bermudez De Castro et al. 1999), *Homo neanderthalensis* and *Homo ergaster* (Wood and Collard 1999), and is considered one of the diagnostic criteria of the genus *Homo*, although the rate of tooth production may vary (Dean et al. 2001). Plio-Pleistocene homonids such as *Australopithecus africanus* and *Paranthropus robustus* and early *Homo* show evidence of a higher rate of enamel formation and possibly a different mechanism of amelogenesis (Lacruz et al. 2006), involving high daily secretion rates and higher numbers of cell secreting

enamel. A suite of dental features such as enamel thickness, occlusal morphology, development rate and duration and enamel-dentine junction shape provide a robust tool for differentiating *Homo* species (Smith et al. 2006).

The enamel of some species grows over long periods and, when analysed with micro-profiling or laser ablation analysis, can be used to trace life histories. This approach has been trialled using strontium by Bentley and Knipper (2005b), who showed that some cattle were seasonally taken to different pastures in Neolithic Germany. Viner et al. (2010) demonstrated a non-seasonal vector of migration in cattle from Durrington Walls. Balasse et al. (2002) showed seasonal mobility of herders in South Africa using a combination of carbon and strontium isotopes. Fraser et al. (2008) showed seasonal vegetation changes along the vector of enamel formation using carbon isotopes from wombat teeth. An important consideration in such research is the potential attenuation of the isotopic signal by the pool of the isotope of interest in the body or the overprinting of the isotopic signal by multiple enamel maturation events (Montgomery et al. 2010).

Dentine, a softer and less mineralised material than tooth enamel, is volumetrically the largest component of human teeth (Driessens and Verbeeck 1990). It comprises 80% mineralised tissue and 20% organic tissue, which is principally collagen (Ross et al. 2002). The majority of mineralised tissue is apatite, with shorter crystallites than are present in enamel (Hillson 2005). Dentine, unlike enamel, is a living tissue and contains odontoblasts lining the sides of the pulp chamber (Hillson 2005), although it does not regenerate as bone does. Dentine is formed (beginning slightly after enamel formation) by the growth of odontoblast processes towards the enamel/dentine junction, followed by fibril formation, matrix maturation and matrix calcification (Sisca and Provenza 1972). The most dominant structure in dentine is the tubules, which extend from the pulp cavity to the enamel-dentine boundary (Hillson 2005). The tubules are surrounded by hyper-mineralised tissue called peritubular dentin, while the remaining mineralised tissue is intertubular tissue (Weiner et al. 1999).

Dentine may show some laminar structures, including von Ebner lines (Dean 1998), Andresen lines (which correspond to cross-striations and Retzius lines in enamel, respectively) (Smith 2008), contour lines of Owen and interglobular spaces (Dean and Scandrett 1996). These may differ in appearance at different locations within the dentine (Kawasaki 1975).

Dentine grows at rates between 1 to 5 μm per day in human teeth, depending on the location within the tooth (Dean 2000). The rate at which the length of dentine in the tooth is extended is governed by: 1) the daily rate at which odontogenic cells produce matrix, 2) the direction of cell movement and 3) the number of mature secretory cells active at one time and their rate of secretion (Dean 2000). Dentine is more susceptible to chemical and physical weathering than enamel, particularly when the collagen is lost (Beeley and Lunt 1980). This may be the result of invading microorganisms, which create foci of diagenetic change and small cavities and can begin a short time after death (Bell et al. 1996).

Cementum (dental cement) serves to hold the tooth into its socket and is composed of approximately 50% inorganic matrix, with most of the inorganic component being collagen (Somerman et al. 1993). Cementum is deposited by cementoblasts, which mineralise around bundles of collagen that extrude from the gum into the narrow space around the tooth (Lieberman 1998). Unlike other dental tissues, cementum growth continues throughout the life of the tooth (Lieberman 1994). In many mammal species, cementum growth follows predictable seasonal cycles, growing faster in summer and slower in winter (Rendu 2010). It can thus indicate the season of death (Wedel 2007).

2.3.5.2. An Introduction to Bone

Bone (in a similar fashion to dentine, enamel and cementum) is composed of small mineral particles within an organic gel. Bone, however, differs in

containing osteocytes, which allow continual replacement of mineralised tissue (Driessens and Verbeeck 1990). This remodelling continues after growth has ceased by continued reabsorption of old bone and formation of new bone (Frost 1964:316). The rate of turnover of compact bone averages 2.5%, increasing to 10% for trabecular bone (Pate et al. 1989). Remodelling rates vary depending on the age of the individual (Cox and Sealy 1997:212).

The precise nature of the mineral component of bone has been the subject of some debate, but it is most likely to be multi-phase apatite (Driessens and Verbeeck 1990). Bone crystals are present in a diversity of forms, including rods and plates, with most having a c-axial length of approximately 30 to 40 nm (Driessens and Verbeeck 1990:186).

2.4. Applications of Strontium Concentration and Isotope Studies

2.4.1.1. Modern Ecological Studies

Modern migration of animals can be traced using strontium isotopes to provide information on ecological systems. The general application of stable isotopes to modern migration studies is reviewed by Hobson (1999) and, specifically for strontium, by Beard and Johnson (2000).

Strontium isotopes have been used to track bird migration such as the black-throated blue warbler (*Dendroica caerulea*) (Chamberlain et al. 1997) and the tree swallow (*Tachycineta bicolor*) (Sellick et al. 2009). Variations in the migration patterns of African elephants have been documented using strontium isotopes (Koch et al. 1995). Britton et al. (2009) reconstructed migration of the caribou (*Rangifer tarandus granti*). The strontium isotope composition of otoliths has been applied extensively to track fish movements (Barnett-Johnson et al. 2005; Kennedy et al. 2002; Lynn Ingram and Weber 1999; Weber et al. 2005).

2.4.1.2. Modern Provenance Studies

Strontium isotopes can be applied as a method of provenance for a variety of materials. This approach has been used to locate the source area for elephant bone (Vogel et al. 1990) and ivory (van der Merwe et al. 1990) to aid in the identification of poached material. Additionally, Beard and Johnson (2000) have applied this technique to the antlers of white-tailed deer and skeletal material from the Vietnam War.

Strontium isotopes have been used as a provenance tool for wine (e.g., Almeida and Vasconcelos 2001; Barbaste et al. 2002; Horn et al. 1993), cider (García-Ruiz et al. 2007), marijuana (West et al. 2009), mineral water (Montgomery et al. 2006) and orange juice (Rummel et al. 2010). These results (with the exception of mineral water) represent bioavailable strontium and therefore can, excepting the effect of fertiliser use, be included in the mapping data for archaeological studies.

2.4.1.3. Hydrogeological Studies

Strontium isotopes can characterise groundwater sources and the extent of water/rock interaction to assist in hydrogeological studies (Shand et al. 2009). The strontium isotope composition of groundwater collected from bores on the western side of Lake Tiberias, Israel, was overwhelmingly characteristic of the Cretaceous rocks of the Judea Group aquifer (Starinsky et al. 1980), and, hence, assisted in provenancing the source of this water (Arad and Bein 1986). A study of secondary calcites from the Negev region in southern Israel showed that precipitates on major faults are enriched in ^{87}Sr relative to the local country rocks, suggesting a non-local fluid source (Avigour et al. 1990). Stein et al. (1997) used strontium isotopes in combination with sedimentological and

chemical evidence to discern the water sources for the Dead Sea and its precursor, Lake Lisan. The results were in the range of 0.70803 to 0.70808 and showed that the Dead Sea and Lake Lisan had varying sources with changing relative importance over time (Stein et al. 1997). In a similar study, Jin et al. (2009) determined the relative sources of water running into Lake Qinghai on the Tibetan Plateau.

Another common application of strontium isotopes is to provide information about the source of groundwater for an aquifer (Négrel et al. 2004). Hamel et al. (2001) used strontium isotopes to determine the extent of interaction between acidic mine waters and grout in an attempt to contain these waters within an abandoned coal mine in West Virginia. Négrel and Petelet-Giraud (2005) used strontium isotopes to quantify the extent of the contribution from groundwater to flooding of the Somme River in France. Klaus et al. (2007) were able to use strontium isotopes to trace the flow paths of purified water injected into the Thon Buri basin aquifer in Thailand. Leung and Jiao (2006) used the same technique to differentiate between natural groundwater and water-main leakage in Hong Kong. Vilomet et al. (2001) were able to quantify the contributions to groundwater chemistry of a leachate plume from a landfill and from fertiliser use. Strontium isotopes can also be used to determine the extent of water-rock interactions in thermal springs (e.g., Négrel and Lachassagne 2000).

2.4.1.4. Dolomitisation Studies

The strontium isotope composition of dolomites has been used to elucidate the source of dolomitising fluids in studies in western Canada (Mountjoy et al. 1992), Eniwetok Atoll in the Marshall Islands (Saller 1984) and Iowa in the United States (Banner et al. 1988). Strontium isotopes have also been used to discern the pre-metamorphism lithology of a dolomite hosting a Fe-Nb-REE deposit in Inner Mongolia (Le Bas et al. 1997).

2.4.1.5. Weathering Studies

Strontium isotope studies are a useful tracer for weathering, pedogenesis and biogeochemical cycling (Stewart et al. (1998). Singh et al. (1998) investigated the high strontium concentration and isotopic composition of some rivers draining the Himalayan-Tibetan Plateau by sampling strontium, oxygen and carbon isotopes and elemental abundances from Precambrian carbonates. Their results suggested that the enrichment in radiogenic strontium in the river waters is more likely to be sourced from the silicates in the drainage basin rather than the carbonates in the headwaters (Singh et al. 1998:754). Strontium can be used as a proxy for calcium weathering, which is an important source of plant nutrition (Jacks et al. 1989). Gierlowski-Kordesch et al. (2008) measured the strontium isotope composition of the Flagstaff Formation in central Utah to examine how the watershed evolved as a proxy for the relative influence of climate and tectonics on sedimentation. Poszwa et al. (2009) used strontium isotopes to determine the source of mineral nutrient for a plant community in French Guiana.

2.4.1.6. Palaeo-Mobility Studies

The use of strontium isotopes to determine past mobility has recently become a much more frequent application of this technique, perhaps driven by the development of MC-ICPMS allowing rapid analysis of large numbers of samples. The method as applied to archaeological studies, reviewed by Bentley (2006), Budd et al. (2004), Montgomery (2010) and Price et al. (2002) was suggested in pioneering paper by Ericson (1985), in which many of the future applications of the technique were envisaged. Selected archaeological case studies are summarised in Table 2.3 through Table 2.10.

To analyse mobility, the strontium isotope composition of biominerals from fossil samples are compared to regional values obtained from local faunal material

(Price et al. 2002) or from the analysis of the bioavailable component of strontium from plants, regolith or bedrock. The most suitable biomineral is tooth enamel, due to its early mineralisation during life and resistance to post-burial diagenesis, although bone and dentine have also been used. Even in conditions of relatively homogenous geology, sufficient contrast may exist for good results to be obtained (Hedman et al. 2009; Montgomery et al. 2007).

Author	Year	Site	Material	Age/Period	Method
Balter et al.	2012	Sterkfontein, Swartkras and Kromdraai B	Enamel	Not Reported	Laser
Britton et al.	2011	Jonzac	Dentine, Enamel	Late Middle Palaeolithic	Solution
Copeland et al.	2010	Gladysvale Cave	Enamel	570 ka	Laser
Copeland et al.	2010	Swartkrans, Sterkfontein	Enamel, Dentine	Pliocene/ Pleistocene	Laser and Solution
Copeland et al.	2011	Swartkrans, Sterkfontein	Enamel	Pliocene/ Pleistocene	Laser
Horn et al.	1994	Mauer	Bone, Dentine, Enamel	Lower Palaeolithic	Solution
Richards et al.	2008	Lakonis	Dentine, Enamel	Middle-Upper Palaeolithic	Laser
Sillen et al.	1995	Swartkrans	Bone	Plio- Pleistocene	Solution
Sillen et al.	1998	Swartkrans	Bone, Enamel	Plio- Pleistocene	Solution

Table 2.3 Selected Strontium Isotope Studies of Palaeolithic or Older Archaeological Material

The question of mobility can be addressed in a number of ways using strontium isotopes. On the most basic level, the method can simply be used to determine if individuals are local or non-local by comparison to a background value obtained from the archaeological site or the surrounding area (Bentley et al. 2007; Conlee et al. 2009; Schweissing and Grupe 2000). This method can be increased in sophistication by combining it with other techniques such as deoxyribonucleic acid (DNA) analysis (e.g., Haak et al. 2008) or other isotopes

(Bentley et al. 2005; Knudson et al. 2009; Montgomery et al. 2005; Müldner et al. 2009; Wright et al. 2010).

Author	Year	Site	Material	Age/Period	Method
Price et al.	2001	Linearbandkeramik Sites	Bones, Teeth	Neolithic	Solution
Bentley et al.	2002	Linearbandkeramik Sites	Enamel	Neolithic	Solution
Bentley et al.	2003	Vaihingen	Bone	Neolithic	Solution
Bentley and Knipper	2005a	Southern German Sites	Enamel	Neolithic	Solution
Bentley and Knipper	2005b	Vaihingen	Enamel	Neolithic	Solution
Bentley et al.	2008	Talheim	Enamel	Neolithic	Solution
Giblin	2009	Hungarian Plains Sites	Enamel	Neolithic-Cooper	Solution
Grupe et al.	1997	Bell Beaker Sites	Enamel, Bone	Neolithic	Solution
Montgomery et al.	2000	Monkton-up-Wimbourne	Enamel, Dentine	Neolithic	Solution
Nehlich et al.	2009	Nieder-Mörlen	Enamel	Neolithic	Solution
Price, Grupe et al.	1994	Bell Beaker Sites	Enamel, Bone	Neolithic	Solution
Price et al.	1998	Bell Beaker Sites	Teeth, Bone	Neolithic	Solution
Sjögren et al.	2009	Megalithic Sites in Sweden	Enamel	Neolithic	Solution
Smits et al.	2010	Schipoluiden, Swifterbant	Enamel	Neolithic	Solution
Viner et al.	2010	Durrington Wells	Enamel, Dentine, Bone	Neolithic	Solution

Table 2.4 Selected Strontium Isotope Studies of European Neolithic Archaeological Material

Some authors (e.g., Richards et al. 2008) make inferences about the strontium isotope composition of the surrounding areas based on their geology and so infer mobility patterns. This approach minimises sampling and laboratory time. Unfortunately, it fails to take into account the complexity of the regolith and strontium bioavailability and so precludes a nuanced understanding of mobility.

Author	Year	Site	Material	Age/Period	Method
Åberg et al.	1998	Norwegian Sites	Teeth, Bone	Medieval	Solution
Bendrey et al.	2009	Rooksdown and Bury Hill	Enamel	Iron	Solution
Budd et al.	2004	British Sites	Enamel	Neolithic- Medieval	Solution
Chenery et al.	2010	Gloucester Sites	Enamel, Dentine	Roman	Solution
Eckardt et al.	2009	Lankhills School Cemetery	Enamel	Roman	Solution
Evans et al.	2012	Many British Sites	Enamel	Neolithic-19th Century	Solution
Giblin et al.	2013	Great Hungarian Plain Sites	Enamel	Neolithic- Copper	Solution
Hoekman-Sites and Giblin	2012	Great Hungarian Plain Sites	Enamel, Bone	Neolithic- Copper	Solution
Hoogewerff et al.	2001	'Ötzi the Iceman'	Bone	3350–3100 BC	Solution
Millard et al.	2005	Eastbourne, Rivenhall and Blackfriars Cemeteries	Teeth	Anglo-Saxon	Solution
Montgomery et al.	2005	West Heslerton Cemetery	Enamel	Neolithic-Early Anglo-Saxon	Solution
Müldner et al.	2009	Whithorn Cathedral Priory	Enamel, Dentine	11th to 14th Century	Solution
Nafplioti	2009	Mycenae	Enamel	Mycenaean	Solution
Schweissing and Grupe	2000	Teuton and Gepid Sites	Teeth and Bone	Iron Age	Solution
Sykes et al.	2006	British Sites	Enamel	Roman	Solution

Table 2.5 Selected Strontium Isotope Studies of Other European Archaeological Material

A more robust approach is to map the surrounding area using plant, regolith, bedrock or faunal samples, and (for bedrock and regolith) leach the samples in a way that mimics the bioavailable component (Capo et al. 1998; Kelly 2007; Montgomery et al. 2007 and many others). Some authors are developing bioavailable strontium maps for regions of archaeological interest, without including case studies, to provide baseline data for other workers (Evans et al.

2009 for the Isle of Skye; Gill et al. 2009 for the Chicxulub in Mexico; Nafplioti 2011 for the Aegean).

Author	Year	Site	Material	Age/Period	Method
Bentley et al.	2005	Ban Chiang	Enamel	Neolithic	Solution
Bentley, Tayles et al.	2007	Khok Phanom Di	Enamel	2100–1500 BC	Solution
Bentley et al.	2009	Ban Lum Khao	Enamel	Bronze	Solution
Valentine et al.	2008	Niah Cave, Gua Sireh, Lobang Angin	Enamel	Neolithic	Solution

Table 2.6 Selected Strontium Isotope Studies of Asian Archaeological Material

Problems with the strontium isotope technique can include an elevation of radiogenic strontium from a high seafood diet (Slovak et al. 2009:163), a lack of suitable contrast between background bioavailable strontium composition, or post-burial diagenesis. As discussed in more detail in section 4.5.1.2, the use of LA-MC-ICPMS provides spatial resolution of the strontium isotope values within an individual sample and reduces sample preparation time; however, results may be offset from solution values due to isobaric interferences (Horstwood et al. 2008; Nowell and Horstwood 2009; Simonetti et al. 2008; Vroon et al. 2008), although the extent of this effect remains contentious (Copeland et al. 2008; 2010).

Author	Year	Site	Material	Age/Period	Method
Bentley et al.	2007	Teouma	Enamel	Lapita	Solution
Lees	2010	Teouma	Enamel, Dentine	Lapita	Laser
Jaric	2004	Sohano, To-At-1, To-At-2	Enamel	Lapita and Post-Lapita	Solution
Shaw et al.	2009	Kamgot, Balbalankin	Enamel	Lapita	Solution
Shaw et al.	2010	Reber-Rakival	Enamel	Lapita	Solution
Shaw et al.	2011	Nebira	Enamel	Lapita	Solution

Table 2.7 Selected Strontium Isotope Studies of Pacific Archaeological Material

Several potential problems with applying the strontium isotope composition to mobility mapping appear not to have been considered in the literature. First, little attention appears to have been given to reconstruction of changes in the bioavailable strontium composition of regolith due to changing climatic conditions. Given the large contribution made by aerosols to regolith strontium isotope composition (as discussed in section 2.3.2), variations in regional wind speed and direction, precipitation and vegetation cover (Pelletier 2007) have the potential to change this value markedly over time. More dramatic processes such as variations in glaciation and the rate of tectonic uplift will vary the rate of bedrock weathering, with implications for regolith strontium composition (Bern et al. 2005; 2007). Additionally, the variation in soil formation processes due to changes in precipitation will have an effect on strontium isotope composition (Stewart et al. 2001).

Author	Year	Site	Material	Age/Period	Method
Conlee et al.	2009	Nasca Sites	Enamel	1–1476 AD	Solution
Ezzo et al.	1997	Grasshopper Pueblo, Walnut Creek	Enamel	1325–1400 AD	Solution
Ezzo and Price	2002	Grasshopper Pueblo, Walnut Creek	Enamel, Bone	1270–1400 AD	Solution
Knudson et al.	2005	Juch'upampa Cave	Enamel, Bone	500–1100 AD	Solution
Knudson et al.	2009	Aja, Cahuachi, Cantayo, Marjoro Chico and Paredones	Enamel	1–800 AD	Solution
Price, Johnson et al.	1994	Grasshopper Pueblo, Walnut Creek	Enamel, Bone	Late Prehistoric	Solution
Price et al.	2000	Teotihuacan	Enamel, Bone	1–650 AD	Solution
Price et al.	2008	Teotihuacan, Tikal, Copan, Palenque and Campeche	Enamel, Bone	Preclassical-Classical	Solution
Price et al.	2010	Copan	Enamel	400–800 AD	Solution
Slovak et al.	2009	Ancón	Enamel,	550–1000 AD	Solution

Author	Year	Site	Material	Age/Period	Method
			Bone		
Tung and Knudson	2011	Conchopata	Enamel, Bone	600–1000 AD	Solution
Turner et al.	2009	Machu Picchu	Enamel	1438–1532 AD	Solution
Wright et al.	2010	Kaminaljuyu	Enamel	600–900 BC	Solution
Wright	2012	Tikal	Enamel	Early-Late Classic	Solution

Table 2.8 Selected Strontium Isotope Studies of American Archaeological Material

Another possible inaccuracy inherent in some strontium isotope studies is the assumption that the strontium isotope composition of the archaeological site is representative of the surrounding area. This manifests particularly in the use of sediment samples from excavations as a ‘local’ value. This approach ignores the genesis of the lithostratigraphic units within archaeological sites as being a unique nexus of geologic, biogenic, anthropogenic and taphonomic agents (Farrand 2001). Clearly, these conditions will operate differently within an archaeological site than outside it; a unique strontium isotope composition for the archaeological site is likely.

Author	Year	Site	Material	Age/Period	Method
Al-Shorman and El-Khoury	2011	Barsinia	Enamel	Late Antiquity	Solution
Perry et al.	2008	Khirbet edh-Dharih	Enamel	100–700 AD	Solution
Perry et al.	2009	Khirbet Faynan	Enamel	Byzantine	Solution
Shewan	2004	Israeli Sites	Bone	Natufian	Solution

Table 2.9 Selected Strontium Isotope Studies of Middle Eastern Archaeological Material

Author	Year	Site	Material	Age/Period	Method
Balasse et al.	2002	Kasteelberg	Enamel	Late Stone Age	Solution
Cox and Sealy	1997	Cape Town Foreshore	Teeth, Bone	1818	Solution
Tafuri et al.	2006	Fezzan	Enamel	Aterian, Acacus, Pastoral, Garamantian	Solution

Table 2.10 Selected Strontium Isotope Studies of Post-Palaeolithic African Archaeological Material

Overall, the use of strontium isotope analysis has wide application in archaeology, with sites from a range of ages and locations being analysed. Unfortunately, only a small proportion of these studies have investigated the heterogeneity of biominerals or utilised a comprehensive mapping programme of bioavailable strontium, suggesting that an increase in methodological rigour is required.

2.4.1.7. Other Archaeological Applications

Several novel applications of the strontium isotope technique to archaeological questions have been undertaken by analysing material other than biominerals. These materials include ancient textiles, as trialled by Frei et al. (2009), and archaeological maize samples from New Mexico, as investigated by Benson et al. (2003).

2.4.1.8. Palaeoecological Studies

Palaeoecological studies can employ strontium isotopes to define mobility of palaeontological material. The need for pre-anthropogenic disturbance baseline data of ecological communities is critical for establishing meaningful conservation and restoration ecology projects (Terry 2010).

Porder et al. (2003) applied the strontium isotope technique to small mammal bones from the Holocene predator accumulated fossil sites of Lamar Cave and Waterfall in Wyoming. The measured $^{87}\text{Sr}/^{86}\text{Sr}$ ratio of local vegetation was used to provide the background values, as they are the principal food sources for the small mammals studied and show only small offsets from the values obtained from the underlying geological units (Porder et al. 2003:198). The results demonstrated that the hunting ranges for the predators found in these 2 sites covered restricted non-overlapping areas and did not vary over time, despite significant climate variations (Porder et al. 2003:202).

Holmden et al. (1997) applied strontium isotopes and strontium concentration and Sr/Ca ratios of carbonate fossil shells to determine the palaeosalinity of ancient estuarine deposits in western Canada. Briot (2008) applied this technique to *Potamides lamarcki* ostracods from the Oligocene Massif Central and suggested that their elevated $^{87}\text{Sr}/^{86}\text{Sr}$ compared to sea water values at this time are indicative of the ostracods living in intracontinental lakes. Further research suggests the importance of establishing the extent of post-burial diagenesis prior to using fossils in this fashion (Cochran et al. 2010).

Strontium isotopes have been applied to tracing the migration of palaeontological material, including a range of fauna (Hoppe and Koch 2007), mammoths and mastodons in the south-western United States (Hoppe et al. 1999), bison in the Great Plains, United States (Widga et al. 2010) and Europe (Julien et al. 2012) and horse and red deer in Italy (Pellegrini et al. 2008), as well as mastodons in Siberia (Arppe et al. 2009).

2.4.1.9. Palaeodietary Studies

The application of elemental abundance studies to the elucidation of diet can provide additional evidence independent to that provided by the archaeological record alone (e.g., Isaac 1971). Palaeodiet studies using strontium have

principally focused on the application of the Sr/Ca ratio to elucidate trophic level (Sillen and Kavanagh 1982) or the Ba/Sr ratio as an indicator of consumption of marine resources (Burton and Price 1990). The Sr/Ca ratio has been proposed to also reflect the degree of marine influence on diet, based on the high strontium level reported for a population with a diet interpreted to be high in molluscs (Schoeninger and Peebles 1981:396). However, Burton and Price (1999) have shown that marine organisms biopurify strontium up the food chain in the same manner and to a similar degree as terrestrial species.

Prior to the acceptance of the Sr/Ca method, strontium concentration was used as a proxy for trophic level with varying degrees of success. Elias (1980) sampled tooth enamel from vegetarian and non-vegetarian human subjects, but could demonstrate no correlation with diet. Schoeninger (1979) calculated the concentration of strontium in bones from the archaeological site of Chalcatzingo in Mexico and compared the results to the nature of their grave goods. The results suggest some correlation between class and diet.

The Sr/Ca ratio reflects the trophic level of an individual's diet as strontium is discriminated against by vertebrate digestive systems. This is undertaken as mammalian proteins involved in calcium transport discriminate in the binding of alkaline earths so that while 40 to 80% of dietary calcium is absorbed, only 20 to 40% of dietary strontium is absorbed (Sillen and Kavanagh 1982). As a result, the Sr/Ca ratios in their tissues, while averaging the ratios of their various dietary components (Burton et al. 1999), are always lower than in the food they consume (Price et al. 1985:420). This process is known as 'discrimination against strontium' in the biochemical literature and 'biopurification of calcium' in the geochemical literature (Sillen and Lee-Thorp 1994). Mammalian controlled diet studies suggest that an animal's Sr/Ca ratio is about 20 to 35% that of its food (Sillen and Lee-Thorp 1994:244).

However, there are a number of complicating factors in the archaeological interpretation of Sr/Ca ratios. They may not linearly reflect the proportion of plant/meat in diet, because they are disproportionately sensitive to high calcium foods (Burton and Wright 1995). Geological substrates influence the Sr/Ca ratio of plants, which leads to variations in the relative ratios of mammals, meaning that local systematic mapping is essential (Alvira et al. 2011). Different parts of the same plant and/or different plant species may incorporate Ca and Sr into their tissues in different ratios (e.g., Dasch et al. 2006; Menzel and Heald 1959; Runia 1987; Wallace and Romney 1971) and so feeding behaviours might affect Sr/Ca ratios in herbivores. Dental enamel has been proposed as a poor candidate for the investigation of Sr/Ca ratios, because it may be formed in juvenile mammals, which do not discriminate against strontium (Sillen and Lee-Thorp 1994:245). Sponheimer et al. (2005) suggested that this potential drawback, which can be avoided by analysing only late developing teeth, is outweighed by the much higher resistance of teeth to post-burial diagenesis than bone.

New advances in analytical technology have allowed rapid, spatially resolved sampling of Sr/Ca ratios, which considerably broadens the field of potential analysis. Micro-scale variations in Sr/Ca ratio during enamel formation may be resolvable in the striae of Retzius, which have a periodicity of 6 to 11 days (Alvira et al. 2011). Spatially resolved micro-analysis has demonstrated that variations due to the degree of mineralisation lead to changes in Sr/Ca ratio within an individual tooth without variations in environmental input (Humphrey et al. 2008).

A derivative of the Sr/Ca method is used to examine whether weaning has taken place in infant remains. This provides information on changes in nursing behaviour through time. This method works on the basis that human milk has an exceptionally low Sr/Ca value (strontium having been discriminated against by the mothers body), while other food is comparatively high in Sr/Ca (Sillen and Smith 1984). This hypothesis was tested on skeletal material from Dor in

Israel (Sillen and Smith 1984) and from Wharram Percy in England (Mays 2003). Humphrey et al. (2008) extended the technique with LA-ICPMS to examine the spatial distribution of Sr/Ca ratios in teeth of children with different nursing strategies. Children fed for prolonged periods with breast milk showed a characteristic reduction in Sr/Ca ratios across the neonatal line (Humphrey et al. 2008:6836). This approach (in combination with strontium and nitrogen isotope data) demonstrated differences in food webs in individuals from Chiribaya affiliated sites in Southern Peru (Knudson et al. 2010).

A recent application of strontium in palaeodietary studies is the use of the $\delta^{88}\text{Sr} / {^{86}\text{Sr}}$ value (Knudson et al. 2010) to define trophic level based on the preferential incorporation of ^{86}Sr in biological systems. Knudson et al. (2010) argued that while the fractionation between ^{86}Sr and ^{88}Sr was small (sufficient to be considered non-existent in many studies) it is sufficient to be used as a palaeothermometer for coral studies (Fietzke and Eisenhauer 2006; Rüggeberg et al. 2008), a tracer of soil production (Halicz et al. 2008) and weathering processes (de Souza et al. 2010) and, hence, can be applied to archaeological studies.

2.4.1.10. Palaeo-Occupation Intensity Studies

The use of strontium abundance, usually as part of a suite of element abundances, is an emerging technique as a marker of human occupation (Jones et al. 2010; Wilson et al. 2005; 2008). The method works on the basis that human occupation frequently leads to a variation in trace element abundance, regardless of the specific function of a site. This effect can be reduced or confused by post-occupation geologic, pedologic, hydrologic or anthropogenic processes (Pierce et al. 1998). Nevertheless, elevated strontium concentrations compared to the surrounding area are often an indication of human occupation.

2.5. Summary

Strontium is a relatively widely distributed element, found in biominerals due to the replacement of calcium. Due to a lack of fractionation of Sr⁸⁷/Sr⁸⁶ ratios in biological systems, strontium is an excellent marker for the geological environment of formation of teeth and bone, despite some complexity between rock, regolith and bioavailable strontium. Strontium has been used as a provenance aid in a wide range of geological, ecological and hydrological studies and has been used widely to investigate the mobility of archaeological materials.

Chapter Three: Background to the Study Areas

3.1. Overview

The research in this thesis was carried out on teeth from the Lower to Middle Palaeolithic archaeological sites of Amud, Holon, Skhul, Tabun and Qafzeh in Israel and Bois Roche, La Chapelle-aux-Saints, Les Fieux, Le Moustier, Rescoundudou, Payre and Pech de l'Azé II in France, shown in Figure 1.1. Soil and rock sampling was undertaken throughout Israel and in the south of France in an east-west transect from Bordeaux to Valence.

These areas, and indeed these sites, contain abundant and important archaeological material and hominin fossils spanning *Homo erectus*, *Homo neanderthalensis* and anatomically modern humans. While both countries have a significant history of investigating archaeological material to answer these questions, strontium isotope led determinations of mobility have thus far only been used sporadically in these regions.

These areas contain a variety of physiographic, geological, pedological and biotic environments that are summarised below. A nuanced understanding of these variables is critical to producing an accurate interpretation and to providing a context for strontium isotope data. Israel and southern France provide a natural laboratory for strontium isotope analysis as these variables are well understood and vary greatly over a comparatively small area.

3.2. Physiography

3.2.1. Topography

3.2.1.1. Israel

Israel can be divided into 4 principal north-south trending physiographic zones, which are (west to east): the coastal plain, the Judean Hills, the Jordan Rift Valley and the Golan Heights (Goldreich 1995:167). Elevations range from 2236 m at Mount Hermon in the Golan Heights to -417 m in the Dead Sea. These topographic zones broadly correspond to geological provinces, with the Judean Hills through the centre of the country (orientated approximately north-south) being dominated by Cretaceous carbonates, the plateaus to the north-east in the Golan Heights being formed by basalts and the depressions to the west and the coastal plain containing principally unconsolidated, comparatively young sediments.

The Israeli coastal plain is up to 50 km wide in the south of the country, and thins until disappearing at Haifa due to the presence of Mount Carmel. The coastal plain thickens in Haifa Bay before thinning again to disappear on the northern border of Israel. The shoreline bends from an east-west orientation to being progressively more north-south in a northwards trend up the country.

The coastal plain in the south (known as the Western Negev coastal plain) is very sandy, dominated by dunes and dissected by several large wadis draining the hinterland (Horowitz 1979). The Pleshet and Sharon coastal plains, through the central part of Israel, are sandy, with abundant hamra red soil and marshes (Horowitz 1979). The coastal plain adjacent to the Carmel Range (known as the Carmel coastal plain) is narrow and principally comprises calcareous aeolian sandstone ridges (kurkar) running parallel with the coastline and interspersed with clay and alluvial silt (Zviely et al. 2009).

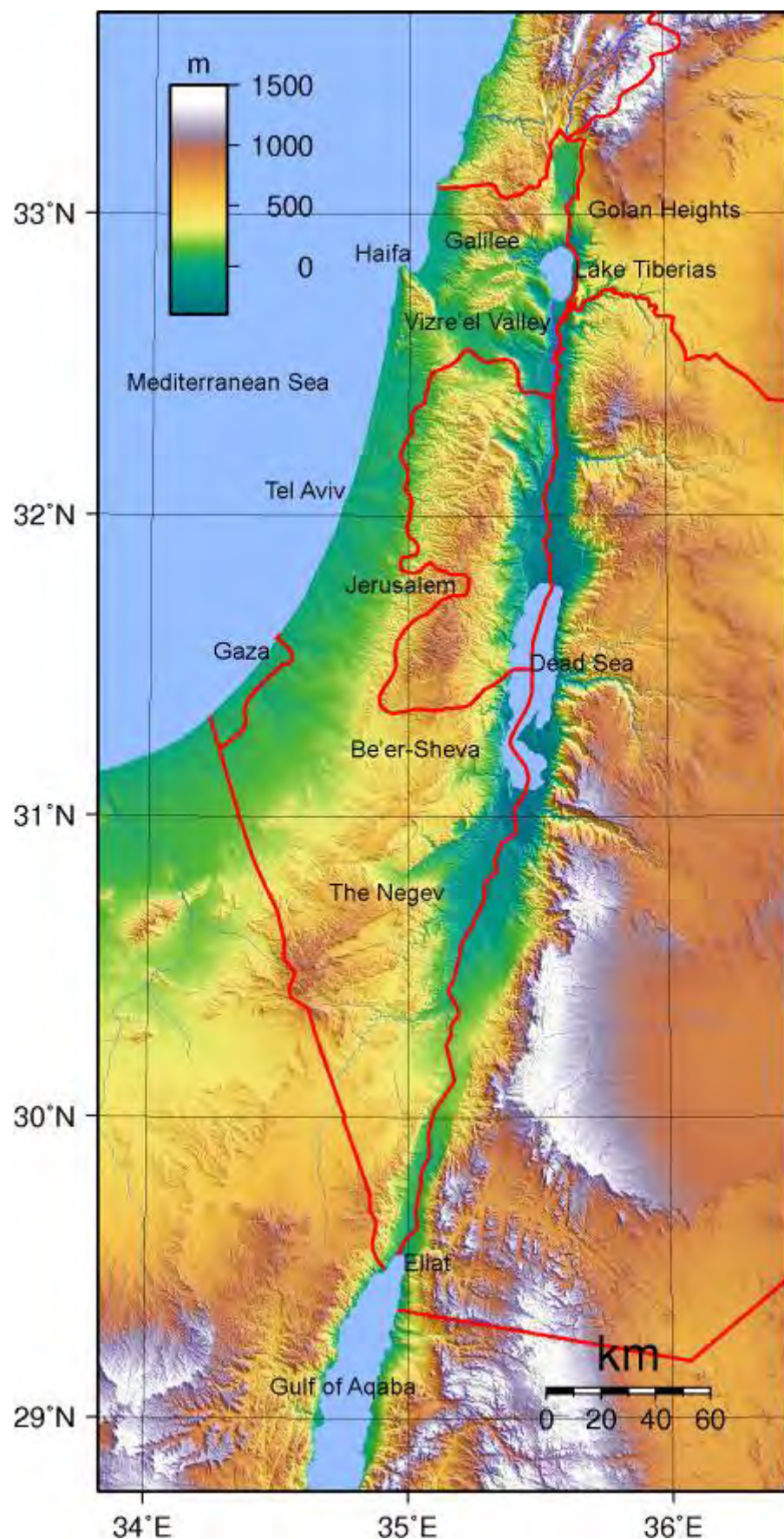


Figure 3.1 Topography of Israel (Image: Modified from Sadalmelik 2007)

The mountainous backbone of Israel, with elevations in the range of 250 to 1200 m, extends from Eilat in the south to the Lebanese mountains, interrupted only by the Vizre'el Valley in the north and the Be-er Sheva Basin in the south (Horowitz 1979). The western edge of these hills generally slopes gently to the coastal plain, particularly in the south (Qumsiyeh 1996). The northern part of this feature is the Galilee Mountains, the central, more arid, section is the Judean Hills and in the south are the Idumea, Negev and Eilat regions. The Eilat block in the south has particularly distinctive steep mountains with no soil, formed by Precambrian basement material.

The Golan Heights is an elevated region bordered by the Hula Basin to the west and the Yarmouk River to the south. The area has a hummocky undulating topography caused by volcanic cones, basalt flows and dykes (Singer 2007). The Jordan Rift Valley encompasses the Hula Basin, the Jordan River Basin, and the Dead Sea. At its deepest, this feature is 400 m below sea level and it expends north-south through the entire country.

Drainage in Israel is minimal, with no perennial streams in the Eilat, Negev and Judean/Samaria mountain regions (Horowitz 1979). The Jordan River is the only significant water course, which drains via the Hula Basin into the fresh Lake Tiberias and subsequently the Dead Sea.

3.2.1.2. France

The areas of southern France considered in this study are divided into a number of broad physiographic zones: the flat coastal plain distributed in a triangular wedge in the west; the moderately elevated, variably incised plateaus in the Dordogne region; the elevated plateau of the Massif Central and the north-south trending valley of the Rhône in the east. These regions have substantial natural physiographic boundaries to the south (the Pyrenees) and to the west (the Alps) and to the east (the Bay of Biscay).



Figure 3.2 Representation of the Topography of France using Shuttle Radar Topography (Modified Image: NASA)

3.2.2. Sea Level

3.2.2.1. Israel

Sea level has varied significantly through the Quaternary in Israel (as shown in Figure 3.3), with the effect of modifying the width of Israel's coastal plain. This process has been significantly affected by active tectonics along this margin, which have caused significant uplift, particularly through the central section (Neev et al. 1987). During the last 250 ka, sea level has risen above its current

level only once (at 125 ka during the peak of interglacial MIS 5e) and has dropped to as much as 100 below its present level (Zviely et al. 2009). Marine coring in Haifa Bay shows that between MIS 5 and MIS 2 and 3 the shelf was regionally exposed and subject to significant erosion (Avnaim-Katav et al. 2012). A similar unconformity is found in between MIS 12, 11 and 10 and MIS 8 and 7 (Avnaim-Katav et al. 2012).

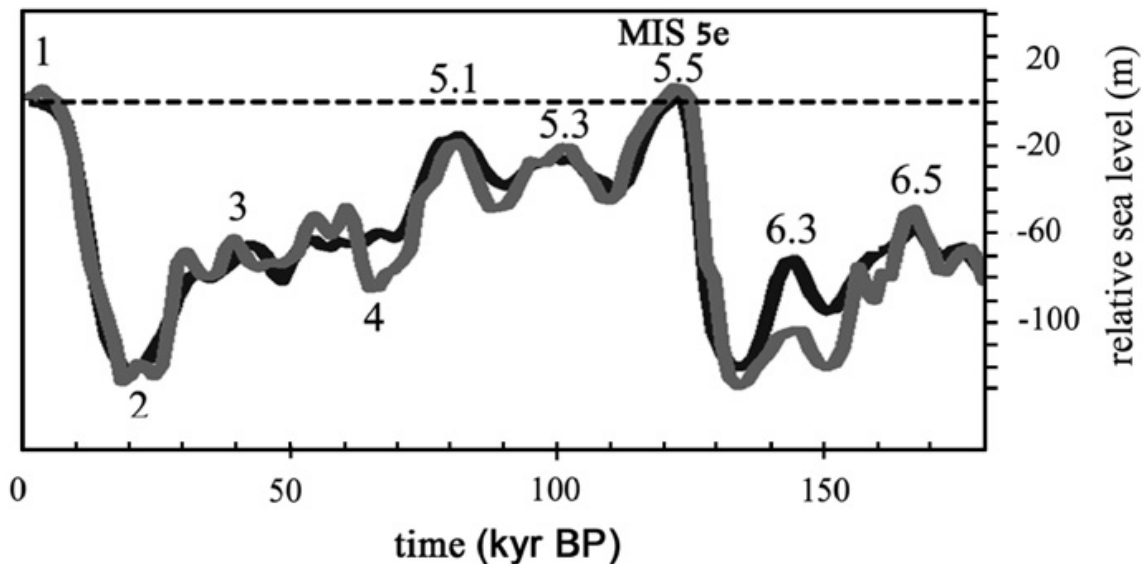


Figure 3.3 Global Sea Level Curve for the Last 200 ka with MIS Noted (Galili et al. 2007)

3.2.2.2. France

Sea level in the Bay of Biscay and the Mediterranean Sea have varied with the ice sheet volume throughout the Quaternary. During sea level lowstands, the Rhône river extended significantly onto the broad, exposed continental shelf (Torres et al. 1997), with the location of the Rhône incised valleys being structurally controlled (Gensous and Tesson 1996). The major reduction of sea level during MIS 4 exposed most of the North Sea, the English Channel and approximately 30 to 40 km of the Atlantic coastal plain as dry land (Mellars 1996). Sea level during MIS 5e was 2 to 12 m higher than today (Van andel and Tzedakis 1996:487). Sea level by the end of MIS 5d reached -50 m and in MIS

5b reached -25 m (Van andel and Tzedakis 1996). Sea level was -50 m for most of MIS 3, then fell to -80 m by the end of MIS 3 (Bard et al. 1990).

3.3. Climate, Vegetation and Fauna

3.3.1. Modern Climate, Vegetation and Fauna

3.3.1.1. Israel

The Mediterranean climate in Israel is characterised by a dry summer and a wet winter. It can be divided into a number of zones, reviewed by Dan and Koyumdjisky (1963). These include a humid and sub-humid Mediterranean climate in the northern part of the country, semi-arid and arid zones in the central region and an extremely arid zone in the south (Dan and Koyumdjisky 1963:14). August is the hottest month in Israel, with mean temperatures ranging from 24 °C in the high mountains to 34 °C near the Dead Sea. January is the coldest month, with mean temperatures ranging from 16 °C near the Dead Sea to 8 °C in the high mountains (Rosenan 1970). The interaction of the humid and arid zones reflects the balance between the effect of the passage of cyclones from the north-east Atlantic into the warm Mediterranean Sea, providing a source for winter rainfall (Roberts and Wright 1993), and the low latitude monsoon system originating in the tropical Atlantic and Indian oceans (Rossignol-Strick 1985) blocking precipitation. Average open water evaporation exceeds long term average rainfall in all months, except December, January and February, based on measurements at Bet Dagan on the central coastal plain (Cohen et al. 2002).

Goldreich (1994; 1995) has reviewed the spatial and temporal distribution of precipitation in Israel. The majority of rain falls between December and January and no rain falls between June and August (Goldreich 1995:167). Snow fall is limited to the tops of the hills. The differences in the spatial distribution of rain in

Israel is one of the most extreme in the world, with great variations in the volume of precipitation occurring over very short distances (Goldreich 1994:45).

The rainfall volume can be divided into several key provinces (shown in Figure 3.4). Rainfall is highest in the north, particularly in the Golan Heights and in the area of Mount Meron. Rainfall is moderate to high in the Carmel Range, the Shomron and the Judean Hills. Rainfall is moderate on the coastal plain and around Beer-Sheva and very low in the Negev and in the Jordan Rift Valley. The marked variations in rainfall are mirrored by variations in humidity, temperature and evapotranspiration (Naveh 1967). There is evidence to suggest that El Niño correlates with precipitation in Israel (Price et al. 1998), although the relationship is complex (e.g., Rimbu et al. 2003). Springtime low pressure systems can send large dust storms from the Sahara (Perry et al. 2008:536).

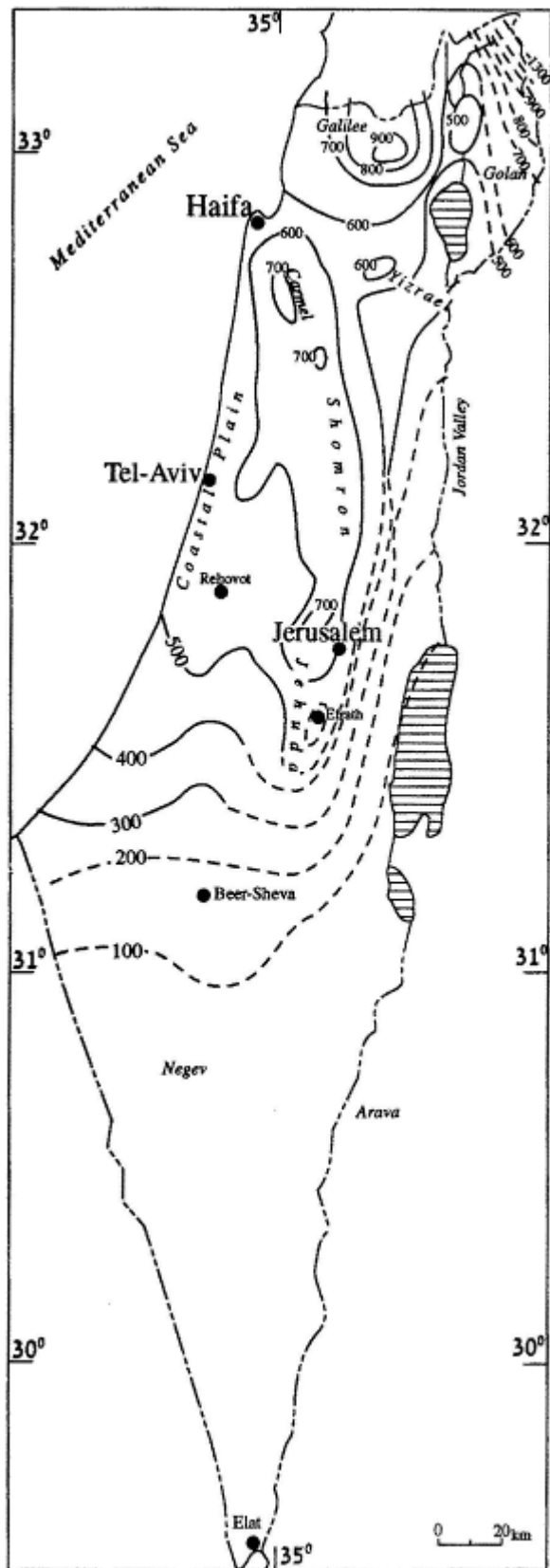


Figure 3.4 Annual Normal (1961 to 1990) Rainfall Map of Israel (Goldreich 1994:46)

Israel has particularly high plant species richness (2700), possibly due its position on a major climate transition (Ronen and Avinoam 1999). The botany of the region was summarised by Zohary (1962). Major plant provinces were initially described by Eig (1931 and 1932) and collated by Zohary (1962), who considered that this vegetation structure has been in place since the Pliocene era. The identified vegetation formations in Israel include: Coniferous Forests, Schlerophyllous Oak Forests and Maquis, Deciduous Broad-Leaved Oak Forests, Evergreen Park-Maquis, Deciduous Steppe-Maquis and Steppe-Forests, Deciduous Thermophilous Scrub, Halophytic Forests, Riparian Woods, Sazaul Woods, Savannah Forests, Mediterranean Batha and Garigue, Dwarf Shrub Steppes, Steppes of Aphyllous, Broomlike Shrubs, Leaf and Stem Succulent Dwarf Shrub Formations and Rush and Reed Vegetation (Zohary 1962:67–69). Overall, the vegetation can be grouped into 3 phytogeographic regions: the Mediterranean, the Irano-Turanian and the Saharo-Sindian.

Pollen investigations show that the northern region is dominated by oak and other Mediterranean trees such as cypress, pistachio and olive, which decrease to the south before becoming absent in the Negev (Horowitz 1979).

3.3.1.2. France

The modern climate of Western Europe is dominated in winter by the North Atlantic oscillation index, which controls the strength and direction of north-westerly winds (Hurrel 1995). If this index is high, these winds are pushed northwards, causing dry winters in the Mediterranean region and rainfall in northern Europe, with the converse being true if the index is low (Sánchez Goñi et al. 2008). In summer, precipitation is suppressed by anti-cyclone cells over the sub-tropical eastern Atlantic ocean (Rodwell and Hoskins 2001).

Temperatures within the study area (measured at Bordeaux) average approximately 5 °C in the winter and approximately 25 °C in the summer.

Precipitation in the region is approximately 1000 mm per year and the mean annual temperature is 10 °C, leading to the dominance of deciduous oak, (*Quercus*) with birch (*Betula*) or hornbeam (*Carpinus*) depending on the mineralogy of the soil (Sánchez Goñi et al. 2008). As elevation increases, beech (*Fagus*) replaces birch/hornbeam until spruce (*Picea abies*), fir (*Abies alba*) and pine (*Pinus sylvestris*) become dominant (Sánchez Goñi et al. 2008).

Two biomes (Prentice et al. 1992) are present within the study area in the modern day; warm mixed and temperate deciduous which each contain a range of plant types as described by Fauquette et al. (1999:6–7).

3.3.2. Quaternary History

The Pleistocene climate has been divided into ‘stages’ (usually termed MIS), controlled by changes in the global ice volume driven by changes in the obliquity, precession and eccentricity of the earth orbit. The stages relevant to this research, as defined by Emiliani (1955; 1956) and Shackleton and Opdyke (1973; 1976), are summarised in Table 3.1. These changes have significant implications for global sea level (Chappell and Shackleton 1986), vegetation and faunal assemblages.

Stage	Age Range	Temperature Trend	North-West Europe Glacial Sequence	Classic Alpine Glacial Sequence
MIS 1	0–13,000	Warmer	Holocene	
MIS 2	13,000–32,000	Colder	Late Weichsellian	Würm
MIS 3	32,000–64,000	Warmer	Middle Weichsellian	
MIS 4	64,000–75,000	Colder		
MIS 5	75,000–128,000	Warmer	Early Weichsellian/Eemian	Riss-Würm Interglacial
MIS 6	128,000–195,000	Colder	Saalian	Riss
MIS 7	195,000–251,000	Warmer		Mindel-Riss Interglacial
MIS 8	251,000–297,000	Colder		

Table 3.1 Original MIS, Temperature Trends and Alpine Glaciations (Data From Gibbard and Van Kolfschoten 2004; Shackleton and Opdyke 1973; 1976)

Subsequent research has demonstrated that major climatic and palaeo-environmental units typically have the duration of the order of 10ka (half a precession cycle), rather than the approximately 50 ka (half an eccentricity cycle) scale suggested in Table 3.1 (Shackleton et al. 2003). This led to the subdivision (within the time scale of interest for this thesis) of MIS 5 into sub-stages 5a to 5e and MIS 7 into 7a to 7e (Gibbard et al. 2005).

Further subdivision of these units has occurred (particularly for MIS 2 to 4), down to the resolution of Dansgaard-Oeschger (DO) cycles (based on Greenland ice cores, see Dansgaard et al. 1984), which have an average period of 1360 years, comprising a cold phase of approximately 600 years followed by a rapid warming (Chappell 2002). These can be grouped into larger packages known as Bond cycles, bounded by ice rafted debris horizons known as Heinrich events (Bond et al. 1993). These high resolution packages can be correlated on a global scale (Voelker 2002). Climate events of any order can have substantial effects on vegetation (Fletcher et al. 2010; Magri and Tzedakis 2000; Tzedakis 2005; Tzedakis et al. 2003) and faunal populations (Discamps et al. 2011), with significant implications for humans.

3.3.2.1. Israel

The regional climate of Israel during the late Pleistocene era varied significantly different to the present day (e.g., Enzel et al. 2008). While the climate has fluctuated significantly, the principal climate trend has been towards progressive desertification.

Frumkin et al. (2011) review a number of paleoclimate proxy from the Levant for the last 200 ka and showed that glacial periods were cool and wet while interterglacials were warm and dry. Waldmann et al. (2009) supported this hypothesis, based on the Dead Sea and its precursors, showing that most glacial periods and even short stadials appeared to be wetter and interglacial and terminations in particular were drier. Horowitz (1989) uses pollen from the Hula and Dead Sea lakes to support this hypothesis, contending that glacials were somewhat cold and had higher rainfall, while interglacials were hot and dry and interstadials had a short, rainy winter and a dry, hot, long summer. During the glacial monsoonal minima, the northern Negev was usually humid and the southern parts of the Saharo-Arabian desert were dry, suggesting that the Mediterranean rather than monsoons was the major source of humidity in the region (Vaks et al. 2006). The oak-terebith-pine woodland present on the Mediterranean Coast and on the flanks of the Jordan Rift Valley was the focus of Pleistocene human settlement in the Levant, because the stable water supply and persistent coverage of woodland vegetation made this the richest habitat in Western Asia (Shea 2007).

MIS 7 was characterised by a variable climate in Israel. A number of sapropels designated S9, S8 and S7, which were dated to 242, 220 and 197 ka, respectively, are present in core MD 84 to 642 from the Nile cone area of the Mediterranean Sea (Cheddadi and Rossignol-Strick 1995). The S9 sapropel contains an evergreen forest assemblage of *Quercus*, *Olea* and *Pistacia* pollen, as well as some mesophyllous trees that require humidity, which suggest a warm and humid climate (Cheddadi and Rossignol-Strick 1995:295). The pollen

in sapropel S8 showed that the Mediterranean forest had declined substantially and had been replaced by a *Artemisia* semi-desert, suggesting a more arid climate (Cheddadi and Rossignol-Strick 1995:295). The S7 sapropel contains a combination of Mediterranean forest and semi-desert species, suggesting composite vegetation with warm summers and cold summers (Cheddadi and Rossignol-Strick 1995:296). During MIS sub-stages 7c and 7b, the climate was arid and cold, with 7b being the more severe (Cheddadi and Rossignol-Strick 1995). $\delta^{13}\text{C}$ values from speleothems in the northern Negev during the humid interglacial interval between 200 to 196 ka suggest a rapid change in the vegetation of the region from desert to Mediterranean steppe forest (Vaks et al. 2006). The presence of travertines dated by the Th/U method in the Negev Highlands (Schwarcz et al. 1979) and the Arava Rift Valley (Livnat and Kronfield 1985) suggests wet conditions in MIS 7, although Horowitz (1987) contended that the presence of these travertines was not related to climate but due to spring water related to fault activity (Horowitz 1987). Speleothem deposition (reflecting higher rainfall than the Holocene) occurred in the Tzavoa Cave in the northern Negev at 200 to 190 ka (Vaks et al. 2006). The period 200 to 190 ka was humid in the Negev, based on the formation of speleothems (Vaks et al. 2006).

The entire MIS 6 of Israel appeared to be cold but not as dry as conditions experienced during MIS 2, on the basis of carbon and oxygen measurements of speleothems from Soreq Cave (Ayalon et al. 2002). Additionally, 2 periods of increased hydrological activity occurred circa 178 and 152 ka (Ayalon et al. 2002). At 178 ka the climate was cold, but probably remained humid because C3 vegetation was dominant (Ayalon et al. 2002:305). Pollen and fauna from sapropel S6, which formed in the Mediterranean Sea during MIS 6, are typical of glacial conditions (although some evidence of refugia oak forests exists) (Cheddadi and Rossignol-Strick 1995; Rossignol-Strick 1985) and alkenones showed cold sea surface temperatures of approximately 15 °C (Emeis et al. 1998). Frumkin et al. (2011:445) suggested that this period had a generally wet climate based on abundant speleothem deposition. Speleothem deposition (reflecting higher rainfall than the Holocene) occurred in the Tzavoa Cave in the

northern Negev between 137 to 123 ka (Vaks et al. 2006). The $\delta^{13}\text{C}$ reflects a Mediterranean steppe forest value, suggesting the desert margin migrated north during these periods (Hallin et al. 2012). At the MIS 6/5 transition, a significant period of soil erosion occurred, suggested by $^{234}\text{U}/^{238}\text{U}$ activity ratios in speleothems from the Jerusalem Cave (Frumkin and Stein 2004). The absence of travertine deposits dating from this period in the Negev led Livnat and Kronfield (1985:171) to conclude that this was a period of low rainfall, similar to the modern climate. The period 190 to 150 ka was humid in the northern Negev region, as demonstrated by the formation of speleothems (Vaks et al. 2006).

MIS 5 in Israel is characterised by a variable climate, with alternating forest and desert. During MIS 5a, oaks are abundant, with medium presence of other Mediterranean, temperate, semi-desert and desert vegetation (Langgut et al. 2011). Interglacial peaks were observed in speleothem fluid inclusion δD values at 129 to 120 ka, a double peak at 108 to 100 ka and 88 to 79 ka, suggesting high average annual surface temperatures at these times (McGarry et al. 2004). Sapropels S5, S4 and S3 were deposited in the Mediterranean Sea during sub-stages 5e, 5c and 5a, respectively (Cheddadi and Rossignol-Strick 1995). During the deposition of S5 (at MIS 5e), an evergreen forest with *Quercus*, *Olea* and *Pistacia* and a deciduous forest was abundant, suggesting mild to warm temperatures and the presence of sufficient moisture (Cheddadi and Rossignol-Strick 1995:296). During the deposition of S4 (at MIS 5c), the semi-desert and desert were more widespread, indicating drier and possibly cooler conditions (Cheddadi and Rossignol-Strick 1995:296). During the deposition of S3 (at MIS 5a), the forest was more abundant than in S4 but less so than in S5, suggesting intermediate climate conditions (Cheddadi and Rossignol-Strick 1995:296). MIS 5 was moderately humid and warm in Israel, as suggested by the presence of sapropel S3 marking the end of MIS 5 (Langgut et al. 2011).

The lack of primary aragonite and gypsum in Lake Lisan compared to Lake Samra and their relative lake levels suggest that the drainage area of the Dead Sea Basin was more arid and characterised by sporadic floods during the

interglacial Samra period (Waldmann et al. 2009). During 78 to 76 ka, the $\delta^{13}\text{C}$ reflects a Mediterranean steppe forest value, indicating the desert margin migrated north during these periods (Hallin et al. 2012). Speleothem deposition (reflecting higher rainfall than the Holocene) occurred in the Tzavaoa Cave in the northern Negev at 84 to 77 ka (Vaks et al. 2006). The presence of travertines dated by the Th/U method in the Negev Highlands (Schwarcz et al. 1979) and the Arava Rift Valley (Livnat and Kronfield 1985) suggests wet conditions in MIS 5. The periods 137 to 123 ka and 84 to 77 ka were humid in the northern Negev, based on the formation of speleothems (Vaks et al. 2006).

The onset of MIS4 in Israel is characterised by a sharp decline in evergreen oak based on pollen from deep-sea core 9509, taken off the southern Israeli coast, with more gradual decreases in other tree species probably due to increasing aridity (Langgut et al. 2011). Pollen analysis of cores 627 and 629 from the Nile cone region of the Mediterranean cone suggests that semi-desert was predominant and the landscape was probably mostly treeless (Cheddadi and Rossignol-Strick 1995:297). This stage represents a transition to glacial conditions.

In contrast, some authors suggested that MIS 4 brought an increase in rainfall, which lasted through to MIS 2 (e.g., Frumkin et al. 2011; Hallin et al. 2012), based on intensive speleothem deposition, high water levels and bicarbonate flux in Lake Lisan (Waldmann et al. 2009) and the deposition of spring carbonates (summarised by Frumkin et al. 2011:445). The difference in these interpretations may reflect a significant climate gradient in Israel during this period, similar to that found today. The average annual temperature during MIS 4 and 3 in Israel was approximately 5 °C colder than today, based on fluid inclusion from the Soreq Cave (McGarry et al. 2004). Some studies suggested that oak woodlands were more widely distributed than today (Horowitz and Gat 1984).

An analysis of rodent assemblages from the Amud Cave shows that a climatic shift during MIS 4 to 3 was not sufficient to cause a shift in the rodent population in the region (Belmaker and Hovers 2011). The period 76 to 25 ka (overlapping MIS4 and 3) was humid in the Negev, based on the formation of speleothems (Vaks et al. 2004).

MIS 3 is characterised by a minor increase in oak species in pollen analysed from core 9509 off southern Israel, suggesting slightly wetter conditions but frequent fluctuations in pollen taxa (Langgut et al. 2011). Some evidence exists for a significant pluvial event during this period, around 56.0 to 54.4 ka (Langgut et al. 2011). Pollen from offshore cores 627, 629 and 642 from the Nile delta suggest that *Artemisia* semi-desert was prevalent, with some evergreen and deciduous forest present in small areas (Cheddadi and Rossignol-Strick 1995:297). Additional evidence for a pluvial event between 55 and 52 ka was obtained by δD measurement from speleothems in the Soreq and Pequiin caves (McGarry et al. 2004:924).

Clumped isotope thermometry of carbonate from a speleothem from the Soreq Cave suggests an annual mean surface temperature of 15 ° at 56 ka (Affek et al. 2008). Hamra soils formed on the coastal plain between 40 to 12.5 ka, suggesting relatively warm and wet conditions (Singer 2007:209). These phases are interspersed with a thick bed of loess material (suggesting dry conditions) covering the coastal plain (Singer 2007). Similarly, dating of calcic palaesols in the Negev showed that wet periods occurred at ~37 ka and ~28 ka (Goodfriend and Magaritz 1988).

Overall, the climate during MIS 4 to 2 was cold and dry, with low tree cover and high levels of semi-desert and desert vegetation (Langgut et al. 2011).

3.3.2.2. France

In the broadest sense, during the period of this study in Europe, MIS 5 and MIS 7 and 8 have been the warmest periods in the study area and MIS 3/4 and MIS 6 were the coldest periods in the study area. There is a broad trend from warmest conditions in MIS 5e to coldest conditions in MIS 2 (Gamble 1992:83). The periods of MIS 4 and especially MIS 3 were characterised by unstable and unpredictable climate systems that would have led to the fragmentation of habitats and possibly the extinction of European Neanderthals (Finlayson and Carrión 2007). In contrast, MIS 5e had the warmest conditions for the last 730 ka (Gamble 1992). The study area of this thesis, while becoming considerably colder during the peak glacial conditions, would never have been subject to ice sheets or permafrost (Poser 1948:65).

The Perigord region in the late Pleistocene era was represented by 4 principal vegetational landscapes, in order of increasing temperature: 1) cold steppe, 2) cold meadowland, 3) cool parkland and 4) temperate forest (Paquereau 1970; summarised by Laville et al. 1980).

The cold steppe was an open landscape of dry-adapted grasses, some shrubs and occasional strands of pines. The arboreal component was not more than 5%. The cold meadowland, which reflects an increase in humidity over the cold steppe, was similar to steppe; however, the open ground was covered with herbaceous vegetation. While the arboreal component was no higher than the steppe, it contained birch and willow, as well as pine. The cool parkland landscape was characterised by an increase in the diversity of open spaces, with meadows alternating with fenland and riverbank communities and an increase to 15% of the arboreal component, including pine, birch, willow, hazel, alder and linden. The temperate forest landscape, reflecting conditions similar to the Perigord today, was more than 60% arboreal, containing all trees found in other ecotypes, as well as oak, beech, elm, maple and a thick forest undergrowth of ferns. The cold steppe and cold meadowland were principally

emplaced during glacials and temperate forests in interstadials and interglacials, while the cool parkland landscape represented an intermediate position between them (Laville et al. 1980:100).

Local Glacial Stage	MIS	Vegetation
Landos Interglacial		Open <i>Pinus</i> Forest
Cayres Stadial	9	Expansion of Steppe
Useel Interstadial	9d	Open Woodland and Herbaceous Grasses
Monteil Stadial	9b & 9c	Steppe
Amargiers Interstadial	9a	Forest
Charbonniers Stadial	8	Very arid Steppe
Bouchet 1 Interstadial	7e	Deciduous Forest
Belvezet Stadial	7d	Steppe with some shrub
Bouchet 2 Interstadial	7c	Montane/ <i>Pinus</i> Forest
Bonnefond Stadial	7b	Steppe
Bouchet 3 Interstadial	7a	Open Mixed oak Forest
Costaros Glacial	6	Steppe
Ribains Interglacial	5e	Dense Woodland
Stadial 1	5d	Steppe
St-Geneys 1 Interstadial	5c	Forest of Varying Types
Stadial 2	5b	Steppe
St-Geneys 2 Interstadial	5a	Forest of Varying Types
Pleniglacial	3	Steppe

Table 3.2 Correlation between Local Glacial Stages, MIS and Vegetation Based on the Palynology of Cores from Velay, Massif Central (Data: Reille et al. 1998; Reille and de Beaulieu 1990)

During MIS 6, the northern ice sheets were among the most extensive of the whole Pleistocene era and persisted much longer than those in MIS 2 (Van andel and Tzedakis 1996:485). Pollen assemblages from a range of locations throughout France suggested very low annual temperatures and very low annual precipitation, with cold steppic environments and/or tundra present in the north of France (Fauquette et al. 1999:9). Pollen from the Dôme Gascogne Seamount (core MD04-2845) showed a period of dominance of steppic plants in MIS 6, with low sea surface temperatures and large amounts of ice rafted debris (Sánchez Goñi et al. 2008), shown in Figure 3.6. Pollen from the Velay lakes in

the Massif Central showed that steppic plants dominated the region (Reille and de Beaulieu 1990; Reille et al. 1998).

In the early MIS 6, the climate in Europe would have been somewhat less severe, before becoming more extreme through MIS 6 (Van andel and Tzedakis 1996:485). Temperatures in south-central France would have had an annual temperature of 1.5 °C and precipitation of around 200 mm (Van andel and Tzedakis 1996). Europe was extensively glaciated, although the Massif Central was not covered by ice (Ehlers and Gibbard 2008).

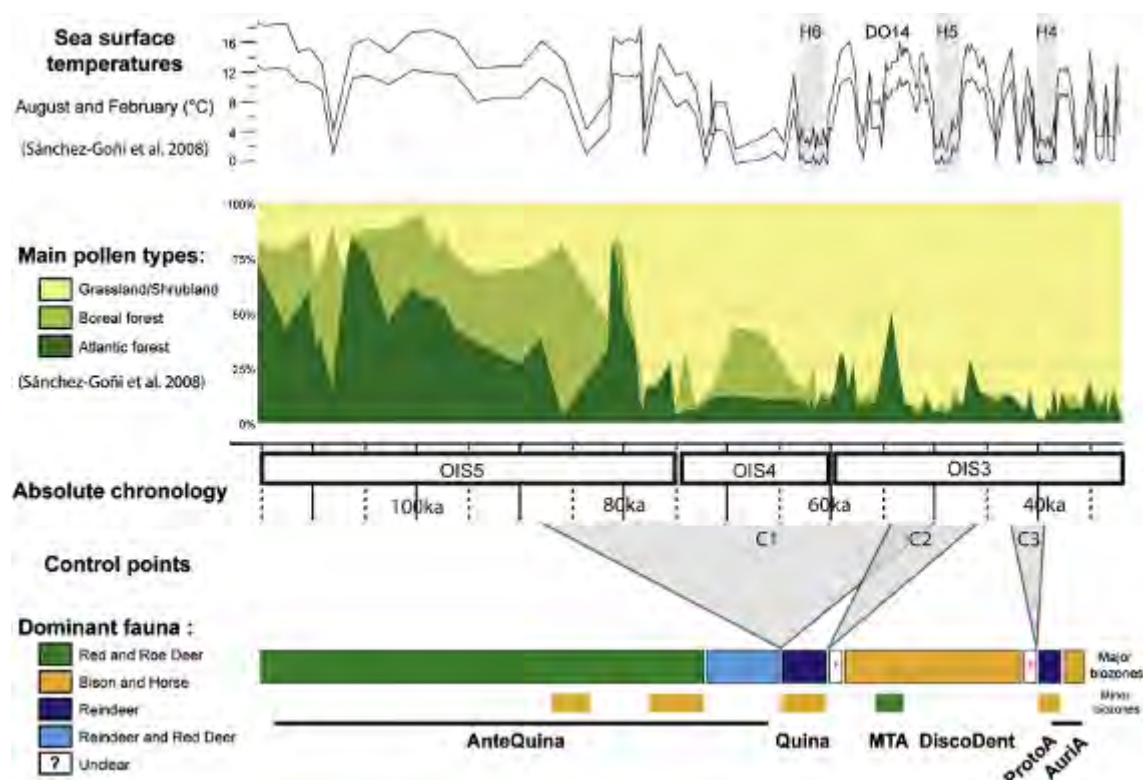


Figure 3.5 Correlation Between MIS 3 to 5, Sea Surface Temperatures, Main Pollen Types on the Western French Margin and Dominant Fauna (Discamps et al. 2011:2770)

The beginning of MIS5 (MIS5e) is characterised by an extremely rapid increase in temperature, with year round temperatures rising by 10 to 15 °C within a period of 5000 years. Overall, vegetation during MIS 5d alternated between expanding open vegetation and forest conditions (Van andel and Tzedakis 1996). The vegetation in France during 5e, based on pollen records, was

characterised by deciduous and mixed biomes (Fauquette et al. 1999:9). Isotherms during July during 5e in the study area would have been in the range of 18 to 20 °C (Zagwijn 1989:61). Only during the very earliest and latest portions of 5e would there have been any area of open vegetation in the study area, with the remainder comprising dense forest (Mellars 1996:11). The vegetation would have been dominated by conifers and Atlantic forest (Sánchez Goñi et al. 2008). During the cold periods of MIS 5 (d and b), the vegetation is dominated by cool conifer forest, taiga and cold steppe, and temperature and precipitation is low (Fauquette et al. 1999:9). In the Massif Central area, 5d and 5b were characterised by steppe vegetation, 5c and 5a by forest and 5e by dense woodland (Reille and de Beaulieu 1990; Reille et al. 1998). Red and roe deer are the dominant fauna in archaeological sites from the study area during MIS 5, with minor sporadic occurrences of bison and horse, shown in Figure 3.5 (Discamps et al. 2011:2770).

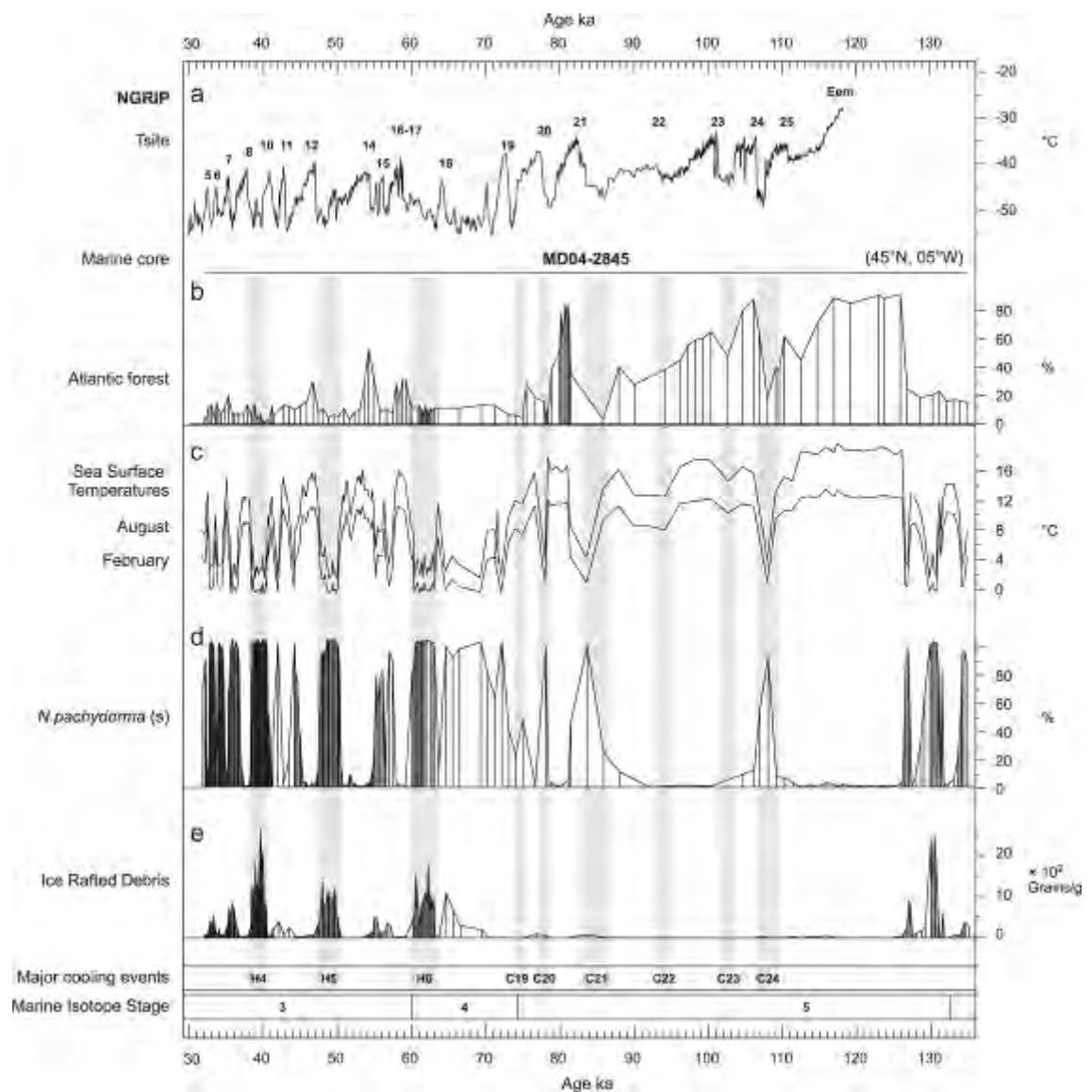


Figure 3.6 Comparison of a) Greenland Temperature Curve to Data from Core MC04–2845 (Bay of Biscay), b) Pollen Percentage Curve for Atlantic Forest, c) Interpreted Sea Surface Temperatures, d) Percentage of Polar Planktic Foraminifera *Neogloboquadrina pachydemata* and e) Ice Rafted Debris (Sánchez Goñi et al. 2008:1144)

MIS 4 in Europe was subject to rigorous climate conditions, with a decrease in surface temperatures by 3 to 4 °C, more than occurred at any period in MIS 5. Pollen from La Grande Pile and Les Echets suggest a steppic vegetation in the study area, in addition to some birch and pine (de Beaulieu and Reille 1984; Woillard 1978; Woillard and Mook 1982). Coring of pollen on the Dôme Gascogne Seamount also suggests steppe vegetation (Sánchez Goñi et al. 2010, 2008). Despite this, periods of rapid warming driven by Dansgaard-Oeschger cycles in this period led to the temporary development of open boreal and/or temperate forest in the study area (Fletcher et al. 2010). Fauna

from the archaeological site of Roc de Marsal from MIS 4 were dominated by red and roe deer, suggesting a wooded environment (Guérin et al. 2012:3080). The faunal assemblage of MIS 4 archaeological sites in the study area were dominated by reindeer and red deer (early MIS 4) and reindeer (late MIS 4), shown in Figure 3.5 (Discamps et al. 2011:2770).

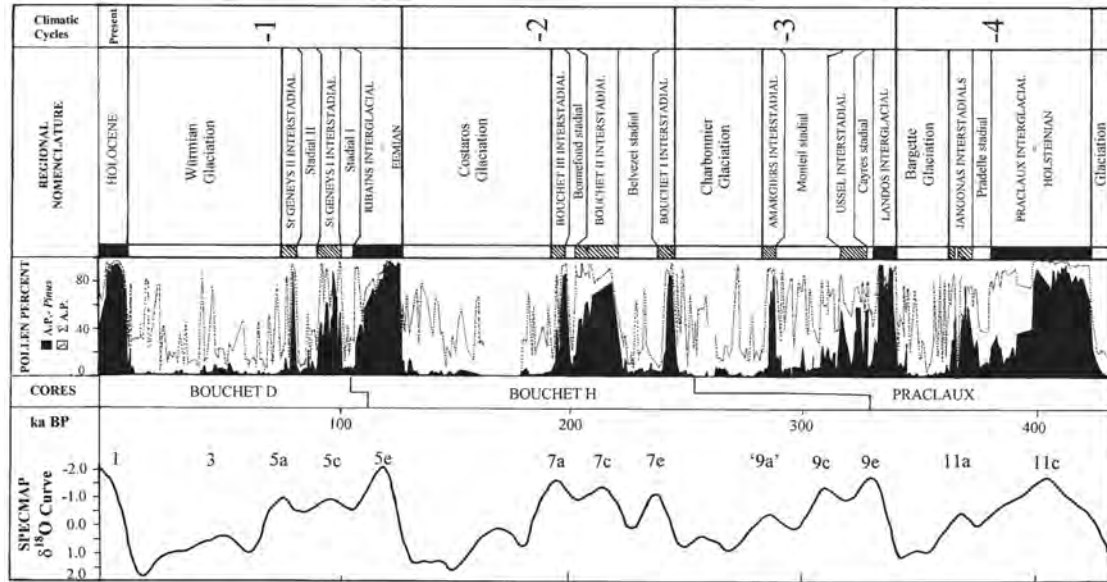


Figure 3.7 Comparison of Stages Identified from Velay Cores to the Oxygen Isotope Curve (Reille et al. 1998:1118)

The study area was subject to sporadic permafrost during early MIS 3 (Vliet-Lanoë 1989). Steppic vegetation dominated during this period, shown from the Velay cores in the Massif Central (Reille and de Beaulieu 1990; Reille et al. 1998) and the Dôme Gascogne Seamount (Sánchez Goñi et al. 2008). Despite this, periods of rapid warming driven by Dansgaard-Oeschger cycles in this period led to the temporary development of open boreal and/or temperate forest in the study area (Fletcher et al. 2010). Faunal assemblages in MIS 3 archaeological sites in France were dominated by bison and horse (Jaubert et al. 2011:5).

3.4. Geology

3.4.1. Geology of the Levant

3.4.1.1. Overview

The geology of Israel can be broken into 5 broad zones, described here as the Southern Igneous Province, the Southern-Central Clastic Province, the Central Carbonate Province, northern Volcanic Province and the coastal sediments, all of which are described in more detail below in sections 3.4.2.1 to 3.4.2.5.

The principal structural elements in the region include the Dead Sea Transform, the Syrian Arc Folds and the Suez Rift, as summarised by Garfunkel (1998) and shown in Figure 3.8. Some of these faults may still be active.

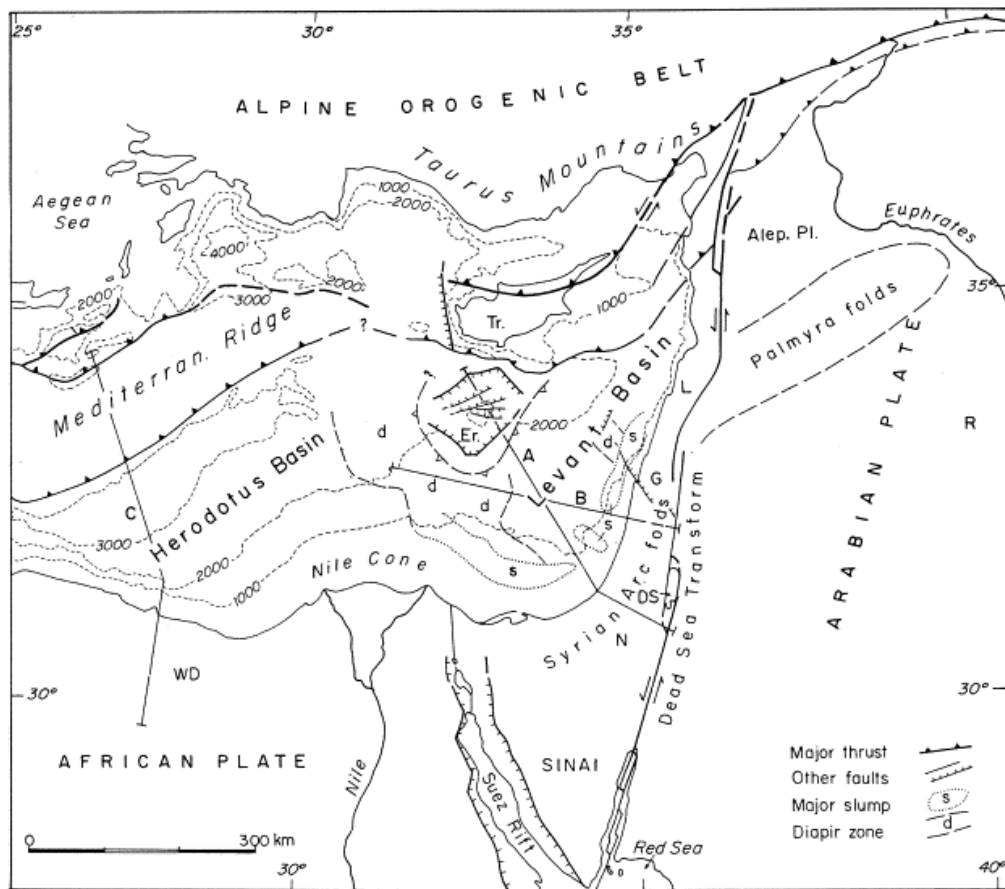


Figure 3.8 Principal Structural Elements of the Eastern Mediterranean Basin (Garfunkel 1998)

3.4.2. Major Geological Provinces

3.4.2.1. Southern Igneous Province

Precambrian plutonic, volcanic and sedimentary rocks characterised by low- to medium-pressure metamorphism are found in the Eilat region in the southern Negev (Shimron and Zwart 1970). The package was formed as part of the Arabo-Nubian Massif (Beyth 1987; Beyth et al. 1994). The units include politic-psammitic schists, orthogenesis and plutonic rock, with compositions from gabbro to granite (Kröner et al. 1990).

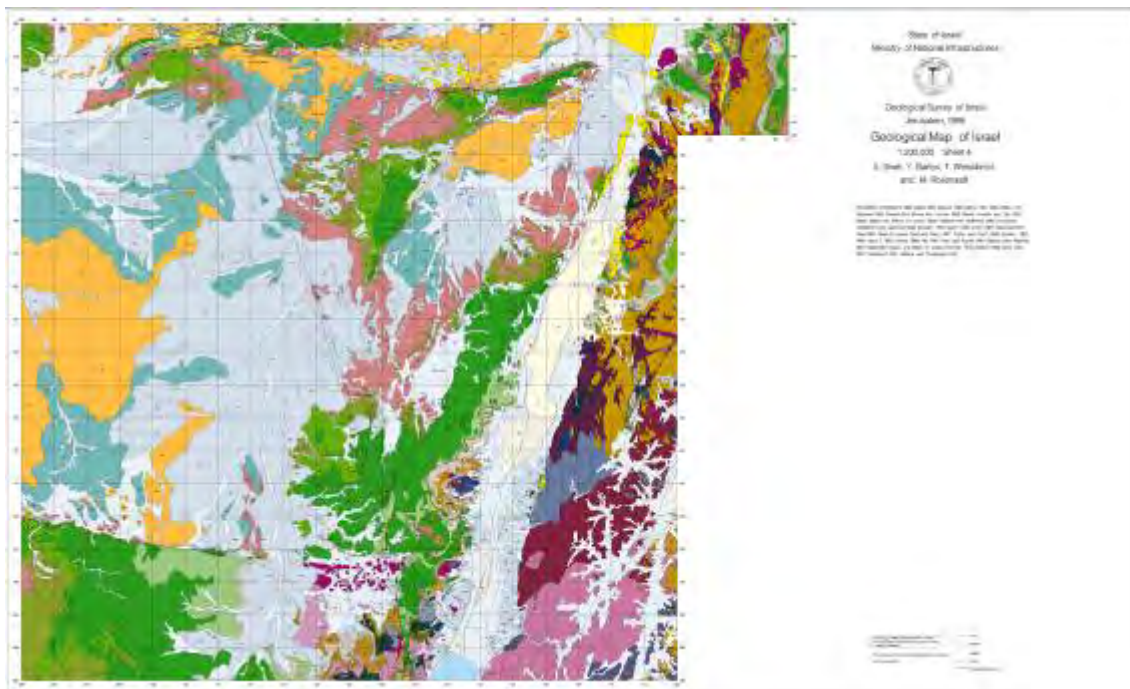


Figure 3.9 Geological Map of Southern Israel (Sneh, Bartov, Weissbrod and Rosenshaft 1998b)

There is significant increase in the initial strontium isotope ratio during the evolution of this package, from 0.703 to 0.709 (Bentor 1985). The older schists appear to contain detritus from a rising island arc rather than mature continental crust (Halpern and Tristan 1981). The younger alkali-rhyolites and their hypabyssal equivalents have undergone potassium metasomatism (Agron and Bentor 1981).

3.4.2.2. Southern-Central Clastic Province

Palaeozoic-recent continental and shallow marine clastic sediments, which rest unconformably on the Precambrian outcrop (described in 3.4.2.1) outcrop in limited areas in the Negev (Singer 2007:9). The ‘Nubian’ continental sediment component of this package becomes progressively more prominent in this unit distal to the underlying Precambrian package (Issar et al. 1972).

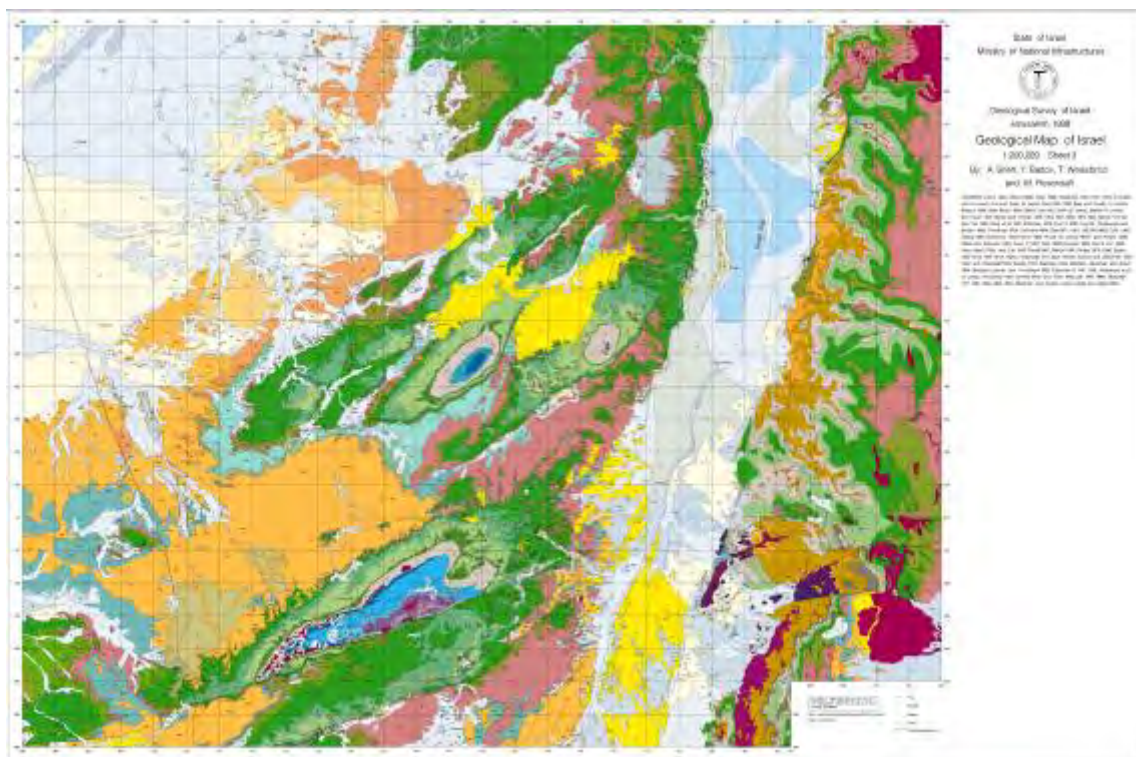


Figure 3.10 Geological Map of Southern-Central Israel (Sneh, Bartov, Weissbrod and Rosensaft 1998a)

3.4.2.3. Central Carbonate Province

The mountainous regions extending from the Hebron Hills in the northern Negev through the Judean Hills to the Samaria in the north, including the Carmel Range, is principally comprised of a large Cretaceous platform complex.

These sediments include dolomites, limestones, clastic sediments and some volcanics (Sass and Bein 1982).

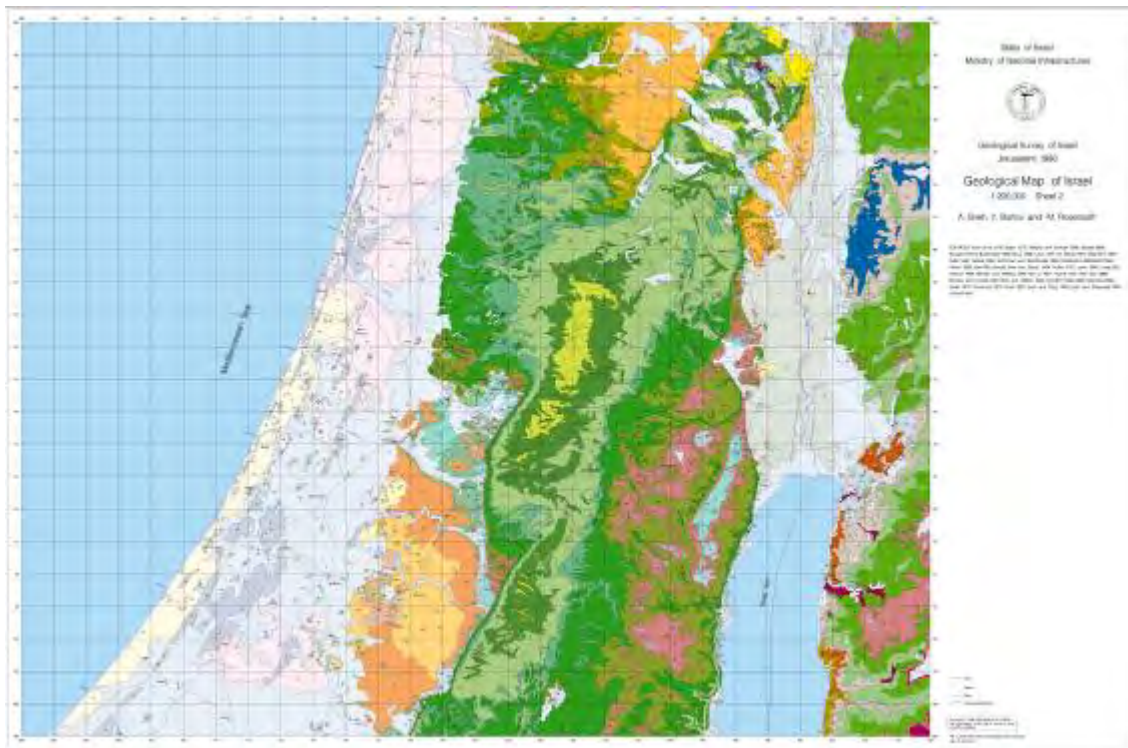


Figure 3.11 Geological Map of Northern Central Israel (Sneh, Bartov and Rosensaft 1998b)

The northern part of the Negev is dominated by north-east to south-west trending asymmetrical anticlines exposing Upper Cretaceous limestones, and dolomites and synclines exposing Senonian-Eocene chalks and marls. Cretaceous marine carbonates exposed in the Dead Sea graben have whole rock strontium isotope values of ~0.707 (Stein 2001). Within the synclines, some Neogene marine clastics are present (Avigour et al. 1990). The eastern boundary of the Negev region is bounded by the Araba valley, a 160 km long depression with a rift geometry inherited from the Neogene extension (Freund et al. 1968). In this valley is the Wadi Araba fault, the local manifestation of the major left-lateral strike slip Dead Sea fault zone (Garfunkel et al. 1981), which locally exhibits stick-slip behaviour (Klinger et al. 2000).

There are also Triassic and Jurassic epicontinental marine sediments outcropping in this area, which have far more significant exposures in the

mountain ranges in Lebanon and Hermon to the north (Singer 2007). Late Cretaceous basalts are also present in this area, probably relating to tectono-magmatic events associated with the break up of Gondwana (Stein and Hofmann 1992). These basalts have whole rock strontium isotope ratios in the range 0.70298 to 0.70322 (Stein and Hofmann 1992:197). Within the Negev, Tertiary volcanic rocks are relatively common, including dolerite dikes, sills and plugs and basal flows (Steinitz et al. 1978:335).

The mountains of Galilee, Carmel, Samaria, Judea and the northern Negev are composed of Cenomanian-Eocene limestones and dolomites interbedded with marls and chalks (Singer 2007). The eastern areas of the Galilee and Golan Heights (excepting those areas covered by volcanics, see section 3.4.2.4) are dominated by shallow platform facies, with the Golan being distal to the ramp slope area (Bachman and Hirsch 2006). The major folding in this region was emplaced in Lower to Middle Tertiary times, although may have begun in the Upper Cretaceous (Singer 2007).

The Carmel Range and proximal regions contain Late Triassic (Stein and Hofmann 1992) and Late Cretaceous volcanism (dated as 5 discrete events in the period of 97.1 ± 1.7 Ma to 82.0 ± 1.3 Ma, see Segev et al. 2002), principally represented by basic pyroclastics with occasional basalt lavas (Sass and Bein 1982). The basalts in the Carmel area have whole rock strontium isotope ratios in the range 0.70312 to 0.70360 (Stein and Hofmann 1992:197).

3.4.2.4. Northern Volcanic Province

The Golan Heights and Galilee region are dominated by material from the Levant Volcanic Province, an extensive volcanic field developed during the Cenozoic era on the north-western part of the Arabian Plate (Mor 1993). This volcanism is part of the Arabian volcanic field Harrat e-Shamah (Weinstein 2000). The Pliocene-Quaternary Bashan Group volcanic sequence in this area

is comprised principally of 5 groups of basalts (the Cover Basalt, the Eitar Basalt, the Ortal Formation and the Golan Formation, see Mor et al. 1997), each of which can be divided into several subsidiary members, which represent discrete periods of volcanic activity covering the period from the Lower Pliocene to the Holocene interbedded with some sedimentary units (Siedner and Horowitz 1974). The members of the Bashan Group, all of which are alkaline olivine basalts, are indistinguishable based on field or laboratory analysis and so their distinction is based on chronostratigraphy (Mor et al. 1997). The basalts are older in the south of the Golan region and younger to the north (Weinstein et al. 2006).

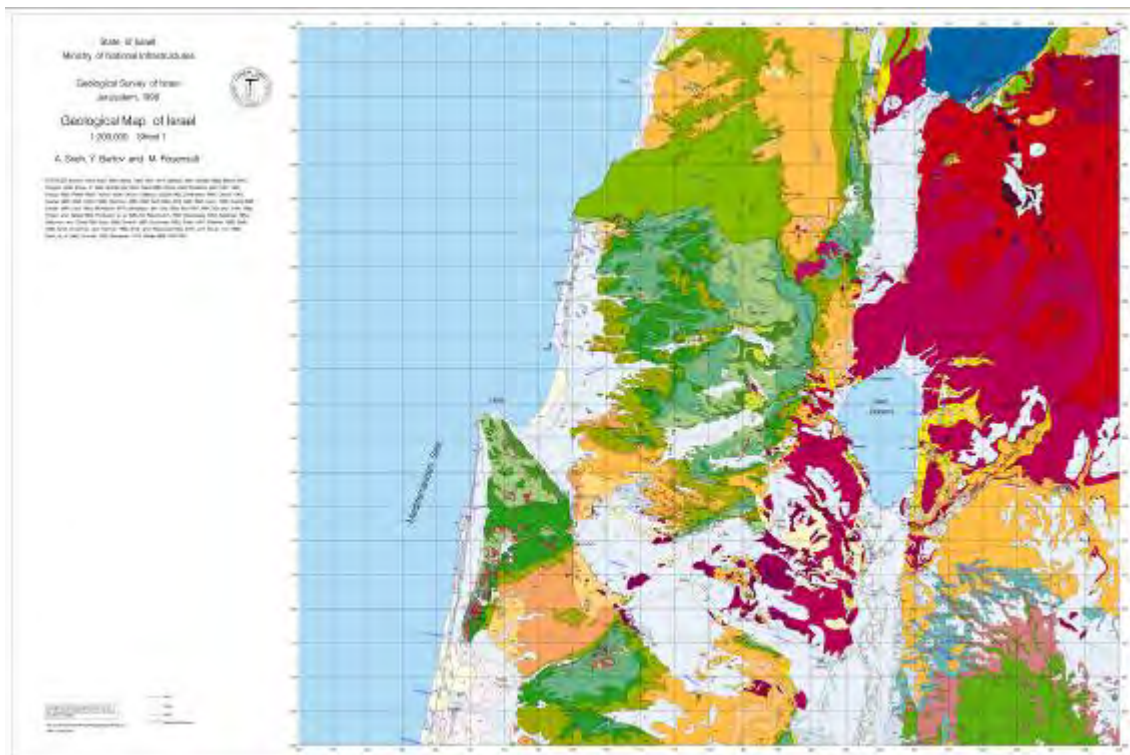


Figure 3.12 Geological Map of Northern Israel (Sneh, Bartov and Rosensaft 1998a)

This volcanism was accompanied by extensive tectonism, principally normal faulting, of the underlying Eocene carbonate units and Oligocene erosional plain to create the current topography (Matmon et al. 2003).

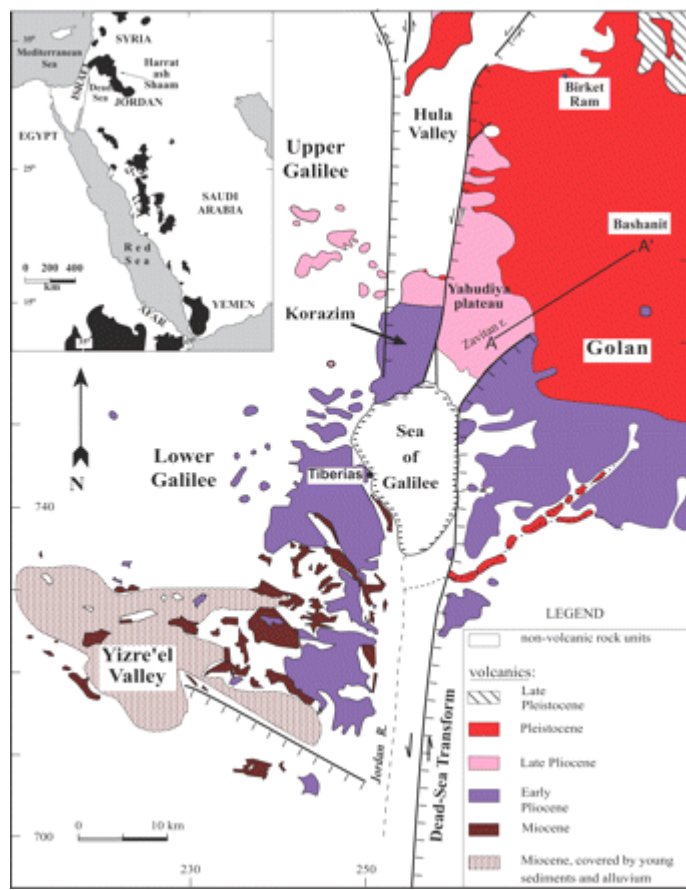


Figure 3.13 Age of Basalts in Northern Israel (Weinstein et al. 2006)

Strontium isotope ratios (whole rock, not bioavailable) for the basalts in this region are summarised by Weinstein et al. (2006:1029–1030). Alkali basalts and basanites from Golan and Galilee show the range 0.7031 to 0.7034 and Miocene basalts from the Yizre'el Valley, southern Galilee and southern Golan have the range 0.7031 to 0.7034 (Weinstein 2000:879). This result is supported by another study of basalts from Golan and Galilee that yielded whole rock strontium isotope values in the range 0.70308 to 0.70334 (Stein and Hofmann 1992:197). Lake Kinneret (Sea of Galilee) is located in the region, but has significant affinities structurally and in lake level to the Dead Sea (Hazan et al. 2005).

3.4.2.5. Dead Sea Rift Sediments

The Dead Sea and its precursors, Lake Lisan (~70 to 15 ka), Lake Samara (~135 to 75 ka), Mid to Late Pleistocene Lake Amora and the Sedom marine lagoon, preserved a complex stratigraphic record of lake level change and tectonics (Stein 2001). The sediments are overall part of the Dead Sea Group, comprising the Ze'elim, Lisan, Samra, Amora, Sedom and Hazeva formations (Waldmann et al. 2009). Sediments of the Sedom lagoon were deposited during the sporadic ingress of the Mediterranean into the Jordan-Arava Valley, creating a package of halite interbedded with gypsum, anhydrite, dolomite and minor silt, marl and clay to a thickness of 1500 to 2000 m (Stein 2001). Strontium isotope composition of these sediments are in the range of 0.7083 to 0.7087 in the halite and 0.7082 to 0.7083 in the dolomite, much lower than the composition of the seawater from which they precipitated (~0.709) (Stein et al. 2000). The Samara Formation was deposited in stream fan deltas, alluvial plains, beach ridges, extensive oolite beds, travertines and lacustrine beds composed of calcitic marls (Waldmann et al. 2009). The sediments in the Lissan Formation are a mosaic of alluvial, delta, beach and offshore sediments comprising clastic sediments and carbonates, with occasional halite and gypsum beds (Bartov et al. 2002).

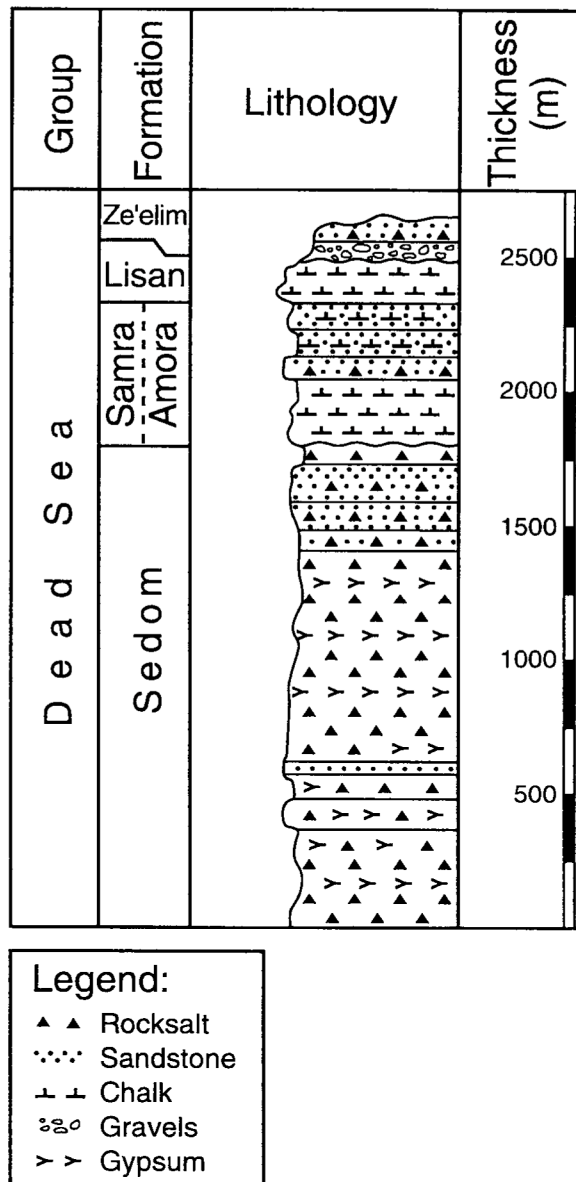


Figure 3.14 Generalised Stratigraphy of the Dead Sea Group (Stein 2001:272)

3.4.2.6. Coastal Sediments

The coastal plain of Israel is dominated by clastic sediments transported from the Nile delta by longshore processes. Sedimentation has been controlled by 6 marine transgressions and regressions since the Pliocene era, interfingering marine and continental material in a complex array (Singer 2007). This material extends from an elevation of up to 150 m abutting the mountains in the east, to a depth of approximately 100 m offshore (Singer 2007).

The most common features on the coastal plain are shore parallel aeolian sandstone ridges known as kurkar, which are cemented by calcium carbonate derived from calcareous skeletal fragments (Yaalon 1967). These are interspersed by reddish sandy-silty soil (known as hamra) formed after kurkar stabilisation by weathering and the accumulation of aeolian dust. A number of these features exist on land as well as offshore (e.g., Galili et al. 1988). These features have been the subject of extensive investigation (e.g., Frenchen et al. 2004; Galili et al. 2007; Gvirtzman et al. 1998; Issar 1968).

Symbol	Area	Geology
Q	North	Alluvium (Gravel; sand, clay) Quaternary
Q	Central	Alluvium (Gravel, sand, clay, loess) Quaternary
Q	Northern Negev	Alluvium (Gravel, sand, silt, loess) Quaternary
Q	Negev	Alluvium (Gravel, sand, silt) Quaternary
QG	General	Sand dunes (Gravel, sand, silt) Quaternary
LS	General	Landslide (Gravel, sand, silt) Quaternary
Tr	General	Trautertiae (Gravel, sand, silt) Quaternary
PD	General	Playa deposits (Clay, silt, sand) Quaternary
RF	General	Red sand and loam ("Hamm") (Clay, silt, sand) Quaternary
Ck	General	Calcareous dolomites ("Burkar") (Clay, silt, sand) Quaternary
Stm	North	Lisan Fm. (Argillite varves, sandstone, gravel, conglomerate, sandstone 25 m) Quaternary
Cm	Central	Lisan Fm. (Argillite varves, sandstone, gravel, conglomerate, sandstone, gypsum 32 m) Quaternary
Cf	Northern Negev	Lisan Fm. (Argillite varves, sandstone, gravel, conglomerate, sandstone, gypsum 45 m) Quaternary
SPM	General	Sarsa Fm. (Sandstone, argillite, sandstone, calcic limestone 25 m) Pliocene - Pleistocene
SPJ	General	Zeliba Fm. Limestone deposits (Jordan) (Marl, sandstone, gravel) Holocene - Quaternary
SPB	General	Besel Ya'akov Fm. (Sand, gravel, clay 5-10) Holocene
SPU	General	Gedot and Shishamar Ha'Yarden fms. Eirk el Ahsar and Hiddeiyi fms. (Conglomerates, sandstone, marlstone, chalk <238 m) Pliocene - Volcanic cone (Basalt, basaltic / flows and volcanoclastic) Quaternary
General	General	Wa'ara Basalt (Basalt, basaltic / flows and volcanoclastic) Quaternary
General	General	Golan Basalt Raqqad Basalt (Basalt, basaltic / flows) Quaternary
General	General	Yarmouk Basalt Naharayim Basalt (Basalt, basaltic / flows) Quaternary
General	General	Yarba Basalt (Basalt, basaltic / flows) Quaternary
General	General	Beaufort Basalt (Basalt, basaltic / flows) Quaternary
PQC	General	Conglomerate units, undifferentiated (Basalt, basaltic / flows, limestone and volcanoclastic) Pliocene - Pliocene
NGF	General	Ar Rish Gravel (Jordan) (Conglomeratic, sandy conglomeratic) Miocene
General	General	Volcanic rock units, undifferentiated (Conglomeratic, sandy conglomeratic) Miocene - Pliocene
D	General	Dalton Basalt (Basalt / flows and pyroclastics) Pliocene
D	North	Bira and Gesher fms. Kardasi Fm. (Marl, oyster limestone, gypsum, conglomerate, sandstone 200 m) Pliocene
D	Central	Bira and Gesher fms. Pleket Fm. (Marl, argillite, sandstone 20 m) Pliocene
D	Northern Negev	Pleket Fm. and Shera Fm. (Upper Mbr.) Mazar Fm. (Conglomerate, sandstone, sand 25 m) Pliocene
D	General	Rhytidic Quartz Porphyry (Sandstone, pebbly sandstone, conglomerate, marlstone, dolomite, limestone) Pliocene
D	General	Yafe Fm. (Marl, Marl) Pliocene
D	General	Sefom and Amora fm. (Silt, sulphite, gypsum, dolomite, sand), sandstone, marlstone, conglomerates 2100 m) Miocene
D	North	Intrusive rocks (Dolomite, gabbro) Miocene
D	Northern Negev	Intrusive and pyroclastic rocks (Basalt). Miocene
D	Negev	Intrusive rocks (Basalt / dykes) Miocene
D	North	Lower Basalt and part of Intermediate Basalt (Basalt, basaltic / flows, intrusion and volcanoclastic) Miocene
D	Central	Lower Basalt and Intermediate Basalt (Basalt, basaltic / flows, intrusion and volcanoclastic) Miocene
D	North	Ziqlag Fm. marlstone carbonates units in Lebanon (Limestone, argillite, dolomitic 1 m) Miocene
D	Central	Ziqlag Fm. (Limestone 50 m) Miocene
D	Northern Negev	Ziqlag and Faith Fms. (Limestone 42 m) Miocene
D	North	Hordos Fm. and Umm Sabae Conglomerate Kefar Giladi Fm. (Sandstone, marlstone, conglomerate, breccia 340 m) Miocene
D	Central	Hordos Fm. and Umm Sabae Conglomerate (Sandstone, marlstone, conglomerate, limestone 230 m) Miocene
D	Northern Negev	Hazeva Fm. Dusa Conglomerate (Jordan) (Sandstone, marlstone, conglomerate, breccia, sand 2800 m) Miocene
D	Negev	Hazeva Fm. Dusa Conglomerate (Jordan) (Conglomerate, sandstone, marlstone, breccia 80 m) Miocene
QI	North	Lakhish Fm. Sella Fm. (Limestone 145 m) Oligocene
QI	Central	Lakhish Fm (Limestone 40 m) Oligocene
S	North	Eocene (Chalk, marlstone) Oligocene
S	Central	Eocene (Jordan) (Limestone, chalk, shew) Oligocene
S	Northern Negev	Umm Rijam Chert-Limestone Fm. (Jordan) (Limestone, chalk, shew) Eocene
S	Negev	Umm Rijam Chert-Limestone Fm. (Jordan) (Limestone, chalk, chert) Eocene
LS	North	Bet Guvrin Fm., Biq Fm. (Chalk, marl 60 m) Upper Eocene
LS	Central	Bet Guvrin Fm. (Chalk, marl 50 m) Upper Eocene
LS	Northern Negev	Bet Guvrin Fm., Qesot and Biq Agur Fm. (Chalk, marl, limestone 240 m) Upper Eocene
LS	Negev	Qesot Fm. (Marl, chalk 22 m) Upper Eocene
AVD	Central	Avedat Group (Chalk, limestone, marl) Lower - Middle Eocene
AVD	Northern Negev	Avedat Group (Chalk, limestone, marl 344 m) Lower - Middle Eocene
AVD	Negev	Avedat Group (Chalk, limestone, marl 314 m) Lower - Middle Eocene
BDK	North	Bar Kokhba Fm. (Limestone 250 m) Middle Eocene
BDK	Central	Bar Kokhba Fm. (Limestone 30 m) Middle Eocene
MRD	North	Marotha Fm. (Chalk 200 m) Middle Eocene
MRD	Central	Marotha Fm. (Chalk 100 m) Middle Eocene
MRD	Northern Negev	Marotha Fm. (Chalk 100 m) Middle Eocene
MRD	North	Tinoret Fm. Meron and Yavne'el Fms. (Limestone, chalk, chert 380 m) Lower - Middle Eocene
MRD	Central	Tinoret Fm. Meron and Yavne'el Fms. (Limestone, chalk, chert 350 m) Lower - Middle Eocene

Figure 3.15 Key to Israeli Geological Maps (1) as Shown in Figure 3.9 to Figure 3.12

at	North	Timna Fm. (Marl, sand, dolomite, chalk, chert 380 m) Lower - Middle Eocene
et	Central	Timna Fm. (Marl and Yav'el Fms) (Limestone, chalk, chert 350 m) Lower - Middle Eocene
ETM	Northern Negev	Nizzana, Horshat, Matred and Nahal Yosef fms. (Limestone, chalk, chert 215 m) Lower - Middle Eocene
ETM	Negev	Nizzana, Horshat and Matred fms. (Chalk, limestone, chert 135 m) Lower - Middle Eocene
ES	Negev	Mor Fm. (Chalk, chert 195 m) Lower - Middle Eocene
ES	North	Adulam Fm. (Chalk, chert 300 m) Lower - Middle Eocene
ES	Central	Adulam Fm. (Chalk, chert 150 m) Lower - Middle Eocene
ES	Northern Negev	Adulam Fm. Mar Fm. (Chalk, chert 150 m) Lower - Middle Eocene
GM	Central	Carmelian - Turonian - Serronian (Jordan) (Limestone, chalk, marl, chert) Lower - Middle Eocene
GM	Negev	Carmelian - Turonian - Serronian (Jordan) (Limestone, dolomite, chalk, marl) Lower - Middle Eocene
LS	General	Volcanic rock units, undifferentiated (Biotite, gabbro, olivine-biotite / pyroxolite and basalt) Upper Cretaceous
ED	North	Mount Scopus Group (Chalk, marl 380 m) Serronian - Paleocene
SD	Central	Mount Scopus Group (Chalk, marl, clay 280 m) Serronian - Paleocene
MP	North	Maastrichtian - Paleocene (Jordan) (Chalk, marl) Serronian - Paleocene
MP	Central	Maastrichtian - Paleocene (Jordan) (Chalk, marl) Serronian - Paleocene
MP	Northern Negev	Ghoreb and Taglye fms. Mar-Mor Fm. (Jordan) (Chalk, marl, clay) Maastrichtian - Paleocene
TT	Negev	Ghoreb and Taglye fms. Mar-Mor Fm. (Jordan) (Chalk, marl 130 m) Maastrichtian - Paleocene
MZ	General	Hatzorit Fm. ("Mortified Zone") (Chalk, marl 130 m) Mortification Hatzorit in Alluvial rocks
PS	Central	Taglye Fm. (Mar, clay, chalk 150 m) Paleocene
PS	Northern Negev	Taglye Fm. (Mar, clay, chalk 63 m) Paleocene
PS	Central	Ghoreb Fm. (Chalk 55 m) Maastrichtian
PS	Northern Negev	Ghoreb Fm. (Chalk 80 m) Maastrichtian
DS	North	Campagne (Jordan) (Chalk, pebbles, sherr) Eocene
DS	Central	Mishash Fm. (Chalk, chalk, phosphatic, limestone 35 m) Campagne
DS	Northern Negev	Mishash Fm. Amman Shk. Lst. And Al Bika Phosphate Fm. (Jordan) (Chalk, chalk, phosphatic, pebbles, marl, limestone, dolomite, conglomerates 25) Campagne
DS	Negev	Mishash Fm. Amman Shk. Lst. And Al Bika Phosphate Fm. (Jordan) (Chalk, chalk, phosphatic, pebbles, marl, limestone, dolomite 100 m) Campagne
DS	Northern Negev	Mendah Fm. Wadi Umm Ghadram (Jordan) (Chalk, marl, chert, sandstone 82 m) Campagne - Campanian
DS	Central	Mendah Fm. (Chalk, chert 164 m) Campagne - Campanian
DS	Negev	Mendah Fm. Wadi Umm Ghadram Fm. (Jordan) (Chalk, chert, sandstone, dolomite 110 m) Campagne - Campanian
DP	Northern Negev	Zibar Fm. (Limestone, dolomite, marl, Chalk) Campanian
DP	Negev	Zibar Fm. (Limestone, dolomite, marl 70 m) Campanian
De	General	Turonian - Santonian (Jordan) (Limestone, marl, chert) Campanian
De	General	Ciocanian - Turonian In Lebanon (Limestone, dolomite) Campanian
De	North	Bita Fm. (Limestone, marl, dolomite) Tortonian
De	Central	Bita Fm. Dervish, Shiva and Neer fms. (Limestone, marl, dolomite 271 m) Tortonian
De	Northern Negev	Bita Fm. Dervish, Shiva and Neer fms. and Gereft fms. Shush' and Wadi es Sir fms.* (Limestone, dolomite, marl, conglomerate, sandstone 271 m) Tortonian
De	Negev	Shua and Gereft fms. Shush' and Wadi es Sir fms. (Jordan) (Marl, limestone, sandstone 276 m) Tortonian
De	Central	Albian - Ciocanian (Jordan) (Limestone, dolomite, chalk, marl) Tortonian
De	Northern Negev	Wendaris Fm. Tamar Fm. (Dolomite 100) Ciocanian
De	Negev	Tamar Fm. (Dolomite 31 m) Ciocanian
De	North	Dele Hamra Fm. Idly Chalk, Bet Umm Limestone, Khurbet Chalk and Jezrely Chalk (Limestone, dolomite, marl, chalk, chert 520 m) Ciocanian
De	Central	Bet Meir, Moab, Ammudim and Kefar Shaul fms. Bi Yorq'at am, Zalt and Avnon fms. (Limestone, dolomite, marl, Chalk) Ciocanian
De	Northern Negev	Bi Yorq'at am, Zalt and Avnon fms. Bi Yorq'at am, Moab, Ammudim and Kefar Shaul fms. (Limestone, dolomite, marl, chalk, chert 210 m) Ciocanian
De	Negev	Bi Yorq'at am, Zalt and Avnon fms. (Limestone, dolomite, chalk, marl, chert 124 m) Ciocanian
De	North	Vagur Fm. Kammon Fm. (Dolomite 197 m) Albian-Ciocanian
De	Central	Girat Yekarim, Soreq and Kedonim fms. Heyon Fm. (Limestone, dolomite, marl, chalk, chert 227 m) Albian-Ciocanian
De	Northern Negev	Heyon Fm. Girat Yekarim, Soreq and Kedonim fms. (Limestone, dolomite, marl, chalk, chert 160 m) Albian-Ciocanian
De	Negev	Heyon Fm. (Limestone, dolomite, marl, chalk, sandstone 44 m) Albian-Ciocanian
Itz	North	Nabi Sa'ad, Ein el Asoud, Hidra, Rama and Kefira fms. (Limestone, chalk, marl, sandstone 430 m) Lower Cretaceous
Itz	Central	Nabi Sa'ad, Ein el Asoud, Hidra, Rama and Kefira fms. (Limestone, marl, chalk, sandstone 670 m) Lower Cretaceous
IK	North	Kurnub Group (Sandstone 85 m) Lower Cretaceous
IK	Central	Kurnub Group (Sandstone, silt) Tithonian 120 m) Lower Cretaceous
IK	Northern Negev	Kurnub Group (Sandstone, pebbly sandstone, marl, mudstone, clay/limestone, dolomite, conglomerates 408 m) Lower Cretaceous
IK	Negev	Kurnub Group (Sandstone, marl, clay, pebbly sandstone, conglomerates 240 m) Lower Cretaceous
IK	North	Intrusions and volcaniclastic rocks (Dikes, intercalated) Miocene
IK	Northern Negev	Intrusions and volcaniclastic rocks (Andesitic and trachytic dykes, scoria, quartz scoria, pumice) Miocene
IK	Negev	Intrusions and volcaniclastic rocks (Basalt) Miocene
IK	North	Basalt flows (Basalt, basanite) Lower Cretaceous
IK	Central	Tuyasitic Volcanics (Basalt flows and volcanicash) Lower Cretaceous
IK	Northern Negev	Basalt flows and volcanicash (Basalt, basanite, tephrite, nepheline) Lower Cretaceous
IK	Negev	Basalt flows (Basalt, basanite, tephrite, nephelite) Lower Cretaceous

Figure 3.16 Key to Israeli Geological Maps (2) as shown in Figure 3.09 to Figure 3.12

31	General	Upper Jurassic (limestone 195 m); Lower Cretaceous
32	North	Ba'er Sheva and Bileam fm. (Limestone, sand 65 m) Upper Archaic
33	Northern Negev	Ba'er Sheva and Bileam fm. (Limestone, sand 160 m) Upper Archaic
34	North	Kidron Fm. (Clay, limestone, dolomite 155 m) Upper Archaic
35	Northern Negev	Kidron Fm. (Clay, limestone, dolomite 30 m) Upper Archaic
36	North	Herman Fm. (Limestone, dolomite 423 m) Middle Archaic
37	Central	Middle Jurassic (Jordan) (Limestone, sand 70m) Middle Archaic
38	Northern Negev	Makhtesh, Zohar and Malmor fm. (Sandstone, limestone, sand, clay) Middle Archaic
39	Northern Negev	Immar Fm. (Sandstone, clay 340 m) Lower Archaic
40	Negev	Immar Fm. (Sandstone, clay 120 m) Lower Archaic
41	Northern Negev	Mishmar and Aradim fms. (Dolomite, limestone, clay, sandstone 90 m) Lower Archaic
42	Negev	Mishmar and Aradim fms. (Dolomite, limestone, clay, sandstone 21 m) Lower Archaic
43	Central	Upper Triassic (Jordan) (Sandstone, limestone, clay, gypsum) Lower Archaic
44	Northern Negev	Makhtesh Fm. (Gypsum, dolomite, limestone, clay 202 m) Middle Triassic
45	Northern Negev	Saharatzin Fm. (Gypsum, clay, sand, dolomite, sandstone, gypsum 178 m) Middle Triassic
46	Negev	Saharatzin Fm. (Gypsum, clay, sand, dolomite, sandstone, gypsum 117 m) Middle Triassic
47	Northern Negev	Gevatim Fm. (Sandstone, clay, quartzic sandstone, limestone, gypsum 130 m) Lower Triassic
48	Negev	Gevatim Fm. (Sandstone, limestone, siltstone, clay 68 m) Lower Triassic
49	General	Ru'el Fm. (Dolomite, sand, limestone +22 m) Lower Triassic
50	General	Peculiar and Triassic (Jordan) (Sandstone; silicate, sandstone) Lower-Triassic
51	Northern Negev	Dab Sandstone Fm. (Jordan) (Sandstone; silicate, sandstone) Ordovician
52	Negev	Dab Sandstone Fm. (Jordan) (Sandstone, pebbly sandstone, dolomite) Ordovician
53	Central	Um el-Barid Sandstone Fm. (Jordan) (Sandstone, sandstone) Cambrian
54	Northern Negev	Um el-Barid Sandstone Fm., with Sallit Fm. where Burj Fm. Almon (Jordan) (Sandstone, sandstone) Cambrian
55	Negev	Um el-Barid Sandstone Fm., with Sallit Archaic Sandstone Fm. where Burj Dolomite-Shale Fm. absent * (Sandstone, sandstone) Cambrian
56	General	Sheheret and Nealinim fms (Pebby sandstone, sandstone, dolomite, limestone, silicate, mudstone, conglomerate 165 m) Cambrian
57	General	Ammud Sheheret and Thusa fms. (Pebby sandstone, sandstone, conglomerate, mudstone, dolomite, limestone, 135 m) Cambrian
58	Central	Burj Dolomite-Shale Fm (Jordan) (Sandstone, dolomite, mudstone) Cambrian
59	Northern Negev	Sallit Archaic Sandstone Fm. and Burj Dolomite-Shale Fm (Jordan) (Sandstone, dolomite, mudstone) Cambrian
60	General	Yam Suf Group (Sandstone, pebbly sandstone, conglomerate, mudstone, dolomite, limestone) Cambrian
61	General	Elat Conglomerate (Sandstone, pebbly sandstone, conglomerate, mudstone, dolomite, limestone) Precambrian
62	General	Tumus Granite, Shalemite Granite, Amram Granite Porphyry (Sandstone, pebbly sandstone, conglomerate, mudstone, dolomite, limestone) Precambrian
63	General	Elat Granite, Roted Granite Porphyry Tumus Granite Porphyry (Sandstone, pebbly sandstone, conglomerate, mudstone, dolomite, limestone) Precambrian
64	General	Syenite, Monzonite and other intermediate rocks (Sandstone, pebbly sandstone, conglomerate, mudstone, dolomite, limestone) Precambrian
65	General	Gabbro, diorite, and other basic rocks (Sandstone, pebbly sandstone, conglomerate, mudstone, dolomite, limestone) Precambrian
66	General	Roted Quartz Diorite (Sandstone, pebbly sandstone, conglomerate, mudstone, dolomite, limestone) Precambrian
67	General	Amphibolite (Sandstone, pebbly sandstone, conglomerate, mudstone, dolomite, limestone) Precambrian
68	General	Granitic Gneiss (Sandstone, pebbly sandstone, conglomerate, mudstone, dolomite, limestone) Precambrian
69	General	Taba Gneiss (Sandstone, pebbly sandstone, conglomerate, mudstone, dolomite, limestone) Precambrian
70	General	Roted and Elat Schist, Gneiss and Migmatite (Sandstone, pebbly sandstone, conglomerate, mudstone, dolomite, limestone, mica-schist) Precambrian
71	General	Akzair Volcanics (Jordan) (Sandstone, pebbly sandstone, conglomerate, mudstone, dolomite, limestone, mica-schist) Precambrian
72	General	Meffaragat Conglomerate (Jordan) (Sandstone, pebbly sandstone, conglomerate, mudstone, dolomite, limestone) Precambrian
73	General	Fman Granite (Jordan) (Sandstone, pebbly sandstone, conglomerate, mudstone, dolomite, limestone) Precambrian
74	General	Qensil Diorite (Jordan) (Sandstone, pebbly sandstone, conglomerate, mudstone, dolomite, limestone) Precambrian
75	General	Sarmad Conglomerate Fm. (incl. Hayala Fm.) (Sandstone, pebbly sandstone, conglomerate, mudstone, dolomite, limestone) Precambrian
76	General	Sarmadaya Microgranite (Sandstone, pebbly sandstone, conglomerate, mudstone, dolomite, limestone) Precambrian
77	General	Yatum Granite (Sandstone, pebbly sandstone, conglomerate, mudstone, dolomite, limestone) Precambrian
78	General	Masdar Monogranite (Jordan) (Sandstone, pebbly sandstone, conglomerate, mudstone, dolomite, limestone, biotite-schist) Precambrian
79	General	Ganivim Volcanics (Jordan) (Sandstone, pebbly sandstone, conglomerate, mudstone, dolomite, limestone, mica-schist) Precambrian
80	General	Erf Porphyry (Jordan) (Sandstone, pebbly sandstone, conglomerate, mudstone, dolomite, limestone) Precambrian
81	General	Thaur Gabbro (Sandstone, pebbly sandstone, conglomerate, mudstone, dolomite, limestone) Precambrian
82	General	Rachaf Bimimetic Quartz Diorite (Sandstone, pebbly sandstone, conglomerate, mudstone, dolomite, limestone) Precambrian
83	General	Roman Granodiorite (Sandstone, pebbly sandstone, conglomerate, mudstone, dolomite, limestone) Precambrian
84	General	Darba Tazalik (Sandstone, pebbly sandstone, conglomerate, mudstone, dolomite, limestone) Precambrian
85	General	Ruhma Flysch Granofels (Jordan) (Sandstone, pebbly sandstone, conglomerate, mudstone, dolomite, limestone) Precambrian
86	General	Tomb Metamorphics (Sandstone, pebbly sandstone, conglomerate, mudstone, dolomite, limestone) Precambrian
87	Negev	Alta Saqa'a Schist (Chalc., chert 105 m) Precambrian
88	Negev	Dukhaya Hornblende (Chalc., chert 105 m) Precambrian
89	General	Alta Barqa Metasediments Biminal Gneiss (Sandstone, pebbly sandstone, conglomerate, mudstone, dolomite, limestone) Precambrian

Figure 3.17 Key to Israeli Geological Maps (3) as Shown in Figure 3.09 to Figure 3.12

3.4.3. Quaternary Landscape Evolution

Pleistocene tectonic activity in the Dead Sea and Lake Kinneret environments has been extensively documented (e.g., Garfunkel et al. 1981; Neev and Emery 1967). This movement is accommodated through strike slip and normal faulting and demonstrates movement in the order of 0.7 to 1.0 cm/a in the Pliocene-Pleistocene era (Garfunkel et al. 1981). Recent tectonic activity is recorded for the Jordan Valley (via an offset staircase) (Ambraseys 1975) and the Hula Basin (Horowitz 1973) and suggested for Galilee (Picard 1943).

The western Carmel Range has been subject to an uplift of no more than 35 to 40 m during approximately the last 600 ka at a maximum rate of 58 to 67 mm/ka (Zviely et al. 2009:243). In contrast, the adjacent Carmel coastal plain has a maximum uplift rate of less than 48 mm/ka (Galili et al. 2007:2553). As no known fault is present between these 2 areas, the variation in motion between these regions may be accommodated by tilting (Zviely et al. 2009). Other authors claimed that the coastal belt of Israel had uplifted appreciably in some place since 6ka, which may be part of a regional post-Pliocene upwarp and associated faulting involving all continental material east of the Mediterranean (Neev et al. 1987).

3.4.4. Soils in the Levant

Israel has a diverse range of soil types, summarised in detail by Dan and Koyumdjisky (1963), Singer (2007) and Shapiro (2006). This diversity is the result of great variability in climate, relief and geology over small distances (Horowitz 1979). The Israeli soil classification system differs from the World Reference Base for Soil Resources and there is much overlap between categories (Krasilnikov et al. 2009). This thesis retains the Israeli terminology as outlined in Singer (2007).

The coastal plain is dominated by red sandy soils, formed on a diverse range of sandy sediments and dark clay soils (vertisols) formed on fine grained alluvial sediments (Singer 2007). The coastal plain also features beach ridges lithified by calcium carbonate known locally as kurkar (Porat et al. 2004) and previously thought to relate to sea level high stands (Horowitz 1979), but more recently shown to develop independent of sea level (Sivan and Porat 2004).

The Negev is dominated by aeolian soils and reg soils (gibber in the Australian context; e.g., Bourman and Milnes 1985) demonstrating the clear dominance of aeolian processes in this region (Singer 2007). The mountain range complex, including the Judean, Samarian and Galilee regions, are dominated by *Terra rossa*, pale rendzina, brown rendzina and calcimorphic brown forest soils (Singer 2007). The formation of *Terra rossa* in Israel remains contentious, with some authors claiming they were forming under current climatic conditions (Reifenberg 1947; Yaalon et al. 1966), others claiming they were relicts formed during more humid conditions (Ravikovitch 1992; Shapiro 2006), while others considered them as palaeosols (Horowitz 1979). The disturbance of these soils can be used to interpret the degree and timing of anthropogenic influence (Tsatskin and Gandler 2002). The Yizre'el and Jordan valleys are dominated by vertisols and calcareous serozem (Singer 2007).

Eastern Galilee and the Golan Heights have soils formed from basalts and pyroclastic deposits dominated by calcareous basaltic dark brown vertisols, basaltic proto-vertisol, basaltic brown Mediterranean clay and red Mediterranean tuffic silt loam (Singer 2007). Weathering rates vary greatly from very slow for basaltic rock to very fast for pyroclastics, leading to a significant difference in soil production (Dan and Singer 1973). The thickest soil cover is present in the south, where the basalts are older (Dan and Singer 1973).

3.4.5. Geology of Southern France

3.4.5.1. Overview

The geology of the study area in southern France is dominated by 4 principal geological provinces: the Massif Central, the sedimentary rocks of the Aquitaine Basin, the sedimentary rocks exposed in the Rhône Valley and the coastal sediments. The principal geological provinces and structural components are illustrated in Figure 3.18.

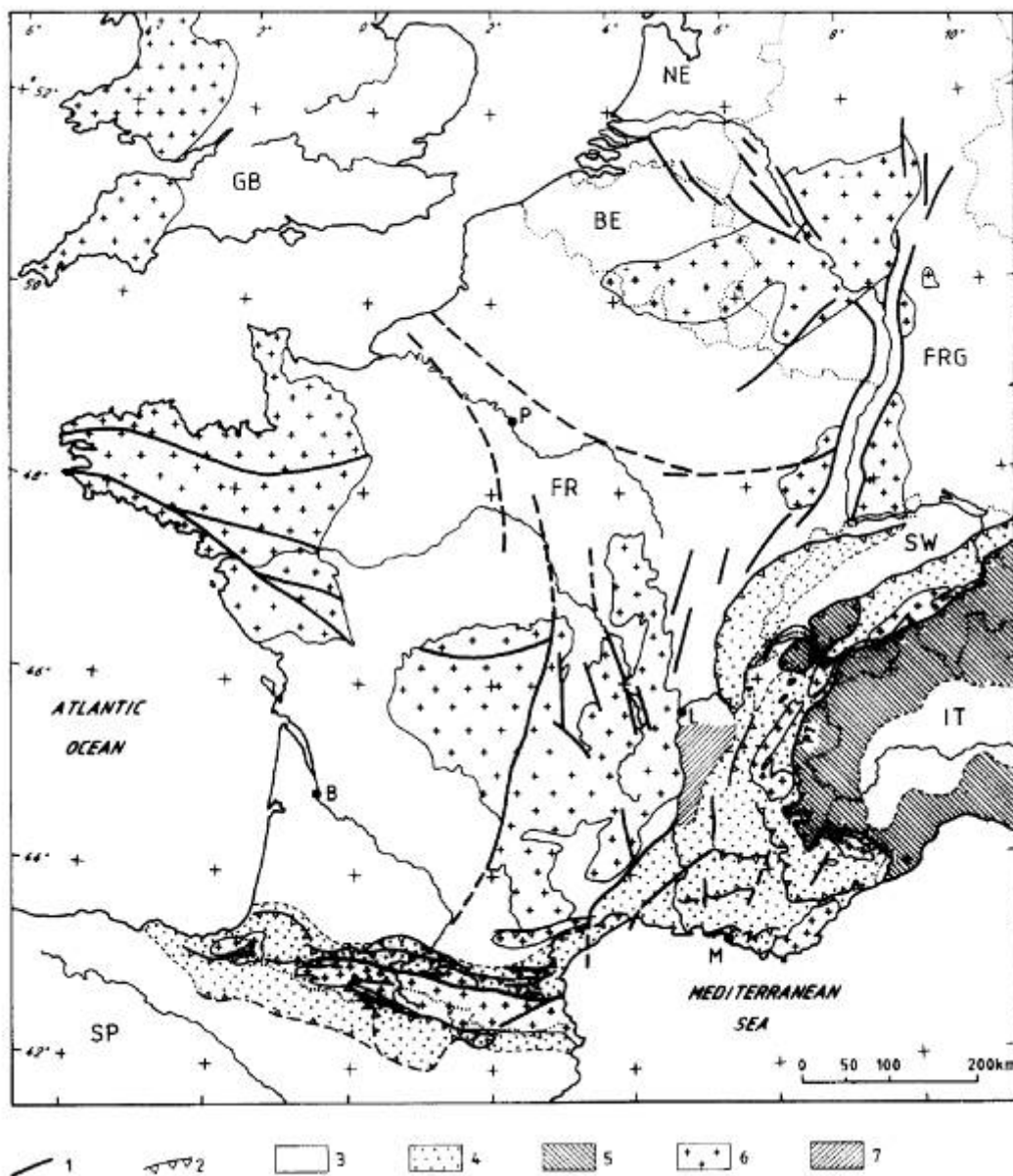


Figure 3.18 Geological Provinces and Structural Elements of France (Blès and Gros 1991:266). 1 = Faults (Normal and Transcurrent), 2 = Principal Thrusts, 3 = Unfolded Post-Palaeozoic Terranes, 4 = Pyrenean and Alpine Folding, 5 = Internal Alps and Apennines, 6 = Old Massifs (Hercynian and Older), 7= Rhône Valley, PT = Pennine Thrust, B = Bordeaux, L = Lyon, P = Paris and M = Marseille

3.4.6. Major Geological Provinces

3.4.6.1. *Massif Central*

The Massif Central formed during the Variscan orogeny, and is almost 2-thirds comprised of granites (Duthou et al. 1984). The metamorphic basement

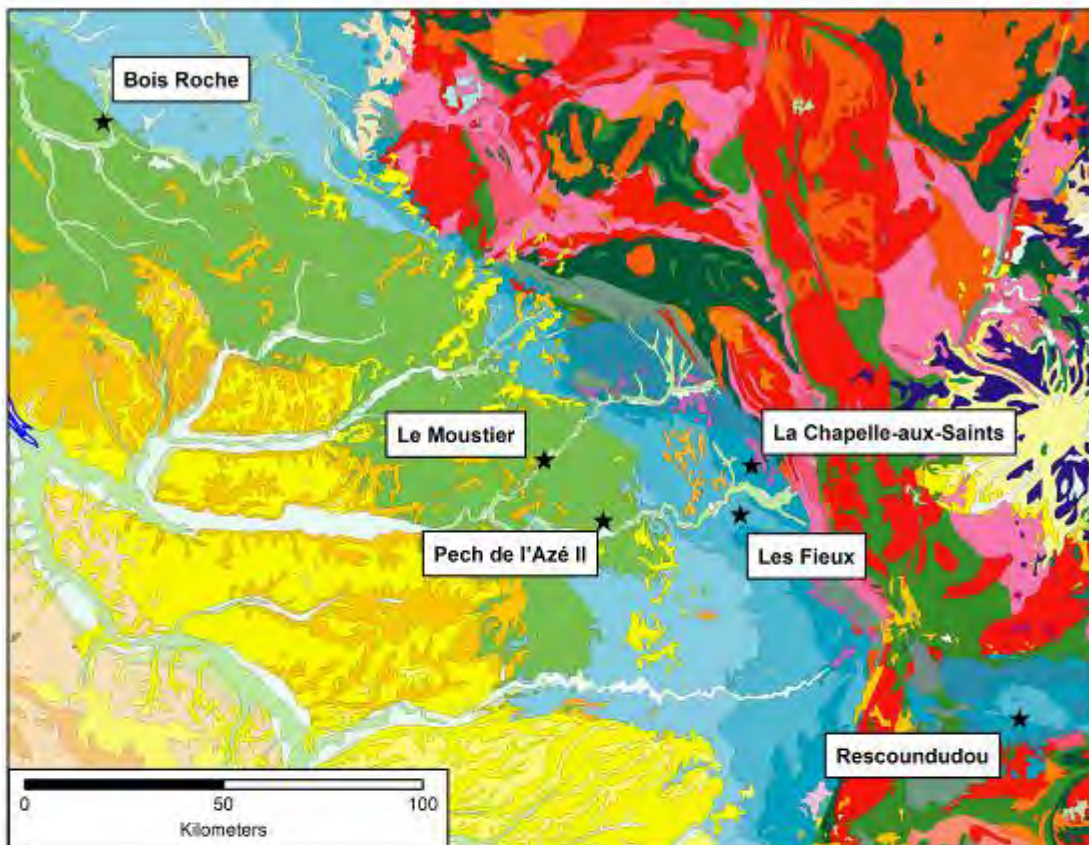
material can be divided into 3 principal zones: 1) the Arverne zone in the north-east, with Devono-Dinantian strata overlying the metamorphic basement, which has been the subject of 2 metamorphic events, 2) the Limousin zone in the west, made up of metamorphic rocks somewhat similar to the Arverne zone and 3) the Cévenole zone in the south characterised by lower grade and younger metamorphism than the other zones (Duthou et al. 1984). Granites in the Massif Central have been emplaced both prior to and following the metamorphic events and are comprised principally of monzogranites/granodiorites and leucogranites, with some Na granites (Duthou et al. 1984). Strontium isotope ratios of the granites are in the range of 0.7033 to 0.7299 (Duthou et al. 1984).

The emplacement of the granites occurred in the Upper Proterozoic era, the Devonian Caledonian orogeny (affecting the Averne zone and the Ruténo-Limousin zone) and the in the Hercynian era (affecting the Cévennes belt) (Pomeral 1980). The area has also been affected by Mio-Pliocene and Quaternary volcanism dominated by alkali basalt flows (Pomeral 1980).

The original Precambrian sequence of the Arverne zone has rhythmically deposited shales and sandstones with volcanic intercalations, which have been principally metamorphosed to the amphibolite facies, although some green schist and granulite facies are present (Pomeral 1980). The Ruténo-Limousin zone is comprised mostly of greywacke detrital beds interbedded with Ordovician and Silurian volcanics (Pomeral 1980). In the Cévennes belt, Cambrian-Ordovician sediments dominate.

The Massif Central was subjected to compression during the Late Hercynian era (late Carboniferous period) leading to the creation of a fracture system, faulting and some small coal-bearing basins in areas of local extension (Blès et al. 1989:81). During the Permian-Triassic era, the region was subject to extension, with thick, lateral basins forming the Autun, Blanzy-Le Creusot, Aumance, Brive, Rodez, St Affrique and Lodeve regions (Blès et al. 1989:88). It

was then significantly planated before being inundated by the ocean during the Jurassic era, leading to the formation of (now poorly preserved) carbonate sediments (Pomeral 1980). The sedimentary and crystalline rocks were sub-aerially exposed and weathered during the Palaeocene and the Eocene eras, before faulting occurred in the Oligocene era, leading to the formation of several deep troughs (Pomeral 1980). Alkali basalt volcanism began in the Miocene era and continued into the Quaternary era, creating much of the present relief (Pomeral 1980).



Geological Units

Holocene unconsolidated sediment	Middle-Upper Triassic sandstone, marl, dolomite, clay
Middle/Upper Pleistocene clay, sand, gravel	Triassic carbonate
Upper Pleistocene/Holocene sand, gravel	Pennian andesitic basalts, splites, basic tuffs
Upper Pleistocene/Holocene basalts, hawaiites, benmoreite, nephrite	Stephanian sediments and igneous
Upper Pleistocene/Holocene trachytes, mugearites, phonolites, pyroclastics	Stephanian/Pennian igneous
Lower Pleistocene sediments	Namurian/Westphalian sediments and metamorphics
Pleistocene sediments	Stephanian granites
Pliocene sediments	Upper Visean/Namurian mazzogranites, granodiorites
Pliocene/Lower Pleistocene gravel, clay, sand	Namurian/Westphalian/Stephanian mazzogranites, granodiorites
Pliocene/Lower Pleistocene basalts, hawaiites, benmoreite, nephrite	Tournaisian/Lower Visean mazzogranites, granodiorites
Pliocene/Lower Pleistocene trachytes, mugearites, phonolites, pyroclastics	Dinantian/Namurian/Westphalian mazzogranites, granodiorites
Miocene sandstones, conglomerates, marls	Middle-Upper Devonian igneous
Miocene/Pliocene sediments	Silurian/Lower Devonian basalts, aprites, dolerites
Oligocene sandstones	Ordovician metamorphics
Oligocene/Miocene basalts, hawaiites, nephrite	Ordovician/Silurian igneous, metamorphic, sedimentary
Oligocene/Miocene mugearites, trachytes, phonolites	Upper Ordovician/Silurian igneous, metamorphic
Middle-Upper Eocene calcareous sands, sandstones, clays	Cambrian sandstones, conglomerates, shales
Middle Eocene/Oligocene carbonate	Cambrian/Ordovician sandstone, conglomerates, arkose sandstones
Paleocene/Lower Eocene clay, marl, limestone, sand	Cambrian/Ordovician metamorphics
Paleocene/Eocene basalts, hawaiites, nephrite	Cambrian-Lower Middle Ordovician metamorphics
Eocene/Oligocene sediments	Upper Silurian/Cambrian igneous
Upper Cretaceous fility clay	Upper Silurian/Cambrian metamorphics
Upper Jurassic carbonate	Bioheric/Cambrian metamorphics
Middle Jurassic carbonate	Bioheric/Cambrian/Ordovician metamorphics
Lower Jurassic carbonate	Rochecourt impactite
Jurassic carbonate	Unknown Age ultrabasalts, peridotites, serpentinites

**Figure 3.19 Geological Units Surrounding the French Archaeological Sites in this Study
(Data: BRGM 2012)**

3.4.6.2. Aquitaine Basin

The Aquitaine Basin is a large Mesozoic and Cenozoic sedimentary basin occupying the south-west quadrant of France. The basin is roughly triangular in shape, with the Bay of Biscay forming the base, the Col de Nauroze the apex and the Pyrenees and the Central Highlands the arms (Laborde 1961). The basin is underlain by extensively folded Hercynian basement comprised of crystalline Precambrian material, as well as Cambrian to Carboniferous sediments with intrusive and volcanic units and Stephano-Permian units of sandstones and shales (Curnelle et al. 1982). The basin reaches a maximum depth of 5 km, contains a sequence of approximately 10 km and joins the Paris basin to the north and the Languedoc basin to the west (Pomeral 1980).

The basin has undergone 2 periods of accelerated subsidence during the Triassic and Late Jurassic to Early Cretaceous periods (Brunet 1984). Many aspects of the Upper Jurassic to Lower Cretaceous depositional history of the Aquitaine Basin are common to the other Mesozoic North Atlantic rift basins (Hiscott et al. 1990). During the Triassic era, continental (particularly alluvial fans and braided streams) and evaporitic sediments dominated, with associated basic magmatism (Curnelle et al. 1982).

The Jurassic-Cretaceous period was dominated by carbonate sedimentation in a variety of facies with considerable lateral and vertical variability, the distribution of which was controlled principally by sea level changes (Pomeral 1980). During the Jurassic era, the basin was a large lagoonal platform, which fragmented during the late Jurassic/early Cretaceous eras when the interplay between the Iberian and European tectonic plates led to the formation of several sub-basins (Curnelle et al. 1982). The most important of these are the Parentis sub-basin to the north and the North Pyrenean Basin complex to the south, which were separated by the east-west trending Central Aquitaine platform (Curnelle et al. 1982). The North Pyrenean Basin, in particular, was the focus of much crustal stretch, rifting, wrenching and orogenic compression

(Bourrouilh et al. 1995). These basins were the subject of rifting during the Albian era, before compression initiated in the eastern Pyrenees in the Cenomanian era (Desegaulx et al. 1991). The late Jurassic and early Cretaceous tectonics also led to the movement of the salt deposited in the Triassic evaporates with significant structural effects on the basin (Curnelle et al. 1982).

Basal Cretaceous strata in the northern part of the basin contain gypsum (often stromatolitic), finely bedded black dolomitic marlstone and limestone, representing depositional environments such as hypersaline tidal flats, lagoon, sabkha and brackish water environments (El Albani et al. 2004). This sequence shows variability in clay mineralogy and distribution (El Albani et al. 2005).

The Pyrenean orogeny developed as a thrust system on top of the European plate in the Tertiary era, leading to the formation of the Aquitaine retro-foreland basin (Vergés et al. 2002). These periodic inundations of the basin ceased in the Tertiary era, where tectonic activity related to the uplift of the Massif Central led to the orientation of anticlinal valleys and the establishment of current drainage patterns (Burke 1995).

3.4.6.3. *Rhône Valley*

The Rhône Valley in south-east France is contained in a graben, which has accumulated sediments of almost 10 km thickness (Prodehl et al. 1995). This region is located on the boundary between the West European plate and the westward thrusting of the Alpine domain (Blès and Gros 1991). The region was subjected to east-west compression at the end of the Miocene era, which did not continue into the Quaternary era (Blès and Gros 1991).

Ludian and Oligocene argillaceous, detrital and evaporitic sediments were deposited in this graben, followed by Middle and Late Miocene marine marls, sandstones and continental conglomerates (Bles and Gros 1991). After the end Miocene compression ceased, marine clays and lacustrine marls were deposited in the Pliocene era, followed by fluviatile sandy and pebbly deposits and then Quaternary loess, silt and pebbles preserved in valley terraces (Bles and Gros 1991:267).

3.4.6.4. Coastal Sediments

The coastal sediments stretching from Biarritz in the south, to the mouth of the Gironde estuary in the north, are a complex interplay of facies relating to the sea level regressions and transgressions since the Miocene era, as well as the control of shallow bedrock in some areas of the region (e.g., Menier et al. 2011).

During the Lower Miocene era, the sea began to transgress to the east and north, creating a complex interplay of marine, littoral and lacustrine facies that were deposited from Landes to the west. During this period, a minor regression led to a large lake formed in the area of Condom, forming extensive carbonate lacustrine sediments. During the Upper Miocene era, a large scale regression led to the significant exposure of these sediments and the beginning of the current fluvial patterns. During the Quaternary era, a large delta developed in the Landes area, dominated by clastic sediments overlain by the windblown ‘Landes sands’ (Pomeral 1980).

The modern Atlantic coastline has a high-energy wave regime, with winter storm waves in excess of 8 m. This, in combination with an insufficient supply of sand, has led to severe erosion of 1 to 10 m/a (Allen and Posamentier 1993). The Gironde estuary, which drains the Dordogne and Garonne rivers, has a large wave and tide dominated delta, which is gradually infilling the MIS 2 to 4 glacial lowstand incised valley (Allen and Posamentier 1993). At present, no

fluvial sand and mud derived from the Gironde catchment makes it to the ocean; instead, they remain in the fluvial system (Allen and Posamentier 1993). This system has extensive overbank systems, reflected as marshes.

Offshore is the Aquitaine continental slope, extended by the marginal Landes Plateau dipping gently to the west (Bourillet et al. 2006). The Gironde palaeo-channel does not extend far offshore (Lericolais et al. 2001), while the Pliocene palaeovalleys of the Landes system reach the head of the Cap-Ferret Canyon system (Bourillet et al. 2006).

3.4.7. Soils in Southern France

The French have a sophisticated soil classification system that is very similar to the Worldwide Reference Base for Soil Resources, although the categories are less well defined in the French system (Krasilnikov et al. 2009). This research applies the Worldwide Reference Base for Soil Resources to all French material (European Soils Bureau Network 2005:28–33).

The coastal plain seaward fringe, extending in a thin band from the France-Spain border to the mouth of the Gironde River is dominated by dystric regosols (European Commission and the European Soil Bureau Network 2004). The wedge of coastal sediments extending from Bayonne in the south to Damazan in the east to the mouth of the Gironde River in the north is dominated by haplic pozols, with minor umbric podzols, dystric regosols and haplic arenosols (European Commission and the European Soil Bureau Network 2004). The dominant mineralogy of the topsoils in this area has the ratio of 1/1 clay (such as kaolinite and serpentine) and quartz (European Commission and the European Soil Bureau Network 2004).

Soils of the Aquitaine Basin sediments in the Dordogne region are mainly calcareous cambisols, dystric cambisols, gleyic luvisols, rendzic leptosols and haplic luvisols, with less common chromic cambisols, chromic luvisols, haplic arenosols, calcareous fluvisols and calcareous leptosols (European Commission and the European Soil Bureau Network 2004). Topsoils in this area are dominated by 2/1 (such as illite or attapulgite) and 2/1/1 non-swelling clays (such as chlorite) and 1/1 clays plus quartz, as well as minor occurrences of 1/1 clays plus oxides and hydroxide clay minerals and swell and non-swelling 2/1 clay minerals (European Commission and the European Soil Bureau Network 2004).

Soils in the Massif Central are dominated by dystric cambisols, with contributions from dystric andosols and haplic leptosols (European Commission and the European Soil Bureau Network 2004). The topsoils in this region are dominated by andic (pyroclastic) minerals, 1/1 clays plus quartz and 2/1 and 2/1/1 non-swelling clays (European Commission and the European Soil Bureau Network 2004).

In the Rhône Valley, chromic cambisols, calcareous cambisols, eutric cambisols, haplic luvisols, chromic luvisols, calcareous leptosols, eutric leptosols and rendzic leptosols are present (European Commission and the European Soil Bureau Network 2004). The topsoil in this area is dominated by swelling and non-swelling 2/1 clays and 2/1 and 2/1/1 non-swelling clays (European Commission and the European Soil Bureau Network 2004).

3.5. Previous Strontium Isotope Studies in Israel

Several investigations of the strontium isotope composition of the study area have been undertaken.

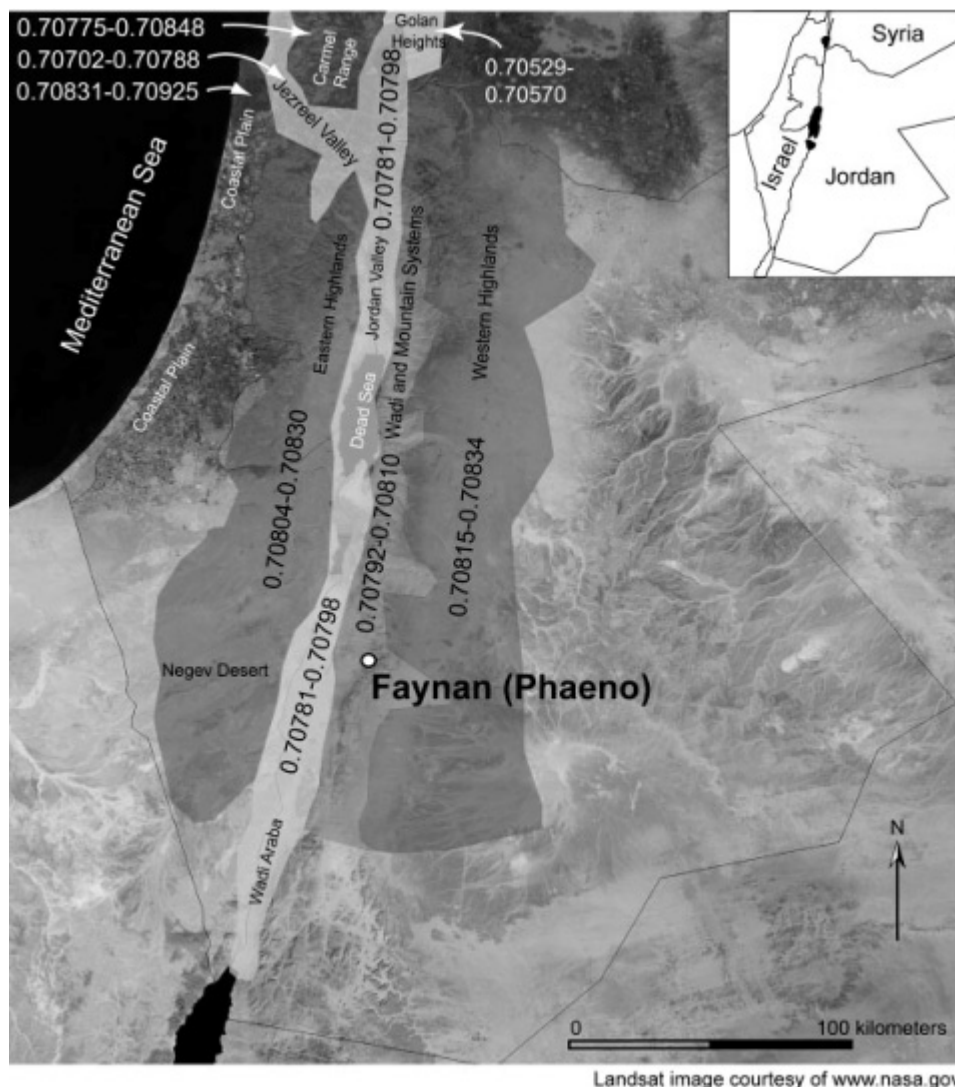


Figure 3.20 Bioavailable Strontium Map of Israel and Jordan (Perry et al. 2009)

Perry et al. (2009) investigated the strontium isotope composition of a rodent tooth and several land snail shell samples recovered from excavations of Wadi Fidan in Jordan to establish the local value for their study of mining labourers. They established a range of 0.70793 to 0.70814, consistent with the range established for the 'Wadi and Mountain systems' in their review of other strontium studies in the region (Perry et al. 2009:430).

They also collated the previous work of Shewan (2004) and Perry et al. (2008) as a bioavailable strontium map for Israel and Jordan (Figure 3.20). The map is based on material collected from archaeological sites as well as modern fauna and flora. The map shows several distinct isotope provinces, with Eastern and

Western Highlands (immediately adjacent to the Jordan Rift Valley) having similar values with a composite range of 0.70804 to 0.7834. The Jordan Valley and the Jezreel Valley forms a separate province, with a range of 0.70781 to 70798 (Jordan) and 0.70702 to 0.70788 (Jezreel), suggesting the alluvial fill in this area is derived from a source other than the adjacent mountain ranges. The author's 'Wadi and Mountain systems' strontium isotope province on the eastern side of the Jordan Valley has a value of 0.70792 to 0.70810. This intermediate value of this province between them adjacent zones suggests that this may be an artefact of fauna migrating between them. The Golan Heights have a value of 0.70529 to 0.70571. A small area of coastal plain has a value of 0.70831 to 0.70925 and the Carmel Range has a value of 0.70775 to 0.70848. Perry et al. (2008) showed more detail of the bioavailable strontium values used for the mapping in this study, reproduced as Figure 3.21 in this text.

Site	UTM E	UTM N	Sample Material	Corrected $^{87}\text{Sr}/^{86}\text{Sr}$ ¹	Region ²	Cluster
Pella	745900	3594500	Rodent enamel	0.707967	JR	1
Pella	745900	3594500	Rodent enamel	0.707924	JR	1
Ya'amoun	773900	3588300	Rodent enamel	0.708336	HM	3
Ya'amoun	773900	3588300	Rodent enamel	0.708250	HM	3
Bedlyeh	756100	3574300	Rodent enamel	0.708012	HM	1
Hesban	766000	3521900	Rodent enamel	0.708185	HM	3
Qasr Bshir	783000	3470900	Rodent enamel	0.708284	HM	3
Rujm Beni Yasser	774200	3459500	Rodent enamel	0.708152	HM	3
Lejjun	773100	3459700	Rodent enamel	0.707535	N/A	4
Lejjun	773100	3459700	Rodent enamel	0.708059	HM	1
Khirbet edh-Dharih	758400	3422200	Rodent enamel	0.707806	HM	2
Khirbet edh-Dharih	758400	3422200	Rodent enamel	0.707862	HM	2
Wadi Fidan	729600	3395000	Rodent enamel	0.708053	JR	1
Da'Janiya	765025	3383020	Rodent enamel	0.708035	HM	1
Khirbet Nawafleh	739000	3357400	Rodent enamel	0.708089	HM	1
Khirbet Nawafleh	739000	3357400	Rodent enamel	0.708102	HM	1
Petra	734600	3357900	Rodent enamel	0.707711	N/A	5
Petra	734600	3357900	Rodent enamel	0.707991	JR	1
Aila/Aqaba	693900	3268400	Rodent enamel	0.707821	JR	2
Aila/Aqaba	693900	3268400	Rodent enamel	0.707852	JR	3
Red Sea ³			Seawater	0.7090		
Red Sea ³			Seawater	0.7091		
Dead Sea ⁴			Seawater	0.708030		

¹ All isotopic ratios reported relative to NBS-987 $^{87}\text{Sr}/^{86}\text{Sr} = 0.710270$.

² HM = Highlands and mountains east of the rift valley; JR = Wadi Araba-Jordan Rift.

³ Starinsky et al. (1980).

⁴ Stein et al. (1997), average of 27 samples.

Figure 3.21 Bioavailable Strontium Isotope Values from Western Jordan (Perry et al. 2008:539)

Rosenthal et al. (1989) undertook a study of the strontium isotope composition of gastropod shells in the Dead Sea Rift area of the Jordan Valley. As part of this study, they summarised the strontium isotope composition of water sources in the Jordan Valley, shown in Figure 3.22. These water values show some agreement with those reported from fauna and flora by Perry et al. (2009), with the most significant offset evident in the basalt values. Stein et al. (1997) sampled water and sediments around the Dead Sea and obtained values in the range of 0.708026 to 0.708075.

Chemical and isotopic composition of the three water sources in the Jordan Valley (meq/l)

Water source	Ca	Sr ($\times 10^3$)	Ba ^d ($\times 10^3$)	Sr/Ca ($\times 10^3$)	Ba/Ca ($\times 10^3$)	$^{87}\text{Sr}/^{86}\text{Sr}$	TDS (mg/l)
carbonate ^a	≈ 4	4–8	0.2–0.6	1–2.5	0.05–0.15	0.7070–0.7080	400
basaltic ^b	≈ 1.2	4–6	0.4–0.7	3–5	0.30–0.50	0.7045–0.7050	250
Rift brines ^c	≈ 17	≈ 220	1.5–2.0	9–12	0.10–0.15	0.7080	>10,000

^aThis study.

^bSandler (1981) and this study.

^cStarinsky (1974); Starinsky and Bielski (1981).

^dSandler et al., 1986.

Figure 3.22: Chemical and Isotopic Composition of the Three Water Sources in the Jordan Valley (Rosenthal et al. 1989:243)

Spiro et al. (2011) investigated the strontium isotope composition of the common snail *Melanopsis* sp. from the Lower to Middle Pleistocene Hula Basin sediments exposed in the archaeological site of Gesher Benot Ya'apov to the north of the Sea of Galilee. The $^{87}\text{Sr}/^{86}\text{Sr}$ values of these snails range from 0.7046–0.7079, varying consistently with time through the Lower-Middle Pleistocene. This change is based on switching of the principal aquifer used as a water source by the snails from the Hermon Jurassic aquifer during colder periods to the Golan basaltic aquifer during warmer periods (Spiro et al. 2011). This changes demonstrates the complexity of the bioavailable strontium isotope system over extended periods.

Shewan (2004) undertook a programme of bioavailable mapping throughout Israel using modern faunal bones and grass samples, which were compared to Natufian human enamel and bones, as well as faunal bones from the sites of El

Wad, Kebara, Ain Mallaba, Hayonim Cave, Wadi Hammeh 27 and Azrag 18. The results from the archaeological sites showed limited mobility and that humans and fauna had similar strontium isotope values. Grasses from the coastal plain near El Wad showed a value of 0.70940, while the Judea, Samaria and Galilee regions had values between 0.70798 to 0.70829 and the Golan regions showed values of 0.70529 to 0.70571. Shewan (2004) undertook analysis of fauna from the Natufian levels of El Wad, which is adjacent to Tabun and Skhul. All samples were treated with the solubility profiling technique in an attempt to remove post-burial strontium (e.g., Sillen 1986). Bone from *Gazella gazelle* showed values of 0.70834 to 0.70843 (n=4). Bone from *Vulpes vulpes* showed values of 0.70841 to 0.70844 (n=4) and bone from a *Panthera sp.* had a value of 0.70841. Human bones had values in the range 0.70836 to 0.70856 (n=9).

3.6. Previous Strontium Isotope Studies in Southern France

A number of studies of the strontium isotope studies of soil, rock, plant or fauna from the study area within France have been undertaken.

Kelly (2007) undertook mapping of the area surrounding the archaeological site of Les Pradelles (located north-east of the town of Angoulême in south-west France) and studied fauna from units 2 to 5. The site is located on the boundary of the limestones of the Aquitaine Basin and the granites of the Massif Central, with the bioavailable component of the limestone having values in the range of 0.7078 to 0.7094 and the bioavailable component of the granites in the range of 0.7098 to 0.7272. Teeth from rat, reindeer, horse, bison, marmot, beaver, wolf and fox were analysed to determine mobility and seasonal variation. No seasonal variation was observed however species with small feeding ranges (such as fox, beaver, marmot) could be mapped to specific geological units, while species with larger ranges (such as wolf, horse, reindeer, bison) gave intermediate values. The results were not able to provide significant information

about Neanderthal hunting strategies, other than to suggest that they could procure marmot up to five km away.

Britton et al. (2011) analysed the strontium isotope composition of Middle Palaeolithic three reindeer teeth and a bison tooth from the archaeological site of Jonzac, located to the south of Cognac in south-west France. This study made multiple intra-tooth samples and showed a range of 0.7095 to 0.7104 for reindeer and 0.7090 to 0.7091 for bison (Britton et al. 2011:181). The reindeer teeth showed a high degree of intra-group strontium isotope variation, suggesting that the group shared similar migration routes and life histories (Britton et al. 2011: 182). All reindeer and bison are interpreted to be non-local and to have migrated biannually over a range of geological environments during tooth formation (Britton et al. 2011: 182).

Hodgkins (2012) analysed the strontium isotope composition of *Equus*, *Cervus* and *Rangifer* teeth from the archaeological sites of Pech de l'Azé (levels I2 and YZ) and Roc de Marsal (levels 8 and 9) as well as a limited number of mapping samples from the area. Results from the teeth ranged from 0.70905 to 0.71378. The results of this study suggested that climate shifts do not have a discernable effect on migration. Furthermore, no clearly defined migratory pattern was evident for any of these samples, with most moving within the area of the Aquitane and/or Paris Basins and some species making occasional incursions into the Massif Central. (Hodgkins 2012: 188).

Strontium isotope values have been obtained for the Massif Central, providing ranges of 0.712954 to 1.981 from granitic and gneissic lithologies (Couturié and Vachette-Caen 1980; Downes and Duthou 1988; Négrel et al. 2000). The strontium isotope value of mineral waters from the Massif Central ranges from 0.71296 to 0.71870, with the lower values interpreted as waters circulating through granites and the upper end reflecting waters circulating through gneissic areas (Négrel and Lachassagne 2000:1359). Stream water draining basic

igneous rocks in the Allanche watershed of the Massif Central has a range of 0.70278 to 0.70352(Négrel and Deschamps 1996).

3.7. Fauna

3.7.1. Fauna of the Levant

Israel is unique in having such a diverse range of habitats in a small area (Qumsiyeh 1996). Its position between Europe, Africa and Asia has served as a corridor for migration and more regularly as a barrier due to climatic and physiographic conditions (Tchernov 1988a). Three principal zoogeographical groups exist in Israel: 1) Mediterranean, 2) Saharo-Sindian and 3) Ethiopian/Afrotropical, with the Mediterranean dominating in the north-west of Israel, the Saharo-Sindian dominating in the south and the centre containing a mixture of all 3 groups (Qumsiyeh 1996).

Common fauna in Israeli archaeological sites over the last 50 ka include gazelle (*Gazella gazelle*), fallow deer (*Dama dama*), wild cattle (*Bos primigenius*), wild goat (*Capra aegagrus*), wild boar (*Sus scrofa*), wolf (*Canis lupus*) and fox (*Vulpes vulpes*) (Davis 1981:101).

Dwarfing of the carnivore (Kurtén 1965) and other mammalian components (Davis 1981) of the fossil record appears to have occurred at the end of the Pleistocene, due to the effects of climate change and then a second event caused by the effects of domestication (Davis 1981).

The Levantine fauna has much in common with African forms based on movement until the desert belt became an effective barrier in the Late Neogene and Pleistocene, later for xerotrophic forms (Tchernov 1979). Central and Western European genera and species were not present in the Levant before

the early Middle Pleistocene (Haas 1968). In the post-glacial period, forest species were pushed northwards by climate and human pressure and desert species invaded from the south once again along the coastal plain (Tchernov 1968).

3.7.2 Fauna of Southern France

Modern fauna in southern France is varied, due to the great diversity of topography and climate in this region. There are 120 extant mammal species in France.

The fauna of this region varied significantly during the Early-Middle Palaeolithic. Zoo-archaeological analysis has demonstrated that a dozen different species ungulates were hunted during Middle and Upper Palaeolithic eras in south-western France, although their individual contribution varies greatly over time as shown in Figure 3.23 (Discamps et al. 2011). The 5 most commonly hunted species were reindeer and caribou, bison, horse, red deer and wapiti and roe deer. During interglacials MIS 5 and MIS 3, dietary diversity (shown by enamel micro and meso wear) was higher than during pleniglacial phases MIS 8 and MIS 4 (Rivals et al. 2009).

The European Middle Pleistocene mammal fauna, represented by large species such as the straight tusked elephant and narrow nosed rhinoceros, was significantly impoverished by the start of MIS 5 due to the effects of a hostile and variable climate (Barnosky et al. 2004). The ‘warm’ component of this fauna was then finally made extinct by the glacial maximum in MIS 2, which the ‘cold’ fauna was able to survive (Finlayson and Carrión 2007). As a result plains mammals such reindeer, bison and horse significantly expanded across Europe following the major extension of the treeless vegetation in the glacial maximum in MIS 2 (Finlayson and Carrión 2007).

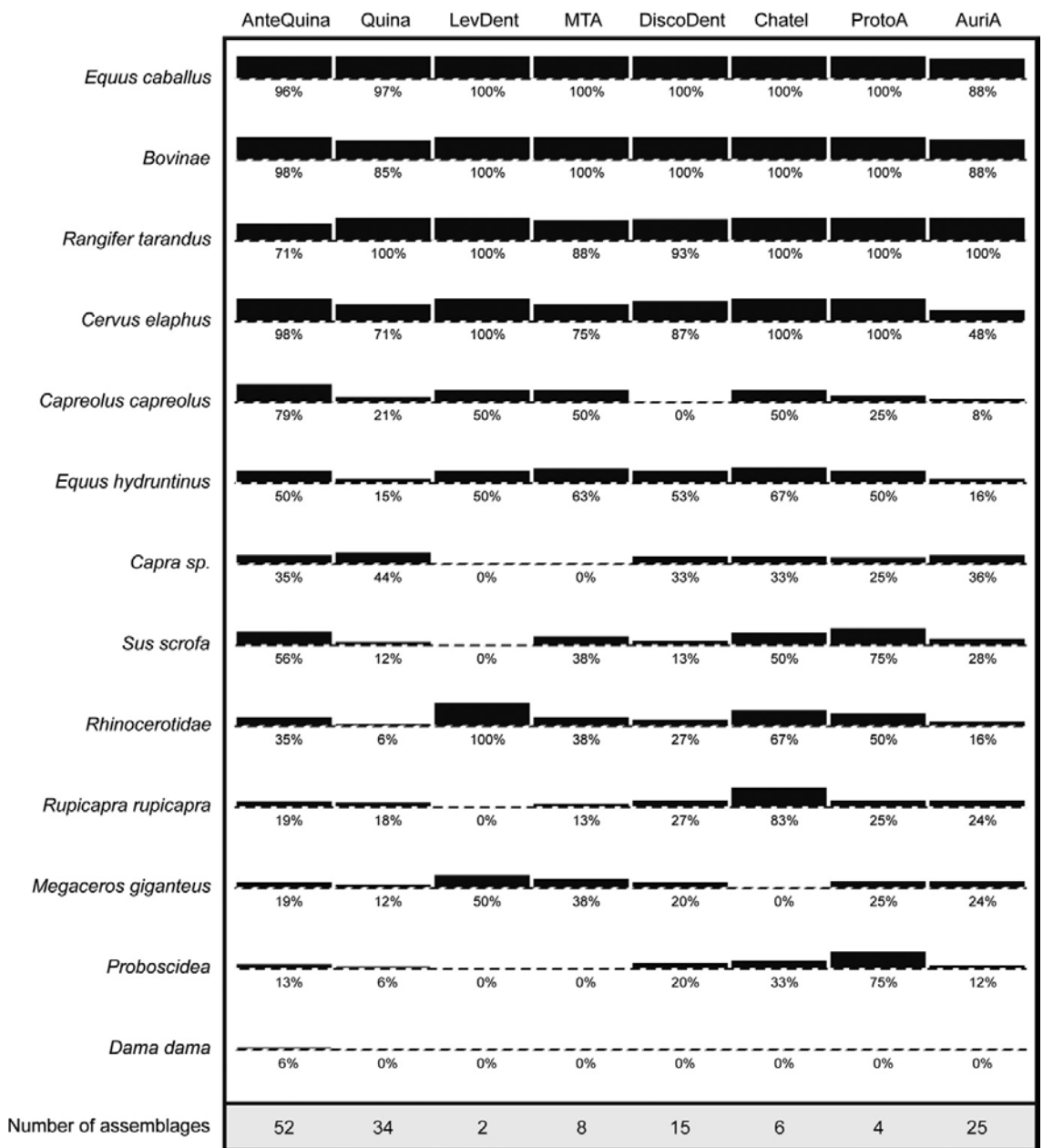


Figure 3.23 Presence/Absence Data for Different Taxon During Different periods of the Mousterian in South-west France (Discamps et al. 2011)

3.8. Fauna Included in this Study

Of the fauna included in this study, the 4 species around which Palaeolithic exploitation strategies by hominins were built (*Bos* and *bison*, *horse*, *red deer*

and reindeer) (Gamble 1992:106) are heavily represented. In addition, pigs, other species of deer, hippopotamus, rhinoceros, hyenas and foxes are included in this study.

3.8.1. Order Artiodactyla

3.8.1.1. Family Suidae (Suborder Suiformes)

Pigs are extant in 9 species (Macdonal and Frädrich 1991), with the wild boar (*Sus scrofa*) species represented in this study. Pigs are omnivores that root food from the substrate using their muzzle (Graves 1984). *Sus scrofa* is mainly herbivorous, with its diet dominated by rhizomes, roots, berries, nuts and water chestnuts, as well as animal food such as rodents, locusts and carrion and birds in some seasons and areas (Groves 1981). Pigs are almost eurytopic and are found in ecozones as diverse as the subarctic, tropical and desert (Baskin and Danell 2003). Breeding can be faster than any other ungulate (Oliver and Fruzinski 1991), but is often regularised by the availability of food (Graves 1984). Farrowing of *Sus scrofa* in modern France occurs principally between February and August (Mauget 1991). Population densities are usually between 1 and 5 individuals per km² (Mauget et al. 1984), and they generally live in groups of 3 to 6 members (Martys 1991).

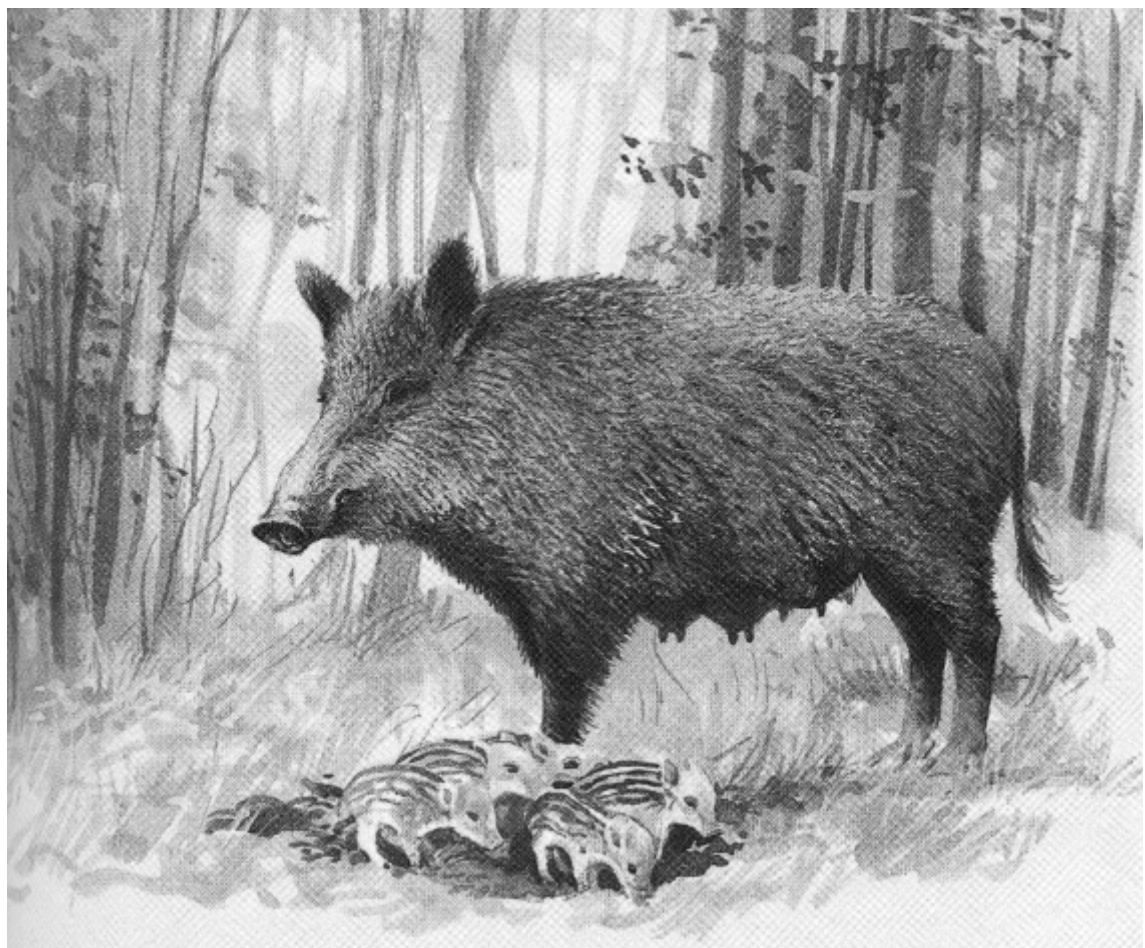


Figure 3.24 *Sus scrofa* (Modified From Groves 2007:19)

The availability (or paucity) of food often controls mobility, which may occur suddenly (d'Huart 1991). The principal ecological impediments to movement are deep snow, frozen ground and water availability, with temperature playing a relatively minor role directly (Groves 1981). Home ranges of pigs can be from less than 100 ha to more than 2500 ha, and tagged pigs are resighted, on average, within 641 m of their original capture site (Graves 1984). In mountainous areas, vertical migration are common and can cover distances of 20 to 50 km. Over a 24-hour period, *Sus scrofa* can travel 30 to 40 km and have been observed to travel 200 to 300 km in 10 to 15 days (Baskin and Danell 2003).

The family Suidae have been traced to the Oligocene era (Thenius 1970). *Sus scrofa* appears in France in the Middle Pleistocene era and becomes a regular,

but not abundant, member of the local fauna (Boyle 1998). *Sus scrofa* in the Pleistocene Perigord favours temperate forest conditions (Laville et al. 1980). *Sus scrofa* appears at the start of MIS 6 in the Middle Pleistocene era (Tchernov 1979) and was, until recently, extremely common in all parts of Israel and particularly so around the Jordan River and the Dead Sea (Tristram 1866). Its modern distribution and abundance is slightly less extensive (Qumsiyeh 1996). Pigs were domesticated in Europe and Asia 5000 to 1000 years ago (Zeuner 1963). In many areas of contemporary South-East Asia and the Pacific, pigs represent one of the most abundant sources of prey in terms of biomass and also often play a significant cultural role as a source of trophies and omens or as an item of trade (Oliver and Fruzinski 1991).

Pigs display considerable sexual dimorphism in their canines, with males having large ever-growing tusks as their upper canines (Hillson 2005). The lower incisions have a chisel-like appearance, while the upper incisors are much smaller and more curved (Hillson 2005). The permanent molars have many subsidiary cusps around a main central cusp and quickly wear down to the dentine (Hillson 2005). The deciduous teeth of pigs erupt immediately following birth and have completed eruption by 120 days (Matschke 1967). The permanent dentition begins to form at birth (McCance et al. 1961), with eruption of the permanent first molar beginning at 4 to 6 months. Enamel maturation occurs between birth and 2 to 3 months for M1, between 1 to 8 months for M2, P2 and P4 and between month 3 to 13 for M3 (Bentley and Knipper 2005a). The European wild boar generally has a slightly later eruption sequence than discussed above, which is based on domestic pigs (Desbiez and Keuroghlian 2001). Because of the heavy wear of enamel in pigs, the amount of dentine exposed can be used as a measure of age (Rolett and Min-yung 1994).

Pig teeth in this study include 3 molars from 1 pig jaw from Skhul and 1 from a wild boar from Les Fieux.

3.8.1.2. Family Cervidae (Suborder Ruminantia (Pecora))

The family Cervidae includes many kinds of deer (17 extant genera, with 36 living species worldwide) (Qumsiyeh 1996), which inhabit diverse ecological niches. They share crescent-shaped ridges on the elongated cusps of their teeth, which are low crowned; there are vacuities between the nasal and lacrimal bones in the skull and their stomachs are in the skull.

Considered in this study are the Mesopotamian fallow deer (*Dama mesopotamica*), the reindeer (*Rangifer tarandu*) and unidentified deer, which are probably red deer (*Cervus elaphus*), given the dominance of this species in France during the period of the study (Boyle 1998).

Dama mesopotamica was formerly distributed in Iran, Iraq, Israel, Jordan, Lebanon, Palestine, Syria and eastern Turkey, but by the 1940s it was thought to be extinct (Chapman and Chapman 1980). In 1956, 2 small populations were discovered in Iran, which has served as the basis for a captive herd and its reintroduction to various areas. *Dama mesopotamica* was formerly thought to be a subspecies of *Dama dama*, but has since been recognised as a separate species diverging in the early Pliocene era (Pitra et al. 2004). It principally occupies riparian forest thickets (McTaggart-Cowan and Holloway 1973).

Reindeers (*Rangifer tarandu*) have an adult body mass of 80 to 180 kg, with females generally being smaller than males (Baskin and Danell 2003). Reindeer occur in a range of ecoregions, including tundra, subarctic, tundra regime mountains, subarctic regime mountains and warm continental environments (Baskin and Danell 2003). They principally inhabit open treeless spaces, although can adapt to boreal forests (Guérin et al. 2012). Extant wild herds of reindeer are both sedentary and migratory, with no morphological or genetic differences between the groups (Banfield 1961). Some herds have ranges as small as a few 100 m², while others undertake seasonal movements over many

1000 km (Britton et al. 2011). Modern reindeer in Eastern Europe and Northern and Central Asia have small ranges in winter and summer and then migrate in spring and autumn (Baskin and Danell 2003:138). Migration usually lags about 15 to 20 days behind the line of melting snow (Baskin and Danell 2003). The teeth, stomach, intestines and physiology of reindeer are equipped for feeding on lichen, although green plants, mushrooms and moss may make a significant contribution to diet (Baskin and Danell 2003). Reindeer are very well adapted to cold conditions, have broad feeding habits and, and while they are plastic in their environmental adaptations, are particularly suited to open, treeless spaces (Discamps et al. 2011:2759). Reindeer are able to live in environments not suited to other ungulates (Discamps et al. 2011).

The red deer (*Cervus elaphus*) is a large deer with a height of more than 1 m to the shoulder and weighing more than 200 kg (Qumsiyeh 1996). It was formerly distributed over much of the Northern Hemisphere; however, it has recently been exterminated from most of its range (Qumsiyeh 1996). This species has a much broader feeding niche than other cervid, consuming a range of grass, herbs and trees (Baskin and Danell 2003). Red deer inhabit open woodland, woodland/forest, moorland and temperate environments and can undertake significant migration (Boyle 1998). They can tolerate steppe (Guérin et al. 2012:3081). The red deer is often split into 2 broad ecological groups, which inhabit either open (American) or woodland (European) areas (Straus 1981). Red deer often live in the upper part of the mountains from summer to early winter, migrating downwards slowly as snow cover becomes heavy (Baskin and Danell 2003). They are ecologically adaptable, as their rumen can be developed to either browse or graze depending on the dominant vegetation available (Stewart 2005). Daily mobility is relatively low, with a maximum of around 8 km (Baskin and Danell 2003). Home ranges are usually smaller in winter and annual migration can be in the range of 10 to 150 km (Baskin and Danell 2003). Red deer lack adaptation to snow but are extremely adaptable, highly eclectic mixed feeders that are best suited to patchy wooded areas (Discamps et al. 2011:2760). They can tolerate a range of climatic conditions, but require

protection from wind and snow, which can be provided either by trees or topographic relief (Discamps et al. 2011).

Palaeolithic reindeer are interpreted to migrate bi-annually, similar to the modern North American caribou (Bahn 1977). Cervid have been common in southern France since ~555 ka, with red deer (*Cervus elaphus*) the dominant species and reindeer (*Rangifer tarandu*) becoming common during colder periods (Boyle 1998). The reindeer played a dominant role in the Upper Palaeolithic economy in the Aquitaine region (Burke 1995). Reindeer appeared to exist in the Palaeolithic Perigord region in conditions less cold than observed for modern examples (Laville et al. 1980). *Dama mesopotamica* and *Cervus elaphus* have been found in Israel since the start of the Riss-Würm period of the Middle Pleistocene era (Tchernov 1979). *Dama mesopotamica* were particularly common in late Palaeolithic caves in Israel and became extinct in the region only during the last century (Qumsiyeh 1996). Red deer favour the subarctic forest, while reindeer favour a slightly more open environment (Gamble 1992:104). Reindeer were very mobile and red deer were somewhat mobile during the last glacial period (Gamble 1992). Reindeer and perhaps red deer and horse migrated principally in an east-west transect, taking advantage of a steepened ecological gradient between the Perigord and the Massif Central during glacial periods (Mellars 1996:53).

All species of the suborder ruminantia (pecora) have persistently growing premolars and molars (Hillson 2005). Deer have very characteristic cheek teeth, with low crowns, prominent roots and a strongly developed cingulum bulge (Hillson 2005). The dentition dimension varies greatly among the cervid (Hillson 2005). Fallow deer are born with 20 deciduous teeth, with permanent molars erupting from 3 to 4 months through 3 years of age and permanent incisors erupting from 7 to 20 months of age (Chapman and Chapman 1970). A very detailed method of scoring dental attrition in fallow deer (*Dama dama*) was devised by Brown and Chapman (1990), which measures type and degree of wear on the 6 lower cheek teeth. The system is suitably detailed to discern the

season of death of cervid found in archaeological sites such as Star Carr (Carter 1998) and Thatcham (Carter 2000).

The following cervid teeth were analysed: 3 Persian fallow deer (*Dama mesopotamica*) teeth from Amud, 2 reindeer (*Rangifer tarandus*) teeth from Les Fieux, 4 deer teeth from Rescoundudou, 3 reindeer teeth from La Chapelle-aux-Saints and 4 deer teeth from layers 8, 6, 4 and 3 from Pech de l'Azé II.

3.8.1.3. Family Bovidae

Bovid in this study include bison, *Bos* (cattle and aurochs) and a large number of samples identified simply as bovid. This ambiguity in identification is due to the difficulty in distinguishing between these species based solely on dental material (Hillson 2005). All of these species are herbivores. The other bovid species included in this study is the chamois (*Rupicapra rupicapra/Rupicapra pyrenaica*) or mountain goat. When a sample is referred to as a bovid in this text, it refers to a sample not distinguished between bison and *Bos*.

Bos primigenius (auruchs) became extinct in 1627 and are the wild ancestors to the modern domestic *Bos taurus* and *Bos indicus* (Beja-Pereira et al. 2006). These species originated in India at around 1.5 to 2 Ma and then spread to Asia, northern Africa and to Europe. Both species were generally sessile and, even when wild, did not make large migrations (Kurtén 1968). Calving occurs in summer. These species were not as well adapted to cold as other Pleistocene species such as woolly mammoth, woolly rhinoceros, steppe bison and horses (van Vuure 2005).



Figure 3.25 Male Bison (*Bison bison*) (Meagher 1986:3)

Bison are represented by 2 extant (*Bison bison* and *Bison bonasus*) and 4 extinct species (*Bison antiquus*, *Bison latifrons*, *Bison occidentalis* and *Bison priscus*). Bison have a variable size (depending on whether they are European or American). Adults are in the range of 2 to 4 m long, 1.5 to 2 m to the shoulder and weigh 350 to 1000 kg (Arthur 1975; Banfield 1974; Bjärvall and Ullström 1986; Lawrence 1974). Bison are a highly migratory species, with modern examples travelling on the order of 100 km (Berger 2004), 250 km (Arthur 1975) or 300 km (Boyle 1990) in long distance migration. In modern Yellowstone National Park, bison annually migrate from higher elevations in summer to lower elevations in winter (Plumb et al. 2009). Bison calving occurs in spring (Berger and Cunningham 1994). Bison are poorly adapted to snow, but can tolerate it for a short time (Discamps et al. 2011). They are grazing specialists that prefer grasses and sedges but can browse on shrubs, forest lichens and trees if

required (Discamps et al. 2011). They are ecologically plastic but are more suited to open grassland environments (Discamps et al. 2011:2759).

Chamois/mountain goats are herbivores that live at moderately high altitudes and are adapted to steep rocky terrain. They weigh 20 to 50 kg and cover a seasonally varying range usually smaller than 100 ha (Boyle 1990). The degree of migration between summer and winter ranges is small, usually of the order of a few km (Hamr 1985). Their modern distribution covers the middle to high mountain ranges of southern Europe, the Balkans and the Near East (Masini and Lovari 1988). In the Plio-Pleistocene era, they were far more widely distributed and their genus was represented by a greater number of species, which occupied a wider range of environments. During the Pleistocene era, in which they occupied their current ecological niche in Europe, they became more widely distributed during interglacials and contracted during glacial periods (Masini and Lovari 1988).

Bison were very common in MIS 2 to 3 in Europe, while *Bos* were comparatively rare in the Pleistocene era (Kurtén 1968); hence, most Pleistocene material is assigned to this taxon. Bison existed in the Mindel to the Riss-Würm during the Middle Pleistocene of Israel, and *Bos* appeared the start of the Riss-Würm and continued until recently (Tchernov 1979). Hunting of bison in the Pleistocene era probably followed Blackfoot Indian practice, in which co-operative hunting is used to surround bison either by hunters (usually in summer) or to corral large numbers of animals and often drive them off cliffs (in winter) (Boyle 1990). Bison favour open, open woodland, woodland/forest, steppe and arctic environments and undertake significant migration (Boyle 1998:17). While the 2 species can co-exist, the bison were more representative of cold steppe and aurochs were indicative of milder conditions (Laville et al. 1980). Bison were mobile and aurochs were somewhat mobile during the glacial (Gamble 1992).

The deciduous dentition of cattle includes incisors, canines and premolars, which erupt before birth (incisors and P3), or soon afterwards (Brown et al. 1960). The permanent dentition includes 0 incisors, 6 molars and 6 premolars and 0 canines on the upper jaw and 6 incisors, 6 molars and 6 premolars and 2 canines on the lower jaw (Hillson 2005). M1 erupts within 9 to 12 months of birth, M2 within 18 months and M3 from 2.25 to 2.5 years (Hillson 2005). For bison, the formation of M1 begins *in utero* and is completed several months after birth, the formation of M2 forms between birth and approximately 13 months of age and the M3 molar forms between 9 months and 2 years of age (Gadbury et al. 2000). By 4.25 years, all permanent teeth have formed and erupted, with the canines being the last to emerge (Brown et al. 1960). Age groups for eruption and wear for chamois were summarised by Pérez-Barbería (1994). The enamel maturation process has been investigated for *Bos taurus* (Balasse 2002), *Bison bison* (Passey and Cerling 2002) and *Bison priscus* (Bernard et al. 2009). Bovid teeth continue to calcify and crystallise after eruption, peripherally and cervically through the enamel (Sakae and Hirai 1982).

Bovid teeth in this study from France include 11 bovid teeth from Bois Roche, 2 bison teeth from Les Fieux, 5 bovid teeth from Rescoundudou, 10 bovid teeth from La Chapelle-aux-Saints, 6 bovid teeth from Le Moustier and 9 bovid teeth from Pech de l'Azé II. Bovid teeth from Israel include 3 bovid teeth from Qafzeh and 9 *Bos* teeth from Tabun, as well as 3 *Bos* teeth and 3 bovid teeth from Skhul and 1 bovid tooth from Holon. The bison teeth in this study include 2 samples from Les Fieux. Chamois/mountain goat teeth include 2 from Les Fieux.

3.8.1.4. Family Hippopotamidae

The hippopotamus spends its days in the water but grazes on land during the day (Eltringham 1993). It requires water to keep its skin moist, but it grazes exclusively on land plants (Eltringham 1993) and so requires both permanent

water and access to riparian vegetation. Its modern distribution is in Sub-Saharan Africa (Eltringham 1993). Hippopotamus were widespread in Europe in the Pleistocene era but have been confined to Africa since the Holocene era (Hillson 2005). Hippopotamuses were probably present in Israel at the start of the Early Pleistocene era and persisted until near the end of the Post-Würm era (Tchernov 1979).

Hippopotamuses have 4 to 6 upper incisors and 2 to 6 lower incisors, 2 upper and lower canines, 8 upper and lower premolars and 6 upper and lower molars (Hillson 2005). The canines grow continually during their lives, and the lower canines have enamel coating only 2 sides (Hillson 2005). Hippopotamuses have a regular eruption sequence and wear history that can be used for aging (Laws 1968).

Two fragments of hippopotamus teeth were analysed in this study, from layer 7 (622) and layer 9 (615) of the French archaeological site of Pech de l'Azé II.

3.8.2. Order Perissodactyla

3.8.2.1. Family Equidae (Suborder Ruminantia/Pecora)

Equids, principally represented by the horse (*Equus caballus*), are herbivores and are common in the archaeological records of France and Israel. Adult horses stand at about 1 to 1.2 m at the shoulder, are about 2 m in length and weigh between 350 to 500 kg (Walker 1968). Horses give birth in May to June in the Northern Hemisphere. They have home ranges of 73 to 303 km² (Miller 1983), which may seasonally adjust (Berger 1986).



Figure 3.26 Przewalski Horse (*Equus caballus przewalskii*) (Bennett and Hoffman 1999:1)

The behaviour of modern feral grassland and desert horses, as well as historical observations of wild horse populations, provides some insight into the behaviour of Pleistocene horse populations (Burke 1995). The Przewalski horse (now extinct in the wild, but originally found in the steppes of Central Asia, see Baskin and Danell 2003) is considered the modern species most similar to the Pleistocene horse, because it has never been successfully domesticated (Boyle 1990). Groups consist of 3 to 100 horses that usually occupy a range of 200 to 250 acres (Spiess 1979). Horses favour grassy and shrubby areas and avoid marshy ground and deep snow (Boyle 1990). Horses are well adapted for steppe and tundra and so were particularly widely geographically distributed

during the Pleistocene glacials (Bennett and Hoffman 1999). Horses can tolerate deep snow, but only for a limited time (Discamps et al. 2011).

The horse is well adapted to running and modern horses can cover long distances in migration (Baskin and Danell 2003). Horse migration in the late Palaeolithic era in south-west France would generally have been over short distances, involved small altitudinal shifts and involved small numbers of animals (Burke 1995). Horses are interpreted to have been mobile during the glacial period (Gamble 1992).

Horses were the second most important prey species during Dryas 1 in south-west France (Burke 1995). Several species of equids appeared in the MIS 7 and 8, but many of them became extinct and were replaced by other equids, which persisted until the Post-Würm era (Tchernov 1979). Horses were first used for riding by humans in approximately 4000 BC (Anthony and Brown 1991).

Equid teeth continue to mineralise for 6 to 12 months after eruption and total amelogenesis for a tooth can span 1.5 to 2.8 years (Hoppe et al. 2004). The deciduous dentition of horses erupt before birth or soon afterwards and may continue for up to 9 months (Hillson 2005). The permanent teeth begin to emerge by about 9 months after birth with the first premolar, followed by the first molar at the end of the first year, then the second molars, second, third and fourth premolars and third molars and then the anterior teeth, with a complete adult dentition being present by 5.5 years at the latest (Hillson 2005). Equids have 6 incisors, 0 to 2 canines, 6 to 8 upper and 6 lower premolars and 6 molars (Hillson 2005). Age can be determined by the degree of dentine exposure due to wear in incisors or the crown height of the cheek teeth (Levine 1982).

Horse teeth in this study include 2 from Les Fieux, 4 from Rescoundudou and 5 from Pech de l'Azé II.

3.8.2.2. Family Rhinocerotidae

Extant species of rhinoceroses include the white rhinoceros (*Ceratotherium simum*), black rhinoceros (*Diceros bicornis*), Indian rhinoceros (*Rhinoceros unicornis*), Javan rhinoceros (*Rhinoceros sondaicus*) and Sumatran rhinoceros (*Dicerorhinus sumatrensis*). Black rhinoceroses are 280 to 290 cm long (including head and body), 132 to 180 cm high and body mass has been reported in the range of 854 to 2896 kg (Hillman-Smith and Groves 1994). White rhinoceroses are 3.35 to 3.77 m long, 1.71 to 1.85 m high to the shoulder and weigh 3200 to 3600 kg (Foster 1980). Sumatran rhinoceroses are 2.36 to 3.175 m long, 1.12 to 1.45 m high to the shoulder and weigh from 800 to 2000 kg (Groves and Kurt 1972). Indian rhinoceroses average 4.12 m long, are 1.4 to 1.9 m high to the shoulder and weigh 1599 to 2132 kg (Laurie et al. 1983).

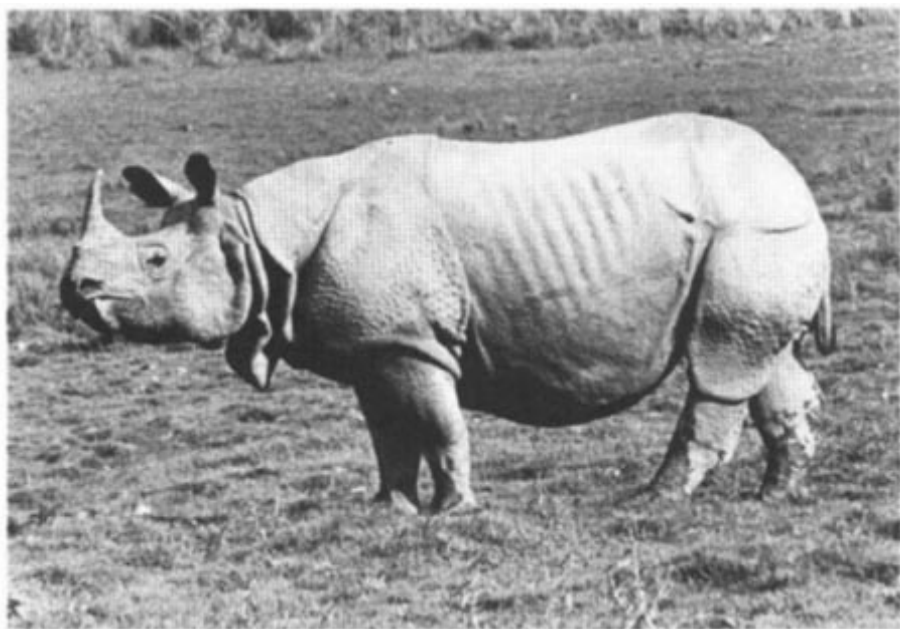


Figure 3.27 Adult Male Indian Rhinoceros (*Rhinoceros unicornis*) (Laurie et al. 1983:1)

Modern black and white rhinoceroses are found in central and southern Africa (Groves 1972; Hillman-Smith and Groves 1994), while Sumatran rhinoceroses live in areas of South-East Asia (Groves and Kurt 1972) and Indian rhinoceroses live in northern India and Nepal (Laurie et al. 1983). They live in a wide range of habitats, including montane forest, savannah, grassland and desert (Hillman-Smith and Groves 1994). Home ranges are 2.6 to 133 km² for black rhinoceroses (Hillman-Smith and Groves 1994) and 2 to 15 km² for white rhinoceroses (Groves 1972). Sumatran rhinoceroses engage in seasonal migration between higher and lower altitudes (Groves and Kurt 1972).

The various species of rhinoceroses in France during the Pleistocene (*Dicerorhinus merki*, *Coelodonta antiquitatis* and *Dicerorhinus hemitoechus*) survived until the end of the Pleistocene era and were particularly adapted to colder conditions (Boyle 1998). Pleistocene mammoths were smaller than their modern counterparts (Boyle 1990) and subsisted on low-growing grasses and other herbaceous elements (Stuart 1982). Rhinoceroses (with some minor variation between species) are thought to have inhabited open, open woodland, woodland/forest, steppe and arctic environments (Boyle 1998:17) during the Pleistocene era. Rhinoceroses were thought to have moderate mobility during the last glacial period (Gamble 1992).

Rhinoceroses have 0 to 4 upper incisors and 0 to 2 lower incisors, no upper canines and 0 to 2 lower canines, 6 to 8 upper and lower premolars and 6 upper and lower molars (Hillson 2005). Deciduous teeth begin erupting from birth beginning with the premolars, and adult teeth begin erupting from the age of 1.5 and have completely erupted by 4 years (Tong 2001).

Two rhinoceros teeth (568 and M038) were included in this study. Sample 568 is from level Ed at the Israeli archaeological site of Tabun, and M038 from layer C1 of the French archaeological site of Rescoundudou.

3.8.3. Order Carnivora

3.8.3.1. Family Hyaenidae

Hyenas (or hyenas) are specialist scavengers of large herbivores, currently distributed in Africa, Central Asia and the Middle East and comprising 4 species: brown hyena (*Hyaena brunnea*), striped hyena (*Hyaena hyaena*), spotted hyena (*Crocuta crocuta*) and aardwolf (*Proteles cristatus*) (Hofer 1998a; 1998b; Mills 1998; Richardson 1998). Striped hyenas weigh from 25 to 55 kg and total body length is 1.1 to 1.8 m (Rieger 1981).

Hyenas were the dominant carnivore in the Middle to Upper Miocene era of Eurasia, with a wide ecological role, while they now act as hunter-scavengers and bone crackers (Jenks and Werdelin 1998). Brown hyenas do not require surface water, although will drink when it is available (Mills 1982); aardwolves will only drink water when food is scarce (Koehler and Richardson 1990). The aardwolf favours open grassy plains but will occupy most habitats in the 100 to 800 mm rainfall range (Koehler and Richardson 1990). Hyena species were abundant in the early Pleistocene era, but by the Middle Pleistocene era had shrunk to their present 4 representatives (Ewer 1967). In Palaeolithic contexts, there is no significant difference between the prey species and proportions between spotted hyenas and humans (Stiner 1992).



Figure 3.28 Striped Hyena (*Hyaena hyaena*) (Rieger 1981:1)

Home range distribution of brown hyenas range from 235 to 480 km² (Mills 1982), while the striped hyena has a range of 72 km² (male) and 44 km² (female) (Kruuk 1972) and the aardwolf, 1 to 4 km² (Koehler and Richardson 1990). Hyenas are associated with open, open woodland, steppe, marsh/river bank and arid environments and are not thought to undertake significant migration (Boyle 1998:17).

The striped hyena (*Hyaena hyaena*) is found in all major habitats of modern Israel (Qumsiyeh 1996) but is extinct in modern France. The striped hyena appears to have replaced the spotted hyena (*Crocuta crocuta*) in Israel, which became extinct approximately 10 ka; however, a period of overlap between the species occurred at this time (Tchernov 1979).

Species of the family Hyaenidae have exceptionally robust upper carnassials with pronounced parastyles, no upper or second lower molars, raised robust

upper third, lower third and lower fourth molars and tall and robust protoconid/paraconid blades with greatly reduced metaconid and taloned on their lower carnassials (Hillson 2005:57). Deciduous incisors and canines of the modern spotted hyena erupt prior to birth and cheek teeth erupt within 2 months of birth (van Horn et al. 2003). Adult teeth begin to emerge for the same species between 6.5 to 9 months and are all present by 13 to 18 months (van Horn et al. 2003).

One sample of a hyena tooth is included in this study, taken from Mousterian level G7 of Les Fieux.

3.8.3.2. Family Canidae

Foxes (principally represented by *Vulpes vulpes*, but many species exist) are omnivores with a wide modern distribution over Europe, North America, North Africa, Asia and Australia (Larivière and Pasitschniak-Arts 1996). *Vulpes vulpes* is a relatively small, slender canid with an elongated muzzle, large pointed ears, a long round bushy tail, long slender legs, relatively small feet and moderately sized eyes with elliptical pupils (Larivière and Pasitschniak-Arts 1996). Body size varies greatly with lengths (excluding tail) from 45 to 90 cm and mass from 2 to 14 kg (Nowak 1991). Foxes breed during the winter and birth after 52 days (Voight 1987). They are principally nocturnal and usually exist as a monogamous pair, which uncommonly interacts with other groups (Larivière and Pasitschniak-Arts 1996).



Figure 3.29 Adult *Vulpes vulpes* (Larivière and Pasitschniak-Arts 1996:2)

Foxes live in a variety of environments, including semi-arid deserts, tundra, farmland and boreal forests; however, they tend to favour heterogeneous and fragmented landscapes (Catling and Burt 1995). They are highly mobile, often covering more than 10 km in a day and dispersing from their home ranges (which can be up to 20 km²) during winter at up to ~300 km (Larivière and Pasitschniak-Arts 1996). Foxes are thought to inhabit open, open woodland, woodland/forest, marsh/riverbank, temperate, arid and humid environments and do not undertake significant migration (Boyle 1998:17).

Foxes are ubiquitous in the archaeological record of southern France since the Riss (MIS 6) (Boyle 1998). Foxes have existed in Israel since the beginning of the Middle Pleistocene era (Tchernov 1979) and remain very common in all but the most arid areas (Qumsiyeh 1996).

All deciduous teeth have emerged by 1 to 2.5 months and all permanent teeth emerge by 6 months (Hillson 2005). The permanent dentition of *Vulpes vulpes* consists of 6 incisors, 2 canines, 8 premolars and 4 molars in the upper jaw and 6 incisors, 2 canines, 8 premolars and 6 molars in the lower jaw. Upper permanent first molar wear can be used to age foxes (Van Bree et al. 1974).

One sample of a fox tooth is included in this study, taken from Mousterian level G7 of the French archaeological site of Les Fieux.

3.9. Archaeology

3.9.1. Hominins Included in this Study

3.9.1.1. Overview

This research examines fauna from archaeological sites that were occupied by *Homo erectus*, *Homo neanderthalensis* and anatomically modern humans. Each of these species has their own chronology, archaeological signature, diet and mobility, which are reviewed in sections 3.9.1.2 to 3.9.1.4. Understanding the characteristics of these individual species is crucial for the accurate interpretation of the archaeological implications of the strontium isotope results.

3.9.1.2. *Homo Erectus*

Definitive *Homo erectus* fossils range in age from 1.8 Ma (possibly 1.9 Ma) in Africa to as recent as 100 ka, or even 50 ka in Indonesia (Antón 2003). Fossils of this species are distributed through Africa, Europe and Asia, although population densities were probably extremely variable and spatially discontinuous (Dennell 2003). The large body size and longer, more linear body form of *Homo erectus* compared to earlier hominins was beneficial for thermoregulation and water balance in xeric (open) forest conditions (Wheeler 1992), and the longer leg length would have increased locomotor efficiency (Kramer and Eck 2000). The ranging patterns of this species would have been significantly enlarged over earlier hominins, and the energetic costs of maintaining a large body and brain suggest a diet with increased emphasis on meat and marrow (Antón 2003).

The Acheulian assemblage is associated with *Homo erectus* both in Europe and Israel, although it is not distributed to the east of the ‘Movius Line’ (Dennell 2003). Some workers consider that *Homo ergaster* is a separate species from *Homo erectus* (Wood 1991), although it is more likely to represent a single evolving species (Ungar et al. 2006). More recently, a new species associated with the Acheulo-Yabudrian industry has been proposed as replacing *Homo erectus* in the Levant at ~400 ka (Hershkovitz et al. 2011).

Homo erectus preferred mosaic environments that contained permanent water, some wood, scrub and grass land (Dennell 2003:423). *Homo erectus* probably favoured aggressive scavenging, augmented by some predation (Domínguez-Rodrigo 2002). Roebroeks (2001) believes that by around 400 ka in Europe, *Homo erectus* were capable and active hunters of large mammals. From MIS 8 and 7 there appears to be an adaptation of hominins to more open and cooler conditions and greater specialisation in hunting (White and Ashton 2003:606). The abilities of *Homo erectus* improved over time, and so the range of environments they could tolerate progressively increased (Dennell 2003). *Homo erectus* have been associated with large and medium sized game (Ben-Dor et al. 2011). Raw material transfer distances in the European Lower Palaeolithic era were generally short (Féblot-Augustins 1999).

3.9.1.3. *Homo Neanderthalensis*

Homo neanderthalensis are present in Western Europe below 55 °N latitude, as far south as Israel and as far east as Southern Siberia, but have not been located in Africa (Hublin 2009). They were present in Europe from at least 200 ka before becoming abruptly extinct between 30 to 40 ka, due to the presence of anatomically modern humans (Mellars 2004). Many of the earlier Neanderthal specimens are regarded as ‘pre’ or ‘proto’ forms, with transitional features from earlier species (Stringer and Gamble 1993). Most authors now accept that

Neanderthals and *Homo sapiens* share a common ancestor in *Homo erectus*, although there may be a diversity of early *Homo* ancestors (Leakey et al. 2012). On this basis, Neanderthals evolved in Europe while *Homo sapiens* evolved in Africa, although the timing and the possibility of transitional species (e.g., *Homo heidelbergensis*, see Mounier et al. 2009) remain under debate (Hublin 2009). While Neanderthals and anatomically modern humans are clearly distinct species, recent DNA analysis has confirmed that some breeding between Neanderthals and anatomically modern humans did take place (Green et al. 2010).

The detailed biological and anatomical features of the Neanderthals have been summarised in detail by Stringer and Gamble (1993) and Trinkaus and Shipman (1993). Overall, they were large bodied species who required a high energetic intake (Steegmann et al. 2002). Neanderthals are distinctive based on their skull and facial regions, including heavily enlarged brow ridges, a low and flattened cranial vault, heavily built jaw and teeth, little chin and a large cranial capacity and brain size (Mellars 1996).

A summary of isotopic evidence of diet from a number of studies (Beauval et al. 2006; Bocherens et al. 2001; Bocherens et al. 2005; Richards and Schmitz 2008; Richards et al. 2008; Richards et al. 2000), shows that the diet of Neanderthals was focused on terrestrial protein and had a trophic level equal to or higher than carnivores (Richards and Trinkaus 2009:16035). Archaeological studies also suggested that Neanderthal hunting focused on large herbivores (Patou-Mathis 2000; Stiner 1994) and that Neanderthals could access seasonal resources such as reindeer (Gaudzinski and Reobroeks 2000). Neanderthals showed adaptability in utilising different hunting strategies through time, possibly due to changes in occupation conditions (Rendu 2010). There has been significant debate over the hunting capabilities of Middle Palaeolithic Neanderthal species, with Binford arguing that these populations were principally scavengers of carnivore kills augmented by limited amounts of opportunistic hunting of small game (Binford 1985). Mellars contended that this

underestimates the capabilities of these populations, although conceded that the hunting was ‘significantly less systematic, less intensive and less logically organised than practised by many of the later, Upper Palaeolithic communities in the same regions’ (Mellars 1989:357). Patou-Mathis (2000:393) took the view that there was little evidence of scavenging behaviour, rather that hunting was specialised and sophisticated particularly during cold phases.

The degree to which Neanderthals were mobile is contentious, with various authors arguing that they moved over long distances in their lifetimes, only moved in a limited area, perhaps to access seasonal resources, or that they stayed in 1 relatively small area for their entire lives (e.g., Richards et al. 2008). Isotopic evidence suggested that Neanderthals were capable of moving distances of at least 20 km during their lifetime (Richards et al. 2008:1254). They predominately lived in cool or cold environments and were limited in their ability to reside in peri-arctic areas (Hublin 2009).

Neanderthals have been variously considered to have different cognitive capacities, with some authors considering that they lacked behaviours such as language, planning their economic and social activities, hunting large animals and modern family structures, while other authors see Neanderthals as only marginally different from anatomically modern humans (summarised by Mellars 1996). Behavioural complexity of Neanderthals appeared to have increased throughout the Middle Palaeolithic era, particularly since 100 ka (Langley et al. 2008).

3.9.1.4. Anatomically Modern Humans

Anatomically modern humans evolved in Africa and subsequently moved over a far greater geographic area at ~40 ka, with the exception of a precocious extension into Israel at ~100 ka, represented by the fossils from Qafzeh and Skhul (Trinkaus 2005). The emergence of this population, seen as an early or

archaic modern human group, in Africa at approximately 200 ka is supported by DNA studies (Forster 2004) and dating of the Omo-Kibish (McDougall et al. 2005) and Middle Awash (White et al. 2003) sites.

Their exact evolutionary lineage has been a source of considerable debate, with both the ‘multi-regional’ and ‘out of Africa’ models being debated widely in the literature (e.g., Schwartz and Tattersall 2010).

3.10. Palaeolithic Archaeology of the Levant

3.10.1. Overview

This section discusses the archaeology of Israel, in general terms, for the Palaeolithic era, as represented by samples in this study. The occupation history of Israel is dynamic, being initially occupied by *Homo erectus*, followed by a possible anatomically modern hominin ancestor, anatomically modern humans, Neanderthals and subsequently anatomically modern humans again (or continually). Overall, with the exception of level B at Tabun, sites with Neanderthal remains in Israel (Amud and Kebara) fall within MIS 4 and MIS 3, while sites with anatomically human remains date to MIS 5 (Hallin et al. 2012). Anatomically modern humans and *Homo erectus* arrived in Israel from Africa, while Neanderthals migrated from Europe.

3.10.2. Key Periods in This Study

3.10.2.1. Lower Palaeolithic, 1.4 Ma to 200 Ka

The Acheulian and Acheulo-Yabrudian industries are characteristic of the Lower Palaeolithic in Israel (Barkai et al. 2002). The earliest human artefacts, based on stratigraphic position, are known from the Erkel Amhar Formation and Nahal Shiqma. The Acheulian is associated with *Homo erectus* (Antón 2003). The

Archeulo-Yabrudian may be associated with a more modern hominins, found at the site of Qesem (Hershkovitz et al. 2011).

The Early Acheulian, best known from the site of Ubeidiya (Bar-Yosef and Tchernov 1972) is characterised by tools of a crude appearance, dominated by chopping tools, with some spheroids, trihedral picks and primitive handaxes (Ronen 1979:296). This site has been dated as being as old as 2.5 Ma (Repennig and Fejfar 1982), but is more likely ~1.4 Ma (Tchernov 1988b). Other sites with similar assemblages in Israel include Kefar Menahem, Negba and Evron Quarry (Ronen 1979).

The Middle Acheulian is known from Holon (Chazan and Horwitz 2007), Gesher Benot Ya'akov (Goren-Inbar et al. 2000), Bar'am, Yir'on, Oumm Qatafa and Tabun (Ronen 1979). It is characterised by the presence of bifaces, the use of a soft hammer and the absence of the Levallois technique (Ronen 1979).

The Late Acheulian era in Israel is characterised by the presence of both handaxes and Levallois products (Goren 1979; Goren-Inbar 1985). It was found at sites such as Avivim (Ohel 1990), Berekhat Ram (Goren-Inbar 1985), Mount Pua (Barkai et al. 2002) and Yrion (Ohel 1986).

The Acheulo-Yabrudian contains 3 major complexes: the Yabrudian, which is dominated by thick scrapers shaped by steep Quina retouch, the Acheuleo-Yabrudian, which has Yabrudian scraper and handaxes and the Pre-Aurignacian, which is dominated by blades and blade-tools (Jelinek 1982b). Sites with Acheulo-Yabrudian material include Jamal (Zaidner et al. 2005), Misliya (Weinstein-Evron et al. 2003) Tabun, (Jelinek 1982b) and Qesem (Barkai et al. 2002; Ben-Dor et al. 2011; Gopher et al. 2010; Hershkovitz et al. 2011). A partial face from a hominin (the ancestry of which is controversial, see Sohn and Wolpoff 1993) was recovered from the site of Zuttiyeh (Gassis and Bar-Yosef 1974), which is associated with the Acheulo-Yabrudian complex. An

incomplete femur from layer Ea and an isolated and worn molar from Tabun layer Eb (McCown and Keith 1939:10) are associated with the Acheulo-Yabrudian and have affinities with archaic *Homo* (Trinkaus 1995). Three permanent mandibular teeth from the lower part of the stratigraphic sequence, and 3 isolated permanent maxillary teeth and 2 isolated deciduous teeth from the Qesam Cave from the Acheulo-Yabrudian era, may show affinities with remains from Skhul and Qafzeh (Hershkovitz et al. 2011).

3.10.2.2. Middle Palaeolithic, 200 to 48 Ka

The Middle Palaeolithic in the Levant is characterised by the Levantine Mousterian that, in Israel, usually employs the Levallois technique (Bar-Yosef 1998), an approach to flaking from cores, which results in large flakes (Holdaway and Stern 2004:61–65) and is practically devoid of handaxes (Ronen 1979). In contrast to Europe, anatomically modern humans appeared precociously and temporarily in Levant far earlier, at approximately 100 ka (Mellars 2004), and so the Mousterian contains material manufactured by both Neanderthals and modern humans (Hovers et al. 1995). The moister MIS 6 to 5 climate conditions in the Saharan climate corridor may have facilitated the access of modern humans to Israel at this time (Frumkin et al. 2011).

Mousterian sites in the Levant concentrate on the coast of northern Israel and Lebanon but extend into southern Israel, Jordan and Syria (Henry 2003:12). The Mousterian layers (B, C and D) of Tabun have been used as a general framework for the subdivision of the Mousterian throughout the Levant (Copeland 1975), although this approach has been criticised (summarised by Hovers 1997) as not being regionally applicable, including diachronic industries and being incorrectly applied at some sites (Henry 2003). Others consider that a suitable degree of typological and technological variation can be included within the Tabun division (Bar-Yosef 1998). The Tabun B assemblage has been linked exclusively with Neanderthals (Bar-Yosef 1994) and the Tabun C assemblage is

considered related to anatomically modern humans, although Neanderthal specimens have been found associated with Tabun C. Elements of modern human behaviour were present in the Levant prior to 100 ka, despite the persistence of Middle Palaeolithic technology in the area (Grün et al. 2005).

The chronology of these industries remains divided between the 'long' (proposed by Mercier et al. 1995 and supported by Schwarcz et al. 1998; Schwarcz and Rink 1998; Valladas et al. 1998) and 'short' chronology (originally proposed by Grün et al. 1991 and slightly extended by advances in the electron spin resonance (ESR) technique by Grün and Stringer 2000).

Hominin remains have been recovered from practically every Levantine cave in which Middle Palaeolithic sediments are found (Hovers et al. 1995), including Amud, Kebara, Tabun, Dederiyeh, Ksar Akil XXV, Skhul and Qafzeh caves (Howell 1998). Of these specimens, those from Amud, Kebara, Ksar Akil XXV, Dederiyeh and the Tabun woman are considered Neanderthals, and those from Skhul, Qafzeh and possibly the Tabun C2 jaw are considered anatomically modern humans (Henry 2003). Uranium series dates obtained from the dentine of faunal material from layers containing late archaic (Neanderthal) and early anatomically modern human fossils from layer C of Tabun and XIX from Qafzeh demonstrated for the first time that these 2 species were living in the same period in the Levant (McDermott et al. 1993:253). The co-existence (though probably not co-habitation) of Neanderthals and modern humans in this region for approximately 20 to 30 ka differs greatly from the situation in Europe (Mellars 1989). The alternate presence of these 2 populations in the area may reflect variations in fauna or climate. No skeletal evidence survived of modern humans in the Levant between 75 ka and 45 ka, leading some authors to suggest that the early modern humans in this area became extinct before a new group arrived in the Upper Palaeolithic era (Shea and Bar-Yosef 2005).

The medium-large fauna at Levantine Mousterian sites includes mountain gazelle (*Gazella gazelle*), red deer (*Cervus elephas*), fallow deer (*Dama mesopotamica*), ibex (*Capra ibex*), wild boar (*Sus scrofa*), aurochs (*Bos primigenius*), equids and roe deer (*Capreolus capreolus*) (Liebermann and Shea 1994:303–304).

Interestingly, the different hominin species in the Levant in the Middle Palaeolithic era were producing and using indistinguishable Mousterian tools, hunting the same animals and behaving in other similar ways (Lieberman and Shea 1994), which has led some researchers to claim that there were few behavioural differences between these *Homo* species in the Levant (e.g., Clark and Lindly 1989). Despite this, cementum increment analysis suggests that modern humans at Qafzeh and Tabun layer C had a circular residential mobility strategy (based on a hunting pattern focused on hunting gazelle only during spring and summer) while Neanderthals practised a more locally intensive radiating mobility pattern at Kebara and Tabun layer B (Lieberman and Shea 1994:301). This is supported by lithic evidence, which suggests that Neanderthals hunted more often than anatomically modern humans (Lieberman and Shea 1994).

3.10.3. Levantine Archaeological Sites in this Study

3.10.3.1. Skhul

The site of Skhul is a small cave with a large associated terrace, which is located in a small valley immediately north of the site of Tabun, approximately 20 km south of Haifa. The site was the subject of a test excavation in 1929 by Kitson-Clark before substantial excavations in 1931 and 1932 by McCown (McCown 1932; 1933). Because of the indurated nature of the site stratigraphy (composed of a limestone breccia), large blocks were removed *in situ* and transported to London, where the skeletal material was extracted (Ronen 1982).

The site contained at least 10 hominins, as well as isolated fragments of skeletal material (McCown and Keith 1939:2–8). These have been classified as anatomically modern humans (Stringer et al. 1989), despite showing morphological variation, which overlaps with the Neanderthal range (Corruccini 1992). The fossils, specifically Skhul I, show distinctly non-European characteristics (Minugh-Purvis 1998).

The site has 4 distinct stratigraphic units: A, B1, B2 and C (Ronen 1982). The B layers contain all hominin fossils (Stringer et al. 1989) and are rich in Levallois Mousterian artefacts (McCown and Keith 1939). Layer C is present in bedrock depressions and contains worn and rolled pre-Mousterian flint implements, which may correlate to the Lower Palaeolithic layers at Tabun (Ronen 1982), although this correlation may be complicated by the complex depositional history of Skhul (McDermott et al. 1993).

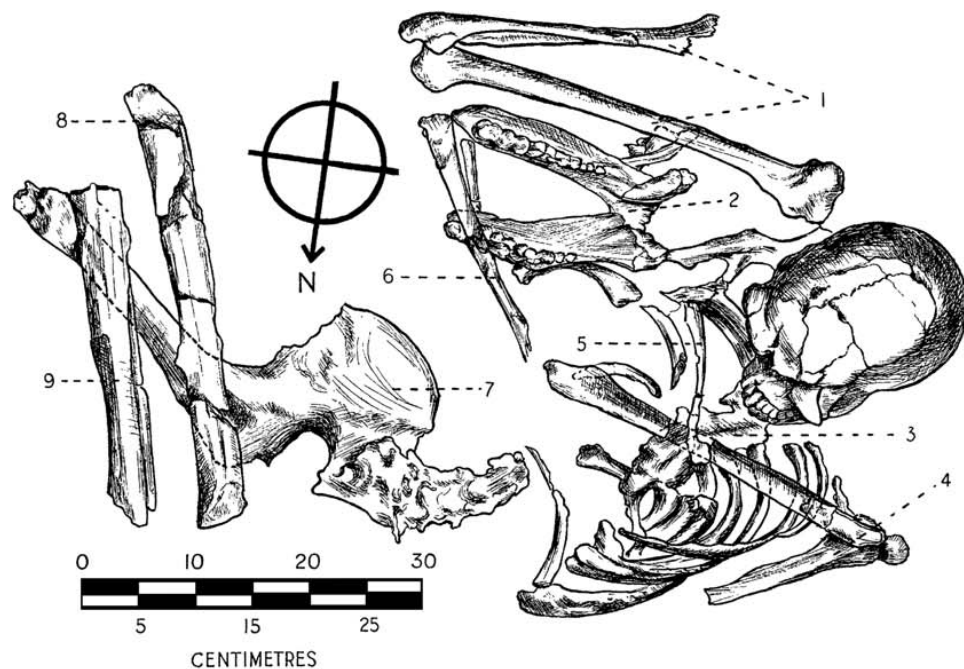
The dating of Skhul is complicated by the apparently intentional nature of the burials, as grave cuts may have penetrated from layer A into layer B (Grün et al. 2005). Thermoluminescence (TL) dating of the flints from layer B provides ages in the range of 99 to 134 ka (Mercier et al. 1993). ESR dating suggests an age of 100 to 135 ka (Grün et al. 2005). Amino acid racemisation provides dates in the range of 35 to 55 ka, although these values may be affected by inaccurate temperature corrections and the use of preservatives on these samples (Masters 1982).

Skhul V is buried with its arms surrounding the lower jar of a boar, suggesting symbolic intent (d'Errico et al. 2010), although it has been claimed that this was inserted after burial (McCown and Keith 1939). In a similar fashion, shells from this site dated to 120 ka are interpreted to have been used for body decoration and possibly as grave goods (Vanhaeren et al. 2006). Ochre located within layer B may have been deliberately heated in order to change its colour,

suggesting possible use for artistic purposes, indicating modern human behaviour (d'Errico et al. 2010). Rock engravings are present at the site and are similar to other Holocene aged features found on the western side of Mount Carmel (Ronen and Barton 1981).

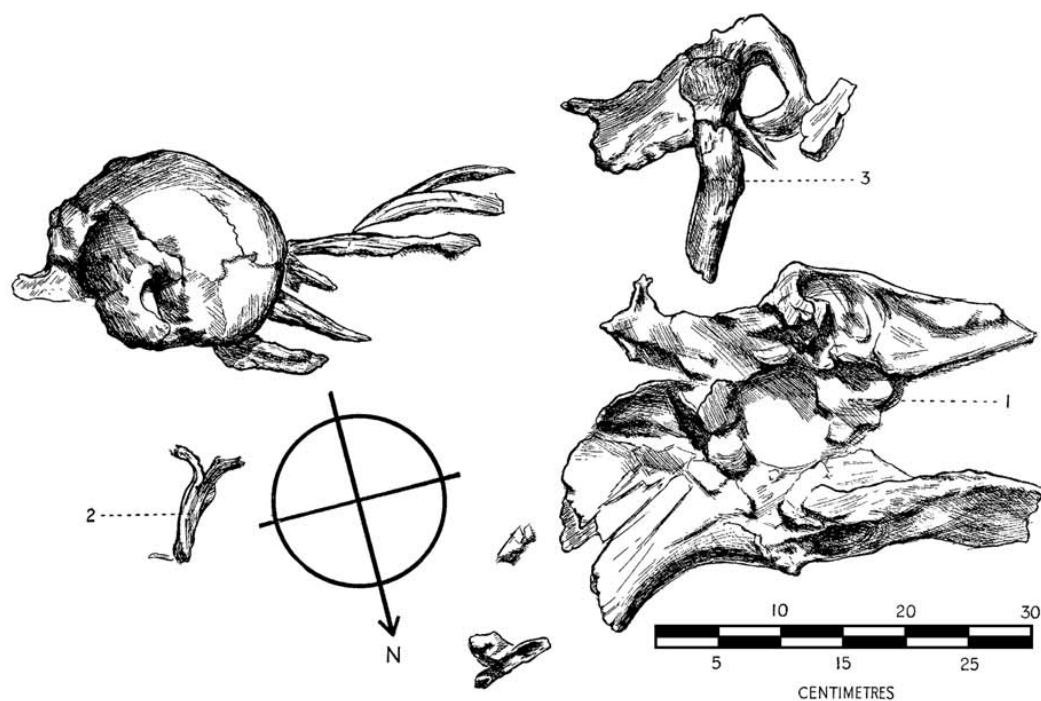
The site of Skhul is located in the Albian-Cenomanian aged Yagur/Kammon Formation Dolostone and is located immediately to the east of the Quaternary coastal sediments and kurkar ridges (Sneh, Bartov and Rosensaft 1998a). There are small outcrops of faulted Upper Cretaceous undifferentiated basalt, gabbro, as well as ultramafic pyroclastics and flows (Sneh, Bartov and Rosensaft 1998a). Turonian aged limestone, marl and dolostone from the Bina Formation is extensively exposed to the north, east and south of the sites, as well as minor outcrops of chalk and marl of the Senonian-Palaeocene Mount Scopus Group, dolostone, limestone and chalk of the Cenomanian Sakhnin and Yanuh formations and Albian-Cenomanian limestone, dolostone, marl, chalk and chert (Sneh, Bartov and Rosensaft 1998a). Soils on the coastal plain are dominated by red sandy soils, including sandy regosols, red sandy loam, red sandy clay loam, Nazaz soils and red sandy 'Husmas' soils, all of which derived their high clay content from aeolian processes (Singer 2007). Soils on Mount Carmel include *Terra rossa* on hard limestone and dolomite, rendzina soils on chalk or marlk and brown forest soils and brown rendzina soils on hard carls or carbonate crusts (Singer 2007:90).

A



2. Plan of the contracted burial of a tall male, Skhul V. 1, right arm; 2, Pig's mandible; 3, dorsal vertebrae; 4, left scapula and humerus; 5, left clavicle; 6, left radius; 7, right ilium; 8, left femur; 9, left tibia and fibula.

B



2. The incompletely preserved skull and skeleton of an adult male, Skhul IX. 1, crushed bovid skull and maxilla; 2, spine of the left scapula; 3, left femur, with adjacent parts of the left pelvis.

Figure 3.30 Plan of A) Skhul V Showing the Pig's Mandible (2) From Which Sample 1058 Derives and B) Skhul IX with the Bovid Skull (1) From Which Sample 1057 Derives (Garrod and Bates 1937)

3.10.3.2. Tabun

The site of Tabun, first excavated by Garrod in the 1930s and located approximately 20 km south of Haifa at the entrance to Wadi Mughara (Schwarcz and Rink 1998) has a long sequence of archaeological material from the Yabrudian to end of the Middle Palaeolithic (Rink et al. 2004). Following the initial excavations in the 1930s (Garrod and Bates 1937) excavations have been undertaken by Jelinek (1982; Jelinek et al. 1973) and Ronen (Ronen and Tsatskin 1995). The site consists of 3 circular chambers, containing a composite sedimentary sequence of approximately 25 m thickness (Jelinek et al. 1973).

The site has one of the most impressive and diverse sequences of archaeological material in the Levant and is used as a reference sequence for the middle and late Pleistocene, although some researchers consider this inappropriate (Hovers 1997). Layers Ed, Ec, Eb and Ea contain Acheulian and Yabrudian industries with the Amudian industry between Eb and Ea, the lower Levantine Mousterian in layer D and the later Levantine Mousterian in layers C and B (Rink et al. 2004). Flint procurement strategies have been studied for this site using cosmogenic isotopes and suggest that artefacts procurement during lower layer E differed markedly from layers above and below (Verri et al. 2005).

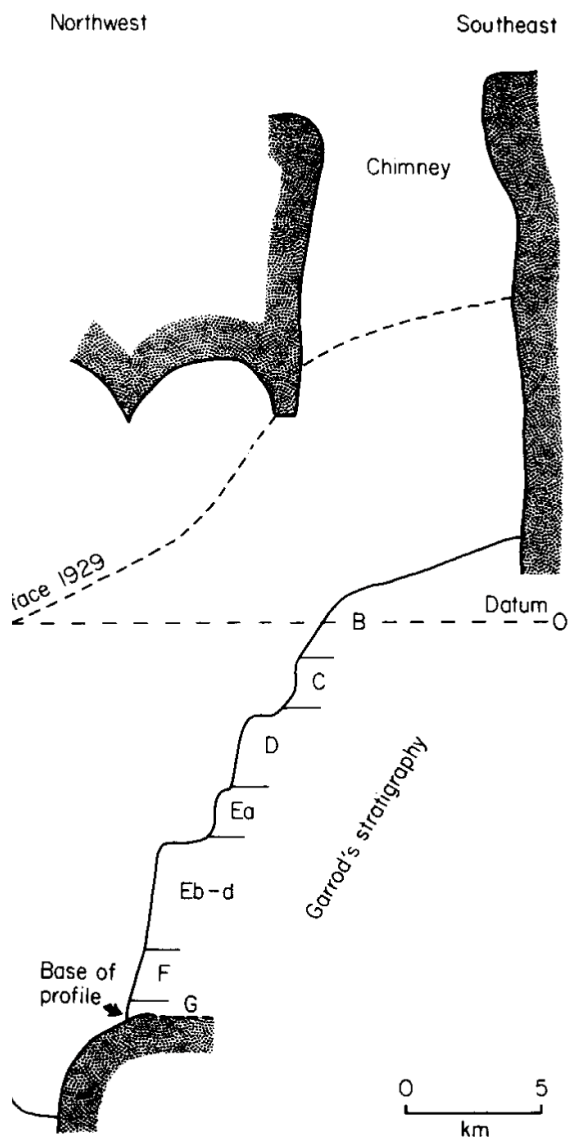


Figure 3.31 Garrod's Stratigraphy of Tabun (Bull and Goldberg 1985)

The stratigraphy of the site, as defined by Garrod, contained 7 principal layers, of which 1 was later subdivided (Ronen 1982). These are summarised in Table 3.3.

Layer	Description
A	1 m thick and disturbed
B	3.5 m thick with an Upper Mousterian industry and abundant <i>Dama mesopotamica</i> remains
C	1.7 m with a Middle Mousterian industry and a complete female hominin skeleton and an additional lower jaw
D	2.3 m thick Lower Mousterian with long and narrow Levallois points
E	5 m thick unit containing handaxes and scrapers divided into layers Ea to Ed. Human femur found in upper level
F	1.9 m thick with Upper Acheulian industry
G	2 m thick, coarse flake industry devoid of handaxes

Table 3.3 Garrod's Stratigraphic Units for Tabun and Original Interpretation of Lithic Technology (Garrod 1934)

These units were further subdivided by Jelinek (1982b: 60) into 130 separate geological contexts, which are grouped into 14 major stratigraphic units, many of which lie within Garrod's layer D. Garrod's stratigraphy is retained in this study, as all sample were collected with reference to this system. The sequence from G to D appears to represent 1 continuous period of deposition, with only occasional interruption (Farrand 1979). Layers G, F and the lower half of E consist of fine well sorted sand while the upper part of E is silty and layer D is 55 to 80% silt (Farrand 1979) and contains pollen suggesting a warm, dry period (Jelinek et al. 1973). The sands in layers G to D are thought to be derived through aeolian delivery of coastal material from a sea level highstand, with the decrease in sand in E and D reflecting the retreat of this source (Bull and Goldberg 1985). In layers G to D, well crystallised hydroxylapatite occurs in vugs and vein, as well as finely disseminated as cement through the sediments (Goldberg and Nathan 1975). Scanning electron microscope (SEM) data suggest that the highest degree of post-depositional chemical alteration of the sediments has occurred in layers F and G (Bull and Goldberg 1985). A dramatic change exists between D and C, as C comprises thinly bedded red, pink, white and black sediment, including ash and charcoal (Goldberg and Nathan 1975). This may be the results of an enlargement of the chimney above the cave, allowing the access of sediments from the plateau above and facilitating a change in the chemical weathering regime (Farrand 1979). Level C

shows evidence of aggregation, has abundant charcoal and its pore contain sparitic coatings, suggesting strong secondary precipitation of calcite (Albert et al. 1999:1255). The white layers in C are composed of ash, with small amounts of *Terra rossa* soil and phosphatised material (Albert et al. 1999). Pollen analysis conducted on the sediments from Tabun indicated that C and D were deposited under cooler and more humid conditions (Jelinek et al. 1973). Layers A and B consist mainly of red clay, limestone fragments and bone breccias (Goldberg and Nathan 1975). Thin section analysis of level B shows the material is a moderately to non-aggregated red clay matrix, which incorporates 15 to 20% quartz silt and sand (Albert et al. 1999:1254). In layers A, B and C, large limestone almost always have a rind of dahllite alternative with amorphous MnO₂, which has precipitate from fluids formed the dissolution of bone by slightly acidic solutions (Goldberg and Nathan 1975). Bone are preserved in layers A and B, rarely in C but not in D-G (Goldberg and Nathan 1975).

The nature of the archaeological assemblages found in the site have been the subject of intense debate. In summary: layer G is interpreted as Acheulian, Layers Ed to Ea are a superposition of Acheulian, Acheuleo-Yabrudian and Yabrudian material, layers Ea and D contain a transitional phase in which the Levallois method appears, layers D to B contain Mousterian, which has been divided in Tabun type D, Tabun type C and Tabun type B (Mercier et al. 1995).

Two hominins plus multiple isolated fragments were recovered from the site of Tabun (McCown and Keith 1939:9–10). There remains significant uncertainty about the stratigraphic and taxonomic position of the important hominins from Tabun, principally due to the thinning of Garrod's units close to the cave wall (Stringer 1998:33). The Tabun C1 skeleton can be robustly attributed to the Neanderthal species (Stringer 1998), however the classification of the Tabun C2 mandible remains more problematic (Stefan and Trinkaus 1998; Quam and Smith 1998:407), and is considered by some authors to be an anatomically modern human (Vandermeersch 1989). While it is found in layer C, it is generally attributed to being intrusive from layer B by Garrod and Bates (1937).

If it is actually *in situ*, it may be more than 100 ka older than the Neanderthal specimens found at Kebara (Valladas et al. 1998). Seven additional human teeth from Tabun were recently located in the collections of the Natural History Museum, which have all been attributed to the same individual, Tabun BC7 (Coppa et al. 2005). This individual has been dated to 82 ± 14 ka (early uptake) and 92 ± 18 ka (linear uptake) and tentatively identified on being associated with layer B both on chronological and uranium concentration grounds (Coppa et al. 2005).

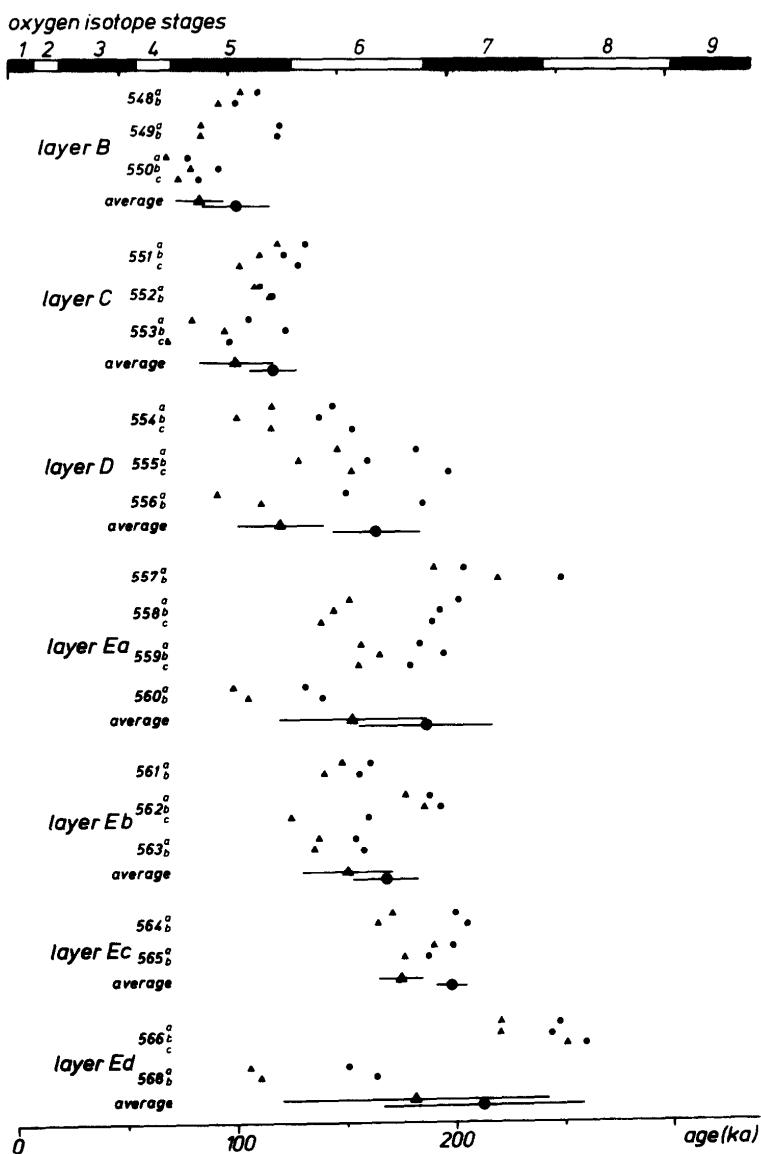


Figure 3.32 Original ESR Chronology for Tabun (Grün et al. 1991:234)

Dating of this site remains controversial, after an initial assessment of Tabun C1 as approximately 50 ka (Jelinek 1982a), approximately doubled by Grün et al. (1991) by dating fauna from Garrod's collection with ESR and subsequently slightly increased by revision of these dates based on improvements in the technique (Grün and Stringer 2000). TL dating of flints by Mercier et al. (1995) has provided a considerably older chronology for all layers with layer C dated at 171 ± 17 ka, layer B dated at 263 ± 27 ka, layers Ea to D 270 ± 22 ka, layers Eb to Ea 306 ± 33 ky, layers Ec to Eb 350 ± 33 ka and layer Ed 331 ± 30 ka (Mercier et al. 1995:501). ESR dating of a cervid tooth found *in situ* revealed a date for the Tabun E industry, which sits between the 'long' and 'short' chronologies (Schwarcz and Rink 1998). An age obtained from direct gamma spectroscopy dating of the Tabun C1 specimen (Schwarcz et al. 1998) is substantially younger than the ESR or TL chronology but has been the subject of methodological criticism (Millard and Pike 1999). Combined ESR/U-series dating by Rink et al. (2004) has provided a date of $387 + 49/-39$ ka for the lowest part of layer Ed, which is in good agreement with the 'long' chronology. Amino acid racemisation dating provides an age of 63 to 81 ka for lower layer C and 83 to 87 ka for the upper part of layer E (Masters 1982).

For this research the revised ESR chronology of Grün and Stringer (2000) is used on the basis that it directly dated the material analysed in this thesis.

Layer	Early Uptake ESR	Linear Uptake ESR	U-Series/ESR
B	102 ± 17	122 ± 16	$104 +33/-18$
C	120 ± 16	140 ± 21	$135 +60/-30$
D	133 ± 13	203 ± 26	$143 +41/-28$
Ea	176 ± 22	213 ± 32	$208 +102/-44$
Eb	180 ± 32	195 ± 37	
Ec	198 ± 51	220 ± 63	
Ed	149 ± 17	191 ± 28	

Table 3.4 Modified ESR Dates for Tabun (Grün and Stringer 2000:602)

Recent controversy has emerged concerning the possible marine inundation of the sites in the Wady el-Mughara valley prior to their uplift to their present position due to elevated sea levels at approximately 120 ka based on the presence of abraded artefacts, marine fossils and interpreted marine sediments (Vita-Finzi et al. 2007b). The interpretation of these features as related to inundation has subsequently been contested (Ronen et al. 2007) and defended (Vita-Finzi et al. 2007b) with the most recent analysis suggesting that the caves were not inundated (Zviely et al. 2009). Regardless of the caves' inundation or otherwise it seems clear that the low lying Carmel coastal plain would have been inundated at 125 ka during the peak of interglacial MIS 5e (Zviely et al. 2009).

The site of Tabun is located in Albian-Cenomanian aged Yagur/Kammon Formation Dolostone and is located immediately to the east of Quaternary coastal sediments and kurkar ridges (Sneh, Bartov and Rosensaft 1998a). Small outcrops of faulted Upper Cretaceous undifferentiated basalt, gabbro, as well as ultramafic pyroclastics and flows (Sneh, Bartov and Rosensaft 1998a). Turonian aged limestone, marl and dolostone from the Bina Formation is extensively exposed to the north, east and south of the sites well as minor outcrops of chalk and marl of the Senonian-Palaeocene Mount Scopus Group, dolostone, limestone and chalk of the Cenomanian Sakhnin and Yanuh formations and Albian-Cenomanian limestone, dolostone, marl, chalk and chert (Sneh, Bartov and Rosensaft 1998a). Soils on the coastal plain are dominated by red sandy soils, including sandy regosols, red sandy loam, red sandy clay loam, nazaz soils and red sandy 'husmas' soils, all of which derived their high clay content from aeolian processes (Singer 2007). Soils on Mount Carmel include *Terra rossa* on hard limestone and dolomite, rendzina soils on chalk or marlk and brown forest soils and brown rendzina soils on hard carls or carbonate crusts (Singer 2007:90).

3.10.3.3. Amud

The Middle Palaeolithic archaeological site of Amud is located approximately 4 km north-west of the Sea of Galilee (Schwarcz and Rink 1998) near Kibutz Hukok. It is a cave site approximately 30 m above the present channel bed of Wadi Amud with a small chamber, a large open middle terrace and a lower sloping terrace (Madella et al. 2002). This cave configuration is relatively recent, probably forming in the late Upper Pleistocene. The archaeological site was originally excavated in the 1960s, and a well preserved, complete Neanderthal skeleton (Amud I) being recovered from the upper layers (Suzuki and Tanaka 1970). Fifteen other, mainly fragmentary, individuals have subsequently been recovered during excavations in the 1990s (Hovers et al. 1995). All hominin skeletal remains were found in layers B2 and B1 (Belmaker and Hovers 2011).

The site of Amud has a highly variable stratigraphy with 2 principal units (subdivided into a total of 6 subunits) reaching a maximum depth of 4 m (Chinzei 1970). Unit A contains archaeological material from the Bronze Age to the present and is broken into 2 subunits (A1 and A2) (Chinzei 1970). The uppermost unit, A1, covers the entire Amud deposit at a relatively uniform thickness and comprises deep brown reddish brown clay with organic material and limestone, basalt and quartz grains (Chinzei 1970). Unit A2 is discontinuous and is found mainly in pits intrusive into the underlying unit B (Valladas et al. 1999). A2 has a variable composition, which varies between pits, however is distinctive based on the presence of many pottery fragments (Chinzei 1970). Unit B comprises layers B1, B2 and B4, which are interbedded calcareous silt, calcareous concretions and black soils probably principally derived from anthropogenic ash and contain Palaeolithic archaeological material (Madella et al. 2002). Layer B3, also a component of unit B, comprises archaeologically sterile limestone gravels (Chinzei 1970). Layer B1 was further divided into horizons 6 and 7 and B2 into horizons 8 to 10 in the later excavation (Valladas et al. 1999). The sediments of units B1-B4 are variably

cemented across site in a fashion that cross cuts stratigraphic boundaries (Shahack-Gross et al. 2008).

Sixteen hominins were found in Amud with this assemblage dominated by infants and young children (Hovers et al. 1995). The almost complete skeleton of Amud 1 (found in layer B1/6) has been interpreted as a Neanderthal (Lavi 1994), although its taxonomic status has been widely discussed (Day 1986; Trinkaus 1983; Wolpoff 1980) based on its mixture of archaic and modern traits (Suzuki and Tanaka 1970). Amud II, found in layer B2/8, is represented by a fragment of the right maxilla and has been identified as an adult Neanderthal (Suzuki and Tanaka 1970). Amud 7, a 10-month-old infant found in layer B2/8 has also been identified as a Neanderthal and was found with a red deer maxilla leaning against its pelvis (Rak et al. 1994). The short duration of sediment accumulation at Amud suggest that all of burials on the site may represent a single, biologically homogeneous sample (Hovers et al. 1995:55).

The lithic industries are broadly from the Levantine Mousterian but are quite variable between stratigraphic units (Hovers 1997). Layer B contains well mixed Levalloisio-Mousterian elements and Upper Palaeolithic tool forms, which are interpreted as a transitional industry (Wantabe 1970).

Faunal analysis, particularly of subunits B1, B2 and B4 has yielded a rich assemblage of material (Takai 1970). The medium-large mammalian fauna is dominated by gazelle (*Gazella gazelle*), fallow deer (*Dama mesopotamica*), wild goat (*Capra aegagrus*), red deer (*Cervus elaphus*), aurochs (*Bos primigenius*), wild boar (*Sus scrofa*) and rhinoceros (*Dicerorhinus hemitoechus*) in diminishing abundance with carnivores, particularly larger species, being rare (Rabinovich and Hovers 2004). This distribution is similar to other late Mousterian Levantine archaeological sites as is the age and body part distribution of gazelles, which is indicative of hunting rather than scavenging as the principal source of meat (Rabinovich and Hovers 2004).

Layer B1/6, believed to be the same level as Amud I (Hovers et al. 1995), was dated with ESR to 43 ± 5 ka (early uptake)/ 48 ± 6 ka (linear uptake) (Schwarcz and Rink 1998) and subsequently to 53 ± 8 ka using combined ESR/U-Series (Rink et al. 2001). The top of level B has been dated based on 2 sub-samples of an artiodactyl tooth collected on the surface as 41 ± 3 and 42 ± 3 (early uptake) and 49 ± 4 and 50 ± 4 (linear uptake) (Grün and Stringer 1991). The underlying B2/8 has been dated as 59 ± 8 (early uptake) and 70 ± 8 (linear uptake) (Schwarcz and Rink 1998), which broadly agree with TL dates of 50 to 60 ka (Rak et al. 1994), 56.5 ± 3.5 ka (Valladas et al. 1999) and a subsequent a combined ESR/U-Series date of 61 ± 11 k (Rink et al. 2001). TL dates for level B4 gave an age of 68.5 ± 3.4 ka (Valladas et al. 1999). Combined ESR/U-series dates for level B5 gave ages of 70 ± 11 ka and 113 ± 18 ka (Rink et al. 2001).

A variety of specialist studies have been undertaken on material from Amud. Oxygen and carbon isotope analysis on calcite material found in possible hearths in this site show a high proportion of wood ash as a source (Shahack-Gross et al. 2008), which may suggest that the site has been subject to low levels of post-depositional diagenesis (Shahack-Gross et al. 2004). Rodent assemblages from MIS 4 and the transition to MIS 3 suggest that climate shifts during this period did not significantly affect small mammals in this region (Belmaker and Hovers 2011). Phytolith studies from Amud show that wood was burnt as fuel by Neanderthals and that fig and wild cereals were utilised as food (Madella et al. 2002).

Environmentally, Amud is on the eastern edge of the present day Mediterranean region (which is dominated by oak-pistachio woodlands and maquis) and so semi-steppic and steppic plants begin to dominate locally (Zohary 1973). This location provided local access to a mosaic of vegetation types, which would have been sensitive to shifts of climate (Madella et al. 2002). Carbon and oxygen isotope results from Qafzeh suggest that the surrounding area was more open than today, containing mesic and semi-arid

woodland and bushland (Hallin et al. 2012). Layers XVI to XXIV are dominated by micro-invertebrates, suggesting more ephemeral use of the site (Tchernov 1981) and isotopic results from these levels suggest extremely arid conditions locally (Hallin et al. 2012:71).

The site is located within the Middle Eocene Bar Kokhba Formation Limestone with Miocene sandstone, mudstone, conglomerate and limestone immediately adjacent to this unit in all directions (Sneh, Bartov and Rosensaft 1998a). Pliocene-Pleistocene basalt is present to the east and west of the site and particularly abundant to the north-east and south in all directions from the site along with smaller outcrops of Quaternary sediments, Lower to Middle carbonates, Senonian-Palaeocene chalk/clay/marl and Turonian Bina Formation carbonates (Sneh, Bartov and Rosensaft 1998a). Basalt derived vertisols, limestone and dolomite derived *Terra rossa*, chalk and marl derived rendzina and hard chalk or carbonate crust derived brown rendzina soils are present locally (Singer 2007).

3.10.3.4. Qafzeh

Qafzeh cave, on Mount Precipice near Nazareth, was excavated by a joint Israeli and French team in the 1960s and 1970s. This site has yielded more than 18 hominin specimens, which are classified as anatomically modern humans with some archaic features (Vandermeersch 1966; 1969a; 1970; 1981). While many of these specimens were fragmented, 3 were articulated partial skeletons. Important for understanding the history of human evolution, ESR and U-series dates from layer XIX in the range of 85 to 110 ka, (McDermott et al. 1993) and isochron analysis (Aitken and Valladas 1993) corroborate earlier TL (Valladas et al. 1987; 1998) and ESR (Schwarcz et al. 1988) in placing the occupation of this site in MIS 5 and suggesting that these anatomically humans may be older than the Kebara Neanderthal and possibly coeval with the Tabun C1 Neanderthal.

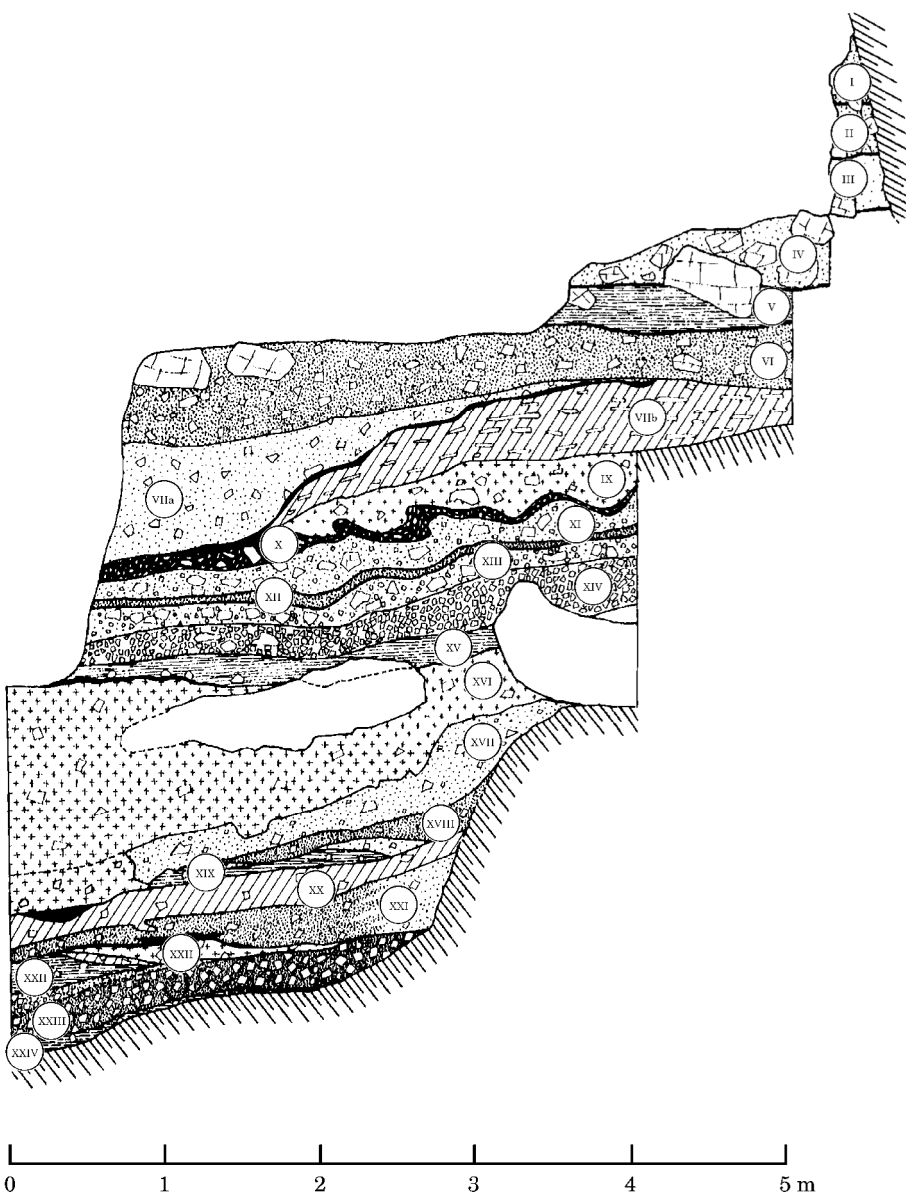


Figure 3.33 North-South Stratigraphic Profile of Qafzeh Cave at Western Excavation Limit (Vandermeersch 1981:28)

The skeletal materials from Qafzeh are quite variable in skeletal morphology, with some displaying primitive features in their cranial morphology despite their clear anatomically modern human origins (Vandermeersch 1981). Most burials (including Qafzeh 8: a partial adult skeleton, Qafzeh 9: an almost complete adult skeleton, Qafzeh 10: a child's skeleton, Qafzeh 12: a child's cranium, Qafzeh 14: a fragmentary child's cranium and Qafzeh 15: the upper portion of a child's skeleton) were located in layer XVII (Gargett 1999). Qafzeh 11; the upper portion of an infant was located in layer XXII (Gargett 1999) associated

with fallow deer antlers (Vandermeersch 1970). Qafzeh 13, an incomplete foetal cranium, was located in layer XVa (Gargett 1999).

The 4.5 m thick Mousterian sequence is broken into 2 major units: the first (layers V-XV) contains abundant broken mammal bones, lithic artefacts, the second (layers XVII-XXIV) contains abundant micro-vertebrate remains and all human skeletal material (Valladas et al. 1988). Layers XXIV to XVII also contain hearths and large mammal remains (Tchernov 1988a). In contrast, the later (currently undated) Middle Palaeolithic stratigraphic layers (XV to III) contain no human remains, micro-fauna and scanty evidence for fire use (Hovers et al. 2003).

The stratigraphy of the talus slope looks superficially quite simple, with cemented calcareous scree with finer grained intervals dominating, although micro-morphological examination demonstrates additional complexity (Goldberg 1980). Layers VII to X are rich in woody fragments and contain voids filled with secondary manganese, layers XI to XVO are rich in secondary soil carbonate, including rinds, cement and nodules suggesting arid conditions, layers XVII to XX have less secondary carbonate and more woody fragments and layers XXI to XXIV consist of loose bedrock scree with little or no fine grained matrix suggesting minimal available water (Goldberg 1980). TL dates exhibited no systematic increase in age in with depth (Valladas et al. 1988) suggesting a very rapid sedimentation rate, possibly by freeze-thaw activity (Farrand 1979:377).

Carbon and oxygen isotopic analysis of gazelle and goat enamel from Qafzeh suggest that in the lower layers conditions were extremely arid surrounding this site while in the upper units the site was surrounded by semi-arid semi-bushland (Hallin et al. 2012). The faunal assemblage from Qafzeh VI to XV suggests a more permanent hominin presence and a more ephemeral/seasonal presence in layers XVI to XXIV (Lieberman and Shea 1994:318).

The lithic assemblage at Qafzeh is Levantine Mousterian (Hovers 2009). The lithic assemblage from the levels associated with most of the hominin fossils (XVII-XXIV) are of the Tabun C type, with a relatively high percentage of radial Levallois flakes and cores with radial/centripetal preparation (Boutié 1989). Ochre has also been found on this site (Vandermeersch 1969b) and the geochemistry and lithology of this ochre may provide information about the mobility of population (Hovers et al. 2003). The presence of (naturally) perforated shells transported over 40 km that may have been strung as a necklace and smeared with ochre in layers XXIV, XXIII, XXII and XXI of Qafzeh has significant implications for the evolution of modern human behaviour (Bar-Yosef Mayer et al. 2009).

The geology immediately surrounding the site is Cenomanian Sakhnin and Yanuh formations comprising dolostone, limestone and chert (Sneh, Bartov and Rosensaft 1998a). To the south, east and west of the site are extensive Quaternary sediments and extensive but often discrete basalt outcrop of both the Pliocene-Pleistocene Cover and Dalwe Basalt and the Miocene Lower and Intermediate Basalt (Sneh, Bartov and Rosensaft 1998a). Carbonate sediments of the Senonian-Palaeocene Mount Scopus Group, Turonian Bina Formation, Lower to Middle Eocene Adulam Formation, Lower to Middle Eocene Timrat, Meroz and Yizre'el Formations are extensively exposed to the north and sparsely exposed to the south (Sneh, Bartov and Rosensaft 1998a). Limestone and dolomite derived *Terra rossa* soil, chalk and marl derived rendzina and hard chalk or carbonate crust derived brown rendzina soils are present locally and to the north of the site (Singer 2007). Vertisols, including non-saline vertisol on alluvium, slightly saline and alkaline vertisol on alluvium and non-saline and non-calcareous vertisol on basalt are common on the Quaternary alluvium and basalt in the area (Singer 2007).

3.10.3.5. Holon

Holon is a Late Lower Palaeolithic site located on the coastal plain immediately south of Tel Aviv (Horwitz et al. 2007). The site was excavated between 1963 and 1970 by Tamar Noy and has been recently re-examined (Chazan and Horwitz 2007). The site extends as a single layer over 150 m² (Yizraeli 1967). The lithic assemblage is considered Middle or Late Acheulian (Yizraeli 1967), with the handaxes and choppers being produced offsite (Chazan 2000a; 2000b). The site has a broad spectrum of faunal material, high minimum numbers of identified species, low incidence of hominin damage to bone, bones and teeth of large sized species, no evidence of fire/hearths or redistribution of food and has thus been interpreted as a multiple mortality/scavenging open-air site (Horwitz et al. 2007).

The site is located in the Quaternary kurkar sediments and the stratigraphy comprises palaeosols and aeolinites (Porat et. al. 1999). Soils on the coastal plain are dominated by red sandy soils, including sandy regosols, red sandy loam, red sandy clay loam, Nazaz soils and red sandy 'Husmas' soils, all of which derived their high clay content from aeolian processes (Singer 2007). ESR dates of *Bos* teeth from the artefact bearing unit (stratum C, see Yizraeli 1967) yielded ages of 204 ± 16 ka and optically stimulated luminescence (OSL) dates of approximately 200 ka (Porat et al. 1999).

3.11. Palaeolithic Archaeology of Southern France

3.11.1. Overview

The Lower to Middle Palaeolithic southern France is a key location for understanding the evolution of modern humans. This region has a rich archaeological record and history of investigation, and research in this area has led to the definition of many of the key periods and raised many of the major

questions in Palaeolithic archaeology. This region has been occupied sequentially by *Homo erectus* and *Homo neanderthalensis*.

3.11.2. Key Periods in This Study

3.11.2.1. Lower Palaeolithic, 2.6 Ma to 250 Ka

Acheulian assemblages are dominated by the presence of handaxes (bifaces), which originated in east Africa approximately 1.5 million years ago (Villa 1983:6). The Archeulian was manufactured by *Homo erectus* and *Homo heidelbergensis* and dates between 1.5 and 0.3 Ma (Ambrose 2001). This term originally designated a particular chronological and technological stage in the stratigraphic succession of the region of Saint Acheul in the Somme Valley (e.g., Flower 1860), extended more broadly within France (de Mortillet 1869) and then extended to other regions (such as the Middle East and Africa, see Clark 1966), where it has come to represent a technocomplex (Clark 1968). Procurement distances of Archeulian stone are rarely more than 20 km away (Hay 1976).

Europe was probably not continuously occupied by hominins until 600 to 500 ka (Roebroeks 2001), although the earliest human presence in Europe has been dated to 1.8 Ma (Gabunia et al. 2000; Vekua et al. 2002). At some stage during the Upper Palaeolithic era, *Homo erectus* were replaced by Neanderthals, possibly with *Homo heidelbergensis* as a transitional species (Mounier et al. 2009).

3.11.2.2. Middle Palaeolithic, ~250 to 48 Ka

In Europe, the Middle Palaeolithic appears to have been exclusively occupied by Neanderthals (Mellars 1996). Distinguishing between the Lower Palaeolithic

and Middle Palaeolithic era is difficult, particularly given the patchy and poorly dated nature of the Lower Palaeolithic record; however, the prime hallmark of Middle Palaeolithic technology is the emergence of more complex and sophisticated patterns of prepared core flaking, such as the Levallois technique (White and Ashton 2003).

The Mousterian stone artefact assemblage shows great variability, having a number of facies, each of which contains broadly the same type of tools, but in different frequencies (Brose and Wolpoff 1971). The interpretation of this assemblage, made famous by the ‘Bordes-Binford’ debate (detailed by Wargo 2009) suggests that the variation between Mousterian tool types is the result of different functional use (Binford and Binford 1966; 1969) or of different cultures (Bordes and Sonneville-Bordes 1970). The currently accepted technocomplex sequence of the Mousterian, from oldest to youngest, is: Asinipodian/Typical/Ferrassie Mousterian, Quina Mousterian, Levallois Denticulate Mousterian, Mousterian of Acheulian tradition and Discoid Denticulate Mousterian (Discamps et al. 2011:2757).

More than 50 cave and rock shelter sites exist in south-west France, many of which have a long and detailed sequence of occupation (Mellars 1996). Strong ecological gradients would have existed, particularly during the cold periods of the Middle Palaeolithic era, and so many different biotic environments would have been accessible within a few days walk of the Perigord region (Mellars 1985).

3.12. French Archaeological Sites in this Study

3.12.1.1. La Chapelle-aux-Saints

The site of La Chapelle-aux-Saints was first excavated in 1908 and yielded a nearly complete specimen of a Neanderthal (Bouyssonie, Bouyssonie and

Bardon 1908; 1913) of around 30 years of age (Dawson and Trinkaus 1997). The excavators identified 6 strata: stratum 1 is a yellowish marly clay with a wide distribution inside the modern cave and out onto the cave apron near the entrance, stratum 2 is clay, stratum 3 represents recent rubble breakdown, stratum 4 is large roofall clasts, stratum 5 is the bedrock of the cave and stratum 6 is a scorched soil at the interface between stratum 1 and 2 (Gargett 1989). More recent excavations by Rendu in the region of bouffia 118, which is 50 m from the burial cave, delineate 2 stratigraphic units known as layers 1 and 2.

The Neanderthal skeleton, which is considered the ‘classic’ example of its type (Trinkaus 1985), has been the subject of extensive investigation, including examination of vertebral osteoarthritis (Dawson and Trinkaus 1997), consideration of the effectiveness and extent of pre-death dentition (Tappen 1985), level of language development (Lieberman and Crelin 1971), pathology (Trinkaus 1985) and the postcranial dimensions (Trinkaus 2011). The stone artefact assemblage of La Chapelle-aux-Saints is characterised as La Quina Mousterian, although a number of Aurignacian elements are present, such as thin retouched blades, carinated end scrapers and long, possibly pressure-flaked blades (Bardon and Bouyssonie 1908).

ESR dates from fauna from stratum 1 show ages of 47 ± 3 ka (early uptake) and 56 ± 4 (linear uptake) (Grün and Stringer 1991).

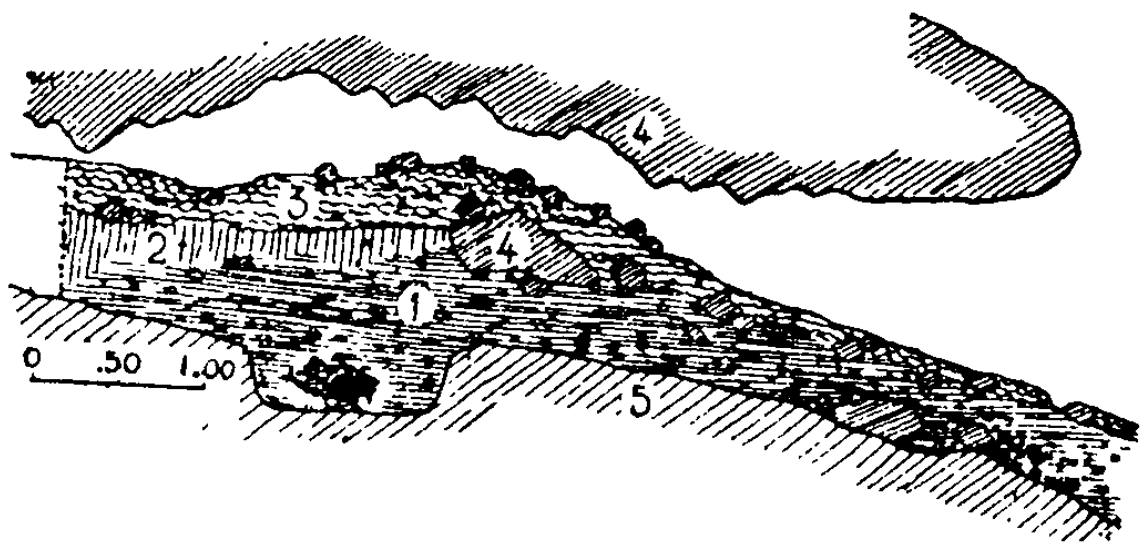


Figure 3.34 Stratigraphic Section of La Chapelle-aux-Saints (Bouyssonie et al. 1908)



Figure 3.35 The Archaeological Site of La Chapelle-aux-Saints During Sample Collection

3.12.1.2. Les Fieux

The archaeological site of Les Fieux is located approximately 3 km north-west of the village of Miers in the department of Lot. The site is contained in an extensive karstic network, and is divided into a number of sectors, each with a varied stratigraphy as shown in Figure 3.37 (Champagne et al. 1990). The site contains archaeological material from the Middle Ages to the Mousterian era and was originally excavated from 1967 to 1991 (Champagne et al. 1990). The site differs from many others in the region by being located on a plateau, rather than in the local river valleys (Guillermin 2006).

A hominin child's molar has been located in layer G7 (Champagne et al. 1990). Stone artefacts from this site have been included in regional analysis of whether hunting became more specialised in the Upper Palaeolithic era (Grayson and Delpech 2002) and if stone artefact richness varies between the Mousterian and the Aurignacian eras (Grayson and Coe 1998). Layer G7 contains many stalagmite fragments and abundant micro-fauna (Champagne et al. 1990). Les Fieux has a faunal assemblage dominated by a single species.

Rock art is an important component of the site, with 14 handprints, dozens of red dots, bone splinters in the wall and a series of figures, including ibex, horse and mammoth (Jaubert 2008). This rock art may include pieces from the Aurignacian, the Gravettian and more recent periods which have been investigated using Raman microscopy (Smith et al. 1999). The site contains a stalagmite, which may have been used as a Palaeolithic 'lithophone' (used as a percussion instrument by striking) (Dams 1985).

Level Fi1 (Porche section) has been dated at $23,900 \pm 33$ BP, and level Sauveterrian (west of the Porche section) is dated at $9,450 \pm 190$ BP (Guillermin 2006).



Figure 3.36 The Archaeological Site of Les Fieux During Sample Collection

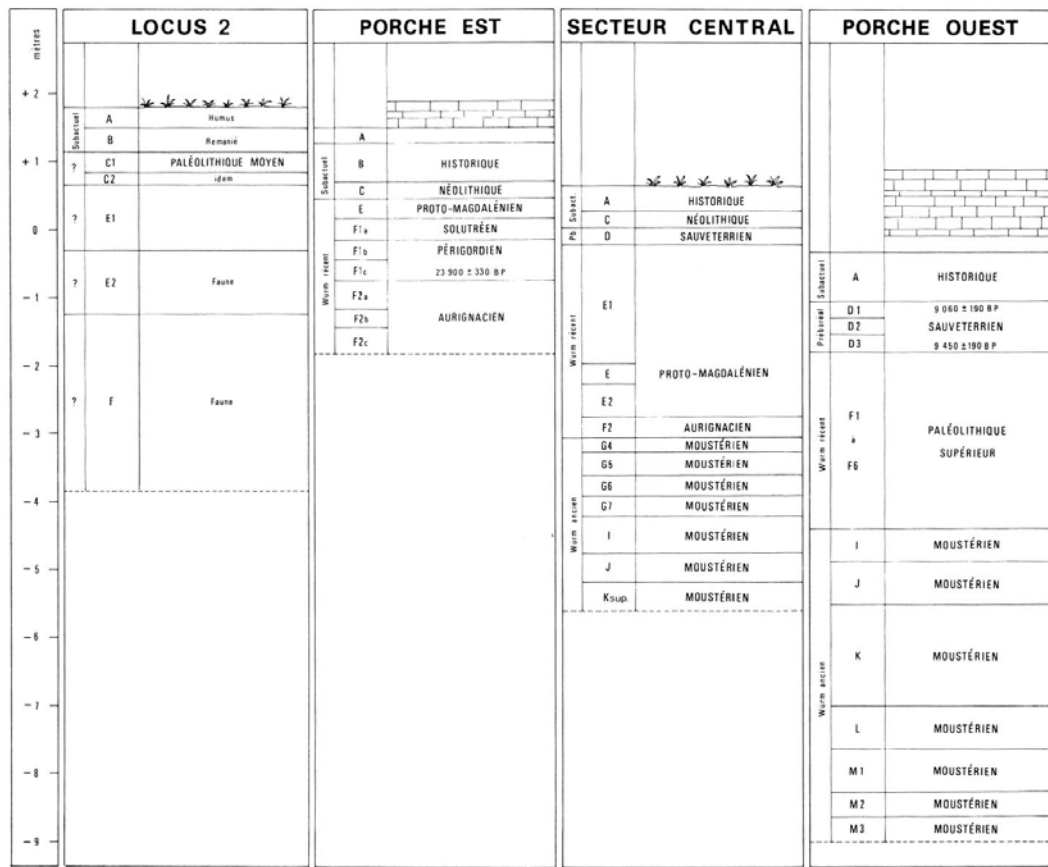


Figure 3.37 Stratigraphy of the Archaeological Site of Les Fieux (Champagne et al. 1990:5)

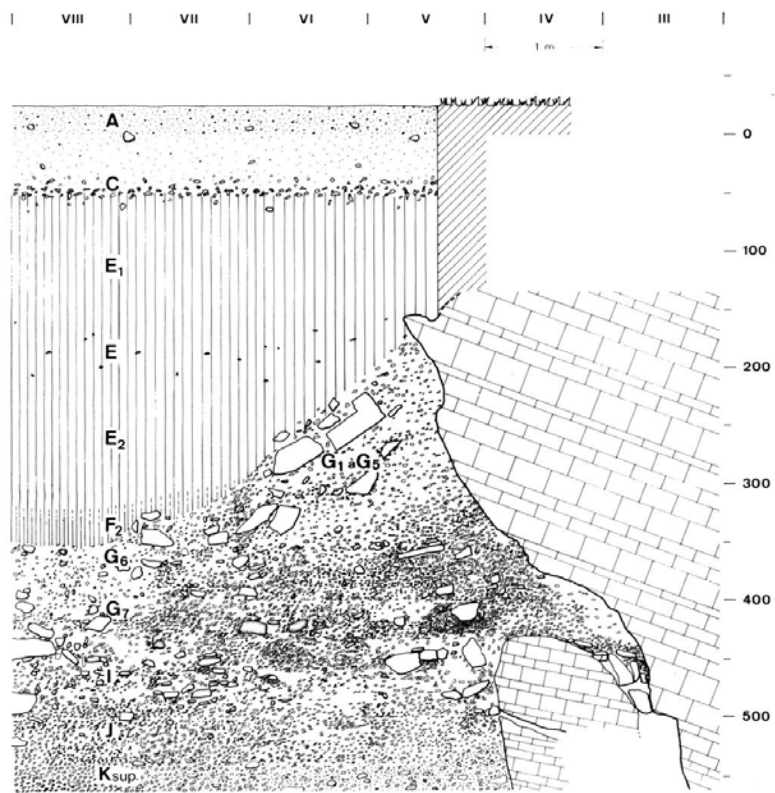


Figure 3.38 Stratigraphic Section of the Secteur Central of the Archaeological Site of Les Fieux (Champagne et al. 1990:6)

The site is located in interbedded Bathonien Jurassic marl, limestone and micrite (BRGM 1996), with similar material present in all directions for a considerable distance.

3.12.1.3. *Le Moustier*

The rock shelter of Le Moustier, near Les Eyzies in the Dordogne region has 2 components: the upper (or ‘classic’) shelter excavated by Lartet and Christy, from which the definition of the Mousterian period is based, and the lower shelter excavated by Hauser and later Peyrony, which yielded 2 Neanderthal skeletons. These include a late adolescent (Le Moustier I) discovered by Hauser in 1908 (Hauser 1909) and an infant (Le Moustier II) excavated by Peyrony in 1914 (Gargett 1989).

Le Moustier I is the only adolescent Neanderthal specimen to preserve associated dental, cranial and postcranial elements (Thompson and Illerhaus 1998). The specimen was nearly destroyed during the Second World War and the skull was only located in 1965 (Ponce De León and Zollikofer 1999). It has been the subject of multiple different physical and computer reconstructions (Ponce De León 2002; Ponce De León and Zollikofer 1999; Thompson and Illerhaus 1998). The neonatal Neanderthal, which was misplaced until 1996, was re-examined and is the youngest Upper Palaeolithic Neanderthal found to date (Maureille 2002).

The stratigraphy of the lower shelter is subdivided into 12 units, of which the lower A to F are fluvial sediments from the Vézère River and the upper G to L contain archaeological material (Valladas et al. 1986). These units have been further subdivided based on sedimentological (Laville 1975) and palynological data (Paquereau 1975).

The principal sedimentary, palynological and archaeological reference on the lower shelter of Le Moustier is Laville et al. (1980), which informs the following description, unless otherwise noted. Layers A to C contains a Typical Mousterian archaeological assemblage and contain abundant fluvial sand with no evidence of cryptoclastic processes suggesting (in combination with the pollen from these layers) relatively temperate and humid conditions. Layers D to E have insufficient archaeological material to permit interpretation. Layer D contains abundant evidence of fluvial activity and the pollen suggests a low percentage of arboreal trees. Layer E is a thick and homogenous clay with a pollen spectrum with 45% arboreal species, suggesting temperate conditions. Denticulate Mousterian is found in layer F, which contains fresh, angular cryoclastic eboulis, suggesting a cold period. Mousterian of Acheulian tradition type A in level G, which is cryptoclastic in nature, suggests moderately cold conditions during its formation and is topped by a well-developed soil profile, which has been truncated before the deposition of layer H. Layer G2 is considered to have been subject to a less cold, more humid climate than the

other G layers. Level H contains a Mousterian of Acheulian Tradition type B assemblage and is considered to have been cold and humid through levels H1 to H2c, as evidenced by the numerous altered eboulis and the clay rich but carbonate impoverished sedimentary matrix. Layers H3 through H9 were cold and dry, as suggested by the voluminous eboulis and absence of matrix leaching in the sediments. Level I contains a Denticulate Mousterian assemblage, and while it is heavily damaged by cryoturbation, is interpreted, due to the presence of water laid sediments, as representing milder and more humid conditions. Level J contains Typical Mousterian and is interpreted to have been deposited under cold and dry conditions due an abundance of cryoclastic eboulis and an unaltered sedimentary matrix. Above level J, a break in sedimentation and period of erosion is interpreted, based on the abrupt truncation of the Mousterian archaeological material. Level L contains an Aurignacian I assemblage. Layer K contains a Chatelperronian assemblage. Layer G, which is the focus this study, is interpreted as being cold and dry.

A subsequent excavation by Geneste in 1982 in the lower shelter recovered material for TL dating of layers G to K (Valladas et al. 1986). This TL dating provided mean ages of 42.6 ± 3.7 ka for layer K, 40.3 ± 2.6 ka for layer J, 40.9 ± 5 ka for layer I, 42.5 ± 2 ka for layers H2 to H9, 46.3 ± 3 ka for layer G4 and 55.8 ± 5 ka for layer G1 (Valladas et al. 1986:452). ESR dating of material from layers G to K was undertaken by Mellars and Grün (1991).

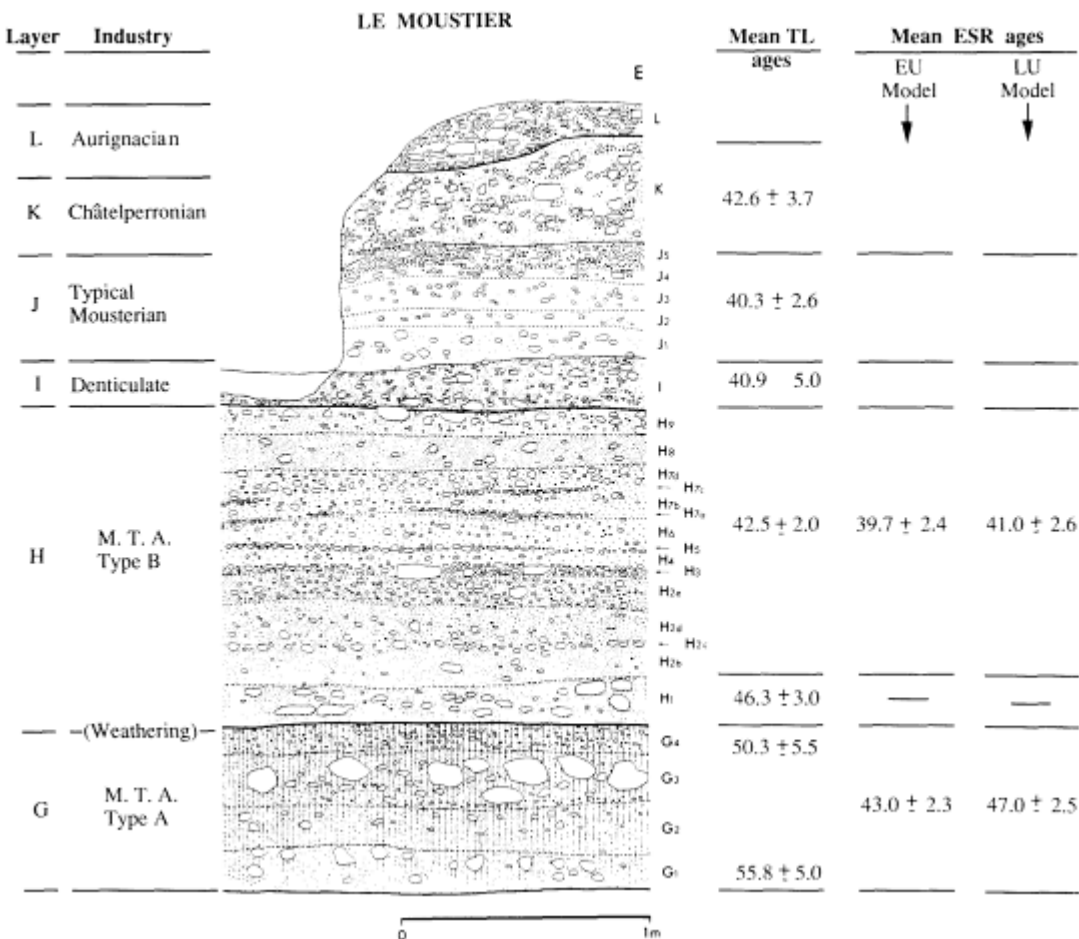


Figure 3.39 Stratigraphic Section of Le Moustier (Mellars and Grün 1991)

The site is located in the formation des Eyzies Coniacian (Late Cretaceous) aged fossiliferous limestone (BRGM 2000). The surrounding area is dominated by shallowly dipping, similar material, with some Jurassic limestone outcropping approximately 10 km to the south (BRGM 2000).

3.12.1.4. Pech de l'Azé II

The archaeological site of Pech de l'Azé II, located approximately 2 km north of the Dordogne Valley and 5 km east of Sarlat, was excavated by Bordes in the period 1950 to 1969 (Bordes 1972b). It is part of a complex of 4 separate rockshelter sites (Pech de l'Azé I to IV), 1 of which has yielded the skull and mandible of a Neanderthal child (Soressi et al. 2007). The site of Pech de l'Azé

II consists of both a large chamber and a now-collapsed rock shelter (Laville et al. 1980). Engraved and perforated artefacts from layer 4a and layer 7, respectively, represent very early occurrences of this kind of artefact (Bordes 1969).

The stratigraphy of the site is divided into 9 units, some of which are further subdivided, shown in Figure 3.40 (Goldberg 1979). The stratigraphy (in contrast to many rock shelters in the region, which are dominated by coarse bedrock debris), is dominated by clay and silty sands with occasional layers of bedrock clasts (Goldberg 1979:19). Detailed sedimentological (Laville et al. 1980), palynological (Paquereau 1975) and micro-morphological (Goldberg 1979) work was undertaken on the section.

The nature of the archaeological assemblages and the climatic interpretation of the sediments from Pech de l'Azé II were summarised by Laville et al. (1980:180–181), and inform all of the information in this paragraph unless otherwise noted. Layers 8 to 9 of this site have 'Meridonal' Acheulian assemblages of a primitive type (Laville et al. 1980). Layer 9 is interpreted to have been deposited in cold and dry climatic conditions based on the presence of stony eboulis of fairly voluminous proportions, although the upper part of this unit may have been subjected to a warmer and more unstable climate. Pollen from layer 9 suggests an environment between cold steppe and cold meadowland, with an arboreal component of less than 5% made up exclusively of pine. Layer 8 is interpreted to have been deposited under cold and very humid conditions on the basis of smaller eboulis than in layer 9 in the lower part of this unit, and less cold and very humid conditions in the upper part. This change is reflected in the pollen from this unit, which shows an increase in arboreal material from 5% at the base to 12% at the top. The assemblage suggests a cool parkland environment, with a more diverse assemblage of trees, including pine, birch and hazel. Layers 7 to 6 both contain an Acheulian assemblage similar to layers 8 to 9. Layer 7B is interpreted to have been deposited under moderately cold and very humid conditions, as reflected by the

presence of sandy material thought to be derived by fluvial action from the adjacent plateau, while layer 7A was deposited under mild and very humid conditions, as suggested by the abundant fluvial sands and gravels. The pollen from layer 7B suggests a cool parkland environment, while in layer 7A a temperate forest exists, with an arboreal component of more than 32%.

Red deer is ubiquitous in the upper layers, dominating in 2A to 2C and 9 and being joined by bovid in 2D, 2F and 8, reindeer in 2E, 2F, 2G, 2G, 3, 4A, 4B, 4D and 4E, horse in 4B and 4C and 8, and rabbit in 5 (Bordes 1972b).

Dating of R was carried out by Grün et al. (1991) using the ESR technique and yielded ages in the range of layer 2 (54 to 59 ka), layer 3 (60 to 72 ka), layer 4 (71 to 87 ka), layer 5 (128–145 ka) and layer 6 to 9 (130 to 162 ka). There is a clear hiatus between layers 5 to 9 and 2 to 4, which reflects the stage 5e climate optimum (Grün et al. 1991).

The site is located in Coniacien (late Cretaceous) sandy bioclastic limestone (BRGM 1986), with shallowly dipping similar material to the north and west. To the east and north-east, Jurassic limestones are extensively exposed (BRGM 1986). To the south, extensive Quaternary sediments are exposed, interspersed with Cretaceous limestones and Jurassic limestones and dolomites (BRGM 1990).

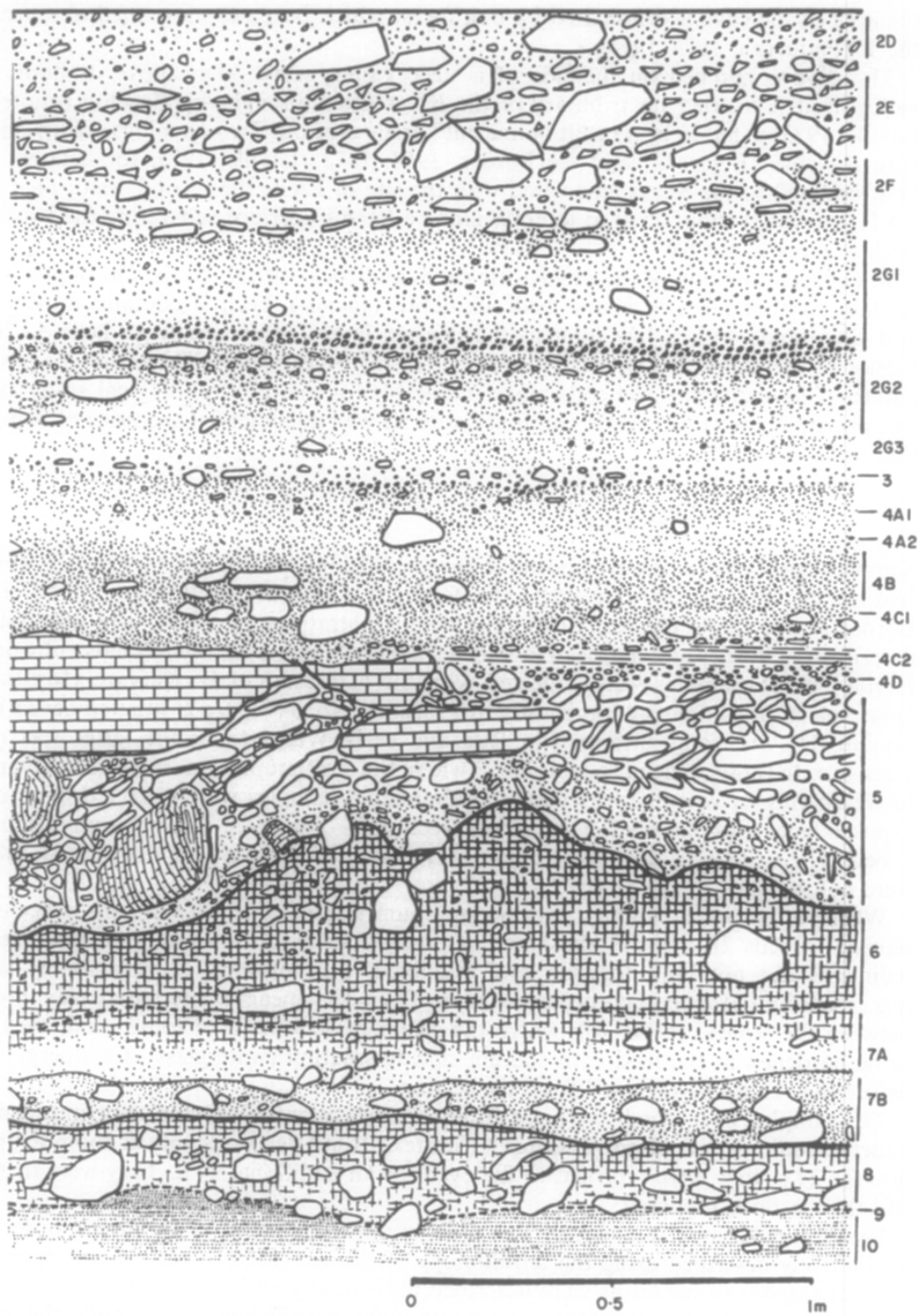


Figure 3.40 Stratigraphic Section of Pech de l'Azé II (Goldberg 1979)

3.12.1.5. Bois Roche

Bois Roche is a small cave located in the ground of a château of the same name, near the city of Cognac in the Charente region of south-central France. The site contains a wide range of faunal material and a very sparse collection of stone artefacts and is interpreted to have been principally a hyena den, with occasional incursion from humans (Villa et al. 2010). The site has 2 principal stratigraphic layers, which have been subdivided into a number of subsidiary units with layer 1c and 2 contain an overwhelming majoring of the faunal material (Villa et al. 2010:922). ESR age estimations from layers 1c and 2 in squares C4, B4, Z4 and Z2 (see Figure 3.41) provide dates that are statistically indistinguishable, with an averaged value of 69.7 ± 4.1 ka (Villa et al. 2010:922).

The site was first excavated by Vandermeersch from 1978 to 1981; however, the results from this investigation remain unpublished. Bartram and Villa and subsequently Villa excavated the site from 1995 to 2000, with the faunal and stone artefact assemblage being described in a number of publications (d'Errico and Villa 1997; Villa and Soressi 2000), which include notable references to flaked bone (Villa and Bartram 1996) and a refutation of the presence of perforated material (d'Errico and Villa 1997). Flint artefacts are rare at this site, with 480 (of 551) smaller than 2 cm and only 20 being flakes or flake fragments (Villa and Soressi 2000). Levallois flakes and a core are present (Villa and Soressi 2000:190).

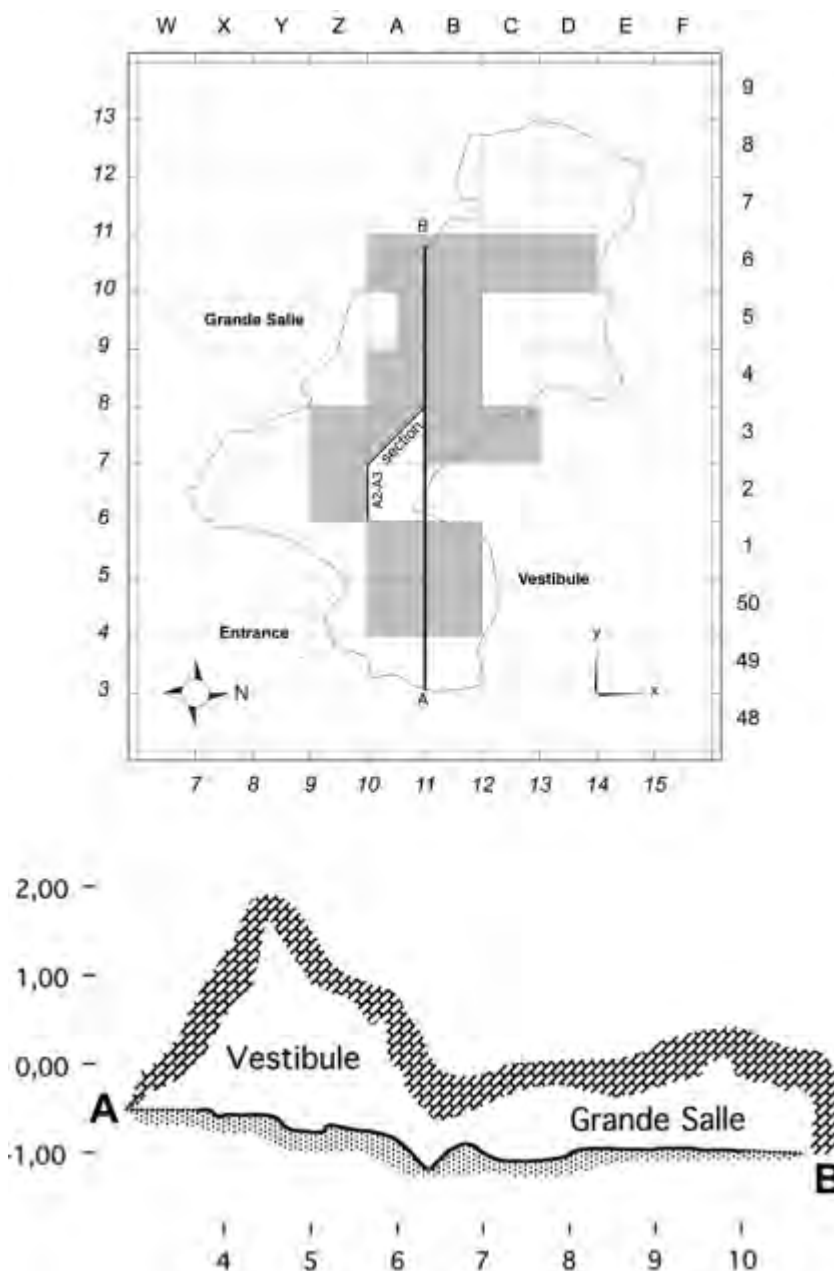


Figure 3.41 Plan View of the Excavation Squares at Bois Roche and a Cross-Section of the Cave

The faunal assemblage is dominated by ungulates with bovid (*Bos* or bison) and horse (*Equus caballus*) making up the principal prey animals. Hyenas, including a large number of juveniles, are the principal carnivores in the assemblage. The lithic artefact assemblage is sparse; however, it contains a very large component of small debris, flakes and flake fragments (Villa and Soressi 2000). Palaeo-environmental conditions during shelter occupation are interpreted to have been cold and dry with *Artemisia*, *Cyperaceae* and *Poaceae*

dominating the plant assemblage. This suggests the region was part of the Central European steppe (Villa et al. 2010:933).

Soil micromorphology in units 1b and 1c show a dominance of laminated silts and clays, while units 1d and 2 show extensive bioturbation (Goldberg 2001:166). Coprolites make a significant contribution to site sediments, as do post-depositional precipitation and dissolution of calcite and phosphate (Goldberg 2001:167).

The site is located within shallowly dipping Santonien (Upper Cretaceous) limestone in a sub-surface cave (BRGM 1968). Limestones surround the site in all directions for more than 10 km, with Jurassic material exposed to the north and north-east (BRGM 1985), Cretaceous to the east and south-east (BRGM 1967), south and south-west (BRGM 1977a), and west and north-west (BRGM 1968).

3.12.1.6. Rescoundudou

The Mousterian site of Rescoundudou is located approximately 10 km north-east of Rodez in the area of Sébazac-Concourès (Aveyron). The site was excavated by J Jaubert in the period 1981 to 1987. It is interpreted as a Neanderthal hunting camp, occupied between 75 to 13 ka, with abundant horse and fallow deer present as game. Five Neanderthal teeth, including 3 maxillary and mandibular deciduous teeth, a fragment of a permanent lower molar and the germ of a permanent upper lateral incisor, were found in unit C1 (Jaubert and Maureille 2008).

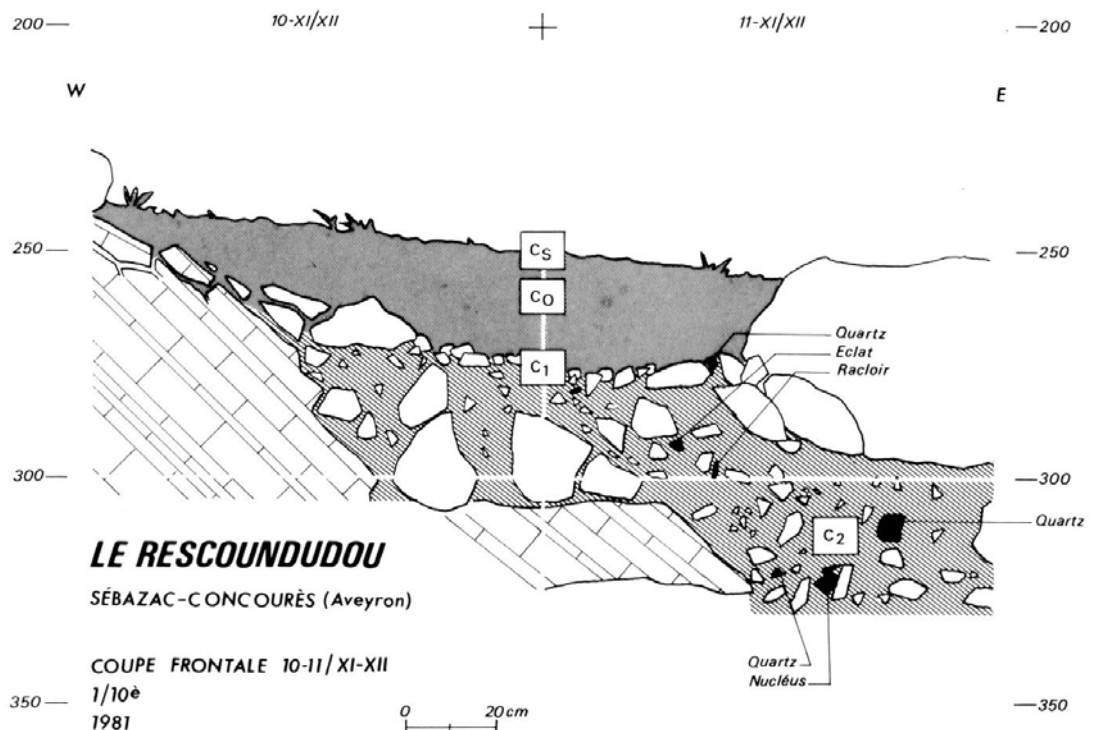


Figure 3.42 Stratigraphy of the Rescoundudou Archaeological Site (Jaubert 1983)

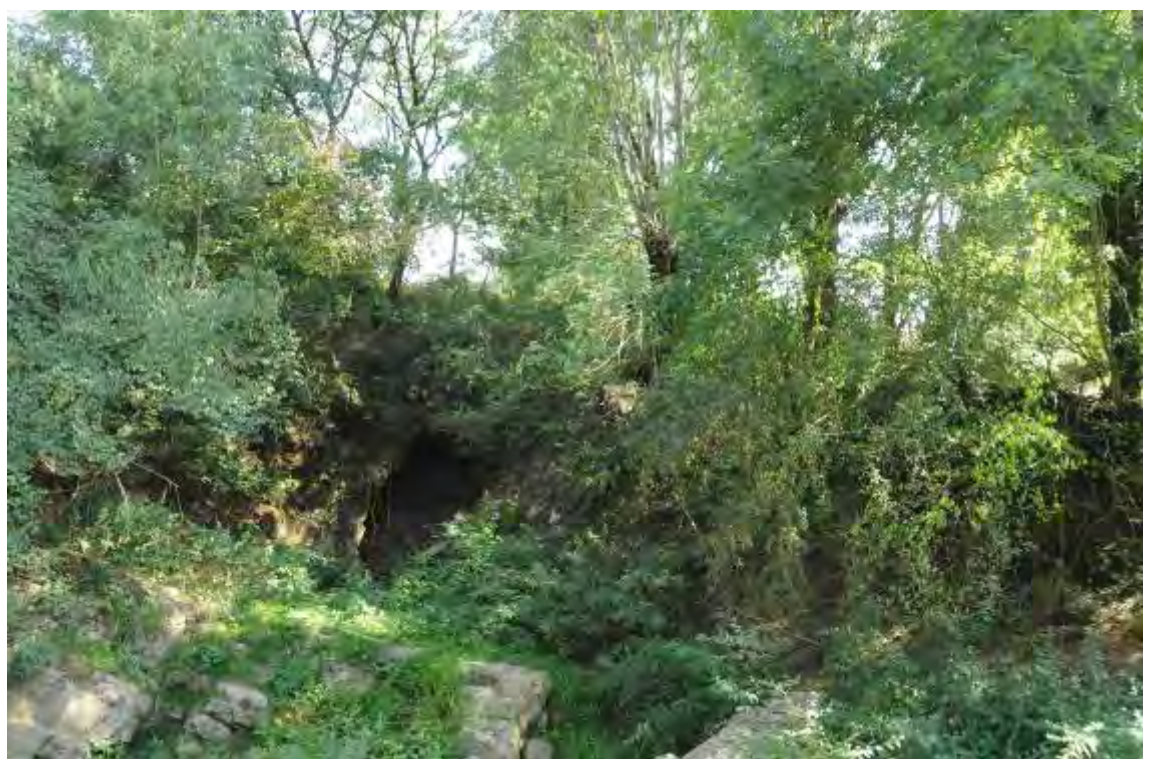


Figure 3.43 Archaeological Site of Rescoundudou During Sample Collection

The original stratigraphy of the site was divided into layers A, B and C, although A and B are soil layers and contain only some protohistoric material. C, which is divided into 3 subunits, contains Mousterian material (Jaubert 1983). Further analysis led to the subdivision of these layers into A1 and A2, B1 to B3, C1a,b,c,d,e,f and g to c and C2 (Jaubert and Maureille 2008). New units were created, including D1, D2, E1, F, E2 and E3, (Jaubert and Maureille 2008), with E2 and E3 containing Mousterian artefacts (Jaubert et al. 1992). A speleothem (layer F) overlays E2 and E3 and has been dated using U-series. This has provided age estimates of 123 +11.7 to 10.2 ka, 139.5 +11.7 to 68.2 ka, 115.6 +16.9 to 14.1 ka and 104.2 +96.8 to 41.7 ka (Jaubert et al. 1992). While layer C1 has not been directly dated, the faunal assemblage reflects the mild conditions of MIS 5C or 5A.

The lithic assemblage with C1 of Rescoundudou is Mousterian (Jaubert 1983). The faunal material, principally from Unit C1 is dominated by horse, daim, red deer, auroches (*Bos primigenius*), rhinoceros, wild cat (*Felis silvestris*) and bear (Jaubert and Maureille 2008).

The site is located within a Jurassic lacustrine limestone (unit J2a), with a conformable contact of Jurassic bioclastic limestone (unit Ji) present immediately to the south of the site (BRGM 1988). Less than 500 m to the south of the site is a reverse faulted contact to Sinemurien (Jurassic) calcarenites (unit I3 to 4) and other Jurassic carbonate sediments (BRGM 1988). Granites, granodiorites, gneisses and amphibolites are present to the south and south-east of the site within approximately 7 km. The granite batholith de la Margeride is exposed within 15 km to the north and schists and micaschists are exposed to the north-east (BRGM 1989). Extensive Miocene-Pleistocene volcanic material outcrops to the east and north-east of the site (BRGM 1989).

3.13. Summary

This chapter reviewed the archaeological, geological, physiographic, biotic and pedological background to southern France and Israel during the Lower to Middle Palaeolithic. Further, detailed consideration was given to the faunal species analysed and the archaeological sites from which these fauna derived.

Chapter Four: Methods

4.1. Overview

This chapter summarises the procedures used for sample collection, processing and analysis of strontium isotope values in this thesis. The relationship of the faunal material analysed using LA-MC-ICPMS to their respective archaeological sites is also discussed.

4.2. Mapping Samples

4.2.1. Israel 2008

Soil and rock samples were collected throughout Israel (excluding the West Bank and Gaza strip) in September and October 2008 by Ian Moffat. Sample locations, shown in Table 4.1 and Figure 4.1 were chosen with reference to a digital 1:200000 geological map of Israel viewed on the Global Positioning System (GPS) Utility program on a Toshiba Satellite Pro laptop in the field with positions being continually updated from a Garmin 12XL GPS using the Old Israel Grid co-ordinate system. Photographs were taken both of the general site and of the geological and pedological features of interest using a Nikon D300 camera with a 18 to 200 mm lens mounted on a Manfrotto tripod. Soil samples were collected for each visible soil layer and grain size, sphericity, roundness, grain sorting, Munsell colour and pH were recorded in the field. Rock samples were taken for the principle geological unit present on each site and a brief description of the lithology made in the field.

Site	Zone	Easting	Northing	Lithology From Field
IS001	36S	682494	3621957	Calcareous Sandstone 'Kurkar'
IS002	36S	675689	3585175	No Bedrock
IS003	36S	680980	3601307	No Bedrock
IS004	36S	681536	3604285	Calcareous Sandstone
IS005	36S	684801	3623556	Reefal Limestone
IS006	36S	685092	3621362	Reefal Limestone
IS007	36S	683780	3603356	Limestone
IS008	36S	687978	3609221	Chalk
IS009	36S	695586	3650202	Calcareous Sandstone 'Kurkar'
IS010	36S	705301	3661995	Limestone
IS011	36S	712541	3662131	Limestone
IS012	36S	719243	3659214	Chalky Limestone
IS013	36S	721813	3649514	Chalky Limestone
IS014	36S	696501	3627390	No Bedrock
IS015	36S	702082	3634803	Limestone
IS016	36S	710374	3639794	Chalky Limestone
IS017	36S	723533	3637663	Chalky Limestone
IS018	36S	712855	3636020	Chalky Limestone
IS019	36S	692598	3615897	Limestone
IS020	36S	690737	3609663	Chalky Limestone
IS021	36S	688498	3621292	Limestone
IS022	36S	689525	3626157	Chalky Limestone
IS023	36S	710592	3607373	No Bedrock
IS024	36S	738739	3623292	Basalt
IS025	36S	733524	3592864	No Bedrock
IS026	36S	726755	3596839	Limestone
IS027	36S	718214	3624458	Limestone Breccia
IS028	36R	694759	3520900	Limestone
IS029	36R	685424	3540358	Limestone
IS030	36S	684603	3564722	No Bedrock
IS031	36S	674516	3554072	No Bedrock
IS032	36R	711495	3520928	Chalk
IS033	36R	670914	3516771	No Bedrock
IS034	36R	656001	3503878	Poorly Consolidated Beach Ridge
IS035	36R	670060	3475507	No Bedrock
IS036	36R	672342	3445622	Chalk
IS037	36R	670360	3419638	Chalky Limestone

Site	Zone	Easting	Northing	Lithology From Field
IS038	36R	650790	3375244	Fossiliferous Limestone
IS039	36R	671031	3396724	Limestone
IS040	36R	678358	3388028	Obsidian
IS041	36R	693961	3345350	Chalky Limestone
IS042	36R	694321	3325656	Limestone
IS043	36R	696254	3302117	No Bedrock
IS044	36R	692862	3296795	Granite/Granodiorite
IS045	36R	683919	3271361	Granite/Granodiorite
IS046	36R	681467	3284927	Semi-Consolidated Sediment
IS047	36R	681161	3283499	Mafic Igneous
IS048	36R	680655	3310200	Chalky Marl
IS049	36R	707921	3372094	Limestone
IS050	36R	714369	3407776	Semi-Consolidated Aeolian Sand
IS051	36R	689994	3426541	Volcanic Glass
IS052	36R	716126	3453916	Limestone/Evaporite
IS053	36S	737222	3610147	Basalt
IS054	36S	731529	3630730	Basalt
IS055	36S	762106	3638757	Vesicular Basalt
IS056	36S	759511	3674122	Vesicular Basalt
IS057	36S	757638	3688033	Limestone
IS058	36S	742215	3672867	No Bedrock
IS059	36S	684176	3631108	No Bedrock
IS060	36S	685379	3623856	Limestone
IS061	36S	734413	3647972	Limestone
IS062	36S	745328	3655402	Basalt

Table 4.1 Israeli Soil/Rock Sample Collection Locations (All Locations WGS-84:36R-36S)



Figure 4.1 Soil/Rock Sample Collection Locations in Israel (Landsat Data Provided by Dr Stephen Savage, Arizona State University 2010)

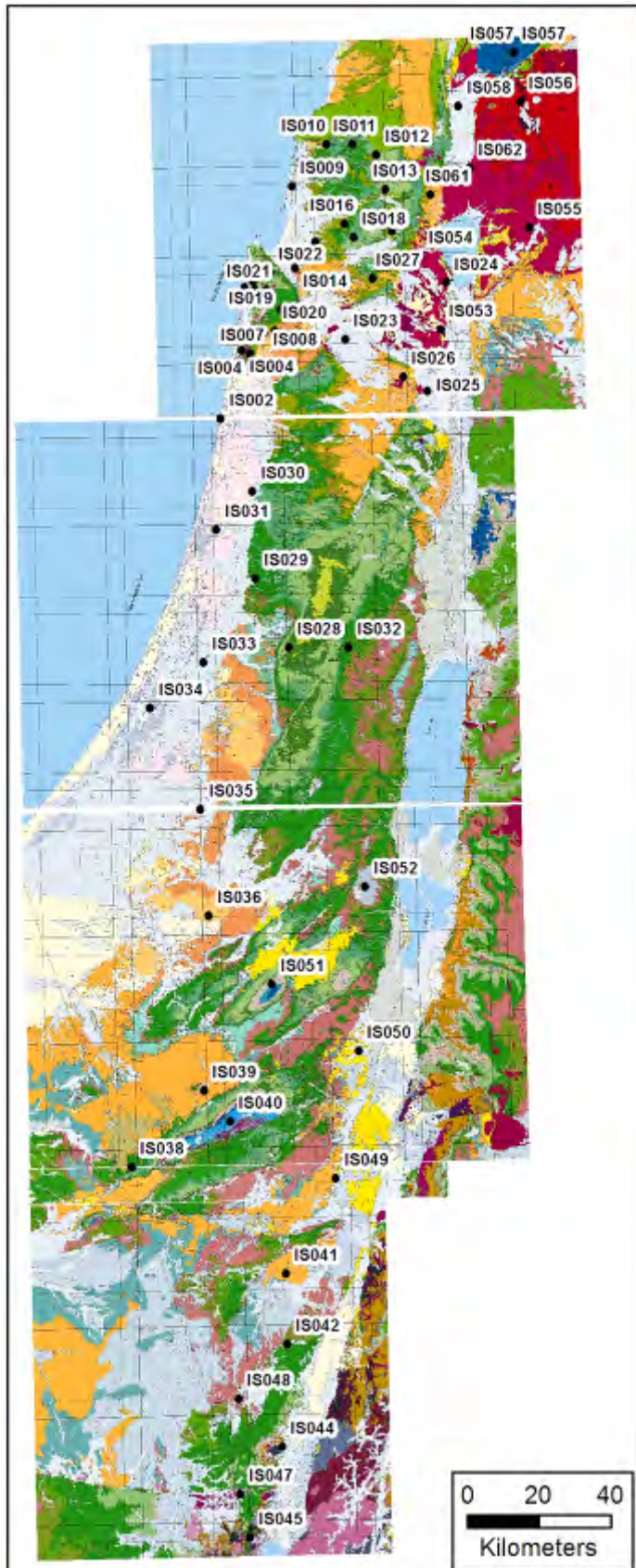


Figure 4.2 Israel Soil/Rock Sample Collection Locations Overlain on Regional Geological Maps (Sneh, Bartov and Rosensaft 1998a and 1998b, Sneh, Bartov, Weissbrod and Rosensaft 1998a and 1998b)

4.2.2. France 2006

Soil, rock and plant samples were collected from areas of France centred on the Rhône Valley between Valance and Orange and the region by Maxime Aubert in 2006, shown in Table 4.1, Figure 4.2, Figure 4.3 and Figure 4.5. Sample locations were chosen with reference to the relevant local 1:50000 geological map to provide a representative cross-section of rock types surrounding the archaeological site of Payre. Site locations were recorded in latitude and longitude using a Garmin Geko 201 GPS. Photographs of all sample collection locations were taken; however, no significant details concerning the soil, rock or plant material were recorded. Plant samples were exclusively taken from grasses located immediately adjacent to the soil sample location, with no attention paid to the species of the grass. The plants were stored in plastic ziplock bags.

Site	Zone	Easting	Northing	Lithology From Map
F1	31T	270113	5062276	Marl, Limestone, Clay
F2	31T	267858	5061775	Marl, Limestone, Clay
F4	31T	269552	5059518	Limestone, Marl, Clay, Sand
F6	31T	268448	5051324	Limestone, Marl, Clay, Sand
F8	31T	276850	5052823	Limestone, Marl, Clay, Sand
F12	31T	288396	5061776	Marl, Limestone, Clay
F16	31T	307742	5053032	Limestone, Marl
F19	31T	312689	5058080	Migmatite
F21	31T	316566	5060204	Monzogranite, Granodiorite
F23	31T	276762	5074376	Marl, Limestone, Clay
F24	31T	278596	5076516	Marl, Limestone, Clay
F25	31T	281821	5076711	Marl, Limestone, Clay
F27	31T	287966	5080184	Basanite, Hawaïite, Tephra
F33	31T	318122	5085533	Monzogranite, Granodiorite
F34	31T	318861	5078299	Paragneiss, Leptynite, Amphibolite
F35	31T	315053	5071792	Paragneiss, Leptynite, Amphibolite
F36	31T	310778	5072387	Paragneiss, Leptynite, Amphibolite

Site	Zone	Easting	Northing	Lithology From Map
F37	31T	315835	5073517	Paragneiss, Leptynite, Amphibolite
F38	31T	320406	5066301	Peraluminous Leucogranite
F40	31T	300215	5068414	Limestone, Marl
P2	31T	636270	4972220	Monzogranite, Granodiorite
P3	31T	613978	4979921	Anatectic Orthogneiss
P4	31T	605305	4977747	Monzogranite, Granodiorite
P5	31T	608043	4977994	Monzogranite, Granodiorite
P6	31T	581185	4983778	Clay, Conglomerate, Sandstone, Marl
P7	31T	588195	4981254	Basanite, Hawaite, Tephra
P8	31T	583541	4982608	Monzogranite, Granodiorite
P9	31T	583488	4982629	Monzogranite, Granodiorite
P10	31T	592176	4970857	Monzogranite, Granodiorite
P11	31T	579265	4953843	Anatectic Orthogneisses
P12	31T	596388	4928948	Schist, Micaschist, Quartzite
P13	31T	593569	4925774	Dolomite, Marl, Evaporite
P14	31T	588209	4926940	Schist, Micaschist, Quartzite
P15	31T	579935	4903929	Sandstone, Conglomerate, Coal, Shale
P16	31T	580827	4906144	Metagranite, Orthogneiss
P17	31T	603549	4903924	Marl, Sandstone, Conglomerate, Limestone
P18	31T	615072	4901240	Limestone Reef Facies Urgonian
P19	31T	615732	4900551	Marl, Sand, Sandstone, Clay, Limestone
P20	31T	630308	4896756	Marl, Sandstone, Chalk, Limestone
P23	31T	613289	4938650	Marl, Limestone, Clay
P24	31T	621739	4931192	Marl, Sand, Sandstone, Clay, Limestone
P25	31T	619053	4939189	Marl, Sand, Sandstone, Clay, Limestone
P26	31T	621056	4938201	Marl, Sand, Sandstone, Clay, Limestone
P27	31T	621678	4947939	Basanite, Hawaite, Tephra
P28	31T	648226	4926782	Marl, Sandstone, Conglomerate, Limestone
P29	31T	647406	4918675	Marl, Conglomerate, Sandstone, Limestone
P30	31T	643842	4899117	Marl, Sandstone, Chalk, Limestone
P31	31T	653617	4899215	Marl, Conglomerate, Sandstone, Limestone
P32	31T	657405	4892315	Sand, Clay, Gravel, Pebble
P33	31T	672108	4904389	Marl, Conglomerate, Sandstone, Limestone
P34	31T	681983	4906777	Marl, Sandstone, Shale, Limestone
P35	31T	681983	4906777	Marl, Sandstone, Shale, Limestone
P36	31T	687076	4920070	Marl, Black Shale, Limestone
P37	31T	706382	4921412	Marl, Sandstone, Shale, Limestone

Site	Zone	Easting	Northing	Lithology From Map
P38	31T	720216	4967508	Marl, Black Shale, Limestone
P39	31T	641335	4965374	Micaschist, Paragneiss
P40	31T	637294	4957464	Marl, Limestone, Clay
P42	31T	637838	4955061	Sand, Clay, Gravel, Pebble
P43	31T	625288	4906215	Sand, Clay, Gravel, Pebble
P44	31T	616838	4904608	Limestone, Marl, Conglomerate, Sandstone
P45	31T	653625	4934020	Marl, Sand, Sandstone, Clay, Limestone
P46	31T	654816	4939806	Sand, Clay, Gravel, Pebble
P47	31T	662743	4953227	Sand, Clay, Gravel, Pebble
P48	31T	689814	4954965	Sand, Clay, Gravel, Pebble
P49	31T	710762	4971827	Marl, Black Shale, Limestone
P50	31T	722254	4969472	Marl, Black Shale, Limestone
P51	31T	728364	4960019	Marl, Sandstone, Conglomerate, Limestone
P52	31T	730957	4969576	Limestone, Calcschist, Marl
P53	31T	734845	4980417	Limestone, Calcschist, Marl
P54	31T	726367	4982172	Amphibolite, Micaschist, Leptynite
P55	31T	634821	4954581	Marl, Limestone, Clay
P56	31T	637537	4954548	Marl, Limestone, Clay
P57	31T	637797	4954224	Sand, Clay, Gravel, Pebble
P58	31T	638372	4954718	Sand, Clay, Gravel, Pebble
P59	31T	639063	4954711	Sand, Clay, Gravel, Pebble
P60	31T	639524	4953538	Sand, Clay, Gravel, Pebble
P61	31T	639548	4953539	Sand, Clay, Gravel, Pebble
P62	31T	638754	4954550	Sand, Clay, Gravel, Pebble

Table 4.2 Soil/Plant Sample Collection Locations, France Collected in 2006 (All Locations in WGS84–31T)

4.2.3. France 2009

Soil and rock samples were collected from the Cognac region of south-eastern France, the Dordogne region of south-central France and the Rodez region of south-central France by Ian Moffat and Rainer Grün, shown in Table 4.3, Figure 4.4 and Figure 4.5. Sample locations were chosen with reference to the relevant local 1:50,000 geological map. Locations were recorded using a Garmin 60CSx

with European geostationary navigation overlay service (EGNOS) corrections enabled. The WGS-84 UTM/UPS co-ordinate system was used for all locations. Photographs were taken both of the general site and of the geological, pedological and botanical features of interest using a Nikon D300 camera with a 18 to 200 mm lens. Soil samples were taken for each visible soil layer. Rock samples were taken for the principle geological unit present on each site and a brief description of the lithology made in the field.

Sample	Zone	Easting	Northing	Lithology From Map
FS001	30T	721160	503407	Limestone, Marl, Clay, Sand
FS006	30T	695046	5060790	Sand, Clay, Gravel, Shingle
FS008	30T	699404	5035025	Sand, Clay, Gravel, Pebble
FS010	30T	722129	5046685	Limestone, Marl, Clay, Sand
FS011	30T	717474	5053975	Limestone, Marl, Clay, Sand
FS016	30T	723956	5084905	Marl, Limestone, Clay
FS018	30T	695487	5079441	Limestone, Marl, Clay, Sand
FS021	30T	700316	5070033	Limestone, Marl, Clay, Sand
FS027	31T	343303	4977631	Limestone, Marl, Clay, Sand
FS027	31T	343303	4977631	Limestone, Marl, Clay, Sand
FS029	31T	339031	4974815	Sand, Clay, Gravel, Shingle
FS031	31T	343614	4968831	Marl, Limestone, Clay
FS032	31T	343902	4969003	Marl, Limestone, Clay
FS032	31T	343902	4969003	Marl, Limestone, Clay
FS032	31T	343902	4969003	Marl, Limestone, Clay
FS035	31T	364413	4964789	Clay, Sand, Gravel, Shingle
FS036	31T	360875	4970271	Limestone, Marl, Clay, Sand
FS037	31T	359240	4977874	Limestone, Marl, Clay, Sand
FS041	31T	398097	4981868	Marl, Limestone, Dolomite
FS041	31T	398097	4981868	Marl, Limestone, Dolomite
FS043	31T	400967	4974223	Sand, Clay, Gravel, Shingle
FS044	31T	411219	4977151	Paragneiss, Leptynite, Amphibolite
FS045	31T	399344	4982356	Marl, Limestone, Dolomite
FS046	31T	399442	4982467	Marl, Limestone, Dolomite
FS047	31T	396434	4970063	Limestone, Marl
FS049	31T	385154	4960867	Marl, Limestone, Clay
FS050	31T	388530	4961960	Marl, Limestone, Clay

Sample	Zone	Easting	Northing	Lithology From Map
FS051	31T	395569	4964432	Marl, Limestone, Dolomite
FS052	31T	403352	4965698	Marl, Limestone, Dolomite
FS052	31T	403352	4965698	Marl, Limestone, Dolomite
FS053	31T	395867	4990680	Sandstone, Conglomerate, Shale, Coal
FS054	31T	400221	4996198	Leptynite, Orthogneiss, Amphibolite
FS055	31T	406773	4995726	Anatectic Orthogneiss
FS056	31T	415656	4992939	Anatectic Orthogneiss
FS057	31T	415617	4992973	Anatectic Orthogneiss
FS058	31T	409561	4984669	Anatectic Orthogneiss
FS059	31T	409401	4984606	Anatectic Orthogneiss
FS060	31T	414875	4967937	Leptynite, Orthogneiss, Amphibolite
FS061	31T	417163	4969334	Paragneiss, Leptynite, Amphibolite
FS063	31T	425397	4972325	Monzogranite, Granodiorite
FS065	31T	430294	4978100	Micaschist, Paragneiss
FS067	31T	437844	4971581	Monzogranite, Granodiorite
FS070	31T	429643	4955208	Micaschist, Paragneiss
FS072	31T	422683	4955326	Leptynite, Orthogneiss, Amphibolite
FS074	31T	410228	4953484	Marl, Limestone, Dolomite
FS076	31T	382579	4987769	Limestone, Marl
FS078	31T	410586	4947189	Limestone, Marl
FS080	31T	398816	4947905	Limestone, Marl
FS081	31T	394242	4947356	Marl, Limestone, Clay
FS083	31T	380555	4955229	Marl, Clay, Limestone, Conglomerate
FS084	31T	369306	4952391	Marl, Limestone, Clay
FS085	31T	364172	4950411	Marl, Limestone, Clay
FS086	31T	360351	4957598	Limestone, Marl, Clay, Sand
FS087	31T	356453	4954771	Marl, Limestone, Clay
FS088	31T	342579	4959745	Limestone, Marl, Clay, Sand
FS089	31T	369850	4973456	Limestone, Marl, Clay, Sand
FS090	31T	466090	4918254	Limestone, Marl
FS092	31T	476904	4923011	Marl, Dolomite, Limestone, Sandstone
FS093	31T	477763	4917559	Limestone, Marl
FS094	31T	473503	4918987	Limestone, Marl
FS096	31T	467072	4912565	Sandstone, Conglomerate, Shale, Coal
FS097	31T	468261	4904608	Marl, Limestone, Dolomite
FS099	31T	472222	4907536	Granite, Orthogneiss
FS100	31T	476284	4906484	Micaschist, Paragneiss

Sample	Zone	Easting	Northing	Lithology From Map
FS102	31T	477133	4907464	Migmatite
FS103	31T	483049	4908159	Anatectic Orthogneiss
FS104	31T	482468	4911339	Micaschist, Paragneiss
FS105	31T	483003	4911985	Granite, Orthogneiss
FS107	31T	478875	4925330	Marl, Dolomite, Limestone, Sandstone
FS108	31T	479023	4928892	Sandstone, Conglomerate, Shale, Coal
FS111	31T	469680	4938102	Monzogranite, Tranodiorite
FS112	31T	464584	4934617	Schist, Mica Schist, Quartzite
FS113	31T	470929	4927979	Sandstone, Conglomerate, Shale, Coal
FS114	31T	470182	4923875	Limestone, Marl, Dolomite
FS115	31T	466355	4920134	Limestone, Marl, Folomite
FS116	31T	480240	4929489	Basanite, Hawaiiite, Tephra
FS118	31T	499737	4941195	Basanite, Hawaiiite, Tephra

Table 4.3 Sample Collection Locations, France 2009 (All Positions WGS84: UTM/UPS)

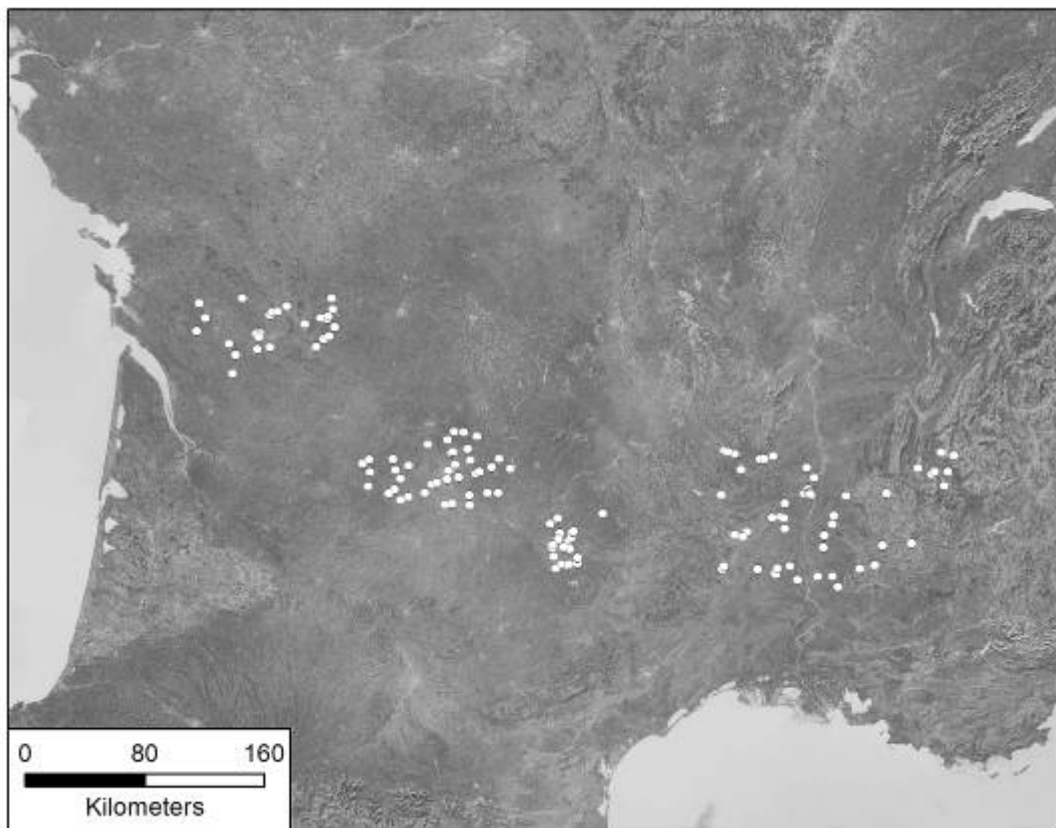


Figure 4.3 Location of all French Sample Collection Sites

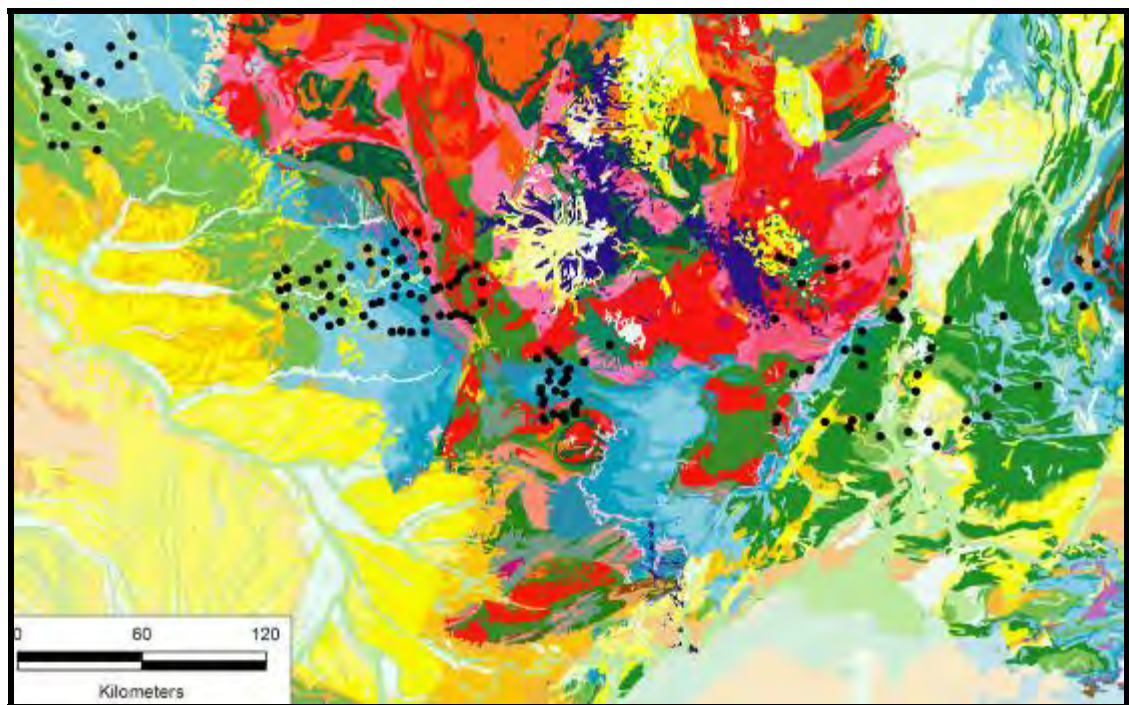


Figure 4.4 Location of Sample Collection Sites Overlain on Geological Units of France

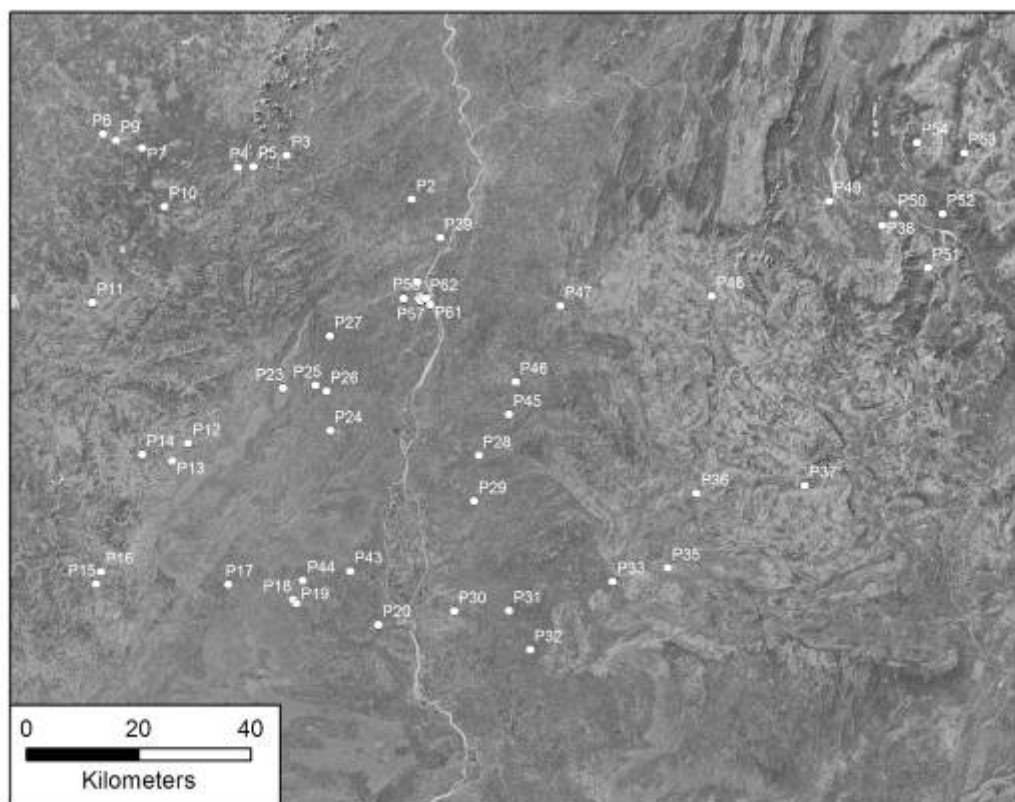


Figure 4.5 Location of Sample Collection Sites in Eastern France

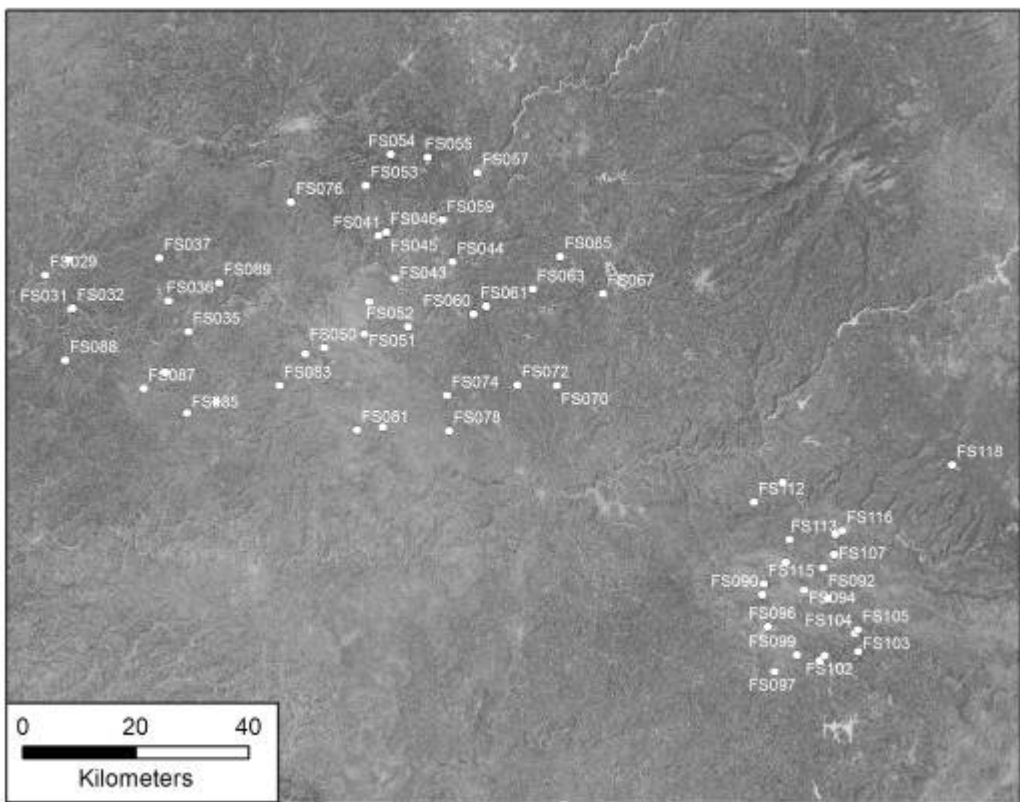


Figure 4.6 Location of Sample Collection Sites in Central France

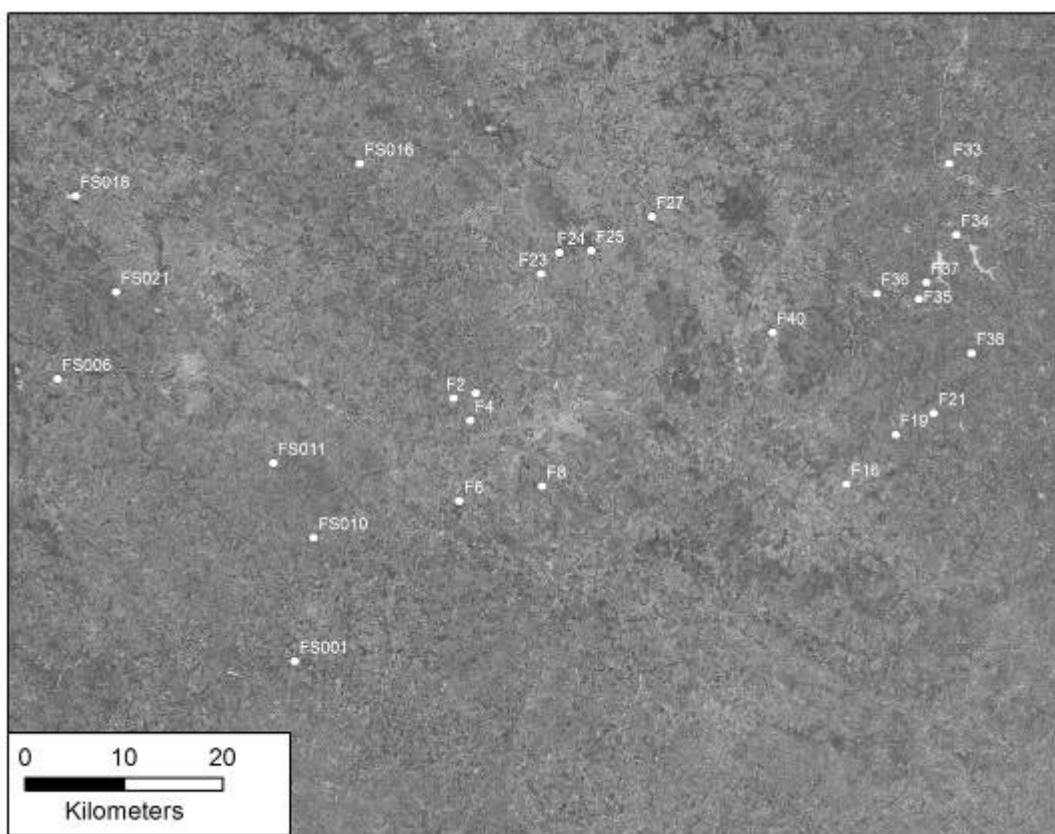


Figure 4.7 Location of Sample Collection Sites in Western France

4.3. Archaeological Samples

4.3.1. Israeli Archaeological Material

4.3.1.1. Skhul

Samples analysed for strontium isotope composition in this study from Skhul include 3 teeth recovered from a bovid jaw (1057A to 1057C), 3 teeth from a pig mandible (1058A to C) and 3 additional bovid teeth (851 to 853), shown prior to sectioning and analysis in section A2.1.1. The bovid skull from which 1057 derives was found directly associated with Skhul IX in a very consolidated breccia at a depth of 2.15 m, nearly touching the rock wall (Grün et al. 2005:318). This was thought by the excavators to have been intrusive to Skhul IX, and that this burial destroyed much of the human skeleton (Garrod and Bates 1937). The pig mandible, which contains samples 1058A to C, was found enclosed in the arms of Skhul V and believed by the excavators to have been deliberately included in the burial (Garrod and Bates 1937). Samples 851, 852 and 853 were not precisely located spatially or stratigraphically during excavation, so their provenance is uncertain.

Sediment samples accompanying samples 1057 and 1058 were analysed for strontium isotope values using MC-ICPMS. All samples in this study have been directly dated using the ESR technique (Grün et al. 2005), as summarised in Table 4.4. In the course of undertaking ESR dating, Grün et al. (2005) analysed the level of uranium in the samples analysed in this research, as summarised in Table 4.5.

Sample	Age ka (Early Uptake)	Age ka (Linear Uptake)
851	45 ± 4	52 ± 5
	42 ± 4	55 ± 6
	49 ± 5	49 ± 5
852	67 ± 7	82 ± 11
	58 ± 6	75 ± 9
	57 ± 5	73 ± 9
853	54 ± 5	64 ± 7
	56 ± 5	66 ± 7
	54 ± 5	63 ± 7
1057	140 ± 21	155 ± 25
	140 ± 21	153 ± 24
	142 ± 22	156 ± 26
1057 (Close to Bedrock)	162 ± 34	182 ± 42
	162 ± 33	181 ± 41
	164 ± 33	184 ± 42
1058	72 ± 8	86 ± 11
	80 ± 10	94 ± 13
	82 ± 10	97 ± 13

Table 4.4 ESR Dates for Samples in this Study from Skhul (Data: Grün et al. 2005)

Sample	Uranium Concentration Enamel (ppm)	Uranium Concentration Dentine (ppm)
851	0.7	24.4
	0.3	27.9
	0.8	20.7
852	1.1	10.9
	1.8	11.4
	1.8	13.2
853	0.5	25.7
	0.4	24.5
	0.3	11.0
1057	0.2	5.7
	0.2	4.9
	0.2	4.7
1058	0.3	28.1
	0.2	31.6
	0.2	31.6

Table 4.5 Uranium Concentration of Samples in this Study from Skhul (Data: Grün et al. 2005)

4.3.1.2. Tabun

Tooth samples analysed using LA-MC-ICPMS in this study include 554 and 556 (layer D), 557 and 558 (layer Ea), 561 and 563 (layer Eb), 564 and 565 (layer Ec) and 567 and 568 (layer Ed), shown prior to sectioning and analysis in section A2.1.2. All samples are *Bos* teeth, except 568, which is a rhino tooth. Uranium concentrations for these samples are summarised in Table 4.6. Soil samples associated with samples 548 to 559, 562, 564, 565 and 567 were analysed for strontium isotope composition using MC-ICPMS.

Sample	Layer	Enamel U (ppm)	Dentine U (ppm)	Sediment U (ppm)
554	D	0.6, 1.31, 0.62	16.1, 18.9, 18.0	4.37, 4.37, 4.37
556	D	8.77, 9.56	23.7, 12.9	4.25, 4.25
557	Ea	0.11, 0.115	1.56, 1.56	2.30, 2.30
558	Ea	0.15, 0.31, 0.36	21.4, 20.7, 24.0	3.41, 3.41, 3.41
561	Eb	0.005, 0.03	6.71, 7.87	7.75, 7.75
563	Eb	0.23, 0.23	4.85, 7.31	3.42, 3.42
564	Ec	0.56, 1.11	3.35, 2.18	2.41, 2.42
565	Ec	0.17, 0.26		0.84, 0.84
567	Ed			
568	Ed	2.04, 2.34	13.4, 16.2	2.66, 2.66

Table 4.6 Uranium Concentration for Samples in this Study from Tabun (Data: Grun et al. 1991:242)

4.3.1.3. Amud

Three teeth (1024 to 1026), identified as fallow deer (*Dama mesopotamica*) originating from layer B1 and dated at as 41 ± 3 and 42 ± 3 ka (early uptake) and 49 ± 4 and 50 ± 4 ka (linear uptake) (Grün and Stringer 1991), were analysed for their strontium isotope composition in this study using LA-MC-ICPMS, shown prior to sectioning and analysis in section A2.1.3. No uranium concentrations were measured for these samples, although concentrations of

less than 0.1 ppm (enamel), 6.5 ppm (dentine) and 1.4 ppm (sediment) have been obtained for another sample from this layer (Rink et al. 2001). Soil samples associated with samples 1024 and 1025, plus an additional soil sample from the same unit (1026) were analysed for strontium isotope composition using MC-ICPMS.

4.3.1.4. Qafzeh

Five enamel fragments (370 to 374) from layer XV (370, 373 and 374), layer XIX (371) and layer XVII (372) were analysed for strontium isotope composition in this study using LA-MC-ICPMS, shown prior to sectioning and analysis in section A2.1.4. Samples 370 to 372 were identified as bovid; however, 373 and 374 were unidentified. Sample 370 was dated at 92.1 ka and 94.2 ka (early uptake) as well as 112.0 ka and 114 ka (linear uptake) using ESR (Schwarcz et al. 1988). The enamel of sample 371 has a uranium concentration of 0.0675 ppm and has been dated at 88.61 +3.24/-3.12 ka using uranium series and 103 ± 19 ka (early uptake) and 125 ± 22 ka (linear uptake) using ESR (McDermott et al. 1993). Sample 372 is dated at 95.2 ka (early uptake) and 103.0 ka (linear uptake) using ESR (Schwarcz et al. 1988). Sample 373 is dated at 95.2 ka (early uptake) and 116.0 ka (linear uptake) using ESR (Schwarcz et al. 1988). Soil samples accompanying samples 371 (layer XIX), 370 (layer XV) and 372 (layer XVII) were analysed for strontium isotope composition using solution MC-ICPMS.

4.3.1.5. Holon

Strontium isotope analysis was undertaken on a single fragment of tooth enamel for strontium isotopes from a *Bos* (1557) from the site of Holon, shown prior to sectioning and analysis in section A2.1.5. This sample from unit C was undertaken in this study, which is estimated to be 200 ka (Joannes-Boyau 2010:109). This sample has been the subject of extensive experimental work in

an effort to improve non-destructive ESR dating (Joannes-Boyau, Bodin and Grün 2010; Grün et al. 2008; Joannes-Boyau and Grün 2009; Joannes-Boyau and Grün 2010; Joannes-Boyau and Grün 2011a, Joannes-Boyau and Grün 2011b; Joannes-Boyau, Grün and Bodin 2010). LA-ICPMS concentration studies or solution analysis of this enamel sample were not undertaken. No soil samples were analysed from this site.

4.3.2. French Archaeological Material

4.3.2.1. La Chapelle-aux-Saints

Samples from the recent excavation from the bouffia 118 region of the site include 6 bovid premolars from layer 1 (samples M005-M010), as well as 2 reindeer molars (sample M001 and M003) and 1 reindeer premolar (M002) from layer 2, shown prior to sectioning and analysis in section A2.2.1. Another suite of bovid teeth (592 to 595), shown prior to sectioning and analysis in section A2.2.1, from stratum 1 of the bouffia Bonneval section of the site and previously dated by (Grün and Stringer 1991:170), were also analysed for Sr isotope composition using LA-MC-ICPMS. Soil samples from Rendu's excavations in the bouffia 118 region of the site include layer 1 (FS045 to S2), layer 2 (FS045 to S1), immediately above the site (FS045 to S3) and the adjacent flood plain (FS046-S1). They were analysed for strontium isotope composition using MC-ICPMS.

4.3.2.2. Les Fieux

LA-MC-ICPMS analysis of samples was conducted, including horse (M011 and M012), wild boar (M013), fox (M014), hyena (M015), bison (M016 and M017), reindeer (M018 and M019), chamois tooth, which may have been digested by a carnivore (M020), and mountain goat/chamois (M021 and M022) from level G7, shown prior to sectioning and analysis in section A2.2.2. Sediment samples

were taken from layers E (FS047 to S3) and G7 (FS047 to S2) from the secteur central and level K on the parche oust wall (FS047 to S1), as well as adjacent to the site (FS047 to S4) and analysed for strontium isotope composition.

4.3.2.3. Le Moustier

Strontium isotope analysis has been undertaken on bovid teeth from layers G1 (sample 845), G2 (sample 846), G3 (sample 847), G4 (sample 848), G5 (sample 849) and G6 (sample 850), shown prior to sectioning and analysis in section A2.2.3. These samples were excavated by Peyrony in the early 1900s and their position within the stratigraphy is not well known, although they are robustly attributed to layer G (Mellars and Grün 1991). These samples have previously been dated (with the exception of 846) using the ESR method by Mellars and Grün (1991:272), returning dates in the range of 40 to 45 ka (early uptake) and 44 to 49 ka (linear uptake). Uranium concentration in these teeth is in the range of 0.01 to 0.62 ppm for enamel and 1.65 to 11.0 ppm for dentine (Mellars and Grün 1991:273), which is considerably higher than layer H, which lies above it in the stratigraphic profile.

4.3.2.4. Pech de l'Azé II

Strontium isotope analysis has been undertaken on bovid (614 and 620), hippopotamus (615, 622), deer (618, 624) and horse (617, 619, 625) specimens, shown prior to sectioning and analysis in section A2.2.4. These samples are from layers 6, 7, 8 and 9 and are dated by Grün et al. (1991:550) as being in the range of 130 to 162 ka, placing these layers in the cold climate conditions of isotope stage 6 (Grün et al. 1991:550). This is supported by the micro-morphological results, which suggest that the high bedrock content in layer 8 is the result of freeze-thaw processes (Goldberg 1979). The uranium concentration of these samples is high, with some (614 and 615) having up to 22 ppm (Grün et al. 1991:46). Grün et al. (1999:1305) conducted detailed U-

series thermal ionisation mass spectrometry (TIMS) analysis using multiple samples on tooth 616, which was shown to have U concentrations of 11.99 to 14.85 ppm in dentine and 0.42 to 0.60 ppm in enamel. These analyses provided U-series ages of 144 ± 44 ka to 89 ± 16 ka. The distribution of U in this tooth suggested that most uranium was diffusing from the dentine into the enamel, rather than directly from outside.

4.3.2.5. Bois Roche

Bovid teeth from layers 1C (samples 2417, 2418, 2422 and 2419) and layer 2 (samples 2421, 2424, 2420, 2423 and 2425A to C), shown prior to sectioning and analysis in section A2.2.6, were analysed for relative strontium isotope abundance. The samples include an upper third premolar (2423), lower third molar (2420), upper second premolar (2421), upper third molar (2422), lower first molar (2419), deciduous upper second premolar (2417), lower first molar (2424) and upper molar (2425). Sediment samples associated with teeth 2417 (layer 1C) and 2424 (layer 2) were analysed using solution MC-ICPMS for ^{87}Sr / ^{86}Sr . Samples 2420, 2425A to C, 2419 and 2424 were analysed for uranium concentration, with results in the range of 0.4 to 1 ppm (Aubert 2011).

4.3.2.6. Rescoundudou

Thirteen samples were analysed from the site of Rescoundudou using LA-MC-ICPMS. All samples in this study (M033 to M045), shown prior to sectioning and analysis in section A2.2.7, are from layer C1. Samples M033, M034, M039, M040 and M041 are bovid and are all molars, with the exception of M041, which is an incisor. Samples M035, M036, M037 and M042 are horse teeth. Sample M038 is a rhinoceros. Samples M042, M043, M044 and M045 are deer. One sediment sample (FS090-S2) from outside of the site was analysed using MC-ICPMS.

4.4. Sample Processing Procedures

4.4.1. Solution Samples

The procedures used in this section are based on those developed for strontium isotope analysis by Dr Graham Mortimer at the Research School of Earth Sciences at the Australian National University, as outlined in Kelly (2007) and Lees (2010).

4.4.1.1. Preparation of Vessels for Analysis

All vessels used for sample preparation were cleaned using a rigorous standard procedure with the aim of minimising sample contamination. Vessels subject to heating during the sample preparation procedures were rinsed after use in Milli-Q water and then soaked in acetone. They were then soaked overnight on a hotplate at approximately 60 °C in each of the following washes sequentially—decon detergent mixed with Milli-Q water, 10% nitric acid, 10% hydrochloric acid and Milli-Q water—before being rinsed with fresh Milli-Q water and dried in an oven overnight. All pipette tips were soaked 2 times in tap water and 3 times in Milli-Q water and then soaked in 10% nitric acid overnight before being washed in Milli-Q water on a further 5 occasions. Strontium and prefilter resins were used in columns on a maximum of 4 occasions. In between uses, columns were soaked 2 times in tap water, 2 times in Milli-Q water, soaked in acetone, rinsed 5 times with Milli-Q water before being soaked in 10% nitric acid for several days and subsequently rinsed in Milli-Q water 5 additional times.

4.4.1.2. Preparation of Samples for Dissolution

Rock and soil samples were heated at 60 °C prior to sample preparation in order to comply with quarantine procedures. After heating, rock samples were crushed to a medium powder using a hand piston. Rock and soil samples were passed through a 2 mm sieve and 1 g of the <2 mm portion was measured out and placed in a 4 ml tube in preparation for leaching.

Tooth samples were prepared for dissolution by removing approximately 0.02 g of enamel or dentine with a dental saw before crushing of this material with a mortar and pestle and placing of this powder in a Teflon beaker.

4.4.1.3. Dissolution of Samples

Soil and rock samples were dissolved by adding 2.5 M ammonium nitrate to 1 g of sample in a 4 ml tube to mimic the extraction of bioavailable strontium by plants (see section 2.3.5.7). Samples were then placed in a Retch shaking machine and agitated continuously for 24 hours. After shaking, samples were placed in a Clements Orbital 310 centrifuge and rotated at 3000 rpm for 5 to 10 minutes. After confirming that the liquid portion of the sample was free of large particulate material, approximately 1 ml of solution was extracted to a Teflon beaker and placed on a hotplate at 60 °C overnight to evaporate all liquid. Subsequent to complete evaporation, 15 drops of high purity concentrated nitric acid was added to each sample before the cap was placed on each beaker for an hour and then removed to allow the sample to evaporate. Then 2 ml of 2 M high purity nitric acid was added to the sample to prepare it for sub-sampling for subsequent analysis.

Plant samples from the Payre mapping programme were prepared by Dr Manfred Thönnessen at the University of Cologne by microwave digestion

following the standard laboratory procedure at this institution in 5 ml of 65% nitric acid at a temperature of 200 °C and a pressure of 7 MPa. The samples were not washed or ashed prior to analysis. The samples were then diluted to 50 ml with double distilled water and mailed to the Australian National University for further analysis.

Tooth enamel and dentine samples were dissolved in 1 ml of concentrated high purity nitric acid and placed on a hotplate at 60 °C in a closed Teflon beaker. After 1 hour, the lid was removed and the sample was allowed to evaporate to dryness. When dry, 2 ml of 2 M high purity nitric acid was added to each sample.

4.4.1.4. Analysis of Concentration

The concentration of each sample was analysed to allow dilutions to be normalised during ion exchange chromatography. To facilitate this measurement, 0.1 ml of solution was sub-sampled from the dissolved plant, soil, rock or teeth samples and diluted with 9.9 ml of 2% high purity nitric acid in a 10 ml vial. The concentration of all samples, excepting those from the Payre area, was then measured with a Varian Vista Pro Axial ICP-AES by Linda McMorrow. The Payre samples were measured using a Varian 820-MS by Les Kinsley.

4.4.1.5. Ion Exchange Chromatography

Ion exchange chromatography was used to separate strontium in the solution from other matrix elements, particularly rubidium (Dicken 2005:17). Eichrom Strontium 50-100 u resins are effective at isolating strontium as it is uptaken preferentially at higher acid concentrations (as shown in Figure 4.6), and can then be removed (once all other ions have been flushed out) by subsequently

lowering the acid wash concentration. An Eichrom prefilter 100-150 μ resin is also used to remove organic material from the solution.

The procedure for column use is to begin with the prefilter resin over the strontium specific resin and wash both by filling them with 0.02 M nitric acid more than 3 times, filling them with 8 M hydrochloric acid 2 times and then filling them with 0.02 M nitric acid at least another 5 times. The strontium resin is then placed over the prefilter and the column is conditioned by passing 0.25 ml of 2 M nitric acid through 3 times. The sample is then loaded into the strontium column in 0.2 ml aliquots up to the required concentration for effective MC-ICPMS analysis, which is dependent on machine setting and instrument performance. Ions other than strontium are then removed by passing a total of 2.5 ml of 2 M nitric acid through the columns. The strontium is then released from the column matrix by passing through a total of 5 ml of 0.02 ml nitric acid in 1 ml aliquots.

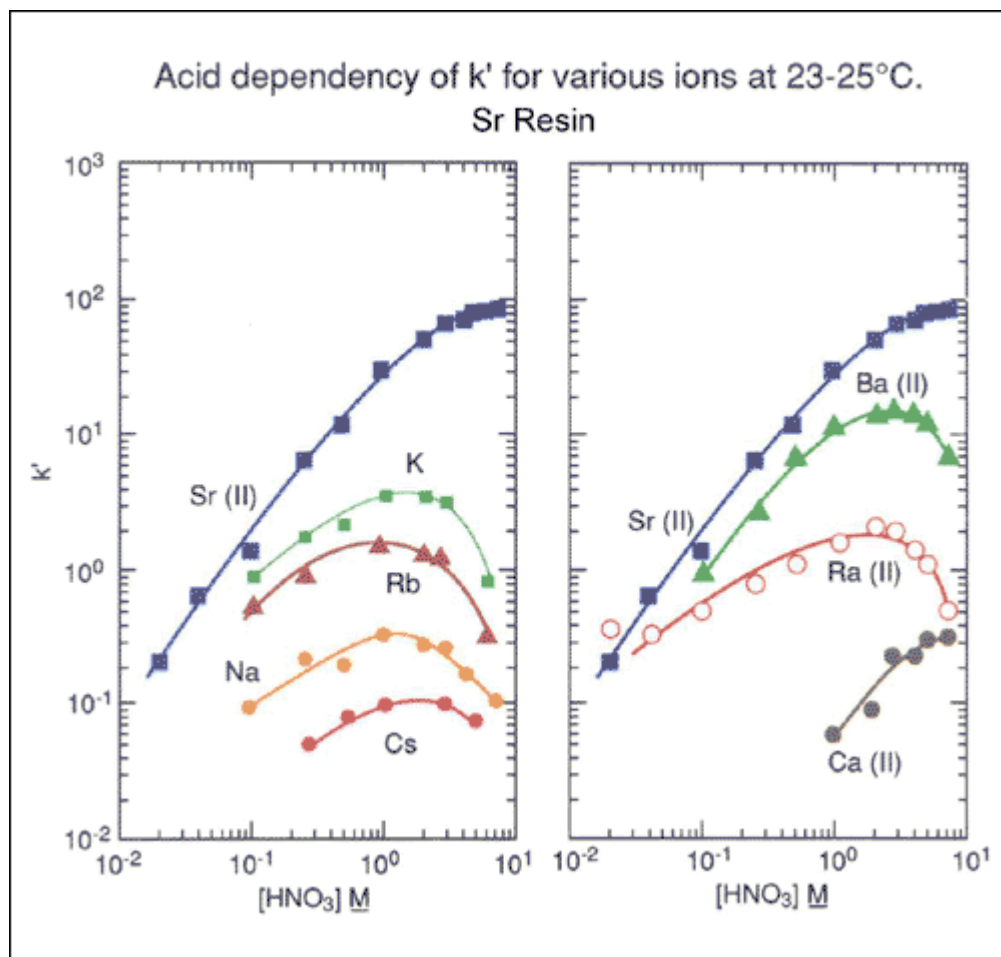


Figure 4.8 Acid Dependency of Various Ions in Strontium Resin (Horwitz et al. 1992)

After the columns are complete, the sample is placed on a hotplate in a Teflon beaker at 60 °C with a drop of phosphoric acid and evaporated to dryness. Immediately prior to sample analysis using the MC-ICPMS, 2 ml of 2% high purity nitric acid is added to the sample and placed on a hotplate at 60 °C for 1 hour with the lid on, before being allowed to cool and being transferred to a 4 ml tube for analysis.

4.4.2. Laser Ablation Samples

Faunal samples for laser ablation analysis are prepared by cutting them longitudinally with a dental saw and smoothing the surface with P800 sandpaper before being cleaned by being wiped with acetone. Following this

preparation, they are mounted in a sample holder using blue tack as shown in Figure 4.7. As discussed in section 4.7.2, all sample spots are cleaned with laser ablation prior to analysis to remove any contamination from the sandpaper or dental saw.



Figure 4.9 Sample Mounted for LA-MC-ICPMS Analysis

4.5. Instrumentation for Strontium Concentration Measurements

4.5.1. ICP-AES/ICP-OES

Inductively coupled atomic/optical emission spectroscopy (ICP-AES/ICP-OES) determines the trace element composition of samples based on their emission of radiation when excited by a plasma torch (Pollard et al. 2007:47). Samples are usually introduced in a liquid state, before being carried by argon into the plasma. All compounds are dissociated by the high plasma temperature and become excited, leading to the emission of characteristic lines in the visible and

ultraviolet state. The emissions for each element can be recorded by a photomultiplier sequentially, allowing fast analysis of a range of elements. Most elements have detection limits in the ppb range.

This technique has been applied to archaeology for the elemental analysis of a range of materials, including bone (Zlateva et al. 2003), clay (Paama et al. 2000), copper ingots (Klemenc et al. 1999), earth floors (Middleton and Price 1996), gold (Hall et al. 1998), hearth fuel (Pierce et al. 1998), pottery (Bruno et al. 2000; Mirti et al. 1994), soil (Knudson et al. 2004; Wells 2004), stoneware (Grave et al. 2005), teeth (Webb et al. 2005) and wood (Durand et al. 1999).

4.5.2. ICPMS

In ICPMS analysis, a sample, introduced either through laser ablation (see section 4.6.1.2 for a detailed discussion) or in solution, is carried into the plasma by argon gas, which is maintained at a temperature of approximately 5000 to 10,000 °C by an external radio frequency current (Pollard and Heron 2008:29). The material is broken down into elements and ionised. These ions enter a magnetic selector device (most often a quadrupole mass filter), which separates them on the basis of their mass to charge ratio before they are collected in a charge sensitive detector (Pollard et al. 2007:199).

ICPMS provides detection limits in the order of parts per 1000 (Pollard et al. 2007:61). Most elements (excepting some with low atomic mass and some actinides) can be analysed. The ICPMS has several advantages over comparable techniques such as neutron activation and X-ray fluorescence as it combines the benefits in ionisation efficiency and convenience inherent to the ICP system with the signal-to-noise ratio and precision of mass spectrometry (Halliday et al. 1998). This method can detect elemental concentrations significantly lower than ICP-AES. The addition of a laser ablation system

provides the opportunity to sample without the need for chemical preparation and allows for spatial resolution within samples.

ICPMS can be used as part of the strontium isotope process both to determine strontium concentration to optimise column chemistry or to measure the concentration of other elements such as uranium that may serve as a proxy for post-burial diagenesis. If measured using a laser ablation system, this may provide a spatial distribution of this overprint.

The applications of ICPMS to archaeology are reviewed by Kennett et al. (2001) and the specific advantages of the laser ablation approach summarised by Resano et al. (2009), Russo et al. (2002) and Speakman and Neff (2005).

Applications of ICPMS in archaeological research include characterising bone (Ghazi 1994; Reinhard and Ghazi 1992), ceramic (Kennett et al. 2002; 2004; Li et al. 2005; 2006; Mallory-Greenough et al. 1998; Marengo et al. 2005), copper (Cooper et al. 2008; Thornton et al. 2002), glaze-paints (Habicht-Mauche et al. 2000), gold (Hall et al. 1998), silver (Longerich et al. 1987), soil (Cook et al. 2006; Entwistle and Abrahams 1997; Entwistle et al. 1998) and wood (Durand et al. 1999).

Specific applications of LA-ICPMS in archaeology include the analysis of ceramics (Cochrane and Neff 2006; Neff 2003), copper (Dussubieux et al. 2008), glass (Shortland et al. 2007), gold (Guerra et al. 1999; Junk 2001), iron (Desaulty et al. 2008; Devos et al. 2000), obsidian (Barca et al. 2007; Gratuze 1999; Pereira et al. 2001; Reepmeyer et al. 2011), paint (Speakman and Neff 2002), pigment (Arnold et al. 2007), silver (Guerra et al. 1999; Sarah et al. 2007) and teeth (Eggins et al. 2003; Simonetti et al. 2008).

4.6. Instrumentation for Strontium Isotope Measurements

4.6.1. MC-ICPMS

The MC-ICPMS, first introduced by Walder and Freedman (1992), operates using a plasma source in a similar fashion to ICPMS; however, rather than utilising a quadrupole filter and a single faraday cup, it uses a magnetic selector and multiple ion beam detectors (Pollard et al. 2007:199). The use of multiple ion beam detectors overcomes the problems of plasma instability inherent in precisely measuring isotopes by ICPMS (Gäbler 2002). This method allows easy sample introduction, high sample throughput, high mass resolution and a precision reaching 0.001%, which is comparable to TIMS (Yang 2009). A schematic of the instrument is shown in Figure 4.8. The applications of this technique were reviewed by Halliday et al. (1998) and Douthitt (2008).

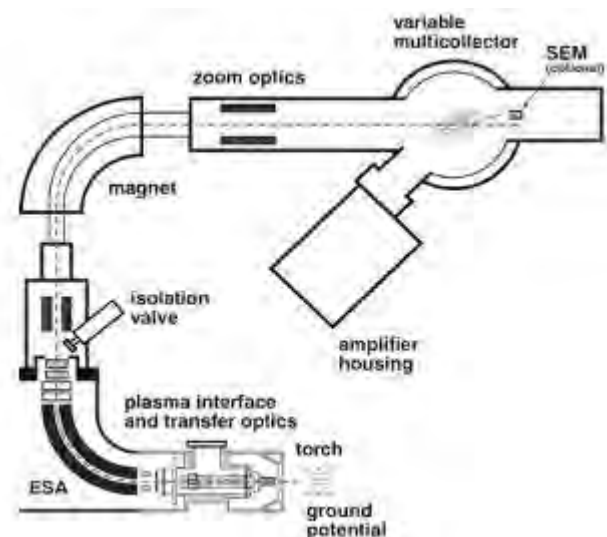


Figure 4.9 Schematic Diagram of Neptune MC-ICPMS (Gäbler 2002:2)

4.6.1.1. Solution MC-ICPMS

Solution MC-ICPMS is overwhelmingly the most common method used in modern studies for measuring the relative abundance of strontium isotopes in archaeology. Other applications of this technique in archaeology include: the

measurement of lead isotopes in bone (Rehkämper and Mezger 2000), copper (Niederschlag et al. 2003) and paints (Fortunato et al. 2005) and uranium series dating of calcretes (Candy et al. 2005), flowstone (Bischoff et al. 2007), rock art (Aubert et al. 2007) and speleothems (Gopher et al. 2010; Vaks et al. 2007).

4.6.1.2. LA-MC-ICPMS

LA-MC-ICPMS potentially provides considerable advantages over traditional or micro-milling techniques because it offers high spatial resolution (around 50 to 100 µm), faster analysis time, less damage to the samples (Horstwood et al. 2008:5659), direct characterisation of solids, requires no chemical dissolution, reduces the risk of contamination and provides a spatial distribution for results (Russo et al. 2002). The minimally destructive nature of this approach is particularly appropriate for rare Palaeolithic samples (Richards et al. 2009). The development of He ablation cells allows the spot size to be further reduced to 10 µm due to the increased transport efficiency away from the ablation site compared to Ar (Eggins et al. 1998:285–286). In addition to strontium isotope analysis, this technique has been applied to many questions within archaeology, including *in situ* U-series dating (Eggins et al. 2005; Grün et al. 2005; 2006; 2008; Mijares et al. 2010; Pike et al. 2006), as well as lead isotope analysis of copper (Cooper et al. 2008), silver (Ponting et al. 2003) and pottery (Iñáñez et al. 2010).

Despite these considerable potential advantages, concerns have been raised about the ability of this technique to obtain accurate and precise data for strontium isotopes (Vroon et al. 2008). In particular, the prospect raised by Simonetti et al. (2008) that $^{87}\text{Sr}/^{86}\text{Sr}$ values obtained by LA-MC-ICPMS show an elevated radiogenic value compared to those from solution MC-ICPMS is relevant to this project. This hypothesis is based on the results of a study of the tooth enamel isotopic compositional and elemental abundance of 37 individuals from the archaeological site of Tombos in Sudan (Simonetti et al. 2008:373).

They reported a correlation between the offset $^{87}\text{Sr}/^{86}\text{Sr}$ ratio and $(\text{Ca} + \text{P})/\text{Sr}$ value, which is hypothesised to yield an isobaric interference to mass 87 based on the composite atomic mass of calcium, phosphorous and oxygen (Simonetti et al. 2008:382). This effect is considered to disappear at strontium concentrations greater than 1900 ppm, which is supported by the results of Bizzarro et al.'s (2003) study of igneous apatite crystals from carbonatites from Greenland. The offset between the strontium ratios obtained by LA-MC-ICPMS and solution MC-ICPMS from the same sample is up to .0025 (Simonetti et al. 2008:381), a value that would make the discrimination between geological environments with a similar strontium isotope ratio impossible. Copeland et al. (2008; 2010) disputed the results of Simonetti et al. (2008) claiming that, while an offset does exist, it is neither of the magnitude claimed nor based on the $\text{Ca} + \text{P} + \text{O}$ isobaric interference.

Horstwood et al. (2008) observed similar results by comparing analysis from LA-MC-ICPMS to those obtained from the same samples using TIMS for a number of teeth, a modern mollusc and 2 igneous apatites. The results show a relationship between decreased accuracy and signal, even after correction for doubly charged rare earth elements, Ca dimmer and Rb (Horstwood et al. 2008:5669). They suggested correcting for this by using a reference material of a well-characterised inorganic phosphate (Horstwood et al. 2008:5672). However, an apatite glass similar to those proposed by Klemme et al. (2008:40), free of strontium, would be appropriate for this purpose.

In contrast, Prohaska et al. (2002) found little difference between bone and teeth analysed using solution data (both with and without the use of strontium specific resin) and with laser ablation sampling. Similarly, Copeland et al. found a difference of 0.0003 ± 0.0002 between laser and solution data for modern rodent teeth (2008) and 0.0005 ± 0.0010 for fossil rodent teeth (2010), well within the acceptable range for discriminating between geological environments in their study area.

The diversity of results from these authors is worrying as this inaccuracy threatens seriously threatens the validity of the use of LA-MC-ICPMS method to analyse the strontium isotope composition of low Sr biominerals such as teeth. As a result, the resolution of this question definitively promises to be an active area of future research.

4.7. MC-ICPMS Sample Analysis

4.7.1. Solution MC-ICPMS

Solution MC-ICPMS analysis was undertaken using a Finnigan Neptune MC-ICPMS under the supervision of Les Kinsley. Samples were run as part of a sequence, which included washes in water, Triton detergent and nitric acid. Prior to each sample, a blank of 2% nitric acid was measured. On multiple occasions during the sample sequence, a SRM987 standard was run to quantify instrument drift.

Faraday Cup	Nominal Mass	Amplifiers
L4	82.5	1
L3	83 (Kr)	6
L2	83.5	2
L1	84 (Sr+Kr)	3
C	85 (Rb)	8
H1	86 (Sr+Kr)	5
H2	86.5	7
H3	87 (Sr+Rb)	4
H4	88 (Sr)	9

Table 4.7 MC-ICMPS Instrument Settings Used For Sample Analysis

4.7.2. LA-MC-ICPMS

LA-MC-ICPMS data were collected with a Finnigan Neptune using the settings described in Table 4.8. Acquisition parameters for the Neptune were optimised using a piece of modern Tridacna shell, which has a known strontium isotope composition. Multiple spots on the Tridacna shell, shown in Appendix Four, were undertaken during analysis to ascertain the accuracy of the data acquisition. All spots were cleaned prior to data collection using laser analysis of a spot diameter larger than was used for analysis. A spot diameter of 233 µm was used with a sample speed of 10 µms⁻¹. Sampling was undertaken in spots to increase the spatial accuracy of the results, despite the possibility that the creation of pits can lead to decreased analyte intensity and increased fractionation (Ramos et al. 2004).

Faraday Cup	Nominal Mass	Amplifiers
L4	82.4652	6
L3	83	3
L2	83.466	1
L1	84	2
C	85	4 + SEM
H1	86	8
H2	86.469	5
H3	87	9
H4	88	7

Table 4.8 LA-MC-ICPMS Instrument Settings Used for Sample Analysis

4.8. Data Analysis

4.8.1. MC-ICPMS

Data collected using the MC-ICPMS were analysed using the Excel spreadsheet developed by Graham Mortimer at the Research School of Earth

Sciences at the Australian National University. The spreadsheet initially corrects the measured intensities of all nominal masses by subtracting the average blank values for each mass from each data point. The spreadsheet then calculates the blank corrected raw ratio for each data point of $^{88}\text{Sr}/^{86}\text{Sr}$, $^{84}\text{Sr}/^{86}\text{Sr}$, $^{85}\text{Rb}/^{86}\text{Sr}$ and $^{87}\text{Sr}/^{86}\text{Sr}$. An interference corrected raw ratio is calculated by subtracting the $^{85}\text{Rb}/^{86}\text{Sr}$ from the $^{87}\text{Sr}/^{86}\text{Sr}$ and dividing the result by 2.463, the known $^{85}\text{Rb}/^{87}\text{Rb}$ ratio. The first step to undertaking a mass bias correction for each data point is to calculate P, which is the natural log of the $^{88}\text{Sr}/^{86}\text{Sr}$ ratio divided by 8.3752, after which the resulting value is divided by the natural log of the mass of 88 (87.9075) divided by the mass of 86 (85.9093). The mass bias corrected ratio of $^{87}\text{Sr}/^{86}\text{Sr}$ for each data point is calculated by dividing the interference corrected raw ratio of $^{87}\text{Sr}/^{86}\text{Sr}$ by the ratio of 86.9089/85.9093 and squaring the result to the power of P. The overall $^{87}\text{Sr}/^{86}\text{Sr}$ value for a solution sample is calculated as the average for all mass bias corrected data points. This correction is necessary because the MC-ICPMS system suffers from high mass bias, deviating from true values by up to 25% (Taylor et al. 1998). This may be the result of supersonic expansion of ions through the sample cone and space charge effects in the skimmer cone, which both favour heavier ions and yield non-uniform sensitivity across the mass range (Yang 2009).

4.8.2. LA-MC-ICPMS

The most challenging aspect of performing accurate analyses using LA-MC-ICPMS is correcting for the multiple interferences with Sr isotope masses, without the advantage of being able to perform chromatographic purification as is possible with solution samples (Ramos et al. 2004). In this research, LA-MC-ICPMS data were corrected using a spreadsheet developed for this project, based on a previous version developed by Dr Steve Eggins from the Research School of Earth Sciences at the Australian National University. This spreadsheet applies a ‘gas blank’ Kr correction, a mass bias correction, a rare earth element correction and a rubidium correction (in that order), as detailed in

sections 4.8.2.1 through 4.8.2.6. This analysis used relative element abundances based on Berglund and Wieser (2011) and relative atomic masses based on Audi et al. (2003).

The accuracy of sample results were evaluated by comparison to values from a Tridacna clam shell, which is a calcite with a homogenous $^{87}\text{Sr}/^{86}\text{Sr}$ composition that corresponds to modern seawater at 0.70918 (Horstwood et al. 2008). LA-MC-ICPMS data were also evaluated with reference to the $^{84}\text{Sr}/^{86}\text{Sr}$ values from each sample, which should correspond to the value of 0.0565 if $^{87}\text{Sr}/^{86}\text{Sr}$ values are robust.

4.8.2.1. Kr Correction

Kr can present a significant isobaric interference during LA-MC-ICPMS analysis due to its unavoidable introduction from Ar and He carrier gas, particularly affecting the measurement of ^{86}Sr and ^{84}Sr (Woodhead et al. 2005). The level of Kr varies between gas supplier and batch; however, Kr interferences in the range of 20 to 50 mV have been reported (Jackson and Hart 2006; Ramos et al. 2004; Waight et al. 2002; Woodhead et al. 2005).

The values used in this research follow the procedure of many authors, as summarised by Vroon et al. (2008:471), of using the ‘gas blank’ or ‘on peak zero’ method to remove this effect. This works by measuring the levels of all cups with gas flows active, but without the laser shutter open and subtracting this value from subsequent analysis. This approach assumes that the laser induced isotope fractionation and instrument discrimination are the same for Sr and Kr and should be effective of Rb/Sr levels of less than 0.1 (Vroon et al. 2008).

4.8.2.2. Mass Bias Correction

A mass bias correction was undertaken on the $^{84}\text{Sr}/^{86}\text{Sr}$ and $^{87}\text{Sr}/^{86}\text{Sr}$ ratios with reference to a $^{86}\text{Sr}/^{88}\text{Sr}$ ratio of 0.1194. This addresses the effects of instrument mass discrimination, which is due to differences in ionisation potentials, space charge effects, matrix effects, preferential transmission of 1 type of ion and reactions within the ICP and isotopic fractionations induced by the laser ablation process (Vroon et al. 2008).

4.8.2.3. REE Interference Correction

The interference of rare earth elements (REEs) is possible through doubly charged species in the Sr mass region (Woodhead et al. 2005). Rare earth elements generally have very low abundance in modern carbonates; however, they can become elevated during burial or diagenesis. The ICP is an effective generator of doubly charged ions, with approximately 2% of REE ions being doubly charged (Ramos et al. 2004). In this research, the values of $^{167}\text{Er}^{++}$, $^{173}\text{Yb}^{++}$ and $^{177}\text{Hf}^{++}$ were measured during analysis and were used to remove the influence of $^{166}\text{Er}^{++}$ from ^{83}Kr , $^{168}\text{Er}^{++}$ from ^{84}Sr , $^{170}\text{Er}^{++}$ from ^{85}Rb , $^{172}\text{Yb}^{++}$ from ^{86}Sr , $^{174}\text{Yb}^{++}$ from ^{87}Sr and $^{176}\text{Yb}^{++}$ from ^{88}Sr .

4.8.2.4. Rb/Sr Correction

The interference of ^{87}Rb on ^{87}Sr presents a significant impediment to accurate Sr isotope determinations, particularly at high Rb concentrations. Rb can be corrected for by calculating a mass bias uncorrected $^{85}\text{Rb}/^{87}\text{Rb}$ ratio using the measured $^{86}\text{Sr}/^{88}\text{Sr}$ ratio and the known $^{85}\text{Rb}/^{87}\text{Rb}$ ratio (0.385713). This value is used with the ^{85}Rb intensity to calculate the ^{87}Rb contribution to mass 87 (Ramos et al. 2004).

4.8.2.5. Ca Argide/Dimmer Correction

The use of a Ca argide or dimmer correction, which removes the possible effect of $^{44,46,48}\text{Ca}(\text{Ca},\text{Ar})^+$ (created on masses 84, 86 and 88, respectively, see Paton et al. 2007) has been applied to other studies utilising LA-MC-ICPMS to analyse Sr isotope composition in biogenic carbonates (e.g., Copeland et al. 2010; Woodhead et al. 2005). It has been omitted in this study. This omission is on the basis that the effect on the $^{87}\text{Sr}/^{86}\text{Sr}$ is likely to be only a very small elevation and thus not significant in determining broad geological provinces, although the potentially much larger effect on the $^{84}\text{Sr}/^{86}\text{Sr}$ should be noted (Paton et al. 2007). Some authors claim that this effect can be removed by appropriate equipment and sampling techniques (e.g., Barnett-Johnson et al. 2005).

4.8.2.6. Other Corrections

A range of other corrections are possible, including for Fe dioxides, Ga oxides, Zn oxides; however, these are not required for biomineral samples.

4.8.2.7. Ca+P+O Offset Correction

As discussed in section 4.6.1.2, an offset is thought to exist between solution and laser values from the same sample due to the effect of a Ca+P+O polyatomic interference on mass 87. This offset is thought to increase, making laser values progressively more radiogenic, with decreasing strontium concentration (Horstwood et al. 2008). In order to correct for this effect, a number of human and faunal tooth samples were examined by both solution and laser analysis at the Australian National University by Boel (2011), Kelly (2007) and Lees (2010). These values were used to define a relationship between solution/laser offset and strontium concentration, shown in Figure 4.9.

Unfortunately, concentration values were not collected for all spots in this study. As an alternative, Tridacna standards collected during each analysis run were used to normalise the strontium 88 voltage between analyses. These normalised values were compared to a Tridacna concentration of 1465 ppm, which was calculated based on the comparison between strontium 88 voltage and a number of known concentration samples. Assuming a linear relationship between strontium 88 voltage and strontium concentration, this value was used to calculate the concentration of each analysis spot. Because of the potential errors associated with this calculation, an average concentration was calculated for the enamel and dentine of each sample and this average value was used to correct all points. By applying this average value, the potential disproportionate effect from small variations in voltage in low concentration samples is avoided. Because the degree of Ca+P+O offset is uncertain (e.g., Copeland et al. 2008), the results are presented both as uncorrected and corrected results.

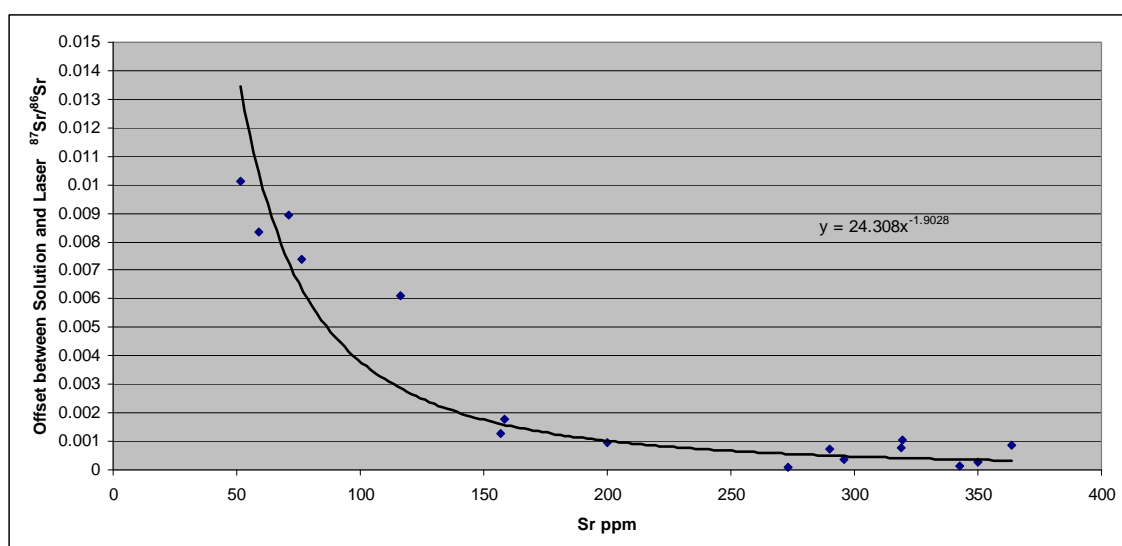


Figure 4.10 Relationship Between Strontium Concentration and Laser/Solution Offset Used for Correction of LA-MC-ICPMS Data in this Study

The degree of offset observed between solution and laser values in this research is more than an order of magnitude greater than observed in Copefland et al (2008, 2010). Furthermore, Copeland et al. (2008, 2010) reveal a linear relationship between concentration and offset while the results from this study show an exponential trend. The relationship between strontium

concentration and offset in the data of Simonetti et al. (2008) corresponds more closely to the data in Figure 4.9, although this data does not show the large increase in offset below 100 ppm. This comparison is however problematic, as only one sample in Simonetti et al.'s study (2008: 376) has a strontium concentration below 100 ppm. The correlation between strontium concentration and offset demonstrated by Nowell and Horstwood (2009) and Horstwood et al. (2008) shows some correlation with the results shown in Figure 4.9 at strontium concentrations higher than 100 ppm. Despite this, the offset between solution and laser data shown in Figure 4.9 are much higher at lower concentrations than is found by Nowell and Horstwood (2009) and Horstwood et al. (2008). The lack of correlation between the results of these studies probably partially reflects the small number of data points analysed as well as the effect of heterogeneous plasma conditions between different instruments and suggests the importance of further research in this area (as discussed in section 7.2.2). The lack of correlation between the results of this study and those of other authors and the very high degree of offset observed at strontium concentrations below 100 ppm suggest that these data should be treated with suspicion.

4.9. Interpretation of Mobility

Strontium isotope data from the faunal teeth in this study are interpreted in a number of ways in order to determine the degree of mobility of a particular sample. Sample with intra-sample enamel $^{87}\text{Sr}/^{86}\text{Sr}$ heterogeneity are considered to be mobile across different geological environments during amelogenesis. Samples with different $^{87}\text{Sr}/^{86}\text{Sr}$ values for their enamel and dentine or which have enamel values which are different for the mapping value for the geological unit which contains the site are considered to be migrants. Corrected strontium isotope values for each distinguishable $^{87}\text{Sr}/^{86}\text{Sr}$ enamel domain were compared to soil, plant and rock values and the distance to the closest outcrop of a geological unit which had a corresponding $^{87}\text{Sr}/^{86}\text{Sr}$ value was measured. In the case of multiple domains existing within a tooth, the distance to the closest corresponding outcrop for each domain was measured

and the greatest of these distances was used for comparison with other samples.

4.10. Overview

This chapter summarised the procedures used for sample collection, processing and analysis of strontium isotope values in this thesis. The relationship of the faunal material analysed using LA-MC-ICPMS to their respective archaeological sites was also discussed.

Chapter Five: Summarised Results

5.1. Overview

This chapter summarises the results from all strontium concentration and isotope analyses and interpretation of mobility undertaken as part of this research. Due to the voluminous nature of the data collected, detailed results for the sample analysis are in Appendix Three and, for the Tridacna analysis, in Appendix Four.

5.2. Regional Mapping Results

A total of 274 soil, rock and plant samples from Israel and France were analysed for strontium isotope composition. These samples have $^{87}\text{Sr}/^{86}\text{Sr}$ values covering the range of 0.701799 ± 0.006234 to 0.817507 ± 0.000013 .

5.2.1. Israel

5.2.1.1. Israeli Soil Samples

There were 67 soil samples analysed for $^{87}\text{Sr}/^{86}\text{Sr}$ from Israel over a range of 0.705772 ± 0.000011 to 0.710199 ± 0.000034 , shown in Table 5.1 and Figure 5.1.

Sample Number	Sample Location	Zone	Easting	Northing	^{88}Sr Volts	$^{87}\text{Sr}/^{86}\text{Sr}$	\pm $^{87}\text{Sr}/^{86}\text{Sr}$	Geology From Field	Geology From Map
151	IS001	36S	682494	3621957	31.76	0.709344	0.000129	Calcareous Sandstone	Clay, Silt, Sand
152	IS002	36S	675689	3585175	22.72	0.709524	0.000118	No Bedrock	Gravel, Sand, Silt
153	IS003	36S	680980	3601307	13.30	0.708952	0.000012	No Bedrock	Clay, Silt, Sand
154	IS004	36S	681536	3604285	39.90	0.708505	0.000114	Sandstone with Carbonate Matrix	Dolostone, Limestone, Chert
155	IS004	36S	681536	3604285	18.80	0.708593	0.000023	Sandstone with Carbonate Matrix	Dolostone, Limestone, Chert
156	IS005	36S	684801	3623556	23.66	0.708958	0.000008	Reefal Limestone	Limestone, Marl, Dolostone
157	IS006	36S	685092	3621362	10.76	0.709149	0.000112	Reefal Limestone	Limestone, Marl, Dolostone
158	IS007	36S	683780	3603356	11.23	0.709282	0.000017	Limestone	Limestone, Marl, Dolostone
159	IS008	36S	687978	3609221	20.11	0.708393	0.000087	Chalk	Chalk, Chert
160	IS009	36S	695586	3650202	13.51	0.709344	0.000012	Calcareous Sandstone 'Kurkar'	Clay, Silt, Sand
161	IS010	36S	705301	3661995	17.58	0.708440	0.000077	Limestone	Limestone, Marl, Dolostone
162	IS011	36S	712541	3662131	2.48	0.710199	0.000034	Very Fine Grained Limestone	Chalk, Marl
163	IS012	36S	719243	3659214	19.91	0.708365	0.000133	Limestone	Limestone, Dolostone, Marl, Chalk, Chert
164	IS013	36S	721813	3649514	13.53	0.709212	0.000011	Chalky Limestone	Limestone, Dolostone, Marl, Chalk, Chert
165	IS014	36S	696501	3627390	14.75	0.708586	0.000011	No Bedrock	Gravel, Sand, Clay
166	IS015	36S	702082	3634803	15.01	0.708776	0.000010	Limestone Breccia	Gravel, Sand, Clay
167	IS016	36S	710374	3639794	27.55	0.708181	0.000133	Chalky Limestone	Chalk, Marl
168	IS017	36S	723533	3637663	17.25	0.708852	0.000084	Chalky White Limestone	Limestone, Chalk, Marl, Sandstone
169	IS018	36S	712855	3636020	14.12	0.708662	0.000011	Chalky Limestone	Dolostone, Limestone, Chert

Sample Number	Sample Location	Zone	Easting	Northing	Sr Volts	$^{87}\text{Sr}/^{86}\text{Sr}$	$^{87}\text{Sr}/^{86}\text{Sr} \pm$	Geology From Field	Geology From Map
170	IS019	36S	692598	3615897	18.51	0.708727	0.000094	Limestone	Limestone, Marl, Dolostone
171	IS020	36S	690737	3609663	14.78	0.708418	0.000012	Chalky Limestone	Chalk, Chert
172	IS021	36S	688498	3621292	16.40	0.708544	0.000010	Limestone	Limestone, Dolostone, Marl, Chalk, Chert
173	IS022	36S	689525	3626157	12.31	0.708140	0.000012	Chalky Limestone	Limestone, Dolostone, Marl, Chalk, Chert
174	IS023	36S	710592	3607373	28.88	0.708231	0.000007	No Bedrock	Gravel, Sand, Clay
175	IS024	36S	738739	3623292	24.01	0.706810	0.000033	Basalt	Basalt, Basanite/Flows, Intrusions and Volcaniclastics
176	IS025	36S	733524	3592864	18.05	0.708430	0.000095	No Bedrock	Gravel, Sand, Clay
177	IS026	36S	726755	3596839	38.20	0.708622	0.000136	Limestone	Limestone, Chalk, Chert
178	IS027	36S	718214	3624458	11.90	0.708464	0.000012	Limestone Breccia	Chalk, Marl
179	IS028	36R	694759	3520900	21.29	0.708733	0.000045	Limestone	Limestone, Dolostone, Marl, Chalk, Chert
180	IS029	36R	685424	3540358	16.87	0.708558	0.000010	Limestone	Limestone, Marl, Dolostone
181	IS030	36S	684603	3564722	13.23	0.709453	0.000011	No Bedrock	Clay, Silt, Sand
182	IS031	36S	674516	3554072	29.18	0.708579	0.000081	No Bedrock	Clay, Silt, Sand
183	IS032	36R	711495	3520928	10.21	0.708774	0.000013	Chalk	Chalk, Chert
184	IS033	36R	670914	3516771	10.71	0.709234	0.000014	No Bedrock	Gravel, Sand, Clay
185	IS034	36R	656001	3503878	12.68	0.708944	0.000012	Poorly Consolidated Beach Ridge	Clay, Silt, Sand
186	IS035	36R	670060	3475507	18.60	0.708470	0.000013	No Bedrock	Gravel, Sand, Clay
187	IS036	36R	672342	3445622	15.98	0.708427	0.000010	Chalk	Chalk, Chert
189	IS038	36R	650790	3375244	31.03	0.708366	0.000140	Limestone	Limestone, Dolostone, Marl
190	IS039	36R	671031	3396724	14.89	0.708464	0.000011	Limestone	Chalk, Limestone, Chert
191	IS041	36R	693961	3345350	26.85	0.708025	0.000078	Chalky Limestone	Chalk, Limestone, Marl

Sample Number	Sample Location	Zone	Easting	Northing	^{88}Sr Volts	$^{87}\text{Sr}/^{86}\text{Sr}$	$^{87}\text{Sr}/^{86}\text{Sr}$ ±	Geology From Field	Geology From Map
192	IS042	36R	694321	3325656	31.26	0.708223	0.000041	Limestone	Marl, Limestone, Sandstone
193	IS043	36R	696254	3302117	12.84	0.708347	0.000013	No Bedrock	Gravel, Sand, Clay
194	IS044	36R	692862	3296795	16.90	0.709414	0.000018	Granite/ Granodiorite	Sandstone, Pebby Sandstone, Conglomerate, Mudstone, Dolostone, Limestone
195	IS045	36R	683919	3271361	14.91	0.708418	0.000010	Granite	Sandstone, Pebby Sandstone, Conglomerate, Mudstone Dolostone, Limestone
196	IS047	36R	681161	3283499	8.49	0.709579	0.000015	Basalt?	Gravel, Sand, Clay
197	IS048	36R	680655	3310200	28.89	0.708297	0.000060	Chalky Marl	Chert, Chalk, Phosphorite, Porcelanite, Marl, Limestone, Dolostone
198	IS049	36R	707921	3372094	20.79	0.708393	0.000031	Chalky Limestone	Chalk, Limestone, Marl
199	IS050	36R	714369	3407776	13.24	0.708784	0.000012	Semi- Consolidated Aeolian Sand	Sandstone, Mudstone, Conglomerate, Limestone and Marl
200	IS051	36R	689994	3426541	12.04	0.708778	0.000014	Basalt/ Volcanic Glass	Dolostone
201	IS052	36R	716126	3453916	11.77	0.708575	0.000013	Evaporite/Limestone	Limestone, Dolostone, Marl, Conglomerate, Sandstone
202	IS053	36S	737222	3610147	18.33	0.707286	0.000033	Basalt	Basalt, Basanite/ Flows, Intrusions and Volcaniclastics
203	IS054	36S	731529	3630730	29.76	0.706600	0.000092	Basalt	Basalt, Basanite/ Flows, Intrusions and Volcaniclastics
204	IS055	36S	762106	3638757	9.79	0.706255	0.000014	Basalt	Basalt, Basanite /Flows, Intrusions and Volcaniclastics

Sample Number	Sample Location	Zone	Easting	Northing	^{88}Sr Volts	$^{87}\text{Sr}/^{86}\text{Sr}$	$^{87}\text{Sr}/^{86}\text{Sr} \pm$	Geology From Field	Geology From Map
205	IS056	36S	759511	3674122	13.69	0.705772	0.000011	Basalt	Basalt, Basanite/Flows
206	IS057	36S	757638	3688033	16.24	0.708304	0.000009	Limestone	Limestone, Dolostone
207	IS057	36S	757638	3688033	15.55	0.709423	0.000126	Limestone	Limestone, Dolostone
208	IS058	36S	742215	3672867	19.65	0.707834	0.000124	No Bedrock	Gravel, Sand, Clay
215	IS061	36S	734413	3647972	12.24	0.709245	0.000013	Limestone	Limestone, Chalk, Chert
216	IS062	36S	745328	3655402	12.80	0.706763	0.000012	Basalt	Basalt, Basanite, Flows
276	IS040	36R	678358	3388028	21.53	0.708230	0.000009	Basalt?	Sandstone, Clay

Table 5.1 Israeli Bioavailable Soil Strontium Isotope Results

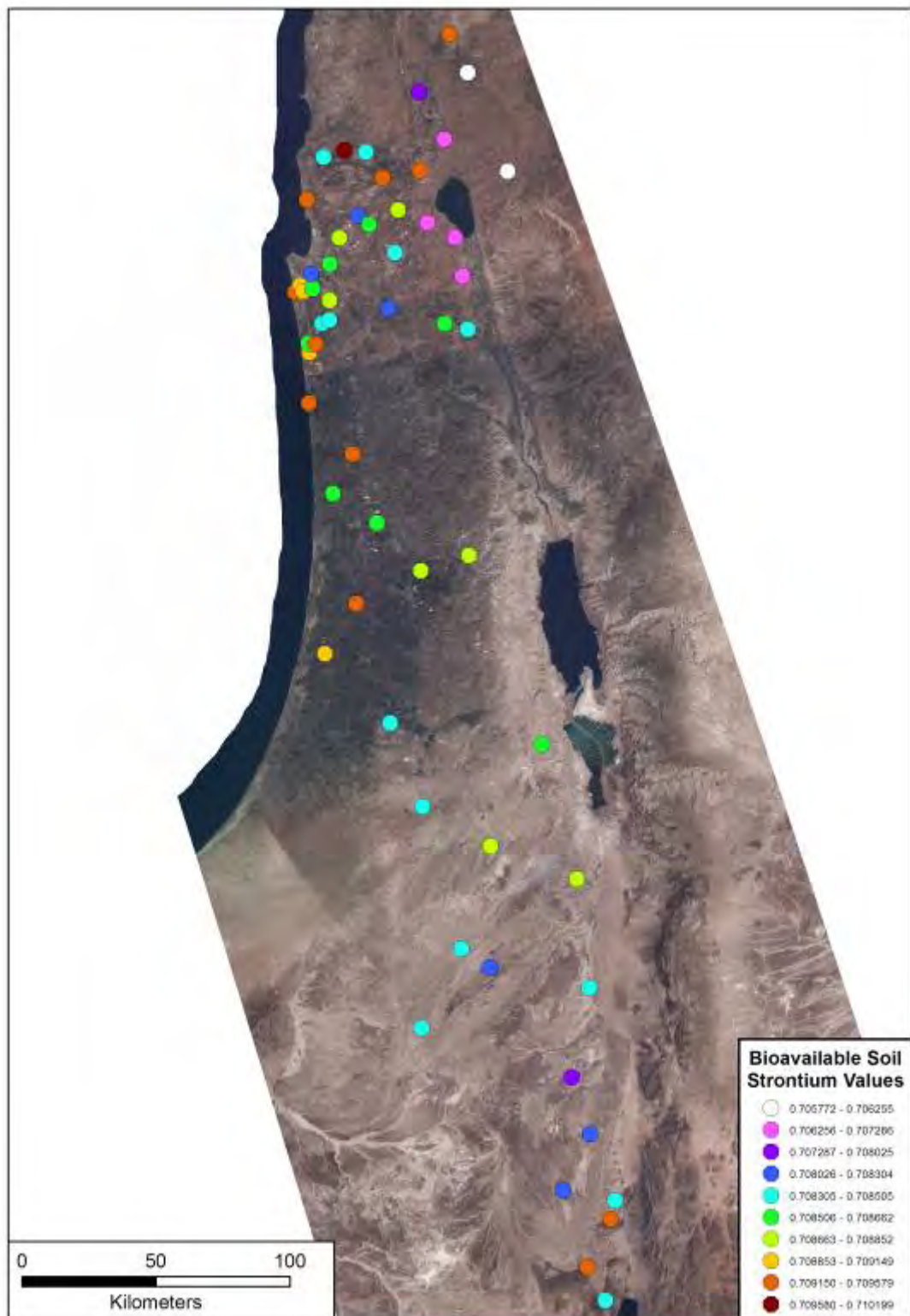


**Figure 5.1 Israeli Bioavailable Soil Strontium Results Overlaid on Landsat Image
(Provided by Dr Stephen Savage, Arizona State University 2010)**

5.2.1.2. Israeli Rock Samples

48 rock samples were analysed for $^{87}\text{Sr}/^{86}\text{Sr}$ values from Israel over a range of 0.705291 ± 0.000006 through 0.740718 ± 0.000014 , shown in Table 5.2 and Figure 5.5.

Sample Number	Sample Location	Zone	Easting	Northing	^{88}Sr Volts	$^{87}\text{Sr}/^{86}\text{Sr}$	$^{87}\text{Sr}/^{86}\text{Sr}^{+}$	Geology From Field	Geology From Map
101	IS004	36S	681536	3604285	17.16	0.709112	0.000010	Sandstone with Carbonate Matrix	Dolostone, Limestone, Chert
102	IS005	36S	684801	3623556	23.21	0.707801	0.000008	Reefal Limestone	Limestone, Marl, Dolostone
103	IS006	36S	685092	3621362	18.78	0.707630	0.000009	Reefal Limestone	Limestone, Marl, Dolostone
104	IS007	36S	683780	3603356	14.93	0.707975	0.000011	Limestone	Limestone, Marl, Dolostone
105	IS008	36S	687978	3609221	33.14	0.707924	0.000007	Chalk	Chalk, Chert
106	IS009	36S	695586	3650202	29.41	0.709103	0.000007	Calcareous Sandstone 'Kurkar'	Clay, Silt, Sand
107	IS010	36S	705301	3661995	30.34	0.707577	0.000007	Limestone	Limestone, Marl, Dolostone
108	IS011	36S	712541	3662131	21.70	0.707328	0.000008	Very Fine Grained Limestone	Chalk, Marl
109	IS012	36S	719243	3659214	27.66	0.707514	0.000008	Limestone	Limestone, Dolostone, Marl, Chalk, Chert
110	IS013	36S	721813	3649514	7.48	0.707795	0.000015	Chalky Limestone	Limestone, Dolostone, Marl, Chalk, Chert
111	IS015	36S	702082	3634803	10.71	0.708449	0.000013	Limestone Breccia	Gravel, Sand, Clay
112	IS016	36S	710374	3639794	17.18	0.708029	0.000010	Chalky Limestone	Chalk, Marl
113	IS017	36S	723533	3637663	23.86	0.708532	0.000008	Chalky White Limestone	Limestone, Chalk, Marl, Sandstone
114	IS018	36S	712855	3636020	18.83	0.708182	0.000009	Chalky Limestone	Dolostone, Limestone, Chert
115	IS019	36S	692598	3615897	2.45	0.708989	0.000031	Limestone	Limestone, Marl, Dolostone
116	IS020	36S	690737	3609663	30.28	0.708000	0.000007	Chalky Limestone	Chalk, Chert

Sample Number	Sample Location	Zone	Easting	Northing	^{88}Sr Volts	$^{87}\text{Sr}/^{86}\text{Sr}$	$^{87}\text{Sr}/^{86}\text{Sr} \pm$	Geology From Field	Geology From Map
117	IS021	36S	688498	3621292	16.10	0.708315	0.000010	Limestone	Limestone, Dolostone, Marl, Chalk, Chert
118	IS022	36S	689525	3626157	18.13	0.707838	0.000009	Chalky Limestone	Limestone, Dolostone, Marl, Chalk, Chert
119	IS024	36S	738739	3623292	34.72	0.706807	0.000007	Basalt	Basalt, Basanite/Flows, Intrusions and Volcaniclastics
120	IS027	36S	718214	3624458	7.58	0.707963	0.000016	Limestone Breccia	Chalk, Marl
121	IS028	36R	694759	3520900	26.19	0.708417	0.000008	Limestone	Limestone, Dolostone, Marl, Chalk, Chert
122	IS026	36S	726755	3596839	25.11	0.708106	0.000008	Limestone	Limestone, Chalk, Chert
123	IS032	36R	711495	3520928	20.21	0.708617	0.000009	Chalk	Chalk, Chert
124	IS034	36R	656001	3503878	39.31	0.708460	0.000006	Poorly Consolidated Beach Ridge	Clay, Silt, Sand
126	IS037	36R	670360	3419638	21.50	0.707696	0.000009	Chalky Limestone	Limestone, Dolostone, Marl, Conglomerate, Sandstone
127	IS038	36R	650790	3375244	25.96	0.707777	0.000008	Limestone	Limestone, Dolostone, Marl
128	IS039	36R	671031	3396724	21.22	0.707963	0.000008	Limestone	Chalk, Limestone, Chert
129	IS040	36R	678358	3388028	20.55	0.707575	0.000008	Basalt?	Sandstone, Clay
131	IS041	36R	693961	3345350	45.02	0.707879	0.000006	Chalky Limestone	Chalk, Limestone, Marl
132	IS041	36R	693961	3345350	21.07	0.707988	0.000009	Silcrete	Chalk, Limestone, Marl
134	IS044	36R	692862	3296795	9.94	0.740718	0.000014	Granite/ Granodiorite	Sandstone, Pebby Sandstone, Conglomerate, Mudstone, Dolostone, Limestone
135	IS045	36R	683919	3271361	24.76	0.711296	0.000007	Granite	Sandstone, Pebby Sandstone, Conglomerate, Mudstone Dolostone, Limestone
136	IS046	36R	681467	3284927	7.09	0.709553	0.000015	Consolidated Quaternary Sediment	Basalt, Basanite/Flows
137	IS047	36R	681161	3283499	10.18	0.714749	0.000013	Basalt?	Gravel, Sand, Clay

Sample Number	Sample Location	Zone	Easting	Northing	88Sr Volts	$^{87}\text{Sr}/^{86}\text{Sr}$	$^{87}\text{Sr}/^{86}\text{Sr} +$	Geology From Field	Geology From Map
138	IS048	36R	680655	3310200	9.13	0.708083	0.000014	Chalky Marl	Chert, Chalk, Phosphorite, Porcelanite, Marl, Limestone, Dolostone
139	IS049	36R	707921	3372094	26.11	0.707840	0.000007	Chalky Limestone	Chalk, Limestone, Marl
140	IS050	36R	714369	3407776	24.43	0.708615	0.000008	Semi-consolidated Aeolian Sand	Sandstone, Mudstone, Conglomerate, Limestone and Marl
141	IS051	36R	689994	3426541	28.88	0.708662	0.000007	Basalt/Volcanic Glass	Dolostone
142	IS052	36R	716126	3453916	24.12	0.708045	0.000007	Evaporite/Limestone	Limestone, Dolostone, Marl, Conglomerate, Sandstone
143	IS053	36S	737222	3610147	15.75	0.706096	0.000010	Basalt	Basalt, Basanite/Flows, Intrusions and Volcaniclastics
144	IS054	36S	731529	3630730	41.72	0.705853	0.000006	Basalt	Basalt, Basanite/Flows, Intrusions and Volcaniclastics
147	IS056	36S	759511	3674122	41.79	0.705291	0.000006	Basalt	Basalt, Basanite/Flows
148	IS060	36S	685379	3623856	16.89	0.708608	0.000010	Limestone	Limestone, Marl, Dolostone
149	IS061	36S	734413	3647972	20.66	0.707868	0.000008	Limestone	Limestone, Chalk, Chert
274	IS042	36R	694321	3325656	25.73	0.707423	0.000009	Limestone	Marl, Limestone, Sandstone
275	IS022	36S	689525	3626157	13.53	0.708036	0.000012	Limestone Breccia	Limestone, Dolostone, Marl, Chalk, Chert
277	IS057	36S	757638	3688033	25.29	0.707584	0.000008	Limestone	Limestone, Dolostone
278	IS062	36S	745328	3655402	27.87	0.705448	0.000008	Basalt	Basalt/Basanite/Flows

Table 5.2 Israeli Bioavailable Rock Strontium Isotope Results

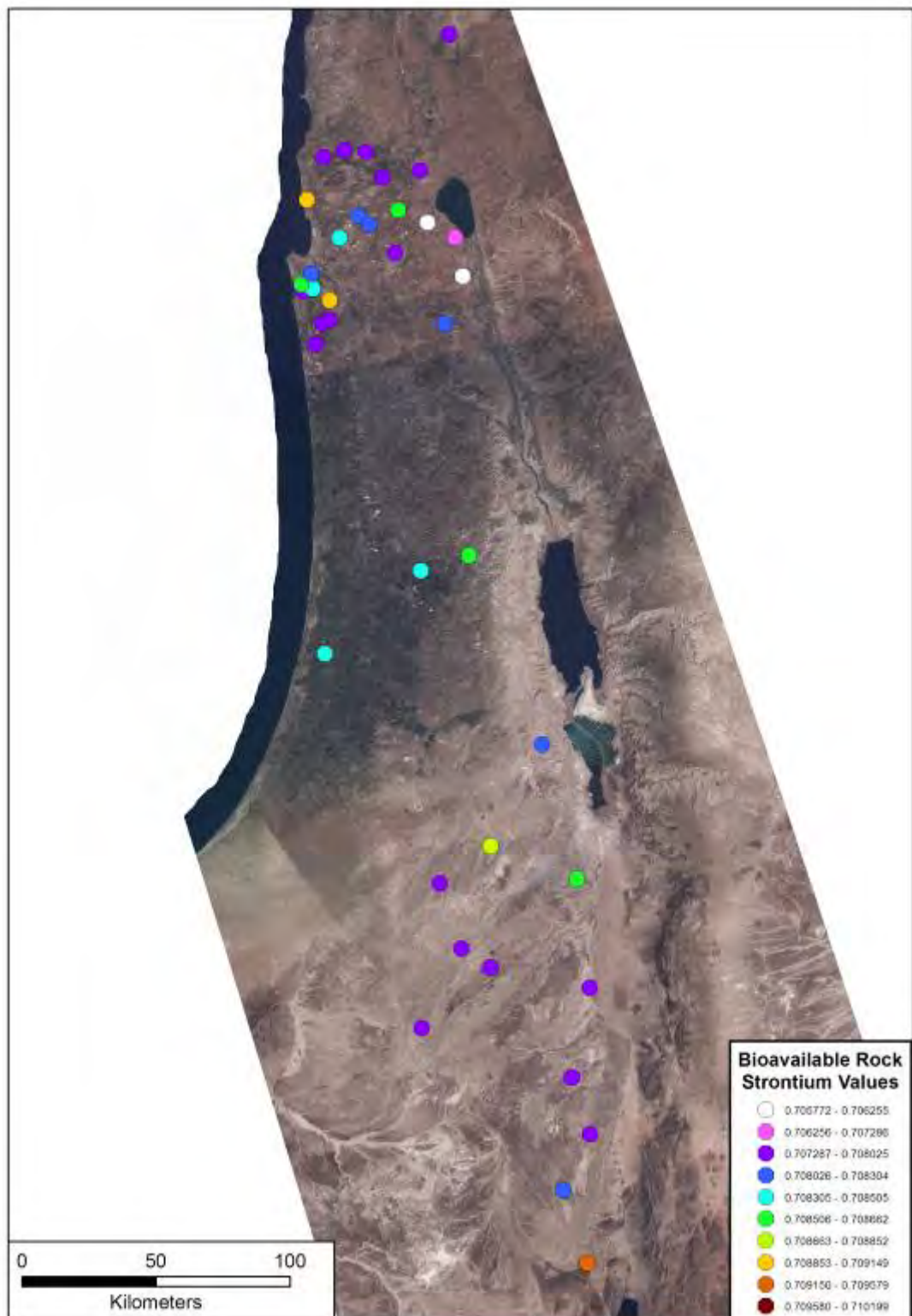


**Figure 5.2 Israeli Bioavailable Rock Strontium Results Overlain on Landsat Image
(Provided by Dr Stephen Savage, Arizona State University 2010)**

5.2.2. France

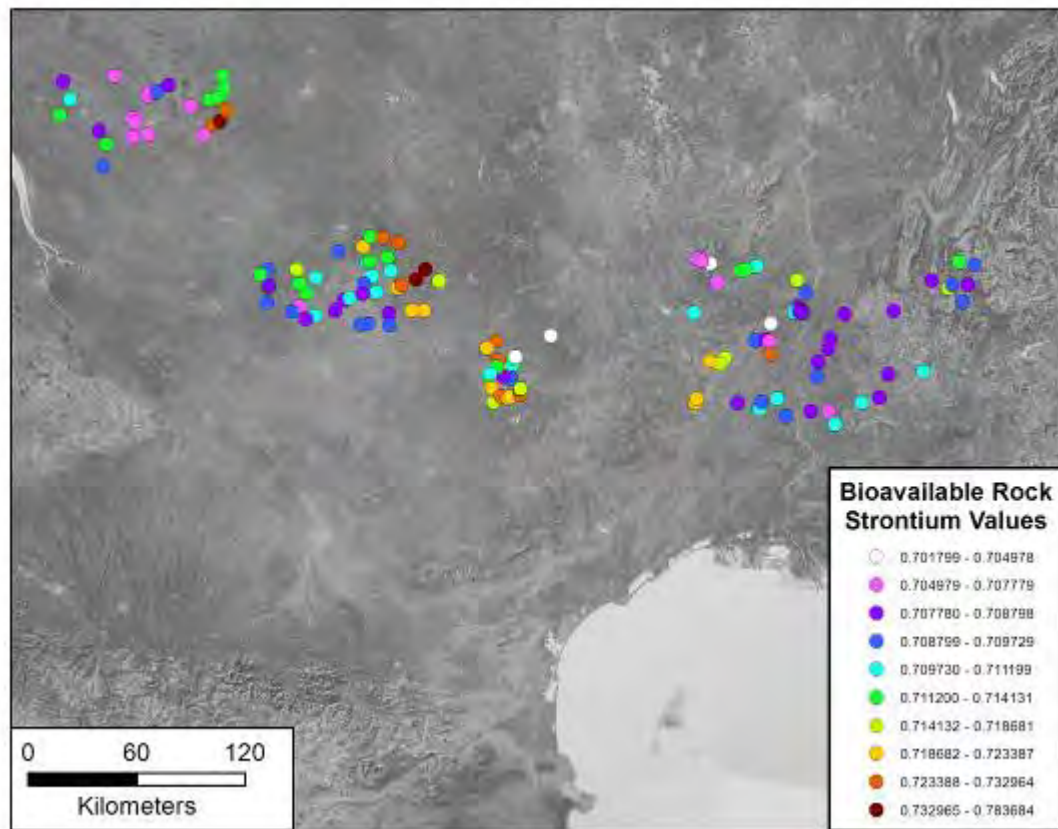


Figure 5.3 French Bioavailable Strontium Results Overlain on Landsat Image

5.2.2.1. French Plant Samples

A total of 59 French grass samples were analysed for $^{87}\text{Sr}/^{86}\text{Sr}$ values over a range of 0.704506 ± 0.000025 through 0.727378 ± 0.000036 , shown in Table 5.3.

Sample Number	Zone	Easting	Northing	^{88}Sr Volts	$^{87}\text{Sr}/^{86}\text{Sr}$	$\pm^{87}\text{Sr}/^{86}\text{Sr}$	Plant Type	Geology From Map
P2P	31T	636270	4972220	4.69	0.715531	0.000026	Grass	Monzogranite, Granodiorite
P3P1	31T	613978	4979921	2.57	0.727378	0.000036	Grass	Anatectic Orthogneiss
P3P2	31T	613978	4979921	5.33	0.710162	0.000026	Grass	Anatectic Orthogneiss
P4P	31T	605305	4977747	5.11	0.713146	0.000039	Grass	Monzogranite, Granodiorite
P5P	31T	608043	4977994	5.12	0.713073	0.000033	Grass	Monzogranite, Granodiorite
P6P	31T	581185	4983778	10.36	0.706023	0.000015	Grass	Clay, Conglomerate, Sandstone, Marl
P7P	31T	588195	4981254	4.15	0.704978	0.000115	Grass	Basanite, Hawaite, Tephra
P8P	31T	583541	4982608	7.87	0.715615	0.000026	Grass	Monzogranite, Granodiorite
P9P	31T	583488	4982629	4.39	0.707561	0.000107	Grass	Monzogranite, Granodiorite
P10P	31T	592176	4970857	5.22	0.705976	0.000029	Grass	Monzogranite, Granodiorite
P11P	31T	579265	4953843	5.13	0.710281	0.000026	Grass	Anatectic Orthogneiss
P12P	31T	596388	4928948	11.69	0.717775	0.000020	Grass	Schist, Micaschist, Quartzite
P13P	31T	593569	4925774	7.97	0.716697	0.000026	Grass	Dolomite, Marl, Evaporite
P14P	31T	588209	4926940	4.68	0.723387	0.000032	Grass	Schist, Micaschist, Quartzite
P15P	31T	579935	4903929	6.38	0.719946	0.000021	Grass	Sandstone, Conglomerate, Coal, Shale
P16P	31T	580827	4906144	4.52	0.719631	0.000031	Grass	Metagranite, Orthogneiss
P17P	31T	603549	4903924	11.34	0.708481	0.000017	Grass	Marl, Sandstone, Conglomerate, Limestone
P19P	31T	615732	4900551	6.38	0.709824	0.000025	Grass	Marl, Sand, Sandstone, Clay, Limestone
P20P	31T	630308	4896756	5.52	0.709391	0.000028	Grass	Marl, Sandstone, Chalk, Limestone
P23P	31T	613289	4938650	3.87	0.709465	0.000120	Grass	Marl, Limestone, Clay
P24P	31T	621739	4931192	4.18	0.724350	0.000119	Grass	Marl, Sand, Sandstone, Clay, Limestone
P25P	31T	619053	4939189	5.84	0.708056	0.000037	Grass	Marl, Sand, Sandstone, Clay, Limestone

Sample Number	Zone	Easting	Northing	^{88}Sr Volts	$^{87}\text{Sr}/^{86}\text{Sr}$	$\pm \frac{^{87}\text{Sr}}{^{86}\text{Sr}}$	Plant Type	Geology From Map
P26P	31T	621056	4938201	12.52	0.707469	0.000019	Grass	Marl, Sand, Sandstone, Clay, Limestone
P27P	31T	621678	4947939	6.60	0.704506	0.000025	Grass	Basanite, Hawaïite, Tephra
P28P	31T	648226	4926782	7.13	0.708191	0.000035	Grass	Marl, Sandstone, Conglomerate, Limestone
P29P	31T	647406	4918675	2.90	0.709561	0.000160	Grass	Marl, Conglomerate, Sandstone, Limestone
P30P	31T	643842	4899117	4.68	0.708595	0.000023	Grass	Marl, Sandstone, Chalk, Limestone
P31P	31T	653617	4899215	14.13	0.707768	0.000269	Grass	Marl, Conglomerate, Sandstone, Limestone
P32P1	31T	657405	4892315	3.55	0.708869	0.000134	Grass	Sand, Clay, Gravel, Pebble
P32P2	31T	657405	4892315	5.44	0.711199	0.000028	Grass	Sand, Clay, Gravel, Pebble
P33P	31T	672108	4904389	5.67	0.709960	0.000090	Grass	Marl, Conglomerate, Sandstone, Limestone
P34P	31T	681983	4906777	4.75	0.709729	0.000027	Grass	Marl, Sandstone, Shale, Limestone
P35P	31T	681983	4906777	10.18	0.708039	0.000012	Grass	Marl, Sandstone, Shale, Limestone
P36P	31T	687076	4920070	11.92	0.708299	0.000018	Grass	Marl, Black Shale, Limestone
P37P	31T	706382	4921412	5.88	0.710581	0.000023	Grass	Marl, Sandstone, Shale, Limestone
P38P	31T	720216	4967508	12.40	0.715361	0.000018	Grass	Marl, Black Shale, Limestone
P39P	31T	641335	4965374	10.21	0.709374	0.000037	Grass	Micaschist, Paragneiss
P40P	31T	637294	4957464	8.20	0.708611	0.000063	Grass	Marl, Limestone, Clay
P42P	31T	637838	4955061	6.43	0.709827	0.000023	Grass	Sand, Clay, Gravel, Pebble
P43P	31T	625288	4906215	6.21	0.710070	0.000028	Grass	Sand, Clay, Gravel, Pebble
P44P	31T	616838	4904608	10.14	0.708921	0.000025	Grass	Limestone, Marl, Conglomerate, Sandstone
P45P	31T	653625	4934020	8.05	0.708744	0.000027	Grass	Marl, Sand, Sandstone, Clay, Limestone
P46P	31T	654816	4939806	5.01	0.708516	0.000090	Grass	Sand, Clay, Gravel, Pebble

Sample Number	Zone	Easting	Northing	^{88}Sr Volts	$^{87}\text{Sr}/^{86}\text{Sr}$	$\pm^{87}\text{Sr}/^{86}\text{Sr}$	Plant Type	Geology From Map
P47P	31T	662743	4953227	8.96	0.708716	0.000029	Grass	Sand, Clay, Gravel, Pebble
P48P	31T	689814	4954965	12.09	0.708016	0.000031	Grass	Sand, Clay, Gravel, Pebble
P49P	31T	710762	4971827	10.30	0.708570	0.000031	Grass	Marl, Black Shale, Limestone
P50P	31T	722254	4969472	7.16	0.708880	0.000028	Grass	Marl, Black Shale, Limestone
P51P	31T	728364	4960019	5.53	0.709114	0.000030	Grass	Marl, Sandstone, Conglomerate, Limestone
P52P	31T	730957	4969576	10.93	0.708496	0.000032	Grass	Limestone, Calcschist, Marl
P53P	31T	734845	4980417	6.11	0.709544	0.000080	Grass	Limestone, Calcschist, Marl
P54P	31T	726367	4982172	6.43	0.711692	0.000023	Grass	Amphibolite, Micaschist, Leptynite
P55P	31T	634821	4954581	3.17	0.710422	0.000038	Grass	Marl, Limestone, Clay
P56P	31T	637537	4954548	10.82	0.707779	0.000019	Grass	Marl, Limestone, Clay
P57P	31T	637797	4954224	3.47	0.709514	0.000033	Grass	Sand, Clay, Gravel, Pebble
P58P	31T	638372	4954718	10.11	0.708046	0.000028	Grass	Sand, Clay, Gravel, Pebble
P59P	31T	639063	4954711	5.55	0.708283	0.000023	Grass	Sand, Clay, Gravel, Pebble
P60P	31T	639524	4953538	6.75	0.709289	0.000081	Grass	Sand, Clay, Gravel, Pebble
P61P	31T	639548	4953539	8.14	0.709065	0.000031	Grass	Sand, Clay, Gravel, Pebble
P62P	31T	638754	4954550	5.17	0.707968	0.000023	Grass	Sand, Clay, Gravel, Pebble

Table 5.3 French Plant (Grass) Bioavailable Strontium Isotope Results

5.2.2.2. French Soil Samples

A total of 81 soil samples from France were analysed for $^{87}\text{Sr}/^{86}\text{Sr}$ values, which have a range of 0.701799 ± 0.006234 through 0.817507 ± 0.000013 , shown in Table 5.4.

Sample Number	Zone	Easting	Northing	^{88}Sr Volts	$^{87}\text{Sr}/^{86}\text{Sr}$	\pm $^{87}\text{Sr}/^{86}\text{Sr}$	Geology From Field	Geology From Map
F19SB	31T	312689	5058080	12.16	0.726320	0.000032	Not Recorded	Migmatite
F38SB	31T	320406	5066301	15.94	0.725510	0.000027	Not Recorded	Peraluminous Leucogranite
SS001F	30T	721160	503407	11.00	0.708985	0.000013	Chalky Limestone	Limestone, Marl, Clay, Sand
SS011F	30T	695046	5060790	7.30	0.711301	0.000020	No Outcrop	Sand, Clay, Gravel, Shingle
FS008-S2	30T	699404	5035025	12.47	0.708559	0.000011	Limestone	Sand, Clay, Gravel, Shingle
FS010-S1	30T	722129	5046685	5.31	0.711507	0.000025	Limestone	Limestone, Marl, Clay, Sand
FS011-S1	30T	717474	5053975	13.73	0.708584	0.000011	Limestone	Limestone, Marl, Clay, Sand
FS016-S1	30T	723956	5084905	15.05	0.707727	0.000010	Limestone	Marl, Limestone, Clay
FS018-S1	30T	695487	5079441	14.12	0.708161	0.000011	Chalky Limestone	Limestone, Marl, Clay, Sand
FS021-S1	30T	700316	5070033	3.99	0.710074	0.000024	Limestone with Siliceous Cobbles	Limestone, Marl, Clay, Sand
FS027-S1	31T	343303	4977631	9.06	0.710389	0.000015	No Bedrock	Limestone, Marl, Clay, Sand
FS027-S2	31T	343303	4977631	18.64	0.709303	0.000009	No Bedrock	Limestone, Marl, Clay, Sand
FS029-S1	31T	339031	4974815	7.77	0.712033	0.000015	No Bedrock	Sand, Clay, Gravel, Shingle
FS031-S1	31T	343614	4968831	2.08	0.714027	0.000050	Limestone	Marl, Limestone, Clay
FS032-S1	31T	343902	4969003	14.12	0.710796	0.000012	No Bedrock	Marl, Limestone, Clay
FS032-S2	31T	343902	4969003	42.45	0.709347	0.000006	No Bedrock	Marl, Limestone, Clay
FS032-S3	31T	343902	4969003	3.65	0.708212	0.000030	No Bedrock	Marl, Limestone, Clay
FS034-S1	31T	351190	4971992	0.26	0.737233	0.000676	Siliceous/Iron Precipitate	Marl, Clay, Limestone, Sandstone, Conglomerate
FS035-S1	31T	364413	4964789	11.53	0.713096	0.000014	No Bedrock	Clay, Sand, Gravel, Shingle
FS036-S1	31T	360875	4970271	3.64	0.712053	0.000025	Limestone	Limestone, Marl, Clay, Sand
FS037-S1	31T	359240	4977874	11.46	0.717308	0.000012	Limestone	Limestone, Marl, Clay, Sand

Sample Number	Zone	Easting	Northing	^{88}Sr Volts	$^{87}\text{Sr}/^{86}\text{Sr}$	$^{87}\text{Sr}/^{86}\text{Sr}^{+}$	Geology From Field	Geology From Map
FS041-S1	31T	398097	4981868	2.00	0.716805	0.000038	Limestone	Marl, Limestone, Dolomite
FS041-S2	31T	398097	4981868	11.48	0.710096	0.000013	Limestone	Marl, Limestone, Dolomite
FS043-S1	31T	400967	4974223	9.71	0.709837	0.000013	No Bedrock	Sand, Clay, Gravel, Shingle
FS044-S1	31T	411219	4977151	11.24	0.710436	0.000012	No Bedrock	Paragneiss, Leptynite, Amphibolite
FS045-S3	31T	399344	4982356	12.25	0.708879	0.000012	Limestone	Marl, Limestone, Dolomite
FS046-S1	31T	399442	4982467	6.89	0.714131	0.000015	No Bedrock	Marl, Limestone, Dolomite
FS047-S4	31T	396434	4970063	4.21	0.709697	0.000025	Limestone, Not <i>In Situ</i>	Limestone, Marl, Clay, Sand
FS049-S1	31T	385154	4960867	7.55	0.708798	0.000186	Limestone	Marl, Limestone, Clay
FS050-S1	31T	388530	4961960	4.60	0.709939	0.000029	Chalky Limestone	Marl, Limestone, Clay
FS051-S1	31T	395569	4964432	11.98	0.708603	0.000012	Limestone	Marl, Limestone, Clay
FS052-S1	31T	403352	4965698	6.21	0.710762	0.000031	Limestone	Marl, Limestone, Clay
FS052-S2	31T	403352	4965698	4.05	0.710286	0.000023	Limestone	Marl, Limestone, Clay
FS053-S1	31T	395867	4990680	3.42	0.719269	0.000027	Red Sandstone/ Schist	Sandstone, Conglomerate, Shale, Coal
FS054-S1	31T	400221	4996198	3.64	0.712245	0.000026	Meta-Sediment	Leptynite, Orthogneiss, Amphibolite
FS055-S2	31T	406773	4995726	6.79	0.725528	0.000017	Heavily Weathered Metamorphics	Anatetic Orthogneiss
FS056-S1	31T	415656	4992939	6.60	0.711984	0.000018	No Bedrock	Granites, Orthogneiss
FS057-S1	31T	415617	4992973	9.27	0.726901	0.000015	Meta-Sediment	Granites, Orthogneiss
FS058-S1	31T	409561	4984669	3.26	0.713898	0.000031	No Bedrock	Granites, Orthogneiss
FS059-S1	31T	409401	4984606	11.29	0.713071	0.000011	Metamorphics	Granites, Orthogneiss
FS060-S1	31T	414875	4967937	5.04	0.720113	0.000020	Metamorphics	Leptynite, Orthogneiss, Amphibolite
FS061-S1	31T	417163	4969334	9.82	0.726981	0.000013	Metamorphics	Paragneiss, Leptynite, Amphibolite

Sample Number	Zone	Easting	Northing	^{88}Sr Volts	$^{87}\text{Sr}/^{86}\text{Sr}$	\pm $^{87}\text{Sr}/^{86}\text{Sr}$	Geology From Field	Geology From Map
FS063-S1	31T	425397	4972325	3.64	0.754291	0.000026	Granite	Monzogranite, Granodiorite
FS065-S1	31T	430294	4978100	2.44	0.783684	0.000041	Granite	Micaschist, Paragneiss
FS065-S2	31T	430294	4978100	11.90	0.817507	0.000013	Granite	Micaschist, Paragneiss
FS067-S1	31T	437844	4971581	19.05	0.717422	0.000010	Granite	Monzogranite, Granodiorite
FS070-S1	31T	429643	4955208	6.51	0.720284	0.000017	Metamorphics	Micaschist, Paragneiss
FS072-S1	31T	422683	4955326	2.94	0.721632	0.000027	Metamorphics	Leptynite, Orthogneiss, Amphibolite
FS074-S1	31T	410228	4953484	17.24	0.708488	0.000009	Limestone	Marl, Limestone, Dolomite
FS076-S1	31T	382579	4987769	5.28	0.708869	0.000038	Chalky Limestone	Limestone, Marl
FS078-S1	31T	410586	4947189	12.03	0.709684	0.000011	Limestone	Limestone, Marl
FS080-S1	31T	398816	4947905	2.24	0.709616	0.000048	Limestone	Limestone, Marl
FS081-S1	31T	394242	4947356	2.85	0.708967	0.000031	Limestone	Marl, Limestone, Clay
FS083-S1	31T	380555	4955229	10.09	0.708452	0.000015	Limestone	Marl, Clay, Limestone, Conglomerate
FS084-S1	31T	369306	4952391	4.91	0.710005	0.000023	Limestone	Marl, Limestone, Clay
FS085-S1	31T	364172	4950411	8.05	0.708299	0.000015	Limestone	Marl, Limestone, Clay
FS086-S1	31T	360351	4957598	9.89	0.707537	0.000015	Limestone	Limestone, Marl, Clay, Sand
FS087-S1	31T	356453	4954771	13.55	0.709055	0.000011	Fossiliferous Limestone	Marl, Limestone, Clay
FS088-S1	31T	342579	4959745	11.25	0.708926	0.000016	Limestone	Limestone, Marl, Clay, Sand
FS089-S1	31T	369850	4973456	12.40	0.710853	0.000011	Limestone	Limestone, Marl, Clay, Sand
FS090-S2	31T	466090	4918254	2.76	0.712240	0.000033	Limestone	Limestone, Marl
FS092-S1	31T	476904	4923011	14.76	0.718681	0.000011	Red Sandstone	Marl, Dolomite, Limestone, Sandstone
FS093-S1	31T	477763	4917559	6.75	0.709320	0.000017	Limestone	Limestone, Marl
FS094-S1	31T	473503	4918987	9.97	0.708000	0.000011	Limestone	Limestone, Marl
FS096-S1	31T	467072	4912565	15.98	0.720050	0.000009	Interbedded Claystone/Sandstone	Sandstone, Conglomerate, Shale, Coal

Sample Number	Zone	Easting	Northing	⁸⁸ Sr Volts	⁸⁸ Sr/ ⁸⁶ Sr	⁸⁷ Sr/ ⁸⁶ Sr	Geology From Field	Geology From Map
FS097-S1	31T	468261	4904608	12.21	0.718429	0.000013	Meta-Sediment	Marl, Limestone, Dolomite
FS099-S1	31T	472222	4907536	15.84	0.728262	0.000011	Metamorphics	Granites, Orthogneiss
FS100-S1	31T	476284	4906484	13.76	0.722192	0.000012	Metamorphics	Micaschist, Paragneiss
FS102-S1	31T	477133	4907464	4.57	0.720363	0.000023	Metamorphics	Migmatite
FS103-S1	31T	483049	4908159	12.30	0.728433	0.000012	Metamorphics	Anatetic Orthogneiss
FS104-S2	31T	482468	4911339	6.91	0.751565	0.000017	Metamorphics	Micaschist, Paragneiss
FS105-S1	31T	483003	4911985	7.25	0.718595	0.000017	Metamorphics	Granite, Orthogneiss
FS107-S1	31T	478875	4925330	17.03	0.711001	0.000010	Limestone	Marl, Dolomite, Limestone, Sandstone
FS108-S1	31T	479023	4928892	27.01	0.713022	0.000009	Red Interbedded Sandstone/ Siltstone	Sandstone, Conglomerate, Shale, Coal
FS111-S1	31T	469680	4938102	13.69	0.727959	0.000011	Granite	Monzogranite, Granodiorite
FS112-S1	31T	464584	4934617	3.69	0.720635	0.000032	Granite	Schist, Mica Schist, Quartzite
FS113-S1	31T	470929	4927979	2.29	0.732964	0.000042	Red Sandstone	Sandstone, Conglomerate, Shale, Coal
FS114-S1	31T	470182	4923875	2.07	0.714013	0.000042	Limestone	Limestone, Marl, Dolomite
FS115-S1	31T	466355	4920134	9.39	0.710655	0.000014	Limestone	Limestone, Marl, Dolomite
FS116-S1	31T	480240	4929489	14.54	0.701799	0.006234	Basalt	Basanite, Hawaïite, Tephra
FS118-S1	31T	499737	4941195	13.55	0.704966	0.000012	Basalt and Tuff	Basanite, Hawaïite, Tephra

Table 5.4 French Soil Bioavailable Strontium Isotope Results

5.2.2.3. French Rock Samples

A total of 19 rock samples from France were analysed for $^{87}\text{Sr}/^{86}\text{Sr}$ values, which have a range of 0.707071 ± 0.000029 through 0.747038 ± 0.000029 , shown in Table 5.5.

Sample Number	Zone	Easting	Northing	^{88}Sr Volts	$^{87}\text{Sr}/^{86}\text{Sr}$	$^{87}\text{Sr}/^{86}\text{Sr} \pm$	Geology From Field	Geology From Map
F12R	31T	288396	5061776	9.17	0.707368	0.000029	Not Recorded	Marl, Limestone, Clay
F16R	31T	307742	5053032	9.55	0.707681	0.000028	Not Recorded	Limestone, Marl
F1R	31T	270113	5062276	10.62	0.707326	0.000031	Not Recorded	Marl, Limestone, Clay
F21R	31T	316566	5060204	12.87	0.747038	0.000029	Not Recorded	Monzogranite, Granodiorite
F23R1	31T	276762	5074376	15.61	0.707129	0.000023	Not Recorded	Marl, Limestone, Clay
F23R2	31T	276762	5074376	9.51	0.707071	0.000029	Not Recorded	Marl, Limestone, Clay
F24R	31T	278596	5076516	8.17	0.707250	0.000033	Not Recorded	Marl, Limestone, Clay
F25R	31T	281821	5076711	4.97	0.708990	0.000185	Not Recorded	Marl, Limestone, Clay
F27R	31T	287966	5080184	7.96	0.708079	0.000028	Not Recorded	Basanite, Hawaïite, Tephra
F2R	31T	267858	5061775	9.81	0.707237	0.000031	Not Recorded	Marl, Limestone, Clay
F33R	31T	318122	5085533	7.35	0.711714	0.000062	Not Recorded	Monzogranite, Granodiorite
F34R	31T	318861	5078299	10.44	0.711919	0.000207	Not Recorded	Paragneiss, Leptynite, Amphibolite
F36R	31T	310778	5072387	28.08	0.712497	0.000008	Not Recorded	Paragneiss, Leptynite, Amphibolite
F37R	31T	315835	5073517	5.08	0.712145	0.000025	Not Recorded	Paragneiss, Leptynite, Amphibolite
F40R	31T	300215	5068414	30.20	0.707617	0.000008	Not Recorded	Limestone, Marl
F4R	31T	269552	5059518	10.46	0.707478	0.000025	Not Recorded	Limestone, Marl, Clay, Sand
F6R	31T	268448	5051324	8.74	0.707582	0.000035	Not Recorded	Limestone, Marl, Clay, Sand
F8R	31T	276850	5052823	9.71	0.707500	0.000031	Not Recorded	Limestone, Marl, Clay, Sand
P18R	31T	615072	4901240	7.99	0.709525	0.000037	Not Recorded	Limestone Reef Facies Urgonian

Table 5.5 French Rock Bioavailable Strontium Isotope Results

5.3. Israeli Archaeological Sites

5.3.1. Skhul

5.3.1.1. LA-ICPMS Results

Samples 851, 852 and 853 from the archaeological site of Skhul were analysed for element concentration and ratios using LA-ICPMS, as summarised in Table 5.6 and shown in detail in section A3.1.1.1.

Sample	Material	Transect	Mg (ppm)	Sr (ppm)	Ba (ppm)	U (ppm)	Mg/Ca	Sr/Ca	Ba/Ca
851	Enamel	One	2090	347	77	2	0.009102	0.000419	0.000060
851	Dentine	One	1633	412	205	31	0.007113	0.000498	0.000158
852	Enamel	One	1603	277	91	1	0.006980	0.000335	0.000070
852	Dentine	One	1176	254	95	19	0.005129	0.000307	0.000073
853	Enamel	One	1630	577	70	3	0.007099	0.000697	0.000054
853	Dentine	One	1606	525	154	24	0.007874	0.000634	0.000119

Table 5.6 Summary Table of LA-ICPMS Elemental Concentrations and Ratios for Faunal Teeth from Skhul

5.3.1.2. MC-ICPMS Results

Two sediment samples, R_1057 and R_1058, from stratigraphic unit B from the archaeological site of Skhul were analysed using MC-ICPMS to determine their $^{87}\text{Sr}/^{86}\text{Sr}$ composition, as summarised in Table 5.7.

Sample Number	Associated with Tooth	Stratigraphic Unit	Age (ky)	$^{87}\text{Sr}/^{86}\text{Sr}$	$^{87}\text{Sr}/^{86}\text{Sr} 2\sigma$ Error
R_1057	1057	B	150 ± 26	0.708636	0.000012
R_1058	1058	B	95 ± 15	0.708722	0.000013

Table 5.7 $^{87}\text{Sr}/^{86}\text{Sr}$ Results from Archaeological Sediments from Skhul

5.3.1.3. Regional Mapping Results

Strontium isotope values from soil samples immediately surrounding the site of Skhul are shown in Figure 5.4.

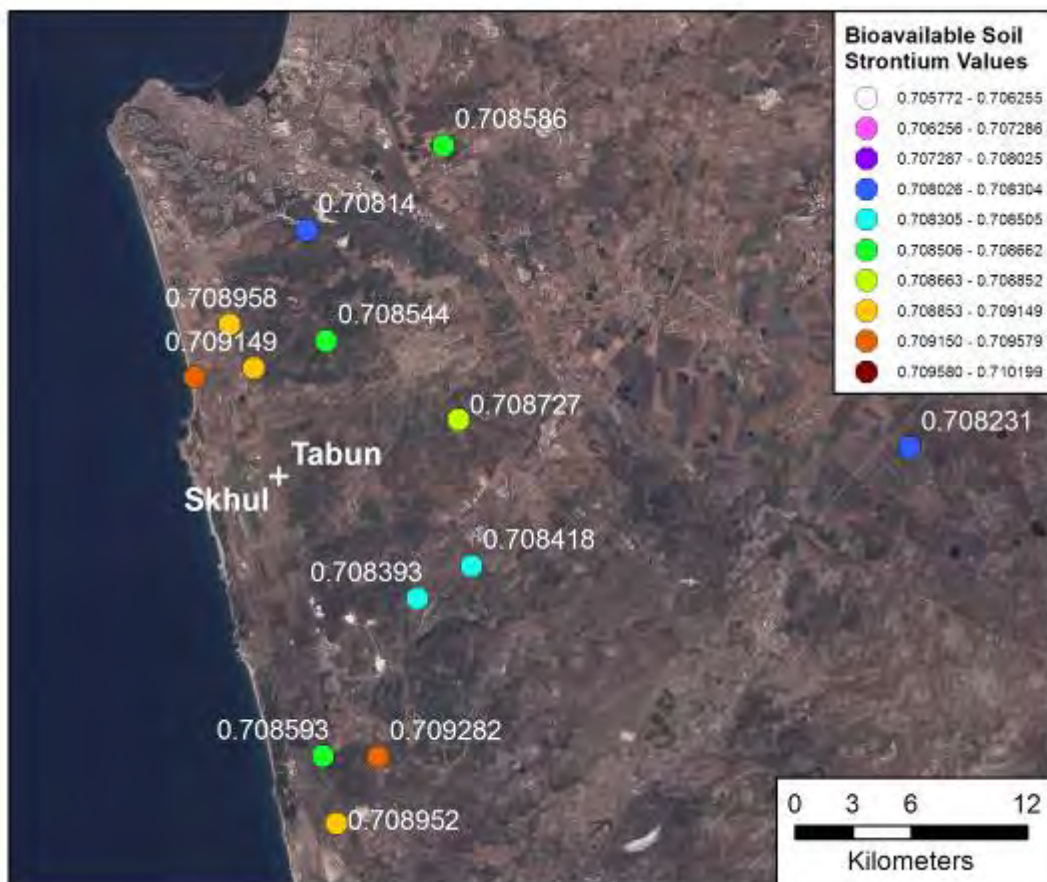


Figure 5.4 Bioavailable Soil Strontium Values Surrounding Tabun and Skhul

5.3.1.4. LA-MC-ICPMS Results

Samples from 5 individuals were analysed from the archaeological site of Skhul using LA-MC-ICPMS. Samples 1057 and 1058 were each analysed in 3 sub-samples. The results from these samples are summarised in Table 5.8 and Figure 5.5. The detailed results and photographs showing the analysis tracks are shown in section A3.2.2.1.

Sample	Material	Track	^{88}Sr Volts	N	$^{84}\text{Sr}/^{86}\text{Sr}$	$^{84}\text{Sr}/^{86}\text{Sr} 2\sigma$ Error	$^{87}\text{Sr}/^{86}\text{Sr}$	$^{87}\text{Sr}/^{86}\text{Sr} 2\sigma$ Error	Corrected $^{87}\text{Sr}/^{86}\text{Sr}$
851	Dentine	1	2.53	27	0.05549	0.00003	0.70947	0.70909	0.00023
851	Enamel	1	2.33	27	0.05549	0.00004	0.70951	0.70900	0.00010
852	Dentine	1	2.85	41	0.05627	0.00002	0.71045	0.70975	0.00017
852	Enamel	1	4.55	39	0.05623	0.00008	0.70963	0.70899	0.00028
853	Dentine	1	3.30	35	0.05646	0.00001	0.70968	0.70951	0.00007
853	Enamel	1	5.14	39	0.05649	0.00000	0.70996	0.70985	0.00008
1057A	Dentine	1	0.43	2	0.05667	0.00030	0.71200	0.71100	0.01300
1057A	Enamel	1	0.54	6	0.05679	0.00015	0.70871	0.70837	0.00039
1057A	Dentine	2	0.43	2	0.05683	0.00014	0.71200	0.71100	0.01300
1057A	Enamel	2	0.52	8	0.05677	0.00023	0.70853	0.70820	0.00029
1057A	Dentine	3	0.34	3	0.05650	0.00039	0.71500	0.71440	0.00850
1057A	Enamel	3	0.51	7	0.05677	0.00013	0.70897	0.70864	0.00031
1057B	Dentine	1	0.35	9	0.05679	0.00031	0.70967	0.70892	0.00094
1057B	Enamel	1	0.39	6	0.05685	0.00019	0.71030	0.70970	0.00120
1057C	Dentine	1	0.25	13	0.05670	0.00021	0.71011	0.70913	0.00065
1057C	Enamel	1	0.26	5	0.05664	0.00033	0.71078	0.70952	0.00037
1057C	Dentine	2	0.28	15	0.05679	0.00020	0.71016	0.70918	0.00051
1057C	Enamel	2	0.26	4	0.05691	0.00077	0.71050	0.70920	0.00100
1058A	Dentine	1	0.29	9	0.05610	0.00024	0.70900	0.70829	0.00037
1058A	Enamel	1	0.14	8	0.05556	0.00048	0.71072	0.70774	0.00057
1058B	Dentine	1	0.32	11	0.05609	0.00018	0.70854	0.70795	0.00020
1058B	Enamel	1	0.13	5	0.05481	0.00063	0.71099	0.70719	0.00067
1058B	Dentine	2	0.32	6	0.05619	0.00026	0.70850	0.70787	0.00028
1058B	Enamel	2	0.12	8	0.05616	0.00054	0.71015	0.70681	0.00061
1058C	Dentine	1	0.33	9	0.05615	0.00020	0.70899	0.70842	0.00058
1058C	Enamel	1	0.12	7	0.05610	0.00053	0.71130	0.70710	0.00230

Table 5.8 Summary Table of Skhul Faunal Teeth LA-MC-ICPMS Sr Isotope Results

Summarised LA-MC-ICPMS Strontium Isotopes Results, Skhul, Israel

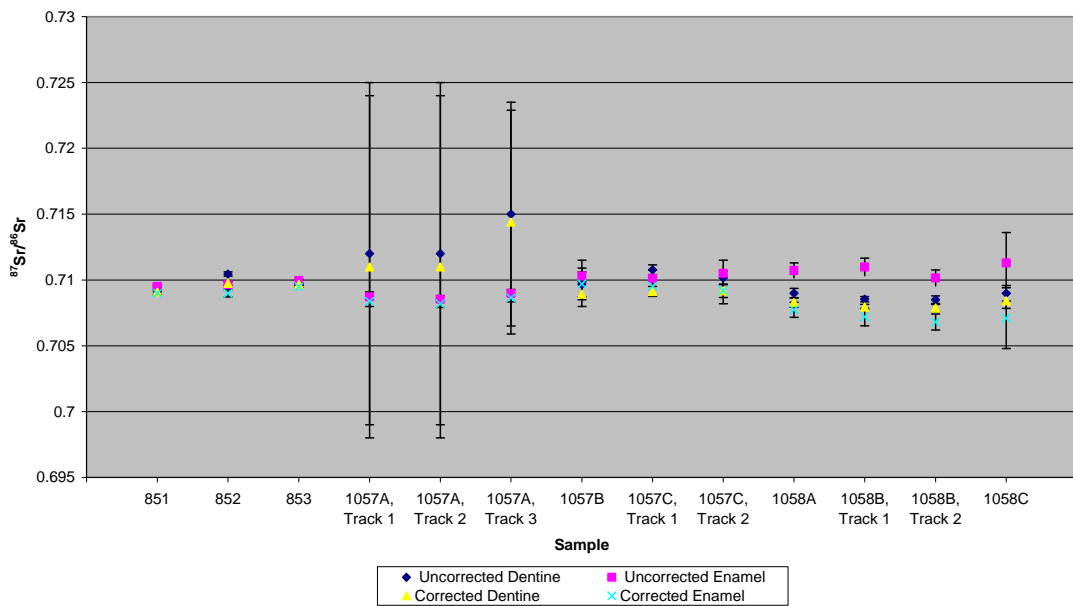


Figure 5.5 Summary Plot of Skhul Faunal Teeth LA-MC-ICPMS Sr Isotope Results

5.3.1.5. Mobility Interpretation

The mobility interpretation of the five teeth analysed from Skhul is summarised in Table 5.9 and discussed in detail in section A3.2.2.1. All bovid samples (851, 852, 853 and 1057) from Skhul show some evidence of being mobile during amelogenesis, have distinct dentine and enamel strontium isotope values and display a $^{87}\text{Sr}/^{86}\text{Sr}$ composition which is different from the geological unit that hosts this site. The pig sample (1058) also has an enamel strontium isotope value that varies from dentine and the local geological environment; however, the enamel does not show evidence of mobility during amelogenesis. All analysed enamel samples from Skhul have corrected $^{87}\text{Sr}/^{86}\text{Sr}$ values which correspond to the bioavailable strontium isotope results from this study for geological units which outcrop within 7.6 km of the archaeological site, suggesting a limited distance of mobility.

Sediment samples from Skhul, shown in detail in section 5.3.1.2, have bioavailable $^{87}\text{Sr}/^{86}\text{Sr}$ values of 0.708636 ± 0.000012 and 0.708722 ± 0.000013 .

Dentine from sample 1058 (with low error) fall within this range; however, all other dentine samples have elevated values. Dentine values of all samples from Skhul are relatively heterogeneous, which may reflect mobility of these individuals during dentine formation, complex post-burial diagenesis or apparent $^{87}\text{Sr}/^{86}\text{Sr}$ variations due to changes in strontium concentration. Of these options, it seems particularly unlikely that the original dentine $^{87}\text{Sr}/^{86}\text{Sr}$ values have been preserved in these samples, as the relatively high uranium concentrations (see sections 5.3.1.1 and A3.1.1.1) suggest that these samples have been overprinted.

Principal Residence During Amelogenesis Based on Corrected Values?								
Principal Residence During Amelogenesis Based on Uncorrected Values?								
Mobile During Amelogenesis?								
Enamel Different from Local Geology (Albian-Cenomanian Yagur/Kammon Formation Dolostone)?								
Dentine/Enamel Different?	MIS	Layer	Species	Sample				
851	Bovid	?	?	Yes	Yes	Yes	Coastal Plain and igneous material near Eilat	Kurkar/Bina Formation and Coastal Plain all within 3.2 km
852	Bovid	?	?	Yes	Yes	Yes	Coastal Plain and area outside of mapping	Carmel Range chalk and Mt Scopus Group and coastal plain sediments all within 3.2 km
853	Bovid	?	?	Yes	Yes	Some what	Mt Scopus Group and area outside of mapping	Mt Scopus Group within 5.4 km
1057A	Bovid	B	5	Yes	Yes	No	Bina Formation, on Mt Carmel Range	Adulam Formation on Mt Carmel Range within 7.6 km
1057B	Bovid	B	5	Yes	Yes	Yes	Unknown and area outside of mapping	Unknown and area outside of mapping
1057C	Bovid	B	5	Yes	Yes	No	Mt Scopus Group sediments? on Mt Carmel Range	Kurkar and Bina Formation within 2.3 km
1058A	Pig	B	5	Yes	Yes	No	Mt Scopus Group sediments? on Mt Carmel Range	Cover/Dalwe Basalt within 1.1 km
1058B	Pig	B	5	Yes	Yes	No	Mt Scopus Group sediments? on Mt Carmel Range	Cover/Dalwe Basalt within 1.1 km
1058C	Pig	B	5	Yes	Yes	No	Mt Scopus Group sediments? on Mt Carmel Range	Cover/Dalwe Basalt within 1.1 km

Table 5.9 Summary of Mobility Results for Analysed Fauna from Skhul

5.3.2. Tabun

5.3.2.1. LA-ICPMS Results

Samples 554, 556, 557, 558, 561, 563, 564, 565 and 567 from the archaeological site of Tabun were analysed for element concentration and ratios using LA-ICPMS, as summarised in Table 5.10 and shown in detail in section A3.1.1.2.

Sample	Material	Transect	Mg (ppm)	P (ppm)	Sr (ppm)	Ba (ppm)	Th (ppm)	U (ppm)	Mg/Ca	Sr/Ca	Ba/Ca
554	Enamel	1	1135	230586	291	54	0	1	0.004943	0.000352	0.000041
556	Enamel	1	1343	197315	264	87	0	10	0.028011	0.001769	0.000363
557	Enamel	1	1204	227453	169	47	0	0	0.005243	0.000204	0.000036
557 (2)	Enamel	1	1151	127521	202	57	0	0	0.005014	0.000243	0.000044
558	Enamel	1	1847	203679	120	37	0	0	0.008042	0.000145	0.000028
561	Enamel	1	1168	208856	163	48	0	0	0.005086	0.000197	0.000037
561	Dentine	1	571	209143	212	148	0	7	0.002487	0.000256	0.000114
563	Enamel	1	1318	192015	244	44	0	0	0.005741	0.000295	0.000034
563	Dentine	1	695	190577	249	113	0	5	0.003027	0.000301	0.000087
564	Dentine	1	844	186233	264	68	0	1	0.003673	0.000318	0.000052
565	Enamel	1	1114	198815	233	106	-5	-4	0.004849	0.000281	0.000280
565	Dentine	1	722	194049	209	83	-4	-3	0.003143	0.000253	0.000252
567	Enamel	1	710	164288	348	112	-5	9	0.003092	0.000420	0.000086
567	Dentine	1	1394	177071	304	14	-3	-3	0.006070	0.000367	0.000011

Table 5.10 Summary Table of LA-ICPMS Elemental Concentrations and Ratios for Faunal Teeth from Tabun

5.3.2.2. MC-ICPMS Results

Sixteen sediment samples from stratigraphic units B to Ed from the archaeological site of Tabun were analysed using MC-ICPMS to determine their $^{87}\text{Sr}/^{86}\text{Sr}$ composition, as summarised in Table 5.11. Strontium isotope analyses

of sediments from layers B to Ed of Tabun are in the range of 0.708331 to 0.708931 and show no systematic change with depth or between stratigraphic units. This result is remarkable considering the significant changes in sedimentation (particularly between layers C and D) and the large variation in the nature of post-burial diagenesis between different layers in the deposit, as summarised in section 3.12.3.2.

Sample Number	Associated with Tooth	Stratigraphic Unit	Age (ky)	$^{87}\text{Sr}/^{86}\text{Sr}$	$^{87}\text{Sr}/^{86}\text{Sr} 2\sigma$ Error
R_548	548	Layer B	102 ± 17/122 ± 16	0.708828	0.000015
R_549	549	Layer B	102 ± 17/122 ± 16	0.708434	0.000009
R_550	550	Layer B	102 ± 17/122 ± 16	0.708506	0.000013
R_551	551	Layer C	120 ± 16/140 ± 21	0.708472	0.000007
R_552	552	Layer C	120 ± 16/140 ± 21	0.708521	0.000010
R_553	553	Layer C	120 ± 16/140 ± 21	0.708633	0.000011
R_554	554	Layer D	133 ± 13/203 ± 26	0.708468	0.000010
R_555	555	Layer D	133 ± 13/203 ± 26	0.708466	0.000013
R_556	556	Layer D	133 ± 13/203 ± 26	0.708490	0.000011
R_557	557	Layer Ea	176 ± 22/213 ± 32	0.708417	0.000009
R_558	558	Layer Ea	176 ± 22/213 ± 32	0.708931	0.000011
R_559	559	Layer Ea	176 ± 22/213 ± 32	0.708385	0.000012
R_562	562	Layer Eb	180 ± 32/195 ± 37	0.708597	0.000014
R_564	564	Layer Ec	198 ± 51/220 ± 63	0.708331	0.000009
R_565	565	Layer Ec	198 ± 51/220 ± 63	0.708371	0.000015
R_567	567	Layer Ed	149 ± 17/191 ± 28	0.708484	0.000011

Table 5.11 $^{87}\text{Sr}/^{86}\text{Sr}$ Results from Archaeological Sediments from Tabun

5.3.2.3. Regional Mapping Results

Strontium isotope values from soil samples immediately surrounding the site of Tabun are shown in Figure 5.6.

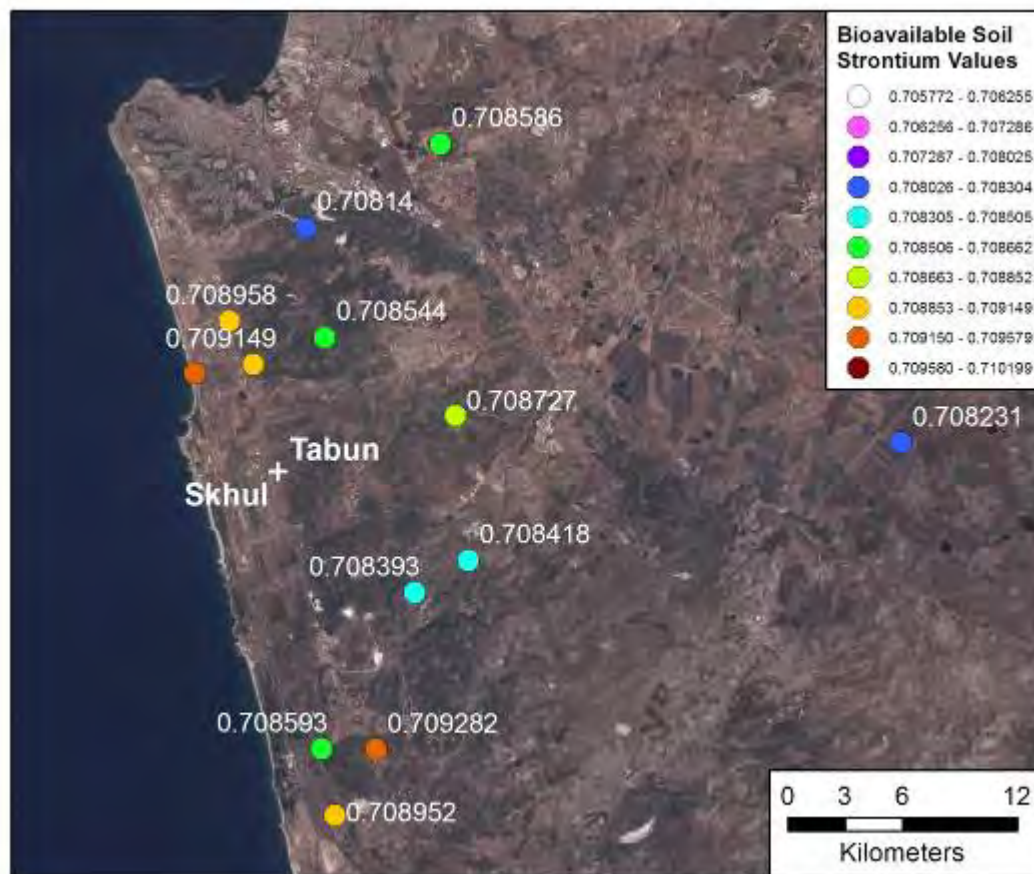


Figure 5.6 Bioavailable Soil Strontium Values Surrounding Tabun

5.3.2.4. LA-MC-ICPMS Results

Samples from 10 individuals were analysed from the archaeological site of Tabun using LA-MC-ICPMS. The results from these samples are summarised in Table 5.12 and Figure 5.7. The detailed results and photographs showing the analysis tracks are shown in section A3.2.2.2.

Sample	Unit	Material	Track	^{88}Sr Volts	n	$^{84}\text{Sr}/^{86}\text{Sr}$	Corrected $^{87}\text{Sr}/^{86}\text{Sr}$	$^{87}\text{Sr}/^{86}\text{Sr}$ 2 σ	Error	
								$^{84}\text{Sr}/^{86}\text{Sr}$ 2 σ	Error	
554	D	Enamel	1	1.90	2	0.05644	0.00008	0.70984	0.70911	0.00042
556	D	Enamel	1	1.58	2	0.05650	0.00160	0.71036	0.70939	0.00049
557	Ea	Enamel	1	1.14	2	0.05635	0.00011	0.71260	0.71140	0.00170
557	Ea	Enamel	2	1.48	2	0.05640	0.00120	0.71197	0.71061	0.00055
558	Ea	Enamel	1	2.65	2	0.05663	0.00009	0.71170	0.70990	0.00220
561	Eb	Dentine	1	1.60	2	0.05656	0.00010	0.70987	0.70845	0.00053
561	Eb	Enamel	1	1.20	3	0.05645	0.00008	0.71260	0.71020	0.00110
563	Eb	Enamel	1	1.42	4	0.05634	0.00007	0.71021	0.70887	0.00034
563	Eb	Dentine	1	1.56	3	0.05644	0.00008	0.70940	0.70844	0.00040
564	Ec	Dentine	1	1.98	2	0.05633	0.00007	0.70988	0.70944	0.00013
565	Ec	Enamel	1	2.14	2	0.05644	0.00072	0.71200	0.71100	0.01000
565	Ec	Dentine	1	1.73	2	0.05638	0.00077	0.71100	0.71050	0.00240
567	Ed	Enamel	1	3.08	2	0.05652	0.00005	0.70944	0.70915	0.00099
567	Ed	Dentine	1	3.18	2	0.05654	0.00005	0.70940	0.70920	0.00150
568	Ed	Enamel	1	0.52	2	0.05694	0.00023	0.70970	0.70900	0.00260
568	Ed	Dentine	1	0.64	12	0.05694	0.00008	0.70887	0.70843	0.00017
568	Ed	Enamel	2	0.42	2	0.05706	0.00031	0.71019	0.70952	0.00043
568	Ed	Dentine	2	0.60	7	0.05678	0.00011	0.70909	0.70865	0.00044
568	Ed	Enamel	3	0.46	4	0.05690	0.00023	0.70964	0.70896	0.00026
568	Ed	Dentine	3	0.50	15	0.05687	0.00015	0.70873	0.70829	0.00015

Table 5.12 Summary Table of Tabun Faunal Teeth LA-MC-ICPMS Sr Isotope Results

Summarised LA-MC-ICPMS Strontium Isotopes Results, Tabun, Israel

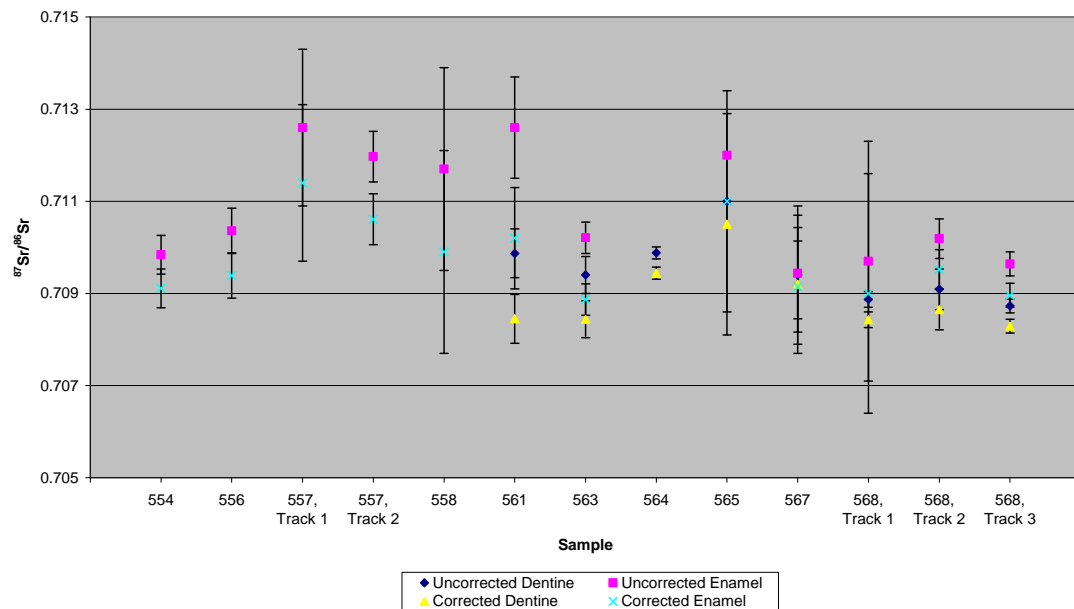


Figure 5.7 Summary Plot of Tabun Faunal Teeth LA-MC-ICPMS Sr Isotope Results

5.3.2.5. Mobility Interpretation

The mobility interpretation for the ten teeth analysed from Tabun is summarised in Table 5.13 and shown in detail in section A3.2.2.2. Of these 10 samples, only 1 shows evidence of mobility during amelogenesis and all (for, which it can be determined) have enamel that differs from the value of the geological unit that contains the site. Two samples out of the 5 (for which this could be determined) have enamel values that differ from their dentine. Five samples (554, 556, 563, 567 and 568) have corrected enamel $^{87}\text{Sr}/^{86}\text{Sr}$ values which correspond to geological units which outcrop within 10km of the site of Tabun. Three samples (557, 558, 561 and 565) have corrected enamel $^{87}\text{Sr}/^{86}\text{Sr}$ values which either do not correspond to strontium values for geological units sampled in this study or that outcrop at least 330 km from the site.

								Principal Residence During Amelogenesis Based on Corrected Values?	
								Principal Residence During Amelogenesis Based on Uncorrected Values?	
								Mobile During Amelogenesis?	
Sample		MIS	Layer	Dentine/Enamel Different?	Enamel Different from Local Geology (Aibian-Cenomanian Yagur/Kammon Formation Dolostone)?			Principal Residence During Amelogenesis Based on Uncorrected Values?	Mobile During Amelogenesis?
554	Bos	D	6	Unknown	Yes	No	Coastal Plain	Mt Carmel carbonates and kurkar within 1 km	
556	Bos	D	6	Unknown	Yes	No	Mt Scopus Group sediments? on Mt Carmel Range	Mt Carmel carbonates and kurkar within 1 km	
557	Bos	Ea	7–9	Unknown	Yes	No	Not found in mapping	Precambrian granite within 350 km	
558	Bos	Ea	7–9	Unknown	Unknown	No	Unknown	Unknown	
561	Bos	Eb	7–9	Yes	Yes	Yes	Unknown	Unknown	
563	Bos	Eb	7–9	No	Yes	No	Mt Scopus Group sediments? on Mt Carmel Range	Bina Formation/ Sakhnin/Yanuh Formation/kurkar within 1km	
564	Bos	Ec	7–9	Unknown	Unknown	Unknown	No enamel	No enamel	
565	Bos	Ec	7–9	Yes	Yes	No	Precambrian granite	Not found in mapping	
567	Bos	Ed	7–9	No	Yes	No	Bina Formation and kurkar	Bina Formation and kurkar within 1 km	
568	Rhino-ceros	Ed	7–9	No	Yes	No	Coastal plain	Bina Formation and kurkar within 1 km	

Table 5.13 Summary of Mobility Results for Analysed Fauna from Tabun

5.3.3. Amud

5.3.3.1. MC-ICPMS Results

Four sediment samples from stratigraphic unit B1 from the archaeological site of Amud were analysed using MC-ICPMS to determine their $^{87}\text{Sr}/^{86}\text{Sr}$ composition, as summarised in Table 5.14. Four sediment samples from Amud were

analysed for strontium isotope composition. The results cover an extremely wide range of values. Samples 1025 and 1027 from Amud are somewhat homogenous, with $^{87}\text{Sr}/^{86}\text{Sr}$ values of 0.707920 ± 0.000010 and 0.708035 ± 0.000009 , respectively. In contrast, sediment samples 1024 and 1026 have significantly different $^{87}\text{Sr}/^{86}\text{Sr}$ values, of 0.719229 ± 0.000009 and 0.721197 ± 0.000010 , respectively, which vary significantly from the strontium isotope value of the other sediment samples from Amud and from the surrounding mapping samples. The stratigraphy of unit B contains interbedded calcareous silt, calcareous concretions and black soils derived from anthropogenic ash (e.g., Madella et al. 2002) suggest that these $^{87}\text{Sr}/^{86}\text{Sr}$ values are elevated compared to expected $^{87}\text{Sr}/^{86}\text{Sr}$ based on lithology, unless the ash is derived from material transported a great distance.

Sample Number	Associated with Tooth	Stratigraphic Unit	Age (ky)	$^{87}\text{Sr}/^{86}\text{Sr}$	$^{87}\text{Sr}/^{86}\text{Sr} 2\sigma$ Error
R_1024	R_1024	B1		0.719229	0.000009
R_1025	R_1025	B1		0.707920	0.000010
R_1026	R_1026	B1		0.721197	0.000010
R_1027	R_1027	B1		0.708035	0.000009

Table 5.14 $^{87}\text{Sr}/^{86}\text{Sr}$ Results from Archaeological Sediments from Amud

5.3.3.2. Regional Mapping Results

Strontium isotope values from soil samples immediately surrounding the site of Amud are shown in Figure 5.8.

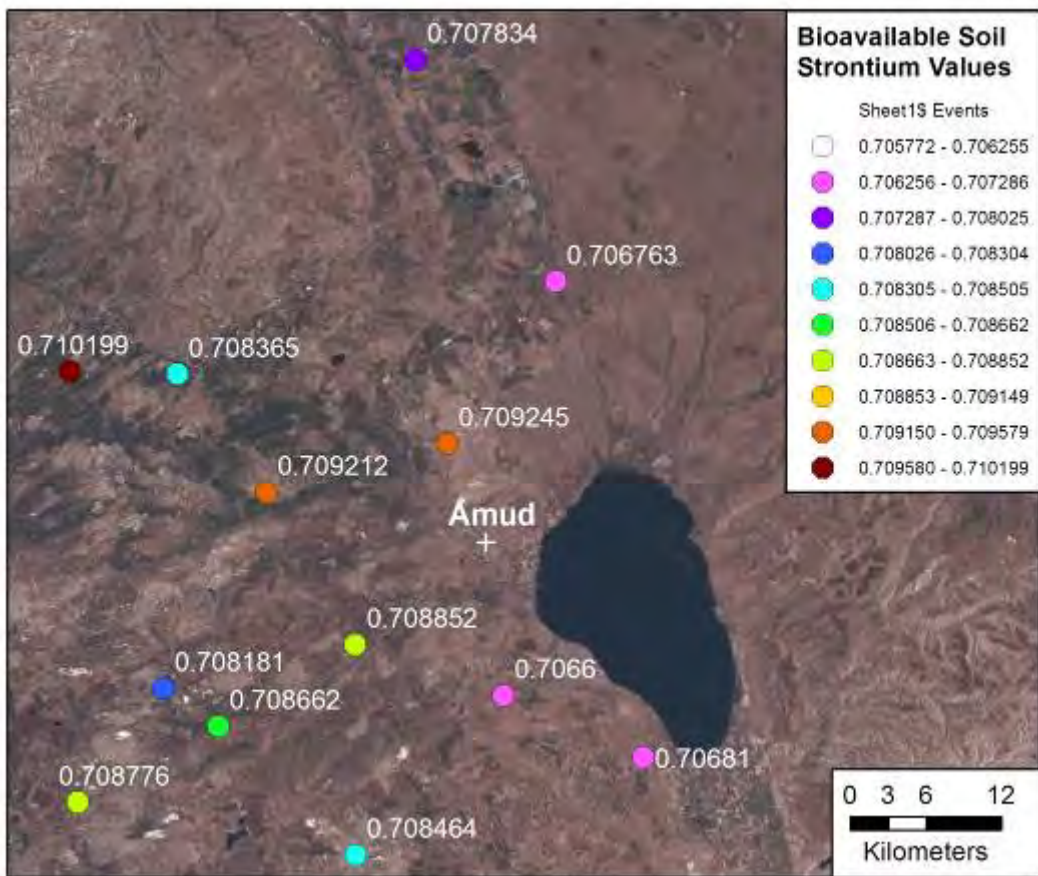


Figure 5.8 Bioavailable Soil Strontium Values Surrounding Amud

5.3.3.3. LA-MC-ICPMS Results

Samples from 3 individuals were analysed from the archaeological site of Amud using LA-MC-ICPMS. The results from these samples are summarised in Table 5.15 and Figure 5.9. The detailed results and photographs showing the analysis tracks are shown in section A3.2.2.3. Overall, uncorrected enamel $^{87}\text{Sr}/^{86}\text{Sr}$ values collected using LA-MC-ICPMS from 3 *Dama mesopotamica* samples from layer B1 from Amud are clustered in 2 domains.

Sample	Unit	Material	Track	^{88}Sr Volts	n	$^{84}\text{Sr}/^{86}\text{Sr}$	$^{84}\text{Sr}/^{86}\text{Sr} 2\sigma$	Corrected $^{87}\text{Sr}/^{86}\text{Sr}$	$^{87}\text{Sr}/^{86}\text{Sr} 2\sigma$ Error
1024	B1	Enamel	1	2.50	4	0.05698	0.00032	0.71098	0.70989
1024	B1	Dentine	1	4.51	6	0.05667	0.00005	0.70899	0.70859
1024	B1	Enamel	2	2.66	2	0.05669	0.00005	0.71190	0.71080
1024	B1	Dentine	2	4.45	7	0.05655	0.00001	0.70911	0.70871
1025	B1	Enamel	1	4.54	15	0.05632	0.00003	0.70887	0.70859
1025	B1	Dentine	1	4.60	15	0.05630	0.00003	0.70856	0.70832
1026	B1	Enamel	1	1.08	4	0.05515	0.00024	0.71071	0.70709
1026	B1	Dentine	1	3.30	9	0.05598	0.00008	0.70887	0.70849
1026	B1	Enamel	2	1.00	3	0.05472	0.00059	0.71050	0.70690
1026	B1	Dentine	2	3.24	10	0.05594	0.00004	0.70876	0.70839

Table 5.15 Summary Table of Amud Faunal Teeth LA-MC-ICPMS Sr Isotope Results

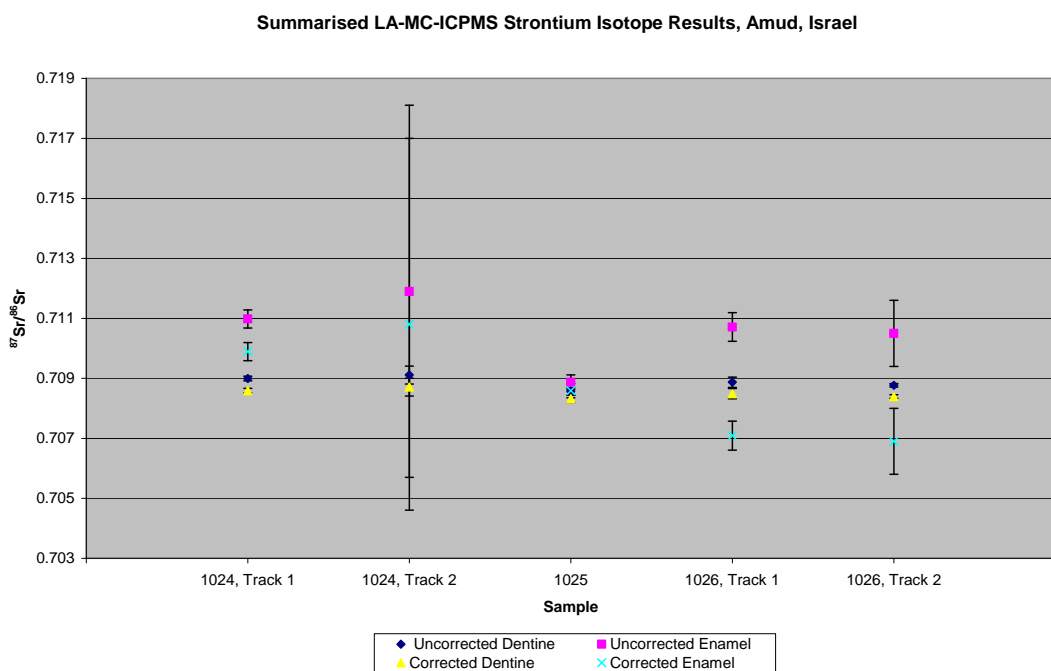


Figure 5.9 Summary Plot of Amud Faunal Teeth LA-MC-ICPMS Sr Isotope Results

5.3.3.4. Mobility Interpretation

The mobility interpretation of the three teeth analysed from Amud is summarised in Table 5.16 and shown in detail in section A3.2.2.3. All three samples have enamel that is heterogeneous in $^{87}\text{Sr}/^{86}\text{Sr}$ composition suggesting mobility during amelogenesis and all have corrected strontium isotope values which corresponds to units outcropping within 2.7 km of the site.

Dentine from the Amud samples have $^{87}\text{Sr}/^{86}\text{Sr}$ values in the range of 0.7085 to 0.7091, suggesting relatively homogeneous post-burial diagenesis. The greatest heterogeneity of dentine values in the Amud samples occurs close to the dentine-enamel junction in samples 1024 and 1026, which probably reflects some enamel being sampled, as well as dentine in these spots.

Sample	Fauna	Dentine/Enamel Different?	Enamel Different from Local Geology (Middle Eocene Bar Kokhba Formation)?	Mobile During Amelogenesis?	Principal Residence During Amelogenesis Based on Uncorrected Values?	Principal Residence During Amelogenesis Based on Corrected Values?
1024	<i>Dama mesopotamica</i>	B1	3	Yes	Yes	Precambrian granite
1025	<i>Dama mesopotamica</i>	B1	3	No	No	Carbonate including the Mount Scopus Group within 1.4 km
1026	<i>Dama mesopotamica</i>	B1	3	No	No	Basalt or carbonate including the Cover/Dalwe Basalt within 0.8 km

Table 5.16 Summary of Mobility Results for Analysed Fauna from Amud

5.3.4. Qafzeh

5.3.4.1. LA-ICPMS Results

Sample 373 from the archaeological site of Qafzeh was analysed for element concentration and ratios using LA-ICPMS, as summarised in Table 5.17 and shown in detail in section A3.1.1.3.

Material	Transect	Mg (ppm)	Sr (ppm)	Ba (ppm)	U (ppm)	Mg/Ca	Sr/Ca	Ba/Ca
Enamel Average	1	2878	561	54	0	0.012535	0.000678	0.000041

Table 5.17 Average Elemental Concentrations and Ratios for Sample 373, an unidentified tooth from layer XV of Qafzeh

5.3.4.2. MC-ICPMS Results

Five sediment samples from stratigraphic units CXV, CXIX, CXVII and CXV from the archaeological site of Qafzeh were analysed using MC-ICPMS to determine their $^{87}\text{Sr}/^{86}\text{Sr}$ composition, as summarised in Table 5.18.

Sample Number	Associated with Tooth	Stratigraphic Unit	Age (ky)	$^{87}\text{Sr}/^{86}\text{Sr}$	$^{87}\text{Sr}/^{86}\text{Sr}$ 2σ Error
R_370	370	Layer CXV	96 ± 13 (EU) 115 ± 15 (LU)	0.708813	0.000015
R_371	371	Layer CXIX	96 ± 13 (EU) 115 ± 15 (LU)	0.708218	0.000006
R_371 (2)	371 (2)	Layer CXIX	96 ± 13 (EU) 115 ± 15 (LU)	0.708203	0.000015
R_372	372	Layer CXVII	96 ± 13 (EU) 115 ± 15 (LU)	0.709446	0.000011
R_374	374	Layer CXV	96 ± 13 (EU) 115 ± 15 (LU)	0.708595	0.000010

Table 5.18 $^{87}\text{Sr}/^{86}\text{Sr}$ Results from Archaeological Sediments from Qafzeh

5.3.4.3. Regional Mapping Results

Strontium isotope values from soil samples immediately surrounding the site of Qafzeh are shown in Figure 5.10.

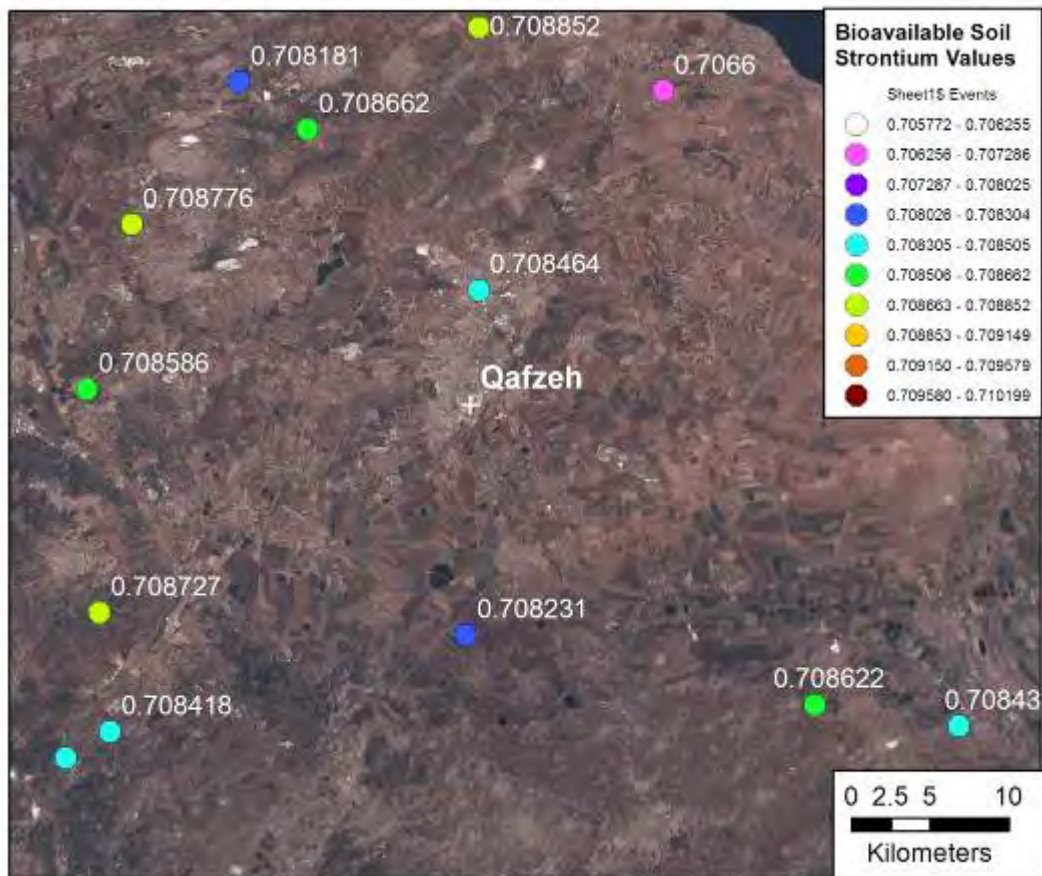


Figure 5.10 Bioavailable Soil Strontium Values Surrounding Qafzeh

5.3.4.4. LA-MC-ICPMS Results

Samples from 5 individuals were analysed from the archaeological site of Qafzeh using LA-MC-ICPMS. The results from these samples are summarised in Table 5.19 and Figure 5.11. The detailed results and photographs showing the analysis tracks are shown in section A3.2.2.4.

Sample	Unit	Material	Track	$^{84}\text{Sr}/^{86}\text{Sr}$	n	$^{84}\text{Sr}/^{86}\text{Sr}$	Corrected $^{87}\text{Sr}/^{86}\text{Sr}$	$^{87}\text{Sr}/^{86}\text{Sr} 2\sigma$	Error
370	CXV	Enamel	1	1.78	9	0.05547	0.00010	0.70992	0.70942
371	CXIX	Enamel	1	1.78	11	0.05486	0.00007	0.70981	0.70922
372	CXVII	Dentine	1	4.91	6	0.05585	0.00005	0.70824	0.70814
372	CXVII	Enamel	2	2.17	13	0.05842	0.00014	0.70742	0.70731
373	CXV	Enamel	1	3.57	3	0.05935	0.00053	0.70831	0.70821
374	CXV	Enamel	1	0.87	14	0.06189	0.00028	0.70983	0.70911

Table 5.19 Summary Table of Qafzeh Faunal Teeth LA-MC-ICPMS Sr Isotope Results

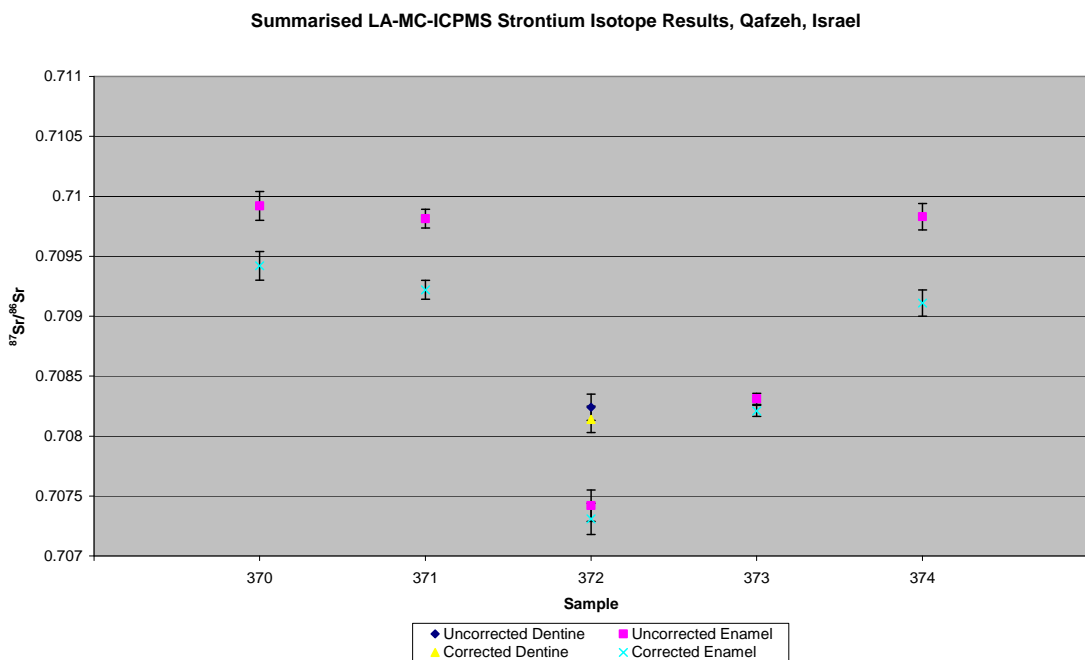


Figure 5.11 Summary Plot of Qafzeh Faunal Teeth LA-MC-ICPMS Sr Isotope Results

5.3.4.5. Mobility Interpretation

The mobility interpretation of the 5 teeth analysed from Qafzeh is summarised in Table 5.20 and shown in detail in section A3.2.2.4. Samples 370, 371, 373 and 374 have relatively homogeneous enamel $^{87}\text{Sr}/^{86}\text{Sr}$ values, suggesting these specimens were not mobile across isotopically distinguishable geological environments during amelogenesis. In contrast, sample 372 has a relatively

heterogeneous enamel $^{87}\text{Sr}/^{86}\text{Sr}$ composition, suggesting that this specimen was mobile during amelogenesis. Corrected $^{87}\text{Sr}/^{86}\text{Sr}$ values from the samples from Qafzeh all correspond to soil mapping sample collected from geological units which outcrop within 1.3 km of the archaeological site, suggesting a relatively small degree of mobility for these samples.

The strontium isotope composition of soil samples from the site of Qafzeh show significant heterogeneity. In particular, the value from layer XVII (0.709446 ± 0.000011) differs from those observed in layers XIX (0.708218 ± 0.000006) or XV (0.708813 ± 0.000015). As discussed in section 3.15.2.2, Goldberg (1980:163) observed that layer XVII lacks the degree of secondary calcite soil cementation (thought to indicate an arid climate) that is found in layers XI to XVI. This soil carbonate may have a strontium isotope value reflecting the groundwater regime during formation, which may explain this variation. Unfortunately, no tooth samples analysed in this study other than 372 have dentine, making it difficult to examine the effect of this variation in secondary cementation on biogenic materials.

Principal Residence During Amelogenesis Based on Corrected Values?								
Principal Residence During Amelogenesis Based on Uncorrected Values?								
Mobile During Amelogenesis? Enamel Different from Local Geology (Cenomanian Sakhnin and Yanuh Formations)?								
Dentine/Enamel Different?	MIS	Layer	Fauna	Sample				
				370	Bovid	XV	5	Unknown
				371	Bovid	XIX	5	Unknown
				372	Bovid	XVII	5	Yes
				373	Unidentified	XV	5	Unknown
				374	Unidentified	XV	5	Unknown

Table 5.20 Summary of Mobility Results for Analysed Fauna from Qafzeh

5.3.5. Holon

5.3.5.1. LA-ICPMS Results

Sample 1557 from the archaeological site of Holon was analysed for element concentration and ratios using LA-ICPMS, as summarised in Table 5.21.

Material	Transect	Mg (ppm)	Sr (ppm)	Ba (ppm)	U (ppm)	Mg/Ca	Sr/Ca	Ba/Ca
Enamel Average	1	1228	315	76	15	0.005348	0.000381	0.000059

Table 5.21 Average Elemental Concentrations and Ratios for Sample 1557, Bovid, Holon

5.3.5.2. Regional Mapping Results

Strontium isotope values from soil samples immediately surrounding the site of Holon are shown in Figure 5.10.

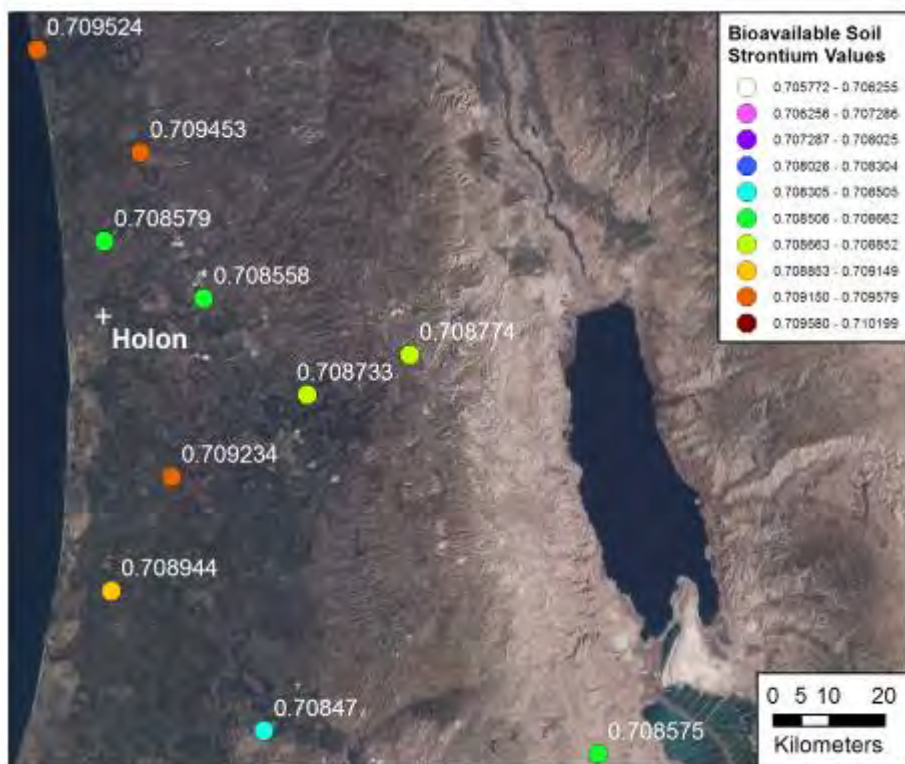


Figure 5.12 Bioavailable Soil Strontium Values Surrounding Holon

5.3.5.3. LA-MC-ICPMS Results

One sample, 1557, was analysed from Holon, with 1 track of 4 enamel spots as shown in Figure 5.13. The enamel spots have an average ^{88}Sr voltage of 1.838, a weighted average $^{87}\text{Sr}/^{86}\text{Sr}$ value of 0.70976 ± 0.00087 and a weighted average $^{84}\text{Sr}/^{86}\text{Sr}$ value of 0.06015 ± 0.00047 , shown in Table 5.22, Table 5.23 and Figure 5.14. Enamel samples are in the range of 0.709229 to 0.710284 and are heterogeneous. Spots 2 and 4 are quite heterogeneous in $^{87}\text{Sr}/^{86}\text{Sr}$ composition, while spots 1 and 3 have significantly lower $^{87}\text{Sr}/^{86}\text{Sr}$ values compared to 2 and 4. These spots are just within 2σ error of each other.

Sample	Unit	Material	Track	^{88}Sr Volts	n	$^{84}\text{Sr}/^{86}\text{Sr}$	$^{84}\text{Sr}/^{86}\text{Sr}$ 2 σ Error	$^{87}\text{Sr}/^{86}\text{Sr}$	Corrected $^{87}\text{Sr}/^{86}\text{Sr}$	$^{87}\text{Sr}/^{86}\text{Sr}$ 2 σ Error
1557	C	Enamel	1	1.83	4	0.06015	0.00047	0.70976	0.70955	0.00087

Table 5.22 Summary Table of Holon Faunal Teeth LA-MC-ICPMS Sr Isotope Results

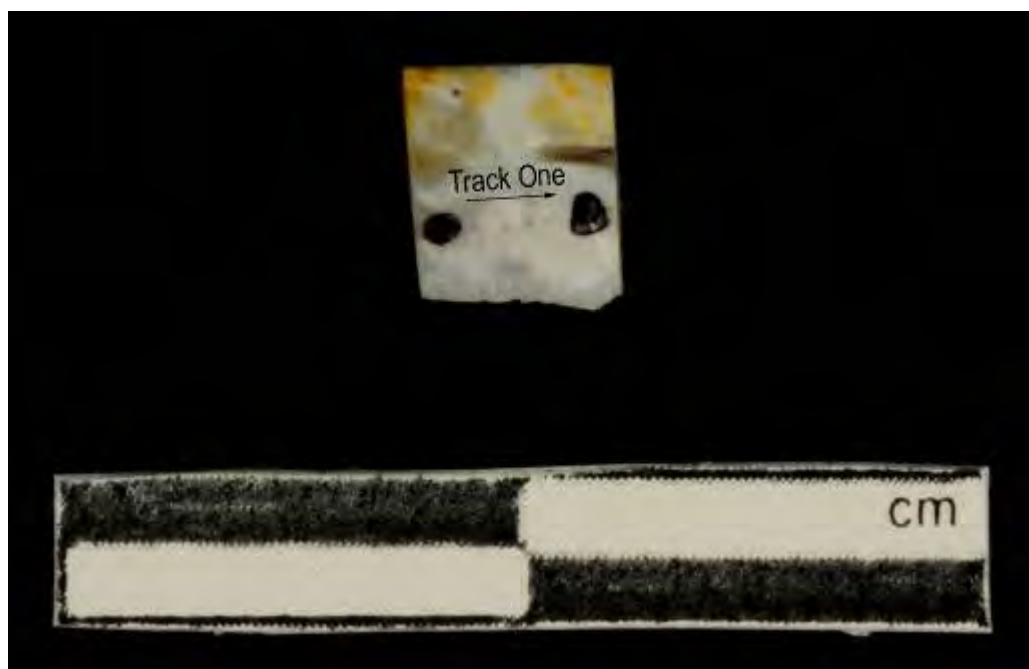


Figure 5.13 LA-MC-ICPMS Track for Sample 1557, Bovid, Holon

Sample	Material	Track	Point	^{88}Sr Volts	$^{84}\text{Sr}/^{86}\text{Sr}$	$^{84}\text{Sr}/^{86}\text{Sr} 2\sigma$ Error	$^{87}\text{Sr}/^{86}\text{Sr}$	Corrected $^{87}\text{Sr}/^{86}\text{Sr}$	$^{87}\text{Sr}/^{86}\text{Sr} 2\sigma$ Error
1557	Enamel	1	1	1.99	0.060215	0.000172	0.709229	0.709017	0.000150
1557	Enamel	1	2	1.90	0.060167	0.000218	0.710223	0.710011	0.000201
1557	Enamel	1	3	1.62	0.060544	0.000257	0.709550	0.709338	0.000215
1557	Enamel	1	4	1.82	0.059734	0.000220	0.710284	0.710072	0.000178

Table 5.23 Sample 1557, Bovid from Holon, Detailed LA-MC-ICPMS Sr Isotope Results

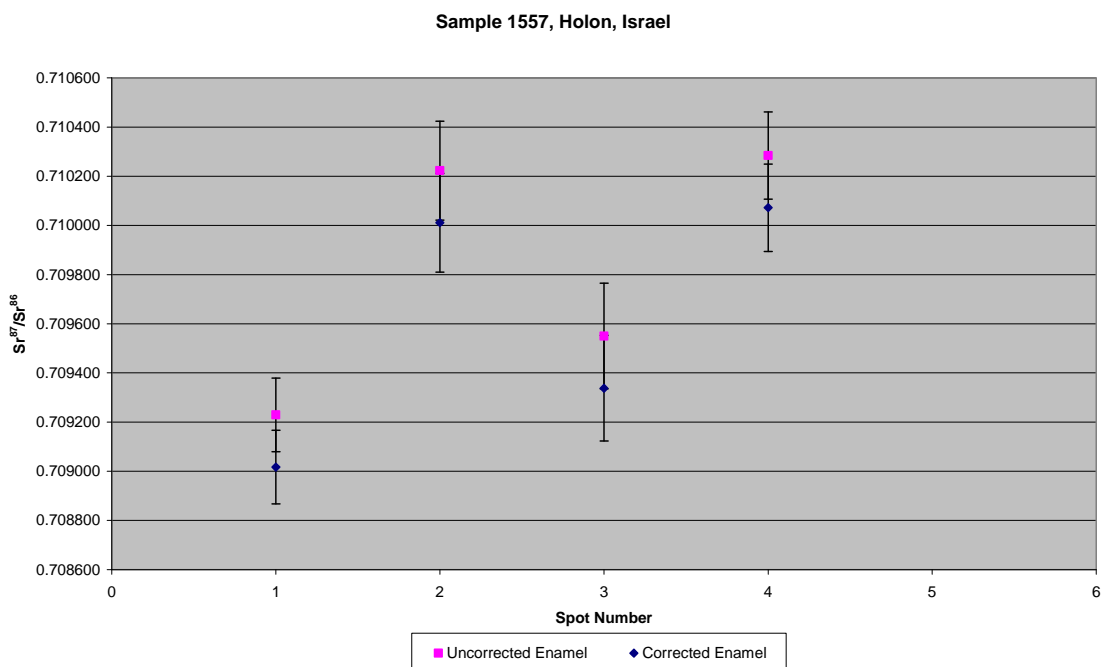


Figure 5.14 Sample 1557, Bovid from Holon, Detailed LA-MC-ICPMS Sr Isotope Results

5.3.5.4. Mobility Interpretation

Sample 1557, a *Bos* tooth from layer C of Holon, was analysed by 4 enamel spots, shown in Figure 5.24. The enamel spots are somewhat heterogeneous, suggesting a sample mobile during amelogenesis. Spots 2 and 4 have statistically indistinguishable strontium isotope values, for which both the uncorrected and corrected weighted mean corresponds with 162 from site

IS011 located within the Senonian-Palaeocene aged Mount Scopus Group. As discussed in section 6.3.1.6, the result from this mapping sample may not be robust. While this analysis site is located 120 km north of Holon, an outcrop of Mount Scopus Group sediments, not sampled in this study, outcrop 32 km to the north-west of the site. Spots 1 and 3 are just within 2σ error. While the error on these data is large, the weighted mean value of spots 1 and 3 correspond to sample 184 from IS033 located on the Quaternary coastal plain which contains the archaeological site. Strontium concentrations are in the range of 306 to 328 ppm and are amenable to the collection of accurate $^{87}\text{Sr}/^{86}\text{Sr}$; however, uranium concentrations of 9 to 17 ppm suggest that this sample may have been the subject of post-burial diagenesis.

Principal Residence During Amelogenesis Based on Corrected Values?						
Principal Residence During Amelogenesis Based on Uncorrected Values?						
Mobile During Amelogenesis?						
Sample	Fauna	Layer	MIS	Dentine/Enamel Different?	Enamel Different from Local Geology (Coastal Plain)?	Mobile During Amelogenesis?
1557	<i>Bos</i>	C	7	Unknown	Some	Yes
					Coastal plain sediments (local) and Mt Scopus Group carbonate (40 km NNW)	Coastal plain sediments within 0 km and Mt Scopus Group carbonate within 32 km

Table 5.24 Summary of Mobility Results for Analysed Fauna from Holon

5.4. French Archaeological Sites

5.4.1. La Chapelle-aux-Saints

5.4.1.1. LA-ICPMS Results

Samples M001, M002, M003, M004, M005, M006, M007, M008, M009 and M010 from the archaeological site of La Chapelle-aux-Saints were analysed for element concentration and ratios using LA-ICPMS, as summarised in Table 5.25 and shown in detail in section A3.1.2.1.

Sample	Material	Transect	Mg (ppm)	P (ppm)	Sr (ppm)	Ba (ppm)	U (ppm)	Mg/Ca	Sr/Ca	Ba/Ca
M001	Enamel	1	1792	168072	276	185	0	16	0.007803	0.000334
M002	Enamel	1	2499	176206	162	91	0	0	0.010883	0.000196
M003	Enamel	1	1418	230640	235	173	0	28	0.006173	0.000284
M003	Dentine	1	1432	239517	267	235	0	18	0.006236	0.000322
M004	Enamel	1	1863	184430	162	106	0	0	0.008110	0.000195
M004	Dentine	1	1416	156099	228	161	0	13	0.006165	0.000276
M005	Dentine	1	1213	204163	222	157	0	17	0.005280	0.000269
M006	Enamel	1	1523	207784	386	310	0	0	0.006634	0.000467
M007	Enamel	1	2332	215517	167	98	0	0	0.010155	0.000202
M008	Enamel	1	1448	198912	293	248	-1	1	0.006305	0.000354
M008	Dentine	1	1049	177611	275	225	-1	55	0.004568	0.000333
M009	Enamel	1	1548	227880	182	214	0	1	0.006741	0.000220
M009	Dentine	1	1154	203197	242	186	0	29	0.005028	0.000292
M009	Enamel	2	1459	223223	187	241	0	0	0.006353	0.000226
M009	Dentine	2	1183	201059	238	202	0	28	0.005153	0.000287
M009	Enamel	3	1549	221539	166	163	0	0	0.006745	0.000201
M009	Dentine	3	1166	200952	237	205	0	24	0.005077	0.000286
M010	Enamel	1	1673	206173	175	180	-13	-13	0.007287	0.000211
M010	Dentine	1	1393	169564	260	192	-12	40	0.006068	0.000315
M010	Enamel	2	1790	196978	185	196	-11	-10	0.007794	0.000223
M010	Dentine	2	1397	168026	239	187	-9	50	0.006084	0.000288
										0.000144

Table 5.25 Summary Table of LA-ICPMS Elemental Concentrations and Ratios for Faunal Teeth from La Chapelle-aux-Saints

5.4.1.2. MC-ICPMS Results

Two sediment samples from, or adjacent to, the archaeological site of La Chapelle-aux-Saints were analysed using MC-ICPMS to determine their $^{87}\text{Sr}/^{86}\text{Sr}$ composition, as summarised in Table 5.26.

Sample Number	Associated with Tooth	Stratigraphic Unit	Age (ky)	$^{87}\text{Sr}/^{86}\text{Sr}$	$^{87}\text{Sr}/^{86}\text{Sr} 2\sigma$ Error
FS045-S2	N/A	Layer 1	Not Dated	0.710098	0.000049
FS045-S3	N/A	Above Excavation	N/A	0.708879	0.000012

Table 5.26 $^{87}\text{Sr}/^{86}\text{Sr}$ Results from Archaeological Sediments from La Chapelle-aux-Saints

5.4.1.3. Regional Mapping Results

Strontium isotope values from soil samples immediately surrounding the site of La Chapelle-aux-Saints are shown in Figure 5.15.

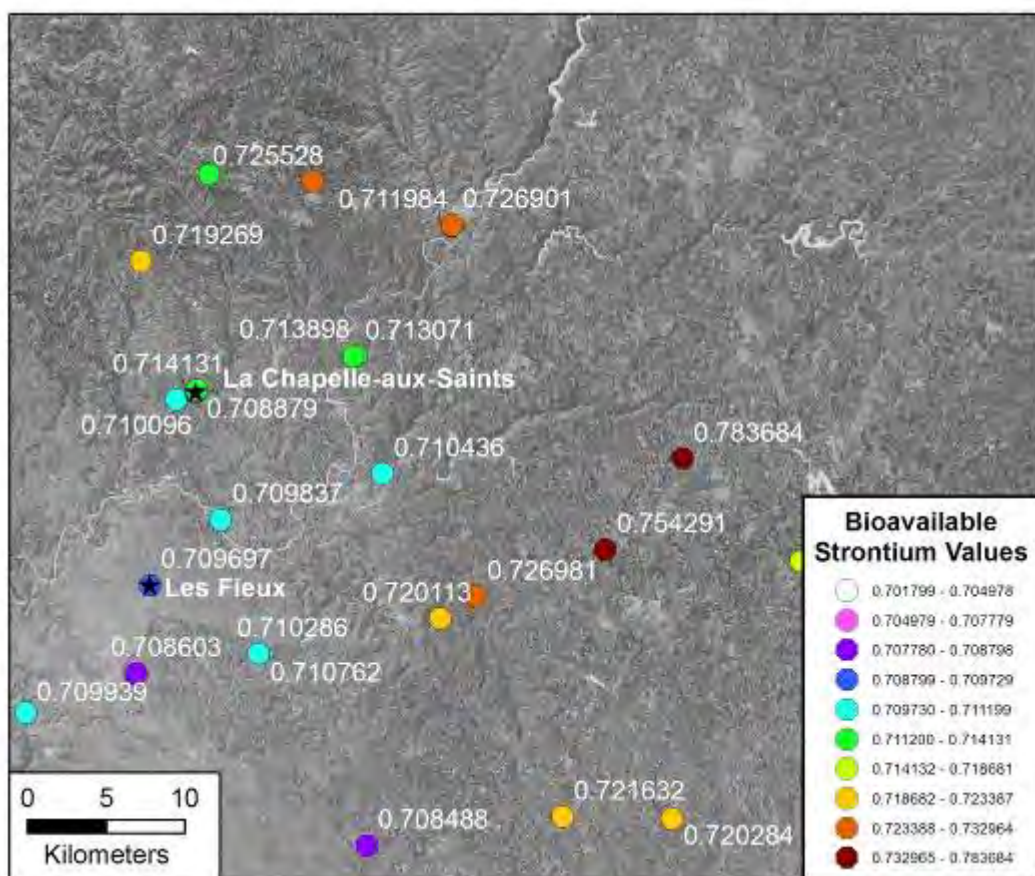


Figure 5.15 Bioavailable Soil Strontium Values Surrounding La Chapelle-aux-Saints

5.4.1.4. LA-MC-ICPMS Results

Samples from 13 individuals were analysed from the archaeological site of La Chapelle-aux-Saints using LA-MC-ICPMS. The results from these samples are summarised in Table 5.27 and Figure 5.16. The detailed results and photographs showing the analysis tracks are shown in section A3.2.3.1.

Sample	Unit	Material	Track	^{88}Sr Volts	n	$^{84}\text{Sr}/^{86}\text{Sr}$	$^{84}\text{Sr}/^{86}\text{Sr}$ 2 σ Error	Corrected $^{87}\text{Sr}/^{86}\text{Sr}$	$^{87}\text{Sr}/^{86}\text{Sr}$ 2 σ Error	
592	BB 1	Enamel	1	0.95	14	0.05733	0.00012	0.71064	0.71018	0.00028
592	BB 1	Dentine	1	1.28	22	0.05710	0.00003	0.70983	0.70958	0.00032
593	BB 1	Enamel	1	1.06	4	0.05671	0.00007	0.71160	0.71140	0.00110
593	BB 1	Dentine	1	2.01	12	0.05666	0.00002	0.70987	0.70978	0.00043
593	BB 1	Enamel	2	1.32	3	0.05705	0.00009	0.71306	0.71281	0.00089
593	BB 1	Dentine	2	1.91	8	0.05678	0.00003	0.70976	0.70967	0.00023
593	BB 1	Enamel	3	1.24	3	0.05732	0.00062	0.71260	0.71230	0.00160
593	BB 1	Dentine	3	1.82	16	0.05697	0.00005	0.70953	0.70944	0.00027
593	BB 1	Enamel	4	1.07	2	0.05707	0.00013	0.71149	0.71124	0.00030
593	BB 1	Dentine	4	1.94	12	0.05683	0.00002	0.71002	0.70993	0.00068
595	BB 1	Enamel	1	1.00	9	0.05690	0.00015	0.71225	0.71182	0.00088
595	BB 1	Dentine	1	1.31	17	0.05690	0.00004	0.71009	0.70981	0.00030
595	BB 1	Enamel	2	0.95	9	0.05663	0.00006	0.71136	0.71049	0.00056
595	BB 1	Dentine	2	1.54	9	0.05661	0.00004	0.70932	0.70904	0.00053
M001	B118 2	Enamel	1	3.15	4	0.05655	0.00010	0.71080	0.71040	0.00180
M001	B118 2	Dentine	1	2.98	1	0.05666	0.00006	0.71042	0.70998	0.00009
M002	B118 2	Enamel	1	0.64	2	0.05774	0.00027	0.71481	0.71284	0.00030
M002	B118 2	Enamel	2	1.26	2	0.05626	0.00011	0.71220	0.71040	0.00290
M003	B118 2	Enamel	1	1.98	2	0.05605	0.00006	0.71030	0.70970	0.00700
M003	B118 2	Dentine	1	2.54	2	0.05612	0.00004	0.71040	0.71000	0.00110
M004	B118 1	Enamel	1	1.18	2	0.05555	0.00012	0.71220	0.71080	0.00210
M004	B118 1	Dentine	1	1.90	2	0.05584	0.00007	0.70980	0.70930	0.00220
M005	B118 1	Enamel	1	1.36	1	0.05546	0.00013	0.71847	0.71781	0.00017

Sample	Unit	Material			n	$^{84}\text{Sr}/^{86}\text{Sr}$	$^{84}\text{Sr}/^{86}\text{Sr} 2\sigma$ Error	$^{87}\text{Sr}/^{86}\text{Sr} 2\sigma$ Error
			Track	^{88}Sr Volts			$^{87}\text{Sr}/^{86}\text{Sr}$	Corrected $^{87}\text{Sr}/^{86}\text{Sr}$
M005	B118 1	Dentine	1	2.11	4	0.05581	0.00005	0.71200
M006	B118 1	Enamel	1	1.62	5	0.05665	0.00005	0.71210
M007	B118 1	Enamel	1	0.73	9	0.05683	0.00013	0.71523
M008	B118 1	Enamel	1	1.33	2	0.05672	0.00009	0.71346
M008	B118 1	Dentine	1	1.48	4	0.05665	0.00008	0.71350
M008	B118 1	Enamel	2	1.16	6	0.05665	0.00011	0.71350
M008	B118 1	Dentine	2	1.33	6	0.05660	0.00006	0.71349
M009	B118 1	Enamel	1	0.80	2	0.05660	0.00150	0.71360
M009	B118 1	Dentine	1	1.26	13	0.05657	0.00005	0.71260
M009	B118 1	Enamel	2	0.61	5	0.05671	0.00014	0.71368
M009	B118 1	Dentine	2	0.96	5	0.05661	0.00010	0.71326
M009	B118 1	Enamel	3	0.66	2	0.05667	0.00022	0.71370
M009	B118 1	Dentine	3	0.95	3	0.05659	0.00013	0.71210
M010	B118 1	Enamel	1	0.75	3	0.05660	0.00016	0.71410
M010	B118 1	Dentine	1	1.32	1	0.05656	0.00012	0.71325
M010	B118 1	Enamel	2	0.58	2	0.05643	0.00027	0.71390
								0.71290
								0.00940

Table 5.27 Summary Table of La Chapelle-aux-Saints Faunal Teeth LA-MC-ICPMS Sr Isotope Results

Summarised LA-MC-ICPMS Strontium Isotope Results, La Chapelle-aux-Saints, France

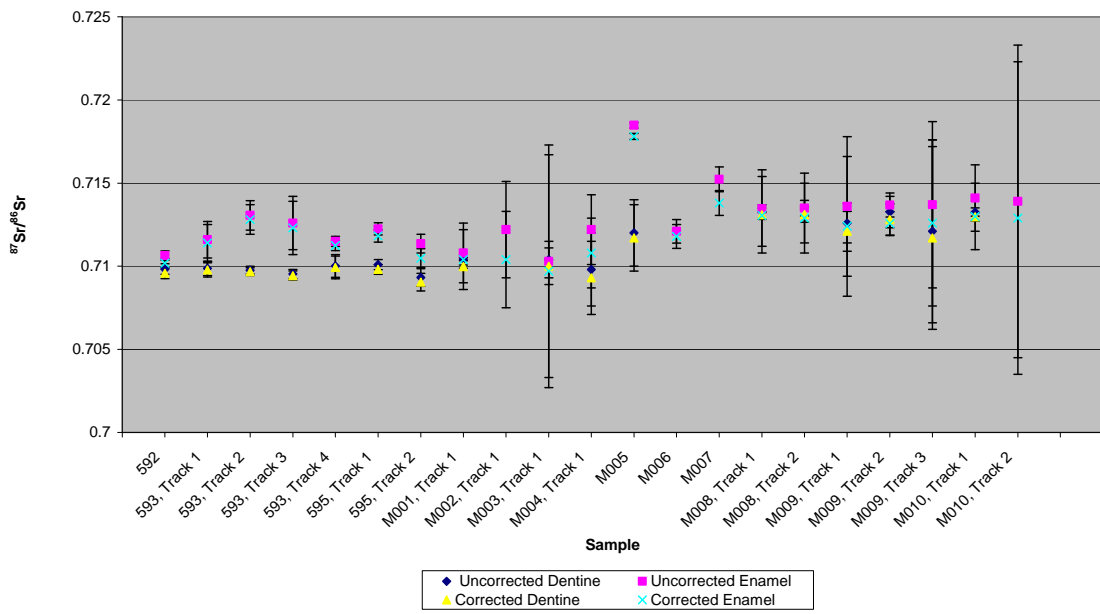


Figure 5.16 Summary Plot of La Chapelle-aux-Saints Faunal Teeth LA-MC-ICPMS Sr Isotope Results

5.4.1.5. Mobility Interpretation

The results from the 13 specimens from the site of La Chapelle-aux-Saints are summarised in Table 5.28 and shown in detail in A3.2.3.1. These samples overwhelmingly show high levels of mobility during amelogenesis. All of the samples (for which this can be determined) show a difference between dentine and enamel $^{87}\text{Sr}/^{86}\text{Sr}$ composition and all are resident at least sometimes on a geological unit other than that which hosts the site.

The corrected $^{87}\text{Sr}/^{86}\text{Sr}$ values of the enamel samples (with the exception of M004) from these samples all correlate with the value of soil samples collected from the Loire, Dordogne or Verezé floodplains and many also correlate with values of Jurassic aged carbonates. Only a small number of the samples (M002, M005, M006 and M007) from La Chapelle-aux-Saints have values which suggest long mobility distances. The corrected value of sample M008 does not correspond with any soil strontium isotope value within this survey.

Overall, samples 593 to 595 from stratum 1 of the bouffia Bonneval and M001 to M004 from layer 1 of the bouffia 118 region have affinities in dentine $^{87}\text{Sr}/^{86}\text{Sr}$ values, lying in the range of 0.7095 to 0.7015, while samples M005 to M010 from layer 2 of the bouffia 118 region have dentine values in the range of 0.712 to 0.7135, suggesting a significantly different regime of post-depositional diagenesis. The strong correlation between stratum 1 of the bouffia Bonneval and layer 1 of the bouffia 118 suggests that they share a similar lithology.

Sample	Fauna	Layer	MIS	Dentine/Enamel Different?		Mobile During Amelogenesis?	Principal Residence During Amelogenesis Based on Uncorrected Values
				Enamel Different from Local Geology (Jurassic Carbonate Sediments)?	Principal Residence During Amelogenesis Based on Uncorrected Values		
592	Bovid	Bouffia Bonneval, stratum 1	3	Yes	Sometimes	Yes	Jurassic carbonate and Dordogne floodplain
593	Bovid	Bouffia Bonneval, stratum 1	3	Yes	Sometimes	Yes	Jurassic or Cretaceous carbonate and Dordogne floodplain
595	Bovid	Bouffia Bonneval, stratum 1	3	Yes	Sometimes	Yes	Jurassic carbonate, Dordogne floodplain and la Chappelle-aux-Saints river floodplain
M001	Reindeer	Bouffia 118, layer 2	?	Yes	Sometimes	Yes	Jurassic carbonate and floodplain sediments
M002	Reindeer	Bouffia 118,	?	Unknown	Yes	Yes	No mapping value and Cambrian metamorphics
							Cambrian metamorphics within 8.3 km

Principal Residence During Amelogenesis Based on Uncorrected Values								
Principal Residence During Amelogenesis Based on Uncorrected Values								
Mobile During Amelogenesis?								
Enamel Different from Local Geology (Jurassic Carbonate Sediments)?								
		layer 2					metamorphics	and Jurassic white clay/ Dordogne floodplain within 0 km
M003	Reindeer	Bouffia 118, layer 2	?	Yes	Yes	Yes	Upper Cretaceous/Lower Jurassic and dordogne floodplain	Dordogne floodplain/Low er Jurassic Carbonate within 0 km and Vereze/ Dordogne floodplain within 3.9 km
M004	Unknown	Bouffia 118, unknown layer	?	Yes	Yes	No	Cambrian metamorphics	Lower Jurassic Carbonate within 0 km
M005	Bovid	Bouffia 118, layer 1	?	Yes	Yes	Unk now n	Metamorphics	Metamorphics within 14.2 km
M006	Bovid	Bouffia 118, layer 1	?	Unknown	Yes	Yes	Dordogne floodplain and Cambrian metamorphics	Dordogne floodplain within 3.9 km and Cambrian metamorphics within 8.5 km
M007	Bovid	Bouffia 118, layer 1	?	Unknown	Yes	Yes	Cambrian sediments and floodplains	Dordogne floodplain within 3.9 km, Carboniferous monzogranite/ granodiorite within 32 km and monzogranite/ granodiorite within 32 km
M008	Bovid	Bouffia 118, layer 1	?	Yes	Yes	No	Dordogne floodplain	Unknown
M009	Bovid	Bouffia 118, layer 1	?	Yes	Yes	Yes	Dordogne and other floodplains	Floodplain within 0.1 km
M0010	Bovid	Bouffia 118,	?	Yes	Yes	Yes	Dordogne floodplain and	Dordogne floodplain

Principal Residence During Amelogenesis Based on Uncorrected Values	
Principal Residence During Amelogenesis Based on Uncorrected Values	
Mobile During Amelogenesis?	
Enamel Different from Local Geology (Jurassic Carbonate Sediments)?	
Dentine/Enamel Different?	
MIS	
Layer	
Fauna	
Sample	

Table 5.28 Summary of Mobility Results for Analysed Fauna from La Chapelle-aux-Saints

5.4.2. Les Fieux

5.4.2.1. MC-ICPMS Results

Three sediment samples from, or adjacent to, the archaeological site of Les Fieux were analysed using MC-ICPMS to determine their $^{87}\text{Sr}/^{86}\text{Sr}$ composition, as summarised in Table 5.29. Sediment samples from Les Fieux have been taken from layer G7, layer K and from the surface adjacent to the site. These values are extremely heterogeneous, with layer G7 having a $^{87}\text{Sr}/^{86}\text{Sr}$ value of 0.708543 ± 0.000042 , layer K a value of 0.711165 ± 0.000049 and the surface a value of 0.709697 ± 0.000025 . While all samples in this study are from layer G7, the presence of this heterogeneity may suggest a complicated sedimentological and/or hydrological regime, which may cause post-burial diagenesis of variable $^{87}\text{Sr}/^{86}\text{Sr}$ composition.

Sample Number	Associated with Tooth	Stratigraphic Unit	Age (ky)	$^{87}\text{Sr}/^{86}\text{Sr}$	$^{87}\text{Sr}/^{86}\text{Sr} 2\sigma$ Error
FS047-S1	N/A	Unit K	Not Dated	0.711165	0.000049
FS047-S2	M011, M012, M013, M014, M015, M016, M017, M018, M019, M020, M021, M022	Unit G	Not Dated	0.708543	0.000042
FS047-S4	N/A	Surface Sediment	N/A	0.709697	0.000025

Table 5.29 $^{87}\text{Sr}/^{86}\text{Sr}$ Results from Archaeological Sediments from Les Fieux

5.4.2.2. *Regional Mapping Samples*

Strontium isotope values from soil samples immediately surrounding the site of Les Fieux are shown in Figure 5.17.

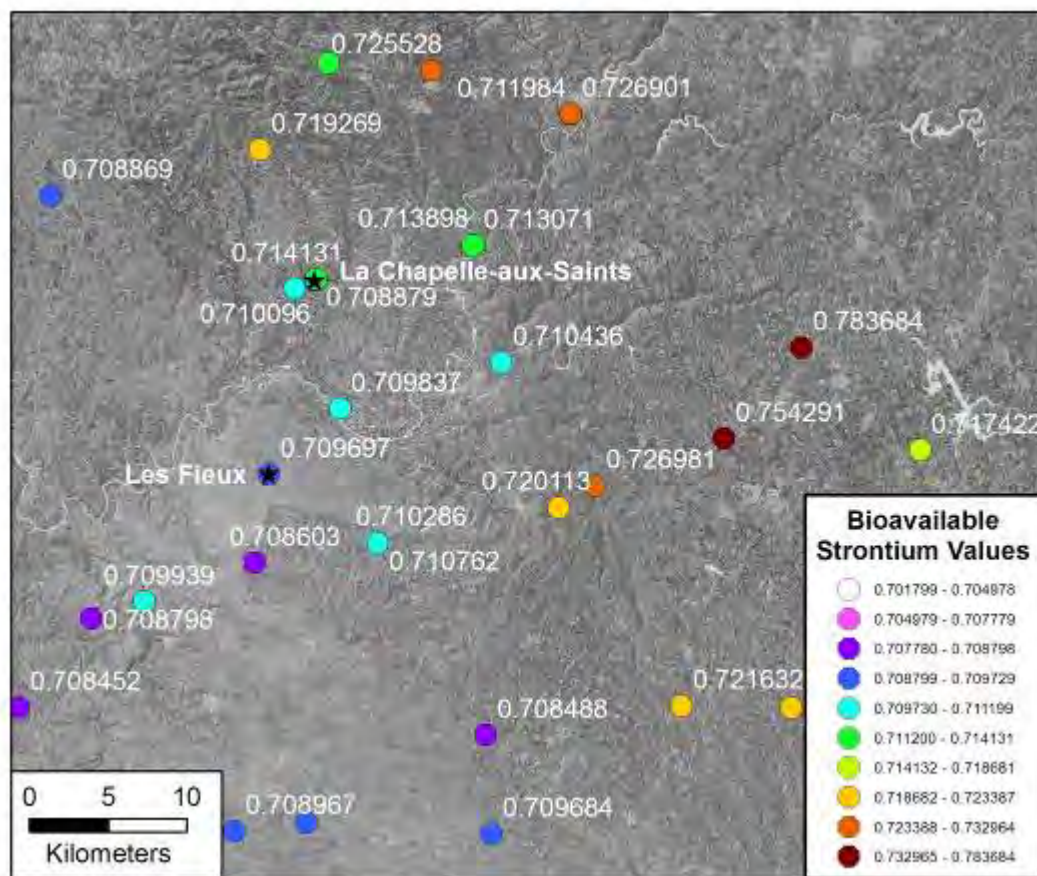


Figure 5.17 Bioavailable Soil Strontium Values Surrounding Les Fieux

5.4.2.3. LA-MC-ICPMS Results

Samples from 12 individuals were analysed from the archaeological site of Les Fieux using LA-MC-ICPMS. The results from these samples are summarised in Table 5.30 and Figure 5.18. The detailed results and photographs showing the analysis tracks are shown in section A3.2.3.2.

Sample	Unit	Material	Track	^{88}Sr Volts	N	$^{84}\text{Sr}/^{86}\text{Sr}$	$^{84}\text{Sr}/^{86}\text{Sr}$ 2 σ Error	$^{87}\text{Sr}/^{86}\text{Sr}$	Corrected $^{87}\text{Sr}/^{86}\text{Sr}$	$^{87}\text{Sr}/^{86}\text{Sr}$ 2 σ Error
M011	G7	Enamel	1	0.50	10	0.05641	0.00032	0.71137	0.70997	0.00074
M011	G7	Dentine	1	0.65	27	0.05644	0.00006	0.71075	0.71013	0.00038
M012	G7	Enamel	1	0.31	5	0.05661	0.00055	0.71112	0.70833	0.00086
M012	G7	Dentine	1	0.59	11	0.05645	0.00009	0.71142	0.71055	0.00079
M012	G7	Enamel	2	0.30	7	0.05633	0.00024	0.71096	0.70817	0.00048
M012	G7	Dentine	2	0.52	9	0.05629	0.00014	0.71144	0.71057	0.00096
M013	G7	Enamel	1	0.29	4	0.05654	0.00035	0.71786	0.71498	0.00040
M013	G7	Dentine	1	0.51	11	0.05655	0.00012	0.71217	0.71099	0.00034
M013	G7	Enamel	2	0.30	4	0.05660	0.00039	0.71730	0.71450	0.00150
M013	G7	Dentine	2	0.50	9	0.05628	0.00013	0.71400	0.71280	0.00110
M014	G7	Enamel	1	0.22	2	0.05700	0.00810	0.71930	0.71220	0.00990
M014	G7	Dentine	1	0.52	9	0.05675	0.00013	0.71143	0.70988	0.00067
M014	G7	Enamel	2	0.19	1	0.05639	0.00064	0.71640	0.70931	0.00087
M014	G7	Dentine	2	0.45	7	0.05644	0.00016	0.71067	0.70912	0.00049
M015	G7	Enamel	1	0.22	1	0.05605	0.00087	0.71751	0.71460	0.00086
M015	G7	Dentine	1	0.26	5	0.05628	0.00034	0.71058	0.70842	0.00089
M016	G7	Enamel	1	0.49	4	0.05679	0.00022	0.71344	0.71238	0.00027
M016	G7	Dentine	1	0.59	3	0.05684	0.00020	0.71070	0.71000	0.00100
M016	G7	Enamel	2	0.42	4	0.05706	0.00049	0.71420	0.71320	0.00190
M016	G7	Dentine	2	0.52	7	0.05694	0.00013	0.71115	0.71046	0.00079
M017	G7	Enamel	1	0.50	6	0.05659	0.00015	0.71260	0.71200	0.00170
M017	G7	Dentine	1	0.57	10	0.05669	0.00009	0.71062	0.71006	0.00089
M017	G7	Enamel	2	0.54	8	0.05656	0.00013	0.71260	0.71200	0.00120
M017	G7	Dentine	2	0.58	10	0.05654	0.00016	0.71080	0.71030	0.00130
M018	G7	Dentine	1	0.34	5	0.05689	0.00026	0.71025	0.70861	0.00037
M018	G7	Enamel	2	0.10	2	0.05900	0.01200	0.71400	0.69910	0.00140
M018	G7	Dentine	2	0.29	4	0.05715	0.00087	0.70978	0.70814	0.00041
M019	G7	Enamel	1	0.23	2	0.05677	0.00056	0.71100	0.70900	0.01100
M019	G7	Dentine	1	0.43	4	0.05657	0.00022	0.70952	0.70876	0.00091
M019	G7	Enamel	2	0.33	4	0.05637	0.00042	0.71270	0.71080	0.00270
M019	G7	Dentine	2	0.52	6	0.05641	0.00017	0.71090	0.71020	0.00230
M020	G7	Enamel	1	0.19	2	0.05610	0.00730	0.71200	0.70900	0.01900
M020	G7	Dentine	1	0.24	3	0.05630	0.00120	0.71000	0.70800	0.00140
M020	G7	Enamel	2	0.24	8	0.05614	0.00034	0.71070	0.70840	0.00140

Sample	Unit	Material	Track	^{88}Sr Volts	N	$^{84}\text{Sr}/^{86}\text{Sr}$	$^{84}\text{Sr}/^{86}\text{Sr}$ 2 σ	$^{87}\text{Sr}/^{86}\text{Sr}$	Corrected $^{87}\text{Sr}/^{86}\text{Sr}$	$^{87}\text{Sr}/^{86}\text{Sr}$ 2 σ Error
M020	G7	Dentine	2	0.29	3	0.05600	0.00110	0.71006	0.70794	0.00052
M021	G7	Enamel	1	0.47	2	0.05644	0.00043	0.71200	0.71100	0.01300
M021	G7	Dentine	1	0.26	7	0.05636	0.00026	0.71060	0.70890	0.00210
M021	G7	Enamel	2	0.42	3	0.05632	0.00020	0.71200	0.71120	0.00360
M021	G7	Dentine	2	0.26	3	0.05650	0.00180	0.71190	0.71020	0.00580
M021	G7	Enamel	3	0.40	2	0.05621	0.00037	0.71300	0.71220	0.00890
M021	G7	Dentine	3	0.30	4	0.05606	0.00069	0.71010	0.70840	0.00160
M022	G7	Dentine	1	0.31	5	0.05637	0.00031	0.70936	0.70778	0.00058

Table 5.30 Summary Table of Les Fieux Faunal Teeth LA-MC-ICPMS Sr Isotope Results

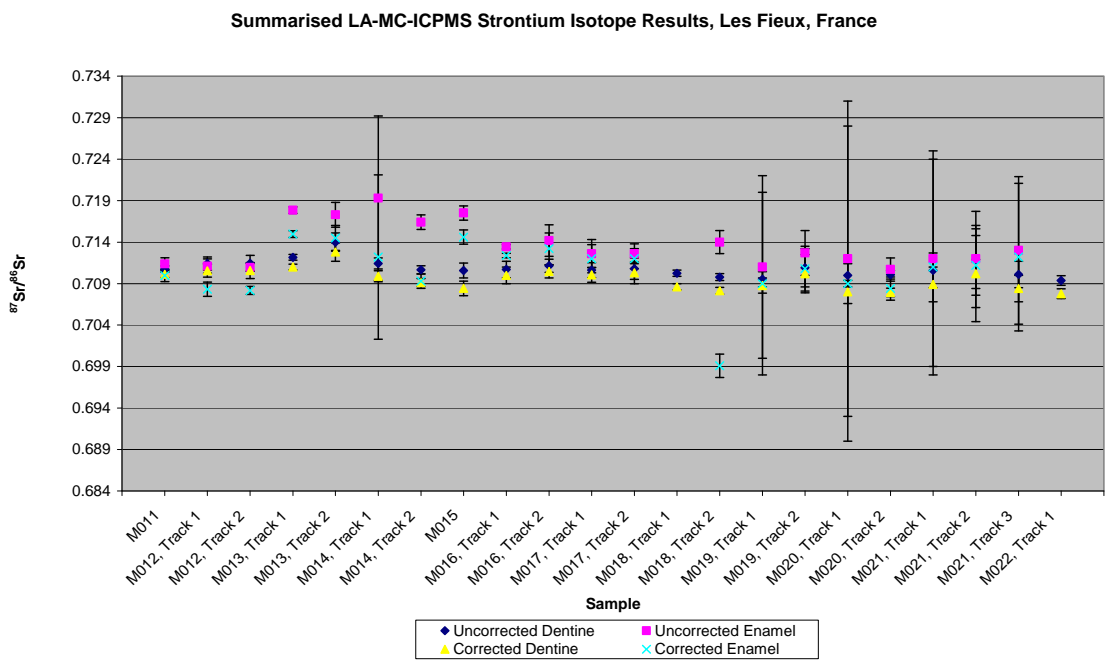


Figure 5.18 Summary Plot of Les Fieux Faunal Teeth LA-MC-ICPMS Sr Isotope Results

5.4.2.4. Mobility Interpretation

The results from the 12 specimens from the site of Les Fieux are summarised in Table 5.31 and shown in detail in A3.2.3.2. These samples show a moderate degree of mobility with 7 of the specimens showing evidence of mobility during

amelogenesis. All samples for which this could be determined lived (at least some time) within a geological unit other than that which contains the archaeological site and have dentine and enamel $^{87}\text{Sr}/^{86}\text{Sr}$ values that are distinct. Six samples (M014, M015, M016, M017, M019 and M021) have values which correlate with soil samples collected from floodplains within the study area. Four samples (M013, M016, M017 and M021) have strontium isotope values which correlate to geological units from outside of the Aquitane Basin, suggesting higher distances of migration.

Principal Residence During Amelogenesis Based on Corrected Values?	Principal Residence During Amelogenesis Based on Uncorrected Values?	Mobile During Amelogenesis?	Enamel Different from Local Geology (Jurassic Carbonate Sediments)?	Dentine/Enamel Different?	MIS	Layer	Fauna	Sample
Lower Jurassic carbonates within 2.8 km and metamorphics within 15 km	Yes	Yes	Sometimes	Yes	G7	3	Horse	M011
Upper Cretaceous carbonate and siliciclastic	No							M012
Carboniferous monzogranite/granodiorite within 36 km west	No						Wild Boar	M013
Metamorphics, Permian sediments and floodplain	Yes						Fox	M014
Carboniferous monzogranite/granodiorite	Unknown						Hyena	M015
Dordogne floodplain and unknown location	Yes						Bison	M016
Floodplain or carboniferous monzogranite/granodiorite and Cambrian metamorphics	Yes						Bison	M017

Principal Residence During Amelogenesis Based on Corrected Values?								
Principal Residence During Amelogenesis Based on Uncorrected Values?								
Mobile During Amelogenesis?								
Dentine/Enamel Different?								
MIS	Layer							
Sample	Fauna							
						Dordogne floodplain	within 15 km and unknown	
M018	Reindeer	G7	3	Yes	Unknown	No	Unknown	Unknown
M019	Reindeer	G7	3	Yes	Sometimes	Yes	Carboniferous monzogranite/granodiorite and Metamorphics, alluvial valley fill and Dordogne floodplain, as well as Jurassic carbonate	Floodplain within 5.3 km and Lower Jurassic carbonate within 2.8 km
M020	Chamois	G7	3	Sometimes	Yes	Yes	Unknown and Dordogne floodplain	Unknown and Lower/Upper Jurassic carbonate within 2.8 km
M021	Mountain goat/ chamois	G7	3	Sometimes	Yes	Yes	Clay within limestone, floodplain, Dordogne floodplain and Lower Jurassic limestone	Floodplain within 5.3 km and Lower Jurassic carbonate within 2.8 km
M022	Mountain goat/ chamois	G7	3	Unknown	Unknown	Unknown	Unknown	Unknown

Table 5.31 Summary of Mobility Results for Analysed Fauna from Les Fieux

5.4.3. Le Moustier

5.4.3.1. Regional Mapping Results

Strontium isotope values from soil samples immediately surrounding the site of Le Moustier are shown in Figure 5.19.

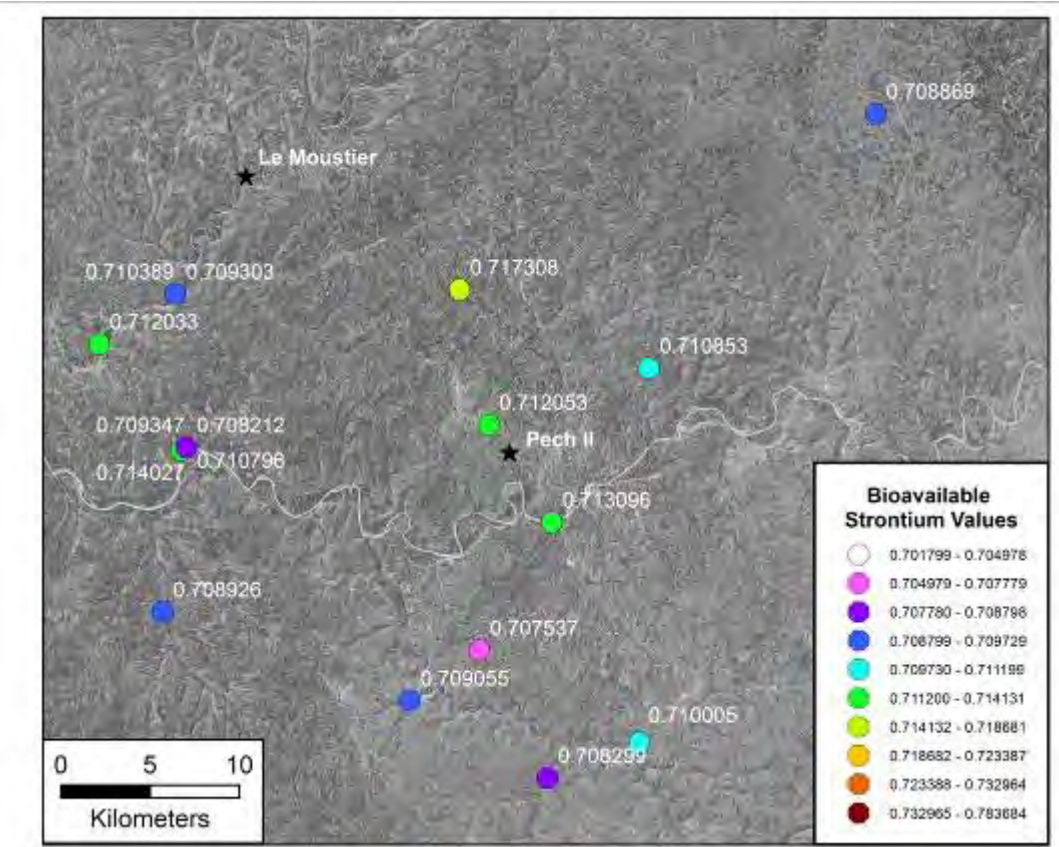


Figure 5.19 Bioavailable Soil Strontium Values Surrounding Le Moustier

5.4.3.2. LA-MC-ICPMS Results

Samples from 6 individuals were analysed from the archaeological site of Le Moustier using LA-MC-ICPMS. The results from these samples are summarised in Table 5.32 and Figure 5.20. The detailed results and photographs showing the analysis tracks are shown in section A3.2.3.3.

Sample	Unit	Material	Track	^{88}Sr Volts	n	$^{84}\text{Sr}/^{86}\text{Sr}$	$^{84}\text{Sr}/^{86}\text{Sr} 2\sigma$ Error	$^{87}\text{Sr}/^{86}\text{Sr}$	Corrected $^{87}\text{Sr}/^{86}\text{Sr}$	$^{87}\text{Sr}/^{86}\text{Sr} 2\sigma$ Error
845	G1	Enamel	1	0.63	5	0.05654	0.00012	0.71570	0.71387	0.00076
845	G1	Dentine	1	0.61	25	0.05655	0.00006	0.71233	0.71070	0.00032
845	G1	Enamel	2	0.43	4	0.05655	0.00022	0.71600	0.71410	0.00140
845	G1	Dentine	2	0.50	10	0.05651	0.00018	0.71252	0.71089	0.00030
846	G2	Enamel	1	1.15	6	0.05659	0.00015	0.71247	0.71187	0.00094
846	G2	Dentine	1	0.85	4	0.05642	0.00009	0.71121	0.71022	0.00057
847	G3	Enamel	1	0.32	3	0.05610	0.00110	0.71710	0.71420	0.00320
847	G3	Dentine	1	0.57	11	0.05651	0.00010	0.71420	0.71280	0.00350
847	G3	Enamel	2	0.37	3	0.05656	0.00027	0.71430	0.71150	0.00180
847	G3	Dentine	2	0.59	10	0.05658	0.00011	0.71209	0.71072	0.00041
848	G4	Enamel	1	0.34	4	0.05628	0.00030	0.71380	0.71000	0.00230
848	G4	Dentine	1	0.43	11	0.05648	0.00017	0.71102	0.70855	0.00033
848	G4	Enamel	2	0.34	3	0.05653	0.00085	0.71390	0.71000	0.00210
848	G4	Dentine	2	0.47	12	0.05635	0.00015	0.71129	0.70882	0.00023
849	G5	Enamel	1	0.52	7	0.05637	0.00028	0.71302	0.71116	0.00046
849	G5	Dentine	1	0.54	10	0.05655	0.00013	0.71191	0.70997	0.00034
849	G5	Enamel	2	0.53	8	0.05639	0.00020	0.71271	0.71085	0.00058
849	G5	Dentine	2	0.53	9	0.05631	0.00013	0.71160	0.70965	0.00033
850	G6	Enamel	1	0.78	5	0.05662	0.00029	0.71261	0.71150	0.00061
850	G6	Dentine	1	0.60	6	0.05654	0.00014	0.71220	0.71060	0.00140
850	G6	Enamel	2	0.65	11	0.05655	0.00016	0.71295	0.71171	0.00029
850	G6	Dentine	2	0.61	15	0.05649	0.00010	0.71164	0.71010	0.00036

Table 5.32 Summary Table of Le Moustier Faunal Teeth LA-MC-ICPMS Sr Isotope Results

Summarised LA-MC-ICPMS Strontium Isotope Results, Le Moustier, France

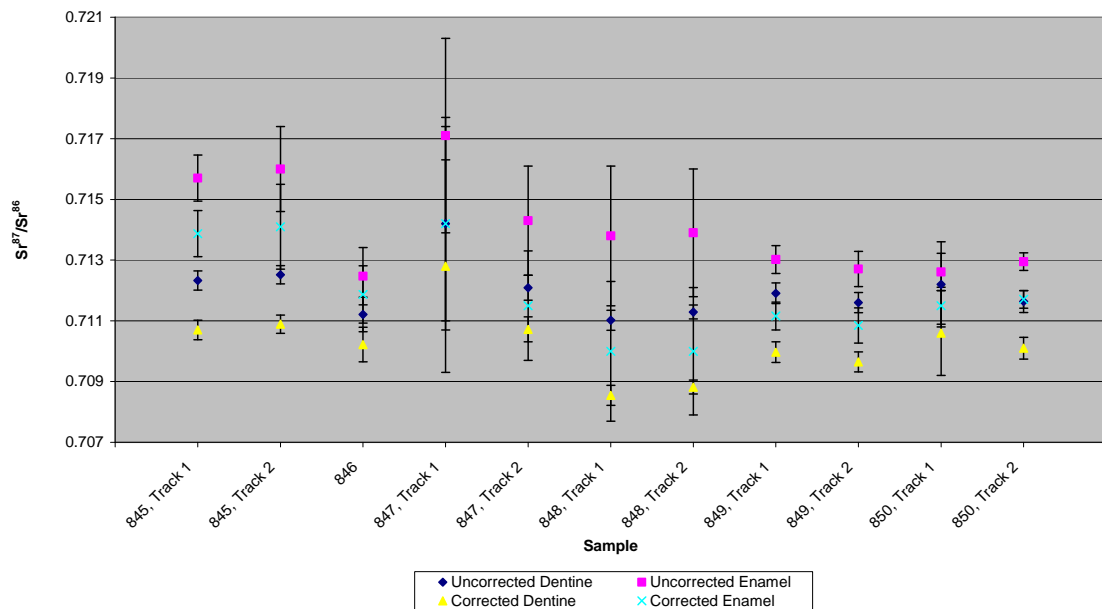


Figure 5.20 Summary Plot of Le Moustier Faunal Teeth LA-MC-ICPMS Sr Isotope Results

5.4.3.3. Mobility Interpretation

The results from the 6 specimens from the site of Le Moustier are summarised in Table 5.33 and shown in detail in A3.2.3.3. All bovid samples analysed from Le Moustier appear to be migrants for at least some portion of their period of amelogenesis, based on the considerable difference between the strontium isotope values of the dentine and enamel and the heterogeneity of email values. All samples from Le Moustier (except 847) have strontium isotope values which suggest that they have spent some of the period of their amelogenesis on floodplains within the study area. Samples 846 and 847 have some domains of enamel strontium isotope composition that don't correspond to any soil samples within the study area. Samples 845 and 849 have $^{87}\text{Sr}/^{86}\text{Sr}$ values corresponding with bioavailable strontium isotope values from the Massif Central, suggesting significant mobility by these animals. Dentine values are slightly different between layers, which may reflect the changes in sediments between the different G units at Le Moustier.

Sample	Fauna	Layer	MIS	Dentine/Enamel Different?		Enamel Different from Local Geology (Cretaceous Carbonate Sediments)?	Mobile During Amelogenesis?	Principal Residence During Amelogenesis Based on Uncorrected Values?	Principal Residence During Amelogenesis Based on Corrected Values?
845	Bovid	G1	3	Yes	Yes	Carboniferous monzogranite/ granodiorite and floodplain	Carboniferous monzogranite/ granodiorite within 85 km and Dordogne floodplain within 14.2 km		
846	Bovid	G2	3	Sometimes	Sometimes	Cambrian metamorphics, Dordogne floodplain and Upper Cretaceous carbonate	Unknown, floodplain within 0.1 km and Dordogne floodplain within 14.2 km		
847	Bovid	G3	3	Yes	Yes	Permian monzogranite/ granodiorite, unknown, as well as Dordogne and another floodplain	Unknown and Middle Jurassic Carbonate within 10 km		
848	Bovid	G4	3	Yes	Yes	Permian monzogranite/ granodiorite, Dordogne river sediments and Vezere river sediments	Floodplain within 0.1 km		
849	Bovid	G5	3	Yes	Yes	Dordogne, unnamed and Vezere river sediments	Floodplain within 0.1 km		
850	Bovid	G6	3	Yes	Yes	Dordogne and Vezere floodplain sediments	Floodplain within 0.1 km, floodplain within 14.2 km, Permian monzogranite/granodiorite within 55 km and Lower Jurassic carbonate within 17.3 km		

Table 5.33 Summary of Mobility Results for Analysed Faunal from Le Moustier

5.4.4. Pech de l'Azé II

5.4.4.1. Regional Mapping Results

Strontium isotope values from soil samples immediately surrounding the site of Pech de l'Azé II are shown in Figure 5.21.

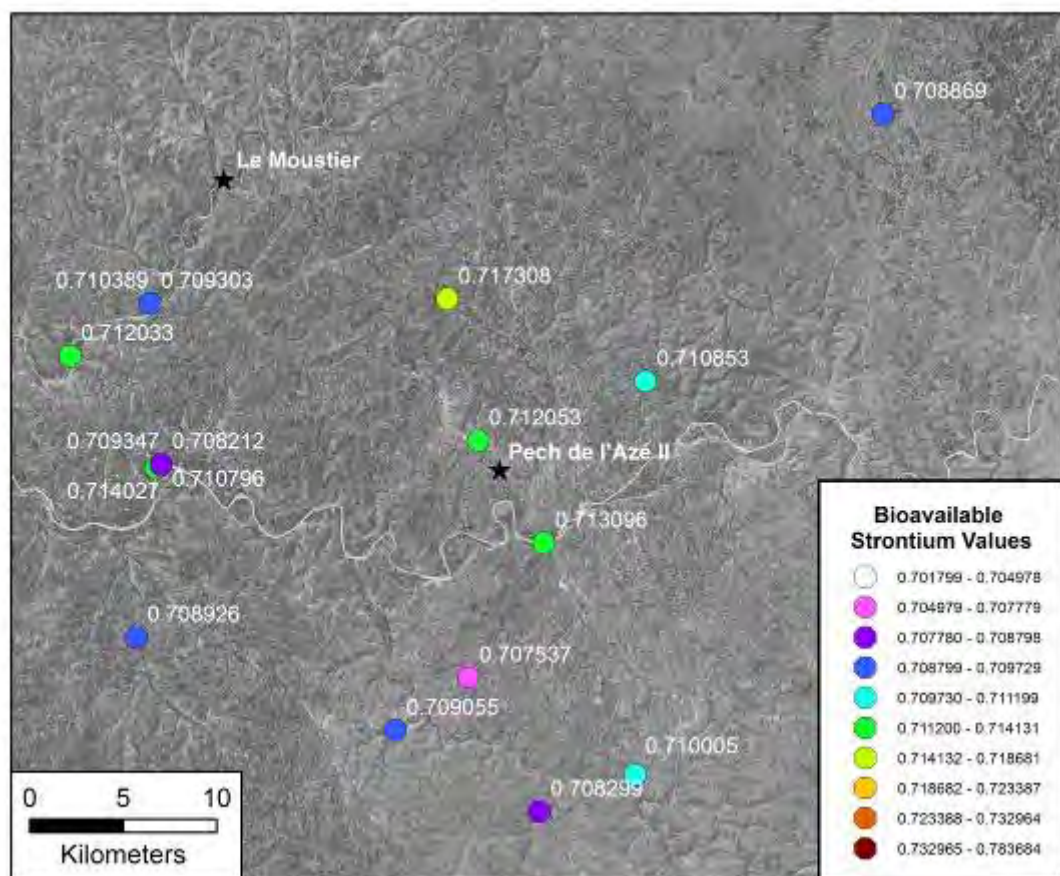


Figure 5.21 Bioavailable Soil Strontium Values Surrounding Pech de l'Azé II

5.4.4.2. LA-MC-ICPMS Results

Samples from 9 individuals were analysed from the archaeological site of Pech de l'Azé II using LA-MC-ICPMS. The results from these samples are

summarised in Table 5.26 and Figure 5.34. The detailed results and photographs showing the analysis tracks are shown in section A3.2.3.4.

Sample	Unit	Material	Track	^{88}Sr Volts	n	$^{84}\text{Sr}/^{86}\text{Sr}$	$^{84}\text{Sr}/^{86}\text{Sr} 2\sigma$ Error	$^{87}\text{Sr}/^{86}\text{Sr}$	Corrected $^{87}\text{Sr}/^{86}\text{Sr}$	$^{87}\text{Sr}/^{86}\text{Sr} 2\sigma$ Error
614	9	Enamel	1	0.40	3	0.05784	0.00030	0.71300	0.71090	0.00560
614	9	Dentine	1	0.38	4	0.05767	0.00046	0.71310	0.71150	0.00120
614	9	Enamel	2	0.27	4	0.05787	0.00039	0.71200	0.70990	0.00590
614	9	Dentine	2	0.34	5	0.05742	0.00028	0.71399	0.71239	0.00068
615	9	Enamel	1	0.40	8	0.05754	0.00037	0.71220	0.71090	0.00130
615	9	Dentine	1	0.35	24	0.05744	0.00015	0.71238	0.71105	0.00041
617	8	Enamel	1	0.28	2	0.05744	0.00045	0.71600	0.71500	0.03000
617	8	Dentine	1	0.29	21	0.05733	0.00014	0.71424	0.71285	0.00079
618	8	Enamel	1	0.48	8	0.05707	0.00024	0.71860	0.71790	0.00120
618	8	Dentine	1	0.34	10	0.05735	0.00018	0.71500	0.71380	0.00110
618	8	Enamel	2	0.44	7	0.05705	0.00020	0.72000	0.71920	0.00260
618	8	Dentine	2	0.36	7	0.05727	0.00022	0.71730	0.71610	0.00210
619	8	Enamel	1	0.75	10	0.05679	0.00014	0.71076	0.71039	0.00033
619	8	Dentine	1	0.70	13	0.05692	0.000081	0.71062	0.71024	0.00022
620	7	Enamel	1	0.31	4	0.05685	0.00028	0.71460	0.71420	0.00100
620	7	Dentine	1	0.35	5	0.05684	0.00027	0.71159	0.71120	0.00062
622	7	Enamel	1	0.36	7	0.05749	0.00034	0.71300	0.71040	0.00130
622	7	Dentine	1	0.40	11	0.05745	0.00026	0.71196	0.70987	0.00041
622	7	Enamel	2	0.29	7	0.05810	0.00047	0.71430	0.71160	0.00180
622	7	Dentine	2	0.35	13	0.05748	0.00027	0.71165	0.70956	0.00037
624	6	Enamel	1	0.35	5	0.05736	0.00056	0.71740	0.71510	0.00710
624	6	Dentine	1	0.27	6	0.05772	0.00054	0.71350	0.70970	0.00190
625	6	Enamel	1	0.34	4	0.05688	0.00027	0.71380	0.70909	0.00082
625	6	Dentine	1	0.36	15	0.05673	0.00024	0.71197	0.71090	0.00064
625	6	Enamel	2	0.37	5	0.05722	0.00022	0.71200	0.70910	0.00140
625	6	Dentine	2	0.37	14	0.05715	0.00024	0.71420	0.71130	0.00100

Table 5.34 Summary Table of Pech de l'Azé II Faunal Teeth LA-MC-ICPMS Sr Isotope Results

Summarised LA-MC-ICPMS Strontium Isotope Results, Pech de l'Azé II, France

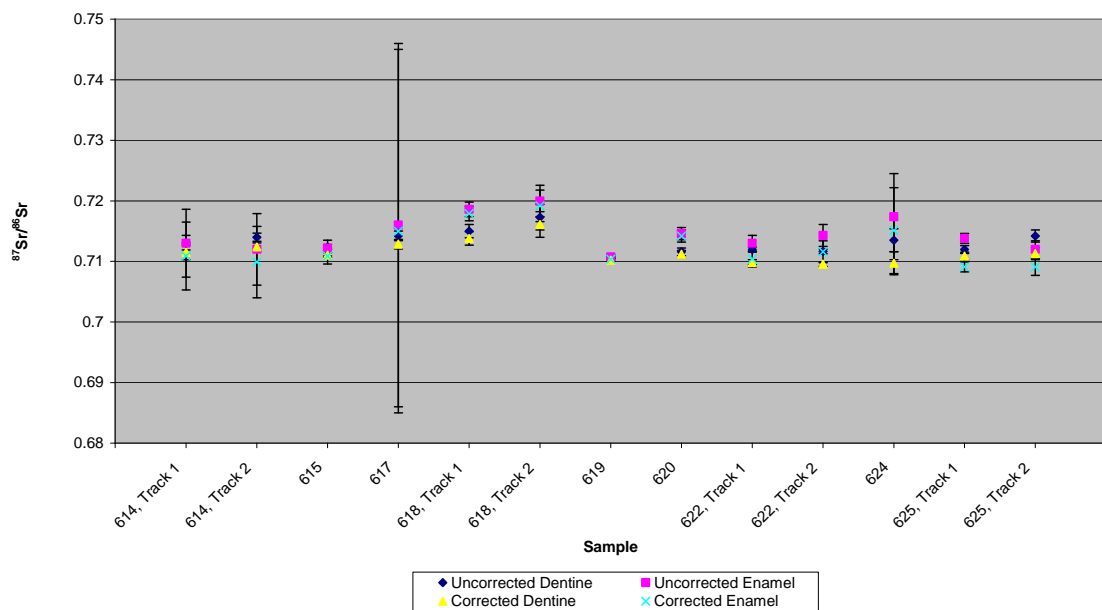


Figure 5.22 Summary Plot of Pech de l'Azé II Faunal Teeth LA-MC-ICPMS Sr Isotope Results

5.4.4.3. Mobility Interpretation

The results from the 9 specimens from the site of Pech de l'Azé II are summarised in Table 5.35 and shown in detail in A3.2.3.4. Five of the samples show evidence of mobility during amelogenesis, based on their heterogeneous enamel composition. Only 1 sample has enamel that has a strontium isotope composition that is entirely different from the geological unit that hosts the site. Seven of the samples have enamel and dentine $^{87}\text{Sr}/^{86}\text{Sr}$ values that are distinct. The strontium isotope samples of five of the samples (614, 617, 619, 620, 622, 624 and 625) show that these specimens spent at least part of their lives on a floodplain with the study area. Four of the samples (614, 615, 617, 618) have enamel values that suggest that they spent some of the period of their amelogenesis in the Massif Central region and 5 of them have enamel $^{87}\text{Sr}/^{86}\text{Sr}$ values that suggest that the samples spent time in the Aquitaine Basin.

Uncorrected dentine values from Pech de l'Azé II are grouped into 2 domains: the first containing samples 614, 617 and 618 (from layer 9, 8 and 8,

respectively) and the second containing samples 615, 619, 620, 622 and 625 (from layer 9, 8, 7, 7 and 6, respectively).

Principal Residence During Amelogenesis Based on Corrected Values?								
Principal Residence During Amelogenesis Based on Uncorrected Values?								
Mobile During Amelogenesis?								
Sample	Fauna	MIS	Layer	Enamel Different from Local Geology (Cretaceous Carbonate Sediments)?	Dentine/Enamel Different?	Mobile During Amelogenesis?	Principal Residence During Amelogenesis Based on Uncorrected Values?	Principal Residence During Amelogenesis Based on Corrected Values?
614	Bovid	9	6	Yes	Sometimes	Yes	Metamorphics, Permian monzogranite/granodiorite, unknown and Cretaceous carbonates	Metamorphics within 45 km, floodplain within 1.4 km, unknown and Upper Cretaceous carbonate within 0 km
615	Hippo-potamus	9	6	Yes	Sometimes	Yes	Metamorphics and Cretaceous carbonates	Unknown and Jurassic carbonates within 8.2 km
617	Horse	8	6	Yes	Yes	Yes	Permian sediments/Lower Jurassic sediments/metamorphic s/ granite and floodplain	Monzogranite/granodiorite within 70 km and floodplain within 1.4 km
618	Deer	8	6	Yes	Yes	Yes	Permian monzogranite/granodiorite and Cambrian/Ordovician anatectic orthogneiss	Permian monzogranite/granodiorite within 70 km and Cambrian/Ordovician anatectic orthogneiss within 46.8 km
619	Horse	8	6	No	No	No	Verezé River/Upper Cretaceous limestone	Upper Cretaceous limestone within 0 km
620	Bovid	7	6	Yes	Yes	No	Floodplain sediments	Floodplain sediments within 1.4 km
622	Hippo-potamus	7	6	Yes	Yes	Yes	Floodplain sediments	Dordonge floodplain within 1.4 km
624	Deer	6	6	Yes	Yes	No	Monzogranite/granodiorite	Dordonge floodplain within 1.4 km
625	Horse	6	6	No	Yes	No	Metamorphics or Floodplain sediments	Dordonge floodplain within 1.4 km

Table 5.35 Summary of Mobility Results for Analysed Fauna from Pech de l'Azé II

5.4.5. Bois Roche

5.4.5.1. LA-ICPMS Results

Samples 2417, 2418, 2421 and 2422 from the archaeological site of Bois Roche were analysed for element concentration and ratios using LA-ICPMS, as summarised in Table 5.36 and shown in detail in section A3.1.2.2.

Sample	Material	Transect	Mg (ppm)	P (ppm)	Sr (ppm)	Ba (ppm)	Th (ppm)	U (ppm)	Mg/Ca	Sr/Ca	Ba/Ca
2417	Enamel	1	2030	191574	240	43	0	0	0.008842	0.000290	0.000033
2417	Dentine	1	979	177285	273	130	0	1	0.004264	0.000330	0.000100
2417	Enamel	2	1680	210222	244	58	0	0	0.007317	0.000295	0.000045
2417	Dentine	2	932	198645	261	129	0	1	0.004059	0.000315	0.000099
2418	Enamel	1	2282	194204	163	42	0	0	0.009939	0.000196	0.000032
2418	Dentine	1	941	171689	182	93	0	0	0.004100	0.000219	0.000072
2421	Enamel	1	1495	211845	235	136	0	0	0.006510	0.000284	0.000105
2421	Dentine	1	534	200034	166	129	0	1	0.002324	0.000200	0.000099
2421	Enamel	2	1466	196756	240	151	0	0	0.006384	0.000290	0.000116
2421	Dentine	2	587	195292	179	139	0	1	0.002555	0.000216	0.000107
2421	Enamel	3	1519	196107	232	138	0	0	0.006617	0.000280	0.000107
2421	Dentine	3	595	216259	157	138	0	1	0.002590	0.000190	0.000106
2422	Dentine	1	717	192454	262	162	-1	8	0.003125	0.000317	0.000125
2422	Enamel	1	1874	209552	165	71	-1	-1	0.008162	0.000199	0.000055
2422	Dentine	2	524	185485	239	141	-1	9	0.002283	0.000289	0.000109

Table 5.36 Summary Table of LA-ICPMS Elemental Concentrations and Ratios from Bois Roche Faunal Teeth

5.4.5.2. MC-ICPMS Results

Five sediment samples from, or adjacent to, the archaeological site of Bois Roche were analysed using MC-ICPMS to determine their $^{87}\text{Sr}/^{86}\text{Sr}$ composition, as summarised in Table 5.37. Sediment samples from the

stratigraphic units of Bois Roche show significant variation in $^{87}\text{Sr}/^{86}\text{Sr}$ value. Samples from layer 1C have a weighted average of 0.70882 ± 0.00029 in a range from 0.708830 ± 0.000009 to 0.709171 ± 0.000018 . The value from layer 2 (0.713459 ± 0.000046) is significantly elevated compared to the values from layer 1C, which may be explained by its position at the back of the cave among very large bedrock blocks (Villa et al. 2010:923), suggesting that different taphonomic processes may be active in this area of the site.

Sample Number	Associated with Tooth	Stratigraphic Unit	Age (ky)	$^{87}\text{Sr}/^{86}\text{Sr}$	$^{87}\text{Sr}/^{86}\text{Sr} 2\sigma$ Error
BR24	2424	Layer 2	$54 \pm 3/55 \pm 3$	0.713459	0.000046
BR81	2417	Layer 1C	$72.5 \pm 12/67 \pm 11$	0.708864	0.000010
BR82	2417	Layer 1C	$72.5 \pm 12/67 \pm 11$	0.709171	0.000018
BR83	2417	Layer 1C	$72.5 \pm 12/67 \pm 11$	0.708830	0.000009
BR85	2417	Layer 1C	$72.5 \pm 12/67 \pm 11$	0.708574	0.000012

Table 5.37 $^{87}\text{Sr}/^{86}\text{Sr}$ Results from Archaeological Sediments from Bois Roche

5.4.5.3. Regional Mapping Results

Strontium isotope values from soil samples immediately surrounding the site of Bois Roche are shown in Figure 5.23.

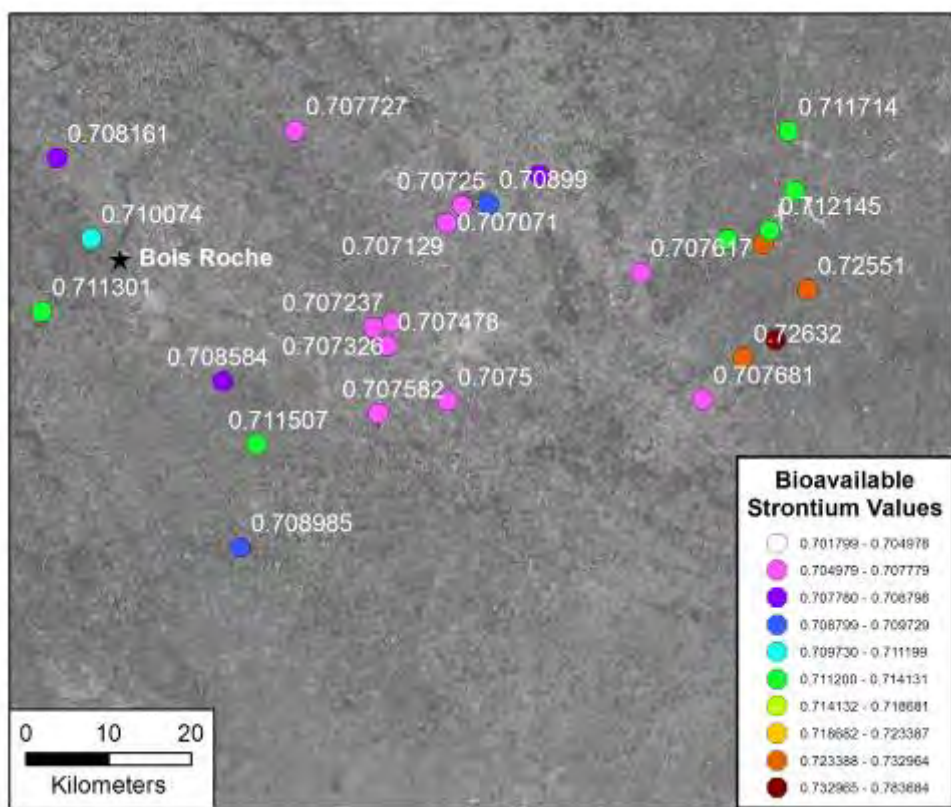


Figure 5.23 Bioavailable Soil Strontium Values Surrounding Bois Roche

5.4.5.4. LA-MC-ICPMS Results

Samples from 9 individuals were analysed from the archaeological site of Bois Roche using LA-MC-ICPMS. The results from these samples are summarised in Table 5.38 and Figure 5.24. The detailed results and photographs showing the analysis tracks are shown in section A3.2.3.5.

Sample	Unit	Material	Track	^{88}Sr Volts	n	$^{84}\text{Sr}/^{86}\text{Sr}$	$^{84}\text{Sr}/^{86}\text{Sr} 2\sigma$ Error	$^{87}\text{Sr}/^{86}\text{Sr}$	Corrected $^{87}\text{Sr}/^{86}\text{Sr}$	$^{87}\text{Sr}/^{86}\text{Sr} 2\sigma$ Error
2417	1C	Enamel	1	0.95	2	0.05631	0.00015	0.71200	0.71200	0.01800
2417	1C	Dentine	1	0.83	5	0.05641	0.00010	0.70967	0.70896	0.00028
2417	1C	Enamel	2	0.90	2	0.05639	0.00014	0.71090	0.71050	0.00510
2417	1C	Dentine	2	0.66	3	0.05617	0.00055	0.70961	0.70890	0.00055
2418	1C	Enamel	1	0.57	6	0.05638	0.00014	0.71292	0.71167	0.00042
2418	1C	Dentine	2	0.80	5	0.05651	0.00022	0.71030	0.70966	0.00032
2419	1C	Enamel	1	0.67	9	0.05607	0.00015	0.71248	0.71095	0.00014
2420	2	Enamel	1	1.03	15	0.05617	0.00008	0.71184	0.71127	0.00027
2421	2	Enamel	1	0.88	4	0.05647	0.00009	0.71158	0.71090	0.00077
2421	2	Dentine	1	0.73	2	0.05649	0.00022	0.71100	0.70990	0.00240
2421	2	Enamel	2	0.77	4	0.05640	0.00029	0.71138	0.71071	0.00034
2421	2	Dentine	2	0.48	3	0.05669	0.00023	0.71080	0.70969	0.00028
2421	2	Enamel	3	0.91	4	0.05652	0.00009	0.71151	0.71084	0.00081
2421	2	Dentine	3	0.67	4	0.05659	0.00024	0.71090	0.70980	0.00130
2422	1C	Enamel	1	0.59	6	0.05641	0.00020	0.71088	0.70965	0.00050
2422	1C	Dentine	1	0.95	11	0.05647	0.00006	0.70963	0.70915	0.00022
2423	2	Enamel	1	0.84	3	0.05640	0.00011	0.71360	0.71280	0.00170
2423	2	Dentine	1	0.60	8	0.05640	0.00012	0.71163	0.70982	0.00027
2423	2	Enamel	2	1.00	3	0.05628	0.00011	0.71600	0.71500	0.01600
2423	2	Dentine	2	0.72	6	0.05623	0.00019	0.71158	0.70978	0.00040
2423	2	Enamel	3	0.93	3	0.05627	0.00013	0.71800	0.71700	0.02400
2423	2	Dentine	3	0.72	8	0.05617	0.00016	0.71165	0.70985	0.00030
2424	2	Enamel	1	0.90	5	0.05660	0.00008	0.71430	0.71270	0.00200
2424	2	Dentine	1	1.08	7	0.05663	0.00010	0.71128	0.71041	0.00029
2424	2	Enamel	2	0.87	4	0.05669	0.00031	0.71460	0.71300	0.00290
2424	2	Dentine	2	1.07	4	0.05655	0.00008	0.71111	0.71024	0.00052
2425A	2	Enamel	1	0.93	10	0.05597	0.00013	0.71232	0.71093	0.00026
2425A	2	Dentine	1	0.89	18	0.05601	0.00004	0.71085	0.70969	0.00018
2425B	2	Enamel	1	1.12	4	0.05633	0.00008	0.71153	0.71078	0.00052
2425B	2	Dentine	1	0.78	10	0.05622	0.00015	0.71055	0.70897	0.00024
2425B	2	Enamel	2	1.23	27	0.05625	0.00004	0.71167	0.71092	0.00011
2425C	2	Enamel	1	1.34	4	0.05643	0.00007	0.71164	0.71109	0.00053
2425C	2	Dentine	1	1.04	7	0.05644	0.00006	0.71050	0.70975	0.00027
2425C	2	Enamel	2	1.29	4	0.05651	0.00015	0.71164	0.71089	0.00055

Sample	Unit	Material	Track	^{88}Sr Volts	n	$^{84}\text{Sr}/^{86}\text{Sr}$	Corrected $^{87}\text{Sr}/^{86}\text{Sr}$	$^{87}\text{Sr}/^{86}\text{Sr}$	$^{87}\text{Sr}/^{86}\text{Sr} 2\sigma$	Error
2425C	2	Dentine	2	1.11	9	0.05643	0.00005	0.71068	0.70993	0.00035

Table 5.38 Summary Table of Bois Roche Faunal Teeth LA-MC-ICPMS Sr Isotope Results

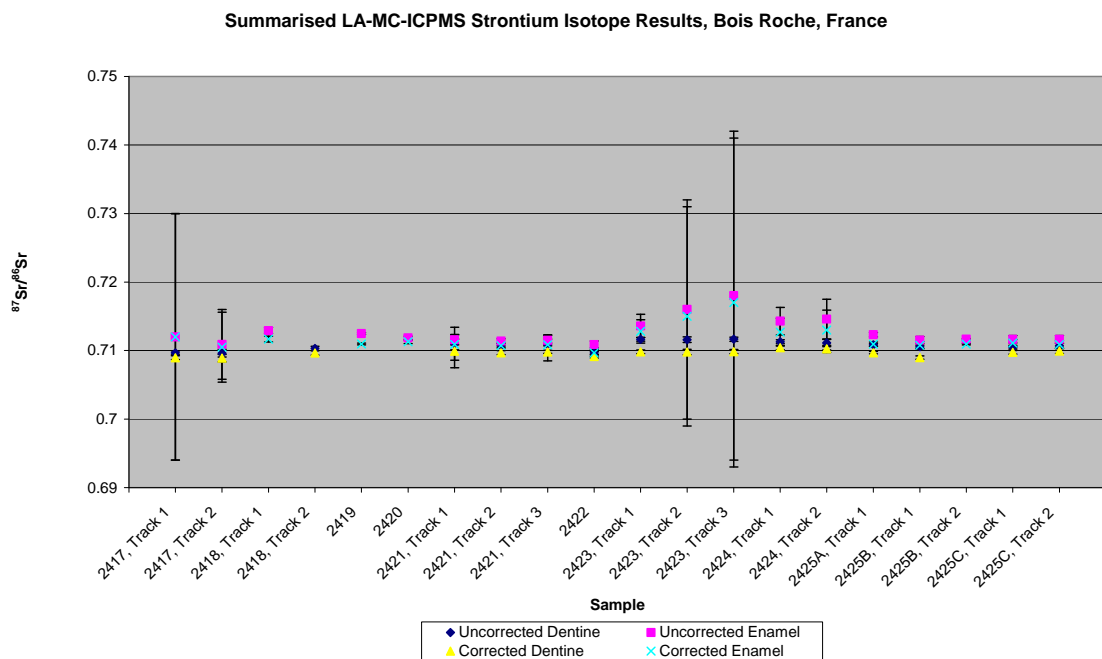


Figure 5.24 Summary Plot of Bois Roche Faunal Teeth LA-MC-ICPMS Sr Isotope Results

5.4.5.5. Mobility Interpretation

The mobility interpretation for the 9 specimens from the site of Bois Roche are summarised in Table 5.39 and shown in detail in A3.2.3.5. Of these samples, 8 are at least somewhat mobile during amelogenesis and all have strontium isotope values that are, at least sometimes, different to the geological unit that hosts this site. All samples (for which this property can be determined) have dentine and enamel $^{87}\text{Sr}/^{86}\text{Sr}$ values that are distinct.

Four of the samples (2417, 2420, 2421 and 2424) have strontium isotope values corresponding to floodplain values mapped within the study area. Seven of the samples (2417, 2418, 2419, 2421, 2422, 2424 and 2425) have enamel values with strontium isotope compositions corresponding to those found in the Aquitaine Basin, which surrounds the site of Bois Roche. Enamel $^{87}\text{Sr}/^{86}\text{Sr}$ values of 3 of the samples (2420, 2423 and 2425) correspond to mapping values found from the Massif Central which suggests mobility over distances of at least 70km.

Sample	Fauna	Layer	MIS	Dentine/Enamel Different?	Enamel Different from Local Geology (Cretaceous Carbonate Sediments)?	Mobile During Amelogenesis?	Principal Residence During Amelogenesis Based on Uncorrected Values?	Principal Residence During Amelogenesis Based on Corrected Values?
2417	Bovid	1C	4	Yes	Sometimes	Yes	Charente River floodplain and Upper Cretaceous carbonate	Upper Cretaceous carbonate within 0 km
2418	Bovid	1C	4	Yes	Yes	Some-what	Cambrian metamorphics within 80 km to the east	Upper Cretaceous carbonate within 0 km
2419	Bovid	1C	4	Unknown	Yes	No	Cambrian metamorphics within 80 km to the east	Upper Cretaceous carbonate within 0 km
2420	Bovid	2	4	Unknown	Yes	Yes	Carboniferous monzogranite/ granodiorite and Cambrian paragneiss/ leptynite/amphibolite	Charente floodplain within 4.6 km and Cambrian paragneiss/ leptynite/ amphibolite within 75 km
2421	Bovid	2	4	Yes	Yes	Yes	Carboniferous monzogranite/ granodiorite/ Cambrian paragneiss/ leptynite/ amphibolite and Charente river floodplain	Charente floodplain within 4.6 km and Upper Cretaceous carbonate within 0 km
2422	Bovid	1C	4	Yes	Sometimes	Yes	Carboniferous monzogranite/ granodiorite/Cambrian paragneiss/leptynite/ amphibolite, Charente river floodplain and Upper Cretaceous carbonate	Upper Cretaceous carbonate within 0 km

Principal Residence During Amelogenesis Based on Corrected Values?						
Principal Residence During Amelogenesis Based on Uncorrected Values?						
Mobile During Amelogenesis?						
2423	Bovid	2	4	Yes	Yes	Dordogne floodplain
2424	Bovid	2	4	Yes	Yes	Carboniferous monzogranite/ granite and unknown
2425	Bovid	2	4	Yes	Yes	Charente river floodplain and Cambrian paragneiss/ leptynite/ amphibolite

Table 5.39 Summary of Mobility Results for Analysed Fauna from Bois Roche

5.4.6. Rescoundudou

5.4.6.1. MC-ICPMS Results

One sediment sample collected adjacent to the archaeological site of Rescoundudou was analysed using MC-ICPMS to determine its $^{87}\text{Sr}/^{86}\text{Sr}$ composition, as summarised in Table 5.40.

Sample Number	Associated with Tooth	Stratigraphic Unit	Age (ky)	$^{87}\text{Sr}/^{86}\text{Sr}$	$^{87}\text{Sr}/^{86}\text{Sr} 2\sigma$ Error
FS090-S2	N/A	Outside of cave	Not dated	0.712240	0.000033

Table 5.40 $^{87}\text{Sr}/^{86}\text{Sr}$ Results from Archaeological Sediments from Rescoundudou

5.4.6.2. Regional Mapping Results

Strontium isotope values from soil samples immediately surrounding the site of Rescoundudou are shown in Figure 5.25.

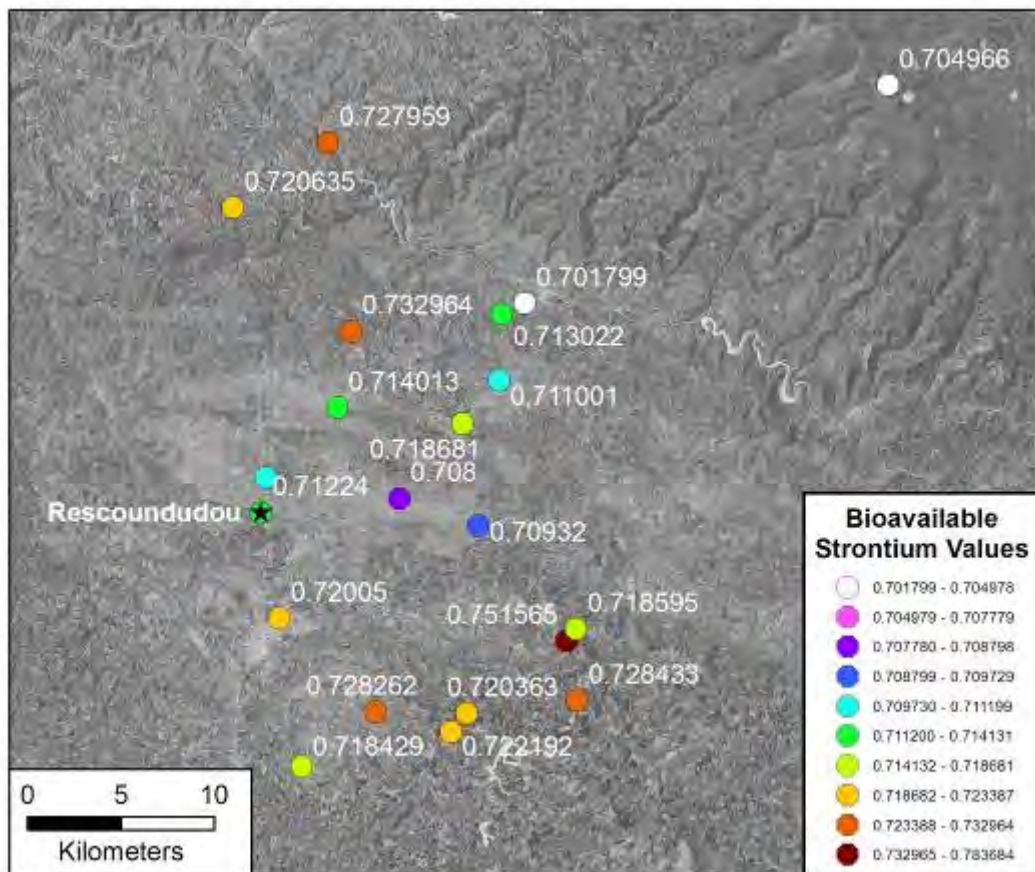


Figure 5.25 Bioavailable Soil Strontium Values Surrounding Rescoundudou

5.4.6.3. LA-MC-ICPMS Results

Samples from 13 individuals were analysed from the archaeological site of Rescoundudou using LA-MC-ICPMS. The results from these samples are summarised in Table 5.41 and Figure 5.26. The detailed results and photographs showing the analysis tracks are pictured in section A3.2.3.6.

Sample	Unit	Material	Track	^{88}Sr Volts	n	$^{84}\text{Sr}/^{86}\text{Sr}$	$^{84}\text{Sr}/^{86}\text{Sr} 2\sigma$ Error	$^{87}\text{Sr}/^{86}\text{Sr}$	Corrected $^{87}\text{Sr}/^{86}\text{Sr}$	$^{87}\text{Sr}/^{86}\text{Sr} 2\sigma$ Error
M33	C1	Enamel	1	0.24	15	0.05708	0.00021	0.71480	0.70360	0.00140
M33	C1	Dentine	1	0.25	27	0.05737	0.00023	0.71500	0.70510	0.00190
M34	C1	Enamel	1	0.23	6	0.05711	0.00035	0.71570	0.70410	0.00130
M34	C1	Dentine	1	0.33	13	0.05675	0.00025	0.71166	0.70572	0.00051
M35	C1	Enamel	1	0.34	9	0.05640	0.00025	0.71324	0.70301	0.00032
M35	C1	Dentine	1	0.53	26	0.05646	0.00009	0.71222	0.70769	0.00029
M36	C1	Enamel	1	0.71	3	0.05652	0.00018	0.71259	0.70994	0.00050
M36	C1	Dentine	1	0.77	16	0.05657	0.00009	0.71190	0.70919	0.00033
M36	C1	Enamel	2	0.69	7	0.05662	0.00012	0.71226	0.70961	0.00062
M36	C1	Dentine	2	0.67	12	0.05662	0.00014	0.71176	0.70906	0.00029
M37	C1	Enamel	1	0.68	2	0.05660	0.00650	0.71190	0.70400	0.00220
M37	C1	Dentine	1	0.67	19	0.05680	0.00031	0.71074	0.70302	0.00044
M37	C1	Enamel	2	0.49	5	0.05530	0.00120	0.71260	0.70473	0.00060
M37	C1	Dentine	2	0.45	31	0.05500	0.00024	0.71090	0.70318	0.00028
M38	C1	Enamel	1	0.29	16	0.05299	0.00041	0.71608	0.71031	0.00021
M38	C1	Enamel	2	0.37	14	0.05304	0.00023	0.71559	0.70982	0.00034
M39	C1	Enamel	1	0.53	7	0.05665	0.00025	0.71364	0.71023	0.00038
M39	C1	Dentine	1	0.48	7	0.05654	0.00027	0.71242	0.70792	0.00062
M40	C1	Enamel	1	0.45	4	0.05661	0.00024	0.71372	0.70769	0.00097
M40	C1	Dentine	1	0.43	4	0.05648	0.00019	0.71320	0.70760	0.00110
M40	C1	Enamel	2	0.39	3	0.05634	0.00028	0.71440	0.70840	0.00400
M40	C1	Dentine	2	0.39	2	0.05680	0.00240	0.71200	0.70600	0.01300
M41	C1	Enamel	1	2.42	5	0.05649	0.00007	0.70788	0.70742	0.00074
M41	C1	Dentine	1	1.54	7	0.05654	0.00004	0.70793	0.70689	0.00073
M41	C1	Enamel	2	2.41	4	0.05651	0.00008	0.70740	0.70694	0.00034
M41	C1	Dentine	2	1.04	5	0.05670	0.00007	0.70816	0.70713	0.00088
M41	C1	Exterior Enamel	3	1.61	13	0.05663	0.00003	0.70768	0.70722	0.00018
M42	C1	Enamel	1	0.73	3	0.05666	0.00015	0.71012	0.70793	0.00068
M42	C1	Dentine	1	0.67	4	0.05693	0.00015	0.70880	0.70620	0.00200
M42	C1	Enamel	2	0.64	6	0.05685	0.00014	0.71090	0.70870	0.00160
M42	C1	Dentine	2	0.60	4	0.05687	0.00031	0.70964	0.70704	0.00095
M42	C1	Exterior Enamel	3	0.60	6	0.05707	0.00021	0.71153	0.70934	0.00051

Sample	Unit	Material	Track	^{88}Sr Volts	n	$^{84}\text{Sr}/^{86}\text{Sr}$	Error	$^{87}\text{Sr}/^{86}\text{Sr} 2\sigma$	$^{87}\text{Sr}/^{86}\text{Sr}$	$^{87}\text{Sr}/^{86}\text{Sr}$
								$^{87}\text{Sr}/^{86}\text{Sr} 2\sigma$	$^{87}\text{Sr}/^{86}\text{Sr}$	$^{87}\text{Sr}/^{86}\text{Sr}$
M43	C1	Enamel	1	0.14	6	0.05837	0.00076	0.72290	0.68700	0.00490
M43	C1	Dentine	1	0.48	9	0.05698	0.00020	0.71084	0.70754	0.00058
M43	C1	Enamel	2	0.11	3	0.05760	0.00140	0.73300	0.69800	0.02600
M43	C1	Dentine	2	0.47	3	0.05690	0.00026	0.71160	0.70830	0.00140
M44	C1	Enamel	1	0.45	12	0.05705	0.00013	0.71920	0.71630	0.00150
M44	C1	Dentine	1	0.42	17	0.05704	0.00016	0.71432	0.71033	0.00082
M45	C1	Enamel	1	0.51	3	0.05707	0.00022	0.71368	0.71131	0.00028
M45	C1	Dentine	1	0.59	6	0.05707	0.00016	0.71060	0.70840	0.00230
M45	C1	Enamel	2	0.57	2	0.05689	0.00023	0.71400	0.71100	0.01000
M45	C1	Dentine	2	0.56	9	0.05698	0.00012	0.71060	0.70840	0.00130

Table 5.41 Summary Table of Rescoundudou Faunal Teeth LA-MC-ICPMS Sr Isotope Results

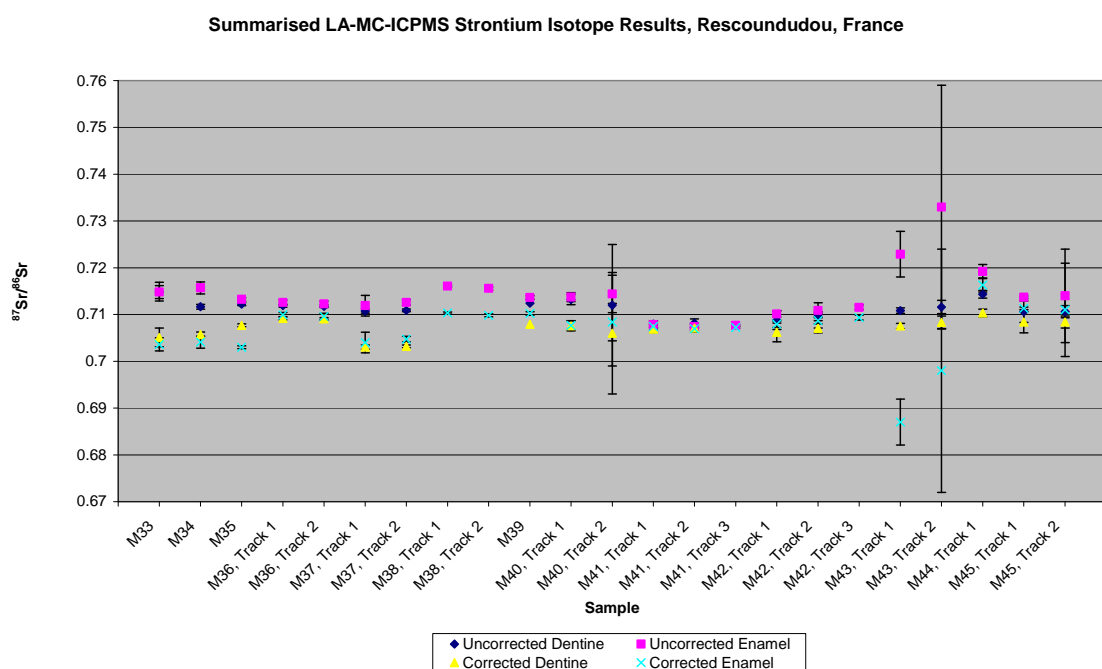


Figure 5.26 Summary Plot of Rescoundudou Faunal Teeth LA-MC-ICPMS Sr Isotope Results

5.4.6.4. Mobility Interpretation

The results from the 9 specimens from the site of Rescoundudou are summarised in Table 5.42 and shown in detail in A3.2.3.6. Only 5 of the 13 specimens are mobile during amelogenesis based on the heterogeneity of their $^{87}\text{Sr}/^{86}\text{Sr}$ enamel values and 7 have strontium isotope values that are the same as the geological unit containing the archaeological site. Nine of 12 samples from which the property can be determined have enamel and dentine values that are distinct. Eight of the samples (M033, M036, M038, M039, M040, M041, M42 and M45) have enamel values that correspond, for at least some analysis spots, with the soil value of the Middle Jurassic carbonate that surrounds the site of Rescoundudou. Three samples (M033, M034 and M037) have $^{87}\text{Sr}/^{86}\text{Sr}$ values that correspond to the mapping results from the Oligocene/Miocene basalt which outcrops within 3 km of the archaeological site.

Principal Residence During Amelogenesis Based on Corrected Values?								
Principal Residence During Amelogenesis Based on Uncorrected Values?								
Mobile During Amelogenesis?								
Enamel Different from Local Geology (Jurassic Carbonate Sediments)?								
Dentine/Enamel Different?	MIS	Layer	Fauna	Sample	Enamel Different from Local Geology (Jurassic Carbonate Sediments)?	Mobile During Amelogenesis?	Principal Residence During Amelogenesis Based on Uncorrected Values?	Principal Residence During Amelogenesis Based on Corrected Values?
M033	Bovid	C1	5	Yes	Sometimes	Yes	Middle Jurassic carbonate and unknown location	Unknown, Oligocene/Miocene basalt within 12.2 km and Middle Jurassic carbonate within 0 km
M034	Bovid	C1	5	Yes	Sometimes	Yes	Middle Jurassic carbonate and metasediment	Unknown and Oligocene/Miocene basalt within 12.2 km
M035	Horse	C1	5	Yes	No	No	Permian siliciclastic	Unknown
M036	Horse	C1	5	No	Yes	Yes	Cambrian paragneiss/leptynite/amphibolite and Devonian amphibolite/micaschist/leptynite	Middle Jurassic carbonate within 0 km
M037	Horse	C1	5	Yes	No	No	Jurassic carbonate sediments	Oligocene/Miocene basalt within 12.2 km
M038	Rhino ceros	C1	5	Unknown	Yes	No	Permian monzogranite/granodiorite	Middle Jurassic carbonate within 0 km
M039	Bovid	C1	5	Yes	No	No	Middle Jurassic carbonate	Middle Jurassic carbonate within 0 km
M040	Bovid	C1	5	No	No	No	Middle Jurassic carbonate	Lower Jurassic carbonate within 75 km and Middle Jurassic carbonate within 0 km
M041	Bovid	C1	5	Yes	Yes	Yes	Unknown and siliciclastic/carbonate sediments	Middle Jurassic carbonate within 0 km and Upper Jurassic carbonate within 36 km
M042	Deer	C1	5	No	No	No	Middle Jurassic carbonate	Middle Jurassic carbonate within 0 km
M043	Deer	C1	5	Yes	Yes	Yes	Many possible geological environments	Unknown
M044	Deer	C1	5	Yes	Yes	No	Permian siliciclastic unit	Carboniferous monzogranite/granodiorite within

								125 km
M045	Deer	C1	5	Yes	No	No	Middle Jurassic carbonate	Middle Jurassic carbonate within 0 km

Table 5.42 Summary of Mobility Results for Analysed Fauna from Rescoundudou

5.5. Standards

5.5.1. Durango Apatite

5.5.1.1. LA-MC-ICPMS Results

Strontium isotope values of Durango apatite collected with LA-MC-ICPMS have a weighted average for 15 points of 0.706134 ± 0.000045 for $^{87}\text{Sr}/^{86}\text{Sr}$ as shown in Table 5.43. The isotope composition of these samples is relatively homogenous, with most samples within error of each other. The $^{84}\text{Sr}/^{86}\text{Sr}$ value is 0.56359 ± 0.000056 .

Sample	Material	Track	^{88}Sr Volts	$^{84}\text{Sr}/^{86}\text{Sr}$	$^{84}\text{Sr}/^{86}\text{Sr} 2\sigma$ Error	Corrected $^{87}\text{Sr}/^{86}\text{Sr}$	$^{87}\text{Sr}/^{86}\text{Sr} 2\sigma$ Error	
Durango	Apatite	1	1.60	0.56359	0.00005	0.70613	0.70592	0.00004

Table 5.43 Durango Apatite LA-MC-ICPMS Sr Isotope Results

5.5.2. Tridacna

There were 631 spots of the Tridacna Australian National University internal standard analysed over the period from 29 November 2010 to 23 June 2011 using LA-MC-ICPMS. The results from these analysis spots are summarised in Table 5.44 and Figure 5.27 and the detailed results are shown in Appendix Four.

Date of Analysis	Pertains to Sample	n	^{88}Sr Volts	$^{84}\text{Sr}/^{86}\text{Sr}$	$^{84}\text{Sr}/^{86}\text{Sr} 2\sigma$ Error	$^{87}\text{Sr}/^{86}\text{Sr}$	$^{87}\text{Sr}/^{86}\text{Sr} 2\sigma$ Error
29/11/10	466, 263	57	21.103	0.056420	0.000015	0.7091715	0.0000055
30/11/10	263, 112, 861, 861E	128	15.304	0.0563698	0.0000045	0.7091650	0.0000031
10/02/11	373E, 1557; 374E, 372E,	40	6.089	0.056463	0.000076	0.709197	0.000015
11/02/11	851, 372D	25	11.271	0.056330	0.000034	0.7091811	0.0000083
12/02/11	371E, 370E	25	9.539	0.056326	0.000023	0.709195	0.000012
7/04/11	852E	11	25.017	0.056246	0.000094	0.70957	0.00029
8/04/11	852D, 853	31	12.409	0.056362	0.000033	0.70961	0.00023
9/04/11	M001, M002, M003, M004, 557E, 558E, 564D, 565, 567	17	8.758	0.056520	0.000029	0.709138	0.000027
10/04/11	557E, 558E, 564D, 565, 567, 554E, 556E, 557E, 561, 563	16	11.532	0.056472	0.000023	0.709145	0.000030
13/05/11	M001, M002, M003, M004, M005, M006, M007, M008, M009, M010, 2421; 2417, 2418; 2422, 2425C, 2425B, 2425A	33	6.946	0.056480	0.000026	0.709149	0.000022
14/05/11	2424, 2423; 2419, 2420,	12	6.658	0.056448	0.000033	0.709031	0.000069
15/05/11	592, 593, 595, M011, M012, M013, M014, M015, M016, M017, M018, M019, M020, M021, M022, 1057; 1058, 568,	63	3.734	0.056513	0.000013	0.709014	0.000036
16/05/11	1057, 1058; 568	15	1.996	0.056511	0.000031	0.708974	0.000060
20/06/11	1024, 1025; 1026, M023, M024, M025, M026, M027, M028, M029, M030	42	12.779	0.056478	0.000018	0.708992	0.000011
21/06/11	M023, M024, M026, M031, M032, M033, M034, M035, M036, M037, M038E	42	8.139	0.056498	0.000024	0.709001	0.000015
22/06/11	M035, M036 M039, M040, M041, M042, M043, M044, M045, 595, 845, 846, 847, 848, 849, 850, Durango, 622, 624, 625	57	6.172	0.056499	0.000020	0.708980	0.000017

Date of Analysis	Pertains to Sample	n	$^{84}\text{Sr}/^{86}\text{Sr}$	$^{84}\text{Sr}/^{86}\text{Sr} 2\sigma$	$^{87}\text{Sr}/^{86}\text{Sr}$	$^{87}\text{Sr}/^{86}\text{Sr} 2\sigma$	Error
23/06/11	Durango, 614, 615, 616, 617, 618, 619, 620, 622, 624, 625,	18	2.977	0.056559	0.000019	0.708935	0.000040
All Dates	All Samples	631	10.716	0.0564097	0.0000076	0.7091560	0.0000060

Table 5.44 Summary Table of Tridacna LA-MC-ICPMS Sr Isotope Results

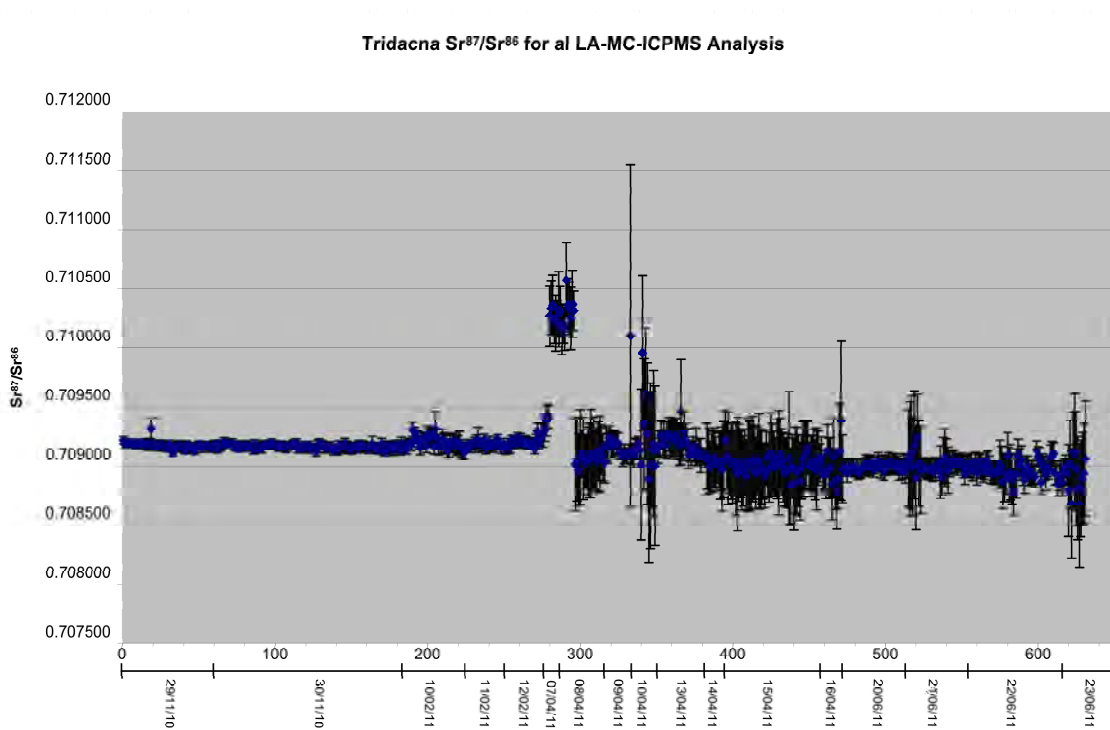


Figure 5.27 Summary Plot of Tridacna LA-MC-ICPMS Sr Isotope Results

5.6. Summary

This chapter summarises the results from all strontium concentration and isotope analyses undertaken on soil, rock, plant mapping samples, archaeological tooth samples and standards. Due to the very large volume of material collected, detailed results for the sample analysis are shown in Appendix Three and, for the Tridacna analysis, in Appendix Four.

The faunal samples from different archaeological sites showed varying patterns of mobility, demonstrated by the heterogeneity of enamel values, the correlation between enamel and dentine values and the degree of correlation of enamel values with the geological unit containing the respective archaeological sites.

The archaeological sites showed high (Bois Roche, La Chapelle-aux-Saints, Le Moustier, Skhul, Amud and Holon), moderate (Rescoundudou, Pech de l'Azé II and Les Fieux) and low (Tabun and Qafzeh) percentages of specimens demonstrating mobility during amelogenesis. The archaeological sites had high (Bois Roche, Pech de l'Azé II, Le Moustier, Les Fieux, La Chapelle-aux-Saints, Skhul, Tabun, Amud, Qafzeh and Holon) and moderate (Rescoundudou) percentages of specimens that showed a difference between enamel strontium isotope values and those of the local geology. Correlation between enamel and dentine was observed to be low (Bois Roche, Pech de l'Azé II, Le Moustier, La Chapelle-aux-Saints, Les Fieux, Skhul and Qafzeh) and moderate (Rescoundudou, Tabun and Amud).

Chapter Six: Discussion

6.1. Overview

This chapter discusses the archaeological and geochemical implications of the results of this research. The patterns of faunal mobility revealed by strontium isotope analysis appear to reflect the influence of a number of variables, including regional physiography, faunal ecology and climate variation.

The results from the LA-MC-ICPMS analysis in this thesis also have significant implications for understanding how best to apply strontium isotope techniques in archaeological research. The large amount of intra-sample heterogeneity in the analysed samples demonstrates that solution analysis of dental material may provide an incomplete representation of mobility.

The results from the mapping programme in Israel and France demonstrate that methodology can have a significant effect on the understanding of regional bioavailable $^{87}\text{Sr}/^{86}\text{Sr}$ ratios. Soil and rock values from the same location vary significantly in strontium isotope values. Further, different geomorphic units such as river floodplains may have very different values from the surrounding area. This suggests that judicious sample site selection is essential to the effective characterisation of regional bioavailable strontium isotope values.

6.2. Mapping Studies

6.2.1. Israel

6.2.1.1. Comparison of Results to Regional Geology

Soil and rock mapping values for Israel (shown in section 5.2.1) show some correlation with geological units, as illustrated in Figure 6.1 and Figure 6.2. Mapping values from basalt units are universally less radiogenic in $^{87}\text{Sr}/^{86}\text{Sr}$ value than all other samples. Overall, soil samples from kurkar, carbonates, granites and areas with no bedrock are statistically indistinguishable. This suggests that inputs other than local bedrock, such as aeolian material or fertiliser (discussed below in section 6.2.1.2), might be important contributors to the strontium isotope composition of Israeli soils.

Percentile Plot of $\text{Sr}^{87}/\text{Sr}^{86}$ Soil Values From Israel Compared to Lithology

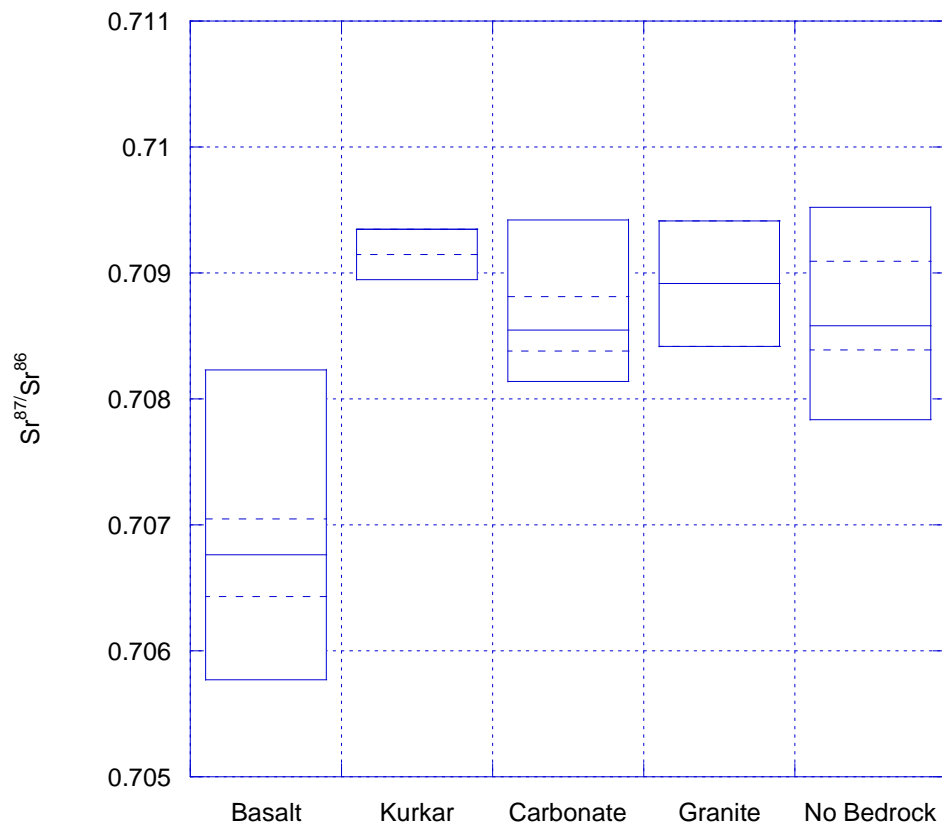


Figure 6.1 Comparison of Israeli Bioavailable Soil Strontium Results to Lithology (Overall Range and Median Value Shown by Solid Lines, 25% and 75% Values Shown by Dotted Lines)

Strontium isotope values from rock samples are far more distinct, with kurkar and carbonate values slightly overlapping, but granite values are significantly elevated (over a large range) compared to all other units.

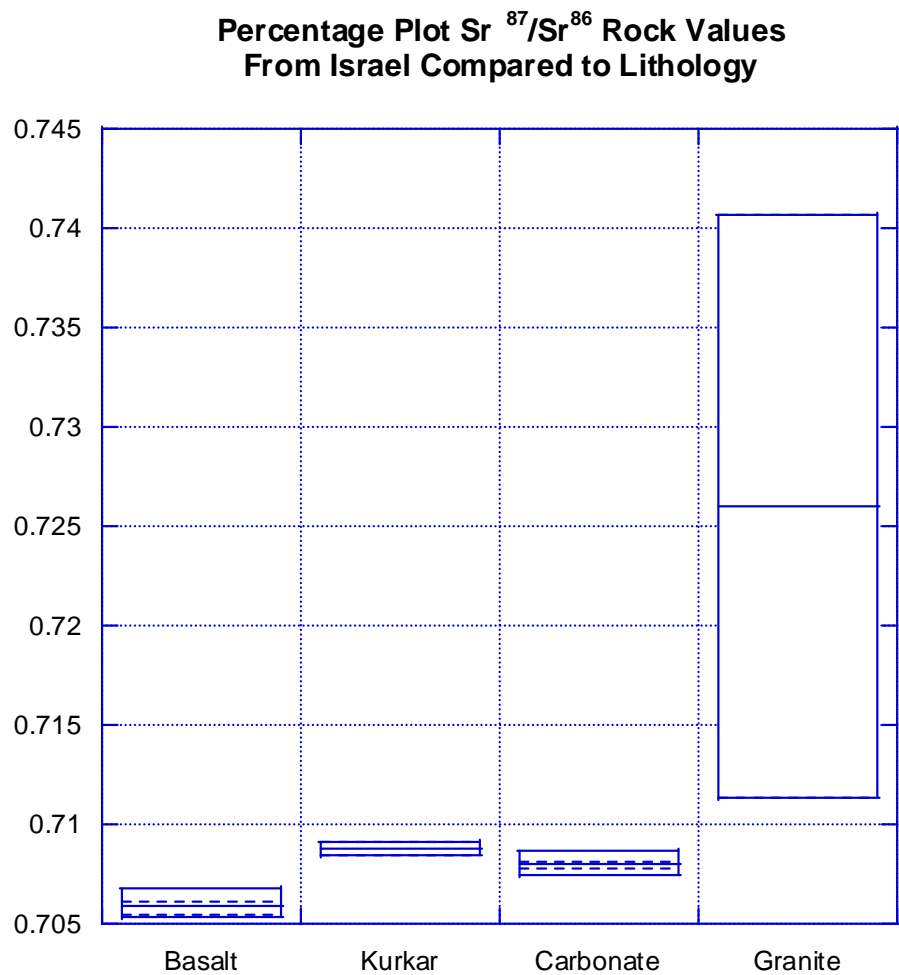


Figure 6.2 Comparison of Israeli Bioavailable Rock Strontium Isotope Results to Lithology (Overall Range and Median Value Shown by Solid Lines, 25% and 75% Values Shown by Dotted Lines)

6.2.1.2. Comparison Between Soil and Rock Results

Forty two survey locations within Israel, which have matched soil and rock samples, are compared in Figure 6.3 and Table 6.1. The variation between soil and rock $^{87}\text{Sr}/^{86}\text{Sr}$ values covers a wide range from 0.031304 to 0.000003. There appears to be no systematic correlation between geology and the variation between the soil/rock values. What is clear is that the variation between soil and rock is, in all cases except 1, greater than error. This variation is probably due to inputs to the soil other than bedrock, such as Saharan aeolian dust ($^{87}\text{Sr}/^{86}\text{Sr}$ values in the range of 0.716-0.7192 (Krom et al. 1999))

or seaspray. Aeolian dust might be particularly significant as aeolian material may make up to 50% of soils formed on hard limestone rocks in Israel (Yaalon 1997).

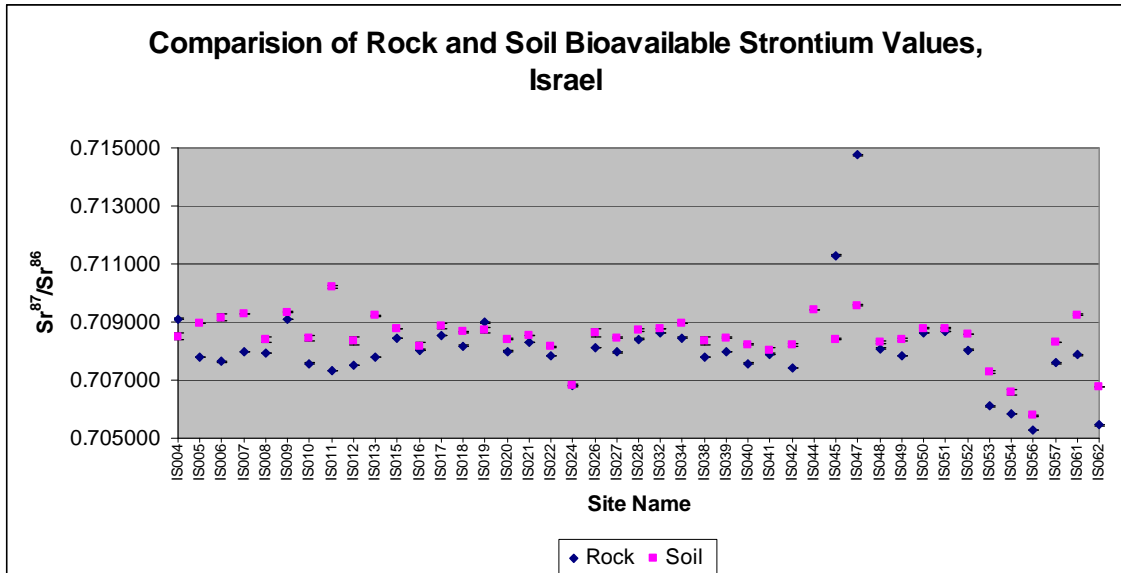


Figure 6.3 Comparison of Bioavailable $^{87}\text{Sr}/^{86}\text{Sr}$ Results from Rock and Soil Samples from Sample Locations in Israel, Excepting Sample IS044

The strontium isotope value of dust in the region is known to have varied over the Pleistocene between a value of 0.711 to 0.712 during MIS 2 and 4 and 0.709 to 0.710 during MIS 1,3 and 5 (Haliva-Cohen et al. 2012). Dust delivery would also have been strongly affected by climate variations in the Pleistocene era (summarised in section 3.4.2.1), in which glacial periods were broadly cool and wet and interglacials were warm and dry (Frumkin et al. 2011). Strontium isotope values have been found to increase at major climate transitions that correspond to sapropel formation in the Mediterranean (Stein et al. 2007). Speleothem analyses show that glacial periods have a higher aeolian strontium isotope contribution than interglacial periods (Frumkin and Stein 2004). This variation makes it unlikely that the mapping samples collected in this thesis accurately reflect the regional strontium isotope values during all of the Palaeolithic era.

The implication of the difference between soil and rock values is that these values cannot be interchangeably used as mapping values without due consideration of this effect.

Site	Rock $^{87}\text{Sr}/^{86}\text{Sr}$	$\pm 2\sigma$ Error	Soil $^{87}\text{Sr}/^{86}\text{Sr}$	$\pm 2\sigma$ Error	Geology from Field	Age of Unit
IS004	0.709112	0.000010	0.708505	0.000114	Sandstone with Carbonate Matrix	Cenomanian
IS005	0.707801	0.000008	0.708958	0.000008	Reefal Limestone	Turonian
IS006	0.707630	0.000009	0.709149	0.000112	Reefal Limestone	Turonian
IS007	0.707975	0.000011	0.709282	0.000017	Limestone	Turonian
IS008	0.707924	0.000007	0.708393	0.000087	Chalk	Lower to Middle Eocene
IS009	0.709103	0.000007	0.709344	0.000012	Calcareous Sandstone 'Kurkar'	Quaternary
IS010	0.707577	0.000007	0.708440	0.000077	Limestone	Turonian
IS011	0.707328	0.000008	0.710199	0.000034	Very Fine Grained Limestone	Senonian-Palaeocene
IS012	0.707514	0.000008	0.708365	0.000133	Limestone	Cenomanian
IS013	0.707795	0.000015	0.709212	0.000011	Chalky Limestone	Cenomanian
IS015	0.708449	0.000013	0.708776	0.000010	Limestone Breccia	Quaternary
IS016	0.708029	0.000010	0.708181	0.000133	Chalky Limestone	Senonian-Palaeocene
IS017	0.708532	0.000008	0.708852	0.000084	Chalky White Limestone	Lower Cretaceous
IS018	0.708182	0.000009	0.708662	0.000011	Chalky Limestone	Cenomanian
IS019	0.708989	0.000031	0.708727	0.000094	Limestone	Turonian
IS020	0.708000	0.000007	0.708418	0.000012	Chalky Limestone	Lower to Middle Eocene
IS021	0.708315	0.000010	0.708544	0.000010	Limestone	Cenomanian
IS022	0.707838	0.000009	0.708140	0.000012	Chalky Limestone	Cenomanian
IS024	0.706807	0.000007	0.706810	0.000033	Basalt	Pliocene-Pleistocene
IS026	0.708106	0.000008	0.708622	0.000136	Limestone	Lower to Middle Eocene
IS027	0.707963	0.000016	0.708464	0.000012	Limestone Breccia	Senonian-Palaeocene
IS028	0.708417	0.000008	0.708733	0.000045	Limestone	Albian-Cenomanian
IS032	0.708617	0.000009	0.708774	0.000013	Chalk	Coniacian-Campanian

Site	Rock $^{87}\text{Sr}/^{86}\text{Sr}$	$\pm 2\sigma$ Error	Soil $^{87}\text{Sr}/^{86}\text{Sr}$	$\pm 2\sigma$ Error	Geology from Field	Age of Unit
IS034	0.708460	0.000006	0.708944	0.000012	Poorly Consolidated Beach Ridge	Quaternary
IS038	0.707777	0.000008	0.708366	0.000140	Limestone	Coniacian
IS039	0.707963	0.000008	0.708464	0.000011	Limestone	Lower to Middle Eocene
IS040	0.707575	0.000008	0.708230	0.000009	Basalt?	Lower Jurassic
IS041	0.707879	0.000006	0.708025	0.000078	Chalky Limestone	Lower to Middle Eocene
IS042	0.707423	0.000009	0.708223	0.000041	Limestone	Turonian
IS044	0.740718	0.000014	0.709414	0.000018	Granite/ Granodiorite	Precambrian
IS045	0.711296	0.000007	0.708418	0.000010	Granite	Precambrian
IS047	0.714749	0.000013	0.709579	0.000015	Basalt?	Quaternary
IS048	0.708083	0.000014	0.708297	0.000060	Chalky Marl	Campanian
IS049	0.707840	0.000007	0.708393	0.000031	Chalky Limestone	Lower to Middle Eocene
IS050	0.708615	0.000008	0.708784	0.000012	Semi-consolidated Aeolian Sand	Miocene
IS051	0.708662	0.000007	0.708778	0.000014	Basalt/Volcanic Glass	Cenomanian
IS052	0.708045	0.000007	0.708575	0.000013	Evaporite/ Limestone	Turonian
IS053	0.706096	0.000010	0.707286	0.000033	Basalt	Pliocene- Pleistocene
IS054	0.705853	0.000006	0.706600	0.000092	Basalt	Pliocene- Pleistocene
IS056	0.705291	0.000006	0.705772	0.000011	Basalt	Quaternary
IS057	0.707584	0.000008	0.708304	0.000009	Limestone	Middle Jurassic
IS061	0.707868	0.000008	0.709245	0.000013	Limestone	Lower to Middle Eocene
IS062	0.705448	0.000008	0.706763	0.000012	Basalt	Quaternary

Table 6.1 Comparison of Rock and Soil Bioavailable $^{87}\text{Sr}/^{86}\text{Sr}$ Results from Matched Sample Locations in Israel

6.2.1.3. Comparison to Other Studies

A number of other studies of bioavailable strontium have been undertaken in Israel, including those of Herut et al. (1993), Perry et al. (2008; 2009), Rosenthal et al. (1989), Shewan (2004) and Spiro et al. (2011).

The results obtained from the analysis of soils deriving from basalts in the Golan Heights from this study are in the range of 0.705772 to 0.706810 for samples (175, 203, 204, 205 and 216) with robust geological provenance. Rock samples (119, 143, 144, 147 and 278) included in this study from this region have the range of 0.705291 to 0.706807. These results differ from those obtained by Shewan (2004:9), which have values in the range of 0.70529 to 0.70571 (n=4). Spiro et al. (2011:412) measured strontium isotope values of a much larger data set of water samples in the Hula valley (adjacent to the Golan Heights) in the range of 0.70467 to 0.70790 (n=37). Strontium isotope sampling of basalt derived groundwater in this region, summarised by Rosenthal et al. (1989:2433), was in the range of 0.7045 to 0.705. Rainwater in the region was analysed to have a strontium isotope composition in the range of 0.70804 to 0.70899 (Herut et al. 1993). The disparity between the results of this study and those of Shewan (2004) are probably a reflection of the limited number of sample sites in her study, as the much larger data set of Spiro et al. (2011) encompass the range in this research. The wide range of strontium isotope results in the Golan Heights can be explained by the rapid depletion of strontium from rocks and soil in this region due to weathering and the large contribution of aeolian dust to soil profiles in this region (Singer 2007:202–206).

Coastal plain grasses were analysed by Shewan (2004:17) in the region of El Wad cave, south of Haifa. These values were in the range of 0.70886 to 0.70965, with an outlying value of 0.71003 attributed to influence from the road base (Shewan 2004:17). Soil samples collected from kurkar (consolidated calcareous sandstone) ridges in this study have values in the range of 0.709344 to 0.709521.

One area of Pleistocene Israel which was not mapped in this study is the coastal plain, which is currently mainly covered by ocean following sea level rise. As discussed in section 3.2.2.1, the sea level has only risen above its current level once during the last 250 ka years (Zviely et al. 2009) and the shelf has been regionally exposed (Avnaim-Katav et al. 2012). Fortunately, a sample has been collected offshore of Atlit by Krom et al. (1999:324), which has a $^{87}\text{Sr}/^{86}\text{Sr}$ value of 0.70951.

6.2.2. France

6.2.2.1. Comparison of Results to Regional Geology

The strontium isotope values from mapping samples in France (summarised in section 5.2.2) compare poorly with lithology, shown in Figure 6.4. These mapping samples were variously analysed from plant, soil or rock samples due to a changing methodology and personnel between field seasons. Unfortunately, no matched samples from the same location in France were analysed and so it is impossible to evaluate the extent of any non-bedrock contribution to soil and plant values. Values from all lithologies other than basic igneous are statistically indistinguishable overall, although samples with a felsic igneous lithology may have significantly more radiogenic value than other samples.

Percentile Plot of $\text{Sr}^{87}/\text{Sr}^{86}$
Mapping Values From France Compared to Lithology

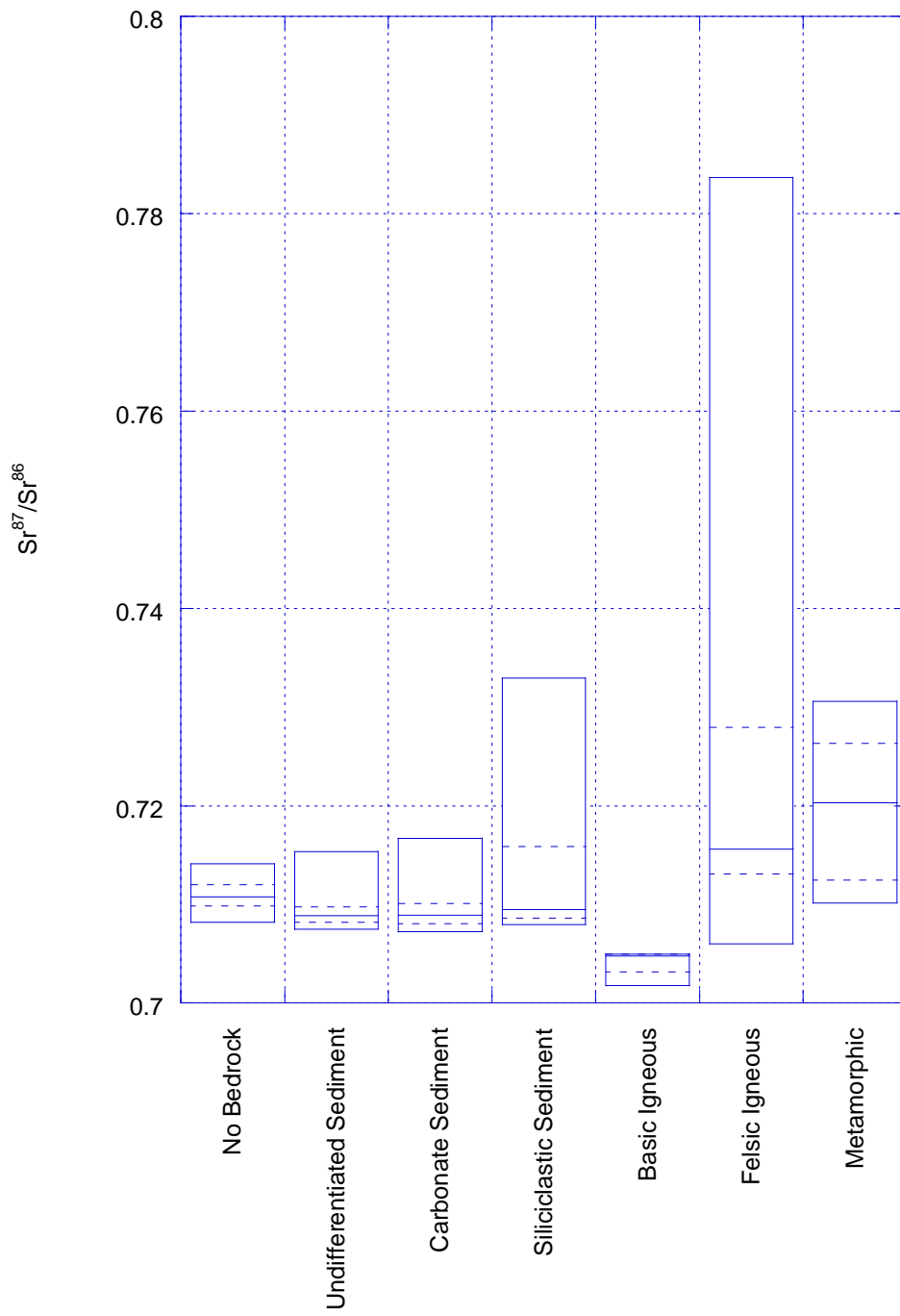


**Figure 6.4 Comparison of French Bioavailable Strontium Isotope Results to Lithology
(Overall Range and Median Value Shown by Solid Lines, 25% and 75% Values Shown by Dotted Lines)**

6.2.2.2. Comparison to Other Studies

Overall the strontium isotope mapping results show some correlation to other studies; however, in all cases, the samples in this study cover a wider range (with the exception of the more radiogenic granite/gneiss samples from the Massif Central) than those in published studies.

Basic igneous samples from the Massif Central in this study cover the range of 0.701799 to 0.704978. This correlates somewhat to results from water sampling in the Allanche watershed (0.70278 to 0.70352), which drains feldspatic basalts and basanites (Négrel and Deschamps 1996).

Samples collected in this study from carbonate sediments in the Aquitaine Basin have a range of 0.707727 to 0.717308 for locations with robust geological provenance. This upper end of this range is considerably more radiogenic than other studies in the region, such as those by Kelly (2007) and Britton et al. (2011), which had a total range of 0.7078 to 0.7104. The elevated values most likely represent the contribution of fertilisers to the soil, which could be verified by comparison to rock samples from the same location.

Previous studies of strontium isotopes from rock and water samples in the Massif Central have an overall range of 0.712954 to 1.981 from granitic and gneissic lithologies (Couturié and Vachette-Caen 1980; Downes and Duthou 1988; Negrel et al. 2000). This compares to a range from this study of 0.705976 to 0.817507, the lower end-member of which is considerably less radiogenic than is found in other studies.

6.3. Geochemical Implications

6.3.1. Analysis of Standards

6.3.1.1. Durango Apatite

The weighted average LA-MC-ICPMS value of 0.706134 ± 0.000045 for $^{87}\text{Sr}/^{86}\text{Sr}$ for Durango Apatite compares favourably, but not exactly, with the value of 0.706327 obtained by Trotter and Eggins (2006) using TIMS and the value of $0.7068 \pm 0.03\%$ obtained by Horstwood et al. (2008). This result demonstrates that relatively accurate $^{87}\text{Sr}/^{86}\text{Sr}$ can be obtained from high strontium concentration apatites, even in the presence of relatively high concentrations of rare earth elements, as are found in this material (Horstwood et al. 2008).

6.3.1.2. Tridacna

The overall weighted average value ($n=631$) for Tridacna spots in this study of 0.7091560 ± 0.0000060 compares favourably with the accepted seawater strontium isotope value of 0.70918 (Horstwood et al. 2008). This results suggests that, overall, the LA-MC-ICPMS results are robust for calcite samples. In contrast to the weighted average value, Tridacna samples collected on 7 and 8 April 2011 are significantly elevated compared to the ideal value, suggesting the strontium isotope values obtained from samples 852 and 853 may not be robust.

6.3.2. Laser Versus Solution Analysis

The methodology used for correcting offset between laser and strontium isotope strontium isotopes values in this research (discussed in section 4.7.2.7) suffers from a number of drawbacks. First, archaeological teeth used to define the

relationship between enamel and dentine can be, shown by the results of this thesis, significantly heterogeneous and so the measured solution values may not represent the true $^{87}\text{Sr}/^{86}\text{Sr}$ composition. Second, the relationship defined between the voltage of the Sr 88 mass and sample strontium concentration used to undertake this correction is probably not absolutely correct. A more robust approach for correcting for Ca+P+O offset would require an alternative sample collection methodology. A series of matrix matched bio-apatites with different strontium concentrations, each of which have a homogenous well defined strontium isotope composition and homogenous strontium concentration within the sample, would need to be analysed during each LA-MC-ICPMS session. This would define the relationship between strontium concentration and offset under the specific plasma conditions of each analysis. Having defined the relationship, each strontium isotope analysis spot should have a matching strontium isotope concentration spot collected to allow the appropriate correction to be applied. The development and application of this methodology is a significant recommendation of this research.

6.3.3. Intra-Tooth Variability

The examination of intra-tooth variability is the principal benefit of applying LA-MC-ICPMS analysis to archaeological material. As discussed by Copeland et al. (2010), only very few published studies have applied LA-MC-ICPMS to determining $^{87}\text{Sr}/^{86}\text{Sr}$ composition, and only slightly more have used micro-drilling to provide spatial resolution for TIMS or MC-ICPMS analysis (e.g., Viner et al. 2010). This research shows that many samples have intra-tooth strontium isotope variability, suggesting that this method should be applied more widely.

While intra-sample enamel or dentine $^{87}\text{Sr}/^{86}\text{Sr}$ heterogeneity has great potential to reveal sample mobility during the formation of these tissues, this may be overprinted by post-burial diagenesis (as discussed in section 2.3.4.8). Dentine is not resistant to this overprinting (Budd et al. 2000) and so its

strontium isotope composition will often reflect this. Enamel is far more resistant to post-burial diagenesis (Trickett et al. 2003) and has been shown to resist overprinting over geological timescales (Bocherens et al. 1994). One approach to determining the degree of overprinting is by measuring the concentration of uranium, which is not present in the teeth when alive but frequently accumulate post-mortem (Eggins et al. 2005). Many of the samples in this thesis were evaluated for post-burial diagenesis using LA-ICPMS measurement of uranium concentration.

LA-MC-ICPMS is particularly promising for some species of herbivore, such as bovid, based on their pattern of enamel mineralisation and relatively high strontium concentration. While cattle share the multistage process of enamel deposition and maturation seen in humans (Brown et al. 1960), the vector of calcification has been demonstrated to progress from the incisal tip to the cervical margin (Sakae and Hirai 1982), suggesting that migration during amelogenesis may be recorded. Similarly, equid enamel have both an enamel matrix and maturation front, which proceed in a ‘down tooth’ direction (Hoppe et al. 2004). Samples 851, 852 and 853 from this study were analysed along the long axis of the tooth and show variations in strontium isotope values, which demonstrate mobility between different geological environments, as discussed in Moffat et al. (2012).

While sampling in a ‘down tooth’ direction is the only way to develop a complete life history for the period of amelogenesis, sampling in other vectors can also provide useful information about mobility. Many samples in this study that were not sampled in a ‘down tooth’ direction show intra-sample strontium isotope variation. These results are sufficient to show some aspect of mobility during amelogenesis; however, they cannot provide a comprehensive record of movement during this period.

Another impediment to the utility of high resolution, spatially resolved strontium isotope analysis is the possibility of “smoothing” of the enamel strontium isotope record by long residence time in the body (Montgomery et al. 2010). This effect may average $^{87}\text{Sr}/^{86}\text{Sr}$ values over a period in the order of months or years (Montgomery et al. 2010). Unfortunately the timing and extent of process remains poorly understood, particularly for fauna, due to a paucity of experimental studies. Despite this uncertainty, it is likely that the $^{87}\text{Sr}/^{86}\text{Sr}$ preserved in enamel represents a time averaged record of strontium isotope values between end-members rather than a complete record of mobility. Nevertheless, this method retains some utility in recording movement between varying geological environments even if some intermediate values contain influence from multiple areas.

While this approach is useful for fauna, the pursuit of evidence for migration in humans at the intra-tooth level based on the *in situ* analysis of rhythmic features such as cross-striae is probably doomed to failure. The basis of the unsuitable of human enamel, as previously discussed by Montgomery (2002), is that the bulk of the mineral content of enamel is formed in the subsequent 3 stages of maturation after this framework is laid down (Robinson et al. 1981). Each of these 4 stages (the total duration of which appears not to have been robustly determined) will involve the formation of enamel crystallites in equilibrium with the body pool of strontium. While these crystallites could potentially be analysed individually, given an average size of 160 nm in length and 20 nm in width for human enamel (Ronnholm 1962), they are 3 orders of magnitude below the resolution of this study (approximately 180 μm pits) or any other analytical technique. Another impediment to the effective application of LA-MC-ICPMS analysis to human material is the generally low concentration of strontium in human teeth, which is generally in the order of $105 \pm 138 \text{ ppm}$ (Evans et al. 2012). It might be expected that Neanderthals have even lower strontium isotope concentrations, due to their interpreted principally carnivorous diet (e.g., Richards and Trinkaus 2009), and so are even less amenable to strontium isotope analysis than modern humans.

6.3.4. Establishing a ‘Local’ Signature

The effective characterisation of the ‘local’ strontium isotope value for an archaeological site is demonstrated by this research to be complex. This is well illustrated by the results surrounding the archaeological site of La Chapelle-aux-Saints, in which layer 1 yields a strontium isotope ratio (FS045-S2) of 0.710098 ± 0.000049 . A soil sample collected from *in situ* material approximately 4 m above the site (FS045-S3) yielded a result of 0.708879 ± 0.00012 , and soil (FS046-S1) taken from 20 cm below the surface of the floodplain of stream, approximately 150 m north-east of the archaeological site, yielded a strontium isotope result of 0.714131 ± 0.000015 . The signal from the river’s floodplain represents a mixing of material from the river’s catchment, rather than the local signal. This suggestion is supported by a sample from this river’s assumed catchment area (FS055-S1), which yields a result of 0.718038 ± 0.000044 . Another possible contribution to the strontium isotope composition of FS046-S1 may be fertiliser use.

An effective sampling programme should then, in theory, concentrate on soil, which is clearly spatially related to the local bedrock. However, this approach has the disadvantage of avoiding flood plain areas that would have been attractive locations for humans and animals as a source of food and water. The results from the LA-MC-ICPMS analysis in France show that many species favoured these areas as habitat during amelogenesis, which could not have been resolved had floodplain sampling not been undertaken. These considerations are less important in Israel, where floodplain sediments are not extensive.

A disadvantage of the methodological approach to strontium isotope mapping used in this research is the focus on soil and rock samples to the exclusion of plant and fauna, meaning that these values may not represent the bio-available

strontium value for these units. The decision to focus on soil and rock samples for analysis (despite plant samples being collected from all locations) was principally the result of the geological background of the researchers undertaking this study. While soil and rock samples do not directly reflect bioavailable strontium isotope values, they were leached using ammonium nitrate following the procedure of Stewart et al. (1998), as discussed in section 2.3.4.5, which replicates the action of plants extracting bioavailable strontium. These results should therefore be robust however future research could compare these to plant and fauna values to provide more nuanced results.

Additionally, the sample preparation procedure used for the preparation of those plants which are included in this study is suboptimal, as while it does focuses exclusively on grasses, a range of species are considered. The analysed samples were also not washed or ashed prior to analysis (following the standard procedure at the University of Cologne where they were prepared) which may result in erroneous strontium values.

6.3.5. External Versus Internal LA-MC-ICPMS

The advantage of the essentially non-destructive nature of LA-MC-ICPMS analysis for rare archaeological samples (Richards et al. 2009) is unfortunately mitigated to some extent by the practise of cutting the samples prior to laser ablation. This is undertaken to obtain a flat surface to facilitate accurate laser focusing (Balter et al. 2012) and to allow access to a cross-section of unaltered enamel and dentine for analysis. Despite the advantages of this approach, many rare archaeological samples are not able to be cut and so, if the results of laser ablation analysis of the exterior of a tooth is demonstrated to be robust, strontium isotope approaches could be applied more widely.

To investigate this possibility, the enamel of 2 archaeological samples (M041 and M042 from Rescoundudou) were analysed both on a cut surface from the

interior and from the exterior of each tooth. Sample M041, a bovid incisor from Rescoundudou, has internal enamel values of 0.70788 ± 0.00074 and 0.70740 ± 0.00034 and exterior enamel values of 0.70768 ± 0.00018 . These values are all within 2σ error. Sample M042, a horse incisor from Rescoundudou, has interior enamel values of 0.71012 ± 0.00068 and 0.7109 ± 0.0016 and an exterior enamel value of 0.71153 ± 0.00051 . The exterior enamel value is within 2σ error of the second enamel track but not the first.

These results show that the analysis of exterior enamel samples may accurately reflect the interior composition in some cases. The fact that some of the exterior $^{87}\text{Sr}/^{86}\text{Sr}$ values do not reflect the interior $^{87}\text{Sr}/^{86}\text{Sr}$ values may not suggest a failure of this approach. This result may instead reflect, as demonstrated by many of the analyses undertaken in this thesis, the significant intra-sample heterogeneity that enamel may contain.

These results suggest that the analysis of exterior enamel may be a suitable method for the relatively non-destructive analysis of archaeological enamel. The disadvantage of this approach is that it may be difficult to capture the degree of $^{87}\text{Sr}/^{86}\text{Sr}$ heterogeneity within the sample, leading to a potentially incomplete understanding of mobility during amelogenesis. Nevertheless, with rare archaeological samples this approach may provide some insights into the provenance of enamel formation.

6.4. Species-Specific Mobility

The fauna analysed in this thesis show mobility patterns that vary between different species, shown in Table 6.2. Persian fallow deer, bison and the mountain goat/chamois and fox in this study were often mobile across a range of geological environments during amelogenesis. In contrast, wild boar and the

rhinoceros (albeit with a very small sample size) remained on the same geological unit during amelogenesis. Some samples of Reindeer, unidentified bovid, horse, unidentified deer and *Bos* show evidence of evidence of mobility over different geological environments during enamel formation. Other than the rhinoceros (which is represented by only 1 sample), moderate (unidentified deer and horses) or high (all other species) percentages of species have enamel which is sometimes or always different from the local geology. Median minimum possible mobility varies from 0 to 18 km. Rhinoceros, *Bos*, unidentified deer and Persian fallow deer have median minimum possible mobility values of less than 2 km while fox, wild boar and bison have values of 15 km or more. A detailed discussion of each fauna is undertaken in sections 7.3.1 to 7.3.7.

Fauna	Enamel $^{87}\text{Sr}/^{86}\text{Sr}$ Values (Sometimes or Always) Different from Local Geology (%)	n	Sample Mobile (Sometimes or Always) During Amelogenesis (%)	n	Median Minimum Possible Mobility (km)	N
Wild Boar	100	2	0	2	16.55	2
Persian Fallow Deer	33	3	100	3	1.4	2
Reindeer	100	4	80	5	4.6	4
Unidentified Deer	67	6	33	6	1.4	5
Unidentified Bovid	95	39	74	39	5	37
Bison	100	2	100	2	15	2
Bos	90	10	22	9	1	6
Mountain Goat/Chamois	100	1	100	1	5.3	1
Horse	56	9	67	9	2.8	9
Rhinoceros	0	1	0	1	0	2
Hippopotamus	100	2	100	2	4.8	2
Hyena	100	1	Unknown	N/A	5.3	2
Fox	100	1	100	1	18	1

Table 6.2 Summary of Faunal Mobility Patterns Based on Strontium Isotope Results

6.4.1. Wild Boar

Wild boar samples in this study include 1058 (3 subsamples) from Skhul and M013 from Les Fieux. Both of these samples have strontium isotope values that differ from their host geological units. Sample 1058, which has a strontium isotope values which correlates with the Cover/Dalwe basalt has a minimum mobility of 1.1 km. Sample M013, whose strontium isotope values correlates with a monzogranite/granodiorite, outcropping in the Massif Central region, was mobile over at least 32 km. Pig mobility of distances of this magnitude is common (as discussed in section 3.8.1.1) and has been observed to occur within a 24 hour period (Baskin and Danell 2003). Neither specimen was mobile during amelogenesis, which in some teeth of *Sus scrofica* may occur up to 13 months after birth (Hillson 2005).

Only a small number of other strontium isotope studies have been undertaken on pig teeth, as discussed in section 2.4.1.7. Shaw et al. (2009; 2010) analysed the strontium isotope composition of pig teeth from the Bismarck Archipelago. These results showed that only a small number of pigs were mobile. A study of Neolithic pig enamel was undertaken by Bentley and Knipper (2005a); however, rather than investigate the mobility of pigs, the enamel was used as a proxy for the local value of human enamel. Unfortunately, all of these studies have been undertaken on samples from domesticated pigs and so the mobility results are not directly comparable to this study.

6.4.2. Deer

*6.4.2.1. Persian Fallow Deer (*Dama Mesopotamica*)*

Three Persian fallow deer were analysed in this study, all from layer B1 at Amud. All 3 specimens were mobile across different geological environments during amelogenesis and two may have lived in the geological unit which

contains Amud. These samples have minimum possible mobility values that place these specimens in the range of 0.8-2.7 km from Amud for some period of their amelogenesis. The mesic humid oak woodland environment interpreted to surround Amud during MIS 3 (Belmaker and Hovers 2011) would have suited the preference of Persian fallow deer for forest thickets (McTaggart-Cowan and Holloway 1973).

No previous published strontium isotope studies on Persian fallow deer were found to compare to the results of this study. The most comparable study is that of Sykes et al. (2006), who undertook strontium isotope analysis on teeth from 2 *Dama dama* specimens in Britain, showing that 1 of these 2 samples were migrants to the study area.

6.4.2.2. Reindeer (*Rangifer Tarandus*)

Five reindeer samples were analysed in this study including samples M001 to M003 from La Chapelle-aux-Saints and samples M018 and M019 from Les Fieux. All reindeer samples, with the exception of the ambiguous M018 (discussed in more detail below), were mobile during amelogenesis. These samples show evidence of amelogenesis occurring in a wide variety of environments, including metamorphic and carbonate bedrock, as well as alluvial sediments. All samples from La Chapelle-aux-Saints resided on geological units which outcrop within 8.3 km of the site and those from Les Fieux within 5.3 km of the site. While this value provides no upper limit on mobility, it differs significantly to those from modern (Bergman et al. 2000) and archaeological (Bahn 1977) ecological studies of reindeer, as these studies report bi-annual episodes of migration, which may occur over several 1000 km.

The enamel from sample M018 has very high error values, making it impossible to define the location of amelogenesis. While these $^{87}\text{Sr}/^{86}\text{Sr}$ values are

statistically indistinguishable, the high error may disguise the fact that this sample was mobile during amelogenesis.

Strontium isotope analysis has previously been undertaken on modern (Britton et al. 2009) and Palaeolithic (Britton et al. 2011, Hodgkins 2012) reindeer. Nearly all of the samples from Britton's studies show a seasonal migration pattern that is not observed in this study. This difference may be due to the use of different sampling methodology, as Britton et al. (2009; 2011) sequentially sampled in a 'down tooth' direction while this study sampled perpendicular to this direction. In contrast, the results of Hodgkins (2012: 190) follow this study in not showing a systematic strontium isotope variation suggesting biannual migration.

Further, the range over which strontium isotope varied in these samples (0.70994 to 0.716770) is much larger than Hodgkins (2012) or Britton et al.'s (2009; 2011) studies. This may partially reflects the high variability of geological environments surrounding La Chapelle-aux-Saints and Les Fieux, which means a wide range of isotope values are available for correlation within a small area although the geology surrounding Pech de l'Azé IV considered in Hodgkins research is similarly diverse.

6.4.2.3. Unidentified Deer

Samples 618 and 624 from Pech de l'Azé II and M042 to M045 from Rescoundudou are deer not identified but likely representing red deer (*Cervus elaphus*). Only 2 of the deer samples, 624 and M043, were mobile across different geological environments during amelogenesis.

These samples have a wide range of minimum mobility values, ranging from 0 km for samples M045 and M042 to 125 km for M044 and 70 km for 618 which,

as discussed in section 3.10.1.2, is within the expected home range of this species (Baskin and Danell 2003). The diversity of mobility distance in these samples may reflect the significant range of environments the red deer inhabit (Boyle 1998). A number of these samples occupied the Massif Central region, including (in the case of sample 618) during the cold Marine Isotope Stage 6. While red deer can tolerate steppic environments (Guérin et al. 2012), they generally migrate down in elevation to avoid heavy snow (Baskin and Danell 2003). During the mild conditions of MIS 5c/5a, corresponding with samples M042 to M045, this region was dominated by forest (Reille and de Beaulieu 1990; Reille et al. 1998) and, therefore, their distribution on the Massif Central might be expected. In contrast, during the glacial MIS 6, corresponding with samples 618 and 624, this region would have been steppic (Reille and de Beaulieu 1990; Reille et al. 1998), although not glaciated (Ehlers and Gibbard 2008).

Strontium isotope studies of red deer are comparatively rare. The enamel of red deer from archaeological sites in central Italy has been analysed for strontium isotope ratios, providing evidence of residence in a limited range of geological environments (Pellegrini et al. 2008). Strontium isotope analysis of *Cervus* teeth by Hodgkins (2012: 185-186) suggest that most individuals remained close to the archaeological sites in which they were found, although a number did live in areas of elevated strontium isotope values

6.4.3. Bovid

6.4.3.1. Unidentified Bovid

Bovid samples in this study from Israel include 851, 852, 853 and 1057 from Skhul and 370, 371 and 372 from Qafzeh. French bovid samples include 592, 593, 595, M005, M006, M007, M008, M009 and M010 from La Chapelle-aux-Saints, samples 845 to 850 from Le Moustier, 614 and 620 from Pech de l'Azé

II, 2417 to 2425 from Bois Roche and M033, M034, M039, M040 and M041 from Rescoundudou.

Of the 7 unidentified bovid samples from Israel, all have enamel spots, which are different from the value of the geological unit which hosts the archaeological site. Additionally, all samples with dentine have $^{87}\text{Sr}/^{86}\text{Sr}$ values that are different from enamel. Four of the 7 samples were mobile across different geological environments during amelogenesis. The lowest minimum distance of mobility was 0.1 km and the greatest was 7.6 km and the median values is 3.2 km.

Of the 32 unidentified bovid samples from France, only 1 has dentine, which is statistically indistinguishable from enamel. Seven have enamel that does not show mobility during amelogenesis and only 2 have enamel that is exclusively the same as the geological unit that hosts their archaeological site. The minimum distance of French bovids is 0 km and the greatest is 85 km and the median value is 9.25 km. These results show that the bovid in this study from France are overwhelmingly mobile, regardless of age or archaeological site.

A comparison between the French and Israeli results shows that samples from both locations are nearly all non-local, based both on the difference in their enamel $^{87}\text{Sr}/^{86}\text{Sr}$ values compared both to dentine and to their host geological unit. The greatest difference between the results from these countries is reflected in the degree of movement between geological environments during amelogenesis and the distance of mobility of minimum mobility. Most obvious is that a number of French samples are mobility over 10 or more kilometres, while no samples from Israel show mobility over this range. This probably reflects the geology of the study area rather than the mobility characteristics of the specimens, as the strontium isotope composition of the bedrock in Israel is far more homogeneous than in France, making it more difficult to observe variation in enamel composition.

6.4.3.2. *Bison*

Bison specimens in this study are samples M016 and M017 from Les Fieux. Both of these specimens were mobile during amelogenesis and lived in an area other than the archaeological site. During amelogenesis these bison spent significant periods of time in floodplain areas and both have a minimum possible mobility of at least 15 km. While these results do represent the maximum mobility of these samples, they differ significantly from modern observations of bison as a highly migratory species (e.g., Arthur 1975; Berger 2004; Boyle 1990).

Strontium isotope analyses of bison enamel has previously been undertaken by Julien et al. (2012) Hodgkins (2012) and Widga et al. (2010). The results of Julien et al. (2012) showed bison that were not mobile during amelogenesis, while the samples from Widga et al. (2010) show limited annual mobility (<50 km) but longer term geographic ‘drift’. Hodgkins’ bison principally lived within sedimentary basins close to their respective archaeological sites, although one specimen may visited the Massif Central. The distance of mobility revealed in these studies is similar to that found in samples M016 and M017.

6.4.3.3. *Bos*

Samples 554, 556, 557, 558, 561, 563, 564, 565 and 567 from Tabun and 1557 from Holon are all *Bos* specimens. Of these 10 samples, 8 have enamel, which is entirely different and 1 has enamel which is somewhat different from the geological unit which hosts their respective archaeological sites. Two of these samples were mobile across different geological environments during amelogenesis. Two of the samples have dentine and enamel values that are statistically distinct and another 2 have values which are indistinct, while 6 are

not able to be determined. These samples were mobile over a minimum possible range of 1-350 km, which a median of 1 km.

If these *Bos* samples are aurochs, the relatively low level of mobility during amelogenesis reflects their generally sessile nature (Kurtén 1968). In contrast to this results, strontium isotope evidence suggests that prehistoric domestic cattle in German (Bentley and Knipper 2005b) and England (Viner et al. 2010) were highly mobile. In the case of samples from Tabun, enamel heterogeneity is probably facilitated by the location of the site immediately adjacent to the boundary of its geological unit.

6.4.3.4. Mountain Goat/Chamois

Two mountain goat/chamois samples, M021 and M022 from Les Fieux, were analysed in this study. No enamel spots were analysed for sample M022; however, the enamel from M021 shows that this sample was mobile across a range of geological environments, including floodplain sediments, Cambrian metamorphics and a Jurassic carbonate package. These areas of residence do not correlate well with the usual ecological niche of this species in moderately high altitudes (Boyle 1990). The minimum possible mobility of 5.3 km from sample M022 is consistent with the expected short distance of migration undertaken by this species (Hamr 1985).

6.4.3.5. Hippopotamus

Two hippopotamus teeth were analysed in this study, samples 615 and 622 from Pech de l'Azé II. Both samples were mobile across geological environments during amelogenesis, have distinct dentine and enamel values and moved over minimum possible distances of 8.2 and 1.4 km. Sample 615 moved between the Massif Central and the area local to the site. Sample

622 was mobile between different floodplains surrounding the site. Residence on floodplain areas is expected, based on the need of hippopotamus to constantly access permanent water and riparian vegetation (Eltringham 1993). It is more difficult to explain the values from sample 615, as little permanent water would have been available on the Massif Central and in the Dordogne region away from the river valleys during the cold and dry conditions in France during MIS 6.

6.4.4. Horse

Horse samples analysed in this study include samples M011 and M012 from layer G7 at Les Fieux, samples M035, M036, M037 and M042 from layer C1 of Rescoundudou and samples 617, 619 and 625 from layers 6, 7 and 8 at Pech de l'Azé II. Horses, discussed in detail in section 3.10.2.1, are a common feature of the archaeological record in Pleistocene France. This species is amenable for tracking mobility, because equid teeth continue to mineralise for 6 to 12 months after eruption and total amelogenesis for a tooth can span 1.5 to 2.8 years (Hoppe et al. 2004).

Isotopic results from this study suggest that horses were somewhat mobile during the Pleistocene era in France, because 5 of the 9 samples have enamel $^{87}\text{Sr}/^{86}\text{Sr}$ values that are distinct from the local geology. Only 3 of the 9 samples have heterogeneous enamel. Horses inhabit a range of geological environments, including the floodplain, carbonate, metamorphic and igneous areas in this study. Sample 617 has been mobile over at least 70 km, moving between the Dordogne region and the Massif Central. Other horse samples are mobile over much smaller distances in the range of 0-15 km. Modern studies, particularly using a Pzewalski horse as a Pleistocene analog (e.g., Boyle 1990), suggest that mobility can be high (Baskin and Danell 2003). Despite this, Pleistocene mobility in France is interpreted to have occurred principally over short distances (Burke 1995). Strontium isotope investigations of horse enamel

by other authors showed low (Pellegrini et al. 2008), variable (Hodgkins 2012) and high (Bendrey et al. 2009) levels of mobility.

Samples M011, M012, M035, M036, M037, M042, 618 and 625 have relatively heterogeneous dentine. The predominance of this heterogeneity in horse enamel from 2 different sites (albeit of similar ages and geological environments) suggests that it may be a characteristic of this material. Indeed, the presence of a heterogeneous primary dentine strontium composition for horses is somewhat expected, given the mobility of horse species; however, the preservation of this signature in the face of potential post-burial diagenesis in archaeological sites is unexpected. A possible reason for the preservation of a heterogeneous strontium isotope composition is the larger (compared to human teeth) peritubular matrix in horse crown dentine (Kodaka et al. 1991; Takuma and Eda 1966), which, as a hyper-mineralised tissue (Bertassoni et al. 2012), may be more resistant to post-burial diagenesis. Different areas of horse teeth contain varying amounts of peritubular dentine, with none being present near the dentine-enamel junction or in the secondary dentine (e.g., Magne et al. 2001:548). This would make different areas of an individual tooth more or less resistant to post-burial diagenesis, which may contribute to a heterogeneous strontium isotope composition. This variable composition will be accentuated in individuals that originally have a heterogeneous dentine composition. The possibility of peritubular dentine preferentially resisting post-burial diagenesis has been previously suggested by Weiner (2010), but has not been tested by previous isotopic investigations.

6.4.5. Rhinoceros

One rhinoceros tooth (568) from level Ed was analysed from the site of Tabun. This sample was not mobile between geological environments during amelogenesis and was resident on the coastal plain or within the Bina Formation, within 1 km of the site of Tabun. One rhinoceros tooth (M038)

analysed from layer C1 from the site of Rescoundudou. This sample was mobile during amelogenesis and was resident on a Middle Jurassic carbonate which contains the site of Rescoundudou. The small degree of mobility shown by these samples is consistent with the small home ranges shown by the black (Hillman-Smith and Groves 1994) and white rhinoceros (Groves 1972). This echoes Richards et al.'s (2008:1254) study of the strontium isotope composition of rhinoceros enamel from the archaeological site of Lakonis, which suggested a limited degree of mobility.

6.4.6. Hyeana

One hyena tooth (M015) from level G7 from the site of Les Fieux was analysed in this study. Only 1 enamel spot was analysed from this sample, making it impossible to define movement during amelogenesis. The single enamel value suggests that this sample was resident within 5.3 km on a floodplain. Modern hyena have a wide range of species-dependant home ranges of 1 to 480 km² (Koehler and Richardson 1990; Kruuk 1972; Mills 1982).

6.4.7. Fox

One fox tooth (M014) from level G7 from the site of Les Fieux was analysed in this study. This sample was mobile across a range of geological environments and physiographic environments within a minimum range of 18 km around the site. This mobility must have occurred over a period of less than 6 months, given the duration of amelogenesis of this species. Fox enamel analysed for strontium isotope values from Les Pradelles showed that this specimen was not local to the archaeological site (Kelly 2007).

6.5. Archaeological Implications

6.5.1. Comparison of Archaeological Sites

The degree of mobility in each archaeological site is compared by a number of proxies shown in Table 6.3, Figure 6.5, 6.6 and 6.7. These include the percentage of fauna that have enamel with a $^{87}\text{Sr}/^{86}\text{Sr}$ value different from the local geology, the percentage of fauna that have a $^{87}\text{Sr}/^{86}\text{Sr}$ value that is heterogeneous indicating mobility during amelogenesis and the minimum possible mobility of each sample. In addition, data from bovids is presented separately to allow the comparison of the results from different sites without introducing bias from the varying mobility behaviour of different fauna. Bovids were chosen for this comparison because of the large number in this study (52) and because they are represented in the analysed fauna from all sites except Amud.

Site	Fauna	Enamel Different from Local Geology (%)	n	Mobile During Amelogenesis (%)	n	Median Minimum Possible Mobility	N
Skhul	All	100	9	44	9	2.75	8
Skhul	Bovid	100	6	67	6	3.2	6
Tabun	All	100	9	11	9	1	6
Tabun	Bovid	100	8	13	8	1	5
Amud	All	33	3	100	3	1.4	3
Amud	Bovid	N/A	0	N/A	0	N/A	0
Qafzeh	All	100	5	20	5	0.8	5
Qafzeh	Bovid	100	5	33	3	0.8	5
Holon	All	100	1	100	1	33	1
Holon	Bovid	100	1	100	1	33	1
La Chapelle-aux-Saints	All	100	12	83	12	3.9	13
La Chapelle-aux-Saints	Bovid	100	9	88	8	6.2	9
Les Fieux	All	100	10	70	10	10.15	10
Les Fieux	Bovid	100	2	100	2	15	2
Le Moustier	All	100	6	100	6	12.1	6
Le Moustier	Bovid	100	6	100	6	12.1	6
Pech de l'Azé II	All	89	9	56	9	1.4	9
Pech de l'Azé II	Bovid	100	2	50	2	23.2	2
Bois Roche	All	100	9	89	9	4.6	9
Bois Roche	Bovid	100	9	89	9	4.6	9
Rescoundudou	All	54	13	38	13	12.2	13
Rescoundudou	Bovid	60	5	60	5	12.2	5

Table 6.3 Mobility Results for all Fauna and for Bovids from all Archaeological Sites in the Study.

A comparison of the percentage of local fauna which have enamel $^{87}\text{Sr}/^{86}\text{Sr}$ values that differ from the local geological is shown in Figure 6.5. This shows that correlation between enamel and host geology is rare, indeed 100% of the samples from most sites, regardless of species, have disparate values.

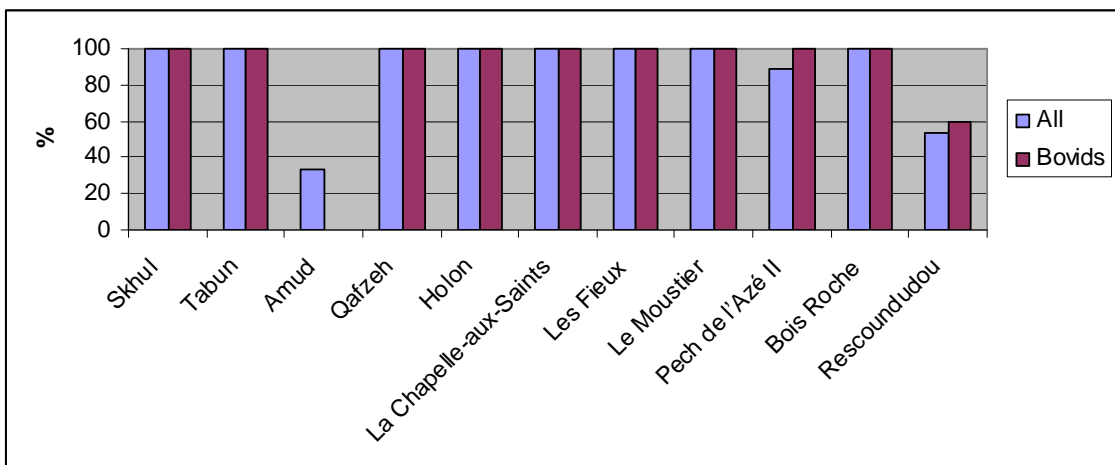


Figure 6.5 Percentages of Archaeological Fauna That Have Enamel $^{87}\text{Sr}/^{86}\text{Sr}$ With A Different Value to the Local Geology.

The comparison of the percentage of archaeological fauna that have heterogeneous enamel values is shown in Figure 6.6. Enamel heterogeneity is interpreted to reflect the mobility of a sample across a variety of different geological environments during amelogenesis. Interestingly, the French sites have a significantly higher percentage of samples displaying heterogeneous enamel (overall 69% ($n=59$) compared to those from Israel (overall 35% ($n=28$)). This correlates with the relatively larger minimum mobility distances observed in French sites as discussed below and shown in Figure 6.7. The significant greater heterogeneity observed in samples from Skhul compared to Tabun is important, given that these sites share the same geological settings. This variation may reflect mobility driven by the alternations in climate during the periodically arid MIS 5 in Israel, given the relative abundance of samples in Skhul from this period.

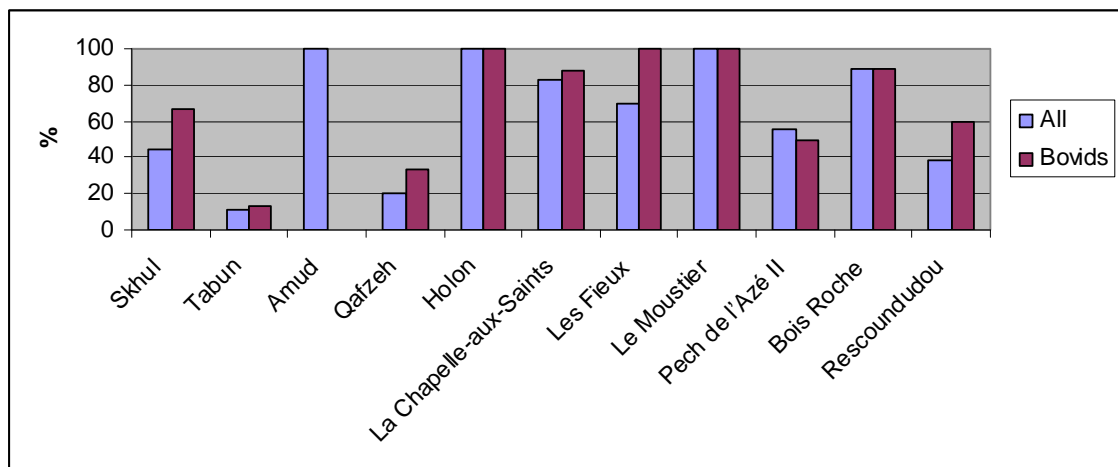


Figure 6.6 Percentage of Archaeological Fauna That Have Heterogeneous Enamel $^{87}\text{Sr}/^{86}\text{Sr}$ Values, Suggesting Mobility across Different Geological Units during Amelogenesis

A comparison of median minimum possible mobility for the archaeological site in this study, shown in detail in Table 6.3 and summarised in Figure 6.7, shows a number of significant variations between sites. All Israeli sites, with the exception of Holon which is discounted due to only having one sample, show median minimum possible mobilities of less than 3.2 km, which as discussed above, correlates to the higher relative percentages of samples mobile across geological environments during amelogenesis. The low minimum distances of mobility in Israeli sites are clear both for all species and for bovids, suggesting it is not an artefact of species assemblage variability. The Israeli sites also cover from MIS 9 through MIS 3, although are more sparsely represented in MIS4 and 3, suggesting that this is not a reflection of behavioural response to varying climate conditions.

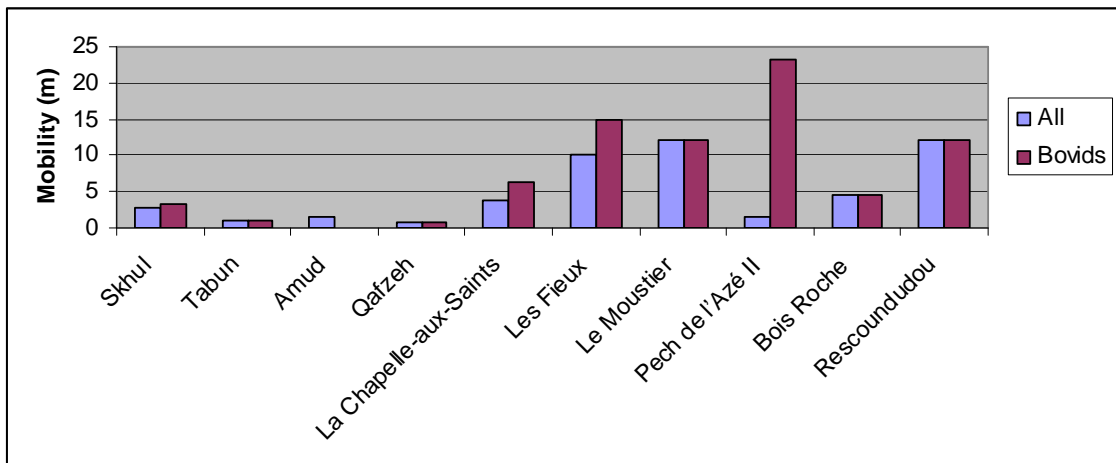


Figure 6.7 Median Minimum Possible Mobility (in kilometres) For Archaeological Fauna in this Study.

The increased median minimum possible mobility distance and increased apparent mobility of French rather than Israeli samples can be interpreted as being due to both geological and b processes. From a geological perspective, the lower distances of migration in the Israeli samples may be an artefact of the spatial relationship between the location of the archaeological sites and the boundaries of the principal geological units. Skhul, Tabun and Qafzeh are located on the boundary between areas of bedrock and unconsolidated Quaternary sediments and all sites (with the exception of Holon) are located proximal to basalt units. This variability close to the site provides the opportunity for a range of strontium isotope domains to be identified within a short distance. In contrast none of the French sites are located on significant geological boundaries, although Le Moustier and La Chapelle-aux-Saints are immediately adjacent to floodplain sediments. While this interpretation may partially account for the median minimum distance of mobility results, it is contradicted by the relatively greater enamel heterogeneity of the French samples. If the results were simply an artefact of the presence of the Israeli sites close to a geological boundary, these samples could be expected to have more heterogeneous enamel composition due to repeatedly crossing this feature.

Another interpretation is that the fauna from French sites was more mobile due to the location of most of these sites adjacent to major rivers including the Dordogne, Vézère and Charente. The principal axis of faunal mobility in this

area in the Palaeolithic is interpreted as east-west, taking advantage of the compression of ecological zones in his orientation, particularly in glacial periods (Mellars 1996). The river valleys follow this orientation and with abundant water, arboreal vegetation and a “generalized” (non-cold specific) fauna even during the most inhospitable MIS 6 (Paquereau 1979), could have served as conduits of faunal mobility between different locations. Furthermore, the entrainment of these valleys between the carbonate plateaus of the Perigord provided, without recourse to long distance mobility, a rich and complex interdigitation of habitats (Mellars 1996: 52) perhaps encouraging their use as a conduit for shorter movement. This interpretation is supported by the results from Rescoududou, the only French site which is not next to a major water course, which has the lowest level of intra enamel heterogeneity for all species and the second lowest for bovids of all French sites. Skhul, Tabun and Amud are located immediately adjacent to small watercourses that would have been more active during some of the Palaeolithic; however these rivers are short and so cannot serve the same function of facilitating longer distance mobility as those in France.

6.5.2. Effect of Climate

The interpretation of mobility derived from all species and archaeological sites in this research for which direct or stratigraphic dating is available is compared to the regional climate regime, shown in Table 6.4. During the period of MIS 9 to 3, climate changed significantly on many occasions in both Israel and France, with significant implications for flora and fauna in these regions. Overall, glacial periods are generally wetter than interglacial periods in the central Levant, as the high atmospheric pressure over Europe pushes the high-latitude climate southwards, leading to a temperate climate as far south as the northern Negev (Frumkin et al. 2011:445). In contrast, glacials are generally cold and dry in south-west France, with a predominance of steppic vegetation. These changes in precipitation, as well as accompanying changes in wind direction and strength, would lead to variations in the isotopic composition and amount of strontium delivered through sea spray and precipitation.

Overall, the results show a significantly higher degree of mobility during MIS 9/8/7, MIS 4 and MIS 3 than in MIS 6 and MIS 5. The correlation between mobility in interglacial MIS 5 and interglacial MIS 6 is particularly interesting given the significant difference in the climate regime between these periods. Similarly, the correlation between MIS 4 and MIS 3 is also notable; however, the climate in MIS 3 did not ameliorate to the degree that it did in MIS 5 (shown in Figure 3.3), which may explain this similarity. The results from MIS 9/8/7 are difficult to compare to other periods because of the large error on these dates, as discussed below.

MIS	Location	Enamel Different from Local Geology (%)	n	Mobile During Amelogenesis (%)	n	Median Minimum Possible Mobility	n
7	All	100	1	100	1	33	1
	Israel	100	1	100	1	33	1
	France	N/A	0	N/A	0	N/A	0
6	All	91	11	45	11	1.4	11
	Israel	100	2	0	2	1	2
	France	89	9	56	9	1.4	9
5	All	74	23	43	23	1.1	21
	Israel	100	6	33	6	2.3	6
	France	54	13	38	13	12.2	11
4	All	100	9	89	9	4.6	9
	Israel	N/A	0	N/A	0	N/A	0
	France	100	9	89	9	4.6	9
3	All	84	31	97	32	5.3	22
	Israel	33	3	100	3	1.4	3
	France	100	19	89	18	5.3	19

Table 6.4 Faunal Mobility of all Samples Compared to Marine Isotope Stages Based on Strontium Isotope Results

6.5.2.1. MIS 9, 8 and 7

The dating of samples from Tabun levels Ea to Ed have large errors, which means that they can only be dated broadly to the period of MIS 9 to 7 (Grün et al. 1991). As a result, it is impossible to make detailed comparisons between the mobility of these samples and the climate. Holon sample 1557 is interpreted as being from MIS 7 and shows evidence of mobility during amelogenesis and has a high minimum possible mobility value of 33 km. Unfortunately, in the absence of other robustly dated samples from this MIS, it is impossible to draw meaningful conclusions about mobility or residency during this period.

6.5.2.2. MIS 6

Samples in this study from MIS 6 are from Pech de l’Azé II layers 8 and 9, Tabun layer D and perhaps from Tabun layers Ea to Ed. Overall, 91% (n=11) of samples have enamel that is different from the geology of their respective archaeological site. Of the samples, 45% have enamel that shows that the sample is mobile during amelogenesis.

The MIS 6 samples collected from France show very distinctive levels of mobility compared to those from Israel. The samples from Pech de l’Azé II show a moderate level of mobility (56%) during amelogenesis and a large number of the samples (89%) are from a geological environment other than the site. The samples from layer D at Tabun show no evidence of mobility (0/2) during amelogenesis and the enamel universally has a $^{87}\text{Sr}/^{86}\text{Sr}$ value different from the geological unit containing the site. The median minimum possible mobility values from France and Israel are virtually indistinguishable, with values of 1 and 1.4 km respectively.

As summarised in sections 3.3.2.1 and 3.3.2.2, the climate in Israel during this period would have been cold but comparatively humid. In contrast, the climate in France would have been both very cold and very dry, with an abundance of steppic vegetation. Despite this, Laville et al. (1980:158–160) considers that the pollen and ‘generalized’ fauna (animals characteristic of mild/temperate conditions, lacking classic ‘cold’ animals) of levels 8 and 9 at Pech de l’Azé II represent a somewhat temperate period. The mild nature of conditions during a glacial probably may reflect, as suggested by Paquereau (1979), that the river valleys of the Perigord would have sustained a mosaic of different vegetation types in the area. As a result, the presence of refugia conditions in the Perigord may have facilitated a level of mobility that is similar to that found in the benign conditions of MIS 5. The comparatively low degree of mobility of samples from level D at Tabun, albeit from a small number of samples, may suggest that the comparatively humid conditions in Israel may have facilitated a lower level of mobility.

6.5.2.3. MIS 5

Samples analysed in this study from MIS 5 include all samples from Rescoundudou, Qafzeh and Skhul. Overall, samples from Rescoundudou are moderately mobile and local, samples from Qafzeh are neither mobile nor local and samples from Skhul are very mobile and non-local.

The analysis of samples from Rescoundudou reveals that 54% (n=13) of samples have enamel that is, at least sometimes, different from the local geology and 38% samples were mobile during amelogenesis. At Rescoundudou, the samples are thought to come from a mild stage MIS 5, probably 5c or 5a (Jaubert, pers. comm. 2011). These periods in the Massif Central were characterised by forest vegetation (Reille and de Beaulieu 1990; Reille et al. 1998). These samples have a relatively high level of median minimum possible value of 12.2 km.

Samples from Qafzeh are overwhelmingly (80%) not mobile during amelogenesis and all lived on a geological unit (100%) different from that which contains the site. In contrast, samples from Skhul show significant evidence for mobility during amelogenesis (80%) and for living in geological environment other than that containing the site (100%). The median minimum possible mobility of these samples is 2.3 km, much lower than observed in the French samples from MIS 5. The difference in mobility patterns between these assemblages may reflect the variable climatic regime in Israel during MIS 5. While the modern annual precipitation regime between these sites is essentially identical (Goldreich 1994:46), several climate proxies suggest significant heterogeneity between these regions in MIS 5. This period was characterised by a more humid regime in Mediterranean regions (near Skhul) and more arid conditions in the Dead Sea area (near Qafzeh), as summarised below and in section 3.4.2.1. Evidence from the Mediterranean suggests that this period was moderately humid and warm in Israel, particularly during sub-stages 5e, 5c and 5a when sapropels were deposited (Cheddadi and Rossignol-Strick 1995; Langgut et al. 2011). In contrast, evidence from the drainage area of the Dead Sea Basin suggests a period of aridity, punctuated by sporadic floods (Waldmann et al. 2009), which is supported by isotope results from Qafzeh (Hallin et al. 2012).

6.5.2.4. MIS 4

Samples in this study from MIS 4 include all samples analysed from Bois Roche. Eight of these 9 samples (89%) are mobile during amelogenesis and all have lived on geological units other than Bois Roche for at least some of their amelogenesis. The median minimum possible mobility of these samples was 4.6 km. The climate during MIS 4 (as discussed in section 3.3.2.2) in Europe was relatively cold and the vegetation was predominantly steppic (de Beaulieu and Reille 1984; Sánchez Goñi et al. 2008; Woillard 1978; Woillard and Mook 1982), interspersed by occasional incursions of temperate and/or boreal forest

(Fletcher et al. 2010). The climate at Bois Roche was ameliorated somewhat by being close to the Atlantic coast (Fauquette et al. 1999).

6.5.2.5. MIS 3

Samples in this study from MIS 3 include all specimens from Les Fieux, Le Moustier, La Chapelle-aux-Saints and Amud. All samples from MIS 3 have $^{87}\text{Sr}/^{86}\text{Sr}$ values that are different from the geological unit that contains the site. Of these samples, 84% (n=31) are mobile during amelogenesis and 97% (n=32) are from geological environments different from their archaeological site.

All French samples from MIS 3 are from a geological environment different from that which contains their archaeological site. These samples (n=26) are relatively mobile during amelogenesis (82%) and have a median minimum possible mobility of 5.3 km. As summarised in section 3.3.2.2, during this period in Europe the vegetation in the study area would have been dominated by grassland (e.g., Discamps et al. 2011) and/or steppe (Reille and de Beaulieu 1990; Reille et al. 1998). Climate would have been changing rapidly and repeatedly, with 15 abrupt warming and increasing precipitation events identified (van Meerbeeck et al. 2011).

The samples from Israel from MIS 3 show a high degree of correlation between enamel and the site geology, a high degree of mobility during amelogenesis and a median minimum possible distance of mobility of 1.4 km. During MIS 3, Israel is interpreted to have been predominately cold, with many large climate transitions. Vegetation was dominated by semi-desert and desert flora (Langgut et al. 2011). Other evidence suggests that the region surrounding Amud Cave was wetter than today based on isotopic values of fauna (Hallin et al. 2012), paleoclimate reconstructions (Frumkin et al. 2011), phytoliths (Madella et al. 2002) and micro-mammals (Belmaker and Hovers 2011), although the composition of the mammalian fauna (Rabinovich and Hovers 2004) suggests a

diversity of environments such as woodlands, open woodlands and bushy regions (Hallin et al. 2012:67–68). Hallin et al. (2012) suggest that this environment meant that prey were available all year round for Neanderthal hunting, a result supported by the results of the strontium isotope analysis in this thesis.

6.6. Summary

The strontium isotope results from this research showed patterns of mobility that were compared to species, climate, vegetation and country. These results suggest that faunal mobility changed along with climate during the Lower and Middle Palaeolithic. Despite this finding it appears that the greatest control on the degree of mobility was the regional physiography, with the river valleys of France providing ideal conduits for mobility regardless of climatic conditions.

The results from the LA-MC-ICPMS analysis in this thesis also have significant implications for understanding how best to apply strontium isotope techniques in archaeological research. The large amount of intra-sample heterogeneity in the analysed samples demonstrates that solution analysis of enamel may provide an incomplete representation of mobility. The results also suggest that the sampling of external enamel may provide some robust, if complete, strontium information which may be useful if cutting the tooth for analysis is impossible.

The results from the mapping programme in Israel and France demonstrate that methodology can have a significant effect on the understanding of regional bioavailable $^{87}\text{Sr}/^{86}\text{Sr}$ ratios. Soil and rock values from the same location vary significantly in strontium isotope values. Further, different geomorphic units such as river floodplains may have very different values from the surrounding area. This suggests that judicious sample site selection is essential to the effective characterisation of regional bioavailable strontium isotope values.

Chapter Seven: Conclusions and Recommendations

7.1. Conclusions

This thesis presents the results of a comprehensive programme of strontium isotope micro-analysis of archaeological fauna from a number of Lower and Middle Palaeolithic archaeological sites in France and Israel. These results were compared to $^{87}\text{Sr}/^{86}\text{Sr}$ results from soil, rock and plant samples in order to define the mobility of these specimens during amelogenesis.

The principal original contribution of this research is that it is the first single study to apply strontium isotope analysis to archaeological samples on such a broad geographic and temporal scale. This approach allows mobility to be compared to parameters such as climate, vegetation, species or regional physiography. Furthermore, this study reveals important new insights into the methodology of strontium isotope analysis, particularly in terms of the application of LA-MC-ICPMS.

The most important methodological finding of this thesis is the demonstration, through the extensive use of micro-analysis, that the degree of heterogeneity in strontium isotope values in mammalian tooth enamel can be significant. This suggests that solution analysis of these samples may provide an incomplete indication of mobility during amelogenesis. Despite this potential, problems clearly remain with the analysis of relatively low strontium materials, which require further research to overcome. Judicious selection of samples with a relatively high strontium concentration and the recognition that some species at a relatively high trophic level, including humans, may be poor candidates for LA-MC-ICPMS are important steps in making this approach robust.

This research also provides significant insights into species-specific mobility during the Lower to Middle Palaeolithic era in Israel and southern France. All Persian fallow deer and reindeer in this study were mobile during amelogenesis, unidentified bovid were principally mobile during amelogenesis and lived in geological environments other than the study area. Bison were mobile during amelogenesis and exclusively occupied floodplains, while *Bos* samples were principally not mobile. Wild boar in this study was not mobile during amelogenesis. Rhinoceroses were not mobile, while hippopotamus samples were all mobile. Of the carnivores in this study, both the hyena and fox lived in geological areas other than the site. During amelogenesis, the fox moved across different geological environments.

The results of this research show varying patterns of mobility during different MIS. Overall, fauna from MIS 4 and 3 are significantly more mobile than samples from MIS 6 and 5. This result is surprising, because climate conditions ameliorated significantly from MIS 6 to MIS 5, which might be expected to yield a change in mobility. The reason for this unexpected correlation is probably the physiographic conditions surrounding the individual sites. The majority of MIS 6 samples in this study come from Pech de l'Azé II, for which independent evidence exists for a comparatively diverse flora during this period, facilitated by refugia conditions in the Perigord valley.

The results show that regional physiography, as discussed in terms of the results from MIS 6, exerts a significant control on regional mobility, with the river valleys of France apparently serving as conduits for faunal movements regardless of climate conditions. This finding has important implications for the predictive modelling of archaeological site locations, as these regions were probably always an abundant source of hominin prey.

While the insights into mobility provided by this research are important, the geographic, climatic, faunal and archaeological breadth of this question is too

large for detailed consideration by the analysis of 100, or even 1000, teeth. Nonetheless, the use of strontium isotopes when applied across a broad temporal and geographic range to answer archaeological questions is shown to have significant potential. This suggests that the usual site-specific approach to the strontium isotope analysis should be broadened for investigation into the history of human evolution in the future.

7.2. Recommendations

Three principal recommendations emerge from this research: firstly, the need to accurately quantify the degree of offset between laser and solution data. Secondly, the need to test the hypotheses proposed in this thesis with a comprehensive species matched suite of samples from an archaeological site and, lastly, to apply the methodology developed in this thesis to examine the evolution of hominin hunting during the Palaeolithic.

The presence of an offset between laser and solution strontium isotope samples when analysing relatively low strontium concentration biominerals remains a contentious issue. A rigorous large scale programme of analysis to quantify this problem is urgently required, involving the analysis of a range of materials with varying strontium concentrations and a known $^{87}\text{Sr}/^{86}\text{Sr}$ composition. Marine mammal teeth present an excellent opportunity for this, as would a series of apatite glasses.

A drawback of this research in terms of understanding the biogeography is the wide range of archaeological sites in different locations with different fauna. This wide focus provides a broad sense of how faunal mobility changes during different climatic and cultural events; however, this approach introduced many variables. A more focused approach would be to analyse multiple samples of the same species from a single archaeological site covering a significant period.

This research has focused on a range of faunal materials, from many archaeological sites in different physiographic region. The materials used for analysis were, in most cases, not necessarily obtained by hunting, instead possibly accumulating in the archaeological sites due to carnivore activity or natural attrition. Because of these many variables it has been impossible in this study to sensibly evaluate the difference in mobility between the various hominin species which occupied these archaeological sites. This is a regrettable omission as the broad temporal scale interpretation of mobility using strontium isotopes pioneered in this research could be used to evaluate the development of hunting strategies, if other variable could be excluded. This would be the case if material from a small number of sites, with long temporal records and abundant fauna from a limited range of species with robust associations with hominin hunting could be analysed.

Chapter Eight: References

- Åberg, G. and F.E. Wickham 1987 Variations in $^{87}\text{Sr}/^{86}\text{Sr}$ in water from streams discharging into the Bothnian Bay, Baltic Sea. *Nordic Hydrology* 18:33–42.
- Åberg, G. and G. Jacks 1987 $\text{Sr}^{87}/\text{Sr}^{86}$ as a tool in studies of weathering rates. In Y. Tardy (ed.), *Geochemistry of the Earth Surface and Processes of Mineral Formation*, pp. 67–76. Madrid: CSIC.
- Åberg, G., Jacks, G., Wickman, T. and P.J. Hamilton 1990 Strontium isotopes in trees as an indicator for calcium availability. *Catena* 17(1):1–11.
- Affek, H.P., Bar-Matthews, M., Ayalon, A., Matthews, A. and J.M. Eiler 2008 Glacial/interglacial temperature variations in Soreq cave speleothems as recorded by ‘clumped isotope’ thermometry. *Geochimica et Cosmochimica Acta* 72:5351–5360.
- Agron, N. and Y.K. Bentor 1981 The volcanic massif of Biq'at Hayareah (Sinai-Negev): A case of potassium metasomatism. *The Journal of Geology* 89(4):479–495.
- Aitken, M.J. and G. Valladas 1993 Luminescence dating relevant to human origins. In M.J. Aitken, C. Stringer and P. Mellars (eds), *The Origins of Modern Humans and the Impact of Chronometric Dating*, pp. 27–39. Princeton: Princeton University Press.
- Albert, R.M., Lavi, O., Estroff, L., Weiner, S., Tsatskin, A., Ronen, A. and S. Lev-Yadun 1999 Mode of occupation of Tabun Cave, Mt Carmel, Israel during the Mousterian period: A study of the sediments and phytoliths. *Journal of Archaeological Science* 26(10):1249–1260.
- Alexander, G.V., Nusbaum, R.E. and N.S. MacDonald 1956 The relative retention of strontium and calcium in bone tissue. *Journal of Biological Chemistry* 218:911–919.

- Allen, G.P. and H.W. Posamentier 1993 Sequence stratigraphy and facies models of an incised valley fill: The Gironde Estuary, France. *Journal of Sedimentary Research* 63(3):378–391.
- Almeida, C.M. and M.T.S.D. Vasconcelos 2001 ICPMS determination of strontium isotope ratio in wine in order to be used as a fingerprint of its regional origin. *Journal of Analytical Atomic Spectrometry* 16(6):607–611.
- Al-Shorman, A. and L. El-Khoury 2011 Strontium isotope analysis of human tooth enamel from Barsinia: A late antiquity site in northern Jordan. *Archaeological and Anthropological Sciences* 3(2):263–269.
- Alvira, F.C., Ramirez Rozzi, F.V., Torchia, G.A., Roso, L. and G.M. Bilmes 2011 A new method for relative Sr determination in human teeth enamel. *Journal of Anthropological Sciences* 89:153–160.
- Ambraseys, N.N. 1975 Studies in historical seismicity and tectonics. *Geodynamics Today*:7–16.
- Ambrose, S.H. 2001 Paleolithic technology and human evolution. *Science* 291:1748–1753.
- Andersson, P., Löfvendahl, R. and Åberg, G. 1990 Major element chemistry, $\delta^2\text{H}$, $\delta^{18}\text{O}$ and $^{87}\text{Sr}/^{86}\text{Sr}$ in a snow profile across central Scandinavia. *Atmospheric Environment. Part A. General Topics* 24(10):2601–2608.
- Anthony, D.W. and D.R. Brown 1991 The origins of horse-back riding. *Antiquity* 65:22–38.
- Antoine, D., Hillson, S. and M.C. Dean 2009 The developmental clock of dental enamel: A test for the periodicity of prism cross-striations in modern humans and an evaluation of the most likely sources of error in histological studies of this kind. *Journal of Anatomy* 214(1):45–55.
- Antón, S.C. 2003 Natural history of *Homo erectus*. *American Journal of Physical Anthropology* 122(S37):126–170.
- Arad, A. and A. Bein 1986 Saline- versus freshwater contribution to the thermal waters of the northern Jordan Rift Valley, Israel. *Journal of Hydrology* 83:49–66.

- Arnold, D.E., Neff, H., Glascock, M. and R.J. Speakman 2007 Sourcing the palygorskite used in Maya blue: A pilot study comparing the results of INAA and LA-ICPMS. *Latin American Antiquity* 18(1):44–58.
- Arppe, L., Karhu, J.A. and S.L. Vartanyan 2009 Bioapatite $^{87}\text{Sr}/^{86}\text{Sr}$ of the last woolly mammoths—Implications for the isolation of Wrangel Island. *Geology* 37(4):347–350.
- Arthur, G.W. 1975 An Introduction to the Ecology of Early Historic Communal Bison Hunting among the Northern Plains Indians. Ottawa: National Museum of Canada.
- Asahara, Y., Tanaka, T., Kamioka, H., Nishimura, A. and T. Yamazaki 1999 Provenance of the north Pacific sediments and process of source material transport as derived from Rb-Sr isotopic systematics. *Chemical Geology* 158(3–4):271–291.
- Aubert, M., O'Connor, S., McCulloch, M., Mortimer, G., Watchman, A. and M. Richer-LaFlèche 2007 Uranium-series dating rock art in East Timor. *Journal of Archaeological Science* 34(6):991–996.
- Audi, G., Wapstra, A.H. and C. Thibault 2003 The AME 2003 atomic mass evaluation (II). Tables, graphs and references. *Nuclear Physics A* 729:337–676.
- Avigour, A., Magaritz, M., Issar, A. and M.H. Dodson 1990 Sr isotope study of vein and cave calcites from southern Israel. *Chemical Geology* 82:69–81.
- Avnaim-Katav, S., Almogi-Labin, A., Sandler, A., Sivan, D., Porat, N. and A. Matmon 2012 The chronostratigraphy of a quaternary sequence at the distal part of the nile littoral cell, Haifa Bay, Israel. *Journal of Quaternary Science* 27(7):675–686.
- Ayalon, A., Bar-Matthews, M. and A. Kaufman 2002 Climatic conditions during marine oxygen isotope stage 6 in the eastern Mediterranean region from the isotopic composition of speleothems of Soreq Cave, Israel. *Geology* 30(4):303–306.

- Bachmann, M. and F. Hirsch 2006 Lower Cretaceous carbonate platform of the eastern Levant (Galilee and the Golan Heights): Stratigraphy and second-order sea-level change. *Cretaceous Research* 27(4):487–512.
- Bahn, P. 1977 Seasonal migration in south-west France during the last glacial period. *Journal of Archaeological Science* 4:245–257.
- Bain, D.C., Midwood, A.J. and J.D. Miller 1998 Strontium isotope ratios in streams and the effect of flow rate in relation to weathering in catchments. *Catena* 32(2):143–151.
- Balasse, M. 2002 Reconstructing dietary and environmental history from enamel isotopic analysis: Time resolution of intra-tooth sequential sampling. *International Journal of Osteoarchaeology* 12:155–165.
- Balasse, M., Ambrose, S.H., Smith, A.B. and T.D. Price 2002 The seasonal mobility model for prehistoric herders in the south-western cape of South Africa assessed by isotopic analysis of sheep tooth enamel. *Journal of Archaeological Science* 29(9):917–932.
- Balter, V., Braga, J., Telouk, P. and J.F. Thackeray 2012 Evidence for dietary change but not landscape use in South African early hominins. *Nature* 489:558–560.
- Banfield, A.W.F. 1961 A revision of the reindeer and caribou, genus Rangifer. *National Museum of Canada Bulletin* 177:1-137.
- Banfield, A.W.F. 1974 *The Mammals of Canada*. Toronto: University of Toronto Press.
- Banner, J.L., Hanson, G.N. and W.J. Meyers 1988 Water-rock interaction history of regionally extensive dolomites of the Burlington-Keokuk Formation (Mississippian): Isotopic evidence. *SEPM Special Publication* 43:97–113.
- Barbaste, M., Robinson, K., Guilfoyle, S., Medina, B. and R. Lobinski 2002 Precise determination of the strontium isotope ratios in wine by inductively coupled plasma sector field multicollector mass spectrometry (ICP-SF-MC-MS). *Journal of Analytical Atomic Spectrometry* 17(2):135–137.

- Barca, D., De Francesco, A.M. and G.M. Crisci 2007 Application of Laser ablation ICPMS for characterization of obsidian fragments from peri-Tyrrhenian area. *Journal of Cultural Heritage* 8(2):141–150.
- Bard, E., Hamelin, B. and R.G. Fairbanks 1990 U-Th ages obtained from mass spectrometry in corals from Barbados: Sea level during the past 130,000 years. *Nature* 346:456–459.
- Bardon, L.J. and A. Bouyssonie 1908 Découverte d'un Squelette Humaine Moustérien à la Bouffia de la Chapelle-Aux-Saints. *L'Anthropologie* 19:513–518.
- Barkai, R., Gopher, A. and P.C. La Porta 2002 Palaeolithic landscape of extraction: Flint surface quarries and workshops at Mt Pua, Israel. *Antiquity* 76(293):672–680.
- Barnett-Johnson, R., Ramos, R.C., Grimes, C.B. and R.B. MacFarlane 2005 Validation of Sr isotopes in otoliths by laser ablation multicollector inductively coupled plasma mass spectrometry (LA-MC-ICPMS): Opening avenues in fisheries science applications. *Canadian Journal of Fisheries and Aquatic Sciences* 62(11):2425–2430.
- Barnosky, A.D., Koch, P.L., Feranec, R.S., Wing, S.L. and A.B. Shabel 2004 Assessing the causes of Late Pleistocene extinctions on the continents. *Science* 306(5693):70–75.
- Bartov, Y., Stein, M., Enzel, Y., Agnon, A. and Z. Reches 2002 Lake levels and sequence stratigraphy of Lake Lisan, the Late Pleistocene precursor of the Dead Sea. *Quaternary Research* 57(1):9–21.
- Bar-Yosef Mayer, D.E., Vandermeersch, B. and O. Bar-Yosef 2009 Shells and ochre in Middle Paleolithic Qafzeh Cave, Israel: Indications for modern behavior. *Journal of Human Evolution* 56(3):307–314.
- Bar-Yosef, O. 1994 The contributions of southwest Asia to the study of the origin of modern humans. In M.H. Nitecki and D.V. Nitecki (eds), *Origins of Anatomically Modern Humans*, pp. 24–66. New York: Plenum Press.

- Bar-Yosef, O. 1998 Chronology of the Middle Paleolithic in the Levant. In T. Akazawa, K. Aoki and O. Bar-Yosef (eds), *Neanderthals and Modern Humans in Western Asia*. pp.39-56. New York: Plenum Press.
- Bar-Yosef, O. 2002 The Upper Paleolithic revolution. *Annual Review of Anthropology* 31:363–393.
- Bar-Yosef, O. and E. Tchernov 1972 *On the paleoecological history of the site of Ubeidiya*. Jerusalem: Israeli Academy of Science and Humanities.
- Baskin, L. and K. Danell 2003 Ecology of Ungulates: A Handbook of Species in Eastern Europe and Northern and Central Asia. Berlin: Springer.
- Beard, B.L. and C.M. Johnson 2000 Strontium isotope composition of skeletal material can determine the birth place and geographic mobility of humans and animals. *Journal of Forensic Science* 45(5):1049–1061.
- Beauval, C., Lacrampe-Cuyaubère, F., Maureille, B. and E. Trinkaus 2006 Direct radiocarbon dating and stable isotopes of the neandertal femur from Les Rochers-de-Villeneuve (Lussac-les-Châteaux, Vienne). *Bulletins et Mémoires de la Société d'Anthropologie de Paris* 18(1–2):35–42.
- Beeley, J.G. and D.A. Lunt 1980 The nature of the biochemical changes in softened dentine from archaeological sites. *Journal of Archaeological Science* 7:371–377.
- Beja-Pereira, A., Caramelli, D., Lalueza-Fox, C., Vernesi, C., Ferrand, N., Casoli, A., Goyache, F., Royo, L.J., Conti, S., Lari, M., Martini, A., Ouragh, L., Magid, A., Atash, A., Zsolnai, A., Boscato, P., Triantaphylidis, C., Ploumi, K., Sineo, L., Mallegni, F., Taberlet, P., Erhardt, G., Sampietro, L., Bertranpetti, J., Barbujani, G., Luikart, G. and G. Bertorelle 2006 The origin of European cattle: Evidence from modern and ancient DNA. *Proceedings of the National Academy of Sciences* 103(21):8113–8118.
- Bell, L.S., Boyde, A. and S.J. Jones 1991 Diagenetic alteration to teeth in situ illustrated by backscattered electron imaging. *Scanning* 13(2):173–183.

Bell, L.S., Skinner, M.F. and S.J. Jones 1996 The speed of post mortem change to the human skeleton and its taphonomic significance. *Forensic Science International* 82(2):129–140.

Belmaker, M. and E. Hovers 2011 Ecological change and the extinction of the Levantine Neanderthals: Implications from a diachronic study of micromammals from Amud Cave, Israel. *Quaternary Science Reviews* 30(21–22):3196–3209.

Ben-Dor, M., Gopher, A., Hershkovitz, I. and R. Barkai 2011 Man the fat hunter: The demise of *Homo erectus* and the emergence of a new hominin lineage in the Middle Pleistocene (ca. 400 kyr) Levant. *PLoS ONE* 6(12):e28689.

Bendrey, R., Hayes, T.E. and M.R. Palmer 2009 Patterns of iron age horse supply: An analysis of strontium isotope ratios of teeth. *Archaeometry* 51(1):140–150.

Bennett, D. and R.S. Hoffman 1999 Equus caballus. *Mammalian Species* 628:1–14.

Benson, L., Cordell, L., Vincent, K., Taylor, H., Stein, J., Lang Farmer, G. and K. Futa 2003 Ancient maize from Chacoan great houses: Where was it grown? *Proceedings of the National Academy of Science* 100(22):13111–13115.

Bentley, R.A. 2006 Strontium Isotopes from the earth to the archaeological skeleton: A review. *Journal of Archaeological Method and Theory* 13(3):135–187.

Bentley, R.A. and C. Knipper 2005a. Geographical patterns in biologically available strontium, carbon and oxygen isotope signatures in prehistoric SW Germany. *Archaeometry* 47(3):629–644.

Bentley, R.A. and C. Knipper 2005b. Transhumance at the early Neolithic settlement at Vaihingen (Germany). *Antiquity* 79.

- Bentley, R.A., Buckley, H.R., Spriggs, M., Bedford, S., Ottley, C.J., Nowell, G.M., Macpherson, C.G. and D.G. Pearson 2007 Lapita migrants in the Pacific's oldest cemetery: Isotopic analysis at Teouma, Vanuatu. *American Antiquity* 72(4):645–656.
- Bentley, R.A., Cox, K., Tayles, N., Higham, C., Macpherson, C., Nowell, G., Cooper, M. and T.E. Hayes 2009 Community diversity at Ban Lum Khao, Thailand: Isotopic evidence from the skeletons. *Asian Perspectives* 48(1):79–97.
- Bentley, R.A., Krause, R., Price, T.D. and B. Kaufmann 2003 Human mobility at the early Neolithic settlement of Vaihingen, Germany: Evidence from strontium isotope analysis. *Archaeometry* 45(3):471–486.
- Bentley, R.A., Pietruszewsky, M., Douglas, M.T. and T.C. Atkinson 2005 Matrilocality during the prehistoric transition to agriculture in Thailand? *Antiquity* 79:865–881.
- Bentley, R.A., Price, T.D. and E. Stephan 2004 Determining the 'local' $^{87}\text{Sr}/^{86}\text{Sr}$ range for archaeological skeletons: A case study from Neolithic Europe. *Journal of Archaeological Science* 31(4):365–375.
- Bentley, R.A., Price, T.D., Lüning, J., Gronenborn, D., Wahl, J. and P.D. Fullagar 2002 Prehistoric migration in Europe: Strontium isotope analysis of early Neolithic skeletons. *Current Anthropology* 43(5):799–804.
- Bentley, R.A., Tayles, N., Higham, C., Macpherson, C. and T.C. Atkinson 2007 Shifting gender relations at Khok Phanom Di, Thailand. *Current Anthropology* 48(2):301–314.
- Bentley, R.A., Wahl, J., Price, T.D. and T.C. Atkinson 2008 Isotopic signatures and hereditary traits: Snapshot of a Neolithic community in Germany. *Antiquity* 82:290–304.
- Bentor, Y.K. 1985 The crustal evolution of the Arabo-Nubian Massif with special reference to the Sinai Peninsula. *Precambrian Research* 28(1):1–74.
- Berger, J. 1986 Wild Horses of the Great Basin: Social Competition and Population Size. Chicago: University of Chicago Press.

- Berger, J. 2004 The last mile: How to sustain long-distance migration in mammals. *Conservation Biology* 18(2):320–331.
- Berger, J. and C. Cunningham 1994 *Bison: Mating and conservation in small populations*. New York: Columbia University Press.
- Berglund, M. and M.E. Wieser 2011 Isotopic compositions of the elements 2009 (IUPAC Technical Report). *Pure and Applied Chemistry* 83(2):397–410.
- Bergman, C.M., Schafer, J.A. and S.N. Luttrell 2000 Caribou movement as a correlated random walk. *Oecologia* 123(3):364–374.
- Bermudez de Castro, J.M., Rosas, A., Carbonell, E., Nicolas, M.E., Rodriguez, J. and J.L. Arsuaga 1999 A modern human pattern of dental development in Lower Pleistocene hominids from Atapuerca-TD6 (Spain). *Proceedings of the National Academy of Science* 96:4210–4213.
- Bern, C.R., Porder, S. and A.R. Townsend 2007 Erosion and landscape development decouple strontium and sulfur in the transition to dominance by atmospheric inputs. *Geoderma* 142(3–4):274–284.
- Bern, C.R., Townsend, A.R. and G.L. Farmer 2005 Unexpected Dominance of parent-material strontium in a tropical forest on highly weathered soils. *Ecology* 86(3):626–632.
- Bernard, A., Daux, V., Lécuyer, C., Brugal, J-P., Genty, D., Wainer, K., Gardien, V., Faourel, F. and J. Jaubert 2009 Pleistocene seasonal variations recorded in the $\delta^{18}\text{O}$ of *Bison priscus* teeth. *Earth and Planetary Science Letters* 283:133-143.
- Bertassoni, L.E., Stankoska, K. and M.V. Swain 2012 Insights into the structure and composition of the peritubular dentin organic matrix and the lamina limitans. *Micron* 43(2–3):229–236.
- Beyth, M. 1987 The Precambrian magmatic rocks of Timna Valley, southern Israel. *Precambrian Research* 36(1):21–38.

- Beyth, M., Stern, R.J., Altherr, R. and A. Kröner 1994 The Late Precambrian Timna igneous complex, southern Israel: Evidence for comagmatic-type sanukitoid monzodiorite and alkali granite magma. *Lithos* 31(3–4):103–124.
- Binford, L. and S. Binford 1969 Stone Tools and Human Behavior. *Scientific American* 220(4):70–84.
- Binford, L.R. 1985 Human ancestors: Changing views of their behavior. *Journal of Anthropological Archaeology* 4(4):292–327.
- Binford, L.R. and S.R. Binford 1966 A preliminary analysis of functional variability in the Mousterian of the Levallois Facies. *American Anthropologist* 68:238–295.
- Bischoff, J.L., Williams, R.W., Rosenbauer, R.J., Aramburu, A., Arsuaga, J.L., Garcia, N. and G. Cuenca-Bescos 2007 High-resolution U-series dates from the Sima de los Huesos hominids yields: Implications for the evolution of the early Neanderthal lineage. *Journal of Archaeological Science* 34(5):763–770.
- Bizzarro, M., Simonetti, A., Stevenson, R.K. and S. Kurszlaukis 2003 In situ $^{87}\text{Sr}/^{86}\text{Sr}$ investigation of igneous apatites and carbonates using laser-ablation MC-ICPMS. *Geochimica et Cosmochimica Acta* 67:289–302.
- Bjärvall, A. and S. Ullström 1986 *The Mammals of Britain and Europe*. Croom Helm, Beckenham.
- Blès, J.L. and Y. Gros 1991 Stress field changes in the Rhone Valley from the Miocene to the present. *Tectonophysics* 194(3):265–277.
- Blès, J.L., Bonijoly, D., Castaing, C. and Y. Gros 1989 Successive post-Variscan stress fields in the French Massif Central and its borders (Western European plate): Comparison with geodynamic data. *Tectonophysics* 169(1–3):79–111.
- Blum, J., Dasch, A., Hamburg, S., Yanai, R. and M. Arthur 2008 Use of foliar Ca/Sr discrimination and $^{87}\text{Sr}/^{86}\text{Sr}$ ratios to determine soil Ca sources to sugar maple foliage in a northern hardwood forest. *Biogeochemistry* 87(3):287–296.

- Blum, J.D., Erel, Y. and K. Brown 1993 $^{87}\text{Sr}/^{86}\text{Sr}$ ratios of Sierra Nevada stream waters: Implications for relative mineral weathering rates. *Geochimica et Cosmochimica Acta* 57(21–22):5019–5025.
- Blum, J.D., Taliaferro, E.H., Weisse, M.T. and R.T. Holmes 2000 Changes in Sr/Ca, Ba/Ca and $^{87}\text{Sr}/^{86}\text{Sr}$ ratios between trophic levels in two forest ecosystems in the northeastern U.S.A. *Biogeochemistry* 49(1):87–101.
- Bocherens, H., Billiou, D., Mariotti, A., Toussaint, M., Patou-Mathis, M., Bonjean, D. and M. Otte 2001 New isotopic evidence for dietary habits of Neanderthals from Belgium. *Journal of Human Evolution* 40(6):497–505.
- Bocherens, H., Brinkmans, D.B., Dauphin, Y. and A. Mariotti 1994 Microstructural and geochemical investigations on Late Cretaceous archosaur teeth from Alberta, Canada. *Canadian Journal of Earth Sciences* 31:783–792.
- Bocherens, H., Drucker, D.G., Billiou, D., Patou-Mathis, M. and B. Vandermeersch 2005 Isotopic evidence for diet and subsistence pattern of the Saint-Césaire I Neanderthal: Review and use of a multi-source mixing model. *Journal of Human Evolution* 49(1):71–87.
- Boel, C. 2011 Identifying Migration: Strontium Isotope Studies on an Early Bell Beaker Population from Le Tumulus des Sables, France. Unpublished Honours thesis, School of Archaeology and Anthropology, Australian National University.
- Böhlke, J.K. and M. Horan 2000 Strontium isotope geochemistry of groundwaters and streams affected by agriculture, Locust Grove, MD. *Applied Geochemistry* 15(5):599–609.
- Bond, G., Broecker, W., Johnsen, S., McManus, J., Labeyrie, L., Jouzel, J. and G. Bonani 1993 Correlations between climate records from North Atlantic sediments and Greenland ice. *Nature* 365(6442):143–147.
- Bordes, F. 1969 Os percé moustérien et os gravé acheuléen du Pech de l'Azé II. *Quaternaria*, XI:1–6.

- Bordes, F. 1972a. Du Paleolithique moyen au Paleolithique superieur: Continuite ou discontinutie? In F. Bordes (ed.), *The origin of Homo sapiens*, pp. 211–218. Paris: UNESCO.
- Bordes, F. 1972b. *A Tale of Two Caves*. New York: Harper and Row.
- Bordes, F. and D.D. Sonneville-Bordes 1970 The Significance of variability in Palaeolithic assemblages. *World Archaeology* 2(1):61–73.
- Bourillet, J.F., Zargrosi, S. and T. Mulder 2006 The French Atlantic margin and deep-sea submarine systems. *Geo-Marine Letters* 26(6):311–315.
- Bourman, R.P. and A.R. Milnes 1985 Gibber Plains. *Australian Geographer* 16(3):229–232.
- Bourrouilh, R., Richert, J-P. and G. Zolnai 1995 The North Pyrenean Aquitaine Basin, France: Evolution and hydrocarbons. *AAPG Bulletin* 79(6):831–853.
- Boutié, P. 1989 Etude technologique de l'industrie moustérienne de la grotte de Qafzeh (prés de Nazareth, Israël). In O. Bar-Yosef and B. Vandermeersch (eds), *Investigations in Southern Levantine Prehistory/Préhistoire du Sud Levant*, pp. 213–230. Oxford: BAR International Series 497.
- Bouyssonie, A., Bouyssonie, J. and L. Bardon 1908 Decouverte d'un squelette humain moustérien a la Bouffia de la Chapelle-aux-Saints (Corrze). *L'Anthropologie* 19:513–518.
- Bouyssonie, A., Bouyssonie, J. and L. Bardon 1913 La station moustérienne de la 'Bouffia' Bonneval, a la Chapelle-sux-Saints. *L'Anthropologie* 24:609–634.
- Boyde, A. 1979 Carbonate concentration, crystal centers, core dissolution, caries, cross striations, circadian rhythms and compositional contrast in the SEM. *Journal of Dental Research* 58:981–983.
- Boyle, K.V. 1990 Upper Palaeolithic Faunas from South-West France: A Zoogeographic Perspective. Oxford: BAR International Series 557.

- Boyle, K.V. 1998 *The Middle Palaeolithic Geography of Southern France*. Oxford: BAR International Series 723.
- Brass, G.W. 1975 The effect of weathering on the distribution of strontium isotopes in weathering profiles. *Geochimica et Cosmochimica Acta* 39(12):1647–1653.
- Brescia, N.J. 1961 *Applied Dental Anatomy*. St. Louis: Mosby.
- BRGM 1967 Cognac. In *Carte Géologique de la France 1/50000*. Orléans: BRGM.
- BRGM 1968 Saintes. In *Carte Géologique de la France 1/50000*. Orléans: BRGM.
- BRGM 1977a. Pons. In *Carte Géologique de la France 1/50000*. Orléans: BRGM.
- BRGM 1985 Matha. In *Carte Géologique de la France 1/50000*. Orléans: BRGM.
- BRGM 1986 Sarlat-La-Caneda. In *Carte Géologique de la France 1/50000*. Orléans: BRGM.
- BRGM 1988 Rodez. In *Carte Géologique de la France 1/50000*. Orléans: BRGM.
- BRGM 1989 Espalion. In *Carte Géologique de la France 1/50000*. Orléans: BRGM.
- BRGM 1990 Gourdon. In *Carte Géologique de la France 1/50000*. Orléans: BRGM.
- BRGM 1996 Souliac. In *Carte Géologique de la France 1/50000*. Orléans: BRGM.
- BRGM 2000 Le Bugue. In *Carte Géologique de la France 1/50000*. Orléans: BRGM.
- BRGM 2008 Montelimar. In *Carte Géologique de la France 1/50000*. Orléans: BRGM.

- Briot, D. 2008 Sr isotopes of the shells of the euryhaline gastropod *Potamides lamarcki* from the Oligocene of the French Massif Central and Paris Basin—A clue to its habitats. *Palaeogeography, Palaeoclimatology, Palaeoecology* 268(1–2):116–122.
- Britton, K., Grimes, V., Dau, J. and M.P. Richards 2009 Reconstructing faunal migrations using intra-tooth sampling and strontium and oxygen isotope analyses: A case study of modern caribou (*Rangifer tarandus granti*). *Journal of Archaeological Science* 36(5):1163–1172.
- Britton, K., Grimes, V., Niven, L., Steele, T.E., McPherron, S., Soressi, M., Kelly, T.E., Jaubert, J., Hublin, J.-J. and M.P. Richards 2011 Strontium isotope evidence for migration in late Pleistocene *Rangifer*: Implications for Neanderthal hunting strategies at the Middle Palaeolithic site of Jonzac, France. *Journal of Human Evolution* 61(2):176–185.
- Britton, K., Grimes, V., Niven, L., Steele, T.E., McPherron, S., Soressi, M., Kelly, T.E., Jaubert, J., Hublin, J.-J. and M.P. Richards 2011 Strontium isotope evidence for migration in late Pleistocene *Rangifer*: Implications for Neanderthal hunting strategies at the Middle Palaeolithic site of Jonzac, France. *Journal of Human Evolution* 61(2):176–185.
- Brose, D.S. and M.H. Wolpoff 1971 Early Upper Paleolithic man and Late Middle Paleolithic tools. *American Anthropologist* 73(5):1156–1194.
- Brown, W.A.B. and N.G. Chapman 1990 The dentition of fallow deer (*Dama dama*): A scoring scheme to assess age from wear of the permanent molariform teeth. *Journal of Zoology* 221:659–682.
- Brown, W.A.B., Christofferson, P.V., Massler, M. and M.B. Weiss 1960 Postnatal tooth development in cattle. *American Journal of Veterinary Research* 21(80):7–34.
- Brunet, M.-F. 1984 Subsidence history of the Aquitaine basin determined from subsidence curves. *Geological Magazine* 121(05):421–428.

- Bruno, P., Caselli, M., Curri, M.L., Genga, A., Striccoli, R. and A. Traini 2000 Chemical characterisation of ancient pottery from south of Italy by Inductively Coupled Plasma Atomic Emission Spectroscopy (ICP-AES): Statistical multivariate analysis of data. *Analytica Chimica Acta* 410(1–2):193–202.
- Budd, P., Millard, A., Chenery, C., Lucy, S. and C.A. Roberts 2004 Investigating population movement by stable isotope analysis: A report from Britain. *Antiquity* 78(299):127–141.
- Budd, P., Montgomery, J., Barreiro, B. and R.G. Thomas 2000 Differential diagenesis of strontium in archaeological human dental tissues. *Applied Geochemistry* 15(5):687–694.
- Bull, P.A. and P. Goldberg 1985 Scanning electron microscope analysis of sediments from Tabun Cave, Mount Carmel, Israel. *Journal of Archaeological Science* 12(3):177–185.
- Burke, A.M. 1995 Prey Movements and Settlement Patterns During the Upper Palaeolithic in Southwestern France. Oxford: BAR International Series 619.
- Burton, J.H. and L.E. Wright 1995 Nonlinearity in the relationship between bone Sr/Ca and diet: Paleodietary implications. *American Journal of Physical Anthropology* 96(3):273–282.
- Burton, J.H. and T.D. Price 1990 The ratio of barium to strontium as a paleodietary indicator of consumption of marine resources. *Journal of Archaeological Science* 17:547–557.
- Burton, J.H. and T.D. Price 1999 Evaluation of bone strontium as a measure of seafood consumption. *International Journal of Osteoarchaeology* 9(4):233–236.
- Burton, J.H. Price, T.D. and W.D. Middleton 1999 Correlation of bone Ba/Ca and Sr/Ca due to biological purification of calcium. *Journal of Archaeological Science* 26(6):609–616.

- Canadell, J., Jackson, R.B., Ehleringer, J.B., Mooney, H.A., Sala, O.E. and E.D. Schulze 1996 Maximum rooting depth of vegetation types at the global scale. *Oecologia* 108(4):583–595.
- Candy, I., Black, S. and B.W. Sellwood 2005 U-series isochron dating of immature and mature calcretes as a basis for constructing Quaternary landform chronologies for the Sorbas basin, southeast Spain. *Quaternary Research* 64(1):100–111.
- Capo, R.C., Stewart, B.W. and O.A. Chadwick 1998 Strontium isotopes as tracers of ecosystem processes: Theory and methods. *Geoderma* 82(1–3):197–225.
- Carter, R.J. 1998 Reassessment of seasonality at the Early Mesolithic site of Star Carr, Yorkshire, based on radiographs of madibular tooth development in red deer (*Cervus elaphus*). *Journal of Archaeological Science* 25:851–856.
- Carter, R.J. 2000 New evidence for seasonal human presence at the Early Mesolithic site of Thatcham, Berkshire, England. *Journal of Archaeological Science* 28:1055–1060.
- Catling, P.C. and R.J. Burt 1995 Why are red foxes absent from some eucalypt forests in eastern New South Wales? *Wildlife Research* 22:535–546.
- Chadwick, O.A., Derry, L.A., Bern, C.R. and P.M. Vitousek 2009 Changing sources of strontium to soils and ecosystems across the Hawaiian Islands. *Chemical Geology* 267(1–2):64–76.
- Chamberlain, C.P., Blum, J.D., Holmes, R.T., Feng, X., Sherry, T.W. and G.R. Graves 1997 The use of isotope tracers for indentifying populations of migratory birds. *Oecologia* 109:132–141.
- Champagne, F., Champagne, C., Jauzon, P. and P. Novel 1990 Le site préhistorique des Fieux a Miers (Lot). *Gallia prehistorie* 32:1–28.
- Chapman, D. and N. Chapman 1980 The distribution of fallow deer: A worldwide review. *Mammal Review* 10:2–138.

- Chapman, D.I. and N.G. Chapman 1970 Development of the teeth and mandibles of fallow deer. *Acta Theriologica* 15:111–131.
- Chappell, J. 2002 Sea level changes forced ice breakouts in the Last Glacial cycle: New results from coral terraces. *Quaternary Science Reviews* 21(10):1229–1240.
- Chappell, J. and N.J. Shackleton 1986 Oxygen isotopes and sea level. *Nature* 324:137–140.
- Chaudhuri, S. and N. Clauer 1986 Fluctuations of isotopic composition of strontium in seawater during the Phanerozoic Eon. *Chemical Geology: Isotope Geoscience* 59:293–303.
- Chazan, M. 2000a. Flake production at the Lower Paleolithic Site of Holon (Israel). Implications for the origin of the Levallois method. *Antiquity* 74:495–499.
- Chazan, M. 2000b. Typological analysis of the Lower Paleolithic Site of Holon, Israel. *Journal of the Israel Prehistoric Society* 30:7–32.
- Chazan, M. and L.K. Horwitz 2007 *Holon: A Lower Paleolithic Site in Israel*. Cambridge: Peabody Museum of Archaeology and Ethnology, Harvard University.
- Cheddadi, R. and M. Rossignol-Strick 1995 Eastern Mediterranean Quaternary paleoclimates from pollen and isotope records of marine cores in the Nile cone area. *Paleoceanography* 10(2):291–300.
- Chenery, C., Müldner, G., Evans, J., Eckardt, H. and M. Lewis 2010 Strontium and stable isotope evidence for diet and mobility in Roman Gloucester, UK. *Journal of Archaeological Science* 37(1):150–163.
- Chinzei, K. 1970 The Amud Cave and its deposits. In H. Suzuki and F. Takai (eds), *The Amud Man and His Cave Site*, pp. 21–51. Tokyo: The University of Tokyo.
- Churchill, S.E. and F.H. Smith 2000 Makers of the early Aurignacian of Europe. *Yearbook of Physical Anthropology* 43:61–115.

- Clark, G.A. and J.M. Lindly 1989 Modern human origins in the Levant and western Asia: The fossil and archeological evidence. *American Anthropologist* 91(4):962–985.
- Clark, J.D. 1966 Acheulian occupation sites in the Middle East and Africa: A study in cultural variability. *American Anthropologist Special Edition* 68(2:2):202–229.
- Clark, J.D. 1968. The Middle Acheulian occupation site of Latamane, Syria (2nd paper). *Quaternaria*, 10:1-72.
- Clauer, N., Hoffert, M., Grimaud, D. and G. Millot 1975 Composition isotopique du strontium d'eaux interstitielles extraites de sédiments récents: Un argument en faveur de l'homogénéisation isotopique des minéraux argileux. *Geochimica et Cosmochimica Acta* 39(11):1579–1582.
- Cochran, J.K., Kallenberg, K., Landman, N.H., Harries, P.J., Weinreb, D., Turekian, K.K., Beck, A.J. and W.A. Cobban 2010 Effect of diagenesis on the Sr, O and C isotope composition of late Cretaceous mollusks from the Western Interior Seaway of North America. *American Journal of Science* 310(2):69–88.
- Cochrane, E.E. and H. Neff 2006 Investigating compositional diversity among Fijian ceramics with laser ablation-inductively coupled plasma-mass spectrometry (LA-ICPMS): Implications for interaction studies on geologically similar islands. *Journal of Archaeological Science* 33(3):378–390.
- Cohen, S., Ianetz, A. and G. Stanhill 2002 Evaporative climate changes at Bet Dagan, Israel, 1964–1998. *Agricultural and Forest Meteorology* 111(2):83–91.
- Conlee, C.A., Buzon, M.R., Gutierrez, A.N., Simonetti, A. and R.A. Creaser 2009 Identifying foreigners versus locals in a burial population from Nasca, Peru: An investigation using strontium isotope analysis. *Journal of Archaeological Science* 36(12):2755–2764.

- Cook, D.E., Kovacevich, B., Beach, T. and R. Bishop 2006 Deciphering the inorganic chemical record of ancient human activity using ICPMS: A reconnaissance study of late Classic soil floors at Cancuén, Guatemala. *Journal of Archaeological Science* 33(5):628–640.
- Cooper, H.K., Duke, M.J.M., Simonetti, A. and G. Chen 2008 Trace element and Pb isotope provenance analyses of native copper in northwestern North America: Results of a recent pilot study using INAA, ICPMS and LA-MC-ICPMS. *Journal of Archaeological Science* 35(6):1732–1747.
- Copeland, J. 1975 The Middle and Upper Paleolithic of Lebanon and Syria in the light of recent research. In F. Wendorf and A.E. Marks (eds), *Problems in Prehistory: North Africa and the Levant*, pp. 317–350. Dallas: Southern Methodist University Press.
- Copeland, S.R., Sponheimer, M., de Ruiter, D.J., Lee-Thorp, J.A., Codron, D., le Roux, P.J., Grimes, V. and M.P. Richards 2011 Strontium isotope evidence for landscape use by early hominins. *Nature* 474(7349):76–78.
- Copeland, S.R., Sponheimer, M., Le Roux, P.J., Grimes, V., Lee-thorp, J.A., de Ruiter, D.J. and M.P. Richards 2008 Strontium isotope ratios ($^{87}\text{Sr}/^{86}\text{Sr}$) of tooth enamel: A comparison of solution and laser ablation multicollector inductively coupled plasma mass spectrometry methods. *Rapid Communications in Mass Spectrometry* 22:3187–3194.
- Copeland, S.R., Sponheimer, M., Lee-Thorp, J.A., de Ruiter, D.J., le Roux, P.J., Grimes, V., Codron, D., Berger, L.R. and M.P. Richards 2010 Using strontium isotopes to study site accumulation processes. *Journal of Taphonomy* 8(2–3):115–127.
- Copeland, S.R., Sponheimer, M., Lee-Thorp, J.A., le Roux, P.J., de Ruiter, D.J. and M.P. Richards 2010 Strontium isotope ratios in fossil teeth from South Africa: Assessing laser ablation MC-ICPMS analysis and the extent of diagenesis. *Journal of Archaeological Science* 37:1437–1446.
- Coppa, A., Grün, R., Stringer, C., Egginis, S. and R. Vargiu 2005 Newly recognized pleistocene human teeth from Tabun Cave, Israel. *Journal of Human Evolution* 49(3):301–315.

- Corruccini, R.S. 1992 Metrical reconsideration of the Skhul IV and IX and Border Cave I crania in the context of modern human origins. *American Journal of Physical Anthropology* 87:433–445.
- Costamagno, S., Meignen, L., Beauval, C., Vandermeersch, B. and B. Maureille 2006 Les Pradelles (Marillac-le-Franc, France): A Mousterian reindeer hunting camp? *Journal of Anthropological Archaeology* 25:466–484.
- Couturié, J.P. and M. Vachette-Caen 1980 Age westphalien des leucogranites recouplant le granite de Margeride (Massif Central français). *Compte Rendus de l'Académie des Sciences, Series II* 291:43–45.
- Cox, G. and J. Sealy 1997 Investigating identity and life histories: Isotopic analysis and historical documentation of slave skeletons found on the Cape Town foreshore, South Africa. *International Journal of Historical Archaeology* 1(3):207–224.
- Curnelle, R., Dubois, P., Seguin, J.C., Whitaker, D., Matthews, D.H., Roberts, D.G., Kent, P., Laughton, A.S. and M.M. Kholief 1982 The Mesozoic-Tertiary evolution of the Aquitaine Basin [and discussion]. *Philosophical Transactions of the Royal Society of London. Series A, Mathematical and Physical Sciences* 305(1489):63–84.
- d'Errico, F. and P. Villa 1997 Holes and grooves: The contribution of microscopy and taphonomy to the problem of art origins. *Journal of Human Evolution* 33:1–31.
- d'Errico, F., Salomon, H., Vignaud, C. and C. Stringer 2010 Pigments from the Middle Palaeolithic levels of Es-Skhul (Mount Carmel, Israel). *Journal of Archaeological Science* 37(12):3099–3110.
- d'Huart, J.P. 1991 Habitat utilization of old world wild pigs. In R.H. Barrett and F. Spitz (eds), *Biology of Suidae*, pp. 30–48. Grenoble: IRGM.
- Dams, L. 1985 Palaeolithic lithophones: Descriptions and comparisons. *Oxford Journal of Archaeology* 4(1):31–46.
- Dan, J. and A. Singer 1973 Soil evolution on basalt and basic pyroclastic materials in the Golan Heights. *Geoderma* 9(3):165–192.

Dan, J. and H. Koyumdjisky 1963 The soils of israel and their distribution. *European Journal of Soil Science* 14(1):12–20.

Dansgaard, W., Johnsen, S., Clausen, H.B., Dahl-Jensen, D., Gunderstrup, N., Hammer, C.U. and H. Oeschger 1984 North Atlantic climatic events revealed by deep Greenland ice cores. In J.E. Hansen and T. Takahashi (eds), *Climate Processes and Climate Sensitivity*, pp. 288–298. Washington: American Geophysical Union.

Dasch, A.A., Blum, J.D., Eagar, C., Fahey, T.J., Driscoll, C.T. and T.G. Siccama 2006 The relative uptake of Ca and Sr into tree foliage using a whole-watershed calcium addition. *Biogeochemistry* 80:21–41.

Dasch, E.J. 1969 Strontium isotopes in weathering profiles, deep-sea sediments and sedimentary rocks. *Geochimica et Cosmochimica Acta* 33(12):1521–1552.

Daux, V., Crovisier, J.L., Hemond, C. and J.C. Petit 1994 Geochemical evolution of basaltic rocks subjected to weathering: Fate of the major elements, rare earth elements and thorium. *Geochimica et Cosmochimica Acta* 58(22):4941–4954.

Davis, S.J.M. 1981 The Effects of temperature change and domestication on the body size of Late Pleistocene to Holocene mammals of Israel. *Paleobiology* 7(1):101–114.

Dawson, J.E. and E. Trinkaus 1997 Vertebral osteoarthritis of the La Chapelle-aux-Saints 1 Neanderthal. *Journal of Archaeological Science* 24(11):1015–1021.

Day, M. 1986 *Guide to Fossil Man*. Chicago: University of Chicago Press.

de Beaulieu, J.L. and M. Reille 1984 A long Upper Pleistocene pollen record from Les Echets, near Lyon, France. *Boreas* 13:111–131.

de Mortillet, G. 1869 Promenades préhistoriques à l'exposition universelle. Paris: Reinwald.

- de Souza, G.F., Reynolds, B.C., Kiczka, M. and B. Bourdon 2010, Evidence for mass-dependent isotopic fractionation of strontium in a glaciated granitic watershed. *Geochimica et Cosmochimica Acta* 74:2596–2614.
- Dean, C. 2000 Progress in understanding hominoid dental development. *Journal of Anatomy* 197:77–101.
- Dean, C., Leakey, M.G., Reid, D., Schrenk, F., Schwartz, G.T., Stringer, C. and A. Walker 2001 Growth processes in teeth distinguish modern humans from *Homo erectus* and earlier hominins. *Nature* 414:628–631.
- Dean, M.C. 1987 Growth layers and incremental markings in hard tissues; a review of the literature and some preliminary observations about enamel structure in *Paranthropus boisei*. *Journal of Human Evolution* 16(2):157–172.
- Dean, M.C. 1998 Comparative observations on the spacing of short-period (von Ebner's) lines in dentine. *Archives of Oral Biology* 43(12):1009–1021.
- Dean, M.C. and A.E. Scandrett 1996 The relation between long-period incremental markings in dentine and daily cross-striations in enamel in human teeth. *Archives of Oral Biology* 41(3):233–241.
- Dennell, R. 2003 Dispersal and colonisation, long and short chronologies: How continuous is the Early Pleistocene record for hominids outside East Africa? *Journal of Human Evolution* 45:421–440.
- Derry, L.A. and O.A. Chadwick 2007 Contributions from earth's atmosphere to soil. *Elements* 3(5):333–338.
- Desaulty, A.-M., Mariet, C., Dillmann, P., Joron, J.L. and P. Fluzin 2008 A provenance study of iron archaeological artefacts by Inductively Coupled Plasma-Mass Spectrometry multi-elemental analysis. *Spectrochimica Acta Part B: Atomic Spectroscopy* 63(11):1253–1262.
- Desbiez, A.L.J. and A. Keuroghlian 2001 Ageing feral pigs (*Sus scrofa*) through tooth eruption and wear. *Suiform Soundings* 9(1):48–55.

- Desegaulx, P., Kooi, H. and S. Cloetingh 1991 Consequences of foreland basin development on thinned continental lithosphere: Application to the Aquitaine basin (SW France). *Earth and Planetary Science Letters* 106(1–4):116–132.
- Devos, W., Senn-Luder, M., Moor, C. and C. Salter 2000 Laser ablation inductively coupled plasma mass spectrometry (LA-ICPMS) for spatially resolved trace analysis of early-medieval archaeological iron finds. *Fresenius' Journal of Analytical Chemistry* 366(8):873–880.
- Dicken, A.P. 2005 *Radiogenic Isotope Geology*. Cambridge: Cambridge University Press.
- Discamps, E., Jaubert, J. and F. Bachellerie 2011 Human choices and environmental constraints: Deciphering the variability of large game procurement from Mousterian to Aurignacian times (MIS 5–3) in southwestern France. *Quaternary Science Reviews* 30(19–20):2755–2775.
- Domínguez-Rodrigo, M. 2002 Hunting and scavenging by early humans: The state of the debate. *Journal of World Prehistory* 16(1):1–54.
- Douglas, G.B., Gray, C.M., Hart, B.T. and R. Beckett 1995 A strontium isotopic investigation of the origin of suspended particulate matter (SPM) in the Murray-Darling River system, Australia. *Geochimica et Cosmochimica Acta* 59(18):3799–3815.
- Douthitt, C. 2008 The evolution and applications of multicollector ICPMS (MC-ICPMS). *Analytical and Bioanalytical Chemistry* 390(2):437–440.
- Downes, H. and J.L. Duthou 1988 Isotopic and trace element arguments for the lower crustal origin of Hercynian granitoids and Pre-Hercynian orthogneiss, massif Central, France. *Chemical Geology* 68:291–308.
- Driessens, F.C.M. and R.M.H. Verbeeck 1990 *Biominerals*. Boca Raton: CRC Press.
- Dupré, B., Négrel, P., Seimbille, F. and C.J. Allegre 1994 $^{87}\text{Sr}/^{86}\text{Sr}$ ratio variation during a rain event. *Atmospheric Environment* 28(4):617–620.

- Durand, S.R., Shelley, P.H., Antweiler, R.C. and H.E. Taylor 1999 Trees, chemistry and prehistory in the American southwest. *Journal of Archaeological Science* 26(2):185–203.
- Dussubieux, L., Deraisme, A., Frot, G., Stevenson, C., Creech, A.M.Y. and Y. Bienvenu 2008 LA–ICP–MS, SEM–EDS and EPMA analysis of Eastern North American copper-based artefacts: Impact of corrosion and heterogeneity on the reliability of the LA–ICP–MS compositional results*. *Archaeometry* 50(4):643–657.
- Duthou, J.L., Cantagrel, J.M., Didier, J. and Y. Viallette 1984 Palaeozoic granitoids from the French Massif Central: Age and origin studied by ^{87}Rb — ^{87}Sr system. *Physics of the Earth and Planetary Interiors* 35(1–3):131–144.
- Eckardt, H., Chenery, C., Booth, P., Evans, J.A., Lamb, A. and G. Müldner 2009 Oxygen and strontium isotope evidence for mobility in Roman Winchester. *Journal of Archaeological Science* 36(12):2816–2825.
- Eggins, S., Grün, R., Pike, A.W.G., Shelley, M. and L. Taylor 2003 U-238, Th-232 profiling and U-series isotope analysis of fossil teeth by laser ablation-ICPMS. *Quaternary Science Reviews* 22(10–13):1373–1382.
- Eggins, S.M., Grün, R., McCulloch, M.T., Pike, A.W.G., Chappell, J., Kinsley, L., Mortimer, G., Shelley, M., Murray-Wallace, C.V., Spotl, C. and L. Taylor 2005 In situ U-series dating by laser-ablation multi-collector ICPMS: New prospects for Quaternary geochronology. *Quaternary Science Reviews* 24(23–24):2523–2538.
- Eggins, S.M., Kinsley, L.P.J. and J.M.G. Shelley 1998 Deposition and element fractionation processes during atmospheric pressure laser sampling for analysis by ICPMS. *Applied Surface Science* 127–129:278–286.
- Ehlers, J. and P. Gibbard 2008 Extent and chronology of Quaternary glaciation. *Episodes* 31(2):211–218.
- Eig, A. 1931 Les éléments et les groupes phytogéographiques auxiliaires dans la flore palestinienne. I Texte. *Feddes Repertorium Specierum Novarum Regni Vegetabilis* 63:1–201.

- Eig, A. 1932 Les éléments et les groupes phytogéographiques auxiliaires dans la flore palestinienne. II Tableauz analytiques. *Feddes Repertorium Specierum Novarum Regni Vegetabilis* 63:21–120.
- El Albani, A., Fürsich, F.T., Colin, J.-P., Meunier, A., Hochuli, P., Martín-Closas, C., Mazin, J.-M. and J.-P. Billon-Bruyat 2004 Palaeoenvironmental reconstruction of the basal Cretaceous vertebrate bearing beds in the Northern part of the Aquitaine Basin (SW France): Sedimentological and geochemical evidence. *Facies* 50(2):195–215.
- El Albani, A., Meunier, A. and F. Fürsich 2005 Unusual occurrence of glauconite in a shallow lagoonal environment (Lower Cretaceous, northern Aquitaine Basin, SW France). *Terra Nova* 17(6):537–544.
- Elderfield, H. 1986 Strontium isotope stratigraphy. *Palaeogeography, Palaeoclimatology, Palaeoecology* 57(1):71–90.
- Elderfield, H. and J.M. Gieskes 1982 Sr isotopes in interstitial waters of marine sediments from Deep Sea Drilling Project cores. *Nature* 300:493–497.
- Elias, M. 1980 The feasibility of dental strontium analysis for diet-assessment of human populations. *American Journal of Physical Anthropology* 53(1):1–4.
- Eltringham, S.K. 1993 The common hippopotamus (*Hippopotamus amphibius*). In W.L.R. Oliver (ed.), *Status Survey and Conservation Action Plan: Pigs, Peccaries and Hippos*, pp. 43–55. Gland: IUCN.
- Emeis, K.-C., Schulz, H.M., Struck, U., Sakamoto, T., Doose, H., Erlenkeuser, H., Howell, M., Kroon, D. and M. Paterne 1998 Stable isotope and alkenone temperature records of sapropels from sites 964 and 967: Constraining the physical environment of sapropel formation in the Eastern Mediterranean Sea. In A.H.F. Robertson, K.-C. Emeis, C. Richter and A. Camerlenghi (eds), *Proceedings of the Ocean Drilling Program, Scientific Results*, pp. 309–331. College Station: Ocean Drilling Program.
- Emiliani, C. 1955 Pleistocene temperatures. *Journal of Geology* 63:538–578.

- Emiliani, C. 1956 Oligocene and miocene temperatures of the equitorial and subtropical Atlantic Ocean. *Journal of Geology* 64(3):281–288.
- Entwistle, J.A. and P.W. Abrahams 1997 Multi-element analysis of soils and sediments from Scottish historical sites. The potential of inductively coupled plasma-mass spectrometry for rapid site investigation. *Journal of Archaeological Science* 24(5):407–416.
- Entwistle, J.A., Abrahams, P.W. and R.A. Dodgshon 1998 Multi-element analysis of soils from Scottish historical sites. Interpreting land-use history through the physical and geochemical analysis of soil. *Journal of Archaeological Science* 25(1):53–68.
- Enzel, Y., Amit, R., Dayan, U., Crouvi, O., Kahana, R., Ziv, B. and D. Sharon 2008 The climatic and physiographic controls of the eastern Mediterranean over the late Pleistocene climates in the southern Levant and its neighboring deserts. *Global and Planetary Change* 60(3–4):165–192.
- Ericson, J.E. 1985 Strontium isotope characterization in the study of prehistoric human ecology. *Journal of Human Evolution* 14(5):503–514.
- European Commission and the European Soil Bureau Network 2004 *The European Soil Database Distribution Version 2.0.* (CD-ROM).
- European Soil Bureau Network 2005 *Soil Atlas of Europe.* Luxembourg: European Commission.
- Evans, J.A., Chinery, C.A. and J. Montgomery 2012 A summary of strontium and oxygen isotope variation in archaeological human tooth enamel excavated from Britain. *Journal of Analytical Atomic Spectrometry* 27:754–764.
- Evans, J.A., Montgomery, J. and G. Wildman 2009 Isotope domain mapping of $^{87}\text{Sr}/^{86}\text{Sr}$ biosphere variation on the Isle of Skye, Scotland. *Journal of the Geological Society* 166(4):617–631.
- Evans, J.A., Montgomery, J., Wildman, G. and N. Boulton 2010 Spatial variations in biosphere $^{87}\text{Sr}/^{86}\text{Sr}$ in Britain. *Journal of the Geological Society* 167(1):1–4.

Ewer, R.F. 1967 The fossil hyaenids of Africa-a reappraisal. In Africa, W.W.

Bishop and J.D. Clark (eds), *Background to Evolution*, pp. 935. Chicago:

University of Chicago Press.

Ezzo, J.A. and T. Douglas Price 2002 Migration, regional reorganization and spatial group composition at Grasshopper Pueblo, Arizona. *Journal of Archaeological Science* 29(5):499–520.

Ezzo, J.A., Johnson, C.M. and T.D. Price 1997 Analytical perspectives on prehistoric migration: A case study from east-central Arizona. *Journal of Archaeological Science* 24(5):447–466.

Farrand, W.R. 1979 Chronology and palaeoenvironment of levantine prehistoric sites as seen from sediment studies. *Journal of Archaeological Science* 6(4):369–392.

Farrand, W.R. 2001 Sediments and stratigraphy in rockshelters and caves: A personal perspective on principles and pragmatics. *Geoarchaeology: An International Journal* 16(5):537–557.

Fauquette, S. v., Guiot, J. I., Menut, M., de Beaulieu, J.-L., Reille, M. and P. Guenet 1999 Vegetation and climate since the last interglacial in the Vienne area (France). *Global and Planetary Change* 20(1):1–17.

Faure, G. 1986, *Principals of Isotope Geology*. New York: John Wiley and Sons.

Faure, G. 1998 *Principles and Applications of Geochemistry*. Upper Saddle River: Prentice Hall.

Faure, G. and J.L. Powell 1972 *Strontium Isotope Geology*. Berlin: Springer-Verlag.

Faure, G. and P.M. Hurley 1963 The isotopic composition of strontium in oceanic and continental basalts: Application to the origin of igneous rocks. *Journal of Petrology* 4(1):31–50.

Faure, G., Bowman, J.R., Elliot, D.H. and L.M. Jones 1974 Strontium isotope composition and petrogenesis of the Kirkpatrick basalt, Queen Alexandra Range, Antarctica. *Contributions to Mineralogy and Petrology* 48(3):153–169.

- Faure, G., Hurley, P.M. and J.L. Powell 1965 The isotopic composition of strontium in surface water from the North Atlantic Ocean. *Geochimica et Cosmochimica Acta* 29:209–220.
- Féblot-Augustins, J. 1999 Raw material transport patterns and settlement systems in the European Lower and Middle Palaeolithic. In W. Roebroeks and C. Gamble (eds), *The Middle Palaeolithic Occupation of Europe*, pp. 193–214. Leiden: Leiden University.
- Feng, J.-L., Zhu, L.-P., Zhen, Z.-L. and Z.-G. Hu 2009 Grain size effect on Sr and Nd isotopic compositions in eolian dust: Implications for tracing dust provenance and Nb model age. *Geochemical Journal* 43:123–131.
- Fietzke, J. and A. Eisenhauer 2006 Determination of temperature-dependent stable strontium isotope ($^{88}\text{Sr}/^{86}\text{Sr}$) fractionation via bracketing standard MC-ICPMS. *Geochemistry Geophysics Geosystems* 7:Q08009.
- Fincham, A.G., Luo, W., Moradian-Oldak, J., Paine, M.L., Snead, M.L. and M. Zeichner-David 2000 Enamel biomineralization: The assembly and disassembly of the protein extracellular organic matrix. In M.F. Teaford, M.M. Smith and M.W. J. Ferguson (eds), *Development, Function and Evolution of Teeth*, p. 314. Cambridge: Cambridge University Press.
- Finlayson, C. and J.S. Carrión 2007 Rapid ecological turnover and its impact on Neanderthal and other human populations. *Trends in Ecology & Evolution* 22(4):213–222.
- Fletcher, W.J., Sánchez Goñi, M.F., Allen, J.R.M., Cheddadi, R., Combourieu-Nebout, N., Huntley, B., Lawson, I., Londeix, L., Magri, D., Margari, V., Müller, U.C., Naughton, F., Novenko, E., Roucoux, K. and P.C. Tzedakis 2010 Millennial-scale variability during the last glacial in vegetation records from Europe. *Quaternary Science Reviews* 29(21–22):2839–2864.
- Flower, J.W. 1860 On a flint implement recently discovered at the base of some beds of drift-gravel and brick-earth at St. Acheul, near Amiens. *Quarterly Journal of the Geological Society* 16(1–2):190–192.

- Forster, P. 2004 Ice ages and the mitochondrial DNA chronology of human dispersals: A review. *Philosophical Transactions of the Royal Society of London Series B-Biological Sciences* 359:255–264.
- Fortunato, G., Ritter, A. and D. Fabian 2005 Old masters' lead white pigments: Investigations of paintings from the 16th to the 17th century using high precision lead isotope abundance ratios. *Analyst* 130(6):898–906.
- Foster, W.E. 1980 The square-lipped rhinoceros. *Lammergeyer* 1:25–35.
- Franzén, L.G. 1990 Transport, deposition and distribution of marine aerosols over southern Sweden during dry westerly storms. *Ambio* 19(4):180–188.
- Fraser, R.A., Grün, R., Privat, K. and M.K. Gagan 2008 Stable-isotope microprofiling of wombat tooth enamel records seasonal changes in vegetation and environmental conditions in eastern Australia. *Palaeogeography, Palaeoclimatology, Palaeoecology* 269(1–2):66–77.
- Frei, K.M., Frei, R., Mannerling, U., Gleba, M., Nosch, M.L. and H. Lyngstrøm 2009 Provenance of ancient textiles-a pilot study evaluating to strontium isotope system in wool. *Archaeometry* 51(2):252–276.
- Frenchen, M., Neber, A., Tsatskin, A., Boenigk, W. and A. Ronen 2004 Chronology of Pleistocene sedimentary cycles in the Carmel Coastal Plain of Israel. *Quaternary International* 121:41–52.
- Freund, R., Zak, I. and Z.W.I. Garfunkel 1968 Age and rate of the sinistral movement along the Dead Sea Rift. *Nature* 220(5164):253–255.
- Frost, C.D. and R.N. Toner 2004 Strontium isotopic identification of water-rock interaction and ground water mixing. *Ground Water* 42(3):418–432.
- Frost, H.M., 1964. Dynamics of bone remodelling. In H.M. Frost (ed.), *Bone Biodynamics*. pp. 315-333. London: Churchill.
- Frumkin, A. and M. Stein 2004 The Sahara-East Mediterranean dust and climate connection revealed by strontium and uranium isotopes in a Jerusalem speleothem. *Earth and Planetary Science Letters* 217(3–4):451–464.

- Frumkin, A., Bar-Yosef, O. and H.P. Schwarcz 2011 Possible paleohydrologic and paleoclimatic effects on hominin migration and occupation of the Levantine Middle Paleolithic. *Journal of Human Evolution* 60(4):437–451.
- Fullagar, P.D. and P.C. Ragland 1975 Chemical weathering and Rb-Sr whole rock ages. *Geochimica et Cosmochimica Acta* 39(9):1245–1252.
- Gäbler, H.-E. 2002 Applications of magnetic sector ICPMS in geochemistry. *Journal of Geochemical Exploration* 75(1–3):1–15.
- Gabunia, L., Vekua, A., Lordkipanidze, D., SwisherIII, C.C., Ferring, R., Justus, A., Nioradze, M., Tvalchrelidze, M., Anton, S.C., Bosinski, G., Jöris, O., Lumley, M.A., de Majsuradze, G. and A. Mouskhelishvili 2000 Earliest Pleistocene hominid cranial remains from Dmanisi, Republic of Georgia: Taxonomy, geological setting and age. *Science* 288:1019–1025.
- Gadbury, C., Todd, L., Jahren, A.H. and R. Amundson 2000 Spatial and temporal variations in the isotopic composition of bison tooth enamel from the Early Holocene Hudson-Meng Bone Bed, Nebraska. *Palaeogeography Palaeoclimatology Palaeoecology* 157:79–93.
- Gaillardet, J., Dupré, B., Allegre, C.J. and P. Négrel 1997 Chemical and physical denudation in the Amazon River Basin. *Chemical Geology* 142(3–4):141–173.
- Galili, E., Weinstein-Evron, M. and A. Ronen 1988 Holocene sea-level changes based on submerged archaeological sites off the northern Carmel Coast in Israel. *Quaternary Research* 29:36–42.
- Galili, E., Zviely, D., Ronen, A. and H.K. Mienis 2007 Beach deposits of MIS 5e high sea stand as indicators for tectonic stability of the Carmel coastal plain, Israel. *Quaternary Science Reviews* 26:2544–2557.
- Gamble, C. 1992 *The Palaeolithic Settlement of Europe*. Cambridge: Cambridge University Press.
- García-Ruiz, S., Moldovan, M., Fortunato, G., Wunderli, S. and J.I.G. Alonso 2007 Evaluation of strontium isotope abundance ratios in combination with multi-elemental analysis as a possible tool to study the geographical origin of ciders. *Analytica Chimica Acta* 590(1):55–66.

- Garfunkel, Z. 1998 Constraints on the origin and history of the Eastern Mediterranean basin. *Tectonophysics* 298(1–3):5–35.
- Garfunkel, Z., Zak, I. and R. Freund 1981 Active faulting in the Dead Sea rift. *Tectonophysics* 80:1–26.
- Gargett, R.H. 1989 Grave shortcomings: The evidence for Neanderthal burial. *Current Anthropology* 30(2):157–190.
- Gargett, R.H. 1999 Middle Palaeolithic burial is not a dead issue: The view from Qafzeh, Saint-Cesaire, Kebara, Amud and Dederiyeh. *Journal of Human Evolution* 37:27–90.
- Garrod, D.A.E. 1934 Excavations at the Wady El-Mughara 1932–1933. *Palestine Exploration Fund Quarterly* 67:85–89.
- Garrod, D.A.E. and D.M.A. Bates 1937 *The Stone Age of Mount Carmel: Description and Archaeology*. Oxford: Clarendon Press.
- Gaudzinski, S. and W. Roebroeks 2000 Adults only. Reindeer hunting at the Middle Palaeolithic site Salzgitter Lebenstedt, Northern Germany. *Journal of Human Evolution* 38(4):497–521.
- Gehler, A., Tütken, T. and A. Pack 2011 Triple oxygen isotope analysis of bioapatite as tracer for diagenetic alteration of bones and teeth. *Palaeogeography Palaeoclimatology Palaeoecology* 310:84–91.
- Gensous, B. and M. Tesson 1996 Sequence stratigraphy, seismic profiles and cores of Pleistocene deposits on the Rhône continental shelf. *Sedimentary Geology* 105(3–4):183–190.
- Ghazi, A.M. 1994 Lead in archaeological samples: An isotopic study by ICPMS. *Applied Geochemistry* 9(6):627–636.
- Gibbard, P. and T. van Kolfschoten 2004 The Pleistocene and Holocene epochs. In F.M. Gradstein, J.G. Ogg and A.G. Smith (eds), *The Geologic Time Scale 2004*. pp. 441–452. Cambridge, Cambridge University Press.
- Gibbard, P.L., Boreham, S., Cohen, K.M. and A. Moscariello 2005 Global chronostratigraphic correlation table for the last 2.7 million years. *Boreas* 34:1

- Giblin, J.I. 2009 Strontium isotope analysis of Neolithic and Copper Age populations on the Great Hungarian Plain. *Journal of Archaeological Science* 36(2):491–497.
- Giblin, J.I., Knudson, K.J., Bereczki, Z., Pálfi, G. and I. Pap 2013 Strontium isotope analysis and human mobility during the Neolithic and Copper Age: A case study from the Great Hungarian Plain. *Journal of Archaeological Science* 40(1):227–239.
- Gierlowski-Kordesch, E.H., Jacobson, A.D., Blum, J.D. and B.L. Valero Garces 2008 Watershed reconstruction of a Paleocene-Eocene lake basin using Sr isotopes in carbonate rocks. *Geological Society of America Bulletin* 120(1–2):85–95.
- Gill, A.M., Hodell, D.A., Kamenov, G.D. and M. Brenner 2009 Geological and archaeological implications of strontium isotope analysis of exposed bedrock in the Chicxulub crater basin, northwestern Yucatán, Mexico. *Geology* 37:723–726.
- Gassis, I. and O. Bar-Yosef 1974 New excavations in Zuttiyeh cave, Wadi Amud, Israel. *Paléorient* 5:175–180.
- Goede, A., McCulloch, M., McDermott, F. and C. Hawkesworth 1998 Aeolian contribution to strontium and strontium isotope variations in a Tasmanian speleothem. *Chemical Geology* 149(1–2):37–50.
- Goldberg, P. 1979 Micromorphology of Pech-de-l'Aze II sediments. *Journal of Archaeological Science* 6(1):17–47.
- Goldberg, P. 1980 Micromorphology in Archaeology and Prehistory. *Paleorient* 6:159–164.
- Goldberg, P. 2001 Some Micromorphological aspects of prehistoric cave deposits. *Cahiers d'Archéologie du CELAT, Quebec* 10:161–175.
- Goldberg, P.S. and Y. Nathan 1975 The phosphate mineralogy of et-Tabun cave, Mount Carmel, Israel. *Mineralogical Magazine* 40:253–258.
- Goldreich, Y. 1994 The spatial distribution of annual rainfall in Israel—A review. *Theoretical and Applied Climatology* 50:45–59.

- Goldreich, Y. 1995 Temporal variations of rainfall in Israel. *Climate Research* 5:167–179.
- Goodfriend, G.A. and M. Magaritz 1988 Palaeosols and late Pleistocene rainfall fluctuations in the Negev Desert. *Nature* 332:144–146.
- Gopher, A., Ayalon, A., Bar-Matthews, M., Barkai, R., Frumkin, A., Karkanas, P. and R. Shahack-Gross 2010 The chronology of the late Lower Paleolithic in the Levant based on U-Th ages of speleothems from Qesem Cave, Israel. *Quaternary Geochronology* 5(6):644–656.
- Goren, N. 1979 An Upper Acheulian industry from the Golan Heights. *Quartär* 29–30:105–121.
- Goren-Inbar, N. 1985 The Lithic assemblage of the Berekhat Ram Acheulian site, Golan Heights. *Paleorient* 11(1):7–28.
- Goren-Inbar, N., Feibel, C.S., Verosub, K.L., Melamed, Y., Kislev, M.E., Tchernov, E. and I. Saragusti 2000 Pleistocene milestones on the Out-of-Africa Corridor at Gesher Benot Ya'aqov, Israel. *Science* 289:944–947.
- Gosz, J.R. and D.I. Moore 1989 Strontium isotope studies of atmospheric inputs to forested watersheds in New Mexico. *Biogeochemistry* 8(2):115–134.
- Gratuze, B. 1999 Obsidian characterization by laser ablation ICPMS and its application to prehistoric trade in the Mediterranean and the Near East: Sources and distribution of obsidian within the Aegean and Anatolia. *Journal of Archaeological Science* 26(8):869–881.
- Graustein, W.C. and R.L. Armstrong 1983 The Use of strontium-87/strontium-86 ratios to measure atmospheric transport into forested watersheds. *Science* 219(4582):289–292.
- Grave, P., Lisle, L. and M. Maccheroni 2005 Multivariate comparison of ICP-OES and PIXE/PIGE analysis of east Asian storage jars. *Journal of Archaeological Science* 32(6):885–896.
- Graves, H.B. 1984 Behavior and ecology of wild and feral swine (*Sus scrofa*). *Journal of Animal Science* 58:482–492.

- Grayson, D.K. and F. Delpech 2002 Specialized Early Upper Palaeolithic hunters in southwestern France? *Journal of Archaeological Science* 29(12):1439–1449.
- Grayson, D.K. and S.C. Coe 1998 Stone tool assemblage richness during the Middle and Early Upper Palaeolithic in France. *Journal of Archaeological Science* 25:927–938.
- Green, R.E., Krause, J., Briggs, A.W., Maricic, T., Stenzel, U., Kircher, M., Patterson, N., Li, H., Zhai, W., Fritz, M. H.-Y., Hansen, N.F., Durand, E.Y., Malaspinas, A.-S., Jensen, J.D., Marques-Bonet, T., Alkan, C., Prüfer, K., Meyer, M., Burbano, H.A., Good, J.M., Schultz, R., Aximu-Petri, A., Butthof, A., Höber, B., Höffner, B., Siegemund, M., Weihmann, A., Nusbaum, C., Lander, E.S., Russ, C., Novod, N., Affourtit, J., Egholm, M., Verna, C., Rudan, P., Brajkovic, D., Kucan, Å., Gušic, I., Doronichev, V.B., Golovanova, L.V., Lalueza-Fox, C., de la Rasilla, M., Fortea, J., Rosas, A., Schmitz, R.W., Johnson, P.L.F., Eichler, E.E., Falush, D., Birney, E., Mullikin, J.C., Slatkin, M., Nielsen, R., Kelso, J., Lachmann, M., Reich, D. and S. Pääbo 2010 A draft sequence of the Neanderthal genome. *Science* 328(5979):710–722.
- Grosbois, C., Négrel, P., Fouillac, C. and D. Grimaud 2000 Dissolved load of the Loire River: Chemical and isotopic characterization. *Chemical Geology* 170(1–4):179–201.
- Grousset, F.E., Biscaye, P.E., Revel, M., Petit, J.-R., Pye, K., Joussaume, S. and J. Jouzel 1992 Antarctic (Dome C) ice-core dust at 18 k.y. B.P.: Isotopic constraints on origins. *Earth and Planetary Science Letters* 111(1):175–182.
- Groves, C. 1981 *Ancestors for the Pigs: Taxonomy and Phylogeny of the Genus Sus*. Technical Bulletin No 3. Canberra: Department of Prehistory, Research School of Pacific Studies, Australian National University.
- Groves, C.P. 1972 Ceratotherium simum. *Mammalian Species* 8:1–6.

- Groves, C.P. 2007 Current views on taxonomy and zoogeography of the genus *Sus*. In U. Albarella, K. Dobney, A. Ervynck and P. Rowley-Conwy (eds), *Pigs and Humans: 10,000 Years of Interaction*, pp. 15–29. Oxford: Oxford University Press.
- Groves, C.P. and F. Kurt 1972 *Dicerorhinus sumatrensis*. *Mammalian Species* 21:1–6.
- Grün, R. and C. Stringer 2000 Tabun revisited: Revised ESR chronology and new ESR and U-series analyses of dental material from Tabun C1. *Journal of Human Evolution* 39(6):601–612.
- Grün, R. and C.B. Stringer 1991 Electron-spin-resonance dating and the evolution of modern humans. *Archaeometry* 33:153–199.
- Grün, R., Aubert, M., Joannes-Boyau, R. and M.H. Moncel 2008 High resolution analysis of uranium and thorium concentration as well as U-series isotope distributions in a Neanderthal tooth from Payre (Ardeche, France) using laser ablation ICPMS. *Geochimica et Cosmochimica Acta* 72(21):5278–5290.
- Grün, R., Maroto, J., Eggins, S., Stringer, C., Robertson, S., Taylor, L., Mortimer, G. and M. McCulloch 2006 ESR and U-series analysis of enamel and dentine fragments of the Banyoles mandible. *Journal of Human Evolution* 50:347–358.
- Grün, R., Stringer, C., McDermott, F., Nathan, R., Porat, N., Robertson, S., Taylor, L., Mortimer, G., Eggins, S. and M. McCulloch 2005 U-series and ESR analyses of bones and teeth relating to the human burials from Skhul. *Journal of Human Evolution* 49(3):316–334.
- Grün, R., Stringer, C.B. and H.P. Schwarcz 1991 ESR dating of teeth from Garrod Tabun Cave collection. *Journal of Human Evolution* 20(3):231–248.
- Grün, R., Yan, G., McCulloch, M.T. and G. Mortimer 1999 Detailed mass spectrometric U-series analyses of two teeth from the archaeological site of Pech de l’Aze II: Implications for uranium migration and dating. *Journal of Archaeological Science* 26(10):1301–1310.

- Grupe, G., Price, T.D., Schröter, P., Söllner, F., Johnson, C.M. and B.L. Beard 1997 Mobility of Bell Beaker people revealed by strontium isotope ratios of tooth and bone: A study of southern Bavarian skeletal remains. *Applied Geochemistry* 12(4):517–525.
- Grynpas, M.D., Hamilton, E., Cheung, R., Tsouderos, Y., Deloffre, P., Hott, M. and P.J. Marie 1996 Strontium increases vertebral bone volume in rats at a low dose that does not induce detectable mineralization defect. *Bone* 18(3):253–259.
- Guérin, G., Discamps, E., Lahaye, C., Mercier, N., Guibert, P., Turq, A., Dibble, H.L., McPherron, S.P., Sandgathe, D., Goldberg, P., Jain, M., Thomsen, K., Patou-Mathis, M., Castel, J.-C. and P. Soulier, M.-C. 2012 Multi-method (TL and OSL), multi-material (quartz and flint) dating of the Mousterian site of Roc de Marsal (Dordogne, France): Correlating Neanderthal occupations with the climatic variability of MIS 5–3. *Journal of Archaeological Science* 39(10):3071–3084.
- Guerra, M.F., Sarthre, C.O., Gondonneau, A. and J.N. Barrandon 1999 Precious metals and provenance enquiries using LA-ICPMS. *Journal of Archaeological Science* 26(8):1101–1110.
- Guillermin 2006 Les Fieux: Une occupation gravettienne du Causse quercinois. *Paleo* 18:69–94.
- Gvirtzman, G., Netser, M. and E. Katsav 1998 Late-Glacial to Holocene Kurkar ridges, Hamra soils and dune fields in the coastal belt of central Israel. *Israel Journal of Earth Sciences* 47:29–46.
- Haak, W., Brandt, G., de Jong, H.N., Meyer, C., Ganslmeier, R., Heyd, V., Hawkesworth, C., Pike, A.W.G., Meller, H. and K.W. Alt 2008 Ancient DNA, Strontium isotopes and osteological analyses shed light on social and kinship organization of the Later Stone Age. *Proceedings of the National Academy of Science* 105(47):18226–18231.
- Haas, G. 1968 *On the Fauna of Ubeidiya*. Jerusalem: Israel Academy of Humanities and Science.

- Habicht-Mauche, J.A., Glenn, S.T., Milford, H. and A.R. Flegal 2000 Isotopic tracing of prehistoric Rio Grande glaze-paint production and trade. *Journal of Archaeological Science* 27(8):709–713.
- Halicz, L., Segal, I., Fruchter, N., Stein, M. and B. Lazar 2008 Strontium stable isotopes fractionate in the soil environments? *Earth and Planetary Science Letters* 272:406–411.
- Hall, M.E., Brimmer, S.P., Li, F.-H. and L. Yablonsky 1998 ICPMS and ICP-OES studies of gold from a Late Sarmatian burial. *Journal of Archaeological Science* 25(6):545–552.
- Halliday, A.N., Lee, D.-C., Christensen, J.N., Rehkämper, M., Yi, W., Luo, X., Hall, C.M., Ballentine, C.J., Pettke, T. and C. Stirling 1998 Applications of multiple collector-ICPMS to cosmochemistry, geochemistry and paleoceanography. *Geochimica et Cosmochimica Acta* 62(6):919–940.
- Hallin, K.A., Schoeninger, M.J. and H.P. Schwarcz 2012 Paleoclimate during Neandertal and anatomically modern human occupation at Amud and Qafzeh, Israel: The stable isotope data. *Journal of Human Evolution* 62(1):59–73.
- Halpern, M. and N. Tristan 1981 Geochronology of the Arabian-Nubian shield in southern Israel and eastern Sinai. *The Journal of Geology* 89(5):639–648.
- Hamel, B.L., Stewart, B.W. and A.G. Kim 2001 Tracing the interaction of acid mine drainage with coal utilization byproducts in a grouted mine: Strontium isotope study of the inactive Omega Coal Mine, West Virginia (USA). *Applied Geochemistry* 25(2):212–223.
- Hamr, J. 1985 Seasonal home range size and utilisation by female chamois (*Rupicapra rupicapra* L.) in Northern Tyrol. In S. Lovari (ed.), *The Biology and Management of Mountain Ungulates*, pp. 106–116. Beckenham: Croom Helm.
- Hart, S.R. 1964 The Petrology and Isotopic-Mineral age relations of a contact zone in the Front Range, Colorado. *The Journal of Geology* 72(5):493–525.

- Hauser, O. 1909 Decouverte d'un squelette du type de Neandertal sous l'abri inferieur du Moustier, Station No 44, Commune de Saint-Leon (Dordogne). *L'Homme Prehistory* 7:1–9.
- Haliva-Cohen, A. Stein, M. Goldstein, S. L. Sandler, A and A. Starinsky 2012 Sources and transport routes of fine detritus material to the Late Quaternary Dead Sea basin. *Quaternary Science Reviews* 50:55–70.
- Hay, R.L. 1976 *Geology of the Olduvai Gorge*. Berkeley: University of California Press.
- Hazan, N., Stein, M., Agnon, A., Marco, S., Nadel, D., Negendank, J.F.W., Schwab, M.J. and D. Neev 2005 The late Quaternary limnological history of Lake Kinneret (Sea of Galilee), Israel. *Quaternary Research* 63(1):60–77.
- Hedge, C.E. 1974 Strontium isotopes in economic geology. *Economic Geology* 69:823–825.
- Hedge, C.E. and F.G. Walthall 1963 Radiogenic strontium-87 as an index of geologic processes. *Science* 140:1214–1217.
- Hedman, K.M., Curry, B.B., Johnson, T.M., Fullagar, P.D. and T.E. Emerson 2009 Variation in strontium isotope ratios of archaeological fauna in the Midwestern United States: A preliminary study. *Journal of Archaeological Science* 36(1):64–73.
- Henry, D.O. 2003 The Levant and the modern human debate. In D.O. Henry (ed.), *Neaderthals in the Levant: Behavioral Organisation and the Beginnings of Human Modernity*, pp. 12–30. London: Continuum.
- Hershkovitz, I., Smith, P., Sarig, R., Quam, R., Rodríguez, L., García, R., Arsuaga, J.L., Barkai, R. and A. Gopher 2011 Middle pleistocene dental remains from Qesem Cave (Israel). *American Journal of Physical Anthropology* 144(4):575–592.
- Herut, B., Starinsky, A. and A. Katz 1993 Strontium in rainwater from Israel: Sources, isotopes and chemistry. *Earth and Planetary Science Letters* 120(1–2):77–84.

- Hiller, C., Robinson, C. and J. Weatherell 1975 Variations in the composition of developing rat incisor enamel. *Calcified Tissue International* 18(1):1–12.
- Hillman-Smith, A.K.K. and C.P. Groves 1994 Diceros bicornis. *Mammalian Species* 455:1–8.
- Hillson, S. 2005 *Teeth*. Cambridge: Cambridge University Press.
- Hiscott, R.N., Wilson, R.C.L., Gradstein, F.M., Pujalte, V., Garcia-Mondejar, J., Boudreau, R.R. and H.A. Wishart 1990 Comparative stratigraphy and Subsidence history of Mesozoic Rift Basins of North Atlantic. *AAPG Bulletin* 74:60–76.
- Hobson, K.A. 1999 Tracing origins and migration of wildlife using stable isotopes: A review. *Oecologia* 120(3):314–326.
- Hodgkins, J.M. 2012 Tracking Climate-Driven Changes in Neanderthal Subsistence Behaviours and Prey Mobility Patterns. Unpublished PhD Thesis. Arizona State University.
- Hoekman-Sites, H.A. and J.I. Giblin 2012 Prehistoric animal use on the Great Hungarian Plain: A synthesis of isotope and residue analyses from the Neolithic and Copper Age. *Journal of Anthropological Archaeology* 31(4):515–527.
- Hofer, H. 1998a Spotted hyaena *Crocuta crocuta* (Erxleben, 1977). In M.G.L. Mills and H. Hofer (eds), *Hyaenas. Status Survey and Conservation Action Plan*, pp. 154. Gland: IUCN.
- Hofer, H. 1998b Striped hyaena *Hyaena (Hyaena) hyaena* (Linnaeus, 1758). In M.G.L. Mills and H. Hofer (eds), *Hyaenas. Status Survey and Conservation Action Plan*, pp. 154. Gland: IUCN.
- Holdaway, S. and N. Stern 2004 *A Record in Stone: The Study of Australia's Flaked Stone Artefacts*. Melbourne: Museum of Victoria.
- Holmden, C., Creaser, R.A. and K. Muehlenbachs 1997 Paleosalinities in ancient brackish water systems determined by $^{87}\text{Sr}/^{86}\text{Sr}$ ratios in carbonate fossils: A case study from the Western Canada sedimentary basin. *Geochimica et Cosmochimica Acta* 61(10):2105–2118.

- Hoogewerff, J., Papesch, W., Kralik, M., Berner, M., Vroon, P., Miesbauer, H., Gaber, O., Künzel, K.-H. and J. Kleinjans 2001 The last domicile of the iceman from Hauslabjoch: A geochemical approach using Sr, C and O isotopes and trace element signatures. *Journal of Archaeological Science* 28(9):983–989.
- Hoppe, K.A. and P.L. Koch 2007 Reconstructing the migration patterns of late Pleistocene mammals from northern Florida, USA. *Quaternary Research* 68(3):347–352.
- Hoppe, K.A., Koch, P.L., Carlson, R.W. and S.D. Webb 1999 Tracking mammoths and mastodons: Reconstruction of migratory behavior using strontium isotope ratios. *Geology* 27(5):439–442.
- Hoppe, K.A., Stover, S., M., Pascoe, J.R. and R. Amundson 2004 Tooth enamel biomineralization in extant horses: Implications for isotopic microsampling. *Palaeogeography Palaeoclimatology Palaeoecology* 206:355–365.
- Horn, P., Hözl, S. and D. Storzer 1994 Habitat determination on a fossil stag's mandible from the site of Homo erectus heidelbergensis at Mauer by use of $^{87}\text{Sr}/^{86}\text{Sr}$. *Naturwissenschaften* 81(8):360–362.
- Horn, P., Schaaf, P., Holbach, B., Hözl, S. and H. Eschnauer 1993 $^{87}\text{Sr}/^{86}\text{Sr}$ from rock and soil into vine and wine. *Zeitschrift für Lebensmitteluntersuchung und -Forschung A* 196(5):407–409.
- Horowitz, A. 1973 Development of the Hula Basin, Israel. *Israel Journal of Earth Sciences* 22:107–139.
- Horowitz, A. 1979 *The Quaternary of Israel*. New York: Academic Press.
- Horowitz, A. 1987 Travertines of the arid regions, oxygen isotope stages and Late Quaternary climates of Israel. *Quaternary Research* 27:103–105.
- Horowitz, A. 1989 Continuous pollen diagrams for the last 3.5 m.y. from Israel: Vegetation, climate and correlation with the oxygen isotope record. *Palaeogeography, Palaeoclimatology, Palaeoecology* 72(0):63–78.

- Horowitz, A. and J.R. Gat 1984 Floral and isotopic indications for possible summer rains in Israel during wetter conditions. *Pollen et Spores* 26:61–68.
- Horstwood, M.S.A., Evans, J.A. and J. Montgomery 2008 Determination of Sr isotopes in calcium phosphates using laser ablation inductively coupled plasma mass spectrometry and their application to archaeological tooth enamel. *Geochimica et Cosmochimica Acta* 72(23):5659–5674.
- Horwitz, E.P., Chiarizia, R. and M.L. Dietz 1992 A novel strontium-selective extraction chromatographic resin. *Solvent Extraction and Ion Exchange* 10(2):313 - 336.
- Horwitz, L.K., Chazan, M., Lister, A., Monchot, H. and N. Porat 2007 The Late Lower Paleolithic site of Holon, Israel: Subsistence, technology and chronology. *Journal of Anthropological Archaeology* 25, 436–447.
- Hovers, E. 1997 Variability of the Levantine Mousterian Assemblages and Settlement Patterns: Implications for the Development of Human Behaviour. Unpublished PhD thesis, Institut of Archaeology, Hebrew University of Jerusalem.
- Hovers, E. 2009 *The Lithic Assemblages of Qafzeh Cave*. Oxford: Oxford University Press.
- Hovers, E., Hani, S., Bar-Yosef, O. and B. Vandermeersch 2003 An early case of colour symbolism-Ochre use by modern humans in Qafzeh cave. *Current Anthropology* 44:491–522.
- Hovers, E., Rak, Y., Lavi, R. and W.H. Kimbel 1995 Homonid remains from Amud cave in the context of the Levantine Middle Paleolithic. *Paleorient* 21(2):47–61.
- Howell, F.C. 1998 Evolutionary implications of altered perspectives on hominin demes and populations in the Later Pleistocene of western Eurasia. In T. Akazawa, K. Aoki and O. Bar-Yosef (eds), *Neanderthals and Modern Humans in Western Asia*, pp. 2–27. New York: Plenum Press.
- Hublin, J.J. 2009 The origin of Neanderthals. *Proceedings of the National Academy of Sciences* 106(38):16022–16027.

- Humphrey, L.T., Dean, M.C., Jeffries, T.E. and M. Penn 2008 Unlocking evidence of early diet from tooth enamel. *Proceedings of the National Academy of Science* 105(19):6834–3839.
- Hurley, P.M., Cormier, R.F., Hower, J., Fairbairn, H.W. and W.H. Pinson 1960 Reliability of glauconite for age measurements by K-Ar and Rb-Sr methods. *American Association of Petroleum Geologists Bulletin* 44:1793–1808.
- Hurrel, J.W. 1995 Decadal trends in the North Atlantic oscillations: Regional temperatures and precipitation. *Science* 269:676–679.
- Hutchin, M.E. and B.E. Vaughan 1967 Relation between calcium and strontium transport rates as determined simultaneously in isolated segments of the primary root of Zea mays. *Plant Physiology* 42:644–650.
- Hutchin, M.E. and B.E. Vaughan 1968 Relation between simultaneous Ca and Sr transport rates in isolated segments of vetch, barley and pine roots. *Plant Physiology* 43:1913–1918.
- Iñañez, J.G., Bellucci, J.J., Rodríguez-Alegría, E., Ash, R., McDonough, W. and R.J. Speakman 2010 Romita pottery revisited: A reassessment of the provenance of ceramics from Colonial Mexico by LA-MC-ICPMS. *Journal of Archaeological Science* 37:2698–2704.
- Isaac, G. 1971 The diet of early man: Aspects of Archaeological evidence from Lower and Middle Pleistocene sites in Africa. *World Archaeology* 2(3):278–299.
- Issar, A. 1968 Geology of central coastal plain of Israel. *Israel Journal of Earth Sciences* 17:16–29.
- Issar, A., Bein, A. and A. Michaeli 1972 On the ancient water of the upper Nubian sandstone aquifer in Central Sinai and southern Israel. *Journal of Hydrology* 17(4):353–374.
- Jacks, G., Åberg, G. and P.J. Hamilton 1989 Calcium budgets for catchments as interpreted by strontium isotopes. *Nordic Hydrology* 90:85–96.

- Jackson, M.G. and S.R. Hart 2006 Strontium isotopes in melt inclusions from Samoan basalts: Implications for heterogeneity in the Samoan plume. *Earth and Planetary Science Letters* 245(1–2):260–277.
- Jackson, S.E. and D. Günther 2003 The nature and sources of laser induced isotopic fractionation in laser ablation-multicollector-inductively coupled plasma-mass spectrometry. *Journal of Analytical Atomic Spectrometry* 18(3):205–212.
- Jaric, J. 2004 Use of Pb and Sr isotopes in human teeth as an indicator of Pacific Islander population dynamics. Unpublished PhD thesis, School of Science, Food and Horticulture, University of Western Sydney
- Jaubert, J. 1983 Le site moustérien du Rescoundudou (Sebazac-Concoures, Aveyron), présentation et problématique. *Bulletin de la Société Préhistorique Française* 80(3):80–87.
- Jaubert, J. 2008 L'art pariétal gravettien en France: Éléments pour un bilan chronologique. *Paleo* 20:439–474.
- Jaubert, J. and B. Maureille 2008 Le gisement moustérien du Rescoundudou (Sebazac-Concoures, Aveyron): Inventaire des restes humains. *Bulletine de la Societe prehistorique francaise* 105(4):677–690.
- Jaubert, J., Bordes, J.-G., Discamps, E. and B. Gravina 2011 A New look at the end of the Middle Palaeolithic sequence in southwestern France. In A.P. Derevianko and M.V. Shunkov (eds), *Characteristic Features of the Middle to Upper Paleolithic Transition in Eurasia*, pp. 102–115. Novosibirsk: Asian Palaeolithic Association.
- Jaubert, J., Kervazo, B., Quinif, Y., Brugal, J-P and W. O'yl 1992 Les Site Paléolithique Moyen Du Rescoundudou (Aveyron, France) Datations U/Th Et Interprétation Chronostratigraphique *L'Anthropologie*, 96(1):103–112.
- Jelinek, A.J. 1982a. The Tabun Cave and Paleolithic man in the Levant. *Science* 216:1369–1375.

- Jelinek, A.J. 1982b. The Middle Paleolithic in the southern Levant, with comments on the appearance of modern Homo sapiens. In A. Ronen (ed.), *The Transition from Lower to Middle Palaeolithic and the Origin of Modern Man*, pp. 57–104. Oxford: BAR International Series 151.
- Jelinek, A.J., Farrand, W.R., Hass, G., Horowitz, A. and P. Goldberg 1973 New excavations at the Tabun cave, Mount Carmel, Israel. 1967–1972: A preliminary report. *Paleorient* 1:151–183.
- Jenks, S.M. and L. Werdelin 1998 Taxonomy and systematics of living hyaenas (family hyaenidae). In M.G.L. Mills and H. Hofer (eds), *Hyenas: Status Survey and Conservation Action Group*, pp. 154pp. Gland: IUCN.
- Jin, Z., Yu, J., Wang, S., Zhang, F., Shi, Y. and C.-F. You 2009 Constraints on water chemistry by chemical weathering in the Lake Qinghai catchment, northeastern Tibetan Plateau (China): Clues from Sr and its isotopic geochemistry. *Hydrogeology Journal* 17(8):2037–2048.
- Joannes-Boyau, R. and R. Grün 2009 Thermal behavior of orientated and non-orientated CO_2^- radicals in tooth enamel. *Radiation Measurements* 44:505-511.
- Joannes-Boyau, R. Bodin, T. and R. Grün 2010 Decomposition of the angular ESR spectra of fossil tooth enamel fragments. *Radiation Measurements* 45:887-898.
- Joannes-Boyau, R., Grün, R. and T. Bodin 2010 Decomposition of the laboratory gamma irradiation component of angular ESR spectra of fossil tooth enamel fragments. *Applied Radiation and Isotopes* 68:1798-1808.
- Joannes-Boyau, R. and R. Grün 2010 Decomposition of UV induced ESR spectra in modern and fossil dental enamel fragments. *Ancient TL* 28(1):23-34.
- Joannes-Boyau, R. and R. Grün 2011a Decomposition of beta-ray induced ESR spectra of fossil tooth enamel. *Radiation Physics and Chemistry* 80(3):335-342.

- Joannes-Boyau, R. and R. Grün 2011b A comprehensive model for CO₂⁻ radicals in fossil tooth enamel: Implications for ESR dating. *Quaternary Geochronology* 6:82-97.
- Jones, R. 1992 Philosophical time travellers. *Antiquity* 66(252):744–757.
- Jones, R., Challands, A., French, C., Card, N., Downes, J. and C. Richards 2010 Exploring the location and function of a Late Neolithic house at Crossiecrown, Orkney by geophysical, geochemical and soil micromorphological methods. *Archaeological Prospection* 17:29–47.
- Julien, M.-A., Bocherens, H., Burke, A., Drucker, D.G., Patou-Mathis, M., Krotava, O. and S. Péan 2012 Were European steppe bison migratory? ¹⁸O, ¹³C and Sr intra-tooth isotopic variations applied to a palaeoethological reconstruction. *Quaternary International* 271:106–119.
- Junk, S.A. 2001 Ancient artefacts and modern analytical techniques-Usefulness of laser ablation ICPMS demonstrated with ancient gold coins. *Nuclear Instruments and Methods in Physics Research Section B: Beam Interactions with Materials and Atoms* 181(1–4):723–727.
- Kawasaki, K. 1975 On the configuration of incremental lines in human dentine as revealed by tetracycline labelling. *Journal of Anatomy* 119(1):61–66.
- Kelly, T.E. 2007 Strontium Isotope Tracing in Animal Teeth at the Neanderthal site of Les Pradelles, Charante, France. Unpublished Honours thesis, Department of Earth and Marine Sciences, Australian National University.
- Kennett, D.J., Anderson, A.J., Cruz, M.J., Clark, G.R. and G.R. Summerhayes 2004 Geochemical characterization of Lapita pottery via inductively coupled plasma–mass spectrometry (ICP–MS). *Archaeometry* 46(1):35–46.
- Kennett, D.J., Neff, H., Glascock, M.D. and A.Z. Mason 2001 A geochemical revolution: Inductively coupled plasma mass spectrometry. *The Archaeological Record* 1:22–26.

- Kennett, D.J., Sakai, S., Neff, H., Gossett, R. and D.O. Larson 2002 Compositional characterization of prehistoric ceramics: A new approach. *Journal of Archaeological Science* 29(5):443–455.
- Kirkham, J., Robinson, C., Weatherell, J.A., Richards, A., Fejerskov, O. and K. Josephsen 1988 Maturation in developing permanent porcine enamel. *Journal of Dental Research* 67(9):1156–1160.
- Klaus, J., Hansen, B. and S. Buapeng 2007 $^{87}\text{Sr}/^{86}\text{Sr}$ ratio: A natural tracer to monitor groundwater flow paths during artificial recharge in the Bangkok area, Thailand. *Hydrogeology Journal* 15(4):745–758.
- Klemenc, S., Budic, B. and J. Zupan 1999 Statistical evaluation of data obtained by inductively coupled plasma atomic emission spectrometry (ICP-AES) for archaeological copper ingots. *Analytica Chimica Acta* 389(1–3):141–150.
- Klemme, S., Prowatke, S., Münker, C., Magee, C.W., Lahaye, Y., Zack, T., Kasemann, S.A., Cabato, E.J.A. and B. Kaeser 2008 Synthesis and preliminary characterisation of new silicate, phosphate and titanite reference glasses. *Geostandards and Geoanalytical Research* 32(1):39–54.
- Klinger, Y., Avouac, J.P., Dorbath, L., Abou Karaki, N. and N. Tisnerat 2000 Seismic behaviour of the Dead Sea fault along Araba valley, Jordan. *Geophysical Journal International* 142:769–782.
- Knudson, K.J., Frink, L., Hoffman, B.W. and T.D. Price 2004 Chemical characterization of Arctic soils: Activity area analysis in contemporary Yup'ik fish camps using ICP-AES. *Journal of Archaeological Science* 31(4):443–456.
- Knudson, K.J., Price, T.D., Buikstra, J.E. and D.E. Blom 2004 The use of strontium isotope analysis to investigate Tiwanaku migration and mortuary ritual in Bolivia and Peru. *Archaeometry* 46(1):5–18.

- Knudson, K.J., Tung, T.A., Nystrom, K.C., Price, T.D. and P.D. Fullagar 2005
The origin of the Juch'upampa Cave mummies: Strontium isotope analysis of archaeological human remains from Bolivia. *Journal of Archaeological Science* 32(6):903–913.
- Knudson, K.J., Williams, H.M., Buikstra, J.E., Tomczak, P.D., Gordon, G.W. and A.D. Anbar 2010 Introducing $\delta^{88/86}\text{Sr}$ analysis in archaeology: A demonstration of the utility of strontium isotope fractionation in paleodietary studies. *Journal of Archaeological Science* 37(9):2352–2364.
- Knudson, K.J., Williams, S.R., Osborn, R., Forgey, K. and P.R. Williams 2009
The geographic origins of Nasca trophy heads using strontium, oxygen and carbon isotope data. *Journal of Anthropological Archaeology* 28(2):244–257.
- Koch, P.L., Heisinger, J., Moss, C., Carlson, R.W., Fogel, M.L. and A.K. Behrensmeyer 1995 Isotopic tracking of change in diet and habitat use in African elephants. *Science* 267(5202):1340–1343.
- Kodaka, T., Debari, K. and M. Yamada 1991 Physico-chemical and morphological studies of horse dentin. *Journal of Electron Microscopy* 40(6):385–391.
- Koehler, C.E. and P.R.K. Richardson 1990 *Proteles cristatus*. *Mammalian Species* 363:1–6.
- Kramer, P.A. and G.G. Eck 2000 Locomotor energetics and leg length in hominid bipedality. *Journal of Human Evolution* 38(5):651–666.
- Krasilnikov, P., Marti, J.-J. I., Arnold, R. and S. Shoba 2009 *Soil Terminology, Correlation and Classification*. London: Earthscan.
- Krom, M.D., Cliff, R.A., Eijnsink, L.M., Herut, B. and R. Chester 1999 The characterisation of Saharan dusts and Nile particulate matter in surface sediments from the Levantine basin using Sr isotopes. *Marine Geology* 155(3–4):319–330.

- Kröner, A., Eyal, M. and Y. Eyal 1990 Early Pan-African evolution of the basement around Elat, Israel, and the Sinai Peninsula revealed by single-zircon evaporation dating and implications for crustal accretion rates. *Geology* 18(6):545–548.
- Kruuk, H. 1972 Feeding and social behaviour of the striped hyaena (*Hyaena vulgaris* Desmarest). *East African Wildlife Journal* 14:91–111.
- Kulp, J.L., Eckelmann, W.R. and A.R. Schulert 1957 Strontium-90 in man. *Science* 125:219–225.
- Kume, T., Akca, E., Nakano, T., Nagano, T., Kapur, S. and T. Watanabe 2010 Seasonal changes of fertilizer impacts on agricultural drainage in a salinized area in Adana, Turkey. *Science of The Total Environment* 408(16):3319–3326.
- Kurtén, B. 1965 Carnivora of the Palestine caves. *Acta Zoologica Fennica* 107:1–74.
- Kurtén, B. 1968 *Pleistocene Mammals of Europe*. London: Weidenfeld and Nicolson.
- Kurtz, A.C., Derry, L.A. and O.A. Chadwick 2001 Accretion of Asian dust to Hawaiian soils: Isotopic, elemental and mineral mass balances. *Geochimica et Cosmochimica Acta* 65(12):1971–1983.
- Laborde, E.D. 1961 *Western Europe*. London: London University Press.
- Lacruz, R.S., Rozzi, F.R. and T.G. Bromage 2006 Variation in enamel development of South African fossil hominids. *Journal of Human Evolution* 51:580–590.
- Langgut, D., Almogi-Labin, A., Bar-Matthews, M. and M. Weinstein-Evron 2011 Vegetation and climate changes in the South Eastern Mediterranean during the Last Glacial-Interglacial cycle (86 ka): New marine pollen record. *Quaternary Science Reviews* 30(27–28):3960–3972.

- Langley, M.C., Clarkson, C. and S. Ulm 2008 Behavioural complexity in Eurasian neanderthal populations: A chronological examination of the archaeological evidence. *Cambridge Archaeological Journal* 18(03):289–307.
- Lasaga, A.C. 1984 Chemical kinetics of water-rock interactions. *Journal of Geophysical Research* 89(B6):4009–4025.
- Larivière, S. and M. Pasitschniak-Arts 1996 *Vulpes vulpes*. *Mammalian Species* 537:1-11.
- Laurie, W.A., Lang, E.M. and C.P. Groves 1983 *Rhinoceros unicornis*. *Mammalian Species* 211:1–6.
- Lavi, R. 1994 The Amud I Skull-Taxonomic Assessment and Phylogenetic Status. Unpublished Masters thesis, Department of Anatomy and Anthropology, Tel-Aviv University.
- Laville, H. 1975 *Climatologie et chronologie du Paleolithiqueen Perigord: Etude sedimentologiquede depots en grottes et sous abris*. Marseilles: Etudes Quaternaires de l'Universite de Provence: Memoire 4.
- Laville, H., Rigaud, J.-P. and J. Sackett 1980 *Rockshelters of the Perigord: Geological Stratigraphy and Archaeological Succession*. London: Academic Press.
- Lawrence, R.D. 1974 *Wildlife in North America: Mammals*. London: Michael Joseph.
- Laws, R.M. 1968 Dentition and ageing of the hippopotamus. *African Journal of Ecology* 6(1):19–52.
- Le Bas, M.J., Spiro, B. and X. Yang 1997 Oxygen, carbon and strontium isotope study of the carbonatitic dolomite host of the Bayan Obo Fe-Nb-REE deposit, Inner Mongolia, N China. *Mineralogical Magazine* 61(4):531–541.
- Leakey, M.G., Spoor, F., Dean, M.C., Feibel, C.S., Anton, S.C., Kiarie, C. and L.N. Leakey 2012 New fossils from Koobi Fora in northern Kenya confirm taxonomic diversity in early Homo. *Nature* 488(7410):201–204.

- Lee, K.M., Appleton, J., Cooke, M., Keenan, F. and K. Sawicka-Kapusta 1999 Use of laser ablation inductively coupled plasma mass spectrometry to provide element versus time profiles in teeth. *Analytica Chimica Acta* 395(1–2):179–185.
- Leeder, M.R., Harris, T. and M.J. Kirkby 1998 Sediment supply and climate change: Implications for basin stratigraphy. *Basin Research* 10(1):7–18.
- Lees, W. 2010 *In situ strontium isotope analysis of human teeth from Teouma, Efate, Vanuatu for tracing Lapita colonization*. Unpublished Masters thesis, School of Archaeology and Anthropology, Australian National University.
- Lee-Thorp, J. 2002 Two decades of progress towards understanding fossilization processes and isotopic signals in calcified tissue minerals. *Archaeometry* 44(3):435–446.
- Lericolais, G., Berné, S. and H. Fenies 2001 Seaward pinching out and internal stratigraphy of the Gironde incised valley on the shelf (Bay of Biscay). *Marine Geology* 175:183–197.
- Leung, C.-M. and J.J. Jiao 2006 Use of strontium isotopes to identify buried water main leakage into groundwater in a highly urbanized coastal area. *Environmental Science & Technology* 40(21):6575–6579.
- Levine, M.A. 1982 The use of crown height measurements and eruption-wear sequences to age horse teeth. In B. Wilson, C. Grigson and S. Payne (eds), *Ageing and Sexing Animal Bones from Archaeological Sites*. pp. 223–250. Oxford: BAR International Series 266.
- Li, B.-P., Greig, A., Zhao, J.-X., Collerson, K.D., Quan, K.-S., Meng, Y.-H. and Z.-l. Ma 2005. ICPMS trace element analysis of Song dynasty porcelains from Ding, Jiexiu and Guantai kilns, north China. *Journal of Archaeological Science* 32(2):251–259.

- Li, B-P., Zhao, J.-X., Greig, A., Collerson, K.D., Feng, Y.-X., Sun, X.-M., Guo, M.-S. and Z.-X. Zhuo 2006 Characterisation of Chinese Tang sancai from Gongxian and Yaozhou kilns using ICPMS trace element and TIMS Sr–Nd isotopic analysis. *Journal of Archaeological Science* 33(1):56–62.
- Lieberman, D.E. 1994 The biological basis for seasonal increments in dental cementum and their application to archaeological research. *Journal of Archaeological Science* 21:525–539.
- Lieberman, D.E. 1998 Neanderthal and early modern human mobility patterns: Comparing archaeological and anatomical evidence. In T. Akazawa, K. Aoki and O. Bar-Yosef (eds), *Neanderthals and Humans in Western Asia*. pp. 263–275. New York: Plenum Press.
- Lieberman, D.E. and J.J. Shea 1994 Behavioral differences between archaic and modern humans in the Levantine Mousterian. *American Anthropologist* 96(2):300–332.
- Lieberman, P. and E.S. Crelin 1971 On the speech of neanderthal man. *Linguistic Inquiry* 2(2):203–222.
- Livnat, A. and J. Kronfeld 1985 Paleoclimatic implications of U-series dates for lake sediments and travertines in the Arava Rift Valley, Israel. *Quaternary Research* 24:164–172.
- Longerich, H.P., Fryer, B.J. and D.F. Strong 1987 Trace analysis of natural alloys by inductively coupled plasma-mass spectrometry (ICPMS): Application to archeological native silver artifacts. *Spectrochimica Acta Part B: Atomic Spectroscopy* 42(1–2):101–109.
- Lynn Ingram, B. and P.K. Weber 1999 Salmon origin in California's Sacramento-San Joaquin river system as determined by otolith strontium isotopic composition. *Geology* 27(9):851–854.
- Macdonal, A.A. and H. Frädrich 1991 Pigs and Peccaries: What are they?. In R.H. Barrett and F. Spitz (eds), *Biology of Suidae*, pp. 7–19. Grenoble: IRGM.

- Macho, G.A. 1994 Variation in enamel thickness and cusp area within human maxillary molars and its bearing on scaling techniques used for studies of enamel thickness between species. *Archives of Oral Biology* 39(9):783–792.
- Madella, M., Jones, M.K., Goldberg, P., Goren, Y. and E. Hovers 2002 The exploitation of plant resources by Neanderthals in Amud Cave (Israel): The evidence from phytolith studies. *Journal of Archaeological Science* 29:703–19.
- Mager, S. 2007 *Botanical Field Guide*. Arcaria Guides, Mullumbimby.
- Magne, D., Pilet, P., Weiss, P. and G. Daculsi 2001 Fourier transform infrared microspectroscopic investigation of the maturation of nonstoichiometric apatites in mineralized tissues: A horse dentin study. *Bone* 29(6):547–552.
- Magri, D. and P.C. Tzedakis 2000 Orbital signatures and long-term vegetation patterns in the Mediterranean. *Quaternary International* 73/74:69–78.
- Mallory-Greenough, L.M., Greenough, J.D. and J.V. Owen 1998 New data for old pots: Trace-element characterization of ancient egyptian pottery using ICPMS. *Journal of Archaeological Science* 25(1):85–97.
- Marengo, E., Aceto, M., Robotti, E., Liparota, M.C., Bobba, M. and G. Pantó 2005 Archaeometric characterisation of ancient pottery belonging to the archaeological site of Novalesa Abbey (Piedmont, Italy) by ICPMS and spectroscopic techniques coupled to multivariate statistical tools. *Analytica Chimica Acta* 537(1–2):359–375.
- Marie, P.J., Ammann, P., Boivin, G. and C. Rey 2001 Mechanisms of action and therapeutic potential of strontium in bone. *Calcified Tissue International* 69:121–129.
- Marie, P.J., Garba, M.T., Hott, M. and L. Miravet 1985 Effect of low doses of stable strontium on bone metabolism in rats. *Mineral and Electrolyte Metabolism* 11:5–13.

- Martys, M.F. 1991 Social organisation and behaviour in the Suidae and Tayassuidae. In R.H. Barrett and F. Spitz (eds), *Biology of Suidae*, pp. 65–77. Grenoble: IRGM.
- Masini, F. and S. Lovari 1988 Systematics, phylogenetic relationships and dispersal of the chamois (*Rupicapra* spp.). *Quaternary Research* 30(3):339–349.
- Masters, P.M. 1982 An amino acid racemization chronology for Tabun. In A. Ronen (ed.), *The Transition from Lower to Middle Paleolithic and the Origin of Modern Man*, pp. 43–54. Oxford: BAR International Series 151.
- Matmon, A., Wdowinski, S. and J.K. Hall 2003 Morphological and structural relations in the Galilee extensional domain, northern Israel. *Tectonophysics* 371(1–4):223–241.
- Matschke, G.H. 1967 Aging european wild hogs by dentition. *The Journal of Wildlife Management* 31(1):109–113.
- Mauget, R. 1991 Reproductive biology of the wild Suidae. In R.H. Barrett and F. Spitz (eds), *Biology of Suidae*, pp. 49–64. Grenoble: IRGM.
- Mauget, R., Campan, R., Spitz, F., Dardaillon, M., Janeau, G. and D. Pepin 1984 Synthèse des connaissances actuelles sur la biologie du sanglier, perspectives et recherches. In F. Spitz and D. Pepin (eds), *Symposium internationale sur le sanglier*, pp. 15–50. Les colloques INRA No 22.
- Maureille, B. 2002 A lost Neanderthal neonate found. *Nature* 419(6902):33–34.
- Mays, S. 2003 Bone strontium: Calcium ratios and duration of breastfeeding in a mediaeval skeletal population. *Journal of Archaeological Science* 30(6):731–741.
- McArthur, J.M. 1994 Recent trends in strontium isotope stratigraphy. *Terra Nova* 6(4):331–358.
- McCance, R.A., Ford, E.H.R. and W.A.B. Brown 1961 Severe undernutrition in growing and adult animals 7. Development of the skull, jaws and teeth in pigs. *British Journal of Nutrition* 15:213–224.

- McCown, T.D. 1932 A note on the excavation and the human remains from the Mugharet Es-Sukhul (cave of the kids), season of 1931. *Bulletin of the American School of Prehistoric Research* 8:12–15.
- McCown, T.D. 1933 Fossil men of the Mugharet Es-Sukhul, near Athlit, Palestine, season of 1932. *Bulletin of the American School of Prehistoric Research* 9:9–15.
- McCown, T.D. and A. Keith 1939 The Stone Age of Mount Carmel: The Fossil Human Remains from the Levalloiso-Mousterian. Oxford: Clarendon.
- McDermott, F. and C. Hawkesworth 1990 The evolution of strontium isotopes in the upper continental crust. *Nature* 344:850–853.
- McDermott, F., Grün, R., Stringer, C.B. and C.J. Hawkesworth 1993 Mass-spectrometric U-series dates for Israeli Neanderthal early-modern Hominid sites. *Nature* 363:252–255.
- McDougall, I., Brown, F.H. and J.G. Fleagle 2005 Stratigraphic placement and age of modern humans from Kibish, Ethiopia. *Nature* 433:733–736.
- McGarry, S., Bar-Matthews, M., Matthews, A., Vaks, A., Schilman, B. and A. Ayalon 2004 Constraints on hydrological and paleotemperature variations in the Eastern Mediterranean region in the last 140 ka given by the δD values of speleothem fluid inclusions. *Quaternary Science Reviews* 23(7–8):919–934.
- McTaggart-Cowan, I. and C.W. Holloway 1973 Threatened deer of the world: Conservation status. *Biological Conservation* 5(4):243–250.
- Meagher, M. 1986 *Bison bison*. *Mammalian Species* 266:1–8.
- Mellars, P. 1985 The ecological basis of social complexity in the Upper Paleolithic of south-western France. In T.D. Price and J.A. Brown (eds), *Prehistoric Hunter-Gatherers: The Emergence of Cultural Complexity*, pp. 271–297. Orlando: Academic Press.
- Mellars, P. 1989 Major issues in the emergence of modern humans. *Current Anthropology* 30(3):349–385.

Mellars, P. 1996 The Neanderthal Legacy: An Archaeological Perspective from Western Europe. Princeton: Princeton University Press.

Mellars, P. 2004 Neanderthals and the modern human colonization of Europe. *Nature* 432:461–465.

Mellars, P. and R. Grün 1991 A comparison of the electron spin resonance and thermoluminescence dating methods: The results of ESR dating at Le Moustier (France). *Cambridge Archaeological Journal* 1(2):269–276.

Menier, D., Tessier, B., Dubois, A., Goubert, E. and M. Sedrati 2011 Geomorphological and hydrodynamic forcing of sedimentary bedforms: Example of Gulf of Morbihan (South Brittany, Bay of Biscay). *Journal of Coastal Research* 64:1530–1534.

Menzel, R.G. and W.R. Heald 1959 Strontium and calcium contents of crop plants in relation to exchangeable strontium and calcium in the soil. *Proceedings of the Soil Science Society of America* 23:110–112.

Menzies, M. and W.E. Seyfried Jr 1979 Basalt-seawater interaction: Trace element and strontium isotopic variations in experimentally altered glassy basalt. *Earth and Planetary Science Letters* 44(3):463–472.

Mercier, H., Valladas, H., Valladas, G., Reyss, J.-L., Jelinek, A., Meignen, L. and J.L. Joron 1995 TL dates of burnt flint from Jelinek's excavations at Tabun and their implications. *Journal of Archaeological Science* 22:495–510.

Mercier, N., Valladas, H., Bar-Yosef, O., Vandermeersch, B., Stringer, C. and J.-L. Joron 1993 Thermoluminescence dates for the Mousterian burials site of Es-Skhul, Mt. Carmel. *Journal of Archaeological Science* 20:169–174.

Meybeck, M. 1979 Concentrations des eaux fluviales en éléments majeurs et apports en solution aux océans. *Revue de Géologie Dynamique et de Géographie Physique* 21(3):215–146.

- Middleton, W.D. and T.D. Price 1996 Identification of Activity Areas by Multi-element Characterization of Sediments from Modern and Archaeological House Floors Using Inductively Coupled Plasma-atomic Emission Spectroscopy. *Journal of Archaeological Science* 23:673–687.
- Mijares, A.S., Detroit, F., Piper, P., Grün, R., Bellwood, P., Aubert, M., Champion, G., Cuevas, N., De Leon, A. and E. Dizon 2010 New evidence for a 67,000-year-old human presence at Callao Cave, Luzon Philippines. *Journal of Human Evolution* 59:123–132.
- Millard, A.R. and A.W.G. Pike 1999 Uranium-series dating of the Tabun Neanderthal: A cautionary note. *Journal of Human Evolution* 36:581–585.
- Millard, A.R., Roberts, C.A. and S.S. Hughes 2005 Isotopic evidence for migration in Medieval England: The potential for tracking the introduction of disease. *Society, Biology and Human Affairs* 70(1):9–14
- Miller, E.K., Blum, J.D. and A.J. Friedland 1993 Determination of soil exchangeable-cation loss and weathering rates using Sr isotopes. *Nature* 362(6419):438–441.
- Miller, R. 1983 Seasonal movements and home ranges of feral horse bands in Wyoming's Red Desert. *Journal of Range Management* 36:199–201.
- Mills, G. 1998 Brown hyaena *Hyaena (Parahyaena) brunnea* (Thunberg, 1820). In M.G.L. Mills and H. Hofer (eds), *Hyaenas. Status Survey and Conservation Action Plan*, pp. 154pp. Gland: IUCN.
- Mills, M.G.L. 1982 *Hyaena brunnea*. *Mammalian Species* 194:1–5.
- Minugh-Purvis, N. 1998 The search for the earliest modern Europeans: A comparison of the Es-Skhul 1 and Krapina 1 juveniles. In T. Akazawa, K. Aoki and O. Bar-Yosef (eds.), *Neanderthals and Modern Humans in Western Asia*. pp. 339–352. New York: Plenum Press.
- Mirti, P., Aruga, R., Appolonia, L., Casoli, A. and M. Oddone 1994 On the role of major, minor and trace elements in provenancing ceramic material. A case study: Roman terra sigillata from Augusta Praetoria. *Fresenius' Journal of Analytical Chemistry* 348(5):396–401.

- Misra, N.K. and V.S. Venkatasubramanian 1977 Strontium diffusion in feldspars—A laboratory study. *Geochimica et Cosmochimica Acta* 41(6):837–838.
- Moffat, I., Stringer, C. and Grün, R. 2012 Spatially Resolved LA-MC-ICPMS Strontium Isotope Analysis of Archaeological Fauna. *Palaios* 27:667-670.
- Montgomery, J. 2002 Lead and Strontium Isotope Compositions of Human Dental Tissues as an Indicator of Ancient Exposure of Population Dynamics. Unpublished PhD thesis, Department of Archaeological Sciences, University of Bradford.
- Montgomery, J. 2010 Passports from the past: Investigating human dispersals using strontium isotope analysis of tooth enamel. *Annals of Human Biology* 37(3):325–346.
- Montgomery, J., Budd, P. and J. Evans 2000 Reconstructing the Lifetime Movements of Ancient People: A Neolithic Case Study from Southern England. *European Journal of Archaeology* 3(3):370–385.
- Montgomery, J., Evans, J.A. and G. Wildman 2006 $^{87}\text{Sr}/^{86}\text{Sr}$ isotope composition of bottled British mineral waters for environmental and forensic purposes. *Applied Geochemistry* 21(10):1626–1634.
- Montgomery, J., Evans, J.A. and R.E. Cooper 2007 Resolving archaeological populations with Sr-isotope mixing models. *Applied Geochemistry* 22(7):1502–1514.
- Montgomery, J., Evans, J.A. and M.S.A. Horstwood 2010 Evidence for long-term averaging of strontium in bovine enamel using TIMS and LA-MC-ICP-MS strontium isotope intra-molar profiles. *Environmental Archaeology* 15(1):32-42.
- Montgomery, J., Evans, J.E., Powlesland, D. and C.A. Roberts 2005 Continuity or colonization in Anglo-Saxon England? Isotope evidence for mobility, subsistence practice and status at West Heslerton. *American Journal of Physical Anthropology* 126(2):123–138.

- Mor, D. 1993 A time-table for the Levant volcanic province, according to K-Ar dating in the Golan heights, Israel. *Journal of African Earth Sciences (and the Middle East)* 16(3):223–234.
- Mor, D., Michelson, H., Druckman, Y., Mimran, Y., Heimann, A., Goldberg, M. and A. Sneh 1997 Notes on the geology of Golan Heights. In *Geological Survey of Israel: Report GSI/15/97*. Jerusalem: Geological Survey of Israel.
- Moss-Salentijn, L., Moss, M.L. and M.S. Yuan 1997 The ontogeny of mammalian enamel. In W. V. Koenigswald and P.M. Sander (eds), *Tooth Enamel Microstructure*. pp.5-30. Rotterdam: A.A. Balkema.
- Mounier, A., Marchal, F. and S. Condemi 2009 Is *Homo heidelbergensis* a distinct species? New insight on the Mauer mandible. *Journal of Human Evolution* 56(3):219–246.
- Mountjoy, E.W., Qing, H. and R.H. McNutt 1992 Strontium isotopic composition of Devonian dolomites, Western Canada Sedimentary Basin: Significance of sources of dolomitizing fluids. *Applied Geochemistry* 7(1):59–75.
- Müldner, G., Montgomery, J., Cook, G.D., Ellam, R., Gledhill, A. and C. Lowe 2009 Isotopes and individuals: Diet and mobility among the medieval Bishops of Whithorn. *Antiquity* 83(322):1119–1133.
- Munro, L.E., Longstaffe, F.J. and C.D. White 2007 Burning and boiling of modern deer bone: Effects of crystallinity and oxygen isotope composition of bioapatite phosphate. *Palaeogeography Palaeoclimatology Palaeoecology* 249:90–102.
- Murdock, G.P. 1967 The ethnographic atlas: A summary. *Ethnology* 6(2):109–236.
- Murray, T. 1993 Elementary Scots. The discovery of strontium. *Scottish Medical Journal* 38(6):188–9.

- Nafplioti, A. 2009 Mycenae revisited part 2. Exploring the local versus non-local geographical origin of the individuals from grave circle a: Evidence from strontium isotope ratio ($^{87}\text{Sr}/^{86}\text{Sr}$) analysis. *Annual of the British School at Athens* 104:279–291.
- Nafplioti, A. 2011 Tracing population mobility in the Aegean using isotope geochemistry: A first map of local biologically available $^{87}\text{Sr}/^{86}\text{Sr}$ signatures. *Journal of Archaeological Science* 38(7):1560–1570.
- Naveh, Z. 1967 Mediterranean ecosystems and vegetation types in California and Israel. *Ecology* 48(3):445–459.
- Neat, P.L., Faure, G. and W.J. Pegram 1979 The isotopic composition of strontium in non-marine carbonate rocks: The Flagstaff Formation of Utah*. *Sedimentology* 26(2):271–282.
- Neev, D. and K.O. Emery 1967 The Dead Sea. *Bulletin of the Geological Survey of Israel* 41:1–147.
- Neev, D., Bakler, N. and K.O. Emery 1987 Mediterranean Coasts of Israel and Sinai: Holocene Tectonism from Geology, Geophysics and Archaeology. New York: Taylor and Francis.
- Neff, H. 2003 Analysis of Mesoamerican plumbate pottery surfaces by laser ablation-inductively coupled plasma-mass spectrometry (LA-ICPMS). *Journal of Archaeological Science* 30(1):21–35.
- Négrel, P. 1999 Geochemical study of a granitic area – the Margeride Mountains, France: chemical element behaviour and $^{87}\text{Sr}/^{86}\text{Sr}$ constraints. *Aquatic Geochemistry* 5:125-165.
- Négrel, P. and P. Deschamps 1996 Natural and Anthropogenic Budgets of a Small Watershed in the Massif Central (France): Chemical and Strontium Isotopic Characterization of Water and Sediments. *Aquatic Geochemistry* 2:1-27.
- Négrel, P. and E. Petelet-Giraud 2005 Strontium isotopes as tracers of groundwater-induced floods: The Somme case study (France). *Journal of Hydrology* 305(1–4):99–119.

- Négrel, P. and P. Lachassagne 2000 Geochemistry of the Maroni River (French Guiana) during the low water stage: Implications for water-rock interaction and groundwater characteristics. *Journal of Hydrology* 237(3–4):212–233.
- Négrel, P. and S. Roy 1998 Chemistry of rainwater in the Massif Central (France): A strontium isotope and major element study. *Applied Geochemistry* 13(8):941–952.
- Négrel, P., Allègre, C.J., Dupré, B. and E. Lewin 1993 Erosion sources determined by inversion of major and trace element ratios and strontium isotopic ratios in river water: The Congo Basin case. *Earth and Planetary Science Letters* 120(1–2):59–76.
- Négrel, P., Guerrot, C. and R. Millot 2007 Chemical and strontium isotope characterization of rainwater in France: Influence of sources and hydrogeochemical implications. *Isotopes in Environmental and Health Studies* 43(3):179 - 196.
- Negrel, P., Guerrot, C., Cocherie, A., Azaroual, M., Brach, M. and C. Fouillac 2000 Rare earth elements, neodymium and strontium isotopic systematics in mineral waters: Evidence from the Massif Central, France. *Applied Geochemistry* 15(9):1345–1367.
- Négrel, P., Petelet-Giraud, E. and D. Widory 2004 Strontium isotope geochemistry of alluvial groundwater: A tracer for groundwater resources characterisation. *Hydrology and Earth System Sciences* 8(5):959–972.
- Nehlich, O., Montgomery, J., Evans, J., Schade-Lindig, S., Pichler, S.L., Richards, M.P. and K.W. Alt 2009 Mobility or migration: A case study from the Neolithic settlement of Nieder-Mörlen (Hessen, Germany). *Journal of Archaeological Science* 36(8):1791–1799.
- Nelson, B.K., Deniro, M.J., Schoeninger, M.J., De Paolo, D.J. and P.E. Hare 1986 Effects of diagenesis on strontium, carbon, nitrogen and oxygen concentration and isotopic composition of bone. *Geochimica et Cosmochimica Acta* 50(9):1941–1949.

- Nesbitt, H.W., Markovics, G. and R.C. Price 1980 Chemical processes affecting alkalis and alkaline earths during continental weathering. *Geochimica et Cosmochimica Acta* 44(11):1659–1666.
- Nezat, C.A., Blum, J.D. and C.T. Driscoll 2010 Patterns of Ca/Sr and $^{87}\text{Sr}/^{86}\text{Sr}$ variation before and after a whole watershed CaSiO_3 addition at the Hubbard Brook Experimental Forest, USA. *Geochimica et Cosmochimica Acta* 74(11):3129–3142.
- Niederschlag, E., Pernicka, E., Seifert, T. and M. Bartelheim 2003 The determination of lead isotope ratios by multiple collector ICPMS: A case study of early Bronze Age artefacts and their possible relation with ore deposits of the Erzgebirge*. *Archaeometry* 45(1):61–100.
- Nier, A.O. 1938 The isotopic constitution of stontium, barium, bismuth, thallium and mercury. *Physical Review* 5:275–278.
- Niven, L.B., Egeland, C.P. and L.C. Todd 2004 An inter-site comparison of enamel hypoplasia in bison: Implications for paleoecology and modeling Late Plains Archaic subsistence. *Journal of Archaeological Science* 31(12):1783–1794.
- Nowak, R., M. 1991 *Walker's Mammals of the World*. Baltimore: The Johns Hopkins Press.
- Nowell, G.M. and M.S.A. Horstwood 2009 Comments on Richards et al., Journal of Archaeological Science 35, 2008 'Strontium isotope evidence of Neanderthal mobility at the site of Lakonis, Greece using laser-ablation PIMMS'. *Journal of Archaeological Science* 36(7):1334–1341.
- Ohel, M. 1986 *The Acheulian industries of Yiron, Israel*. Oxford: BAR International Series 307.
- Ohel, M. 1990 Lithic Analysis of of Acheulian Assemblages from the Avivim Sites, Israel. Oxford: BAR International Series 562.
- Oliver, W.L.R. and B. Fruzinski 1991 People and pigs. In R.H. Barrett and F. Spitz (eds), *Biology of Suidae*, pp. 93–116. Grenoble: IRGM.

- Oprea, C., Szalanski, P.J., Gustova, M.V., Oprea, I.A. and V. Buzguta 2009 Multivariate comparison of elemental concentrations in human teeth. *Applied Radiation and Isotopes* 67(12):2142–2145.
- Paama, L., Pitkänen, I. and P. Perämäki 2000 Analysis of archaeological samples and local clays using ICP-AES, TG-DTG and FTIR techniques. *Talanta* 51(2):349–357.
- Palmer, M.R. and J.M. Edmond 1992 Controls over the strontium isotope composition of river water. *Geochimica et Cosmochimica Acta* 56(5):2099–2111.
- Pankhurst, R.J. 1977 Strontium isotope evidence for mantle events in the continental lithosphere. *Journal of the Geological Society* 134:255–268.
- Paquereau, M.-M. 1970 Flores et climats paléolithiques dans le Sud-Ouest de la France. *Revue de Géographie Physique et Géologie Dynamique* 2(12):109–116.
- Paquereau, M.-M. 1975 Le Wurm ancien en Perigord. Etude palynologique. Première partie: Les diagrammes palynologiques: La zonation climatique. *Quaternaria* 18:67–116.
- Paquereau, M.-M. 1979 Quelques types de flores tardi-glaciaires dans le sud-ouest de la France. In D. de Sonneville-Bordes (ed.), *La Fin des Temps Glaciaires en Europe*, pp. 51–59. Paris: Centre National de la Recherche Scientifique.
- Passey, B.H. and T.E. Cerling 2002 Tooth enamel mineralization in ungulates: Implications for recovering a primary isotopic time-series. *Geochimica et Cosmochimica Acta* 66:3225–3234.
- Pate, D. and K.A. Brown 1985 The stability of bone strontium in the geochemical environment. *Journal of Human Evolution* 14(5):483–491.
- Pate, D., Hutton, J.T. and K. Norrish 1989 Ionic exchange between soil solution and bone: Towards a predictive model. *Applied Geochemistry* 4:303–316.

- Paton, C., Woodhead, J.D., Hergt, J.M., Philips, D. and S. Shee 2007 Strontium isotope analysis of Kimberlitic groundmass Perovskite via LA-MC-ICPMS. *Geostandards and Geoanalytical Research* 31(4):321–330.
- Patou-Mathis, M. 2000 Neanderthal subsistence behaviours in Europe. *International Journal of Osteoarchaeology* 10(5):379–395.
- Pellegrini, M., Donahue, R.E., Chinery, C., Evans, J., Lee-Thorp, J., Montgomery, J. and M. Mussi 2008 Faunal migration in late-glacial central Italy: Implications for human resource exploitation. *Rapid Communications in Mass Spectrometry* 22(11):1714–1726.
- Pelletier, J.D. 2007 Cantor set model of eolian dust deposits on desert alluvial fan terraces. *Geology* 35(5):439–442.
- Pereira, C.E.B., Miekeley, N., Poupeau, G. and I.L. Küchler 2001 Determination of minor and trace elements in obsidian rock samples and archaeological artifacts by laser ablation inductively coupled plasma mass spectrometry using synthetic obsidian standards. *Spectrochimica Acta Part B: Atomic Spectroscopy* 56(10):1927–1940.
- Pérez-Barbería, F.J. 1994 Determination of age in Cantabrian chamois (*Rupicapra pyrenaica pavva*) from jaw tooth-row eruption and wear. *Journal of Zoology* 233(4):649–656.
- Perry, M.A., Coleman, D. and N. Delhopital 2008 Mobility and exile at 2nd century A.D. Khirbet edh-Dharih: Strontium isotope analysis of human migration in western Jordan. *Geoarchaeology-an International Journal* 23(4):528–549.
- Perry, M.A., Coleman, D.S., Dettman, D.L. and A.H. al-Shiyab 2009 An isotopic perspective on the transport of Byzantine mining camp laborers into southwestern Jordan. *American Journal of Physical Anthropology* 140(3):429–441.
- Petelet-Giraud, E., Négrel, P. and J. Casanova 2003 Variability of $^{87}\text{Sr}/^{86}\text{Sr}$ in water draining granite revealed after a double correction for atmospheric and anthropogenic inputs. *Hydrological Sciences Journal* 48(5):729 - 742.

- Pett-Ridge, J.C., Derry, L.A. and A.C. Kurtz 2009 Sr isotopes as a tracer of weathering processes and dust inputs in a tropical granitoid watershed, Luquillo Mountains, Puerto Rico. *Geochimica et Cosmochimica Acta* 73(1):25–43.
- Picard, L. 1943 *Structure and Evolution of Palestine*. Jerusalem: Hebrew University.
- Pierce, C., Adams, K.R. and J.D. Stewart 1998 Determining the fuel constituents of ancient hearth ash via ICP-AES analysis. *Journal of Archaeological Science* 25(6):493–503.
- Pike, A.W.G. and R.E.M. Hedges 2001 Sample geometry and U uptake in archaeological teeth: Implications for U-series and ESR dating. *Quaternary Science Reviews* 20:1021–1025.
- Pike, A.W.G., Foster, G.L., Stringer, C., Eggins, S.M. and R. Grün 2006 Direct U-series dating of fossil human bone by laser ablation MC-ICPMS. *Geochimica et Cosmochimica Acta* 70(18):A494–A494.
- Pitra, C., Fickel, J., Meijaard, E. and C.P. Groves 2004 Evolution and phylogeny of old world deer. *Molecular Phylogenetics and Evolution* 33:880–895.
- Plumb, G.E., White, P.J., Coughenour, M.B. and R.L. Wallen 2009 Carrying capacity, migration and dispersal in Yellowstone bison. *Biological Conservation* 142:2377–2387.
- Pollard, A.M. and C. Heron 2008 *Archaeological Chemistry*. Cambridge: The Royal Society of Chemistry.
- Pollard, M., Batt, C., Stern, B. and S.M.M. Young 2007 *Analytical Chemistry in Archaeology*. Cambridge: Cambridge University Press.
- Pomeral, C. 1980 Geology of France with Twelve Itineraries. Paris: Masson.
- Ponce De León, M.S. 2002 Computerized paleoanthropology and Neanderthals: The case of Le Moustier 1. *Evolutionary Anthropology: Issues, News and Reviews* 11(S1):68–72.

- Ponce De León, M.S. and C.P.E. Zollikofer 1999 New evidence from Le Moustier 1: Computer-assisted reconstruction and morphometry of the skull. *The Anatomical Record* 254(4):474–489.
- Ponting, M., Evans, J.A. and V. Pashley 2003 Fingerprinting of Roman mints using laser-ablation MC-ICPMS lead isotope analysis. *Archaeometry* 45(4):591–597.
- Porat, N., Wintle, A.G. and M. Ritte 2004 Mode and timing of kurkar and hamra formation, central coastal plain, Israel. *Israel Journal of Earth Sciences* 53(1).
- Porat, N., Zhou, L.P., Chazan, M., Noy, T. and L.K. Horwitz 1999 Dating the Lower Paleolithic open-air site of Holon, Israel by luminescence and ESR techniques. *Quaternary Research* 51(3):328–341.
- Porder, S., Paytan, A. and E.A. Hadly 2003 Mapping the origin of faunal assemblages using strontium isotopes. *Paleobiology* 29(2):197–204.
- Pors Nielsen, S. 2004 The biological role of strontium. *Bone* 35(3):583–588.
- Poser, H. 1948 Aeolische Ablagerungen und Klima des Spätglazials im Mittel- und Westeuropa. *Naturwissenschaften* 35(269–276):307–312.
- Poszwa, A., Ferry, B., Pollie, B., Grimaldi, C., Charles-Dominique, P., Loubet, M. and E. Dambrine 2009 Variations of plant and soil $^{87}\text{Sr}/^{86}\text{Sr}$ along the slope of a tropical inselberg. *Annals of Forest Science* 66(5):512.
- Prentice, I.C., Cramer, W., Harrison, S.P., Leemans, R., Monserud, R.A. and A.M. Solomon 1992 A global biome model based on plant physiology and dominance, soil properties and climate. *Journal of Biogeography* 19:117–134.
- Price, C., Stone, L., Huppert, A., Rajagopalan, B. and P. Alpert 1998 A possible link between El Niño and precipitation in Israel. *Geophysical Research Letters* 25(1):3963–3966.
- Price, T.D., Bentley, R.A., Gronenborn, D., Lüning, J. and J. Wahl 2001 Human migration in the Linearbandkeramik of central Europe. *Antiquity* 75:593–603.

- Price, T.D., Burton, J.H. and R.A. Bentley 2002 The characterization of biologically available strontium isotope ratios for the study of prehistoric migration. *Archaeometry* 44(1):117–135.
- Price, T.D., Burton, J.H., Fullagar, P.D., Wright, L.E., Buikstra, J.E. and V. Tiesler 2008 Strontium isotopes and the study of human mobility in ancient Mesoamerica. *Latin American Antiquity* 19(2):167–180.
- Price, T.D., Burton, J.H., Sharer, R.J., Buikstra, J.E., Wright, L.E., Traxler, L.P. and K.A. Miller 2010 Kings and commoners at Copan: Isotopic evidence for origins and movement in the Classic Maya period. *Journal of Anthropological Archaeology* 29(1):15–32.
- Price, T.D., Connor, M. and J.D. Parsen 1985 Bone chemistry and the reconstruction of diet: Strontium discrimination in white-tailed deer. *Journal of Archaeological Science* 12(6):419–442.
- Price, T.D., Grupe, G. and P. Schröter 1994 Reconstruction of migration patterns in the Bell Beaker period by stable strontium isotope analysis. *Applied Geochemistry* 9(4):413–417.
- Price, T.D., Grupe, G. and P. Schröter 1998 Migration in the Bell Beaker period of central Europe. *Antiquity* 72:405–411.
- Price, T.D., Johnson, C.M., Ezzo, J.A., Ericson, J. and J.H. Burton 1994 Residential mobility in the prehistoric southwest United States: A preliminary study using strontium isotope analysis. *Journal of Archaeological Science* 21(3):315–330.
- Price, T.D., Manzanilla, L. and W.D. Middleton 2000 Immigration and the ancient city of Teotihuacan in Mexico: A study using strontium isotope ratios in human bone and teeth. *Journal of Archaeological Science* 27(10):903–913.
- Prodehl, C., Mueller, S. and V. Haak 1995 The European Cenozoic rift system. In K.H. Olsen (ed.), *Continental Rifts: Evolution, Structure, Tectonics*, pp. 133–201. Amsterdam: Elsevier.

- Prohaska, T., Latkoczy, C., Schultheis, G., Teschler-Nicola, M. and G. Stigeder 2002 Investigation of Sr isotope ratios in prehistoric human bones and teeth using laser ablation ICPMS and ICPMS after Rb/Sr separation. *Journal of Analytical Atomic Spectrometry* 17(8):887–891.
- Quade, J., Chivas, A.R. and M.T. McCulloch 1995 Strontium and carbon isotope tracers and the origins of soil carbonate in South Australia and Victoria. *Palaeogeography, Palaeoclimatology, Palaeoecology* 113(1):103–117.
- Quam, R.M. and F.H. Smith 1998 A reassessment of the Tabun C2 mandible. In T. Akazawa, K. Aoki and O. Bar-Yosef (eds), *Neanderthals and Modern Humans in Western Asia*. pp. 405-421 New York: Plenum Press.
- Qumsiyeh, M.B. 1996 *Mammals of the Holy Land*. Lubbock: Texas Tech University Press.
- Rabinovich, R. and E. Hovers 2004 Faunal analysis from Amud Cave: Preliminary results and interpretations. *International Journal of Osteoarchaeology* 14:287–306.
- Rahill, W.J. and M. Walser 1965 Renal tubular reabsorption of trace alkaline earths compared with calcium. *American Journal of Physiology* 208:1165–1170.
- Raiber, M., Webb, J.A. and D.A. Bennetts 2009 Strontium isotopes as tracers to delineate aquifer interactions and the influence of rainfall in the basalt plains of southeastern Australia. *Journal of Hydrology* 367(3–4):188–199.
- Rak, Y., Hovers, E. and W.H. Kimbel 1994 A Neanderthal infant from Amud Cave, Israel. *Journal of Human Evolution* 26:313–324.
- Ramos, F.C., Wolff, J.A. and D.L. Tollstrup 2004 Measuring $^{87}\text{Sr}/^{86}\text{Sr}$ variations in minerals and groundmass from basalts using LA-MC-ICPMS. *Chemical Geology* 211(1–2):135–158.
- Ravikovitch, S. 1992 *The Soils of Israel: Formation, Nature and Properties*. Tel Aviv: Hakibbutz Hameuchad Publishing House,.

- Raymond, L.A. 1995 Petrology: The Study of Igneous, Sedimentary and Metamorphic Rocks. Dubuque: Wm C. Brown.
- Reepmeyer, C., Spriggs, M., Anggraeni, Lape, P., Neri, L., Ronquillo, W.P., Simanjuntak, T., Summerhayes, G., Tanudirjo, D. and A. Tiauzon 2011 Obsidian sources and distribution systems in Island Southeast Asia: New results and implications from geochemical research using LA-ICPMS. *Journal of Archaeological Science* 38(11):2995–3005.
- Rehkämper, M. and K. Mezger 2000 Investigation of matrix effects for Pb isotope ratio measurements by multiple collector ICPMS: Verification and application of optimized analytical protocols. *Journal of Analytical Atomic Spectrometry* 15(11):1451–1460.
- Reifenberg, A. 1947 *The Soils of Palestine*. London: Thomas Murby.
- Reille, M. and J.L. de Beaulieu 1990 Pollen analysis of a long upper Pleistocene continental sequence in a Velay maar (Massif Central, France). *Palaeogeography, Palaeoclimatology, Palaeoecology* 80(1):35–48.
- Reille, M., andrieu, V.R., De Beaulieu, J.-L., Guenet, P. and C. Goeury 1998 A long pollen record from Lac du Bouchet, Massif Central, France: For the period ca. 325 TO 100 ka BP (OIS 9c to OIS 5e). *Quaternary Science Reviews* 17(12):1107–1123.
- Reinhard, K.J. and A.M. Ghazi 1992 Evaluation of lead concentrations in 18th-century Omaha Indian skeletons using ICPMS. *American Journal of Physical Anthropology* 89(2):183–195.
- Rendu, W. 2010 Hunting behaviour and Neanderthal adaptability in the Late Pleistocene site of Pech-de-l’Azé I. *Journal of Archaeological Science* 37, 1798–1810.
- Repennig, C.A. and O. Fejfar 1982 Evidence for earlier date of Ubeidiya, Israel, homonid site. *Nature* 299:344–347.
- Resano, M., García-Ruiz, E. and F. Vanhaecke 2009 Laser ablation-inductively coupled plasma mass spectrometry in archaeometric research. *Mass Spectrometry Reviews* 29(1):55–78.

- Richards, M., Grimes, V., Smith, C., Smith, T., Harvati, K., Hublin, J.-J., Karkanas, P. and E. Panagopoulou 2009 Response to Nowell and Horstwood (2009). *Journal of Archaeological Science* 36(7):1657–1658.
- Richards, M.P. and E. Trinkaus 2009 Isotopic evidence for the diets of European Neanderthals and early modern humans. *Proceedings of the National Academy of Science* 106:16034–16039.
- Richards, M.P. and R.W. Schmitz 2008 Isotope evidence for the diet of the Neanderthal type specimen. *Antiquity* 82:553–559.
- Richards, M.P., Harvati, K., Grimes, V., Smith, C., Smith, T., Hublin, J.J., Karkanas, P. and E. Panagopoulou 2008 Strontium isotope evidence of Neanderthal mobility at the site of Lakonis, Greece using laser-ablation PIMMS. *Journal of Archaeological Science* 35:1251–1256.
- Richards, M.P., Pettitt, P.B., Trinkaus, E., Smith, F.H., Paunović, M. and I. Karavanić 2000 Neanderthal diet at Vindija and Neanderthal predation: The evidence from stable isotopes. *Proceedings of the National Academy of Sciences* 97(13):7663–7666.
- Richards, M.P., Taylor, G., Steele, T., McPherron, S.P., Soressi, M., Jaubert, J., Orschiedt, J., Mallye, J.B., Rendu, W. and J.J. Hublin 2008 Isotopic dietary analysis of a Neanderthal and associated fauna from the site of Jonzac (Charente-Maritime), France. *Journal of Human Evolution* 55(1):179–185.
- Richardson, P. 1998 Aardwolf *Proteles cristatus* (Sparrman 1783). In M.G.L. Mills and H. Hofer (eds), *Hyaenas: Status Survey and Conservation Action Plan*, pp. 154pp. Gland: IUCN.
- Rieger, I. 1981 *Hyaena hyaena*. *Mammalian Species* 150:1–5.
- Rimbu, N., Lohmann, G., Felis, T. and J. Pätzold 2003 Shift in ENSO teleconnections recorded by a northern Red Sea coral. *Journal of Climate* 16(9):1414–1422.

- Rink, W.J., Schwarcz, H.P., Lee, H.K., Rees-Jones, J., Rabinovich, R. and E. Hovers 2001 Electron spin resonance (ESR) and thermal ionization mass spectrometric (TIMS) $^{230}\text{Th}/^{234}\text{U}$ dating of teeth in Middle Paleolithic layers at Amud Cave, Israel. *Geoarchaeology-an International Journal* 16(6):701–717.
- Rink, W.J., Schwarcz, H.P., Ronen, A. and A. Tsatskin 2004 Confirmation of a near 400 ka age for the Yabrudian industry at Tabun Cave, Israel. *Journal of Archaeological Science* 31(1):15–20.
- Rivals, F., Schulz, E. and T.M. Kaiser 2009 Late and middle Pleistocene ungulates dietary diversity in Western Europe indicate variations of Neanderthal paleoenvironments through time and space. *Quaternary Science Reviews* 28(27–28):3388–3400.
- Roberts, N. and H.E. Wright 1993 Vegetational, lake level and climatic history of the Near East and South west Asia. In H.E. Wright, J.E. Kutzbach, T. Webb, F.A. Ruddiman, F.A. Street-Perrott and P.J. Bartlein (eds), *Global Climates since the Last Glacial Maximum*, pp. 194–220. Minneapolis: University of Minnesota.
- Robinson, C., Briggs, H.D., Atkinson, P.J. and J.A. Weatherell 1981 Chemical changes during formation and maturation of human deciduous enamel. *Archives of Oral Biology* 26(12):1027–1033.
- Robinson, C., Weatherell, J.A., El-Attar, I. and D. Deutsch 1980 Pattern of mineral uptake in developing bovine incisors. *Caries Research* 14:389–393.
- Robinson, R.G., Spicer, J.A., Preston, D.F., Wegst, A.V. and N.L. Martin 1987 Treatment of metastatic bone pain with strontium-89. *International Journal of Radiation Applications and Instrumentation. Part B. Nuclear Medicine and Biology* 14(3):219–222.
- Roddick, J.C. and W. Compston 1977 Strontium isotopic equilibration: A solution to a paradox. *Earth and Planetary Science Letters* 34(2):238–246.

- Rodwell, M.J. and B.J. Hoskins 2001 Subtropical anticyclones and summer monsoons. *Journal of Climate* 14:3192–3211.
- Roebroeks, W. 2001 Hominid behaviour and the earliest occupation of Europe: An exploration. *Journal of Human Evolution* 41(5):437–461.
- Rolett, B.V. and M.-Y. Chiu 1994 Age estimation of prehistoric pigs (*Sus scrofa*) by molar eruption and attrition. *Journal of Archaeological Science* 21(3):377–386.
- Ronen, A. 1979 Paleolithic industries. In A. Horowitz (ed.), *The Quaternary of Israel*. pp. 296-307. New York: Academic Press.
- Ronen, A. 1982 Mt Carmel caves: The first excavations. In A. Ronen (ed.), *The Transition from Lower to Middle Palaeolithic and the Origin of Upper Man*. pp. 7-28. Oxford: BAR International Series 151.
- Ronen, A. 1984a. Sefunim Prehistoric sites: Mount Carmel, Israel. *British Archaeological Reports International Series* 230(i).
- Ronen, A. 1984b. Sefunim Prehistoric sites: Mount Carmel, Israel. *British Archaeological Reports International Series* 230(ii).
- Ronen, A. and A. Tsatskin 1995 New interpretation of the oldest part of the Tabun cave sequence, Mount Carmel, Israel. In H. Ullrich (ed.), *Man and Environment in the Paleolithic*, pp. 265–281. Liege: ERAUL.
- Ronen, A. and G.M. Barton 1981 Rock engravings on western Mount Carmel, Israel. *Quartär* 31/32:121–137.
- Ronen, A., Kaufman, A., Gophna, R., Bakler, N., Smith, P. and A. Amiel 1975 The Epi-Paleolithic site of Hefziba, central coastal plain of Israel. *Quartär* 26:53–72.
- Ronen, A., Zviely, D. and E. Galili 2007 Did the Last Interglacial sea penetrate Mount Carmel caves? Comments on ‘The setting of the Mt. Carmel caves reassessed’ by C. Vita-Finzi and C. Stringer. *Quaternary Science Reviews* 26:2684–2685.

- Ronen, K. and D. Avinoam 1999 Distribution of plant species in Israel in relation to spatial variation in rainfall. *Journal of Vegetation Science* 10(3):421–432.
- Ronnholm, E. 1962 *The Amelogenesis in Embryonic Human Teeth*. Uppsala: Almqvist Wiksell.
- Rosenan, N. 1970 *Climate*. In M. Ha-medidot (ed.), *Atlas of Israel: Cartography, Physical Geography, Human and Economic Geography, History*. Amsterdam: Elsevier.
- Rosenthal, Y., Katz, A. and E. Tchernov 1989 The reconstruction of Quaternary freshwater lakes from the chemical and isotopic composition of gastropod shells: The Dead Sea rift, Israel. *Palaeogeography, Palaeoclimatology, Palaeoecology* 74(3–4):241–253.
- Ross, M.H., Kaye, G.I. and W. Pawlina 2002 *Histology: A Text and Atlas*. Philadelphia: Lippincott, Williams and Wilkins.
- Rossignol-Strick, M. 1985 Mediterranean Quaternary sapropels, an immediate response of the African monsoon to variation of insolation. *Palaeogeography, Palaeoclimatology, Palaeoecology* 49:237–263.
- Rüggeberg, A., Fietzke, J., Liebetrau, V., Eisenhauer, A., Dullo, W.-C. and A. Freiwald 2008 Stable strontium isotopes ($\delta^{88/86}\text{Sr}$) in cold-water corals—A new proxy for reconstruction of intermediate ocean water temperatures. *Earth and Planetary Science Letters* 269:570–575.
- Rummel, S., Hoelzl, S., Horn, P., Rossmann, A. and C. Schlicht 2010 The combination of stable isotope abundance ratios of H, C, N and S with $^{87}\text{Sr}^{86}\text{Sr}$ for geographical origin assignment of orange juices. *Food Chemistry* 118(4):890–900.
- Runia, L.J. 1987 Strontium and calcium distribution in plants: Effect on paleodietary studies. *Journal of Archaeological Science* 14:599–608.
- Russell, R.S. and J. Sanderson 1967 Nutrient uptake by different parts of the intact roots of plants. *Journal of Experimental Botany* 18(56):491–508.

- Russo, R.E., Mao, X., Liu, H., Gonzalez, J. and S.S. Mao 2002 Laser ablation in analytical chemistry—a review. *Talanta* 57(3):425–451.
- Sadalmelik, I. 2007 *Topographic Map of Israel*, Retrieved on 13/10/2011 from http://en.wikipedia.org/wiki/File:Israel_Topography.png.
- Sakae, T. and G. Hirai 1982 Calcification and crystallization in bovine enamel. *Journal of Dental Research* 61(1):57–59.
- Sakae, T., Suzuki, K. and Y. Kozawa 1997 A short review of studies on chemical and physical properties of enamel crystallites. In W. V. Koenigswald and P.M. Sander (eds), *Tooth Enamel Microstructure*, pp. 31–39. Rotterdam: A.A. Balkema.
- Saller, A.H. 1984 Petrologic and geochemical constraints on the origin of subsurface dolomite, Enewetak Atoll: An example of dolomitization by normal seawater. *Geology* 12(4):217–220.
- Sánchez Goñi, M.F., Landais, A., Fletcher, W.J., Naughton, F., Desprat, S. and J. Duprat 2008 Contrasting impacts of Dansgaard-Oeschger events over a western European latitudinal transect modulated by orbital parameters. *Quaternary Science Reviews* 27(11–12):1136–1151.
- Sander, P.M. 1997 Non-mammalian synapsid enamel and the origin of mammalian enamel prisms: The bottom-up perspective. In W. V. Koenigswald and P.M. Sander (eds), *Tooth Enamel Microstructure*, pp. 41–62. Rotterdam: A.A. Balkema.
- Sarah, G., Gratuze, B. and J.-N. Barrandon 2007 Application of laser ablation inductively coupled plasma mass spectrometry (LA-ICPMS) for the investigation of ancient silver coins. *Journal of Analytical Atomic Spectrometry* 22(9):1163–1167.
- Sass, E. and A. Bein 1982 The Cretaceous carbonate platform in Israel. *Cretaceous Research* 3(1–2):135–144.
- Sass, E. and A. Starinsky 1979 Behaviour of strontium in subsurface calcium chloride brines: Southern Israel and Dead Sea rift valley. *Geochimica et Cosmochimica Acta* 43(6):885–895.

- Schoeninger, M.J. 1979 Diet and status at Chalcatzingo: Some empirical and technical aspects of strontium analysis. *American Journal of Physical Anthropology* 51(3):295–309.
- Schoeninger, M.J. and C.S. Peebles 1981 Effect of mollusc eating on human bone strontium levels. *Journal of Archaeological Science* 8(4):391–397.
- Schroeder, H.A., Tipton, I.H. and A.P. Nason 1972 Trace metals in man:
- Schwarcz, H.P. and W.J. Rink 1998 Progress in ESR and U-series chronology of the Levantine Paleolithic. In T. Akazawa, K. Aoki and O. Bar-Yosef (eds), *Neanderthals and Modern Humans in Western Asia*. pp. 57-67. New York: Plenum Press.
- Schwarcz, H.P., Blackwell, B., Goldberg, P. and A.E. Marks 1979 Uranium series dating of travertine from archaeological sites, Nahal Zin, Israel. *Nature* 277:558–560.
- Schwarcz, H.P., Buhay, W.M., Grün, R., Valladas, H., Tchernov, E., Bar-Yosef, O. and B. Vandermeersch 1989 ESR dating of the Neanderthal site, Kebara Cave, Israel. *Journal of Archaeological Science* 16(6):653–659.
- Schwarcz, H.P., Buhay, W.M., Grün, R., Vandermeersch, B., Bar-Yosef, O., Valladas, H. and E. Tchernov 1988 ESR dates for the homonid burial site of Qafzeh in Israel. *Journal of Human Evolution* 17:733–737.
- Schwarcz, H.P., Simpson, J.J. and C. Stringer 1998 Neanderthal skeleton from Tabun: U-series data by gamm-ray spectrometry. *Journal of Human Evolution* 35:635–645.
- Schwartz, J.H. and I. Tattersall 2010 Fossil evidence for the origin of Homo sapiens. *American Journal of Physical Anthropology* 143(S51):94–121.
- Schweissing, M.M. and G. Grupe 2000 Local or nonlocal? A research of strontium isotope ratios of teeth and bones on skeletal remains with artificial deformed skulls. *Anthropologischer Anzeiger; Bericht über die biologisch-anthropologische Literatur* 58(1):99–103.

- Schweissing, M.M. and G. Grupe 2003 Tracing migration events in man and cattle by stable strontium isotope analysis of appositionally grown mineralized tissue. *International Journal of Osteoarchaeology* 13:96–103.
- Scott, R.B., Nesbitt, R.W., Julius Dasch, E. and R.A. Armstrong 1971 A strontium isotope evolution model for Cenozoic magma genesis, Eastern Great Gasin, U.S.A. *Bulletin of Volcanology* 35(1):1–26.
- Segev, A., Sass, E., Ron, H., Lang, B., Kolodny, Y. and M. McWilliams 2002 Stratigraphic, geochronologic and paleomagnetic constraints on Late Cretaceous volcanism in northern Israel. *Israel Journal of Earth Sciences* 51(3–4):297–309.
- Sellick, M.J., Kyser, T.K., Wunder, M.B., Chipley, D. and D.R. Norris 2009 Geographic variation of strontium and hydrogen isotopes in avian tissue: Implications for tracking migration and dispersal. *PLoS ONE* 4(3):e4735.
- Shackleton, N.J. and N.D. Opdyke 1973 Oxygen isotope and palaeomagnetic stratigraphy of Equatorial Pacific core V28–238: Oxygen isotope temperatures and ice Volume on a 10^5 and 10^6 year time scale. *Quaternary Research* 3(1):39–55.
- Shackleton, N.J. and N.D. Opdyke 1976 Oxygen isotope and paleomagnetic strigraphy of Pacific core V28–238: Late Pliocene to Latest Pleistocene. *Memoir (Geological Society of America)* 145:449–464.
- Shackleton, N.J. and Pisias, N.G. 1985 Atmospheric carbon dioxide, orbital forcing, and climate. In: E.T. Sundquist and W.S. Broecker (eds.) *The Carbon Cycle and Atmospheric CO₂: Natural Variations Archean to Present*. pp. 303-317. Washington D.C.: American Geophysical Union.
- Shackleton, N.J., Chapman, M., Sanchez-Goni, M.F., Pailler, D. and Y. Lancelot 2002 The classic marine isotope substage 5e. *Quaternary Research* 58:14–16.
- Shackleton, N.J., Sanchez-Goni, M.F., Pailler, D. and Y. Lancelot 2003 Marine isotope substage 5e and the Eemian interglacial. *Global and Planetary Change* 36:151–155.

- Shahack-Gross, R., Ayalon, A., Goldberg, P., Goren, Y., Rabinovich, R. and E. Hovers 2008 Formation processes of cemented features in Karstic cave sites revealed using stable oxygen and carbon isotopic analyses: A case study at Middle Paleolithic Amud Cave, Israel. *Geoarchaeology: An International Journal* 23(1):43–62.
- Shahack-Gross, R., Berna, F., Karkanas, P. and S. Weiner 2004 Bat guano and preservation of archaeological remains in cave sites. *Journal of Archaeological Science* 31:1259–1272.
- Shand, P., Darbyshire, D.P.F., Love, A.J. and W.M. Edmunds 2009 Sr isotopes in natural waters: Applications to source characterisation and water-rock interaction in contrasting landscapes. *Applied Geochemistry* 24(4):574–586.
- Shapiro, M. 2006 Soils of Israel. *Eurasian Soil Science* 39(11):1170–1175.
- Shaw, B., Buckley, H., Summerhayes, G., Anson, D., Garling, S., Valentin, F., Mandui, H., Stirling, C. and M. Reid 2010 Migration and mobility at the Late Lapita site of Reber-Rakival (SAC), Watom Island using isotope and trace element analysis: A new insight into Lapita interaction in the Bismarck Archipelago. *Journal of Archaeological Science* 37(3):605–613.
- Shaw, B., Buckley, H., Summerhayes, G., Stirling, C. and M. Reid 2011 Prehistoric migration at Nebira, South Coast of Papua New Guinea: New insights into interaction using isotope and trace element concentration analyses. *Journal of Anthropological Archaeology* 30(3):344–358.
- Shaw, B.J., Summerhayes, G.R., Buckley, H.R. and J.A. Baker 2009 The use of strontium isotopes as an indicator of migration in human and pig Lapita populations in the Bismarck Archipelago, Papua New Guinea. *Journal of Archaeological Science* 36(4):1079–1091.
- Shea, J.J. 2007 Behavioral differences between Middle and Upper Paleolithic Homo sapiens in the East Mediterranean Levant: The roles of intraspecific competition and dispersal from Africa. *Journal of Anthropological Research* 63(4):449–488.

- Shea, J.J. and O. Bar-Yosef 2005 Who were the Skhul/Qafzeh people? An archaeological perspective on Eurasia's earliest modern humans. *Journal of the Israel Prehistoric Society* 35:449–466.
- Shellis, R.P. 1984 Variations in growth of the enamel crown in human teeth and a possible relationship between growth and enamel structure. *Archives of Oral Biology* 29(9):697–705.
- Shellis, R.P. and G.H. Dibdin 2000 Enamel microporosity and its functional implications. In M.F. Teaford, M.M. Smith and M.W. J. Ferguson (eds), *Development, Function and Evolution of Teeth*. pp.242-251. Cambridge: Cambridge University Press.
- Shewan, L. 2004 Natufian settlement systems and adaptive strategies: The issue of sedentism and the potential of strontium isotope analysis. In C. Delage (ed.), *The Last Hunter-Gatherer Societies in the Near East*. Oxford: BAR International Series. John and Erica Hedges.
- Shimron, A.E. and H.J. Zwart 1970 The occurrence of low pressure metamorphism in the Precambrian of the Middle East and North East Africa. *Geologie En Mijnbouw* 49:369–374.
- Shinoda, H. 1984 Faithful records of biological rhythms in dental hard tissues. *Chemistry Today* 162:43–40.
- Shortland, A., Rogers, N. and K. Eremin 2007 Trace element discriminants between Egyptian and Mesopotamian Late Bronze Age glasses. *Journal of Archaeological Science* 34(5):781–789.
- Siedner, G. and A. Horowitz 1974 Radiometric ages of late Cainozoic basalts from northern Israel: Chronostratigraphic implications. *Nature* 250:23–26.
- Sillen, A. 1986 Biogenic and diagenetic Sr/Ca in Plio-Pleistocene fossils of the Omo Shungura Formation. *Paleobiology* 12(3):311–323.
- Sillen, A. and J.A. Lee-Thorp 1994 Trace element and isotopic aspects of predator-prey relationships in terrestrial foodwebs. *Palaeogeography, Palaeoclimatology, Palaeoecology* 107(3–4):243–255.

- Sillen, A. and M. Kavanagh 1982 Strontium and paleodietary research: A review. *American Journal of Physical Anthropology* 25:67–90.
- Sillen, A. and P. Smith 1984 Weaning patterns are reflected in strontium-calcium ratios of juvenile skeletons. *Journal of Archaeological Science* 11(3):237–245.
- Sillen, A., Hall, G. and R. Armstrong 1995 Strontium calcium ratios (Sr/Ca) and strontium isotopic ratios ($^{87}\text{Sr}/^{86}\text{Sr}$) of Australopithecus robustus and Homo sp. from Swartkrans. *Journal of Human Evolution* 28(3):277–285.
- Sillen, A., Hall, G., Richardson, S. and R. Armstrong 1998 $^{87}\text{Sr}/^{86}\text{Sr}$ ratios in modern and fossil food-webs of the Sterkfontein Valley: Implications for early hominid habitat preference. *Geochimica et Cosmochimica Acta* 62(14):2463–2473.
- Simmer, J.P. and J.C. Hu 2001 Dental enamel formation and its impact on clinical dentistry. *Journal of Dental Education* 65:896–905.
- Simonetti, A., Buzon, M.R. and R.A. Creaser 2008 In-situ elemental and Sr isotope investigation of human tooth enamel by laser ablation-(MC)-ICPMS: Successes and Pitfalls*. *Archaeometry* 50:371–385.
- Singer, A. 2007 *The Soils of Israel*. Berlin: Springer.
- Singer, A. and E. Ben-Dor 1987 Origin of red clay layers interbedded with basalts of the Golan Heights. *Geoderma* 39(293–306).
- Singh, S.K., Trivedi, J.R., Pande, K., Ramesh, R. and S. Krishnaswami 1998 Chemical and strontium, oxygen and carbon isotopic compositions of carbonates from the lesser Himalaya: Implications to the strontium isotope composition of the source waters of the Ganga, Ghaghara and the Indus Rivers. *Geochimica et Cosmochimica Acta* 62(5):743–755.
- Sips, A.J.A.M., van der Vijgh, W.J.F., Barto, R. and J.C. Netelenbos 1996 Intestinal absorption of strontium chloride in healthy volunteers: Pharmacokinetics and reproducibility. *British Journal of Clinical Pharmacology* 41(6):543–549.

- Sisca, R.F. and D.V. Provenza 1972 Initial dentin formation in human deciduous teeth. *Calcified Tissue International* 9(1):1–16.
- Sivan, D. and N. Porat 2004 Evidence from luminescence for Late Pleistocene formation of calcareous aeolianite (kurkar) and paleosol (hamra) in the Carmel Coast, Israel. *Palaeogeography, Palaeoclimatology, Palaeoecology* 211(1–2):95–106.
- Sjögren, K.-G., Price, T.D. and T. Ahlström 2009 Megaliths and mobility in south-western Sweden. Investigating relationships between a local society and its neighbours using strontium isotopes. *Journal of Anthropological Archaeology* 28(1):85–101.
- Skinner, H.C.W. 2000 In praise of phosphates, or why vertebrates chose apatite to mineralize their skeletal elements. *International Geology Review* 42:232–240.
- Slovak, N.M., Paytan, A. and B.A. Wiegand 2009 Reconstructing Middle Horizon mobility patterns on the coast of Peru through strontium isotope analysis. *Journal of Archaeological Science* 36(1):157–165.
- Smith, D.C., Bouchard, M. and M. Lorblanchett 1999 An initial raman microscopic investigation of prehistoric rock art in caves of the Quercy District, S.W. France. *Journal of Raman Spectroscopy* 30:347–354.
- Smith, H. 1994 Patterns of dental development in *Homo*, *Australopithecus*, *Pan* and *Gorilla*. *American Journal of Physical Anthropology* 94:307–325.
- Smith, T.M. 2008 Incremental dental development: Methods and applications in hominoid evolutionary studies. *Journal of Human Evolution* 54:205–224.
- Smith, T.M., Olejniczak, A.J., Reid, D.J., Ferrell, R.J. and J.J. Hublin 2006 Modern human molar enamel thickness and enamel-dentine junction shape. *Archives of Oral Biology* 51:974–995.
- Smits, E., Millard, A.R., Nowell, G. and G.D. Pearson 2010 Isotopic investigation of diet and residential mobility in the Neolithic of the lower Rhine Basin. *European Journal of Archaeology* 13(1):5–31.

- Sneh, A., Bartov, Y, Weissbrod, T. and M. Rosensaft 1998a. *Geological Map of Israel, 1:200,000, Sheet 3*. Geological Survey of Israel.
- Sneh, A., Bartov, Y, Weissbrod, T. and M. Rosensaft 1998b. *Geological Map of Israel, 1:200,000, Sheet 4*. Geological Survey of Israel.
- Sneh, A., Bartov, Y. and M. Rosensaft 1998a. *Geological Map of Israel, 1:200,000, Sheet 1*. Geological Survey of Israel.
- Sneh, A., Bartov, Y. and M. Rosensaft 1998b. *Geological Map of Israel, 1:200,000, Sheet 2*. Geological Survey of Israel.
- Sohn, S. and M.H. Wolpoff 1993 Zuttiyeh face: A view from the east. *American Journal of Physical Anthropology* 91(3):325–347.
- Somerman, M.J., Morrison, G.M., Alexander, M.B. and R.A. Foster 1993 Structure and composition of cementum. In W.H. Bowen and L.A. Tabak (eds), *Cariology for the Nineties*. pp. 155-171. Rochester: University of Rochester Press.
- Soressi, M., Jones, H.L., Rink, W.J., Maureille, B. and A.M. Tillier 2007 The Pech-de-l'Azé I Neandertal child: ESR, uranium-series and AMS ^{14}C dating of its MTA type B context. *Journal of Human Evolution* 52:455–466.
- Speakman, R.J. and H. Neff 2002 Evaluation of painted pottery from the Mesa Verde region using laser ablation-inductively coupled plasma mass spectrometry (LA-ICPMS). *American Antiquity* 67(1):137–144.
- Speakman, R.J. and H. Neff 2005 *Laser Ablation-ICPMS in Archaeological Research*. Albuquerque; University of Mexico Press.
- Speth, J.D. 2004 News flash: Negative evidence convicts Neanderthals of gross mental incompetence. *World Archaeology* 36(4):519–526.
- Spiess, A.E. 1979 *Reindeer and Caribou Hunters: An Archaeological Study*. London: Academic Press.

- Spiro, B., Ashkenazi, S., Starinsky, A. and A. Katz 2011 Strontium isotopes in *Melanopsis* sp. as indicators of variation in hydrology and climate in the Upper Jordan Valley during the Early-Middle Pleistocene and wider implications. *Journal of Human Evolution* 60(4):407–416.
- Sponheimer, M., de Ruiter, D.J., Lee-Thorp, J. and A. Späth 2005 Sr/Ca and early hominin diets revisited: New data from modern and fossil tooth enamel. *Journal of Human Evolution* 48:147–156.
- Spooner, E.T.C. 1976 The strontium isotopic composition of seawater and seawater-oceanic crust interaction. *Earth and Planetary Science Letters* 31(1):167–174.
- Spooner, E.T.C., Chapman, H.J. and J.D. Smewing 1977 Strontium isotopic contamination and oxidation during ocean floor hydrothermal metamorphism of the ophiolitic rocks of the Troodos Massif, Cyprus. *Geochimica et Cosmochimica Acta* 41(7):873–877, 879–890.
- Starinsky, A., Bielski, M., Lazar, B., Wakshal, E. and G. Steinitz 1980 Marine $^{87}\text{Sr}/^{86}\text{Sr}$ ratios from the Jurassic to Pleistocene: Evidence from groundwaters in Israel. *Earth and Planetary Science Letters* 47:75–80.
- Steegmann, A.T., Cerny, F.J. and T.W. Holliday 2002 Neanderthal cold adaptation: Physiological and energetic factors. *American Journal of Human Biology* 14:566–583.
- Stefan, V.H. and E. Trinkaus 1998 Discrete trait and dental morphometric affinities of the Tabun 2 mandible. *Journal of Human Evolution* 34(5):443–468.
- Steiger, R.H. and E. Jäger 1977 Subcommision on geochronology: Convention on the use of decay constants in geo- and cosmochronology. *Earth and Planetary Science Letters* 36(3):359–362.
- Stein, M. 2001 The sedimentary and geochemical record of Neogene-Quaternary water bodies in the Dead Sea Basin: Inferences for the regional paleoclimatic history. *Journal of Paleolimnology* 26(3):271–282.
- Stein, M. and A.W. Hofmann 1992 Fossil plume head beneath the Arabian lithosphere? *Earth and Planetary Science Letters* 114(1):193–209.

- Stein, M., Almogi-Labin, A., Goldstein, S.L., Hemleben, C. and A. Starinsky 2007 Late Quaternary changes in desert dust inputs to the Red Sea and Gulf of Aden from $^{87}\text{Sr}/^{86}\text{Sr}$ ratios in deep-sea cores. *Earth and Planetary Science Letters* 261(1–2):104–119.
- Stein, M., Starinsky, A., Agnon, A., Katz, A., Raab, M., Spiro, B. and I. Zak 2000 The impact of brine-rock interaction during marine evaporite formation on the isotopic Sr record in the oceans: Evidence from Mt. Sedom, Israel. *Geochimica et Cosmochimica Acta* 64(12):2039–2053.
- Stein, M., Starinsky, A., Katz, A., Goldstein, S.L., Machlus, M. and A. Schramm 1997 Strontium isotopic, chemical and sedimentological evidence for the evolution of Lake Lisan and the Dead Sea. *Geochimica et Cosmochimica Acta* 61(18):3975–3992.
- Steinitz, G., Bartov, Y. and J.C. Hunziker 1978 K-Ar determinations of some Miocene-Pliocene basalts in Israel: Their significance to the tectonics of the Rift Valley. *Geological Magazine* 115:329–340.
- Sterk, G. 2003 Causes, consequences and control of wind erosion in Sahelian Africa: A review. *Land Degradation & Development* 14(1):95–108.
- Stewart, B.W., Capo, R.C. and O.A. Chadwick 1998 Quantitative strontium isotope models for weathering, pedogenesis and biogeochemical cycling. *Geoderma* 82(1–3):173–195.
- Stewart, B.W., Capo, R.C. and O.A. Chadwick 2001 Effects of rainfall on weathering rate, base cation provenance and Sr isotope composition of Hawaiian soils. *Geochimica et Cosmochimica Acta* 65(7):1087–1099.
- Stewart, J.R. 2005 The ecology and adaptation of Neanderthals during the non-analogue environment of Oxygen Isotope Stage 3. *Quaternary International* 137(1):35–46.
- Stiner, M.C. 1992 Overlapping species ‘choice’ by Italian Upper Pleistocene predators. *Current Anthropology* 33:433–451.
- Stiner, M.C. 1994 *Honor Among Thieves: A Zooarchaeological Study of Neanderthal Ecology*. Princeton: Princeton University Press.

- Stoll, H.M. and D.P. Schrag 1998 Effects of Quaternary sea level cycles on strontium in seawater. *Geochimica et Cosmochimica Acta* 62(7):1107–1118.
- Straus, L.G. 1981 On the habitat and diet of *Cervus elaphus*. *Munibe* 33:175–182.
- Stringer, C. 1998 Chronological and biogeographic perspectives on later human evolution. In T. Akazawa, K. Aoki and O. Bar-Yosef (eds), *Neanderthals and Modern Humans in Western Asia*. pp.29-37. New York: Plenum Press.
- Stringer, C. and C. Gamble 1993 *In Search of the Neanderthals: Solving the puzzle of human origins*. London: Thames and Hudson.
- Stringer, C.B., Grün, R., Schwarcz, H.P. and P. Goldberg 1989 ESR dates for the Hominid burial site of ES Skull in Israel. *Nature* 338(6218):756–758.
- Stuart, A.J. 1982 *Pleistocene Vertebrates in the British Isles*. London: Longman.
- Stockdale, J. 1800 Translator's Preface to Labillardiere, M. *Voyage in Search of La Pérouse*. London: John Stockdale.
- Suga, S. 1982 Progressive mineralization pattern of developing enamel during the maturation stage. *Journal of Dental Research* 61:1532–1542.
- Suga, S. 1989 Enamel hypomineralization viewed from the pattern of progressive mineralization of human and monkey developing enamel. *Advances in Dental Research* 3:188–198.
- Suzuki, H. and F. Takai 1970 *The Amud Man and His Cave Site*. Tokyo: The University of Tokyo.
- Sykes, N.J., White, J., Hayes, T.E. and M.R. Palmer 2006 Tracking animals using strontium isotopes in teeth: The role of fallow deer (*Dama dama*) in Roman Britain. *Antiquity* 80(310):948–959.
- Tafuri, M.A., Bentley, R.A., Manzi, G. and S. di Lernia 2006 Mobility and kinship in the prehistoric Sahara: Strontium isotope analysis of Holocene human skeletons from the Acacus Mts. (southwestern Libya). *Journal of Anthropological Archaeology* 25(3):390–402.

- Takai, F. 1970 Fossil mammals from the Amud Cave. In H. Suzuki and F. Takai (eds), *The Amud Man and His Cave Site*, pp. 53–76. Tokyo: The University of Tokyo.
- Takuma, S. and S. Eda 1966 Structure and development of the peritubular matrix in dentin. *Journal of Dental Research* 45(3):683–692.
- Tappen, N.C. 1985 The dentition of the ‘old man’ of La Chapelle-aux-Saints and inferences concerning Neandertal behavior. *American Journal of Physical Anthropology* 67(1):43–50.
- Taylor, H.E., Huff, R.A. and A. Montaser 1998 Novel applications of ICPMS. In A. Montaser (ed.), *Inductively Coupled Plasma Mass Spectrometry*. pp. 681–808. New York: Wiley-VCH.
- Tchernov, E. 1968 A Preliminary Investigation of the Birds in the Pleistocene Deposits of Ubeidiya, Israel. Jerusalem: Israel Academy of Science and Humanities.
- Tchernov, E. 1979 Quaternary fauna. In A. Horowitz (ed.), *The Quaternary of Israel*, pp. 259–290. New York: Academic Press.
- Tchernov, E. 1984 The fauna of Sefunim Cave, Mt Carmel. In A. Ronen (ed.), *Sefunim Prehistoric Sites Mount Carmel, Israel*, pp. 401–419. Oxford: BAR International Series 230 (ii).
- Tchernov, E. 1988a. Biochronology of the Middle Paleolithic and dispersal events of hominids in the Levant. In M. Otte (ed.), *L'homme de Neandertal: L'environnement*. pp. 153–168. Liege: University de Liege.
- Tchernov, E. 1988b. The age of Ubeidiya Formation (Jordan Valley, Israel) and the earliest Homonids in the Levant. *Paleorient* 14(2):63–65.
- Teagle, D.A.H., Alt, J.C., Chiba, H. and A.N. Halliday 1998 Dissecting an active hydrothermal deposit: The strontium and oxygen isotopic anatomy of the TAG hydrothermal mound-anhydrite. In M. Herzig, S.E. Humphris, D.J. Miller and R.A. Zierenberg (eds), *Proceedings of the Ocean Drilling Program, Scientific Results*. pp. 129–141. Ocean Drilling Program, College Station.

- Terry, R.C. 2010 The dead do not lie: Using skeletal remains for rapid assessment of historical small-mammal community baselines. *Proceedings of the Royal Society B* 277(1685):1193–1201.
- Thenius, E. 1970 Zur Evolution und Verbreitungsgeschichte der Suidae (Artiodactyla, Mammalia). *Zeitschrift für Säugetierkunde* 35:321–342.
- Thompson, J.L. and B. Illerhaus 1998 A new reconstruction of the Le Moustier 1 skull and investigation of internal structures using 3-D- μ CT data. *Journal of Human Evolution* 35(6):647–665.
- Thornton, C.P., Lamberg-Karlovsky, C.C., Liezers, M. and S.M.M. Young 2002 On pins and needles: Tracing the Evolution of copper-base alloying at Tepe Yahya, Iran, via ICPMS analysis of common-place items. *Journal of Archaeological Science* 29(12):1451–1460.
- Tong, H. 2001 Age profiles of rhino fauna from the Middle Pleistocene Nanjing Man site, South China: Explained by the rhino specimens of living species. *International Journal of Osteoarchaeology* 11:231–237.
- Torres, J., Droz, L., Savoye, B., Terentieva, E., Cochonat, P., Kenyon, N.H. and M. Canals 1997 Deep-sea avulsion and morphosedimentary evolution of the Rhône Fan Valley and Neofan during the Late Quaternary (north-western Mediterranean Sea). *Sedimentology* 44(3):457–477.
- Trickett, M.A., Budd, P., Montgomery, J. and J. Evans 2003 An assessment of solubility profiling as a decontamination procedure for the $^{87}\text{Sr}/^{86}\text{Sr}$ analysis of archaeological human skeletal tissue. *Applied Geochemistry* 18(5):653–658.
- Trinkaus, E. 1983 *The Shanidar Neanderthals*. New York: Academic Press.
- Trinkaus, E. 1985 Pathology and the posture of the La Chapelle-aux-Saints Neandertal. *American Journal of Physical Anthropology* 67(1):19–41.
- Trinkaus, E. 1995 Near Eastern late Archaic Humans. *Paleorient* 21(2):9–24.
- Trinkaus, E. 2005 Early modern humans. *Annual Review of Anthropology* 34:207–230.

- Trinkaus, E. 2011 The postcranial dimensions of the La Chapelle-aux-saints 1 Neandertal. *American Journal of Physical Anthropology* 145(3):461–468.
- Trinkaus, E. and P. Shipman 1993 *The Neanderthals: Changing the image of mankind*. London: Jonathan Cape.
- Tristram, H.B. 1866 Report on the mammals of Palestine. *Proceedings of the Zoological Society of London* 1866:84–93.
- Trotter, J.A. and S.M. Eggins 2006 Chemical systematics of conodont apatite determined by laser ablation ICPMS. *Chemical Geology* 233:196–216.
- Trueman, C.N.G., Behrensmeyer, A.K., Tuross, N. and S. Weiner 2004 Mineralogical and compositional changes in bones exposed on soil surfaces in Amboseli National Park, Kenya: Diagenetic mechanisms and the role of sediment pore fluids. *Journal of Archaeological Science* 31(6):721–739.
- Tsatskin, A. 1998 A paleopedological examination of the sediments in Tabun Cave, Mount Carmel, Israel. *Quaternary International* 51–52:75–77.
- Tsatskin, A. and T.S. Gandler 2002 Further notes on Terra Rossa and related soils near Kfar Hahoresh archaeological site, Israel. *Options méditerranéennes* 50:109–120.
- Tung, T.A. and K.J. Knudson 2011 Identifying locals, migrants and captives in the Wari Heartland: A bioarchaeological and biogeochemical study of human remains from Conchopata, Peru. *Journal of Anthropological Archaeology* 30(3):247–261.
- Turner, B.L., Kamenov, G.D., Kingston, J.D. and G.J. Armelagos 2009 Insights into immigration and social class at Machu Picchu, Peru based on oxygen, strontium and lead isotopic analysis. *Journal of Archaeological Science* 36(2):317–332.
- Tzedakis, P.C. 2005 Towards an understanding of the response of southern European vegetation to orbital and suborbital climate variability. *Quaternary Science Reviews* 24(14–15):1585–1599.

Tzedakis, P.C., McManus, P.C., Hooghiemstra, H., Oppo, D.W. and T.A.

Wijmstra 2003 Comparison of changes in vegetation in northeast Greece with records of climate variability on orbital and suborbital frequencies over the last 450,000 years. *Earth and Planetary Science Letters* 212:197–212.

Ungar, P.S., Grine, F.E. and M.F. Teaford 2006 Diet in early *Homo*: A review of the evidence and a new model of adaptive versatility. *Annual Review of Anthropology* 35:209–228.

Vaks, A., Bar-Matthews, M., Ayalon, A., Matthews, A., Frumkin, A., Dayan, U., Halicz, L., Almogi-Labin, A. and B. Schilman 2006 Paleoclimate and location of the border between Mediterranean climate region and the Saharo-Arabian Desert as revealed by speleothems from the northern Negev Desert, Israel. *Earth and Planetary Science Letters* 249(3–4):384–399.

Vaks, A., Bar-Matthews, M., Ayalon, A., Matthews, A., Halicz, L. and A. Frumkin 2007 Desert speleothems reveal climatic window for African exodus of early modern humans. *Geology* 35(9):831–834.

Valentine, B., Kamenov, G.D. and J. Krigbaum 2008 Reconstructing Neolithic groups in Sarawak, Malaysia through lead and strontium isotope analysis. *Journal of Archaeological Science* 35(6):1463–1473.

Valladas, H., Geneste, J.M., Joron, J.L. and J.P. Chadelle 1986 Thermoluminescence dating of Le Moustier (Dordogne, France). *Nature* 322:452–454.

Valladas, H., Joron, J.L., Valladas, G., Arensburg, B., Bar-Yosef, O., Belfer-Cohen, A., Goldberg, P., Laville, H., Meignen, L., Rak, Y., Tchernov, E., Tilier, A.M. and B. Vandermeersch 1987 Thermoluminscence dates for the Neanderthal burial site at Kebara in Israel. *Nature* 330:159–160.

Valladas, H., Mercier, H., Joron, J.-L. and J.-L. Reyss 1998 GIF laboratory dates for Middle Paleolithic Levant. In T. Akazawa, K. Aoki and O. Bar-Yosef (eds), *Neanderthals and Modern Humans in Western Asia*, pp. 69–75. New York: Plenum Press.

- Valladas, H., Mercier, N., Ayliffe, L.K., Falguères, C., Bahain, J.J., Dolo, J.M., Froget, L., Joron, J.L., Masaoudi, H., Reyss, J.L. and M.H. Moncel 2008 Radiometric dates for the Middle Palaeolithic sequence of Payre (Ardèche, France). *Quaternary Geochronology* 3(4):377–389.
- Valladas, H., Mercier, N., Froget, L., Hovers, E., Joron, J.L., Kimbel, W.H. and Y. Rak 1999 TL Dates for the Neanderthal site of the Amud Cave, Israel. *Journal of Archaeological Science* 26(3):259–268.
- Valladas, H., Reyss, J.-L., Valladas, G., Bar-Yosef, O. and B. Vandermeersch 1988 Thermoluminescence dating of Mousterian ‘Proto-Cro-Magnon’ remains from Israel and the origins of modern man. *Nature* 331:614–616.
- Van andel, T.H. and P.C. Tzedakis 1996 Palaeolithic landscapes of Europe and environs, 150,000–25,000 years ago: An overview. *Quaternary Science Reviews* 15(5–6):481–500.
- van Bree, P.J.H., van Soest, R.M.W. and L. Strongman 1974 Tooth wear as an indication of age in badgers (*Meles meles*, L.) and red foxes (*Vulpes vulpes*, L.). *Zeitschrift fur Saugetierk* 39:243–248.
- van der Merwe, N.J., Lee-Thorp, J.A., Thackeray, J.F., Hall-Martin, A., Kruger, F.J., Coetze, H., Bell, R.H.V. and M. Lindeque 1990 Source-area determination of elephant ivory by isotopic analysis. *Nature* 346(6286):744–746.
- van Horn, R.C., McElhinny, T.L. and K.E. Holekamp 2003 Age estimation and dispersal in the spotted hyena (*Crocuta crocuta*). *Journal of Mammalogy* 84(3):1019–1019–1030.
- Van Meerbeeck, C.J., Renssen, H., Roche, D.M., Wohlfarth, B., Bohncke, S.J.P., Bos, J.A.A., Engels, S., Helmens, K.F., Sáinzchez-Goñi, M.F., Svensson, A. and J. Vandenbergh 2011 The nature of MIS 3 stadial-interstadial transitions in Europe: New insights from model-data comparisons. *Quaternary Science Reviews* 30(25–26):3618–3637.
- van Vuure, T. 2005 Retracing the Aurochs: History, Morphology and Ecology of an Extinct Wild Ox. Sofia: Pensoft.

- Vandermeersch, B. 1966 Nouvelles découvertes de restes humains dans les couches Levalloisomoustériennes du gisement de Qafzeh (Israël). *Compte Rendus de l'Academie des Sciences*, D:262:1434–1436.
- Vandermeersch, B. 1969a. Les nouveaux squelettes moustériens découverts à Qafzeh (Israël) et leur signification. *Compte Rendus de l'Academie des Sciences* D(268):2562–2565.
- Vandermeersch, B. 1969b. Decouverte d'un object en ocre avec trace d'utilisation dans le moustérien de Qafzeh (Israel). *Bulletin de la Société Préhistorique Française* 66:157–158.
- Vandermeersch, B. 1970 Une sepulture moustérienne avec offrandes découverte dans la grotte de Qafzeh. *Compte Rendus de l'Academie des Sciences* 268:298–301.
- Vandermeersch, B. 1981 *Les Hommes Fossiles de Qafzeh, Israel*. Paris: CNRS.
- Vandermeersch, B. 1989 The evolution of modern humans: Recent evidence from southwest Asia. In P. Mellars and C.B. Stringer (eds), *The Human Revolution*, pp. 155–164. Edinburgh: Edinburgh University Press.
- Vanhaeren, M., d'Errico, F., Stringer, C., James, S.L., Todd, J.A. and H.K. Mienis 2006 Middle Paleolithic shell beads in Israel and Algeria. *Science* 312:1785–1788.
- Vaughan, B.E., Evans, E.C. and M.E. Hutchin 1967 Polar transport characteristics of radiostronium and radiocalcium in isolated corn root segments. *Plant Physiology* 42:747–750.
- Veizer, J. 1989 Strontium isotopes in seawater through time. *Annual Review of Earth and Planetary Science* 17:141–167.
- Vekua, A., Lordkipanidze, D., Rightmire, G.P., Agusti, J., Ferring, R., Maisuradze, G., Mouskhelishvili, A., Noriadze, M., Ponce de Leon, M., Tappen, M., Tvalchrelidze, M. and C. Zollikofer 2002 A new skull of early homo from Dmanisi, Georgia. *Science* 297:85–89.

- Vergés, J., Fernàndez, M. and A. Martínez 2002 The Pyrenean orogen: Pre-, syn- and post-collisional evolution. *Journal of the Virtual Explorer* 8:55–74.
- Verri, G., Barkai, R., Gopher, A., Hass, M., Kubik, P.W., Paul, M., Ronen, A., Weiner, S. and E. Boaretto 2005 Flint procurement strategies in the Late Lower Palaeolithic recorded by in situ produced cosmogenic Be-10 in Tabun and Qesem Caves (Israel). *Journal of Archaeological Science* 32(2):207–213.
- Villa, P. 1983 Terra Amata and the Middle Pleistocene Archaeological Record of Southern France. Berkeley: University of California Press.
- Villa, P. and L. Bartram 1996 Flaked bone from a hyena den. *Paleo* 8:143–159.
- Villa, P. and M. Soressi 2000 Stone tools in carnivore sites: The case of Bois Roche. *Journal of Anthropological Research* 56:187–215.
- Villa, P., Sánchez Goñi, M.F., Bescós, G.C., Grün, R., Ajas, A., García Pimienta, J.C. and W. Lees 2010 The archaeology and paleoenvironment of an Upper Pleistocene hyena den: An integrated approach. *Journal of Archaeological Science* 37:919–935.
- Vilomet, J.D., Angeletti, B., Moustier, S., Ambrosi, J.P., Wiesner, M., Bottero, J.Y. and L. Chatelet-Snidaro 2001 Application of strontium isotopes for tracing landfill leachate plumes in groundwater. *Environmental Science & Technology* 35(23):4675–4679.
- Viner, S., Evans, J., Albarella, U. and M.P. Pearson 2010 Cattle mobility in prehistoric Britain: Strontium isotope analysis of cattle teeth from Durrington Walls (Wiltshire, Britain). *Journal of Archaeological Science* 37(11):2812–2820.
- Vita-Finzi, C. and C. Stringer 2007a The setting of the Mt. Carmel caves reassessed. *Quaternary Science Reviews* 26:436–440.
- Vita-Finzi, C. and C. Stringer 2007b Reply to Ronen et al. *Quaternary Science Reviews* 26:2685–2686.

- Vliet-Lanoë, B.V. 1989 Dynamics and extent of the Weichselian permafrost in western Europe (Substage 5E to stage 1). *Quaternary International* 3–4(0):109–113.
- Voelker, A.H.L. 2002 Global distribution of centennial-scale records for Marine Isotope Stage (MIS) 3: A database. *Quaternary Science Reviews* 21(10):1185–1212.
- Vogel, J.C., Eglington, B. and J.M. Auret 1990 Isotope fingerprints in elephant bone and ivory. *Nature* 346(6286):747–749.
- Voight, E.A. 1987 Red fox. In M. Nowak, J.A. Baker, M.E. Obbard and B. Malloch (eds), *Wild Furbearer Management and Conservation in North America*. pp. 379–382. Ontario: Ministry of Natural Resources.
- von Koenigswald, W. 2000 Two different strategies in enamel differentiation: Marsupialia versus Eutheria. In M.F. Teaford, M.M. Smith and M.W. J. Ferguson (eds), *Development, Function and Evolution of Teeth*, p. 314. Cambridge: Cambridge University Press.
- Vroon, P.Z., van der Wagt, B., Koornneef, J.M. and G.R. Davies 2008 Problems in obtaining precise and accurate Sr isotope analysis from geological materials using laser ablation MC-ICPMS. *Analytical and Bioanalytical Chemistry* 390:463–476.
- Waught, T., Baker, J. and D. Peate 2002 Sr isotope ratio measurements by double-focusing MC-ICPMS: Techniques, observations and pitfalls. *International Journal of Mass Spectrometry* 221(3):229–244.
- Walder, A.J. and P.A. Freedman 1992 Isotopic ratio measurement using a double focusing magnetic sector mass analyser with an inductively coupled plasma as an ion source. *Journal of Analytical Atomic Spectrometry* 7:571–575.
- Waldmann, N., Stein, M., Ariztegui, D. and A. Starinsky 2009 Stratigraphy, depositional environments and level reconstruction of the last interglacial Lake Samra in the Dead Sea basin. *Quaternary Research* 72(1):1–15.
- Walker, E.P. 1968 *Mammals of the World*. Baltimore: The Johns Hopkins Press.

- Wallace, A. and E.M. Romney 1971 Some interactions of Ca, Sr and Ba in plants. *Agronomy Journal* 63(2):245–248.
- Wantabe, H. 1970 A Palaeolithic industry from the Amud Cave. In H. Suzuki and F. Takai (eds), *The Amud Man and His Cave Site*, pp. 77–95. Tokyo: The University of Tokyo.
- Wargo, M.C. 2009 The Bordes-Binford Debate: Transatlantic Interpretative Traditions in Paleolithic Archaeology. Unpublished PhD thesis, The Graduate School, University of Texas at Arlington.
- Webb, E., Amarasinghe, D., Tauch, S., Green, E.F., Jones, J. and A.H. Goodman 2005 Inductively coupled plasma-mass (ICPMS) and atomic emission spectrometry (ICP-AES): Versatile analytical techniques to identify the archived elemental information in human teeth. *Microchemical Journal* 81(2):201–208.
- Weber, P.K., Bacon, C.R., Hutcheon, I.D., Ingram, B.L. and J.L. Wooden 2005 Ion microprobe measurement of strontium isotopes in calcium carbonate with application to salmon otoliths. *Geochimica et Cosmochimica Acta* 69(5):1225–1239.
- Wedel, V.L. 2007 Determination of season at death using dental cementum increment analysis. *Journal of Forensic Sciences* 52(6):1334–1337.
- Weiner, S. 2010 Microarchaeology: Beyond the Visible Archaeological Record. Cambridge: Cambridge University Press.
- Weiner, S., Veis, A., Beniash, E., Arad, T., Dillon, J.W., Sabsay, B. and F. Siddiqui 1999 Peritubular dentin formation: Crystal organization and the macromolecular constituents in human teeth. *Journal of Structural Biology* 126(1):27–41.
- Weinstein, Y. 2000 Spatial and temporal geochemical variability in basin-related volcanism, northern Israel. *Journal of African Earth Sciences* 30(4):865–886.

- Weinstein, Y., Navon, O., Altherr, R. and M. Stein 2006 The role of lithospheric mantle heterogeneity in the generation of Plio-Pleistocene Alkali Basaltic suites from NW Harrat Ash Shaam (Israel). *Journal of Petrology* 47(5):1017–1050.
- Weinstein-Evron, M., Bar-Oz, G., Zaidner, Y., Tsatskin, A., Druck, D., Porat, N. and I. Hershkovitz 2003 Introducing Misliya Cave, Mount Carmel, Israel: A New continuous Lower/Middle Paleolithic sequence in the Levant. *Eurasian Prehistory* 1(1):31–55.
- Wells, E.C. 2004 Investigating activity patterns in prehispanic plazas: Weak acid-extraction ICP–AES analysis of anthrosols at Classic period El Coyote, northwestern Honduras. *Archaeometry* 46(1):67–84.
- West, J.B., Hurley, J.M., Dudás, F.Ö. and J.R. Ehleringer 2009 The stable isotope ratios of marijuana. II. Strontium isotopes relate to geographic origin. *Journal of Forensic Sciences* 54(6):1261–1269.
- Wheeler, P.E. 1992 The thermoregulatory advantages of large body size for hominids foraging in savannah environments. *Journal of Human Evolution* 23(4):351–362.
- Whipkey, C.E., Capo, R.C., Chadwick, O.A. and B.W. Stewart 2000 The importance of sea spray to the cation budget of a coastal Hawaiian soil: A strontium isotope approach. *Chemical Geology* 168(1–2):37–48.
- White, M. and N. Ashton 2003 Lower Palaeolithic core technology and the origins of the Levallois method in northwestern Europe. *Current Anthropology* 44(4):598–609.
- White, T.D. and P.A. Folkens 2005 *The Human Bone Manual*. California: Elsevier Press.
- White, T.D., Asfaw, B., DeGusta, D., Gilbert, H., Richards, G.D., Suwa, G. and F.C. Howell 2003 Pleistocene *Homo sapiens* from middle Awash, Ethiopia. *Nature* 423:742–747.
- Wickman, F.E. 1948 Isotope ratios: A clue to the age of certain marine sediments. *The Journal of Geology* 56:61–66.

- Wickman, F.E. and Åberg, G. 1987 Variations in the $^{87}\text{Sr}/^{86}\text{Sr}$ ratio in lake waters from central Sweden. *Nordic Hydrology* 18:21–32.
- Widga, C., Walker, J.D. and L.D. Stockli 2010 Middle Holocene Bison diet and mobility in the eastern Great Plains (USA) based on $\delta^{13}\text{C}$, $\delta^{18}\text{O}$ and $^{87}\text{Sr}/^{86}\text{Sr}$ analyses of tooth enamel carbonate. *Quaternary Research* 73(3):449–463.
- Williams, R.A.D. and J.C. Elliot 1989 *Basic and Applied Dental Biochemistry*. Edinburgh: Churchill Livingstone.
- Wilson, C.A., Davidson, D.A. and M.S. Cresser 2005 An evaluation of multielement analysis of historic soil contamination to differentiate space use and former function in and around abandoned farms. *The Holocene* 15(7):1094–1099.
- Wilson, C.A., Davidson, D.A. and M.S. Cresser 2008 Multi-element soil analysis: An assessment of its potential as an aid to archaeological interpretation. *Journal of Archaeological Science* 35:412–424.
- Woillard, G.M. 1978 Grande Pile peat bog: A continuous pollen record for the last 140,000 years. *Quaternary Research* 9:1–21.
- Woillard, G.M. and W.G. Mook 1982 Carbon-14 dates at Grand Pile: Correlation of land and sea chronologies. *Science* 215:159–161.
- Wolpoff, M.H. 1980 *Paleoanthropology*. New York: Alfred Knopf.
- Wood, B. and M. Collard 1999 The human genus. *Science* 284:65–71.
- Wood, B.A. 1991 Hominid Cranial Remains. Koobi Fora Research Project. Oxford: Clarendon.
- Woodhead, J., Swearer, S., Hergt, J. and R. Maas 2005 In situ Sr-isotope analysis of carbonates by LA-MC-ICPMS: Interference corrections, high spatial resolution and an example from otolith studies. *Journal of Analytical Atomic Spectrometry* 20(1):22–27.
- Wright, L.E. 2012 Immigration to Tikal, Guatemala: Evidence from stable strontium and oxygen isotopes. *Journal of Anthropological Archaeology* 31(3):334–352.

- Wright, L.E., Valdés, J.A., Burton, J.H., Douglas Price, T. and H.P. Schwarcz
2010 The children of Kaminaljuyu: Isotopic insight into diet and long
distance interaction in Mesoamerica. *Journal of Anthropological
Archaeology* 29(2):155–178.
- Yaalon, D.H. 1967 Factors affecting the lithification of eolianite and
interpretation of its environmental significance in the Coastal Plain of
Israel. *Journal of Sedimentary Petrology* 37:1189–1199.
- Yaalon, D.H. 1997 Soils in the Mediterranean region: What makes them
different? *Catena* 28:157–169.
- Yaalon, D.H., Nathan, Y., Koyumdjisky, H. and J. Dan 1966 Weathering and
catenary differentiation of clay minerals in soils on various parent
materials in Israel. In Heller, L and A. Weiss (eds), *Proceedings of the
International Clay Conference, Jerusalem*, pp. 187–198. Jerusalem:
Israel Program for Scientific Translations.
- Yang, L. 2009 Accurate and precise determination of isotopic ratios by MC-
ICPMS: A review. *Mass Spectrometry Reviews* 28(6):990–1011.
- Yizraeli, T. 1967 A lower Paleolithic site at Holon. *Israel Exploration Journal*
17:144–152.
- Zagwijn, W.H. 1989 Vegetation and climate during warmer intervals in the Late
Pleistocene of western and central Europe. *Quaternary International* 3–
4(0):57–67.
- Zaidner, Y., Druck, Y., Nadler, M. and M. Weinstein-Evron 2005 The Archeulo-
Yabrudian of Jamal Cave, Mount Carmel, Israel. *Journal of the Israel
Prehistoric Society* 35:93–116.
- Zapata, J., Pérez-Sirvent, C., Martínez-Sánchez, M.J. and P. Tovar 2006
Diagenesis, not biogenesis: Two late Roman skeletal examples. *Science
of The Total Environment* 369(1–3):357–368.
- Zeuner, F.E. 1963 *A History of Domesticated Animals*. New York: Harper and
Row.

- Zlateva, B., Djingova, R. and I. Kuleff 2003 On the possibilities of ICP-AES for analysis of archaeological bones. *Central European Journal of Chemistry* 1(3):201–221.
- Zohary, M. 1962 *Plant life of Palestine: Israel and Jordan*. New York: Ronald Press.
- Zohary, M. 1973 *Geobotanical Foundations of the Middle East*. Stuttgart: Gustav Fischer Verlag.
- Zumdahl, S.S. 1997 *Chemistry*. Boston: Houghton Mifflin.
- Zviely, D., Galili, E., Ronen, A., Salamon, A. and Z. Ben-Avraham 2009 Reevaluating the tectonic uplift of western Mount Carmel, Israel, since the middle Pleistocene. *Quaternary Research* 71:239–245.

Appendix One: Sample Collection Locations

A1.1. Israeli Sites

A1.1.1. IS001

Easting: 682494

Northing: 3621957

Zone: 36S

Elevation: 5

Description of Site Location: On the highway from Haifa-Tel Aviv under a railway bridge at 'railway' archaeological site.

Date Collected: 27/09/2008

Collected By: Ian Moffat

Samples in Study: SS002

Sample Types in Study: Soil

Soil Described in Field: Very thin, poorly developed soil on lithified sand dune with a maximum thickness of 5 cm.

Geology Observed in the Field: Calcareous sandstone

Geology Name from Map: Calcareous sandstone 'kurkar'

Lithology from Map: Clay, silt, sand

Age from Map: Quaternary



A1.1.2. IS002

Easting: 682494

Northing: 3621957

Zone: 36S

Elevation: 0

Description of Site Location: Unconsolidated coastal dune between Highway 2 and the beach near Hadera.

Date Collected: 27/09/2008

Collected By: Ian Moffat

Samples in Study: SS003

Sample Types in Study: Soil

Soil Described in Field: No soil formation evident.

Geology Observed in the Field: No bedrock

Geology Name from Map: Sand dunes

Lithology from Map: Gravel, sand, silt

Age from Map: Quaternary



A1.1.3. IS003

Easting: 680980

Northing: 3601307

Zone: 36S

Elevation: 5

Description of Site Location: On the edge of the olive grove, off Highway 4 near Bet Hanayan, near the foot of Carmel Range.

Date Collected: 27/09/2008

Collected By: Ian Moffat

Samples in Study: SS004

Sample Types in Study: Soil

Soil Described in Field: Sample from 5 cm below surface in material with abundant clay pellets and carbonate nodules.

Geology Observed in the Field: No bedrock

Geology Name from Map: Calcareous sandstone 'kurkar'

Lithology from Map: Clay, silt, sand

Age from Map: Quaternary



A1.1.4. IS004

Easting: 681536

Northing: 3604285

Zone: 36S

Elevation: 7

Description of Site Location: Adjacent to Highway 2 in the new construction near Kebara Cave.

Date Collected: 27/09/2008

Collected By: Ian Moffat

Samples in Study: RS002, SS005, SS006

Sample Types in Study: Rock, soil

Soil Described in Field: Dark, organic rich, friable soil with some carbonate nodules (SS005) and more consolidated, less organic soil with large limestone blocks (SS06).

Geology Observed in the Field: Sandstone with carbonate matrix

Geology Name from Map: Sakhnin and Yanuh Formation

Lithology from Map: Dolostone, limestone, chert

Age from Map: Cenomanian



A1.1.5. IS005

Easting: 684801

Northing: 3623556

Zone: 36S

Elevation: 93

Description of Site Location: Msylia Cave in the Carmel Range, east of Highway 4 south of Haifa.

Date Collected: 29/09/2008

Collected By: Ian Moffat

Samples in Study: RS003, SS007

Sample Types in Study: Rock, soil

Soil Described in Field: Thin veneer of sediment overlaying cave sediment located near excavation.

Geology Observed in the Field: Reefal limestone

Geology Name from Map: Bina Formation

Lithology from Map: Limestone, marl, dolostone

Age from Map: Turonian



A1.1.6. IS006

Easting: 685092

Northing: 3621362

Zone: 36S

Elevation: 52

Description of Site Location: Cave of Nahal Oren, off Highway 4 south of Haifa. Material collected about 5 m into cave on east edge.

Date Collected: 29/09/2008

Collected By: Ian Moffat

Samples in Study: RS004, SS008

Sample Types in Study: Rock, soil

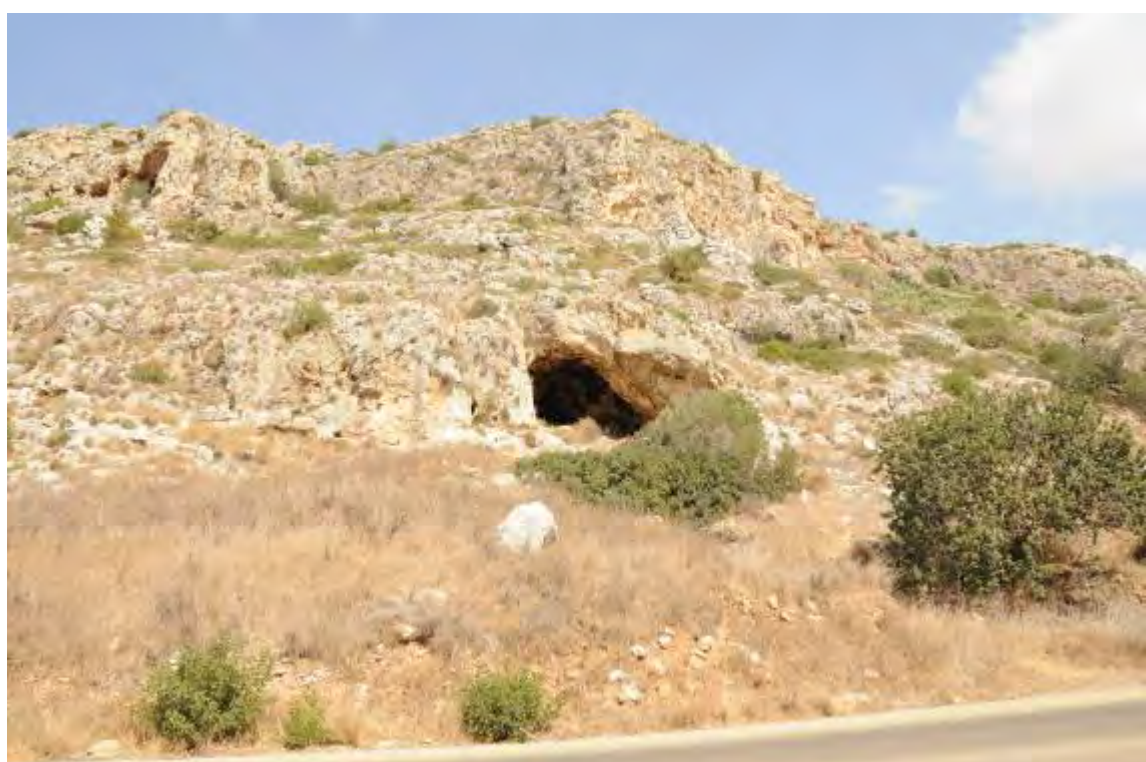
Soil Described in Field: Very fine grained powdery cave sediment with abundant goat faeces.

Geology Observed in the Field: Reefal limestone

Geology Name from Map: Bina Formation

Lithology from Map: Limestone, marl, dolostone

Age from Map: Turonian



A1.1.7. IS007

Easting: 683780

Northing: 3603356

Zone: 36S

Elevation: 66

Description of Site Location: Off Highway 652, south of Neve Sharel.

Date Collected: 29/09/2008

Collected By: Ian Moffat

Samples in Study: RS005, SS009

Sample Types in Study: Rock, soil

Soil Described in Field: Thin soil developed on top of a limestone with many rock fragments.

Geology Observed in the Field: Limestone

Geology Name from Map: Bina Formation

Lithology from Map: Limestone, marl, dolostone

Age from Map: Turonian



A1.1.8. IS008

Easting: 687978

Northing: 3609221

Zone: 36S

Elevation: 101

Description of Site Location: On the track into forest north of Bat Shlomo.

Date Collected: 29/09/2008

Collected By: Ian Moffat

Samples in Study: RS006, SS010

Sample Types in Study: Rock, soil

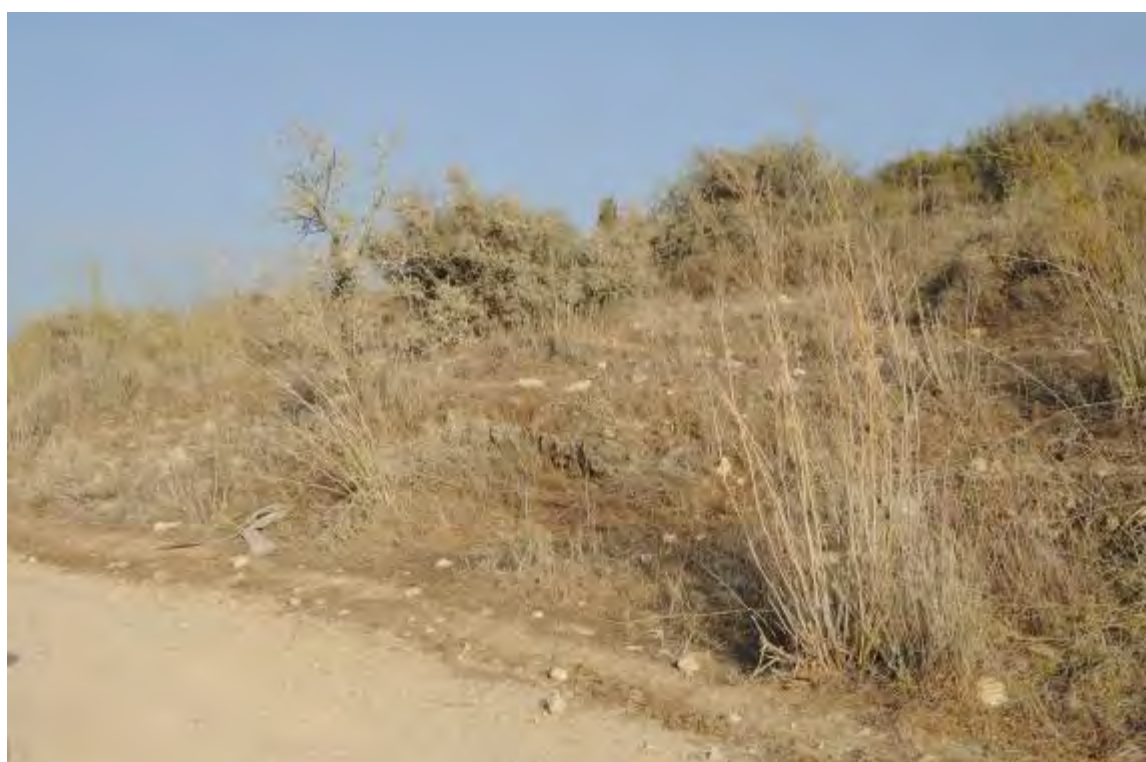
Soil Described in Field: Some chalk fragments with pellet clays dominating.

Geology Observed in the Field: Chalk

Geology Name from Map: Adulam Formation

Lithology from Map: Chalk, chert

Age from Map: Lower-Middle Eocene



A1.1.9. IS009

Easting: 695586

Northing: 3650202

Zone: 36S

Elevation: 9

Description of Site Location: North of Akko near turnoff to Regba and Nes Ammin (8611).

Date Collected: 30/09/2008

Collected By: Ian Moffat

Samples in Study: RS007, SS010*

Sample Types in Study: Rock, soil

Soil Described in Field: Very thin soil with many rock fragments.

Geology Observed in the Field: Chalk

Geology Name from Map: Adulam Formation

Lithology from Map: Chalk, chert

Age from Map: Lower-Middle Eocene



A1.1.10. IS010

Easting: 705301

Northing: 3661995

Zone: 36S

Elevation: 397

Description of Site Location: In small park on the Lebanese border.

Date Collected: 30/09/2008

Collected By: Ian Moffat

Samples in Study: RS008, SS011

Sample Types in Study: Rock, soil

Soil Described in Field: Thin *Terra rossa* soil with abundant limestone fragments.

Geology Observed in the Field: Limestone

Geology Name from Map: Bina Formation

Lithology from Map: Limestone, marl, dolostone

Age from Map: Turonian



A1.1.11. IS011

Easting: 712541

Northing: 3662131

Zone: 36S

Elevation: 555

Description of Site Location: On Highway 899 at turnoff to Shomeral/Zarit.

Date Collected: 30/09/2008

Collected By: Ian Moffat

Samples in Study: RS009, SS012

Sample Types in Study: Rock, soil

Soil Described in Field: Thin soil developed on top of limestone. Soil sample taken next to orchard and fence. May be disturbed and have fertilizer.

Geology Observed in the Field: Very fine grained limestone

Geology Name from Map: Mount Scopus Group

Lithology from Map: Chalk, marl

Age from Map: Senonian-Paleocene



A1.1.12. IS012

Easting: 719243

Northing: 3659214

Zone: 36S

Elevation: 674

Description of Site Location: On Road 8994 just south of turnoff from Road 899 at Har Biranit.

Date Collected: 30/09/2008

Collected By: Ian Moffat

Samples in Study: RS010, SS013

Sample Types in Study: Rock, soil

Soil Described in Field: Thin reddish mantle on limestone, very thin poorly developed soil with some limestone fragments.

Geology Observed in the Field: Limestone

Geology Name from Map: Deir Hanna Formation, Isfiya Chalk, Bet Oren Limestone, Khureibe Chalk and Junediya Chalk

Lithology from Map: Limestone, dolostone, marl, chalk, chert

Age from Map: Cenomanian



A1.1.13. IS013

Easting: 721813

Northing: 3649514

Zone: 36S

Elevation: 935

Description of Site Location: On north side of road near a quarry on the way to Beit Jan.

Date Collected: 30/09/2008

Collected By: Ian Moffat

Samples in Study: RS011, SS014

Sample Types in Study: Rock, soil

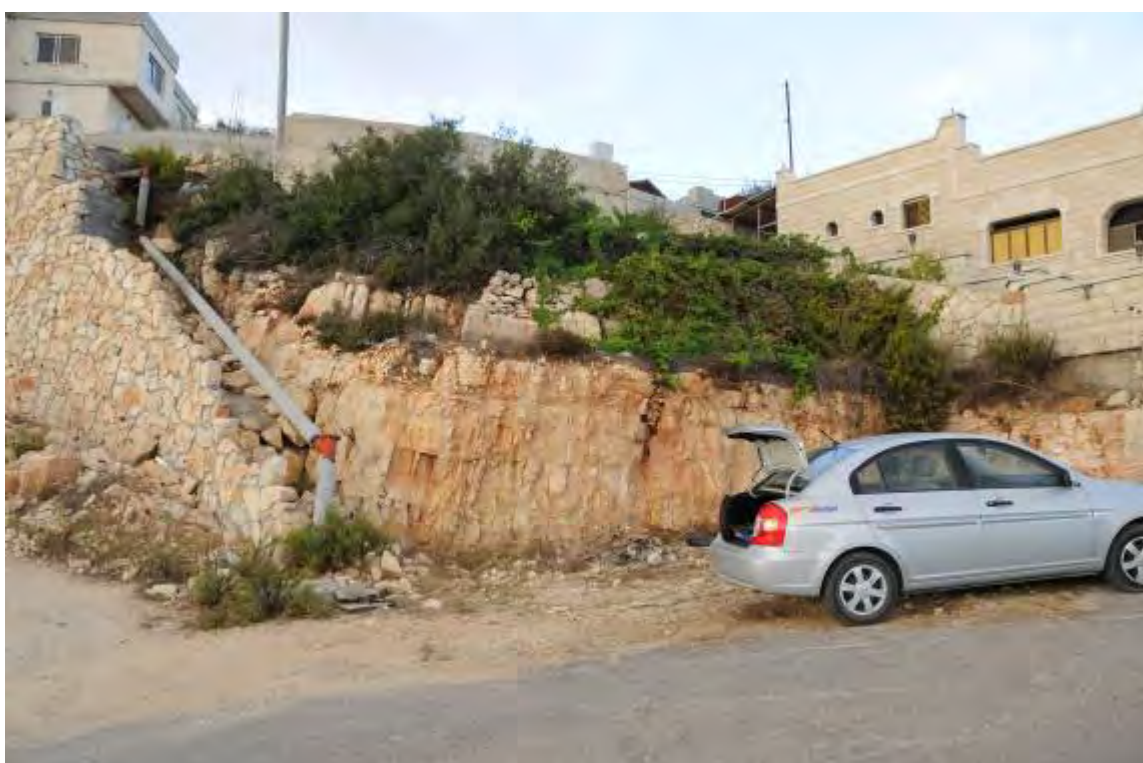
Soil Described in Field: Thinly developed soil on limestone. Sampled near garden and recent earthworks.

Geology Observed in the Field: Chalky limestone

Geology Name from Map: Deir Hanna Formation, Isfiya Chalk, Bet Oren Limestone, Khureibe Chalk and Junediya Chalk

Lithology from Map: Limestone, dolostone, marl, chalk, chert

Age from Map: Cenomanian



A1.1.14. IS014

Easting: 696501

Northing: 3627390

Zone: 36S

Elevation: 9

Description of Site Location: In paddock to the east of Highway 70 heading north from Haifa.

Date Collected: 01/10/2008

Collected By: Ian Moffat

Samples in Study: SS015

Sample Types in Study: Soil

Soil Described in Field: Nearly all cracking clay, recently ploughed agricultural land. Almost certainly has had fertilizer applied.

Geology Observed in the Field: No bedrock

Geology Name from Map: Alluvium

Lithology from Map: Gravel, sand, clay

Age from Map: Quaternary



A1.1.15. IS015

Easting: 702082

Northing: 3634803

Zone: 36S

Elevation: 63

Description of Site Location: On small side road parallel to Highway 70 near Shafar'am.

Date Collected: 01/10/2008

Collected By: Ian Moffat

Samples in Study: RS012, SS016

Sample Types in Study: Rock, soil

Soil Described in Field: Thin soil developed on limestone. There has been some disturbance and dumping of rubbish in the area.

Geology Observed in the Field: Limestone breccia

Geology Name from Map: Alluvium

Lithology from Map: Gravel, sand, clay

Age from Map: Quaternary



A1.1.16. IS016

Easting: 710374

Northing: 3639794

Zone: 36S

Elevation: 272

Description of Site Location: Off Highway 805 on the way to Ya'aa.

Date Collected: 01/10/2008

Collected By: Ian Moffat

Samples in Study: RS013, SS017

Sample Types in Study: Rock, soil

Soil Described in Field: Thin brown soil on limestone, composed of clay with occasional limestone fragments.

Geology Observed in the Field: Chalky limestone

Geology Name from Map: Mount Scopus Group

Lithology from Map: Chalk, marl

Age from Map: Senonian-Paleocene



A1.1.17. IS017

Easting: 723533

Northing: 3637663

Zone: 36S

Elevation: 169

Description of Site Location: East of Deir Hana on Road 805, next to Muslim shrine in olive grove.

Date Collected: 01/10/2008

Collected By: Ian Moffat

Samples in Study: RS014, SS018

Sample Types in Study: Rock, soil

Soil Described in Field: Thin red soil on limestone mainly composed of clay with limestone pieces. In olive grove, so may be fertilized.

Geology Observed in the Field: Chalky white limestone

Geology Name from Map: Nabi Sa'id, Ein el Assad, Hidra, Rama and Kefira Formations

Lithology from Map: Limestone, chalk, marl, sandstone

Age from Map: Lower Cretaceous



A1.1.18. IS018

Easting: 712855

Northing: 3636020

Zone: 36S

Elevation: 421

Description of Site Location: On Road 7955 just west of turnoff to Yodfat.

Date Collected: 01/10/2008

Collected By: Ian Moffat

Samples in Study: RS015, SS019

Sample Types in Study: Rock, soil

Soil Described in Field: Thin, poorly developed soil on limestone.

Geology Observed in the Field: Chalky limestone

Geology Name from Map: Sakhnin and Yanuh Formation

Lithology from Map: Dolostone, limestone, chert

Age from Map: Cenomanian



A1.1.19. IS019

Easting: 692598

Northing: 3615897

Zone: 36S

Elevation: 308

Description of Site Location: On Road 672 south of Carmel, in firing range.

Date Collected: 02/10/2008

Collected By: Ian Moffat

Samples in Study: RS016, SS020

Sample Types in Study: Rock, soil

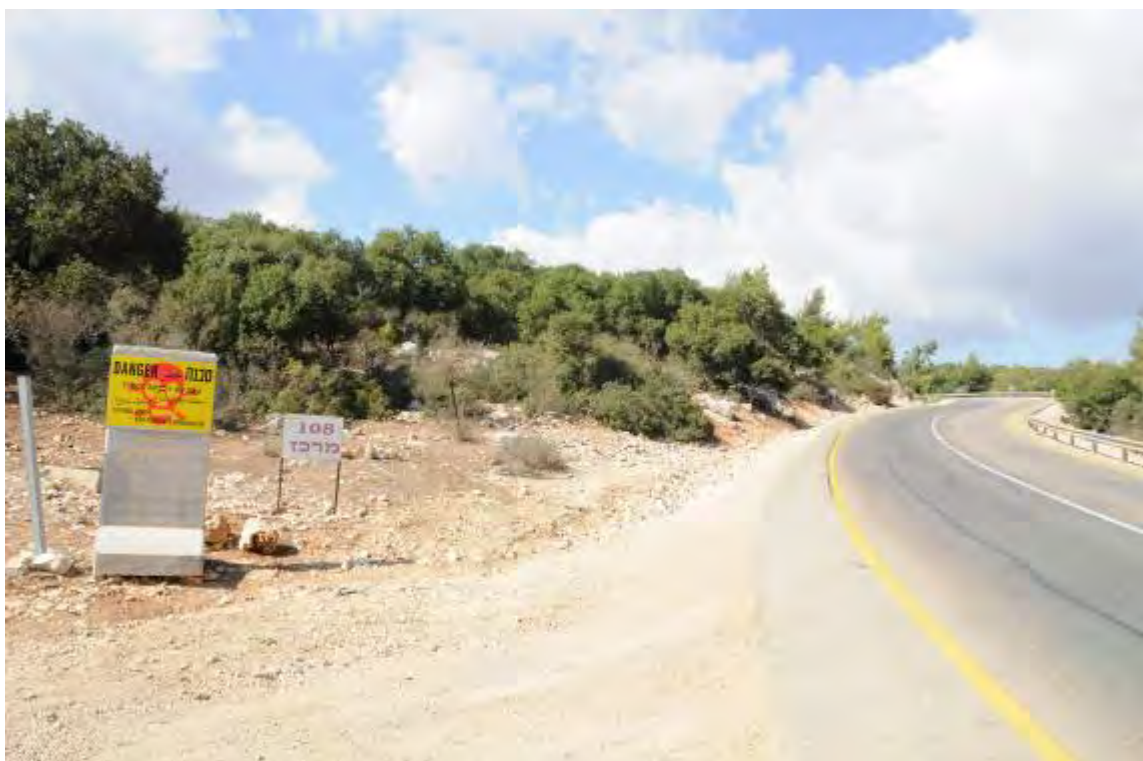
Soil Described in Field: Thin red poorly developed soil on top of limestone with no obvious soil horizons and quite abundant limestone fragments.

Geology Observed in the Field: Limestone

Geology Name from Map: Bina Formation

Lithology from Map: Limestone, marl, dolostone

Age from Map: Turonian



A1.1.20. IS020

Easting: 690737

Northing: 3609663

Zone: 36S

Elevation: 110

Description of Site Location: On Highway 70 to the west of the Elyakim interchange.

Date Collected: 02/10/2008

Collected By: Ian Moffat

Samples in Study: RS017, SS021

Sample Types in Study: Rock, soil

Soil Described in Field: Thin poorly developed soil with very abundant limestone fragments and organic material.

Geology Observed in the Field: Chalky limestone

Geology Name from Map: Adulam Formation

Lithology from Map: Chalk, chert

Age from Map: Lower-Middle Eocene



A1.1.21. IS021

Easting: 688498

Northing: 3621292

Zone: 36S

Elevation: 336

Description of Site Location: Off Road 721 in Carmel Range near the Spa Resort.

Date Collected: 02/10/2008

Collected By: Ian Moffat

Samples in Study: RS018, SS022

Sample Types in Study: Rock, soil

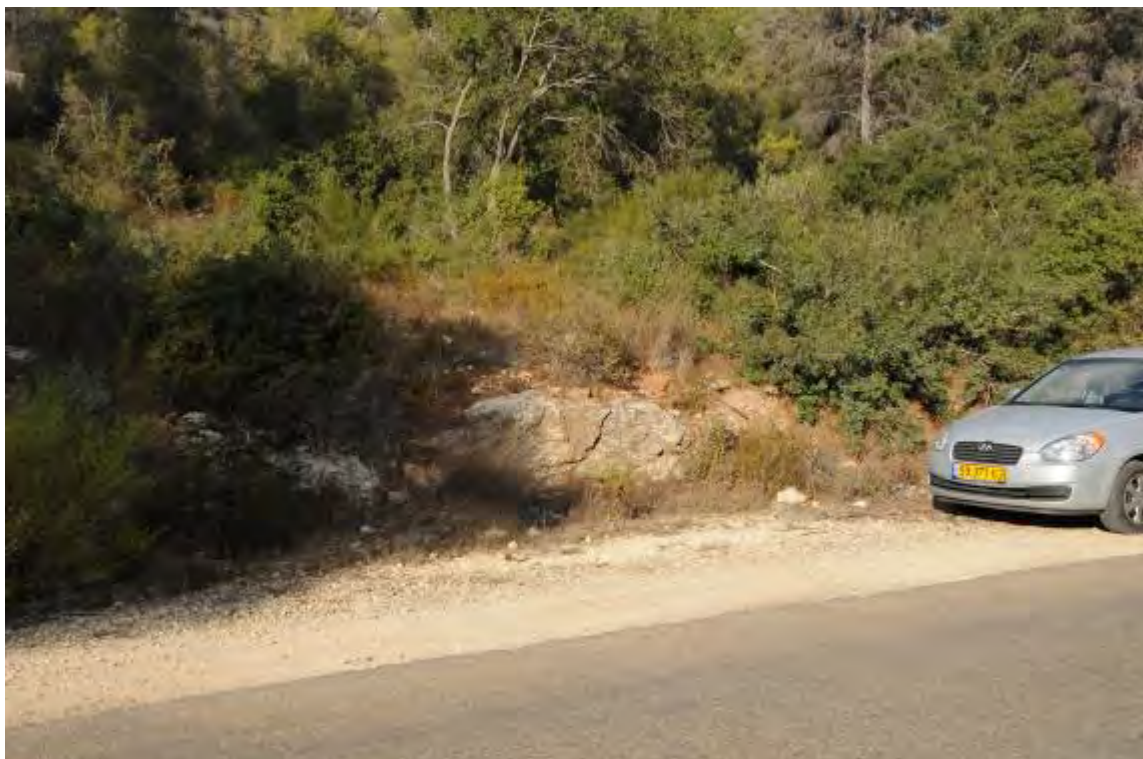
Soil Described in Field: Very thin soil on limestone with moderate amount of limestone fragments.

Geology Observed in the Field: Limestone

Geology Name from Map: Deir Hanna Formation, Isfiya Chalk, Bet Oren Limestone, Khureibe Chalk and Junediya Chalk

Lithology from Map: Limestone, dolostone, marl, chalk, chert

Age from Map: Cenomanian



A1.1.22. IS022

Easting: 689525

Northing: 3626157

Zone: 36S

Elevation: 445

Description of Site Location: On Highway 672 next to Haifa University.

Date Collected: 02/10/2008

Collected By: Ian Moffat

Samples in Study: RS019, RS019*, SS023

Sample Types in Study: Rock, soil

Soil Described in Field: Soil is thin (<2 cm), patchy and extremely poorly developed.

Geology Observed in the Field: Chalky limestone

Geology Name from Map: Deir Hanna Formation, Isfiya Chalk, Bet Oren Limestone, Khureibe Chalk and Junediya Chalk

Lithology from Map: Limestone, dolostone, marl, chalk, chert

Age from Map: Cenomanian



A1.1.23. IS023

Easting: 710592

Northing: 3607373

Zone: 36S

Elevation: 54

Description of Site Location: New service station on Road 675 just east of the turnoff from Highway 65.

Date Collected: 03/10/2008

Collected By: Ian Moffat

Samples in Study: SS024

Sample Types in Study: Soil

Soil Described in Field: Pure clay soil cracked heavily in places to depth of 5 cm. In agricultural field, so may be fertilized.

Geology Observed in the Field: No bedrock

Geology Name from Map: Alluvium

Lithology from Map: Gravel, sand, clay

Age from Map: Quaternary



A1.1.24. IS024

Easting: 738739

Northing: 3623292

Zone: 36S

Elevation: 72

Description of Site Location: Off Highway 768 just north of Alumot junction.

Date Collected: 04/10/2008

Collected By: Ian Moffat

Samples in Study: RS021, SS025

Sample Types in Study: Rock, soil

Soil Described in Field: Poorly developed soil composed of basalt fragments and clay.

Geology Observed in the Field: Basalt

Geology Name from Map: Cover Basalt and Dalwe Basalt

Lithology from Map: Basalt, basanite/flows, intrusions and volcaniclastics

Age from Map: Pliocene-Pleistocene



A1.1.25. IS025

Easting: 733524

Northing: 3592864

Zone: 36S

Elevation: 122

Description of Site Location: In the village of Rekhov on Highway 90.

Date Collected: 04/10/2008

Collected By: Ian Moffat

Samples in Study: SS026

Sample Types in Study: Soil

Soil Described in Field: Very poorly developed soil with many angular limestone fragments.

Geology Observed in the Field: No bedrock

Geology Name from Map: Alluvium

Lithology from Map: Gravel, sand, clay

Age from Map: Quaternary



A1.1.26. IS026

Easting: 726755

Northing: 3596839

Zone: 36S

Elevation: 313

Description of Site Location: At turnoff of Road 6666 from 667 in Gilboa Mountains.

Date Collected: 04/10/2008

Collected By: Ian Moffat

Samples in Study: RS023, SS027

Sample Types in Study: Rock, soil

Soil Described in Field: Organic rich, friable soil with 20% limestone fragments and some quartz.

Geology Observed in the Field: Limestone

Geology Name from Map: Timrat Formation, Meroz and Yizre'el Formations

Lithology from Map: Limestone, chalk, chert

Age from Map: Lower-Middle Eocene



A1.1.27. IS027

Easting: 718214

Northing: 3624458

Zone: 36S

Elevation: 305

Description of Site Location: North of Nazareth on 754 near village of Kafr Kara.

Date Collected: 04/10/2008

Collected By: Ian Moffat

Samples in Study: RS021, SS028

Sample Types in Study: Rock, soil

Soil Described in Field: Undifferentiated soil with 20% limestone fragments.

Geology Observed in the Field: Limestone breccia

Geology Name from Map: Mount Scopus Group

Lithology from Map: Chalk, marl

Age from Map: Senonian-Paleocene



A1.1.28. IS028

Easting: 694759

Northing: 3520900

Zone: 36R

Elevation: 487

Description of Site Location: On Highway 1 near village of Shar Hugay.

Date Collected: 08/10/2008

Collected By: Ian Moffat

Samples in Study: RS022, SS029

Sample Types in Study: Rock, soil

Soil Described in Field: Soil is poorly developed and perched on hill. There are a large number of limestone clasts.

Geology Observed in the Field: Limestone

Geology Name from Map: Givat Ye'arim, Soreq and Kesalon Formations, Hevyon Formation

Lithology from Map: Limestone, dolostone, marl, chalk, chert

Age from Map: Albian-Cenomanian



A1.1.29. IS029

Easting: 685424

Northing: 3540358

Zone: 36S

Elevation: 85

Description of Site Location: On Highway 6 south of the Giv'at Ko'akh junction.

Date Collected: 08/10/2008

Collected By: Ian Moffat

Samples in Study: SS030

Sample Types in Study: Soil

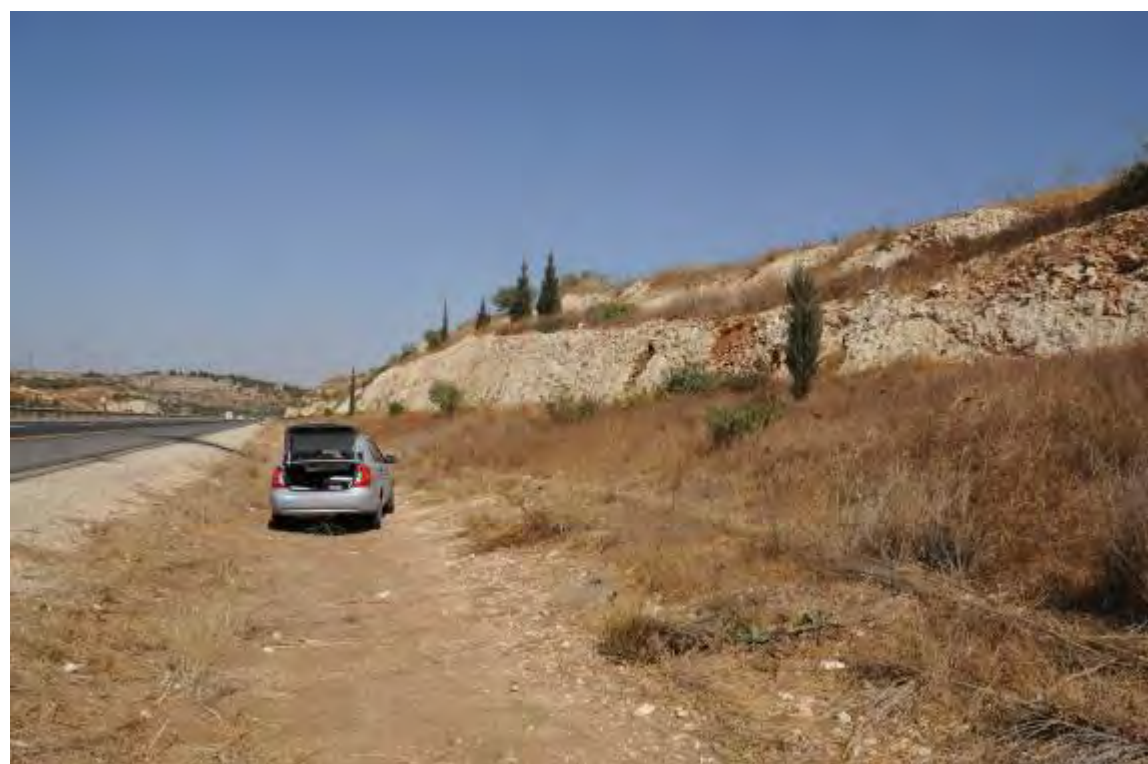
Soil Described in Field: Poorly developed thin soil overlying another with many cobble sized limestone fragments.

Geology Observed in the Field: Limestone

Geology Name from Map: Bina Formation

Lithology from Map: Limestone, marl, dolostone

Age from Map: Turonian



A1.1.30. IS030

Easting: 684603

Northing: 3564722

Zone: 36S

Elevation: 53

Description of Site Location: At Eyal interchange of Highway 6 on side of Road 5504.

Date Collected: 08/10/2008

Collected By: Ian Moffat

Samples in Study: SS031

Sample Types in Study: Soil

Soil Described in Field: Well-developed soil near area of agricultural and road construction, so may be disturbed.

Geology Observed in the Field: No bedrock

Geology Name from Map: Red sand and loam 'hamra'

Lithology from Map: Clay, silt, sand

Age from Map: Quaternary



A1.1.31. IS031

Easting: 674516

Northing: 3554072

Zone: 36S

Elevation: 6

Description of Site Location: On Highway 4, just south of Marasha interchange in orchard on west of road.

Date Collected: 08/10/2008

Collected By: Ian Moffat

Samples in Study: SS032

Sample Types in Study: Soil

Soil Described in Field: Soil is in orchard so probably has some fertilizer added.

Geology Observed in the Field: No bedrock

Geology Name from Map: Red sand and loam 'hamra'

Lithology from Map: Clay, silt, sand

Age from Map: Quaternary



A1.1.32. IS032

Easting: 711495

Northing: 3520928

Zone: 36R

Elevation: 797

Description of Site Location: Near Bed and Breakfast on Sheshet Hayamin Street in Jerusalem in excavations for light rail.

Date Collected: 09/10/2008

Collected By: Ian Moffat

Samples in Study: RS024, SS033

Sample Types in Study: Rock, soil

Soil Described in Field: Sample taken 10 cm above sediment/rock interface. Area of tended grass so may contain fertilizer.

Geology Observed in the Field: Chalk

Geology Name from Map: Menuha Formation

Lithology from Map: Chalk, chert

Age from Map: Coniacian-Campanian



A1.1.33. IS033

Easting: 670914

Northing: 3516771

Zone: 36R

Elevation: 67

Description of Site Location: Off Highway 3, near Revadim.

Date Collected: 10/10/2008

Collected By: Ian Moffat

Samples in Study: SS034

Sample Types in Study: Soil

Soil Described in Field: Well-developed agricultural soil sample taken from the side of ditch. May be fertilized.

Geology Observed in the Field: No bedrock

Geology Name from Map: Alluvium

Lithology from Map: Gravel, sand, clay

Age from Map: Quaternary



A1.1.34. IS034

Easting: 656001

Northing: 3503878

Zone: 36R

Elevation: 74

Description of Site Location: On Highway 35 in road cutting just east of Ashkelon.

Date Collected: 10/10/2008

Collected By: Ian Moffat

Samples in Study: RS025, SS035

Sample Types in Study: Rock, soil

Soil Described in Field: Very poorly developed thin soil with some cracking clay from underlying rock on surface.

Geology Observed in the Field: Poorly consolidated beach ridge

Geology Name from Map: Calcareous sandstone 'kurkar'

Lithology from Map: Clay, silt, sand

Age from Map: Quaternary



A1.1.35. IS035

Easting: 670060

Northing: 3475507

Zone: 36R

Elevation: 264

Description of Site Location: On Highway 40 north of Be'er Sheva.

Date Collected: 10/10/2008

Collected By: Ian Moffat

Samples in Study: SS036

Sample Types in Study: Soil

Soil Described in Field: Undifferentiated semi-consolidated Quaternary very fine sand and silt/clay taken 20 cm below surface.

Geology Observed in the Field: No bedrock

Geology Name from Map: Alluvium

Lithology from Map: Gravel, sand, clay

Age from Map: Quaternary



A1.1.36. IS036

Easting: 672342

Northing: 3445622

Zone: 36R

Elevation: 320

Description of Site Location: On Highway 40 near Ramot Khovav Industrial Zone south of Be'er Sheva.

Date Collected: 10/10/2008

Collected By: Ian Moffat

Samples in Study: SS037

Sample Types in Study: Soil

Soil Described in Field: Thin soil on limestone, sample taken from surface.

Geology Observed in the Field: Chalk

Geology Name from Map: Adulam Formation

Lithology from Map: Chalk, chert

Age from Map: Lower-Middle Eocene



A1.1.37. IS037

Easting: 670360

Northing: 3419638

Zone: 36R

Elevation: 522

Description of Site Location: On Highway 40 to the North of Sde Boker.

Date Collected: 10/10/2008

Collected By: Ian Moffat

Samples in Study: RS027

Sample Types in Study: Rock

Soil Described in Field: N/A

Geology Observed in the Field: Chalky limestone

Geology Name from Map: Bina Formation, Derorim, Shvta and Nezer Formations, Ora and Gerofit Formations, Shuay;b and Wadi as Sir Formations

Lithology from Map: Limestone, dolostone, marl, conglomerate, sandstone

Age from Map: Turonian



A1.1.38. IS038

Easting: 650790

Northing: 3375244

Zone: 36R

Elevation: 951

Description of Site Location: At Har Kharif border post on Road 171.

Date Collected: 11/10/2008

Collected By: Ian Moffat

Samples in Study: RS028, SS039

Sample Types in Study: Rock, soil

Soil Described in Field: Very thin, patchy soil developed on limestone.

Geology Observed in the Field: Limestone

Geology Name from Map: Zihor Formation

Lithology from Map: Limestone, dolostone, marl

Age from Map: Coniacian



A1.1.39. IS039

Easting: 671031

Northing: 3396724

Zone: 36R

Elevation: 756

Description of Site Location: North of Mitze Ramon on Highway 40.

Date Collected: 11/10/2008

Collected By: Ian Moffat

Samples in Study: RS029, SS040

Sample Types in Study: Rock, soil

Soil Described in Field: Thin poorly developed soil on limestone with some disturbance from road building.

Geology Observed in the Field: Limestone

Geology Name from Map: Nizzana, Horsha and Matred Formations

Lithology from Map: Chalk, limestone, chert

Age from Map: Lower-Middle Eocene



A1.1.40. IS040

Easting: 678358

Northing: 3388028

Zone: 36R

Elevation: 486

Description of Site Location: In floor of Mitze Ramon Crator on Highway 40.

Date Collected: 11/10/2008

Collected By: Ian Moffat

Samples in Study: RS030, SS040*

Sample Types in Study: Rock, soil

Soil Described in Field: Poorly developed soil on top of basalt flow.

Geology Observed in the Field: Basalt?

Geology Name from Map: Inmar Formation

Lithology from Map: Sandstone, clay

Age from Map: Lower Jurassic



A1.1.41. IS041

Easting: 693961

Northing: 3345350

Zone: 36R

Elevation: 286

Description of Site Location: On Highway 40 just south of Tsikhor junction.

Date Collected: 11/10/2008

Collected By: Ian Moffat

Samples in Study: RS032, RS033, SS041

Sample Types in Study: Rock, soil

Soil Described in Field: Poorly developed chalky soil with lots of silcrete and some evidence of disturbance.

Geology Observed in the Field: Chalky limestone

Geology Name from Map: Avedat Group

Lithology from Map: Chalk, limestone, marl

Age from Map: Lower-Middle Eocene



A1.1.42. IS042

Easting: 694321

Northing: 3325656

Zone: 36R

Elevation: 398

Description of Site Location: At Shiafon junction on Highway 40.

Date Collected: 12/10/2008

Collected By: Ian Moffat

Samples in Study: RS034, SS042

Sample Types in Study: Rock, soil

Soil Described in Field: Very thin poorly developed soil on limestone.

Geology Observed in the Field: Limestone

Geology Name from Map: Ora and Gerofit Formations, Shuay'b and Wadi as Sir Formations

Lithology from Map: Marl, limestone, sandstone

Age from Map: Turonian



A1.1.43. IS043

Easting: 696254

Northing: 3302117

Zone: 36R

Elevation: 75

Description of Site Location: In rift valley, off Highway 90 in side road to 'Predator's Centre'.

Date Collected: 12/10/2008

Collected By: Ian Moffat

Samples in Study: SS043

Sample Types in Study: Soil

Soil Described in Field: Soil with contribution from granites to the east and sedimentary rocks to the west. Soil has been deflated and has had water running over it. Many angular cobbles.

Geology Observed in the Field: No bedrock

Geology Name from Map: Alluvium

Lithology from Map: Gravel, sand, clay

Age from Map: Quaternary



A1.1.44. IS044

Easting: 692862

Northing: 3296795

Zone: 36R

Elevation: 179

Description of Site Location: On side road to Timna Park off Highway 90.

Date Collected: 12/10/2008

Collected By: Ian Moffat

Samples in Study: RS035, SS044

Sample Types in Study: Rock, soil

Soil Described in Field: Thin part of alluvial fan with very poorly developed soil on granite/granodiorite with many angular clasts.

Geology Observed in the Field: Granite/Granodiorite

Geology Name from Map: Timna Granite, Shahmon Granite, Yehoshafat Granite, Amram Granite Porphyry

Lithology from Map: Sandstone, pebbly sandstone, conglomerate, mudstone, dolostone, limestone

Age from Map: Precambrian



A1.1.45. IS045

Easting: 683919

Northing: 3271361

Zone: 36R

Elevation: 294

Description of Site Location: Down canyon to the south of Highway 12 to the west of Eilat.

Date Collected: 12/10/2008

Collected By: Ian Moffat

Samples in Study: RS036, SS045

Sample Types in Study: Rock, soil

Soil Described in Field: Soil is present at bottom of outcrop in gully floor so will have input from surrounding rocks. Many large clasts.

Geology Observed in the Field: Granite

Geology Name from Map: Timna Granite, Shahmon Granite, Yehoshafat Granite, Amram Granite Porphyry

Lithology from Map: Sandstone, pebbly sandstone, conglomerate, mudstone dolostone, limestone

Age from Map: Precambrian



A1.1.46. IS046

Easting: 681467

Northing: 3284927

Zone: 36R

Elevation: 666

Description of Site Location: In Red Canyon National Park off Highway 12 north of Netafim.

Date Collected: 12/10/2008

Collected By: Ian Moffat

Samples in Study: RS037

Sample Types in Study: Rock

Soil Described in Field: N/A

Geology Observed in the Field: Consolidated Quaternary sediment

Geology Name from Map: Conglomerate units, undifferentiated

Lithology from Map: Basalt, basanite/flows

Age from Map: Neogene-Quaternary



A1.1.47. IS047

Easting: 681161

Northing: 3283499

Zone: 36R

Elevation: 739

Description of Site Location: Next to Highway 12 at upper carpark for Red Canyon.

Date Collected: 12/10/2008

Collected By: Ian Moffat

Samples in Study: RS038, SS046

Sample Types in Study: Rock, soil

Soil Described in Field: Thin soil, developed on basalt. 30% coarse angular basalt fragments, 40% fine-very fine sand and 30% clay.

Geology Observed in the Field: Basalt?

Geology Name from Map: Alluvium

Lithology from Map: Gravel, sand, clay

Age from Map: Quaternary



A1.1.48. IS048

Easting: 680655

Northing: 3310200

Zone: 36R

Elevation: 523

Description of Site Location: On Highway 12 just south of Uvda Airforce Base.

Date Collected: 12/10/2008

Collected By: Ian Moffat

Samples in Study: RS039, SS047

Sample Types in Study: Rock, soil

Soil Described in Field: Thin patchy soil on limestone.

Geology Observed in the Field: Chalky marl

Geology Name from Map: Mishash Formation, Anman Silic Lst and Al Hisa Phosforite Formations

Lithology from Map: Chert, chalk, phosphorite, porcelanite, marl, limestone, dolostone

Age from Map: Campanian



A1.1.49. IS049

Easting: 707921

Northing: 3372094

Zone: 36R

Elevation: 41

Description of Site Location: On Highway 90 south of Tsukim.

Date Collected: 13/10/2008

Collected By: Ian Moffat

Samples in Study: RS040, SS048

Sample Types in Study: Rock, soil

Soil Described in Field: Very thin patchy soil on limestone. 30% angular limestone fragments, 30% very fine-fine sand and 40% clay/silt.

Geology Observed in the Field: Chalky limestone

Geology Name from Map: Avedat Group

Lithology from Map: Chalk, limestone, marl

Age from Map: Lower-Middle Eocene



A1.1.50. IS050

Easting: 714369

Northing: 3407776

Zone: 36R

Elevation: 136

Description of Site Location: On Highway 90 just north of turnoff to Khatseva.

Date Collected: 13/10/2008

Collected By: Ian Moffat

Samples in Study: RS041, SS049

Sample Types in Study: Rock, soil

Soil Described in Field: Unconsolidated sediment collected from the bottom of outcrop.

Geology Observed in the Field: Semi-consolidated Aeolian Sand

Geology Name from Map: Hazeva Formation, Dana Conglomerate

Lithology from Map: Sandstone, mudstone, conglomerate, limestone and marl

Age from Map: Miocene



A1.1.51. IS051

Easting: 689994

Northing: 3426541

Zone: 36R

Elevation: 385

Description of Site Location: Inside Ha-Makhtesh Ha-Gadol off Road 225.

Date Collected: 13/10/2008

Collected By: Ian Moffat

Samples in Study: RS042, SS050

Sample Types in Study: Rock, soil

Soil Described in Field: Thin, sparsely distributed soil with many angular fragments present. 10% clay, 90% medium-cobble sized fragments.

Geology Observed in the Field: Basalt/Volcanic Glass

Geology Name from Map: Weradim Formation, Tamar Formation

Lithology from Map: Dolostone

Age from Map: Cenomanian



A1.1.52. IS052

Easting: 716126

Northing: 3453916

Zone: 36R

Elevation: 260

Description of Site Location: On Road 31, east of Khatrurim junction.

Date Collected: 13/10/2008

Collected By: Ian Moffat

Samples in Study: RS043, SS051

Sample Types in Study: Rock, soil

Soil Described in Field: Thin, partially cemented soil developed on top of rock.

Geology Observed in the Field: Evaporite/limestone

Geology Name from Map: Bina Formation, Derorim, Shivta and Nezer Formations, Ora and Gerofit Formations, Shuay;b and Wadi as Sir Formations

Lithology from Map: Limestone, dolostone, marl, conglomerate, sandstone

Age from Map: Turonian



A1.1.53. IS053

Easting: 737222

Northing: 3610147

Zone: 36R

Elevation: 20

Description of Site Location: Off Highway 90, on side Road 717 to Kokhav ho-Yarden.

Date Collected: 14/10/2008

Collected By: Ian Moffat

Samples in Study: RS044, SS052

Sample Types in Study: Rock, soil

Soil Described in Field: Soil appears to have creped with basalt blocks.

Geology Observed in the Field: Basalt

Geology Name from Map: Cover Basalt and Dalwe Basalt

Lithology from Map: Basalt, basanite/flows, intrusions and volcaniclastics

Age from Map: Pliocene-Pleistocene



A1.1.54. IS054

Easting: 731529

Northing: 3630730

Zone: 36R

Elevation: 185

Description of Site Location: On turnoff ramp to the Ha-Galil Takhton Industries park from Highway 77.

Date Collected: 14/10/2008

Collected By: Ian Moffat

Samples in Study: RS045, SS053

Sample Types in Study: Rock, soil

Soil Described in Field: Thin (0.5 m) soil developed on basalt.

Geology Observed in the Field: Basalt

Geology Name from Map: Cover Basalt and Dalwe Basalt

Lithology from Map: Basalt, basanite/flows, intrusions and volcaniclastics

Age from Map: Pliocene-Pleistocene



A1.1.55. IS055

Easting: 762106

Northing: 3638757

Zone: 36R

Elevation: 432

Description of Site Location: On Road 808 just north of turnoff to 98, near Syrian border.

Date Collected: 15/10/2008

Collected By: Ian Moffat

Samples in Study: SS054

Sample Types in Study: Soil

Soil Described in Field: Red basaltic soil mixed with large basalt pieces.

Geology Observed in the Field: Basalt

Geology Name from Map: Cover Basalt and Dalwe Basalt

Lithology from Map: Basalt, basanite/flows, intrusions and volcaniclastics

Age from Map: Pliocene-Pleistocene



A1.1.56. IS056

Easting: 759511

Northing: 3674122

Zone: 36R

Elevation: 65

Description of Site Location: Off Road 98 to the east from the El-Rom junction.

Date Collected: 15/10/2008

Collected By: Ian Moffat

Samples in Study: RS047, SS055

Sample Types in Study: Rock, soil

Soil Described in Field: Well-developed soil intermingled with basalt at depth.

Geology Observed in the Field: Basalt

Geology Name from Map: Golan Basalt, Raqqad Basalt

Lithology from Map: Basalt, basanite/flows

Age from Map: Quaternary



A1.1.57. IS057

Easting: 757638

Nothing: 3688033

Zone: 36R

Elevation: 582

Description of Site Location: On Road 98 near ski resort.

Date Collected: 15/10/2008

Collected By: Ian Moffat

Samples in Study: RS048, SS056, SS057

Sample Types in Study: Rock, soil

Soil Described in Field: A thin red layer of no more than 3 cm. Very friable (SS056) and thin light, very clay rich consolidated layer of 5 to 10 cm overlying limestone (SS057).

Geology Observed in the Field: Limestone

Geology Name from Map: Hermon Formation

Lithology from Map: Limestone, dolostone

Age from Map: Middle Jurassic



A1.1.58. IS058

Easting: 742215

Northing: 3672867

Zone: 36R

Elevation: 76

Description of Site Location: On Road 9778 near village of Gonen.

Date Collected: 15/10/2008

Collected By: Ian Moffat

Samples in Study: SS058

Sample Types in Study: Soil

Soil Described in Field: Alluvial material from Jordan River.

Geology Observed in the Field: No bedrock

Geology Name from Map: Alluvium

Lithology from Map: Gravel, sand, clay

Age from Map: Quaternary



A1.1.59. IS060

Easting: 685379

Northing: 3623856

Zone: 36R

Elevation: 116

Description of Site Location: Sefunim Cave, up a wadi to the north of Msylia.

Date Collected: 16/10/2008

Collected By: Ian Moffat

Samples in Study: RS049

Sample Types in Study: Rock

Soil Described in Field: N/A

Geology Observed in the Field: Limestone

Geology Name from Map: Bina Formation

Lithology from Map: Limestone, marl, dolostone

Age from Map: Turonian



A1.1.60. IS061

Easting: 734413

Northing: 3647972

Zone: 36R

Elevation: 598

Description of Site Location: Off Highway 89 to the south of Tsefat.

Date Collected: 17/10/2008

Collected By: Ian Moffat

Samples in Study: RS050 SS065

Sample Types in Study: Rock, soil

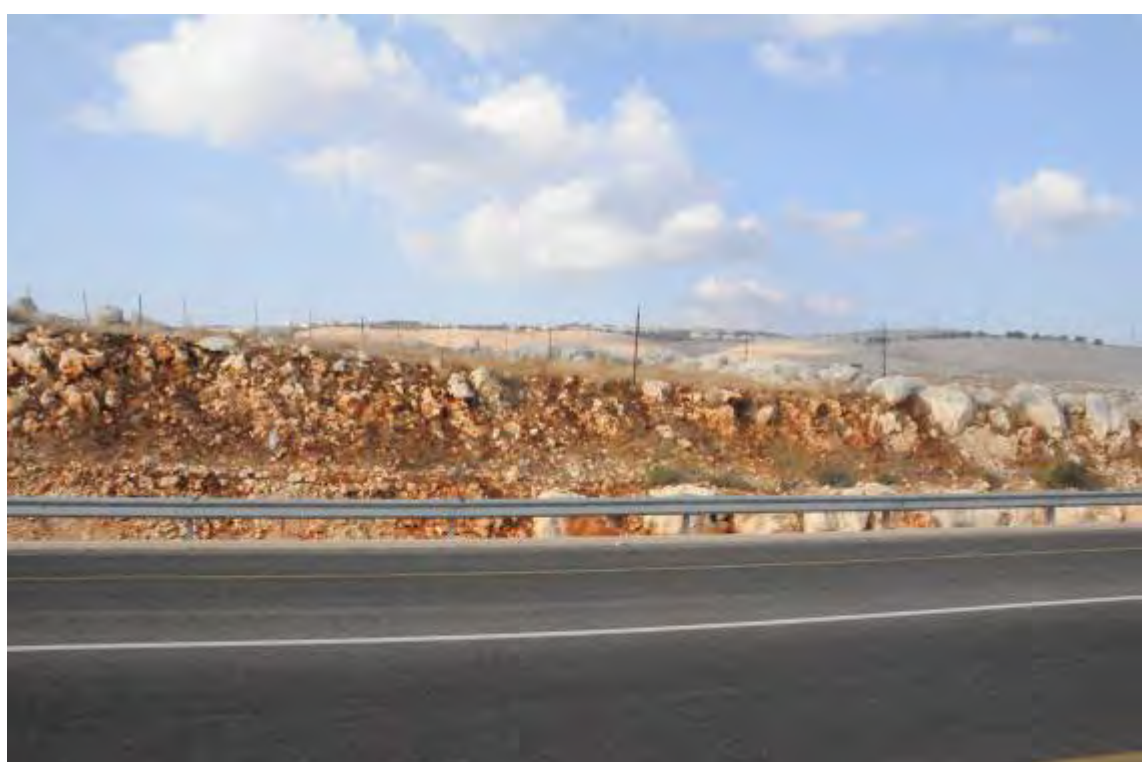
Soil Described in Field: Thick zone (3 m) of mixed *Terra rossa* soil and limestone.

Geology Observed in the Field: Limestone

Geology Name from Map: Timrat Formation, Meroz and Yizre'el Formations

Lithology from Map: Limestone, chalk, chert

Age from Map: Lower-Middle Eocene



A1.1.61. IS062

Easting: 745328

Northing: 3655402

Zone: 36R

Elevation: 100

Description of Site Location: On Highway 91, just west of Gadot junction near the bottom of rift valley.

Date Collected: 17/10/2008

Collected By: Ian Moffat

Samples in Study: RS051, SS066

Sample Types in Study: Soil

Soil Described in Field: Soil intermingled with basalt block, appears to have been a fire in the area recently.

Geology Observed in the Field: Basalt

Geology Name from Map: Yarda Basalt

Lithology from Map: Basalt/basanite/flows

Age from Map: Quaternary



A1.2. French Sites

A1.2.1. F01

Easting: 270113

Northing: 5062276

Zone: 31T

Elevation: N/A

Description of Site Location: N/A

Date Collected: N/A

Collected By: Maxime Aubert

Samples in Study: R

Sample Types in Study: Rock

Soil Described in Field: N/A

Geology Observed in the Field: N/A

Geology Name from Map: N/A

Lithology from Map: Marl, limestone, clay

Age from Map: Upper Jurassic



A1.2.2. F02

Easting: 267858

Northing: 5061775

Zone: 31T

Elevation: N/A

Description of Site Location: N/A

Date Collected: N/A

Collected By: Maxime Aubert

Samples in Study: R

Sample Types in Study: Rock

Soil Described in Field: N/A

Geology Observed in the Field: N/A

Geology Name from Map: N/A

Lithology from Map: Marl, limestone, clay

Age from Map: Upper Jurassic



A1.2.3. F04

Easting: 269552

Northing: 5059518

Zone: 31T

Elevation: N/A

Description of Site Location: N/A

Date Collected: N/A

Collected By: Maxime Aubert

Samples in Study: R

Sample Types in Study: Rock

Soil Described in Field: N/A

Geology Observed in the Field: N/A

Geology Name from Map: N/A

Lithology from Map: Limestone, marl, clay, sand

Age from Map: Upper Cretaceous



A1.2.4. F06

Easting: 268448

Northing: 5051324

Zone: 31T

Elevation: N/A

Description of Site Location: N/A

Date Collected: N/A

Collected By: Maxime Aubert

Samples in Study: R

Sample Types in Study: Rock

Soil Described in Field: N/A

Geology Observed in the Field: N/A

Geology Name from Map: N/A

Lithology from Map: Limestone, marl, clay, sand

Age from Map: Upper Cretaceous



A1.2.5. F08

Easting: 268448

Northing: 5051324

Zone: 31T

Elevation: N/A

Description of Site Location: N/A

Date Collected: N/A

Collected By: Maxime Aubert

Samples in Study: R

Sample Types in Study: Rock

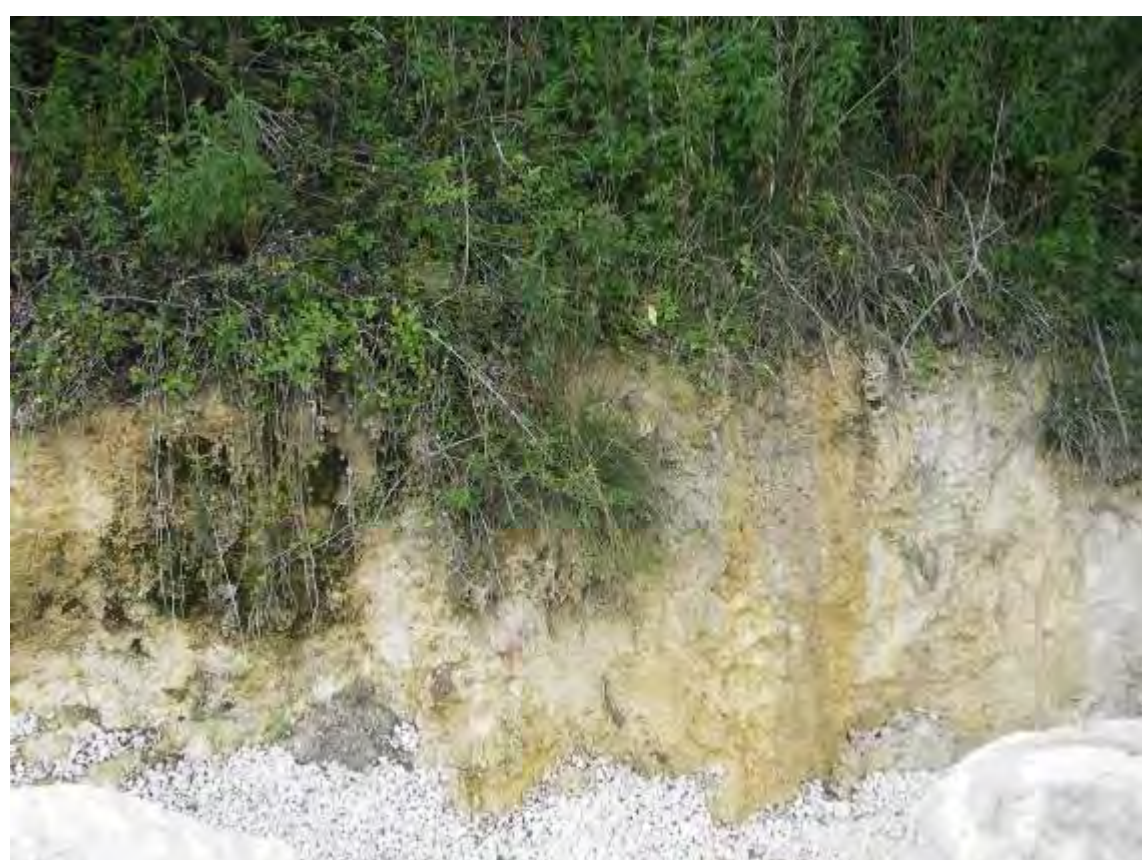
Soil Described in Field: N/A

Geology Observed in the Field: N/A

Geology Name from Map: N/A

Lithology from Map: Limestone, marl, clay, sand

Age from Map: Upper Cretaceous



A1.2.6. F12

Easting: 288396

Northing: 5061776

Zone: 31T

Elevation: N/A

Description of Site Location: N/A

Date Collected: N/A

Collected By: Maxime Aubert

Samples in Study: R

Sample Types in Study: Rock

Soil Described in Field: N/A

Geology Observed in the Field: N/A

Geology Name from Map: N/A

Lithology from Map: Marl, limestone, clay

Age from Map: Upper Jurassic



A1.2.7. F16

Easting: 307742

Northing: 5053032

Zone: 31T

Elevation: N/A

Description of Site Location: N/A

Date Collected: N/A

Collected By: Maxime Aubert

Samples in Study: R

Sample Types in Study: Rock

Soil Described in Field: N/A

Geology Observed in the Field: N/A

Geology Name from Map: N/A

Lithology from Map: Limestone, marl

Age from Map: Middle Jurassic



A1.2.8. F19

Easting: 312689

Northing: 5058080

Zone: 31T

Elevation: N/A

Description of Site Location: River, about 25 m from F18.

Date Collected: N/A

Collected By: Maxime Aubert

Samples in Study: SB

Sample Types in Study: Rock

Soil Described in Field: N/A

Geology Observed in the Field: N/A

Geology Name from Map: N/A

Lithology from Map: Migmatite

Age from Map: Brioherian, Cambrian



A1.2.9. F21

Easting: 316566

Northing: 5060204

Zone: 31T

Elevation: N/A

Description of Site Location: N/A

Date Collected: N/A

Collected By: Maxime Aubert

Samples in Study: R

Sample Types in Study: Rock

Soil Described in Field: N/A

Geology Observed in the Field: N/A

Geology Name from Map: N/A

Lithology from Map: Monzogranite, granodiorite

Age from Map: Upper Visean, Namurian



A1.2.10. F23

Easting: 276762

Northing: 5074376

Zone: 31T

Elevation: N/A

Description of Site Location: N/A

Date Collected: N/A

Collected By: Maxime Aubert

Samples in Study: R1, R2

Sample Types in Study: Rock

Soil Described in Field: N/A

Geology Observed in the Field: N/A

Geology Name from Map: N/A

Lithology from Map: Marl, limestone, clay

Age from Map: Upper Jurassic



A1.2.11. F24

Easting: 278596

Northing: 5076516

Zone: 31T

Elevation: N/A

Description of Site Location: N/A

Date Collected: N/A

Collected By: Maxime Aubert

Samples in Study: R

Sample Types in Study: Rock

Soil Described in Field: N/A

Geology Observed in the Field: N/A

Geology Name from Map: N/A

Lithology from Map: Marl, limestone, clay

Age from Map: Upper Jurassic



A1.2.12. F25

Easting: 281821

Northing: 5076711

Zone: 31T

Elevation: N/A

Description of Site Location: N/A

Date Collected: N/A

Collected By: Maxime Aubert

Samples in Study: R

Sample Types in Study: Rock

Soil Described in Field: N/A

Geology Observed in the Field: N/A

Geology Name from Map: N/A

Lithology from Map: Marl, limestone, clay

Age from Map: Upper Jurassic



A1.2.13. F27

Easting: 287966

Northing: 5080184

Zone: 31T

Elevation: N/A

Description of Site Location: N/A

Date Collected: N/A

Collected By: Maxime Aubert

Samples in Study: R

Sample Types in Study: Rock

Soil Described in Field: N/A

Geology Observed in the Field: N/A

Geology Name from Map: N/A

Lithology from Map: Basanite, hawaiite, tephra

Age from Map: Oligocene, Miocene



A1.2.14. F33

Easting: 318122

Northing: 5085533

Zone: 31T

Elevation: N/A

Description of Site Location: N/A

Date Collected: N/A

Collected By: Maxime Aubert

Samples in Study: R

Sample Types in Study: Rock

Soil Described in Field: N/A

Geology Observed in the Field: N/A

Geology Name from Map: N/A

Lithology from Map: Monzogranite, Granodiorite

Age from Map: Upper Visean, Namurian



A1.2.15. F34

Easting: 318861

Northing: 5078299

Zone: 31T

Elevation: N/A

Description of Site Location: N/A

Date Collected: N/A

Collected By: Maxime Aubert

Samples in Study: R

Sample Types in Study: Rock

Soil Described in Field: N/A

Geology Observed in the Field: N/A

Geology Name from Map: N/A

Lithology from Map: Paragneiss, leptynite, amphibolite

Age from Map: Brioherian, Cambrian



A1.2.16. F35

Easting: 315053

Northing: 5071792

Zone: 31T

Elevation: N/A

Description of Site Location: N/A

Date Collected: N/A

Collected By: Maxime Aubert

Samples in Study: SB

Sample Types in Study: Rock

Soil Described in Field: N/A

Geology Observed in the Field: N/A

Geology Name from Map: N/A

Lithology from Map: Paragneiss, leptynite, amphibolite

Age from Map: Brioherian, Cambrian



A1.2.17. F36

Easting: 310778

Northing: 5072387

Zone: 31T

Elevation: N/A

Description of Site Location: N/A

Date Collected: N/A

Collected By: Maxime Aubert

Samples in Study: R

Sample Types in Study: Rock

Soil Described in Field: N/A

Geology Observed in the Field: N/A

Geology Name from Map: N/A

Lithology from Map: Paragneiss, leptynite, amphibolite

Age from Map: Brioherian, Cambrian



A1.2.18. F37

Easting: 315835

Northing: 5073517

Zone: 31T

Elevation: N/A

Description of Site Location: N/A

Date Collected: N/A

Collected By: Maxime Aubert

Samples in Study: R

Sample Types in Study: Rock

Soil Described in Field: N/A

Geology Observed in the Field: N/A

Geology Name from Map: N/A

Lithology from Map: Paragneiss, leptynite, amphibolite

Age from Map: Brioherian, Cambrian



A1.2.19. F38

Easting: 320406

Northing: 5066301

Zone: 31T

Elevation: N/A

Description of Site Location: N/A

Date Collected: N/A

Collected By: Maxime Aubert

Samples in Study: SB

Sample Types in Study: Rock

Soil Described in Field: N/A

Geology Observed in the Field: N/A

Geology Name from Map: N/A

Lithology from Map: Peraluminous leucogranite

Age from Map: Upper Visean, Namurian



A1.2.20. F40

Easting: 300215

Northing: 5068414

Zone: 31T

Elevation: N/A

Description of Site Location: N/A

Date Collected: N/A

Collected By: Maxime Aubert

Samples in Study: R

Sample Types in Study: Rock

Soil Described in Field: N/A

Geology Observed in the Field: N/A

Geology Name from Map: N/A

Lithology from Map: Limestone, marl

Age from Map: Middle Jurassic



A1.2.21. FS001

Easting: 721160

Northing: 5034074

Zone: 30T

Elevation: 110

Description of Site Location: Adjacent to N10 Freeway near village.

Date Collected: 4/09/2009

Collected By: Ian Moffat, Rainer Grün

Samples in Study: SS001F

Sample Types in Study: Soil

Soil Described in Field: Thin layer of light brown soil overlying bedrock.

Geology Observed in the Field: Chalky limestone

Geology Name from Map: N/A

Lithology from Map: Limestone, marl, clay, sand

Age from Map: Upper Cretaceous



A1.2.22. FS006

Easting: 695046

Northing: 5060790

Zone: 30T

Elevation: 10

Description of Site Location: In cut bank of river, which has cut approximately 2 m.

Date Collected: 5/09/2009

Collected By: Ian Moffat, Rainer Grün

Samples in Study: SS010F

Sample Types in Study: Soil

Soil Described in Field: Sample taken from 30 cm below floodplain surface.

Geology Observed in the Field: No outcrop

Geology Name from Map: N/A

Lithology from Map: Sand, clay, gravel, shingle

Age from Map: Holocene



A1.2.23. FS008

Easting: 699404

Northing: 5035025

Zone: 30T

Elevation: 30

Description of Site Location: In road cutting just south of Jonzac.

Date Collected: 5/09/2009

Collected By: Ian Moffat, Rainer Grün

Samples in Study: S2

Sample Types in Study: Soil

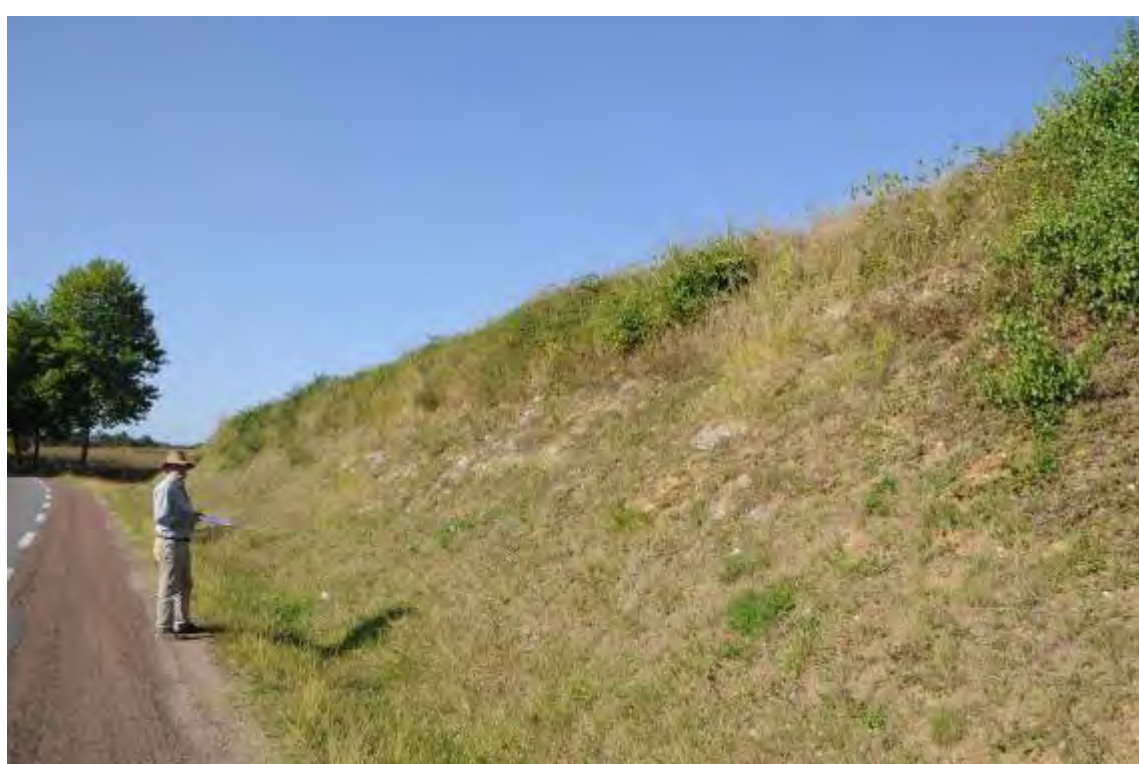
Soil Described in Field: Taken on ground surface.

Geology Observed in the Field: Limestone

Geology Name from Map: N/A

Lithology from Map: Sand, clay, gravel, pebble

Age from Map: Holocene



A1.2.24. FS010

Easting: 722129

Northing: 5046685

Zone: 30T

Elevation: 75

Description of Site Location: On small road cutting at entrance to chateau, just north of village of La Roche.

Date Collected: 5/09/2009

Collected By: Ian Moffat, Rainer Grün

Samples in Study: S1

Sample Types in Study: Soil

Soil Described in Field: Collected about 0.5 m below surface. May be slope wash.

Geology Observed in the Field: Limestone

Geology Name from Map: N/A

Lithology from Map: Limestone, marl, clay, sand

Age from Map: Upper Cretaceous



A1.2.25. FS011

Easting: 717474

Northing: 5053975

Zone: 30T

Elevation: 92

Description of Site Location: In small road cut near village of Peron Janac.

Date Collected: 5/09/2009

Collected By: Ian Moffat, Rainer Grün

Samples in Study: S1

Sample Types in Study: Soil

Soil Described in Field: Collected about 0.5 m below surface. May be slope wash.

Geology Observed in the Field: Limestone

Geology Name from Map: N/A

Lithology from Map: Sand, clay, gravel, pebble

Age from Map: Holocene



A1.2.26. FS016

Easting: 723956

Northing: 5084905

Zone: 30T

Elevation: 120

Description of Site Location: Just west of village of Verdille in small cut for a drain.

Date Collected: 5/09/2009

Collected By: Ian Moffat, Rainer Grün

Samples in Study: S1

Sample Types in Study: Soil

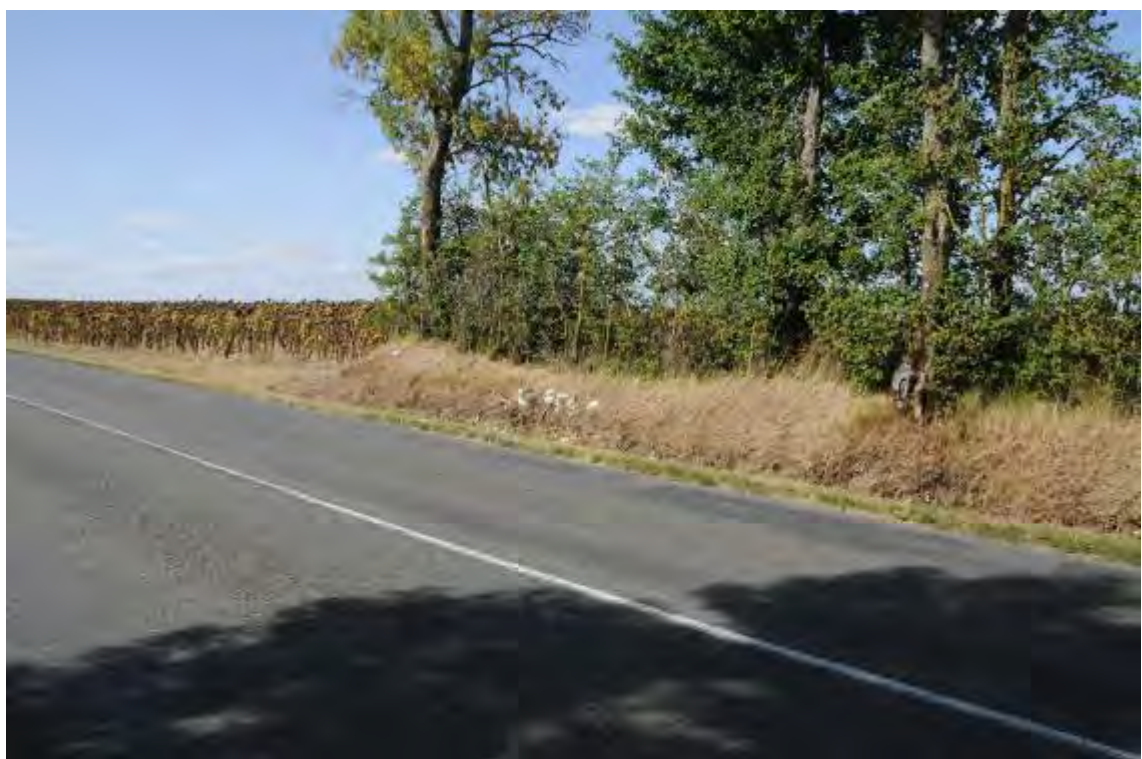
Soil Described in Field: Taken from rock/soil interface, 0.5 m below surface.

Geology Observed in the Field: Limestone

Geology Name from Map: N/A

Lithology from Map: Marl, limestone, clay

Age from Map: Upper Jurassic



A1.2.27. FS018

Easting: 695487

Northing: 507944

Zone: 30T

Elevation: 53

Description of Site Location: Base of large, knocked over tree with rock and soil in roots.

Date Collected: 5/09/2009

Collected By: Ian Moffat, Rainer Grün

Samples in Study: S1

Sample Types in Study: Soil

Soil Described in Field: Taken from among roots, would have been <0.5 m deep when *in situ*.

Geology Observed in the Field: Chalky limestone

Geology Name from Map: N/A

Lithology from Map: Limestone, marl, clay, sand

Age from Map: Upper Cretaceous



A1.2.28. FS021

Easting: 700316

Northing: 5070033

Zone: 30T

Elevation: 92

Description of Site Location: Ditch near intersection of D122 and D55, in forest.

Date Collected: 5/09/2009

Collected By: Ian Moffat, Rainer Grün

Samples in Study: S2

Sample Types in Study: Soil

Soil Described in Field: Soil profile is approximately 1 m, grey-looking sample taken on surface.

Geology Observed in the Field: Limestone with siliceous cobbles

Geology Name from Map: N/A

Lithology from Map: Limestone, marl, clay, sand

Age from Map: Upper Cretaceous



A1.2.29. FS027

Easting: 343303

Northing: 4977631

Zone: 31T

Elevation: 77

Description of Site Location: Taken from small lane off main street in Les Eyzies, this appears to be a terrace about the elevation of the current village.

Date Collected: 6/09/2009

Collected By: Ian Moffat, Rainer Grün

Samples in Study: S1, S2

Sample Types in Study: Soil

Soil Described in Field: Collected 1 m below surface of bench.

Geology Observed in the Field: No bedrock

Geology Name from Map: N/A

Lithology from Map: Limestone, marl, clay, sand

Age from Map: Upper Cretaceous

A1.2.30. FS029

Easting: 339031

Northing: 4974815

Zone: 31T

Elevation: 70

Description of Site Location: On riverbank of Vezere, near village of Campagne.

Date Collected: 7/09/2009

Collected By: Ian Moffat, Rainer Grün

Samples in Study: S1

Sample Types in Study: Soil

Soil Described in Field: Taken from river bank about 0.5 m below floodplain surface.

Geology Observed in the Field: No bedrock

Geology Name from Map: N/A

Lithology from Map: Sand, clay, gravel, shingle

Age from Map: Holocene



A1.2.31. FS031

Easting: 343614

Northing: 4968831

Zone: 31T

Elevation: 75

Description of Site Location: On bend of river near village of Mouzens in road cutting.

Date Collected: 7/09/2009

Collected By: Ian Moffat, Rainer Grün

Samples in Study: S1

Sample Types in Study: Soil

Soil Described in Field: Taken from clays between the limestone horizons approximately 1 m above ground. May be slope wash.

Geology Observed in the Field: Limestone

Geology Name from Map: N/A

Lithology from Map: Marl, limestone, clay

Age from Map: Upper Jurassic



A1.2.32. FS033

Easting: 343902

Northing: 4969003

Zone: 31T

Elevation: 68

Description of Site Location: Adjacent to Dordogne river in village of Monsec, at least 3 terraces exist with the upper most extensive but heavily agricultural.

Date Collected: 7/09/2009

Collected By: Ian Moffat, Rainer Grün

Samples in Study: S1, S2, S3

Sample Types in Study: Soil

Soil Described in Field: Taken from lowest terrace, approximately 2 m above river level (S1), taken from middle terrace, approximately 5 m above river level (S2) and taken from upper terrace, approximately 10 m above river level (S3).

Geology Observed in the Field: No bedrock

Geology Name from Map: N/A

Lithology from Map: Marl, limestone, clay

Age from Map: Upper Jurassic



A1.2.33. FS035

Easting: 364413

Northing: 4964789

Zone: 31T

Elevation: 84

Description of Site Location: Sampled from river bank of Dordogne near St Rome.

Date Collected: 7/09/2009

Collected By: Ian Moffat, Rainer Grün

Samples in Study: S1

Sample Types in Study: Soil

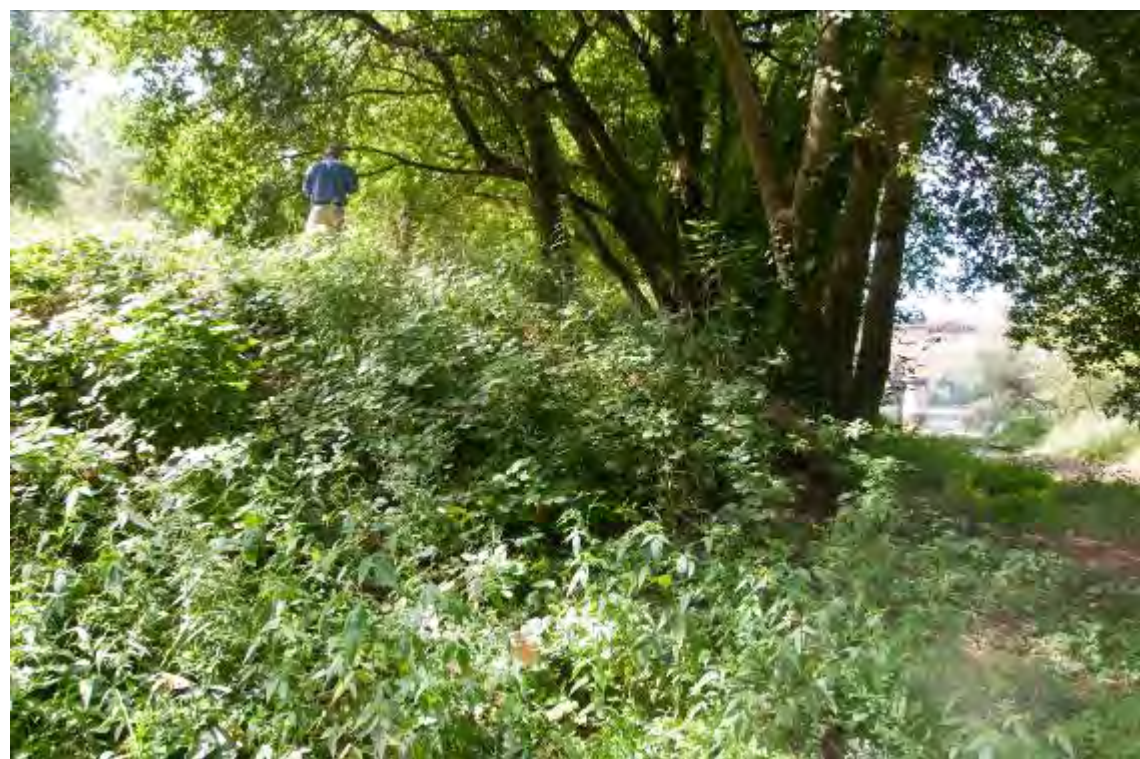
Soil Described in Field: Sample taken 30 cm below surface of floodplain. Thickness of approximately 5 m above river level.

Geology Observed in the Field: No bedrock

Geology Name from Map: N/A

Lithology from Map: Clay, sand, gravel, shingle

Age from Map: Middle-Upper Pleistocene



A1.2.34. FS036

Easting: 360875

Northing: 4970271

Zone: 31T

Elevation: 143

Description of Site Location: Road cutting at entrance to quarry.

Date Collected: 7/09/2009

Collected By: Ian Moffat, Rainer Grün

Samples in Study: S1

Sample Types in Study: Soil

Soil Described in Field: Strange clay that may be part of the formation or valley fill.

Geology Observed in the Field: Limestone

Geology Name from Map: N/A

Lithology from Map: Limestone, marl, clay, sand

Age from Map: Upper Cretaceous



A1.2.35. FS037

Easting: 359240

Northing: 4977874

Zone: 31T

Elevation: 316

Description of Site Location: In large road cutting near village of Maneyral.

Date Collected: 7/09/2009

Collected By: Ian Moffat, Rainer Grün

Samples in Study: S1

Sample Types in Study: Soil

Soil Described in Field: Taken from light coloured clay unit apparently interbedded in limestone.

Geology Observed in the Field: Limestone

Geology Name from Map: N/A

Lithology from Map: Limestone, marl, clay, sand

Age from Map: Upper Cretaceous



A1.2.36. FS041

Easting: 398097

Northing: 4981868

Zone: 31T

Elevation: 316

Description of Site Location: Small road cutting near village of Le Maraud.

Date Collected: 7/09/2009

Collected By: Ian Moffat, Rainer Grün

Samples in Study: S1

Sample Types in Study: Soil

Soil Described in Field: White clay, taken from within limestone unit.

Geology Observed in the Field: Limestone

Geology Name from Map: N/A

Lithology from Map: Marl, limestone, dolomite

Age from Map: Lower Jurassic



A1.2.37. FS043

Easting: 400967

Northing: 4974223

Zone: 31T

Elevation: 133

Description of Site Location: Taken from river bank of Dordogne near town of Cabrette.

Date Collected: 7/09/2009

Collected By: Ian Moffat, Rainer Grün

Samples in Study: S1

Sample Types in Study: Soil

Soil Described in Field: Collected from floodplain surface, approximately 3 to 4 m above river level.

Geology Observed in the Field: No bedrock

Geology Name from Map: N/A

Lithology from Map: Sand, clay, gravel, shingle

Age from Map: Holocene



A1.2.38. FS044

Easting: 411219

Northing: 4977151

Zone: 31T

Elevation: 149

Description of Site Location: Collected in village on floodplain.

Date Collected: 7/09/2009

Collected By: Ian Moffat, Rainer Grün

Samples in Study: S1

Sample Types in Study: Soil

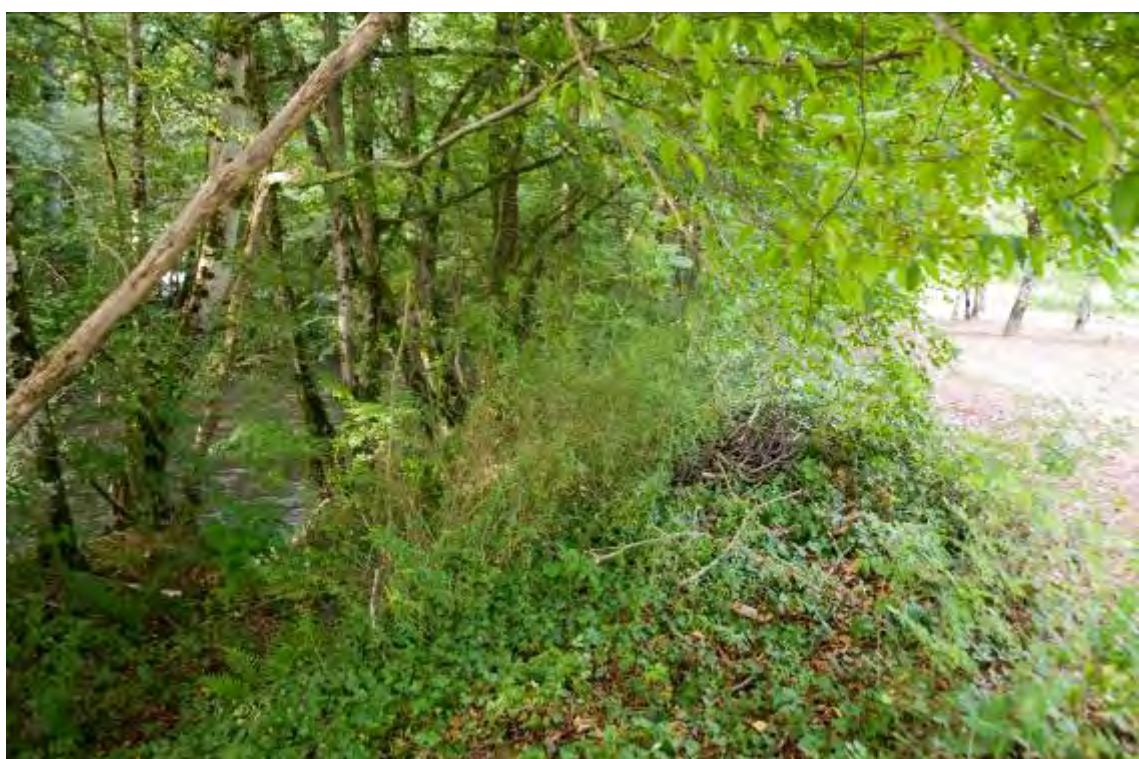
Soil Described in Field: Taken from surface of floodplain, may have agricultural input.

Geology Observed in the Field: No bedrock

Geology Name from Map: N/A

Lithology from Map: Paragneiss, leptynite, amphibolite

Age from Map: Brioverian, Cambrian



A1.2.39. FS045

Easting: 399344

Northing: 4982356

Zone: 31T

Elevation: 153

Description of Site Location: Archaeological site of La Chappelle-aux-Saints.

Date Collected: 8/09/2009

Collected By: Ian Moffat, Rainer Grün

Samples in Study: S3

Sample Types in Study: Soil

Soil Described in Field: Soil sample taken above (3 to 4 m) excavation.

Geology Observed in the Field: Limestone

Geology Name from Map: N/A

Lithology from Map: Marl, limestone, dolomite

Age from Map: Lower Jurassic



A1.2.40. FS046

Easting: 399442

Northing: 4982467

Zone: 31T

Elevation: 146

Description of Site Location: Sample taken from creek adjacent to archaeological site of La Chappelle-aux-Saints.

Date Collected: 8/09/2009

Collected By: Ian Moffat, Rainer Grün

Samples in Study: S1

Sample Types in Study: Soil

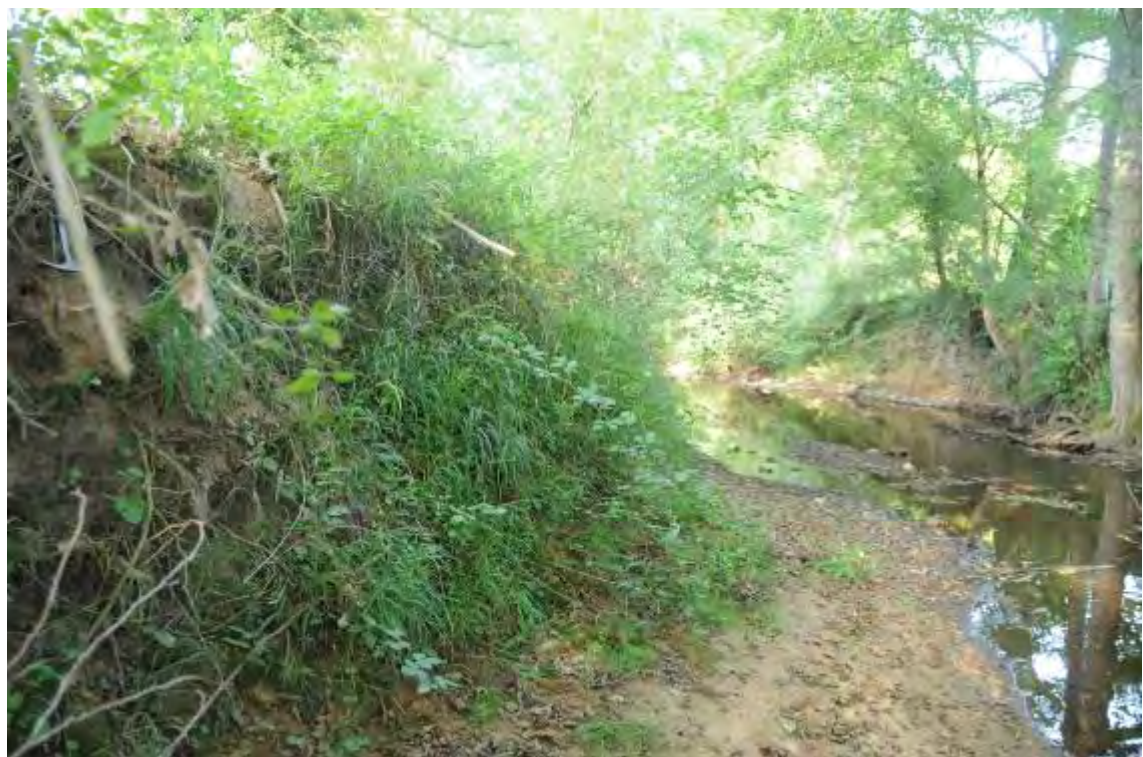
Soil Described in Field: Sample taken from sediment 20 cm below floodplain surface, adjacent to river.

Geology Observed in the Field: No bedrock

Geology Name from Map: N/A

Lithology from Map: Marl, limestone, dolomite

Age from Map: Lower Jurassic



A1.2.41. FS047

Easting: 396434

Northing: 4970063

Zone: 31T

Elevation: 146

Description of Site Location: Archaeological site of les Fieux.

Date Collected: 8/09/2009

Collected By: Ian Moffat, Rainer Grün

Samples in Study: S4

Sample Types in Study: Soil

Soil Described in Field: Taken from surface sediment above north side of archaeological site.

Geology Observed in the Field: Limestone, not *in situ*

Geology Name from Map: N/A

Lithology from Map: Marl, Limestone, marl

Age from Map: Middle Jurassic



A1.2.42. FS049

Easting: 385154

Northing: 4960867

Zone: 31T

Elevation: 240

Description of Site Location: Small road cutting near village.

Date Collected: 8/09/2009

Collected By: Ian Moffat, Rainer Grün

Samples in Study: S1

Sample Types in Study: Soil

Soil Described in Field: Thin soil.

Geology Observed in the Field: Limestone

Geology Name from Map: N/A

Lithology from Map: Marl, limestone, clay

Age from Map: Upper Jurassic



A1.2.43. FS050

Easting: 388530

Northing: 4961960

Zone: 31T

Elevation: 187

Description of Site Location: In road cutting in possible old quarry.

Date Collected: 8/09/2009

Collected By: Ian Moffat, Rainer Grün

Samples in Study: S1

Sample Types in Study: Soil

Soil Described in Field: Very thin mantle of red soil on limestone.

Geology Observed in the Field: Chalky limestone

Geology Name from Map: N/A

Lithology from Map: Marl, limestone, clay

Age from Map: Upper Jurassic



A1.2.44. FS051

Easting: 395569

Northing: 4964432

Zone: 31T

Elevation: 314

Description of Site Location: Small road cutting, west of Alvignac.

Date Collected: 8/09/2009

Collected By: Ian Moffat, Rainer Grün

Samples in Study: S1

Sample Types in Study: Soil

Soil Described in Field: 0.5 m of soil cover over limestone in front of chateau, no obvious agriculture.

Geology Observed in the Field: Limestone

Geology Name from Map: N/A

Lithology from Map: Marl, limestone, dolomite

Age from Map: Lower Jurassic



A1.2.45. FS052

Easting: 403352

Northing: 4965698

Zone: 31T

Elevation: 372

Description of Site Location: Very new cutting at intersection of D142 and D73 near St Cere.

Date Collected: 8/09/2009

Collected By: Ian Moffat, Rainer Grün

Samples in Study: S1, S2

Sample Types in Study: Soil

Soil Described in Field: Sampled from within limestone unit (S1) and sampled from surface of the cutting from thin soil less than 10 cm thick (S2).

Geology Observed in the Field: Limestone

Geology Name from Map: N/A

Lithology from Map: Marl, limestone, dolomite

Age from Map: Lower Jurassic



A1.2.46. FS053

Easting: 395867

Northing: 4990680

Zone: 31T

Elevation: 226

Description of Site Location: Road cutting and picnic spot north of Meyssac and on the way to house.

Date Collected: 10/09/2009

Collected By: Ian Moffat, Rainer Grün

Samples in Study: S1

Sample Types in Study: Soil

Soil Described in Field: Very thin poorly developed soil mantling bedrock.

Geology Observed in the Field: Red sandstone/schist

Geology Name from Map: N/A

Lithology from Map: Sandstone, conglomerate, shale, coal

Age from Map: Permian



A1.2.47. FS054

Easting: 400221

Northing: 4996198

Zone: 31T

Elevation: 355

Description of Site Location: On road cutting near La Roanne river.

Date Collected: 10/09/2009

Collected By: Ian Moffat, Rainer Grün

Samples in Study: S1

Sample Types in Study: Soil

Soil Described in Field: Thin mantle of soil, on steep slope. May be slope wash.

Geology Observed in the Field: Meta-sediment

Geology Name from Map: N/A

Lithology from Map: Leptynite, orthogneiss, amphibolite

Age from Map: Brioherian, Cambrian



A1.2.48. FS055

Easting: 406773

Northing: 4995726

Zone: 31T

Elevation: 546

Description of Site Location: In road cutting west of village of Neuville.

Date Collected: 10/09/2009

Collected By: Ian Moffat, Rainer Grün

Samples in Study: S2

Sample Types in Study: Soil

Soil Described in Field: Sampled from 1 m below FS055-S1.

Geology Observed in the Field: Heavily weathered metamorphics

Geology Name from Map: N/A

Lithology from Map: Anatetic orthogneiss

Age from Map: Cambrian/Lower-Middle Ordovician



A1.2.49. FS056

Easting: 415656

Northing: 4992939

Zone: 31T

Elevation: 173

Description of Site Location: Taken from bank of Dordogne river near Argentat.

Date Collected: 10/09/2009

Collected By: Ian Moffat, Rainer Grün

Samples in Study: S1

Sample Types in Study: Soil

Soil Described in Field: No bedrock.

Geology Observed in the Field: No bedrock

Geology Name from Map: N/A

Lithology from Map: Anatectic orthogneiss

Age from Map: Brioverian, Upper Cambrian



A1.2.50. FS057

Easting: 415617

Northing: 4992973

Zone: 31T

Elevation: 182

Description of Site Location: Road Cutting near Argentat.

Date Collected: 10/09/2009

Collected By: Ian Moffat, Rainer Grün

Samples in Study: S1

Sample Types in Study: Soil

Soil Described in Field: Collected at top of section.

Geology Observed in the Field: Meta-sediment

Geology Name from Map: N/A

Lithology from Map: Anatectic orthogneiss

Age from Map: Brioverian, Upper Cambrian



A1.2.51. FS058

Easting: 409561

Northing: 4984669

Zone: 31T

Elevation: 157

Description of Site Location: Bank of Dordogne river on D12.

Date Collected: 10/09/2009

Collected By: Ian Moffat, Rainer Grün

Samples in Study: S1

Sample Types in Study: Soil

Soil Described in Field: Taken from mole hill on river bank approximately 3 m above river level.

Geology Observed in the Field: No bedrock

Geology Name from Map: N/A

Lithology from Map: Anatectic orthogneiss

Age from Map: Cambrian, Lower-Middle Ordovician



A1.2.52. FS059

Easting: 409401

Northing: 4984606

Zone: 31T

Elevation: 150

Description of Site Location: In road cutting near river on D12.

Date Collected: 10/09/2009

Collected By: Ian Moffat, Rainer Grün

Samples in Study: S1

Sample Types in Study: Soil

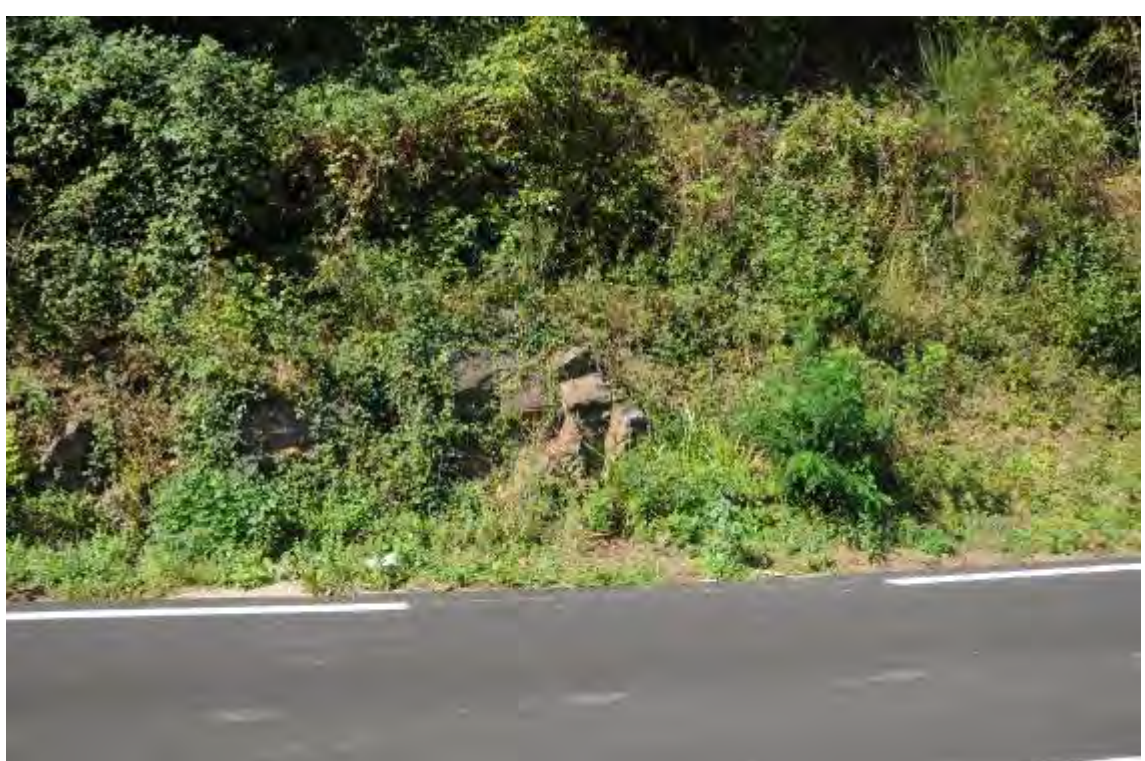
Soil Described in Field: Thin soil mantle on a steep slope, may be slope wash.

Geology Observed in the Field: Metamorphics

Geology Name from Map: N/A

Lithology from Map: Anatectic orthogneiss

Age from Map: Cambrian, Lower-Middle Ordovician



A1.2.53. FS060

Easting: 414875

Northing: 4967937

Zone: 31T

Elevation: 199

Description of Site Location: In old quarry, just past village of Siramon.

Date Collected: 10/09/2009

Collected By: Ian Moffat, Rainer Grün

Samples in Study: S1

Sample Types in Study: Soil

Soil Described in Field: N/A

Geology Observed in the Field: Metamorphics

Geology Name from Map: N/A

Lithology from Map: Leptynite, orthogneiss, amphibolite

Age from Map: Brioherian, Cambrian



A1.2.54. FS061

Easting: 417163

Northing: 4969334

Zone: 31T

Elevation: 421

Description of Site Location: Just east of village of Frayssinhes. In a small road cutting.

Date Collected: 10/09/2009

Collected By: Ian Moffat, Rainer Grün

Samples in Study: S1

Sample Types in Study: Soil

Soil Described in Field: Very thin poorly developed soil on top of cutting containing extensive rock fragments.

Geology Observed in the Field: Metamorphics

Geology Name from Map: N/A

Lithology from Map: Paragneiss, leptynite, amphibolite

Age from Map: Brioverian, Cambrian



A1.2.55. FS063

Easting: 425397

Nothing: 4972325

Zone: 31T

Elevation: 645

Description of Site Location: Small road cutting south of Calviac.

Date Collected: 10/09/2009

Collected By: Ian Moffat, Rainer Grün

Samples in Study: S1

Sample Types in Study: Soil

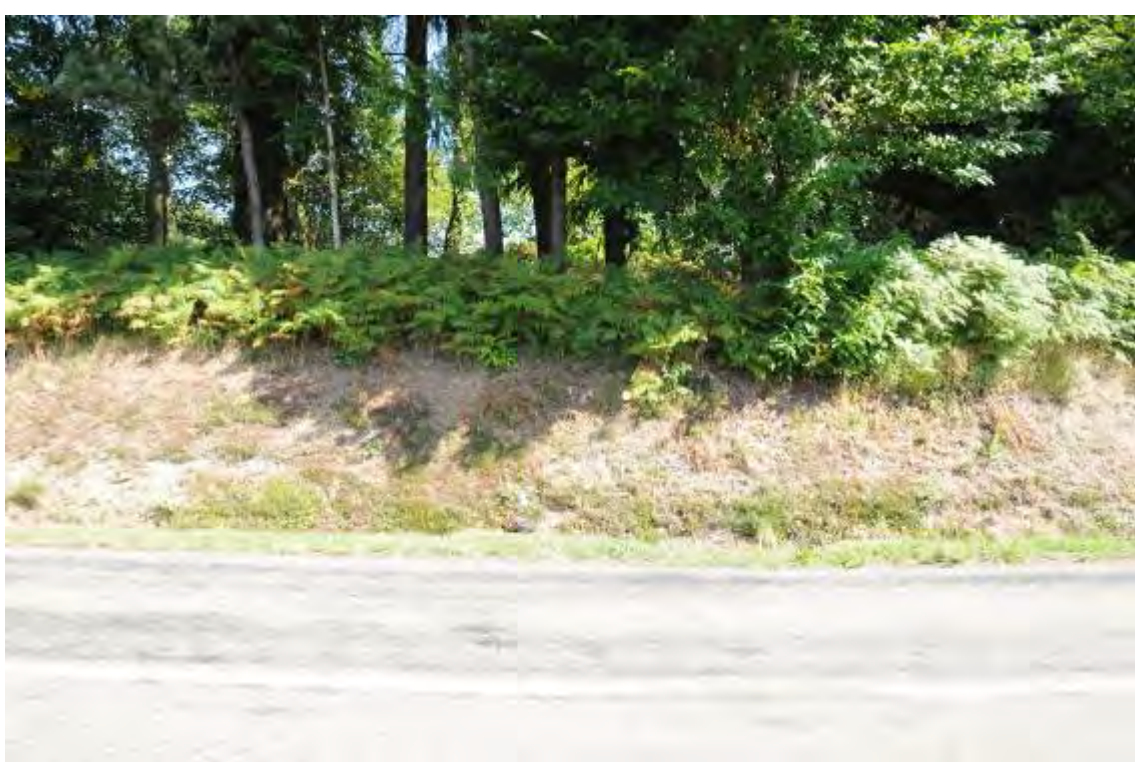
Soil Described in Field: Very thick (2 m) soil profile. Sample collected approximately 10 cm from top.

Geology Observed in the Field: Granite

Geology Name from Map: N/A

Lithology from Map: Monzogranite, granodiorite

Age from Map: Upper Visean, Namurian



A1.2.56. FS065

Easting: 430294

Northing: 4978100

Zone: 31T

Elevation: 597

Description of Site Location: Granite outcrop near Siran.

Date Collected: 10/09/2009

Collected By: Ian Moffat, Rainer Grün

Samples in Study: S1

Sample Types in Study: Soil

Soil Described in Field: Thin layer of soil developed on granite. Sample taken on top of outcrop.

Geology Observed in the Field: Granite

Geology Name from Map: N/A

Lithology from Map: Micaschist, paragneiss

Age from Map: Upper Brioherian, Cambrian, Ordovician



A1.2.57. FS067

Easting: 437844

Northing: 4971581

Zone: 31T

Elevation: 640

Description of Site Location: Road cutting near village of Souli.

Date Collected: 10/09/2009

Collected By: Ian Moffat, Rainer Grün

Samples in Study: S1

Sample Types in Study: Soil

Soil Described in Field: N/A

Geology Observed in the Field: Granite

Geology Name from Map: N/A

Lithology from Map: Monzogranite, granodiorite

Age from Map: Carboniferous



A1.2.58. FS070

Easting: 429643

Northing: 4955208

Zone: 31T

Elevation: 531

Description of Site Location: In road cutting, next to creek north-west of village of Saint-Cirgues.

Date Collected: 10/09/2009

Collected By: Ian Moffat, Rainer Grün

Samples in Study: S1

Sample Types in Study: Soil

Soil Described in Field: Thin soil over rocks on slope, may be slope wash.

Geology Observed in the Field: Metamorphics

Geology Name from Map: N/A

Lithology from Map: Micaschist, paragneiss

Age from Map: Brioverian, Cambrian, Ordovician



A1.2.59. FS072

Easting: 422683

Northing: 4955326

Zone: 31T

Elevation: 576

Description of Site Location: Road cutting near village of Bourial.

Date Collected: 10/09/2009

Collected By: Ian Moffat, Rainer Grün

Samples in Study: S1

Sample Types in Study: Soil

Soil Described in Field: Taken at top of outcrop approximately 1 m above ground.

Geology Observed in the Field: Metamorphics

Geology Name from Map: N/A

Lithology from Map: Leptynite, orthogneiss, amphibolite

Age from Map: Brioherian, Cambrian



A1.2.60. FS074

Easting: 410228

Northing: 4953484

Zone: 31T

Elevation: 371

Description of Site Location: Road cutting near Gramat.

Date Collected: 10/09/2009

Collected By: Ian Moffat, Rainer Grün

Samples in Study: S1

Sample Types in Study: Soil

Soil Described in Field: Taken from top of section; poor, thin soil with many limestone frags.

Geology Observed in the Field: Limestone

Geology Name from Map: N/A

Lithology from Map: Marl, limestone, dolomite

Age from Map: Lower Jurassic



A1.2.61. FS076

Easting: 382579

Northing: 4987769

Zone: 31T

Elevation: 313

Description of Site Location: On side road with large road cutting west of Sarrazac.

Date Collected: 10/09/2009

Collected By: Ian Moffat, Rainer Grün

Samples in Study: S1

Sample Types in Study: Soil

Soil Described in Field: Very thin, poorly developed red soil sample from top of section.

Geology Observed in the Field: Chalky limestone

Geology Name from Map: N/A

Lithology from Map: Limestone, marl

Age from Map: Middle Jurassic



A1.2.62. FS078

Easting: 410586

Northing: 4947189

Zone: 31T

Elevation: 342

Description of Site Location: In small road cutting next to railway line in Assier.

Date Collected: 11/09/2009

Collected By: Ian Moffat, Rainer Grün

Samples in Study: S1

Sample Types in Study: Soil

Soil Described in Field: Very thin poorly developed red soil on top of section.

Geology Observed in the Field: Limestone

Geology Name from Map: N/A

Lithology from Map: Limestone, marl

Age from Map: Middle Jurassic



A1.2.63. FS080

Easting: 398816

Northing: 4947905

Zone: 31T

Elevation: 333

Description of Site Location: Road cutting near town of Tartabelle.

Date Collected: 11/09/2009

Collected By: Ian Moffat, Rainer Grün

Samples in Study: S1

Sample Types in Study: Soil

Soil Described in Field: Very thin poorly developed red soil with abundant limestone fragments.

Geology Observed in the Field: Limestone

Geology Name from Map: N/A

Lithology from Map: Limestone, marl

Age from Map: Middle Jurassic



A1.2.64. FS081

Easting: 394242

Northing: 4947356

Zone: 31T

Elevation: 399

Description of Site Location: Road cutting near village of Fontanes du Causse.

Date Collected: 11/09/2009

Collected By: Ian Moffat, Rainer Grün

Samples in Study: S1

Sample Types in Study: Soil

Soil Described in Field: Very thin poorly developed red soil with abundant limestone fragments.

Geology Observed in the Field: Limestone

Lithology from Map: Marl, limestone, clay

Age from Map: Upper Jurassic



A1.2.65. FS083

Easting: 380555

Northing: 4955229

Zone: 31T

Elevation: 321

Description of Site Location: In road cutting at turnoff to St Project.

Date Collected: 11/09/2009

Collected By: Ian Moffat, Rainer Grün

Samples in Study: S1

Sample Types in Study: Soil

Soil Described in Field: Very thin red soil over limestone.

Geology Observed in the Field: Limestone

Geology Name from Map: N/A

Lithology from Map: Marl, clay, limestone, conglomerate

Age from Map: Oligocene



A1.2.66. FS084

Easting: 369306

Northing: 4952391

Zone: 31T

Elevation: 196

Description of Site Location: Small road cutting west of Gourdon.

Date Collected: 11/09/2009

Collected By: Ian Moffat, Rainer Grün

Samples in Study: S1

Sample Types in Study: Soil

Soil Described in Field: Thin poorly developed soil on small rock outcrop.

Geology Observed in the Field: Limestone

Geology Name from Map: N/A

Lithology from Map: Marl, limestone, clay

Age from Map: Upper Jurassic



A1.2.67. FS085

Easting: 364172

Northing: 4950411

Zone: 31T

Elevation: 170

Description of Site Location: In small road cutting on side road north-east of Salviac.

Date Collected: 11/09/2009

Collected By: Ian Moffat, Rainer Grün

Samples in Study: S1

Sample Types in Study: Soil

Soil Described in Field: Very thin, light brown soil on limestone.

Geology Observed in the Field: Limestone

Geology Name from Map: N/A

Lithology from Map: Marl, limestone, clay

Age from Map: Upper Jurassic



A1.2.68. FS086

Easting: 360351

Northing: 4957598

Zone: 31T

Elevation: 154

Description of Site Location: Small road cutting near village of Le Creze.

Date Collected: 11/09/2009

Collected By: Ian Moffat, Rainer Grün

Samples in Study: S1

Sample Types in Study: Soil

Soil Described in Field: Thin red, poorly developed soil with abundant limestone fragments.

Geology Observed in the Field: Limestone

Geology Name from Map: N/A

Lithology from Map: Limestone, marl, clay, sand

Age from Map: Upper Cretaceous



A1.2.69. FS087

Easting: 356453

Northing: 4954771

Zone: 31T

Elevation: 120

Description of Site Location: Small quarry south of Daglan. On side of road.

Date Collected: 11/09/2009

Collected By: Ian Moffat, Rainer Grün

Samples in Study: S1

Sample Types in Study: Soil

Soil Described in Field: Very thin brown/grey soil forming on isolated outcrop of rock 20 m west of rock outcrop.

Geology Observed in the Field: Fossiliferous limestone

Geology Name from Map: N/A

Lithology from Map: Marl, limestone, clay

Age from Map: Upper Jurassic



A1.2.70. FS088

Easting: 342579

Northing: 4959745

Zone: 31T

Elevation: 106

Description of Site Location: In large road cutting south of Belves.

Date Collected: 11/09/2009

Collected By: Ian Moffat, Rainer Grün

Samples in Study: S1

Sample Types in Study: Soil

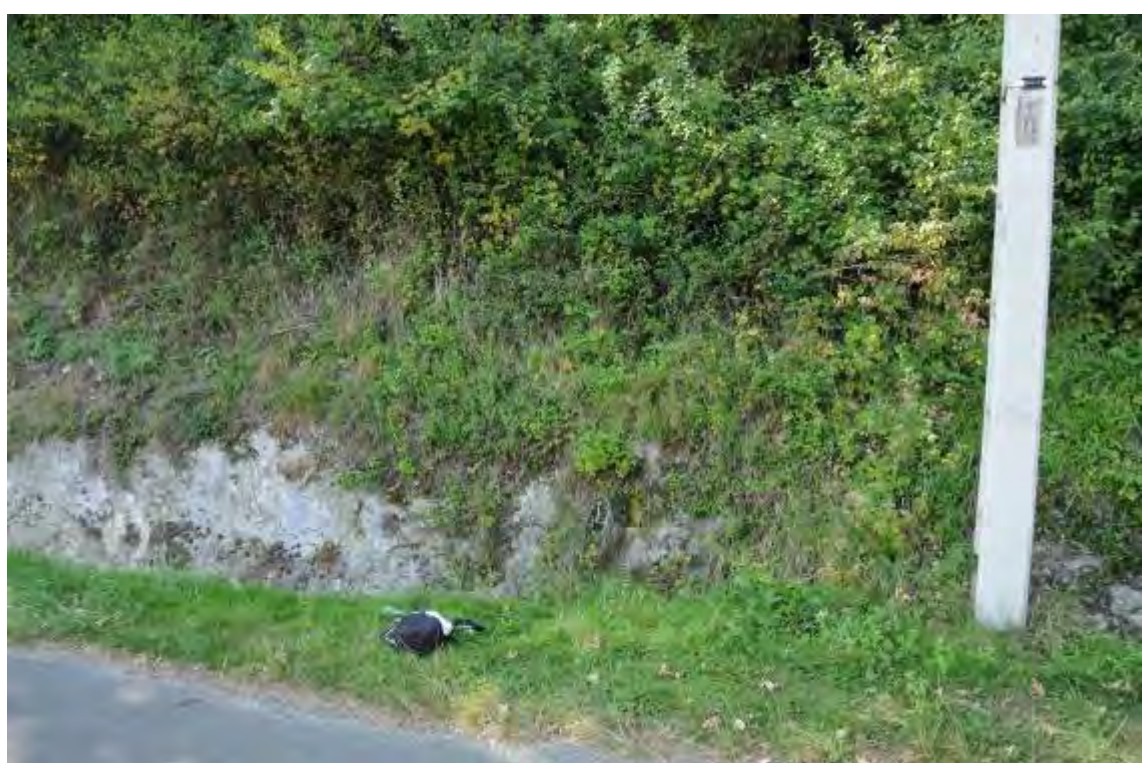
Soil Described in Field: Very thin soil mantling slope, probably includes a contribution from slope wash.

Geology Observed in the Field: Limestone

Geology Name from Map: N/A

Lithology from Map: Limestone, marl, clay, sand

Age from Map: Upper Cretaceous



A1.2.71. FS089

Easting: 369850

Northing: 4973456

Zone: 31T

Elevation: 228

Description of Site Location: Small cutting on side of road near village of Carlux.

Date Collected: 11/09/2009

Collected By: Ian Moffat, Rainer Grün

Samples in Study: S1

Sample Types in Study: Soil

Soil Described in Field: Well-developed red soil on limestone. May be artificially mounded.

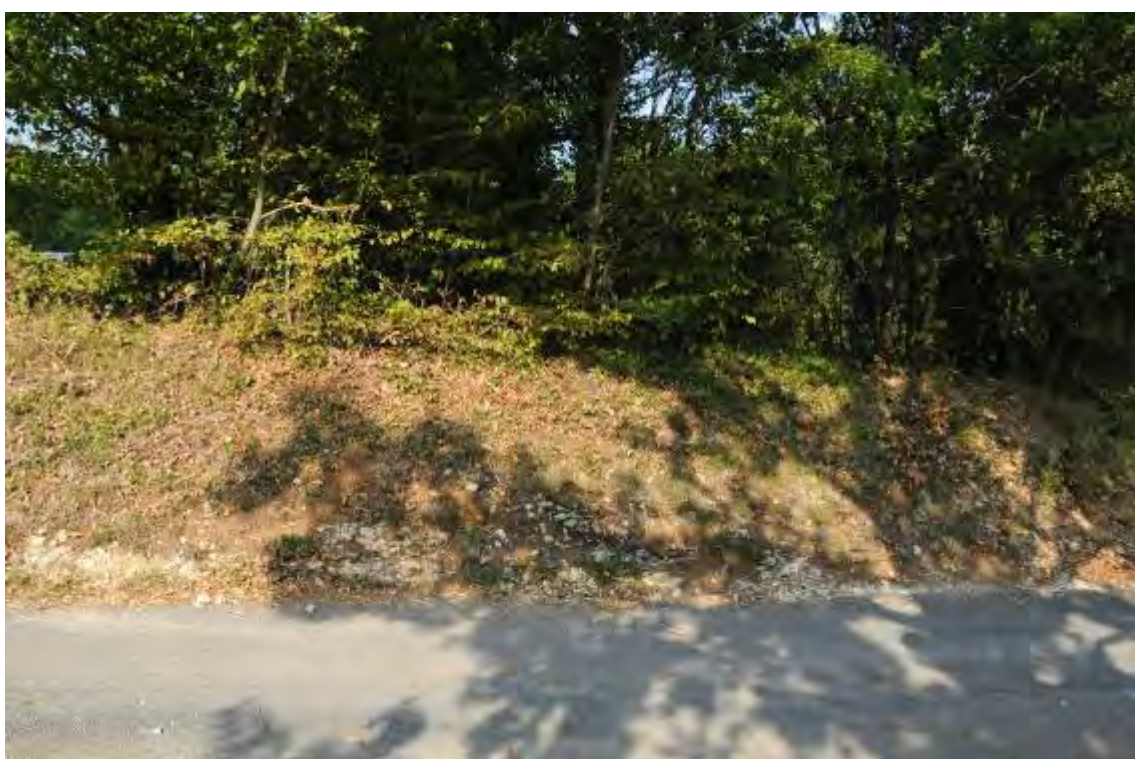
Geology Observed in the Field: Limestone

Geology Name from Map: N/A

Geology Name from Map: N/A

Lithology from Map: Limestone, marl, clay, sand

Age from Map: Upper Cretaceous



A1.2.72. FS090

Easting: 466090

Northing: 4918254

Zone: 31T

Elevation: 568

Description of Site Location: Southeast of village of Le Rescoundudou.

Date Collected: 12/09/2009

Collected By: Ian Moffat, Rainer Grün

Samples in Study: S2

Sample Types in Study: Soil

Soil Described in Field: Taken south-east of the grate covered cave above large open cave at surface level.

Geology Observed in the Field: Limestone

Geology Name from Map: N/A

Lithology from Map: Limestone, marl

Age from Map: Middle Jurassic



A1.2.73. FS092

Easting: 476904

Northing: 4923011

Zone: 31T

Elevation: 559

Description of Site Location: South of the village of St Catherine.

Date Collected: 13/09/2009

Collected By: Ian Moffat, Rainer Grün

Samples in Study: S1

Sample Types in Study: Soil

Soil Described in Field: Thick chocolate brown, well-developed soil on slope, may have slope wash component.

Geology Observed in the Field: Red sandstone

Geology Name from Map: N/A

Lithology from Map: Marl, dolomite, limestone, sandstone

Age from Map: Lower Jurassic



A1.2.74. FS093

Easting: 477763

Northing: 4917559

Zone: 31T

Elevation: 608

Description of Site Location: Small outcrop in field south of the village of Grioudas.

Date Collected: 13/09/2009

Collected By: Ian Moffat, Rainer Grün

Samples in Study: S1

Sample Types in Study: Soil

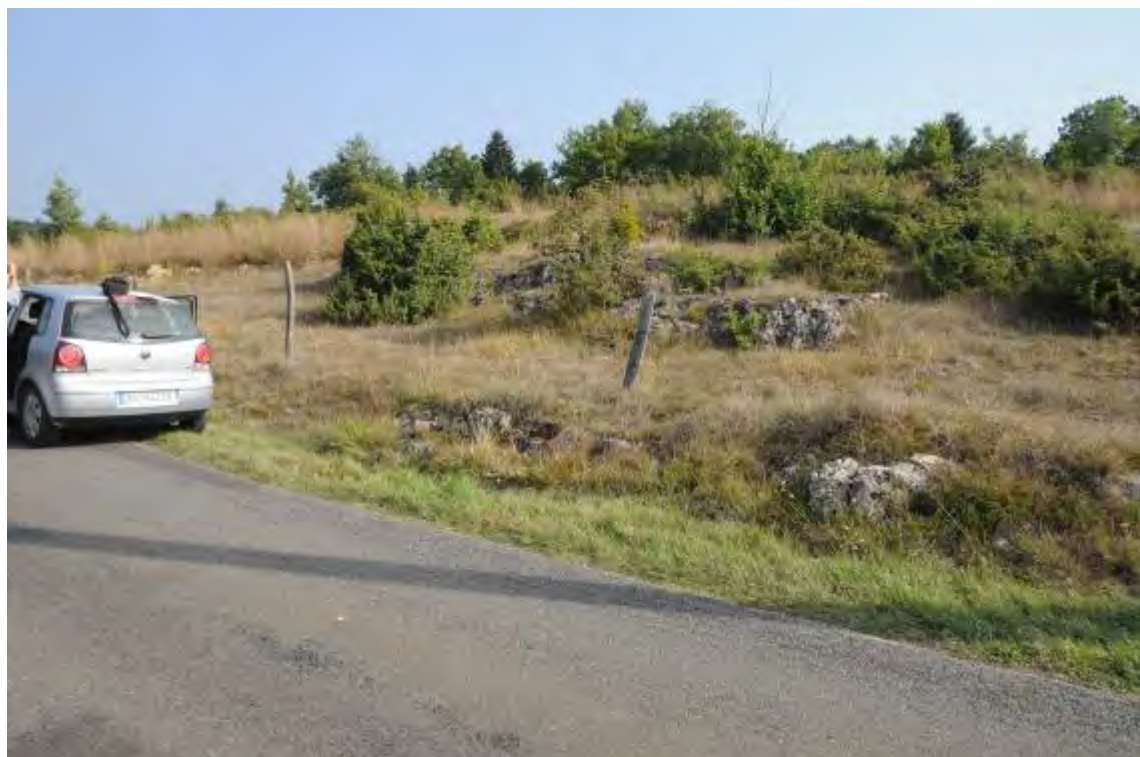
Soil Described in Field: Well-developed red soil.

Geology Observed in the Field: Limestone

Geology Name from Map: N/A

Lithology from Map: Limestone, marl

Age from Map: Middle Jurassic



A1.2.75. FS094

Easting: 473503

Northing: 4918987

Zone: 31T

Elevation: 614

Description of Site Location: North of turnoff to Comtal in small road cutting in carpark.

Date Collected: 13/09/2009

Collected By: Ian Moffat, Rainer Grün

Samples in Study: S1

Sample Types in Study: Soil

Soil Described in Field: Thin, poorly developed brown soil with abundant limestone fragments.

Geology Observed in the Field: Limestone

Geology Name from Map: N/A

Lithology from Map: Limestone, marl

Age from Map: Middle Jurassic



A1.2.76. FS096

Easting: 467072

Northing: 4912565

Zone: 31T

Elevation: 551

Description of Site Location: In carpark of Lidl south of Rodez.

Date Collected: 13/09/2009

Collected By: Ian Moffat, Rainer Grün

Samples in Study: S1

Sample Types in Study: Soil

Soil Described in Field: Moderately developed red soil.

Geology Observed in the Field: Inter-bedded claystone/sandstone

Geology Name from Map: N/A

Lithology from Map: Sandstone, conglomerate, shale, coal

Age from Map: Permian



A1.2.77. FS097

Easting: 468261

Northing: 4904608

Zone: 31T

Elevation: 650

Description of Site Location: North of Flavin in small road cutting.

Date Collected: 13/09/2009

Collected By: Ian Moffat, Rainer Grün

Samples in Study: S1

Sample Types in Study: Soil

Soil Described in Field: Well-developed grey soil, agricultural activity behind sample location.

Geology Observed in the Field: Meta-sediment

Geology Name from Map: N/A

Lithology from Map: Marl, limestone, dolomite

Age from Map: Lower Jurassic



A1.2.78. FS099

Easting: 472222

Northing: 4907536

Zone: 31T

Elevation: 696

Description of Site Location: East of 5-way intersection at Comps.

Date Collected: 13/09/2009

Collected By: Ian Moffat, Rainer Grün

Samples in Study: S1

Sample Types in Study: Soil

Soil Described in Field: Poorly developed light brown soil.

Geology Observed in the Field: Metamorphics

Geology Name from Map: N/A

Lithology from Map: Granite, orthogenesis

Age from Map: Cambrian, Lower-Middle Ordovician



A1.2.79. FS100

Easting: 476284

Northing: 4906484

Zone: 31T

Elevation: 830

Description of Site Location: South of Frayssinhes on side of road in a small cutting.

Date Collected: 13/09/2009

Collected By: Ian Moffat, Rainer Grün

Samples in Study: S1

Sample Types in Study: Soil

Soil Described in Field: Very thin (<5 cm), light brown, poorly developed soil.

Geology Observed in the Field: Metamorphics

Geology Name from Map: N/A

Lithology from Map: Micaschist, paragneiss

Age from Map: Brioverian, Cambrian, Ordovician



A1.2.80. FS102

Easting: 477133

Northing: 4907464

Zone: 31T

Elevation: 853

Description of Site Location: On dirt track west of Le Panque.

Date Collected: 13/09/2009

Collected By: Ian Moffat, Rainer Grün

Samples in Study: S1

Sample Types in Study: Soil

Soil Described in Field: Light brown soil, sample taken in field 5 m away from FS102-R1.

Geology Observed in the Field: Metamorphics

Geology Name from Map: N/A

Lithology from Map: Migmatite

Age from Map: Cambrian, Ordovician



A1.2.81. FS103

Easting: 483049

Northing: 4908159

Zone: 31T

Elevation: 857

Description of Site Location: Small road cutting south of St-Martin-de-Conieres.

Date Collected: 13/09/2009

Collected By: Ian Moffat, Rainer Grün

Samples in Study: S1

Sample Types in Study: Soil

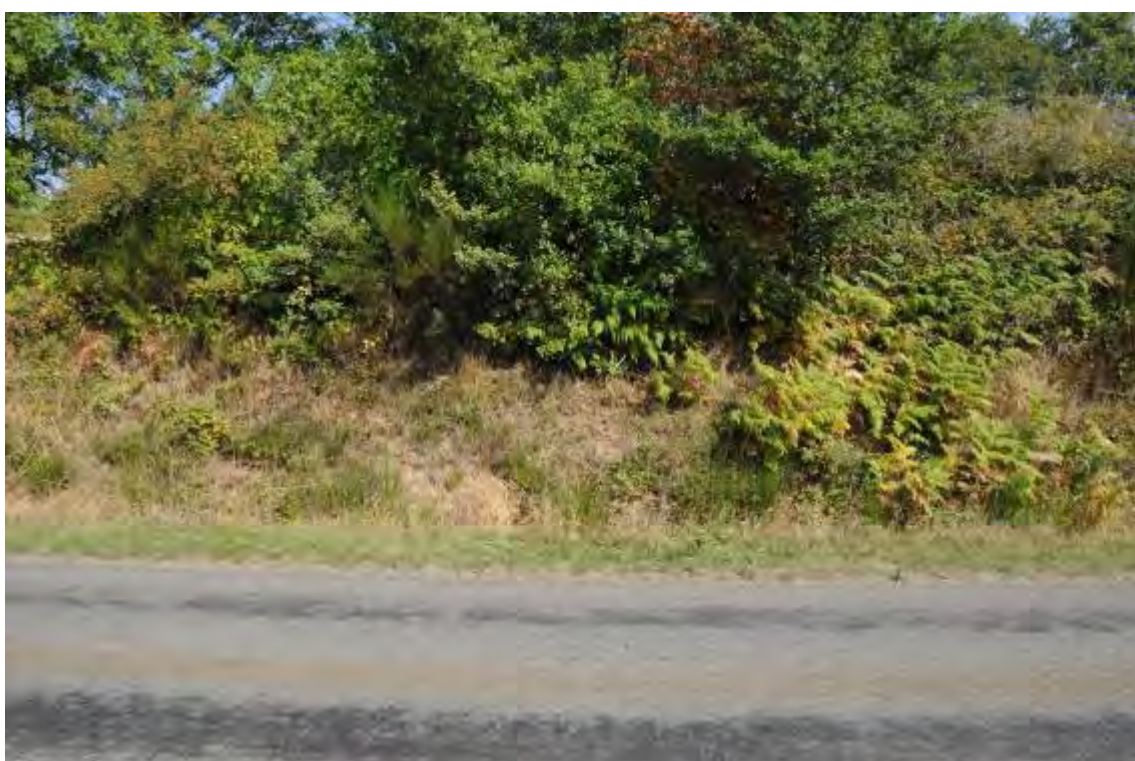
Soil Described in Field: Thin, poorly developed soil.

Geology Observed in the Field: Metamorphics

Geology Name from Map: N/A

Lithology from Map: Anatectic orthogneiss

Age from Map: Cambrian, Lower-Middle Ordovician



A1.2.82. FS104

Easting: 482468

Northing: 4911339

Zone: 31T

Elevation: 803

Description of Site Location: In small road cutting on corner north of La Boulloire.

Date Collected: 13/09/2009

Collected By: Ian Moffat, Rainer Grün

Samples in Study: S2

Sample Types in Study: Soil

Soil Described in Field: *In situ* weather of bedrock to form thin poorly developed soil on outcrop.

Geology Observed in the Field: Metamorphics

Geology Name from Map: N/A

Lithology from Map: Micaschist, paragneiss

Age from Map: Brioverian, Cambrian, Ordovician



A1.2.83. FS105

Easting: 483003

Northing: 4911985

Zone: 31T

Elevation: 773

Description of Site Location: In road cutting on curve north of La Boulloire.

Date Collected: 13/09/2009

Collected By: Ian Moffat, Rainer Grün

Samples in Study: S1

Sample Types in Study: Soil

Soil Described in Field: Very thin poorly developed soil with abundant rock fragments.

Geology Observed in the Field: Metamorphics

Geology Name from Map: N/A

Lithology from Map: Granite, orthogneiss

Age from Map: Brioherian upper Cambrian



A1.2.84. FS107

Easting: 478875

Northing: 4925330

Zone: 31T

Elevation: 590

Description of Site Location: In large cutting, north of Bozouls.

Date Collected: 14/09/2009

Collected By: Ian Moffat, Rainer Grün

Samples in Study: S1

Sample Types in Study: Soil

Soil Described in Field: Very thin light brown soil with abundant lithic fragments.

Geology Observed in the Field: Limestone

Geology Name from Map: N/A

Lithology from Map: Marl, dolomite, limestone, sandstone

Age from Map: Lower Jurassic



A1.2.85. FS108

Easting: 479023

Northing: 4928892

Zone: 31T

Elevation: 516

Description of Site Location: On curved section of road south of town of Espalion.

Date Collected: 14/09/2009

Collected By: Ian Moffat, Rainer Grün

Samples in Study: S1

Sample Types in Study: Soil

Soil Described in Field: Moderately well-developed chocolate brown soil on artificial bench cut in rock.

Geology Observed in the Field: Red inter-bedded sandstone/siltstone

Geology Name from Map: N/A

Lithology from Map: Sandstone, conglomerate, shale, coal

Age from Map: Permian



A1.2.86. FS111

Easting: 469680

Northing: 4938102

Zone: 31T

Elevation: 282

Description of Site Location: In Lot river gorge, south-east of Entrayques.

Date Collected: 14/09/2009

Collected By: Ian Moffat, Rainer Grün

Samples in Study: S1

Sample Types in Study: Soil

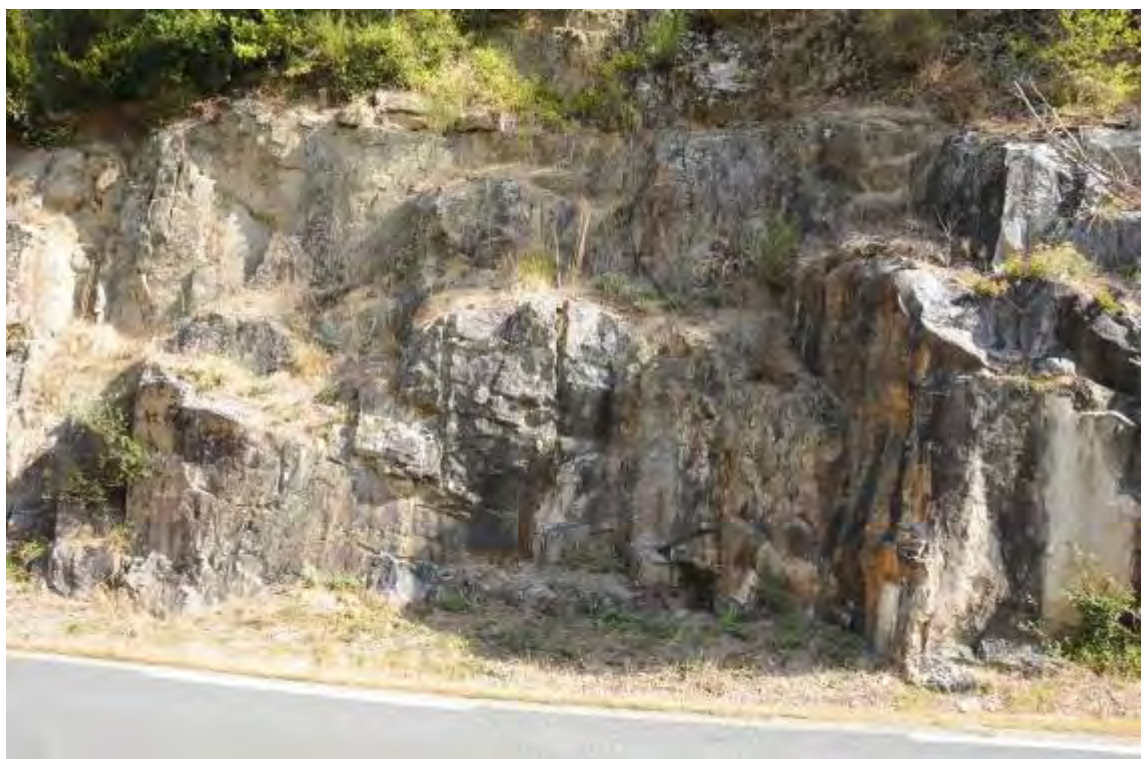
Soil Described in Field: Very thin soil, developed on rock ledge.

Geology Observed in the Field: Granite

Geology Name from Map: N/A

Lithology from Map: Monzogranite, granodiorite

Age from Map: Upper Visean, Namurian



A1.2.87. FS112

Easting: 464584

Northing: 4934617

Zone: 31T

Elevation: 577

Description of Site Location: In small road cutting in little forest south of Nacoulargues.

Date Collected: 14/09/2009

Collected By: Ian Moffat, Rainer Grün

Samples in Study: S1

Sample Types in Study: Soil

Soil Described in Field: Very thin poorly developed soil on top of outcrop.

Geology Observed in the Field: Granite

Geology Name from Map: N/A

Lithology from Map: Schist, mica schist, quartzite

Age from Map: Brioherian, Cambrian, Ordovician



A1.2.88. FS113

Easting: 470929

Northing: 4927979

Zone: 31T

Elevation: 529

Description of Site Location: In small road cutting north of Rodille.

Date Collected: 14/09/2009

Collected By: Ian Moffat, Rainer Grün

Samples in Study: S1

Sample Types in Study: Soil

Soil Described in Field: Thick, well-developed red soil.

Geology Observed in the Field: Red sandstone

Geology Name from Map: N/A

Lithology from Map: Sandstone, conglomerate, shale, coal

Age from Map: Permian



A1.2.89. FS114

Easting: 470182

Northing: 4923875

Zone: 31T

Elevation: 563

Description of Site Location: In driveway south of Rodelle.

Date Collected: 14/09/2009

Collected By: Ian Moffat, Rainer Grün

Samples in Study: S1

Sample Types in Study: Soil

Soil Described in Field: Well-developed thin red soil.

Geology Observed in the Field: Limestone

Geology Name from Map: N/A

Lithology from Map: Limestone, marl, dolomite

Age from Map: Middle Jurassic



A1.2.90. FS115

Easting: 466355

Northing: 4920134

Zone: 31T

Elevation: 597

Description of Site Location: North of Le Rescoundudou.

Date Collected: 14/09/2009

Collected By: Ian Moffat, Rainer Grün

Samples in Study: S1

Sample Types in Study: Soil

Soil Described in Field: Well-developed red soil of unknown thickness.

Geology Observed in the Field: Limestone

Geology Name from Map: N/A

Lithology from Map: Limestone, marl, dolomite

Age from Map: Middle Jurassic



A1.2.91. FS116

Easting: 480240

Northing: 4929489

Zone: 31T

Elevation: 520

Description of Site Location: Just below castle of Calment d'Olt.

Date Collected: 14/09/2009

Collected By: Ian Moffat, Rainer Grün

Samples in Study: S1

Sample Types in Study: Soil

Soil Described in Field: Thin red soil on basalt.

Geology Observed in the Field: Basalt

Geology Name from Map: N/A

Lithology from Map: Basanite, hawaiite, tephra

Age from Map: Oligocene, Miocene



A1.2.92. FS118

Easting: 499737

Northing: 4941195

Zone: 31T

Elevation: 132

Description of Site Location: Just east of village of Aubrac.

Date Collected: 14/09/2009

Collected By: Ian Moffat, Rainer Grün

Samples in Study: S1

Sample Types in Study: Soil

Soil Described in Field: Thin, well-developed chocolate brown soil immediately on top of tuff.

Geology Observed in the Field: Basalt and tuff

Geology Name from Map: N/A

Lithology from Map: Basanite, hawaiite, tephra

Age from Map: Oligocene, Miocene



A1.2.93. P2

Easting: 636270

Northing: 4972220

Zone: 31T

Elevation: N/A

Description of Site Location: N/A

Date Collected: N/A

Collected By: Maxime Aubert

Samples in Study: P

Sample Types in Study: Plant

Soil Described in Field: N/A

Geology Observed in the Field: N/A

Geology Name from Map: N/A

Lithology from Map: Monzogranite, granodiorite

Age from Map: Dinantien, Namurien, Westphalien



A1.2.94. P3

Easting: 613978

Northing: 4979921

Zone: 31T

Elevation: N/A

Description of Site Location: N/A

Date Collected: N/A

Collected By: Maxime Aubert

Samples in Study: P1, P2

Sample Types in Study: Plant

Soil Described in Field: N/A

Geology Observed in the Field: N/A

Geology Name from Map: N/A

Lithology from Map: Anatectic orthogneiss

Age from Map: Briovertien, Cambrian, Ordovician



A1.2.95. P4

Easting: 605305

Northing: 4977747

Zone: 31T

Elevation: N/A

Description of Site Location: N/A

Date Collected: N/A

Collected By: Maxime Aubert

Samples in Study: P1, P2

Sample Types in Study: Plant

Soil Described in Field: N/A

Geology Observed in the Field: N/A

Geology Name from Map: N/A

Lithology from Map: Monzogranite, granodiorite

Age from Map: Namurien, Westphalien, Stephanien



A1.2.96. P5

Easting: 608043

Northing: 4977994

Zone: 31T

Elevation: N/A

Description of Site Location: N/A

Date Collected: N/A

Collected By: Maxime Aubert

Samples in Study: P1, P2

Sample Types in Study: Plant

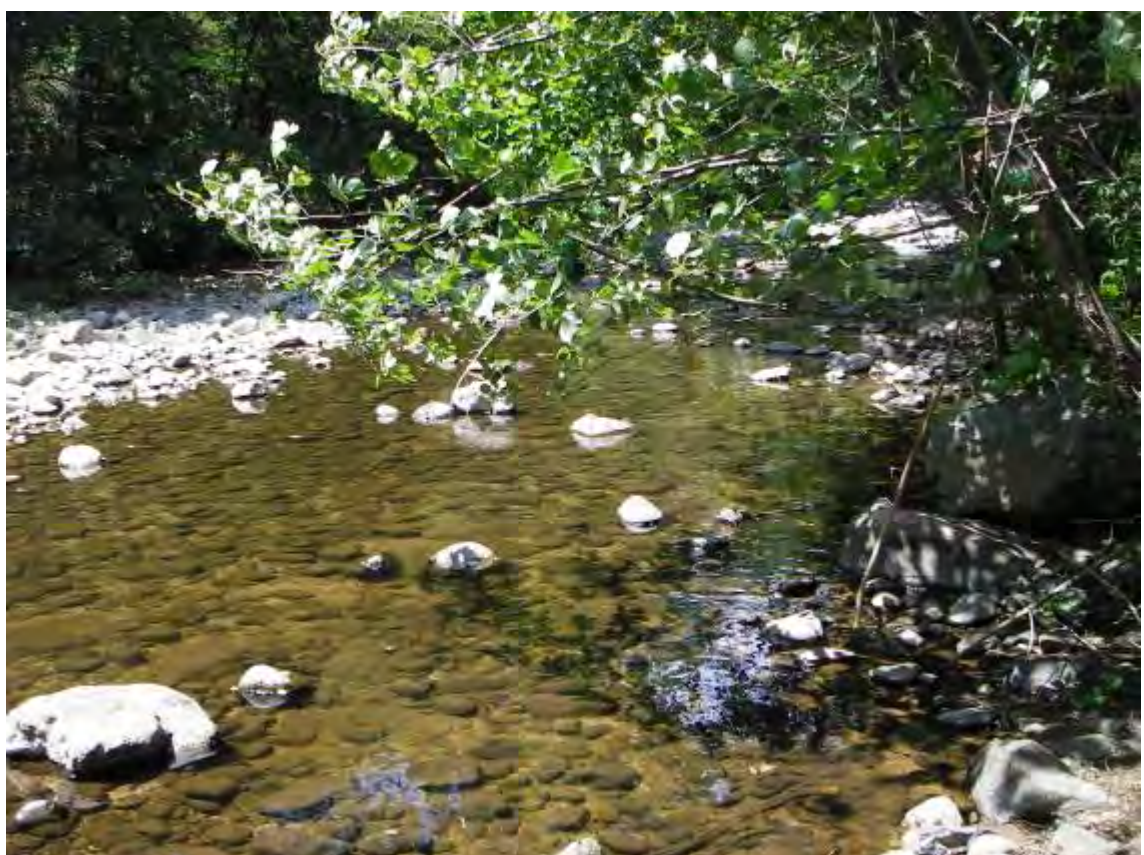
Soil Described in Field: N/A

Geology Observed in the Field: N/A

Geology Name from Map: N/A

Lithology from Map: Monzogranite, granodiorite

Age from Map: Namurien, Westphalien, Stephanien



A1.2.97. P6

Easting: 581185

Northing: 4983778

Zone: 31T

Elevation: N/A

Description of Site Location: N/A

Date Collected: N/A

Collected By: Maxime Aubert

Samples in Study: P1, P2

Sample Types in Study: Plant

Soil Described in Field: N/A

Geology Observed in the Field: N/A

Geology Name from Map: N/A

Lithology from Map: Clay, conglomerate, sandstone, marl

Age from Map: Clay, conglomerate, sandstone, marl



A1.2.98. P7

Easting: 588195

Northing: 4981254

Zone: 31T

Elevation: N/A

Description of Site Location: N/A

Date Collected: N/A

Collected By: Maxime Aubert

Samples in Study: P1, P2

Sample Types in Study: Plant

Soil Described in Field: N/A

Geology Observed in the Field: N/A

Geology Name from Map: N/A

Lithology from Map: Basanite, hawaiite, tephra

Age from Map: Oligocene, Miocene



A1.2.99. P8

Easting: 583541

Northing: 4982608

Zone: 31T

Elevation: N/A

Description of Site Location: N/A

Date Collected: N/A

Collected By: Maxime Aubert

Samples in Study: P1, P2

Sample Types in Study: Plant

Soil Described in Field: N/A

Geology Observed in the Field: N/A

Geology Name from Map: N/A

Lithology from Map: Monzogranite, granodiorite

Age from Map: Namurien, Westphalien, Stephanien



A1.2.100. P9

Easting: 583488

Northing: 4982629

Zone: 31T

Elevation: N/A

Description of Site Location: N/A

Date Collected: N/A

Collected By: Maxime Aubert

Samples in Study: P1, P2

Sample Types in Study: Plant

Soil Described in Field: N/A

Geology Observed in the Field: N/A

Geology Name from Map: N/A

Lithology from Map: Monzogranite, granodiorite

Age from Map: Namurien, Westphalien, Stephanien



A1.2.101. P10

Easting: 592176

Northing: 4970857

Zone: 31T

Elevation: N/A

Description of Site Location: Les Estables.

Date Collected: N/A

Collected By: Maxime Aubert

Samples in Study: P

Sample Types in Study: Plant

Soil Described in Field: N/A

Geology Observed in the Field: N/A

Geology Name from Map: N/A

Lithology from Map: Monzogranite, granodiorite

Age from Map: Namurien, Westphalien, Stephanien



A1.2.102. P11

Easting: 579265

Northing: 4953843

Zone: 31T

Elevation: N/A

Description of Site Location: Lanarche.

Date Collected: N/A

Collected By: Maxime Aubert

Samples in Study: P

Sample Types in Study: Plant

Soil Described in Field: N/A

Geology Observed in the Field: N/A

Geology Name from Map: N/A

Lithology from Map: Anatectic orthogneisses

Age from Map: Upper Brioerien, Cambrian



A1.2.103. P12

Easting: 596388

Northing: 4928948

Zone: 31T

Elevation: N/A

Description of Site Location: River.

Date Collected: N/A

Collected By: Maxime Aubert

Samples in Study: P

Sample Types in Study: Plant

Soil Described in Field: N/A

Geology Observed in the Field: N/A

Geology Name from Map: N/A

Lithology from Map: Schist, micaschist, quartzite

Age from Map: Brioverien, Cambrian, Ordovician



A1.2.104. P13

Easting: 593569

Northing: 4925774

Zone: 31T

Elevation: N/A

Description of Site Location: N/A

Date Collected: N/A

Collected By: Maxime Aubert

Samples in Study: P

Sample Types in Study: Plant

Soil Described in Field: N/A

Geology Observed in the Field: N/A

Geology Name from Map: N/A

Lithology from Map: Dolomite, marl, evaporite

Age from Map: Middle-Upper Triassic



A1.2.105. P14

Easting: 588209

Northing: 4926940

Zone: 31T

Elevation: N/A

Description of Site Location: St-Jean de Poncharesse.

Date Collected: N/A

Collected By: Maxime Aubert

Samples in Study: P

Sample Types in Study: Plant

Soil Described in Field: N/A

Geology Observed in the Field: N/A

Geology Name from Map: N/A

Lithology from Map: Schist, micaschist, quartzite

Age from Map: Brioverien, Cambrian, Ordovician



A1.2.106. P15

Easting: 579935

Northing: 4903929

Zone: 31T

Elevation: N/A

Description of Site Location: La Vernarede.

Date Collected: N/A

Collected By: Maxime Aubert

Samples in Study: P

Sample Types in Study: Plant

Soil Described in Field: N/A

Geology Observed in the Field: N/A

Geology Name from Map: N/A

Lithology from Map: Sandstone, conglomerate, coal, shale

Age from Map: Stephanien



A1.2.107. P16

Easting: 580827

Northing: 4906144

Zone: 31T

Elevation: N/A

Description of Site Location: River at Chambon.

Date Collected: N/A

Collected By: Maxime Aubert

Samples in Study: P

Sample Types in Study: Plant

Soil Described in Field: N/A

Geology Observed in the Field: N/A

Geology Name from Map: N/A

Lithology from Map: Metagranite, orthogneiss

Age from Map: Cambrian, Lower-Middle Ordovician



A1.2.108. P17

Easting: 603549

Northing: 4903924

Zone: 31T

Elevation: N/A

Description of Site Location: Canviac.

Date Collected: N/A

Collected By: Maxime Aubert

Samples in Study: P

Sample Types in Study: Plant

Soil Described in Field: N/A

Geology Observed in the Field: N/A

Geology Name from Map: N/A

Lithology from Map: Marl, sandstone, conglomerate, limestone

Age from Map: Oligocene



A1.2.109. P18

Easting: 615072

Northing: 4901240

Zone: 31T

Elevation: N/A

Description of Site Location: River.

Date Collected: N/A

Collected By: Maxime Aubert

Samples in Study: P

Sample Types in Study: Plant

Soil Described in Field: N/A

Geology Observed in the Field: N/A

Geology Name from Map: N/A

Lithology from Map: Limestone reef facies urgonian

Age from Map: Lower Cretaceous



A1.2.110. P19

Easting: 615732

Northing: 4900551

Zone: 31T

Elevation: N/A

Description of Site Location: Near a river.

Date Collected: N/A

Collected By: Maxime Aubert

Samples in Study: P

Sample Types in Study: Plant

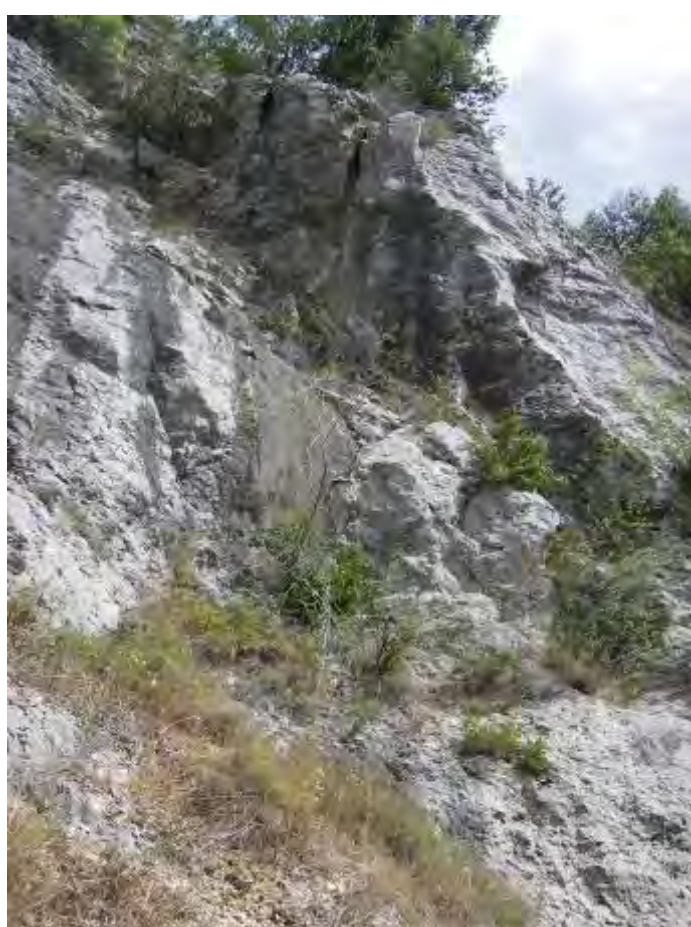
Soil Described in Field: N/A

Geology Observed in the Field: N/A

Geology Name from Map: N/A

Lithology from Map: Marl, sand, sandstone, clay, limestone

Age from Map: Lower Cretaceous



A1.2.111. P20

Easting: 630308

Northing: 4896756

Zone: 31T

Elevation: N/A

Description of Site Location: St Nazaire.

Date Collected: N/A

Collected By: Maxime Aubert

Samples in Study: P

Sample Types in Study: Plant

Soil Described in Field: N/A

Geology Observed in the Field: N/A

Geology Name from Map: N/A

Lithology from Map: Marl, sandstone, chalk, limestone

Age from Map: Upper Cretaceous



A1.2.112. P23

Easting: 613289

Northing: 4938650

Zone: 31T

Elevation: N/A

Description of Site Location: St Nazaire.

Date Collected: N/A

Collected By: Maxime Aubert

Samples in Study: P

Sample Types in Study: Plant

Soil Described in Field: N/A

Geology Observed in the Field: N/A

Geology Name from Map: N/A

Lithology from Map: Marl, limestone, clay

Age from Map: Upper Jurassic



A1.2.113. P24

Easting: 621739

Northing: 4931192

Zone: 31T

Elevation: N/A

Description of Site Location: St-Andreol-de-Berg.

Date Collected: N/A

Collected By: Maxime Aubert

Samples in Study: P

Sample Types in Study: Plant

Soil Described in Field: N/A

Geology Observed in the Field: N/A

Geology Name from Map: N/A

Lithology from Map: Marl, sand, sandstone, clay, limestone

Age from Map: Lower Cretaceous



A1.2.114. P25

Easting: 619053

Northing: 4939189

Zone: 31T

Elevation: N/A

Description of Site Location: St Nazaire.

Date Collected: N/A

Collected By: Maxime Aubert

Samples in Study: P

Sample Types in Study: Plant

Soil Described in Field: N/A

Geology Observed in the Field: N/A

Geology Name from Map: N/A

Lithology from Map: Marl, sand, sandstone, clay, limestone

Age from Map: Lower Cretaceous



A1.2.115. P26

Easting: 621056

Northing: 4938201

Zone: 31T

Elevation: N/A

Description of Site Location: N/A

Date Collected: N/A

Collected By: Maxime Aubert

Samples in Study: P

Sample Types in Study: Plant

Soil Described in Field: N/A

Geology Observed in the Field: N/A

Geology Name from Map: N/A

Lithology from Map: Marl, sand, sandstone, clay, limestone

Age from Map: Lower Cretaceous



A1.2.116. P27

Easting: 621678

Northing: 4947939

Zone: 31T

Elevation: N/A

Description of Site Location: Freyssenet.

Date Collected: N/A

Collected By: Maxime Aubert

Samples in Study: P

Sample Types in Study: Plant

Soil Described in Field: N/A

Geology Observed in the Field: N/A

Geology Name from Map: N/A

Lithology from Map: Basanite, hawaiite, tephra

Age from Map: Oligocene, Miocene



A1.2.117. P28

Easting: 648226

Northing: 4926782

Zone: 31T

Elevation: N/A

Description of Site Location: Near Montjoyen.

Date Collected: N/A

Collected By: Maxime Aubert

Samples in Study: P

Sample Types in Study: Plant

Soil Described in Field: N/A

Geology Observed in the Field: N/A

Geology Name from Map: N/A

Lithology from Map: Marl, sandstone, conglomerate, limestone

Age from Map: Oligocene



A1.2.118. P29

Easting: 647406

Northing: 4918675

Zone: 31T

Elevation: N/A

Description of Site Location: N/A

Date Collected: N/A

Collected By: Maxime Aubert

Samples in Study: P

Sample Types in Study: Plant

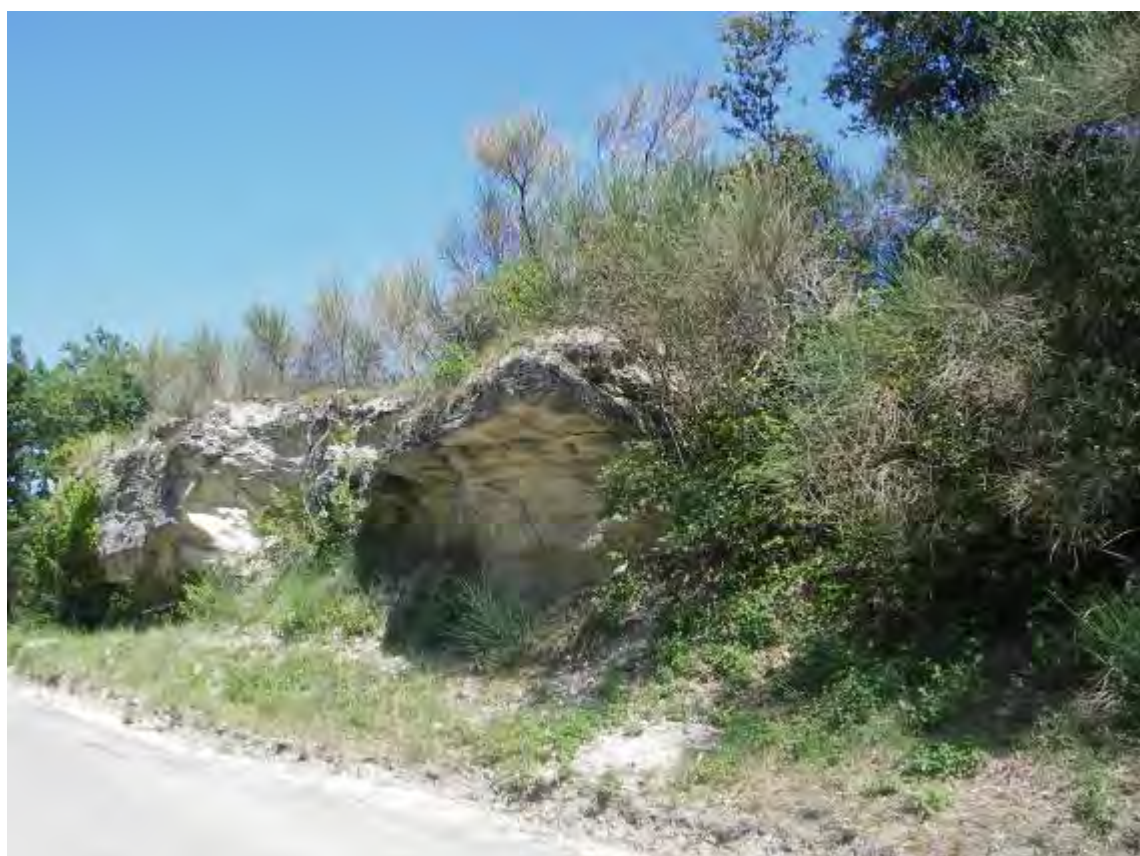
Soil Described in Field: N/A

Geology Observed in the Field: N/A

Geology Name from Map: N/A

Lithology from Map: Marl, sandstone, conglomerate, limestone

Age from Map: Miocene



A1.2.119. P30

Easting: 643842

Northing: 4899117

Zone: 31T

Elevation: N/A

Description of Site Location: North of Uchany.

Date Collected: N/A

Collected By: Maxime Aubert

Samples in Study: P

Sample Types in Study: Plant

Soil Described in Field: N/A

Geology Observed in the Field: N/A

Geology Name from Map: N/A

Lithology from Map: Marl, sandstone, chalk, limestone

Age from Map: Upper Cretaceous



A1.2.120. P31

Easting: 653617

Northing: 4899215

Zone: 31T

Elevation: N/A

Description of Site Location: River at Cairanne.

Date Collected: N/A

Collected By: Maxime Aubert

Samples in Study: P

Sample Types in Study: Plant

Soil Described in Field: N/A

Geology Observed in the Field: N/A

Geology Name from Map: N/A

Lithology from Map: Marl, conglomerate, sandstone, limestone

Age from Map: Miocene



A1.2.121. P32

Easting: 657405

Northing: 4892315

Zone: 31T

Elevation: N/A

Description of Site Location: River near Violes.

Date Collected: N/A

Collected By: Maxime Aubert

Samples in Study: P1, P2

Sample Types in Study: Plant

Soil Described in Field: N/A

Geology Observed in the Field: N/A

Geology Name from Map: N/A

Lithology from Map: Sand, clay, gravel, pebble

Age from Map: Holocene



A1.2.122. P33

Easting: 672108

Northing: 4904389

Zone: 31T

Elevation: N/A

Description of Site Location: Merindol-les-oliviers.

Date Collected: N/A

Collected By: Maxime Aubert

Samples in Study: P

Sample Types in Study: Plant

Soil Described in Field: N/A

Geology Observed in the Field: N/A

Geology Name from Map: N/A

Lithology from Map: Marl, conglomerate, sandstone, limestone

Age from Map: Miocene



A1.2.123. P34

Easting: 681983

Northing: 4906777

Zone: 31T

Elevation: N/A

Description of Site Location: Near Buis-les-Bayonniers.

Date Collected: N/A

Collected By: Maxime Aubert

Samples in Study: P

Sample Types in Study: Plant

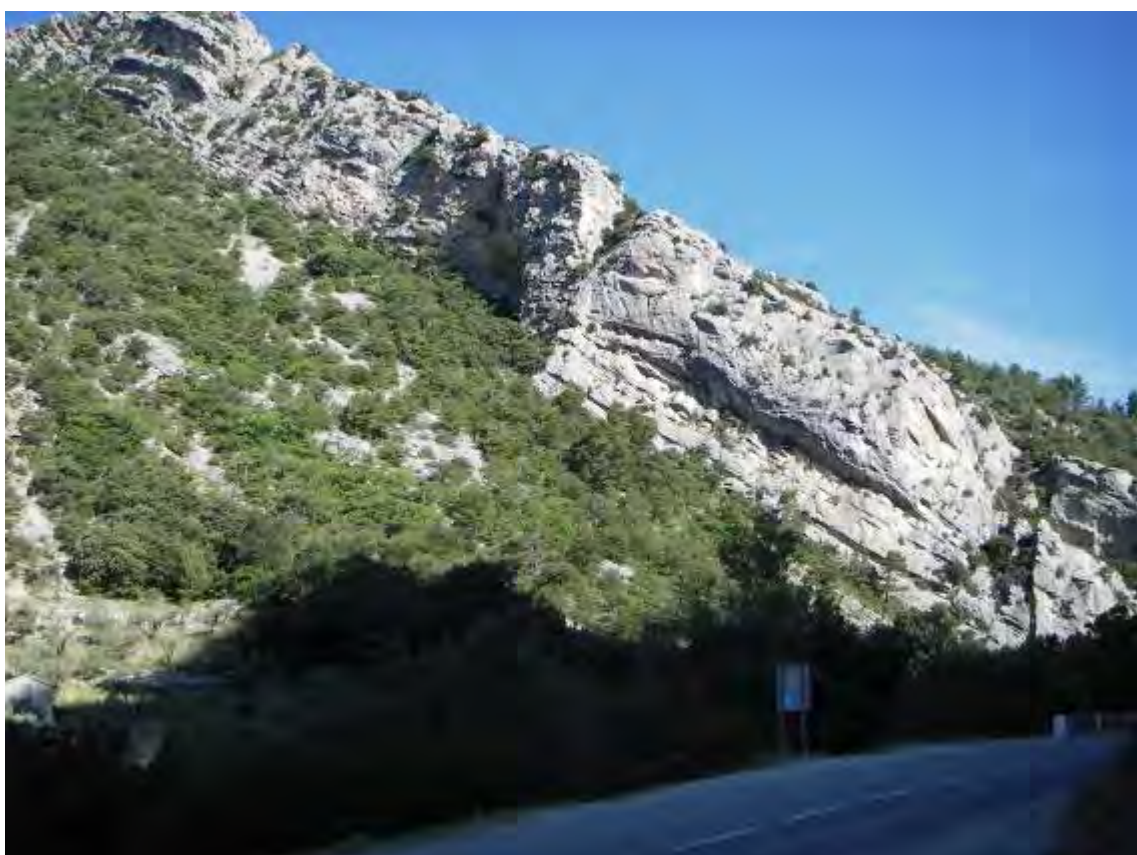
Soil Described in Field: N/A

Geology Observed in the Field: N/A

Geology Name from Map: N/A

Lithology from Map: Marl, sandstone, shale, limestone

Age from Map: Lower Cretaceous



A1.2.124. P35

Easting: 681983

Northing: 4906777

Zone: 31T

Elevation: N/A

Description of Site Location: River, near P34.

Date Collected: N/A

Collected By: Maxime Aubert

Samples in Study: P

Sample Types in Study: Plant

Soil Described in Field: N/A

Geology Observed in the Field: N/A

Geology Name from Map: N/A

Lithology from Map: Marl, sandstone, shale, limestone

Age from Map: Lower Cretaceous



A1.2.125. P36

Easting: 687076

Northing: 4920070

Zone: 31T

Elevation: N/A

Description of Site Location: River near Reimuzat Eyques.

Date Collected: N/A

Collected By: Maxime Aubert

Samples in Study: P

Sample Types in Study: Plant

Soil Described in Field: N/A

Geology Observed in the Field: N/A

Geology Name from Map: N/A

Lithology from Map: Marl, black shale, limestone

Age from Map: Upper Jurassic



A1.2.126. P37

Easting: 706382

Northing: 4921412

Zone: 31T

Elevation: N/A

Description of Site Location: N/A

Date Collected: N/A

Collected By: Maxime Aubert

Samples in Study: P

Sample Types in Study: Plant

Soil Described in Field: N/A

Geology Observed in the Field: N/A

Geology Name from Map: N/A

Lithology from Map: Marl, sandstone, shale, limestone

Age from Map: Lower Cretaceous



A1.2.127. P38

Easting: 720216

Northing: 4967508

Zone: 31T

Elevation: N/A

Description of Site Location: River near Beancharted.

Date Collected: N/A

Collected By: Maxime Aubert

Samples in Study: P

Sample Types in Study: Plant

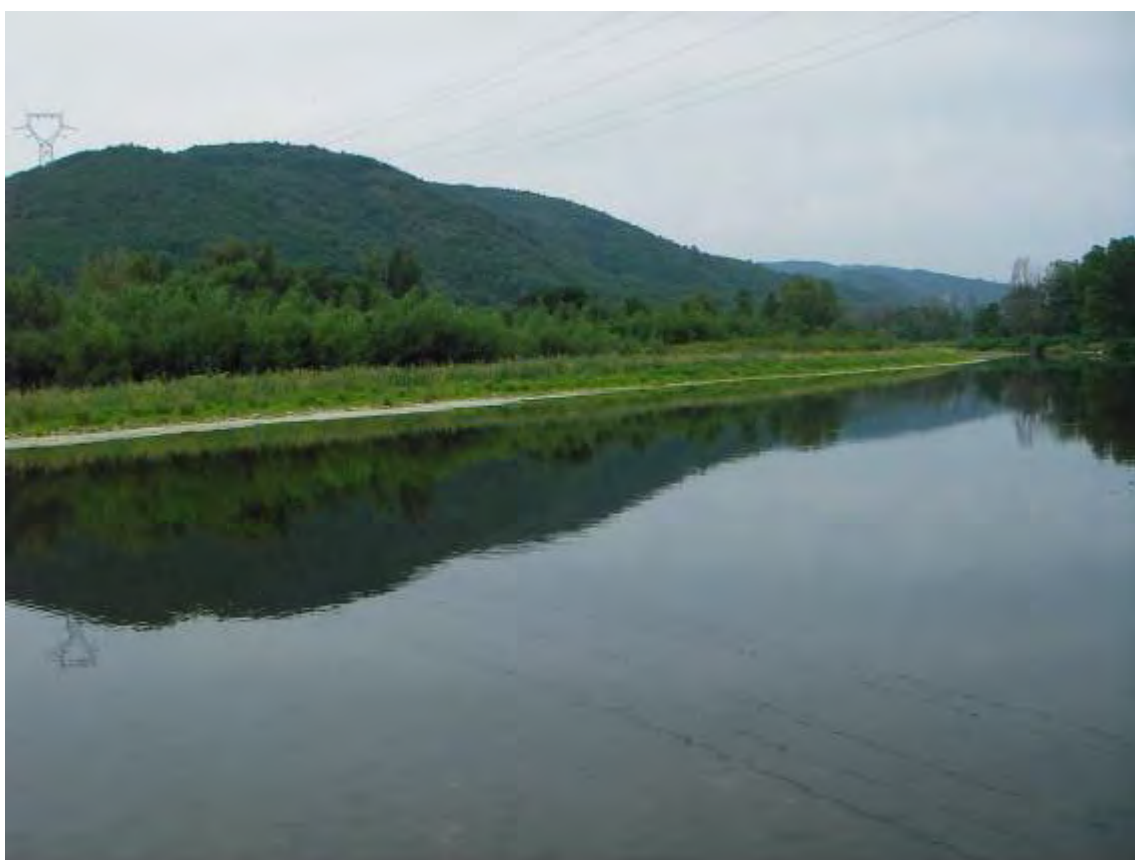
Soil Described in Field: N/A

Geology Observed in the Field: N/A

Geology Name from Map: N/A

Lithology from Map: Marl, black shale, limestone

Age from Map: Upper Jurassic



A1.2.128. P39

Easting: 641335

Northing: 4965374

Zone: 31T

Elevation: N/A

Description of Site Location: N/A

Date Collected: N/A

Collected By: Maxime Aubert

Samples in Study: P

Sample Types in Study: Plant

Soil Described in Field: N/A

Geology Observed in the Field: N/A

Geology Name from Map: N/A

Lithology from Map: Micaschist, paragneiss

Age from Map: Brioverien, Cambrian, Ordovician



A1.2.129. P40

Easting: 637294

Northing: 4957464

Zone: 31T

Elevation: N/A

Description of Site Location: River.

Date Collected: N/A

Collected By: Maxime Aubert

Samples in Study: P

Sample Types in Study: Plant

Soil Described in Field: N/A

Geology Observed in the Field: N/A

Geology Name from Map: N/A

Lithology from Map: Marl, limestone, clay

Age from Map: Upper Jurassic



A1.2.130. P42

Easting: 637838

Northing: 4955061

Zone: 31T

Elevation: N/A

Description of Site Location: Le Payre.

Date Collected: N/A

Collected By: Maxime Aubert

Samples in Study: P

Sample Types in Study: Plant

Soil Described in Field: N/A

Geology Observed in the Field: N/A

Geology Name from Map: N/A

Lithology from Map: Sand, clay, gravel, pebble

Age from Map: Holocene



A1.2.131. P43

Easting: 625288

Northing: 4906215

Zone: 31T

Elevation: N/A

Description of Site Location: Ardito river downstream.

Date Collected: N/A

Collected By: Maxime Aubert

Samples in Study: P

Sample Types in Study: Plant

Soil Described in Field: N/A

Geology Observed in the Field: N/A

Geology Name from Map: N/A

Lithology from Map: Sand, clay, gravel, pebble

Age from Map: Holocene



A1.2.132. P44

Easting: 616838

Northing: 4904608

Zone: 31T

Elevation: N/A

Description of Site Location: N/A

Date Collected: N/A

Collected By: Maxime Aubert

Samples in Study: P

Sample Types in Study: Plant

Soil Described in Field: N/A

Geology Observed in the Field: N/A

Geology Name from Map: N/A

Lithology from Map: Limestone, marl, conglomerate, sandstone

Age from Map: Middle-Upper Eocene



A1.2.133. P45

Easting: 653625

Northing: 4934020

Zone: 31T

Elevation: N/A

Description of Site Location: River.

Date Collected: N/A

Collected By: Maxime Aubert

Samples in Study: P

Sample Types in Study: Plant

Soil Described in Field: N/A

Geology Observed in the Field: N/A

Geology Name from Map: N/A

Lithology from Map: Marl, sand, sandstone, clay, limestone

Age from Map: Lower Cretaceous



A1.2.134. P46

Easting: 654816

Northing: 4939806

Zone: 31T

Elevation: N/A

Description of Site Location: River.

Date Collected: N/A

Collected By: Maxime Aubert

Samples in Study: P

Sample Types in Study: Plant

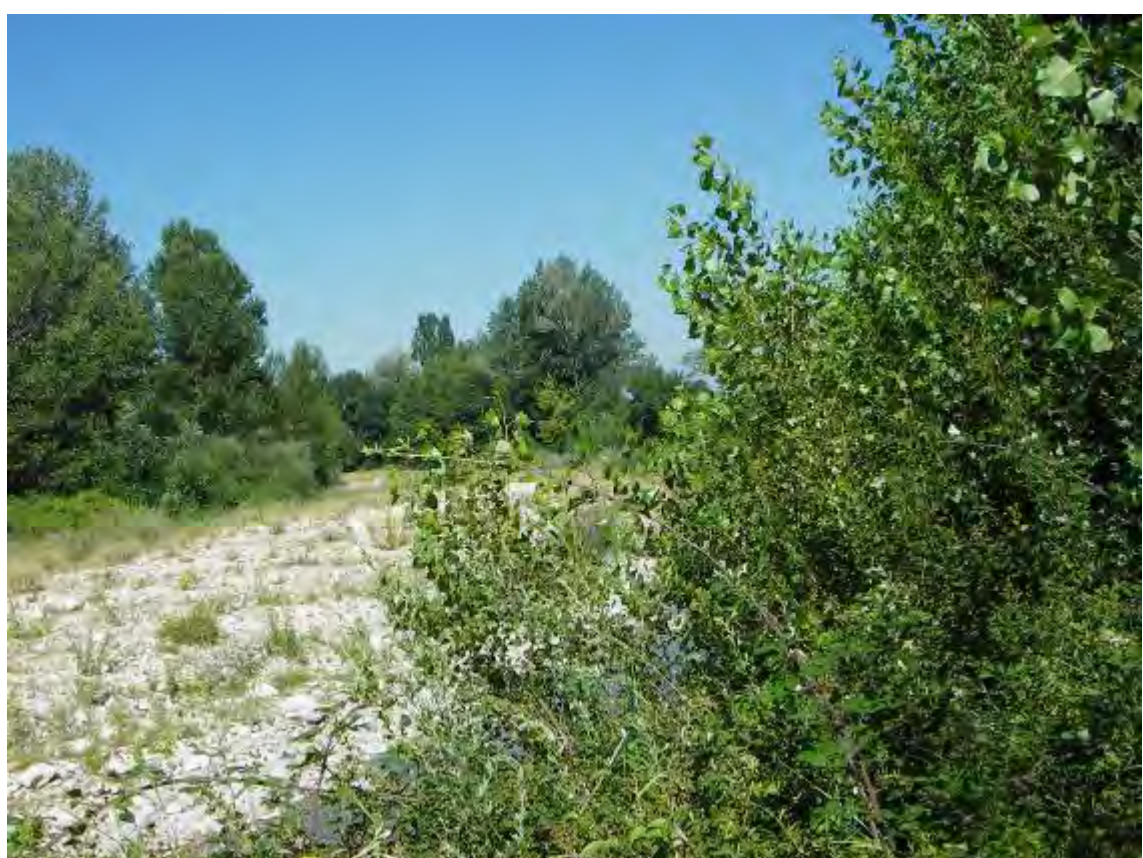
Soil Described in Field: N/A

Geology Observed in the Field: N/A

Geology Name from Map: N/A

Lithology from Map: Sand, clay, gravel, pebble

Age from Map: Holocene



A1.2.135. P47

Easting: 662743

Northing: 4953227

Zone: 31T

Elevation: N/A

Description of Site Location: Drone river near Crest.

Date Collected: N/A

Collected By: Maxime Aubert

Samples in Study: P

Sample Types in Study: Plant

Soil Described in Field: N/A

Geology Observed in the Field: N/A

Geology Name from Map: N/A

Lithology from Map: Sand, clay, gravel, pebble

Age from Map: Holocene



A1.2.136. P48

Easting: 689814

Northing: 4954965

Zone: 31T

Elevation: N/A

Description of Site Location: N/A

Date Collected: N/A

Collected By: Maxime Aubert

Samples in Study: P

Sample Types in Study: Plant

Soil Described in Field: N/A

Geology Observed in the Field: N/A

Geology Name from Map: N/A

Lithology from Map: Sand, clay, gravel, pebble

Age from Map: Holocene



A1.2.137. P49

Easting: 710762

Northing: 4971827

Zone: 31T

Elevation: N/A

Description of Site Location: N/A

Date Collected: N/A

Collected By: Maxime Aubert

Samples in Study: P

Sample Types in Study: Plant

Soil Described in Field: N/A

Geology Observed in the Field: N/A

Geology Name from Map: N/A

Lithology from Map: Marl, black shale, limestone

Age from Map: Upper Jurassic



A1.2.138. P50

Easting: 722254

Northing: 4969472

Zone: 31T

Elevation: N/A

Description of Site Location: N/A

Date Collected: N/A

Collected By: Maxime Aubert

Samples in Study: P

Sample Types in Study: Plant

Soil Described in Field: N/A

Geology Observed in the Field: N/A

Geology Name from Map: N/A

Lithology from Map: Marl, black shale, limestone

Age from Map: Upper Jurassic



A1.2.139. P51

Easting: 728364

Northing: 4960019

Zone: 31T

Elevation: N/A

Description of Site Location: Not certain that rock is *in situ*.

Date Collected: N/A

Collected By: Maxime Aubert

Samples in Study: P

Sample Types in Study: Plant

Soil Described in Field: N/A

Geology Observed in the Field: N/A

Geology Name from Map: N/A

Lithology from Map: Marl, sandstone, conglomerate, limestone

Age from Map: Upper Cretaceous



A1.2.140. P52

Easting: 730957

Northing: 4969576

Zone: 31T

Elevation: N/A

Description of Site Location: N/A

Date Collected: N/A

Collected By: Maxime Aubert

Samples in Study: P

Sample Types in Study: Plant

Soil Described in Field: N/A

Geology Observed in the Field: N/A

Geology Name from Map: N/A

Lithology from Map: Limestone, calcschist, marl

Age from Map: Lower Jurassic



A1.2.141. P53

Easting: 734845

Northing: 4980417

Zone: 31T

Elevation: N/A

Description of Site Location: N/A

Date Collected: N/A

Collected By: Maxime Aubert

Samples in Study: P

Sample Types in Study: Plant

Soil Described in Field: N/A

Geology Observed in the Field: N/A

Geology Name from Map: N/A

Lithology from Map: Limestone, calcschist, marl

Age from Map: Lower Jurassic



A1.2.142. P54

Easting: 726367

Northing: 4982172

Zone: 31T

Elevation: N/A

Description of Site Location: N/A

Date Collected: N/A

Collected By: Maxime Aubert

Samples in Study: P

Sample Types in Study: Plant

Soil Described in Field: N/A

Geology Observed in the Field: N/A

Geology Name from Map: N/A

Lithology from Map: Amphibolite, micaschist, leptynite

Age from Map: Marl, limestone, clay



A1.2.143. P55

Easting: 634821

Northing: 4954581

Zone: 31T

Elevation: N/A

Description of Site Location: Payre Site.

Date Collected: N/A

Collected By: Maxime Aubert

Samples in Study: P

Sample Types in Study: Plant

Soil Described in Field: N/A

Geology Observed in the Field: N/A

Geology Name from Map: N/A

Lithology from Map: Devonian

Age from Map: Upper Jurassic



A1.2.144. P56

Easting: 637537

Northing: 4954548

Zone: 31T

Elevation: N/A

Description of Site Location: Payre River.

Date Collected: N/A

Collected By: Maxime Aubert

Samples in Study: P

Sample Types in Study: Plant

Soil Described in Field: N/A

Geology Observed in the Field: N/A

Geology Name from Map: N/A

Lithology from Map: Devonian

Age from Map: Upper Jurassic



A1.2.145. P57

Easting: 637797

Northing: 4954224

Zone: 31T

Elevation: N/A

Description of Site Location: N/A

Date Collected: N/A

Collected By: Maxime Aubert

Samples in Study: P

Sample Types in Study: Plant

Soil Described in Field: N/A

Geology Observed in the Field: N/A

Geology Name from Map: N/A

Lithology from Map: Sand, clay, gravel, pebble

Age from Map: Holocene



A1.2.146. P58

Easting: 638372

Northing: 4954718

Zone: 31T

Elevation: N/A

Description of Site Location: N/A

Date Collected: N/A

Collected By: Maxime Aubert

Samples in Study: P

Sample Types in Study: Plant

Soil Described in Field: N/A

Geology Observed in the Field: N/A

Geology Name from Map: N/A

Lithology from Map: Sand, clay, gravel, pebble

Age from Map: Holocene



A1.2.147. P59

Easting: 639063

Northing: 4954711

Zone: 31T

Elevation: N/A

Description of Site Location: N/A

Date Collected: N/A

Collected By: Maxime Aubert

Samples in Study: P

Sample Types in Study: Plant

Soil Described in Field: N/A

Geology Observed in the Field: N/A

Geology Name from Map: N/A

Lithology from Map: Clay, conglomerate, sandstone, marl

Age from Map: Eocene, Oligocene



A1.2.148. P60

Easting: 639524

Northing: 4953538

Zone: 31T

Elevation: N/A

Description of Site Location: Rhone Banks.

Date Collected: N/A

Collected By: Maxime Aubert

Samples in Study: P

Sample Types in Study: Plant

Soil Described in Field: N/A

Geology Observed in the Field: N/A

Geology Name from Map: N/A

Lithology from Map: Sand, clay, gravel, pebble

Age from Map: Holocene



A1.2.149. P61

Easting: 639548

Northing: 4953539

Zone: 31T

Elevation: N/A

Description of Site Location: 25 m to the east of P60 and 15 m up the slope.

Date Collected: N/A

Collected By: Maxime Aubert

Samples in Study: P

Sample Types in Study: Plant

Soil Described in Field: N/A

Geology Observed in the Field: N/A

Geology Name from Map: N/A

Lithology from Map: Sand, clay, gravel, pebble

Age from Map: Holocene



A1.2.150. P62

Easting: 638754

Northing: 4954550

Zone: 31T

Elevation: N/A

Description of Site Location: N/A

Date Collected: N/A

Collected By: Maxime Aubert

Samples in Study: P

Sample Types in Study: Plant

Soil Described in Field: N/A

Geology Observed in the Field: N/A

Geology Name from Map: N/A

Lithology from Map: Sand, clay, gravel, pebble

Age from Map: Holocene



Appendix Two: Fauna

A2.1. Israeli Archaeological Material

A2.1.1. Skhul



Figure A2.1 Sample 851, Bovid, Unknown Stratigraphic Provenance, Skhul, Israel



Figure A2.2 Sample 852, Bovid, Unknown Stratigraphic Provenance, Skhul, Israel



Figure A2.3 Sample 853, Bovid, Unknown Stratigraphic Provenance, Skhul, Israel



Figure A2.4 Sample 1057A, Bovid, Unit B, Skhul, Israel



Figure A2.5 Sample 1057B, Bovid, Unit B, Skhul, Israel



Figure A2.6 Sample 1057C, Bovid, Unit B, Skhul, Israel

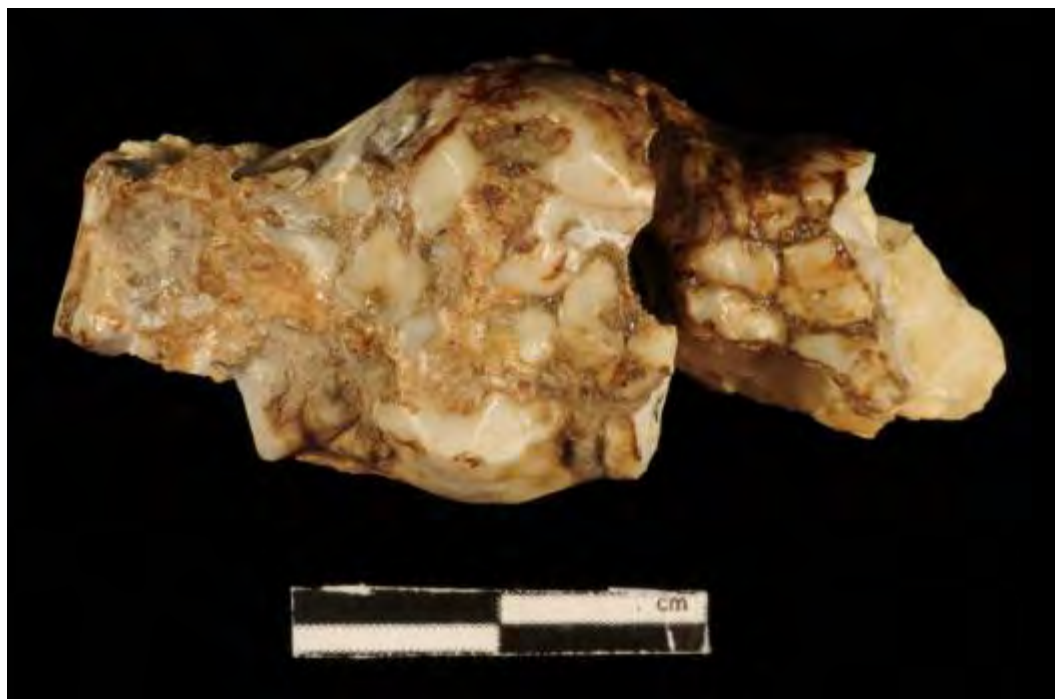


Figure A2.7 Sample 1058A, Wild Boar, Unit B, Skhul, Israel



Figure A2.8 Sample 1058B, Wild Boar, Unit B, Skhul, Israel



Figure A2.9 Sample 1058C, Wild Boar, Unit B, Skhul, Israel

A2.1.2. Tabun



Figure A2.10 Sample 554, *Bos*, Layer D, Tabun, Israel



Figure A2.11 Sample 556, *Bos*, Layer D, Tabun, Israel



Figure A2.12 Sample 557, *Bos*, Layer Ea, Tabun, Israel



Figure A2.13 Sample 557 (2), *Bos*, Layer Ea, Tabun, Israel



Figure A2.14 Sample 558, *Bos*, Layer Ea, Tabun, Israel



Figure A2.15 Sample 561, *Bos*, Layer Eb, Tabun, Israel



Figure A2.16 Sample 563, *Bos*, Layer Eb, Tabun, Israel



Figure A2.17 Sample 564, *Bos*, Layer Ec, Tabun, Israel



Figure A2.18 Sample 565, *Bos*, Layer Ec, Tabun, Israel



Figure A2.19 Sample 567, *Bos*, Layer Ed, Tabun, Israel



Figure A2.20 Sample 568, Rhinoceros, Layer Ed, Tabun, Israel

A2.1.3. Amud



Figure A2.21 Sample 1024, *Dama mesopotamica*, Layer B1, Amud, Israel



Figure A2.22 Sample 1025, *Dama mesopotamica*, Layer B1, Amud, Israel



Figure A2.23 Sample 1026, *Dama mesopotamica*, Layer B1, Amud, Israel

A2.1.4. Qafzeh



Figure A2.24 Sample 371, Bovid, Layer XIX, Qafzeh, Israel



Figure A2.25 Sample 372, Bovid, Layer XVII, Qafzeh, Israel



Figure A2.26 Sample 373, Unidentified Species, Layer XV, Qafzeh, Israel

A2.1.5. Holon



Figure A2.27 Sample 1557, *Bos*, Layer C, Holon, Israel

A2.2. French Archaeological Material

A2.2.1. La Chapelle-aux-Saints



Figure A2.28 Sample 592, Bovid, Bouffia Bonneval: Straum 1, La Chapelle-aux-Saints, France



Figure A2.29 Sample 593, Bovid, Bouffia Bonneval: Straum 1, La Chapelle-aux-Saints, France



Figure A2.30 Sample 595, Bovid, Bouffia Bonneval: Straum 1, La Chapelle-aux-Saints, France



Figure A2.31 Sample M001, Reindeer, Bouffia 118: Layer 2, La Chapelle-aux-Saints, France



Figure A2.32 Sample M002, Reindeer, Bouffia 118: Layer 2, La Chapelle-aux-Saints, France



Figure A2.33 Sample M003, Reindeer, Bouffia 118: Layer 2, La Chapelle-aux-Saints, France



Figure A2.34 Sample M004, Unknown Species, Bouffia 118: Unknown Layer, La Chapelle-aux-Saints, France



Figure A2.35 Sample M005, Bovid, Bouffia 118: Layer 1, La Chapelle-aux-Saints, France



Figure A2.36 Sample M006, Bovid, Bouffia 118: Layer 1, La Chapelle-aux-Saints, France



Figure A2.37 Sample M007, Bovid, Bouffia 118: Layer 1, La Chapelle-aux-Saints, France



Figure A2.38 Sample M008, Bovid, Bouffia 118: Layer 1, La Chapelle-aux-Saints, France



Figure A2.39 Sample M009, Bovid, Bouffia 118: Layer 1, La Chapelle-aux-Saints, France



Figure A2.40 Sample M010, Bovid, Bouffia 118: Layer 1, La Chapelle-aux-Saints, France

A2.2.2. Les Fieux



Figure A2.41 Sample M011, Horse, Layer G7, Les Fieux, France



Figure A2.42 Sample M012, Horse, Layer G7, Les Fieux, France



Figure A2.43 Sample M013, Wild Boar, Layer G7, Les Fieux, France



Figure A2.44 Sample M014, Fox, Layer G7, Les Fieux, France



Figure A2.45 Sample M015, Hyena, Layer G7, Les Fieux, France



Figure A2.46 Sample M016, Bison, Layer G7, Les Fieux, France



Figure A2.47 Sample M017, Bison, Layer G7, Les Fieux, France



Figure A2.48 Sample M018, Reindeer, Layer G7, Les Fieux, France



Figure A2.49 Sample M019, Reindeer, Layer G7, Les Fieux, France

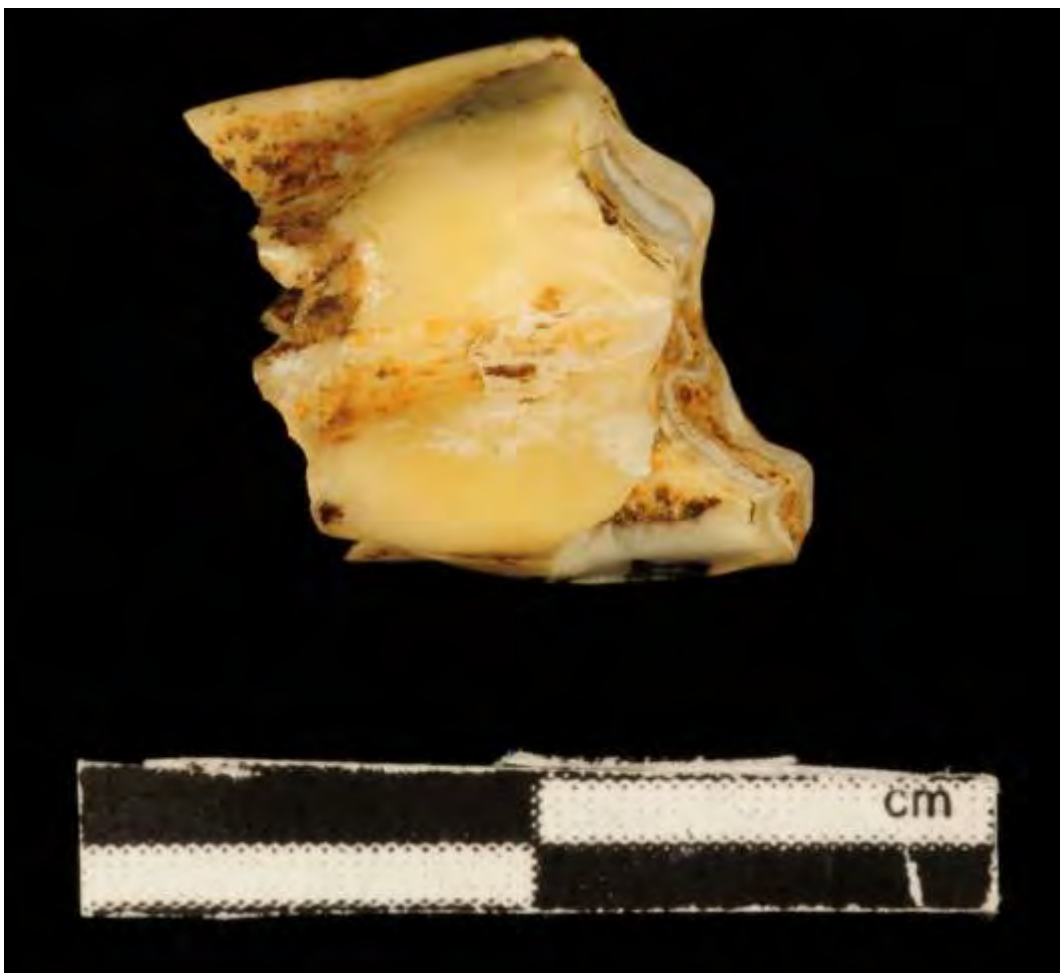


Figure A2.50 Sample M020, Chamois, Layer G7, Les Fieux, France



Figure A2.51 Sample M021, Mountain Goat/Chamois, Layer G7, Les Fieux, France

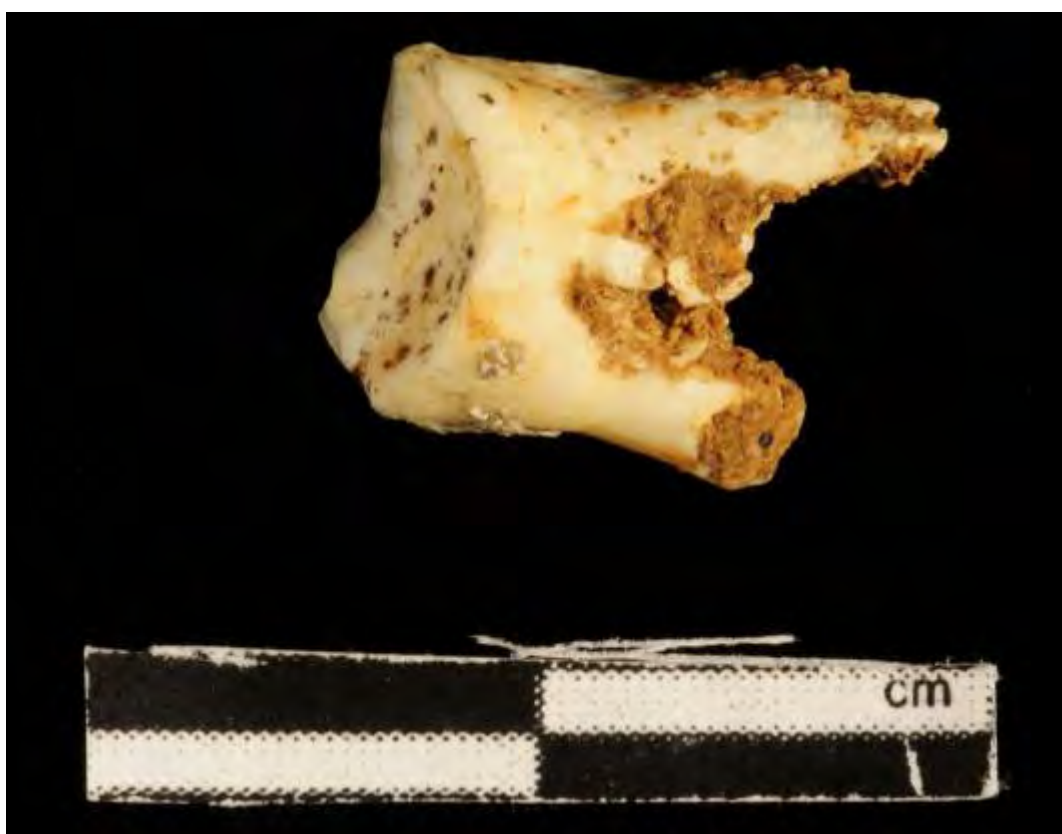


Figure A2.52 Sample M022, Mountain Goat/Chamois, Layer G7, Les Fieux, France

A2.2.3. Le Moustier



Figure A2.53 Sample 845, Bovid, Layer G1, Le Moustier, France



Figure A2.54 Sample 846, Bovid, Layer G2, Le Moustier, France



Figure A2.55 Sample 847, Bovid, Layer G3, Le Moustier, France



Figure A2.56 Sample 848, Bovid, Layer G4, Le Moustier, France



Figure A2.57 Sample 849, Bovid, Layer G5, Le Moustier, France



Figure A2.58 Sample 850, Bovid, Layer G6, Le Moustier, France

A2.2.4. Pech de l'Azé II



Figure A2.59 Sample 614, Bovid, Layer 9, Pech de l'Azé II, France



Figure A2.60 Sample 615, Hippopotamus, Layer 9, Pech de l'Azé II, France



Figure A2.61 Sample 617, Horse, Layer 8, Pech de l'Azé II, France



Figure A2.62 Sample 618, Deer, Layer 8, Pech de l'Azé II, France



Figure A2.63 Sample 619, Horse, Layer 8, Pech de l'Azé II, France



Figure A2.64 Sample 620, Bovid, Layer 7, Pech de l'Azé II, France



Figure A2.65 Sample 622, Hippopotamus, Layer 7, Pech de l'Azé II, France



Figure A2.66 Sample 624, Deer, Layer 6, Pech de l'Azé II, France



Figure A2.67 Sample 625, Horse, Layer 6, Pech de l'Azé II, France

A2.2.5. Bois Roche



Figure A2.68 Sample 2417, Bovid, Layer 1C, Bois Roche, France



Figure A2.69 Sample 2418, Bovid, Layer 1C, Bois Roche, France



Figure A2.70 Sample 2419, Bovid, Layer 1C, Bois Roche, France



Figure A2.71 Sample 2420, Bovid, Layer 2, Bois Roche, France



Figure A2.72 Sample 2421, Bovid, Layer 2, Bois Roche, France



Figure A2.73 Sample 2422, Bovid, Layer 1C, Bois Roche, France



Figure A2.74 Sample 2423, Bovid, Layer 2, Bois Roche, France



Figure A2.75 Sample 2424, Bovid, Layer 2, Bois Roche, France



Figure A2.76 Sample 2425A, Bovid, Layer 2, Bois Roche, France



Figure A2.77 Sample 2425B, Bovid, Layer 2, Bois Roche, France



Figure A2.78 Sample 2425C, Bovid, Layer 2, Bois Roche, France

A2.2.6. Rescoundudou



Figure A2.79 Sample M033, Bovid, Layer C1, Rescoundudou, France



Figure A2.80 Sample M034, Bovid, Layer C1, Rescoundudou, France



Figure A2.81 Sample M035, Horse, Layer C1, Rescoundudou, France



Figure A2.82 Sample M036, Horse, Layer C1, Rescoundudou, France



Figure A2.83 Sample M037, Horse, Layer C1, Rescoundudou, France



Figure A2.84 Sample M038, Bovid, Layer C1, Rescoundudou, France



Figure A2.85 Sample M039, Bovid, Layer C1, Rescoundudou, France



Figure A2.86 Sample M040, Bovid, Layer C1, Rescoundudou, France



Figure A2.87 Sample M041, Bovid, Layer C1, Rescoundudou, France

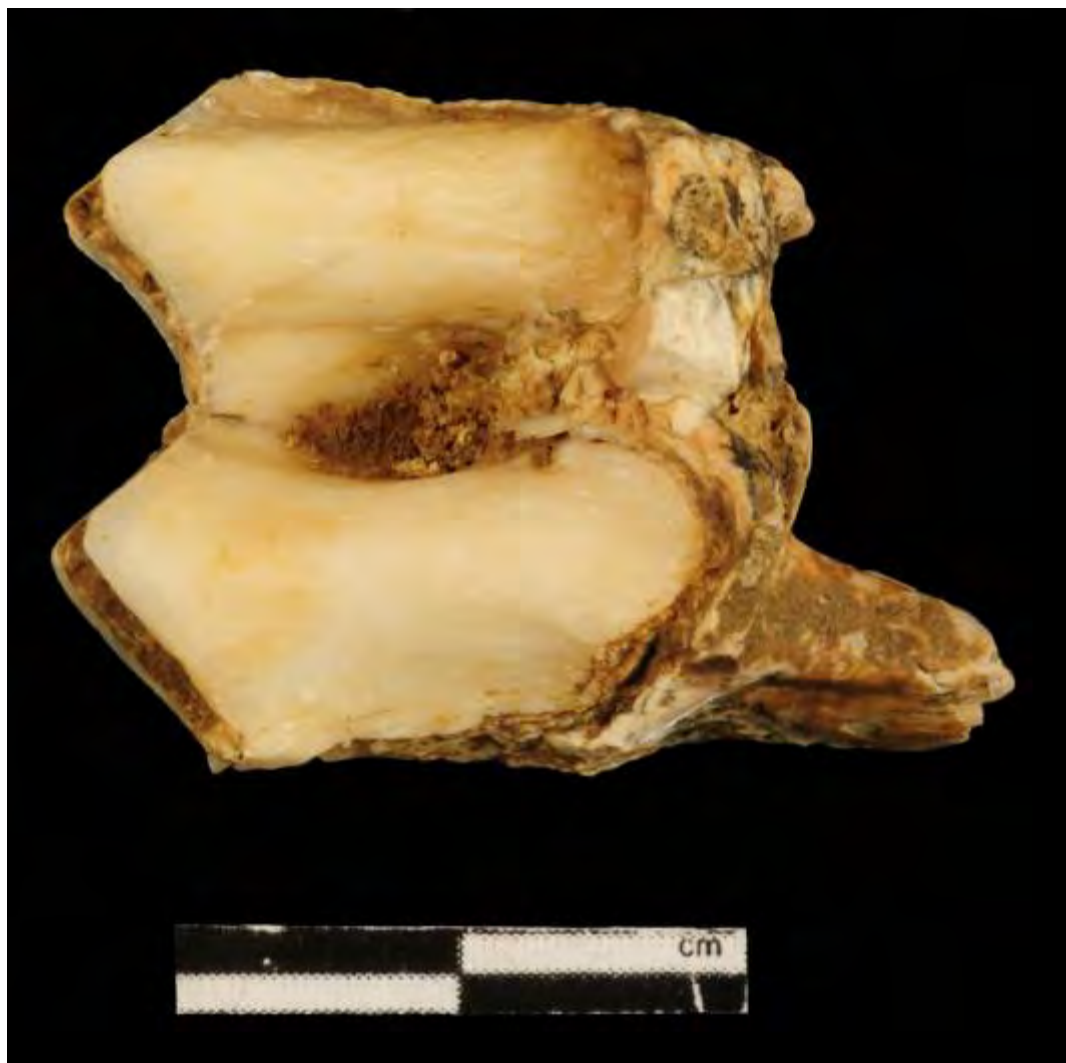


Figure A2.88 Sample M042, Deer, Layer C1, Rescoundudou, France



Figure A2.89 Sample M043, Deer, Layer C1, Rescoundudou, France



Figure A2.90 Sample M044, Deer, Layer C1, Rescoundudou, France



Figure A2.91 Sample M045, Deer, Layer C1, Rescoundudou, France

Appendix Three: Detailed Results

A3.1. LA-ICPMS Concentration Results

A3.1.1. Israeli Archaeological Samples

A3.1.1.1. Skhul

Element concentrations were collected for 29 spots within the enamel and dentine of sample 851 from the archaeological site of Skhul, shown in Figure A2.1. The results are summarised in Table 5.6 and shown in detail in Table A3.1 and Table A3.2. Strontium concentration for enamel ranges from 283 to 415 ppm and does not vary in a systematic fashion. Uranium concentration for enamel varies from 0 to 6 ppm. Strontium concentration for dentine ranges from 362 to 445 ppm and uranium concentration ranges from a minimum of 22 ppm to a maximum of 38 ppm.

Spot	Material	Mg (ppm)	Sr (ppm)	Ba (ppm)	U (ppm)	Mg/Ca	Sr/Ca	Ba/Ca
1	Enamel	1962	345	82	2	0.008547	0.000417	0.000063
2	Enamel	1771	392	86	1	0.007715	0.000473	0.000066
3	Enamel	2053	346	70	1	0.008939	0.000418	0.000054
4	Enamel	1732	390	87	0	0.007543	0.000471	0.000067
5	Enamel	1857	363	70	0	0.008087	0.000439	0.000054
6	Enamel	1813	373	74	0	0.007898	0.000451	0.000057
7	Enamel	1676	387	82	1	0.007298	0.000467	0.000063
8	Enamel	1621	389	86	1	0.007061	0.000470	0.000066
9	Enamel	1789	336	72	1	0.007793	0.000406	0.000055
10	Enamel	1627	360	82	1	0.007087	0.000435	0.000063
11	Enamel	1700	324	67	1	0.007404	0.000392	0.000051
12	Enamel	1907	297	57	0	0.008304	0.000359	0.000044
13	Enamel	1601	342	77	2	0.006974	0.000413	0.000060
14	Enamel	1672	320	74	1	0.007283	0.000387	0.000057
15	Enamel	1851	323	60	1	0.008062	0.000390	0.000046
16	Enamel	1995	343	63	1	0.008688	0.000415	0.000049
17	Enamel	1772	360	71	1	0.007717	0.000435	0.000054
18	Enamel	2145	316	81	2	0.009342	0.000381	0.000062
19	Enamel	2220	371	103	4	0.009669	0.000449	0.000079
20	Enamel	2096	388	116	6	0.009128	0.000469	0.000089
21	Enamel	7108	349	93	4	0.030958	0.000422	0.000072
22	Enamel	1813	415	92	4	0.007896	0.000502	0.000071
23	Enamel	1924	373	97	6	0.008379	0.000451	0.000075
24	Enamel	2048	378	101	5	0.008918	0.000457	0.000078
25	Enamel	2040	305	67	2	0.008885	0.000368	0.000052
26	Enamel	2673	292	55	1	0.011640	0.000353	0.000043
27	Enamel	2072	283	51	1	0.009024	0.000342	0.000039
28	Enamel	2083	298	61	1	0.009073	0.000360	0.000047
29	Enamel	1985	295	66	2	0.008643	0.000357	0.000051

Table A3.1 Elemental Concentrations and Ratios for Enamel, Sample 851, Bovid, Unknown Layer, Skhul

Spot	Material	Mg (ppm)	Sr (ppm)	Ba (ppm)	U (ppm)	Mg/Ca	Sr/Ca	Ba/Ca
1	Dentine	1579	362	178	29	0.006878	0.000437	0.000137
2	Dentine	1568	383	189	30	0.006828	0.000463	0.000146
3	Dentine	1439	373	181	30	0.006266	0.000451	0.000140
4	Dentine	1534	382	174	30	0.006681	0.000461	0.000134
5	Dentine	1435	390	186	31	0.006251	0.000471	0.000143
6	Dentine	1547	363	178	31	0.006738	0.000439	0.000137
7	Dentine	1476	381	186	30	0.006428	0.000460	0.000144
8	Dentine	1483	381	181	29	0.006457	0.000460	0.000139
9	Dentine	1622	383	193	31	0.007063	0.000463	0.000149
10	Dentine	1493	424	209	32	0.006503	0.000513	0.000161
11	Dentine	1574	415	200	32	0.006855	0.000502	0.000154
12	Dentine	1537	431	214	32	0.006693	0.000520	0.000165
13	Dentine	1538	415	211	31	0.006696	0.000501	0.000163
14	Dentine	1520	418	204	29	0.006620	0.000505	0.000157
15	Dentine	1606	426	210	30	0.006996	0.000515	0.000162
16	Dentine	1626	440	224	34	0.007080	0.000532	0.000173
17	Dentine	1607	423	200	29	0.006999	0.000511	0.000154
18	Dentine	1795	431	221	31	0.007818	0.000521	0.000170
19	Dentine	1934	436	217	30	0.008424	0.000527	0.000167
20	Dentine	2009	422	213	27	0.008751	0.000510	0.000164
21	Dentine	1714	437	224	33	0.007465	0.000528	0.000172
22	Dentine	1671	445	226	37	0.007278	0.000538	0.000174
23	Dentine	1543	422	214	33	0.006722	0.000509	0.000165
24	Dentine	1668	441	239	38	0.007264	0.000533	0.000184
25	Dentine	1720	436	218	34	0.007492	0.000527	0.000168
26	Dentine	1541	450	209	28	0.006712	0.000544	0.000161
27	Dentine	1823	431	234	37	0.007940	0.000521	0.000180
28	Dentine	1984	418	217	31	0.008639	0.000505	0.000167
29	Dentine	1776	393	183	22	0.007736	0.000474	0.000141

Table A3.2 Elemental Concentrations and Ratios for Dentine, Sample 851, Bovid, Unknown Layer, Skhul

Element concentrations for sample 852 from the archaeological site of Skhul, shown in Figure A2.2, were collected for 38 enamel and 42 dentine spots. The results are summarised in Table 5.6 and shown in detail in Table A3.3 and Table A3.4. Strontium concentration for enamel ranges from 242 to 324 ppm and uranium concentration varies from 0 to 5 ppm. Strontium concentration for dentine ranges from 187 to 324 ppm and uranium concentration ranges from 12 to 40 ppm.

Spot	Material	Mg (ppm)	Sr (ppm)	Ba (ppm)	U (ppm)	Mg/Ca	Sr/Ca	Ba/Ca
1	Enamel	1668	242	88	2	0.007265	0.000292	0.000067
2	Enamel	1684	250	85	1	0.007334	0.000302	0.000066
3	Enamel	1567	258	89	0	0.006824	0.000311	0.000069
4	Enamel	1606	274	95	1	0.006996	0.000331	0.000073
5	Enamel	1841	267	104	3	0.008019	0.000323	0.000080
6	Enamel	1919	317	122	4	0.008358	0.000383	0.000094
7	Enamel	1911	324	124	5	0.008323	0.000391	0.000096
8	Enamel	1922	314	122	5	0.008370	0.000379	0.000094
9	Enamel	1919	305	115	5	0.008359	0.000368	0.000088
10	Enamel	1831	291	91	2	0.007976	0.000352	0.000070
11	Enamel	1628	280	85	1	0.007090	0.000339	0.000065
12	Enamel	1595	278	80	1	0.006945	0.000335	0.000061
13	Enamel	1581	281	87	1	0.006884	0.000339	0.000067
14	Enamel	1766	279	88	2	0.007693	0.000338	0.000068
15	Enamel	1634	275	84	1	0.007118	0.000333	0.000065
16	Enamel	1573	277	75	1	0.006852	0.000335	0.000058
17	Enamel	1600	262	70	1	0.006970	0.000316	0.000054
18	Enamel	1485	304	93	1	0.006469	0.000367	0.000072
19	Enamel	1467	312	98	1	0.006391	0.000377	0.000075
20	Enamel	1485	311	98	0	0.006465	0.000376	0.000075
21	Enamel	1538	297	87	0	0.006699	0.000359	0.000067
22	Enamel	1484	287	84	0	0.006464	0.000347	0.000065
23	Enamel	1438	291	83	0	0.006263	0.000352	0.000064
24	Enamel	1421	286	83	0	0.006190	0.000346	0.000064
25	Enamel	1453	282	80	0	0.006328	0.000341	0.000062

Spot	Material	Mg (ppm)	Sr (ppm)	Ba (ppm)	U (ppm)	Mg/Ca	Sr/Ca	Ba/Ca
26	Enamel	1444	255	79	0	0.006287	0.000309	0.000061
27	Enamel	1420	264	78	1	0.006183	0.000320	0.000060
28	Enamel	1416	260	82	1	0.006167	0.000314	0.000063
29	Enamel	1533	262	90	2	0.006675	0.000317	0.000070
30	Enamel	1486	263	92	1	0.006471	0.000318	0.000071
31	Enamel	1491	278	101	2	0.006494	0.000336	0.000078
32	Enamel	1493	268	86	1	0.006501	0.000323	0.000067
33	Enamel	1526	256	81	1	0.006645	0.000309	0.000062
34	Enamel	1547	257	81	1	0.006739	0.000310	0.000062
35	Enamel	1648	267	99	1	0.007177	0.000323	0.000076
36	Enamel	1608	263	93	1	0.007003	0.000317	0.000072
37	Enamel	1640	249	85	0	0.007140	0.000301	0.000065
38	Enamel	1637	247	84	1	0.007129	0.000298	0.000065

Table A3.3 Elemental Concentrations and Ratios for Enamel, Sample 852, Bovid, Unknown Layer, Skhul

Spot	Material	Mg (ppm)	Sr (ppm)	Ba (ppm)	U (ppm)	Mg/Ca	Sr/Ca	Ba/Ca
1	Dentine	1052	219	82	20	0.004583	0.000264	0.000064
2	Dentine	956	227	81	20	0.004163	0.000275	0.000063
3	Dentine	1500	187	62	15	0.006534	0.000226	0.000047
4	Dentine	906	227	72	19	0.003944	0.000275	0.000055
5	Dentine	1021	223	74	18	0.004444	0.000270	0.000057
6	Dentine	1147	215	70	17	0.004996	0.000260	0.000054
7	Dentine	962	223	71	17	0.004190	0.000269	0.000055
8	Dentine	1010	222	78	17	0.004401	0.000268	0.000060
9	Dentine	1159	245	86	16	0.005048	0.000295	0.000066
10	Dentine	1100	244	83	16	0.004790	0.000294	0.000064
11	Dentine	1107	254	90	16	0.004819	0.000307	0.000069
12	Dentine	1146	240	82	16	0.004991	0.000290	0.000063
13	Dentine	1142	240	80	15	0.004974	0.000290	0.000062
14	Dentine	1117	236	74	15	0.004865	0.000285	0.000057
15	Dentine	1038	239	79	16	0.004521	0.000288	0.000061
16	Dentine	1065	258	80	16	0.004640	0.000311	0.000062
17	Dentine	1099	243	81	15	0.004786	0.000294	0.000063

Spot	Material	Mg (ppm)	Sr (ppm)	Ba (ppm)	U (ppm)	Mg/Ca	Sr/Ca	Ba/Ca
18	Dentine	1115	259	76	15	0.004857	0.000312	0.000059
19	Dentine	1244	249	88	15	0.005416	0.000301	0.000068
20	Dentine	1594	226	94	13	0.006941	0.000273	0.000072
21	Dentine	1104	239	91	14	0.004807	0.000289	0.000070
22	Dentine	2025	229	70	12	0.008819	0.000277	0.000054
23	Dentine	1111	265	89	16	0.004839	0.000320	0.000069
24	Dentine	1034	270	82	15	0.004503	0.000327	0.000063
25	Dentine	944	263	76	15	0.004113	0.000317	0.000059
26	Dentine	978	233	80	15	0.004259	0.000282	0.000062
27	Dentine	1028	229	79	13	0.004477	0.000277	0.000061
28	Dentine	893	252	79	16	0.003889	0.000305	0.000061
29	Dentine	949	251	84	16	0.004132	0.000304	0.000065
30	Dentine	932	253	80	16	0.004059	0.000306	0.000062
31	Dentine	983	261	85	16	0.004280	0.000315	0.000065
32	Dentine	1281	284	102	16	0.005897	0.000343	0.000079
33	Dentine	1221	270	106	18	0.005317	0.000327	0.000081
34	Dentine	1308	283	119	21	0.005695	0.000342	0.000092
35	Dentine	1324	280	122	23	0.005765	0.000338	0.000094
36	Dentine	1302	279	135	27	0.005670	0.000337	0.000104
37	Dentine	1473	319	149	32	0.006414	0.000385	0.000115
38	Dentine	1313	294	149	35	0.005716	0.000356	0.000115
39	Dentine	1312	298	149	37	0.005713	0.000360	0.000115
40	Dentine	1348	308	160	39	0.005873	0.000372	0.000124
41	Dentine	1423	313	163	40	0.006198	0.000379	0.000126
42	Dentine	1622	324	158	39	0.007066	0.000391	0.000121

Table A3.4 Elemental Concentrations and Ratios for Dentine, Sample 852, Bovid, Unknown Layer, Skhul

Element concentrations for sample 853 from the archaeological site of Skhul, shown in Figure A2.3, were collected for 32 enamel and 35 dentine spots. The results are summarised in Table 5.6 and shown in detail in Table A3.5 and Table A3.6. Strontium concentration for enamel ranges from 496 to 699 ppm and uranium concentration varies from 1 to 33 ppm. Strontium concentration for dentine ranges from 400 to 606 ppm and uranium concentration ranges from 15 to 34 ppm.

Spot	Material	Mg (ppm)	Sr (ppm)	Ba (ppm)	U (ppm)	Mg/Ca	Sr/Ca	Ba/Ca
1	Enamel	2055	590	78	5	0.008948	0.000713	0.000060
2	Enamel	2163	513	83	4	0.009420	0.000619	0.000064
3	Enamel	2047	496	75	5	0.008914	0.000599	0.000058
4	Enamel	1996	513	94	6	0.008694	0.000619	0.000072
5	Enamel	1946	536	106	7	0.008476	0.000648	0.000082
6	Enamel	1828	553	85	4	0.007961	0.000668	0.000065
7	Enamel	1573	588	63	2	0.006849	0.000711	0.000048
8	Enamel	1719	584	58	1	0.007485	0.000706	0.000045
9	Enamel	1653	592	55	1	0.007197	0.000715	0.000043
10	Enamel	1583	620	55	1	0.006895	0.000750	0.000042
11	Enamel	1748	561	84	4	0.007612	0.000677	0.000065
12	Enamel	1582	556	47	1	0.006891	0.000672	0.000036
13	Enamel	1550	556	43	1	0.006750	0.000672	0.000033
14	Enamel	1475	546	40	1	0.006426	0.000660	0.000031
15	Enamel	1556	566	46	1	0.006777	0.000683	0.000035
16	Enamel	1511	549	60	2	0.006579	0.000663	0.000046
17	Enamel	1439	546	69	2	0.006266	0.000659	0.000053
18	Enamel	1491	531	52	1	0.006493	0.000642	0.000040
19	Enamel	1466	547	69	2	0.006385	0.000661	0.000053
20	Enamel	1564	548	80	3	0.006813	0.000662	0.000062
21	Enamel	1472	531	63	2	0.006408	0.000641	0.000049
22	Enamel	1513	537	56	1	0.006590	0.000649	0.000043
23	Enamel	1549	517	51	1	0.006747	0.000625	0.000039
24	Enamel	1492	533	56	2	0.006497	0.000643	0.000043
25	Enamel	1516	625	61	1	0.006603	0.000755	0.000047
26	Enamel	1553	630	58	1	0.006764	0.000761	0.000045
27	Enamel	1508	683	61	1	0.006568	0.000825	0.000047

Spot	Material	Mg (ppm)	Sr (ppm)	Ba (ppm)	U (ppm)	Mg/Ca	Sr/Ca	Ba/Ca
28	Enamel	1593	699	70	1	0.006937	0.000844	0.000054
29	Enamel	1555	651	67	1	0.006774	0.000786	0.000051
30	Enamel	1577	676	63	1	0.006866	0.000816	0.000048
31	Enamel	1596	692	64	1	0.006950	0.000836	0.000050
32	Enamel	1294	589	217	33	0.005636	0.000711	0.000168

Table A3.5 Elemental Concentrations and Ratios for Enamel, Sample 853, Bovid, Unknown Layer, Skhul

Spot	Material	Mg (ppm)	Sr (ppm)	Ba (ppm)	U (ppm)	Mg/Ca	Sr/Ca	Ba/Ca
1	Dentine	2373	484	149	18	0.041140	0.000584	0.000115
2	Dentine	2114	481	157	19	0.009207	0.000581	0.000121
3	Dentine	1930	495	155	19	0.008403	0.000598	0.000120
4	Dentine	1889	509	156	19	0.008225	0.000615	0.000120
5	Dentine	2201	511	153	18	0.009584	0.000617	0.000118
6	Dentine	2105	527	130	17	0.009168	0.000637	0.000100
7	Dentine	1856	432	105	15	0.008084	0.000522	0.000081
8	Dentine	1393	481	115	17	0.006067	0.000581	0.000088
9	Dentine	1403	456	100	16	0.006110	0.000551	0.000077
10	Dentine	1258	516	113	18	0.005481	0.000624	0.000087
11	Dentine	1328	445	94	15	0.005784	0.000538	0.000073
12	Dentine	1267	532	124	21	0.005519	0.000642	0.000096
13	Dentine	1404	554	138	23	0.006116	0.000669	0.000106
14	Dentine	1477	507	152	24	0.006432	0.000612	0.000117
15	Dentine	1569	563	123	21	0.006831	0.000680	0.000095
16	Dentine	1482	606	141	22	0.006456	0.000732	0.000109
17	Dentine	1524	558	148	25	0.006637	0.000674	0.000114
18	Dentine	1478	443	113	18	0.006436	0.000535	0.000087
19	Dentine	1587	578	162	25	0.006911	0.000699	0.000125
20	Dentine	1579	572	157	24	0.006877	0.000691	0.000121
21	Dentine	1505	596	152	24	0.006553	0.000720	0.000117
22	Dentine	1332	537	160	25	0.005800	0.000649	0.000124
23	Dentine	1650	400	111	16	0.007185	0.000483	0.000086

Spot	Material	Mg (ppm)	Sr (ppm)	Ba (ppm)	U (ppm)	Mg/Ca	Sr/Ca	Ba/Ca
24	Dentine	1577	528	179	29	0.006870	0.000637	0.000138
25	Dentine	1500	556	158	27	0.006531	0.000672	0.000122
26	Dentine	1623	586	163	27	0.007067	0.000708	0.000126
27	Dentine	1687	582	176	29	0.007347	0.000703	0.000136
28	Dentine	1548	546	177	29	0.006742	0.000660	0.000136
29	Dentine	1515	515	178	30	0.006597	0.000622	0.000137
30	Dentine	1562	532	195	33	0.006802	0.000643	0.000150
31	Dentine	1644	517	197	33	0.007158	0.000625	0.000152
32	Dentine	1434	529	193	34	0.006244	0.000640	0.000149
33	Dentine	1512	549	220	33	0.006584	0.000663	0.000170
34	Dentine	1433	557	211	30	0.006239	0.000673	0.000162
35	Dentine	1467	589	243	33	0.006389	0.000711	0.000187

Table A3.6 Elemental Concentrations and Ratios for Dentine, Sample 853, Bovid, Unknown Layer, Skhul

A3.1.1.2. Tabun

Element concentrations for sample 554 from the archaeological site of Tabun, shown in Figure A2.10, were collected for 2 enamel spots. The results are summarised in Table 5.10 and shown in detail in Table A3.7. Strontium concentration for enamel ranges from 288 to 295 ppm and uranium concentration is 1 ppm.

Spot	Material	Mg (ppm)	P (ppm)	Sr (ppm)	Ba (ppm)	Th (ppm)	U (ppm)	Mg/Ca	Sr/Ca	Ba/Ca
1	Enamel	1208	249500	295	57	0	1	0.005260	0.000356	0.000044
2	Enamel	1062	211672	288	50	0	1	0.004626	0.000348	0.000039

Table A3.7 Elemental Concentrations and Ratios for Enamel, Sample 554, Bos, Layer D, Tabun

Element concentrations for sample 556 from the archaeological site of Tabun, shown in Figure A2.11, were collected for 2 enamel spots. The results are

summarised in Table 5.10 and shown in detail in Table A3.8. Strontium concentration for enamel ranges from 261 to 267 ppm and uranium concentration is 10 ppm.

Spot	Material	Mg (ppm)	P (ppm)	Sr (ppm)	Ba (ppm)	Th (ppm)	U (ppm)	Mg/Ca	Sr/Ca	Ba/Ca
1	Enamel	1131	190718	267	85	0	10	0.049251	0.003222	0.000657
2	Enamel	1555	203912	261	89	0	10	0.006770	0.000315	0.000068

Table A3.8 Elemental Concentrations and Ratios for Enamel, Sample 556, Bos, Layer D, Tabun

Element concentrations for sample 557 from the archaeological site of Tabun, shown in Figure A2.12, were collected for 2 enamel spots. The results are summarised in Table 5.10 and shown in detail in Table A3.9. Strontium concentration for enamel ranges from 168 to 170 ppm and uranium concentration is 0 ppm.

Spot	Material	Mg (ppm)	P (ppm)	Sr (ppm)	Ba (ppm)	Th (ppm)	U (ppm)	Mg/Ca	Sr/Ca	Ba/Ca
1	Enamel	1229	222207	168	46	0	0	0.005352	0.000203	0.000035
2	Enamel	1179	232699	170	48	0	0	0.005133	0.000205	0.000037

Table A3.9 Elemental Concentrations and Ratios for Enamel, Sample 557, Bos, Layer Ea, Tabun

Element concentrations for sample 557 (2) from the archaeological site of Tabun, shown in Figure A2.13, were collected for 2 enamel spots. The results are summarised in Table 5.10 and shown in detail in Table A3.10. Strontium concentration for enamel ranges from 199 to 204 ppm and uranium concentration is 0 ppm.

Spot	Material	Mg (ppm)	P (ppm)	Sr (ppm)	Ba (ppm)	Th (ppm)	U (ppm)	Mg/Ca	Sr/Ca	Ba/Ca
1	Enamel	1143	123832	204	59	0	0	0.004978	0.000246	0.000046
2	Enamel	1159	131210	199	54	0	0	0.005049	0.000240	0.000042

Table A3.10 Elemental Concentrations and Ratios for Enamel, Sample 557 (2), Bos, Layer Ea, Tabun

Element concentrations for sample 558 from the archaeological site of Tabun, shown in Figure A2.14, were collected for 2 enamel spots. The results are summarised in Table 5.10 and shown in detail in Table A3.11. Strontium concentration for enamel ranges from 119 to 121 ppm and uranium concentration is 0 ppm.

Spot	Material	Mg (ppm)	P (ppm)	Sr (ppm)	Ba (ppm)	Th (ppm)	U (ppm)	Mg/Ca	Sr/Ca	Ba/Ca
1	Enamel	1748	201404	121	37	0	0	0.007615	0.000146	0.000028
2	Enamel	1945	205954	119	36	0	0	0.008469	0.000144	0.000027

Table A3.11 Elemental Concentrations and Ratios for Enamel, Sample 558, Bos, Layer Ea, Tabun

Element concentrations for sample 561 from the archaeological site of Tabun, shown in Figure A2.15, were collected for 3 enamel and 2 dentine spots. The results are summarised in Table 5.10 and shown in detail in Table A3.12. Strontium concentration for enamel ranges from 157 to 173 ppm and uranium concentration is 0 ppm. Strontium concentration for dentine ranges from 209 to 215 ppm and uranium concentration ranges from 5 to 8 ppm.

Spot	Material	Mg (ppm)	P (ppm)	Sr (ppm)	Ba (ppm)	Th (ppm)	U (ppm)	Mg/Ca	Sr/Ca	Ba/Ca
1	Enamel	1144	208274	157	45	0	0	0.004981	0.000189	0.000035
2	Enamel	1231	208041	173	49	0	0	0.005363	0.000209	0.000037
3	Enamel	1128	210254	159	50	0	0	0.004913	0.000192	0.000038
4	Dentine	603	202138	209	147	0	8	0.002626	0.000252	0.000113
5	Dentine	539	216148	215	150	0	5	0.002347	0.000260	0.000116

Table A3.12 Elemental Concentrations and Ratios for Enamel and Dentine, Sample 561, Bos, Layer Eb, Tabun

Element concentrations for sample 563 from the archaeological site of Tabun, shown in Figure A2.16, were collected for 4 enamel and 3 dentine spots. The results are summarised in Table 5.10 and shown in detail in Table A3.13. Strontium concentration for enamel ranges from 240 to 253 ppm and uranium concentration is 0 ppm. Strontium concentration for dentine ranges from 245 to 252 ppm and uranium concentration ranges from 5 to 6 ppm.

Spot	Material	Mg (ppm)	P (ppm)	Sr (ppm)	Ba (ppm)	Th (ppm)	U (ppm)	Mg/Ca	Sr/Ca	Ba/Ca
1	Enamel	1374	202277	241	45	0	0	0.005982	0.000291	0.000035
2	Enamel	1231	186568	241	45	0	0	0.005360	0.000292	0.000035
3	Enamel	1314	184590	253	43	0	0	0.005722	0.000306	0.000033
4	Enamel	1354	194626	240	42	0	0	0.005899	0.000290	0.000032
5	Dentine	673	194123	252	110	0	5	0.002929	0.000304	0.000085
6	Dentine	730	186933	250	126	0	6	0.003178	0.000302	0.000097
7	Dentine	683	190674	245	104	0	5	0.002974	0.000296	0.000080

Table A3.13 Elemental Concentrations and Ratios for Enamel and Dentine, Sample 563, Bos, Layer Eb, Tabun

Element concentrations for sample 564 from the archaeological site of Tabun, shown in Figure A2.17, were collected for 2 dentine spots. The results are summarised in Table 5.10 and shown in detail in Table A3.14. Strontium

concentration for dentine ranges from 254 to 273 ppm and uranium concentration is 1 ppm.

Spot	Material	Mg (ppm)	P (ppm)	Sr (ppm)	Ba (ppm)	Th (ppm)	U (ppm)	Mg/Ca	Sr/Ca	Ba/Ca
1	Dentine	799	187024	254	49	0	1	0.003478	0.000306	0.000038
2	Dentine	888	185442	273	86	0	1	0.003867	0.000330	0.000066

Table A3.14 Elemental Concentrations and Ratios for Dentine, Sample 564, Bos, Layer Ec, Tabun

Element concentrations for sample 565 from the archaeological site of Tabun, shown in Figure A2.18, were collected for 2 enamel and 2 dentine spots. The results are summarised in Table 5.10 and shown in detail in Table A3.15. Strontium concentration for enamel ranges from 232 to 233 ppm and uranium concentration ranges from -4 to -3 ppm. Strontium concentration for dentine ranges from 205 to 213 ppm and uranium concentration is -3 ppm. As a negative value for concentration is not possible, this suggests an error in the acquisition or processing of the LA-ICPMS data set.

Spot	Material	Mg (ppm)	P (ppm)	Sr (ppm)	Ba (ppm)	Th (ppm)	U (ppm)	Mg/Ca	Sr/Ca	Ba/Ca
1	Enamel	1015	198940	233	99	-5	-4	0.004419	0.000281	0.000279
2	Enamel	1212	198690	232	113	-4	-3	0.005278	0.000280	0.000281
3	Dentine	731	192068	213	86	-4	-3	0.003186	0.000257	0.000256
4	Dentine	712	196029	205	80	-4	-3	0.003099	0.000248	0.000248

Table A3.15 Elemental Concentrations and Ratios for Enamel and Dentine, Sample 565, Bos, Layer Ec, Tabun

Element concentrations for sample 567 from the archaeological site of Tabun, shown in Figure A2.19, were collected for 2 enamel and 2 dentine spots. The results are summarised in Table 5.10 and shown in detail in Table A3.16. Strontium concentration for enamel ranges from 344 to 352 ppm and uranium concentration is 7 to 10 ppm. Strontium concentration for dentine ranges from 301 to 307 ppm and uranium concentration is -3 ppm. As a negative value for

concentration is not possible, this suggests an error in the acquisition or processing of the LA-ICPMS data set.

Spot	Material	Mg (ppm)	P (ppm)	Sr (ppm)	Ba (ppm)	Th (ppm)	U (ppm)	Mg/Ca	Sr/Ca	Ba/Ca
1	Enamel	702	162066	352	108	-5	7	0.003057	0.000425	0.000083
2	Enamel	718	166510	344	115	-4	10	0.003127	0.000415	0.000089
3	Dentine	1426	179429	301	14	-3	-3	0.006208	0.000363	0.000011
4	Dentine	1362	174712	307	13	-2	-3	0.005931	0.000370	0.000010

Table A3.16 Elemental Concentrations and Ratios for Enamel and Dentine, Sample 567, Bos, Layer Ed, Tabun

A3.1.1.3. Qafzeh

Element concentrations for sample 373 from the archaeological site of Qafzeh, shown in Figure A2.26, were collected for 3 enamel spots. The results are summarised in Table 5.17 and shown in detail in Table A3.17. Strontium concentration for enamel ranges from 556 to 566 ppm and uranium concentration is 0 ppm.

Spot	Material	Mg (ppm)	Sr (ppm)	Ba (ppm)	U (ppm)	Mg/Ca	Sr/Ca	Ba/Ca
1	Enamel	2869	562	57	0	0.012497	0.000679	0.000044
2	Enamel	2878	556	49	0	0.012536	0.000671	0.000038
3	Enamel	2887	566	55	0	0.012571	0.000684	0.000042

Table A3.17 Elemental Concentrations and Ratios for Enamel, Sample 373, Unidentified Species, Layer XVII, Qafzeh

A3.1.1.4. Holon

Element concentrations for sample 1557 from the archaeological site of Holon, shown in Figure A2.27, were collected for 5 enamel spots. The results are summarised in Table 5.21 and shown in detail in Table A3.18. Strontium concentration for enamel ranges from 308 to 328 ppm and uranium concentration ranges from 9 to 19 ppm.

Spot	Material	Mg (ppm)	Sr (ppm)	Ba (ppm)	U (ppm)	Mg/Ca	Sr/Ca	Ba/Ca
1	Enamel	1300	314	76	9	0.005662	0.000380	0.000059
2	Enamel	1203	308	71	17	0.005238	0.000373	0.000055
3	Enamel	1267	306	78	13	0.005517	0.000369	0.000060
4	Enamel	1162	322	76	19	0.005061	0.000389	0.000058
5	Enamel	1208	328	82	19	0.005260	0.000396	0.000063

Table A3.18 Elemental Concentrations and Ratios for Enamel, Sample 1557, Bovid, Unit C, Holon

A3.1.2. French Archaeological Samples

A3.1.2.1. La Chapelle-aux-Saints

Element concentrations for sample M001 from the archaeological site of La Chapelle-aux-Saints, shown in Figure A2.31, were collected for 5 enamel spots. The results are summarised in Table 5.25 and shown in detail in Table A3.19. Strontium concentration for enamel ranges from 251 to 353 ppm and uranium concentration ranges from 1 to 21 ppm.

Spot	Material	Mg (ppm)	P (ppm)	Sr (ppm)	Ba (ppm)	Th (ppm)	U (ppm)	Mg/Ca	Sr/Ca	Ba/Ca
1	Enamel	1757	163506	252	173	0	20	0.007654	0.000304	0.000133
2	Enamel	1983	163884	353	223	0	21	0.008636	0.000426	0.000172
3	Enamel	1529	162904	272	208	0	20	0.006658	0.000329	0.000160

4	Enamel	1541	165135	251	174	0	19	0.006713	0.000304	0.000134
5	Enamel	2148	184931	252	146	0	1	0.009355	0.000305	0.000113

Table A3.19 Elemental Concentrations and Ratios for Enamel, Sample M001, Reindeer, Bouffia 118: Layer 2, La Chapelle-aux-Saints

Element concentrations for sample M002 from the archaeological site of La Chapelle-aux-Saints, shown in Figure A2.32, were collected for 2 enamel spots. The results are summarised in Table 5.25 and shown in detail in Table A3.20. Strontium concentration for enamel is 162 ppm and uranium concentration ranges is 0 ppm.

Spot	Material	Mg (ppm)	P (ppm)	Sr (ppm)	Ba (ppm)	Th (ppm)	U (ppm)	Mg/Ca	Sr/Ca	Ba/Ca
1	Enamel	2547	175543	162	94	0	0	0.011093	0.000196	0.000072
2	Enamel	2451	176868	162	88	0	0	0.010673	0.000196	0.000068

Table A3.20 Elemental Concentrations and Ratios for Enamel, Sample M002, Reindeer, Bouffia 118: Layer 2, La Chapelle-aux-Saints

Element concentrations for sample M003 from the archaeological site of La Chapelle-aux-Saints, shown in Figure A2.33, were collected for 2 enamel and 2 dentine spots. The results are summarised in Table 5.25 and shown in detail in Table A3.21. Strontium concentration for enamel is 214 to 255 ppm and uranium concentration ranges from 26 to 29 ppm. Strontium concentration for dentine is 256 to 277 ppm and uranium concentration ranges from 16 to 19 ppm.

Spot	Material	Mg (ppm)	P (ppm)	Sr (ppm)	Ba (ppm)	Th (ppm)	U (ppm)	Mg/Ca	Sr/Ca	Ba/Ca
1	Enamel	1471	221765	255	211	0	29	0.006405	0.000308	0.000162
2	Enamel	1364	239514	214	134	0	26	0.005940	0.000259	0.000103
3	Dentine	1456	232411	277	241	0	19	0.006343	0.000335	0.000186
4	Dentine	1407	246622	256	229	0	16	0.006128	0.000309	0.000176

Table A3.21 Elemental Concentrations and Ratios for Enamel and Dentine, Sample M003, Reindeer, Bouffia 118: Layer 2, La Chapelle-aux-Saints

Element concentrations for sample M004 from the archaeological site of La Chapelle-aux-Saints, shown in Figure A2.34, were collected for 2 enamel and 2 dentine spots. The results are summarised in Table 5.25 and shown in detail in Table A3.22. Strontium concentration for enamel is 161 to 162 ppm and uranium concentration is 0 ppm. Strontium concentration for dentine is 225 to 231 ppm and uranium concentration ranges from 12 to 13 ppm.

Spot	Material	Mg (ppm)	P (ppm)	Sr (ppm)	Ba (ppm)	Th (ppm)	U (ppm)	Mg/Ca	Sr/Ca	Ba/Ca
1	Enamel	1867	183943	161	107	0	0	0.008129	0.000195	0.000082
2	Enamel	1858	184916	162	105	0	0	0.008091	0.000195	0.000081
3	Dentine	1428	154265	225	150	0	12	0.006221	0.000272	0.000115
4	Dentine	1403	157933	231	172	0	13	0.006108	0.000279	0.000132

Table A3.22 Elemental Concentrations and Ratios for Enamel and Dentine, Sample M004, Unknown Species, Bouffia 118: Unknown Layer, La Chapelle-aux-Saints

Element concentrations for sample M005 from the archaeological site of La Chapelle-aux-Saints, shown in Figure A2.35, were collected for 4 dentine spots. The results are summarised in Table 5.25 and shown in detail in Table A3.23. Strontium concentration for dentine is 186 to 253 ppm and uranium concentration ranges from 16 to 18 ppm.

Spot	Material	Mg (ppm)	P (ppm)	Sr (ppm)	Ba (ppm)	Th (ppm)	U (ppm)	Mg/Ca	Sr/Ca	Ba/Ca
1	Dentine	1160	194475	186	131	0	18	0.005050	0.000225	0.000101
2	Dentine	1170	201776	211	163	0	16	0.005095	0.000255	0.000126
3	Dentine	1239	209617	253	172	0	17	0.005394	0.000306	0.000132
4	Dentine	1281	210785	238	162	0	18	0.005580	0.000288	0.000125

Table A3.23 Elemental Concentrations and Ratios for Dentine, Sample M005, Bovid, Bouffia 118: Layer 1, La Chapelle-aux-Saints

Element concentrations for sample M006 from the archaeological site of La Chapelle-aux-Saints, shown in Figure A2.36, were collected in a continuous transect in enamel. The results are shown in Table 5.25 and Table A3.24. Strontium concentration for enamel has an average of 386 ppm and uranium concentration of 1 ppm.

Material	Mg (ppm)	P (ppm)	Sr (ppm)	Ba (ppm)	U (ppm)	Th (ppm)	Mg/Ca	Sr/Ca	Ba/Ca
Enamel	1523	207784	386	310	0	0	0.006634	0.000467	0.000239

Table A3.24 Elemental Concentrations and Ratios for Enamel Transect, Sample M006, Bovid, Bouffia 118: Layer 1, La Chapelle-aux-Saints

Element concentrations for sample M007 from the archaeological site of La Chapelle-aux-Saints, shown in Figure A2.37, were collected in a continuous transect in enamel. The results are shown in Table 5.25 and Table A3.25. Strontium concentration for enamel has an average of 167 ppm and uranium concentration of 1 ppm.

Material	Mg (ppm)	P (ppm)	Sr (ppm)	Ba (ppm)	U (ppm)	Th (ppm)	Mg/Ca	Sr/Ca	Ba/Ca
Enamel	2332	215517	167	98	0	0	0.010155	0.000202	0.000076

Table A3.25 Elemental Concentrations and Ratios for Enamel Transect, Sample M007, Bovid, Bouffia 118: Layer 1, La Chapelle-aux-Saints

Element concentrations for sample M008 from the archaeological site of La Chapelle-aux-Saints, shown in Figure A2.38, were collected in a continuous transect in enamel and dentine. The results are shown in Table 5.25 and Table A3.26. Strontium concentration for enamel has an average of 293 ppm and uranium concentration of 1 ppm.

Material	Mg (ppm)	P (ppm)	Sr (ppm)	Ba (ppm)	Th (ppm)	U (ppm)	Mg/Ca	Sr/Ca	Ba/Ca
Enamel	1448	198912	293	248	-1	1	0.006305	0.000354	0.000356
Dentine	1049	177611	275	225	-1	55	0.004568	0.000333	0.000334

Table A3.26 Elemental Concentrations and Ratios for Enamel and Dentine Transects, Sample M008, Bovid, Bouffia 118: Layer 1, La Chapelle-aux-Saints

Element concentrations for sample M009 from the archaeological site of La Chapelle-aux-Saints, shown in Figure A2.39, were collected in 3 continuous transects in enamel and dentine. The results are shown in Table 5.25 and Table A3.27. Strontium concentration for enamel has average transect values of 166 to 187 ppm and uranium concentration of 0 to 1 ppm. Strontium concentration for dentine has average transect values of 237 to 242 ppm and uranium concentration of 24 to 29 ppm.

Material	Transect	Mg (ppm)	P (ppm)	Sr (ppm)	Ba (ppm)	Th (ppm)	U (ppm)	Mg/Ca	Sr/Ca	Ba/Ca
Enamel Average	One	1548	227880	182	214	0	1	0.006741	0.000220	0.000165
Dentine Average	One	1154	203197	242	186	0	29	0.005028	0.000292	0.000144
Enamel Average	Two	1459	223223	187	241	0	0	0.006353	0.000226	0.000186
Dentine Average	Two	1183	201059	238	202	0	28	0.005153	0.000287	0.000156
Enamel Average	Three	1549	221539	166	163	0	0	0.006745	0.000201	0.000125
Dentine Average	Three	1166	200952	237	205	0	24	0.005077	0.000286	0.000158

Table A3.27 Elemental Concentrations and Ratios for Enamel and Dentine Transects, Sample M009, Bovid, Bouffia 118: Layer 1, La Chapelle-aux-Saints

Element concentrations for sample M010 from the archaeological site of La Chapelle-aux-Saints, shown in Figure A2.40, were collected in 2 continuous transects in enamel and dentine. The results are shown in Table 5.25 and Table A3.28. Strontium concentration for enamel has average transect values of 175 and 185 ppm and uranium concentration of -13 and -10 ppm. As a negative

value for concentration is not possible, this suggests an error in the acquisition or processing of the LA-ICPMS data set. Strontium concentration for dentine has average transect values of 239 and 260 ppm and uranium concentration of 40 and 50 ppm.

Material	Transect	Mg (ppm)	P (ppm)	Sr (ppm)	Ba (ppm)	Th (ppm)	U (ppm)	Mg/Ca	Sr/Ca	Ba/Ca
Enamel Average	One	1673	206173	175	180	-13	-13	0.007287	0.000211	0.000139
Dentine Average	One	1393	169564	260	192	-12	40	0.006068	0.000315	0.000148
Enamel Average	Two	1790	196978	185	196	-11	-10	0.007794	0.000223	0.000151
Dentine Average	Two	1397	168026	239	187	-9	50	0.006084	0.000288	0.000144

Table A3.28 Elemental Concentrations and Ratios for Enamel and Dentine Transects, Sample M010, Bovid, Bouffia 118: Layer 1, La Chapelle-aux-Saints

A3.1.2.2. Bois Roche

Element concentrations for sample 2417 from the archaeological site of Bois Roche, shown in Figure A2.68, were collected in 2 continuous transects in enamel and dentine. The results are shown in Table 5.36 and Table A3.29. Strontium concentration for enamel has average transect values of 240 and 244 ppm and uranium concentration of 0 ppm. Strontium concentration for dentine has average transect values of 261 and 273 ppm and uranium concentration of 1 ppm.

Material	Transect	Mg (ppm)	P (ppm)	Sr (ppm)	Ba (ppm)	Th (ppm)	U (ppm)	Mg/Ca	Sr/Ca	Ba/Ca
Enamel Average	One	2030	191574	240	43	0	0	0.008842	0.000290	0.000033
Dentine Average	One	979	177285	273	130	0	1	0.004264	0.000330	0.000100

Enamel Average	Two	1680	210222	244	58	0	0	0.007317	0.000295	0.000045
Dentine Average	Two	932	198645	261	129	0	1	0.004059	0.000315	0.000099

Table A3.29 Elemental Concentrations and Ratios for Enamel and Dentine Transects, Sample 2417, Bovid, Layer 1C, Bois Roche

Element concentrations for sample 2418 from the archaeological site of Bois Roche, shown in Figure A2.69, were collected in 1 continuous transect in enamel and dentine. The results are shown in Table 5.36 and Table A3.30. Strontium concentration for enamel has an average value of 163 ppm and uranium has an average concentration of 0 ppm. Strontium concentration for dentine has an average value of 182 ppm and a uranium concentration of 0 ppm.

Material	Transect	Mg (ppm)	P (ppm)	Sr (ppm)	Ba (ppm)	Th (ppm)	U (ppm)	Mg/Ca	Sr/Ca	Ba/Ca
Enamel Average	One	2282	194204	163	42	0	0	0.009939	0.000196	0.000032
Dentine Average	One	941	171689	182	93	0	0	0.004100	0.000219	0.000072

Table A3.30 Elemental Concentrations and Ratios for Enamel and Dentine Transects, Sample 2418, Bovid, Layer 1C, Bois Roche

Element concentrations for sample 2421 from the archaeological site of Bois Roche, shown in Figure A2.72, were collected in 3 continuous transects in enamel and dentine. The results are shown in Table 5.36 and Table A3.31. Strontium concentration for enamel has average transect values that range from 232 to 240 ppm and uranium concentration of 0 ppm. Strontium concentration for dentine has average transect values that range from 157 to 179 ppm and uranium concentration of 1 ppm.

Material	Transect	Mg (ppm)	P (ppm)	Sr (ppm)	Ba (ppm)	Mg/Ca	Sr/Ca	Ba/Ca
Enamel Average	One	1495	211845	235	136	0	0.006510	0.000284
Dentine Average	One	534	200034	166	129	0	1	0.002324
Enamel Average	Two	1466	196756	240	151	0	0	0.006384
Dentine Average	Two	587	195292	179	139	0	1	0.002555
Enamel Average	Three	1519	196107	232	138	0	0	0.006617
Dentine Average	Three	595	216259	157	138	0	1	0.002590
								0.000190
								0.000106

Table A3.31 Elemental Concentrations and Ratios for Enamel and Dentine Transects, Sample 2421, Bovid, Layer 2, Bois Roche

Element concentrations for sample 2422 from the archaeological site of Bois Roche, shown in Figure A2.73, were collected in 3 continuous transects in dentine and 1 continuous transect in enamel. The results are shown in Table 5.36 and Table A3.32. Strontium concentration for enamel has an average transect value of 165 ppm and uranium concentration of -1 ppm. As a negative value for concentration is not possible, this suggests an error in the acquisition or processing of the LA-ICPMS data set. Strontium concentration for dentine has average transect values of 239 and 262 ppm and uranium concentration of 8 and 9 ppm.

Material	Transect	Mg (ppm)	P (ppm)	Sr (ppm)	Ba (ppm)	Mg/Ca	Sr/Ca	Ba/Ca
Dentine (1) Average	One	717	192454	262	162	-1	8	0.003125
Enamel Average	One	1874	209552	165	71	-1	-1	0.008162
Dentine (2) Average	One	524	185485	239	141	-1	9	0.002283

Table A3.32 Elemental Concentrations and Ratios for Enamel and Dentine Transects, Sample 2422, Bovid, Layer 1C, Bois Roche

A3.2. LA-MC-ICPMS Strontium Isotope Results

A3.2.1. Non-Archaeological Material

A3.2.1.1. Durango Apatite

Strontium isotope values of Durango apatite collected with LA-MC-ICPMS have a weighted average of 15 points, shown in Figure A3.1, of 0.706134 ± 0.000045 for uncorrected $^{87}\text{Sr}/^{86}\text{Sr}$ and 0.70592 ± 0.000045 for corrected $^{87}\text{Sr}/^{86}\text{Sr}$. The isotope composition of these samples is relatively homogenous, with most samples within error of each other, shown in Table 5.43, Table A3.33 and Figure A3.2. Uncorrected $^{87}\text{Sr}/^{86}\text{Sr}$ values range from 0.705969 to 0.706239 and corrected values range from 0.705759 to 0.706029. The weighted average $^{84}\text{Sr}/^{86}\text{Sr}$ value is 0.56359 ± 0.000056 .

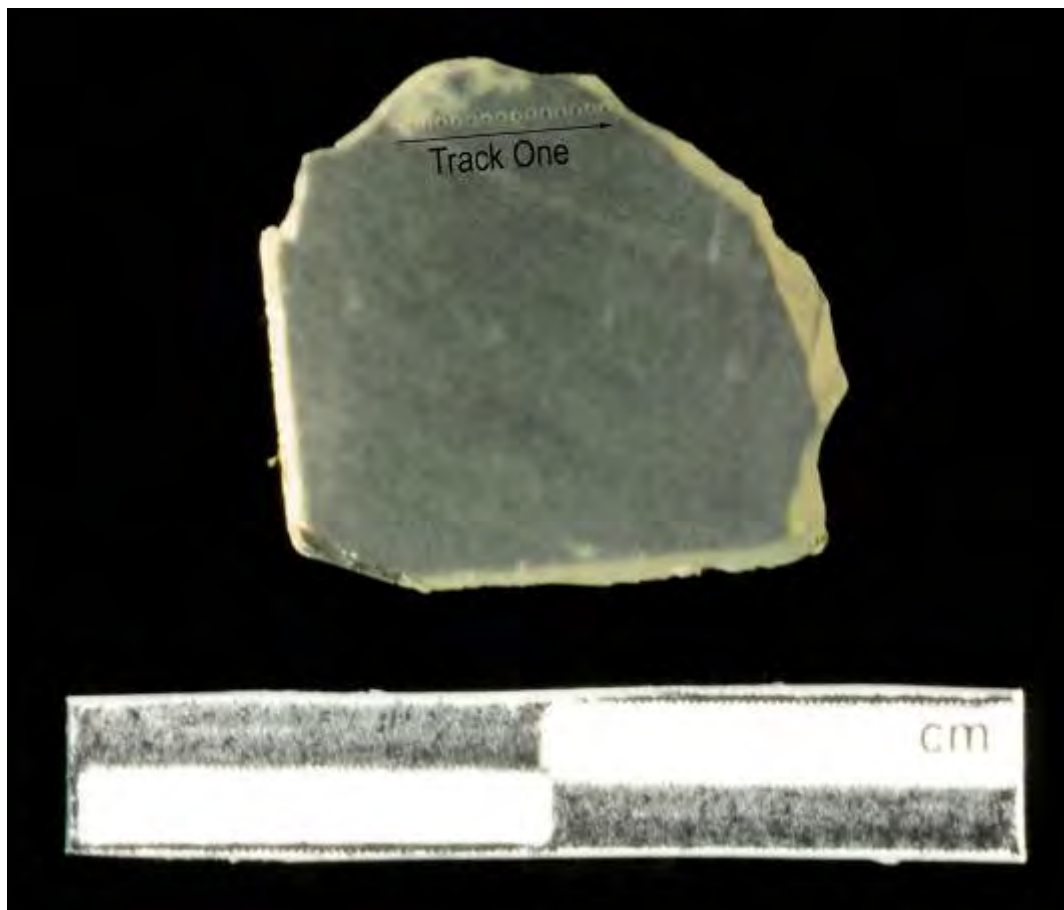


Figure A3.1 LA-MC-ICPMS Track for Durango Apatite

Sample	Material	Track	Point	^{88}Sr Volts	$^{84}\text{Sr}/^{86}\text{Sr}$	$^{84}\text{Sr}/^{86}\text{Sr} 2\sigma$ Error	Corrected $^{87}\text{Sr}/^{86}\text{Sr}$	$^{87}\text{Sr}/^{86}\text{Sr} 2\sigma$ Error
Durango	Apatite	1	1	1.728	0.056227	0.000133	0.706228	0.706018
Durango	Apatite	1	2	1.707	0.056248	0.000100	0.706071	0.705861
Durango	Apatite	1	3	1.896	0.056237	0.000099	0.706158	0.705948
Durango	Apatite	1	4	1.778	0.056366	0.000108	0.705966	0.705756
Durango	Apatite	1	5	1.723	0.056241	0.000144	0.706190	0.705980
Durango	Apatite	1	6	1.757	0.056394	0.000108	0.706239	0.706029
Durango	Apatite	1	7	1.624	0.056643	0.000400	0.706180	0.705970
Durango	Apatite	1	8	1.459	0.056422	0.000133	0.705969	0.705759
Durango	Apatite	1	9	1.444	0.056334	0.000198	0.706102	0.705892
Durango	Apatite	1	10	1.455	0.056334	0.000141	0.706229	0.706019
Durango	Apatite	1	11	1.539	0.056451	0.000146	0.706091	0.705881
Durango	Apatite	1	12	1.788	0.056452	0.000096	0.706197	0.705987
Durango	Apatite	1	13	1.567	0.056410	0.000111	0.706111	0.705901
Durango	Apatite	1	14	1.371	0.056386	0.000135	0.706159	0.705949
Durango	Apatite	1	15	1.297	0.056573	0.000148	0.706100	0.705890

Table A3.33 Durango Apatite LA-MC-ICPMS Sr Isotope Results

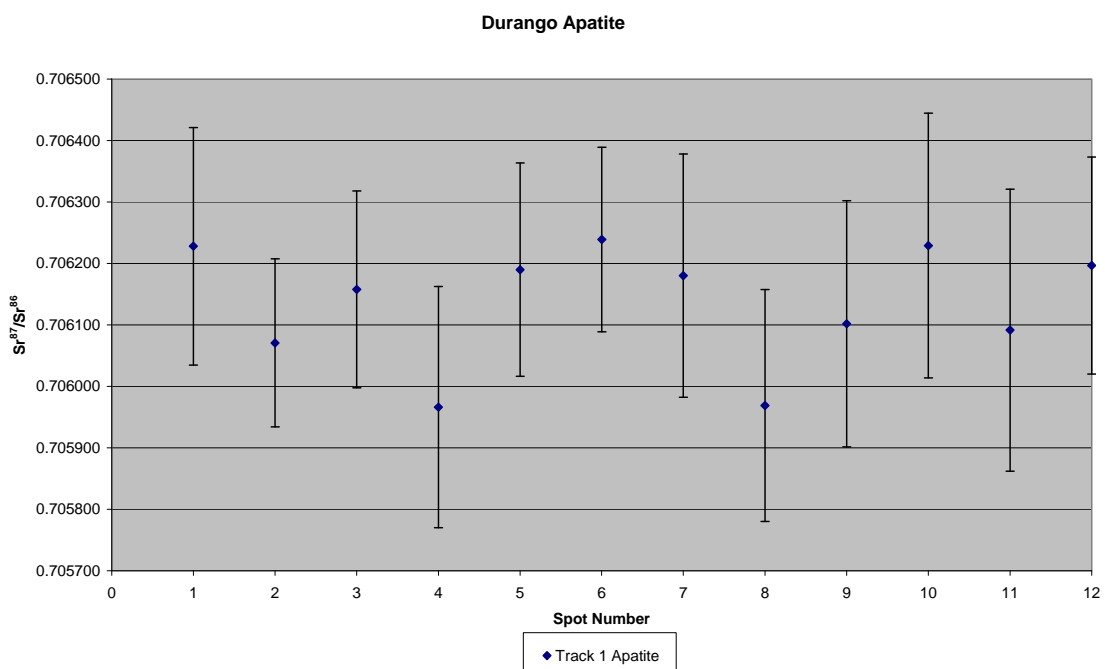


Figure A3.2 Durango Apatite LA-MC-ICPMS Uncorrected Sr Isotope Results

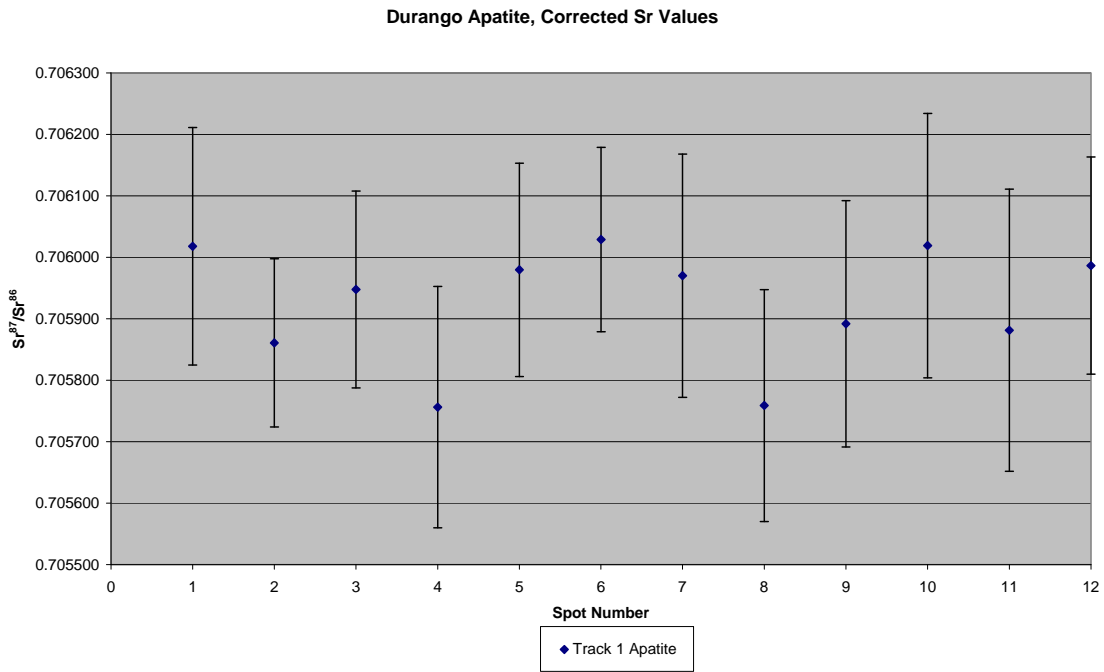


Figure A3.3 Durango Apatite LA-MC-ICPMS Uncorrected Sr Isotope Results

A3.2.2. Israeli Archaeological Sites

A3.2.2.1. Skhul

Sample 851, a bovid sample with unknown stratigraphic provenance from Skhul shown in Figure A2.1, was analysed by 1 track comprising 27 enamel and 27 dentine spots, shown in Figure A3.4. This sample has a weighted average uncorrected $^{87}\text{Sr}/^{86}\text{Sr}$ value for dentine of 0.70947 ± 0.00023 , a weighted average corrected $^{87}\text{Sr}/^{86}\text{Sr}$ value for dentine of 0.70909 ± 0.00023 , a weighted average $^{84}\text{Sr}/^{86}\text{Sr}$ value of 0.055493 ± 0.000036 and an average ^{88}Sr voltage of 2.533 volts ($n=27$), shown in Table 5.8 and Figure 5.5. The enamel of sample 851 has a weighted average uncorrected $^{87}\text{Sr}/^{86}\text{Sr}$ value of 0.70951 ± 0.00010 , a weighted average corrected $^{87}\text{Sr}/^{86}\text{Sr}$ value of 0.70900 ± 0.00010 , an average ^{88}Sr voltage of 2.337 and a weighted average $^{84}\text{Sr}/^{86}\text{Sr}$ value of 0.055494 ± 0.000047 ($n=27$), shown in Table A3.34 and Figures A3.5 and A3.6. The dentine $^{87}\text{Sr}/^{86}\text{Sr}$ values range from 0.708982 to 0.711292 (uncorrected) and 0.708606 to 0.710916 (corrected), and the enamel $^{87}\text{Sr}/^{86}\text{Sr}$ values range from 0.709143 to 0.710928 (uncorrected) and 0.708638 to 0.710423 (corrected), shown in Table A3.35 and Figures A3.5 and A3.6. The enamel shows a rhythmic patterning of $^{87}\text{Sr}/^{86}\text{Sr}$ values over a period of approximately 20 spots,

which corresponds to approximately 1 cm in the direction from root to the occlusal surface, shown in Figure A3.5.

This sample has $^{87}\text{Sr}/^{86}\text{Sr}$ values for dentine and enamel that are statistically indistinguishable. Enamel spot 24 has the most radiogenic uncorrected strontium isotope value (0.710928 ± 0.002618); however, the very high error on this sample means that it is difficult to use this spot for mobility analysis. Excluding this spot, enamel values are principally in a domain with an uncorrected weighted average of 0.70951 ± 0.00010 , which is in excellent agreement with the value of unconsolidated coastal sediment from sample 152 from IS022 which outcrops within 3.2 km from the site. This domain has a corrected value of 0.708951 ± 0.000080 , which corresponds to a number of mapping samples in the region, including from the Bina Formation (sample 156 from IS005) and kurkar (sample 153 from IS003) which outcrop within 1 km and 2.3 km from the site, respectively. Spots 15 to 18, which increase up to a maximum uncorrected value of 0.71064 ± 0.000214 , are more elevated than any soil samples in Israel in this study and correspond only to rock values from the Eilat located approximately 400 km from Skhul and so is considered an unlikely source of this value. The corrected value of this domain (0.70955 ± 0.00043) corresponds to sample 152 from IS002 from an unconsolidated coastal dune which outcrops within 3.2 km from the site. Overall, both the corrected and uncorrected values suggest that this specimen was principally resident on or near the coastal plain during amelogenesis, although made a short incursion to an unknown location.

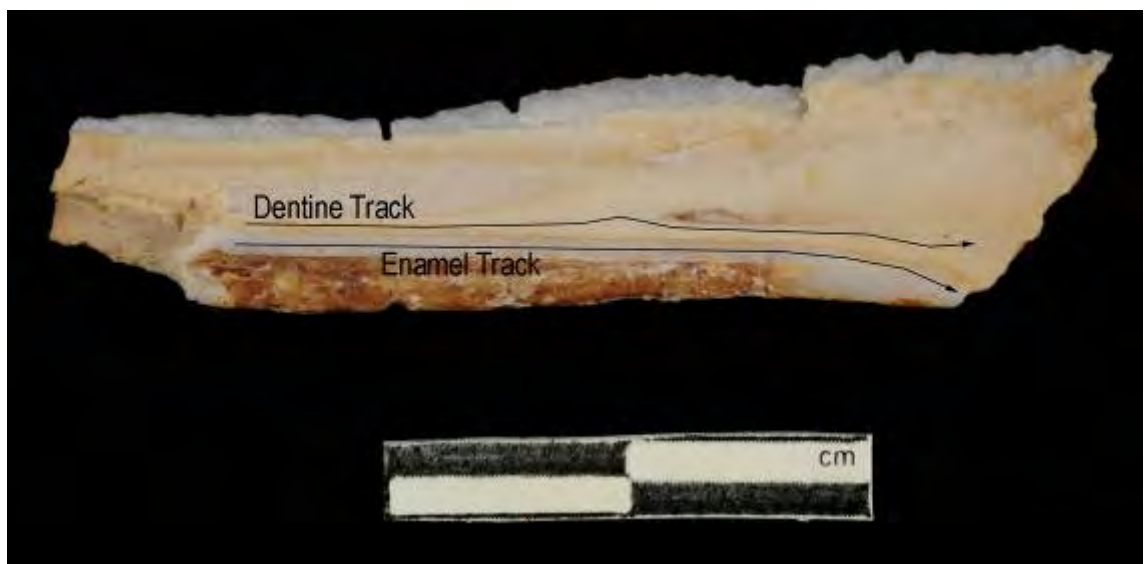


Figure A3.4 LA-MC-ICPMS Track for Sample 851, Bovid, Unknown Stratigraphic Provenance, Skhul

Sample	Material	Track	Point	^{88}Sr Volts	$^{84}\text{Sr}/^{86}\text{Sr}$	$^{84}\text{Sr}/^{86}\text{Sr} 2\sigma$ Error	$^{87}\text{Sr}/^{86}\text{Sr}$	Corrected $^{87}\text{Sr}/^{86}\text{Sr}$	$^{87}\text{Sr}/^{86}\text{Sr} 2\sigma$ Error
851	Dentine	1	1	2.918	0.055334	0.000094	0.710181	0.709804	0.000113
851	Dentine	1	2	2.897	0.055441	0.000085	0.710655	0.710278	0.000218
851	Dentine	1	3	2.258	0.055296	0.000131	0.711292	0.710916	0.000111
851	Dentine	1	4	2.725	0.055379	0.000094	0.710451	0.710074	0.000117
851	Dentine	1	5	2.787	0.055380	0.000094	0.710128	0.709751	0.000138
851	Dentine	1	6	2.357	0.055465	0.000132	0.710325	0.709948	0.000136
851	Dentine	1	7	2.209	0.055588	0.000105	0.709553	0.709176	0.000144
851	Dentine	1	8	3.012	0.055656	0.000098	0.709373	0.708996	0.000102
851	Dentine	1	9	2.388	0.055411	0.000144	0.709364	0.708987	0.000119
851	Dentine	1	10	2.839	0.055523	0.000083	0.709197	0.708820	0.000084
851	Dentine	1	11	2.485	0.055563	0.000124	0.709545	0.709169	0.000137
851	Dentine	1	12	2.058	0.055408	0.000194	0.709299	0.708922	0.000136
851	Dentine	1	13	2.319	0.055485	0.000140	0.709453	0.709076	0.000144
851	Dentine	1	14	2.225	0.055521	0.000107	0.709278	0.708902	0.000109
851	Dentine	1	15	2.192	0.055461	0.000143	0.709201	0.708824	0.000131
851	Dentine	1	16	2.443	0.055514	0.000108	0.709146	0.708769	0.000161
851	Dentine	1	17	2.548	0.055486	0.000103	0.709127	0.708750	0.000115
851	Dentine	1	18	2.373	0.055567	0.000124	0.709179	0.708802	0.000118
851	Dentine	1	19	2.667	0.055579	0.000105	0.709138	0.708761	0.000103
851	Dentine	1	20	2.951	0.055617	0.000080	0.708982	0.708606	0.000126
851	Dentine	1	21	2.418	0.055430	0.000125	0.709427	0.709050	0.000494
851	Dentine	1	22	2.637	0.055545	0.000115	0.709122	0.708745	0.000094
851	Dentine	1	23	2.695	0.055548	0.000097	0.709034	0.708657	0.000094
851	Dentine	1	24	2.514	0.055449	0.000127	0.709121	0.708744	0.000310
851	Dentine	1	25	2.284	0.055412	0.000134	0.709106	0.708730	0.000151
851	Dentine	1	26	2.366	0.055504	0.000128	0.709007	0.708630	0.000086
851	Dentine	1	27	2.826	0.055541	0.000132	0.709329	0.708952	0.000130

Table A3.34 Detailed LA-MC-ICPMS Sr Isotope Results for Dentine, Sample 851, Bovid, Unknown Stratigraphic Provenance, Skhul

Sample	Material	Track	Point	⁸⁸ Sr Volts	⁸⁴ Sr/ ⁸⁶ Sr	⁸⁴ Sr/ ⁸⁶ Sr 2σ Error	⁸⁷ Sr/ ⁸⁶ Sr	Corrected ⁸⁷ Sr/ ⁸⁶ Sr	⁸⁷ Sr/ ⁸⁶ Sr 2σ Error
851	Enamel	1	1	2.455	0.055505	0.000123	0.709395	0.708890	0.000167
851	Enamel	1	2	2.316	0.055643	0.000116	0.709460	0.708955	0.000113
851	Enamel	1	3	2.308	0.055580	0.000149	0.709529	0.709025	0.000117
851	Enamel	1	4	2.519	0.055585	0.000105	0.709598	0.709094	0.000132
851	Enamel	1	5	2.037	0.055617	0.000129	0.709496	0.708991	0.000160
851	Enamel	1	6	2.438	0.055616	0.000122	0.709439	0.708934	0.000115
851	Enamel	1	7	2.262	0.055544	0.000118	0.709324	0.708819	0.000150
851	Enamel	1	8	2.336	0.055641	0.000131	0.709221	0.708717	0.000140
851	Enamel	1	9	2.117	0.055530	0.000146	0.709228	0.708723	0.000154
851	Enamel	1	10	2.119	0.055539	0.000139	0.709262	0.708757	0.000130
851	Enamel	1	11	1.902	0.055302	0.000141	0.709436	0.708931	0.000162
851	Enamel	1	12	2.283	0.055406	0.000109	0.709280	0.708775	0.000140
851	Enamel	1	13	2.040	0.055429	0.000156	0.709143	0.708638	0.000145
851	Enamel	1	14	1.951	0.055449	0.000142	0.709648	0.709143	0.000182
851	Enamel	1	15	2.378	0.055375	0.000135	0.709959	0.709454	0.000145
851	Enamel	1	16	2.416	0.055492	0.000143	0.710640	0.710136	0.000214
851	Enamel	1	17	2.425	0.055496	0.000131	0.709886	0.709381	0.000137
851	Enamel	1	18	2.451	0.055516	0.000138	0.710080	0.709575	0.000138
851	Enamel	1	19	2.485	0.055506	0.000120	0.709639	0.709135	0.000140
851	Enamel	1	20	2.549	0.055472	0.000125	0.709465	0.708961	0.000134
851	Enamel	1	21	2.526	0.055476	0.000113	0.709530	0.709025	0.000128
851	Enamel	1	22	2.916	0.055520	0.000098	0.709414	0.708909	0.000108
851	Enamel	1	23	2.712	0.055553	0.000094	0.709333	0.708828	0.000108
851	Enamel	1	24	2.479	0.055615	0.000151	0.710928	0.710423	0.002618
851	Enamel	1	25	2.332	0.055183	0.000126	0.709542	0.709038	0.000127
851	Enamel	1	26	2.075	0.055159	0.000213	0.709693	0.709189	0.000149
851	Enamel	1	27	2.267	0.055241	0.000138	0.709396	0.708892	0.000124

Table A3.35 Detailed LA-MC-ICPMS Sr Isotope Results for Enamel, Sample 851, Bovid, Unknown Stratigraphic Provenance, Skhul

Sample 851, Skhul, Israel

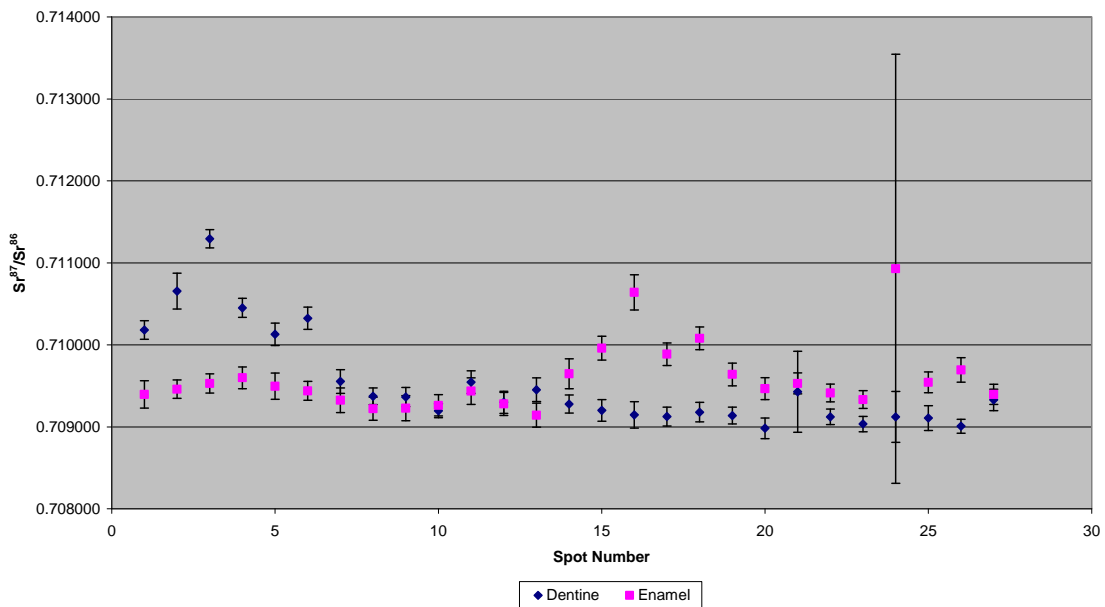


Figure A3.5 Detailed LA-MC-ICPMS Uncorrected Sr Isotope Results, Sample 851, Bovid, Unknown Stratigraphic Provenance, Skhul

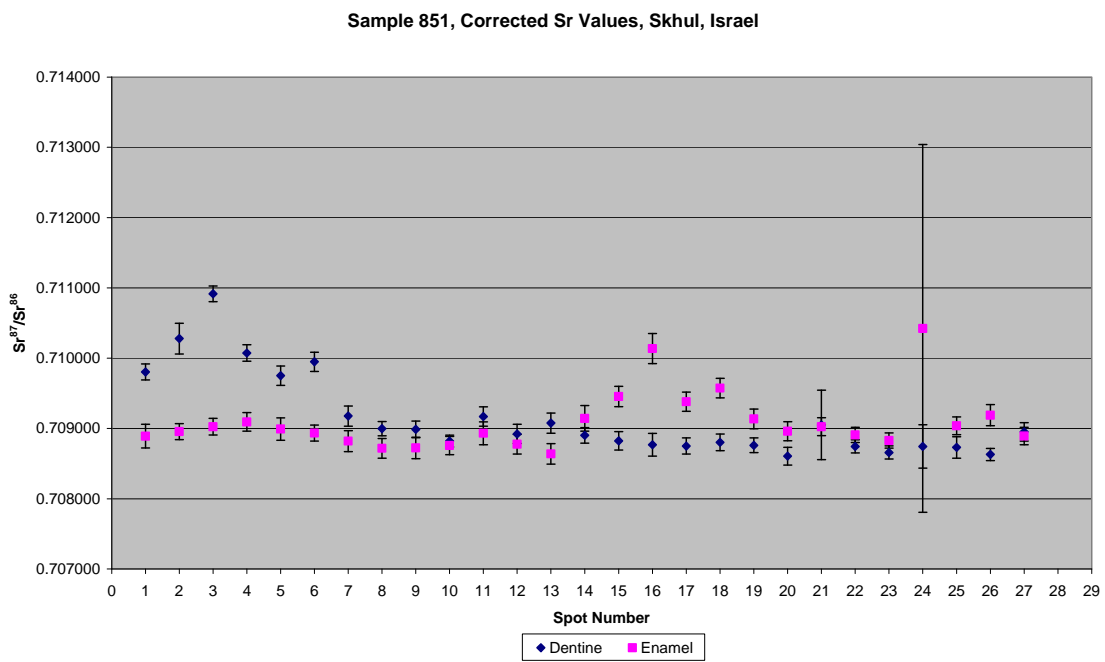


Figure A3.6 Detailed LA-MC-ICPMS Corrected Sr Isotope Results, Sample 851, Bovid, Unknown Stratigraphic Provenance, Skhul

Sample 852, a bovid sample with unknown stratigraphic provenance from Skhul shown in Figure A2.2 was analysed by 1 track comprising 39 enamel and 42 dentine spots, shown in Figure A3.7. This sample has a weighted average uncorrected $^{87}\text{Sr}/^{86}\text{Sr}$ value for dentine of 0.71045 ± 0.00017 , weighted average corrected $^{87}\text{Sr}/^{86}\text{Sr}$ value for dentine of 0.70975 ± 0.00017 , a weighted average $^{84}\text{Sr}/^{86}\text{Sr}$ value of 0.056272 ± 0.000024 and an average ^{88}Sr voltage of 2.856 ($n=41$), shown in Table 5.8 and Figure 5.5. The enamel of sample 852 has a weighted average uncorrected $^{87}\text{Sr}/^{86}\text{Sr}$ value of 0.70963 ± 0.00028 , a weighted average corrected $^{87}\text{Sr}/^{86}\text{Sr}$ value of 0.70899 ± 0.00028 , a weighted average $^{84}\text{Sr}/^{86}\text{Sr}$ value of 0.056235 ± 0.000085 and an average ^{88}Sr voltage of 4.556 ($n=39$), shown in Table 5.8 and Figure 5.5. Dentine has uncorrected values of 0.709536 to 0.719987 and corrected values of 0.708837 to 0.719288 for $^{87}\text{Sr}/^{86}\text{Sr}$, shown in Table A3.36, Figure A3.8 and Figure A3.9. $^{87}\text{Sr}/^{86}\text{Sr}$ values and 2σ error values are significantly elevated for the first spot of the transect before stabilising for the rest of the transect. After spot 31, $^{87}\text{Sr}/^{86}\text{Sr}$ values decrease suddenly and then remain depressed for the remainder of the transect. The enamel $^{87}\text{Sr}/^{86}\text{Sr}$ values range from 0.708451 to 0.714782 (uncorrected) and 0.707812 to 0.714143 (corrected), shown in Table A3.37, Figure A3.8 and Figure A3.9. Spots 2 and particularly 1 have elevated $^{87}\text{Sr}/^{86}\text{Sr}$ values compared to the rest of the tooth. $^{87}\text{Sr}/^{86}\text{Sr}$ varies rhythmically over approximately 13 spots from a minimum value of approximately 0.708500 to a maximum value of approximately 0.710900, which represents about 1.5 cm in the direction from the root to the occlusal surface.

Sample 852, a bovid sample with unknown stratigraphic provenance from Skhul, was analysed by 1 track containing 39 spots of enamel and 42 spots of dentine, shown in Figure A3.7. The strontium isotope values of this sample are summarised in Table 5.8 and Figure 5.5 and shown in detail in Table A3.36, Table A3.37, Figure A3.8 and Figure A3.9. This sample has weighted average $^{87}\text{Sr}/^{86}\text{Sr}$ values for dentine and enamel that are distinct. The rhythmic changes in the $^{87}\text{Sr}/^{86}\text{Sr}$ values in 852 may represent regular mobility between 2 distinct geological environments by the specimen during amelogenesis. As bovid molars continue to form after birth up to an age of approximately 12 months (see section 3.10.1.3) this would represent sub-annual mobility. The location of

Skhul between the coastal plain ($^{87}\text{Sr}/^{86}\text{Sr}$ value in the range of 0.708952 to 0.709522) and carbonate highlands of the Mount Carmel Range (in the range of 0.708393 to 0.708727) should allow these locations to be distinguished. The many uncorrected values greater than 0.710 from this tooth (even if the $^{87}\text{Sr}/^{86}\text{Sr}$ values of enamel spots 1 and 2— 0.714782 ± 0.000722 and 0.712290 ± 0.000344 , respectively—are considered sample collection artefacts) cannot be explained based on any local geology sampled in this study. In contrast, the corrected values of this sample vary between end-members of approximately 0.710 and 0.708. Values in the range of 0.708 includes a number of soil samples, including sample 173 from IS022, sample 171 from IS020 and sample 159 from IS008, all from chalky limestone on the Carmel Range which outcrop within 0.6 km from the site. The upper domain corresponds either to soil sample 162 from site IS011 collected from the Mount Scopus Group limestone approximately 62 km north-north-east of Skhul or sample 152 from site IS002 from the coastal plain which outcrop within 5.4 km and 3.2 km from the site, respectively.

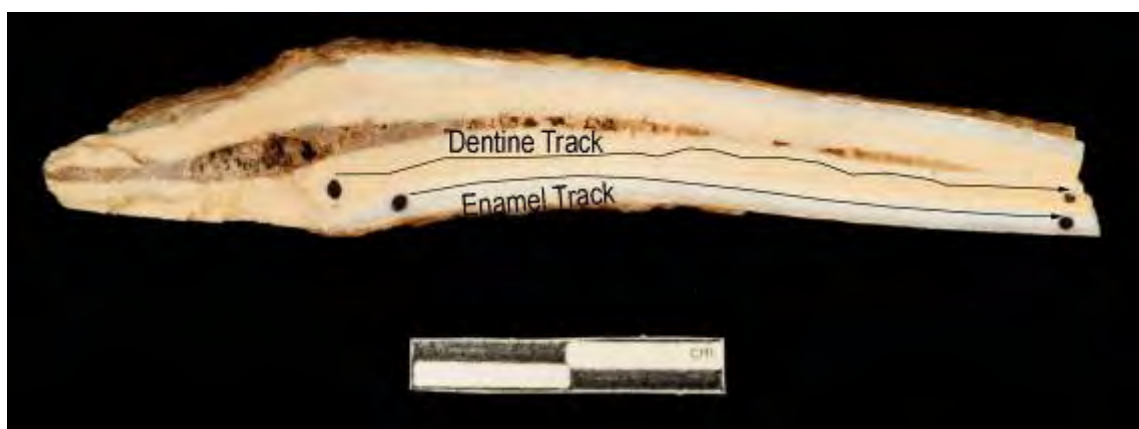


Figure A3.7 LA-MC-ICPMS Track for Sample 852, Bovid, Unknown Stratigraphic Provenance, Skhul

Sample	Material	Track	Point	88 Sr Volts	84 Sr/⁸⁶Sr	84 Sr/⁸⁶Sr 2σ Error	87 Sr/⁸⁶Sr	Corrected 87 Sr/⁸⁶Sr	87 Sr/⁸⁶Sr 2σ Error
852	Dentine	1	1	2.882	0.056256	0.000072	0.719987	0.719288	0.001625
852	Dentine	1	2	2.710	0.056302	0.000075	0.711251	0.710552	0.000236
852	Dentine	1	3	2.948	0.056329	0.000057	0.710726	0.710027	0.000283
852	Dentine	1	4	2.572	0.056365	0.000080	0.710514	0.709815	0.000244
852	Dentine	1	5	2.666	0.056382	0.000076	0.710848	0.710149	0.000327
852	Dentine	1	6	2.713	0.056326	0.000079	0.710512	0.709813	0.000181
852	Dentine	1	7	2.969	0.056322	0.000072	0.711062	0.710363	0.000276
852	Dentine	1	8	3.343	0.056243	0.000063	0.710423	0.709724	0.000322
852	Dentine	1	9	3.238	0.056288	0.000065	0.710280	0.709581	0.000153
852	Dentine	1	10	3.277	0.056337	0.000078	0.710740	0.710041	0.000261
852	Dentine	1	11	3.361	0.056315	0.000066	0.711019	0.710320	0.000275
852	Dentine	1	12	2.892	0.056382	0.000079	0.710742	0.710043	0.000288
852	Dentine	1	13	2.829	0.056268	0.000077	0.710905	0.710206	0.000228
852	Dentine	1	14	2.752	0.056216	0.000084	0.711197	0.710498	0.000371
852	Dentine	1	15	3.099	0.056284	0.000088	0.712502	0.711803	0.001078
852	Dentine	1	16	3.131	0.056356	0.000064	0.711045	0.710346	0.000160
852	Dentine	1	17	3.166	0.056302	0.000055	0.710556	0.709857	0.000180
852	Dentine	1	18	3.080	0.056400	0.000056	0.710983	0.710284	0.000593
852	Dentine	1	19	2.889	0.056396	0.000069	0.710177	0.709478	0.000216
852	Dentine	1	20	2.493	0.056355	0.000090	0.710907	0.710208	0.000251
852	Dentine	1	21	2.395	0.056377	0.000088	0.711059	0.710360	0.000388
852	Dentine	1	22	2.447	0.056273	0.000082	0.710815	0.710116	0.000296
852	Dentine	1	23	2.595	0.056339	0.000081	0.710614	0.709915	0.000218
852	Dentine	1	24	2.216	0.056234	0.000098	0.710801	0.710102	0.000273
852	Dentine	1	25	2.369	0.056304	0.000092	0.711105	0.710406	0.000326
852	Dentine	1	26	2.439	0.056337	0.000099	0.711262	0.710563	0.000447
852	Dentine	1	27	2.006	0.056222	0.000100	0.710901	0.710202	0.000351
852	Dentine	1	28	2.014	0.056190	0.000121	0.711668	0.710969	0.000323
852	Dentine	1	29	2.507	0.056230	0.000060	0.710233	0.709534	0.000314
852	Dentine	1	30	2.461	0.056219	0.000095	0.710241	0.709542	0.000217
852	Dentine	1	31	2.445	0.056173	0.000092	0.710083	0.709384	0.000261
852	Dentine	1	32	2.808	0.056219	0.000069	0.710033	0.709334	0.000231
852	Dentine	1	33	2.542	0.056241	0.000070	0.710021	0.709322	0.000203
852	Dentine	1	34	3.095	0.056242	0.000075	0.710133	0.709434	0.000192
852	Dentine	1	35	3.085	0.056271	0.000059	0.710119	0.709420	0.000259
852	Dentine	1	36	3.248	0.056177	0.000056	0.710098	0.709399	0.000190

							$^{87}\text{Sr}/^{86}\text{Sr}$ 2 σ	Error
							$^{87}\text{Sr}/^{86}\text{Sr}$	Corrected
							$^{87}\text{Sr}/^{86}\text{Sr}$	$^{87}\text{Sr}/^{86}\text{Sr}$ 2 σ
852	Dentine	1	37	3.489	0.056214	0.000064	0.709895	0.709196
852	Dentine	1	38	3.249	0.056109	0.000055	0.709689	0.708990
852	Dentine	1	39	3.388	0.056232	0.000064	0.710838	0.710139
852	Dentine	1	40	3.280	0.056190	0.000058	0.709552	0.708853
852	Dentine	1	41	3.234	0.056147	0.000069	0.709536	0.708837
852	Dentine	1	42	3.647	0.056207	0.000062	0.709637	0.708938

Table A3.36 Detailed LA-MC-ICPMS Sr Isotope Results for Dentine, Sample 852, Bovid, Unknown Stratigraphic Provenance, Skhul

							$^{87}\text{Sr}/^{86}\text{Sr}$ 2 σ	Error
							$^{87}\text{Sr}/^{86}\text{Sr}$	Corrected
							$^{87}\text{Sr}/^{86}\text{Sr}$	$^{87}\text{Sr}/^{86}\text{Sr}$ 2 σ
852	Enamel	1	1	7.078	0.056531	0.000054	0.714782	0.714143
852	Enamel	1	2	6.063	0.056591	0.000043	0.712290	0.711651
852	Enamel	1	3	6.379	0.056600	0.000034	0.710831	0.710192
852	Enamel	1	4	6.107	0.056480	0.000030	0.710749	0.710110
852	Enamel	1	5	6.122	0.056523	0.000040	0.709539	0.708900
852	Enamel	1	6	6.471	0.056491	0.000029	0.709894	0.709255
852	Enamel	1	7	5.549	0.056453	0.000041	0.710304	0.709665
852	Enamel	1	8	5.384	0.056402	0.000039	0.711094	0.710455
852	Enamel	1	9	5.211	0.056438	0.000044	0.709994	0.709355
852	Enamel	1	10	5.158	0.056378	0.000042	0.710480	0.709841
852	Enamel	1	11	4.665	0.056346	0.000049	0.710000	0.709362
852	Enamel	1	12	4.620	0.056357	0.000044	0.710576	0.709938
852	Enamel	1	13	4.650	0.056263	0.000052	0.710880	0.710241
852	Enamel	1	14	4.437	0.056208	0.000046	0.710919	0.710280
852	Enamel	1	15	5.823	0.056241	0.000069	0.710122	0.709483
852	Enamel	1	16	3.879	0.056192	0.000056	0.710951	0.710312
852	Enamel	1	17	3.798	0.056101	0.000052	0.709859	0.709220
852	Enamel	1	18	4.325	0.056095	0.000059	0.709130	0.708492
852	Enamel	1	19	4.595	0.056181	0.000055	0.708800	0.708161
852	Enamel	1	20	4.375	0.056056	0.000040	0.708467	0.707828
852	Enamel	1	21	4.628	0.056093	0.000060	0.708451	0.707812

Sample	Material	Track	Point	88Sr Volts	84Sr/⁸⁶Sr	84Sr/⁸⁶Sr 2σ Error	Corrected 87Sr/⁸⁶Sr	87Sr/⁸⁶Sr	87Sr/⁸⁶Sr 2σ Error
852	Enamel	1	22	4.573	0.056095	0.000064	0.708726	0.708087	0.000216
852	Enamel	1	23	3.962	0.055988	0.000064	0.708867	0.708228	0.000292
852	Enamel	1	24	3.738	0.055988	0.000053	0.709993	0.709354	0.000245
852	Enamel	1	25	3.876	0.056001	0.000060	0.710702	0.710063	0.000294
852	Enamel	1	26	3.734	0.055942	0.000065	0.710476	0.709838	0.000267
852	Enamel	1	27	3.555	0.055932	0.000070	0.710640	0.710001	0.000343
852	Enamel	1	28	3.931	0.055907	0.000062	0.710888	0.710249	0.000383
852	Enamel	1	29	3.887	0.055908	0.000057	0.710056	0.709417	0.000335
852	Enamel	1	30	3.436	0.055881	0.000063	0.709830	0.709191	0.000223
852	Enamel	1	31	3.780	0.055884	0.000070	0.709253	0.708614	0.000204
852	Enamel	1	32	4.078	0.055946	0.000060	0.708635	0.707996	0.000245
852	Enamel	1	33	3.555	0.055835	0.000066	0.709033	0.708394	0.000198
852	Enamel	1	34	3.634	0.055836	0.000057	0.709016	0.708377	0.000194
852	Enamel	1	35	3.766	0.055902	0.000049	0.709033	0.708394	0.000177
852	Enamel	1	36	3.572	0.055812	0.000060	0.709344	0.708706	0.000185
852	Enamel	1	37	3.447	0.055777	0.000068	0.709183	0.708545	0.000221
852	Enamel	1	38	3.876	0.055893	0.000071	0.708877	0.708238	0.000201
852	Enamel	1	39	3.984	0.055872	0.000045	0.709120	0.708481	0.000209

Table A3.37 Detailed LA-MC-ICPMS Sr Isotope Results for Enamel, Sample 852, Bovid, Unknown Stratigraphic Provenance, Skhul

Sample 852, Skhul, Israel

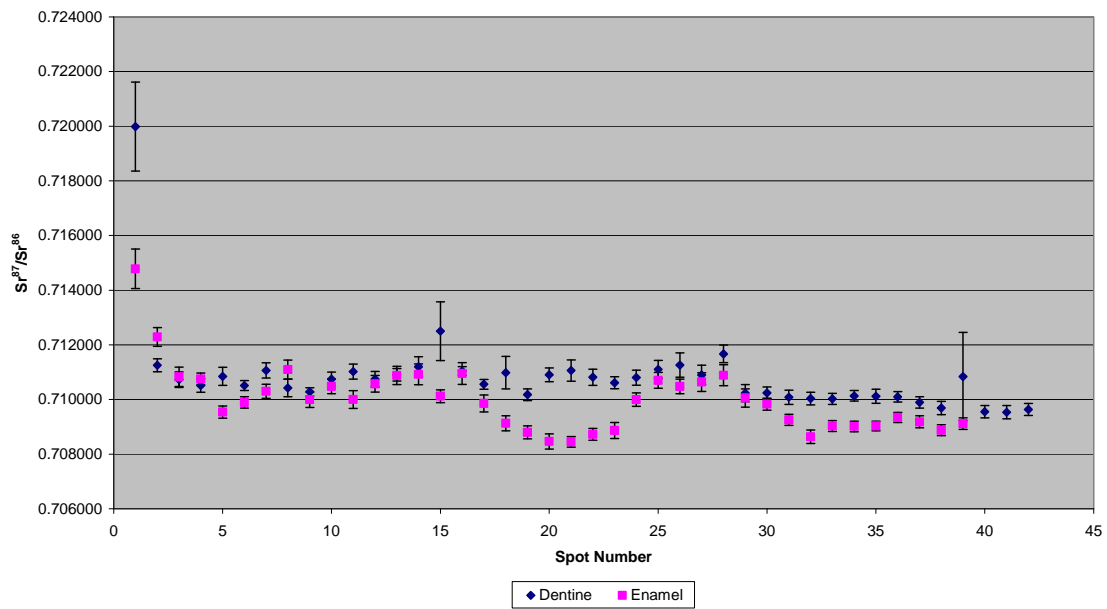


Figure A3.8 Detailed LA-MC-ICPMS Uncorrected Sr Isotope Results, Sample 852, Bovid, Unknown Stratigraphic Provenance, Skhul

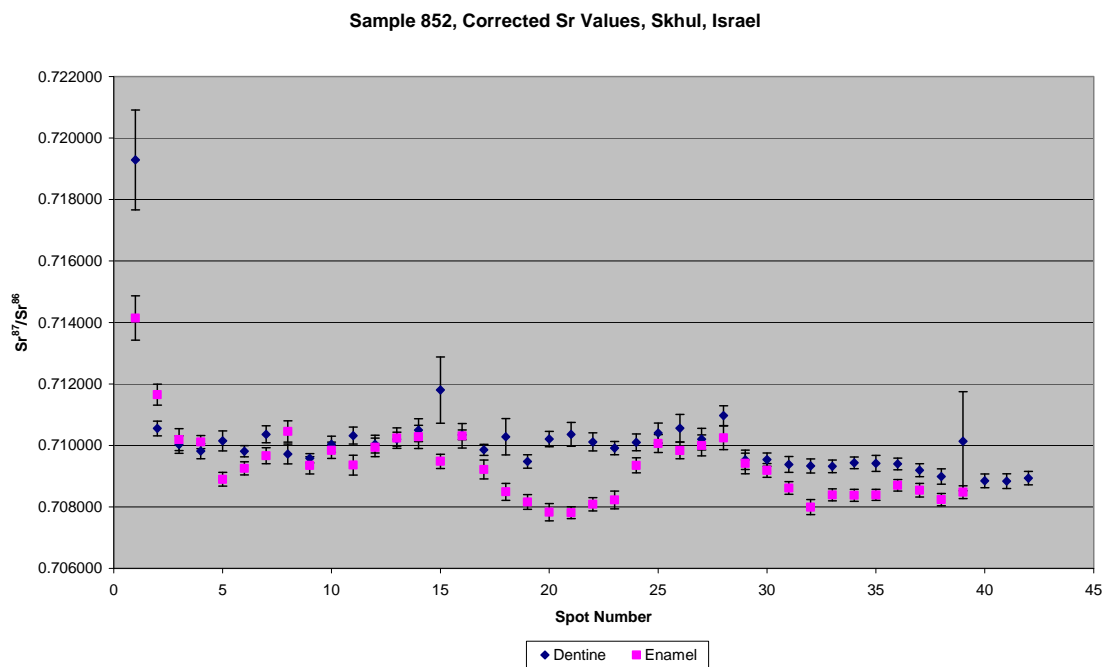


Figure A3.9 Detailed LA-MC-ICPMS Corrected Sr Isotope Results, Sample 852, Bovid, Unknown Stratigraphic Provenance, Skhul

Sample 853, a bovid sample with unknown stratigraphic provenance from Skhul, shown in Figure A2.3, was analysed by 1 track comprising 39 enamel and 35 dentine spots, shown in Figure A3.10. The dentine of this sample has an average ^{88}Sr voltage of 3.301, a weighted average uncorrected $^{87}\text{Sr}/^{86}\text{Sr}$ value of 0.709684 ± 0.000075 , a weighted average corrected $^{87}\text{Sr}/^{86}\text{Sr}$ value of 0.70951 ± 0.000075 and a weighted average $^{84}\text{Sr}/^{86}\text{Sr}$ value of 0.056468 ± 0.000017 ($n=35$), shown in Table 5.8 and Figure 5.5. Sample 853 enamel has an average ^{88}Sr voltage of 5.144, a weighted average uncorrected $^{87}\text{Sr}/^{86}\text{Sr}$ value of 0.709962 ± 0.000081 , a weighted average corrected $^{87}\text{Sr}/^{86}\text{Sr}$ value of 0.70985 ± 0.000081 and a weighted average $^{84}\text{Sr}/^{86}\text{Sr}$ value of 0.0564923 ± 0.0000095 ($n=39$), shown in Table 5.8 and Figure 5.5. Dentine values range from 0.709285 to 0.710228 (uncorrected) and 0.709112 to 0.710055 (corrected), shown in Table A3.38 and enamel values range from 0.709573 to 0.710866 (uncorrected) and 0.709466 to 0.710759 (corrected), shown in Table A3.39. With the exception of spot 21, which is elevated in $^{87}\text{Sr}/^{86}\text{Sr}$ value, dentine trends from spot 1 to spot 31, before jumping up in value to spot 32 and then remaining stable until the end of the transect, shown in Figure A3.11 and Figure A3.12. Enamel broadly trends from an elevated $^{87}\text{Sr}/^{86}\text{Sr}$ value from the start of the transect to a depressed $^{87}\text{Sr}/^{86}\text{Sr}$ value at the end of the transect, shown in Figure A3.11 and Figure A3.12.

This sample has weighted average values for dentine and enamel that are distinct, with the exception of spot 21, which is elevated compared to the rest of the track. The $^{87}\text{Sr}/^{86}\text{Sr}$ values show a gradual decrease in uncorrected values from a domain of approximately 0.7102 to a domain of approximately 0.7098; however, nearly all samples are within 2σ error. The closest comparable value to this domain is found in the Senonian-Palaeocene aged Mount Scopus Group limestone sample 162 from site IS011, which has a value of 0.710199 ± 0.000034 , although, as discussed in section 6.3.1.6, this value may not be robust. While this analysis site is located 60 km north-north-east of Skhul, an outcrop of Mount Scopus Group sediments, not sampled in this study, outcrop within 10 km of the site on the top of the Mount Carmel Range. The corrected values from this sample have a weighted average of 0.70985 ± 0.00008 , which

also correlates with sample 162 from site IS011 in the Senonian-Palaeocene aged Mount Scopus Group which outcrops within 5.4 km of the site.

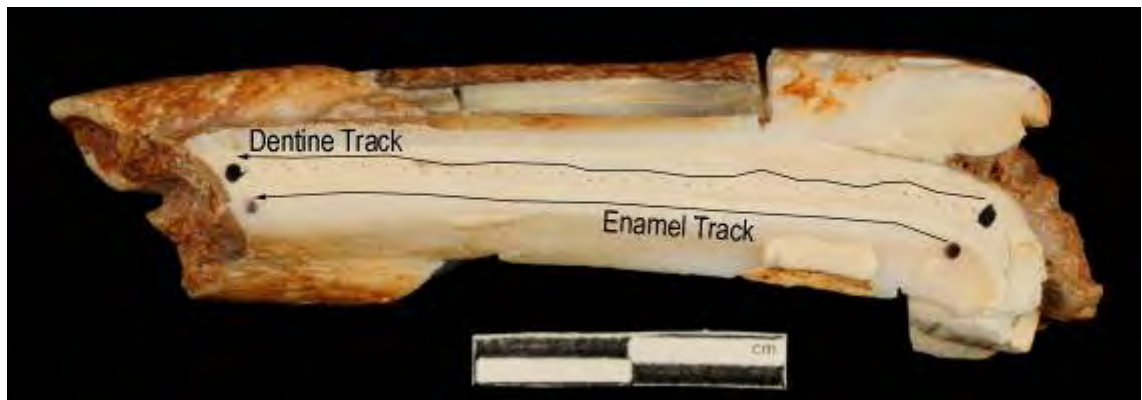


Figure A3.10 LA-MC-ICPMS Track for Sample 853 Bovid, Unknown Stratigraphic Provenance, Skhul

Sample	Material	Track	Point	^{88}Sr Volts	$^{84}\text{Sr}/^{86}\text{Sr}$	$^{84}\text{Sr}/^{86}\text{Sr} 2\sigma$ Error	$^{87}\text{Sr}/^{86}\text{Sr}$ Corrected $^{87}\text{Sr}/^{86}\text{Sr}$	$^{87}\text{Sr}/^{86}\text{Sr} 2\sigma$ Error
853	Dentine	1	1	3.581	0.056460	0.000062	0.709978	0.709805
853	Dentine	1	2	3.767	0.056438	0.000047	0.710228	0.710055
853	Dentine	1	3	3.557	0.056449	0.000053	0.709791	0.709618
853	Dentine	1	4	4.072	0.056506	0.000049	0.709772	0.709599
853	Dentine	1	5	3.889	0.056491	0.000052	0.709681	0.709508
853	Dentine	1	6	4.165	0.056440	0.000057	0.709970	0.709797
853	Dentine	1	7	3.829	0.056485	0.000046	0.710030	0.709857
853	Dentine	1	8	3.428	0.056466	0.000055	0.709752	0.709579
853	Dentine	1	9	3.053	0.056418	0.000068	0.709975	0.709802
853	Dentine	1	10	3.064	0.056521	0.000060	0.709684	0.709511
853	Dentine	1	11	3.891	0.056516	0.000057	0.709869	0.709696
853	Dentine	1	12	2.736	0.056427	0.000068	0.709874	0.709701
853	Dentine	1	13	2.939	0.056538	0.000069	0.709780	0.709607
853	Dentine	1	14	3.313	0.056584	0.000062	0.710093	0.709920
853	Dentine	1	15	2.826	0.056464	0.000071	0.709590	0.709417
853	Dentine	1	16	3.091	0.056470	0.000054	0.709684	0.709511
853	Dentine	1	17	3.418	0.056582	0.000052	0.709828	0.709655
853	Dentine	1	18	3.009	0.056453	0.000076	0.709663	0.709490
853	Dentine	1	19	3.281	0.056471	0.000066	0.709533	0.709360
853	Dentine	1	20	3.091	0.056518	0.000059	0.709377	0.709204
853	Dentine	1	21	3.323	0.056523	0.000059	0.709576	0.709403
853	Dentine	1	22	3.110	0.056452	0.000065	0.709713	0.709539
853	Dentine	1	23	2.602	0.056533	0.000102	0.709812	0.709639
853	Dentine	1	24	2.483	0.056441	0.000082	0.709562	0.709389
853	Dentine	1	25	2.981	0.056429	0.000067	0.709568	0.709395
853	Dentine	1	26	3.062	0.056473	0.000068	0.709410	0.709237
853	Dentine	1	27	3.227	0.056436	0.000075	0.709435	0.709262
853	Dentine	1	28	3.621	0.056451	0.000048	0.709524	0.709351
853	Dentine	1	29	3.239	0.056399	0.000049	0.709474	0.709301
853	Dentine	1	30	3.402	0.056430	0.000065	0.709617	0.709444
853	Dentine	1	31	3.413	0.056433	0.000058	0.709464	0.709291
853	Dentine	1	32	3.229	0.056438	0.000062	0.709445	0.709272
853	Dentine	1	33	3.005	0.056497	0.000063	0.709919	0.709746
853	Dentine	1	34	3.468	0.056401	0.000045	0.709285	0.709112
853	Dentine	1	35	3.380	0.056404	0.000053	0.709656	0.709483
								0.000164

Table A3.38 Detailed LA-MC-ICPMS Sr Isotope Results for Dentine, Sample 853, Bovid, Unknown Stratigraphic Provenance, Skhul

Sample	Material	Track	Point	^{88}Sr Volts	$^{84}\text{Sr}/^{86}\text{Sr}$	$^{84}\text{Sr}/^{86}\text{Sr} 2\sigma$ Error	$^{87}\text{Sr}/^{86}\text{Sr}$	Corrected $^{87}\text{Sr}/^{86}\text{Sr}$	$^{87}\text{Sr}/^{86}\text{Sr} 2\sigma$ Error
853	Enamel	1	1	4.903	0.056488	0.000055	0.710612	0.710505	0.000260
853	Enamel	1	2	4.918	0.056472	0.000034	0.710211	0.710104	0.000177
853	Enamel	1	3	4.208	0.056510	0.000048	0.710247	0.710140	0.000197
853	Enamel	1	4	4.246	0.056499	0.000049	0.710214	0.710107	0.000205
853	Enamel	1	5	4.774	0.056466	0.000044	0.710154	0.710047	0.000244
853	Enamel	1	6	4.755	0.056503	0.000044	0.710332	0.710225	0.000231
853	Enamel	1	7	4.101	0.056468	0.000040	0.710078	0.709971	0.000315
853	Enamel	1	8	4.281	0.056474	0.000052	0.709950	0.709843	0.000210
853	Enamel	1	9	5.297	0.056520	0.000036	0.709836	0.709729	0.000241
853	Enamel	1	10	5.645	0.056484	0.000042	0.710001	0.709894	0.000225
853	Enamel	1	11	5.139	0.056476	0.000046	0.709890	0.709783	0.000258
853	Enamel	1	12	5.632	0.056499	0.000039	0.710022	0.709915	0.000365
853	Enamel	1	13	5.279	0.056550	0.000036	0.709907	0.709800	0.000205
853	Enamel	1	14	5.179	0.056478	0.000032	0.709874	0.709767	0.000304
853	Enamel	1	15	5.157	0.056512	0.000037	0.709939	0.709832	0.000292
853	Enamel	1	16	5.029	0.056554	0.000042	0.709865	0.709758	0.000275
853	Enamel	1	17	5.151	0.056509	0.000041	0.709893	0.709786	0.000226
853	Enamel	1	18	4.778	0.056530	0.000044	0.710027	0.709920	0.000245
853	Enamel	1	19	4.565	0.056528	0.000039	0.710040	0.709933	0.000254
853	Enamel	1	20	4.552	0.056471	0.000043	0.709856	0.709749	0.000295
853	Enamel	1	21	4.555	0.056530	0.000040	0.710866	0.710759	0.000239
853	Enamel	1	22	4.931	0.056510	0.000042	0.709758	0.709651	0.000225
853	Enamel	1	23	5.003	0.056454	0.000040	0.709783	0.709676	0.000262
853	Enamel	1	24	4.785	0.056552	0.000043	0.709979	0.709872	0.000187
853	Enamel	1	25	5.267	0.056476	0.000046	0.709822	0.709715	0.000235
853	Enamel	1	26	5.276	0.056489	0.000035	0.709796	0.709689	0.000273
853	Enamel	1	27	5.150	0.056529	0.000041	0.709891	0.709784	0.000248
853	Enamel	1	28	5.158	0.056454	0.000040	0.709770	0.709663	0.000250
853	Enamel	1	29	5.462	0.056466	0.000042	0.709637	0.709530	0.000222
853	Enamel	1	30	5.895	0.056509	0.000031	0.709787	0.709680	0.000203
853	Enamel	1	31	5.733	0.056489	0.000030	0.709573	0.709466	0.000227
853	Enamel	1	32	4.938	0.056464	0.000048	0.709809	0.709702	0.000210
853	Enamel	1	33	5.758	0.056456	0.000034	0.709759	0.709652	0.000215
853	Enamel	1	34	6.001	0.056487	0.000047	0.709954	0.709847	0.000314

Sample	Material	Track	Point	^{88}Sr Volts	$^{84}\text{Sr}/^{86}\text{Sr}$	$^{87}\text{Sr}/^{86}\text{Sr} 2\sigma$	Corrected $^{87}\text{Sr}/^{86}\text{Sr}$	Error
853	Enamel	1	35	5.977	0.056442	0.000036	0.709804	0.709697
853	Enamel	1	36	6.623	0.056475	0.000037	0.709939	0.709832
853	Enamel	1	37	5.523	0.056481	0.000044	0.709751	0.709644
853	Enamel	1	38	5.657	0.056459	0.000034	0.709803	0.709696
853	Enamel	1	39	5.355	0.056501	0.000038	0.709886	0.709779

Table A3.39 Detailed LA-MC-ICPMS Sr Isotope Results for Enamel, Sample 853, Bovid, Unknown Stratigraphic Provenance, Skhul

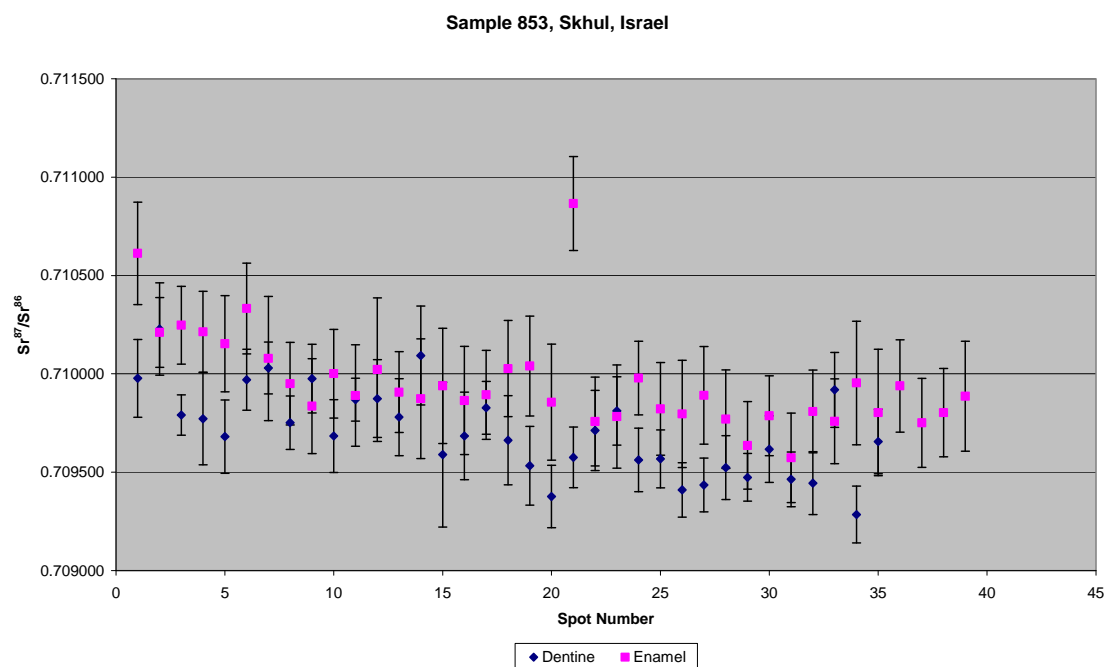


Figure A3.11 Detailed LA-MC-ICPMS Uncorrected Sr Isotope Results, Sample 853, Bovid, Unknown Stratigraphic Provenance, Skhul

Sample 853, Corrected Sr Values, Skhul, Israel

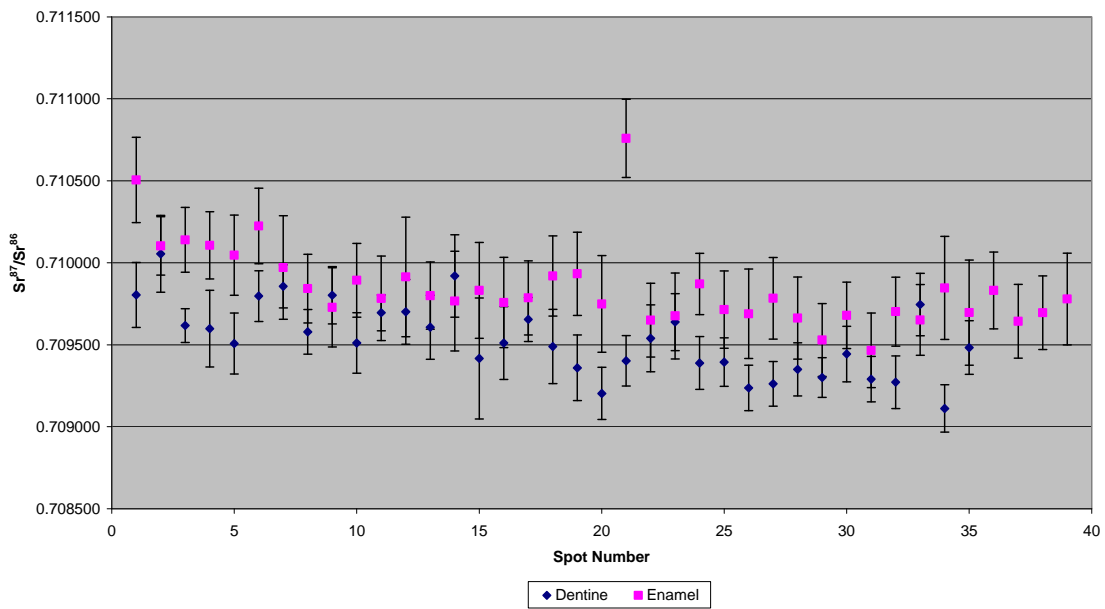


Figure A3.12 Detailed LA-MC-ICPMS Corrected Sr Isotope Results, Sample 853, Bovid, Unknown Stratigraphic Provenance, Skhul

Sample 1057, shown in Figure A2.4, Figure A2.5 and Figure A2.6 was analysed as 3 subsamples: 1057A, 1057B and 1057C with the tracks shown in Figure A3.13, Figure A3.16, and Figure A3.19.

These 3 teeth are from a bovid jaw that was buried intrusively into the Skhul IX hominin. The dentine of track 1 of 1057A has an average ^{88}Sr voltage of 0.434, a weighted average uncorrected $^{87}\text{Sr}/^{86}\text{Sr}$ value of 0.712 ± 0.013 , a weighted average corrected $^{87}\text{Sr}/^{86}\text{Sr}$ value of 0.71100 ± 0.013 and a weighted average $^{84}\text{Sr}/^{86}\text{Sr}$ value of 0.05667 ± 0.00030 ($n=2$), shown in Table 5.8 and Figure 5.5. The enamel of track 1 of 1057A has an average ^{88}Sr voltage of 0.542, a weighted average uncorrected $^{87}\text{Sr}/^{86}\text{Sr}$ value of 0.70871 ± 0.00039 , a weighted average corrected $^{87}\text{Sr}/^{86}\text{Sr}$ value of 0.70837 ± 0.00039 and a weighted average $^{84}\text{Sr}/^{86}\text{Sr}$ value of 0.05679 ± 0.00015 ($n=6$), shown in Table 5.8 and Figure 5.5. Dentine values for track 1 of sample 1057A are 0.710830 and 0.713003 (uncorrected) and 0.710245 and 0.712419 (corrected), enamel values range from 0.708317 to 0.709706 (uncorrected) and 0.707980 to 0.709369 (corrected), shown in Figure A3.14, Figure A3.15 and Table A3.40. Enamel

values increase from spot 1 until spot 6, shown in Figure A3.14, Figure A3.15 and Table A3.40.

The dentine of track 2 of 1057A has an average ^{88}Sr voltage of 0.438, a weighted average uncorrected $^{87}\text{Sr}/^{86}\text{Sr}$ value of 0.712 ± 0.013 , a weighted average corrected $^{87}\text{Sr}/^{86}\text{Sr}$ value of 0.71100 ± 0.013 and a weighted average $^{84}\text{Sr}/^{86}\text{Sr}$ value of 0.05683 ± 0.00014 ($n=2$), shown in Table 5.8 and Figure 5.5. The enamel of track 2 of 1057A has an average ^{88}Sr voltage of 0.524, a weighted average uncorrected $^{87}\text{Sr}/^{86}\text{Sr}$ value of 0.70853 ± 0.00029 , a weighted average corrected $^{87}\text{Sr}/^{86}\text{Sr}$ value of 0.70820 ± 0.00029 and a weighted average $^{84}\text{Sr}/^{86}\text{Sr}$ value of 0.05677 ± 0.00023 ($n=8$), shown in Table 5.8 and Figure 5.5. Dentine $^{87}\text{Sr}/^{86}\text{Sr}$ values for track 2 of 1057A are 0.711107 and 0.713849 (uncorrected), 0.710523 and 0.713265 (corrected), and enamel values are 0.708084 to 0.708981 (uncorrected) and 0.707747 to 0.708643 (corrected), shown in Figure A3.14, Figure A3.15 and Table A3.40.

The dentine of track 3 of 1057A has an average ^{88}Sr voltage of 0.343, a weighted average uncorrected $^{87}\text{Sr}/^{86}\text{Sr}$ value of 0.7150 ± 0.0085 , a weighted average corrected $^{87}\text{Sr}/^{86}\text{Sr}$ value of 0.71440 ± 0.0085 and a weighted average $^{84}\text{Sr}/^{86}\text{Sr}$ value of 0.05650 ± 0.00039 ($n=3$), shown in Table 5.8 and Figure 5.5. The enamel of track 3 of 1057A has an average ^{88}Sr voltage of 0.510, a weighted average uncorrected $^{87}\text{Sr}/^{86}\text{Sr}$ value of 0.70897 ± 0.00031 , a weighted average uncorrected $^{87}\text{Sr}/^{86}\text{Sr}$ value of 0.70864 ± 0.00031 and a weighted average $^{84}\text{Sr}/^{86}\text{Sr}$ value of 0.05677 ± 0.00013 ($n=7$), shown in Table 5.8 and Figure 5.5. Track 3 of 1057A has dentine $^{87}\text{Sr}/^{86}\text{Sr}$ values in the range of 0.712770 to 0.719279 (uncorrected) and 0.712185 to 0.718694 (corrected), and enamel $^{87}\text{Sr}/^{86}\text{Sr}$ values in the range of 0.708284 to 0.709439 (uncorrected) and 0.707946 to 0.709102 (corrected), shown in Figure A3.14, Figure A3.15 and Table A3.40.

The 3 tracks of sample 1057A have homogenous enamel $^{87}\text{Sr}/^{86}\text{Sr}$ values. The uncorrected weighted average of all 1057A enamel values is 0.70873 ± 0.00018 , which correlates with sample 170 from site IS019 from the Turonian

age Bina Formation. This unit is extensively distributed over the Carmel Range. The corrected weighted average enamel of this sample is 0.70839 ± 0.00018 , which correlates to values from sample 159 from site IS008 and sample 171 from site IS020, both from the Lower to Middle Eocene Adulam Formation, which outcrops on the Carmel Range within 7.6km of the site.

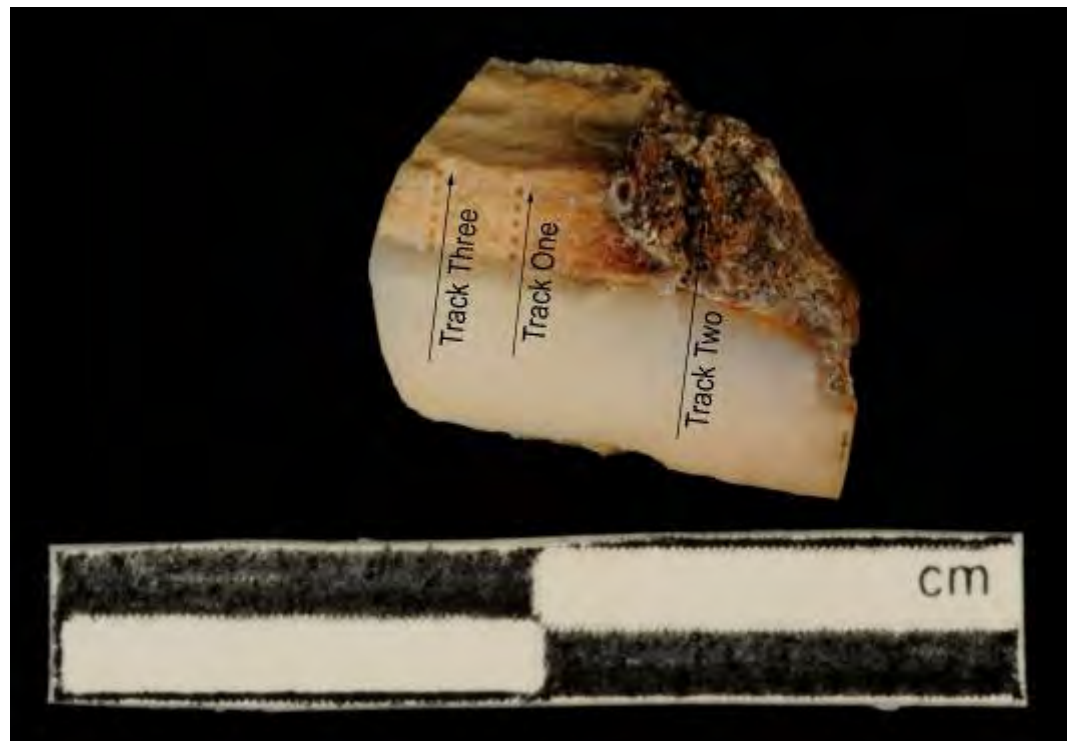


Figure A3.13 LA-MC-ICPMS Track for Sample 1057A, Bovid, Layer B, Skhul

Sample	Material	Track	Point	^{88}Sr Volts	$^{84}\text{Sr}/^{86}\text{Sr}$	$^{84}\text{Sr}/^{86}\text{Sr} 2\sigma$ Error	$^{87}\text{Sr}/^{86}\text{Sr}$	Corrected $^{87}\text{Sr}/^{86}\text{Sr}$	$^{87}\text{Sr}/^{86}\text{Sr} 2\sigma$ Error
1057A	Enamel	1	1	0.629	0.056791	0.000348	0.708317	0.707980	0.000573
1057A	Enamel	1	2	0.596	0.056826	0.000357	0.708479	0.708141	0.000436
1057A	Enamel	1	3	0.577	0.056650	0.000277	0.708718	0.708381	0.000440
1057A	Enamel	1	4	0.562	0.056874	0.000380	0.708682	0.708345	0.000396
1057A	Enamel	1	5	0.454	0.056789	0.000442	0.708980	0.708642	0.000641
1057A	Enamel	1	6	0.437	0.057081	0.000502	0.709706	0.709369	0.000728
1057A	Dentine	1	7						
1057A	Dentine	1	8						

Sample	Material	Track	Point	^{88}Sr Volts	$^{84}\text{Sr}/^{86}\text{Sr}$	$^{84}\text{Sr}/^{86}\text{Sr} 2\sigma$ Error	$^{87}\text{Sr}/^{86}\text{Sr}$	Corrected $^{87}\text{Sr}/^{86}\text{Sr}$	$^{87}\text{Sr}/^{86}\text{Sr} 2\sigma$ Error
1057A	Dentine	1	9	0.432	0.056581	0.000432	0.713003	0.712419	0.000607
1057A	Dentine	1	10	0.435	0.056750	0.000430	0.710830	0.710245	0.000452
1057A	Dentine	1	11						
1057A	Enamel	2	1	0.559	0.056576	0.000343	0.708764	0.708427	0.000548
1057A	Enamel	2	2	0.575	0.057006	0.000279	0.708981	0.708643	0.000460
1057A	Enamel	2	3	0.579	0.056829	0.000295	0.708358	0.708020	0.000461
1057A	Enamel	2	4	0.581	0.057030	0.000367	0.708099	0.707761	0.000469
1057A	Enamel	2	5	0.569	0.056494	0.000260	0.708084	0.707747	0.000502
1057A	Enamel	2	6	0.503	0.057034	0.000308	0.708643	0.708306	0.000454
1057A	Enamel	2	7	0.439	0.056704	0.000504	0.708539	0.708201	0.000536
1057A	Enamel	2	8	0.385	0.056146	0.000518	0.708939	0.708602	0.000597
1057A	Dentine	2	9	0.426	0.056532	0.000527	0.711107	0.710523	0.000433
1057A	Dentine	2	10						
1057A	Dentine	2	11						
1057A	Dentine	2	12						
1057A	Dentine	2	13						
1057A	Dentine	2	14						
1057A	Dentine	2	15						
1057A	Dentine	2	16	0.450	0.056827	0.000737	0.713849	0.713265	0.000950
1057A	Dentine	2	17						
1057A	Enamel	3	1	0.565	0.056763	0.000353	0.709439	0.709102	0.000477
1057A	Enamel	3	2	0.541	0.056986	0.000342	0.708860	0.708523	0.000412
1057A	Enamel	3	3	0.533	0.056868	0.000340	0.709210	0.708872	0.000580
1057A	Enamel	3	4	0.499	0.056709	0.000351	0.708914	0.708577	0.000550
1057A	Enamel	3	5	0.498	0.056662	0.000420	0.709063	0.708725	0.000522
1057A	Enamel	3	6	0.441	0.056862	0.000440	0.708986	0.708649	0.000452
1057A	Enamel	3	7	0.491	0.056607	0.000272	0.708284	0.707946	0.000550
1057A	Dentine	3	8						
1057A	Dentine	3	9	0.377	0.056494	0.000456	0.712770	0.712185	0.000687
1057A	Dentine	3	10	0.318	0.056622	0.001118	0.715748	0.715163	0.001294
1057A	Dentine	3	11						
1057A	Dentine	3	12	0.335	0.056445	0.001193	0.719279	0.718694	0.001001
1057A	Dentine	3	13						

Table A3.40 Detailed LA-MC-ICPMS Sr Isotope Results for Dentine, Sample 1057A, Bovid, Layer B, Skhul

Sample 1057A, Skhul, Israel

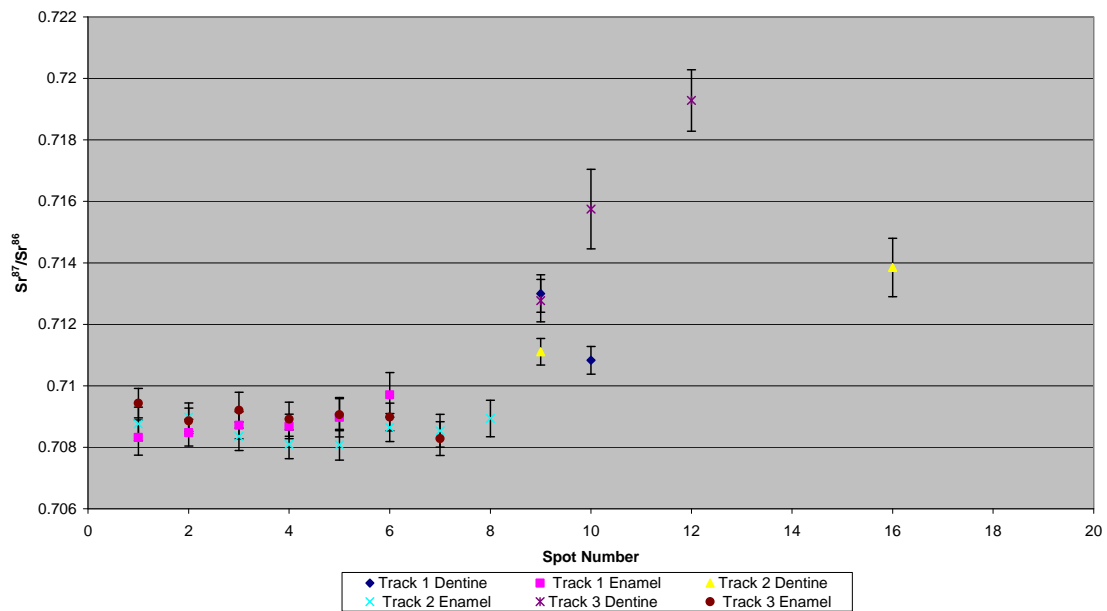


Figure A3.14 Detailed LA-MC-ICPMS Uncorrected Sr Isotope Results, Sample 1057A, Bovid, Layer B, Skhul

Sample 1057A, Corrected Sr Values, Skhul, Israel

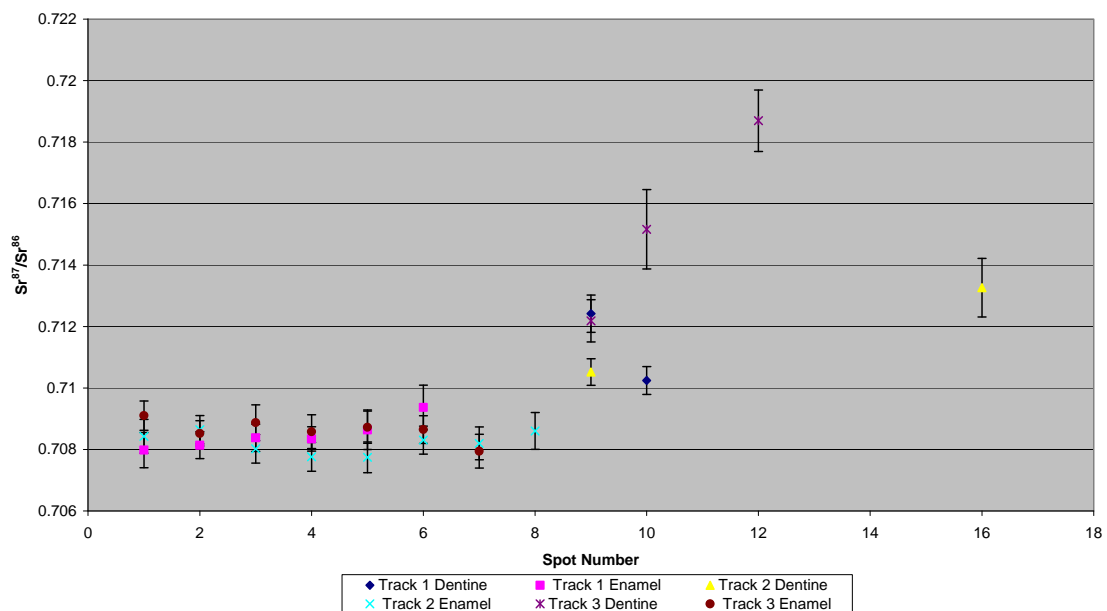


Figure A3.15 Detailed LA-MC-ICPMS Corrected Sr Isotope Results, Sample 1057A, Bovid, Layer B, Skhul

Sample 1057B, shown in Figure A2.5, was analysed as 1 track, with 9 spots in dentine and 6 spots in enamel, each collected in 2 discontinuous sections, shown in Figure A3.16. The dentine track has a weighted average uncorrected $^{87}\text{Sr}/^{86}\text{Sr}$ value of 0.70967 ± 0.00094 , a weighted average corrected $^{87}\text{Sr}/^{86}\text{Sr}$ value of 0.70892 ± 0.00094 , a weighted average $^{84}\text{Sr}/^{86}\text{Sr}$ value of 0.05679 ± 0.00031 and an average ^{88}Sr voltage of 0.351 (n=9), shown in Table 5.8 and Figure 5.5. Dentine values range from 0.708065 to 0.713162 (uncorrected) and 0.707315 to 0.712411 (corrected), shown in Figure A3.17, Figure A3.18 and Table A3.41. Dentine values show significant heterogeneity; however, the variations show some regularity, increasing from spot 1 to spot 3, then decreasing to spot 7. Spots 13 and 14 have an elevated $^{87}\text{Sr}/^{86}\text{Sr}$ value, with spot 14 showing values similar to the surrounding enamel. Enamel values for sample 1057B have an average ^{88}Sr voltage of 0.396, a weighted average uncorrected $^{87}\text{Sr}/^{86}\text{Sr}$ value of 0.7103 ± 0.0012 , a weighted average corrected $^{87}\text{Sr}/^{86}\text{Sr}$ value of 0.70970 ± 0.0012 and a weighted average $^{84}\text{Sr}/^{86}\text{Sr}$ value of 0.05685 ± 0.00019 (n=6), shown in Table 5.8 and Figure 5.5. Enamel $^{87}\text{Sr}/^{86}\text{Sr}$ value range from 0.708700 to 0.712403 (uncorrected) and 0.708130 to 0.711832 (corrected), shown in Table A3.41, Figure A3.17 and Figure A3.18, have significant heterogeneity increasing in a linear fashion from point 8 to point 12 up to the dentine-enamel junction before decreasing from sample 17 to sample 19.

The 1 track of sample 1057B has very heterogeneous enamel values, suggesting a sample mobile during amelogenesis. Enamel values are distributed in 2 somewhat homogenous domains with an uncorrected weighted average of 0.7095 ± 0.0010 (points 8, 9, 10 and 19) and 0.71193 ± 0.00042 (12, 17 and 18), respectively. The corrected value of domain 1 is 0.7089 ± 0.0010 , which is within 2σ error of the corrected value. These values cover a wide range of mapping samples surrounding the site, making it impossible to define the location of residence during amelogenesis. Neither uncorrected and corrected values from the second domain have local equivalent values in the soil and rock mapping data from this study. As this tooth is cut perpendicular to the growth direction, it suggests that bovid tooth $^{87}\text{Sr}/^{86}\text{Sr}$ heterogeneity exists in all directions.

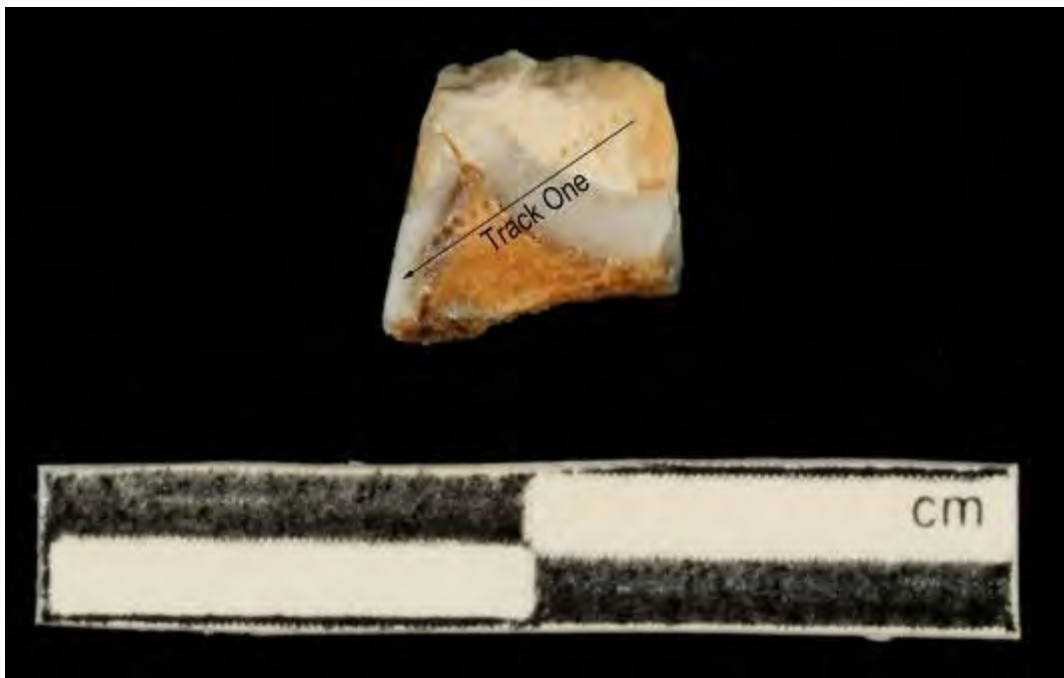


Figure A3.16 LA-MC-ICPMS Track for Sample 1057B, Bovid, Layer B, Skhul

Sample	Material	Track	Point	^{88}Sr Volts	$^{84}\text{Sr}/^{86}\text{Sr}$	$^{84}\text{Sr}/^{86}\text{Sr}$ Error	$^{87}\text{Sr}/^{86}\text{Sr}$ Corrected	$^{87}\text{Sr}/^{86}\text{Sr}$	$^{87}\text{Sr}/^{86}\text{Sr}$ 2σ Error
1057B	Dentine	1	1	0.441	0.056872	0.000508	0.709177	0.708427	0.000630
1057B	Dentine	1	2	0.213	0.056962	0.000828	0.709083	0.708333	0.001085
1057B	Dentine	1	3	0.304	0.057824	0.001107	0.711284	0.710534	0.001050
1057B	Dentine	1	4	0.299	0.057315	0.001015	0.709825	0.709075	0.000886
1057B	Dentine	1	5	0.255	0.056875	0.000779	0.709930	0.709180	0.000780
1057B	Dentine	1	6	0.340	0.056730	0.000582	0.708388	0.707638	0.000653
1057B	Dentine	1	7	0.371	0.057049	0.000733	0.708065	0.707315	0.000904
1057B	Enamel	1	8	0.549	0.056799	0.000388	0.708700	0.708130	0.000615
1057B	Enamel	1	9	0.424	0.056504	0.000566	0.709148	0.708577	0.000602
1057B	Enamel	1	10	0.317	0.056851	0.000591	0.709939	0.709368	0.000569
1057B	Enamel	1	11						
1057B	Enamel	1	12	0.354	0.057059	0.000560	0.711785	0.711214	0.000701
1057B	Dentine	1	13	0.404	0.056303	0.000502	0.710183	0.709433	0.000503
1057B	Dentine	1	14	0.287	0.056119	0.001156	0.713162	0.712411	0.001157
1057B	Dentine	1	15						

1057B	Dentine	1	16						
1057B	Enamel	1	17	0.260	0.057259	0.000875	0.712403	0.711832	0.000783
1057B	Enamel	1	18	0.323	0.057003	0.000572	0.711647	0.711076	0.000753
1057B	Enamel	1	19	0.548	0.056829	0.000404	0.710075	0.709504	0.000541

Table A3.41 Detailed LA-MC-ICPMS Sr Isotope Results for Enamel and Dentine, Sample 1057B, Bovid, Layer B, Skhul

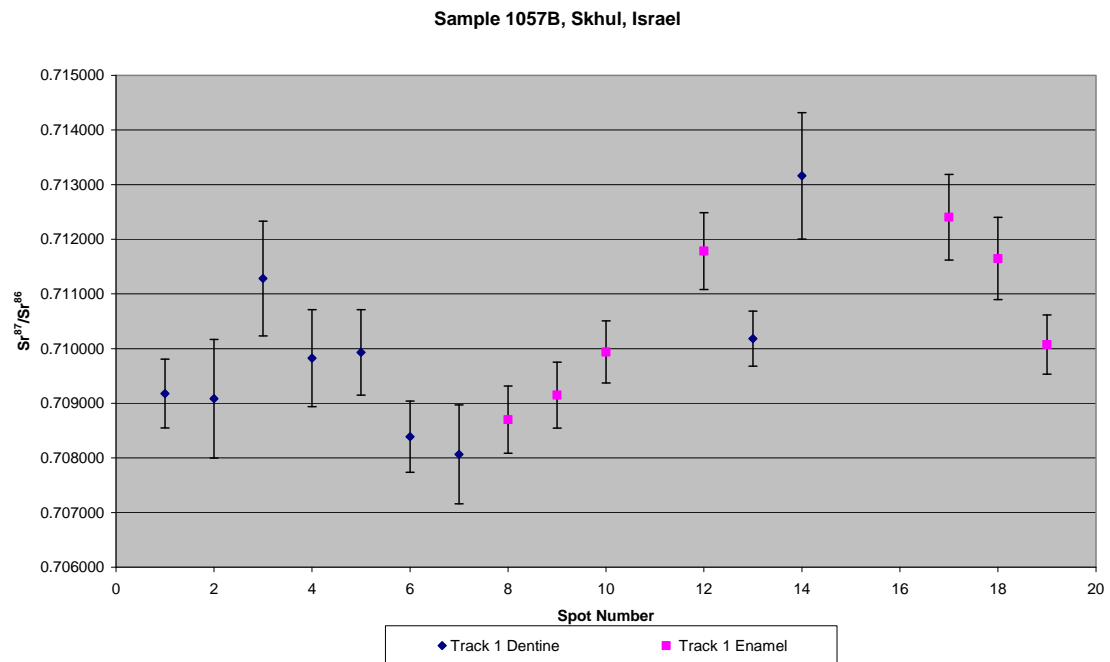


Figure A3.17 Detailed LA-MC-ICPMS Uncorrected Sr Isotope Results, Sample 1057B, Bovid, Layer B, Skhul

Sample 1057B, Corrected Sr Values, Skhul, Israel

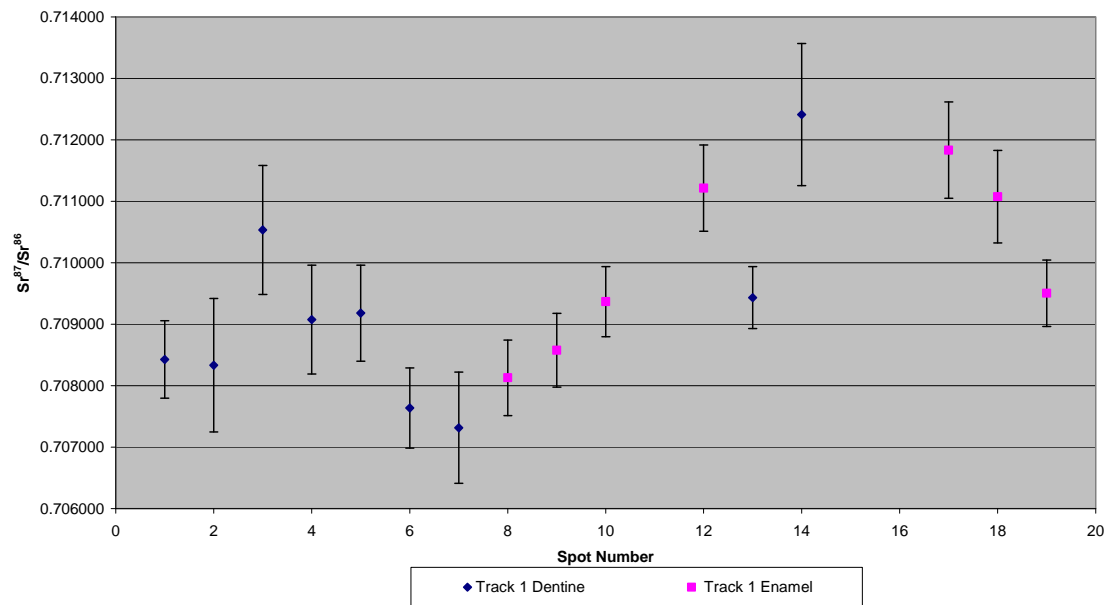


Figure A3.18 Detailed LA-MC-ICPMS Corrected Sr Isotope Results, Sample 1057B, Bovid, Layer B, Skhul

Sample 1057C, shown in Figure A2.6, was analysed in 2 tracks shown in Figure A3.19. The dentine of track 1 has an average ^{88}Sr voltage of 0.257, a weighted average uncorrected $^{87}\text{Sr}/^{86}\text{Sr}$ value of 0.71011 ± 0.00065 , a weighted average uncorrected $^{87}\text{Sr}/^{86}\text{Sr}$ value of 0.70913 ± 0.00065 and a weighted average $^{84}\text{Sr}/^{86}\text{Sr}$ value of 0.05670 ± 0.00021 ($n=13$), shown in Table 5.8 and Figure 5.5. The enamel in track 1 of sample 1057C has a weighted average uncorrected $^{87}\text{Sr}/^{86}\text{Sr}$ value of 0.71078 ± 0.00037 , a weighted average uncorrected $^{87}\text{Sr}/^{86}\text{Sr}$ value of 0.70952 ± 0.00037 , a weighted average $^{84}\text{Sr}/^{86}\text{Sr}$ value of 0.05664 ± 0.00033 and an average ^{88}Sr voltage of 0.264 ($n=5$), shown in Table 5.8 and Figure 5.5. Dentine in track 2 has a weighted average uncorrected $^{87}\text{Sr}/^{86}\text{Sr}$ value of 0.71016 ± 0.00051 , a weighted average corrected $^{87}\text{Sr}/^{86}\text{Sr}$ value of 0.70918 ± 0.00051 , a weighted average $^{84}\text{Sr}/^{86}\text{Sr}$ value of 0.05679 ± 0.00020 and an average ^{88}Sr voltage of 0.282 ($n=15$), shown in Table 5.8 and Figure 5.5. Enamel in track 2 has a weighted average uncorrected $^{87}\text{Sr}/^{86}\text{Sr}$ value of 0.7105 ± 0.0010 , a weighted average corrected $^{87}\text{Sr}/^{86}\text{Sr}$ value of 0.70920 ± 0.0010 , a weighted average $^{84}\text{Sr}/^{86}\text{Sr}$ value of 0.05691 ± 0.00077 and an average ^{88}Sr voltage of 0.264 ($n= 6$), shown in Table 5.8 and Figure 5.5. Track 1 enamel values for sample 1057C range from 0.710534 to 0.710907 (uncorrected), 0.709277 to 0.709649 (corrected), and track 1 dentine values range from 0.708399 to 0.712239 (uncorrected), 0.707419 to 0.711259 (corrected), shown in Figure A3.20, Figure A3.21 and Table A3.45. Track 2 enamel values range are 0.710023- 0.711276 (uncorrected) and 0.708766 to 0.710018 (corrected), while track 2 dentine ranges from 0.709252 to 0.712849 (uncorrected) and 0.708272 to 0.711870 (corrected), shown in Figure A3.20, Figure A3.21 and Table A3.42. The enamel values for both tracks are homogeneous within 2σ error, while dentine values are significantly more heterogeneous.

The 2 enamel tracks of sample 1057C have values that are homogenous within 2σ error. The weighted average uncorrected strontium isotope value for this sample is 0.71064 ± 0.00034 . The closest comparable value is found in the soil strontium results from the Senonian-Palaeocene aged Mount Scopus Group limestone from site IS011, which has a value of 0.710199 ± 0.000034 , although, as discussed in section 6.3.1.6, this value may not be robust. While this

analysis site is located 60 km north-north-east of Skhul, an outcrop of Mount Scopus Group sediments, not sampled in this study, outcrop within 10 km of the site on the top of the Mount Carmel Range. The weighted average corrected value of this sample is 0.70938 ± 0.00034 , which corresponds to local soil mapping values from kurkar (sample 151 from site IS001) and the Turonian Bina Formation (sample 158 from site IS007) within 2.3 km and 1 km from the site, respectively.

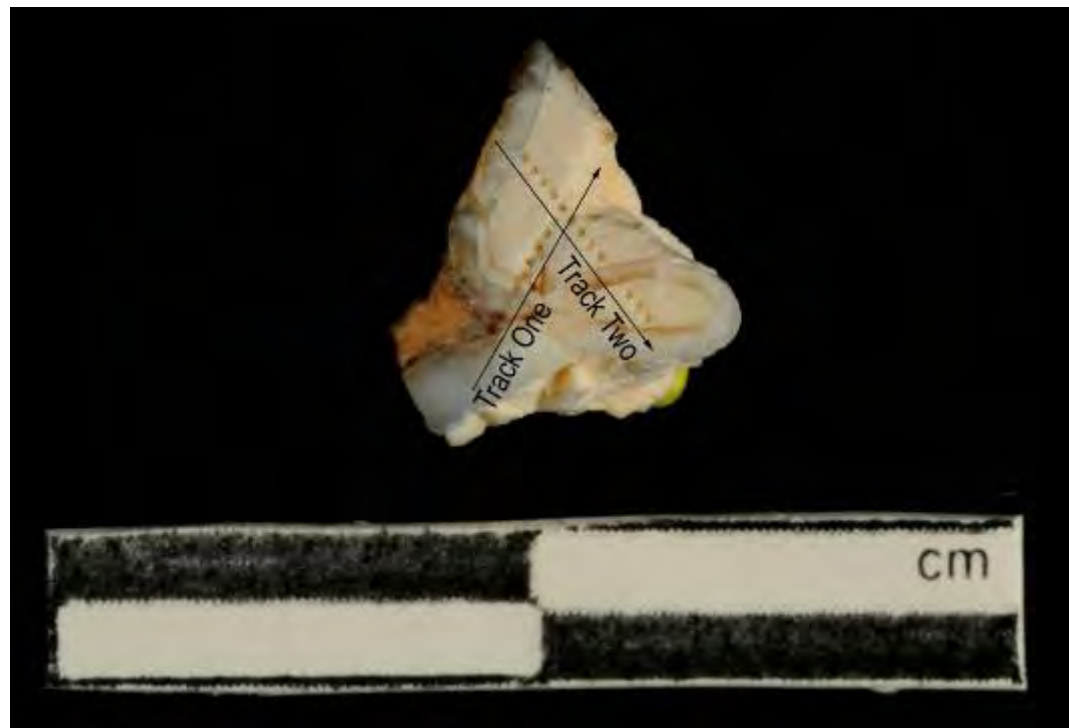


Figure A3.19 LA-MC-ICPMS Track for Sample 1057C, Bovid, Layer B, Skhul

Sample	Material	Track	Point	^{88}Sr Volts	$^{84}\text{Sr}/^{86}\text{Sr}$	$^{84}\text{Sr}/^{86}\text{Sr} 2\sigma$ Error	$^{87}\text{Sr}/^{86}\text{Sr}$ Corrected	$^{87}\text{Sr}/^{86}\text{Sr} 2\sigma$ Error
1057C	Enamel	1	1					
1057C	Enamel	1	2	0.3945	0.056823	0.000537	0.710907	0.709649
1057C	Enamel	1	3	0.241	0.056159	0.000846	0.710670	0.709413
1057C	Enamel	1	4	0.235	0.056276	0.000883	0.710669	0.709412
1057C	Enamel	1	5	0.238	0.057039	0.000830	0.710811	0.709553
1057C	Enamel	1	6	0.213	0.056588	0.000914	0.710534	0.709277
								0.000969

Sample	Material	Track	Point	88Sr Volts	84Sr/ ⁸⁶ Sr	84Sr/ ⁸⁶ Sr 2σ Error	87Sr/ ⁸⁶ Sr	Corrected 87Sr/ ⁸⁶ Sr	87Sr/ ⁸⁶ Sr 2σ Error
1057C	Dentine	1	7	0.186	0.056165	0.000952	0.711187	0.710207	0.001193
1057C	Dentine	1	8						
1057C	Enamel	1	9						
1057C	Dentine	1	10	0.248	0.056637	0.000689	0.710613	0.709633	0.000927
1057C	Dentine	1	11	0.254	0.056484	0.001135	0.712239	0.711259	0.001167
1057C	Dentine	1	12	0.204	0.057506	0.000850	0.711412	0.710433	0.001147
1057C	Dentine	1	13	0.245	0.056835	0.000853	0.709032	0.708052	0.000807
1057C	Dentine	1	14	0.263	0.056136	0.000872	0.710368	0.709389	0.000811
1057C	Dentine	1	15	0.259	0.056727	0.000919	0.709693	0.708713	0.000885
1057C	Dentine	1	16	0.280	0.056770	0.000611	0.711349	0.710370	0.000838
1057C	Dentine	1	17	0.265	0.056401	0.000920	0.710954	0.709975	0.001099
1057C	Dentine	1	18	0.291	0.056880	0.000777	0.709030	0.708051	0.000916
1057C	Dentine	1	19	0.312	0.056992	0.000606	0.708399	0.707419	0.000779
1057C	Dentine	1	20	0.220	0.056221	0.000852	0.710180	0.709201	0.001333
1057C	Dentine	1	21	0.315	0.056733	0.000644	0.709884	0.708904	0.000656
1057C	Enamel	2	1	0.247	0.057008	0.000866	0.711104	0.709846	0.000894
1057C	Enamel	2	2	0.240	0.056161	0.000780	0.710023	0.708766	0.000749
1057C	Dentine	2	3	0.290	0.056843	0.000623	0.710847	0.709867	0.000876
1057C	Dentine	2	4	0.278	0.056561	0.000648	0.711270	0.710291	0.001024
1057C	Dentine	2	5	0.288	0.056807	0.000711	0.709580	0.708601	0.000808
1057C	Dentine	2	6	0.270	0.056613	0.000605	0.709544	0.708565	0.001003
1057C	Dentine	2	7	0.288	0.057000	0.000505	0.709516	0.708537	0.000722
1057C	Dentine	2	8	0.309	0.057472	0.000763	0.709563	0.708583	0.000687
1057C	Dentine	2	9	0.333	0.056676	0.000592	0.709738	0.708758	0.000714
1057C	Dentine	2	10	0.203	0.056852	0.001006	0.710239	0.709259	0.001042
1057C	Dentine	2	11	0.268	0.057306	0.000787	0.709654	0.708675	0.000801
1057C	Enamel	2	12	0.288	0.057285	0.000536	0.710122	0.708865	0.000618
1057C	Enamel	2	13	0.283	0.056813	0.000748	0.711276	0.710018	0.000853
1057C	Dentine	2	14	0.238	0.056635	0.000751	0.709252	0.708272	0.000980
1057C	Dentine	2	15	0.271	0.056557	0.000738	0.712849	0.711870	0.000925
1057C	Dentine	2	16	0.268	0.057392	0.000573	0.710486	0.709506	0.001010
1057C	Dentine	2	17	0.234	0.056186	0.000892	0.711712	0.710732	0.001108
1057C	Dentine	2	18	0.305	0.056136	0.000694	0.710408	0.709428	0.000802
1057C	Dentine	2	19	0.380	0.056637	0.000507	0.709882	0.708903	0.000710

Table A3.42 Detailed LA-MC-ICPMS Sr Isotope Results for Enamel and Dentine, Sample 1057C, Bovid, Layer B, Skhul

Sample 1057C, Skhul, Israel

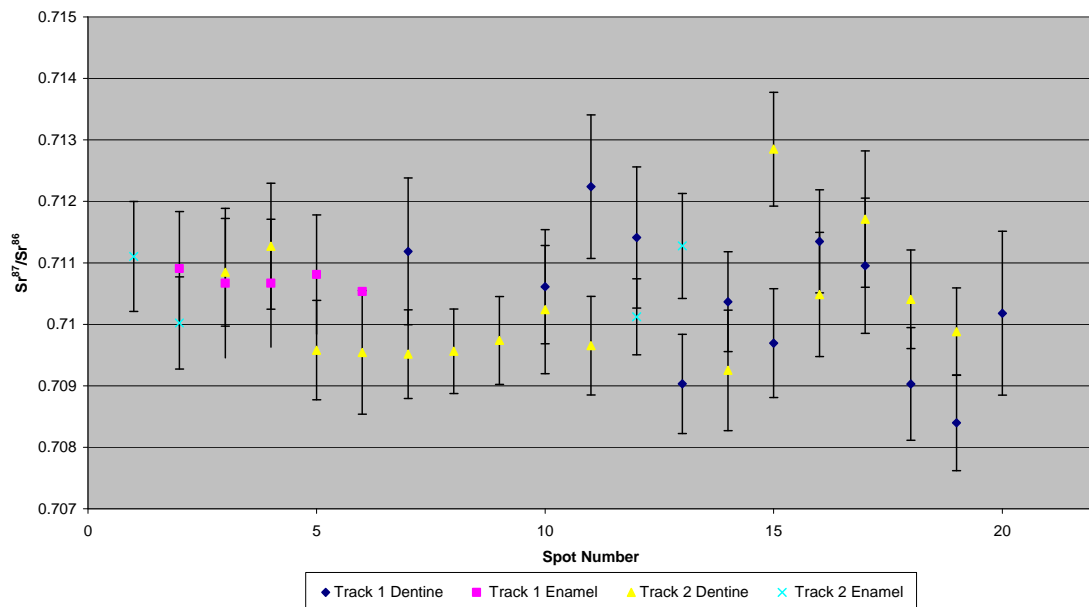


Figure A3.20 Detailed LA-MC-ICPMS Uncorrected Sr Isotope Results, Sample 1057C, Bovid, Layer B, Skhul

Sample 1057C, Corrected Sr Values, Skhul, Israel

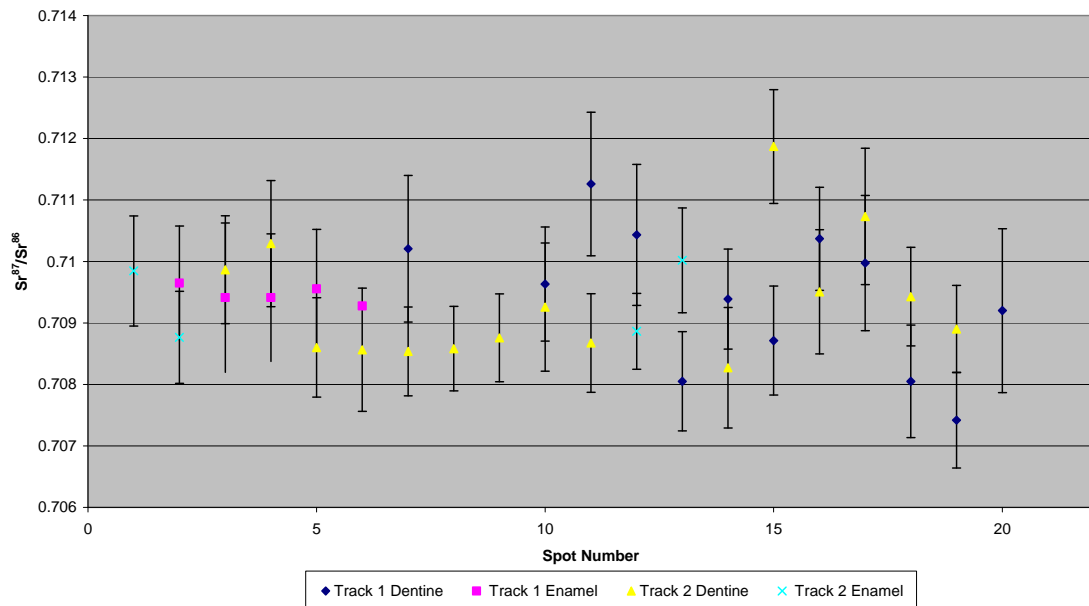


Figure A3.21 Detailed LA-MC-ICPMS Corrected Sr Isotope Results, Sample 1057C, Bovid, Layer B, Skhul

Skhul 1058 comprises 3 teeth (A, B and C) from a pig mandible buried in the arms of the Skhul V hominin in layer 2 of Skhul. Sample 1058A, shown in Figure A2.7, was analysed as 1 track, with 9 spots in dentine and 8 spots in enamel, shown in Figure A3.22. The enamel has an average ^{88}Sr voltage of 0.141, a weighted average uncorrected $^{87}\text{Sr}/^{86}\text{Sr}$ value of 0.71072 ± 0.00057 , a weighted average corrected $^{87}\text{Sr}/^{86}\text{Sr}$ value of 0.70774 ± 0.00057 and a weighted average $^{84}\text{Sr}/^{86}\text{Sr}$ value of 0.05556 ± 0.00048 ($n=8$), shown in Table 5.8 and Figure 5.5. Sample 1058A dentine has an average ^{88}Sr voltage of 0.292, a weighted average uncorrected $^{87}\text{Sr}/^{86}\text{Sr}$ value of 0.70900 ± 0.00037 , a weighted average corrected $^{87}\text{Sr}/^{86}\text{Sr}$ value of 0.70829 ± 0.00037 and a weighted average $^{84}\text{Sr}/^{86}\text{Sr}$ value of 0.05610 ± 0.00024 ($n=9$), shown in Table 5.8 and Figure 5.5. Enamel values range from 0.709738 to 0.712163 (uncorrected) and 0.706763 to 0.709188 (corrected), while dentine values range from 0.708609 to 0.709800 (uncorrected) and 0.707897 to 0.709088 (corrected), shown in Table A3.43, Figure A3.23 and Figure A3.24. Enamel and dentine values are homogeneous with 2σ error.

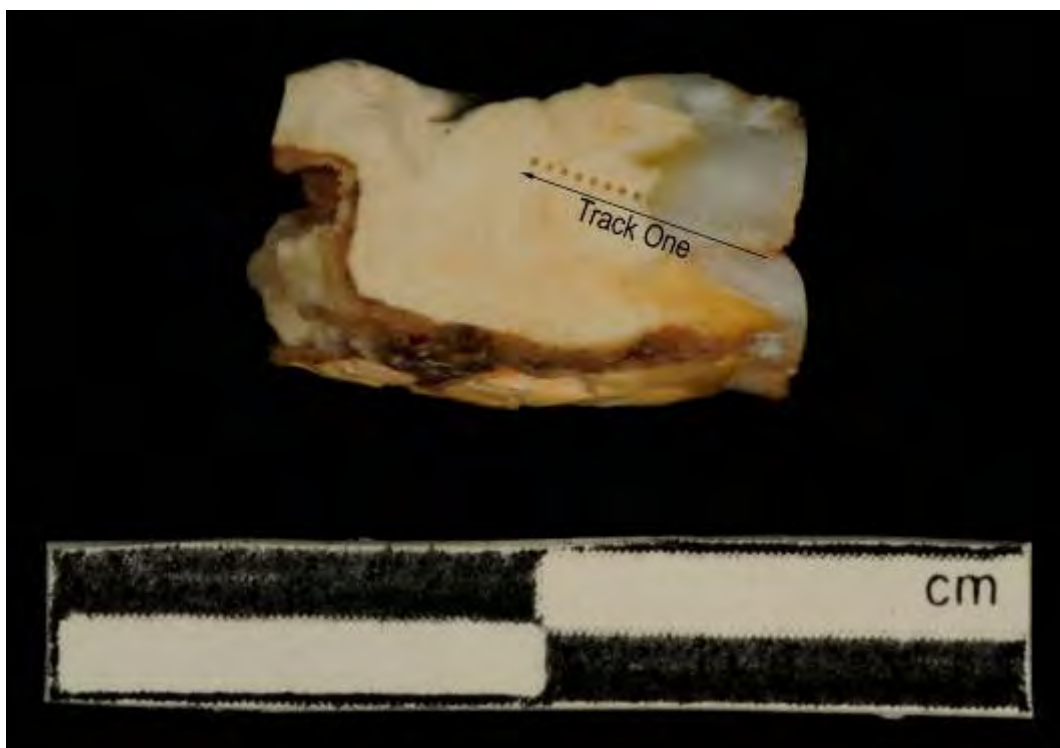


Figure A3.22 LA-MC-ICPMS Track for Sample 1058A, Wild Boar, Layer B, Skhul

Sample	Material	Track	Point	^{88}Sr Volts	$^{84}\text{Sr}/^{86}\text{Sr}$	$^{84}\text{Sr}/^{86}\text{Sr} 2\sigma$ Error	$^{87}\text{Sr}/^{86}\text{Sr}$	Corrected $^{87}\text{Sr}/^{86}\text{Sr}$	$^{87}\text{Sr}/^{86}\text{Sr} 2\sigma$ Error
1058A	Enamel	1	1						
1058A	Enamel	1	2	0.130	0.055981	0.001294	0.712163	0.709188	0.001623
1058A	Enamel	1	3	0.138	0.054790	0.001611	0.709738	0.706763	0.001782
1058A	Enamel	1	4	0.146	0.055712	0.001328	0.709990	0.707015	0.001638
1058A	Enamel	1	5	0.144	0.056614	0.001660	0.709992	0.707017	0.001751
1058A	Enamel	1	6	0.137	0.054873	0.001482	0.711275	0.708300	0.001461
1058A	Enamel	1	7	0.131	0.055234	0.001721	0.711466	0.708491	0.001779
1058A	Enamel	1	8	0.140	0.054989	0.001737	0.709956	0.706981	0.001816
1058A	Enamel	1	9	0.165	0.055698	0.000906	0.710704	0.707729	0.001492
1058A	Dentine	1	10	0.258	0.056213	0.000702	0.709800	0.709088	0.000825
1058A	Dentine	1	11	0.226	0.056703	0.001155	0.708609	0.707897	0.001000
1058A	Dentine	1	12	0.331	0.056593	0.000655	0.708804	0.708093	0.000821
1058A	Dentine	1	13	0.340	0.056256	0.000674	0.709099	0.708387	0.000772
1058A	Dentine	1	14	0.308	0.056016	0.000678	0.708174	0.707463	0.000720
1058A	Dentine	1	15	0.305	0.055863	0.000691	0.708816	0.708104	0.000788
1058A	Dentine	1	16	0.289	0.056067	0.000687	0.709310	0.708599	0.000811
1058A	Dentine	1	17	0.299	0.055699	0.000905	0.709311	0.708599	0.000750
1058A	Dentine	1	18	0.275	0.055579	0.000720	0.709160	0.708448	0.000799

Table A3.43 Detailed LA-MC-ICPMS Sr Isotope Results for Enamel and Dentine, Wild Boar, Layer B, Skhul

Sample 1058A, Skhul, Israel

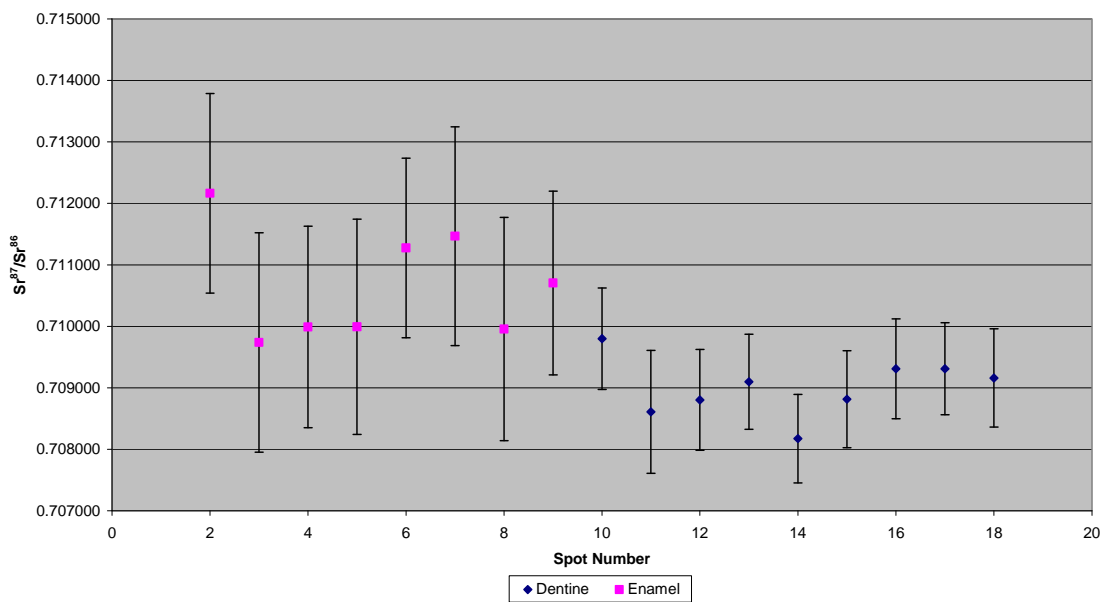


Figure A3.23 Detailed LA-MC-ICPMS Uncorrected Sr Isotope Results, Sample 1058A, Wild Boar, Layer B, Skhul

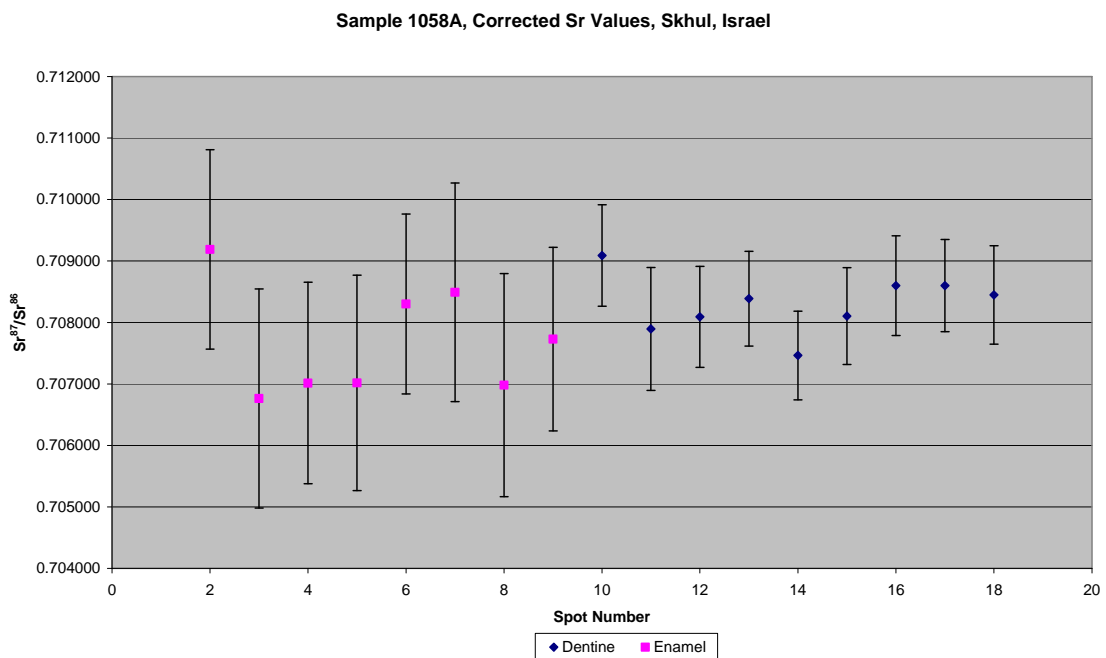


Figure A3.24 Detailed LA-MC-ICPMS Corrected Sr Isotope Results, Sample 1058A, Wild Boar, Layer B, Skhul

Sample 1058B, shown in Figure A2.8, was analysed with 2 tracks: track 1 has 11 dentine spots and 5 enamel spots and track 2 has 6 dentine spots and 8 enamel spots, shown in Figure A3.25. Track 1 in dentine has an average ^{88}Sr voltage of 0.329, a weighted average uncorrected $^{87}\text{Sr}/^{86}\text{Sr}$ value of 0.70854 ± 0.00020 , a weighted average corrected $^{87}\text{Sr}/^{86}\text{Sr}$ value of 0.70795 ± 0.00020 and a weighted average $^{84}\text{Sr}/^{86}\text{Sr}$ value of 0.05609 ± 0.00018 ($n=11$), shown in Table 5.8 and Figure 5.5. The enamel in this track has an average ^{88}Sr voltage of 0.131, a weighted average uncorrected $^{87}\text{Sr}/^{86}\text{Sr}$ value of 0.71099 ± 0.00067 , a weighted average corrected $^{87}\text{Sr}/^{86}\text{Sr}$ value of 0.70719 ± 0.00067 and a weighted average $^{84}\text{Sr}/^{86}\text{Sr}$ value of 0.05481 ± 0.00063 ($n=5$), shown in Table 5.8 and Figure 5.5. The dentine in track 2 has an average ^{88}Sr voltage of 0.321, a weighted average uncorrected $^{87}\text{Sr}/^{86}\text{Sr}$ value of 0.70850 ± 0.00028 , a weighted average corrected $^{87}\text{Sr}/^{86}\text{Sr}$ value of 0.70787 ± 0.00028 and a weighted average $^{84}\text{Sr}/^{86}\text{Sr}$ value of 0.05619 ± 0.00026 ($n=6$), shown in Table 5.8 and Figure 5.5. The enamel in track 2 has an average ^{88}Sr voltage of 0.129, a weighted average uncorrected $^{87}\text{Sr}/^{86}\text{Sr}$ value of 0.71015 ± 0.00061 , a weighted average corrected $^{87}\text{Sr}/^{86}\text{Sr}$ value of 0.70681 ± 0.00061 and a weighted average $^{84}\text{Sr}/^{86}\text{Sr}$ value of 0.05616 ± 0.00054 ($n=8$), shown in Table 5.8 and Figure 5.5. Enamel values for track 1 of sample 1058B are in the range of 0.709898 to 0.711723 (uncorrected) and 0.706105 to 0.707929 (corrected), as well as 0.709083 to 0.711442 (uncorrected) and 0.705741 to 0.708100 (corrected) for track 2, shown in Table A3.44, Figure A3.26 and Figure A3.27. Sample 1058B has dentine values for track 1 of 0.708197 to 0.708845 (uncorrected) and 0.707598 to 0.708246 (corrected), as well as for track 2 of 0.708229 to 0.708788 (uncorrected) and 0.707598 to 0.708157 (corrected). Dentine values for tracks 1 and 2 are homogeneous within 2σ error range, enamel values for tracks 1 and 2 are also homogeneous within 2σ error; however, the error range is significantly larger for enamel than for dentine.

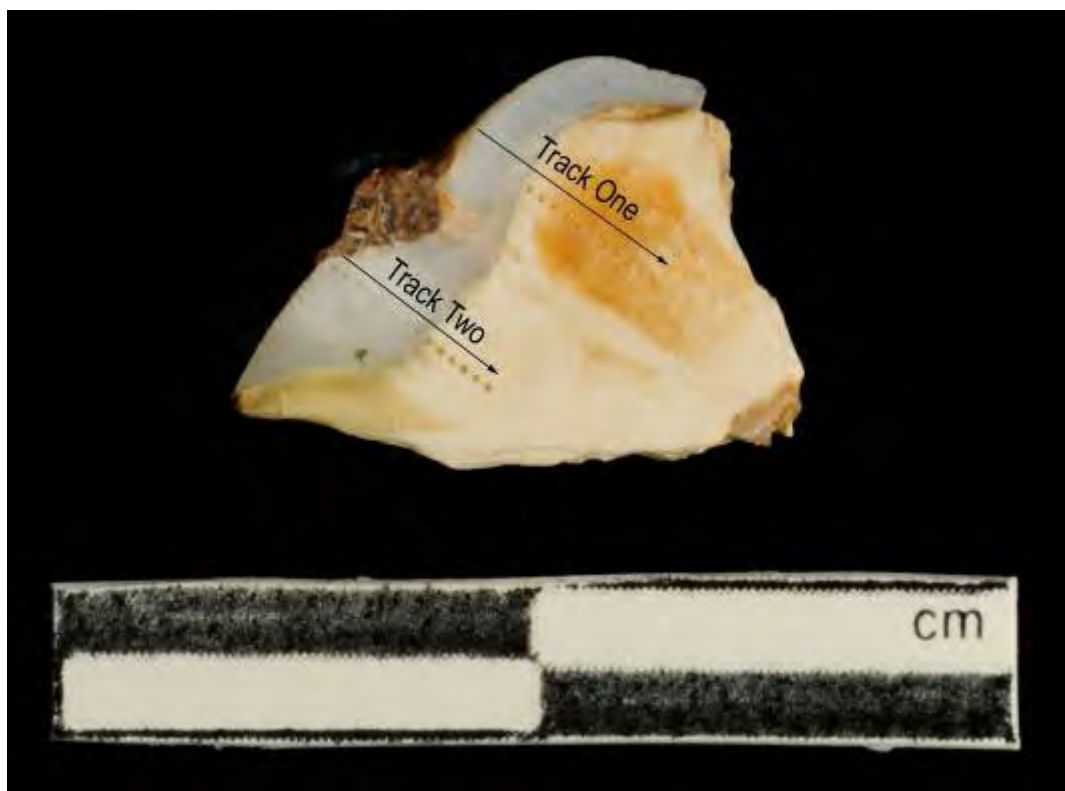


Figure A3.25 LA-MC-ICPMS Track for Sample 1058B, Wild Boar, Layer B, Skhul

Sample	Material	Track	Point	^{88}Sr Volts	$^{84}\text{Sr}/^{86}\text{Sr}$	$^{84}\text{Sr}/^{86}\text{Sr} 2\sigma$ Error	$^{87}\text{Sr}/^{86}\text{Sr}$	Corrected $^{87}\text{Sr}/^{86}\text{Sr}$	$^{87}\text{Sr}/^{86}\text{Sr} 2\sigma$ Error
1058B	Enamel	1	1	0.119	0.055059	0.001555	0.711723	0.707929	0.001510
1058B	Enamel	1	2	0.124	0.053462	0.001472	0.711448	0.707655	0.001902
1058B	Enamel	1	3	0.119	0.055197	0.001729	0.711512	0.707719	0.002724
1058B	Enamel	1	4	0.139	0.055191	0.001693	0.711113	0.707320	0.001187
1058B	Enamel	1	5	0.156	0.055120	0.001092	0.709898	0.706105	0.001338
1058B	Dentine	1	6	0.380	0.055934	0.000543	0.708471	0.707871	0.000697
1058B	Dentine	1	7	0.276	0.056545	0.000746	0.708834	0.708235	0.000820
1058B	Dentine	1	8	0.308	0.055869	0.000637	0.708515	0.707915	0.000590
1058B	Dentine	1	9	0.322	0.056252	0.000871	0.708197	0.707598	0.000595
1058B	Dentine	1	10	0.360	0.056258	0.000528	0.708845	0.708246	0.000879
1058B	Dentine	1	11	0.333	0.055676	0.000654	0.708660	0.708060	0.000564
1058B	Dentine	1	12	0.336	0.056203	0.000531	0.708710	0.708111	0.000686
1058B	Dentine	1	13	0.318	0.056139	0.000660	0.708656	0.708057	0.000685
1058B	Dentine	1	14	0.322	0.055928	0.000624	0.708720	0.708120	0.000656
1058B	Dentine	1	15	0.330	0.056065	0.000519	0.708265	0.707665	0.000754
1058B	Dentine	1	16	0.329	0.056220	0.000521	0.708243	0.707644	0.000808
1058B	Enamel	2	1						
1058B	Enamel	2	2	0.117	0.055957	0.001856	0.709431	0.706089	0.001869
1058B	Enamel	2	3	0.110	0.056668	0.001447	0.709083	0.705741	0.001973
1058B	Enamel	2	4	0.117	0.056714	0.002099	0.711194	0.707852	0.001948
1058B	Enamel	2	5	0.130	0.056635	0.001700	0.711213	0.707871	0.002171
1058B	Enamel	2	6	0.140	0.056202	0.001393	0.710012	0.706670	0.001582
1058B	Enamel	2	7	0.148	0.055954	0.001345	0.709675	0.706333	0.001626
1058B	Enamel	2	8	0.133	0.055693	0.001352	0.711442	0.708100	0.001831
1058B	Enamel	2	9	0.138	0.055713	0.001780	0.709829	0.706487	0.001420
1058B	Dentine	2	10	0.314	0.056210	0.000855	0.708788	0.708157	0.000768
1058B	Dentine	2	11	0.321	0.056300	0.000557	0.708229	0.707598	0.000590
1058B	Dentine	2	12	0.321	0.056299	0.000644	0.708239	0.707608	0.000804
1058B	Dentine	2	13	0.310	0.055708	0.000673	0.708471	0.707840	0.000772
1058B	Dentine	2	14	0.328	0.056284	0.000568	0.708751	0.708120	0.000676
1058B	Dentine	2	15	0.335	0.056256	0.000642	0.708589	0.707958	0.000729

Table A3.44 Detailed LA-MC-ICPMS Sr Isotope Results for Enamel and Dentine, Wild Boar, Layer B, Skhul

Sample 1058B, Skhul, Israel

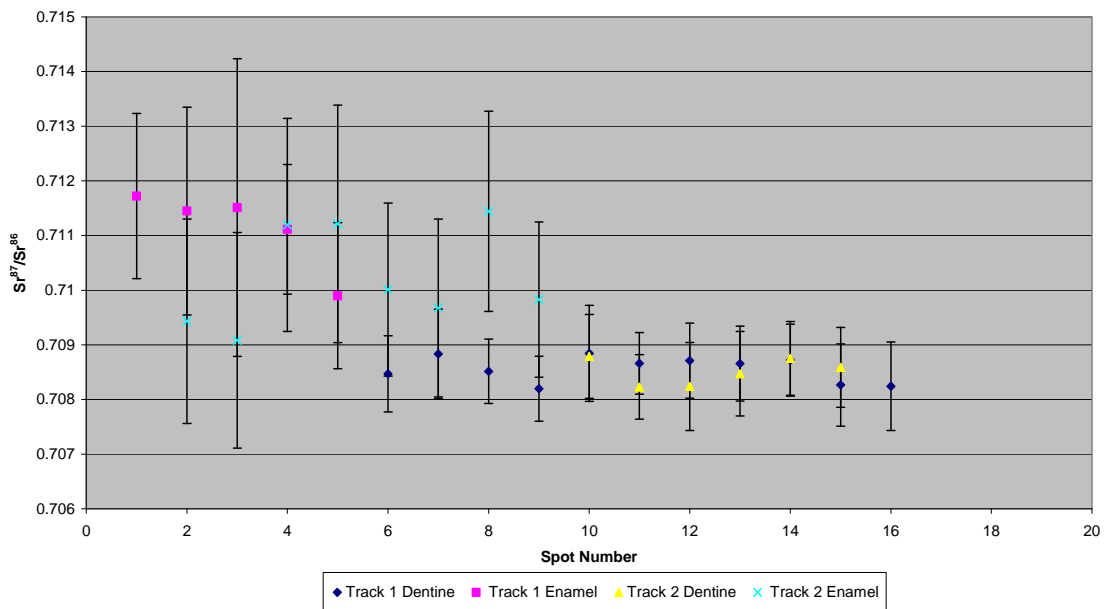


Figure A3.26 Detailed LA-MC-ICPMS Uncorrected Sr Isotope Results, Sample 1058B, Wild Boar, Layer B, Skhul

Sample 1058B, Corrected Sr Values, Skhul, Israel

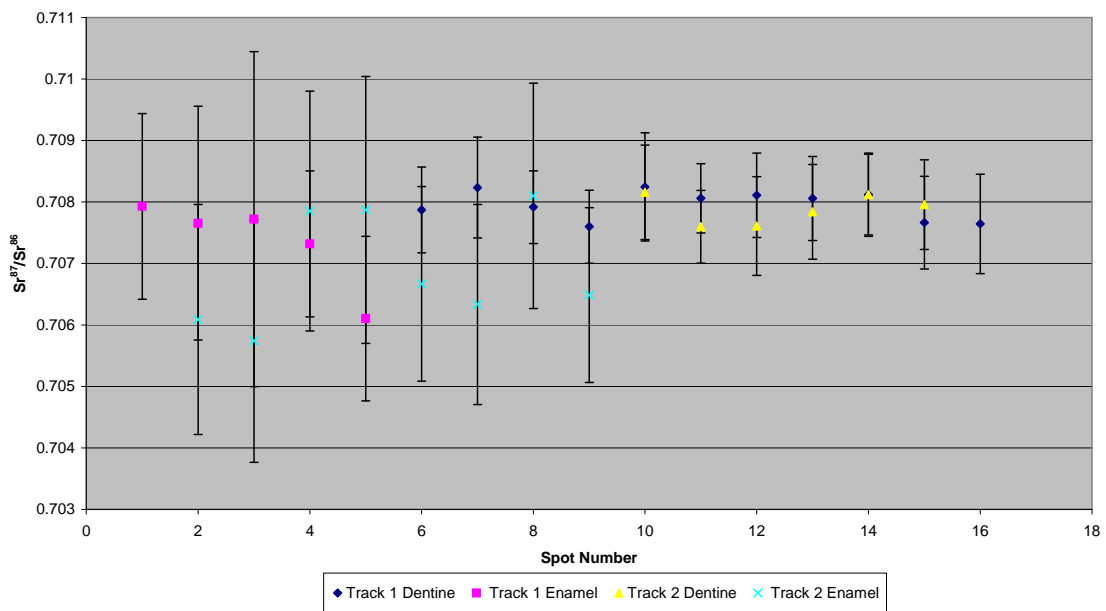


Figure A3.27 Detailed LA-MC-ICPMS Corrected Sr Isotope Results, Sample 1058B, Wild Boar, Layer B, Skhul

Sample 1058C, shown in Figure A2.9, was analysed in 1 track, with 9 spots in dentine and 7 spots in enamel, shown in Figure A3.28. Dentine from sample 1058C has an average ^{88}Sr voltage of 0.331, a weighted average uncorrected $^{87}\text{Sr}/^{86}\text{Sr}$ value of 0.70899 ± 0.00058 , a weighted average corrected $^{87}\text{Sr}/^{86}\text{Sr}$ value of 0.70842 ± 0.00058 and a weighted average $^{84}\text{Sr}/^{86}\text{Sr}$ value of 0.05615 ± 0.00020 ($n=9$), shown in Table 5.8 and Figure 5.5. Sample 1058C enamel has an average ^{88}Sr voltage of 0.129, a weighted average uncorrected $^{87}\text{Sr}/^{86}\text{Sr}$ value of 0.7113 ± 0.0023 , a weighted average corrected $^{87}\text{Sr}/^{86}\text{Sr}$ value of 0.70710 ± 0.0023 and a weighted average $^{84}\text{Sr}/^{86}\text{Sr}$ value of 0.05610 ± 0.00053 ($n=7$), shown in Table 5.8 and Figure 5.5. Enamel $^{87}\text{Sr}/^{86}\text{Sr}$ values for sample 1058C range from 0.708304 to 0.715464 (uncorrected) and 0.704170 to 0.711329 (corrected), while dentine $^{87}\text{Sr}/^{86}\text{Sr}$ values range from 0.708710 to 0.712346 (uncorrected) and 0.708144 to 0.711780 (corrected), shown in Table A3.45, Figure A3.29 and Figure A3.30. Enamel strontium isotope values, with the exception of spot 1, are homogeneous within 2σ error and dentine strontium isotope values, with the exception of spot 16, are also homogeneous within 2σ error.



Figure A3.28 LA-MC-ICPMS Track for Sample 1058C, Wild Boar, Layer B, Skhul

Sample	Material	Track	Point	^{88}Sr Volts	$^{84}\text{Sr}/^{86}\text{Sr}$	$^{84}\text{Sr}/^{86}\text{Sr} 2\sigma$ Error	Corrected $^{87}\text{Sr}/^{86}\text{Sr}$	$^{87}\text{Sr}/^{86}\text{Sr}$	$^{87}\text{Sr}/^{86}\text{Sr} 2\sigma$ Error
1058C	Enamel	1	1	0.180	0.056240	0.000876	0.715464	0.711329	0.001408
1058C	Enamel	1	2	0.114	0.056567	0.002095	0.710188	0.706054	0.001864
1058C	Enamel	1	3	0.116	0.055682	0.001411	0.709347	0.705213	0.001792
1058C	Enamel	1	4	0.123	0.055119	0.001617	0.710895	0.706761	0.001542
1058C	Enamel	1	5	0.114	0.055663	0.001934	0.709802	0.705668	0.001532
1058C	Enamel	1	6	0.119	0.056387	0.001911	0.708304	0.704170	0.001960
1058C	Enamel	1	7	0.135	0.056817	0.001485	0.711879	0.707745	0.001410
1058C	Dentine	1	8	0.341	0.056217	0.000609	0.708710	0.708144	0.000539
1058C	Dentine	1	9	0.346	0.055814	0.000562	0.708848	0.708282	0.000717
1058C	Dentine	1	10	0.340	0.056334	0.000596	0.708676	0.708109	0.000606
1058C	Dentine	1	11	0.290	0.056149	0.000660	0.708641	0.708074	0.000882
1058C	Dentine	1	12	0.292	0.055644	0.000720	0.709382	0.708816	0.000897
1058C	Dentine	1	13	0.348	0.056085	0.000539	0.709044	0.708477	0.000718
1058C	Dentine	1	14	0.371	0.056182	0.000512	0.709253	0.708687	0.000757
1058C	Dentine	1	15	0.344	0.056678	0.000619	0.708721	0.708155	0.000564
1058C	Dentine	1	16	0.303	0.056297	0.001190	0.712346	0.711780	0.001191
1058C	Dentine	1	17						

Table A3.45 Detailed LA-MC-ICPMS Sr Isotope Results for Enamel and Dentine, Sample 1058C, Wild Boar, Layer B, Skhul

Sample 1058A, Skhul, Israel

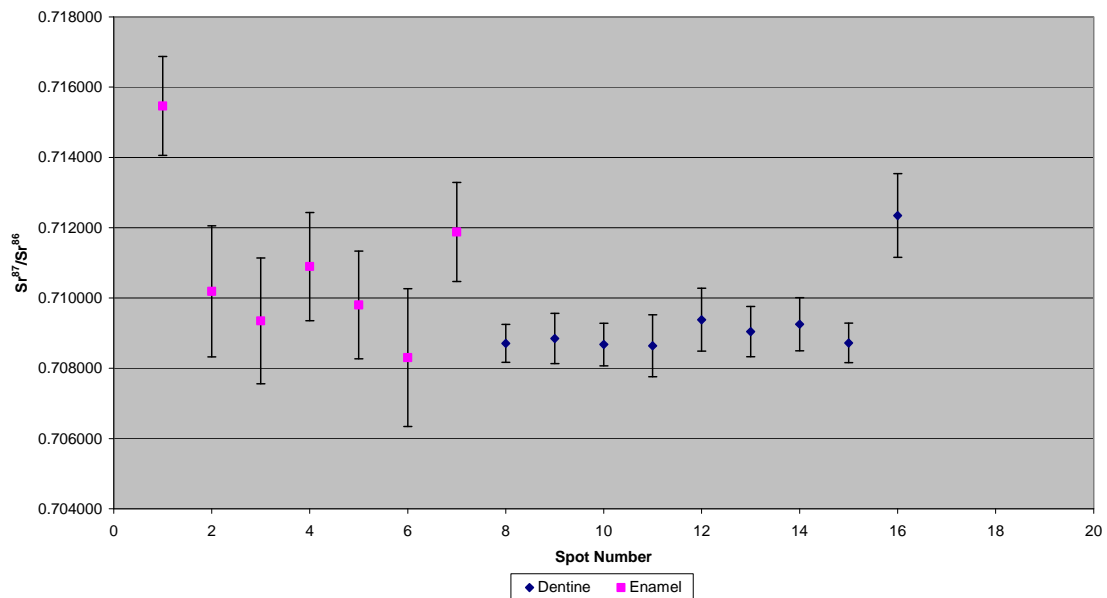


Figure A3.29 Detailed LA-MC-ICPMS Uncorrected Sr Isotope Results, Sample 1058A, Wild Boar, Layer B, Skhul

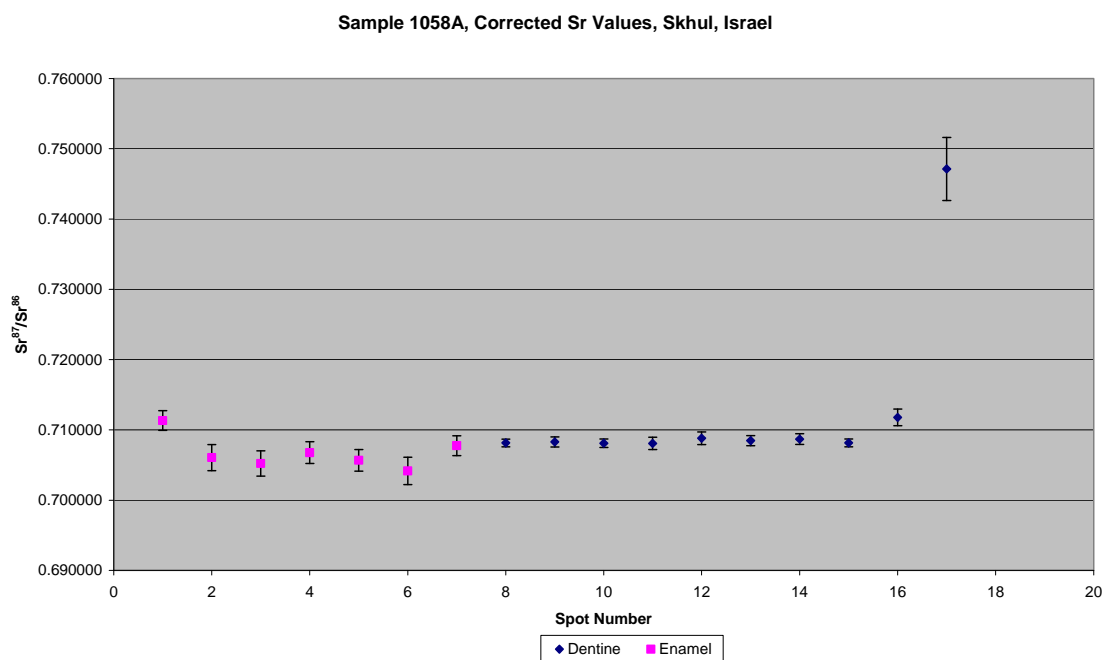


Figure A3.30 Detailed LA-MC-ICPMS Corrected Sr Isotope Results, Sample 1058A, Wild Boar, Layer B, Skhul

The $^{87}\text{Sr}/^{86}\text{Sr}$ values for the enamel spots in 1058A, 1058B and 1058C vary considerably, the 2σ errors are large and so the samples from all tracks on

samples 1058A, B and C are statistically indistinguishable. The weighted average uncorrected value of these spots is 0.71053 ± 0.00037 . The only exception is spot 1 from sample 1058C, which probably reflects an unfocused laser, due to being partially off the edge of the sample. The closest comparable value is found in the soil strontium results from the Senonian-Palaeocene aged Mount Scopus Group limestone from sample 162 at site IS011, which has a value of 0.710199 ± 0.000034 , although, as discussed in section 6.3.1.6, this value may not be robust. While this analysis site is located 60 km north-north-east of Skhul, an outcrop of Mount Scopus Group sediments, not sampled in this study, outcrop within 5.4 km of the site on the top of the Mount Carmel Range. The corrected weighted average value of sample 1058 is 0.70723 ± 0.00054 , which corresponds to sample 175 from site IS024 and sample 202 from site IS053, both from the Cover/Dalwe Basalt and located approximately 65 km east of Skhul. This unit outcrops within 25 km of Skhul; however, Upper Cretaceous basalts, unsampled in this study, which probably has a similar strontium isotope composition, outcrop within 1.1 km of the site.

A3.2.2.2. Tabun

Sample 554, a *Bos* tooth from layer D at Tabun shown in Figure A2.10, was analysed using 1 track with 2 spots collected in enamel, shown in Figure A3.31. Enamel from sample 554 has an average ^{88}Sr voltage of 1.904, a weighted average uncorrected $^{87}\text{Sr}/^{86}\text{Sr}$ value of 0.70984 ± 0.00042 , a weighted average corrected $^{87}\text{Sr}/^{86}\text{Sr}$ value of 0.70911 ± 0.00042 and a weighted average $^{84}\text{Sr}/^{86}\text{Sr}$ value of 0.056447 ± 0.000080 ($n=2$), shown in Table 5.12 and Figure 5.7. The 2 spots have a relatively homogeneous $^{87}\text{Sr}/^{86}\text{Sr}$ composition within 2σ error, shown in Table A3.46, Figure A3.32 and Figure A3.33.

The strontium isotope values of this sample are summarised in Table 5.51 and Figure 5.7 and shown in detail in Table A3.46, Figure A3.32 and Figure A3.33. Enamel from this sample has relatively homogenous enamel strontium isotope composition with a weighted average uncorrected value of 0.70984 ± 0.00042 . This value is slightly elevated compared to, but within 2σ error of, local unconsolidated coastal plain sediments, such as sample 152 from site IS002, suggesting that this specimen lived local to Tabun during amelogenesis. The weighted average corrected enamel value for this sample is 0.70911 ± 0.00042 , which corresponds to a large number of mapping samples surrounding the site, including from carbonates of the Mount Carmel Range IS005, IS006, IS007, IS019 and IS021, as well as kurkar from the coastal plain, including IS001 and IS003, the closest of which outcrops within 1 km of the archaeological site.

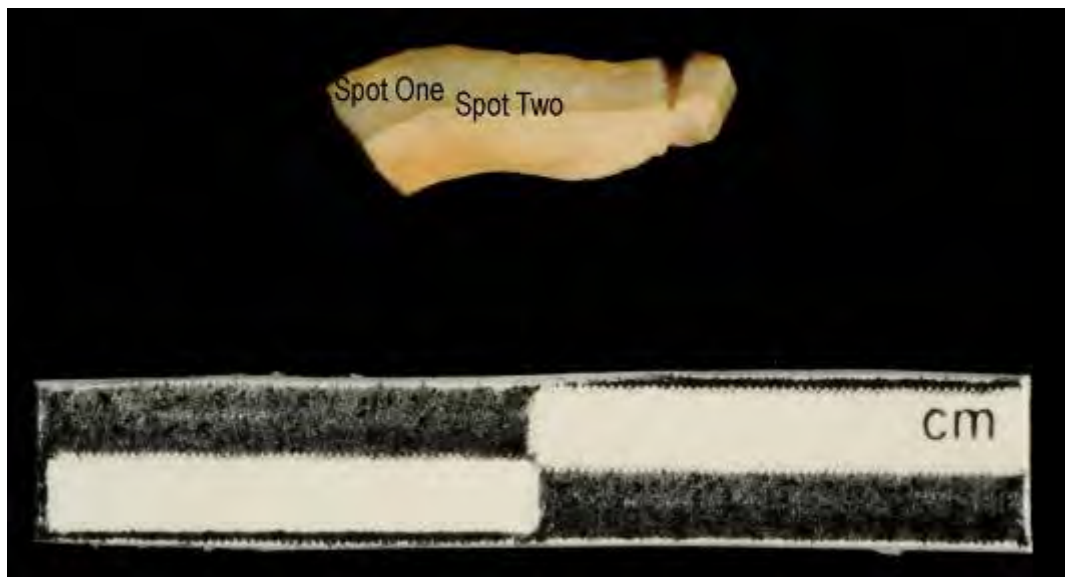


Figure A3.31 LA-MC-ICPMS Track for Sample 554, *Bos*, Layer D, Tabun

Sample	Material	Track	Point	^{88}Sr Volts	$^{84}\text{Sr}/^{86}\text{Sr}$	Corrected $^{87}\text{Sr}/^{86}\text{Sr}$	$^{87}\text{Sr}/^{86}\text{Sr}$ Error	$^{87}\text{Sr}/^{86}\text{Sr}$ 2σ
554	Enamel	1	1	2.143	0.056430	0.000096	0.709811	0.709077
554	Enamel	1	2	1.665	0.056491	0.000152	0.709889	0.709155

Table A3.46 Detailed LA-MC-ICPMS Sr Isotope Results for Enamel, Sample 554, *Bos*, Layer D, Tabun

Sample 554, Tabun, Israel

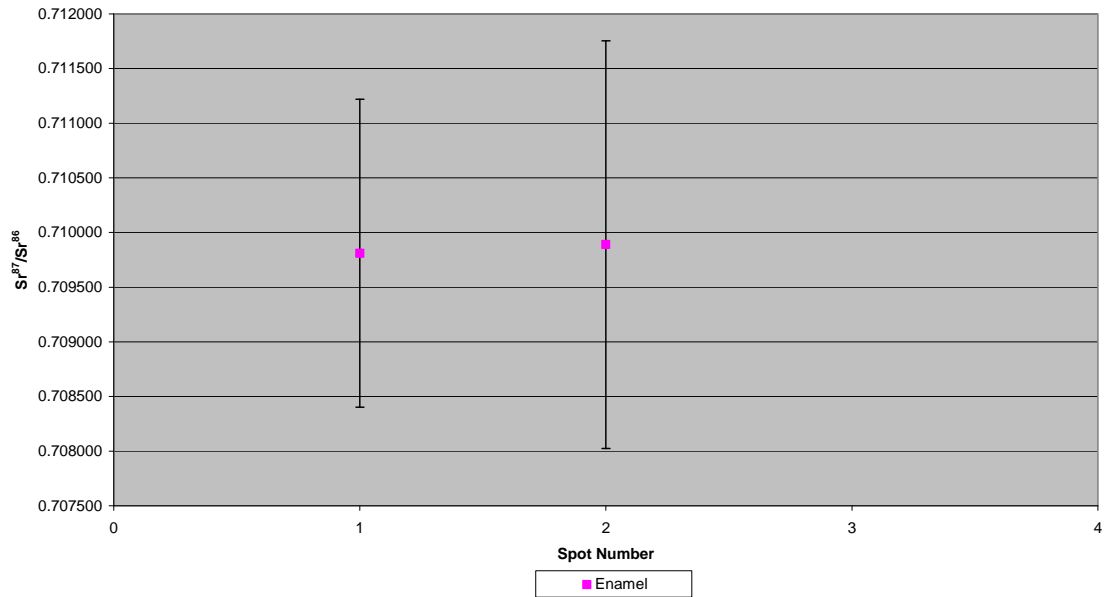


Figure A3.32 Detailed LA-MC-ICPMS Uncorrected Sr Isotope Results, Sample 554, *Bos*, Layer D, Tabun

Sample 554, Corrected Sr Values, Tabun, Israel

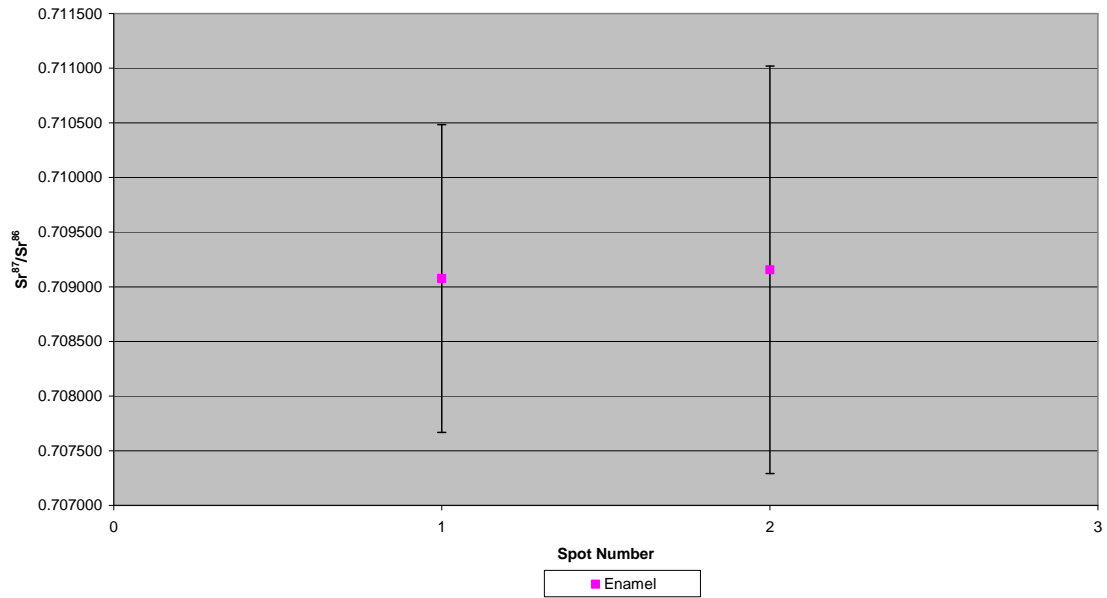


Figure A3.33 Detailed LA-MC-ICPMS Corrected Sr Isotope Results, Sample 554, *Bos*, Layer D, Tabun

Sample 556, a *Bos* tooth from layer D at Tabun shown in Figure A2.11, was analysed using 1 track with 2 spots, collected in enamel shown in Figure A3.34. Enamel from sample 556 has an average ^{88}Sr voltage of 1.589, a weighted average uncorrected $^{87}\text{Sr}/^{86}\text{Sr}$ value of 0.71036 ± 0.00049 , a weighted average corrected $^{87}\text{Sr}/^{86}\text{Sr}$ value of 0.70939 ± 0.00049 and a weighted average $^{84}\text{Sr}/^{86}\text{Sr}$ value of 0.0565 ± 0.0016 ($n=2$), shown in Table 5.12 and Figure 5.7. The 2 spots have a relatively homogenous composition, within 2σ error, shown in Figure A3.35, Figure A3.36 and Table A3.47.

The strontium isotope values of this sample are summarised in Table 5.51 and Figure 5.7 and shown in detail in Table A3.47, Figure A3.35 and Figure A3.36. The uncorrected weighted average of enamel is 0.71036 ± 0.00049 . This composition is within 2σ error of soil strontium results from the Senonian-Palaeocene aged Mount Scopus Group limestone from site IS011, which has a value of 0.710199 ± 0.000034 , although, as discussed in section 6.3.1.6, this value may not be robust. While this analysis site is located 60 km north-north-east of Skhul, an outcrop of Mount Scopus Group sediments, not sampled in this study, outcrop within 10 km of the site on the top of the Mount Carmel Range. The corrected weighted average of enamel is 0.70939 ± 0.00049 , which corresponds to a large number of mapping samples surrounding the site, including from carbonates of the Mount Carmel Range IS005, IS006, IS007, IS019 and IS021, as well as kurkar from the coastal plain, including IS001 and IS003, the closest of which outcrops within 1km of the site.

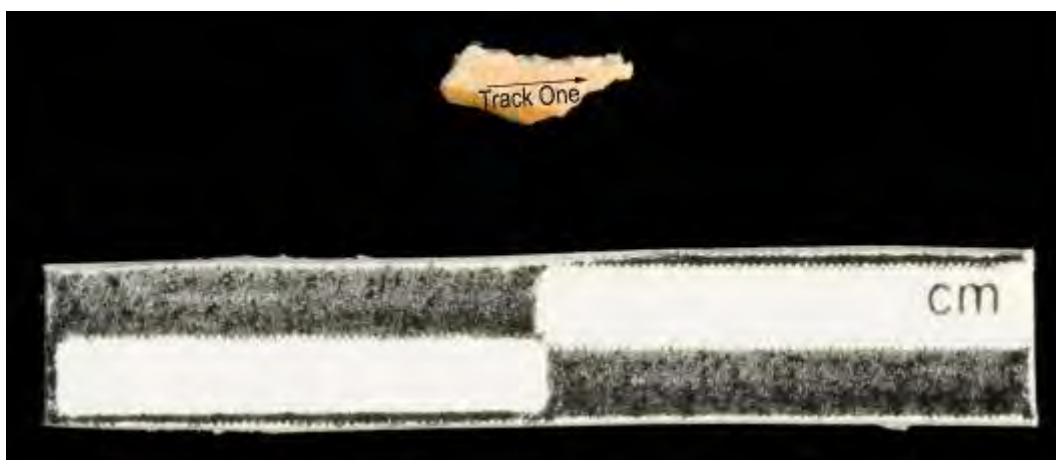


Figure A3.34 LA-MC-ICPMS Track for Sample 556, *Bos*, Layer D, Tabun

Sample	Material	Track	Point	$^{84}\text{Sr}/^{86}\text{Sr}$	Error	$^{87}\text{Sr}/^{86}\text{Sr}$	2σ	Error
556	Enamel	1	1	1.543	0.056435	0.000144	0.710218	0.709254
556	Enamel	1	2	1.636	0.056704	0.000213	0.710554	0.709590

Table A3.47 Detailed LA-MC-ICPMS Sr Isotope Results for Enamel, Sample 556, *Bos*, Layer D, Tabun

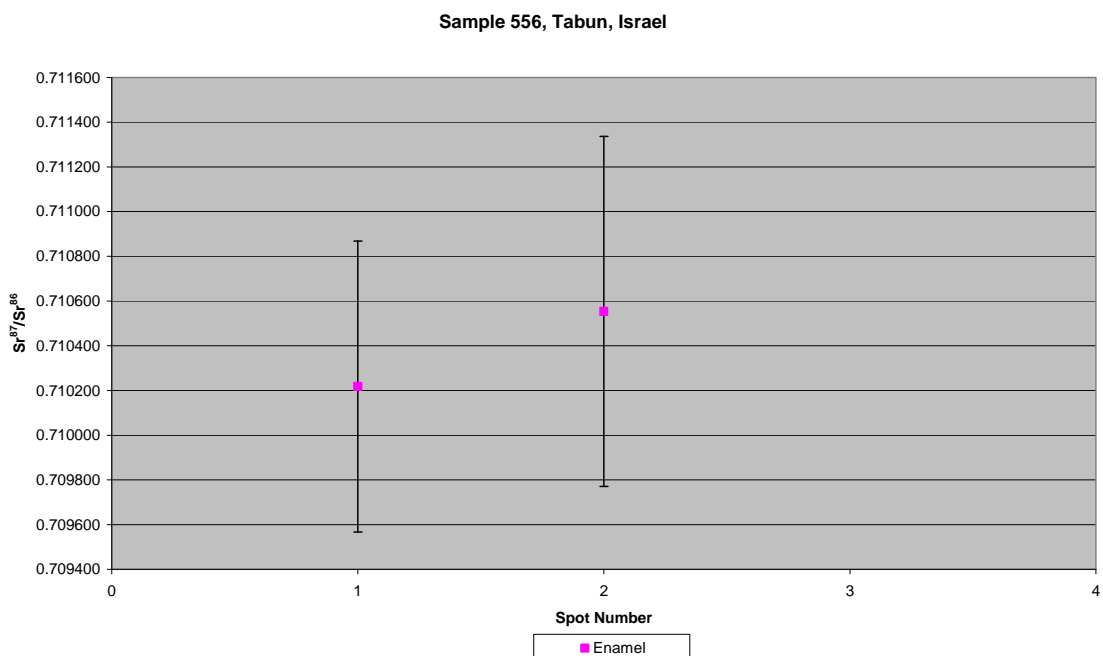


Figure A3.35 Detailed LA-MC-ICPMS Uncorrected Sr Isotope Results, Sample 556, *Bos*, Layer D, Tabun

Sample 556, Corrected Sr Values, Tabun, Israel

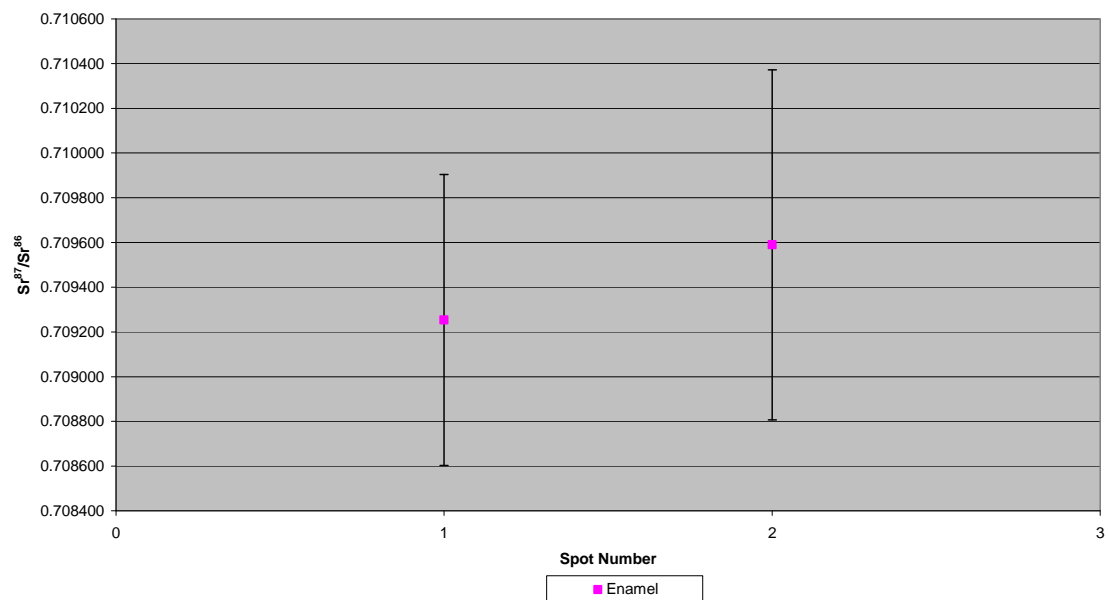


Figure A3.36 Detailed LA-MC-ICPMS Corrected Sr Isotope Results, Sample 556, *Bos*, Layer D, Tabun

Sample 557, a *Bos* tooth from layer Ea at Tabun shown in A2.12 and A2.13, was analysed by 2 tracks each with 2 spots that are all collected in enamel, shown in Figure A3.37 and Figure A3.38. Enamel from track 1 in sample 557 has an average ^{88}Sr voltage of 1.149, a weighted average uncorrected $^{87}\text{Sr}/^{86}\text{Sr}$ value of 0.7126 ± 0.0017 , a weighted average corrected $^{87}\text{Sr}/^{86}\text{Sr}$ value of 0.71140 ± 0.0017 and a weighted average $^{84}\text{Sr}/^{86}\text{Sr}$ value of 0.05635 ± 0.00011 ($n=2$), shown in Table 5.12 and Figure 5.7. Enamel from track 2 in sample 557 has an average ^{88}Sr voltage of 1.481, a weighted average uncorrected $^{87}\text{Sr}/^{86}\text{Sr}$ value of 0.71197 ± 0.00055 , a weighted average corrected $^{87}\text{Sr}/^{86}\text{Sr}$ value of 0.71061 ± 0.00055 and a weighted average $^{84}\text{Sr}/^{86}\text{Sr}$ value of 0.0564 ± 0.0012 ($n=2$), shown in Table 5.12 and Figure 5.7. All spots from the enamel of sample 557 are relatively homogeneous, with a $^{87}\text{Sr}/^{86}\text{Sr}$ composition within 2σ error of each other, shown in Table A3.48, Figure A3.39 and Figure A3.40.

The strontium isotope values of this sample are summarised in Table 5.51 and Figure 5.7 and shown in detail in Table A3.48, Figure A3.39 and Figure A3.40. The individual fragments have uncorrected weighted average values of 0.7126 ± 0.0017 and 0.71197 ± 0.00055 and are statistically indistinguishable based on 2σ error. The much higher error and elevated mean results in enamel fragment 1 are probably the result of the lower strontium concentration in this sample. The weighted average corrected value of enamel from this sample is 0.71133 ± 0.00045 . The only mapping sample that might correlate with these enamel values is the rock sample from location IS045, which has the value of 0.711296 ± 0.000007 from a Precambrian granite. As unit outcrops approximately 350 km from the site, this is not a credible location for this sample to have lived during amelogenesis.

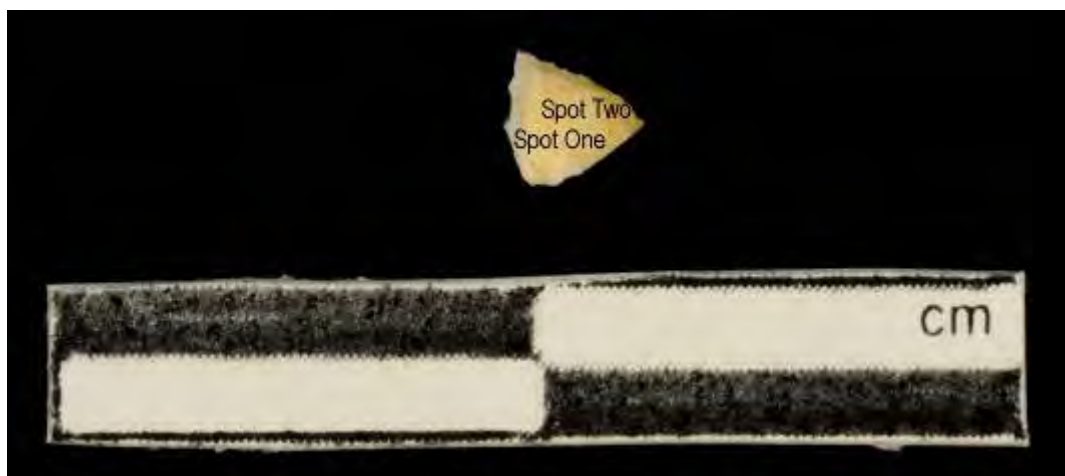


Figure A3.37 LA-MC-ICPMS Track for Sample 557, Track 1, *Bos*, Layer Ea, Tabun

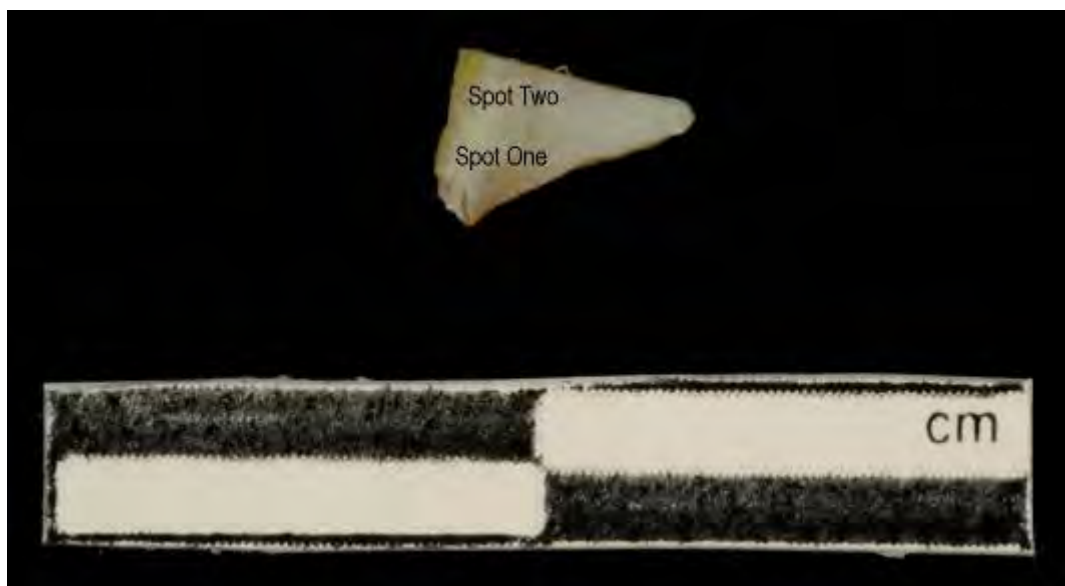


Figure A3.38 LA-MC-ICPMS Track for Sample 557, Track 2, *Bos*, Layer Ea, Tabun

Sample	Material	Track	Point	^{88}Sr Volts	$^{84}\text{Sr}/^{86}\text{Sr}$	$^{84}\text{Sr}/^{86}\text{Sr} 2\sigma$	Corrected $^{87}\text{Sr}/^{86}\text{Sr}$	$^{87}\text{Sr}/^{86}\text{Sr} 2\sigma$
557	Enamel	1	1	1.137	0.056329	0.000152	0.712491	0.711259
557	Enamel	1	2	1.161	0.056390	0.000175	0.712760	0.711528
557	Enamel	2	1	1.553	0.056281	0.000170	0.711996	0.710637
557	Enamel	2	2	1.408	0.056481	0.000132	0.711942	0.710583

Table A3.48 Detailed LA-MC-ICPMS Sr Isotope Results for Enamel, Sample 557, *Bos*, Layer Ea, Tabun

Sample 557, Tabun, Israel

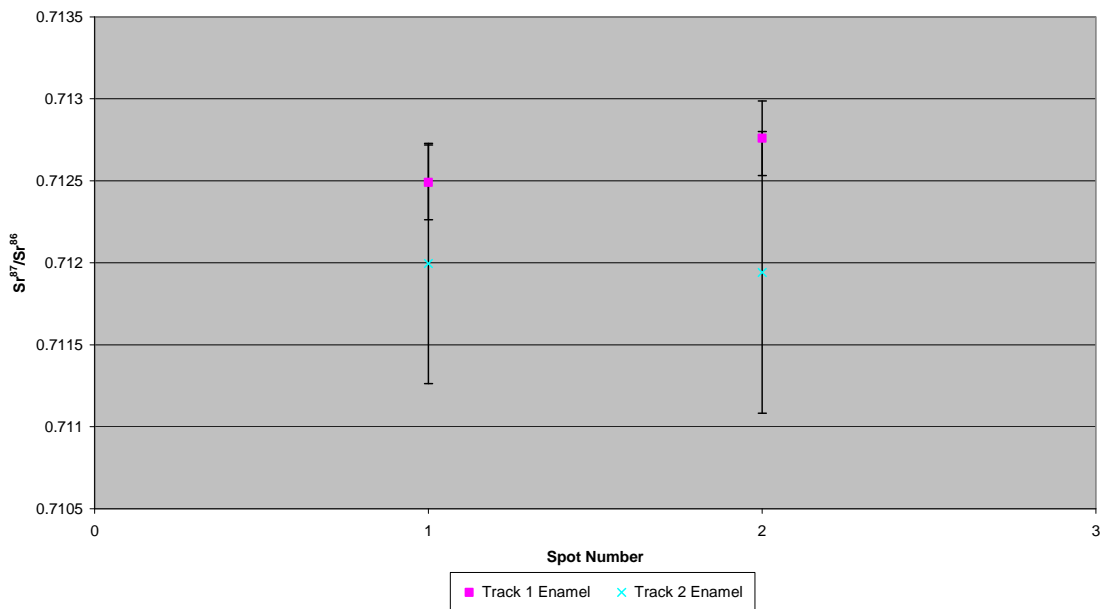


Figure A3.39 Detailed LA-MC-ICPMS Uncorrected Sr Isotope Results, Sample 557, *Bos*, Layer Ea, Tabun

Sample 557, Corrected Sr Values, Tabun, Israel

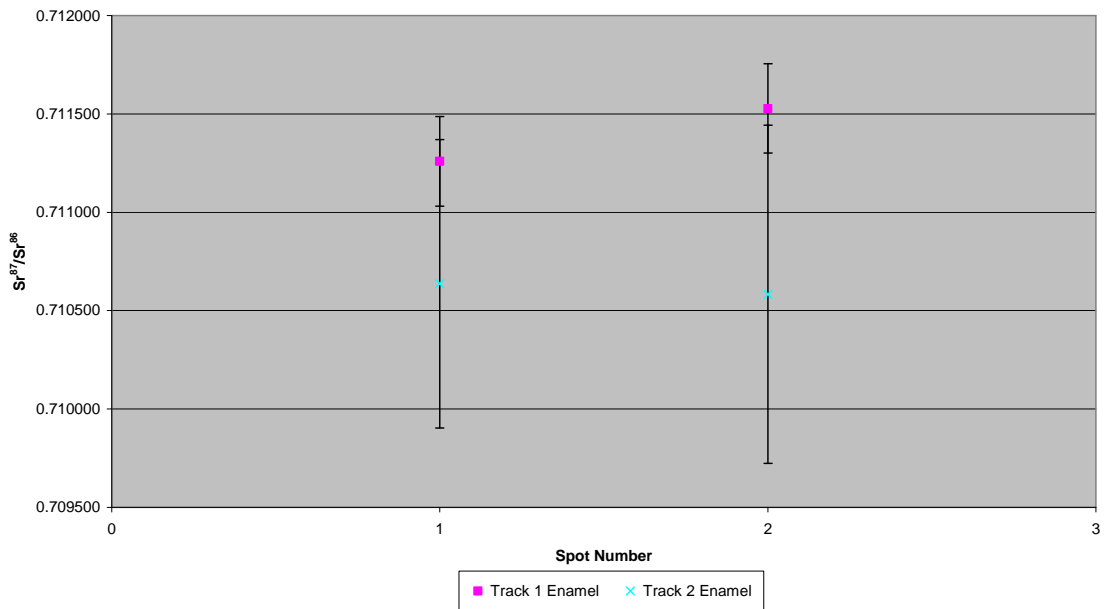


Figure A3.40 Detailed LA-MC-ICPMS Corrected Sr Isotope Results, Sample 557, *Bos*, Layer Ea, Tabun

Sample 558, a *Bos* tooth from layer Ea at Tabun shown in Figure A2.14, was analysed by 1 track that has 2 enamel spots, shown in Figure A3.41. Enamel from track 1 in sample 558 has an average ^{88}Sr voltage of 2.658, a weighted average uncorrected $^{87}\text{Sr}/^{86}\text{Sr}$ value of 0.7117 ± 0.0022 , a weighted average corrected $^{87}\text{Sr}/^{86}\text{Sr}$ value of 0.70990 ± 0.0022 and a weighted average $^{84}\text{Sr}/^{86}\text{Sr}$ value of 0.056635 ± 0.000099 ($n=2$), shown in Table 5.12 and Figure 5.7. The 2 spots have a relatively homogenous $^{87}\text{Sr}/^{86}\text{Sr}$ composition within 2σ error of each other, shown in Figure A3.42, Figure A3.43 and Table A3.49.

The strontium isotope values of this sample are summarised in Table 5.51 and Figure 5.7 and shown in detail in Table A3.49, Figure A3.42 and Figure A3.43. The enamel has an uncorrected weighted average value of 0.7117 ± 0.0022 and a corrected value of 0.70990 ± 0.00220 . These sample spots are all within 2σ error, suggesting that this specimen was not mobile during amelogenesis. The large 2σ error of the $^{87}\text{Sr}/^{86}\text{Sr}$ LA-MC-ICPMS results makes the use of this sample as an indicator of mobility very difficult. This large error is probably the result of the relatively low strontium concentration of this sample with values of 121 ppm and 119 ppm.



Figure A3.41 LA-MC-ICPMS Track for Sample 558, *Bos*, Layer Ea, Tabun

Sample	Material	Track	Point	^{88}Sr Volts	$^{84}\text{Sr}/^{86}\text{Sr}$	$^{87}\text{Sr}/^{86}\text{Sr}$	Corrected $^{87}\text{Sr}/^{86}\text{Sr}$	$^{87}\text{Sr}/^{86}\text{Sr} 2\sigma$ Error
558	Enamel	1	1	1.352	0.056677	0.000162	0.711572	0.709774
558	Enamel	1	2	1.306	0.056607	0.000130	0.711945	0.710147

Table A3.49 Detailed LA-MC-ICPMS Sr Isotope Results for Enamel, Sample 558, *Bos*, Layer Ea, Tabun

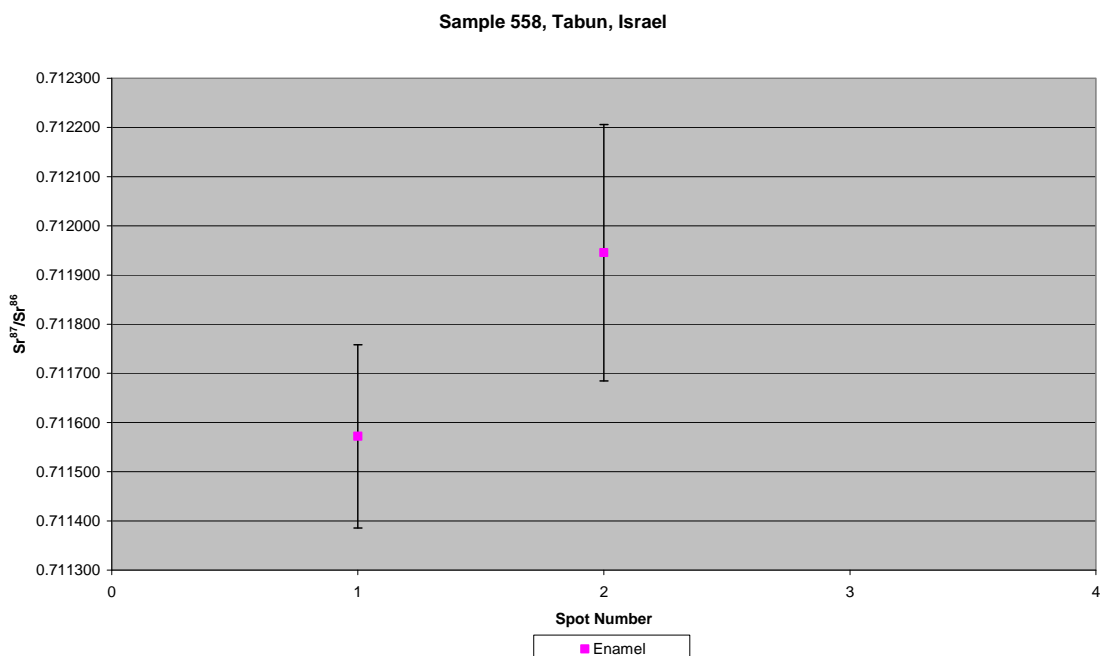


Figure A3.42 Detailed LA-MC-ICPMS Uncorrected Sr Isotope Results, Sample 558, *Bos*, Layer Ea, Tabun

Sample 558, Corrected Sr Values, Tabun, Israel

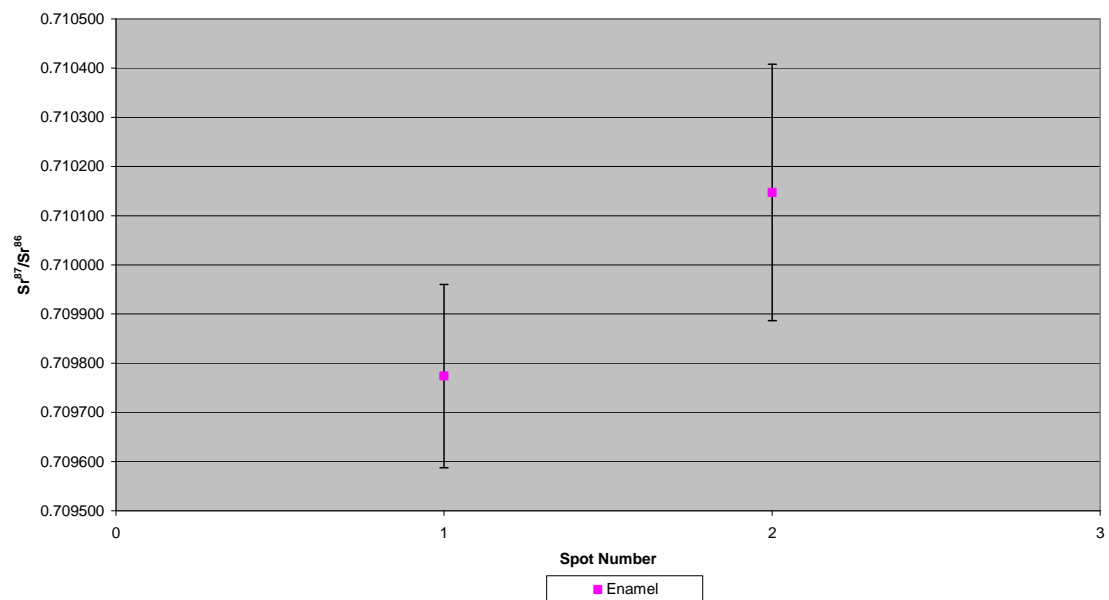


Figure A3.43 Detailed LA-MC-ICPMS Corrected Sr Isotope Results, Sample 558, *Bos*, Layer Ea, Tabun

Sample 561, a *Bos* tooth from layer Ea at Tabun shown in Figure A2.15, was analysed by 1 track that has 3 enamel spots and 2 dentine spots, shown in Figure A3.44. The dentine spots have an average ^{88}Sr voltage of 1.600, a weighted average uncorrected $^{87}\text{Sr}/^{86}\text{Sr}$ value of 0.70987 ± 0.00053 , a weighted average corrected $^{87}\text{Sr}/^{86}\text{Sr}$ value of 0.70845 ± 0.00053 and a weighted average $^{84}\text{Sr}/^{86}\text{Sr}$ value of 0.05656 ± 0.00010 ($n=2$), shown in Table 5.12 and Figure 5.7. The enamel spots have an average ^{88}Sr voltage of 1.201, a weighted average uncorrected $^{87}\text{Sr}/^{86}\text{Sr}$ value of 0.7126 ± 0.0011 , a weighted average corrected $^{87}\text{Sr}/^{86}\text{Sr}$ value of 0.71020 ± 0.0011 and a weighted average $^{84}\text{Sr}/^{86}\text{Sr}$ value of 0.056452 ± 0.000082 ($n=3$), shown in Table 5.12 and Figure 5.7. Enamel has a range of $^{87}\text{Sr}/^{86}\text{Sr}$ value of 0.711728 to 0.712736, with spots 2 and 3 showing a relatively homogenous isotopic composition that is within 2σ error, shown in Table A3.50, Figure A3.45 and Figure A3.46. The dentine has a relatively homogeneous $^{87}\text{Sr}/^{86}\text{Sr}$ isotope composition, with the 2 spots showing values within 2σ error of each other.

The strontium isotope values of this sample are summarised in Table 5.51 and Figure 5.7 and shown in detail in Table A3.50, Figure A3.45 and Figure A3.46. The 3 enamel spots have a weighted average value of 0.7126 ± 0.0011 . Spot 1 has a significantly elevated $^{87}\text{Sr}/^{86}\text{Sr}$ value compared to the other 2 spots, suggesting the sample was mobile during amelogenesis. This interpretation is supported by the relatively homogenous strontium concentration in this enamel, suggesting that the variation in values is not an artefact of the laser ablation process. The high 2σ error makes the use of these values as an indicator of geographic mobility very difficult. The dentine spots have a weighted average value of 0.70987 ± 0.00053 . This is significantly more radiogenic compared to sediment samples from this archaeological layer, which have values of 0.708417 ± 0.000009 , 0.708931 ± 0.000011 and 0.708385 ± 0.000012 .

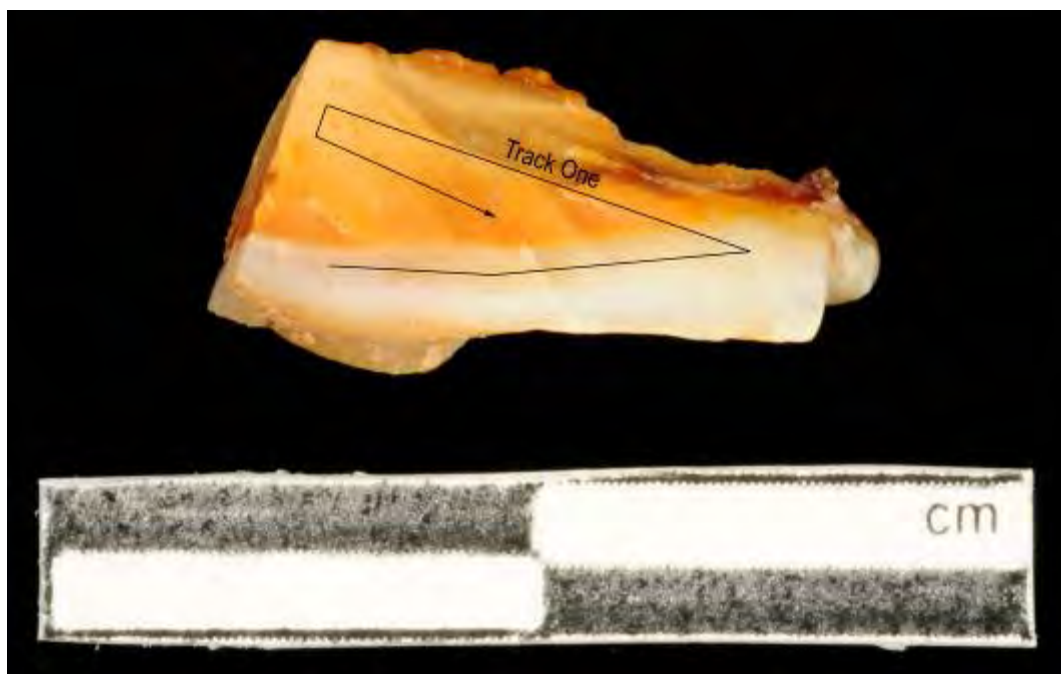


Figure A3.44 LA-MC-ICPMS Track for Sample 561, *Bos*, Layer Eb, Tabun

Sample	Material	Track	Point	^{88}Sr /Volts	$^{84}\text{Sr}/^{86}\text{Sr}$	$^{84}\text{Sr}/^{86}\text{Sr}$ 2 σ Error	Corrected $^{87}\text{Sr}/^{86}\text{Sr}$	$^{87}\text{Sr}/^{86}\text{Sr}$ 2 σ Error
561	Enamel	1	1	1.224	0.056486	0.000117	0.712736	0.710381
561	Enamel	1	2	1.214	0.056467	0.000185	0.711806	0.709451
561	Enamel	1	3	1.164	0.056379	0.000158	0.711728	0.709374
561	Dentine	1	4	1.690	0.056518	0.000134	0.709721	0.708299
561	Dentine	1	5	1.510	0.056609	0.000162	0.710193	0.708771

Table A3.50 Detailed LA-MC-ICPMS Sr Isotope Results for Enamel and Dentine, Sample 561, *Bos*, Layer Eb, Tabun

Sample 561, Tabun, Israel

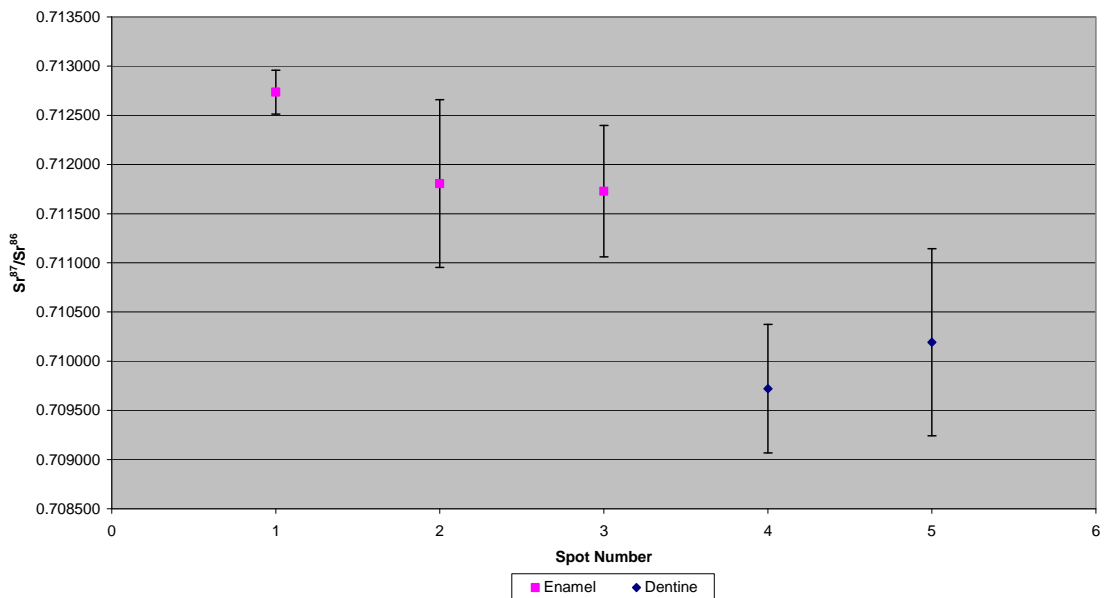


Figure A3.45 Detailed LA-MC-ICPMS Uncorrected Sr Isotope Results, *Bos*, Layer Eb, Tabun

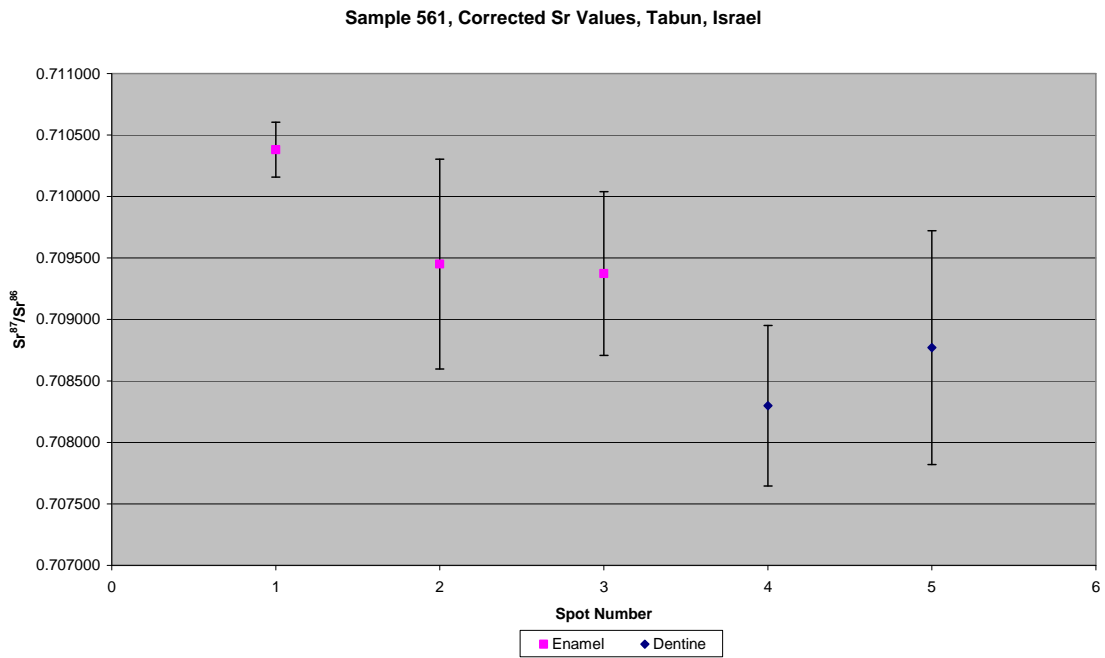


Figure A3.46 Detailed LA-MC-ICPMS Corrected Sr Isotope Results, *Bos*, Layer Eb, Tabun

Sample 563, a *Bos* tooth from layer Eb at Tabun shown in Figure A2.16, was analysed by 1 track that has 4 enamel spots and 3 dentine spots, shown in Figure A3.47. The dentine spots have an average ^{88}Sr voltage of 1.565, a

weighted average uncorrected $^{87}\text{Sr}/^{86}\text{Sr}$ value of 0.70940 ± 0.00040 , a weighted average corrected $^{87}\text{Sr}/^{86}\text{Sr}$ value of 0.70844 ± 0.00040 and a weighted average $^{84}\text{Sr}/^{86}\text{Sr}$ value of 0.056442 ± 0.000080 ($n=3$), shown in Table 5.12 and Figure 5.7. The enamel spots have an average ^{88}Sr voltage of 1.420, a weighted average uncorrected $^{87}\text{Sr}/^{86}\text{Sr}$ value of 0.71021 ± 0.00034 , a weighted average corrected $^{87}\text{Sr}/^{86}\text{Sr}$ value of 0.70887 ± 0.00034 and a weighted average $^{84}\text{Sr}/^{86}\text{Sr}$ value of 0.056342 ± 0.000070 ($n=4$), shown in Table 5.12 and Figure 5.7. The enamel and dentine $^{87}\text{Sr}/^{86}\text{Sr}$ values are relatively homogeneous, covering the range of 0.710008 to 0.710466 (uncorrected enamel), 0.708668 to 0.709126 (corrected enamel), 0.709155 to 0.709593 (uncorrected dentine) and 0.708189 to 0.708628 (corrected dentine), shown in Table A3.51, Figure A3.48 and Figure A3.49. There is a small offset between the dentine and enamel $^{87}\text{Sr}/^{86}\text{Sr}$ values, although all remain within 2σ error of each other.

Enamel values for this sample are all homogenous within 2σ error and so no mobility during amelogenesis is evident. The weighted average uncorrected $^{87}\text{Sr}/^{86}\text{Sr}$ value for this sample is 0.71021 ± 0.00034 . The closest comparable value is found in the soil strontium results from the Senonian-Palaeocene aged Mount Scopus Group very fine grained limestone from site IS011, which has a value of 0.710199 ± 0.000034 , although, as discussed in section 6.3.1.6, this value may not be robust. While this analysis site is located 60 km north-north-east of Skhul, an outcrop of Mount Scopus Group sediments, not sampled in this study, occurs within 10 km of the site on the top of the Mount Carmel Range. The weighted average uncorrected $^{87}\text{Sr}/^{86}\text{Sr}$ value 0.70887 ± 0.00034 corresponds to a number of mapping samples surrounding the site, including sample 156 from IS005 and sample 170 from IS019, both located within the Bina Formation and sample 154 from IS004 located within the Sakhnin/Yanuh Formation from the Mount Carmel Range, as well as sample 153 from IS003 from kurkar from the coastal plain. Dentine is slightly elevated compared to the $^{87}\text{Sr}/^{86}\text{Sr}$ value of 0.708597 ± 0.000014 for sediments from this layer. Weighted average $^{84}\text{Sr}/^{86}\text{Sr}$ values of this sample are 0.056342 ± 0.000070 , suggesting that the $^{87}\text{Sr}/^{86}\text{Sr}$ values may not be robust.

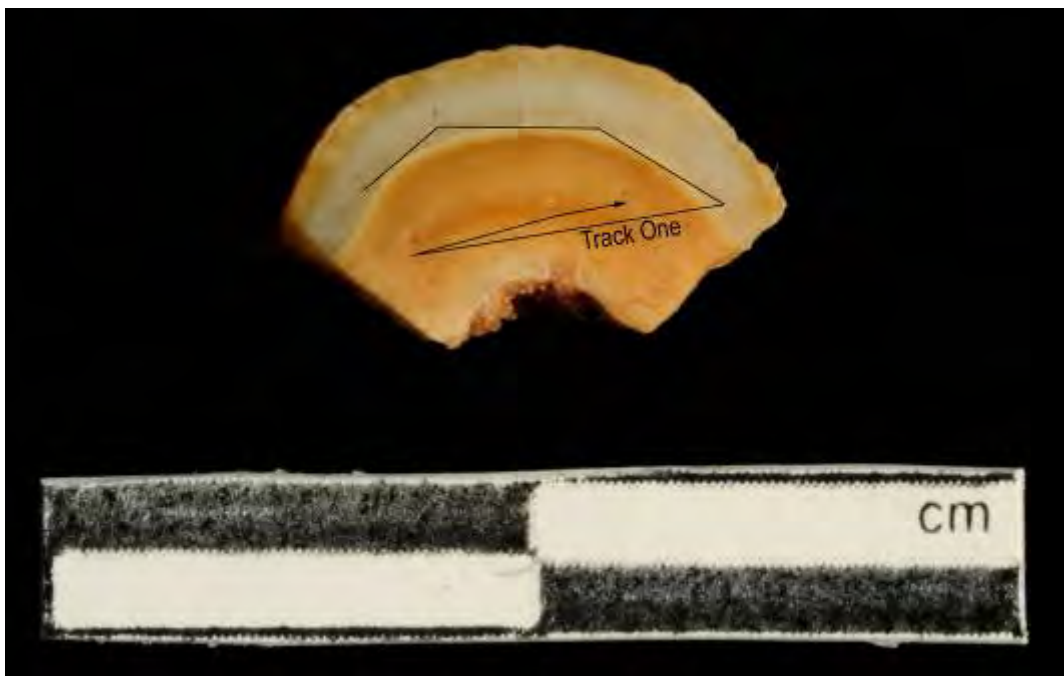


Figure A3.47 LA-MC-ICPMS Track for Sample 563, *Bos*, Layer Eb, Tabun

Sample	Material	Track	Point	^{88}Sr Volts	$^{84}\text{Sr}/^{86}\text{Sr}$	$^{84}\text{Sr}/^{86}\text{Sr}$ 2 σ Error	$^{87}\text{Sr}/^{86}\text{Sr}$ Corrected	$^{87}\text{Sr}/^{86}\text{Sr}$ 2 σ Error	
563	Enamel	1	1	1.603	0.056361	0.000112	0.710042	0.708702	0.000611
563	Enamel	1	2	1.401	0.056370	0.000182	0.710008	0.708668	0.000848
563	Enamel	1	3	1.368	0.056395	0.000163	0.710256	0.708917	0.000851
563	Enamel	1	4	1.306	0.056252	0.000145	0.710466	0.709126	0.000607
563	Dentine	1	5	1.436	0.056358	0.000190	0.709155	0.708189	0.000950
563	Dentine	1	6	1.662	0.056460	0.000123	0.709392	0.708427	0.000556
563	Dentine	1	7	1.597	0.056464	0.000135	0.709593	0.708628	0.000791

Table A3.51 Detailed LA-MC-ICPMS Sr Isotope Results for Enamel and Dentine, Sample 563, *Bos*, Layer Eb, Tabun

Sample 563, Tabun, Israel

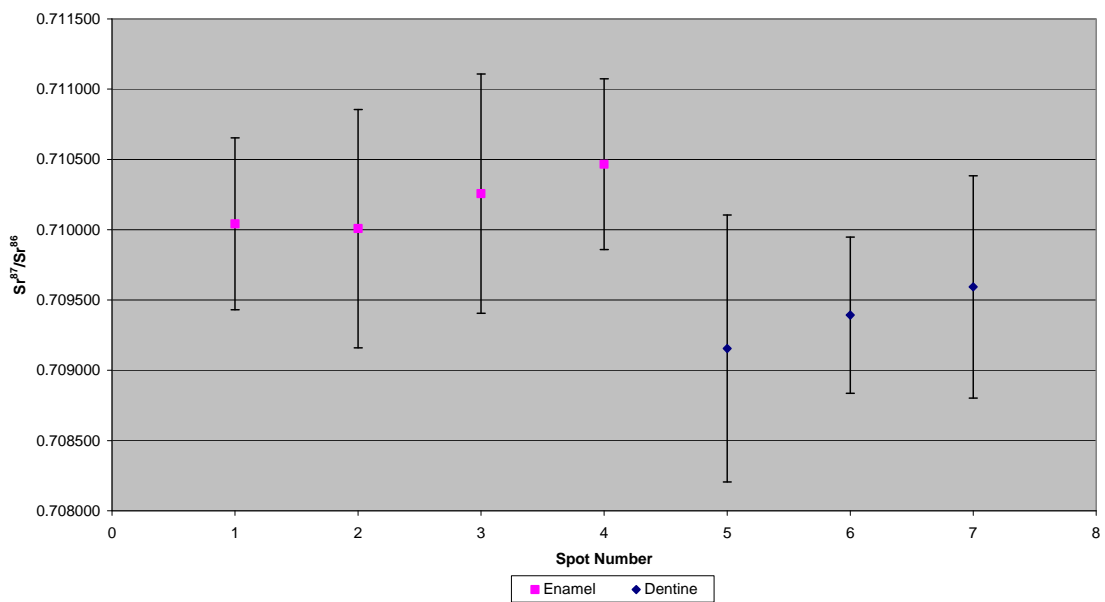


Figure A3.48 Detailed LA-MC-ICPMS Uncorrected Sr Isotope Results, Sample 563, *Bos*, Layer Eb, Tabun

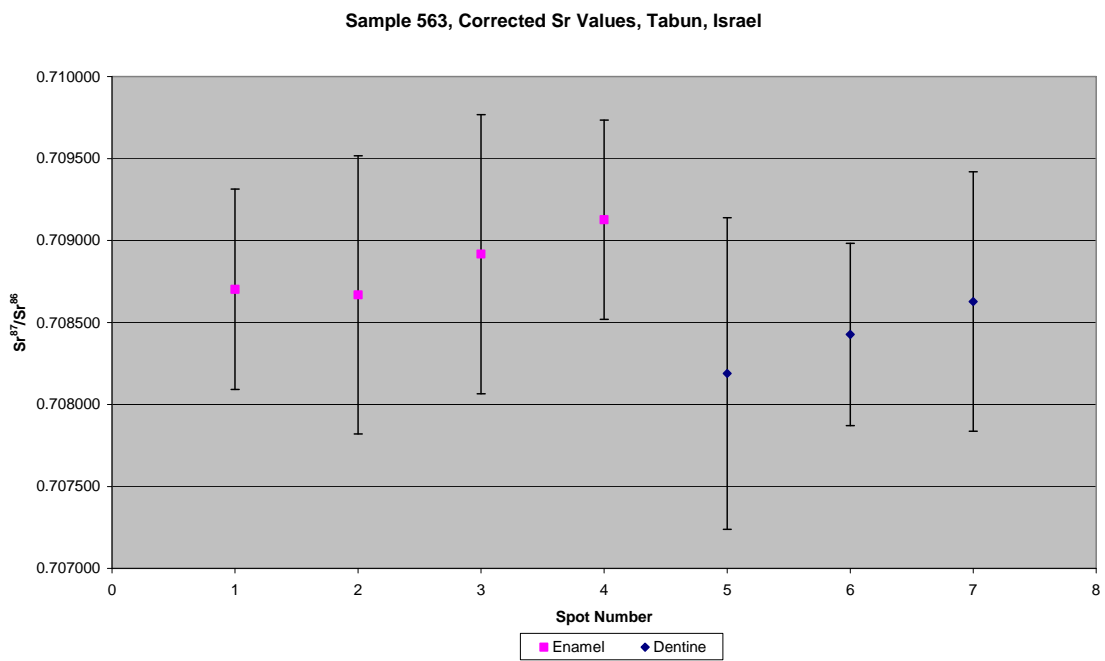


Figure A3.49 Detailed LA-MC-ICPMS Corrected Sr Isotope Results, Sample 563, *Bos*, Layer Eb, Tabun

Sample 564, a *Bos* tooth from layer Ec at Tabun shown in Figure A2.17, was analysed by 1 track, which consists of 2 spots collected in dentine, shown in Figure A3.50. The dentine spots have an average ^{88}Sr voltage of 1.986, a weighted average uncorrected $^{87}\text{Sr}/^{86}\text{Sr}$ value of 0.70988 ± 0.00013 , a weighted average corrected $^{87}\text{Sr}/^{86}\text{Sr}$ value of 0.70944 ± 0.00013 and a weighted average $^{84}\text{Sr}/^{86}\text{Sr}$ value of 0.056331 ± 0.000077 ($n=2$), shown in Table 5.12 and Figure 5.7. The $^{87}\text{Sr}/^{86}\text{Sr}$ values of the spots are extremely homogeneous, shown in Table A3.52, Figure A3.51 and Figure A3.52.

Uncorrected dentine spots have a weighted average $^{87}\text{Sr}/^{86}\text{Sr}$ value of 0.70988 ± 0.00013 . This differs significantly from the strontium isotope value of 0.708597 ± 0.000014 obtained from the archaeological sediment from this layer. Average strontium concentration in this sample is 264 ppm and so the results should be robust.

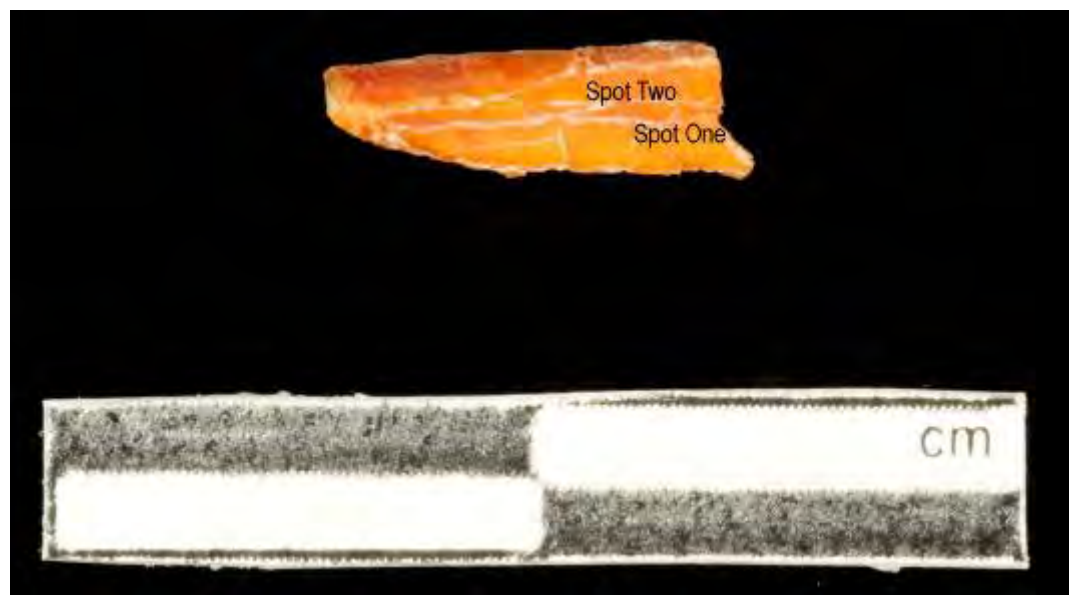


Figure A3.50 LA-MC-ICPMS Track for Sample 564, *Bos*, Layer Ec, Tabun

Sample	Material	Track	Point	^{88}Sr Volts	$^{84}\text{Sr}/^{86}\text{Sr}$	$^{84}\text{Sr}/^{86}\text{Sr}$ Error	$^{87}\text{Sr}/^{86}\text{Sr}$	Corrected $^{87}\text{Sr}/^{86}\text{Sr}$	$^{87}\text{Sr}/^{86}\text{Sr}$ Error	$^{87}\text{Sr}/^{86}\text{Sr}$ 2σ
--------	----------	-------	-------	------------------------	---------------------------------	---------------------------------------	---------------------------------	---	---------------------------------------	---

564	Dentine	1	1	1.995	0.056329	0.000093	0.709888	0.709077	0.000173
564	Dentine	1	2	1.977	0.056334	0.000144	0.709880	0.709155	0.000217

Table A3.52 Detailed LA-MC-ICPMS Sr Isotope Results, Sample 564, *Bos*, Layer Ec, Tabun

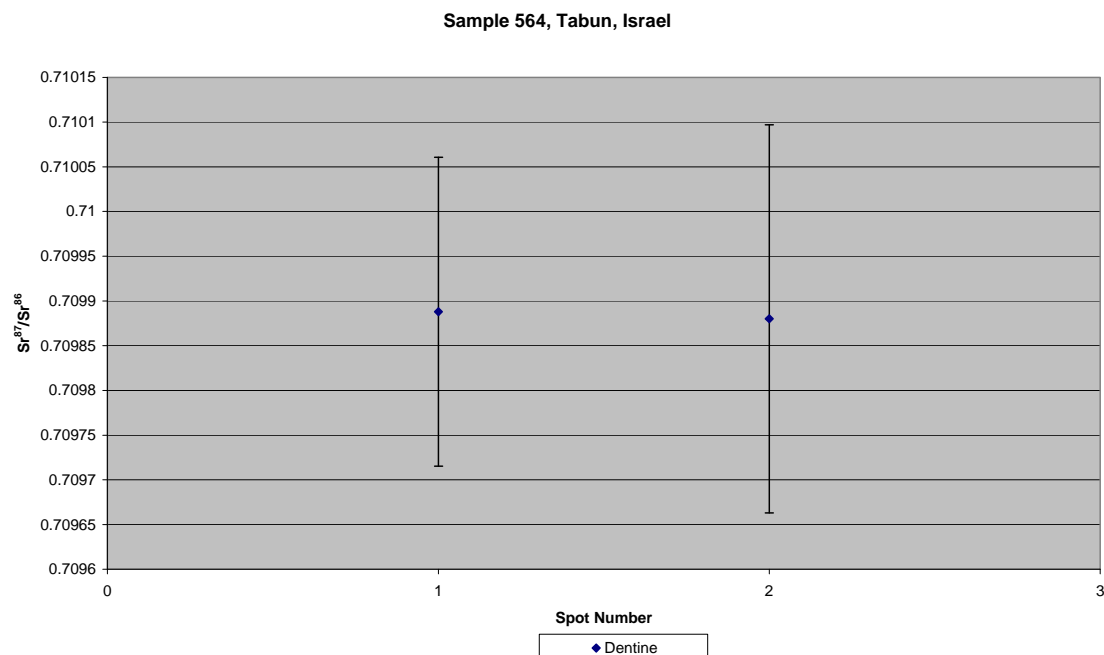


Figure A3.51 Detailed LA-MC-ICPMS Uncorrected Sr Isotope Results, Sample 564, *Bos*, Layer Ec, Tabun

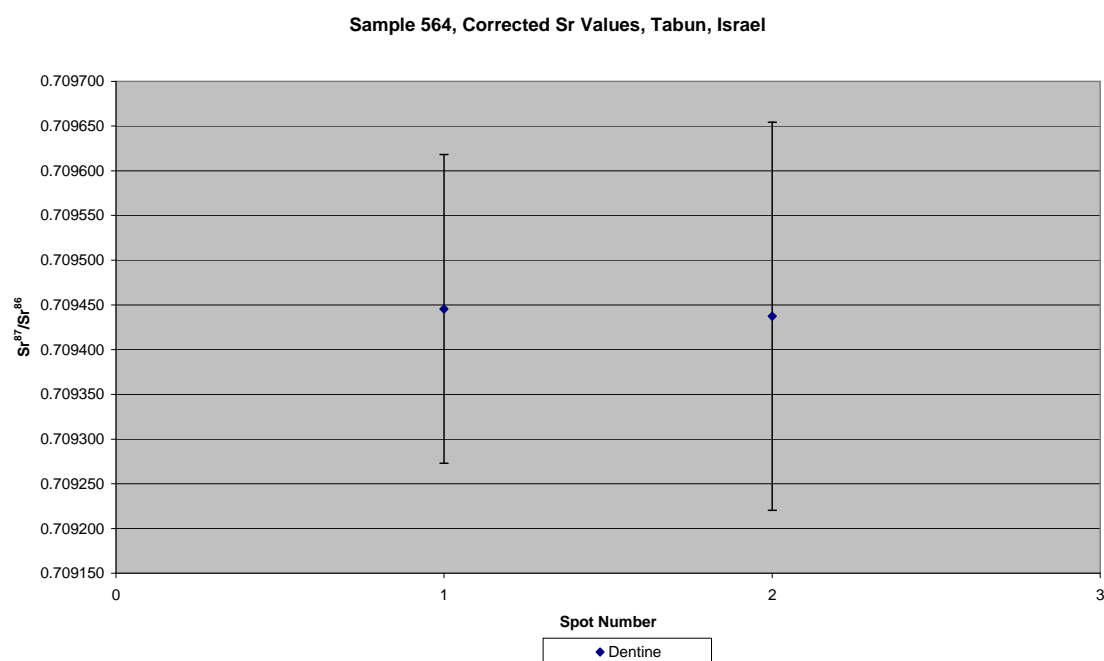


Figure A3.52 Detailed LA-MC-ICPMS Corrected Sr Isotope Results, Sample 564, *Bos*, Layer Ec, Tabun

Sample 565, a *Bos* tooth from layer Ec at Tabun shown in Figure A2.18, was analysed by 1 track, which consists of 2 spots collected in enamel and 2 spots collected in dentine, shown in Figure A3.53. The enamel spots have an average ^{88}Sr voltage of 2.149, a weighted average uncorrected $^{87}\text{Sr}/^{86}\text{Sr}$ value of 0.7120 ± 0.010 , a weighted average corrected $^{87}\text{Sr}/^{86}\text{Sr}$ value of 0.71100 ± 0.010 and a weighted average $^{84}\text{Sr}/^{86}\text{Sr}$ value of 0.05644 ± 0.00072 , shown in Table 5.12 and Figure 5.7. The dentine spots have an average ^{88}Sr voltage of 1.733, a weighted average uncorrected $^{87}\text{Sr}/^{86}\text{Sr}$ value of 0.7110 ± 0.0024 , a weighted average corrected $^{87}\text{Sr}/^{86}\text{Sr}$ value of 0.71050 ± 0.0024 and a weighted average $^{84}\text{Sr}/^{86}\text{Sr}$ value of 0.05638 ± 0.00077 , shown in Table 5.12 and Figure 5.7. Enamel $^{87}\text{Sr}/^{86}\text{Sr}$ values are very heterogeneous, with spot 1 being very elevated compared to spot 2, shown in Table A3.53, Figure A3.54 and Figure A3.55. Spot 2 (enamel) has a $^{87}\text{Sr}/^{86}\text{Sr}$ value within 2σ error of spot 3 (dentine). Spot 3 and 4 have $^{87}\text{Sr}/^{86}\text{Sr}$ values within 2σ error of each other.

The enamel $^{87}\text{Sr}/^{86}\text{Sr}$ values for this sample are very heterogeneous, indicating a sample mobile during amelogenesis. The only appropriate mapping value for the uncorrected enamel values is IS045, a Precambrian granite located near Eilat; however, this result implies an unreasonable distance of migration. No mapping samples correspond to corrected enamel values for this sample. The dentine has values of 0.711203 ± 0.000202 and 0.710831 ± 0.000210 , which have divergent mean values, although they are just within 2σ error. This variation cannot be explained by changes in strontium concentration, as the LA-ICPMS values for these spots are relatively homogeneous.

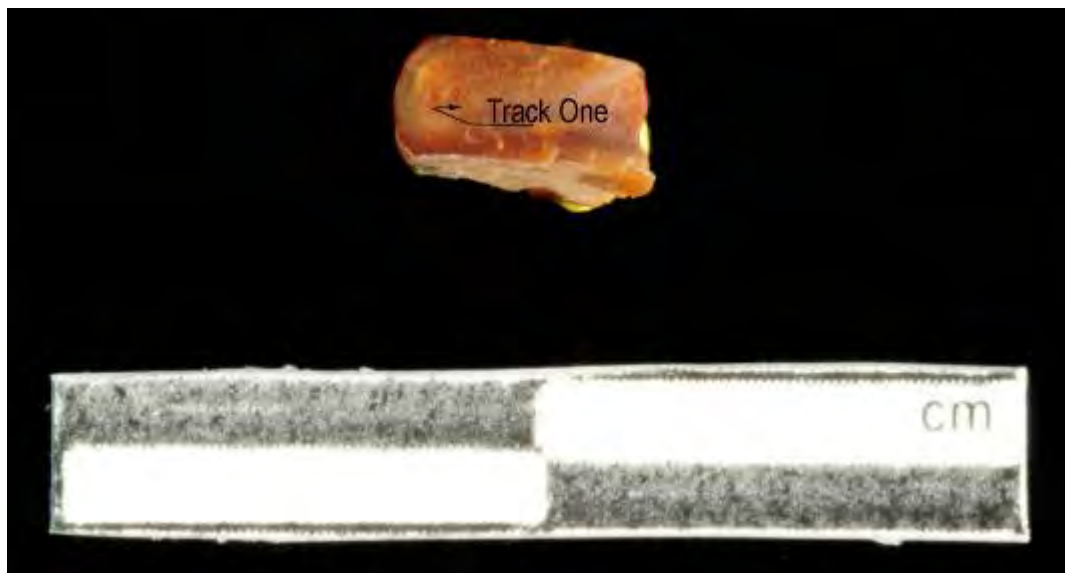


Figure A3.53 LA-MC-ICPMS Track for Sample 565, *Bos*, Layer Ec, Tabun

Sample	Material	Track	Point	⁸⁸ Sr Volts	⁸⁴ Sr/ ⁸⁶ Sr	Corrected ⁸⁷ Sr/ ⁸⁶ Sr	⁸⁷ Sr/ ⁸⁶ Sr	⁸⁷ Sr/ ⁸⁶ Sr 2σ Error
565	Enamel	1	1	2.142	0.056366	0.000108	0.712907	0.712575
565	Enamel	1	2	2.156	0.056484	0.000083	0.711204	0.710873
565	Dentine	1	3	1.775	0.056447	0.000113	0.711203	0.710705
565	Dentine	1	4	1.690	0.056325	0.000110	0.710831	0.710334

Table A3.53 Detailed LA-MC-ICPMS Sr Isotope Results for Enamel and Dentine, Sample 565, *Bos*, Layer Eb, Tabun

Sample 565, Tabun, Israel

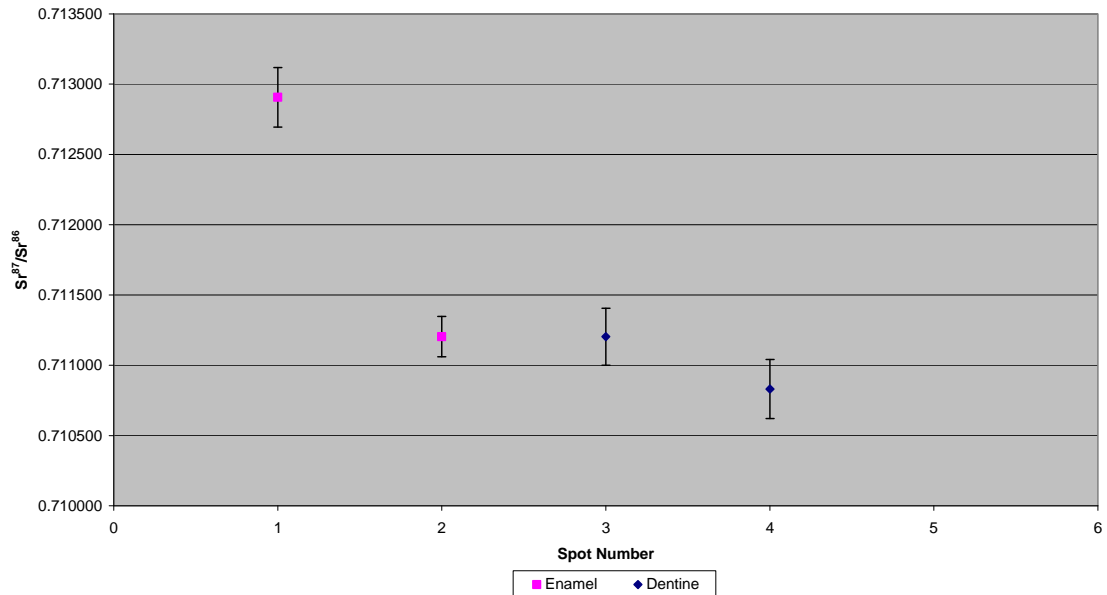


Figure A3.54 Detailed LA-MC-ICPMS Uncorrected Sr Isotope Results, Sample 565, *Bos*, Layer Ec, Tabun

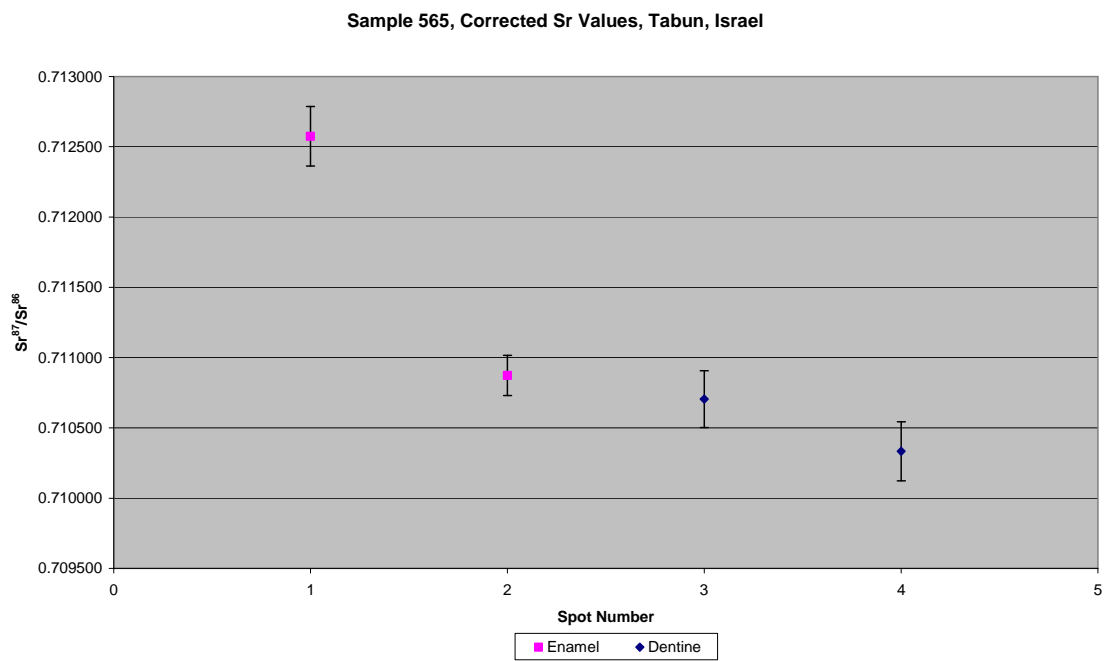


Figure A3.55 Detailed LA-MC-ICPMS Corrected Sr Isotope Results, Sample 565, *Bos*, Layer Ec, Tabun

Sample 567, a *Bos* tooth from layer Ed at Tabun shown in Figure A2.19, was analysed by 1 track, which consists of 2 spots collected in enamel and 2 spots collected in dentine, shown in Figure A3.56. The enamel spots have an average ^{88}Sr voltage of 3.084, a weighted average uncorrected $^{87}\text{Sr}/^{86}\text{Sr}$ value of 0.70944 ± 0.00099 , a weighted average corrected $^{87}\text{Sr}/^{86}\text{Sr}$ value of 0.70915 ± 0.00099 and a weighted average $^{84}\text{Sr}/^{86}\text{Sr}$ value of 0.056528 ± 0.000051 ($n=2$), shown in Table 5.12 and Figure 5.7. The dentine spots have an average ^{88}Sr voltage of 3.185, a weighted average uncorrected $^{87}\text{Sr}/^{86}\text{Sr}$ value of 0.7094 ± 0.0015 , a weighted average corrected $^{87}\text{Sr}/^{86}\text{Sr}$ value of 0.70920 ± 0.0015 and a weighted average $^{84}\text{Sr}/^{86}\text{Sr}$ value of 0.056549 ± 0.000059 ($n=2$), shown in Table 5.12 and Figure 5.7. Enamel values are 0.709369 and 0.709527 (uncorrected), as well as 0.709078 and 0.709235 (corrected), which are within 2σ error, while dentine values are 0.709292 and 0.709531 (uncorrected), as well as 0.709057 and 0.709296 (corrected) which are just slightly outside of 2σ error, shown in Table A3.54, Figure A3.57 and Figure A3.58.

The enamel $^{87}\text{Sr}/^{86}\text{Sr}$ values are within 2σ error, suggesting that this specimen was not mobile during amelogenesis. This uncorrected and corrected weighted average enamel value for this sample corresponds to values 157 from IS006 and 158 from IS007, sampled from the Bina Formation from the Mount Carmel Range, as well as 151 from IS001 from kurkar from the coastal plain, which outcrop within 1 km and 2.3 km of the site, respectively. Strontium concentrations of these samples are high, suggesting that the values are robust. Dentine $^{87}\text{Sr}/^{86}\text{Sr}$ values are somewhat heterogeneous, with values of 0.709531 ± 0.000120 and 0.709292 ± 0.000108 , with homogeneous strontium concentrations suggesting that this heterogeneity is accurate.

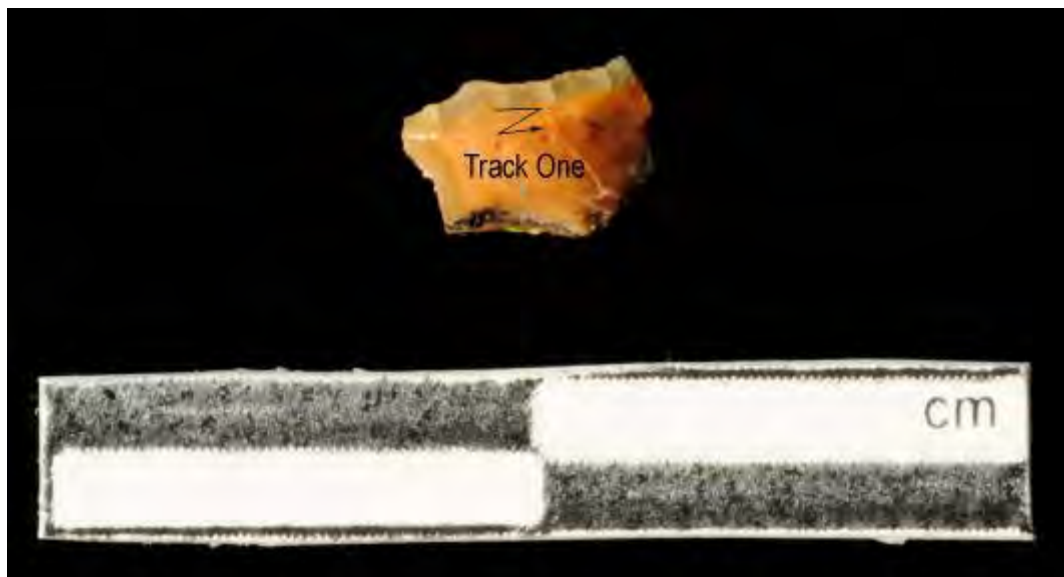


Figure A3.56 LA-MC-ICPMS Track for Sample 567, *Bos*, Layer Ed, Tabun

Sample	Material	Point	Track	^{88}Sr Volts	$^{84}\text{Sr}/^{86}\text{Sr}$	$^{84}\text{Sr}/^{86}\text{Sr} 2\sigma$	Corrected $^{87}\text{Sr}/^{86}\text{Sr}$	$^{87}\text{Sr}/^{86}\text{Sr}$ Error
567	Enamel	1	1	3.157	0.056510	0.000074	0.709369	0.709078
567	Enamel	1	2	3.012	0.056545	0.000074	0.709527	0.709235
567	Dentine	1	3	3.119	0.056570	0.000079	0.709531	0.709296
567	Dentine	1	4	3.251	0.056521	0.000092	0.709292	0.709057

Table A3.54 Detailed LA-MC-ICPMS Sr Isotope Results for Enamel and Dentine, *Bos*, Layer Ed, Tabun

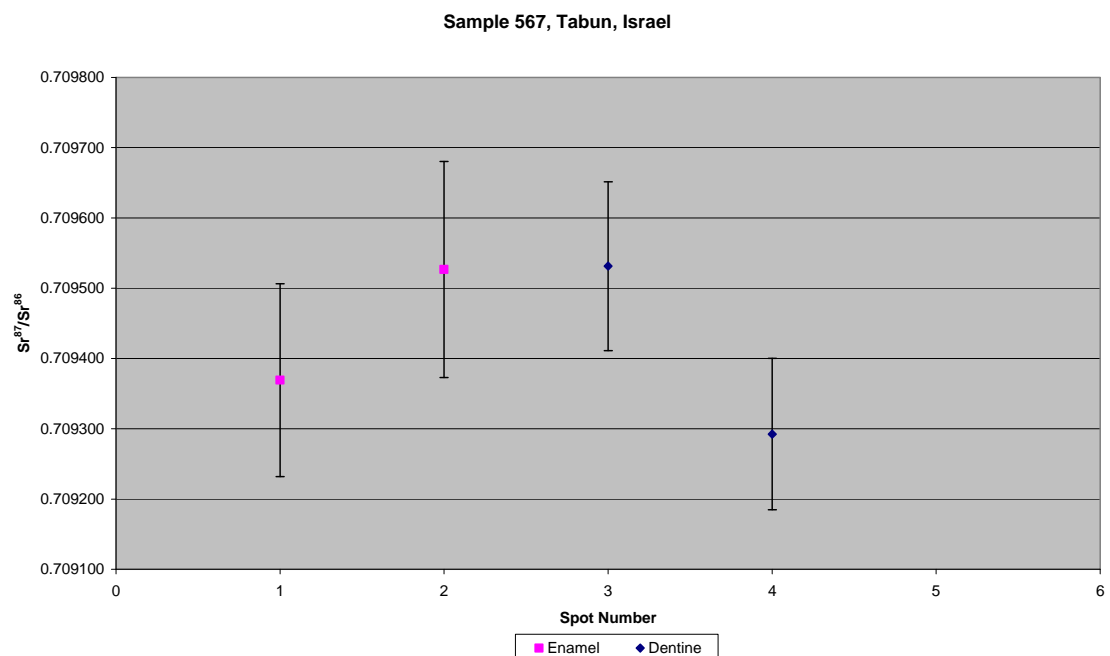


Figure A3.57 Detailed LA-MC-ICPMS Uncorrected Sr Isotope Results, Sample 567, *Bos*, Layer Eb, Tabun

Sample 567, Corrected Sr Values, Tabun, Israel

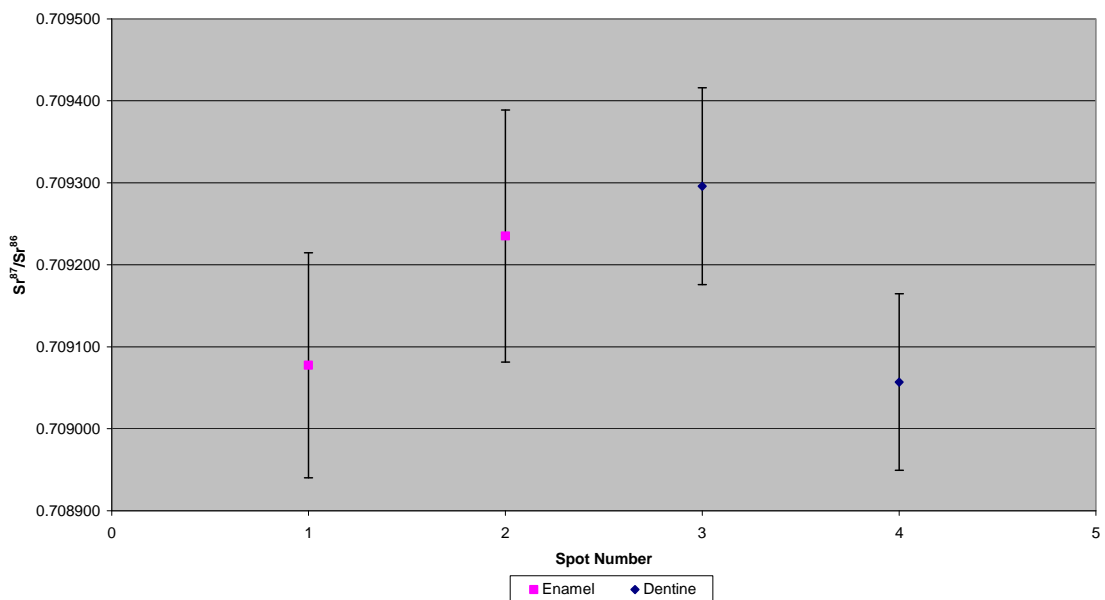


Figure A3.58 Detailed LA-MC-ICPMS Uncorrected Sr Isotope Results, Sample 567, *Bos*, Layer Ed, Tabun

Sample 568, a rhinoceros tooth from layer Ed shown in Figure A2.20, was analysed by 3 tracks, which contain 2 spots of enamel and 12 spots of dentine, 2 spots of enamel and 7 spots of dentine and 4 spots of enamel and 15 spots of dentine, respectively, shown in Figure A3.59. The weighted average values of enamel and dentine for tracks in this sample are shown in Table 5.12 and Figure 5.7. The enamel spots of track 1 have an average ^{88}Sr voltage of 0.529, a weighted average uncorrected $^{87}\text{Sr}/^{86}\text{Sr}$ value of 0.7097 ± 0.0026 , a weighted average corrected $^{87}\text{Sr}/^{86}\text{Sr}$ value of 0.70900 ± 0.0026 and a weighted average $^{84}\text{Sr}/^{86}\text{Sr}$ value of 0.05694 ± 0.00023 ($n=2$). The dentine spots of track 1 have an average ^{88}Sr voltage of 0.708, a weighted average uncorrected $^{87}\text{Sr}/^{86}\text{Sr}$ value of 0.70887 ± 0.00017 , a weighted average corrected $^{87}\text{Sr}/^{86}\text{Sr}$ value of 0.70843 ± 0.00017 and a weighted average $^{84}\text{Sr}/^{86}\text{Sr}$ value of 0.056942 ± 0.000082 ($n=12$). The enamel spots of track 2 have an average ^{88}Sr voltage of 0.424, a weighted average uncorrected $^{87}\text{Sr}/^{86}\text{Sr}$ value of 0.71019 ± 0.00043 , a weighted average corrected $^{87}\text{Sr}/^{86}\text{Sr}$ value of 0.70952 ± 0.00043 and a weighted average $^{84}\text{Sr}/^{86}\text{Sr}$ value of 0.05706 ± 0.00031 ($n=2$). The dentine spots of track 2 have an average ^{88}Sr voltage of 0.607, a weighted average uncorrected $^{87}\text{Sr}/^{86}\text{Sr}$ value of 0.70909 ± 0.00044 , a weighted average corrected

$^{87}\text{Sr}/^{86}\text{Sr}$ value of 0.70865 ± 0.00044 and a weighted average $^{84}\text{Sr}/^{86}\text{Sr}$ value of 0.05678 ± 0.00011 ($n=7$). The enamel spots of track 3 have an average ^{88}Sr voltage of 0.462, a weighted average uncorrected $^{87}\text{Sr}/^{86}\text{Sr}$ value of 0.70964 ± 0.00026 , a weighted average corrected $^{87}\text{Sr}/^{86}\text{Sr}$ value of 0.70896 ± 0.00026 and a weighted average $^{84}\text{Sr}/^{86}\text{Sr}$ value of 0.05690 ± 0.00023 ($n=4$). The dentine spots of track 3 have an average ^{88}Sr voltage of 0.506, a weighted average uncorrected $^{87}\text{Sr}/^{86}\text{Sr}$ value of 0.70873 ± 0.00015 , a weighted average corrected $^{87}\text{Sr}/^{86}\text{Sr}$ value of 0.70829 ± 0.00015 and a weighted average $^{84}\text{Sr}/^{86}\text{Sr}$ value of 0.05687 ± 0.00015 ($n=15$). Enamel values range from 0.709432 to 0.710229 (uncorrected) and 0.708760 to 0.709556 (corrected), while dentine values range from 0.708269 to 0.709833 (uncorrected) and 0.707831 to 0.709394 (corrected), shown in Table A3.55, Figure A3.60 and Figure A3.61. Both enamel and dentine $^{87}\text{Sr}/^{86}\text{Sr}$ values are relatively heterogeneous; however, enamel values are generally elevated compared to the dentine.

All enamel spots from the 3 analysis tracks are within 2σ error, suggesting that this specimen was not mobile during amelogenesis. The enamel values have an overall uncorrected weighted average of 0.70975 ± 0.00023 , which is within error of the value of sample 152 from IS002 from unconsolidated coastal plain sediments. The weighted average corrected enamel value is 0.70908 ± 0.00023 , which corresponds to samples 156 from IS005 and 157 from IS006 located in the Bina Formation, as well as 153 from IS003 located in kurkar, which outcrop within 1 km and 2.3 km of the site, respectively. While many of the dentine and enamel values have overlapping 2σ error, the weighted average value for dentine is considerably less radiogenic than the enamel value. The strontium isotope values for the sediment in this stratigraphic unit is 0.708484 ± 0.000011 , which is slightly more radiogenic than the value obtained for dentine.



Figure A3.59 LA-MC-ICPMS Track for Sample 568, Rhinoceros, Layer Ed, Tabun

Sample	Material	Track	Point	^{88}Sr Volts	$^{84}\text{Sr}/^{86}\text{Sr}$	$^{84}\text{Sr}/^{86}\text{Sr} 2\sigma$ Error	Corrected $^{87}\text{Sr}/^{86}\text{Sr}$	$^{87}\text{Sr}/^{86}\text{Sr} 2\sigma$ Error
568	Enamel	1	1	0.530	0.056980	0.000316	0.709889	0.709216
568	Enamel	1	2	0.527	0.056880	0.000353	0.709473	0.708800
568	Dentine	1	3	0.701	0.057102	0.000300	0.709405	0.708967
568	Dentine	1	4	0.914	0.056933	0.000184	0.709061	0.708623
568	Dentine	1	5	0.749	0.057063	0.000252	0.708755	0.708317
568	Dentine	1	6	0.710	0.056721	0.000254	0.708800	0.708361
568	Dentine	1	7	0.545	0.057036	0.000377	0.708976	0.708537
568	Dentine	1	8	0.513	0.057084	0.000425	0.708842	0.708403
568	Dentine	1	9	0.530	0.057154	0.000487	0.708875	0.708436
568	Dentine	1	10	0.608	0.056754	0.000317	0.708269	0.707831
568	Dentine	1	11	0.582	0.056979	0.000371	0.708828	0.708390
568	Dentine	1	12	0.612	0.056925	0.000309	0.708546	0.708108
568	Dentine	1	13	0.625	0.057112	0.000312	0.708727	0.708288
568	Dentine	1	14	0.624	0.056802	0.000246	0.708844	0.708405
568	Dentine	1	15					
568	Enamel	2	1	0.407	0.057152	0.000435	0.710229	0.709556
568	Enamel	2	2	0.441	0.056960	0.000464	0.710149	0.709477
568	Dentine	2	3	0.661	0.056761	0.000279	0.709013	0.708574
568	Dentine	2	4	0.539	0.056826	0.000329	0.708765	0.708327
568	Dentine	2	5	0.527	0.056765	0.000347	0.708737	0.708298
568	Dentine	2	6	0.568	0.056850	0.000329	0.708796	0.708357
568	Dentine	2	7	0.549	0.056826	0.000352	0.708715	0.708277
568	Dentine	2	8	0.602	0.056894	0.000297	0.709278	0.708839
568	Dentine	2	9	0.804	0.056639	0.000253	0.709833	0.709394
568	Enamel	3	1	0.418	0.057073	0.000430	0.710050	0.709378
568	Enamel	3	2	0.438	0.056821	0.000513	0.709602	0.708930
568	Enamel	3	3	0.447	0.056754	0.000428	0.709626	0.708953
568	Enamel	3	4	0.547	0.056960	0.000536	0.709432	0.708760
568	Dentine	3	5	0.476	0.057012	0.000406	0.708798	0.708359
568	Dentine	3	6	0.406	0.057073	0.000525	0.708793	0.708355
568	Dentine	3	7	0.415	0.057384	0.000441	0.708766	0.708327
568	Dentine	3	8	0.396	0.057208	0.000469	0.708513	0.708074
568	Dentine	3	9	0.431	0.057436	0.000472	0.708600	0.708162
568	Dentine	3	10	0.440	0.057045	0.000439	0.708617	0.708179
568	Dentine	3	11	0.449	0.057317	0.000628	0.708474	0.708036
568	Dentine	3	12	0.485	0.057074	0.000518	0.708320	0.707882
568	Dentine	3	13	0.513	0.056748	0.000382	0.708529	0.708091

Sample	Material	Track	Point	^{88}Sr Volts	$^{84}\text{Sr}/^{86}\text{Sr}$	$^{84}\text{Sr}/^{86}\text{Sr} 2\sigma$	Corrected $^{87}\text{Sr}/^{86}\text{Sr}$	$^{87}\text{Sr}/^{86}\text{Sr} 2\sigma$	Error
568	Dentine	3	14	0.523	0.056914	0.000394	0.708802	0.708364	0.000398
568	Dentine	3	15	0.553	0.056762	0.000328	0.708564	0.708126	0.000395
568	Dentine	3	16	0.587	0.056806	0.000263	0.708679	0.708240	0.000418
568	Dentine	3	17	0.592	0.056719	0.000350	0.708879	0.708440	0.000543
568	Dentine	3	18	0.620	0.056678	0.000296	0.709216	0.708778	0.000580
568	Dentine	3	19	0.710	0.056422	0.000302	0.709333	0.708895	0.000431

Table A3.55 Detailed LA-MC-ICPMS Sr Isotope Results for Enamel and Dentine, Sample 568, Rhinoceros, Layer Ed, Tabun

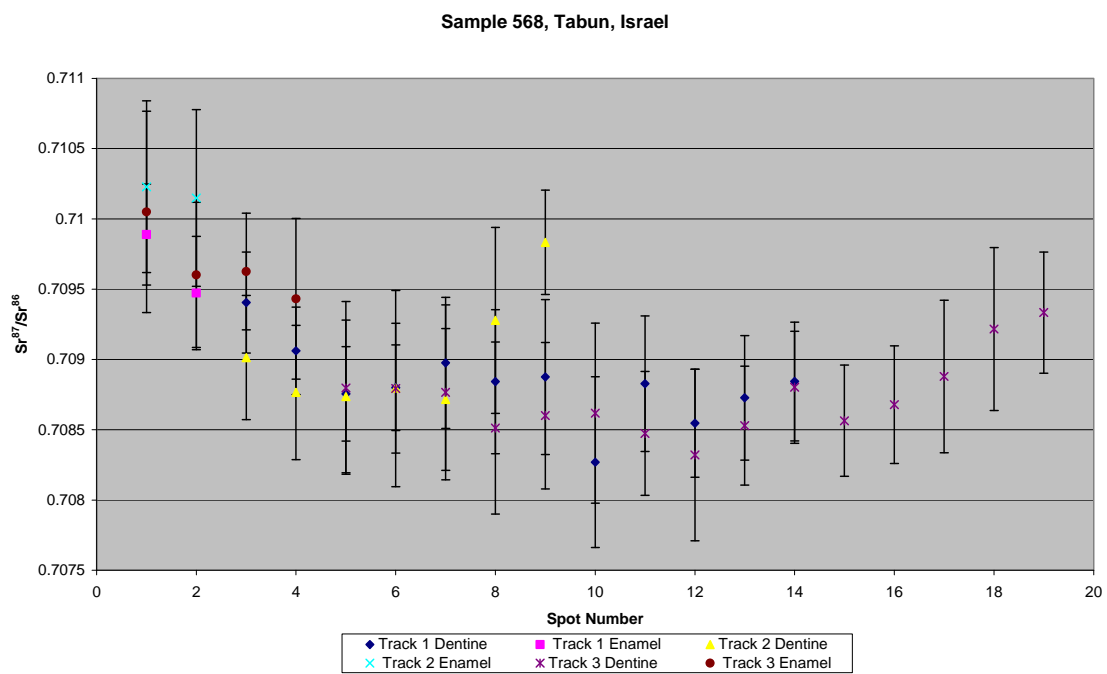


Figure A3.60 Detailed LA-MC-ICPMS Uncorrected Sr Isotope Results, Sample 568, Rhinoceros, Layer Ed, Tabun

Sample 568, Corrected Sr Values, Tabun, Israel

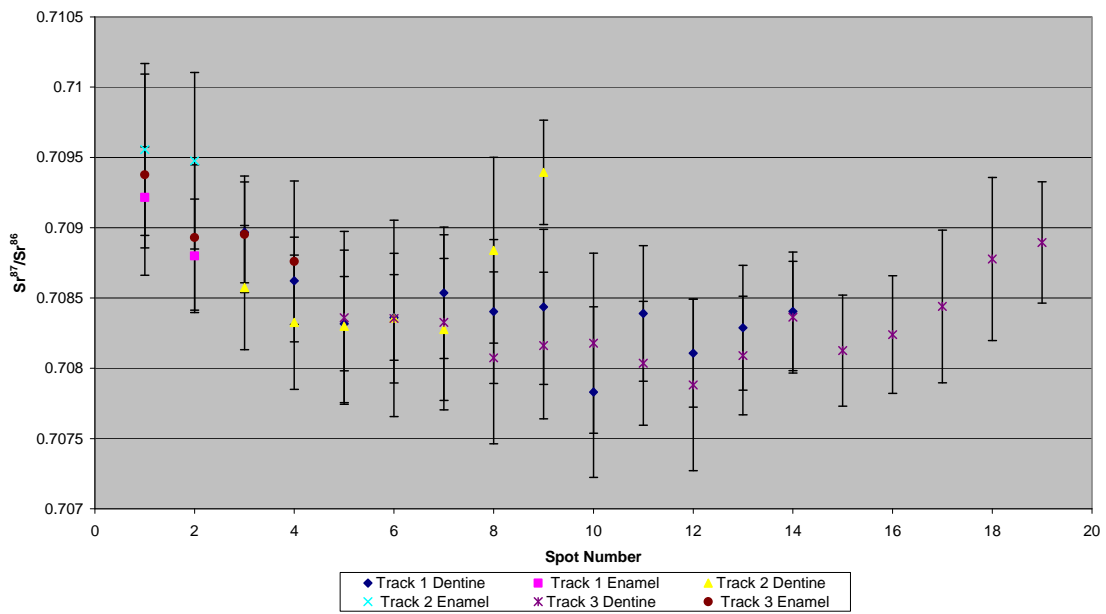


Figure A3.61 Detailed LA-MC-ICPMS Corrected Sr Isotope Results, Sample 568, *Bos*, Layer Ed, Tabun

A3.2.2.3. Amud

Sample 1024, a *Dama mesopotamica* tooth from layer B1 at Amud shown in Figure A2.21, was analysed in 2 tracks shown in Figure A3.62, with track 1 comprising 4 spots of enamel and 6 spots of dentine and track 2 comprising 2 spots of enamel and 7 spots of dentine, the strontium isotope results of which are summarised in Table 5.15 and Figure 5.9. The enamel spots of track 1 have an average ⁸⁸Sr voltage of 2.504, a weighted average uncorrected ⁸⁷Sr/⁸⁶Sr value of 0.71098 ± 0.00030 , a weighted average corrected ⁸⁷Sr/⁸⁶Sr value of 0.70989 ± 0.00030 and a weighted average ⁸⁴Sr/⁸⁶Sr value of 0.05698 ± 0.00032 ($n=4$). The dentine spots of track 1 have an average ⁸⁸Sr voltage of 4.512, a weighted average uncorrected ⁸⁷Sr/⁸⁶Sr value of 0.708994 ± 0.000078 , a weighted average corrected ⁸⁷Sr/⁸⁶Sr value of 0.70859 ± 0.000078 and a weighted average ⁸⁴Sr/⁸⁶Sr value of 0.056672 ± 0.000050 ($n=6$). The enamel spots of track 2 have an average ⁸⁸Sr voltage of 2.664, a weighted average uncorrected ⁸⁷Sr/⁸⁶Sr value of 0.7119 ± 0.0062 , a weighted average corrected ⁸⁷Sr/⁸⁶Sr value of 0.71080 ± 0.0062 and a weighted average ⁸⁴Sr/⁸⁶Sr value of 0.056691 ± 0.000051 ($n=2$). The dentine spots of track 2 have an average ⁸⁸Sr voltage of 4.454, a weighted average uncorrected ⁸⁷Sr/⁸⁶Sr value of 0.70911 ± 0.0062 , a weighted average corrected ⁸⁷Sr/⁸⁶Sr value of 0.70879 ± 0.0062 and a weighted average ⁸⁴Sr/⁸⁶Sr value of 0.056689 ± 0.000051 ($n=2$).

0.00030, a weighted average corrected $^{87}\text{Sr}/^{86}\text{Sr}$ value of 0.70871 ± 0.00030 and a weighted average $^{84}\text{Sr}/^{86}\text{Sr}$ value of 0.056558 ± 0.000016 ($n=7$). Enamel $^{87}\text{Sr}/^{86}\text{Sr}$ values cover the range of 0.710742 to 0.711174 (uncorrected) and 0.709653 to 0.710086 (corrected) for track 1 and 0.711586 and 0.712708 (uncorrected), as well as 0.710498 and 0.711620 (corrected) for track 2, shown in Table A3.56, Figure A3.63 and Figure A3.64. The $^{87}\text{Sr}/^{86}\text{Sr}$ values for enamel for track 1 are relatively homogeneous, being principally within 2σ error. In contrast, track 2 has heterogeneous $^{87}\text{Sr}/^{86}\text{Sr}$ values with point 1 being particularly elevated compared with the rest of the sample. Dentine $^{87}\text{Sr}/^{86}\text{Sr}$ values for track 1 cover the range of 0.708925 to 0.709132 (uncorrected) and 0.708530 to 0.708737 (corrected), while track 2 cover the range of 0.708698 to 0.709685 (uncorrected) and 0.708302 to 0.709290 (corrected), shown in Table A3.56, Figure A3.63 and Figure A3.64.

Enamel values are somewhat heterogeneous, particularly track 2, suggesting that this sample was mobile during amelogenesis. The enamel has an uncorrected weighted average $^{87}\text{Sr}/^{86}\text{Sr}$ value of 0.71122 ± 0.00056 , for which the only comparable mapping value is associated with a Precambrian granite rock sample near Eilat, although mobility of this distance (~440 km) is probably not credible. The corrected enamel value for this sample is 0.71013 ± 0.00056 , which corresponds to sample 162 from IS011 in the Bina Formation, which outcrops within 2.7 km from the site. Unfortunately no strontium concentration information was collected for this sample; however, the $^{84}\text{Sr}/^{86}\text{Sr}$ ratio of enamel is 0.05685 ± 0.00022 , which suggests that the analysis is relatively robust.



Figure A3.62 LA-MC-ICPMS Track for Sample 1024, *Dama mesopotamica*, Layer B1, Amud

Sample	Material	Track	Point	^{88}Sr Volts	$^{84}\text{Sr}/^{86}\text{Sr}$	$^{84}\text{Sr}/^{86}\text{Sr}$ 2 σ Error	$^{87}\text{Sr}/^{86}\text{Sr}$	Corrected $^{87}\text{Sr}/^{86}\text{Sr}$	$^{87}\text{Sr}/^{86}\text{Sr}$ 2 σ Error
1024	Enamel	1	1	1.890	0.057329	0.000109	0.711028	0.709940	0.000177
1024	Enamel	1	2	2.319	0.057010	0.000117	0.710963	0.709875	0.000156
1024	Enamel	1	3	2.746	0.056908	0.000082	0.711174	0.710086	0.000147
1024	Enamel	1	4	3.058	0.056852	0.000078	0.710742	0.709653	0.000155
1024	Dentine	1	5	4.169	0.056706	0.000049	0.709132	0.708737	0.000091
1024	Dentine	1	6	4.431	0.056701	0.000039	0.708925	0.708530	0.000070
1024	Dentine	1	7	4.414	0.056717	0.000056	0.709013	0.708618	0.000118
1024	Dentine	1	8	4.567	0.056684	0.000048	0.708955	0.708560	0.000085
1024	Dentine	1	9	4.592	0.056683	0.000038	0.709012	0.708617	0.000092
1024	Dentine	1	10	4.900	0.056598	0.000035	0.708990	0.708595	0.000097
1024	Enamel	2	1	2.689	0.056682	0.000061	0.712708	0.711620	0.000258
1024	Enamel	2	2	2.640	0.056714	0.000102	0.711586	0.710498	0.000150
1024	Dentine	2	3	3.703	0.056575	0.000047	0.709685	0.709290	0.000092
1024	Dentine	2	4	4.548	0.056517	0.000040	0.708698	0.708302	0.000086
1024	Dentine	2	5	4.666	0.056577	0.000050	0.708873	0.708478	0.000095
1024	Dentine	2	6	4.735	0.056578	0.000038	0.708943	0.708548	0.000084
1024	Dentine	2	7	4.273	0.056574	0.000050	0.709154	0.708759	0.000108
1024	Dentine	2	8	4.054	0.056548	0.000046	0.709189	0.708794	0.000088
1024	Dentine	2	9	5.197	0.056549	0.000042	0.709288	0.708893	0.000087

Table A3.56 Detailed LA-MC-ICPMS Sr Isotope Results for Enamel and Dentine, Sample 1024, *Dama mesopotamica*, Layer B1, Amud

Sample 1024, Amud, Israel

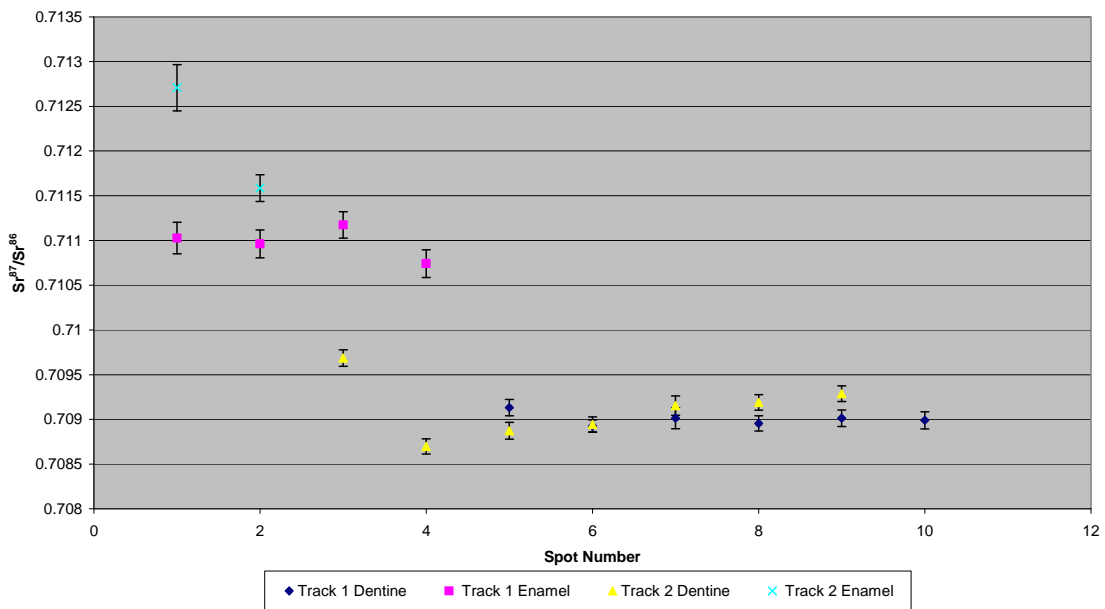


Figure A3.63 Detailed LA-MC-ICPMS Uncorrected Sr Isotope Results, Sample 1024, *Dama mesopotamica*, Layer B1, Amud

Sample 1024, Corrected Sr Values, Amud, Israel

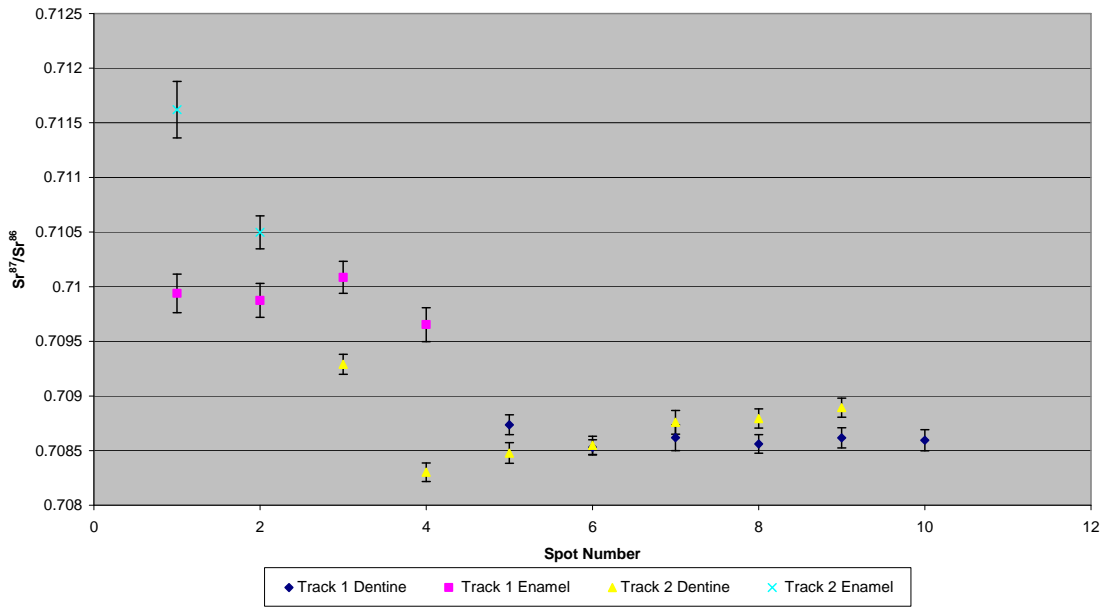


Figure A3.64 Detailed LA-MC-ICPMS Corrected Sr Isotope Results, Sample 1024, *Dama mesopotamica*, Layer B1, Amud

Sample 1025, a *Dama mesopotamica* tooth from layer B1 at Amud shown in Figure A2.22, was analysed by 1 track containing 15 spots of enamel and 15 spots of dentine, shown in Figure A3.65. The enamel spots of sample 1025 have an average ^{88}Sr voltage of 4.544, a weighted average uncorrected

$^{87}\text{Sr}/^{86}\text{Sr}$ value of 0.70887 ± 0.00024 , a weighted average corrected $^{87}\text{Sr}/^{86}\text{Sr}$ value of 0.70859 ± 0.00024 and a weighted average $^{84}\text{Sr}/^{86}\text{Sr}$ value of 0.056323 ± 0.000037 ($n=15$), shown in Table 5.15 and Figure 5.9. The dentine spots of sample 1025 have an average ^{88}Sr voltage of 4.607039, a weighted average uncorrected $^{87}\text{Sr}/^{86}\text{Sr}$ value of 0.70856 ± 0.00012 , a weighted average corrected $^{87}\text{Sr}/^{86}\text{Sr}$ value of 0.70832 ± 0.00012 and a weighted average $^{84}\text{Sr}/^{86}\text{Sr}$ value of 0.056309 ± 0.000039 ($n=15$), shown in Table 5.15 and Figure 5.9. Enamel $^{87}\text{Sr}/^{86}\text{Sr}$ values for sample 1025 are in the range of 0.708597 to 0.711611 (uncorrected) and 0.708326 to 0.711340 (corrected), shown in Table A3.57, Figure A3.66 and Figure A3.67. The values are relatively heterogeneous, particularly spot 1, which is significantly elevated compared to the other samples. Dentine $^{87}\text{Sr}/^{86}\text{Sr}$ values for sample 1025 are in the range of 0.708252 to 0.709243 (uncorrected) and 0.708554 to 0.709004 (corrected), shown in Table A3.57, Figure A3.66 and Figure A3.67.

The enamel spots are somewhat homogenous, although spot 1 has a particularly elevated value compared to other samples. The degree of heterogeneity suggests that this sample was somewhat mobile during amelogenesis. The enamel has an uncorrected weighted average $^{87}\text{Sr}/^{86}\text{Sr}$ value of 0.70887 ± 0.00024 , which corresponds to a bioavailable soil value from sample location IS017 of $0.708852 + 0.000084$ from the local limestone grouped as part of the Nabi Sa'id, Ein el Assad, Hidra, Rama and Kefira Formations by Sneh, Bartov and Rosensaft, (1998a). This combination of units outcrops only in a very small area to the west of Amud, providing a very specific location for this specimen during amelogenesis. The corrected weighted average value of this sample is 0.70860 ± 0.00024 , which corresponds to a number of carbonate mapping samples, including the Mount Scopus Group (value from sample 178 from site IS027) which outcrops within 1.4 km of the site. Dentine in sample 1025 is relatively heterogeneous, suggesting a complex regime of post-burial diagenesis or significant variations in strontium concentration.

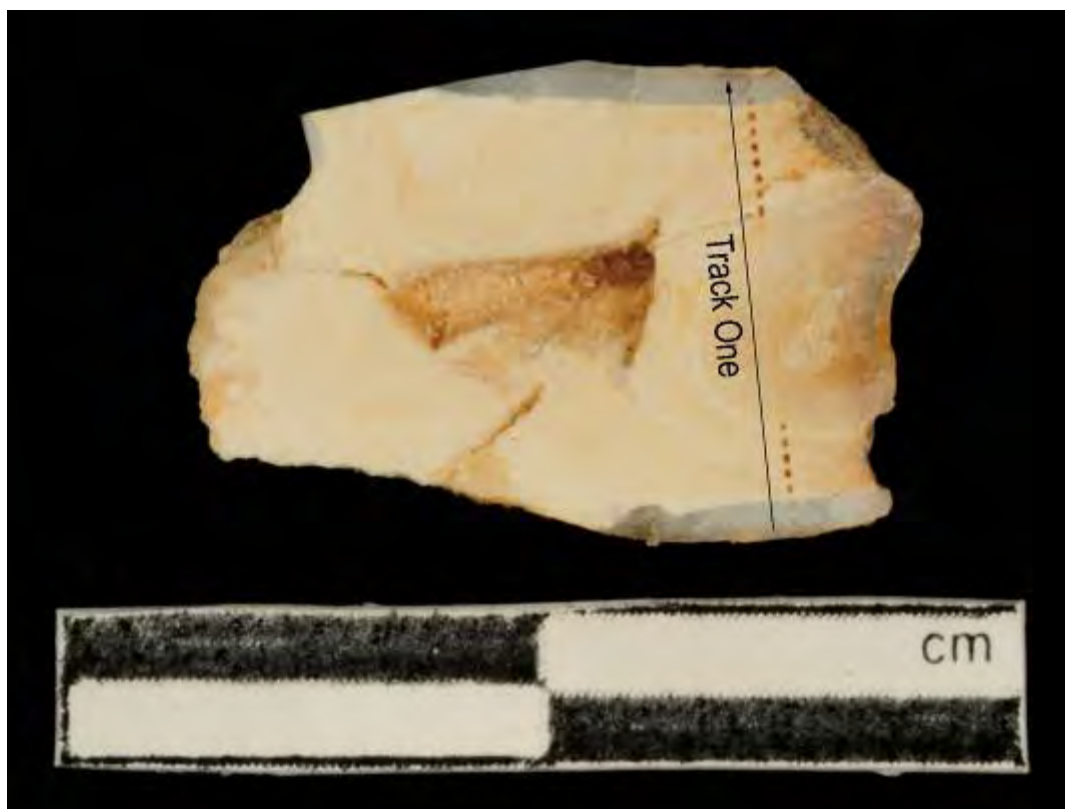


Figure A3.65 LA-MC-ICPMS Track for Sample 1025, *Dama mesopotamica*, Layer B1, Amud

Sample	Material	Track	Point	^{88}Sr Volts	$^{84}\text{Sr}/^{86}\text{Sr}$	$^{84}\text{Sr}/^{86}\text{Sr} 2\sigma$	Corrected $^{87}\text{Sr}/^{86}\text{Sr}$	$^{87}\text{Sr}/^{86}\text{Sr} 2\sigma$	Error
1025	Enamel	1	1	3.683	0.056351	0.000059	0.711611	0.711340	0.000185
1025	Enamel	1	2	4.541	0.056398	0.000050	0.708970	0.708699	0.000086
1025	Enamel	1	3	4.698	0.056410	0.000047	0.708599	0.708328	0.000095
1025	Enamel	1	4	5.943	0.056399	0.000029	0.708685	0.708413	0.000098
1025	Dentine	1	5	5.558	0.056398	0.000050	0.708765	0.708526	0.000084
1025	Dentine	1	6	4.073	0.056323	0.000044	0.708946	0.708707	0.000145
1025	Dentine	1	7	6.217	0.056413	0.000037	0.708593	0.708354	0.000076
1025	Dentine	1	8	5.336	0.056384	0.000039	0.708409	0.708171	0.000071
1025	Enamel	1	9	5.171	0.056362	0.000046	0.708801	0.708530	0.000096
1025	Enamel	1	10	4.748	0.056334	0.000035	0.708834	0.708563	0.000109
1025	Enamel	1	11	4.769	0.056343	0.000044	0.708868	0.708597	0.000098
1025	Dentine	1	12	3.755	0.056297	0.000064	0.709060	0.708822	0.000124
1025	Dentine	1	13	3.400	0.056304	0.000056	0.708794	0.708556	0.000136
1025	Dentine	1	14	3.179	0.056200	0.000073	0.708763	0.708524	0.000178
1025	Dentine	1	15	3.489	0.056186	0.000082	0.709243	0.709004	0.000189
1025	Enamel	1	16	3.641	0.056216	0.000078	0.709077	0.708805	0.000135

1025	Enamel	1	17	5.068	0.056291	0.000048	0.708927	0.708656	0.000088
1025	Enamel	1	18	5.039	0.056305	0.000037	0.708825	0.708554	0.000075
1025	Enamel	1	19	4.525	0.056301	0.000040	0.708849	0.708577	0.000102
1025	Enamel	1	20	4.325	0.056280	0.000044	0.708675	0.708403	0.000112
1025	Enamel	1	21	3.932	0.056255	0.000060	0.708658	0.708387	0.000125
1025	Dentine	1	22	3.962	0.056236	0.000055	0.708507	0.708268	0.000104
1025	Dentine	1	23	5.919	0.056367	0.000037	0.708602	0.708364	0.000087
1025	Dentine	1	24	4.030	0.056229	0.000056	0.708379	0.708140	0.000077
1025	Dentine	1	25	5.048	0.056285	0.000043	0.708252	0.708014	0.000100
1025	Dentine	1	26	4.636	0.056235	0.000040	0.708345	0.708106	0.000087
1025	Dentine	1	27	5.024	0.056240	0.000037	0.708584	0.708345	0.000078
1025	Dentine	1	28	5.474	0.056292	0.000046	0.708484	0.708245	0.000101
1025	Enamel	1	29	3.512	0.056181	0.000056	0.708597	0.708326	0.000089
1025	Enamel	1	30	4.560	0.056207	0.000044	0.709057	0.708785	0.000108

Table A3.57 Detailed LA-MC-ICPMS Sr Isotope Results for Enamel and Dentine, Sample 1025, *Dama mesopotamica*, Layer B1, Amud

Sample 1025, Amud, Israel

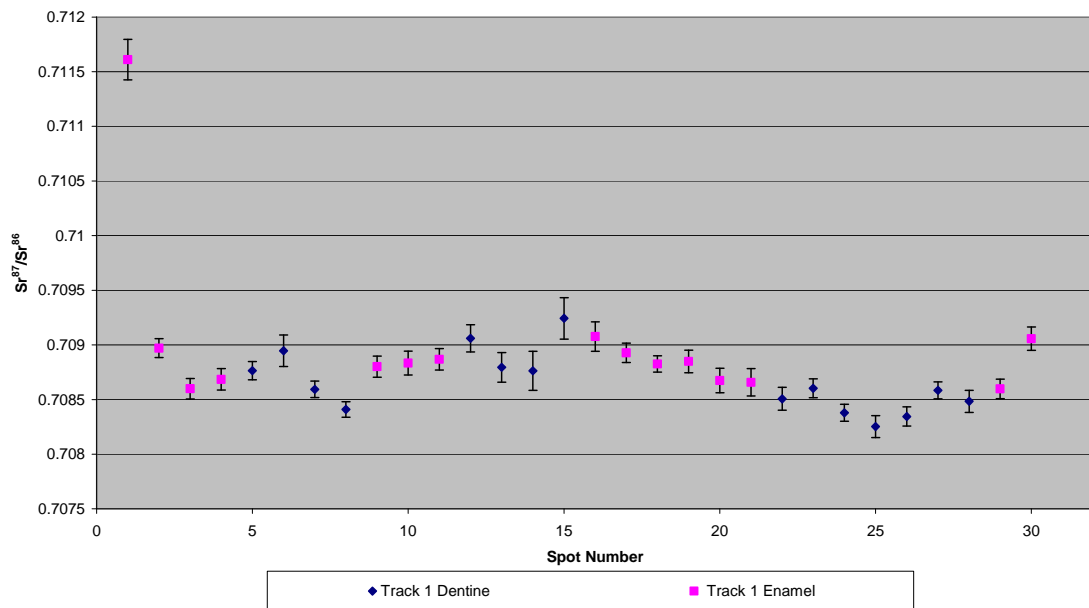


Figure A3.66 Detailed LA-MC-ICPMS Uncorrected Sr Isotope Results, Sample 1025, *Dama mesopotamica*, Layer B1, Amud

Sample 1025, Corrected Sr Values, Amud, Israel

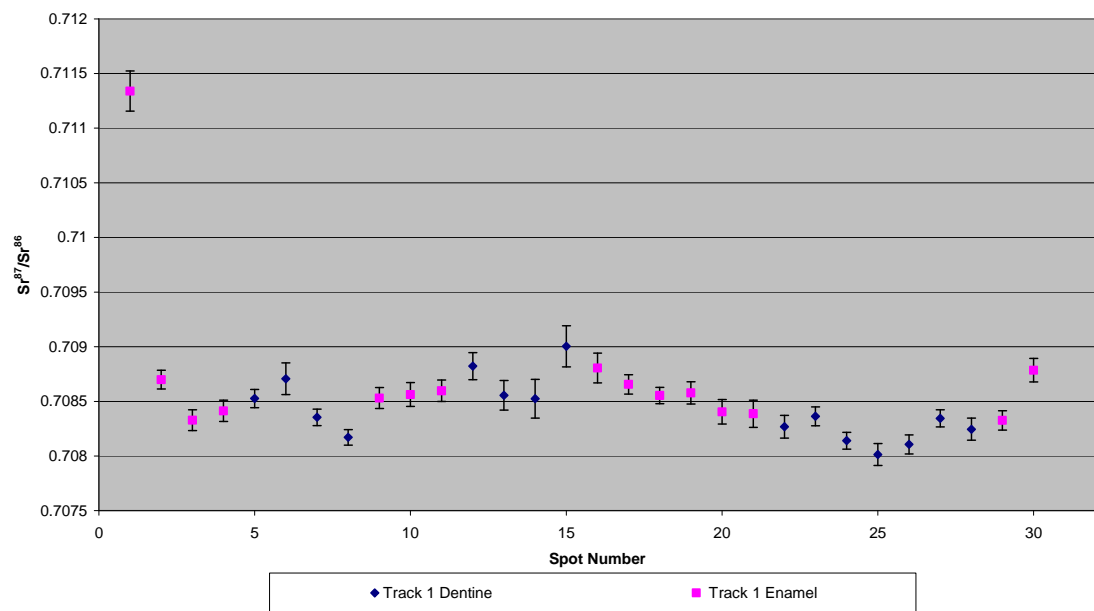


Figure A3.67 Detailed LA-MC-ICPMS Corrected Sr Isotope Results, Sample 1025, *Dama mesopotamica*, Layer B1, Amud

Sample 1026, a *Dama mesopotamica* tooth from layer B1 at Amud shown in Figure A2.23, was analysed in 2 tracks, with track 1 comprising 4 spots of enamel and 9 spots of dentine and track 2 comprising 3 spots of enamel and 11 spots of dentine, which is shown in Figure A3.68, the strontium isotope results of which are summarised in Table 5.15 and Figure 5.9. The enamel spots of track 1 have an average ^{88}Sr voltage of 1.080, a weighted average uncorrected $^{87}\text{Sr}/^{86}\text{Sr}$ value of 0.71071 ± 0.00048 , a weighted average corrected $^{87}\text{Sr}/^{86}\text{Sr}$ value of 0.70709 ± 0.00048 and a weighted average $^{84}\text{Sr}/^{86}\text{Sr}$ value of 0.05515 ± 0.00024 ($n=4$). The dentine spots of track 1 have an average ^{88}Sr voltage of 3.301740, a weighted average uncorrected $^{87}\text{Sr}/^{86}\text{Sr}$ value of 0.70887 ± 0.00017 , a weighted average corrected $^{87}\text{Sr}/^{86}\text{Sr}$ value of 0.70849 ± 0.00017 and a weighted average $^{84}\text{Sr}/^{86}\text{Sr}$ value of 0.055988 ± 0.000088 ($n=6$). The enamel spots of track 2 have an average ^{88}Sr voltage of 1.005, a weighted average uncorrected $^{87}\text{Sr}/^{86}\text{Sr}$ value of 0.7105 ± 0.0011 , a weighted average corrected $^{87}\text{Sr}/^{86}\text{Sr}$ value of 0.70690 ± 0.0011 and a weighted average $^{84}\text{Sr}/^{86}\text{Sr}$ value of 0.05472 ± 0.00059 ($n=3$). The dentine spots of track 2 have an average ^{88}Sr voltage of 3.2452, a weighted average uncorrected $^{87}\text{Sr}/^{86}\text{Sr}$ value of 0.708767 ± 0.000059 , a weighted average corrected $^{87}\text{Sr}/^{86}\text{Sr}$ value of 0.70839 ± 0.000059 and a weighted average $^{84}\text{Sr}/^{86}\text{Sr}$ value of 0.055942 ± 0.000045 ($n=10$). Enamel $^{87}\text{Sr}/^{86}\text{Sr}$ values are in the range of 0.710467 to 0.711105 (uncorrected) and 0.706842 to 0.707480 (corrected) for track 1 as well as 0.708751 to 0.710981 (uncorrected) and 0.708379 to 0.707355 (corrected) for track 2, shown in Table A3.58, Figure A3.69 and Figure A3.70. Dentine $^{87}\text{Sr}/^{86}\text{Sr}$ values are in the range of 0.708650 to 0.709620 (uncorrected) and 0.708278 to 0.709248 (corrected) for track 1 as well as 0.708640 to 0.709030 (uncorrected) and 0.708268 to 0.708659 (corrected) for track 2, shown in Table A3.58, Figure A3.69 and Figure A3.70. Dentine values are principally homogenous, with the greatest variation being the first dentine spot of both tracks, which have a significantly elevated $^{87}\text{Sr}/^{86}\text{Sr}$ value. Enamel values are relatively heterogeneous, becoming progressively elevated in $^{87}\text{Sr}/^{86}\text{Sr}$ value along track 1 and become depressed along track 2.

Enamel values are relatively heterogeneous, suggesting a specimen mobile during amelogenesis. The weighted average of all enamel spots is 0.71062 ± 0.00032 , which corresponds to bioavailable results from the Senonian-Palaeocene aged Mount Scopus Group limestone from site IS011, which has a value of 0.710199 ± 0.000034 , although, as discussed in section 6.3.1.6, this value may not be robust. While this analysis site is located 35 km west-north-west of Amud, an outcrop of Mount Scopus Group sediments, not sampled in this study, outcrop within 2 km east of the site. The corrected enamel weighted average value of 0.70739 ± 0.00091 is within 2σ error of a large number of mapping samples from basalt (175 from IS024, 202 from IS053, 203 from IS054 and 216 from IS062) and carbonates (163 from IS012, 167 from IS016, 168 from IS017 and 169 from IS018) surrounding the site. Of the unit above, the closest to Amud is the Cover and Dalwe Basalt which outcrops within 0.8 km of the site. With the exception of spot 5 on track 1, which may have partially sampled enamel, the dentine values are relatively homogenous, with an overall weighted average 0.708811 ± 0.000085

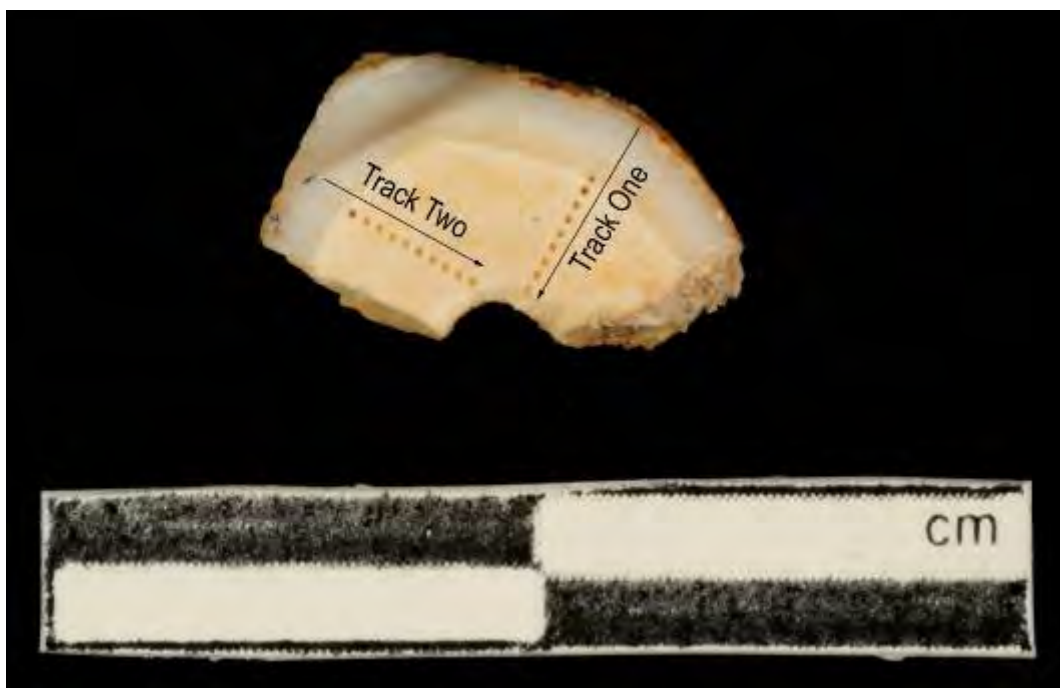


Figure A3.68 LA-MC-ICPMS Track for Sample 1026, *Dama mesopotamica*, Layer B1, Amud

Sample	Material	Track	Point	^{88}Sr Volts	$^{84}\text{Sr}/^{86}\text{Sr}$	$^{84}\text{Sr}/^{86}\text{Sr} 2\sigma$ Error	$^{87}\text{Sr}/^{86}\text{Sr}$	Corrected $^{87}\text{Sr}/^{86}\text{Sr}$	$^{87}\text{Sr}/^{86}\text{Sr} 2\sigma$ Error
1026	Enamel	1	1	1.025	0.055075	0.000180	0.710467	0.706842	0.000243
1026	Enamel	1	2	1.098	0.055292	0.000136	0.710567	0.706942	0.000258
1026	Enamel	1	3	1.095	0.055038	0.000198	0.710989	0.707364	0.000287
1026	Enamel	1	4	1.102	0.054957	0.000255	0.711105	0.707480	0.000357
1026	Dentine	1	5	1.492	0.055476	0.000104	0.709620	0.709248	0.000175
1026	Dentine	1	6	2.948	0.055953	0.000055	0.708758	0.708386	0.000104
1026	Dentine	1	7	3.787	0.056078	0.000060	0.708650	0.708278	0.000096
1026	Dentine	1	8	3.297	0.055997	0.000067	0.708879	0.708508	0.000089
1026	Dentine	1	9	3.473	0.056014	0.000049	0.708795	0.708424	0.000088
1026	Dentine	1	10	3.541	0.056014	0.000064	0.708835	0.708463	0.000117
1026	Dentine	1	11	4.160	0.056081	0.000044	0.708684	0.708313	0.000081
1026	Dentine	1	12	3.600	0.055976	0.000049	0.708946	0.708574	0.000096
1026	Dentine	1	13	3.414	0.055920	0.000051	0.709181	0.708809	0.000092
1026	Enamel	2	1	0.896	0.054452	0.000240	0.710981	0.707355	0.000269
1026	Enamel	2	2	0.967	0.054556	0.000242	0.710373	0.706748	0.000246
1026	Enamel	2	3	1.154	0.054891	0.000151	0.710109	0.709738	0.000296
1026	Dentine	2	4	2.833	0.055863	0.000076	0.708751	0.708379	0.000109
1026	Dentine	2	5	3.404	0.055968	0.000063	0.708640	0.708268	0.000100
1026	Dentine	2	6	3.445	0.056000	0.000055	0.708743	0.708371	0.000090
1026	Dentine	2	7	3.126	0.055926	0.000075	0.708825	0.708453	0.000092
1026	Dentine	2	8	3.525	0.055959	0.000072	0.708784	0.708412	0.000148
1026	Dentine	2	9	3.436	0.056007	0.000056	0.708757	0.708385	0.000090
1026	Dentine	2	10	3.482	0.055905	0.000053	0.708716	0.708344	0.000082
1026	Dentine	2	11	3.246	0.055929	0.000075	0.708807	0.708435	0.000098
1026	Dentine	2	12	3.270	0.055979	0.000058	0.708800	0.708428	0.000117
1026	Dentine	2	13	2.685	0.055800	0.000071	0.709030	0.708659	0.000149

Table A3.58 Detailed LA-MC-ICPMS Sr Isotope Results for Enamel and Dentine, Sample 1026, *Dama mesopotamica*, Layer B1, Amud

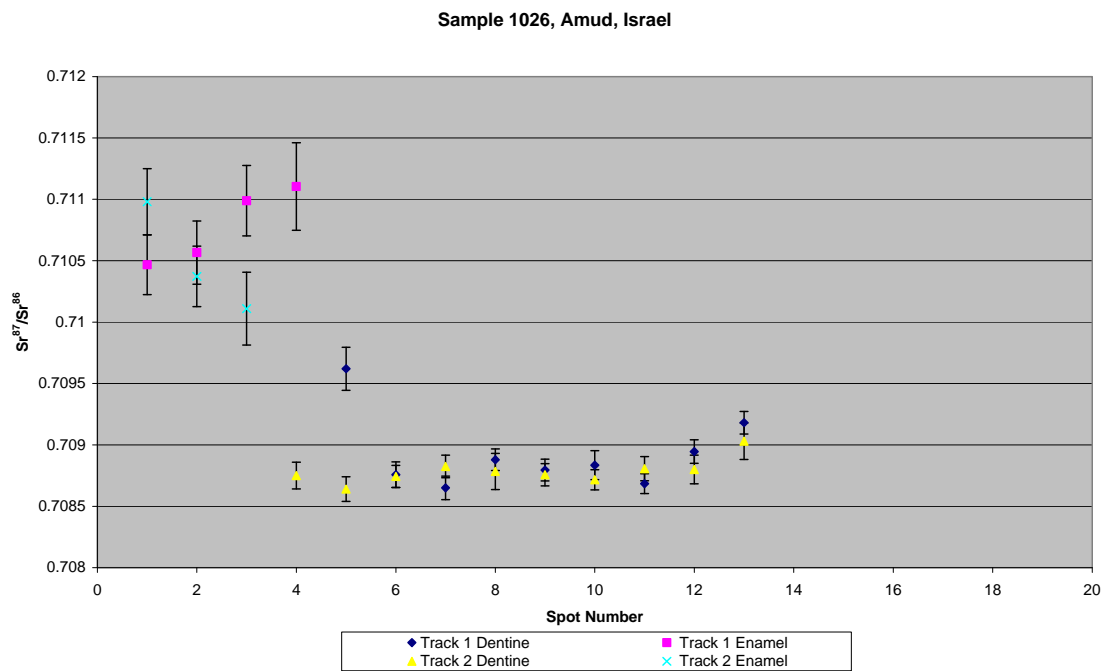


Figure A3.69 Detailed LA-MC-ICPMS Uncorrected Sr Isotope Results, Sample 1026, *Dama mesopotamica*, Layer B1, Amud

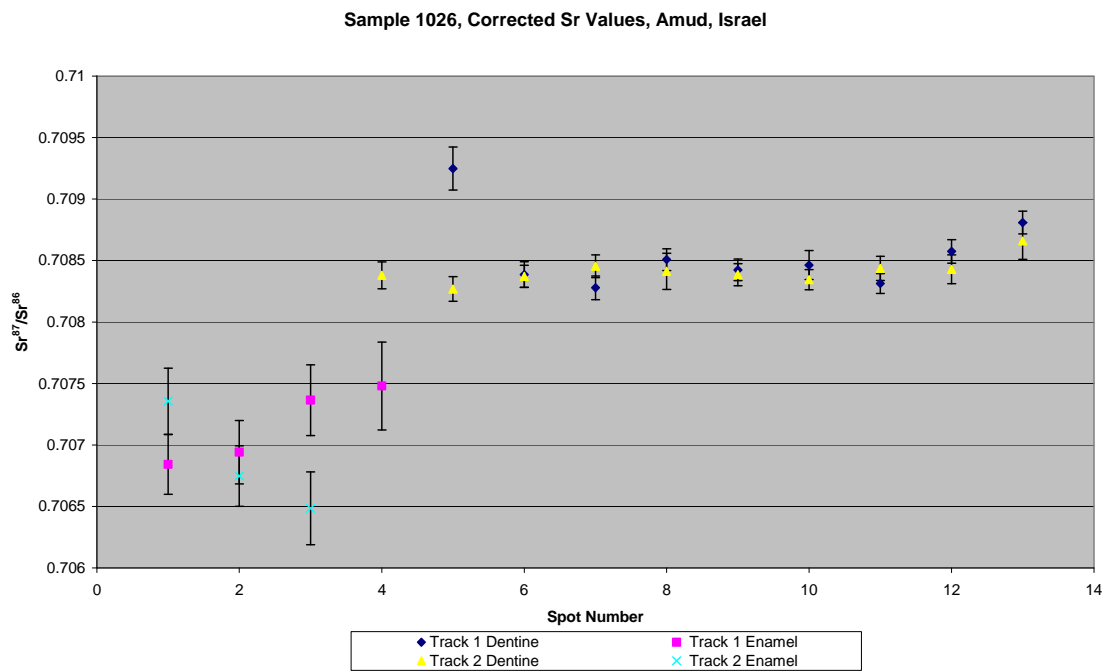


Figure A3.70 Detailed LA-MC-ICPMS Corrected Sr Isotope Results, Sample 1026, *Dama mesopotamica*, Layer B1, Amud

A3.2.2.4. Qafzeh

Sample 370, a bovid tooth from layer XV of Qafzeh, was analysed by 1 track comprising 9 spots of enamel. The enamel spots of sample 370 have an average ^{88}Sr voltage of 1.782, a weighted average uncorrected $^{87}\text{Sr}/^{86}\text{Sr}$ value of 0.70992 ± 0.00012 , a weighted average corrected $^{87}\text{Sr}/^{86}\text{Sr}$ value of 0.70942 ± 0.00012 and a weighted average $^{84}\text{Sr}/^{86}\text{Sr}$ value of 0.05547 ± 0.00010 ($n=9$), shown in Table 5.19 and Figure 5.11. Enamel $^{87}\text{Sr}/^{86}\text{Sr}$ values for sample 370 are in the range of 0.709663 to 0.710195 (uncorrected) and 0.709160 to 0.709692 (corrected), shown in Table A3.59, Figure A3.71 and Figure A3.72. The enamel values are relatively homogenous, with most being within 2σ error of each other.

The enamel from this sample has a relatively homogeneous strontium isotope composition, within 2σ error. The uncorrected weighted average of all enamel spots is 0.71062 ± 0.00032 , which corresponds with sample 162 from site IS011 located in the Senonian-Palaeocene aged Mount Scopus Group although, as discussed in section 6.3.1.6, this value may not be robust. While this analysis site is located 50 km north-north-west of Qafzeh, outcrop of Mount Scopus Group sediments, not sampled in this study, outcrop less than 1 km to the north and south of Qafzeh, suggesting that this sample is local. The corrected weighted average value for this sample is 0.70942 ± 0.00012 , which correlates with a number of different mapping samples surrounding the site, including from kurkar (151 from IS001 and 160 from IS009) and carbonates (157 from IS006, 158 from IS007, 164 from IS013 and 215 from IS061). Of these units, the Bina Formation (sampled from location IS006 and IS007) outcrops within 0.1 km of the site. No strontium concentration data were collected for this sample; however, the $^{84}\text{Sr}/^{86}\text{Sr}$ weighted average value for enamel of 0.05547 ± 0.00010 suggests that this analysis is not robust.

Sample	Material	Track	Point	^{88}Sr Volts	$^{84}\text{Sr}/^{86}\text{Sr}$	Corrected $^{87}\text{Sr}/^{86}\text{Sr}$	$^{87}\text{Sr}/^{86}\text{Sr} 2\sigma$	Error
370	Enamel	1	1	2.128	0.055443	0.000132	0.709843	0.709340
370	Enamel	1	2	1.862	0.055414	0.000143	0.709946	0.709443
370	Enamel	1	3	2.063	0.055699	0.000145	0.709850	0.709347
370	Enamel	1	4	1.860	0.055580	0.000174	0.709867	0.709364
370	Enamel	1	5	1.967	0.055372	0.000140	0.709663	0.709160
370	Enamel	1	6	1.551	0.055407	0.000162	0.709865	0.709362
370	Enamel	1	7	1.587	0.055578	0.000194	0.710087	0.709584
370	Enamel	1	8	1.436	0.055394	0.000254	0.710195	0.709692
370	Enamel	1	9	1.587	0.055218	0.000211	0.710094	0.709591

Table A3.59 Detailed LA-MC-ICPMS Sr Isotope Results for Enamel, Sample 370, Bovid, Layer XV, Qafzeh

Sample 370, Qafzeh, Israel

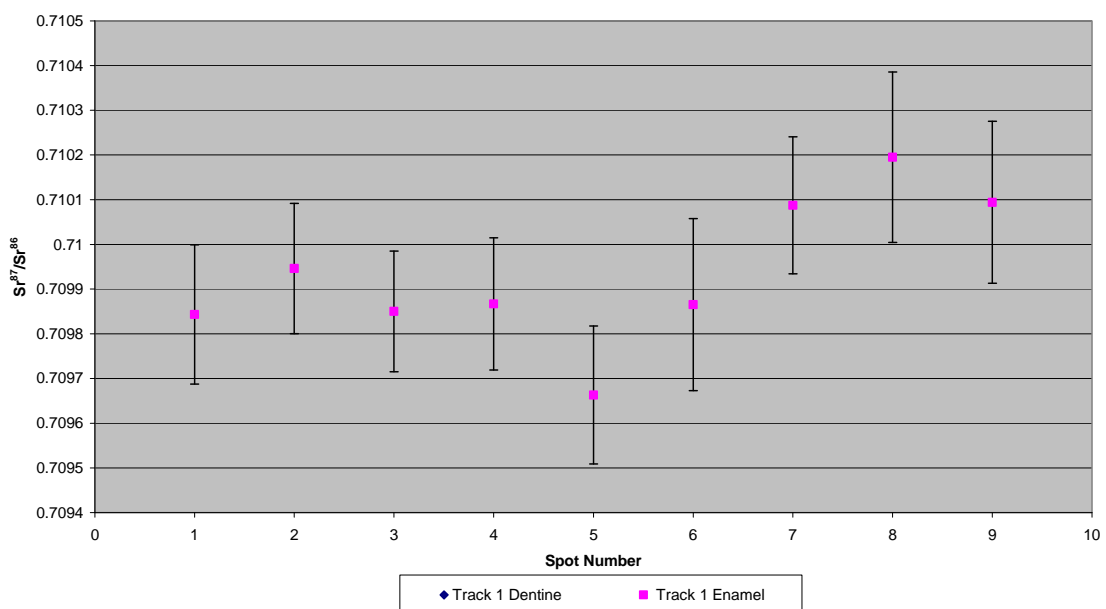


Figure A3.71 Detailed LA-MC-ICPMS Uncorrected Sr Isotope Results, Sample 370, Bovid, Layer XV, Qafzeh

Sample 370, Corrected Sr Values, Qafzeh, Israel

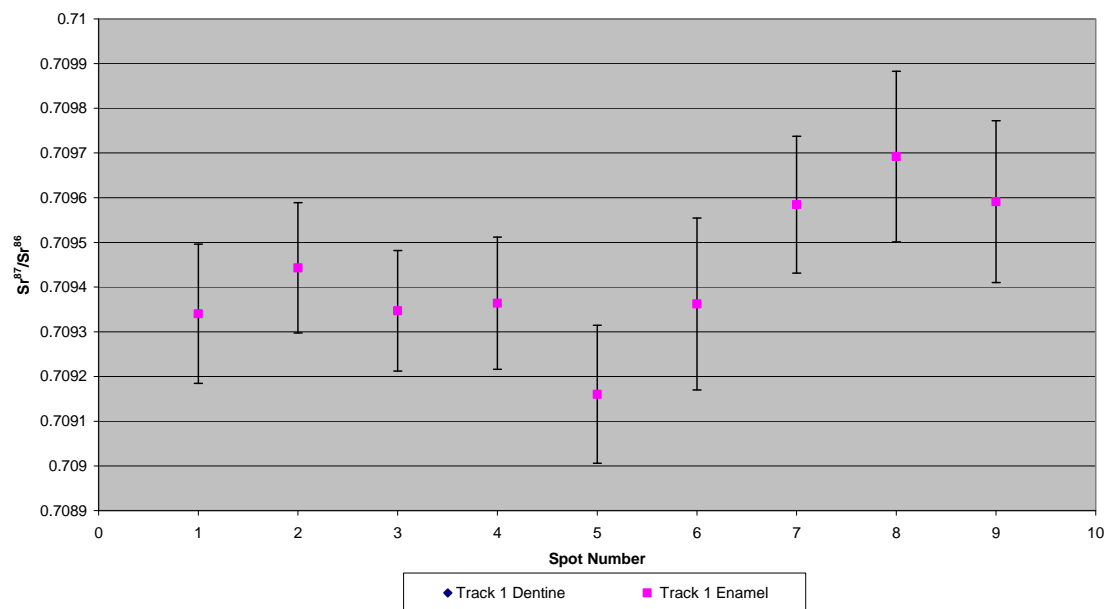


Figure A3.72 Detailed LA-MC-ICPMS Corrected Sr Isotope Results, Sample 370, Bovid, Layer XV, Qafzeh

Sample 371, a bovid tooth from layer XIX at Qafzeh shown in Figure A2.24, was analysed as 1 track containing 11 spots of enamel, shown in Figure A3.73. The enamel spots of sample 371 have an average ^{88}Sr voltage of 1.787, a weighted average uncorrected $^{87}\text{Sr}/^{86}\text{Sr}$ value of 0.709814 ± 0.000078 , a weighted average uncorrected $^{87}\text{Sr}/^{86}\text{Sr}$ value of 0.70922 ± 0.000078 and a weighted average $^{84}\text{Sr}/^{86}\text{Sr}$ value of 0.054867 ± 0.000072 ($n=11$), shown in Table 5.19 and Figure 5.11. Enamel $^{87}\text{Sr}/^{86}\text{Sr}$ values for sample 371 are in the range of 0.709605 to 0.710016 (uncorrected) and 0.709016 to 0.709427 (corrected), shown in Table A3.60, Figure A3.74 and Figure A3.75. The enamel values are relatively homogenous, with most being within 2σ error of each other.

These spots are principally statistically indistinguishable, suggesting a sample not mobile during amelogenesis. The weighted uncorrected average strontium isotope value of this sample (0.709814 ± 0.000078) does not correspond to any mapped soil or rock strontium isotope values in this study, although it is statistically indistinguishable from Qafzeh sample 374. The weighted average corrected value of this sample is 0.70922 ± 0.00007 , which corresponds to carbonate values from sample 215 from site IS061 from a Lower-Eocene carbonate package containing the Timrat, Meroz and Yizre'el Formation and sample 164 from IS013 from a combined Cenomanian carbonate package containing the Deir Hanna Formation, Isfiya Chalk, Bet Oren Limestone, Khureibe Chalk and Junediya Chalk. Of the units, the Cenomanian carbonate package outcrops closest to Qafzeh, within 0.8 km. The weighted average $^{84}\text{Sr}/^{86}\text{Sr}$ value from this sample is 0.05486 ± 0.00007 , which suggests that the $^{87}\text{Sr}/^{86}\text{Sr}$ values may not be robust.

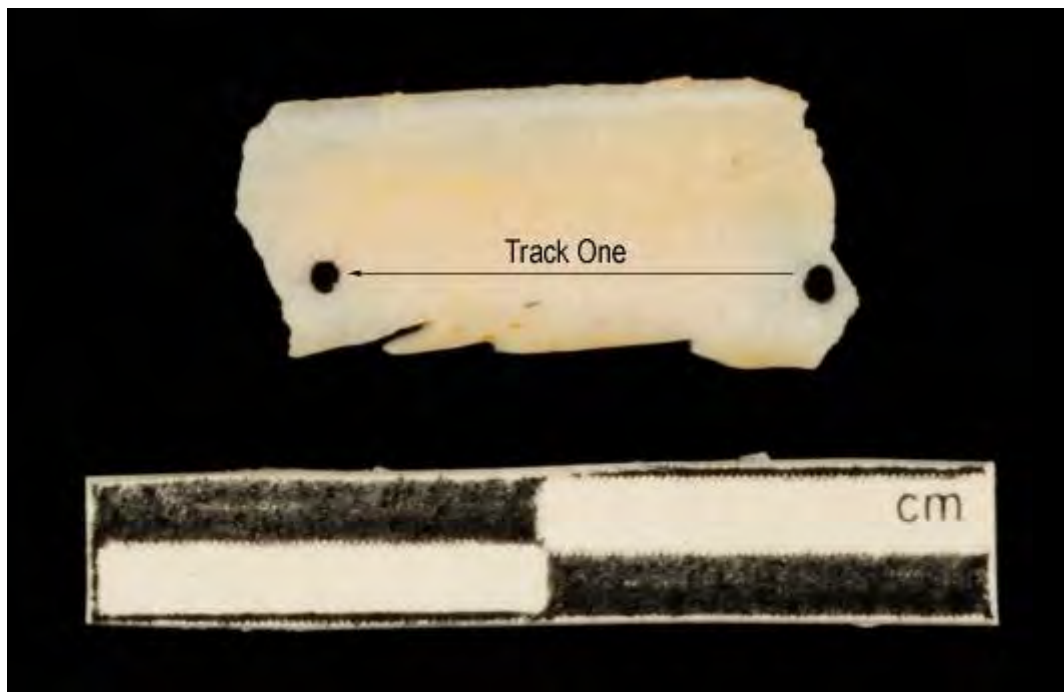


Figure A3.73 LA-MC-ICPMS Track for Sample 371, Bovid, Layer XIX, Qafzeh

Sample	Material	Track	Point	^{88}Sr Volts	$^{84}\text{Sr}/^{86}\text{Sr}$	$^{84}\text{Sr}/^{86}\text{Sr} 2\sigma$	Corrected $^{87}\text{Sr}/^{86}\text{Sr}$	$^{87}\text{Sr}/^{86}\text{Sr}$	$^{87}\text{Sr}/^{86}\text{Sr} 2\sigma$	Error
371	Enamel	1	1	1.889	0.054780	0.000197	0.709779	0.709190	0.000147	
371	Enamel	1	2	1.910	0.054646	0.000186	0.709874	0.709285	0.000162	
371	Enamel	1	3	1.874	0.054802	0.000141	0.709605	0.709016	0.000143	
371	Enamel	1	4	1.909	0.054886	0.000173	0.709782	0.709193	0.000151	
371	Enamel	1	5	1.843	0.054846	0.000166	0.709739	0.709150	0.000205	
371	Enamel	1	6	1.776	0.054908	0.000179	0.709729	0.709140	0.000154	
371	Enamel	1	7	1.847	0.054971	0.000154	0.709831	0.709242	0.000146	
371	Enamel	1	8	1.760	0.055048	0.000189	0.709802	0.709213	0.000178	
371	Enamel	1	9	1.700	0.054979	0.000197	0.710016	0.709427	0.000189	
371	Enamel	1	10	1.532	0.054795	0.000179	0.709983	0.709394	0.000181	
371	Enamel	1	11	1.617	0.054887	0.000177	0.709912	0.709323	0.000138	

Table A3.60 Detailed LA-MC-ICPMS Sr Isotope Results for Enamel, Sample 371, Bovid, Layer XIX, Qafzeh

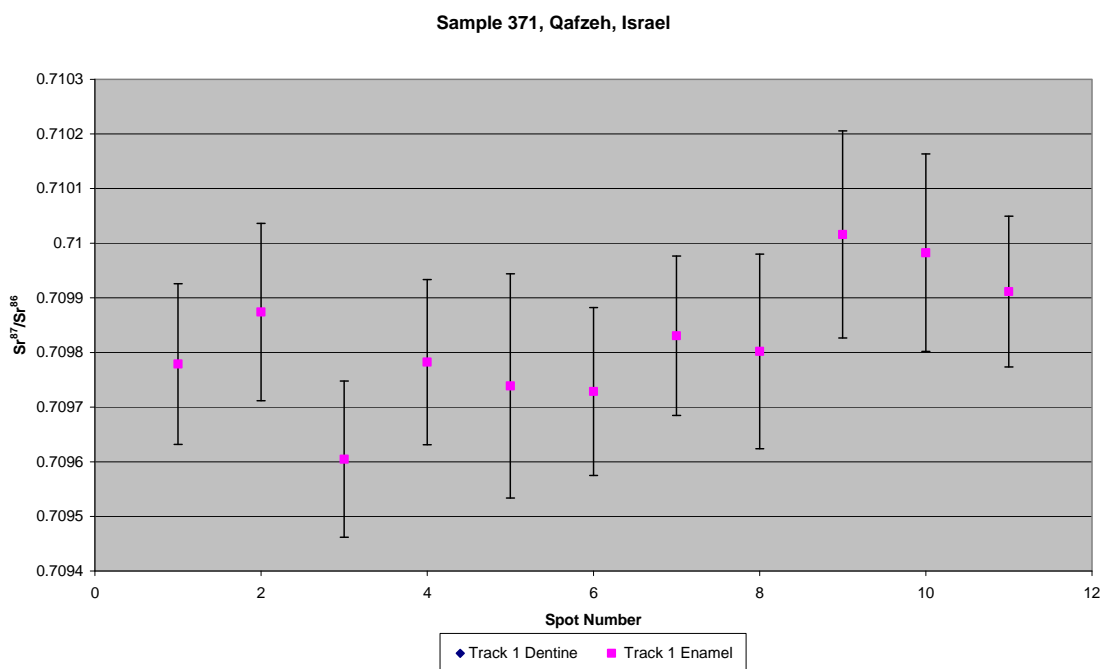


Figure A3.74 Detailed LA-MC-ICPMS Uncorrected Sr Isotope Results, Sample 371, Bovid, Layer XIX, Qafzeh

Sample 371, Corrected Sr Values, Qafzeh, Israel

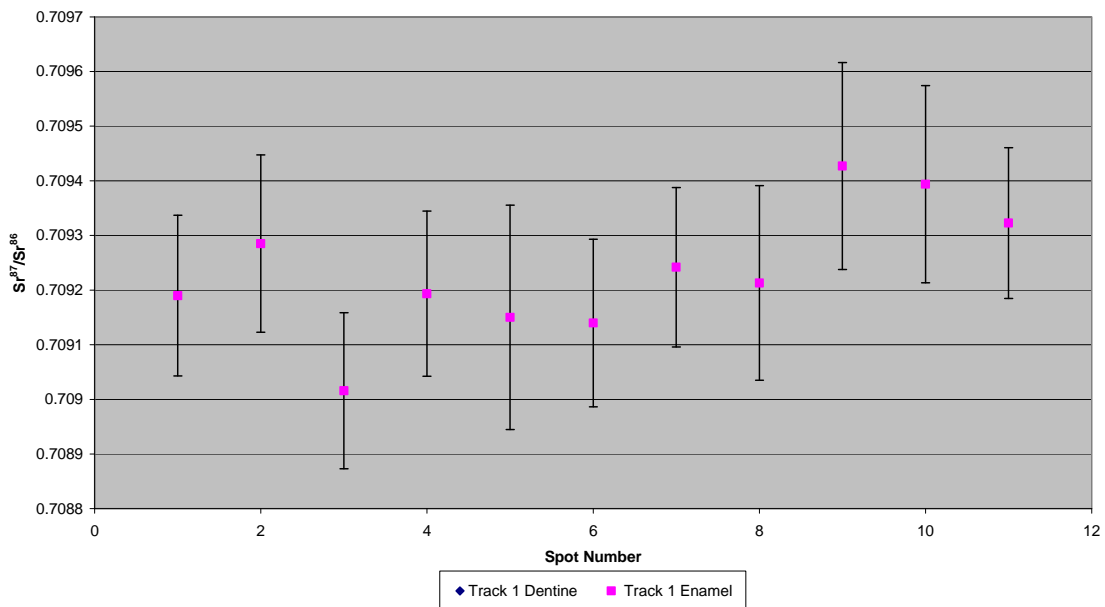


Figure A3.75 Detailed LA-MC-ICPMS Corrected Sr Isotope Results, Sample 371, Bovid, Layer XIX, Qafzeh

Sample 372, a bovid tooth from layer XVII of Qafzeh shown in Figure A2.25, was analysed as 2 tracks containing 6 spots of dentine and 13 spots of enamel respectively, shown in Figure A3.76. The dentine spots of sample 372 have an average ^{88}Sr voltage of 4.913, a weighted average uncorrected $^{87}\text{Sr}/^{86}\text{Sr}$ value of 0.70824 ± 0.00011 , a weighted average corrected $^{87}\text{Sr}/^{86}\text{Sr}$ value of 0.70814 ± 0.00011 and a weighted average $^{84}\text{Sr}/^{86}\text{Sr}$ value of 0.055854 ± 0.000055 ($n=6$), shown in Table 5.19 and Figure 5.11. The enamel spots of sample 372 have an average ^{88}Sr voltage of 2.175, a weighted average uncorrected $^{87}\text{Sr}/^{86}\text{Sr}$ value of 0.70742 ± 0.00013 , a weighted average corrected $^{87}\text{Sr}/^{86}\text{Sr}$ value of 0.70731 ± 0.00013 and a weighted average $^{84}\text{Sr}/^{86}\text{Sr}$ value of 0.05842 ± 0.00014 ($n=13$), shown in Table 5.19 and Figure 5.11. Dentine $^{87}\text{Sr}/^{86}\text{Sr}$ values for sample 372 are in the range of 0.708115 to 0.708379 (uncorrected) and 0.708017 to 0.708280 (corrected), shown in Table A3.61, Figure A3.77 and Figure A3.78 . Dentine values are extremely homogeneous, all being within 2σ error of each other. Enamel $^{87}\text{Sr}/^{86}\text{Sr}$ values for sample 372 are in the range of 0.706996 to 0.708273 (uncorrected) and 0.706887 to 0.708164 (corrected), shown in Table A3.61, Figure A3.77 and Figure A3.78. The enamel values are

somewhat heterogeneous and appear to change in a rhythmic manner broadly increasing in value from sample 1 to 7 then decreasing to point 10 and then broadly increasing to point 13. The values in sample 12 appear elevated, although the error is significantly larger than all other spots in this track.

Enamel values are somewhat heterogeneous (with the exception of spot 12, which is excluded from consideration based on its very high 2σ error), suggesting a sample mobile during amelogenesis. The lower uncorrected and corrected enamel $^{87}\text{Sr}/^{86}\text{Sr}$ end-member of enamel values correlates very well with mapping values from the Pliocene-Pleistocene Cover/Dalwe Basalt from location IS024, which has values of 0.70681 ± 0.000033 (soil) and 0.706807 ± 0.000007 (rock). This sample location is 28 km to the east-north-east of Qafzeh; however, this unit outcrops in an arc in multiple directions within 4 km of the site. The higher uncorrected and corrected enamel end-member correlates with the mapping value from the bioavailable rock sample, which has a value of 0.707795 ± 0.000015 from a Cenomanian carbonate package comprising the Deir Hanna Formation, Isfiya Chalk, Bet Oren Limestone, Khureibe Chalk and Junediya Chalk. This unit outcrops extensively to the north and west of the site and has small areas of outcrop as close 0.8 km to the south-east. These units exist within 1 km of each other, suggesting that this sample could have been mobile only over a relatively limited area during amelogenesis. $^{84}\text{Sr}/^{86}\text{Sr}$ values for the enamel of sample 372 have a weighted average value of 0.05842 ± 0.00014 , which is considerably elevated compared to the ideal value of 0.0565. This suggests that the $^{87}\text{Sr}/^{86}\text{Sr}$ data are not robust. Dentine values are extremely homogeneous, all being within 2σ error of each other, have a weighted average uncorrected value of 0.70824 ± 0.00011 and a corrected value of 0.70814 ± 0.00011 . This corresponds poorly with the soil value of 0.709446 ± 0.000011 .



Figure A3.76 LA-MC-ICPMS Track for Sample 372, Bovid, Layer XVII, Qafzeh

Sample	Material	Track	Point	^{88}Sr Volts	$^{84}\text{Sr}/^{86}\text{Sr}$	$^{87}\text{Sr}/^{86}\text{Sr}$	Corrected $^{87}\text{Sr}/^{86}\text{Sr}$	$^{87}\text{Sr}/^{86}\text{Sr} 2\sigma$	Error
372	Dentine	1	1	5.008	0.055913	0.000055	0.708218	0.708120	0.000080
372	Dentine	1	2	4.691	0.055880	0.000069	0.708258	0.708160	0.000070
372	Dentine	1	3	5.423	0.055891	0.000067	0.708115	0.708017	0.000071
372	Dentine	1	4	5.050	0.055782	0.000062	0.708162	0.708063	0.000080
372	Dentine	1	5	4.540	0.055826	0.000073	0.708287	0.708188	0.000119
372	Dentine	1	6	4.764	0.055820	0.000060	0.708379	0.708280	0.000067
372	Enamel	2	1	2.091	0.058521	0.000117	0.707129	0.707020	0.000154
372	Enamel	2	2	1.731	0.059163	0.000143	0.707471	0.707362	0.000180
372	Enamel	2	3	2.083	0.058555	0.000115	0.707397	0.707288	0.000120
372	Enamel	2	4	2.067	0.058482	0.000116	0.707498	0.707389	0.000117
372	Enamel	2	5	2.325	0.058494	0.000097	0.707585	0.707476	0.000127
372	Enamel	2	6	2.341	0.058338	0.000116	0.707545	0.707436	0.000131
372	Enamel	2	7	2.321	0.058268	0.000110	0.707659	0.707550	0.000115
372	Enamel	2	8	2.298	0.058320	0.000102	0.707342	0.707233	0.000124
372	Enamel	2	9	2.016	0.058423	0.000127	0.707218	0.707109	0.000131
372	Enamel	2	10	1.946	0.058504	0.000114	0.706996	0.706887	0.000129
372	Enamel	2	11	2.139	0.058422	0.000109	0.707291	0.707182	0.000143
372	Enamel	2	12	2.250	0.058423	0.000132	0.708273	0.708164	0.001326
372	Enamel	2	13	2.669	0.058068	0.000089	0.707624	0.707515	0.000098

Table A3.61 Detailed LA-MC-ICPMS Sr Isotope Results, Sample 372, Bovid, Layer XVII, Qafzeh

Sample 372, Qafzeh, Israel

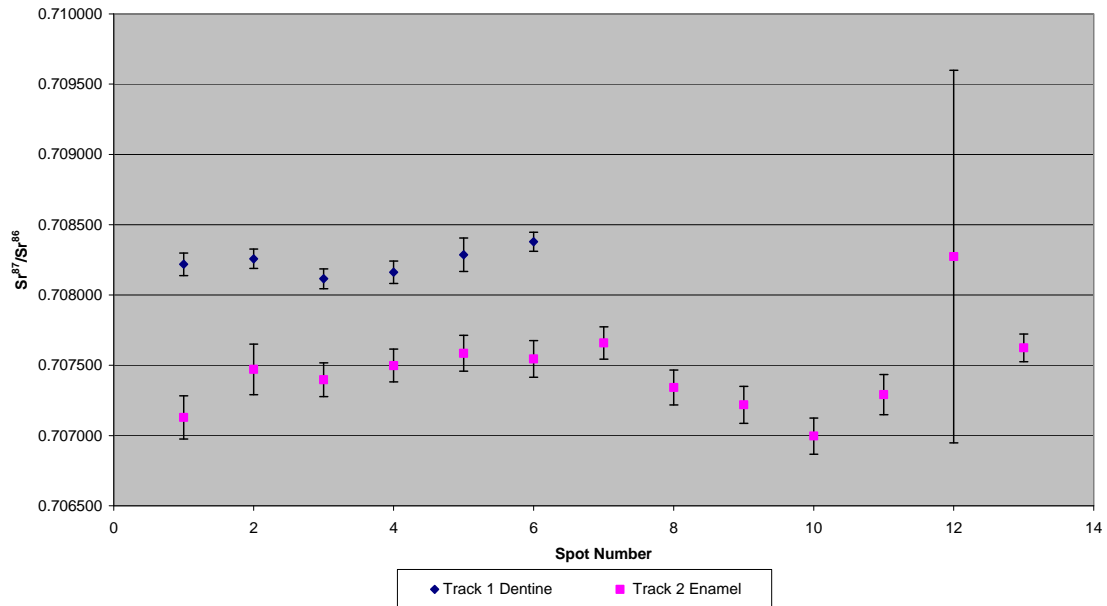


Figure A3.77 Detailed LA-MC-ICPMS Uncorrected Sr Isotope Results, Sample 372, Bovid, Layer XVII, Qafzeh

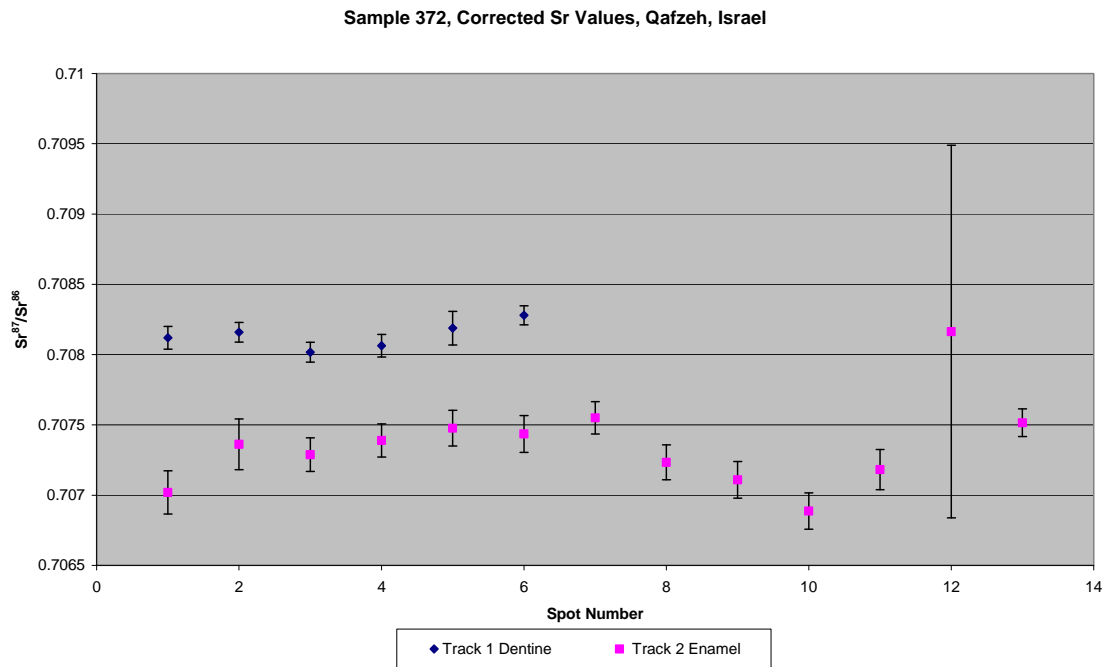


Figure A3.78 Detailed LA-MC-ICPMS Corrected Sr Isotope Results, Sample 372, Bovid, Layer XVII, Qafzeh

Sample 373, an unidentified tooth from layer XV of Qafzeh shown in Figure A2.26, was analysed as 1 track containing 3 spots of enamel, shown in Figure A3.79. The enamel spots of sample 373 have an average ^{88}Sr voltage of 3.577, a weighted average uncorrected $^{87}\text{Sr}/^{86}\text{Sr}$ value of 0.708311 ± 0.000046 , a weighted average corrected $^{87}\text{Sr}/^{86}\text{Sr}$ value of 0.70821 ± 0.000046 and a weighted average $^{84}\text{Sr}/^{86}\text{Sr}$ value of 0.05935 ± 0.00053 ($n=3$), shown in Table 5.19 and Figure 5.11. Enamel spots are extremely homogenous, covering the range of 0.708295 to 0.708328 (uncorrected) and 0.708197 to 0.708230 (corrected), and are well within 2σ error of each other, shown in Table A3.62, Figure A3.80 and Figure A3.81.

The enamel samples are extremely homogenous, suggesting a sample not mobile during amelogenesis. The corrected and uncorrected weighted average $^{87}\text{Sr}/^{86}\text{Sr}$ values correspond best with those of the local Quaternary alluvium sample from location IS023, approximately 15 km south of Qafzeh, which has a value of 0.708231 ± 0.000007 . Similar Quaternary sediments are extensively exposed to the south of Qafzeh, as close as 1.3 km from the site. These enamel spots have a $^{84}\text{Sr}/^{86}\text{Sr}$ weighted average value of 0.05935 ± 0.00053 , which is considerably elevated compared to 0.0565. In contrast, strontium concentration of enamel from sample 373 are very high, with values in the range of 556 to 566 ppm, and the sample contains no uranium, suggesting that the strontium isotope values should be robust.



Figure A3.79 LA-MC-ICPMS Track for Sample 373

Sample	Material	Track	Point	^{88}Sr Volts	$^{84}\text{Sr}/^{86}\text{Sr}$	$^{84}\text{Sr}/^{86}\text{Sr} 2\sigma$ Error	Corrected $^{87}\text{Sr}/^{86}\text{Sr}$	$^{87}\text{Sr}/^{86}\text{Sr} 2\sigma$ Error
373	Enamel	1	1	3.868	0.059295	0.000072	0.708295	0.708197
373	Enamel	1	2	3.156	0.059638	0.000121	0.708304	0.708206
373	Enamel	1	3	3.706	0.059064	0.000174	0.708328	0.708230

Table A3.62 Sample 373, Qafzeh, Detailed LA-MC-ICPMS Sr Isotope Results

Sample 373, Qafzeh, Israel

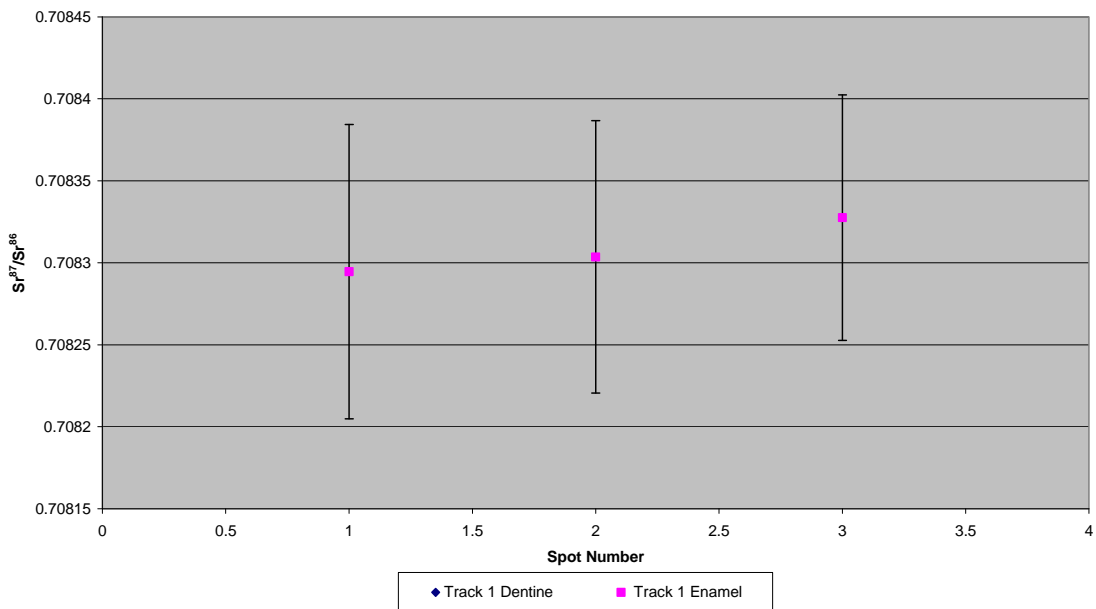


Figure A3.80 Sample 373, Qafzeh, Detailed LA-MC-ICPMS Uncorrected Sr Isotope Results

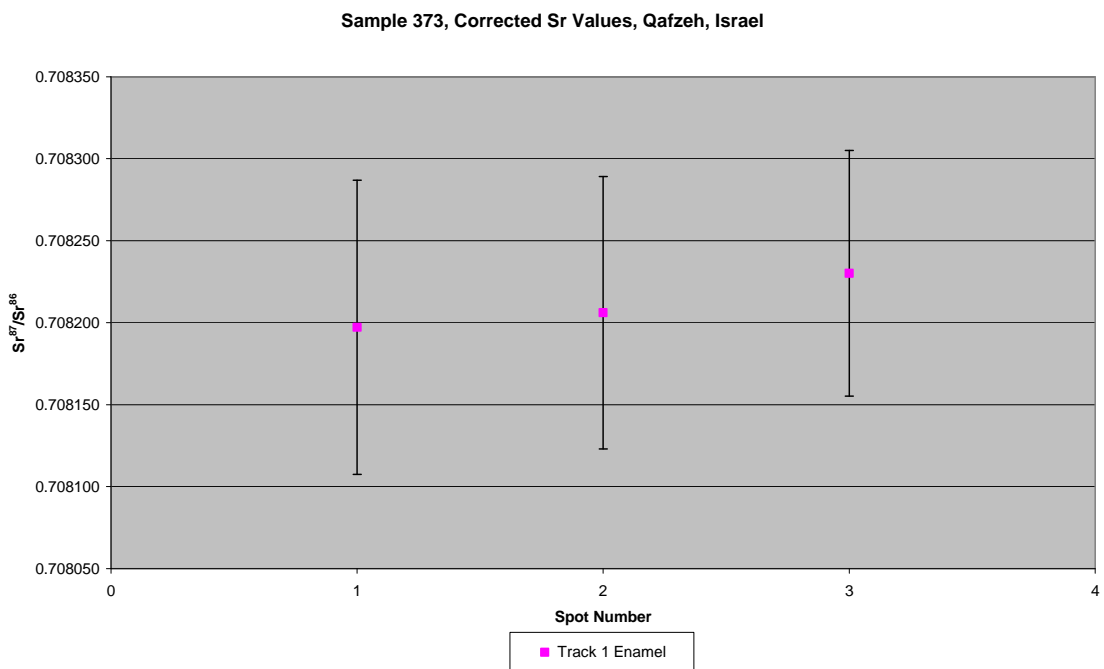


Figure A3.81 Sample 373, Qafzeh, Detailed LA-MC-ICPMS Corrected Sr Isotope Results

Sample 374, an unidentified tooth from layer XV of Qafzeh, was analysed as 1 track containing 14 spots of enamel, shown in Figure A3.82. The enamel spots have an average ^{88}Sr voltage of 0.876, a weighted average uncorrected $^{87}\text{Sr}/^{86}\text{Sr}$ value of 0.70983 ± 0.00011 , a weighted average corrected $^{87}\text{Sr}/^{86}\text{Sr}$ value of 0.70911 ± 0.00011 and a weighted average $^{84}\text{Sr}/^{86}\text{Sr}$ value of 0.06189 ± 0.00028 ($n=14$), shown in Table 5.19 and Figure 5.11. Enamel samples are in the range of 0.709653 to 0.710131 (uncorrected) and 0.708933 to 0.709411 (corrected), and are well within 2σ error of each other, shown in Table A3.63, Figure A3.83 and Figure A3.84.

Enamel spots are homogeneous within 2σ error, suggesting that the specimen was not mobile during amelogenesis. The weighted average $^{87}\text{Sr}/^{86}\text{Sr}$ value from this sample (0.70983 ± 0.00011) does not correspond to any mapping samples in this study; however, it is statistically indistinguishable from the results from sample 371. The corrected weighted average $^{87}\text{Sr}/^{86}\text{Sr}$ value from this sample (0.70911 ± 0.00011) correlates to the value from 164 from IS013, which is located in a Cenomanian carbonate unit comprising the Deir Hanna Formation, Isfiya Chalk, Bet Oren Limestone, Khureibe Chalk and Junediya Chalk which outcrops within 0.8 km of the site. $^{84}\text{Sr}/^{86}\text{Sr}$ weighted average values in the enamel of 0.06189 ± 0.00028 are extremely unfavourable, suggesting that the $^{87}\text{Sr}/^{86}\text{Sr}$ values are not robust.



Figure A3.82 LA-MC-ICPMS Track for Sample 374, Unidentified Species, Layer XV, Qafzeh

Sample	Material	Track	Point	^{88}Sr Volts	$^{84}\text{Sr}/^{86}\text{Sr}$	$^{84}\text{Sr}/^{86}\text{Sr} 2\sigma$ Error	$^{87}\text{Sr}/^{86}\text{Sr}$	Corrected $^{87}\text{Sr}/^{86}\text{Sr}$	$^{87}\text{Sr}/^{86}\text{Sr} 2\sigma$ Error
374	Enamel	1	1	1.080	0.062160	0.000267	0.709701	0.708981	0.000191
374	Enamel	1	2	0.924	0.062465	0.000248	0.709997	0.709277	0.000278
374	Enamel	1	3	0.955	0.062270	0.000252	0.709669	0.708949	0.000315
374	Enamel	1	4	0.874	0.062431	0.000288	0.709972	0.709252	0.000302
374	Enamel	1	5	0.779	0.062534	0.000350	0.709653	0.708933	0.000249
374	Enamel	1	6	0.788	0.062236	0.000276	0.710097	0.709377	0.000269
374	Enamel	1	7	0.825	0.062337	0.000258	0.709938	0.709218	0.000228
374	Enamel	1	8	0.856	0.061675	0.000226	0.709747	0.709027	0.000302
374	Enamel	1	9	0.851	0.061596	0.000251	0.709867	0.709147	0.000292
374	Enamel	1	10	0.918	0.061591	0.000268	0.709862	0.709142	0.000310
374	Enamel	1	11	0.807	0.061337	0.000302	0.710131	0.709411	0.000378
374	Enamel	1	12	0.845	0.061467	0.000263	0.709856	0.709136	0.000275
374	Enamel	1	13	0.924	0.061202	0.000283	0.709430	0.708710	0.000284
374	Enamel	1	13	0.841150	0.061180	0.000307	0.709903	0.709183	0.000307

Table A3.63 Detailed LA-MC-ICPMS Sr Isotope Results for Enamel, Sample 374, Unidentified Species, Layer XV, Qafzeh

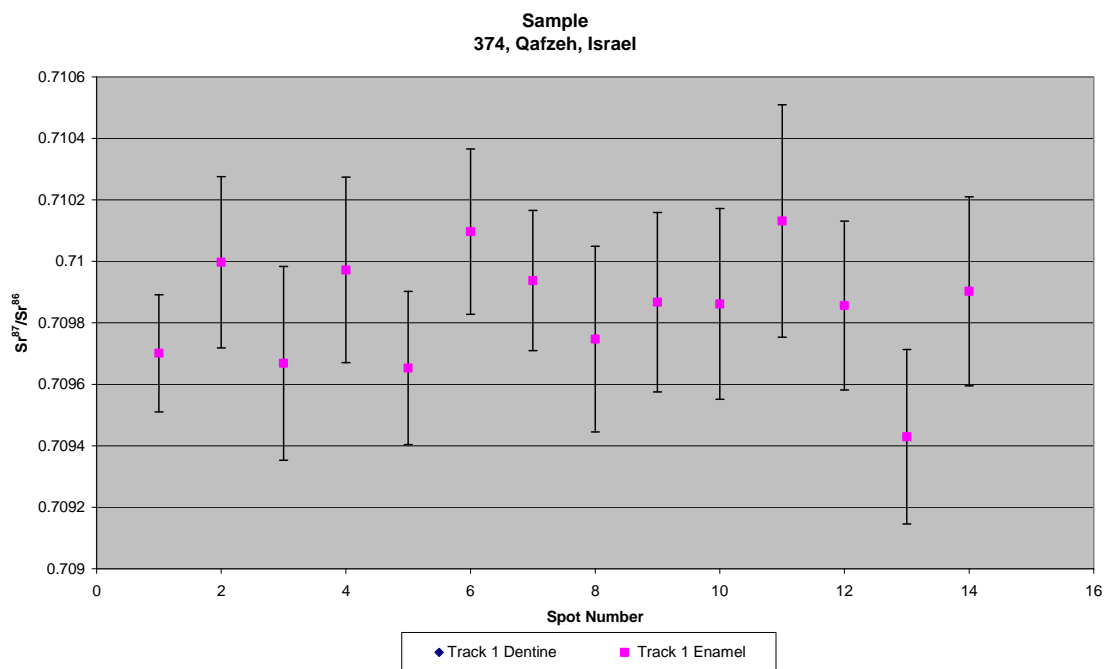


Figure A3.83 Detailed LA-MC-ICPMS Uncorrected Sr Isotope Results, Sample 374, Unidentified Species, Layer XV, Qafzeh

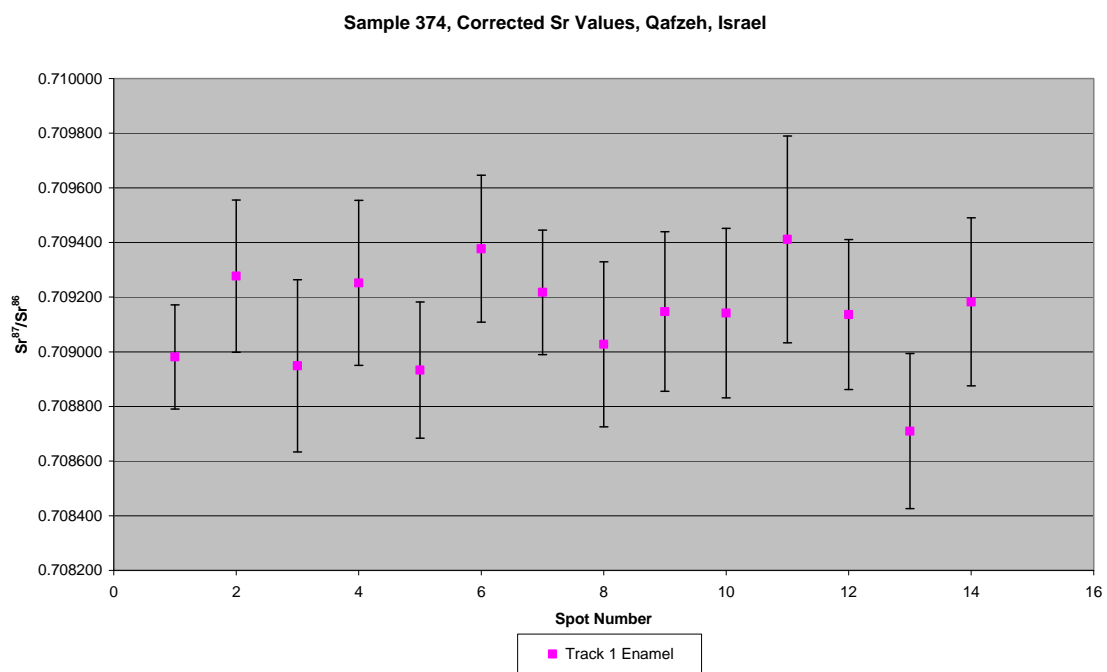


Figure A3.84 Detailed LA-MC-ICPMS Corrected Sr Isotope Results, Sample 374, Unidentified Species, Layer XV, Qafzeh

A3.2.3. French Archaeological Sites

A3.2.3.1. *La Chapelle-aux-Saints*

Sample 592, a bovid tooth from stratum 1 of the bouffia Bonneval section of La Chapelle-aux-Saints shown in Figure A2.28, was analysed in 1 track shown in Figure A3.85 comprising 14 spots of enamel in 4 discontinuous sections and 22 spots of dentine in 3 discontinuous sections, the strontium isotope results of which are summarised in Table 5.27 and Figure 5.16. The enamel spots of track 1 have an average ^{88}Sr voltage of 0.957, a weighted average uncorrected $^{87}\text{Sr}/^{86}\text{Sr}$ value of 0.71064 ± 0.00028 , a weighted average corrected $^{87}\text{Sr}/^{86}\text{Sr}$ value of 0.71018 ± 0.00028 and a weighted average $^{84}\text{Sr}/^{86}\text{Sr}$ value of 0.05733 ± 0.00012 ($n=14$). The dentine spots of track 1 have an average ^{88}Sr voltage of 1.281, a weighted average uncorrected $^{87}\text{Sr}/^{86}\text{Sr}$ value of 0.70983 ± 0.00032 , a weighted average corrected $^{87}\text{Sr}/^{86}\text{Sr}$ value of 0.70958 ± 0.00032 and a weighted average $^{84}\text{Sr}/^{86}\text{Sr}$ value of 0.057105 ± 0.000034 ($n=22$). Enamel values range from 0.710091 to 0.711789 (uncorrected) and 0.709634 to 0.711332 (corrected), and are relatively heterogeneous, appearing to vary systematically along the track. Dentine values range from 0.709256 to 0.711418 (uncorrected) and 0.709004 to 0.711166 (corrected), and are distributed in a number of discrete domains. Dentine values in the centre of the sample are homogenous, with all samples having $^{87}\text{Sr}/^{86}\text{Sr}$ values within 2σ error values of each other. Dentine values in the dentine of the tooth, which is external to the enamel are considerably more heterogeneous. Detailed values for enamel and dentine for sample 592 are shown in Table A3.64, Figure A3.86 and Figure A3.87.

Enamel values are relatively heterogeneous, with a rhythmic variation ranging from 0.710091 ± 0.000490 to 0.711789 ± 0.00046 for uncorrected values and 0.709634 ± 0.000490 to 0.711332 ± 0.00046 for corrected values, suggesting that this sample was mobile during amelogenesis, shown in Table A3.64, Figure A3.86 and Figure A3.87. The lower $^{87}\text{Sr}/^{86}\text{Sr}$ value of both the uncorrected and corrected enamel corresponds to the value of 0.710096 ± 0.000013 from FS041-S2, taken from a white clay within a limestone unit within the Lower

Jurassic carbonate package that contains La Chapelle-aux-Saints. This unit is quite heterogeneous, with values ranging from 0.708488 ± 0.000009 to 0.716805 ± 0.000038 . Heterogeneity at the higher end of this range probably reflects the input of fertilisers and material taken from alluvial plains, which drain more radiogenic materials to the east. The higher $^{87}\text{Sr}/^{86}\text{Sr}$ uncorrected value of the enamel is within the range of the Lower Jurassic unit, but correlates well with the value of 0.711984 ± 0.000018 from the floodplain soil of FS056-S1 adjacent to the Dordogne river. The bedrock in this location is Upper Cambrian anatetic orthogneiss, although this flood plain sample is a poor reflection of the surrounding area, shown by the value of 0.726901 ± 0.000015 found above bedrock at FS057-S1, which is approximately 50 m from FS056-S1. This sample location is approximately 20 km from the site of La Chapelle-aux-Saints. The higher corrected $^{87}\text{Sr}/^{86}\text{Sr}$ is slightly outside of the error range of FS056-S1; however, given the heterogeneity displayed by Dordogne floodplain samples in this research, this sample may have derived from another unsampled location of this unit. The value correlates with the value of 0.711001 ± 0.00001 from sample FS107-S1, collected approximately 100 km from the archaeological site, which is located within the same Lower Jurassic carbonate unit that contains the site of La Chapelle-aux-Saints. This corrected data suggests that the specimen has values either exclusively from the Lower Jurassic carbonate containing La Chapelle-aux-Saints or also including values from the Dordongne floodplain. Overall, both corrected and uncorrected strontium isotope values suggest that this specimen moved either within the bedrock surrounding the site or between local bedrock and the Dordogne river floodplain which is within 3.9 km from the site. There is a significant difference in $^{87}\text{Sr}/^{86}\text{Sr}$ composition between enamel and dentine, suggesting this sample may be a migrant. The dentine $^{87}\text{Sr}/^{86}\text{Sr}$ values are relatively heterogeneous, particularly in the outer sections of the dentine. The overall weighted average uncorrected dentine values are 0.70967 ± 0.00024 and corrected values are 0.70958 ± 0.00032 , within error of each other. This might suggest differences in the post-depositional diagenesis, possibly relating to the accessibility of different parts of the sample to fluid, or that the analysis spots include some enamel. The $^{84}\text{Sr}/^{86}\text{Sr}$ values from the enamel and dentine have weighted average values of

0.05733 ± 0.00012 , 0.057105 ± 0.000034 , respectively, which is significantly elevated compared to the expected value of 0.0565, suggesting that the $^{87}\text{Sr}/^{86}\text{Sr}$ analyses of these samples may not be robust.

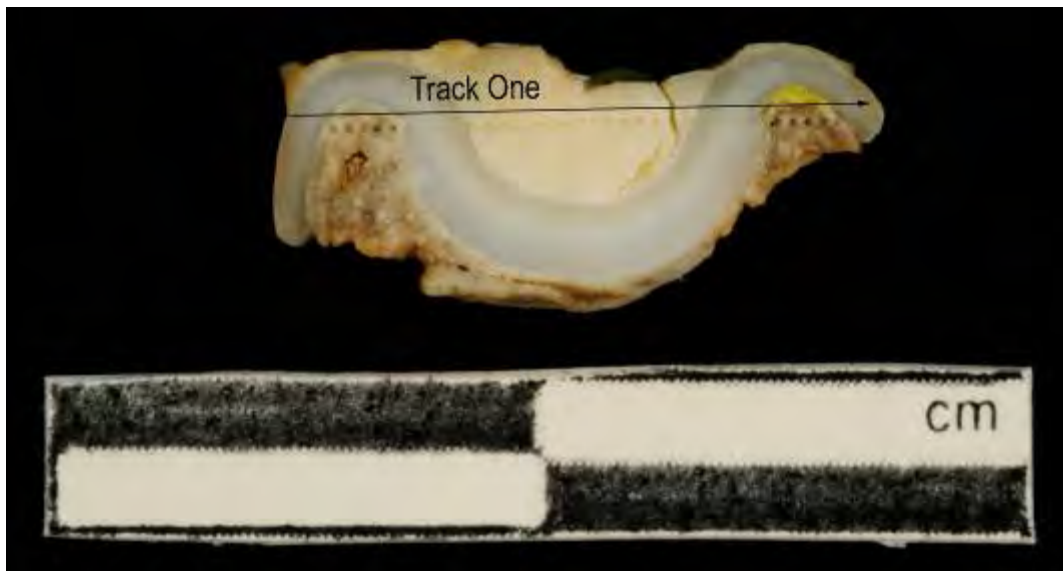


Figure A3.85 LA-MC-ICPMS Track for Sample 592, Bovid, Bouffia Bonneval: Stratum 1, La Chapelle-aux-Saints

Sample	Material	Track	Point	^{88}Sr Volts	$^{84}\text{Sr}/^{86}\text{Sr}$	$^{84}\text{Sr}/^{86}\text{Sr}$ Error	Corrected $^{87}\text{Sr}/^{86}\text{Sr}$	$^{87}\text{Sr}/^{86}\text{Sr} 2\sigma$ Error
592	Enamel	1	1	1.494609	0.057117	0.000126	0.710323	0.709866
592	Enamel	1	2	0.951847	0.057480	0.000209	0.710091	0.709634
592	Enamel	1	3	0.644129	0.057689	0.000296	0.710875	0.710418
592	Dentine	1	4	1.451233	0.057049	0.000148	0.709785	0.709534
592	Dentine	1	5	1.397749	0.057167	0.000201	0.711418	0.711166
592	Dentine	1	6	1.319672	0.057119	0.000141	0.709802	0.709551
592	Dentine	1						
592	Dentine	1						
592	Enamel	1	9	0.642620	0.057777	0.000278	0.711789	0.711332
592	Enamel	1	10	0.845721	0.057477	0.000249	0.710460	0.710003
592	Enamel	1	11	0.911424	0.057454	0.000231	0.710270	0.709813
592	Enamel	1	12	0.990826	0.057594	0.000309	0.710184	0.709727
592	Dentine	1	13	1.398358	0.057094	0.000122	0.709520	0.709268
592	Dentine	1	14	1.268425	0.056988	0.000116	0.709402	0.709150
592	Dentine	1	15	1.202069	0.057179	0.000196	0.709519	0.709268
592	Dentine	1	16	1.305515	0.057081	0.000163	0.709256	0.709004

Sample	Material	Track	Point	^{88}Sr Volts	$^{84}\text{Sr}/^{86}\text{Sr}$	$^{84}\text{Sr}/^{86}\text{Sr} 2\sigma$ Error	$^{87}\text{Sr}/^{86}\text{Sr}$	Corrected $^{87}\text{Sr}/^{86}\text{Sr}$	$^{87}\text{Sr}/^{86}\text{Sr} 2\sigma$ Error
592	Dentine	1	17	1.246356	0.057105	0.000127	0.709450	0.709198	0.000215
592	Dentine	1	18	1.218207	0.057299	0.000196	0.709519	0.709268	0.000248
592	Dentine	1	19	1.287223	0.057025	0.000148	0.709477	0.709225	0.000223
592	Dentine	1	20	1.256524	0.057168	0.000209	0.709411	0.709160	0.000310
592	Dentine	1	21	1.250931	0.057113	0.000158	0.709363	0.709112	0.000248
592	Dentine	1	22	1.282505	0.057137	0.000171	0.709367	0.709116	0.000243
592	Dentine	1	23	1.280911	0.057118	0.000144	0.709588	0.709336	0.000289
592	Dentine	1	24	1.350904	0.057711	0.001085	0.709952	0.709700	0.000653
592	Dentine	1	25	1.330765	0.057337	0.000201	0.709688	0.709437	0.000233
592	Dentine	1	26	0.941090	0.057236	0.000230	0.709959	0.709707	0.000328
592	Dentine	1	27	1.484657	0.057049	0.000153	0.709604	0.709353	0.000224
592	Enamel	1	28	1.223270	0.057284	0.000174	0.710444	0.709987	0.000359
592	Enamel	1	29	0.975840	0.057466	0.000217	0.710301	0.709844	0.000522
592	Enamel	1	30	0.926923	0.057408	0.000174	0.710550	0.710093	0.000494
592	Enamel	1	31	0.810278	0.057408	0.000293	0.711334	0.710877	0.000510
592	Enamel	1	32	0.958828	0.057290	0.000174	0.711167	0.710710	0.000432
592	Enamel	1	33	1.214324	0.057127	0.000157	0.712052	0.711801	0.000360
592	Enamel	1	34	1.270183	0.057017	0.000155	0.711255	0.711004	0.000293
592	Enamel	1	35						
592	Enamel	1	36	1.326969	0.057082	0.000166	0.711353	0.711102	0.000293
592	Dentine	1	37	1.111124	0.057140	0.000167	0.710862	0.710610	0.000305
592	Enamel	1	38	0.877755	0.057434	0.000218	0.711331	0.710874	0.000395
592	Enamel	1	39	1.154983	0.056986	0.000170	0.710590	0.710133	0.000297

Table A3.64 Detailed LA-MC-ICPMS Sr Isotope Results for Enamel and Dentine, Sample 592, Bovid, Bouffia Bonneval: Stratum 1, La Chapelle-aux-Saints

Sample 592, La Chapelle-aux-Saints, France

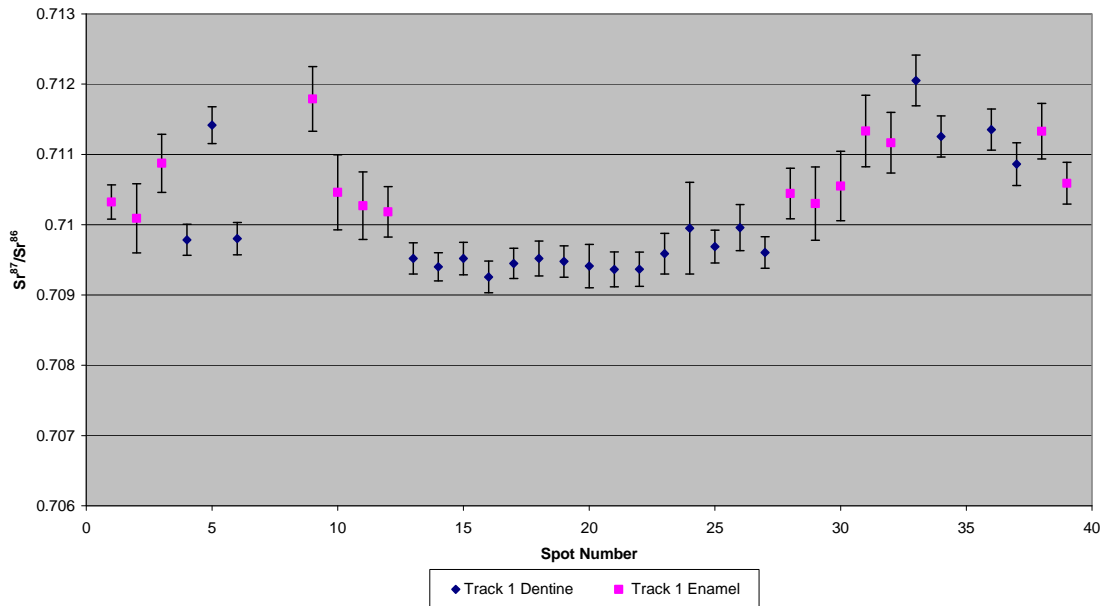


Figure A3.86 Detailed LA-MC-ICPMS Uncorrected Sr Isotope Results, Sample 592, Bovid, Bouffia Bonneval: Stratum 1, La Chapelle-aux-Saints

Sample 592, Corrected Sr Values, La Chapelle-aux-Saints, France

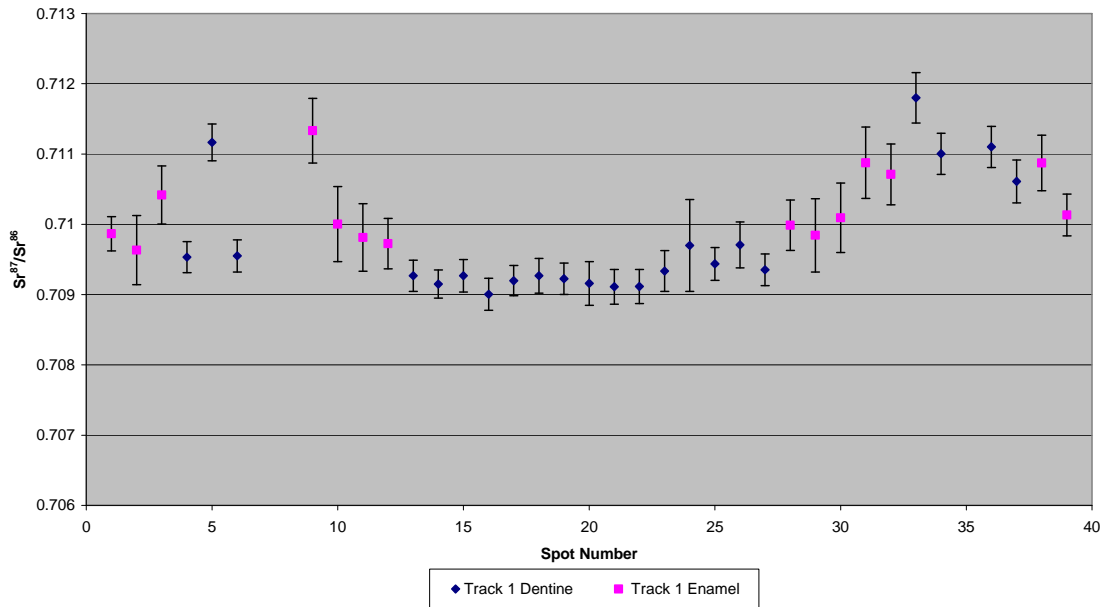


Figure A3.87 Detailed LA-MC-ICPMS Corrected Sr Isotope Results, Sample 592, Bovid, Bouffia Bonneval: Stratum 1, La Chapelle-aux-Saints

Sample 593, a bovid tooth, from stratum 1 of the bouffia Bonneval section of La Chapelle-aux-Saints shown in Figure A2.29, was analysed in 4 tracks, with track 1 comprising 4 spots of enamel and 12 spots of dentine, track 2 comprising 3 spots of enamel and 8 spots of dentine, track 3 comprising 3 spots of enamel and 16 spots of dentine and track 4 comprising 2 spots of enamel and 12 spots of dentine, which are shown in Figure A3.88. The strontium isotope results of sample 593 are summarised in Table 5.27 and Figure 5.16. The enamel spots of track 1 have an average ^{88}Sr voltage of 1.065, a weighted average uncorrected $^{87}\text{Sr}/^{86}\text{Sr}$ value of 0.7116 ± 0.0011 , a weighted average corrected $^{87}\text{Sr}/^{86}\text{Sr}$ value of 0.71140 ± 0.0011 and a weighted average $^{84}\text{Sr}/^{86}\text{Sr}$ value of 0.056716 ± 0.000074 ($n=4$). The dentine spots of track 1 have an average ^{88}Sr voltage of 2.014, a weighted average uncorrected $^{87}\text{Sr}/^{86}\text{Sr}$ value of 0.70987 ± 0.00043 , a weighted average corrected $^{87}\text{Sr}/^{86}\text{Sr}$ value of 0.70978 ± 0.00043 and a weighted average $^{84}\text{Sr}/^{86}\text{Sr}$ value of 0.056668 ± 0.000028 ($n=12$). The enamel spots of track 2 have an average ^{88}Sr voltage of 1.327, a weighted average uncorrected $^{87}\text{Sr}/^{86}\text{Sr}$ value of 0.71306 ± 0.00089 , a weighted average corrected $^{87}\text{Sr}/^{86}\text{Sr}$ value of 0.71281 ± 0.00089 and a weighted average $^{84}\text{Sr}/^{86}\text{Sr}$ value of 0.057051 ± 0.000097 ($n=3$). The dentine spots of track 2 have an average ^{88}Sr voltage of 1.916, a weighted average uncorrected $^{87}\text{Sr}/^{86}\text{Sr}$ value of 0.70976 ± 0.00023 , a weighted average corrected $^{87}\text{Sr}/^{86}\text{Sr}$ value of 0.70967 ± 0.00023 and a weighted average $^{84}\text{Sr}/^{86}\text{Sr}$ value of 0.056780 ± 0.000034 ($n=8$). The enamel spots of track 3 have an average ^{88}Sr voltage of 1.244, a weighted average uncorrected $^{87}\text{Sr}/^{86}\text{Sr}$ value of 0.7126 ± 0.0016 , a weighted average corrected $^{87}\text{Sr}/^{86}\text{Sr}$ value of 0.71230 ± 0.0016 and a weighted average $^{84}\text{Sr}/^{86}\text{Sr}$ value of 0.05732 ± 0.00062 ($n=3$). The dentine spots of track 3 have an average ^{88}Sr voltage of 1.820, a weighted average uncorrected $^{87}\text{Sr}/^{86}\text{Sr}$ value of 0.70953 ± 0.00027 , a weighted average corrected $^{87}\text{Sr}/^{86}\text{Sr}$ value of 0.70944 ± 0.00027 and a weighted average $^{84}\text{Sr}/^{86}\text{Sr}$ value of 0.056971 ± 0.000058 ($n=16$). The enamel spots of track 4 have an average ^{88}Sr voltage of 1.070, a weighted average uncorrected $^{87}\text{Sr}/^{86}\text{Sr}$ value of 0.71149 ± 0.00030 , a weighted average corrected $^{87}\text{Sr}/^{86}\text{Sr}$ value of 0.71124 ± 0.00030 and a weighted average $^{84}\text{Sr}/^{86}\text{Sr}$ value of 0.05707 ± 0.00013 ($n=2$). The dentine spots of track 4 have an average ^{88}Sr voltage of 1.949, a weighted average

uncorrected $^{87}\text{Sr}/^{86}\text{Sr}$ value of 0.71002 ± 0.00068 , a weighted average corrected $^{87}\text{Sr}/^{86}\text{Sr}$ value of 0.70993 ± 0.00068 and a weighted average $^{84}\text{Sr}/^{86}\text{Sr}$ value of 0.056834 ± 0.000028 ($n=12$).

Enamel values of track 1 are in the range of 0.711067 to 0.712462 (uncorrected), as well as 0.710812 to 0.712207 (corrected), and the values are slightly heterogeneous, increasing in $^{87}\text{Sr}/^{86}\text{Sr}$ value from spot 1 to spot 4. Dentine values of track 1 are in the range of 0.709247 to 0.711746 (uncorrected), as well as 0.709158 to 0.711657 (corrected), and are moderately homogenous, although spot 5 (the first dentine spot in this track) is elevated compared to the other dentine spots. Enamel values of track 2 are in the range of 0.712682 to 0.713401 (uncorrected), as well as 0.712427 to 0.713146 (corrected), and are moderately heterogeneous. Dentine values of track 2 are in the range of 0.709388 to 0.710207 (uncorrected), as well as 0.709298 to 0.710118 (corrected), and are moderately homogenous. Enamel values of track 3 are in the range of 0.712125 to 0.713271 (uncorrected), as well as 0.711870 to 0.713016 (corrected), and are moderately heterogeneous. Dentine values of track 3 are in the range of 0.708931 to 0.710909 (uncorrected), as well as 0.708841 to 0.710820 (corrected) are moderately homogeneous. Enamel values of track 4 are 0.711389 and 0.711590 (uncorrected), as well as 0.711134 and 0.711335 (corrected) are relatively homogenous. Dentine values of track 4 are in the range of 0.709375 to 0.720467 (uncorrected), as well as 0.709285 to 0.720377 (corrected), and are relatively homogenous, with the exception of spot 15, which is significantly elevated in $^{87}\text{Sr}/^{86}\text{Sr}$ value. Detailed values for enamel and dentine for sample 593 are shown in Table A3.65, Figure A3.89 and Figure A3.90.

The strontium isotope composition of enamel and dentine are significantly different, suggesting that this sample is a migrant. Enamel values are relatively heterogeneous between, and within, tracks with an overall range from 0.711067 ± 0.000412 to 0.713401 ± 0.000279 (uncorrected) and 0.710812 ± 0.000412 to 0.713146 ± 0.000279 (corrected), suggesting a sample mobile during amelogenesis, shown in Table A3.65, Figure A3.89 and Figure A3.90. Corrected and uncorrected values for enamel are within 2σ error, and so the

mobility interpretation is the same for both sets of values. The upper range of the values correlate best with sample FS059-S1 (0.713071 ± 0.000011) collected near the Dordogne river. Bedrock in this area is a Cambrian-Ordovician anatectic orthogneiss, which other samples (e.g., FS055-S2 with a value of 0.725528 ± 0.000017) suggest would have a much higher $^{87}\text{Sr}/^{86}\text{Sr}$ value. This suggests that sample FS059-S1 is, in contrast with the field notes, a floodplain sample. The Dordogne floodplain is present within 3.9 km of the archaeological site. The lower range of the enamel correlates well with the value of 0.710762 ± 0.000031 from FS052-S1, which is collected in the Lower Jurassic carbonate package that also contains La Chapelle-aux-Saints. This sample location is approximately 17 km from La Chapelle-aux-Saints. Another possible suitable value of 0.710853 ± 0.000011 is found at FS089-S1 in an Upper Cretaceous carbonate package, which is approximately 30 km from La Chapelle-aux-Saints. The dentine values of all tracks are relatively homogenous (with the exception of point 15 on track 4, which is probably an erroneous value), with an overall weighted average value of 0.70978 ± 0.00018 .

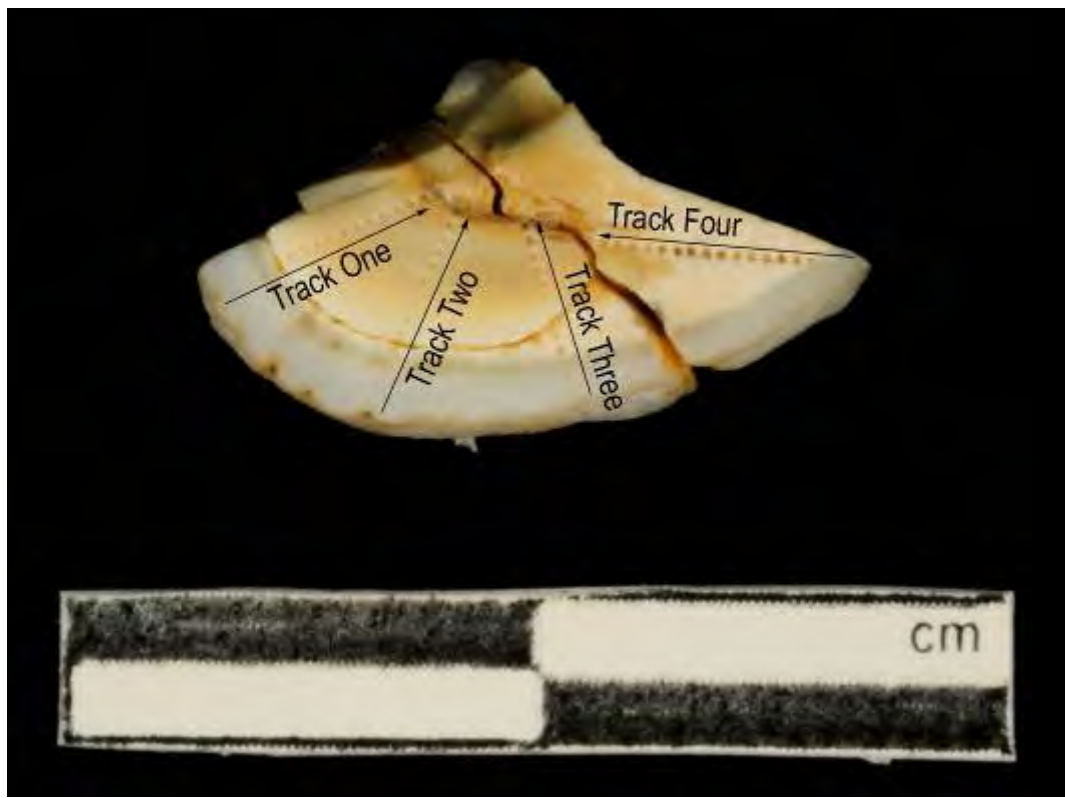


Figure A3.88 LA-MC-ICPMS Track for Sample 593, Bovid, Bouffia Bonneval: Stratum 1, La Chapelle-aux-Saints

Sample	Material	Track	Point	^{88}Sr Volts	$^{84}\text{Sr}/^{86}\text{Sr}$	Corrected $^{87}\text{Sr}/^{86}\text{Sr}$	$^{87}\text{Sr}/^{86}\text{Sr} 2\sigma$	Error	
593	Enamel	1	1	1.016	0.056763	0.000174	0.711110	0.710855	0.000372
593	Enamel	1	2	0.978	0.056727	0.000245	0.711067	0.710812	0.000412
593	Enamel	1	3	0.999	0.056869	0.000245	0.711502	0.711246	0.000326
593	Enamel	1	4	1.266	0.056676	0.000096	0.712462	0.712207	0.000315
593	Dentine	1	5	1.478	0.056770	0.000147	0.711746	0.711657	0.000168
593	Dentine	1	6	1.813	0.056691	0.000087	0.710360	0.710271	0.000166
593	Dentine	1	7	1.927	0.056692	0.000112	0.709844	0.709755	0.000167
593	Dentine	1	8	1.965	0.056660	0.000092	0.709567	0.709477	0.000182
593	Dentine	1	9	2.179	0.056664	0.000084	0.709247	0.709158	0.000137
593	Dentine	1	10	2.196	0.056679	0.000090	0.709467	0.709378	0.000161
593	Dentine	1	11	2.054	0.056577	0.000109	0.710245	0.710155	0.000229
593	Dentine	1	12	2.030	0.056608	0.000119	0.710126	0.710037	0.000227
593	Dentine	1	13	2.019	0.056619	0.000110	0.709687	0.709597	0.000217
593	Dentine	1	14	2.149	0.056734	0.000091	0.709472	0.709383	0.000190
593	Dentine	1	15	2.090	0.056670	0.000100	0.709371	0.709281	0.000156
593	Dentine	1	16	2.266	0.056658	0.000081	0.709834	0.709745	0.000115
593	Enamel	2	1	1.180	0.057014	0.000197	0.713090	0.712835	0.000305

Sample	Material	Track	Point	^{88}Sr Volts	$^{84}\text{Sr}/^{86}\text{Sr}$	$^{84}\text{Sr}/^{86}\text{Sr} 2\sigma$ Error	$^{87}\text{Sr}/^{86}\text{Sr}$	Corrected $^{87}\text{Sr}/^{86}\text{Sr}$	$^{87}\text{Sr}/^{86}\text{Sr} 2\sigma$ Error
593	Enamel	2	2	1.187	0.057166	0.000178	0.712682	0.712427	0.000311
593	Enamel	2	3	1.613	0.056993	0.000148	0.713401	0.713146	0.000307
593	Dentine	2	4	1.845	0.056773	0.000131	0.709894	0.709804	0.000190
593	Dentine	2	5	1.759	0.056829	0.000090	0.709959	0.709870	0.000242
593	Dentine	2	6	1.816	0.056701	0.000112	0.709601	0.709512	0.000205
593	Dentine	2	7	2.013	0.056788	0.000104	0.709388	0.709298	0.000200
593	Dentine	2	8	2.007	0.056736	0.000100	0.710207	0.710118	0.000199
593	Dentine	2	9	2.010	0.056730	0.000107	0.709743	0.709654	0.000225
593	Dentine	2	10	1.919	0.056806	0.000089	0.709545	0.709455	0.000182
593	Dentine	2	11	1.955	0.056818	0.000083	0.709899	0.709810	0.000247
593	Dentine	2	12						
593	Enamel	3	1	1.065	0.057626	0.000204	0.712292	0.712037	0.000288
593	Enamel	3	2	1.114	0.057392	0.000200	0.712125	0.711870	0.000290
593	Enamel	3	3	1.555	0.057135	0.000142	0.713271	0.713016	0.000279
593	Dentine	3	4	2.242	0.056915	0.000089	0.710909	0.710820	0.000181
593	Dentine	3	5	2.022	0.056974	0.000124	0.709711	0.709622	0.000223
593	Dentine	3	6	1.701	0.057123	0.000104	0.709185	0.709096	0.000194
593	Dentine	3	7	1.746	0.056993	0.000109	0.709192	0.709103	0.000191
593	Dentine	3	8	1.673	0.057055	0.000115	0.709368	0.709279	0.000177
593	Dentine	3	9	1.812	0.056922	0.000111	0.709501	0.709411	0.000203
593	Dentine	3	10	1.468	0.057073	0.000129	0.708931	0.708841	0.000221
593	Dentine	3	11	1.601	0.057056	0.000140	0.709517	0.709427	0.000195
593	Dentine	3	12	1.598	0.057054	0.000125	0.709393	0.709303	0.000191
593	Dentine	3	13	1.584	0.057159	0.000107	0.708997	0.708908	0.000204
593	Dentine	3	14	1.439	0.057103	0.000131	0.709097	0.709007	0.000271
593	Dentine	3	15	2.312	0.056909	0.000093	0.709444	0.709354	0.000199
593	Dentine	3	16	2.134	0.056859	0.000078	0.709330	0.709241	0.000180
593	Dentine	3	17	2.008	0.056797	0.000089	0.709686	0.709597	0.000186
593	Dentine	3	18	2.105	0.056899	0.000101	0.709503	0.709414	0.000169
593	Dentine	3	19	1.669	0.057006	0.000109	0.710254	0.710165	0.000193
593	Enamel	4	1						
593	Enamel	4	2	1.011	0.057020	0.000188	0.711389	0.711134	0.000440
593	Enamel	4	3	1.129	0.057129	0.000188	0.711590	0.711335	0.000422
593	Dentine	4	4	1.473	0.056942	0.000165	0.712709	0.712619	0.000507
593	Dentine	4	5	1.601	0.056858	0.000124	0.711334	0.711245	0.000175
593	Dentine	4	6	1.902	0.056863	0.000095	0.710539	0.710449	0.000152

Sample	Material	Track	Point	^{88}Sr Volts	$^{84}\text{Sr}/^{86}\text{Sr}$	Corrected $^{87}\text{Sr}/^{86}\text{Sr}$	$^{87}\text{Sr}/^{86}\text{Sr}$ 2 σ	Error
593	Dentine	4	7	1.950	0.056779	0.000092	0.709748	0.709658
593	Dentine	4	8	2.017	0.056813	0.000096	0.709592	0.709503
593	Dentine	4	9	2.097	0.056847	0.000110	0.709375	0.709285
593	Dentine	4	10	1.947	0.056908	0.000108	0.709677	0.709588
593	Dentine	4	11	1.887	0.056800	0.000087	0.710213	0.710123
593	Dentine	4	12	2.006	0.056835	0.000118	0.709717	0.709627
593	Dentine	4	13	1.967	0.056849	0.000084	0.709608	0.709519
593	Dentine	4	14	2.082	0.056793	0.000089	0.709446	0.709357
593	Dentine	4	15	2.458	0.056839	0.000093	0.720467	0.720377

Table A3.65 Detailed LA-MC-ICPMS Sr Isotope Results for Enamel and Dentine, Sample 593, Bovid, Bouffia Bonneval: Stratum 1, La Chapelle-aux-Saints

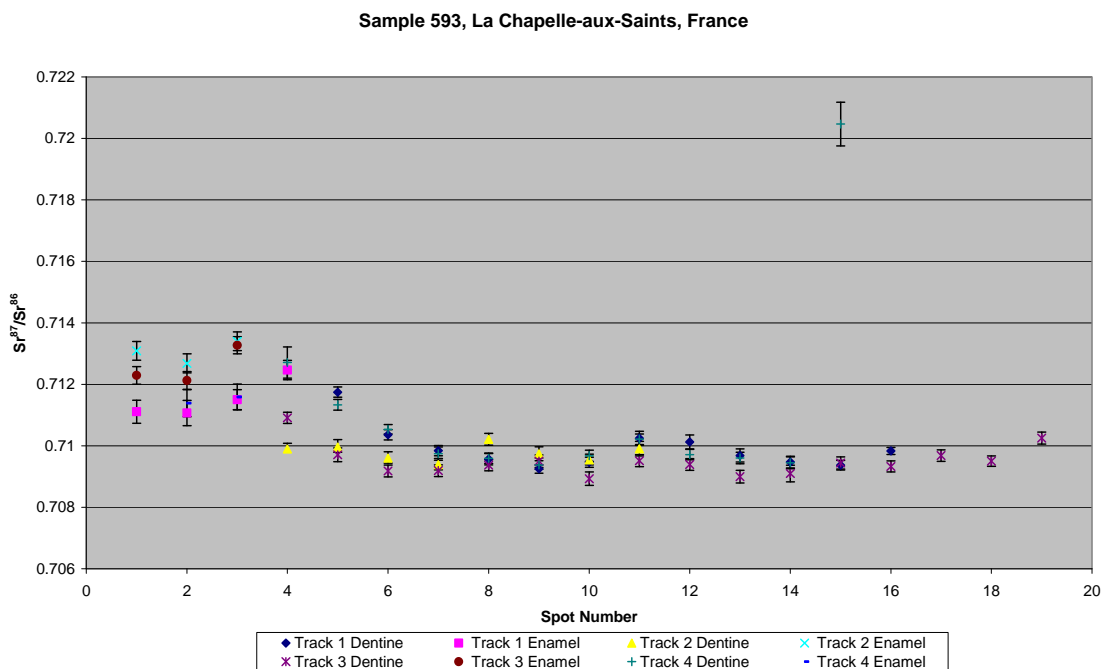


Figure A3.89 Detailed LA-MC-ICPMS Uncorrected Sr Isotope Results, Sample 593, Bovid, Bouffia Bonneval: Stratum 1, La Chapelle-aux-Saints

Sample 593, Corrected Sr Values, La Chapelle-aux-Saints, France

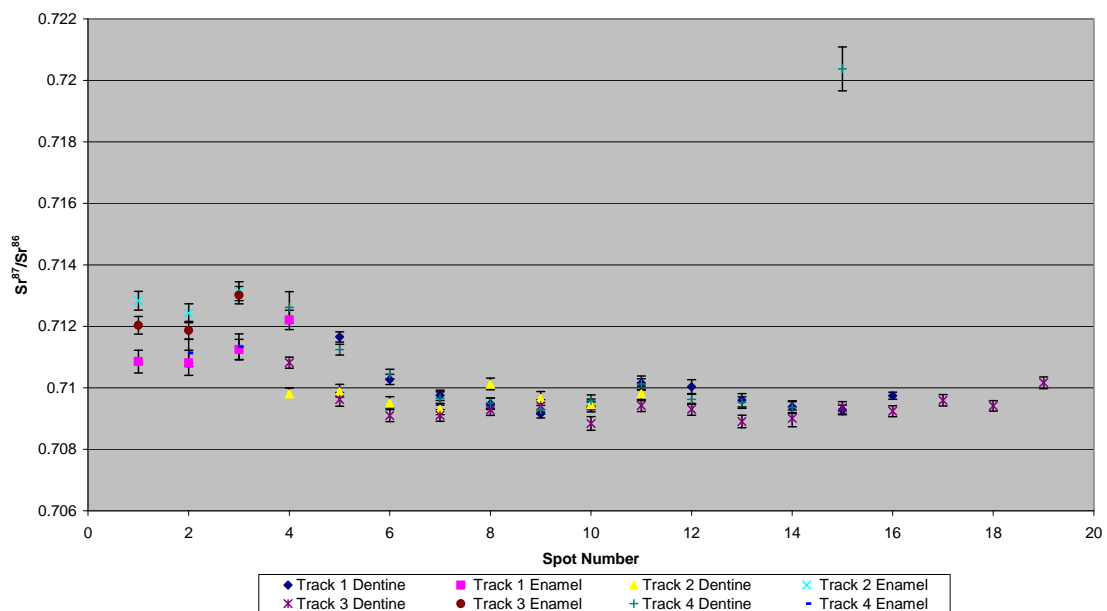


Figure A3.90 Detailed LA-MC-ICPMS Corrected Sr Isotope Results, Sample 593, Bovid, Bouffia Bonneval: Stratum 1, La Chapelle-aux-Saints

Sample 595, a bovid tooth from stratum 1 of the bouffia Bonneval section of La Chapelle-aux-Saints shown in Figure A2.30 was analysed in 2 tracks, with track 1 comprising 9 spots of enamel and 17 spots of dentine, each in 3 discontinuous sections and track 2 comprising 9 spots of enamel and 9 spots of dentine, each in 2 discontinuous sections, shown in Figure A3.91. The strontium isotope results of these 2 tracks are summarised in Table 5.27 and Figure 5.16. The enamel spots of track 1 have an average ^{88}Sr voltage of 1.007, a weighted average uncorrected $^{87}\text{Sr}/^{86}\text{Sr}$ value of 0.71225 ± 0.00088 , a weighted average corrected $^{87}\text{Sr}/^{86}\text{Sr}$ value of 0.71182 ± 0.00088 and a weighted average $^{84}\text{Sr}/^{86}\text{Sr}$ value of 0.056900 ± 0.000157 ($n=9$). The dentine spots of track 1 have an average ^{88}Sr voltage of 1.317, a weighted average uncorrected $^{87}\text{Sr}/^{86}\text{Sr}$ value of 0.71009 ± 0.00030 , a weighted average corrected $^{87}\text{Sr}/^{86}\text{Sr}$ value of 0.70981 ± 0.00030 and a weighted average $^{84}\text{Sr}/^{86}\text{Sr}$ value of 0.056906 ± 0.000047 ($n=17$). The enamel spots of track 2 have an average ^{88}Sr voltage of 0.959, a weighted average uncorrected $^{87}\text{Sr}/^{86}\text{Sr}$ value of 0.71136 ± 0.00056 , a weighted average corrected $^{87}\text{Sr}/^{86}\text{Sr}$ value of 0.71049 ± 0.00056 and a weighted average $^{84}\text{Sr}/^{86}\text{Sr}$ value of 0.056635 ± 0.000063 ($n=9$). The dentine spots of track 2 have an average ^{88}Sr voltage of 1.543, a weighted average

uncorrected $^{87}\text{Sr}/^{86}\text{Sr}$ value of 0.70932 ± 0.00053 , a weighted average corrected $^{87}\text{Sr}/^{86}\text{Sr}$ value of 0.70904 ± 0.00053 and a weighted average $^{84}\text{Sr}/^{86}\text{Sr}$ value of 0.056611 ± 0.000046 ($n=9$). Enamel values of track 1, which are in 3 discontinuous sections, are in the range of 0.711795 to 0.714482 (uncorrected), as well as 0.711366 to 0.714053 (corrected), and are heterogeneous. Dentine values of track 1, which are in 3 discontinuous sections, are in the range of 0.709365 to 0.711747 (uncorrected), as well as 0.709086 to 0.711468 (corrected), and are heterogeneous, particularly the outside sections of the dentine. Enamel values of track 2 are in the range of 0.709727 to 0.712046 (uncorrected), as well as 0.708855 and 0.711174 (corrected), and are somewhat heterogeneous. Dentine values of track 2 are in the range of 0.708042 to 0.710668 (uncorrected), as well as 0.707766 to 0.710391 (corrected), and are somewhat heterogeneous. Detailed values for enamel and dentine for sample 595 are shown in Table A3.66, Figure A3.92 and Figure A3.93.

This sample has very heterogeneous $^{87}\text{Sr}/^{86}\text{Sr}$ values of dentine and enamel and significant difference between the weighted average values between tracks, suggesting a sample mobile during amelogenesis. Enamel $^{87}\text{Sr}/^{86}\text{Sr}$ values are in the range of 0.709727 ± 0.000623 - 0.714482 ± 0.000489 for uncorrected data and 0.708855 ± 0.000623 to 0.714053 ± 0.000489 , with the majority of values in the range 0.710 to 0.713 (uncorrected) and 0.7095 to 0.7135 (corrected), shown in Table A3.66, Figure A3.92 and Figure A3.93. This suggests that, across both uncorrected and corrected results, the specimen could have lived in a Middle Jurassic unit (FS078-S1: 0.709684 ± 0.000011), a Lower Jurassic unit which includes the archaeological site (FS052-S1: 0.710762 ± 0.000031), the Dordogne river floodplain (FS058-S1: 0.713898 ± 0.000031) or the floodplain of the small river adjacent to La Chapelle-aux-Saints (FS046-S1: 0.714131 ± 0.000015). It is difficult to define domains within these values, as while they have relatively heterogeneous mean values, they are indistinguishable within 2σ error. The overall weighted average value for dentine is 0.71003 ± 0.00025 (uncorrected) and 0.70975 ± 0.00025 (corrected). The heterogeneity of dentine value, which is particularly apparent in the outermost sections of dentine, suggests multiple episodes of post-burial diagenesis.

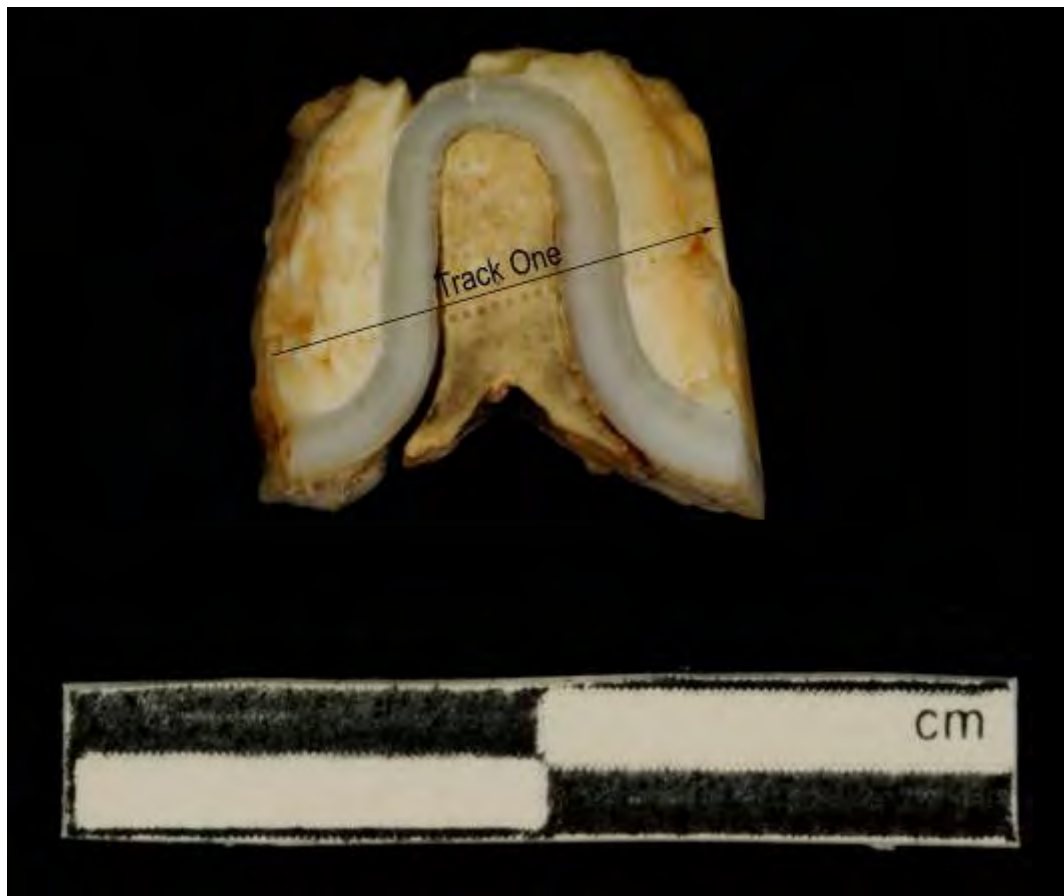


Figure A3.91 LA-MC-ICPMS Track for Sample 595, Bovid, Bouffia Bonneval: Stratum 1, La Chapelle-aux-Saints

Sample	Material	Track	Point	^{88}Sr Volts	$^{84}\text{Sr}/^{86}\text{Sr}$	$^{84}\text{Sr}/^{86}\text{Sr}$ 2σ Error	$^{87}\text{Sr}/^{86}\text{Sr}$	Corrected $^{87}\text{Sr}/^{86}\text{Sr}$	$^{87}\text{Sr}/^{86}\text{Sr}$ 2σ Error
595	Dentine	1	1	2.262	0.056791	0.000113	0.709365	0.709086	0.000197
595	Dentine	1	2	1.614	0.056786	0.000115	0.709661	0.709382	0.000365
595	Dentine	1	3	1.679	0.056823	0.000093	0.709603	0.709324	0.000291
595	Dentine	1	4	1.173	0.056949	0.000142	0.710233	0.709954	0.000336
595	Dentine	1	5	1.133	0.057017	0.000144	0.710580	0.710301	0.000300
595	Enamel	1	6	1.254	0.057031	0.000167	0.713018	0.712589	0.000322
595	Enamel	1	7	1.114	0.057012	0.000164	0.712057	0.711629	0.000388
595	Enamel	1	8	1.012	0.057284	0.000390	0.711795	0.711366	0.000632
595	Enamel	1	9	0.850	0.056949	0.000238	0.714482	0.714053	0.000489
595	Dentine	1	10	1.371	0.056855	0.000129	0.709990	0.709711	0.000289
595	Dentine	1	11	1.257	0.057019	0.000131	0.710008	0.709728	0.000246
595	Dentine	1	12	1.322	0.056982	0.000138	0.710131	0.709852	0.000243
595	Dentine	1	13	1.301	0.056943	0.000209	0.709735	0.709456	0.000283
595	Dentine	1	14	1.293	0.056954	0.000219	0.710035	0.709756	0.000277
595	Dentine	1	15	1.215	0.057202	0.000700	0.710326	0.710047	0.000504
595	Dentine	1	16	1.223	0.057029	0.000191	0.709904	0.709624	0.000271
595	Dentine	1	17	1.117	0.056923	0.000183	0.710419	0.710139	0.000244
595	Enamel	1	18	0.756	0.057892	0.000902	0.713045	0.712617	0.001084
595	Enamel	1	19	0.852	0.057380	0.000307	0.711828	0.711399	0.000439
595	Enamel	1	20	0.924	0.057209	0.000258	0.711888	0.711459	0.000404
595	Enamel	1	21	1.054	0.056993	0.000168	0.712712	0.712284	0.000414
595	Dentine	1	22	1.235	0.056963	0.000212	0.711747	0.711468	0.000248
595	Dentine	1	23	1.081	0.056976	0.000210	0.710550	0.710271	0.000250
595	Dentine	1	24	0.976	0.056947	0.000190	0.709850	0.709571	0.000371
595	Dentine	1	25	1.140	0.056985	0.000191	0.709730	0.709451	0.000204
595	Enamel	1	26	1.250	0.056900	0.000157	0.710397	0.709968	0.000371
595	Enamel	2	1	1.565	0.056524	0.000124	0.710845	0.709973	0.000766
595	Enamel	2	2	1.051	0.056697	0.000153	0.711020	0.710148	0.000606
595	Enamel	2	3	0.820	0.056690	0.000326	0.711728	0.710856	0.000510
595	Enamel	2	4	0.702	0.056787	0.000280	0.712046	0.711174	0.000389
595	Enamel	2	5	0.816	0.056759	0.000285	0.711374	0.710502	0.000502
595	Dentine	2	6	1.508	0.056687	0.000203	0.709951	0.709674	0.000630
595	Dentine	2	7	1.480	0.056758	0.000187	0.709176	0.708899	0.000698
595	Dentine	2	8						
595	Dentine	2	9	1.396	0.056640	0.000137	0.709522	0.709245	0.000640
595	Dentine	2	10	1.308	0.056567	0.000174	0.710668	0.710391	0.000924

Sample	Material	Track	Point	^{88}Sr Volts	$^{84}\text{Sr}/^{86}\text{Sr}$	Error	$^{87}\text{Sr}/^{86}\text{Sr}$	Corrected $^{87}\text{Sr}/^{86}\text{Sr}$	$^{87}\text{Sr}/^{86}\text{Sr} 2\sigma$ Error
595	Enamel	2	11	0.592	0.056672	0.000328	0.711962	0.711090	0.000401
595	Enamel	2	12	0.789	0.056803	0.000259	0.710928	0.710056	0.000489
595	Enamel	2	13	1.059	0.056624	0.000183	0.710533	0.709661	0.000640
595	Enamel	2	14	1.241	0.056592	0.000150	0.709727	0.708855	0.000623
595	Dentine	2	15	1.626	0.056620	0.000112	0.708042	0.707766	0.000577
595	Dentine	2	16	1.402	0.056647	0.000159	0.708949	0.708673	0.000778
595	Dentine	2	17	1.494	0.056544	0.000141	0.709183	0.708906	0.000727
595	Dentine	2	18	1.814	0.056600	0.000115	0.709297	0.709020	0.000540
595	Dentine	2	19	1.860	0.056542	0.000129	0.709789	0.709513	0.000572

Table A3.66 Detailed LA-MC-ICPMS Sr Isotope Results for Enamel and Dentine, Sample 595, Bovid, Bouffia Bonneval: Stratum 1, La Chapelle-aux-Saints

Sample 595, La Chapelle-aux-Saints, France

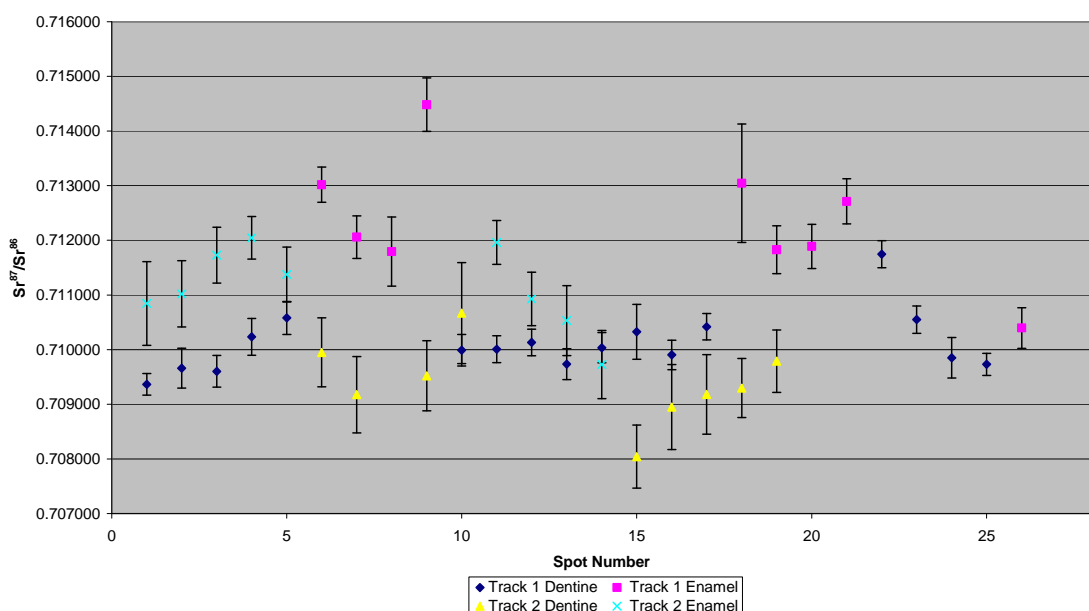


Figure A3.92 Detailed LA-MC-ICPMS Uncorrected Sr Isotope Results, Sample 595, Bovid, Bouffia Bonneval: Stratum 1, La Chapelle-aux-Saints

Sample 595, Corrected Sr Values, La Chapelle-aux-Saints, France

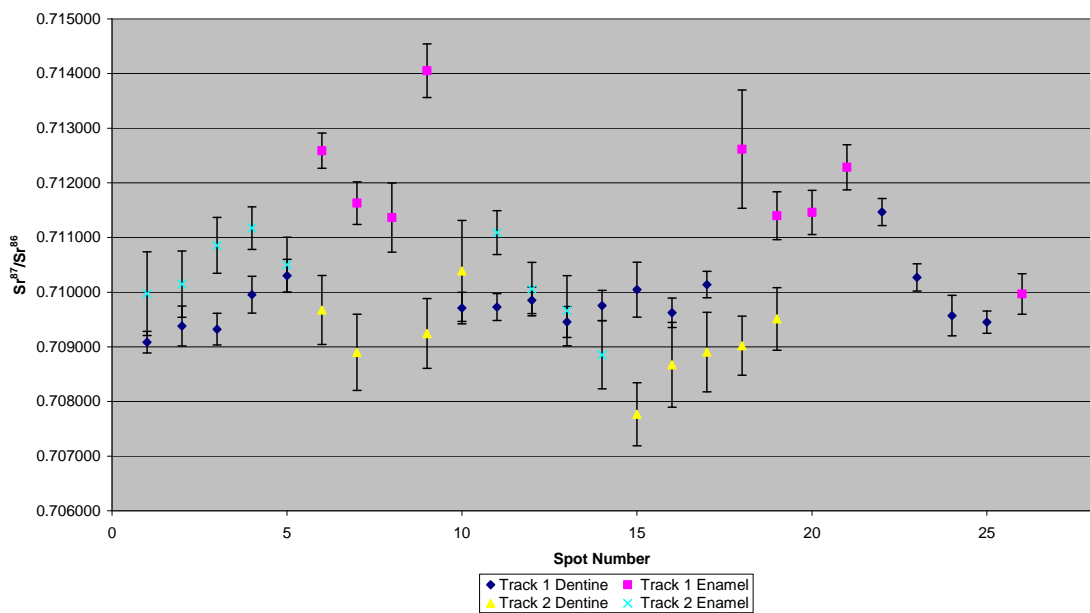


Figure A3.93 Detailed LA-MC-ICPMS Corrected Sr Isotope Results, Sample 595, Bovid, Bouffia Bonneval: Stratum 1, La Chapelle-aux-Saints

Sample M001, a reindeer upper first molar from layer 1 of the bouffia 118 section of La Chapelle-aux-Saints shown in Figure A2.31, was analysed in 1 track, with 4 spots of enamel and 1 spot of dentine, shown in Figure A3.94. The strontium isotope results from this sample are summarised in Table 5.27 and Figure 5.16. The enamel spots are in 2 discontinuous sections with 1 dentine spot in between. The enamel spots have an average ^{88}Sr voltage of 3.159, a weighted average uncorrected $^{87}\text{Sr}/^{86}\text{Sr}$ value of 0.7108 ± 0.0018 , a weighted average corrected $^{87}\text{Sr}/^{86}\text{Sr}$ value of 0.71040 ± 0.0018 and a weighted average $^{84}\text{Sr}/^{86}\text{Sr}$ value of 0.05655 ± 0.00010 ($n=4$). The dentine spots have an average ^{88}Sr voltage of 2.982, a weighted average uncorrected $^{87}\text{Sr}/^{86}\text{Sr}$ value of 0.710422 ± 0.000096 , a weighted average corrected $^{87}\text{Sr}/^{86}\text{Sr}$ value of 0.70998 ± 0.000096 and a weighted average $^{84}\text{Sr}/^{86}\text{Sr}$ value of 0.056668 ± 0.000068 ($n=1$). Enamel values are in the range of 0.709936 to 0.713529 (uncorrected), as well as 0.709520 to 0.713113 (corrected), and are extremely heterogeneous, while the dentine value of track 1 is 0.710422. Detailed values for enamel and dentine for sample M001 are shown in Table A3.67, Figure A3.95 and Figure A3.96.

Enamel values are heterogeneous, suggesting that this individual was extremely mobile across varying geological environments during amelogenesis. Enamel values range from a minimum uncorrected $^{87}\text{Sr}/^{86}\text{Sr}$ value of 0.709936 ± 0.000118 to a maximum of 0.713529 ± 0.000181 and a minimum corrected $^{87}\text{Sr}/^{86}\text{Sr}$ value of 0.709520 ± 0.000118 to a maximum value of 0.713113 ± 0.000181 , shown in Table A3.67, Figure A3.95 and Figure A3.96. The extent of this range suggests a specimen mobile from the area local to the site to a location to the east. The 2 lower uncorrected enamel values, spots 3 and 5, have a weighted average value of 0.709961 ± 0.000080 , which corresponds to the mapping value of 0.710096 ± 0.000013 from FS041-S2, which is less than 2 km from the site of La Chapelle-aux-Saints. A number of other mapping locations from 8 to 17 km to the south of the site, including Dordogne floodplain samples FS043-S1 and FS044-S1 and carbonate samples FS047-S4 and FS052-S1, have values that also correspond to this value. The 2 lower corrected enamel values have a weighted average uncorrected value of 0.709545 ± 0.000080 , which corresponds to the value of FS080-S1 (0.709616 ± 0.000048) from the Middle Jurassic unit, which outcrops within approximately 5.5 km to the south-west of La Chapelle-aux-Saints. The highest uncorrected enamel value from this specimen (spot 4) has no corresponding value from the mapping programme in France, although probably represents a value from the Dordogne floodplain that is intermediate between the more radiogenic values of the metamorphic/igneous province to the east and the carbonate province surrounding the site of La Chapelle-aux-Saints. The corrected value from this sample corresponds either to the Dordogne floodplain sample of 0.713096 ± 0.000014 at FS035-S1 or 0.713071 ± 0.000011 at FS059-S1, which outcrops within 3.9 km of the site. Overall, this range of values for the enamel from sample M001 suggests that this specimen has been mobile in the area surrounding the archaeological site and in the Dordogne floodplain. The 1 spot of dentine from this sample has a $^{87}\text{Sr}/^{86}\text{Sr}$ value of 0.710422 ± 0.000096 .

Strontium concentrations for track 1 of sample M001, as summarised in Table 5.20 and shown in detail in Table A3.19, have a mean of 276 ppm but are somewhat heterogeneous. Spot 2 (353 ppm) is significantly elevated compared

to the other spots, which range from 251 to 272 ppm. Uranium concentrations of this sample are relatively high, with a mean of 16 ppm; however, the value of point 5 is significantly depressed compared to the other spots, with a value of 1 ppm compared to a range for the other spots of 19 to 21 ppm. The relatively high level of uranium suggests that the sample may have been subject to post-burial diagenesis, although the degree of this may have been heterogeneous. $^{84}\text{Sr}/^{86}\text{Sr}$ values of enamel and dentine for this specimen have a weighted average of 0.056572 ± 0.000091 , suggesting that the $^{87}\text{Sr}/^{86}\text{Sr}$ values of this sample are robust.

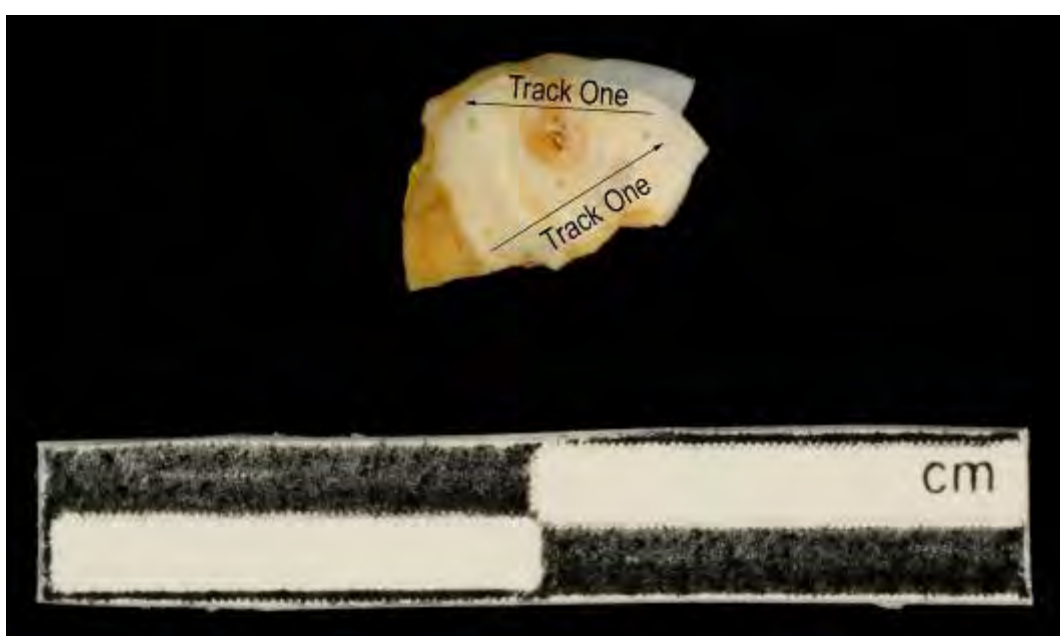


Figure A3.94 LA-MC-ICPMS Track for Sample M001, Reindeer, Bouffia 118: Layer 2, La Chapelle-aux-Saints

Sample	Material	Track	Point	^{88}Sr Volts	$^{84}\text{Sr}/^{86}\text{Sr}$	$^{84}\text{Sr}/^{86}\text{Sr} 2\sigma$ Error	$^{87}\text{Sr}/^{86}\text{Sr}$	Corrected $^{87}\text{Sr}/^{86}\text{Sr}$	$^{87}\text{Sr}/^{86}\text{Sr} 2\sigma$ Error
M001	Enamel	1	1	4.438	0.056596	0.000039	0.711103	0.710687	0.000076
M001	Dentine	1	2	2.982	0.056668	0.000068	0.710422	0.709987	0.000096
M001	Enamel	1	3	2.936	0.056547	0.000073	0.709936	0.709520	0.000118
M001	Enamel	1	4	2.314	0.056575	0.000101	0.713529	0.713113	0.000181
M001	Enamel	1	5	2.950	0.056456	0.000060	0.709985	0.709569	0.000114

Table A3.67 Detailed LA-MC-ICPMS Sr Isotope Results for Dentine and Enamel, Sample M001, Reindeer, Bouffia 118: Layer 2, La Chapelle-aux-Saints

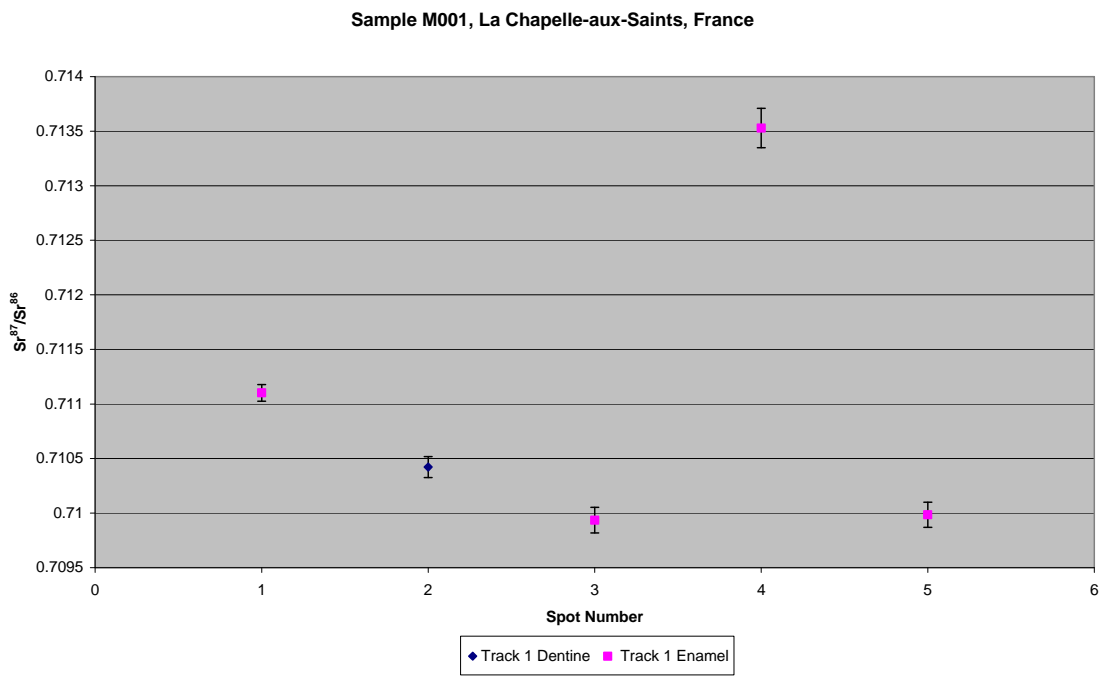


Figure A3.95 Detailed LA-MC-ICPMS Uncorrected Sr Isotope Results, Sample M001, Reindeer, Bouffia 118: Layer 2, La Chapelle-aux-Saints

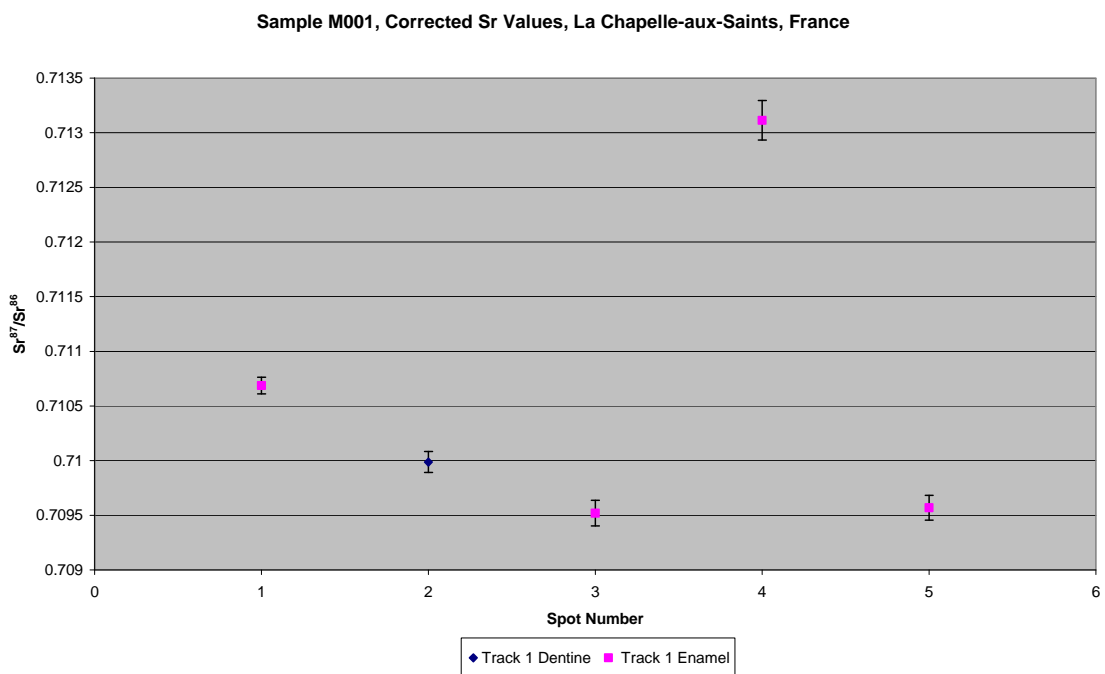


Figure A3.96 Detailed LA-MC-ICPMS Corrected Sr Isotope Results, Sample M001, Reindeer, Bouffia 118: Layer 2, La Chapelle-aux-Saints

Sample M002, a reindeer upper premolar from layer 2 of the bouffia 18 section of La Chapelle-aux-Saints shown in Figure A2.32, was analysed in 2 tracks consisting of 2 spots of enamel each, shown in Figure A3.97. The strontium isotope results of this sample are summarised in Table 5.27 and Figure 5.16. The enamel spots of track 1 have an average ^{88}Sr voltage of 0.642, a weighted average uncorrected $^{87}\text{Sr}/^{86}\text{Sr}$ value of 0.71481 ± 0.00030 , a weighted average corrected $^{87}\text{Sr}/^{86}\text{Sr}$ value of 0.71284 ± 0.00030 and a weighted average $^{84}\text{Sr}/^{86}\text{Sr}$ value of 0.05774 ± 0.00027 ($n=2$). Enamel values for track 1 including 0.714873 and 0.714725 (uncorrected), as well as 0.712900 and 0.712752 (corrected), are heterogeneous between samples, shown in Table A3.68, Figure A3.98 and Figure A3.99. The enamel spots of track 2 have an average ^{88}Sr voltage of 1.261, a weighted average uncorrected $^{87}\text{Sr}/^{86}\text{Sr}$ value of 0.7122 ± 0.0029 , a weighted average corrected $^{87}\text{Sr}/^{86}\text{Sr}$ value of 0.71040 ± 0.0029 and a weighted average $^{84}\text{Sr}/^{86}\text{Sr}$ value of 0.05626 ± 0.00011 ($n=2$). Enamel values for track 2 include 0.712026 and 0.712486 (uncorrected), as well as 0.710689 and 0.710228 (corrected), and are heterogeneous between samples, shown in Table A3.68, Figure A3.98 and Figure A3.99.

The enamel $^{87}\text{Sr}/^{86}\text{Sr}$ values from this sample are very heterogeneous between tracks and somewhat homogenous within tracks. Track 1 has a weighted average $^{87}\text{Sr}/^{86}\text{Sr}$ uncorrected value of 0.71481 ± 0.00030 and corrected value of 0.71284 ± 0.00030 . The uncorrected value from this track does not correspond to any mapping value in the study area, with the most similar mapping sample being FS046-S1 from the floodplain of the small river adjacent to La Chapelle-aux-Saints. Given the heterogeneity of floodplain samples observed in this study, this value may reflect the source of this enamel. The corrected value from this track corresponds to the $^{87}\text{Sr}/^{86}\text{Sr}$ value of 0.712245 ± 0.000026 from FS054-S1, which is located approximately 14 km to the north of La Chapelle-aux-Saints in Cambrian metamorphic rocks which outcrops within 8.3 km of the site. Track 2 has a weighted average $^{87}\text{Sr}/^{86}\text{Sr}$ uncorrected value of 0.7122 ± 0.0029 and a corrected value of 0.7104 ± 0.0029 . The uncorrected value from this track corresponds best to the $^{87}\text{Sr}/^{86}\text{Sr}$ value of 0.712245 ± 0.000026 from FS054-S1 (as does the corrected value of track 1), which is located approximately 14 km to the north of La Chapelle-aux-Saints in

Cambrian metamorphics. The corrected value from this track is similar in value to sample FS041-S2 from a white clay within the Lower Jurassic unit (0.710096 ± 0.000013), which contains the archaeological site, as well as the Dordogne floodplain value from FS044-S1 (0.710436 ± 0.000012).

Elemental concentrations for sample M002, summarised in Table 5.20 and shown in detail in Table A3.20, suggest that the results are somewhat robust. While the concentration of strontium is somewhat low at 162 ppm. This sample has no uranium, suggesting that it has not been subjected to post-burial diagenesis. The $^{84}\text{Sr}/^{86}\text{Sr}$ values have a weighted average value of 0.05626 ± 0.00011 , which is sub-optimal compared to the ideal value of 0.0565.

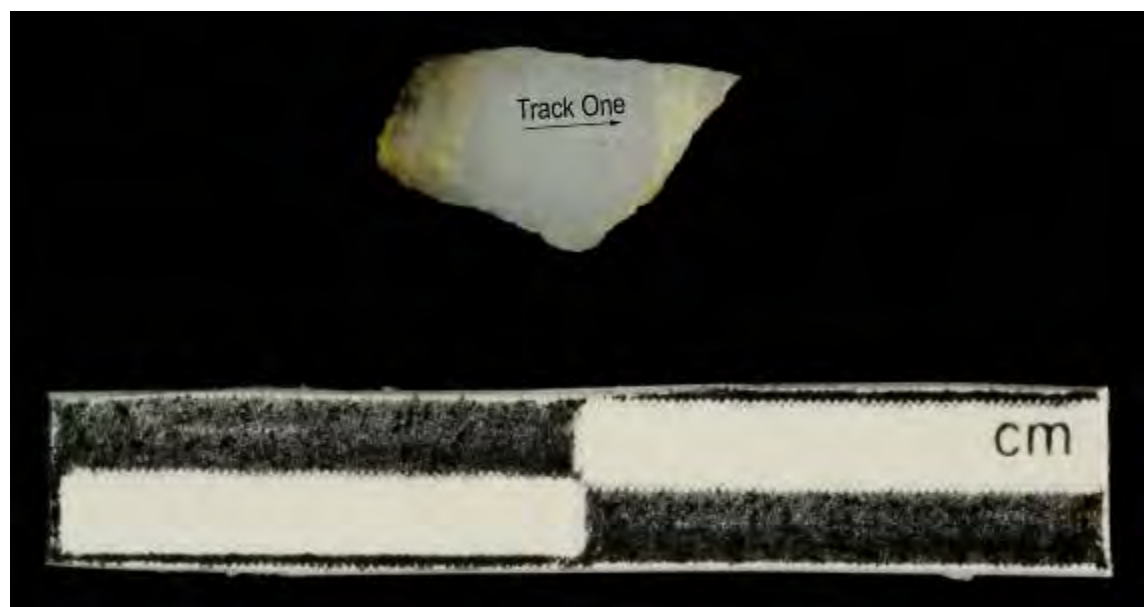


Figure A3.97 LA-MC-ICPMS Track for Sample M002, Reindeer, Bouffia 118: Layer 2, La Chapelle-aux-Saints

Sample	Material	Track	Point	^{88}Sr Volts	$^{84}\text{Sr}/^{86}\text{Sr}$	Error	$^{87}\text{Sr}/^{86}\text{Sr}$	Corrected $^{87}\text{Sr}/^{86}\text{Sr}$	$^{87}\text{Sr}/^{86}\text{Sr} 2\sigma$
M002	Enamel	1	1	0.639	0.057700	0.000335	0.714873	0.712900	0.000407
M002	Enamel	1	2	0.645	0.057827	0.000472	0.714725	0.712752	0.000462

M002	Enamel	2	1	1.151	0.056242	0.000151	0.712486	0.710689	0.000211
M002	Enamel	2	2	1.370	0.056271	0.000160	0.712026	0.710228	0.000192

Table A3.68 Detailed LA-MC-ICPMS Sr Isotope Results for Enamel, Sample M002, Reindeer, Bouffia 118: Layer 2, La Chapelle-aux-Saints

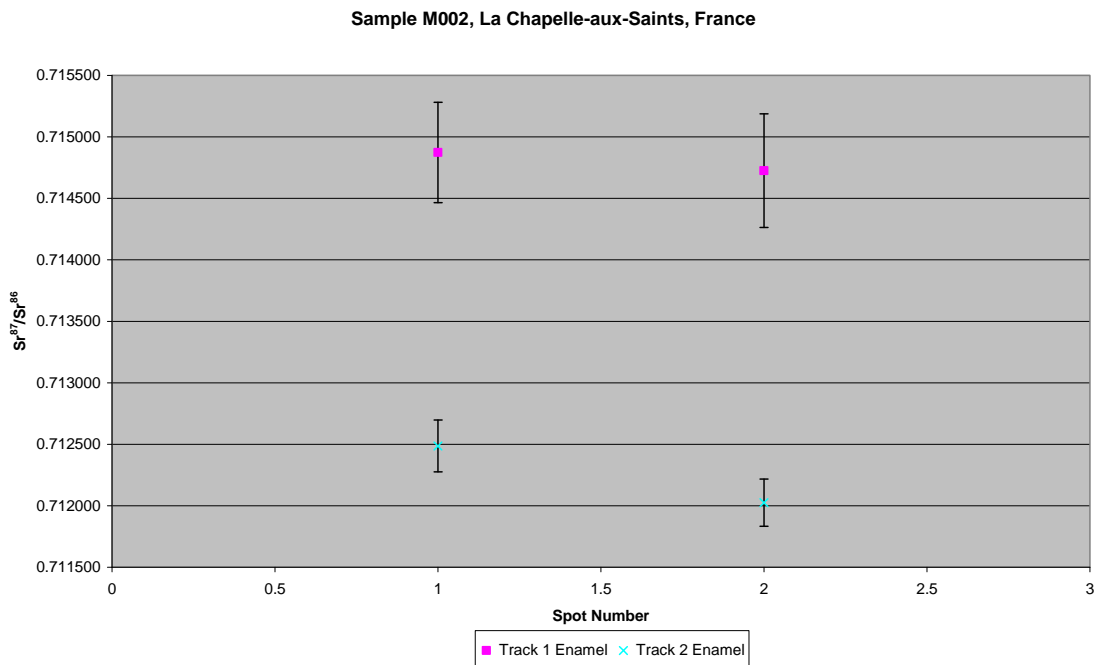


Figure A3.98 Detailed LA-MC-ICPMS Uncorrected Sr Isotope Results, Sample M002, Reindeer, Bouffia 118: Layer 2, La Chapelle-aux-Saints

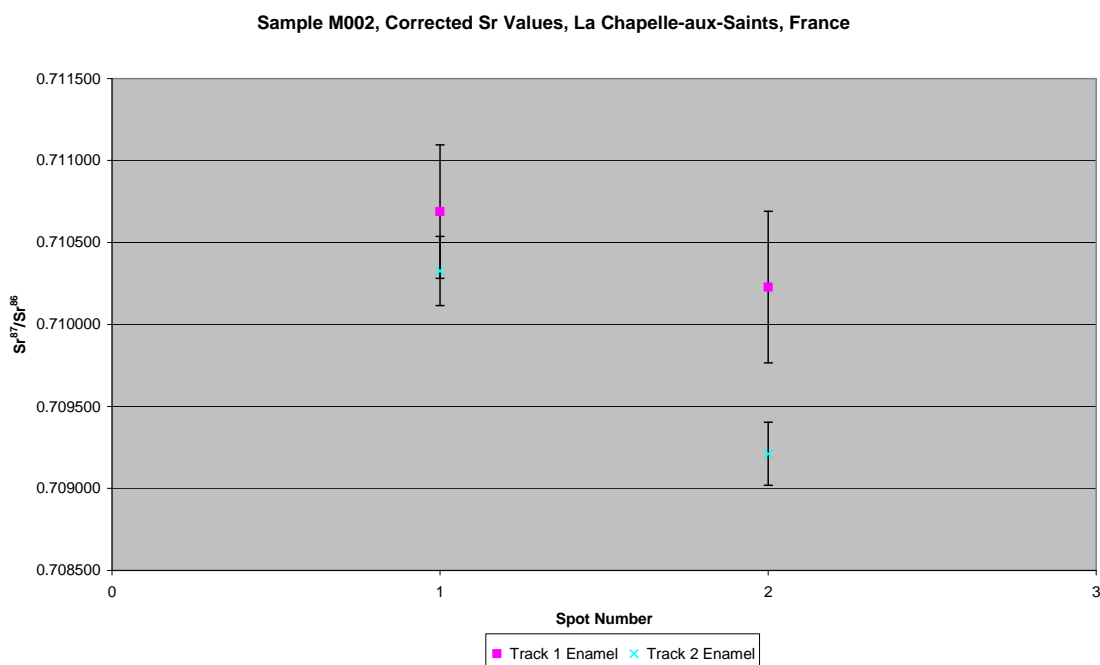


Figure A3.99 Detailed LA-MC-ICPMS Corrected Sr Isotope Results, Sample M002, Reindeer, Bouffia 118: Layer 2, La Chapelle-aux-Saints

Sample M003, a reindeer upper second molar from layer 2 of the bouffia 18 section of La Chapelle-aux-Saints shown in Figure 2.33, was analysed in 1 track consisting of 2 spots of enamel and 2 spots of dentine, shown in Figure A3.100. The strontium isotope results of this sample are summarised in Table 5.27 and Figure 5.16. The enamel spots of track 1 have an average ^{88}Sr voltage of 1.982, a weighted average uncorrected $^{87}\text{Sr}/^{86}\text{Sr}$ value of 0.7103 ± 0.0070 , a weighted average uncorrected $^{87}\text{Sr}/^{86}\text{Sr}$ value of 0.70970 ± 0.0070 and a weighted average $^{84}\text{Sr}/^{86}\text{Sr}$ value of 0.056059 ± 0.000064 ($n=2$). The dentine spots of track 1 have an average ^{88}Sr voltage of 2.544, a weighted average uncorrected $^{87}\text{Sr}/^{86}\text{Sr}$ value of 0.7104 ± 0.0011 , a weighted average corrected $^{87}\text{Sr}/^{86}\text{Sr}$ value of 0.71000 ± 0.0011 and a weighted average $^{84}\text{Sr}/^{86}\text{Sr}$ value of 0.056128 ± 0.000049 ($n=2$). Enamel values for track 1 are 0.710990 and 0.709874 (uncorrected), as well as 0.709211 and 0.710327 (corrected), and dentine values are 0.710326 and 0.710492 (uncorrected), as well as 0.709948 and 0.710115 (corrected). The dentine values are homogeneous; however, the enamel values are heterogeneous. Detailed values for enamel and dentine for sample M003 are shown in Table A3.69, Figure A3.101 and Figure A3.102.

The enamel $^{87}\text{Sr}/^{86}\text{Sr}$ values (shown in detail in Table A3.69, Figure A3.101 and Figure A3.102) are somewhat heterogeneous, with uncorrected values of 0.710990 ± 0.000210 and 0.709874 ± 0.000173 and corrected values of 0.710327 ± 0.000210 and 0.709211 ± 0.000173 . The value of the first uncorrected spot correlates to values from samples Upper Cretaceous FS089-S1 and Lower Jurassic FS052-S1. The value of the first corrected spot corresponds to values from a number of locations surrounding La Chapelle-aux-Saints, including FS041-S2 and FS052-S2 (Lower Jurassic limestone which contains the site) and FS044-S1 (Dordogne floodplain). The value of the second uncorrected spot corresponds to mapping sample FS043-S1, with a $^{87}\text{Sr}/^{86}\text{Sr}$ value of 0.709837 ± 0.000013 , which is a floodplain sample from the Dordogne river approximately 12 km south of the site of La Chapelle-aux-Saints. The second corrected spot has a value that correlates to floodplain samples from

the Vezere (FS027-S2) and Dordogne (FS032-S2) rivers which outcrop within 3.9 km of the archaeological site. The dentine values are relatively heterogeneous, with a weighted average uncorrected value of 0.7104 ± 0.0011 .

Elemental concentrations of sample M003, summarised in Table 5.20 and shown in detail in Table A3.21, suggest that the $^{87}\text{Sr}/^{86}\text{Sr}$ values of this sample are robust. The enamel and dentine strontium concentrations are relatively high. Uranium has a relatively high concentration in this sample, with values of 29 and 26 ppm for enamel and 19 and 16 ppm for dentine. This suggests that this specimen may have been subject to post-burial diagenesis. $^{84}\text{Sr}/^{86}\text{Sr}$ values, shown in Table A3.78, have a weighted average value of 0.056102 ± 0.000074 , which is significantly lower than the optimum value of 0.0565.

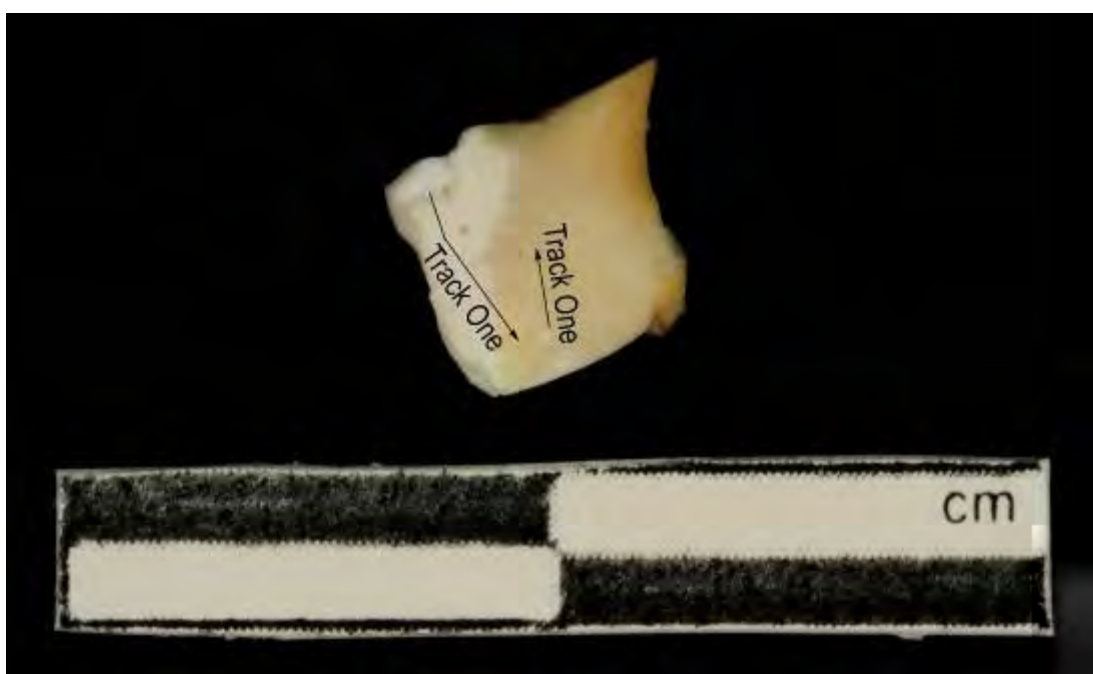


Figure A3.100 LA-MC-ICPMS Track for Sample M003, Reindeer, Bouffia 118: Layer 2, La Chapelle-aux-Saints

Sample	Material	Track	Point	^{88}Sr Volts	$^{84}\text{Sr}/^{86}\text{Sr}$	$^{84}\text{Sr}/^{86}\text{Sr} 2\sigma$	Corrected $^{87}\text{Sr}/^{86}\text{Sr}$	$^{87}\text{Sr}/^{86}\text{Sr} 2\sigma$	Error
M003	Enamel	1	1	2.179	0.056082	0.000081	0.710990	0.710327	0.000210

M003	Enamel	1	2	1.784	0.056016	0.000109	0.709874	0.709211	0.000173
M003	Dentine	1	3	2.533	0.056143	0.000071	0.710326	0.709948	0.000098
M003	Dentine	1	4	2.555	0.056113	0.000070	0.710492	0.710115	0.000105

Table A3.69 Detailed LA-MC-ICPMS Sr Isotope Results for Enamel and Dentine, Reindeer, Bouffia 118: Layer 2, La Chapelle-aux-Saints

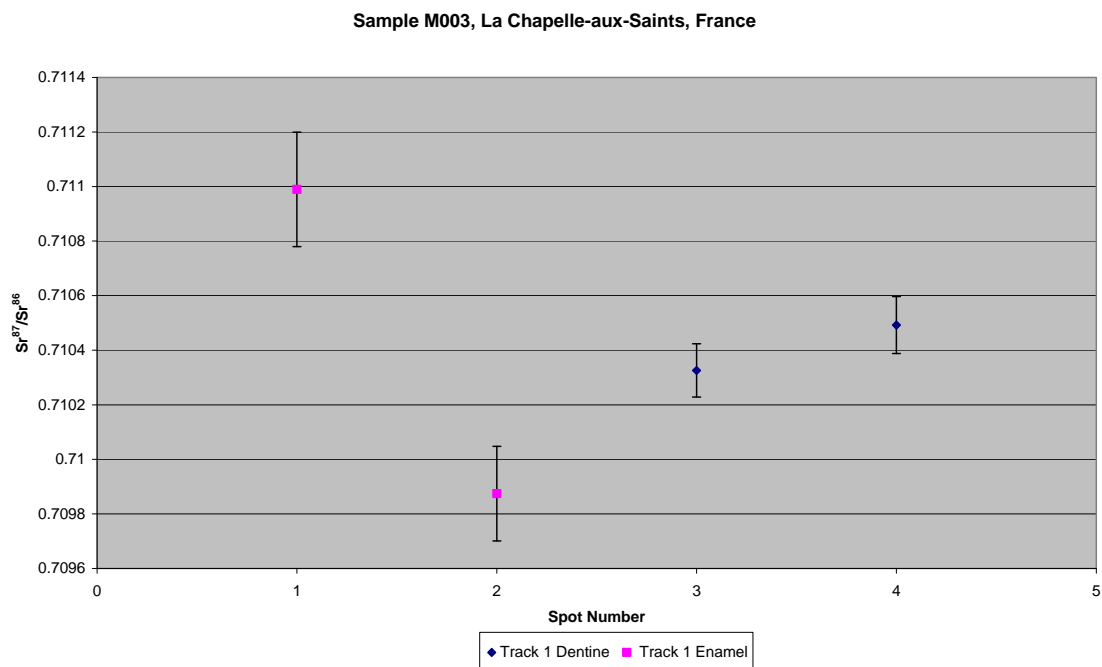


Figure A3.101 Detailed LA-MC-ICPMS Uncorrected Sr Isotope Results, Reindeer, Bouffia 118: Layer 2, La Chapelle-aux-Saints

Sample M003, Corrected Sr Values, La Chapelle-aux-Saints, France

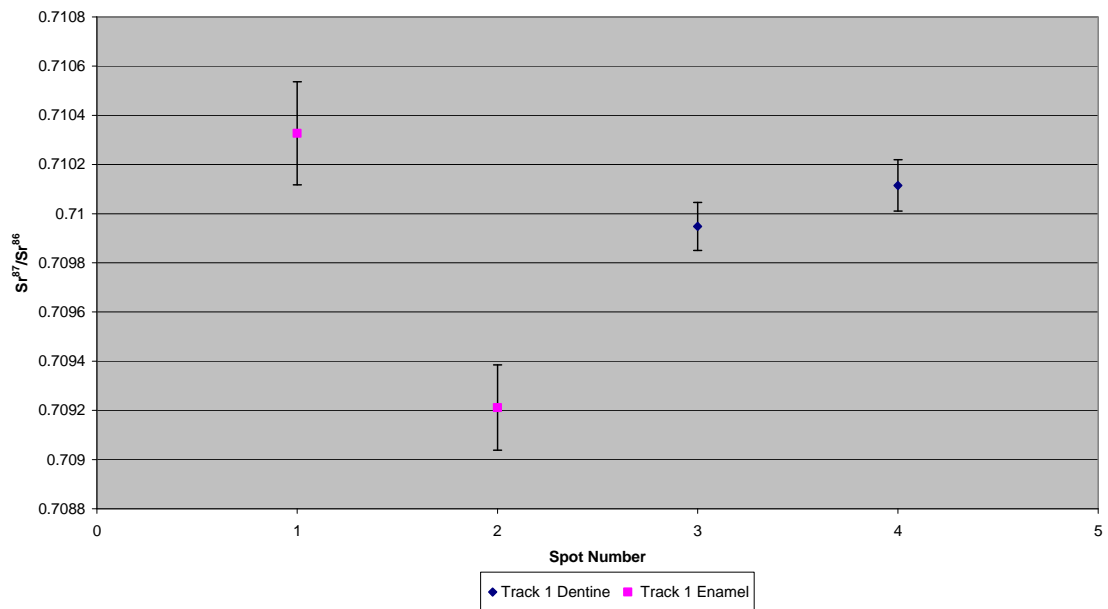


Figure A3.102 Detailed LA-MC-ICPMS Corrected Sr Isotope Results, Reindeer, Bouffia 118: Layer 2, La Chapelle-aux-Saints

Sample M004, an unidentified tooth from an unknown layer of the bouffia 18 section of La Chapelle-aux-Saints shown in Figure A2.34, was analysed by 1 track consisting of 2 spots of enamel and 2 spots of dentine, shown in Figure A3.103. The strontium isotope results of this sample are summarised in Table 5.27 and Figure 5.16. The enamel spots have an average ^{88}Sr voltage of 1.189, a weighted average uncorrected $^{87}\text{Sr}/^{86}\text{Sr}$ value of 0.7122 ± 0.0021 , a weighted average corrected $^{87}\text{Sr}/^{86}\text{Sr}$ value of 0.71080 ± 0.0021 and a weighted average $^{84}\text{Sr}/^{86}\text{Sr}$ value of 0.05555 ± 0.00012 ($n=2$). The dentine spots have an average ^{88}Sr voltage of 1.900, a weighted average uncorrected $^{87}\text{Sr}/^{86}\text{Sr}$ value of 0.7098 ± 0.0022 , a weighted average corrected $^{87}\text{Sr}/^{86}\text{Sr}$ value of 0.70930 ± 0.0022 and a weighted average $^{84}\text{Sr}/^{86}\text{Sr}$ value of 0.055844 ± 0.000072 ($n=2$). Enamel values are homogenous within 2σ error within the track and dentine values are heterogeneous. Detailed values for enamel and dentine for sample M004 are shown in Table A3.70, Figure A3.104 and Figure A3.105.

Enamel $^{87}\text{Sr}/^{86}\text{Sr}$ are homogenous within 2σ error, with a weighted average uncorrected value of 0.7122 ± 0.0021 and corrected value of 0.71080 ± 0.0021 . The uncorrected values correspond to the $^{87}\text{Sr}/^{86}\text{Sr}$ value of 0.712245 ± 0.000026 from FS054-S1, a Cambrian metamorphic package containing leptynite, orthogneiss and amphibolite, which is located approximately 14 km to the north of La Chapelle-aux-Saints. The corrected values correlate with mapping values from Upper Cretaceous (FS089-S1) and Lower Jurassic (FS052-S1) carbonates. This Lower Jurassic unit contains the archaeological site. Dentine values are just outside of 2σ error, with uncorrected values of 0.710010 ± 0.000161 and 0.709655 ± 0.000135 and corrected values of 0.709500 ± 0.000161 and 0.709145 ± 0.000135 . The disparity in $^{87}\text{Sr}/^{86}\text{Sr}$ values between enamel and dentine (which is greater between the uncorrected than corrected samples) suggests that this individual is a migrant.

Elemental concentrations from sample M004, summarised in Table 5.20 and shown in detail in Table A3.22, show strontium values for enamel of 161 and 162 ppm and 225 and 231 ppm. Uranium concentrations are 0 ppm for the

enamel spots and 12 and 13 ppm for dentine spots, suggesting that the dentine may have been subject to post-burial diagenesis. $^{84}\text{Sr}/^{86}\text{Sr}$ values have a weighted average of 0.05576 ± 0.00024 , which is significantly lower than the ideal value of 0.0565.

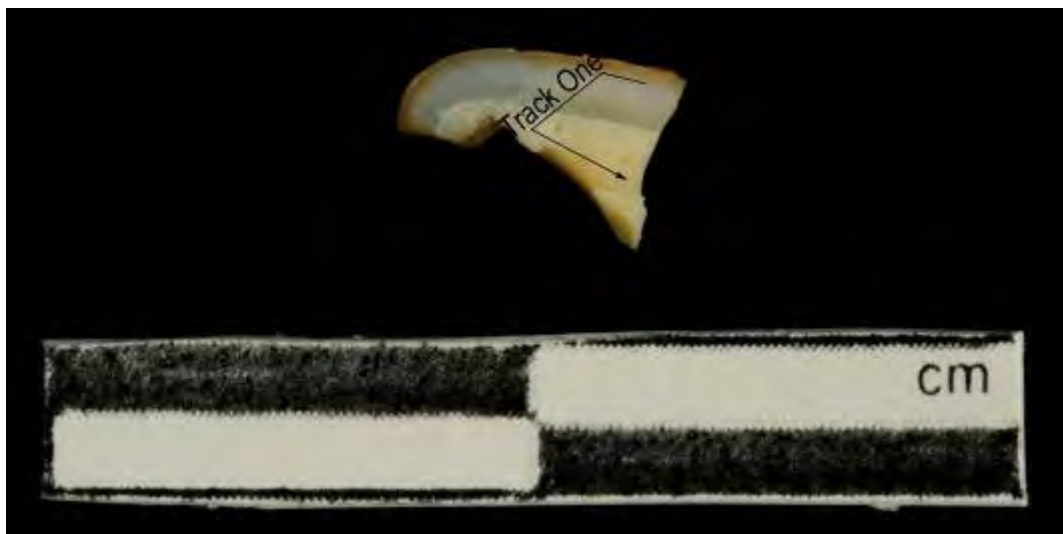


Figure A3.103 LA-MC-ICPMS Track for Sample M004, Unknown Species, Bouffia 118: Unknown Layer, La Chapelle-aux-Saints

Sample	Material	Track	Point	^{88}Sr Volts	$^{84}\text{Sr}/^{86}\text{Sr}$	$^{84}\text{Sr}/^{86}\text{Sr} 2\sigma$	Corrected $^{87}\text{Sr}/^{86}\text{Sr}$	$^{87}\text{Sr}/^{86}\text{Sr}$	$^{87}\text{Sr}/^{86}\text{Sr} 2\sigma$
M004	Enamel	1	1	1.140	0.055587	0.000182	0.712322	0.710956	0.000171
M004	Enamel	1	2	1.238	0.055525	0.000156	0.711994	0.710628	0.000165
M004	Dentine	1	3	1.870	0.055843	0.000138	0.710010	0.709500	0.000161
M004	Dentine	1	4	1.929	0.055844	0.000086	0.709655	0.709145	0.000135

Table A3.70 Detailed LA-MC-ICPMS Sr Isotope Results for Enamel and Dentine, Sample M004, Unknown Species, Bouffia 118: Unknown Layer, La Chapelle-aux-Saints

Sample M004, La Chapelle-aux-Saints, France

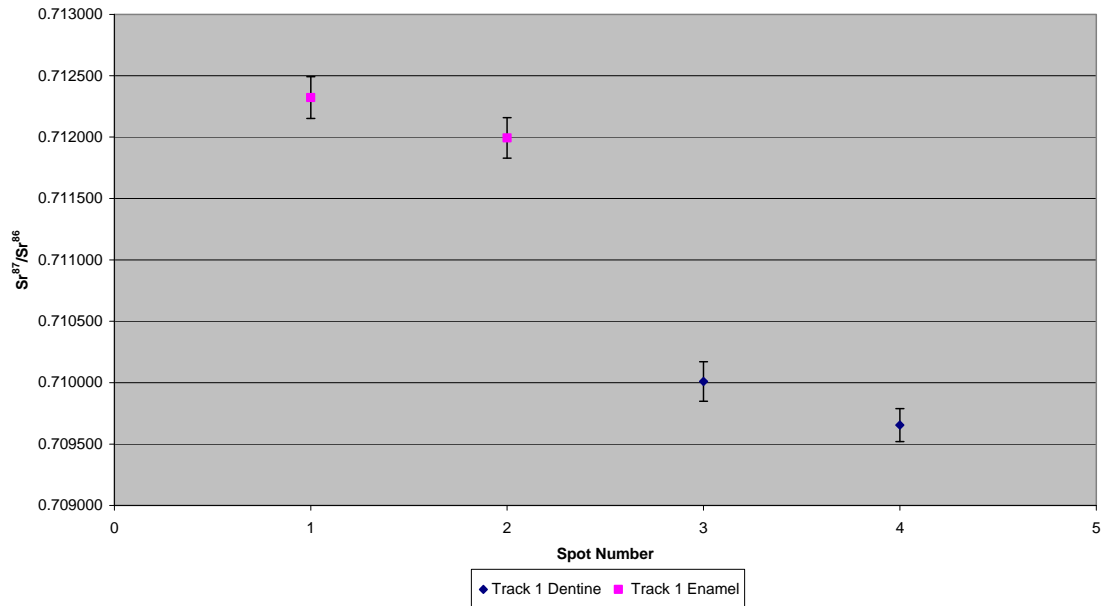


Figure A3.104 Detailed LA-MC-ICPMS Uncorrected Sr Isotope Results, Sample M004, Unknown Species, Bouffia 118: Unknown Layer, La Chapelle-aux-Saints

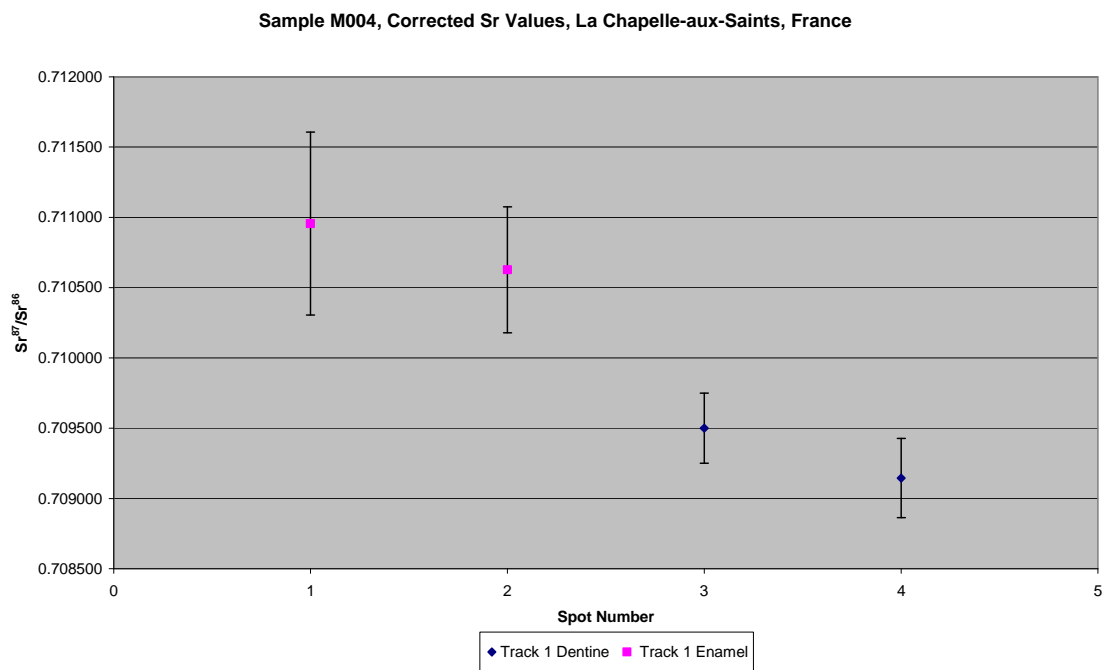


Figure A3.105 Detailed LA-MC-ICPMS Corrected Sr Isotope Results, Sample M004, Unknown Species, Bouffia 118: Unknown Layer, La Chapelle-aux-Saints

Sample M005, a bovid upper fourth premolar from layer 1 from the bouffia 118 section of La Chapelle-aux-Saints shown in Figure A2.35, was analysed in 1

track consisting of 4 spots of dentine and 1 of enamel, shown in Figure A3.106. The strontium isotope results from this sample are summarised in Table 5.27 and Figure 5.16. The enamel spot of M005 has a ^{88}Sr voltage of 1.362, a weighted average uncorrected $^{87}\text{Sr}/^{86}\text{Sr}$ value of 0.718474 ± 0.000174 , a weighted average corrected $^{87}\text{Sr}/^{86}\text{Sr}$ value of 0.71781 ± 0.000174 and a weighted average $^{84}\text{Sr}/^{86}\text{Sr}$ value of 0.055465 ± 0.000130 ($n=1$). The dentine spots have an average ^{88}Sr voltage of 2.116, a weighted average uncorrected $^{87}\text{Sr}/^{86}\text{Sr}$ value of 0.7120 ± 0.0020 , a weighted average corrected $^{87}\text{Sr}/^{86}\text{Sr}$ value of 0.71170 ± 0.0020 and a weighted average $^{84}\text{Sr}/^{86}\text{Sr}$ value of 0.055817 ± 0.000051 ($n=4$). Dentine values are in the range 0.710665 to 0.714934 (uncorrected), as well as 0.710346 to 0.714615 (corrected), and are very heterogeneous. Detailed values for enamel and dentine for sample M005 are shown in Table A3.71, Figure A3.107 and Figure A3.108.

The enamel spot has an uncorrected $^{87}\text{Sr}/^{86}\text{Sr}$ value of 0.718474 ± 0.000174 and a corrected value of 0.717818 ± 0.000174 , which is far more elevated than any other enamel sample from La Chapelle-aux-Saints. The mapping locations corresponding to the uncorrected value are found approximately 100 km to the south-east of La Chapelle-aux-Saints and include FS097-S1 (0.718429 ± 0.000013) and FS105-S1 (0.718595 ± 0.000017), while P12P (0.717775 ± 0.00002) located approximately 200 km to the east of the site within a Brioerian/Cambrian/Ordovician metamorphic package, corresponds to the corrected value. This unit outcrops within 14.2 km of the archaeological site. Dentine values are extremely heterogeneous, which may suggest multiple episodes of post-burial diagenesis.

Elemental concentrations from sample M005, summarised in Table 5.20 and shown in detail in Table A3.23, were collected only from dentine. These have strontium concentrations in the range of 186 to 253 ppm and uranium concentrations in the range of 16 to 18 ppm. $^{84}\text{Sr}/^{86}\text{Sr}$ values for sample M005 have a weighted average of 0.05577 ± 0.00018 , which is less than the ideal value of 0.0565, suggesting that the $^{87}\text{Sr}/^{86}\text{Sr}$ values may not be robust.

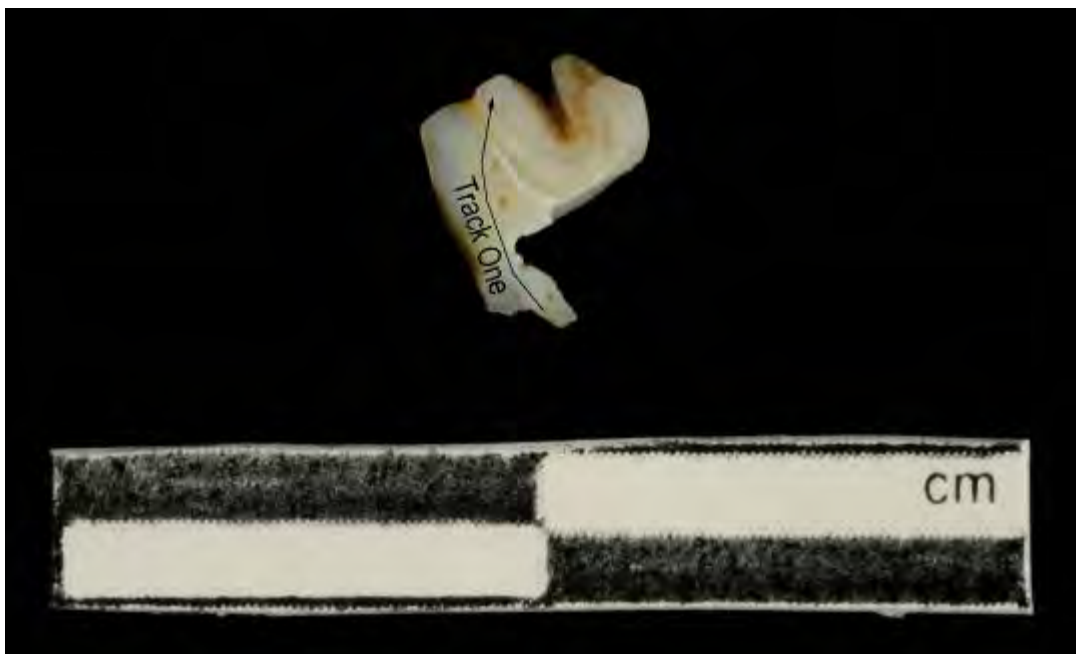


Figure A3.106 LA-MC-ICPMS Track for Sample M005, Bovid, Bouffia 118: Layer 1, La Chapelle-aux-Saints

Sample	Material	Track	Point	^{88}Sr Volts	$^{84}\text{Sr}/^{86}\text{Sr}$	$^{84}\text{Sr}/^{86}\text{Sr} 2\sigma$ Error	$^{87}\text{Sr}/^{86}\text{Sr}$	Corrected $^{87}\text{Sr}/^{86}\text{Sr}$	$^{87}\text{Sr}/^{86}\text{Sr} 2\sigma$ Error
M005	Dentine	1	1	1.848	0.055812	0.000102	0.710665	0.710346	0.000167
M005	Dentine	1	2	2.453	0.055917	0.000158	0.714934	0.714615	0.000306
M005	Dentine	1	3	2.128	0.055827	0.000091	0.712439	0.712120	0.000146
M005	Dentine	1	4	2.036	0.055777	0.000092	0.711946	0.711627	0.000145
M005	Enamel	1	5	1.362	0.055465	0.000130	0.718474	0.717818	0.000174

Table A3.71 Detailed LA-MC-ICPMS Sr Isotope Results for Dentine and Enamel, Sample M005, Bovid, Bouffia 118: Layer 1, La Chapelle-aux-Saints

Sample M005, La Chapelle-aux-Saints, France

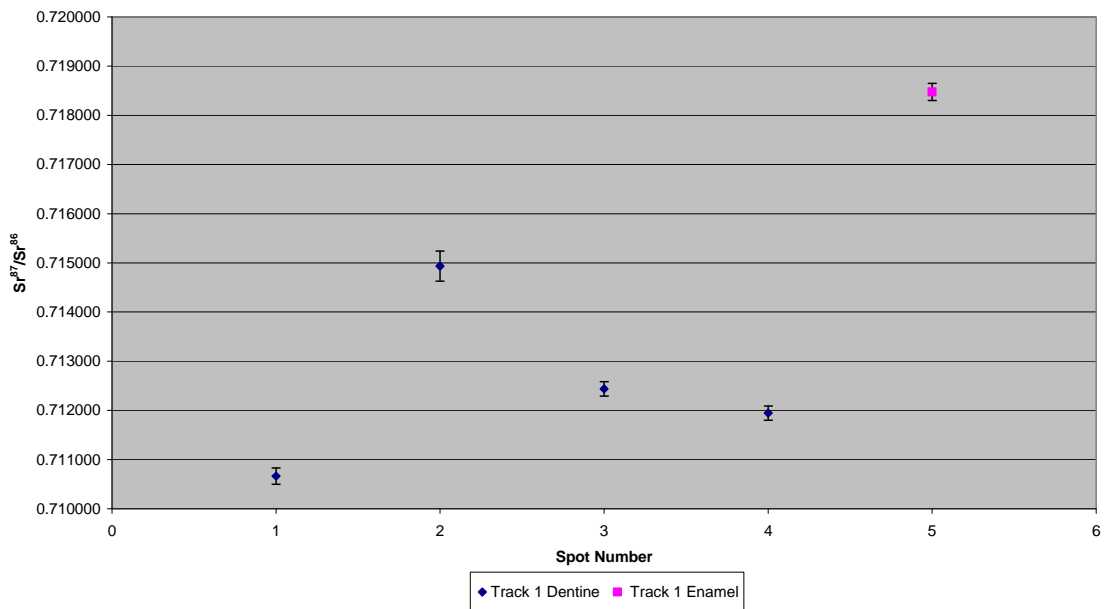


Figure A3.107 Detailed LA-MC-ICPMS Uncorrected Sr Isotope Results, Sample M005, Bovid, Bouffia 118: Layer 1, La Chapelle-aux-Saints

Sample M005, Corrected Sr Values, La Chapelle-aux-Saints, France

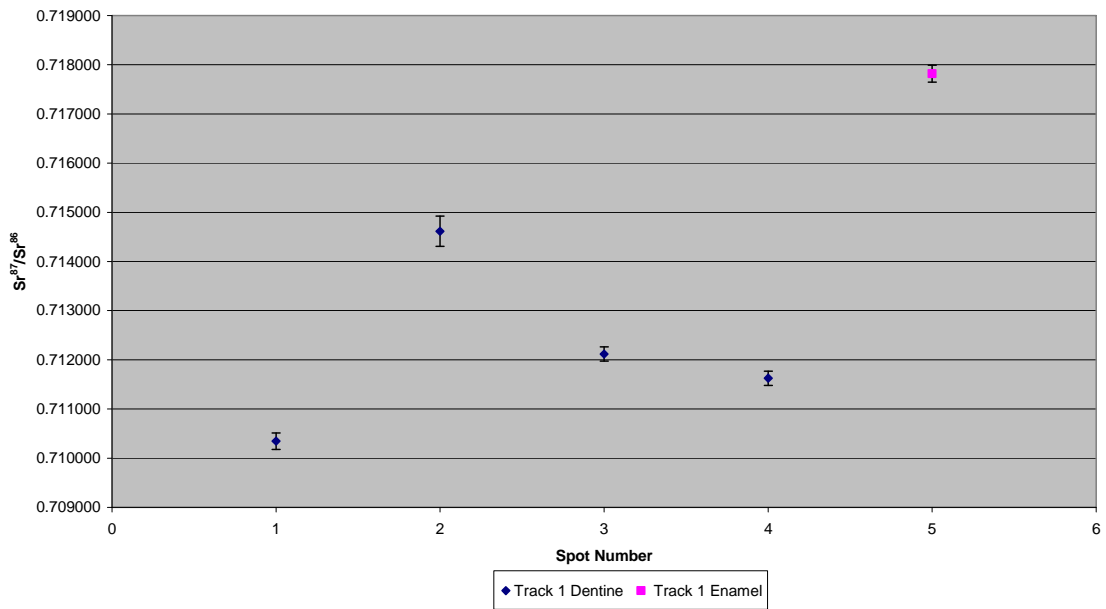


Figure A3.108 Detailed LA-MC-ICPMS Corrected Sr Isotope Results, Sample M005, Bovid, Bouffia 118: Layer 1, La Chapelle-aux-Saints

Sample M006, a bovid upper second premolar from layer 1 of the bouffia 118 section of La Chapelle-aux-Saints shown in Figure A2.36, was analysed in 1 track consisting of 5 spots of enamel, shown in Figure A3.109. The strontium isotope results of this sample are summarised in Table 5.27 and Figure 5.16. The enamel of M006 has an average ^{88}Sr voltage of 1.623, a weighted average uncorrected $^{87}\text{Sr}/^{86}\text{Sr}$ value of 0.71210 ± 0.00071 , a weighted average corrected $^{87}\text{Sr}/^{86}\text{Sr}$ value of 0.71179 ± 0.00071 and a weighted average $^{84}\text{Sr}/^{86}\text{Sr}$ value of 0.056650 ± 0.000056 . Enamel values are in the range of 0.711401 to 0.712725 (uncorrected) and 0.711092 to 0.712416 (corrected). The values are somewhat heterogeneous, with spots 1 and 5 and spots 2, 3 and 4 within 2σ error. Detailed values for enamel for sample M006 are shown in Table A3.72, Figure A3.110 and Figure A3.111.

This sample has 2 domains of enamel $^{87}\text{Sr}/^{86}\text{Sr}$ composition with an uncorrected range of 0.711401 to 0.711728 and 0.712471 to 0.712725 and a corrected range of 0.711092 to 0.711420 and 0.712162 to 0.712416, suggesting that this specimen was mobile during amelogenesis. The uncorrected and corrected values are within 2σ error, and so the mapping interpretation is the same for both values. The lower domain corresponds somewhat to the value of 0.711984 ± 0.000018 from the Dordogne floodplain at FS056-S1. This suggests that this sample may have been resident on the floodplain in an area where its inputs are slightly different. The higher domain corresponds to mapping location F36R, with a value of 0.712497 ± 0.000008 , which is collected within Cambrian metamorphics containing paragneiss, leptynites and amphibolites. This sample location is 125 km to the north-west of the site of La Chapelle-aux-Saints; however, the same unit outcrops within 8.5 km of this site. One mapping location (FS044-S1) is found within this unit close to La Chapelle-aux-Saints, with a value of 0.710436 ± 0.000012 , which is significantly different from the value of F36R; however, it is located on a floodplain and so probably does not reflect the local bedrock.

Enamel from sample M006, summarised in Table 5.20 and Table A3.24, has a very high mean strontium concentration (310 ppm) and very low uranium concentration (0 ppm), suggesting that strontium isotope results are very robust. The $^{84}\text{Sr}/^{86}\text{Sr}$ value is 0.056651 ± 0.000057 , only slightly elevated compared to the ideal value of 0.0565, suggesting that the results are probably robust.

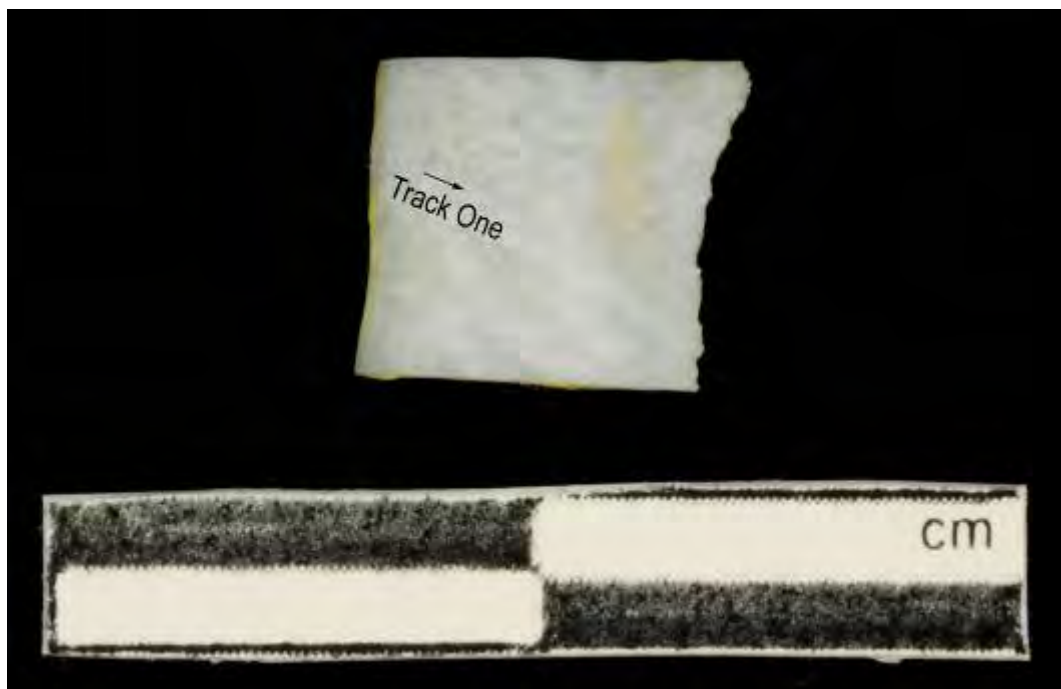


Figure A3.109 LA-MC-ICPMS Track for Sample M006, Bovid, Bouffia 118: Layer 1, La Chapelle-aux-Saints

Sample	Material	Track	Point	^{88}Sr Volts	$^{84}\text{Sr}/^{86}\text{Sr}$	Error	$^{87}\text{Sr}/^{86}\text{Sr}$	2σ	Error
M006	Enamel	1	1	1.695	0.056579	0.000155	0.711401	0.711092	0.000223
M006	Enamel	1	2	1.536	0.056659	0.000116	0.712471	0.712162	0.000224
M006	Enamel	1	3	1.656	0.056745	0.000126	0.712725	0.712416	0.000244
M006	Enamel	1	4	1.583	0.056644	0.000130	0.712504	0.712195	0.000268
M006	Enamel	1	5	1.647	0.056600	0.000127	0.711728	0.711420	0.000198

Table A3.72 Detailed LA-MC-ICPMS Sr Isotope Results for Dentine and Enamel, Sample M006, Bovid, Bouffia 118: Layer 1, La Chapelle-aux-Saints

Sample M006, La Chapelle-aux-Saints, France

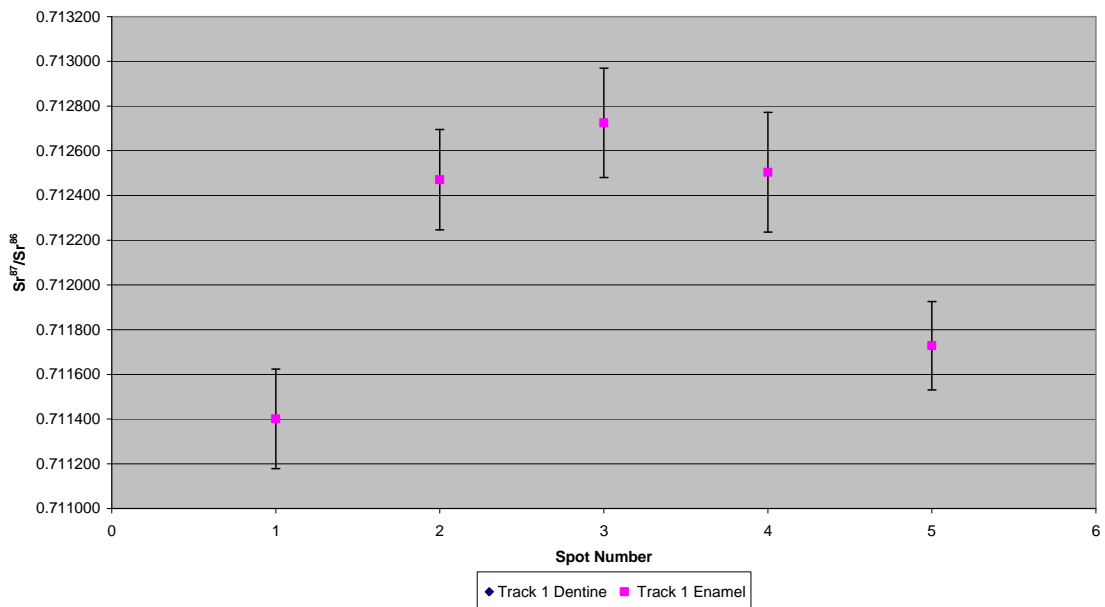


Figure A3.110 Detailed LA-MC-ICPMS Uncorrected Sr Isotope Results, Sample M006, Bovid, Bouffia 118: Layer 1, La Chapelle-aux-Saints

Sample M006, Corrected Sr Values, La Chapelle-aux-Saints, France

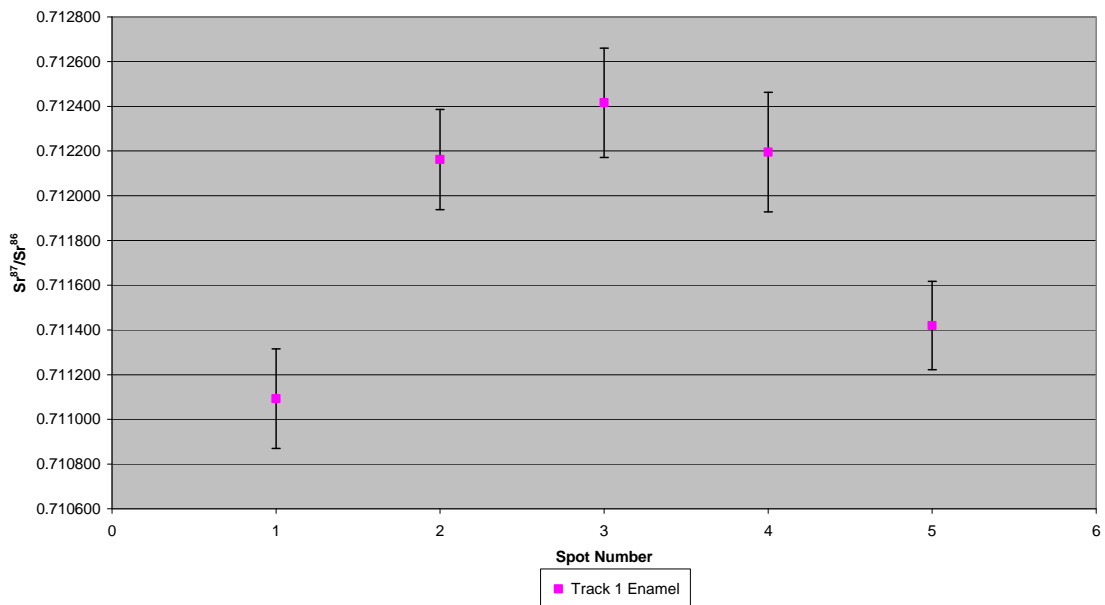


Figure A3.111 Detailed LA-MC-ICPMS Corrected Sr Isotope Results, Sample M006, Bovid, Bouffia 118: Layer 1, La Chapelle-aux-Saints

Sample M007, a bovid upper second premolar from layer 1 from the bouffia 118 section of La Chapelle-aux-Saints shown in Figure A2.37, was analysed in 1 track consisting of 9 spots of enamel, shown in Figure A3.112. The strontium isotope results of this sample are summarised in Table 5.27 and Figure 5.16. The enamel of M007 has an average ^{88}Sr voltage of 0.734, a weighted average uncorrected $^{87}\text{Sr}/^{86}\text{Sr}$ value of 0.71523 ± 0.00075 , a weighted average corrected $^{87}\text{Sr}/^{86}\text{Sr}$ value of 0.71380 ± 0.00075 and a weighted average $^{84}\text{Sr}/^{86}\text{Sr}$ value of 0.05683 ± 0.00013 ($n=9$). Enamel values are in the range of 0.714578 to 0.718720 (uncorrected), as well as 0.713153 to 0.717295 (corrected), and are relatively homogeneous, with the exception of spots 2 and 3, which have an elevated $^{87}\text{Sr}/^{86}\text{Sr}$ composition. Detailed values for enamel for sample M007 are shown in Table A3.73, Figure A3.113 and Figure A3.114.

The enamel of this sample has 2 $^{87}\text{Sr}/^{86}\text{Sr}$ domains. The first contains spots 1 and 4 to 9, and has a range of 0.714578 to 0.715076 (uncorrected) and 0.713153 to 0.713642 (corrected). The mapping sample that corresponds best to this uncorrected domain is P38P, which has a value of 0.715361 ± 0.000018 . Unfortunately, this location is more than 320 km to the east of La Chapelle-aux-Saints. A more parsimonious location for this sample may be suggested by the

value of 0.714131 ± 0.000015 from location FS046-S1, a floodplain of a small stream adjacent to the archaeological site. While the mapping value from this site is lower than the enamel domain from sample M007, it drains significantly more radiogenic regions to the east and north (up to 0.725528 ± 0.000017 at FS055-S2), suggesting that floodplain sediments upstream of FS046-S1 may have elevated $^{87}\text{Sr}/^{86}\text{Sr}$ values. The corrected domain comprising these spots does not correspond to any mapping values; however, it may reflect floodplain values from the Dordogne river, which locally include values such as 0.713071 ± 0.000011 (FS059-S1) and 0.713096 ± 0.000014 (FS035-S1) which outcrops within 3.9 km of the site. Spots 2 and 3 have significantly elevated $^{87}\text{Sr}/^{86}\text{Sr}$ values of 0.718720 ± 0.000613 and 0.716440 ± 0.000378 (uncorrected) and 0.717295 ± 0.000613 and 0.715015 ± 0.000378 (corrected). The uncorrected value of spot 2 is within 2σ error of mapping sample FS053-S1 with a value of 0.719269 ± 0.000027 , which is located within a Cambrian sedimentary package less than 10 km north-north-west of La Chapelle-aux-Saints. The corrected value of spot 2 corresponds with mapping sample FS067-S1 (0.717422 ± 0.00001) from a Carboniferous monzogranite/granodiorite outcropping approximately 32 km to the east. The uncorrected value of spot 3 correlates to a value of 0.716805 ± 0.000038 from location FS041-S1, which is located less than 1.5 km from the site nominally within a Lower Jurassic carbonate package. Examination of the detailed geological map (Astruc and Lefavrais-Raymond 1996) shows that this location is within an area of alluvial sediment and so may reflect a contribution not related to the local bedrock. The corrected value from spot 3 corresponds to the value of P38P located within a Jurassic sedimentary/metamorphic unit outcropping within approximately 280 km east of the site and location P8P from a monzogranite/granodiorite located approximately 190 km east of the site. Of these values, the $^{87}\text{Sr}/^{86}\text{Sr}$ seems more credible, as the value from P38P is very elevated for a principally carbonate unit. The unit containing P8P outcrops within 32 km of the archaeological site. The heterogeneity of the enamel strontium isotope values probably reflects a sample mobile during amelogenesis.

Enamel from sample M007, summarised in Table 5.20 and Table A3.25, has a mean strontium concentration of 167 ppm and a uranium concentration of 0 ppm. These values suggest that the sample has not been subject to post-burial diagenesis; however, its strontium concentration is lower than some other samples and so a higher C+P+O interference may exist. $^{84}\text{Sr}/^{86}\text{Sr}$ values for this sample are slightly elevated, with a weighted average of 0.05683 ± 0.00013 .



Figure A3.112 LA-MC-ICPMS Track for Sample M007, Bovid, Bouffia 118: Layer 1, La Chapelle-aux-Saints

Sample	Material	Track	Point	^{88}Sr Volts	$^{84}\text{Sr}/^{86}\text{Sr}$	$^{84}\text{Sr}/^{86}\text{Sr} 2\sigma$ Error	Corrected $^{87}\text{Sr}/^{86}\text{Sr}$	$^{87}\text{Sr}/^{86}\text{Sr} 2\sigma$ Error
M007	Enamel	1	1	0.881	0.057011	0.000233	0.715076	0.713651
M007	Enamel	1	2	0.728	0.057045	0.000277	0.718720	0.717295
M007	Enamel	1	3	0.750	0.057000	0.000295	0.716440	0.715015
M007	Enamel	1	4	0.703	0.056670	0.000242	0.715067	0.713642
M007	Enamel	1	5	0.697	0.056695	0.000265	0.714911	0.713486
M007	Enamel	1	6	0.706	0.056956	0.000291	0.714971	0.713546
M007	Enamel	1	7	0.706	0.056721	0.000290	0.714985	0.713560
M007	Enamel	1	8	0.722	0.056743	0.000293	0.714744	0.713319
M007	Enamel	1	9	0.710	0.056669	0.000232	0.714578	0.713153

Table A3.73 Detailed LA-MC-ICPMS Sr Isotope Results for Dentine and Enamel, Sample M007, Bovid, Bouffia 118: Layer 1, La Chapelle-aux-Saints

Sample M007, La Chapelle-aux-Saints, France

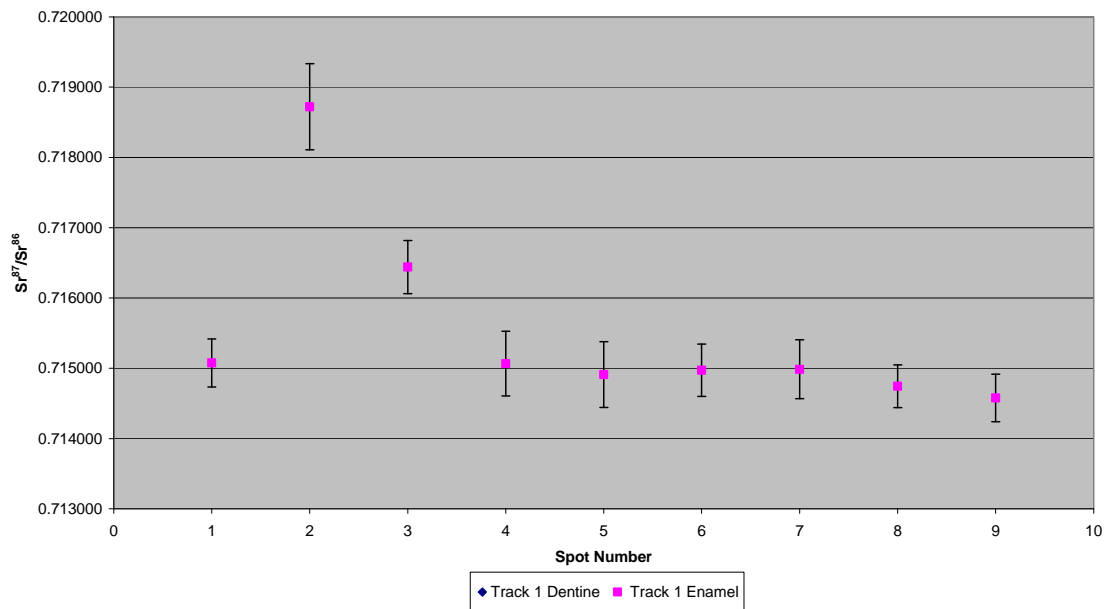


Figure A3.113 Detailed LA-MC-ICPMS Uncorrected Sr Isotope Results, Sample M007, Bovid, Bouffia 118: Layer 1, La Chapelle-aux-Saints

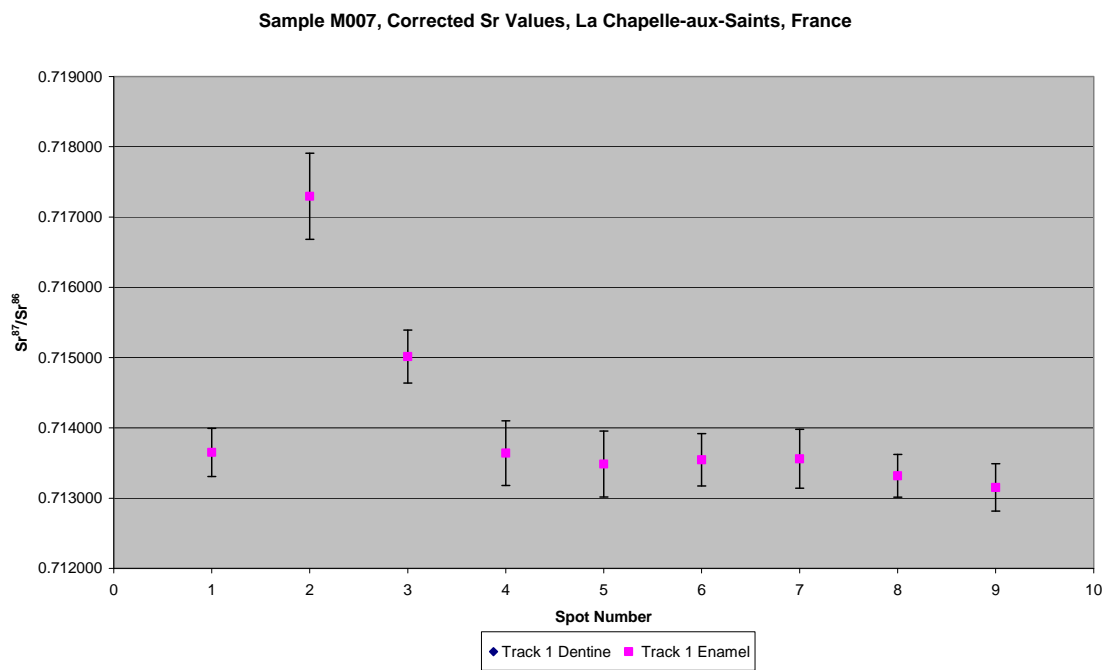


Figure A3.114 Detailed LA-MC-ICPMS Corrected Sr Isotope Results, Sample M007, Bovid, Bouffia 118: Layer 1, La Chapelle-aux-Saints

Sample M008, a bovid upper third premolar from layer 1 from the bouffia 118 section of La Chapelle-aux-Saints shown in Figure A2.38, was analysed in 2 tracks, with the first consisting of 2 spots of enamel and 4 spots of dentine and the second consisting of 6 spots of enamel in 2 discontinuous sections and 6 spots of dentine in between, shown in Figure A3.115. The strontium isotope results of sample M008 are summarised in Table 5.27 and Figure 5.16. The enamel spots of track 1 have an average ^{88}Sr voltage of 1.339, a weighted average uncorrected $^{87}\text{Sr}/^{86}\text{Sr}$ value of 0.71346 ± 0.00023 , a weighted average corrected $^{87}\text{Sr}/^{86}\text{Sr}$ value of 0.71305 ± 0.00023 and a weighted average $^{84}\text{Sr}/^{86}\text{Sr}$ value of 0.056729 ± 0.000098 ($n=2$). The dentine spots of track 1 have an average ^{88}Sr voltage of 1.487, a weighted average uncorrected $^{87}\text{Sr}/^{86}\text{Sr}$ value of 0.7135 ± 0.0023 , a weighted average corrected $^{87}\text{Sr}/^{86}\text{Sr}$ value of 0.71310 ± 0.0023 and a weighted average $^{84}\text{Sr}/^{86}\text{Sr}$ value of 0.056658 ± 0.000082 ($n=4$). The enamel spots of track 2 have an average ^{88}Sr voltage of 1.163, a weighted average uncorrected $^{87}\text{Sr}/^{86}\text{Sr}$ value of 0.7135 ± 0.0021 , a weighted average corrected $^{87}\text{Sr}/^{86}\text{Sr}$ value of 0.71290 ± 0.0021 and a weighted average $^{84}\text{Sr}/^{86}\text{Sr}$ value of 0.05665 ± 0.00011 ($n=6$). The dentine spots of track 2 have an average ^{88}Sr voltage of 1.330, a weighted average uncorrected $^{87}\text{Sr}/^{86}\text{Sr}$ value of 0.71349 ± 0.00047 , a weighted average corrected $^{87}\text{Sr}/^{86}\text{Sr}$ value of 0.71311 ± 0.00047 and a weighted average $^{84}\text{Sr}/^{86}\text{Sr}$ value of 0.056603 ± 0.000060 ($n=6$). Enamel values of track 1 are extremely homogeneous, with values of 0.713453 and 0.713475 (uncorrected), as well as 0.713035 and 0.713058 (corrected). Enamel values of track 2 are 0.712815 to 0.743104 (uncorrected), as well as 0.712242 to 0.742531 (corrected), and are extremely homogeneous, with the exception of spots 1 and 12. Dentine values of track 2 are 0.713076 to 0.714701 and are relatively homogeneous, with the exception of spot 5. Detailed values for enamel for sample M008 are shown in Table A3.74, Figure A3.116 and Figure A3.117.

The majority of enamel $^{87}\text{Sr}/^{86}\text{Sr}$ spots from this sample are in the range of 0.712815 ± 0.000210 to 0.713475 ± 0.000327 (uncorrected) and 0.712242 ± 0.000210 to 0.713058 ± 0.000327 (uncorrected), with the exception of outlying values on the edges of enamel in track 2. The domain containing most of the spots has a weighted average of 0.71316 ± 0.00035 (uncorrected) and 0.71263

± 0.00042 (corrected). The uncorrected value corresponds to the $^{87}\text{Sr}/^{86}\text{Sr}$ ratio of 0.713071 ± 0.000011 obtained from FS059-S1 located in a Cambrian-Ordovician anatetic orthogneiss. As discussed above with reference to sample 593, the strontium isotope composition of this location probably reflects floodplain sediments from the Dordogne river rather than the local bedrock. The corrected value for this domain does not correspond to any mapping sample in this study.

Both the corrected and uncorrected values from spots 1, 11 and 12 from track 2 do not have exactly corresponding values with mapping samples analysed within this study; however, they are within the range of $^{87}\text{Sr}/^{86}\text{Sr}$ ratios obtained in this (e.g., FS063-S1: 0.754291 ± 0.000026 and FS065-S1: 0.783684 ± 0.000041) and other investigations (Couturié and Vachette-Caen 1980; Downes and Duthou 1988). This may suggest that this specimen was mobile from 1 of these areas towards a less radiogenic province during amelogenesis, creating an intermediate strontium isotope value. More likely is that the 2 spots on the outside of track 2 (and to a lesser extent on spot 11) are located somewhat off of the flat analysis surface causing the laser to become unfocused, leading to variations in the particle size of the ablated material and, hence, possibly erroneous isotope values (Jackson and Günther 2003). This hypothesis is supported by the image of the sample after analysis (Figure A3.115), which shows that these 3 analysis spots appear somewhat off the edge of the sample. Excluding the outlying spots, the enamel $^{87}\text{Sr}/^{86}\text{Sr}$ is relatively homogenous, suggesting an individual not mobile during amelogenesis. Dentine values for track 1 and track 2 are relatively and somewhat heterogeneous, respectively, suggesting a complicated regime of post-burial diagenesis.

Enamel and dentine element concentrations of M008, summarised in Table 5.20 and Table A3.26, have relatively high strontium values with a mean of 293 ppm for enamel and 275 ppm for dentine. Uranium concentrations are very heterogeneous, with a value of 1 ppm for enamel and 55 ppm for dentine, which suggests that the dentine was probably subject to post-burial diagenesis.

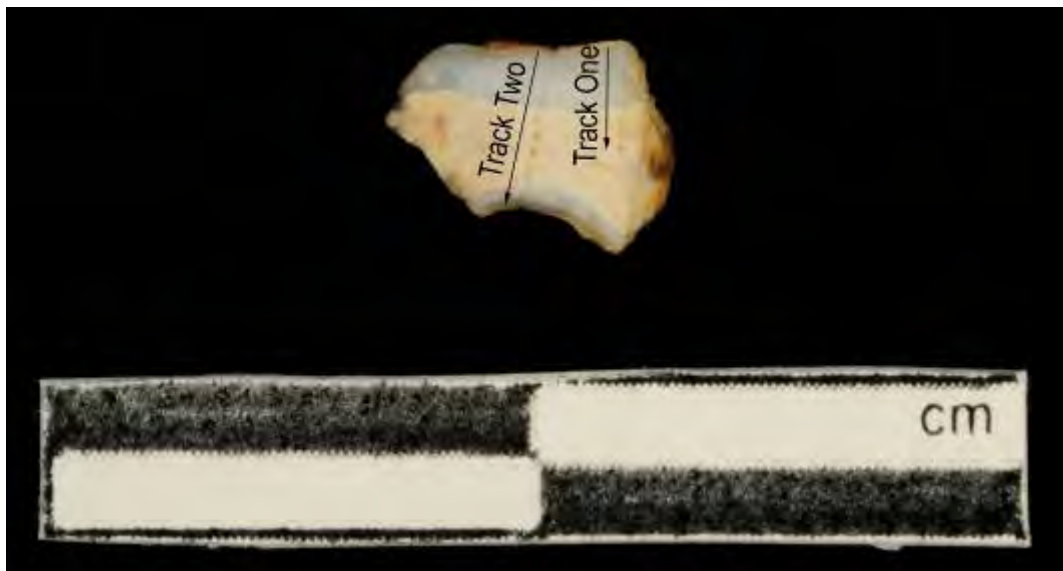


Figure A3.115 LA-MC-ICPMS Track for Sample M008, Bovid, Bouffia 118: Layer 1, La Chapelle-aux-Saints

Sample	Material	Track	Point	^{88}Sr Volts	$^{84}\text{Sr}/^{86}\text{Sr}$	Corrected $^{87}\text{Sr}/^{86}\text{Sr}$	$^{87}\text{Sr}/^{86}\text{Sr} 2\sigma$
					Error		Error
M008	Enamel	1	1	1.227	0.056661	0.000170	0.713453
M008	Enamel	1	2	1.452	0.056765	0.000124	0.713475
M008	Dentine	1	3	1.488	0.056633	0.000207	0.713700
M008	Dentine	1	4	1.654	0.056679	0.000158	0.711623
M008	Dentine	1	5	1.462	0.056600	0.000158	0.714382
M008	Dentine	1	6	1.343	0.056712	0.000161	0.714804
M008	Enamel	2	1	1.027	0.056789	0.000165	0.743104
M008	Enamel	2	2	1.160	0.056684	0.000137	0.713343
M008	Enamel	2	3	1.361	0.056544	0.000132	0.713157
M008	Enamel	2	4	1.542	0.056697	0.000134	0.712815
M008	Dentine	2	5	1.417	0.056684	0.000120	0.714701
M008	Dentine	2	6	1.372	0.056617	0.000156	0.713541
M008	Dentine	2	7	1.362	0.056586	0.000149	0.713076
M008	Dentine	2	8	1.449	0.056521	0.000140	0.713385
M008	Dentine	2	9	1.061	0.056517	0.000235	0.713219
M008	Dentine	2	10	1.317	0.056610	0.000160	0.713750
M008	Enamel	2	11	1.025	0.056692	0.000243	0.715885
M008	Enamel	2	12	0.865	0.056487	0.000225	0.731907

Table A3.74 Detailed LA-MC-ICPMS Sr Isotope Results for Dentine and Enamel, Sample M008, Bovid, Bouffia 118: Layer 1, La Chapelle-aux-Saints

Sample M008, La Chapelle-aux-Saints, France

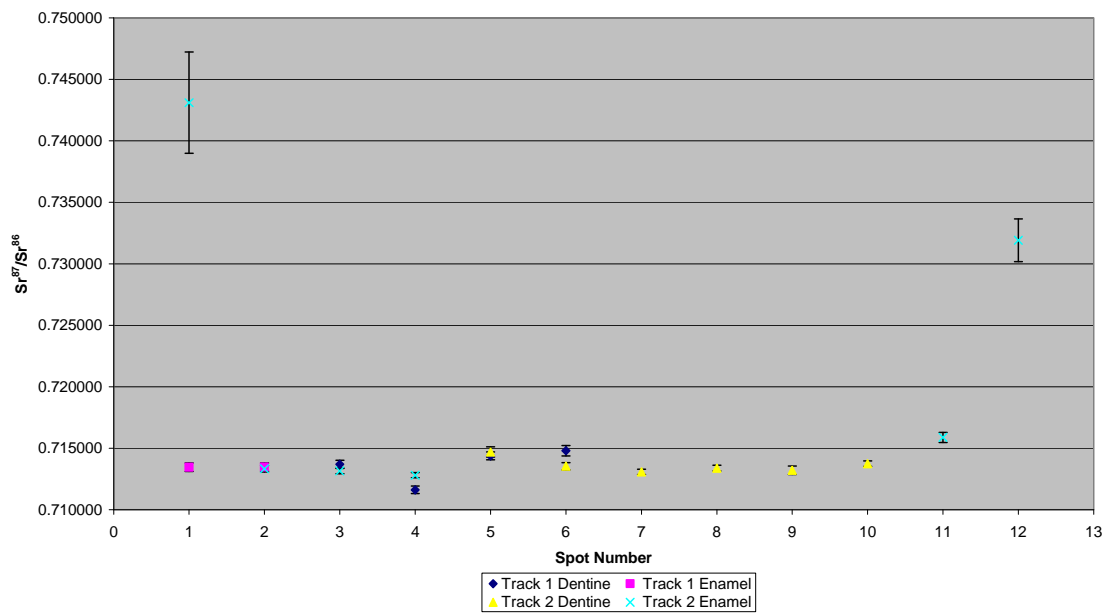


Figure A3.116 Detailed LA-MC-ICPMS Uncorrected Sr Isotope Results, Sample M008, Bovid, Bouffia 118: Layer 1, La Chapelle-aux-Saints

Sample M008, Corrected Sr Values, La Chapelle-aux-Saints, France

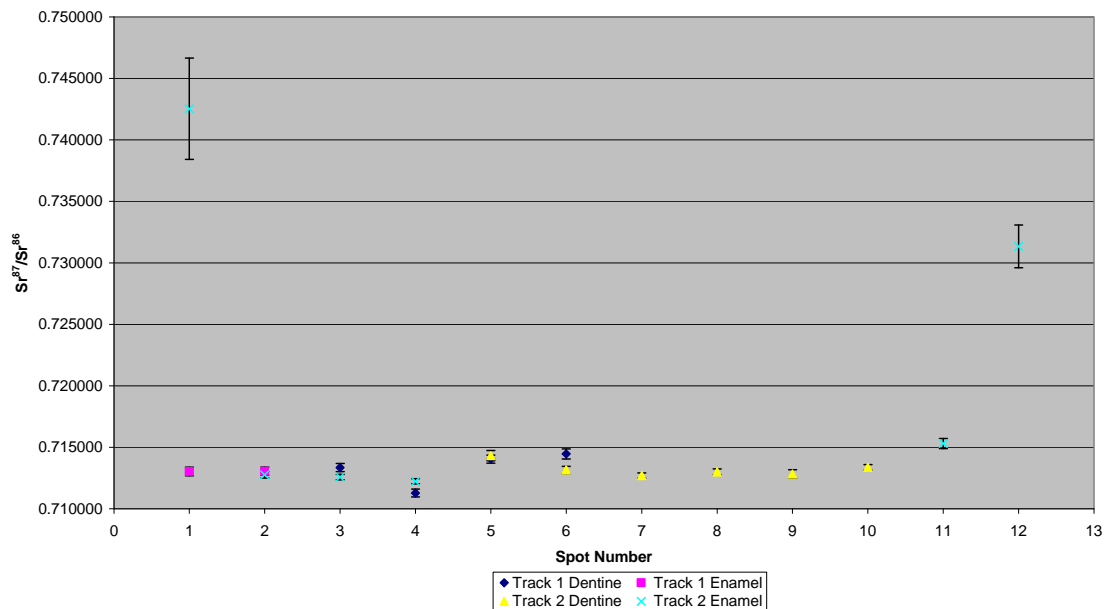


Figure A3.117 Detailed LA-MC-ICPMS Corrected Sr Isotope Results, Sample M008, Bovid, Bouffia 118: Layer 1, La Chapelle-aux-Saints

Sample M009, a bovid lower third premolar from layer 1 from the bouffia 118 section of La Chapelle-aux-Saints shown in Figure A2.39, was analysed in 3 tracks, with the first consisting of 2 spots of enamel and 13 spots of dentine, the second consisting of 5 spots of enamel and 5 spots of dentine and the third consisting of 2 spots of enamel and 3 spots of dentine, as summarised in Figure A3.118. The strontium isotope results of this sample are summarised in Table 5.27 and Figure 5.16. The enamel spots of track 1 have an average ^{88}Sr voltage of 0.809, a weighted average uncorrected $^{87}\text{Sr}/^{86}\text{Sr}$ value of 0.7136 ± 0.0042 , a weighted average corrected $^{87}\text{Sr}/^{86}\text{Sr}$ value of 0.71240 ± 0.0042 and a weighted average $^{84}\text{Sr}/^{86}\text{Sr}$ value of 0.0566 ± 0.0015 ($n=2$). The dentine spots of track 1 have an average ^{88}Sr voltage of 1.264, a weighted average uncorrected $^{87}\text{Sr}/^{86}\text{Sr}$ value of 0.7126 ± 0.0012 , a weighted average corrected $^{87}\text{Sr}/^{86}\text{Sr}$ value of 0.71210 ± 0.0012 and a weighted average $^{84}\text{Sr}/^{86}\text{Sr}$ value of 0.056571 ± 0.000053 ($n=13$). The enamel spots of track 2 have an average ^{88}Sr voltage of 0.617, a weighted average uncorrected $^{87}\text{Sr}/^{86}\text{Sr}$ value of 0.71368 ± 0.00072 , a weighted average corrected $^{87}\text{Sr}/^{86}\text{Sr}$ value of 0.71257 ± 0.00072 and a weighted average $^{84}\text{Sr}/^{86}\text{Sr}$ value of 0.05671 ± 0.00014 ($n=5$). The dentine spots of track 2 have an average ^{88}Sr voltage of 0.967, a weighted average uncorrected $^{87}\text{Sr}/^{86}\text{Sr}$ value of 0.71326 ± 0.00094 , a weighted average corrected $^{87}\text{Sr}/^{86}\text{Sr}$ value of 0.71281 ± 0.00094 and a weighted average $^{84}\text{Sr}/^{86}\text{Sr}$ value of 0.05661 ± 0.00010 ($n=5$). The enamel spots of track 3 have an average ^{88}Sr voltage of 0.664, a weighted average uncorrected $^{87}\text{Sr}/^{86}\text{Sr}$ value of 0.7137 ± 0.0050 , a weighted average corrected $^{87}\text{Sr}/^{86}\text{Sr}$ value of 0.71260 ± 0.0050 and a weighted average $^{84}\text{Sr}/^{86}\text{Sr}$ value of 0.05667 ± 0.00022 ($n=2$). The dentine spots of track 3 have an average ^{88}Sr voltage of 0.956, a weighted average uncorrected $^{87}\text{Sr}/^{86}\text{Sr}$ value of 0.7121 ± 0.0055 , a weighted average corrected $^{87}\text{Sr}/^{86}\text{Sr}$ value of 0.71170 ± 0.0055 and a weighted average $^{84}\text{Sr}/^{86}\text{Sr}$ value of 0.05659 ± 0.00013 ($n=3$). Enamel of sample M009 has $^{87}\text{Sr}/^{86}\text{Sr}$ values in track 1 of 0.713075 and 0.713778 (uncorrected), as well as 0.711969 and 0.712672 (corrected), in track 2 of 0.713164 to 0.714503 (uncorrected), as well as 0.712058 to 0.713397 (corrected), and in track 3 of 0.713445 and 0.714268 (uncorrected), as well as 0.712339 and 0.713162 (corrected).

Enamel values are relatively homogenous, all being within 2σ error. Dentine of sample M009 has $^{87}\text{Sr}/^{86}\text{Sr}$ values in track 1 of 0.709847 to 0.717940 (uncorrected) and 0.709391 to 0.717484 (corrected), in track 2 of 0.712541 to 0.714147 (uncorrected), as well as 0.712086 to 0.713692 (corrected), and in track 3 of 0.710246 to 0.714028 (uncorrected) and 0.709791 to 0.713573 (corrected). Dentine values are very heterogeneous, both within and between tracks. Detailed values for enamel for sample M009 are shown in Table A3.75, Figure A3.119 and Figure A3.120.

Enamel $^{87}\text{Sr}/^{86}\text{Sr}$ values for this sample range from 0.713075 ± 0.000408 to 0.714503 ± 0.000372 (uncorrected) and 0.711969 ± 0.000408 to 0.713397 ± 0.000372 (corrected). These values are outside of 2σ error within their respective analyses, suggesting that the sample was somewhat mobile during amelogenesis. Both uncorrected and corrected values correlate with mapping values from the Dordogne (e.g., FS056-S1 0.711984 ± 0.000018 , FS058-S1 0.713898 ± 0.000031 and FS059-S1 0.713071 ± 0.000011) and other floodplains (e.g., FS046-S1 0.714131 ± 0.000015) in the region, suggesting that this specimen lived relatively near the site of La Chapelle-aux-Saints. The floodplain from which sample FS046-S1 outcrops within 0.1 km of the archaeological site. The dentine of this sample is extremely heterogeneous, suggesting variable post-burial diagenesis.

Elemental concentrations for the 3 tracks of M009 are shown in Table 5.20 and Table A3.27. Strontium concentrations are moderate for enamel and slightly elevated for dentine. Uranium concentrations are 0 or 1 ppm for enamel, suggesting that these samples are probably free from post-burial diagenesis. Uranium concentrations are more elevated for dentine with mean values of 29, 28 and 24 ppm for tracks 1, 2 and 3, respectively. The weighted average value for $^{84}\text{Sr}/^{86}\text{Sr}$ is 0.056647 ± 0.000036 , which is slightly elevated compared to the ideal value.

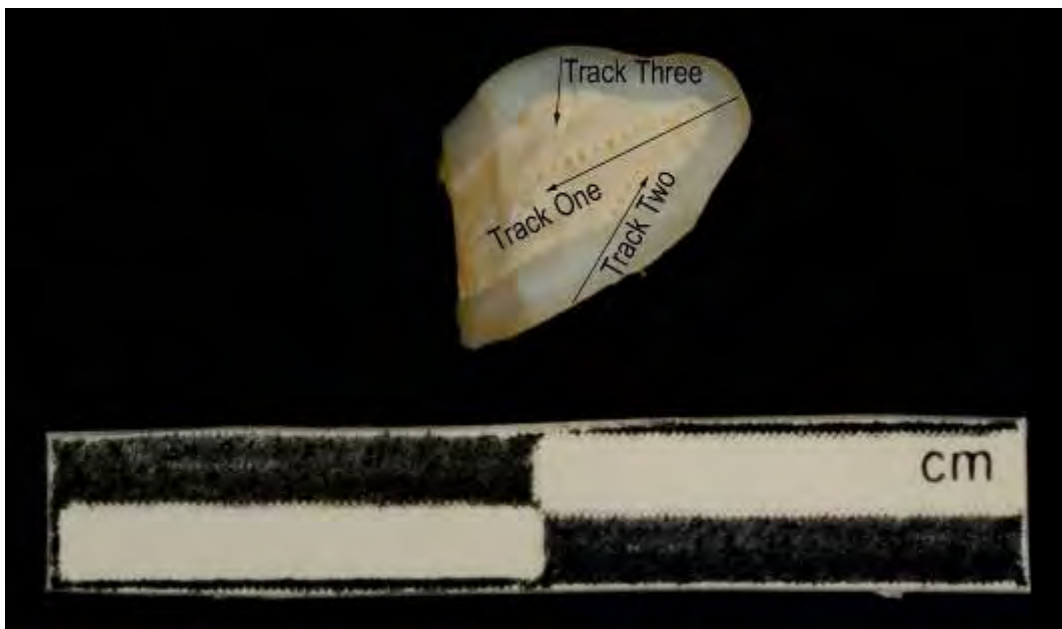


Figure A3.118 LA-MC-ICPMS Track for Sample M009, Bovid, Bouffia 118: Layer 1, La Chapelle-aux-Saints

Sample	Material	Track	Point	^{88}Sr Volts	$^{84}\text{Sr}/^{86}\text{Sr}$	$^{84}\text{Sr}/^{86}\text{Sr}$ 2 σ Error	$^{87}\text{Sr}/^{86}\text{Sr}$	Corrected $^{87}\text{Sr}/^{86}\text{Sr}$	$^{87}\text{Sr}/^{86}\text{Sr}$ 2 σ Error
M009	Enamel	1	1	0.836	0.056738	0.000282	0.713778	0.712672	0.000282
M009	Enamel	1	2	0.782	0.056494	0.000245	0.713075	0.711969	0.000408
M009	Dentine	1	3	1.129	0.056636	0.000204	0.714933	0.714478	0.000280
M009	Dentine	1	4	1.189	0.056710	0.000247	0.715518	0.715063	0.000420
M009	Dentine	1	5						
M009	Dentine	1	6	1.068	0.056437	0.000166	0.710690	0.710235	0.000223
M009	Dentine	1	7	1.320	0.056514	0.000134	0.712538	0.712082	0.000261
M009	Dentine	1	8	1.212	0.056465	0.000182	0.713072	0.712616	0.000316
M009	Dentine	1	9	1.218	0.056600	0.000202	0.717940	0.717484	0.000357
M009	Dentine	1	10	1.103	0.056770	0.000216	0.712649	0.712193	0.000297
M009	Dentine	1	11	1.186	0.056699	0.000147	0.712801	0.712345	0.000245
M009	Dentine	1	12	1.0476	0.056564	0.000206	0.711798	0.711342	0.000317
M009	Dentine	1	13						
M009	Dentine	1	14	1.268	0.056544	0.000147	0.713611	0.713155	0.000249
M009	Dentine	1	15	1.333	0.056627	0.000159	0.713959	0.713504	0.000196
M009	Dentine	1	16	1.594	0.056509	0.000114	0.712934	0.712479	0.000154
M009	Dentine	1	17	1.769	0.056578	0.000116	0.709847	0.709391	0.000152
M009	Enamel	2	1	0.507	0.056660	0.000478	0.713594	0.712488	0.000523
M009	Enamel	2	2	0.527	0.057107	0.000477	0.713956	0.712850	0.000509
M009	Enamel	2	3	0.611	0.056729	0.000290	0.714503	0.713397	0.000372
M009	Enamel	2	4	0.662	0.056593	0.000281	0.713164	0.712058	0.000485
M009	Enamel	2	5						
M009	Enamel	2	6	0.777	0.056687	0.000271	0.713281	0.712175	0.000296
M009	Dentine	2	7	0.682	0.056729	0.000309	0.714060	0.713605	0.000390
M009	Dentine	2	8	0.937	0.056514	0.000249	0.714147	0.713692	0.000258
M009	Dentine	2	9	1.071	0.056697	0.000189	0.713166	0.712710	0.000319
M009	Dentine	2	10	1.043	0.056442	0.000220	0.712674	0.712218	0.000222
M009	Dentine	2	11	1.104	0.056658	0.000220	0.712541	0.712086	0.000357
M009	Enamel	3	1	0.576	0.056816	0.000368	0.714268	0.713162	0.000474
M009	Enamel	3	2	0.751	0.056587	0.000284	0.713445	0.712339	0.000359
M009	Dentine	3	3	0.794	0.056706	0.000298	0.713621	0.713166	0.000319
M009	Dentine	3	4	1.001	0.056471	0.000247	0.714028	0.713573	0.000282
M009	Dentine	3	5	1.072	0.056610	0.000178	0.710246	0.709791	0.000221

Table A3.75 Detailed LA-MC-ICPMS Sr Isotope Results for Dentine and Enamel, Sample M009, Bovid, Bouffia 118: Layer 1, La Chapelle-aux-Saints

Sample M009, La Chapelle-aux-Saints, France

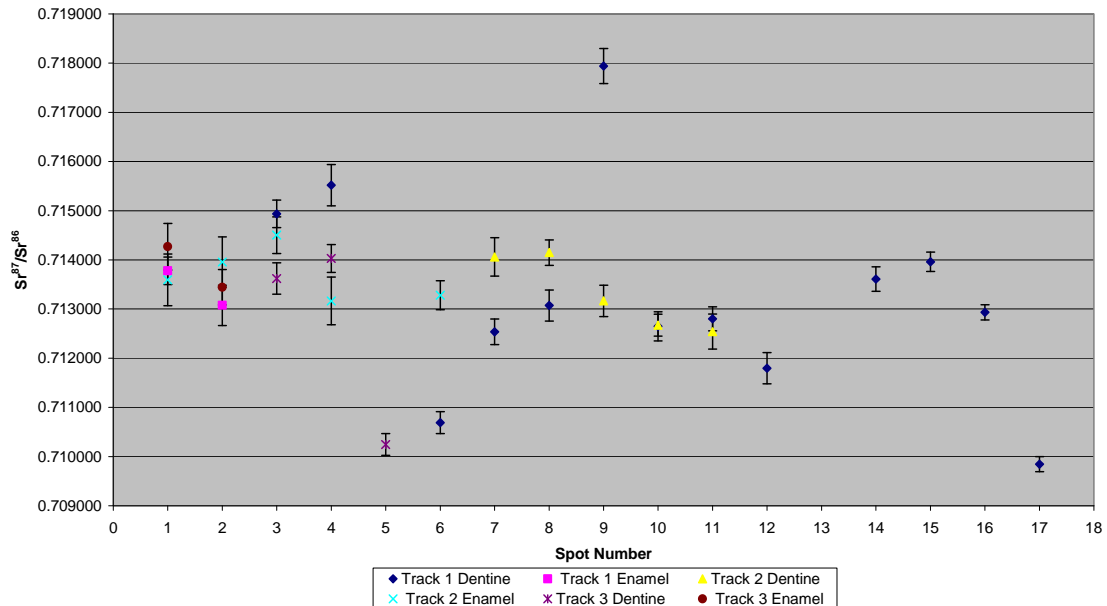


Figure A3.119 Detailed LA-MC-ICPMS Uncorrected Sr Isotope Results, Sample M009, Bovid, Bouffia 118: Layer 1, La Chapelle-aux-Saints

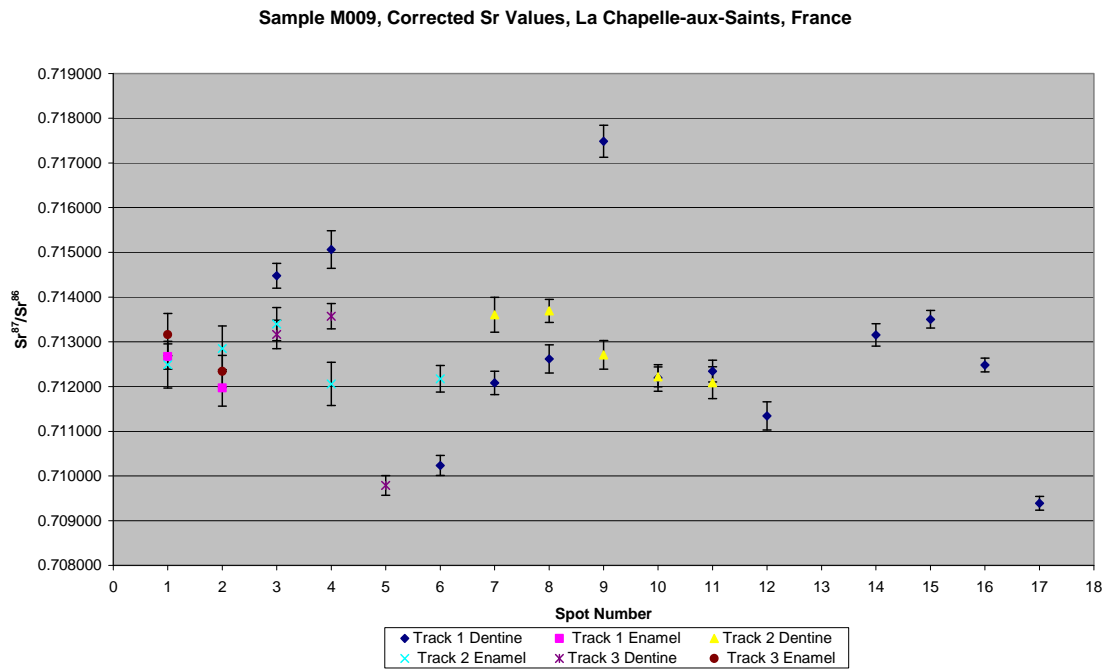


Figure A3.120 Detailed LA-MC-ICPMS Corrected Sr Isotope Results, Sample M009, Bovid, Bouffia 118: Layer 1, La Chapelle-aux-Saints

Sample M010, a bovid upper second premolar from layer 1 from the bouffia 118 section of La Chapelle-aux-Saints shown in Figure A2.40, was analysed in 2 tracks, with the first containing 3 spots of enamel and 1 spot of dentine and the second containing 2 spots of enamel shown in Figure A3.121. The results from this sample are summarised in Table 5.27 and Figure 5.16. The enamel spots of track 1 have an average ^{88}Sr voltage of 0.751, a weighted average uncorrected $^{87}\text{Sr}/^{86}\text{Sr}$ value of 0.7141 ± 0.0020 , a weighted average corrected $^{87}\text{Sr}/^{86}\text{Sr}$ value of 0.71300 ± 0.0020 and a weighted average $^{84}\text{Sr}/^{86}\text{Sr}$ value of 0.05660 ± 0.00016 ($n=3$). The dentine spots of track 1 have an average ^{88}Sr voltage of 1.322, a weighted average uncorrected $^{87}\text{Sr}/^{86}\text{Sr}$ value of 0.713259 ± 0.000249 , a weighted average corrected $^{87}\text{Sr}/^{86}\text{Sr}$ value of 0.71297 ± 0.000249 and a weighted average $^{84}\text{Sr}/^{86}\text{Sr}$ value of 0.056560 ± 0.000125 ($n=1$). The enamel spots of track 2 have an average ^{88}Sr voltage of 0.581, a weighted average uncorrected $^{87}\text{Sr}/^{86}\text{Sr}$ value of 0.7139 ± 0.0094 , a weighted average corrected $^{87}\text{Sr}/^{86}\text{Sr}$ value of 0.71290 ± 0.0094 and a weighted average $^{84}\text{Sr}/^{86}\text{Sr}$ value of 0.05643 ± 0.00027 ($n=2$). Enamel values for track 1 are in the range of 0.713475 to 0.715025 (uncorrected), as well as 0.712417 to 0.713967 (corrected), and are 0.713490 and 0.715187 (uncorrected), as well as 0.714128 and 0.712431 (corrected), for track 2. Dentine has a value of 0.713259 (corrected), and 0.712978 (uncorrected), with 4 dentine points being excluded from consideration because of very unstable $^{87}\text{Sr}/^{86}\text{Sr}$ values. Spots 1 and 2 have excellent agreement between strontium isotope values between tracks 1 and 2, however, are significantly different from each other. Spot 3 from track 1 is also heterogeneous compared to the other enamel spots. Detailed values for enamel for sample M010 are shown in Table A3.76, Figure A3.122 and Figure A3.123.

The enamel values of this sample are in the range of 0.713490 ± 0.000324 to 0.715187 ± 0.000553 (uncorrected) and 0.712431 ± 0.000324 to 0.714128 ± 0.000553 (corrected), suggesting an individual mobile during amelogenesis. Spots 1 from track 1 and 2 and spot 3 from track 1 are within 2σ error and have an overall weighted average value of uncorrected value of 0.71485 ± 0.00090 and a corrected value of 0.71379 ± 0.00090 . The uncorrected value does not correspond to any mapping results from this survey; however, the corrected value corresponds with the Dordogne floodplain value from FS058-S1, located

approximately 10 km east-north-east of La Chapelle-aux-Saints. This unit outcrops within 3.9 km of the archaeological site. The values of spot 2 from tracks 1 and 2 has a weighted average uncorrected value of 0.71348 ± 0.00022 , which are intermediate values between 2 adjacent Dordogne floodplain samples (FS058-S1 and FS059-S1). In the absence of any other mapping sample with a suitable value, this seems the most likely source of this value. The corrected value of spot 2 from tracks 1 and 2 has a value of 0.71242 ± 0.00022 , which corresponds to the value of metamorphic rocks outcropping within 8.5 km of the site, represented by mapping sample FS054-S1. The close match between spots 1 and 2 between tracks 1 and 2 in an orientation perpendicular to the enamel growth direction suggests lateral continuity in enamel maturation times. The enamel values are, with the exception of spot 2 from track 1 and track 2, distinct from the dentine value for this sample.

Elemental concentrations for M010, shown in Table 5.20 and Table A3.28, are considerably higher for dentine than for enamel. The uranium and thorium concentrations for this sample appear to be erroneous, with some negative values being returned from this analysis. The weighted average $^{84}\text{Sr}/^{86}\text{Sr}$ value for all spots in this sample is 0.056558 ± 0.000091 , suggesting that the $^{87}\text{Sr}/^{86}\text{Sr}$ values for this sample are robust.

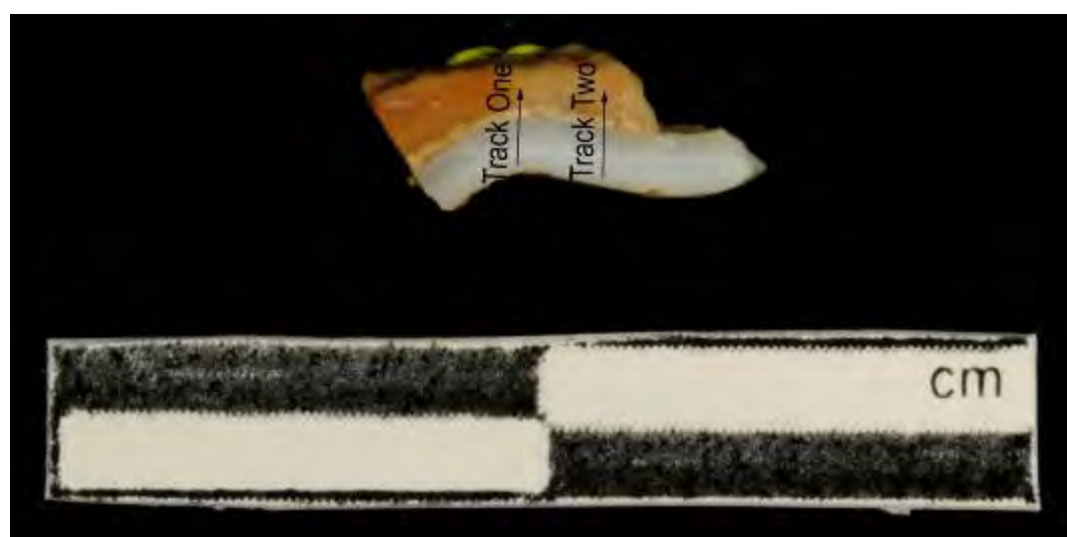


Figure A3.121 LA-MC-ICPMS Track for Sample M010, Bovid, Bouffia 118: Layer 1, La Chapelle-aux-Saints

Sample	Material	Track	Point	^{88}Sr Volts	$^{84}\text{Sr}/^{86}\text{Sr}$	$^{84}\text{Sr}/^{86}\text{Sr} 2\sigma$ Error	Corrected $^{87}\text{Sr}/^{86}\text{Sr}$	$^{87}\text{Sr}/^{86}\text{Sr}$ 2 σ Error
M010	Enamel	1	1	0.512	0.056928	0.000587	0.715025	0.713967
M010	Enamel	1	2	0.712	0.056643	0.000294	0.713475	0.712417
M010	Enamel	1	3	1.028	0.056539	0.000217	0.714510	0.713452
M010	Dentine	1	4					
M010	Dentine	1	5	1.322	0.056560	0.000125	0.713259	0.712978
M010	Enamel	2	1	0.510	0.056597	0.000497	0.715187	0.714128
M010	Enamel	2	2	0.653	0.056359	0.000331	0.713490	0.712431
M010	Dentine	2	3					
M010	Dentine	2	4					
M010	Dentine	2	5					

Table A3.76 Detailed LA-MC-ICPMS Sr Isotope Results for Dentine and Enamel, Sample M010, Bovid, Bouffia 118: Layer 1, La Chapelle-aux-Saints

Sample M010, La Chapelle-aux-Saints, France

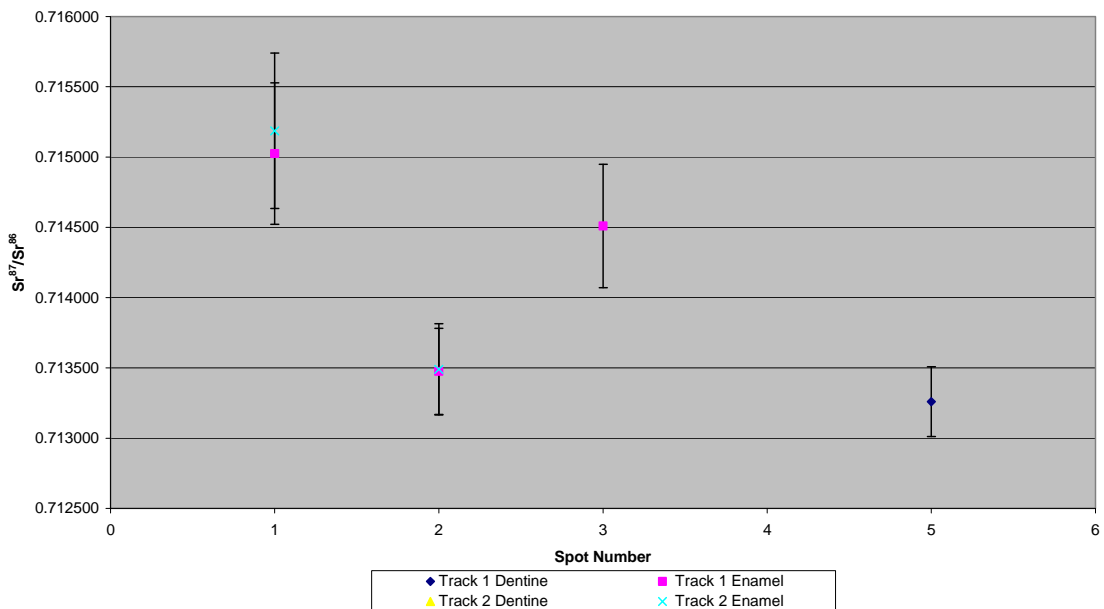


Figure A3.122 Detailed LA-MC-ICPMS Uncorrected Sr Isotope Results, Sample M010, Bovid, Bouffia 118: Layer 1, La Chapelle-aux-Saints

Sample M010, Corrected Sr Values, La Chapelle-aux-Saints, France

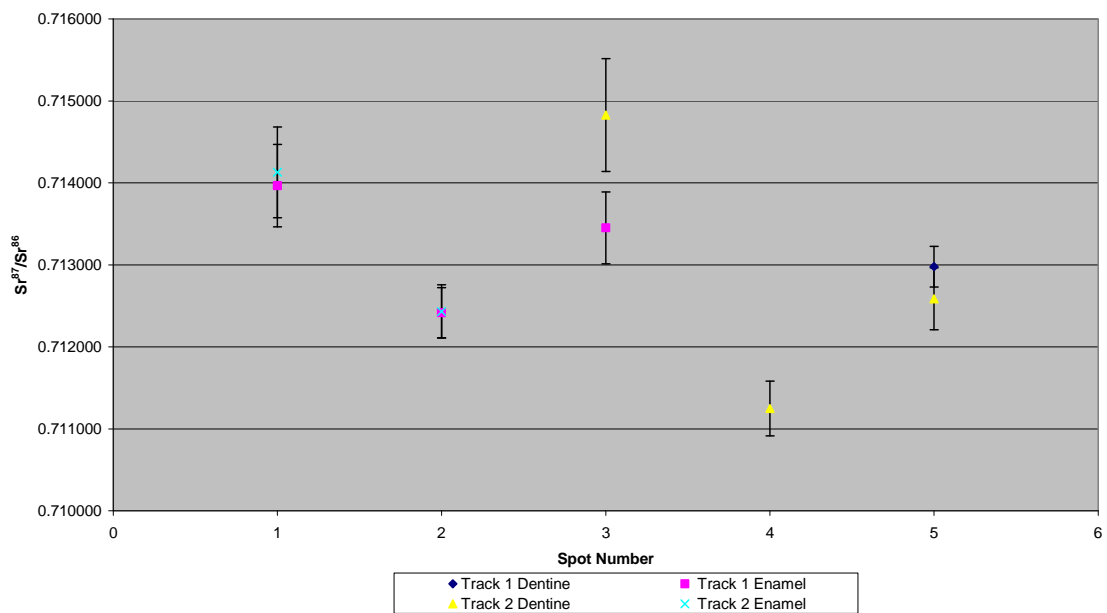


Figure A3.123 Detailed LA-MC-ICPMS Corrected Sr Isotope Results, Sample M010, Bovid, Bouffia 118: Layer 1, La Chapelle-aux-Saints

A3.2.3.2. Les Fieux

Sample M011, a horse from layer G7 of Les Fieux shown in Figure A2.41, was analysed in 1 track with 10 spots of enamel in 4 discontinuous sections and 27 spots of dentine in 5 discontinuous sections, shown in Figure A3.124. The results from this sample are summarised in Table 5.30 and Figure 5.18. The enamel spots have an average ^{88}Sr voltage of 0.502, a weighted average uncorrected $^{87}\text{Sr}/^{86}\text{Sr}$ value of 0.71137 ± 0.00074 , a weighted average corrected $^{87}\text{Sr}/^{86}\text{Sr}$ value of 0.70997 ± 0.00074 and a weighted average $^{84}\text{Sr}/^{86}\text{Sr}$ value of 0.05641 ± 0.00032 ($n=10$). The dentine spots have an average ^{88}Sr voltage of 0.650, a weighted average uncorrected $^{87}\text{Sr}/^{86}\text{Sr}$ value of 0.71075 ± 0.00038 , a weighted average corrected $^{87}\text{Sr}/^{86}\text{Sr}$ value of 0.71013 ± 0.00038 and a weighted average $^{84}\text{Sr}/^{86}\text{Sr}$ value of 0.056442 ± 0.000063 ($n=27$). Enamel values range from 0.710173 to 0.713859 (uncorrected), as well as 0.708773 to 0.713859 (corrected), and are very heterogeneous, with no systematic variation along the track. Dentine values range from 0.709682 to 0.713802 (uncorrected), as well as 0.709056 to 0.713176 (corrected), and are very heterogeneous, with no systematic variation along the track. Detailed values for enamel and dentine for sample M011 are shown in

Table A3.77, Figure A3.125 and Figure A3.126.

The enamel from this sample has very heterogeneous $^{87}\text{Sr}/^{86}\text{Sr}$ values in the range of 0.710173 ± 0.000420 to 0.713859 ± 0.000876 (uncorrected) and 0.708773 ± 0.000420 to 0.712459 ± 0.000876 (corrected), suggesting that this individual was mobile during amelogenesis. Enamel values do not vary in a systematic fashion, suggesting irregular vectors of enamel formation compared to the direction of the sample track. The lower end-member of the uncorrected range corresponds to the mapping value of 0.710762 ± 0.000031 from FS052-S1 located within a Lower Jurassic carbonate province, which outcrops within 3 km of Les Fieux. The entire uncorrected range corresponds with values from the Dordogne floodplain (including 0.709837 ± 0.000013 from FS043-S1, 0.713096 ± 0.000014 from FS035-S1, 0.713898 ± 0.000031 from FS058-S1). These uncorrected values suggest a sample mobile either between the area

local to the site and the nearby Dordogne floodplain or exclusively within the Dordogne floodplain. The lower range of the corrected range corresponds to mapping values, such as from FS049-S1, FS051-S1 and FS081-S1, from lower and upper Jurassic carbonates outcropping to the south through east of Les Fieux. The closest of these units outcrop within 2.8 km of the archaeological site. The upper end of the corrected range corresponds to the mapping value from metamorphic rocks (sampled by FS054-S1) which outcrop within 15 km of the site. The corrected values suggest a sample mobile between the carbonate province to the south and west of the site and the metamorphic province to the east and north of the site. No elemental concentrations were collected for this sample; however, the weighted average of $^{84}\text{Sr}/^{86}\text{Sr}$ values for enamel and dentine spots for this sample of 0.056438 ± 0.000077 suggests that the analysis is relatively robust.

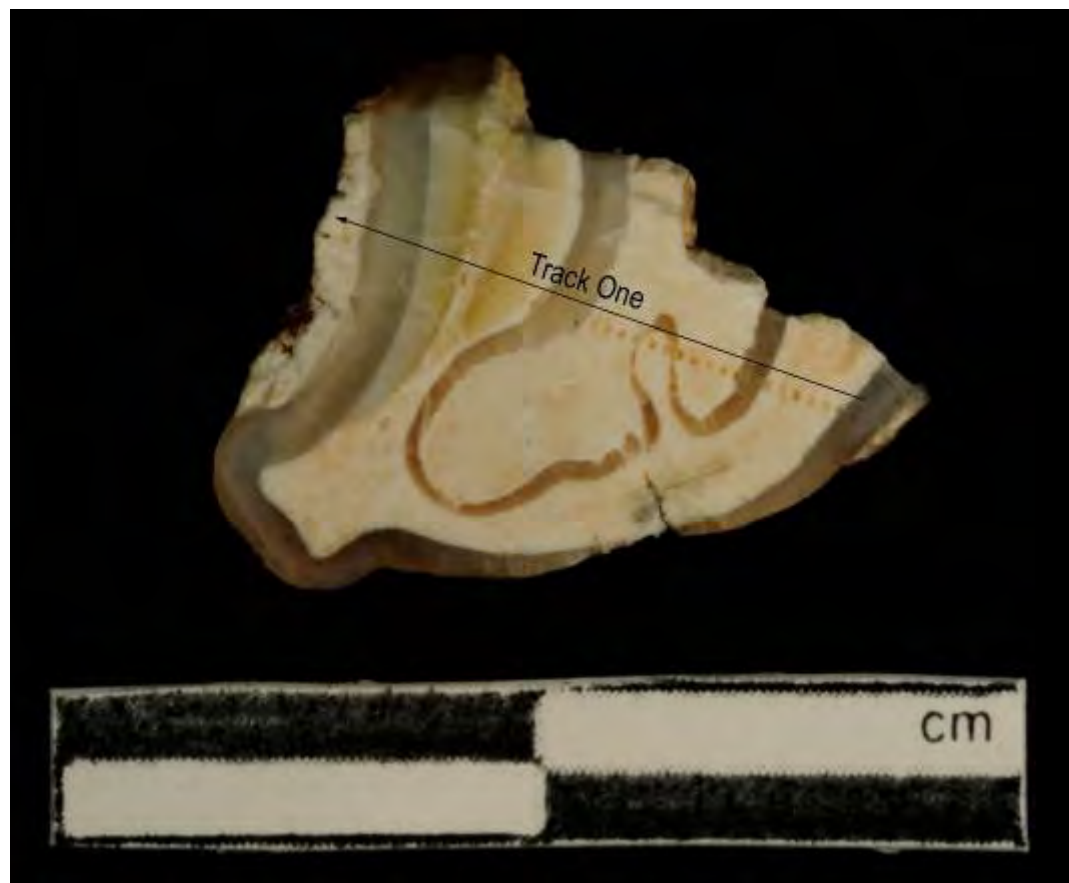


Figure A3.124 LA-MC-ICPMS Track for Sample M011, Horse, Layer G7, Les Fieux

Sample	Material	Track	Point	^{88}Sr Volts	$^{84}\text{Sr}/^{86}\text{Sr}$	$^{84}\text{Sr}/^{86}\text{Sr}$ 2σ Error	Corrected $^{87}\text{Sr}/^{86}\text{Sr}$	$^{87}\text{Sr}/^{86}\text{Sr}$	$^{87}\text{Sr}/^{86}\text{Sr}$ 2σ Error
M011	Enamel	1	1	0.337	0.056561	0.000647	0.711698	0.710298	0.000560
M011	Dentine	1	2	0.385	0.056606	0.000547	0.712258	0.711633	0.000852
M011	Dentine	1	3	0.742	0.056457	0.000359	0.712056	0.711430	0.000610
M011	Dentine	1	4	0.729	0.056317	0.000315	0.713620	0.712994	0.000667
M011	Dentine	1	5	0.594	0.056513	0.000302	0.710667	0.710042	0.000503
M011	Dentine	1	6	0.603	0.056355	0.000440	0.710644	0.710019	0.000495
M011	Dentine	1	7	0.625	0.056572	0.000362	0.711688	0.711062	0.000426
M011	Enamel	1	8	0.704	0.056208	0.000291	0.710849	0.709448	0.000322
M011	Dentine	1	9	0.423	0.056012	0.000494	0.712665	0.712039	0.000529
M011	Dentine	1	10	0.461	0.056087	0.000469	0.710393	0.709767	0.000715
M011	Dentine	1	11	0.863	0.056577	0.000257	0.710402	0.709776	0.000375
M011	Dentine	1	12	0.906	0.056488	0.000208	0.709735	0.709109	0.000373
M011	Dentine	1	13	0.855	0.056680	0.000253	0.709831	0.709205	0.000495
M011	Dentine	1	14	0.556	0.056315	0.000358	0.710994	0.710368	0.000378
M011	Dentine	1	15	0.797	0.056558	0.000285	0.710710	0.710084	0.000328
M011	Enamel	1	16	0.705	0.056454	0.000350	0.710173	0.708773	0.000420
M011	Dentine	1	17	0.583	0.056833	0.000378	0.711812	0.711186	0.000414
M011	Dentine	1	18	0.772	0.056466	0.000260	0.710159	0.709533	0.000409
M011	Dentine	1	19	0.869	0.056448	0.000290	0.709682	0.709056	0.000387
M011	Enamel	1	20	0.877	0.057754	0.000610	0.711139	0.709739	0.000410
M011	Enamel	1	21	0.386	0.056291	0.000977	0.713237	0.711837	0.000578
M011	Enamel	1	22	0.369	0.057019	0.000658	0.713859	0.712459	0.000876
M011	Dentine	1	23	0.394	0.056071	0.000520	0.712905	0.712279	0.000559
M011	Dentine	1	24	0.528	0.056244	0.000478	0.710730	0.710104	0.000438
M011	Dentine	1	25	0.764	0.056399	0.000326	0.710606	0.709980	0.000423
M011	Dentine	1	26	0.643	0.056521	0.000225	0.710284	0.709658	0.000540
M011	Dentine	1	27	0.833	0.056472	0.000292	0.710399	0.709774	0.000325
M011	Dentine	1	28	0.853	0.056318	0.000381	0.710443	0.709817	0.000516
M011	Dentine	1	29	0.613	0.056360	0.000502	0.709851	0.709225	0.000372
M011	Dentine	1	30	0.597	0.056294	0.000410	0.709945	0.709319	0.000500
M011	Dentine	1	31	0.532	0.056039	0.000386	0.710972	0.710346	0.000473
M011	Enamel	1	32	0.599	0.056175	0.000405	0.711051	0.709651	0.000464
M011	Enamel	1	33	0.420	0.056538	0.000530	0.712099	0.710699	0.000758
M011	Enamel	1	34	0.329	0.055824	0.000599	0.712235	0.710835	0.000730
M011	Enamel	1	35	0.293	0.056150	0.000769	0.713417	0.712016	0.001039
M011	Dentine	1	36	0.318	0.056178	0.000730	0.713802	0.713176	0.000690
M011	Dentine	1	37	0.709	0.056254	0.000328	0.710278	0.709652	0.000401

Table A3.77 Detailed LA-MC-ICPMS Sr Isotope Results for Dentine and Enamel, Sample M011, Horse, Layer G7, Les Fieux

Sample M011, Les Fieux, France

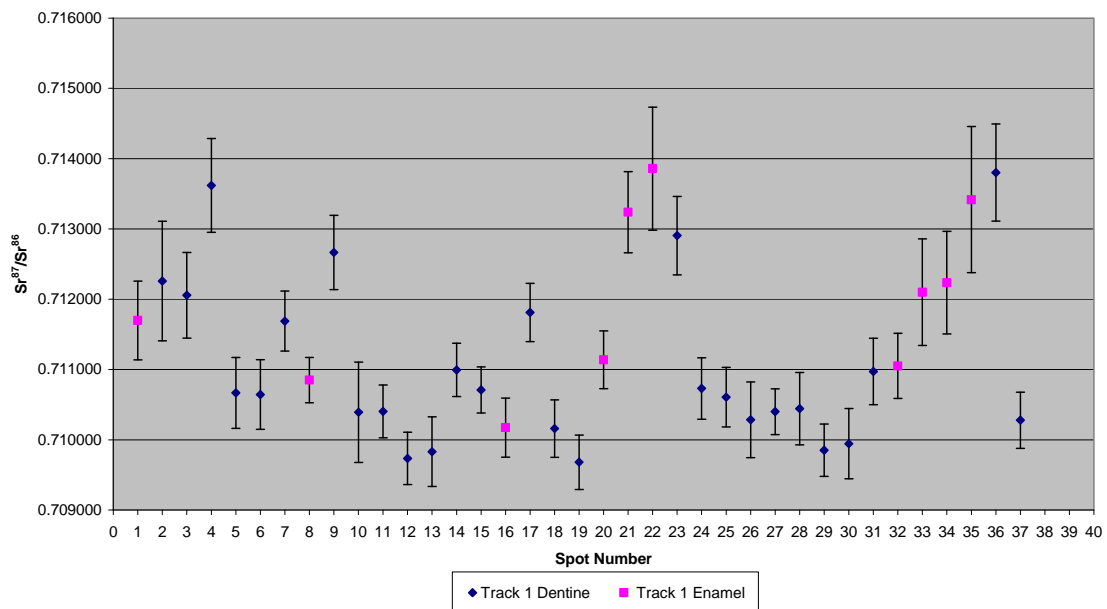


Figure A3.125 Detailed LA-MC-ICPMS Uncorrected Sr Isotope Results, Sample M011, Horse, Layer G7, Les Fieux

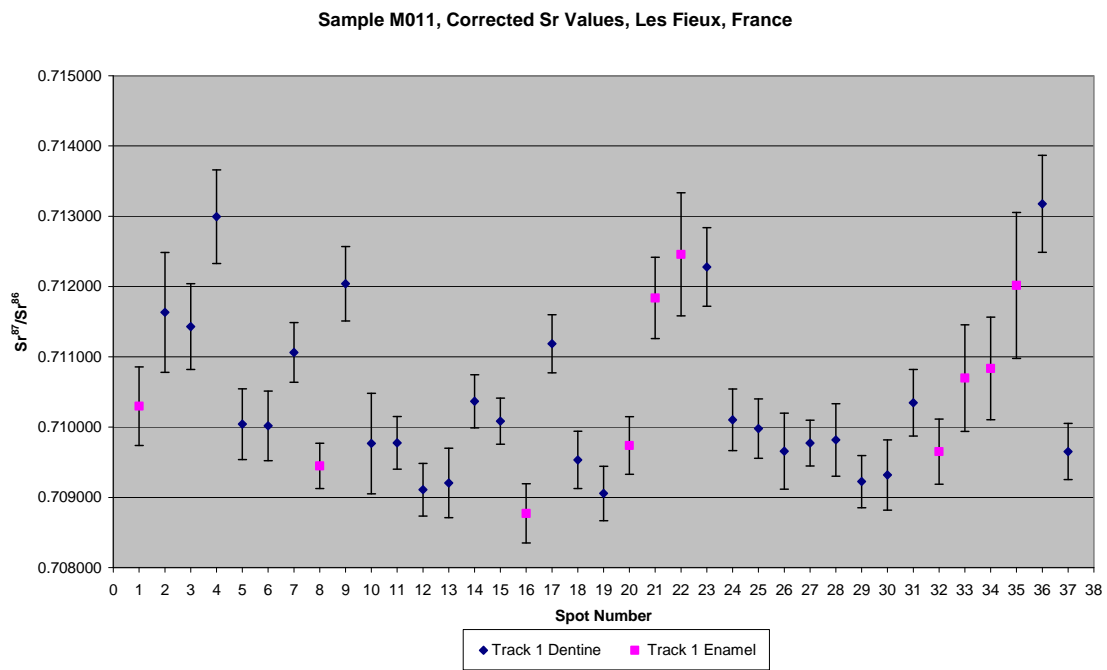


Figure A3.126 Detailed LA-MC-ICPMS Corrected Sr Isotope Results, Sample M011, Horse, Layer G7, Les Fieux

Sample M012, a horse from layer G7 of Les Fieux, was collected in 2 tracks, with the first containing 5 spots of enamel in 2 discontinuous sections and 11 spots of dentine in 2 discontinuous sections and the second containing 7 spots of enamel in 2 discontinuous sections and 9 spots of dentine in 2 discontinuous sections, shown in Figure A3.127. The results from this sample are summarised in Table 5.30 and Figure 5.18. The enamel spots of track 1 have an average ^{88}Sr voltage of 0.311, a weighted average uncorrected $^{87}\text{Sr}/^{86}\text{Sr}$ value of 0.71112 ± 0.00086 , a weighted average corrected $^{87}\text{Sr}/^{86}\text{Sr}$ value of 0.70833 ± 0.00086 and a weighted average $^{84}\text{Sr}/^{86}\text{Sr}$ value of 0.05661 ± 0.00055 ($n=5$). The dentine spots of track 1 have an average ^{88}Sr voltage of 0.596, a weighted average uncorrected $^{87}\text{Sr}/^{86}\text{Sr}$ value of 0.71142 ± 0.00079 , a weighted average corrected $^{87}\text{Sr}/^{86}\text{Sr}$ value of 0.71055 ± 0.00079 and a weighted average $^{84}\text{Sr}/^{86}\text{Sr}$ value of 0.056459 ± 0.000099 ($n=11$). The enamel spots of track 2 have an average ^{88}Sr voltage of 0.306, a weighted average uncorrected $^{87}\text{Sr}/^{86}\text{Sr}$ value of 0.71096 ± 0.00048 , a weighted average corrected $^{87}\text{Sr}/^{86}\text{Sr}$ value of 0.70817 ± 0.00048 and a weighted average $^{84}\text{Sr}/^{86}\text{Sr}$ value of 0.05633 ± 0.00024 ($n=7$). The dentine spots of track 2 have an average ^{88}Sr voltage of 0.527, a weighted average uncorrected $^{87}\text{Sr}/^{86}\text{Sr}$ value of 0.71144 ± 0.00096 , a weighted average corrected $^{87}\text{Sr}/^{86}\text{Sr}$ value of 0.71057 ± 0.00096 and a weighted average $^{84}\text{Sr}/^{86}\text{Sr}$ value of 0.05629 ± 0.00014 ($n=9$). Enamel values of track 1 range from 0.710343 to 0.711876 (uncorrected), as well as 0.707561 to 0.709093 (corrected), and are homogenous within 2σ error. Enamel values of track 2 range from 0.710263 to 0.711465 (uncorrected), as well as 0.707480 to 0.708683 (corrected), and are homogenous within 2σ error. Dentine values of track 1 are in the range of 0.709747 to 0.712234 (uncorrected), as well as 0.708882 to 0.711368 (corrected), and are extremely heterogeneous. Dentine values of track 2 are in the range of 0.711066 to 0.713724 (uncorrected), as well as 0.710200 to 0.712858, and are relatively heterogeneous. Detailed values for enamel and dentine for sample M012 are shown in Table A3.78, Figure A3.128 and Figure A3.129.

This sample has homogeneous enamel values within 2σ error, which are in the range 0.710343 ± 0.001048 to 0.711876 ± 0.000537 (uncorrected) and 0.707561 ± 0.001048 to 0.709093 ± 0.000537 (corrected). The uncorrected

values have an overall weighted average of 0.71103 ± 0.00037 , which locally corresponds to the value of 0.710853 ± 0.000011 from sample location FS089-S1 in the Upper Cretaceous carbonate and siliciclastic unit, which outcrops within 20 km of the site to the west of Les Fieux. The corrected values have an overall weighted average of 0.70825 ± 0.00037 , which corresponds to the value of lower and upper Jurassic and Oligocene carbonates south of the Les Fieux represented by FS074-S1, FS085-S1 and FS083-S1 which outcrop within 2.7 km from the site. Dentine values are extremely heterogeneous, in the range of 0.709747 to 0.713724 (uncorrected) and 0.708882 to 0.712858 (corrected) with no systematic variation in values along the track. The large range of dentine values makes it difficult to determine if there is a significant difference in enamel and dentine values for this sample.

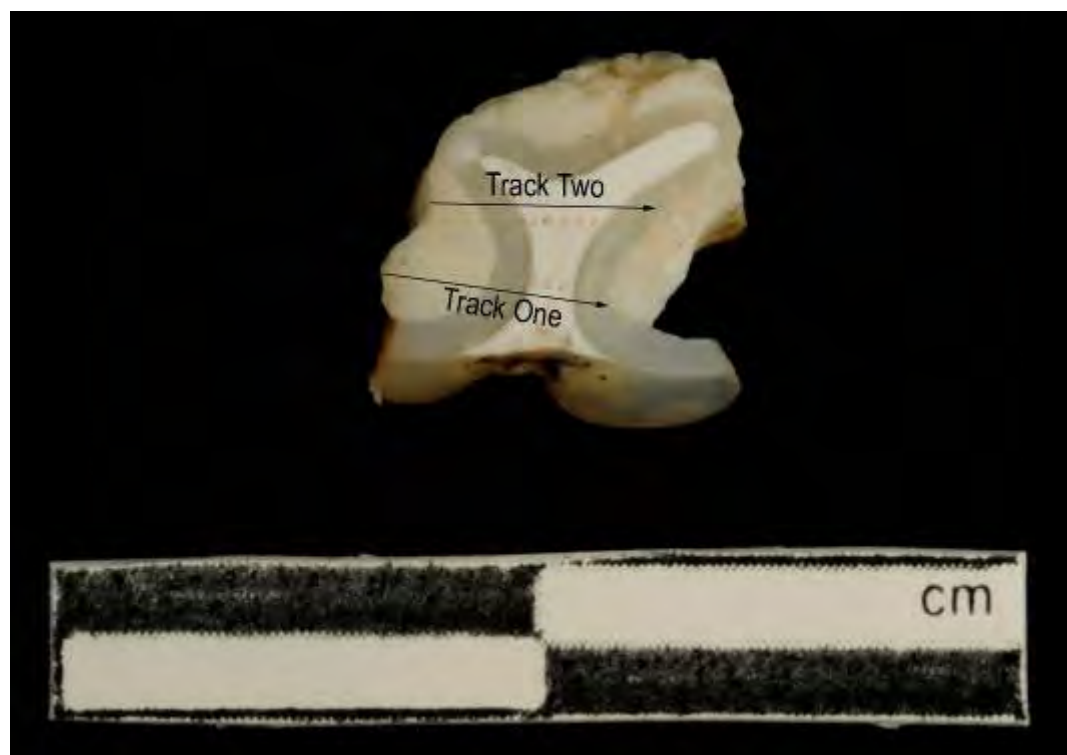


Figure A3.127 LA-MC-ICPMS Track for Sample M012, Horse, Layer G7, Les Fieux

Sample	Material	Track	Point	^{88}Sr Volts	$^{84}\text{Sr}/^{86}\text{Sr}$	$^{84}\text{Sr}/^{86}\text{Sr}$ 2 σ Error	Corrected $^{87}\text{Sr}/^{86}\text{Sr}$	$^{87}\text{Sr}/^{86}\text{Sr}$ 2 σ Error
M012	Dentine	1	1	0.966	0.056592	0.000191	0.712698	0.711832
M012	Dentine	1	2	0.623	0.056483	0.000388	0.711661	0.710795
M012	Dentine	1	3	0.584	0.056606	0.000325	0.711222	0.710357
M012	Dentine	1	4	0.586	0.056139	0.000430	0.711824	0.710958
M012	Dentine	1	5	0.590	0.056559	0.000374	0.711098	0.710233
M012	Dentine	1	6	0.973	0.056435	0.000221	0.709747	0.708882
M012	Dentine	1	7	0.600	0.056205	0.000417	0.710663	0.709798
M012	Dentine	1	8	0.337	0.056600	0.000746	0.711421	0.710556
M012	Enamel	1	9	0.340	0.056520	0.000612	0.711024	0.708242
M012	Enamel	1	10	0.265	0.055827	0.000824	0.711074	0.708291
M012	Dentine	1	11	0.453	0.056022	0.000489	0.713517	0.712651
M012	Dentine	1	12	0.382	0.056504	0.000466	0.710815	0.709950
M012	Dentine	1	13	0.462	0.056274	0.000450	0.712234	0.711368
M012	Enamel	1	14	0.285	0.056537	0.000621	0.711876	0.709093
M012	Enamel	1	15	0.325	0.057247	0.000725	0.710343	0.707561
M012	Enamel	1	16	0.339	0.056768	0.000622	0.710359	0.707576
M012	Dentine	2	1	0.809	0.056113	0.000424	0.712228	0.711363
M012	Dentine	2	2	0.545	0.056476	0.000491	0.710330	0.709464
M012	Dentine	2	3	0.562	0.056391	0.000345	0.710391	0.709525
M012	Dentine	2	4	0.581	0.056284	0.000389	0.710235	0.709370
M012	Enamel	2	5	0.313	0.056538	0.000681	0.711044	0.708262
M012	Enamel	2	6	0.285	0.056815	0.000657	0.711459	0.708677
M012	Enamel	2	7	0.225	0.056299	0.000894	0.711465	0.708683
M012	Dentine	2	8	0.427	0.056600	0.000578	0.713724	0.712858
M012	Dentine	2	9	0.475	0.056088	0.000471	0.711066	0.710200
M012	Dentine	2	10	0.455	0.056320	0.000461	0.711814	0.710948
M012	Dentine	2	11	0.451	0.056159	0.000681	0.712220	0.711355
M012	Dentine	2	12	0.440	0.056249	0.000365	0.713352	0.712487
M012	Enamel	2	13	0.316	0.056092	0.000858	0.711386	0.708604
M012	Enamel	2	14	0.274	0.056078	0.000815	0.711144	0.708362
M012	Enamel	2	15	0.288	0.056379	0.000797	0.711144	0.708361
M012	Enamel	2	16	0.443	0.056186	0.000392	0.710263	0.707480

Table A3.78 Detailed LA-MC-ICPMS Sr Isotope Results for Dentine and Enamel, Sample M012, Horse, Layer G7, Les Fieux

Sample M012, Les Fieux, France

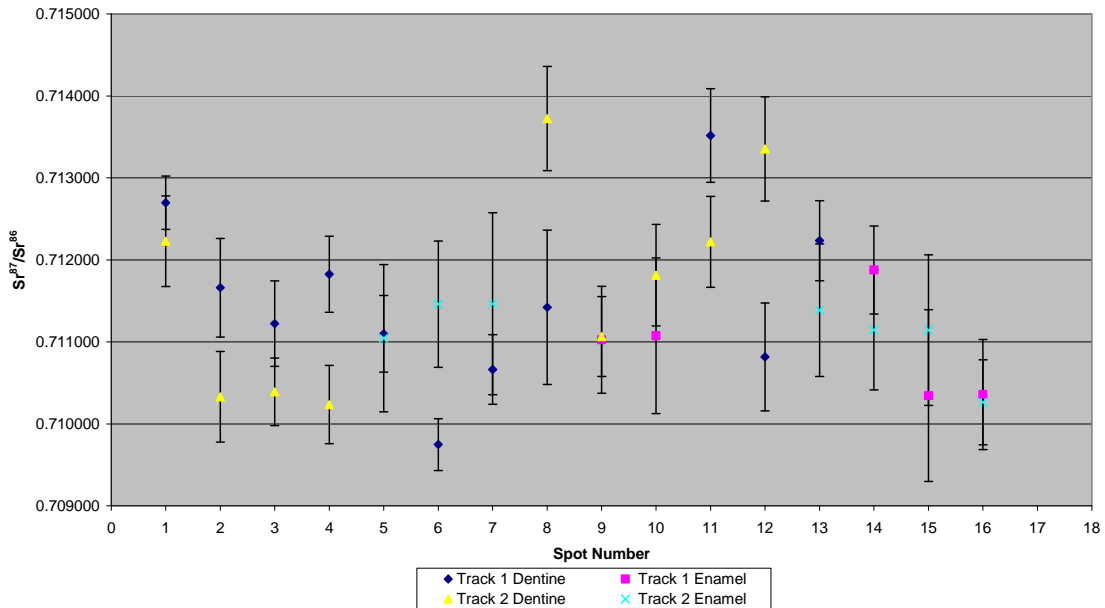


Figure A3.128 Detailed LA-MC-ICPMS Uncorrected Sr Isotope Results, Sample M012, Horse, Layer G7, Les Fieux

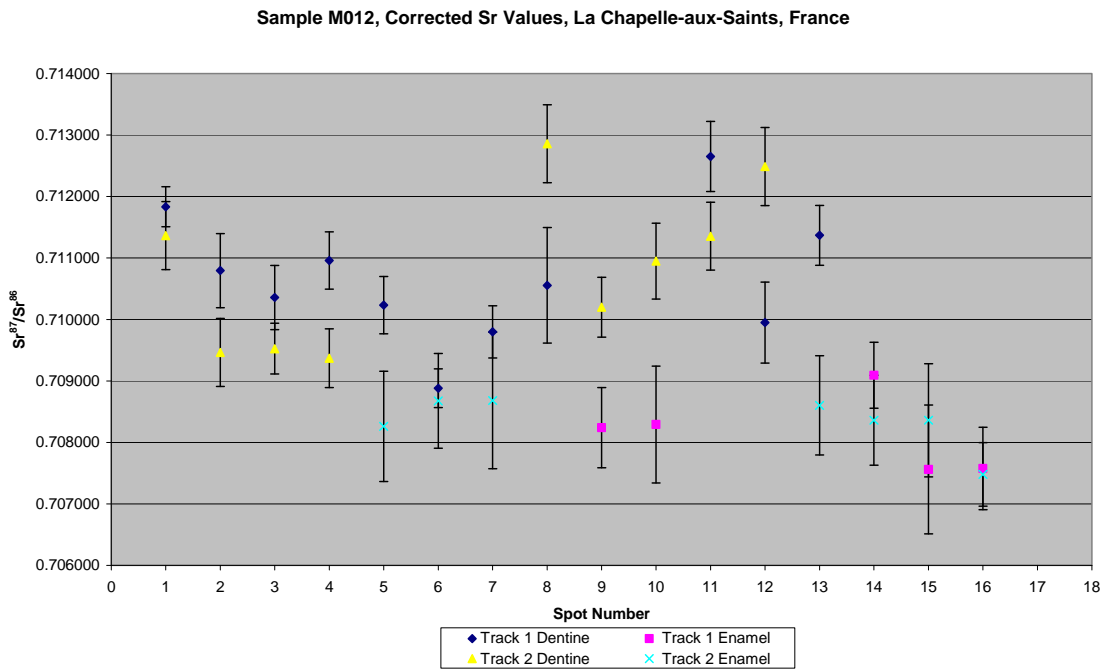


Figure A3.129 Detailed LA-MC-ICPMS Corrected Sr Isotope Results, Sample M012, Horse, Layer G7, Les Fieux

Sample M013, a wild boar from layer G7 of Les Fieux was analysed in 2 tracks, with the first containing 4 spots of enamel and 11 spots of dentine and the second containing 4 spots of enamel in 2 discontinuous sections and 9 spots of dentine, shown in Figure A3.130. The results from this sample are summarised in Table 5.30 and Figure 5.18. The enamel spots of track 1 have an average ^{88}Sr voltage of 0.292, a weighted average uncorrected $^{87}\text{Sr}/^{86}\text{Sr}$ value of 0.71786 ± 0.00040 , a weighted average corrected $^{87}\text{Sr}/^{86}\text{Sr}$ value of 0.71498 ± 0.00040 and a weighted average $^{84}\text{Sr}/^{86}\text{Sr}$ value of 0.05654 ± 0.00035 ($n=4$). The dentine spots of track 1 have an average ^{88}Sr voltage of 0.516, a weighted average uncorrected $^{87}\text{Sr}/^{86}\text{Sr}$ value of 0.71217 ± 0.00034 , a weighted average corrected $^{87}\text{Sr}/^{86}\text{Sr}$ value of 0.71099 ± 0.00034 and a weighted average $^{84}\text{Sr}/^{86}\text{Sr}$ value of 0.05655 ± 0.00012 ($n=11$). The enamel spots of track 2 have an average ^{88}Sr voltage of 0.305, a weighted average uncorrected $^{87}\text{Sr}/^{86}\text{Sr}$ value of 0.7173 ± 0.0015 , a weighted average corrected $^{87}\text{Sr}/^{86}\text{Sr}$ value of 0.71450 ± 0.0015 and a weighted average $^{84}\text{Sr}/^{86}\text{Sr}$ value of 0.05660 ± 0.00039 ($n=4$). The dentine spots of track 2 have an average ^{88}Sr voltage of 0.505, a weighted average uncorrected $^{87}\text{Sr}/^{86}\text{Sr}$ value of 0.7140 ± 0.0011 , a weighted average corrected $^{87}\text{Sr}/^{86}\text{Sr}$ value of 0.71280 ± 0.0011 and a weighted average $^{84}\text{Sr}/^{86}\text{Sr}$ value of 0.05628 ± 0.00013 ($n=9$). Enamel values of track 1 range from 0.717497 to 0.718136 (corrected), as well as 0.714620 to 0.715258 and are homogenous within 2σ error. Enamel values of track 2 range from 0.716169 to 0.718220 (uncorrected), as well as 0.713292 to 0.715343 (corrected), and are homogenous within 2σ error, although values decrease from point 1 to point 4. Dentine values of track 1 range from 0.711606 to 0.712987 (uncorrected), as well as 0.710422 to 0.711803 (corrected), and are moderately heterogeneous. Dentine values of track 2 range from 0.712735 to 0.717960 (uncorrected), as well as 0.711551 to 0.716777 (corrected), and are extremely heterogeneous. Detailed values for enamel and dentine for sample M013 are shown in Table A3.79, Figure A3.131 and Figure A3.132.

This sample has a significant difference in $^{87}\text{Sr}/^{86}\text{Sr}$ values between enamel (overall uncorrected weighted average 0.71765 ± 0.00056) and dentine (overall uncorrected weighted average 0.71291 ± 0.00062). Enamel spots in the range 0.716169 ± 0.000881 to 0.718220 ± 0.000869 (uncorrected) and 0.713292 ± 0.000869 (corrected) and dentine in the range 0.712735 ± 0.000869 to 0.717960 ± 0.000869 (uncorrected) and 0.716777 ± 0.000869 (corrected).

0.000881 to 0.715343 \pm 0.000869 (corrected) are within 2σ error, although the error range is large. The overall weighted average uncorrected enamel value corresponds to mapping sample FS067-S1, which has a $^{87}\text{Sr}/^{86}\text{Sr}$ value of 0.717422 \pm 0.00001 and is located within a Carboniferous monzogranite/granodiorite region, which outcrops within 36 km of Les Fieux. Mapping samples which correspond to the overall weighted average corrected enamel value include the upper Jurassic sedimentary/metamorphic unit sampled in P38P, which outcrops approximately 300 km to the east of the site and location P8P from a monzogranite/granodiorite located approximately 190 km east of the site. Of these values, the $^{87}\text{Sr}/^{86}\text{Sr}$ seems more credible, as the value from P38P is very elevated for a principally carbonate unit. The unit containing P8P outcrops within 32 km of the archaeological site. Dentine values are in the range 0.711226 \pm 0.000509 to 0.717960 \pm 0.000799 (uncorrected) and 0.710043 \pm 0.000509 to 0.716777 \pm 0.000799 (corrected), and are extremely heterogeneous, particularly track 2. This may reflect multiple episodes of post-burial diagenesis. $^{84}\text{Sr}/^{86}\text{Sr}$ values have an overall weighted average of 0.056445 \pm 0.000084, suggesting that the $^{87}\text{Sr}/^{86}\text{Sr}$ values for this specimen are robust.

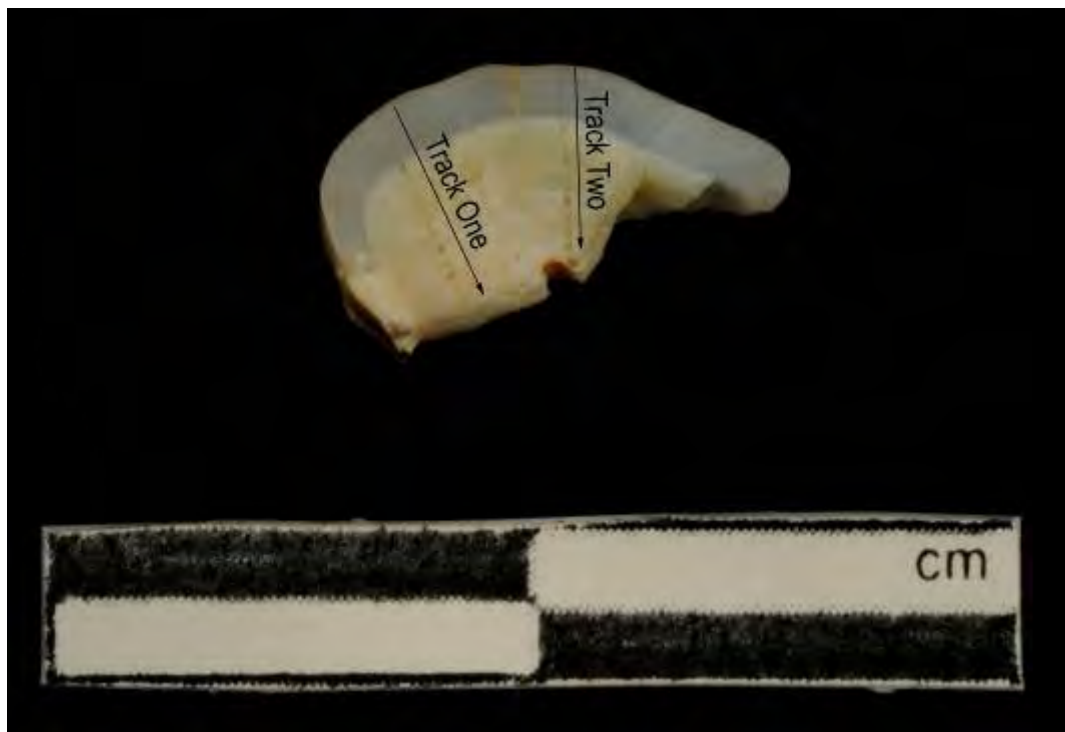


Figure A3.130 LA-MC-ICPMS Track for Sample M013, Wild Boar, Layer G7, Les Fieux

Sample	Material	Track	Point	^{88}Sr Volts	$^{84}\text{Sr}/^{86}\text{Sr}$	$^{84}\text{Sr}/^{86}\text{Sr} 2\sigma$ Error	$^{87}\text{Sr}/^{86}\text{Sr}$	Corrected $^{87}\text{Sr}/^{86}\text{Sr}$	$^{87}\text{Sr}/^{86}\text{Sr} 2\sigma$ Error
M013	Enamel	1	1	0.328	0.056367	0.000683	0.717497	0.714620	0.000760
M013	Enamel	1	2	0.249	0.056456	0.000714	0.718136	0.715258	0.000911
M013	Enamel	1	3	0.278	0.056666	0.000686	0.718093	0.715215	0.000702
M013	Enamel	1	4	0.313	0.056726	0.000807	0.717712	0.714834	0.000930
M013	Dentine	1	5	0.601	0.056445	0.000325	0.712194	0.711011	0.000498
M013	Dentine	1	6	0.650	0.056530	0.000421	0.712987	0.711803	0.000511
M013	Dentine	1	7	0.699	0.056813	0.000287	0.712492	0.711309	0.000346
M013	Dentine	1	8	0.499	0.056364	0.000332	0.711606	0.710422	0.000613
M013	Dentine	1	9	0.436	0.056468	0.000548	0.711620	0.710437	0.000449
M013	Dentine	1	10	0.466	0.056692	0.000496	0.712539	0.711355	0.000639
M013	Dentine	1	11	0.417	0.056456	0.000531	0.711893	0.710710	0.000621
M013	Dentine	1	12	0.452	0.056468	0.000509	0.711226	0.710043	0.000509
M013	Dentine	1	13	0.450	0.056608	0.000469	0.712321	0.711138	0.000626
M013	Dentine	1	14	0.421	0.056350	0.000602	0.712312	0.711129	0.000431
M013	Dentine	1	15	0.585	0.056580	0.000331	0.712388	0.711204	0.000551
M013	Enamel	2	1	0.312	0.056266	0.000647	0.718220	0.715343	0.000869
M013	Enamel	2	2	0.268	0.056774	0.000908	0.717758	0.714881	0.001134
M013	Enamel	2	3	0.312	0.056862	0.000879	0.717301	0.714424	0.001159
M013	Enamel	2	4	0.329	0.056761	0.000808	0.716169	0.713292	0.000881
M013	Dentine	2	5	0.558	0.056216	0.000426	0.712735	0.711551	0.000471
M013	Dentine	2	6	0.626	0.056476	0.000332	0.714545	0.713361	0.000455
M013	Dentine	2	7	0.599	0.056363	0.000319	0.714141	0.712958	0.000421
M013	Dentine	2	8	0.453	0.055901	0.000539	0.712943	0.711760	0.000707
M013	Dentine	2	9	0.440	0.055773	0.000490	0.715443	0.714259	0.000599
M013	Dentine	2	10	0.418	0.056094	0.000671	0.711515	0.710331	0.000747
M013	Dentine	2	11	0.472	0.056329	0.000396	0.713696	0.712513	0.000475
M013	Dentine	2	12	0.488	0.056398	0.000374	0.713832	0.712648	0.000586
M013	Dentine	2	13	0.492	0.056339	0.000414	0.717960	0.716777	0.000799

Table A3.79 Detailed LA-MC-ICPMS Sr Isotope Results for Dentine and Enamel, Sample M013, Wild Boar, Layer G7, Les Fieux

Sample M013, Les Fieux, France

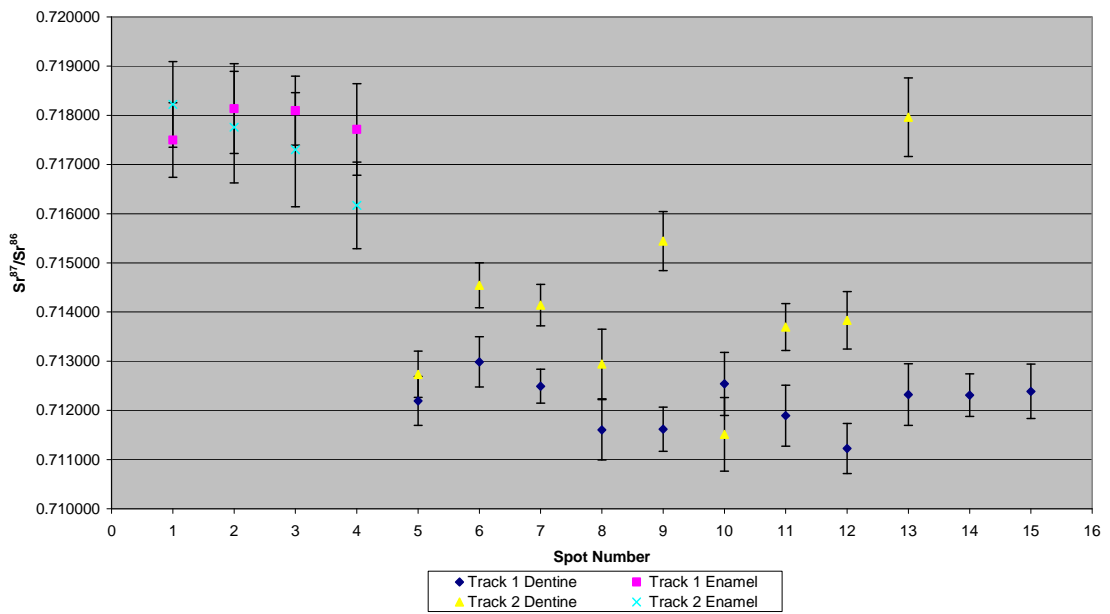


Figure A3.131 Detailed LA-MC-ICPMS Uncorrected Sr Isotope Results, Sample M013, Wild Boar, Layer G7, Les Fieux

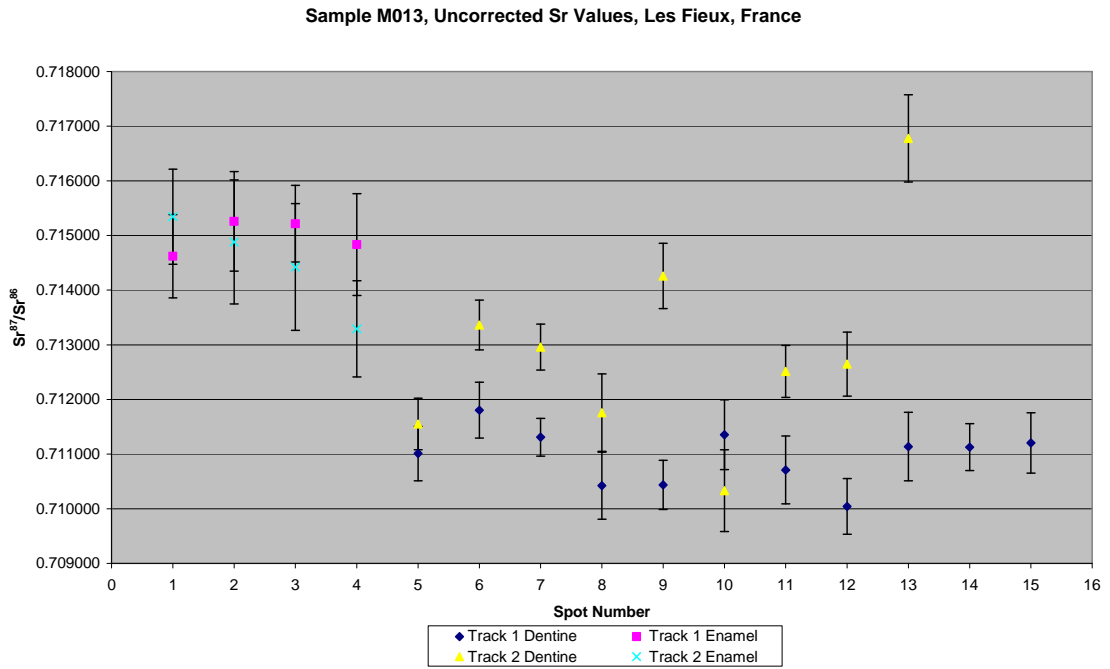


Figure A3.132 Detailed LA-MC-ICPMS Corrected Sr Isotope Results, Sample M013, Wild Boar, Layer G7, Les Fieux

Sample M014, a fox from layer G7 of Les Fieux, was analysed in 2 tracks, with the first containing 2 discontinuous spots of enamel and 9 spots of dentine and the second containing 1 spot of enamel and 7 spots of dentine, shown in Figure A3.133. The results from this sample are summarised in Table 5.30 and Figure 5.18. The enamel spots of track 1 have an average ^{88}Sr voltage of 0.227, a weighted average uncorrected $^{87}\text{Sr}/^{86}\text{Sr}$ value of 0.7193 ± 0.0099 , a weighted average corrected $^{87}\text{Sr}/^{86}\text{Sr}$ value of 0.71220 ± 0.0099 and a weighted average $^{84}\text{Sr}/^{86}\text{Sr}$ value of 0.0570 ± 0.0081 ($n=2$). The dentine spots of track 1 have an average ^{88}Sr voltage of 0.523, a weighted average uncorrected $^{87}\text{Sr}/^{86}\text{Sr}$ value of 0.71143 ± 0.00067 , a weighted average corrected $^{87}\text{Sr}/^{86}\text{Sr}$ value of 0.70988 ± 0.00067 and a weighted average $^{84}\text{Sr}/^{86}\text{Sr}$ value of 0.05675 ± 0.00013 ($n=9$). The enamel spot of track 2 has a ^{88}Sr voltage of 0.195, an uncorrected $^{87}\text{Sr}/^{86}\text{Sr}$ value of 0.717 ± 0.018 , a corrected $^{87}\text{Sr}/^{86}\text{Sr}$ value of 0.70931 ± 0.018 and a $^{84}\text{Sr}/^{86}\text{Sr}$ value of 0.05639 ± 0.00064 ($n=1$). The dentine spots of track 2 have an average ^{88}Sr voltage of 0.455, a weighted average uncorrected $^{87}\text{Sr}/^{86}\text{Sr}$ value of 0.71067 ± 0.00049 , a weighted average corrected $^{87}\text{Sr}/^{86}\text{Sr}$ value of 0.70912 ± 0.00049 and a weighted average $^{84}\text{Sr}/^{86}\text{Sr}$ value of 0.05644 ± 0.00016 ($n=7$). Enamel values of track 1 are 0.718578 and 0.720142 (uncorrected), as well as 0.711492 and 0.713056 (corrected), which are homogeneous within 2σ error. Dentine values for track 1 are in the range of 0.710305 to 0.713444 (uncorrected), as well as 0.708752 to 0.711891 (corrected), and are heterogeneous. Dentine values for track 2 are in the range of 0.709858 to 0.711148 (uncorrected), as well as 0.708306 to 0.709595 (corrected), and are heterogeneous. Detailed values for enamel and dentine for sample M014 are shown in Table A3.80, Figure A3.134 and Figure A3.135.

This sample has a very significant difference between enamel and dentine values. Enamel values are heterogeneous, in the range 0.716403 ± 0.000874 to 0.720142 ± 0.001075 (uncorrected) and 0.709317 ± 0.000874 to 0.713056 ± 0.001075 (corrected). Spots 1 and 11 on track 1 are homogenous within 2σ error and the uncorrected values correspond to mapping samples from locations FS060-S1 (0.720113 ± 0.00002) and FS070-S1 ($0.7202840.000017$) from metamorphic units, and FS053-S1 (0.718578 ± 0.001006) from a Permian siliciclastic unit, all of which outcrop within 19 km of Les Fieux. The corrected

values from these spots correspond to mapping sample FS036-S1 from a Upper Cretaceous limestone which outcrops within 18 km from the site. Spot 9 from track 2 has an uncorrected value of 0.716403 ± 0.000874 , which corresponds to FS041-S1, which, as discussed above with reference to sample M007, reflects floodplain sediments. The same spot has a corrected value of 0.709317 ± 0.000874 , which reflects floodplain sediments from the Verezee or Dordogne rivers, based on values from FS027-S2 and FS032-S2. The floodplain outcrops within 5.3 km of the archaeological site. Dentine values are somewhat heterogeneous, being slightly outside of 2σ error. $^{84}\text{Sr}/^{86}\text{Sr}$ have a weighted average 0.05663 ± 0.00012 , suggesting that the $^{87}\text{Sr}/^{86}\text{Sr}$ values are robust.



Figure A3.133 LA-MC-ICPMS Track for Sample M014, Fox, Layer G7, Les Fieux

Sample	Material	Track	Point	^{88}Sr Volts	$^{84}\text{Sr}/^{86}\text{Sr}$	$^{84}\text{Sr}/^{86}\text{Sr} 2\sigma$	Corrected $^{87}\text{Sr}/^{86}\text{Sr}$	$^{87}\text{Sr}/^{86}\text{Sr} 2\sigma$
M014	Enamel	1	1	0.183	0.058019	0.001156	0.720142	0.713056
M014	Dentine	1	2	0.492	0.056794	0.000438	0.710305	0.708752
M014	Dentine	1	3	0.551	0.056799	0.000339	0.711616	0.710063
M014	Dentine	1	4	0.560	0.056715	0.000329	0.711792	0.710239
M014	Dentine	1	5	0.569	0.056793	0.000422	0.712029	0.710476
M014	Dentine	1	6	0.510	0.056968	0.000392	0.711538	0.709986
M014	Dentine	1	7	0.471	0.056343	0.000550	0.712410	0.710858
M014	Dentine	1	8	0.519	0.056716	0.000411	0.710140	0.708587
								0.000500

M014	Dentine	1	9	0.559	0.056735	0.000468	0.710939	0.709387	0.000417
M014	Dentine	1	10	0.475	0.056698	0.000518	0.713444	0.711891	0.000792
M014	Enamel	1	11	0.270	0.056586	0.000703	0.718578	0.711492	0.001006
M014	Enamel	2	1						
M014	Dentine	2	2	0.445	0.056477	0.000357	0.710443	0.708891	0.000600
M014	Dentine	2	3	0.428	0.056359	0.000446	0.709858	0.708306	0.000749
M014	Dentine	2	4	0.421	0.056137	0.000554	0.710822	0.709270	0.000529
M014	Dentine	2	5	0.462	0.056317	0.000355	0.711250	0.709697	0.000471
M014	Dentine	2	6	0.465	0.056644	0.000457	0.710426	0.708873	0.000524
M014	Dentine	2	7	0.451	0.056529	0.000522	0.709863	0.708310	0.000723
M014	Dentine	2	8	0.511	0.056625	0.000466	0.711148	0.709595	0.000604
M014	Enamel	2	9	0.243	0.056525	0.000714	0.716403	0.709317	0.000874

Table A3.80 Detailed LA-MC-ICPMS Sr Isotope Results for Dentine and Enamel, Sample M014, Fox, Layer G7, Les Fieux

Sample M014, Les Fieux, France

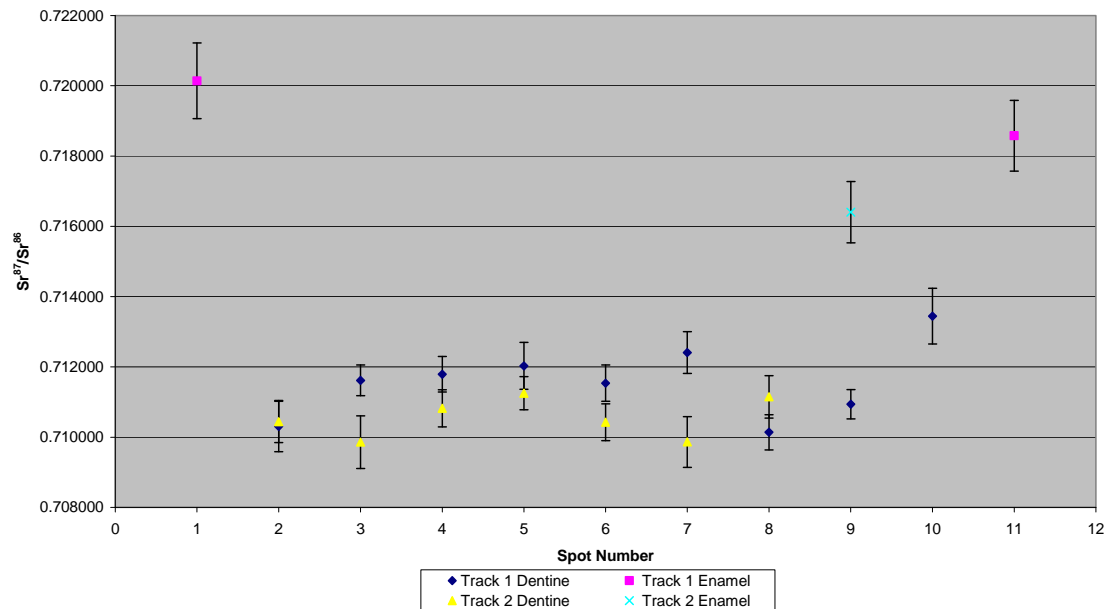


Figure A3.134 Detailed LA-MC-ICPMS Uncorrected Sr Isotope Results, Sample M014, Fox, Layer G7, Les Fieux

Sample M014, Corrected Sr Values, Les Fieux, France

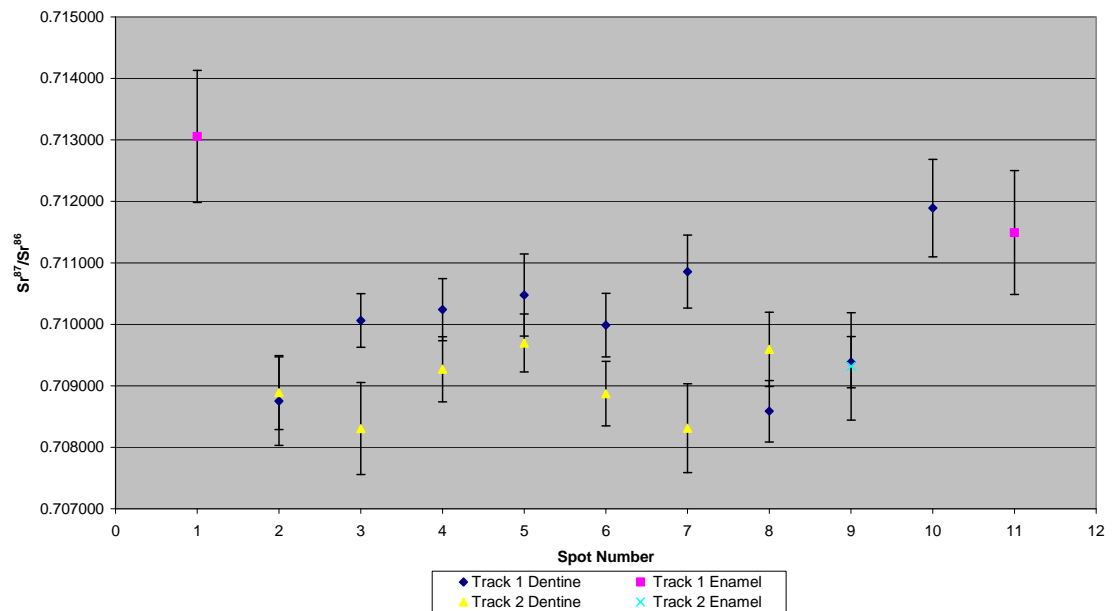


Figure A3.135 Detailed LA-MC-ICPMS Corrected Sr Isotope Results, Sample M014, Fox, Layer G7, Les Fieux

Sample M015, a hyena from layer G7 of Les Fieux, was analysed in 1 track, with 1 spot in enamel and 5 spots in dentine, shown in Figure A3.136. The results from this sample are summarised in Table 5.30 and Figure 5.18. The enamel spot has a ^{88}Sr voltage of 0.226, an uncorrected $^{87}\text{Sr}/^{86}\text{Sr}$ value of 0.717513 ± 0.000860 , an corrected $^{87}\text{Sr}/^{86}\text{Sr}$ value of 0.71460 ± 0.000860 and a $^{84}\text{Sr}/^{86}\text{Sr}$ value of 0.056059 ± 0.000876 ($n=1$). The dentine spots have an average ^{88}Sr voltage of 0.268, a weighted average uncorrected $^{87}\text{Sr}/^{86}\text{Sr}$ value of 0.71058 ± 0.00089 , a weighted average corrected $^{87}\text{Sr}/^{86}\text{Sr}$ value of 0.70842 ± 0.00089 and a weighted average $^{84}\text{Sr}/^{86}\text{Sr}$ value of 0.05628 ± 0.00034 ($n=5$). Dentine values are in the range of 0.709631 to 0.711354 (uncorrected), as well as 0.707465 to 0.709188 (corrected), and are relatively homogenous. Detailed values for enamel and dentine for sample M015 are shown in Table A3.81, Figure A3.137 and Figure A3.138.

There is a very significant difference between enamel and dentine $^{87}\text{Sr}/^{86}\text{Sr}$ values for this sample. The uncorrected dentine values are in the range of 0.709631 ± 0.000992 to 0.711354 ± 0.000686 , which are within 2σ error and have a weighted average value of 0.71058 ± 0.00089 . The enamel spot has an uncorrected value of 0.717513 ± 0.000860 , which corresponds to mapping samples FS067-S1 (0.717422 ± 0.00001) and FS037-S1 (0.717308 ± 0.000012). These samples are collected from a Carboniferous monzogranite/granodiorite and a clay package within an Upper Cretaceous interbedded limestone/clay, respectively. These values suggest that the sample is from either 38 km to the west (FS037-S1) or 41 km to the east (FS067-S1). As sample FS037-S1 is a clay unit interbedded within a limestone, it would not be expected to contribute significantly to regional bioavailable values being taken up by plants and animals. The corrected value of the enamel spot has a value of 0.714609 ± 0.000860 , which correlates to floodplain sediment samples, including FS046-S1 and FS058-S1 which outcrop within 5.3 km of the site. $^{84}\text{Sr}/^{86}\text{Sr}$ values have a weighted average of 0.05625 ± 0.00032 , which is within 2σ error of the expected value of 0.0565.



Figure A3.136 LA-MC-ICPMS Track for Sample M015, Hyena, Layer G7, Les Fieux

Sample	Material	Track	Point	^{88}Sr Volts	$^{84}\text{Sr}/^{86}\text{Sr}$	$^{87}\text{Sr}/^{86}\text{Sr} 2\sigma$	$^{87}\text{Sr}/^{86}\text{Sr}$	$^{87}\text{Sr}/^{86}\text{Sr} 2\sigma$	$^{87}\text{Sr}/^{86}\text{Sr} 2\sigma$
					Error	Corrected $^{87}\text{Sr}/^{86}\text{Sr}$	Error	Corrected $^{87}\text{Sr}/^{86}\text{Sr}$	Error
M015	Enamel	1	1	0.226	0.056059	0.000876	0.717513	0.714609	0.000860
M015	Dentine	1	2	0.297	0.056560	0.000723	0.711354	0.709188	0.000686
M015	Dentine	1	3	0.275	0.056167	0.000732	0.710947	0.708780	0.000760
M015	Dentine	1	4	0.263	0.056341	0.000837	0.710018	0.707851	0.000788
M015	Dentine	1	5	0.256	0.056134	0.000717	0.709631	0.707465	0.000992
M015	Dentine	1	6	0.249	0.056170	0.000950	0.710190	0.708024	0.001005

Table A3.81 Detailed LA-MC-ICPMS Sr Isotope Results for Dentine and Enamel, Sample M015, Hyena, Layer G7, Les Fieux

Sample M015, Les Fieux, France

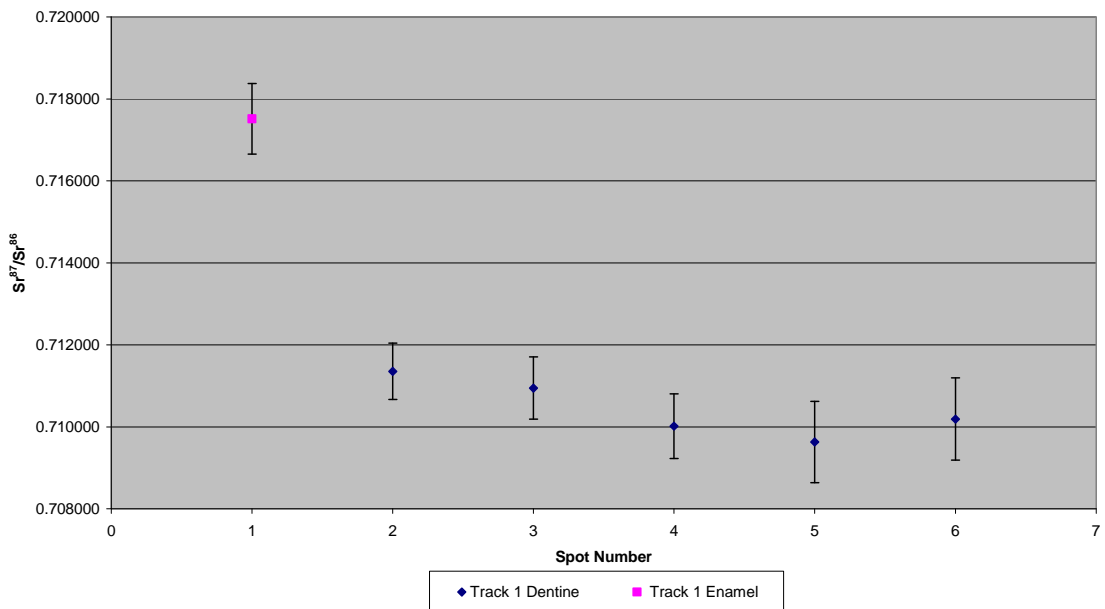


Figure A3.137 Detailed LA-MC-ICPMS Uncorrected Sr Isotope Results, Sample M015, Hyena, Layer G7, Les Fieux

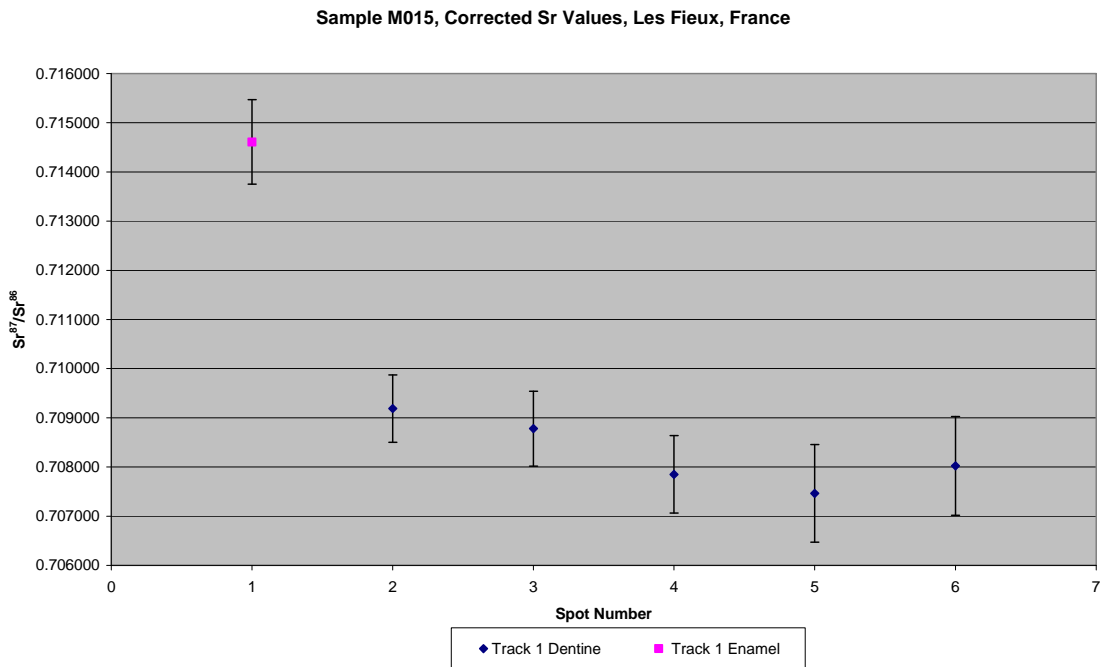


Figure A3.138 Detailed LA-MC-ICPMS Corrected Sr Isotope Results, Sample M015, Hyena, Layer G7, Les Fieux

Sample M016, a bison from layer G7 of Les Fieux shown in Figure A2.46, was analysed in 2 tracks, with track 1 comprising 4 spots of enamel and 3 spots of

dentine and track 2 comprising 4 spots of enamel and 7 spots of dentine, shown in Figure A3.139. The results from this sample are summarised in Table 5.30 and Figure 5.18. The enamel spots of track 1 have an average ^{88}Sr voltage of 0.497, a weighted average uncorrected $^{87}\text{Sr}/^{86}\text{Sr}$ value of 0.71344 ± 0.00027 , a weighted average corrected $^{87}\text{Sr}/^{86}\text{Sr}$ value of 0.71238 ± 0.00027 and a weighted average $^{84}\text{Sr}/^{86}\text{Sr}$ value of 0.05679 ± 0.00022 ($n=4$). The dentine spots of track 1 have an average ^{88}Sr voltage of 0.597, a weighted average uncorrected $^{87}\text{Sr}/^{86}\text{Sr}$ value of 0.7107 ± 0.0010 , a weighted average corrected $^{87}\text{Sr}/^{86}\text{Sr}$ value of 0.71000 ± 0.0010 and a weighted average $^{84}\text{Sr}/^{86}\text{Sr}$ value of 0.05684 ± 0.00020 ($n=3$). The enamel spots of track 2 have an average ^{88}Sr voltage of 0.428, a weighted average uncorrected $^{87}\text{Sr}/^{86}\text{Sr}$ value of 0.7142 ± 0.0019 , a weighted average corrected $^{87}\text{Sr}/^{86}\text{Sr}$ value of 0.71320 ± 0.0019 and a weighted average $^{84}\text{Sr}/^{86}\text{Sr}$ value of 0.05706 ± 0.00049 ($n=4$). The dentine spots of track 2 have an average ^{88}Sr voltage of 0.520, a weighted average uncorrected $^{87}\text{Sr}/^{86}\text{Sr}$ value of 0.71115 ± 0.00079 , a weighted average corrected $^{87}\text{Sr}/^{86}\text{Sr}$ value of 0.71046 ± 0.00079 and a weighted average $^{84}\text{Sr}/^{86}\text{Sr}$ value of 0.05694 ± 0.00013 ($n=7$). Enamel values from track 1 are in the range of 0.713146 to 0.713988 (uncorrected), as well as 0.712085 to 0.712926 (corrected), and are homogenous within 2σ error. Enamel values from track 2 are in the range of 0.713023 to 0.715883 (uncorrected), as well as 0.711961 to 0.714821 (corrected), and are relatively heterogeneous, with the values decreasing progressively along the track. Spots 3 and 4 from the enamel in tracks 1 and 2 are relatively homogenous with each other. Dentine values of track 1 are in the range of 0.710385 to 0.711251 (uncorrected), as well as 0.709689 to 0.710555 (corrected), and are relatively homogenous within 2σ error. Dentine values of track 2 are in the range of 0.710581 to 0.712907 (uncorrected), as well as 0.709886 to 0.712211 (corrected), and are relatively homogenous and within 2σ error, with the exception of spot 11. Detailed values for enamel and dentine for sample M016 are shown in Table A3.82, Figure A3.140 and Figure A3.141.

Enamel values for this sample are in the range of 0.713023 ± 0.000609 to 0.715883 ± 0.000651 (uncorrected) and 0.711961 ± 0.000609 to 0.714821 ± 0.000651 (corrected), suggesting that this specimen was moving across

variable geological environments during ameleteogenesis. Spots 1 to 4 of track 1 and spots 3 and 4 of track 2 are within 2σ error and have a weighted average uncorrected value of 0.71343 ± 0.00033 and a corrected value of 0.71237 ± 0.00033 . The uncorrected value corresponds to mapping location FS035-S1 (0.713096 ± 0.000014) from the Dordogne floodplain approximately 32 km to the west of Les Fieux. The corrected value corresponds to mapping location FS054-S1 from metamorphic rocks which outcrops within 15 km of the archaeological site. The 2 additional spots, 1 and 2 from track 2, are within 2σ error and have a weighted average uncorrected value of 0.7153 ± 0.007 . This value corresponds to a wide range of mapping locations surrounding the site; however, the generally elevated value suggests a location to the east of Les Fieux. The corrected value from these spots has a value of 0.7142 ± 0.0070 , which corresponds to floodplain sediments adjacent to the site of La Chapelle-aux-Saints. There is a significant variation between dentine and enamel strontium isotope values, suggesting that this sample is a migrant. Dentine values are relatively homogenous, with the exception of 1 outlying value, and have an overall weighted average value of 0.71100 ± 0.00053 . $^{84}\text{Sr}/^{86}\text{Sr}$ have an overall weighted average value of 0.056908 ± 0.000092 , which is significantly elevated, suggesting that the $^{87}\text{Sr}/^{86}\text{Sr}$ values may not be robust.



Figure A3.139 LA-MC-ICPMS Track for Sample M016, Bison, Layer G7, Les Fieux

Sample	Material	Track	Point	88Sr Volts	84Sr/86Sr	84Sr/86Sr 2σ Error	Corrected 87Sr/86Sr	87Sr/86Sr Error
M016	Enamel	1	1	0.640	0.056534	0.000593	0.713363	0.712302
M016	Enamel	1	2	0.380	0.057118	0.000513	0.713410	0.712348
M016	Enamel	1	3	0.432	0.056707	0.000556	0.713988	0.712926
M016	Enamel	1	4	0.538	0.056762	0.000331	0.713146	0.712085
M016	Dentine	1	5	0.525	0.056682	0.000369	0.711251	0.710555
M016	Dentine	1	6	0.610	0.056953	0.000342	0.710672	0.709977
M016	Dentine	1	7	0.656	0.056862	0.000339	0.710385	0.709689
M016	Enamel	2	1	0.389	0.056995	0.000592	0.715883	0.714821
M016	Enamel	2	2	0.427	0.057312	0.000451	0.714770	0.713709
M016	Enamel	2	3	0.425	0.057217	0.000517	0.713699	0.712638
M016	Enamel	2	4	0.472	0.056654	0.000496	0.713023	0.711961
M016	Dentine	2	5	0.486	0.056753	0.000334	0.710967	0.710271
M016	Dentine	2	6	0.525	0.056745	0.000349	0.710680	0.709984
M016	Dentine	2	7	0.564	0.057075	0.000405	0.710922	0.710226
M016	Dentine	2	8	0.491	0.056965	0.000324	0.710743	0.710047
M016	Dentine	2	9	0.500	0.056918	0.000397	0.711034	0.710338
M016	Dentine	2	10	0.517	0.057152	0.000343	0.710581	0.709886
M016	Dentine	2	11	0.554	0.056984	0.000359	0.712907	0.712211

Table A3.82 Detailed LA-MC-ICPMS Sr Isotope Results for Dentine and Enamel, Sample M016, Bison, Layer G7, Les Fieux

Sample M016, Les Fieux, France

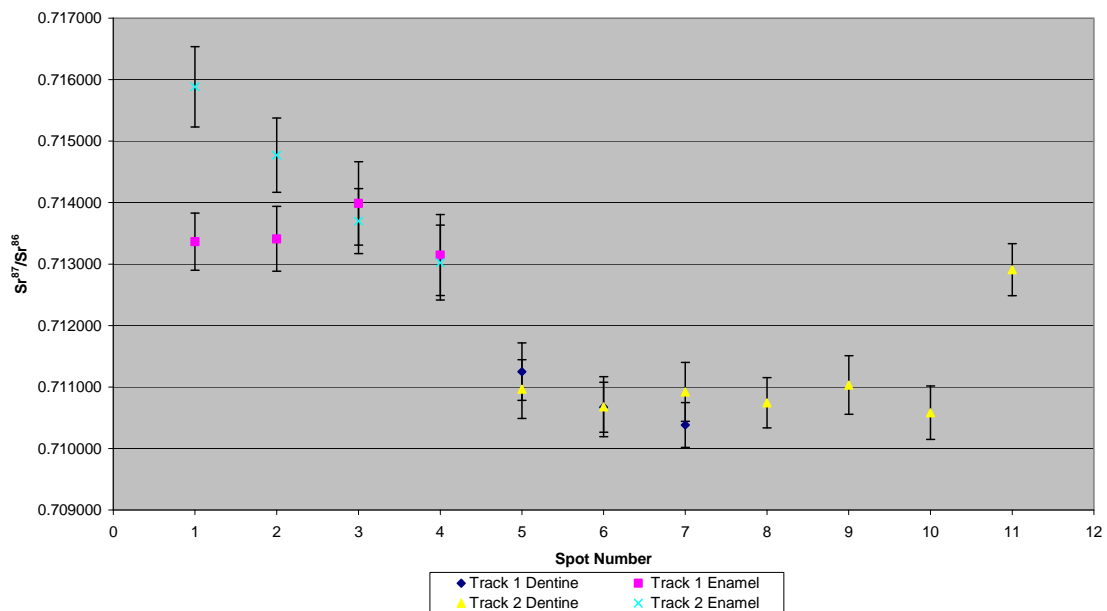


Figure A3.140 Detailed LA-MC-ICPMS Uncorrected Sr Isotope Results, Sample M016, Bison, Layer G7, Les Fieux

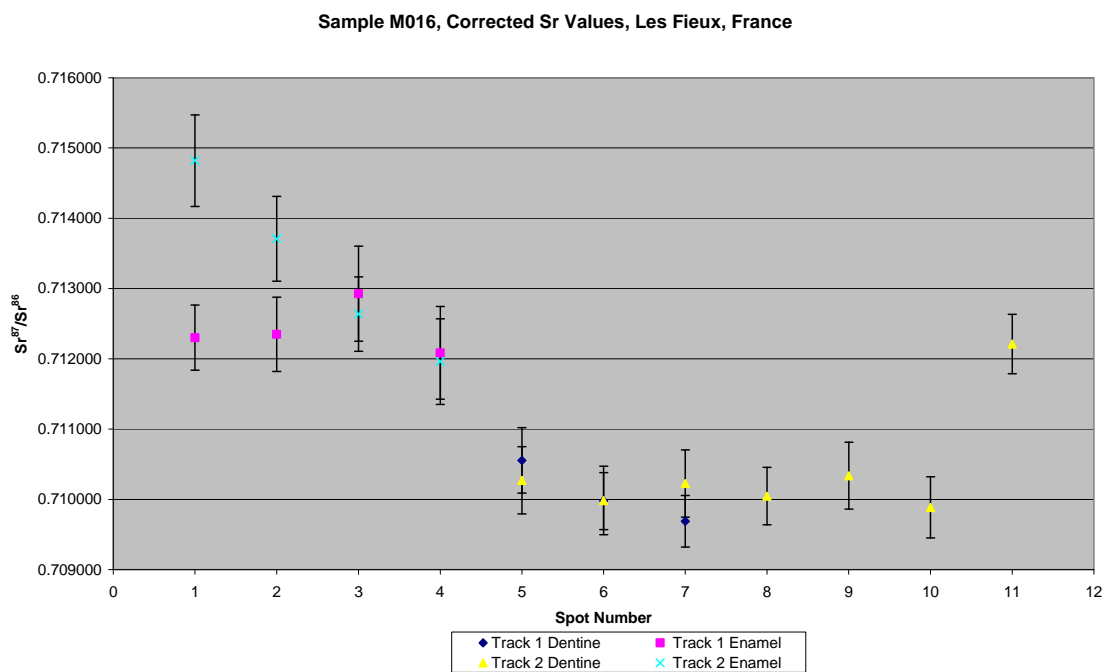


Figure A3.141 Detailed LA-MC-ICPMS Corrected Sr Isotope Results, Sample M016, Bison, Layer G7, Les Fieux

Sample M017, a bison from layer G7 of Les Fieux shown in Figure A2.47, was analysed in 2 tracks, with track 1 comprising 6 spots of enamel in 2 discontinuous sections and 10 spots of dentine in 2 discontinuous sections and track 2 comprising 8 spots of enamel in 3 discontinuous sections and 10 spots of dentine in 3 discontinuous sections, shown in Figure A3.142. The results from this sample are summarised in Table 5.30 and Figure 5.18. The enamel spots of track 1 have an average ^{88}Sr voltage of 0.505, a weighted average uncorrected $^{87}\text{Sr}/^{86}\text{Sr}$ value of 0.7126 ± 0.0017 , a weighted average corrected $^{87}\text{Sr}/^{86}\text{Sr}$ value of 0.71200 ± 0.0017 and a weighted average $^{84}\text{Sr}/^{86}\text{Sr}$ value of 0.05659 ± 0.00015 ($n=6$). The dentine spots of track 1 have an average ^{88}Sr voltage of 0.572, a weighted average uncorrected $^{87}\text{Sr}/^{86}\text{Sr}$ value of 0.71062 ± 0.00089 , a weighted average corrected $^{87}\text{Sr}/^{86}\text{Sr}$ value of 0.71006 ± 0.00089 and a weighted average $^{84}\text{Sr}/^{86}\text{Sr}$ value of 0.056699 ± 0.000098 . The enamel spots of track 2 have an average ^{88}Sr voltage of 0.540, a weighted average uncorrected $^{87}\text{Sr}/^{86}\text{Sr}$ value of 0.7126 ± 0.0012 , a weighted average corrected $^{87}\text{Sr}/^{86}\text{Sr}$ value of 0.71200 ± 0.0012 and a weighted average $^{84}\text{Sr}/^{86}\text{Sr}$ value of 0.05656 ± 0.00013 . The dentine spots of track 2 have an average ^{88}Sr voltage of 0.585, a weighted average uncorrected $^{87}\text{Sr}/^{86}\text{Sr}$ value of 0.7108 ± 0.0013 , a weighted average corrected $^{87}\text{Sr}/^{86}\text{Sr}$ value of 0.71030 ± 0.0013 and a weighted average $^{84}\text{Sr}/^{86}\text{Sr}$ value of 0.05654 ± 0.00016 . Enamel values for track 1 are in the range of 0.711340 to 0.717378 (uncorrected), as well as 0.710754 to 0.712692 (corrected), and they are relatively heterogeneous. Enamel values for track 2 are in the range of 0.711775 to 0.720176 (corrected), as well as 0.711189 to 0.719590 (corrected), and are relatively homogeneous, with the exception of spot 11. Dentine values for track 1 are in the range of 0.709621 to 0.714920 (uncorrected), as well as 0.709065 to 0.714363 (corrected), and are relatively heterogeneous, particularly spots 3 through 5. Dentine values for track 2 are in the range of 0.709799 to 0.720176 (uncorrected), as well as 0.709242 to 0.719590 (corrected), and are relatively homogenous, with the exception of spot 8. Detailed values for enamel and dentine for sample M017 are shown in Table A3.83, Figure A3.143 and Figure A3.144.

Enamel for this sample is in the range of 0.711340 ± 0.000593 to 0.720176 ± 0.001181 (uncorrected) and 0.710754 ± 0.000593 to 0.719590 ± 0.001181

(corrected), this high degree of variability suggests that this specimen was extremely mobile during amelogenesis. Three enamel spots have values that are significantly elevated compared to the other values; spot 1 and 6 from track 1 and spot 11 of track 2. Spot 1 from track 1 has an uncorrected $^{87}\text{Sr}/^{86}\text{Sr}$ value of 0.717378 ± 0.000836 , which corresponds to 3 possible values in the mapping area. These include those of FS037-S1, with a value of 0.717308 ± 0.000012 , located in an Upper Cretaceous carbonate and siliciclastic unit, FS041-S1, with a value of 0.716805 ± 0.000038 , located on a floodplain and FS067-S1, with a value of 0.717422 ± 0.00001 , located in a Carboniferous monzogranite/granodiorite. As discussed with reference to sample M015 above, it is unlikely that FS037-S1 contributed to regional bioavailable values. The corrected value of the same spot is 0.712692 ± 0.000836 , which corresponds to Dordogne floodplain samples, including FS035-S1, FS056-S1 and FS058-S1. This floodplain outcrops within 4.2 km of the site. There is a domain of enamel spots that have an intermediate $^{87}\text{Sr}/^{86}\text{Sr}$ value, including spot 2 of track 1 and spot 1 and 6 of track 2, which have a weighted average uncorrected value of 0.71316 ± 0.00031 . This value corresponds to 2 mapping samples from the floodplain of the Dordogne near the site of Les Fieux: FS058-S1 (0.713898 ± 0.000031) and FS035-S1 (0.713096 ± 0.000014), which are 20 km north-east and 33 km east-south-east, respectively, from the site. This intermediate domain has a corrected weighted average value of 0.71257 ± 0.00031 , which correlates with mapping sample FS054-S1 from a Cambrian metamorphic unit east and north from the site. There is a final domain of enamel values, including spot 7, 8 and 9 from track 1 and spot 2, 5, 12, 13 and 14 from track 2 that has a weighted average uncorrected value of 0.71189 ± 0.00018 . This corresponds to the mapping value from FS056-S1 (0.711984 ± 0.000018), a location on the Dordogne floodplain approximately 30 km north-east of Les Fieux. The corrected values from this final domain have a weighted average value of 0.71135 ± 0.00016 , which does not correlate with any mapping samples in this study. The degree of heterogeneity in the dentine suggests a complicated regime of post-burial diagenesis. The enamel and dentine spots have an overall weighted average value of 0.056604 ± 0.000065 , suggesting they have robust $^{87}\text{Sr}/^{86}\text{Sr}$ values.



Figure A3.142 LA-MC-ICPMS Track for Sample M017, Bison, Layer G7, Les Fieux

Sample	Material	Track	Point	^{88}Sr Volts	$^{84}\text{Sr}/^{86}\text{Sr}$	$^{84}\text{Sr}/^{86}\text{Sr}$ 2 σ	Corrected $^{87}\text{Sr}/^{86}\text{Sr}$	$^{87}\text{Sr}/^{86}\text{Sr}$ 2 σ
M017	Enamel	1	1	0.452	0.056507	0.000379	0.717378	0.712692
M017	Enamel	1	2	0.511	0.056890	0.000347	0.712925	0.712339
M017	Dentine	1	3	0.560	0.056368	0.000357	0.713249	0.716792
M017	Dentine	1	4	0.583	0.056761	0.000340	0.714920	0.714363
M017	Dentine	1	5	0.537	0.057019	0.000531	0.711412	0.710855
M017	Enamel	1	6	0.447	0.056501	0.000448	0.714607	0.714021
M017	Enamel	1	7	0.498	0.056457	0.000433	0.711340	0.710754
M017	Enamel	1	8	0.538	0.056572	0.000343	0.711895	0.711309
M017	Enamel	1	9	0.583	0.056520	0.000325	0.711960	0.711373
M017	Dentine	1	10	0.554	0.056601	0.000392	0.710440	0.709883

Sample	Material	Track	Point	^{88}Sr Volts	$^{84}\text{Sr}/^{86}\text{Sr}$	$^{84}\text{Sr}/^{86}\text{Sr} 2\sigma$ Error	$^{87}\text{Sr}/^{86}\text{Sr}$	Corrected $^{87}\text{Sr}/^{86}\text{Sr}$	$^{87}\text{Sr}/^{86}\text{Sr} 2\sigma$ Error
M017	Dentine	1	11	0.599	0.056775	0.000375	0.709812	0.709255	0.000318
M017	Dentine	1	12	0.484	0.056683	0.000343	0.710608	0.710052	0.000468
M017	Dentine	1	13	0.533	0.056829	0.000302	0.710791	0.710234	0.000382
M017	Dentine	1	14	0.749	0.056784	0.000191	0.709621	0.709065	0.000464
M017	Dentine	1	15	0.505	0.056659	0.000310	0.710153	0.709596	0.000501
M017	Dentine	1	16	0.612	0.056481	0.000318	0.710399	0.709842	0.000449
M017	Enamel	2	1	0.471	0.056732	0.000457	0.713080	0.712493	0.000603
M017	Enamel	2	2	0.535	0.056536	0.000305	0.711988	0.711402	0.000518
M017	Dentine	2	3	0.616	0.056710	0.000287	0.710067	0.709511	0.000444
M017	Dentine	2	4	0.503	0.056548	0.000362	0.710743	0.710186	0.000590
M017	Enamel	2	5	0.636	0.056626	0.000331	0.712210	0.711624	0.000486
M017	Enamel	2	6	0.572	0.056665	0.000374	0.713376	0.712790	0.000495
M017	Dentine	2	7	0.795	0.056402	0.000264	0.710274	0.709717	0.000545
M017	Dentine	2	8	0.524	0.056772	0.000448	0.717674	0.717117	0.000644
M017	Dentine	2	9						
M017	Dentine	2	10						
M017	Enamel	2	11	0.430	0.056341	0.000748	0.720176	0.719590	0.001181
M017	Enamel	2	12	0.530	0.056779	0.000425	0.712253	0.711667	0.000520
M017	Enamel	2	13	0.567	0.056475	0.000272	0.711775	0.711189	0.000508
M017	Enamel	2	14	0.582	0.056248	0.000413	0.711995	0.711409	0.000568
M017	Dentine	2	15	0.515	0.056300	0.000407	0.710900	0.710343	0.000520
M017	Dentine	2	16	0.632	0.056950	0.000301	0.710514	0.709957	0.000502
M017	Dentine	2	17	0.554	0.056318	0.000345	0.711385	0.710828	0.000494
M017	Dentine	2	18	0.742	0.056447	0.000236	0.710321	0.709764	0.000392
M017	Dentine	2	19	0.537	0.056283	0.000436	0.709799	0.709242	0.000442
M017	Dentine	2	20	0.435	0.056596	0.000417	0.709967	0.709410	0.000550

Table A3.83 Detailed LA-MC-ICPMS Sr Isotope Results for Dentine and Enamel, Sample M017, Bison, Layer G7, Les Fieux

Sample M017, Les Fieux, France

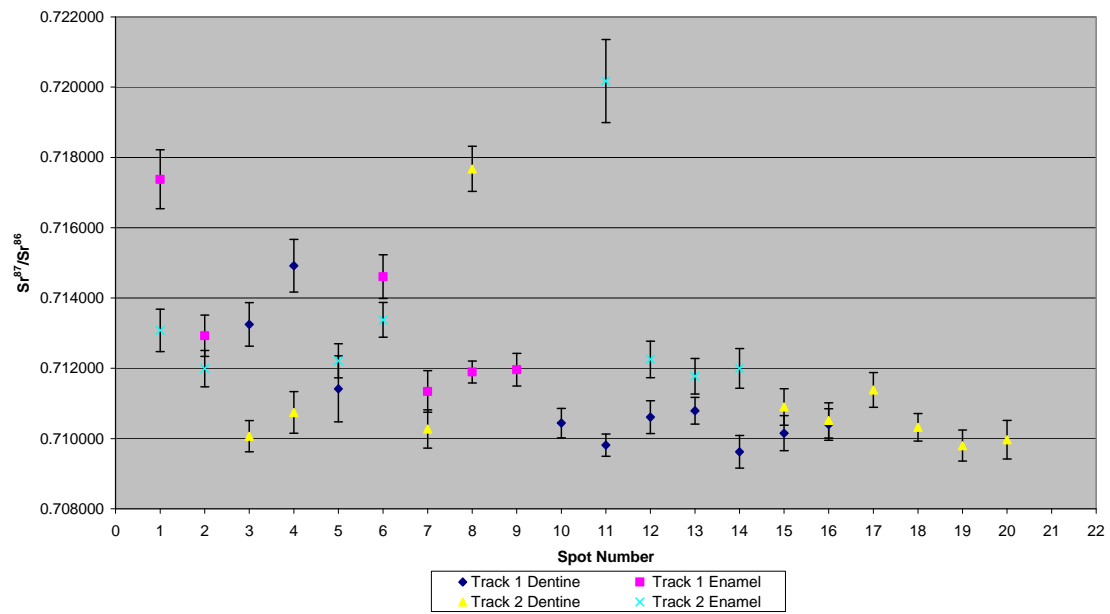


Figure A3.143 Detailed LA-MC-ICPMS Uncorrected Sr Isotope Results, Sample M017, Bison, Layer G7, Les Fieux

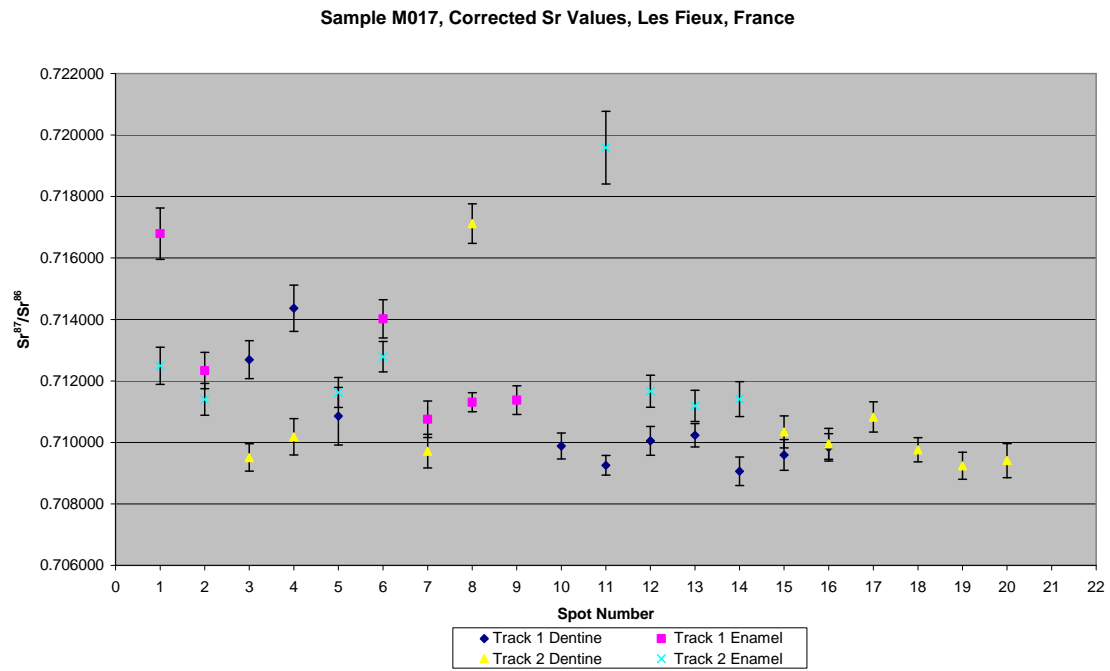


Figure A3.144 Detailed LA-MC-ICPMS Corrected Sr Isotope Results, Sample M017, Bison, Layer G7, Les Fieux

Sample M018, a reindeer from layer G7 of Les Fieux shown in Figure A2.48, was analysed in 2 tracks, with track 1 comprising 5 spots of dentine and track 2 comprising 2 spots of enamel and 4 spots of dentine, shown in Figure A3.145. The results from this sample are summarised in Table 5.30 and Figure 5.18. The dentine spots of track 1 have an average ^{88}Sr voltage of 0.344, a weighted average uncorrected $^{87}\text{Sr}/^{86}\text{Sr}$ value of 0.71025 ± 0.00037 , a weighted average corrected $^{87}\text{Sr}/^{86}\text{Sr}$ value of 0.70861 ± 0.00037 and a weighted average $^{84}\text{Sr}/^{86}\text{Sr}$ value of 0.05689 ± 0.00026 ($n=5$). The enamel spots of track 2 have an average ^{88}Sr voltage of 0.100, a weighted average uncorrected $^{87}\text{Sr}/^{86}\text{Sr}$ value of 0.7140 ± 0.0014 , a weighted average corrected $^{87}\text{Sr}/^{86}\text{Sr}$ value of 0.69910 ± 0.0014 and a weighted average $^{84}\text{Sr}/^{86}\text{Sr}$ value of 0.059 ± 0.012 ($n=2$). The dentine spots of track 2 have an average ^{88}Sr voltage of 0.292, a weighted average uncorrected $^{87}\text{Sr}/^{86}\text{Sr}$ value of 0.70978 ± 0.00041 , a weighted average corrected $^{87}\text{Sr}/^{86}\text{Sr}$ value of 0.70814 ± 0.00041 and a weighted average $^{84}\text{Sr}/^{86}\text{Sr}$ value of 0.05715 ± 0.00087 ($n=4$). Dentine values for track 1 are in the range of 0.709752 to 0.710717 (uncorrected), as well as 0.708108 to 0.709074 (corrected), and are very heterogeneous, all being within 2σ error. Enamel values for track 2 are in the range of 0.713704 to 0.715212 (uncorrected), as well as 0.698800 to 0.700307 (corrected), and while the average values are somewhat homogenous, the high error of these samples means that they are heterogeneous within 2σ error. Dentine values for track 2 are in the range of 0.709334 to 0.710324 (uncorrected), as well as 0.707690 to 0.708680 (corrected), and are heterogeneous within 2σ error. Detailed values for enamel and dentine for sample M018 are shown in Table A3.84, Figure A3.146 and Figure A3.147.

This sample shows a significant difference between the $^{87}\text{Sr}/^{86}\text{Sr}$ values of enamel and dentine as summarised in Table 5.24 and Figure 5.18 and shown in detail in Table A3.84, Figure A3.146 and Figure A3.147. The 2 enamel spots have values that are within 2σ error. The errors on these samples are too high to allow effective characterisation of the location of these samples during amelogenesis, probably due to the low voltages during acquisition (0.078 and

0.122 Sr⁸⁸ volts). Dentine values are very heterogeneous, in the range of 0.709334 ± 0.001064 to 0.710717 ± 0.000855.

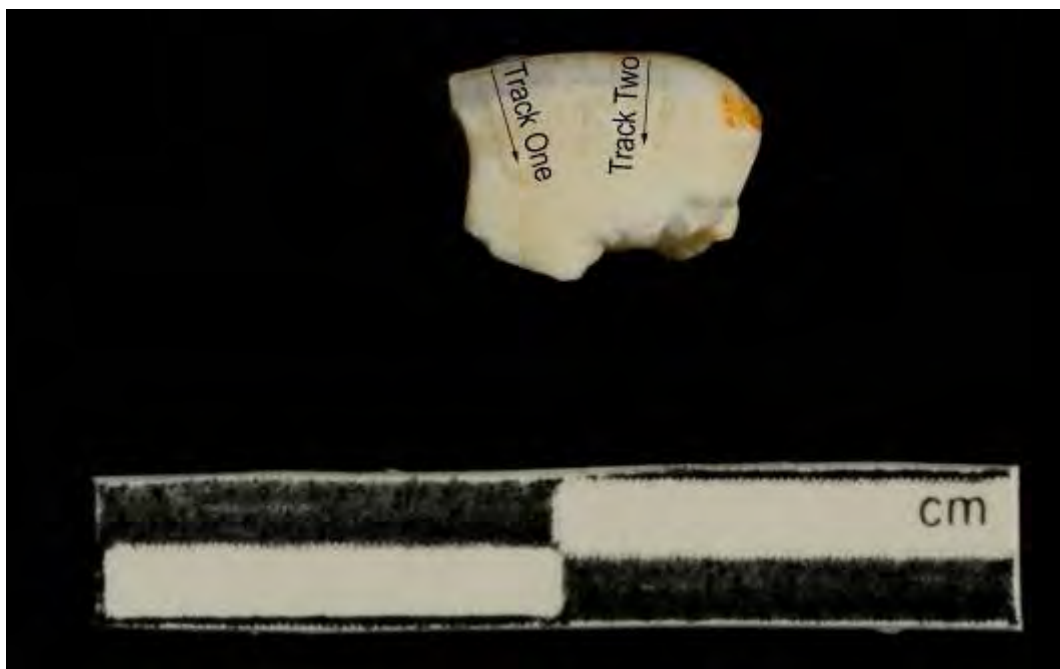


Figure A3.145 LA-MC-ICPMS Track for Sample M018, Reindeer, Layer G7, Les Fieux

Sample	Material	Track	Point	⁸⁸ Sr Volts	⁸⁴ Sr/ ⁸⁶ Sr	Corrected ⁸⁷ Sr/ ⁸⁶ Sr	⁸⁷ Sr/ ⁸⁶ Sr Error	⁸⁷ Sr/ ⁸⁶ Sr 2σ	⁸⁷ Sr/ ⁸⁶ Sr Error
M018		1	1						
M018		1	2						
M018	Dentine	1	3	0.323	0.056775	0.000668	0.709752	0.708108	0.000868
M018	Dentine	1	4	0.342	0.056981	0.000583	0.710095	0.708451	0.000748
M018	Dentine	1	5	0.351	0.056810	0.000669	0.710717	0.709074	0.000855
M018	Dentine	1	6	0.377	0.057011	0.000701	0.710072	0.708428	0.000997
M018	Dentine	1	7	0.327	0.056858	0.000475	0.710573	0.708929	0.000815
M018	Enamel	2	1	0.078	0.060580	0.002391	0.715212	0.700307	0.003360
M018	Enamel	2	2	0.122	0.058576	0.001571	0.713704	0.698800	0.001601
M018	Dentine	2	3	0.280	0.056376	0.000826	0.709334	0.707690	0.001064
M018	Dentine	2	4	0.293	0.057778	0.000875	0.709616	0.707972	0.000840
M018	Dentine	2	5	0.317	0.057220	0.000818	0.709648	0.708004	0.000732
M018	Dentine	2	6	0.279	0.057260	0.000691	0.710324	0.708680	0.000785

Table A3.84 Detailed LA-MC-ICPMS Sr Isotope Results, Sample M018, Reindeer, Layer G7, Les Fieux

Sample M018, Les Fieux, France

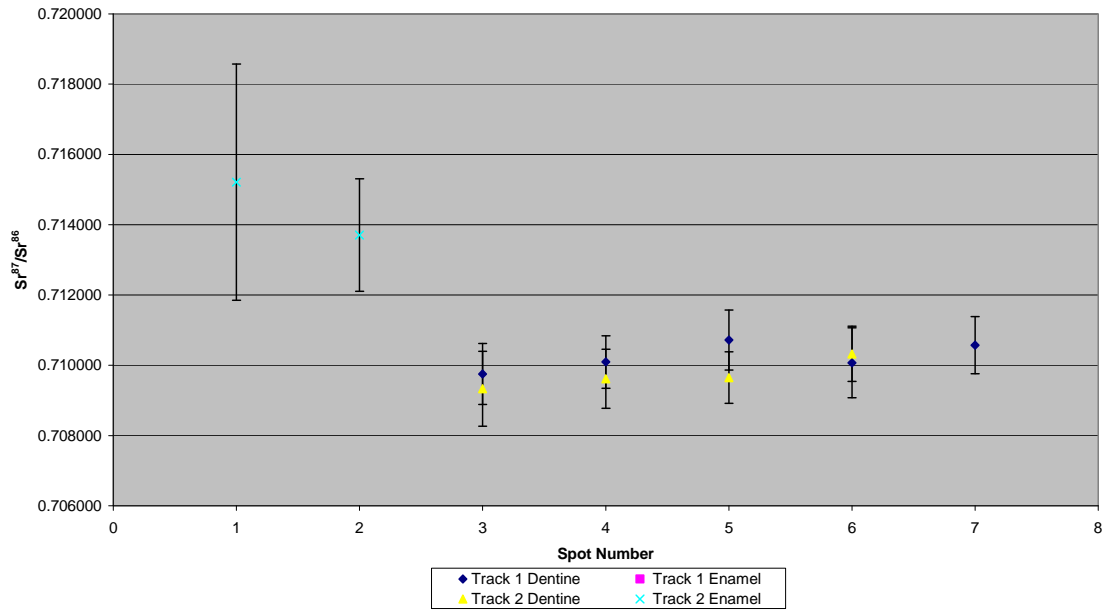


Figure A3.146 Detailed LA-MC-ICPMS Uncorrected Sr Isotope Results, Sample M018, Reindeer, Layer G7, Les Fieux

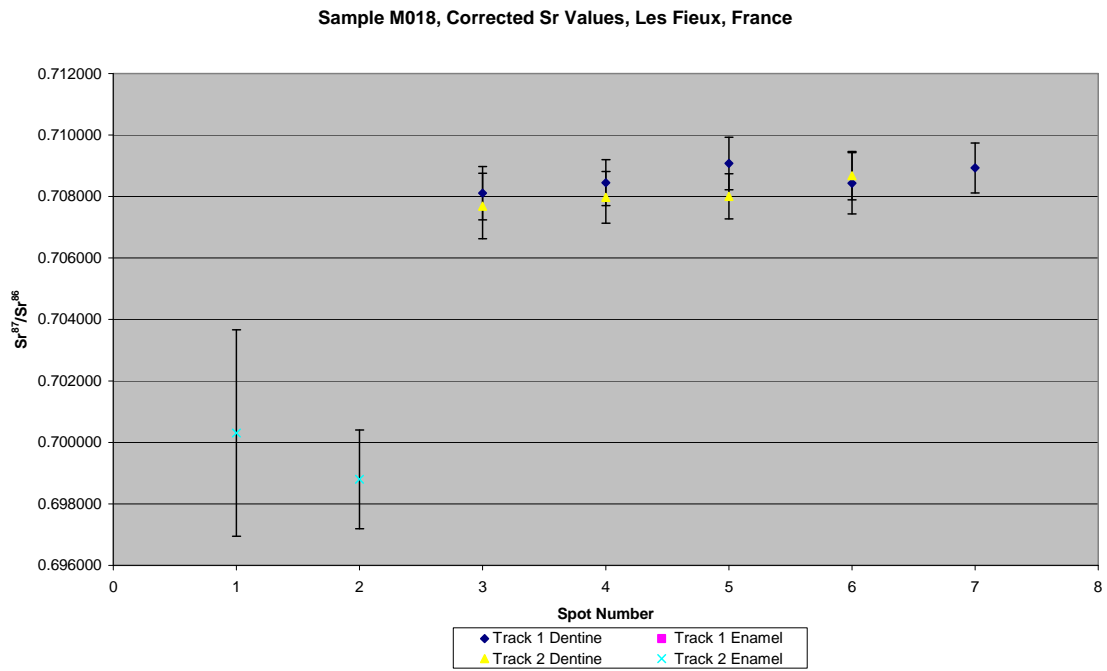


Figure A3.147 Detailed LA-MC-ICPMS Corrected Sr Isotope Results, Sample M018, Reindeer, Layer G7, Les Fieux

Sample M019, a reindeer from layer G7 from Les Fieux shown in Figure A2.49, was analysed in 2 tracks, with track 1 comprising 2 spots of enamel and 4 spots of dentine and track 2 comprising 4 spots of enamel and 6 spots of dentine, shown in Figure A3.148. The results from this sample are summarised in Table 5.30 and Figure 5.18. The enamel spots of track 1 have an average ^{88}Sr voltage of 0.239, a weighted average uncorrected $^{87}\text{Sr}/^{86}\text{Sr}$ value of 0.711 ± 0.011 , a weighted average corrected $^{87}\text{Sr}/^{86}\text{Sr}$ value of 0.70900 ± 0.011 and a weighted average $^{84}\text{Sr}/^{86}\text{Sr}$ value of 0.05677 ± 0.00056 ($n=2$). The dentine spots of track 1 have an average ^{88}Sr voltage of 0.432, a weighted average uncorrected $^{87}\text{Sr}/^{86}\text{Sr}$ value of 0.70952 ± 0.00091 , a weighted average corrected $^{87}\text{Sr}/^{86}\text{Sr}$ value of 0.70876 ± 0.00091 and a weighted average $^{84}\text{Sr}/^{86}\text{Sr}$ value of 0.05657 ± 0.00022 ($n=4$). The enamel spots of track 2 have an average ^{88}Sr voltage of 0.339, a weighted average uncorrected $^{87}\text{Sr}/^{86}\text{Sr}$ value of 0.7127 ± 0.0027 , a weighted average corrected $^{87}\text{Sr}/^{86}\text{Sr}$ value of 0.71080 ± 0.0027 and a weighted average $^{84}\text{Sr}/^{86}\text{Sr}$ value of 0.05637 ± 0.00042 ($n=4$). The dentine spots of track 2 have an average ^{88}Sr voltage of 0.521, a weighted average uncorrected $^{87}\text{Sr}/^{86}\text{Sr}$ value of 0.7109 ± 0.0023 , a weighted average corrected $^{87}\text{Sr}/^{86}\text{Sr}$ value of 0.71020 ± 0.0023 and a weighted average $^{84}\text{Sr}/^{86}\text{Sr}$ value of 0.05641 ± 0.00017 ($n=6$). Enamel values for track 1 are in the range of 0.710020 to 0.711827 (uncorrected), as well as 0.708148 to 0.709955 (corrected), with the values being somewhat homogenous, just outside of 2σ error. Dentine values for track 1 are in the range of 0.708958 to 0.710437 (uncorrected), as well as 0.708198 to 0.709678 (corrected), and are slightly heterogeneous, being just outside of 2σ error. Enamel values for track 2 are in the range of 0.711817 to 0.716770 (uncorrected), as well as 0.709945 to 0.714898 (corrected), and are moderately homogeneous, with the exception of spot 1, which is elevated in value compared to the other spots. Dentine values for track 2 are in the range of 0.709077 to 0.726637 (uncorrected), as well as 0.708318 to 0.725878 (corrected), which are somewhat heterogeneous, being just outside of 2σ error, with the exception of spot 10, which is significantly elevated compared to all other values in sample M019. Detailed values for enamel and dentine for sample M019 are shown in Table A3.85, Figure A3.149 and Figure A3.150.

This sample has enamel and dentine $^{87}\text{Sr}/^{86}\text{Sr}$ values that, with the exception of outliers, are overlapping in range. Spot 1 from track 2 is elevated compared to the other enamel spots in this sample, with an uncorrected value of 0.716770 ± 0.001352 . This value corresponds to a number of mapping sites, including FS037-S1 with a value of 0.717308 ± 0.000012 located in a Upper Cretaceous carbonate and siliciclastic unit, FS041-S1 with a value of 0.716805 ± 0.000038 located on a floodplain and FS067-S1 with a value of 0.717422 ± 0.00001 located in a Carboniferous monzogranite/granodiorite. As discussed with reference to sample M015, it is unlikely that location FS037-S1 represents the source of this enamel value. The corrected value for the same spot is 0.714898 ± 0.001352 , which correlates with floodplain samples FS031-S1 and FS046-S1. Spot 2, 3 and 4 from track 2 are within the same domain of values, all being within 2σ error, and have a weighted average uncorrected value of 0.71211 ± 0.00042 . This corresponds to the mapping value from a number of locations, including FS056-S1 (0.711984 ± 0.000018) from the Dordogne floodplain, FS054-S1 (0.712245 ± 0.000026) from a Cambrian metamorphic unit and FS036-S1 (0.712053 ± 0.000025), which is alluvial valley fill. The corrected value of this domain is 0.71029 ± 0.00046 , which corresponds to mapping values such as FS052-S2 from the Lower Jurassic carbonate unit, which outcrops south, east and north of the site within a minimum distance of 2.8 km. Spot 2 of track 1 has the much less radiogenic uncorrected $^{87}\text{Sr}/^{86}\text{Sr}$ value of 0.710020 ± 0.000758 , which corresponds to the local area of Les Fieux (sample FS047-S4), which has a value of 0.79697 ± 0.000025 . The corrected value of this spot is 0.708148 ± 0.000758 , which corresponds to mapping values such as FS049-S1, FS051-S1 and FS074-S1 from lower and upper Jurassic carbonates to the south-east and west of the site. The dentine value from spot 10 on track 2 is extremely elevated compared to the others samples in this track, which given its position on the edge of the sample suggests that the laser is not correctly focused (as discussed above with reference to sample M008).



Figure A3.148 LA-MC-ICPMS Track for Sample M019, Reindeer, Layer G7, Les Fieux

Sample	Material	Track	Point	^{88}Sr Volts	$^{84}\text{Sr}/^{86}\text{Sr}$	Corrected $^{87}\text{Sr}/^{86}\text{Sr}$	$^{87}\text{Sr}/^{86}\text{Sr}$ Error	$^{87}\text{Sr}/^{86}\text{Sr} 2\sigma$
M019	Enamel	1	1	0.200	0.057102	0.001142	0.711827	0.709955
M019	Enamel	1	2	0.279	0.056655	0.000659	0.710020	0.708148
M019	Dentine	1	3	0.345	0.056246	0.000616	0.710437	0.709678
M019	Dentine	1	4	0.476	0.056405	0.000437	0.709733	0.708973
M019	Dentine	1	5	0.459	0.056676	0.000415	0.708958	0.708198
M019	Dentine	1	6	0.447	0.056737	0.000404	0.709457	0.708697
M019	Enamel	2	1	0.241	0.056809	0.001109	0.716770	0.714898
M019	Enamel	2	2	0.315	0.056614	0.000685	0.712335	0.710463
M019	Enamel	2	3	0.411	0.055806	0.000834	0.712191	0.710319
M019	Enamel	2	4	0.389	0.056315	0.000985	0.711817	0.709945
M019	Dentine	2	5	0.474	0.056340	0.000488	0.711449	0.710689
M019	Dentine	2	6	0.487	0.056027	0.000403	0.711935	0.711175
M019	Dentine	2	7	0.487	0.056488	0.000479	0.711965	0.711206
M019	Dentine	2	8	0.424	0.056562	0.000633	0.710983	0.710224
M019	Dentine	2	9	0.486	0.056711	0.000470	0.709077	0.708318
M019	Dentine	2	10	0.765	0.056469	0.000284	0.726637	0.725878
								0.003110

Table A3.85 Detailed LA-MC-ICPMS Sr Isotope Results, Sample M019, Reindeer, Layer G7, Les Fieux

Sample M019, Les Fieux, France

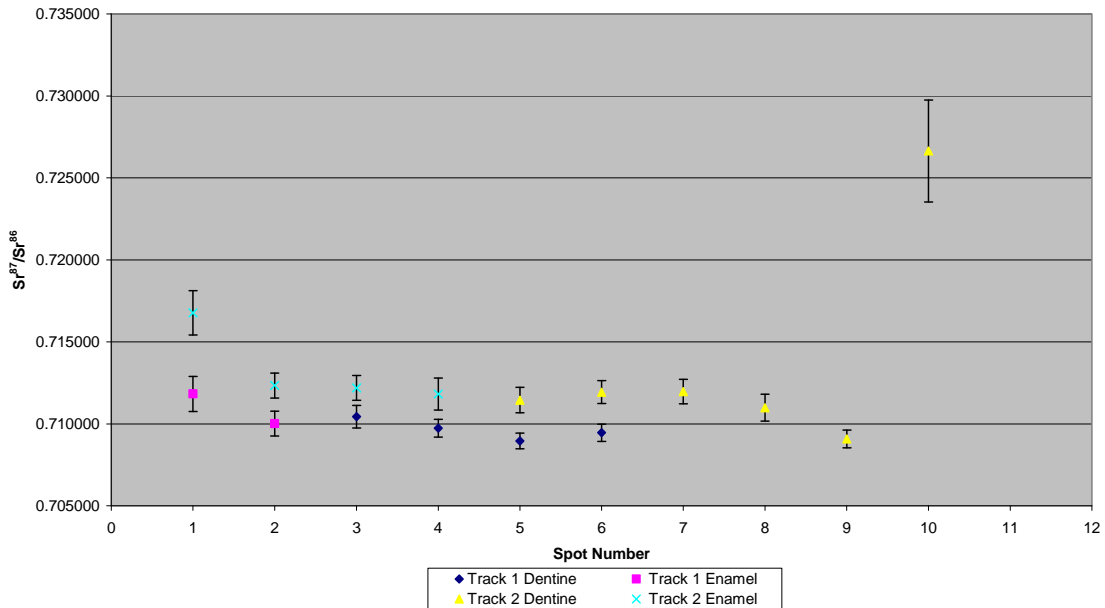


Figure A3.149 Detailed LA-MC-ICPMS Uncorrected Sr Isotope Results, Sample M019, Reindeer, Layer G7, Les Fieux

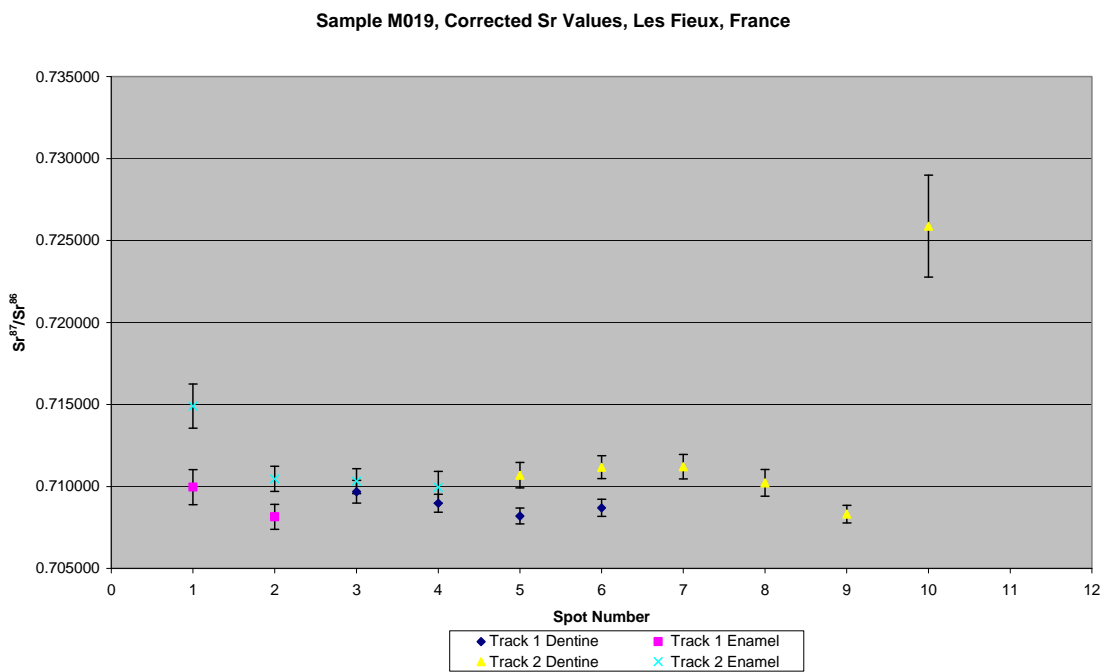


Figure A3.150 Detailed LA-MC-ICPMS Corrected Sr Isotope Results, Sample M019, Reindeer, Layer G7, Les Fieux

Sample M020, a chamois from layer G7 of Les Fieux, was analysed in 2 tracks, with track 1 comprising 2 spots of enamel and 3 spots of dentine and track 2 comprising 8 spots of enamel in 2 discontinuous sections and 3 spots of dentine, shown in Figure A3.151. The results from this sample are summarised in Table 5.30 and Figure 5.18. The enamel spots of track 1 have an average ^{88}Sr voltage of 0.191, a weighted average uncorrected $^{87}\text{Sr}/^{86}\text{Sr}$ value of 0.712 ± 0.019 , a weighted average corrected $^{87}\text{Sr}/^{86}\text{Sr}$ value of 0.70900 ± 0.019 and a weighted average $^{84}\text{Sr}/^{86}\text{Sr}$ value of 0.0561 ± 0.0073 ($n=2$). The dentine spots of track 1 have an average ^{88}Sr voltage of 0.240, a weighted average uncorrected $^{87}\text{Sr}/^{86}\text{Sr}$ value of 0.7100 ± 0.0014 , a weighted average corrected $^{87}\text{Sr}/^{86}\text{Sr}$ value of 0.70800 ± 0.0014 and a weighted average $^{84}\text{Sr}/^{86}\text{Sr}$ value of 0.0563 ± 0.0012 ($n=3$). The enamel spots of track 2 have an average ^{88}Sr voltage of 0.245, a weighted average uncorrected $^{87}\text{Sr}/^{86}\text{Sr}$ value of 0.7107 ± 0.0014 , a weighted average corrected $^{87}\text{Sr}/^{86}\text{Sr}$ value of 0.70840 ± 0.0014 and a weighted average $^{84}\text{Sr}/^{86}\text{Sr}$ value of 0.05614 ± 0.00034 ($n=8$). The dentine spots of track 2 have an average ^{88}Sr voltage of 0.298, a weighted average uncorrected $^{87}\text{Sr}/^{86}\text{Sr}$ value of 0.71006 ± 0.00052 , a weighted average corrected $^{87}\text{Sr}/^{86}\text{Sr}$ value of 0.70794 ± 0.00052 and a weighted average $^{84}\text{Sr}/^{86}\text{Sr}$ value of 0.0560 ± 0.0011 . Enamel values for track 1 are 0.710363 and 0.713435 (uncorrected), as well as 0.708075 and 0.711148, and the samples are moderately heterogeneous, being just outside of 2σ error. Dentine values are in the range of 0.709377 to 0.710482 (uncorrected), as well as 0.707361 to 0.708465 (corrected), and are relatively homogeneous, all being within 2σ error and decreasing in value from spot 4 to 6. Enamel values for track 2 are in the range of 0.709638 to 0.717025 (uncorrected), as well as 0.707350 to 0.714738 (corrected), and are heterogeneous for spot 1 and spot 2 and homogenous for spots 3 to 5 and 9 to 11. Dentine values for track 2 are in the range of 0.709762 to 0.710101 (uncorrected), as well as 0.707746 to 0.708084 (corrected), and are homogenous, being within 2σ error. Detailed values for enamel and dentine for sample M020 are shown in Table A3.86, Figure A3.152 and Figure A3.153.

The enamel $^{87}\text{Sr}/^{86}\text{Sr}$ values for this sample from spot 2 for track 1 and spots 1 and 2 for track 2 are heterogeneous, with uncorrected values of 0.713435 ± 0.001593 , 0.717025 ± 0.002145 and 0.714558 ± 0.001577 , respectively. The

error of these values is too high to correlate these values to mapping locations. The remaining enamel spots are homogeneous within 2σ error, with a weighted average uncorrected value of 0.71032 ± 0.00036 , which corresponds to the value of the Dordogne floodplain at mapping location FS044-S1 (0.710436 ± 0.000012). The weighted average corrected value of these spots is 0.70803 ± 0.00036 , which correlates to lower and upper Jurassic and Oligocene carbonate sediments outcropping to the south of the site, such as from sample sites FS074-S1, FS085-S1 and FS083-S1 within a mime distance of 2.8 km. The presence of divergent enamel values suggests that the specimen was a migrant at some stage during amelogenesis but also lived in the local area. Dentine values suggest relatively homogenous post-burial diagenesis. $^{84}\text{Sr}/^{86}\text{Sr}$ values have a weighted average value of 0.05612 ± 0.00022 , which is considerably less than the ideal value of 0.0656, suggesting that the $^{87}\text{Sr}/^{86}\text{Sr}$ values for this sample are not robust.

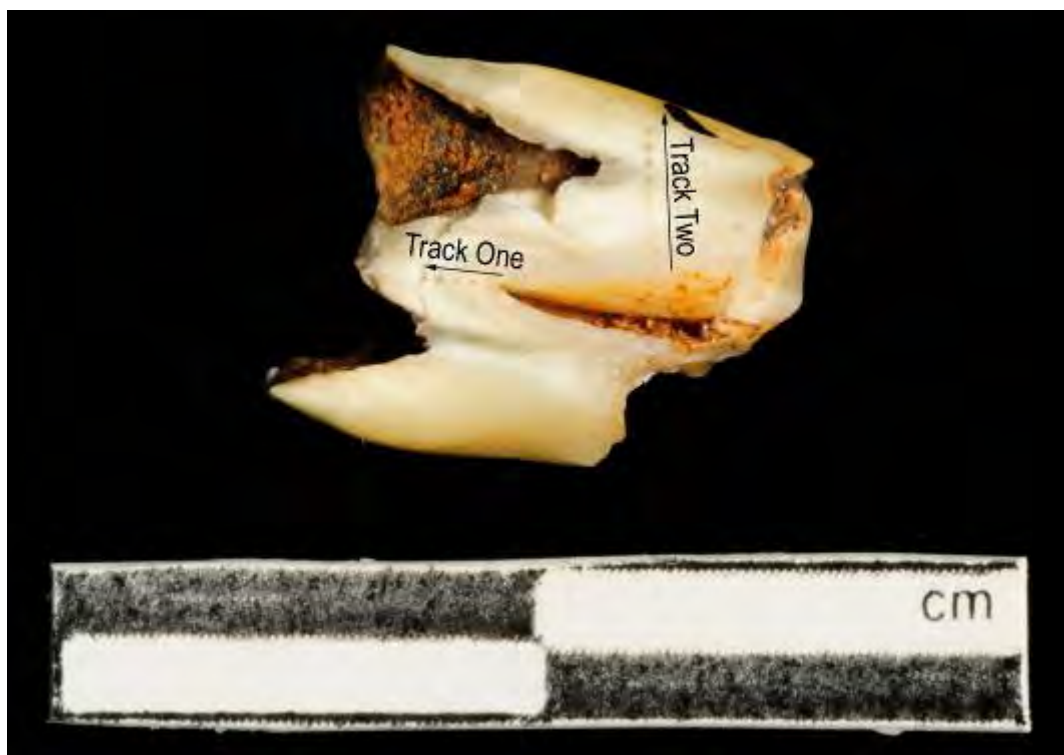


Figure A3.151 LA-MC-ICPMS Track for Sample M020, Chamois, Layer G7, Les Fieux

Sample	Material	Track	Point	^{88}Sr Volts	$^{84}\text{Sr}/^{86}\text{Sr}$	Error	$^{87}\text{Sr}/^{86}\text{Sr}$	Corrected $^{87}\text{Sr}/^{86}\text{Sr}$	$^{87}\text{Sr}/^{86}\text{Sr} 2\sigma$ Error
M020	Enamel	1	1						
M020	Enamel	1	2	0.142	0.054640	0.001683	0.713435	0.711148	0.001593
M020	Enamel	1	3	0.239	0.056346	0.000646	0.710363	0.708075	0.001227
M020	Dentine	1	4	0.249	0.056281	0.000870	0.710482	0.708465	0.000792
M020	Dentine	1	5	0.222	0.056815	0.000930	0.709953	0.707937	0.000899
M020	Dentine	1	6	0.250	0.055807	0.000815	0.709377	0.707361	0.000904
M020	Enamel	2	1	0.098	0.056709	0.002314	0.717025	0.714738	0.002145
M020	Enamel	2	2	0.125	0.055336	0.001799	0.714558	0.712271	0.001577
M020	Enamel	2	3	0.247	0.056328	0.001243	0.710170	0.707883	0.001242
M020	Enamel	2	4	0.263	0.055813	0.001014	0.711299	0.709011	0.000869
M020	Enamel	2	5	0.311	0.055921	0.000789	0.710099	0.707811	0.000847
M020	Dentine	2	6	0.299	0.056075	0.000673	0.709762	0.707746	0.000779
M020	Dentine	2	7	0.318	0.056320	0.000774	0.710101	0.708084	0.000666
M020	Dentine	2	8	0.277	0.055395	0.000910	0.709968	0.707952	0.000903
M020	Enamel	2	9	0.256	0.056229	0.000770	0.710290	0.708003	0.000960
M020	Enamel	2	10	0.308	0.056266	0.000728	0.710114	0.707826	0.000763
M020	Enamel	2	11	0.349	0.056440	0.000986	0.709638	0.707350	0.001133

Table A3.86 Detailed LA-MC-ICPMS Sr Isotope Results, Sample M020, Chamois, Layer G7, Les Fieux

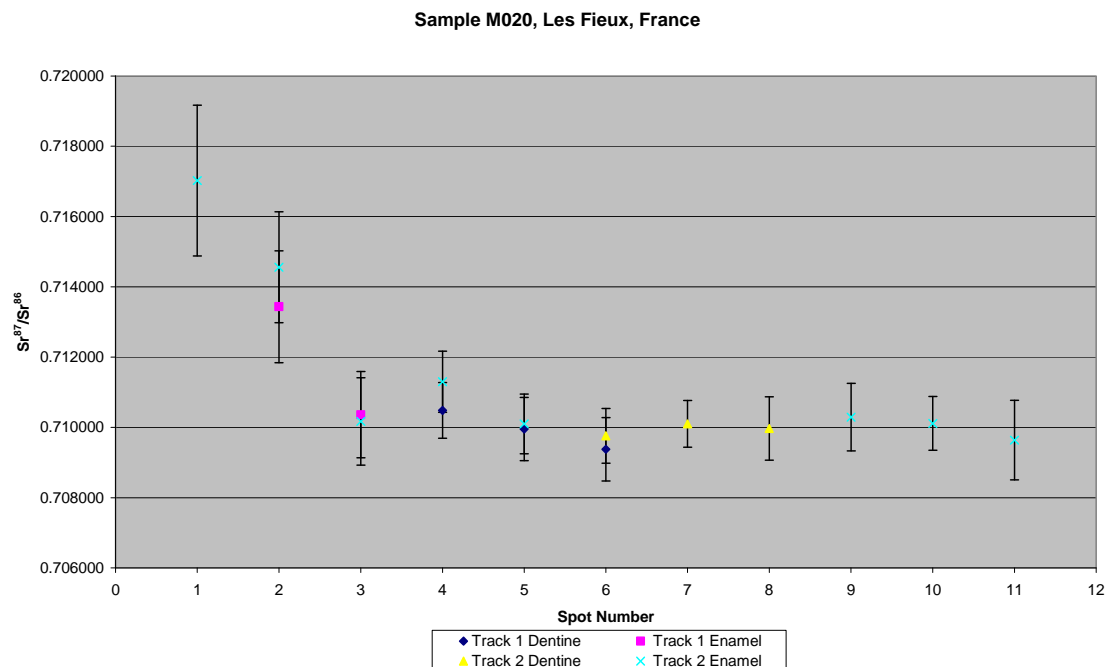


Figure A3.152 Detailed LA-MC-ICPMS Uncorrected Sr Isotope Results, Sample M020, Chamois, Layer G7, Les Fieux

Sample M020, Corrected Sr Values, Les Fieux, France

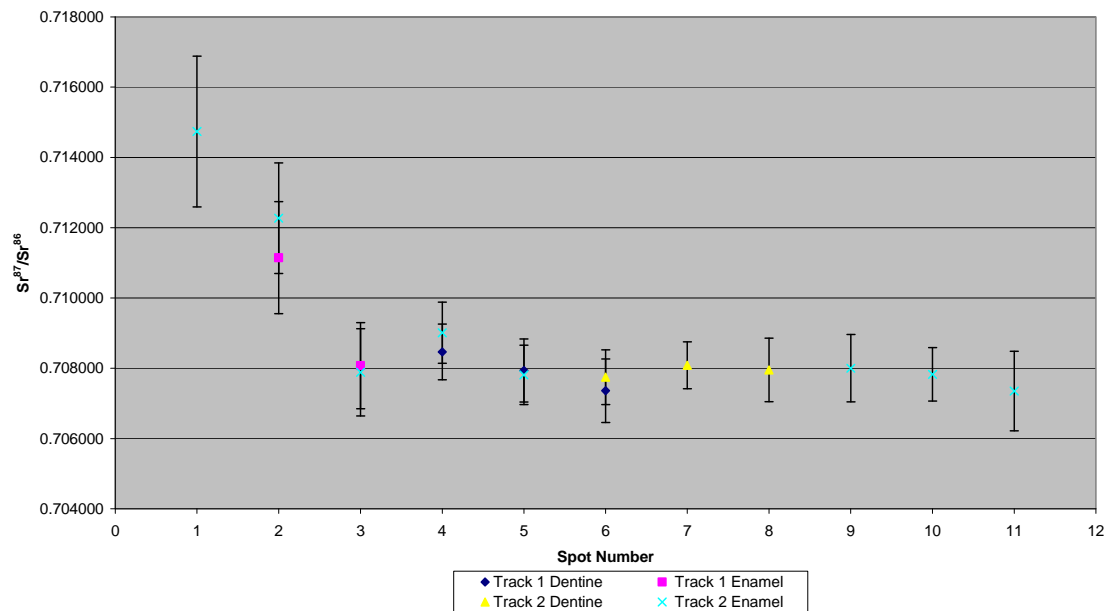


Figure A3.153 Detailed LA-MC-ICPMS Corrected Sr Isotope Results, Sample M020, Chamois, Layer G7, Les Fieux

Sample M021, a mountain goat/chamois from layer G7 from Les Fieux shown in Figure A2.51, was analysed in 3 tracks, with track 1 comprising 2 spots of enamel and 7 spots of dentine, track 2 comprising 8 spots of enamel in 3 discontinuous sections and 3 spots of dentine and track 3 comprising 2 spots of enamel and 4 spots of dentine, shown in Figure A3.155. The results from this sample are summarised in Table 5.30 and Figure 5.18. The enamel spots of track 1 have an average ^{88}Sr voltage of 0.471, a weighted average uncorrected $^{87}\text{Sr}/^{86}\text{Sr}$ value of 0.712 ± 0.013 , a weighted average corrected $^{87}\text{Sr}/^{86}\text{Sr}$ value of 0.71100 ± 0.013 and a weighted average $^{84}\text{Sr}/^{86}\text{Sr}$ value of 0.05644 ± 0.00043 ($n=2$). The dentine spots of track 1 have an average ^{88}Sr voltage of 0.269, a weighted average uncorrected $^{87}\text{Sr}/^{86}\text{Sr}$ value of 0.7106 ± 0.0021 , a weighted average corrected $^{87}\text{Sr}/^{86}\text{Sr}$ value of 0.70890 ± 0.0021 and a weighted average $^{84}\text{Sr}/^{86}\text{Sr}$ value of 0.05636 ± 0.00026 ($n=7$). The enamel spots of track 2 have an average ^{88}Sr voltage of 0.428, a weighted average uncorrected $^{87}\text{Sr}/^{86}\text{Sr}$ value of 0.7120 ± 0.0036 , a weighted average corrected $^{87}\text{Sr}/^{86}\text{Sr}$ value of 0.71120 ± 0.0036 and a weighted average $^{84}\text{Sr}/^{86}\text{Sr}$ value of 0.05632 ± 0.00020 ($n=3$). The dentine spots of track 2 have an average ^{88}Sr voltage of 0.263, a weighted average uncorrected $^{87}\text{Sr}/^{86}\text{Sr}$ value of 0.7119 ± 0.0058 , a weighted average corrected $^{87}\text{Sr}/^{86}\text{Sr}$ value of 0.71020 ± 0.0058 and a weighted average $^{84}\text{Sr}/^{86}\text{Sr}$ value of 0.0565 ± 0.0018 ($n=3$). The enamel spots of track 3 have an average ^{88}Sr voltage of 0.401, a weighted average uncorrected $^{87}\text{Sr}/^{86}\text{Sr}$ value of 0.7130 ± 0.0089 , a weighted average corrected $^{87}\text{Sr}/^{86}\text{Sr}$ value of 0.71220 ± 0.0089 and a weighted average $^{84}\text{Sr}/^{86}\text{Sr}$ value of 0.05621 ± 0.00037 ($n=2$). The dentine spots of track 3 have an average ^{88}Sr voltage of 0.303, a weighted average uncorrected $^{87}\text{Sr}/^{86}\text{Sr}$ value of 0.7101 ± 0.0016 , a weighted average corrected $^{87}\text{Sr}/^{86}\text{Sr}$ value of 0.70840 ± 0.0016 and a weighted average $^{84}\text{Sr}/^{86}\text{Sr}$ value of 0.05606 ± 0.00069 . Enamel values for track 1 are 0.710919 and 0.713018 (uncorrected), as well as 0.710103 and 0.713649 (corrected), outside of 2σ error. Dentine values for track 1 are in the range of 0.708909 to 0.715892 (uncorrected), as well as 0.707215 to 0.714199, and are heterogeneous overall; however, spots 3 and 4 are homogenous within 2σ error with each other, as are spots 5 through 9. Enamel values for track 2 are in the range of 0.710929 to 0.714418 (uncorrected), as well as 0.710113 to 0.713601 (corrected), and are extremely heterogeneous, increasing in value from spot 1 to 3. Dentine values for track 2 are in the range of 0.710529 to 0.715048 (uncorrected), as well as

0.708836 to 0.713355 (corrected), with spots 4 and 5 being within 2σ error, while spot 3 is outside of error. Enamel values for track 3 are 0.712725 and 0.714769 (uncorrected), as well as 0.711908 and 0.713953 (corrected), which are outside of 2σ error. Dentine values for track 3 are in the range of 0.709367 to 0.712762 (uncorrected), as well as 0.707674 to 0.711069 (corrected), with spots 4 to 6 being within 2σ error. Detailed values for enamel and dentine for sample M021 are shown in Table A3.87, Figure A3.155 and Figure A3.156.

The enamel values of this sample are heterogeneous and are distributed within 3 domains, the first comprising spot 2 on track 3 and spot 3 on track 2, the second comprising spot 1 on track 3, spot 2 on track 2 and spot 10 on track 1, and the third containing spot 1 from track 2 and spot 1 on track 1. The first domain has an uncorrected weighted average value of 0.71452 ± 0.00090 and a corrected weighted average value of 0.71370 ± 0.00090 . The corrected value corresponds to FS031-S1 (a clay layer probably derived from Dordogne river sediments), FS046-S1 (floodplain sediments adjacent to La Chapelle-aux-Saints) and FS058-S1 (floodplain sediments from the Dordogne river) which outcrop within a minimum distance of 5.3 km. The uncorrected value of this domain correlates with Dordogne floodplain samples FS035-S1 and FS059-S1. The second domain has an uncorrected weighted average of 0.71279 ± 0.00037 , which corresponds to the mapping values of 0.713096 ± 0.000014 from FS035-S1 and 0.713071 ± 0.000011 from FS059-S1, both from the Dordogne floodplain. The corrected weighted average value of the second domain is 0.71198 ± 0.00037 , which correlates to mapping samples, including FS029-S1 from the Verezé floodplain, FS036-S1 from alluvial valley fill, FS054-S1 from a Cambrian metamorphic unit and FS056-S1 from the Dordogne floodplain. The third domain has a weighted average uncorrected value of 0.71093 ± 0.00041 , which corresponds to 0.710762 ± 0.000031 from FS052-S1, which is located within a Lower Jurassic carbonate package outcropping within 3 km of Les Fieux. The weighted average corrected value of the third domain is 0.71011 ± 0.00041 , which corresponds with lower and upper Jurassic carbonate units such as FS052-S2 and FS050-S1 which outcrop within a minimum

distance of 2.8 km. Dentine values are relatively homogenous, with the exception of near the dentine-enamel junction where the values are elevated.

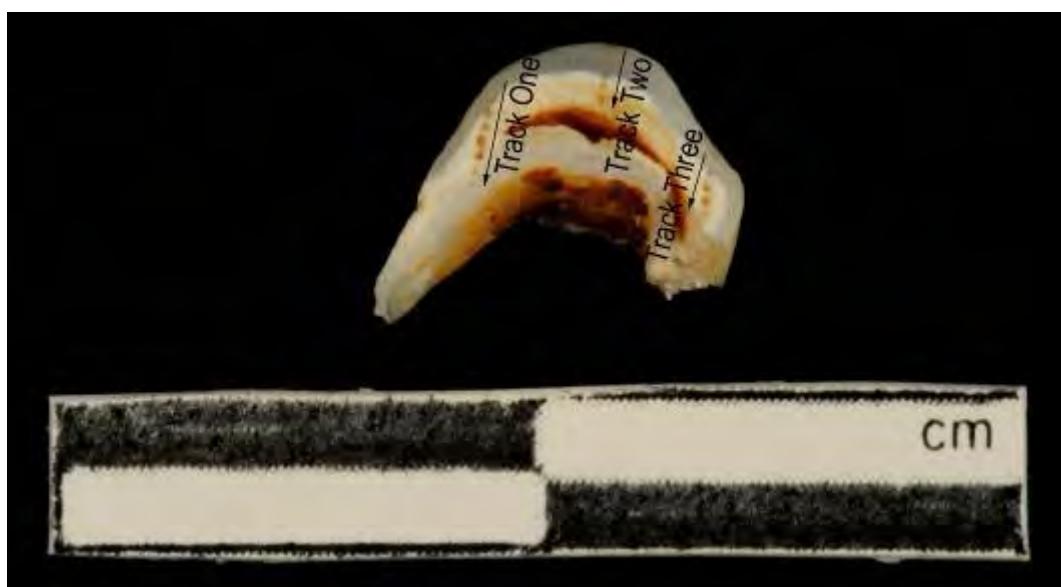


Figure A3.154 LA-MC-ICPMS Track for Sample M021, Mountain Goat/Chamois, Layer G7, Les Fieux

Sample	Material	Track	Point	^{88}Sr Volts	$^{84}\text{Sr}/^{86}\text{Sr}$	$^{84}\text{Sr}/^{86}\text{Sr} 2\sigma$ Error	$^{87}\text{Sr}/^{86}\text{Sr}$	Corrected $^{87}\text{Sr}/^{86}\text{Sr}$	$^{87}\text{Sr}/^{86}\text{Sr} 2\sigma$ Error
M021	Enamel	1	1	0.721	0.056411	0.000510	0.710919	0.710103	0.000803
M021	Enamel	1	2						
M021	Dentine	1	3	0.155	0.056002	0.001377	0.715342	0.713649	0.001332
M021	Dentine	1	4	0.182	0.056336	0.000926	0.715892	0.714199	0.001262
M021	Dentine	1	5	0.312	0.056523	0.000541	0.710608	0.708915	0.000836
M021	Dentine	1	6	0.306	0.056646	0.000605	0.708984	0.707291	0.000688
M021	Dentine	1	7	0.354	0.056102	0.000727	0.708909	0.707215	0.000977
M021	Dentine	1	8	0.265	0.056276	0.000734	0.709640	0.707947	0.001029
M021	Dentine	1	9	0.307	0.056196	0.000577	0.710674	0.708981	0.000629
M021	Enamel	1	10	0.220	0.056520	0.000851	0.713018	0.712201	0.000898
M021	Enamel	2	1	0.772	0.056365	0.000219	0.710929	0.710113	0.000489
M021	Enamel	2	2	0.340	0.056106	0.000558	0.712756	0.711939	0.000540
M021	Enamel	2	3	0.173	0.055793	0.001296	0.714418	0.713601	0.001083
M021	Dentine	2	4	0.184	0.055915	0.001068	0.715048	0.713355	0.001238
M021	Dentine	2	5	0.263	0.056370	0.000613	0.710529	0.708836	0.000937
M021	Dentine	2	6	0.343	0.057815	0.001214	0.711155	0.709462	0.001214
M021	Enamel	3	1	0.677	0.056229	0.000384	0.712725	0.711908	0.000678
M021	Enamel	3	2	0.124	0.055767	0.001919	0.714769	0.713953	0.001711
M021	Dentine	3	3	0.179	0.055119	0.001274	0.712762	0.711069	0.001316
M021	Dentine	3	4	0.314	0.056119	0.000719	0.709367	0.707674	0.000626
M021	Dentine	3	5	0.288	0.055761	0.000723	0.710329	0.708636	0.000804
M021	Dentine	3	6	0.431	0.056396	0.000574	0.710086	0.708393	0.000616

Table A3.87 Detailed LA-MC-ICPMS Sr Isotope Results for Dentine and Enamel, Sample M021, Mountain Goat/Chamois, Layer G7, Les Fieux

Sample M021, Les Fieux, France

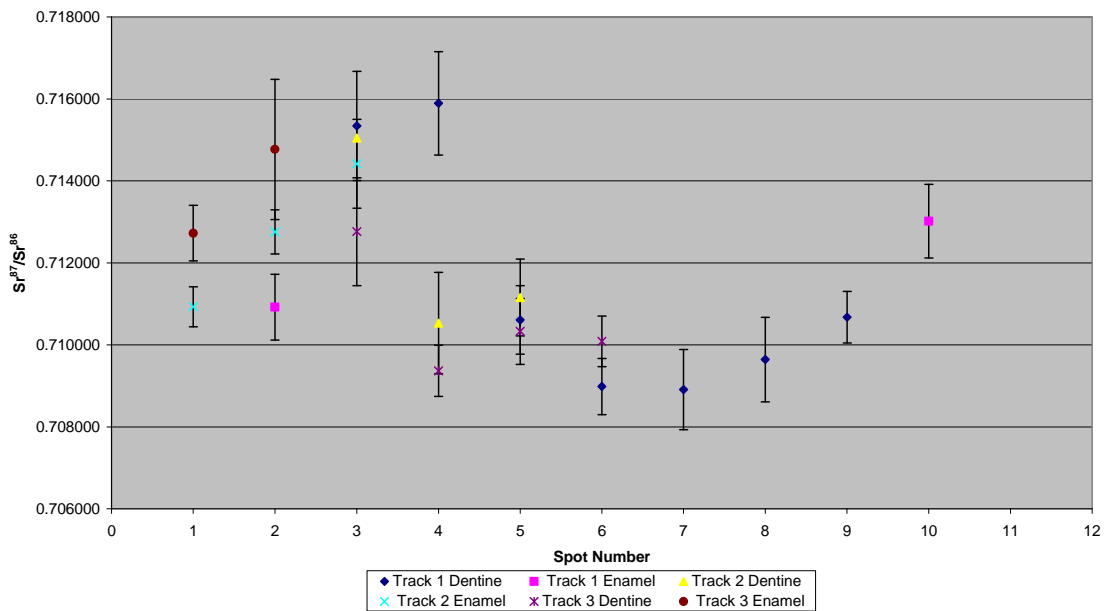


Figure A3.155 Detailed LA-MC-ICPMS Uncorrected Sr Isotope Results, Sample M021, Mountain Goat/Chamois, Layer G7, Les Fieux

Sample M021, Corrected Sr Values, Les Fieux, France

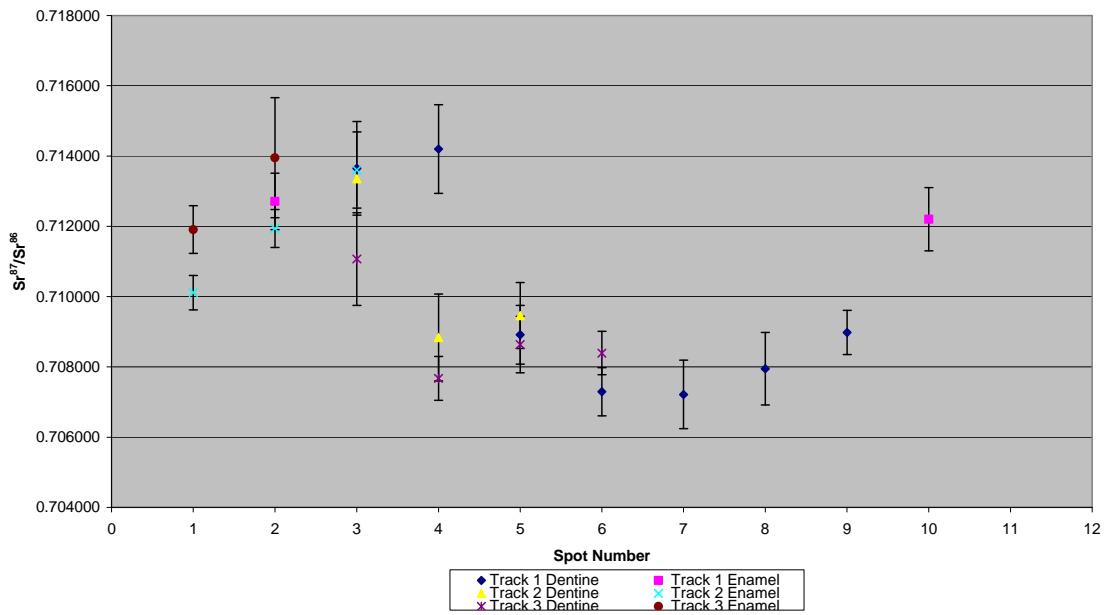


Figure A3.156 Detailed LA-MC-ICPMS Corrected Sr Isotope Results, Sample M021, Mountain Goat/Chamois, Layer G7, Les Fieux

Sample M022, a mountain goat/chamois from layer G7 of Les Fieux shown in Figure A2.52, was analysed in 1 track comprising 5 spots of dentine, shown in Figure A3.157. The results from this sample are summarised in Table 5.30 and Figure 5.18. The dentine spots have an average ^{88}Sr voltage of 0.319, a weighted average uncorrected $^{87}\text{Sr}/^{86}\text{Sr}$ value of 0.70936 ± 0.00058 , a weighted average corrected $^{87}\text{Sr}/^{86}\text{Sr}$ value of 0.70778 ± 0.00058 and a weighted average $^{84}\text{Sr}/^{86}\text{Sr}$ value of 0.05637 ± 0.00031 ($n=5$). Dentine values are in the range of 0.708784 to 0.710033 (uncorrected), as well as 0.707204 to 0.708452 (corrected), and are homogenous within 2σ error. Detailed values for dentine for sample M022 are shown in Table A3.88, Figure A3.158 and Figure A3.159.

No enamel is present in this sample and so no mobility analysis was attempted. The dentine $^{87}\text{Sr}/^{86}\text{Sr}$ and $^{84}\text{Sr}/^{86}\text{Sr}$ values for this sample are all within 2σ error with a range of 0.708784 ± 0.000613 to 0.710033 ± 0.000880 . This suggests a relatively homogenous regime of post-burial diagenesis.



Figure A3.157 LA-MC-ICPMS Track for Sample M022, Mountain Goat/Chamois, Layer G7, Les Fieux

Sample	Material	Track	Point	^{88}Sr Volts	$^{84}\text{Sr}/^{86}\text{Sr}$		$^{87}\text{Sr}/^{86}\text{Sr}$ 2 σ	Corrected $^{87}\text{Sr}/^{86}\text{Sr}$	$^{87}\text{Sr}/^{86}\text{Sr}$ Error
					$^{84}\text{Sr}/^{86}\text{Sr}$ 2 σ	Error			
M022	Enamel	1	1						
M022	Dentine	1	2	0.313	0.056765	0.000705	0.709625	0.708045	0.000759
M022	Dentine	1	3	0.317	0.056346	0.000669	0.708784	0.707204	0.000613
M022	Dentine	1	4	0.306	0.056075	0.000719	0.709597	0.708017	0.000810
M022	Dentine	1	5	0.325	0.055786	0.000864	0.710033	0.708452	0.000880
M022	Dentine	1	6	0.333	0.056644	0.000674	0.709296	0.707715	0.000638

Table A3.88 Detailed LA-MC-ICPMS Sr Isotope Results, Sample M022, Mountain Goat/Chamois, Layer G7, Les Fieux

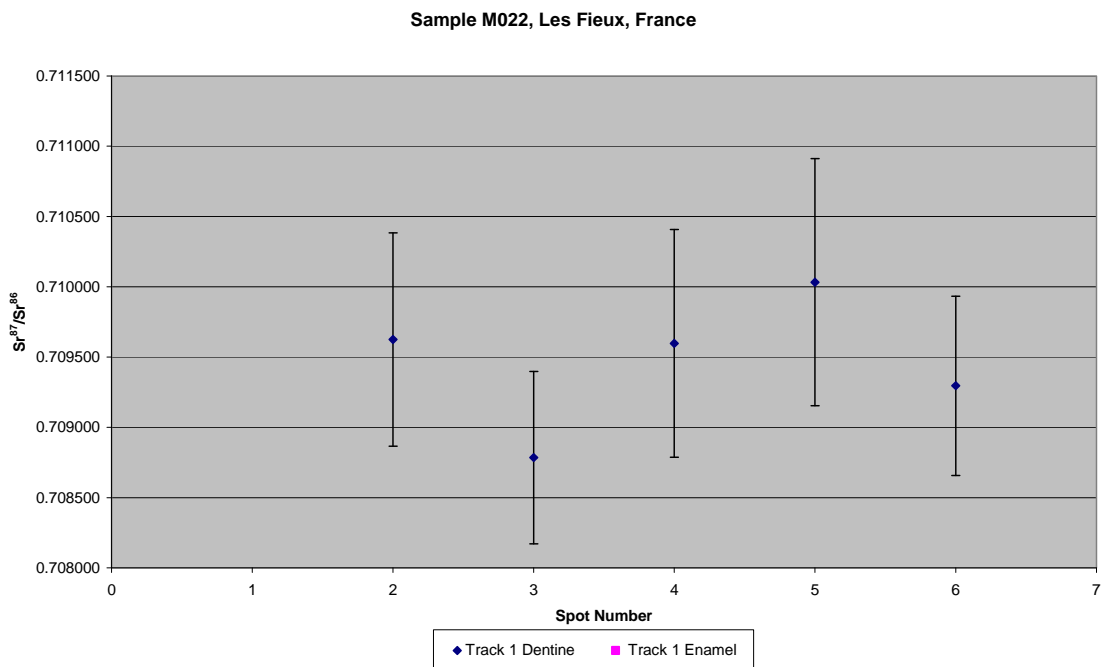


Figure A3.158 Detailed LA-MC-ICPMS Uncorrected Sr Isotope Results, Sample M022, Mountain Goat/Chamois, Layer G7, Les Fieux

Sample M022, Corrected Sr Values, Les Fieux, France

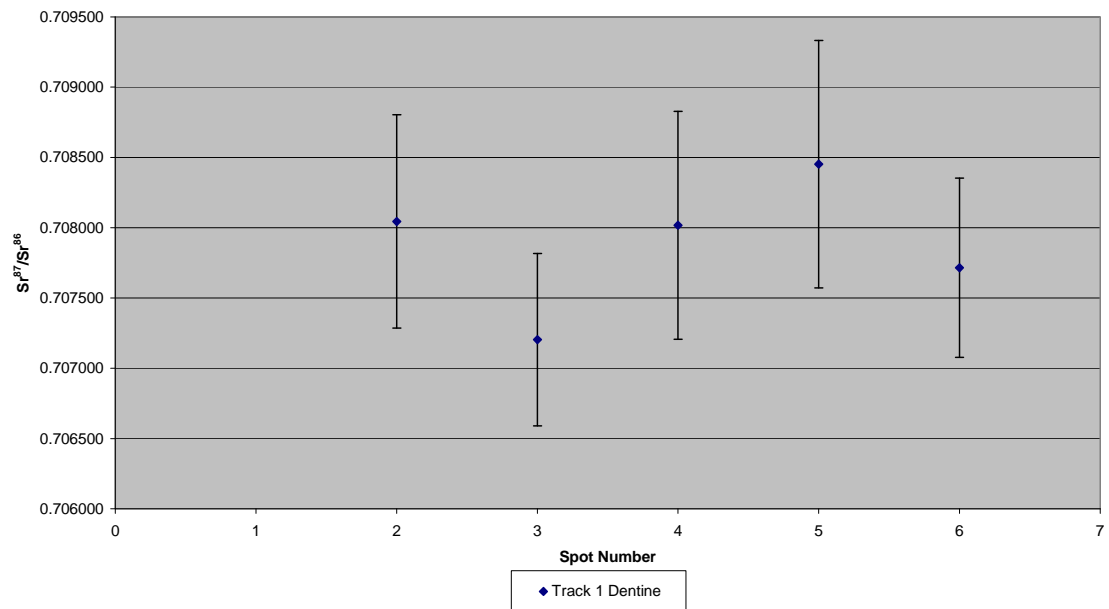


Figure A3.159 Detailed LA-MC-ICPMS Corrected Sr Isotope Results, Sample M022, Mountain Goat/Chamois, Layer G7, Les Fieux

A3.2.3.3. *Le Moustier*

Sample 845, a bovid tooth from layer G1 of Le Moustier shown in Figure A2.53, was analysed in 2 tracks, with track 1 comprising 5 spots of enamel and 25 spots of dentine, track 2 comprising 4 spots of enamel and 10 spots of dentine, shown in Figure A3.160. The results from this sample are summarised in Table 5.32 and Figure 5.20. The enamel spots of track 1 have an average ^{88}Sr voltage of 0.637, a weighted average uncorrected $^{87}\text{Sr}/^{86}\text{Sr}$ value of 0.71570 ± 0.00076 , a weighted average corrected $^{87}\text{Sr}/^{86}\text{Sr}$ value of 0.71387 ± 0.00076 and a weighted average $^{84}\text{Sr}/^{86}\text{Sr}$ value of 0.05654 ± 0.00012 ($n=5$). The dentine spots of track 1 have an average ^{88}Sr voltage of 0.613, a weighted average uncorrected $^{87}\text{Sr}/^{86}\text{Sr}$ value of 0.71233 ± 0.00032 , a weighted average corrected $^{87}\text{Sr}/^{86}\text{Sr}$ value of 0.71070 ± 0.00032 and a weighted average $^{84}\text{Sr}/^{86}\text{Sr}$ value of 0.056553 ± 0.000063 ($n=25$). The enamel spots of track 2 have an average ^{88}Sr voltage of 0.439, a weighted average uncorrected $^{87}\text{Sr}/^{86}\text{Sr}$ value of 0.7160 ± 0.0014 , a weighted average corrected $^{87}\text{Sr}/^{86}\text{Sr}$ value of 0.71410 ± 0.0014 and a weighted average $^{84}\text{Sr}/^{86}\text{Sr}$ value of 0.05655 ± 0.00022 ($n=4$). The dentine spots of track 2 have an average ^{88}Sr voltage of 0.501, a weighted average uncorrected $^{87}\text{Sr}/^{86}\text{Sr}$ value of 0.71252 ± 0.00030 , a weighted average corrected $^{87}\text{Sr}/^{86}\text{Sr}$ value of 0.71089 ± 0.00030 and a weighted average $^{84}\text{Sr}/^{86}\text{Sr}$ value of 0.05651 ± 0.00018 ($n=10$). Enamel values for track 1 are in the range of 0.714741 to 0.716452 (uncorrected), as well as 0.712906 to 0.714617 (corrected), and are somewhat homogenous, decreasing from spot 1 to spot 5. Dentine values for track 1 are in the range of 0.710589 to 0.714945 (uncorrected), as well as 0.708957 to 0.713312 (corrected), and are relatively heterogeneous. Enamel values for track 2 are in the range of 0.715104 to 0.717531 (uncorrected), as well as 0.713269 to 0.715696 (corrected), and are relatively heterogeneous, decreasing in value from spot 1 to spot 4. Dentine values for track 2 are in the range of 0.711909 to 0.712886 (uncorrected), as well as 0.710277 to 0.711253 (corrected), and are somewhat homogenous, being just outside of 2σ error. Detailed values for enamel and dentine for sample 845 are shown in Table A3.89, Figure A3.161 and Figure A3.162.

This sample has enamel and dentine $^{87}\text{Sr}/^{86}\text{Sr}$ values that are distinct, with uncorrected weighted average values of 0.71578 ± 0.00051 and 0.71238 ± 0.00024 , respectively. Enamel values from both tracks show significant variability with $^{87}\text{Sr}/^{86}\text{Sr}$ values decreasing from spot 1 to spot 5 and spot 1 to spot 4 in tracks 1 and 2, respectively. This suggests that this individual moved across isotopically distinct geological environments during amelogenesis. The steady descent in values may reflect a delayed transition in the strontium isotope composition of enamel being laid down after crossing a distinct geological boundary, due to the pool of strontium within the specimen's body. The higher end-member enamel uncorrected $^{87}\text{Sr}/^{86}\text{Sr}$ value of 0.717531 ± 0.000771 corresponds to FS037-S1 (0.717308 ± 0.000012) and FS067-S1 (0.717422 ± 0.00001). While the location of FS037-S1 (13.5 km south-east) is much closer to Le Moustier than FS067-S1 (90 km east), this value comes from a clay unit interbedded within a limestone and so is probably not representative of the surrounding area. It is more likely that this specimen was resident in the area of FS067-S1, which is located within a Carboniferous monzogranite/granodiorite. The corrected $^{87}\text{Sr}/^{86}\text{Sr}$ value of the higher end-member is 0.715696 ± 0.000771 , which corresponds to P8P, which is located within a Carboniferous monzogranite/granodiorite but outcrop within 85 km. The lower end-member of the enamel $^{87}\text{Sr}/^{86}\text{Sr}$ has an uncorrected value of 0.714741 ± 0.000377 , which does not correspond to any mapping value within the study area; however, it is slightly outside of the value of FS046-S1 (0.714131 ± 0.000015), which is located in the floodplain sediments of the small stream near La Chapelle-aux-Saints. Given the wide range of values within the Dordogne floodplain (as discussed above with reference to sample M011), it is likely that this, or other similar streams, draining from the Massif Central have values in this range. The corrected enamel value of this lower end-member is 0.712906 ± 0.000377 , which corresponds to Dordogne floodplain values such as FS035-S1 and FS059-S1. The floodplain outcrops within 14.2 km. The overall range of enamel values in this sample suggests a specimen moving from the Massif Central in an easterly direction down a river valley. All enamel and dentine spots in this sample have a $^{84}\text{Sr}/^{86}\text{Sr}$ weighted average value of 0.056544 ± 0.000049 , suggesting that the $^{87}\text{Sr}/^{86}\text{Sr}$ results are robust.

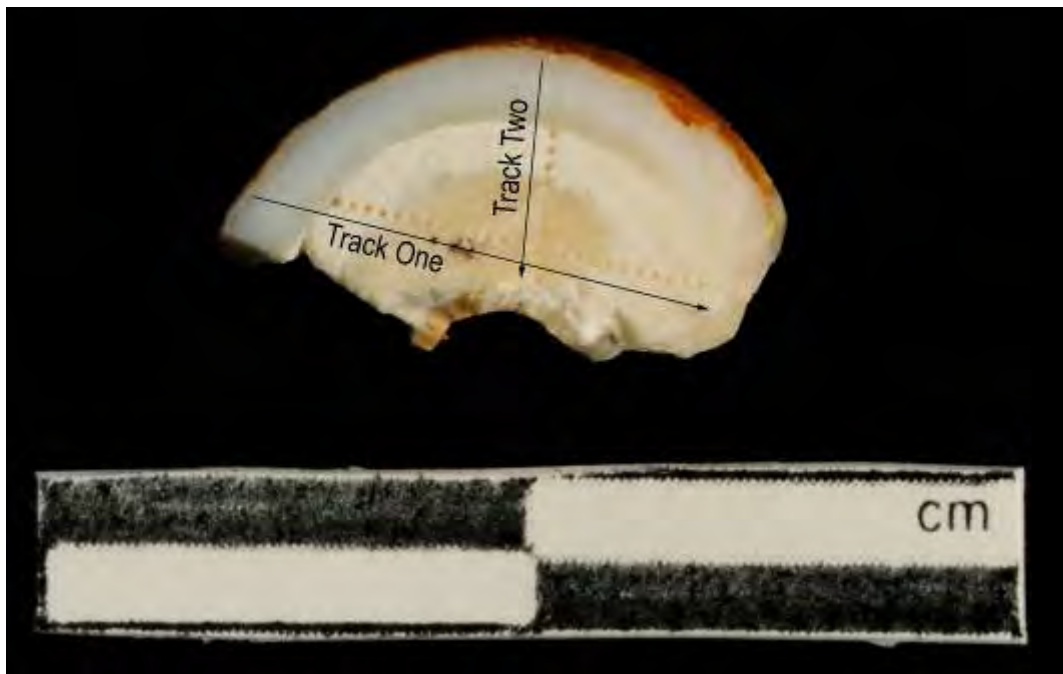


Figure A3.160 LA-MC-ICPMS Track for Sample 845, Bovid, Layer G1, Le Moustier

Sample	Material	Track	Point	88Sr Volts	$^{84}\text{Sr}/^{86}\text{Sr}$	$^{84}\text{Sr}/^{86}\text{Sr} 2\sigma$ Error	Corrected $^{87}\text{Sr}/^{86}\text{Sr}$	$^{87}\text{Sr}/^{86}\text{Sr} 2\sigma$ Error
845	Enamel	1	1	0.584	0.056326	0.000362	0.716452	0.714617
845	Enamel	1	2	0.625	0.056597	0.000280	0.715969	0.714133
845	Enamel	1	3	0.649	0.056697	0.000273	0.715781	0.713946
845	Enamel	1	4	0.655	0.056506	0.000198	0.715492	0.713657
845	Enamel	1	5	0.672	0.056529	0.000311	0.714741	0.712906
845	Dentine	1	6	0.473	0.056728	0.000445	0.710589	0.708957
845	Dentine	1	7	0.612	0.056545	0.000297	0.711609	0.709977
845	Dentine	1	8	0.631	0.056390	0.000477	0.713023	0.711391
845	Dentine	1	9	0.533	0.056390	0.000294	0.711496	0.709864
845	Dentine	1	10	0.596	0.056316	0.000317	0.714945	0.713312
845	Dentine	1	11	0.782	0.056876	0.000283	0.713056	0.711424
845	Dentine	1	12	0.600	0.056571	0.000368	0.712528	0.710896
845	Dentine	1	13	0.727	0.056590	0.000278	0.713380	0.711747
845	Dentine	1	14	0.737	0.056578	0.000236	0.712267	0.710634
845	Dentine	1	15	0.635	0.056753	0.000363	0.712274	0.710641
845	Dentine	1	16	0.620	0.056586	0.000356	0.711650	0.710018
845	Dentine	1	17	0.622	0.056462	0.000296	0.712434	0.710802
845	Dentine	1	18	0.658	0.056531	0.000235	0.712134	0.710502

Sample	Material	Track	Point	^{88}Sr Volts	$^{84}\text{Sr}/^{86}\text{Sr}$	$^{84}\text{Sr}/^{86}\text{Sr} 2\sigma$ Error	$^{87}\text{Sr}/^{86}\text{Sr}$	Corrected $^{87}\text{Sr}/^{86}\text{Sr}$	$^{87}\text{Sr}/^{86}\text{Sr} 2\sigma$ Error
845	Dentine	1	19	0.602	0.056517	0.000316	0.711936	0.710303	0.000498
845	Dentine	1	20	0.656	0.056422	0.000292	0.711940	0.710307	0.000325
845	Dentine	1	21	0.623	0.056547	0.000311	0.712109	0.710477	0.000380
845	Dentine	1	22	0.588	0.056671	0.000335	0.712268	0.710636	0.000472
845	Dentine	1	23	0.644	0.056321	0.000341	0.712622	0.710990	0.000402
845	Dentine	1	24	0.641	0.056500	0.000235	0.712735	0.711103	0.000391
845	Dentine	1	25	0.536	0.057021	0.000660	0.711265	0.709633	0.000493
845	Dentine	1	26	0.589	0.056305	0.000313	0.711849	0.710217	0.000421
845	Dentine	1	27	0.519	0.056546	0.000365	0.711255	0.709623	0.000384
845	Dentine	1	28	0.506	0.056868	0.000561	0.711964	0.710331	0.000510
845	Dentine	1	29	0.564	0.056732	0.000367	0.712357	0.710724	0.000481
845	Dentine	1	30	0.624	0.056782	0.000360	0.714342	0.712710	0.000656
845	Enamel	2	1	0.351	0.056823	0.000504	0.717531	0.715696	0.000771
845	Enamel	2	2	0.418	0.056683	0.000543	0.716110	0.714275	0.000668
845	Enamel	2	3	0.470	0.056459	0.000461	0.716194	0.714359	0.000410
845	Enamel	2	4	0.519	0.056394	0.000365	0.715104	0.713269	0.000460
845	Dentine	2	5	0.427	0.056615	0.000641	0.712191	0.710558	0.000672
845	Dentine	2	6	0.515	0.056711	0.000416	0.712464	0.710831	0.000519
845	Dentine	2	7	0.372	0.056549	0.000612	0.712099	0.710466	0.000506
845	Dentine	2	8	0.474	0.056775	0.000399	0.711909	0.710277	0.000416
845	Dentine	2	9	0.554	0.056689	0.000357	0.712983	0.711350	0.000435
845	Dentine	2	10	0.533	0.056643	0.000380	0.712830	0.711198	0.000356
845	Dentine	2	11	0.589	0.056343	0.000308	0.712886	0.711253	0.000475
845	Dentine	2	12	0.506	0.056501	0.000460	0.712251	0.710619	0.000518
845	Dentine	2	13	0.536	0.056518	0.000342	0.712130	0.710498	0.000480
845	Dentine	2	14	0.508	0.055918	0.000389	0.712874	0.711242	0.000375

Table A3.89 Detailed LA-MC-ICPMS Sr Isotope Results for Dentine and Enamel, Sample 845, Bovid, Layer G1, Le Moustier

Sample 845, Le Moustier, France

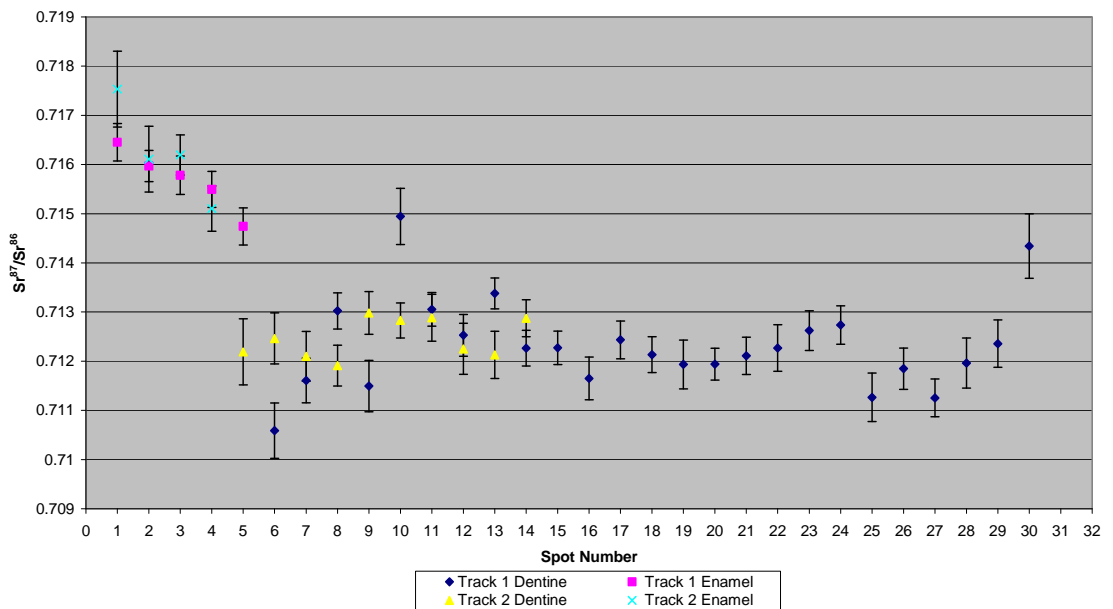


Figure A3.161 Detailed LA-MC-ICPMS Uncorrected Sr Isotope Results, Sample 845, Bovid, Layer G1, Le Moustier

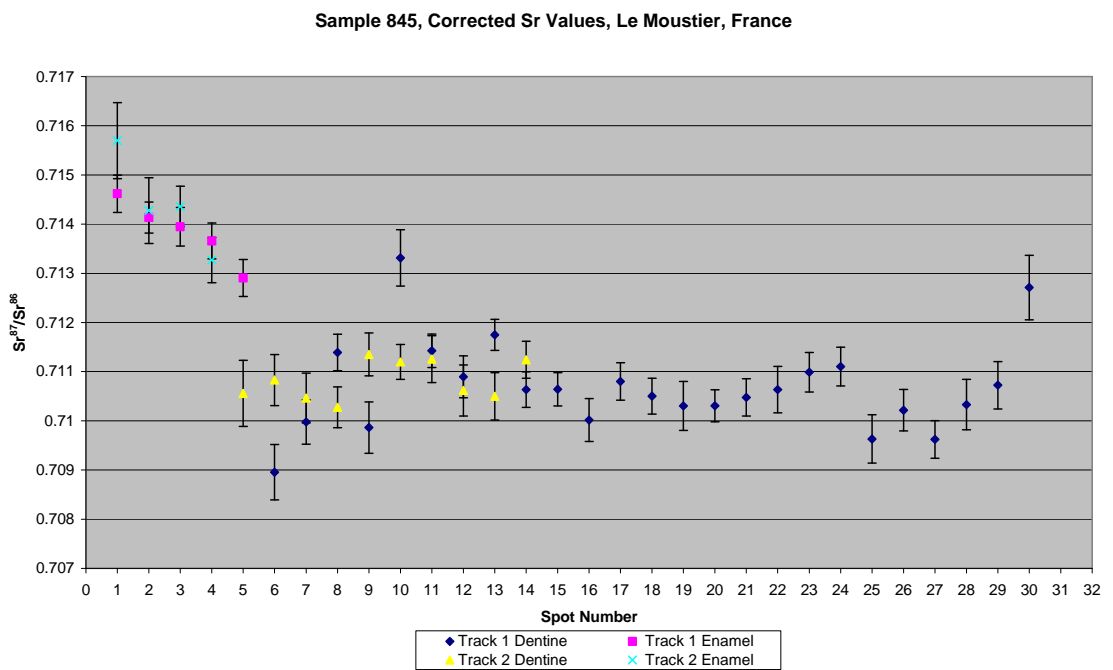


Figure A3.162 Detailed LA-MC-ICPMS Corrected Sr Isotope Results, Sample 845, Bovid, Layer G1, Le Moustier

Sample 846, a bovid tooth from layer G2 of Le Moustier shown in Figure A2.54, was analysed in 1 track comprising 6 spots of enamel and 4 spots of dentine, shown in Figure A3.163. The results from this sample are summarised in Table 5.32 and Figure 5.20. The enamel spots have an average ^{88}Sr voltage of 1.157, a weighted average uncorrected $^{87}\text{Sr}/^{86}\text{Sr}$ value of 0.71247 ± 0.00094 , a weighted average corrected $^{87}\text{Sr}/^{86}\text{Sr}$ value of 0.71187 ± 0.00094 and a weighted average $^{84}\text{Sr}/^{86}\text{Sr}$ value of 0.05659 ± 0.00015 ($n=6$). The dentine spots have an average ^{88}Sr voltage of 0.859, a weighted average uncorrected $^{87}\text{Sr}/^{86}\text{Sr}$ value of 0.71121 ± 0.00057 , a weighted average corrected $^{87}\text{Sr}/^{86}\text{Sr}$ value of 0.71022 ± 0.00057 and a weighted average $^{84}\text{Sr}/^{86}\text{Sr}$ value of 0.056427 ± 0.000097 ($n=4$). Enamel values are in the range of 0.711427 to 0.713535 (uncorrected), as well as 0.710823 to 0.712931 (corrected), and are heterogeneous overall, although spots 3 to 5 are homogenous within 2σ error. Dentine values are in the range 0.710698 to 0.711552 (uncorrected), as well as 0.709707 to 0.710561 (corrected), and are homogeneous within 2σ error. Detailed values for enamel and dentine for sample 846 are shown in Table A3.90, Figure A3.164 and Figure A3.165.

This sample has enamel and dentine $^{87}\text{Sr}/^{86}\text{Sr}$ values that are statistically indistinguishable. There are 3 domains in the weighted average uncorrected enamel strontium composition; the first of 0.7117 ± 0.0030 containing spots 1 and 2, the second of 0.712722 ± 0.000312 from spot 6 and the third of 0.71334 ± 0.00040 comprising spots 3 through 5. These domains have corrected values of 0.7111 ± 0.0030 , 0.712118 ± 0.000312 and 0.71274 ± 0.00039 . This heterogeneity suggests that amelogenesis occurred in at least 2 distinct geological environments, 1 of which was probably local to the site given the similarity between the values of spots 1 and 2 and dentine from this sample. The high 2σ error on the first spot makes it impossible to define a discrete geological unit that correlates either with the corrected or uncorrected value. The second uncorrected domain correlates to the mapping location of FS054-S1, which is located in metamorphic bedrock (0.712245 ± 0.000026), and the corrected value of this domain corresponds to floodplain and alluvial valley fill values such as FS029-S1, FS036-S1, FS056-S1 located within 0.1 km of the

site. Both the uncorrected and corrected values of the third domain correlate to FS035-S1 (0.713096 ± 0.000014) and FS059-S1 (0.713071 ± 0.000011), both from the Dordogne floodplain which outcrops within 14.2 km of the site. $^{84}\text{Sr}/^{86}\text{Sr}$ values from all spots are 0.056534 ± 0.000099 , suggesting that the $^{87}\text{Sr}/^{86}\text{Sr}$ values are very robust.

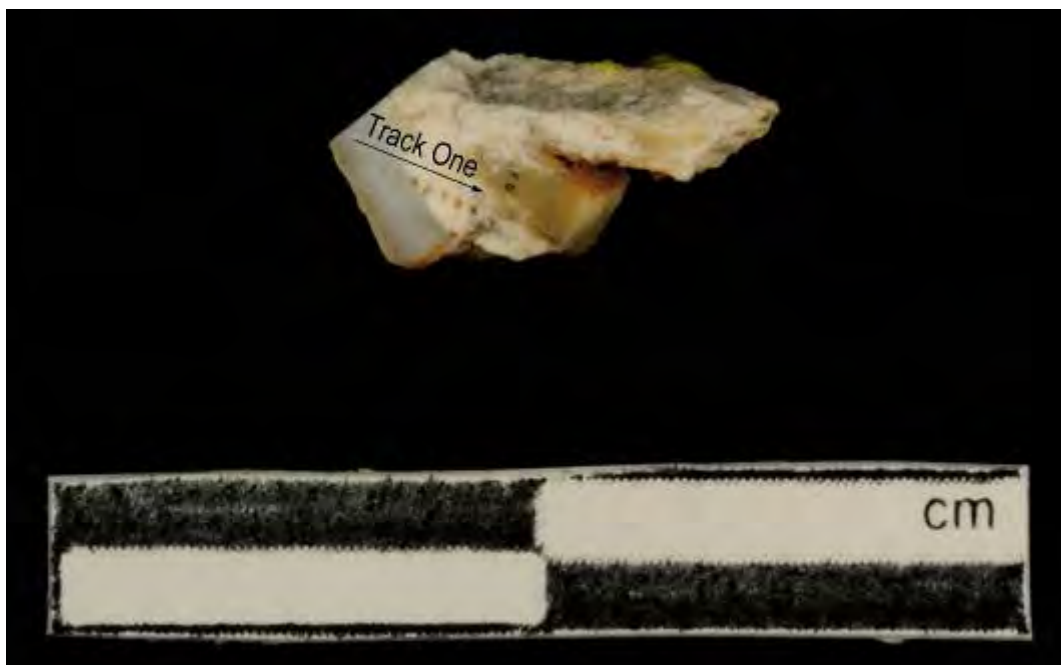


Figure A3.163 LA-MC-ICPMS Track for Sample 846, Bovid, Layer G2, Le Moustier

Sample	Material	Track	Point	^{88}Sr Volts	$^{84}\text{Sr}/^{86}\text{Sr}$	$^{84}\text{Sr}/^{86}\text{Sr} 2\sigma$ Error	$^{87}\text{Sr}/^{86}\text{Sr}$	Corrected $^{87}\text{Sr}/^{86}\text{Sr}$	$^{87}\text{Sr}/^{86}\text{Sr} 2\sigma$ Error
846	Enamel	1	1	1.376	0.056767	0.000135	0.711427	0.710823	0.000202
846	Enamel	1	2	1.229	0.056564	0.000183	0.711906	0.711302	0.000198
846	Enamel	1	3	1.113	0.056573	0.000162	0.713197	0.712594	0.000273
846	Enamel	1	4	1.192	0.056650	0.000350	0.713328	0.712724	0.000237
846	Enamel	1	5	1.101	0.056403	0.000161	0.713535	0.712931	0.000290
846	Enamel	1	6	0.930	0.056528	0.000204	0.712722	0.712118	0.000312
846	Dentine	1	7	0.757	0.056459	0.000236	0.711436	0.710445	0.000381
846	Dentine	1	8	0.849	0.056373	0.000205	0.711552	0.710561	0.000318
846	Dentine	1	9	0.887	0.056459	0.000227	0.711006	0.710016	0.000282
846	Dentine	1	10	0.941	0.056428	0.000158	0.710698	0.709707	0.000457

Table A3.90 Detailed LA-MC-ICPMS Sr Isotope Results, Sample 846, Bovid, Layer G2, Le Moustier

Sample 846, Le Moustier, France

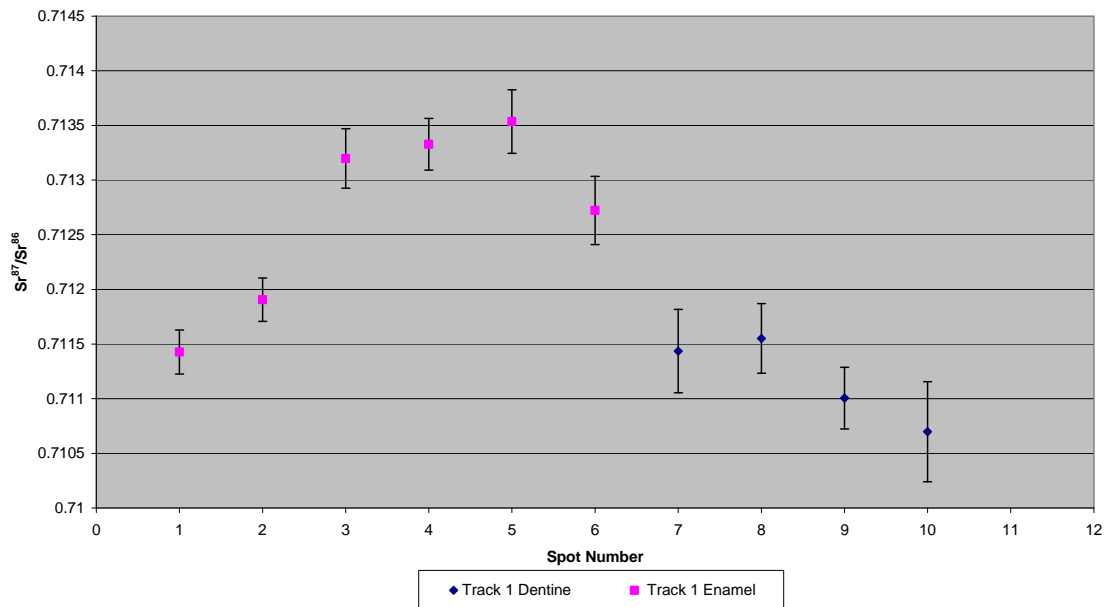


Figure A3.164 Detailed LA-MC-ICPMS Uncorrected Sr Isotope Results, Sample 846, Bovid, Layer G2, Le Moustier

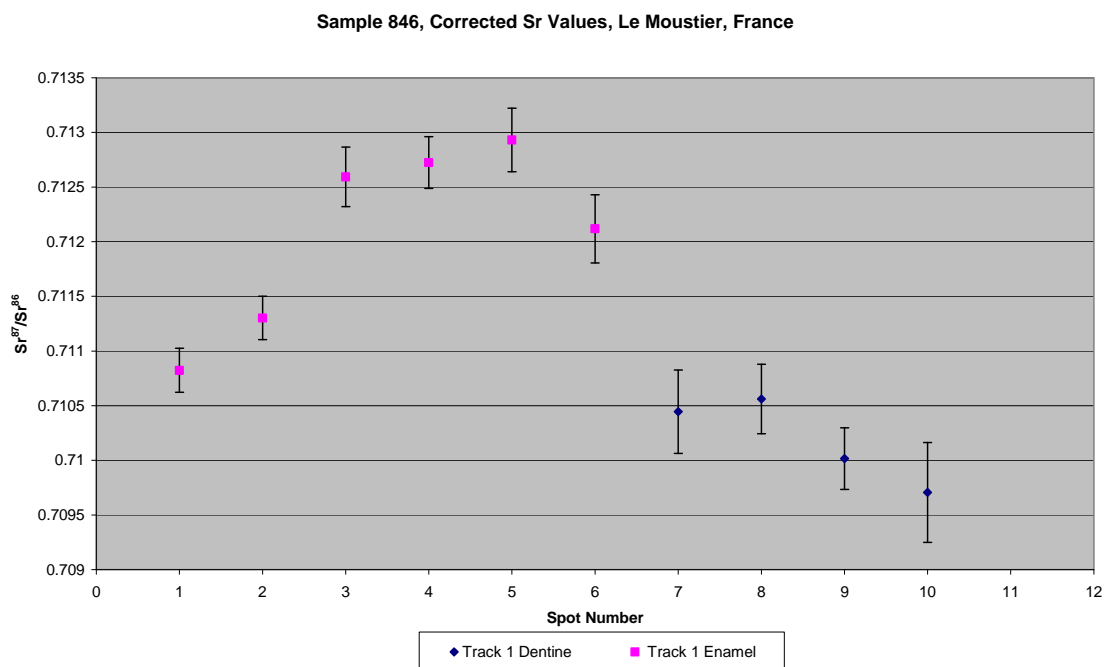


Figure A3.165 Detailed LA-MC-ICPMS Uncorrected Sr Isotope Results, Sample 846, Bovid, Layer G2, Le Moustier

Sample 847, a bovid from layer G3 of Le Moustier shown in Figure A2.55, was analysed in 2 tracks, with track 1 comprising 3 spots of enamel and 11 spots of dentine, track 2 comprising 3 spots of enamel and 10 spots of dentine, shown in Figure A3.166. The results from this sample are summarised in Table 5.32 and Figure 5.20. The enamel spots of track 1 have an average ^{88}Sr voltage of 0.322, a weighted average uncorrected $^{87}\text{Sr}/^{86}\text{Sr}$ value of 0.7171 ± 0.0032 , a weighted average corrected $^{87}\text{Sr}/^{86}\text{Sr}$ value of 0.71420 ± 0.0032 and a weighted average $^{84}\text{Sr}/^{86}\text{Sr}$ value of 0.0561 ± 0.0011 ($n=3$). The dentine spots of track 1 have an average ^{88}Sr voltage of 0.574, a weighted average uncorrected $^{87}\text{Sr}/^{86}\text{Sr}$ value of 0.7142 ± 0.0035 , a weighted average corrected $^{87}\text{Sr}/^{86}\text{Sr}$ value of 0.71280 ± 0.0035 and a weighted average $^{84}\text{Sr}/^{86}\text{Sr}$ value of 0.05651 ± 0.0001 ($n=11$). The enamel spots of track 2 have an average ^{88}Sr voltage of 0.376, a weighted average uncorrected $^{87}\text{Sr}/^{86}\text{Sr}$ value of 0.7143 ± 0.0018 , a weighted average corrected $^{87}\text{Sr}/^{86}\text{Sr}$ value of 0.71150 ± 0.0018 and a weighted average $^{84}\text{Sr}/^{86}\text{Sr}$ value of 0.05656 ± 0.00027 ($n=3$). The dentine spots of track 2 have an average ^{88}Sr voltage of 0.594, a weighted average uncorrected $^{87}\text{Sr}/^{86}\text{Sr}$ value of 0.71209 ± 0.00041 , a weighted average corrected $^{87}\text{Sr}/^{86}\text{Sr}$ value of 0.71072 ± 0.00041 and a weighted average $^{84}\text{Sr}/^{86}\text{Sr}$ value of 0.05658 ± 0.00011 . Enamel values for track 1 are in the range of 0.714850 to 0.717614 (uncorrected), as well as 0.712001 to 0.714764 (corrected), and are relatively heterogeneous, although spots 1 and 3 are within 2σ error. Dentine values of track 1 are in the range of 0.711352 to 0.726839 (uncorrected), as well as 0.709980 to 0.725468 (corrected), and are somewhat homogenous, with the exception of spot 15, which is extremely elevated compared to all other spots of 847. Enamel values for track 2 are in the range of 0.713981 to 0.715556 (uncorrected), as well as 0.711132 to 0.712707 (corrected), with spots 2 and 3 being relatively homogenous. Dentine values for track 2 are in the range of 0.711619 to 0.713981 (uncorrected), as well as 0.710248 to 0.711132 (corrected), and are somewhat homogenous. Detailed values for enamel and dentine for sample 847 are shown in Table A3.91, Figure A3.167 and Figure A3.168.

Enamel values for this sample are heterogeneous, suggesting that this sample was mobile during amelogenesis. These are distributed in 3 domains, with domains 2 and 3 overlapping. Domain 1 contains spots 1 and 3 from track 1 and

has a weighted average uncorrected value of 0.71755 ± 0.00046 , which corresponds to the values of mapping samples FS037-S1 (0.717308 ± 0.000012) and FS067-S1 (0.717422 ± 0.00001), although as discussed with reference to sample M0015, the value from FS067-S1 is more likely to reflect the location of residence during amelogenesis. The corrected value of this domain is 0.71470 ± 0.00046 , which does not correlate to any mapping sample in this study. Domain 2, containing spots 1 from track 2 and spot 2 from track 1, has a weighted average uncorrected value of 0.7153 ± 0.0044 and a weighted average corrected value of 0.7124 ± 0.0044 . The large 2σ error on these values makes it impossible to correlate this domain with a mapping sample. Domain 3, containing spots 2 and 3 from track 2, has a weighted uncorrected average value of 0.71405 ± 0.00038 , which corresponds to samples from the Dordogne (FS031-S1: 0.714027 ± 0.00005) and another floodplain (FS046-S1: 0.714131 ± 0.000015). The corrected value of this domain is 0.71120 ± 0.00038 , which correlates to mapping sample FS107-S1 from a Middle Jurassic carbonate unit, which outcrops within 10 km of Le Moustier. Dentine values vary somewhat, but are overall almost within 2σ error, with the exception of spot 15, suggesting a relatively homogenous regime of post-burial diagenesis. Uncorrected dentine $^{87}\text{Sr}/^{86}\text{Sr}$ values have an overall weighted value of (0.7131 ± 0.0017) ; however, if the very elevated value of spot 15 on track 1 is excluded, the weighted average is reduced significantly (0.71214 ± 0.00027). Using this reduced value, the uncorrected dentine and enamel (0.7155 ± 0.0018) values are statistically distinguishable.

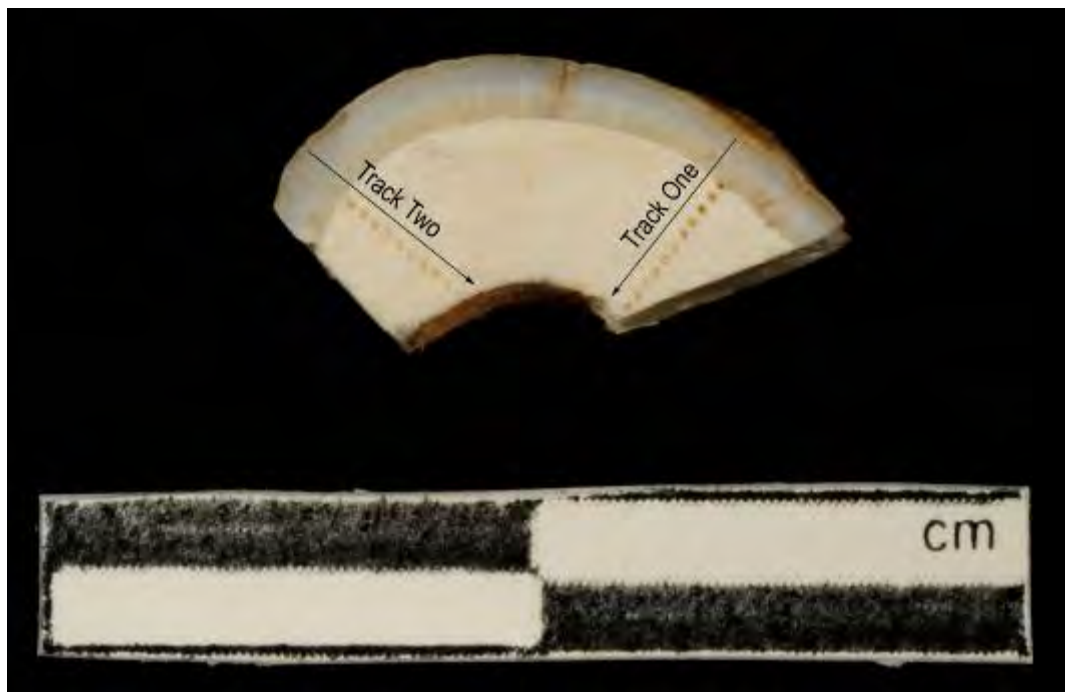


Figure A3.166 LA-MC-ICPMS Track for Sample 847, Bovid, Layer G3, Le Moustier

Sample	Material	Track	Point	^{88}Sr Volts	$^{84}\text{Sr}/^{86}\text{Sr}$	$^{84}\text{Sr}/^{86}\text{Sr} 2\sigma$ Error	$^{87}\text{Sr}/^{86}\text{Sr}$	Corrected $^{87}\text{Sr}/^{86}\text{Sr}$	$^{87}\text{Sr}/^{86}\text{Sr} 2\sigma$ Error
847	Enamel	1	1	0.244	0.055782	0.000733	0.717614	0.714764	0.000836
847	Enamel	1	2	0.329	0.055879	0.000602	0.714850	0.712001	0.000975
847	Enamel	1	3	0.394	0.056569	0.000562	0.717522	0.714672	0.000559
847	Dentine	1	4	0.456	0.056392	0.000369	0.712293	0.710921	0.000487
847	Dentine	1	5	0.522	0.056374	0.000478	0.712273	0.710902	0.000564
847	Dentine	1	6	0.471	0.056373	0.000343	0.711440	0.710069	0.000460
847	Dentine	1	7	0.493	0.056508	0.000374	0.711352	0.709980	0.000504
847	Dentine	1	8	0.533	0.056594	0.000398	0.711823	0.710452	0.000452
847	Dentine	1	9						
847	Dentine	1	10	0.675	0.056710	0.000357	0.712265	0.710894	0.000437
847	Dentine	1	11	0.641	0.056305	0.000360	0.712333	0.710961	0.000298
847	Dentine	1	12	0.572	0.056545	0.000345	0.713889	0.712517	0.000518
847	Dentine	1	13	0.571	0.056235	0.000372	0.711925	0.710554	0.000396
847	Dentine	1	14	0.606	0.056726	0.000279	0.712520	0.711149	0.000392
847	Dentine	1	15	0.773	0.056591	0.000287	0.726839	0.725468	0.000346
847	Enamel	2	1	0.287	0.056743	0.000834	0.715556	0.712707	0.000799
847	Enamel	2	2	0.379	0.056492	0.000473	0.714191	0.711342	0.000676
847	Enamel	2	3	0.462	0.056567	0.000377	0.713981	0.711132	0.000482
847	Dentine	2	4	0.464	0.056776	0.000427	0.711755	0.710384	0.000392
847	Dentine	2	5	0.587	0.056757	0.000338	0.711731	0.710360	0.000350
847	Dentine	2	6	0.599	0.056696	0.000454	0.712246	0.710875	0.000472
847	Dentine	2	7	0.585	0.056289	0.000507	0.712005	0.710634	0.000543
847	Dentine	2	8	0.627	0.056396	0.000347	0.711716	0.710345	0.000310
847	Dentine	2	9	0.608	0.056695	0.000298	0.711619	0.710248	0.000392
847	Dentine	2	10	0.546	0.056456	0.000388	0.712003	0.710632	0.000335
847	Dentine	2	11	0.557	0.056734	0.000419	0.713682	0.712311	0.000429
847	Dentine	2	12	0.572	0.056601	0.000458	0.712275	0.710904	0.000466
847	Dentine	2	13	0.792	0.056438	0.000268	0.712446	0.711075	0.000345

Table A3.91 Detailed LA-MC-ICPMS Sr Isotope Results for Dentine and Enamel, Sample 847, Bovid, Layer G3, Le Moustier

Sample 847, Le Moustier, France

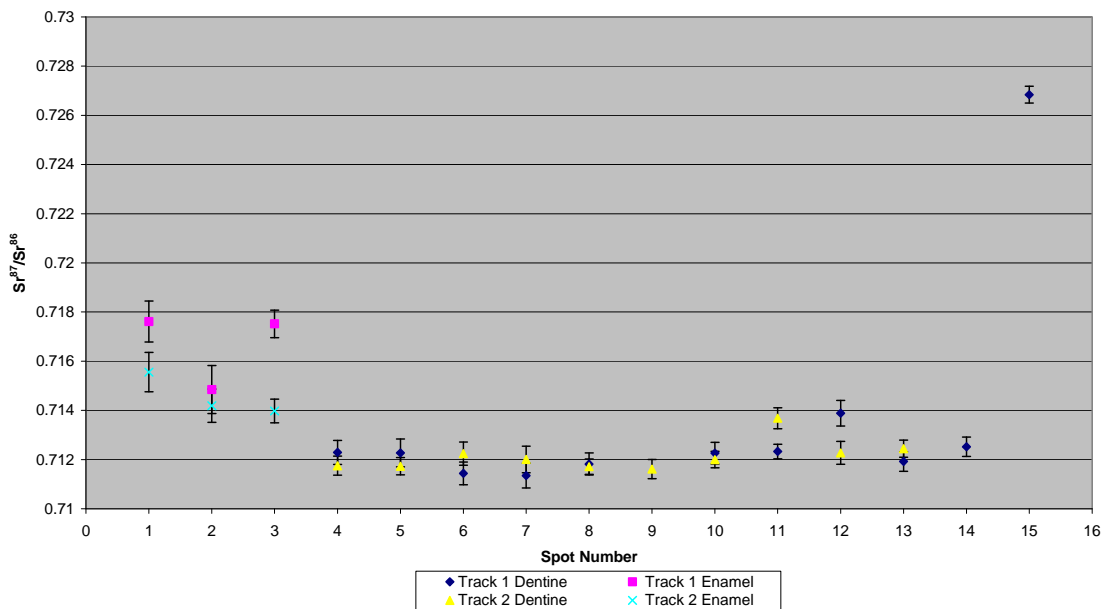


Figure A3.167 Detailed LA-MC-ICPMS Uncorrected Sr Isotope Results, Sample 847, Bovid, Layer G3, Le Moustier

Sample 847, Corrected Sr Values, Le Moustier, France

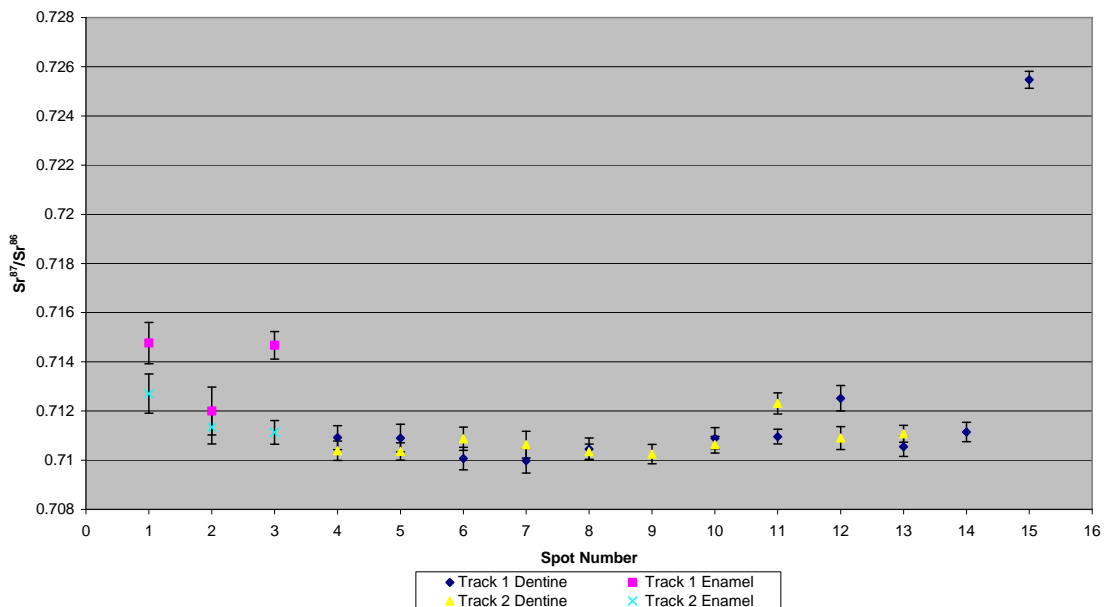


Figure A3.168 Detailed LA-MC-ICPMS Corrected Sr Isotope Results, Sample 847, Bovid, Layer G3, Le Moustier

Sample 848, a bovid from layer G4 of Le Moustier shown in Figure A2.56, was analysed in 2 tracks, with track 1 comprising 4 spots of enamel and 11 spots of dentine and track 2 comprising 3 spots of enamel and 12 spots of dentine, shown in Figure A3.170. The results from this sample are summarised in Table 5.32 and Figure 5.20. The enamel spots of track 1 have an average ^{88}Sr voltage of 0.343, a weighted average uncorrected $^{87}\text{Sr}/^{86}\text{Sr}$ value of 0.7138 ± 0.0023 , a weighted average corrected $^{87}\text{Sr}/^{86}\text{Sr}$ value of 0.71000 ± 0.0023 and a weighted average $^{84}\text{Sr}/^{86}\text{Sr}$ value of 0.05628 ± 0.0003 ($n=4$). The dentine spots of track 1 have an average ^{88}Sr voltage of 0.436, a weighted average uncorrected $^{87}\text{Sr}/^{86}\text{Sr}$ value of 0.71102 ± 0.00033 , a weighted average corrected $^{87}\text{Sr}/^{86}\text{Sr}$ value of 0.70855 ± 0.00033 and a weighted average $^{84}\text{Sr}/^{86}\text{Sr}$ value of 0.05648 ± 0.00017 ($n=11$). The enamel spots of track 2 have an average ^{88}Sr voltage of 0.349, a weighted average uncorrected $^{87}\text{Sr}/^{86}\text{Sr}$ value of 0.7139 ± 0.0021 , a weighted average corrected $^{87}\text{Sr}/^{86}\text{Sr}$ value of 0.71000 ± 0.0021 and a weighted average $^{84}\text{Sr}/^{86}\text{Sr}$ value of 0.05653 ± 0.00085 ($n=3$). The dentine spots of track 2 have an average ^{88}Sr voltage of 0.472, a weighted average uncorrected $^{87}\text{Sr}/^{86}\text{Sr}$ value of 0.71129 ± 0.00023 , a weighted average corrected $^{87}\text{Sr}/^{86}\text{Sr}$ value of 0.70882 ± 0.00023 and a weighted average $^{84}\text{Sr}/^{86}\text{Sr}$ value of 0.05635 ± 0.00015 . Enamel values for track 1 are in the range of 0.712144 to 0.715815 (uncorrected), as well as 0.708314 and 0.711985 (corrected), and are heterogeneous except for spots 2 and 3, which are within 2σ error. Enamel spots decrease in value from 1 to 4. Dentine values for track 1 are in the range of 0.710252 to 0.711797 (uncorrected), as well as 0.707779 to 0.709324 (corrected), and are somewhat homogenous, all being within 2σ error. Enamel values for track 2 are in the range of 0.713478 to 0.715361 (uncorrected), as well as 0.709648 to 0.711531 (corrected), and are mostly within 2σ error. Dentine values for track 2 are in the range of 0.710802 to 0.712250 (uncorrected), as well as 0.708329 to 0.709777 (corrected), and are mostly within 2σ error. Detailed values for enamel and dentine for sample 848 are shown in Table A3.92, Figure A3.170 and Figure A3.171.

This sample has dentine (0.71118 ± 0.00019) and enamel (0.7138 ± 0.0010) weighted average uncorrected strontium isotope values that are significantly

different from each other. The variation of enamel $^{87}\text{Sr}/^{86}\text{Sr}$ values between spots suggests that this specimen was mobile during amelogenesis. The enamel $^{87}\text{Sr}/^{86}\text{Sr}$ values can be grouped into 3 domains, with domain 1, including spot 1 from track 1 and track 2, with a weighted average uncorrected value of 0.71560 ± 0.00059 and a weighted average corrected value of 0.71177 ± 0.00059 . Domain 2 includes spot 2 and 3 from track 1 and track 2 and has a weighted average uncorrected value of 0.71377 ± 0.00030 and a weighted average corrected value of 0.70994 ± 0.00030 . Domain 3 includes spot 4 of track 1 and has an uncorrected value of 0.712144 ± 0.000647 and a corrected value of 0.708314 ± 0.000647 . The mapping unit, which correlates best to the uncorrected value from domain 1, is P8P (0.715615 ± 0.000026), which is located within a Permian monzogranite/granodiorite. P8P is located approximately 240 km west of Le Moustier; however, the same unit (which has a very heterogeneous $^{87}\text{Sr}/^{86}\text{Sr}$ composition) outcrops within 80 km of the site. The corrected value from this sample correlates to mapping values from the Verezé (FS029-S1) and Dordogne (FS056-S1) floodplain, as well as alluvial valley fill (FS036-S1). The second uncorrected domain corresponds to mapping values from FS059-S1 (0.713071 ± 0.000011) or FS031-S1 (0.714027 ± 0.00005) from Dordogne river sediments and the corrected value correlates with a floodplain sample from the Verezé river located approximately 7 km southwest of Le Moustier. The corrected third domain correlates to a number of mapping values; however, the most likely source is FS029-S1 (0.712033 ± 0.000015) on the floodplain on the Vezere river, while the uncorrected value corresponds to a number of values to the east and south of the site.

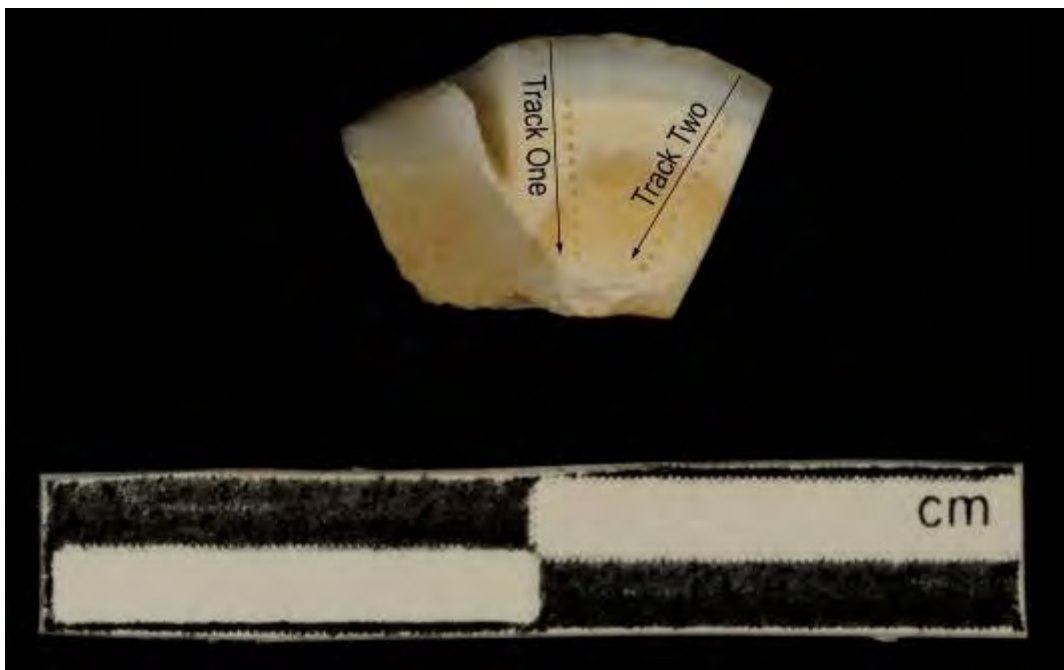


Figure A3.169 LA-MC-ICPMS Track for Sample 848, Bovid, Layer G4, Le Moustier

Sample	Material	Track	Point	^{88}Sr Volts	$^{84}\text{Sr}/^{86}\text{Sr}$	$^{84}\text{Sr}/^{86}\text{Sr} 2\sigma$ Error	Corrected $^{87}\text{Sr}/^{86}\text{Sr}$	$^{87}\text{Sr}/^{86}\text{Sr} 2\sigma$ Error
848	Enamel	1	1	0.299	0.056156	0.000678	0.715815	0.711985
848	Enamel	1	2	0.327	0.056174	0.000635	0.714307	0.710476
848	Enamel	1	3	0.377	0.056256	0.000573	0.713958	0.710128
848	Enamel	1	4	0.368	0.056474	0.000556	0.712144	0.708314
848	Dentine	1	5	0.323	0.056471	0.000592	0.711262	0.708788
848	Dentine	1	6	0.473	0.056257	0.000385	0.710252	0.707779
848	Dentine	1	7	0.492	0.056376	0.000417	0.710752	0.708279
848	Dentine	1	8	0.459	0.056398	0.000412	0.710915	0.708442
848	Dentine	1	9	0.418	0.056334	0.000454	0.710884	0.708410
848	Dentine	1	10	0.425	0.056073	0.000505	0.710648	0.708174
848	Dentine	1	11	0.454	0.056489	0.000376	0.711502	0.709029
848	Dentine	1	12	0.439	0.056999	0.000468	0.710471	0.707997
848	Dentine	1	13	0.447	0.056881	0.000472	0.710867	0.708394
848	Dentine	1	14	0.477	0.056582	0.000377	0.711797	0.709324
848	Dentine	1	15	0.391	0.056506	0.000461	0.711647	0.709173
848	Enamel	2	1	0.285	0.056066	0.000816	0.715361	0.711531
848	Enamel	2	2	0.394	0.056493	0.000428	0.713478	0.709648
848	Enamel	2	3	0.367	0.056954	0.000681	0.713627	0.709796
848	Dentine	2	4	0.468	0.056628	0.000426	0.711275	0.708802
848	Dentine	2	5	0.498	0.056784	0.000486	0.711073	0.708600
848	Dentine	2	6	0.490	0.056430	0.000446	0.711188	0.708715
848	Dentine	2	7	0.475	0.056217	0.000329	0.711130	0.708657
848	Dentine	2	8	0.507	0.056344	0.000341	0.711427	0.708953
848	Dentine	2	9	0.445	0.056803	0.000528	0.711632	0.709159
848	Dentine	2	10	0.444	0.056589	0.000528	0.710802	0.708329
848	Dentine	2	11	0.456	0.056056	0.000574	0.712250	0.709777
848	Dentine	2	12	0.488	0.056207	0.000360	0.711386	0.708913
848	Dentine	2	13	0.479	0.056194	0.000402	0.711631	0.709158
848	Dentine	2	14	0.521	0.056068	0.000370	0.710804	0.708331
848	Dentine	2	15	0.393	0.056277	0.000528	0.711262	0.708788

Table A3.92 Detailed LA-MC-ICPMS Sr Isotope Results for Dentine and Enamel, Sample 848, Bovid, Layer G4, Le Moustier

Sample 848, Le Moustier, France

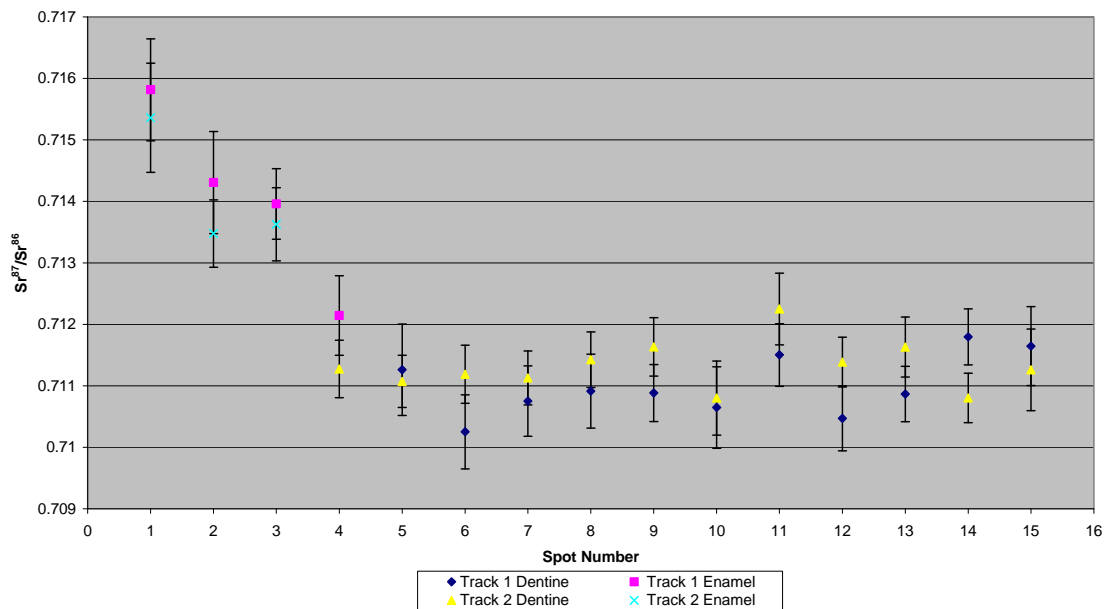


Figure A3.170 Detailed LA-MC-ICPMS Uncorrected Sr Isotope Results, Sample 848, Bovid, Layer G4, Le Moustier

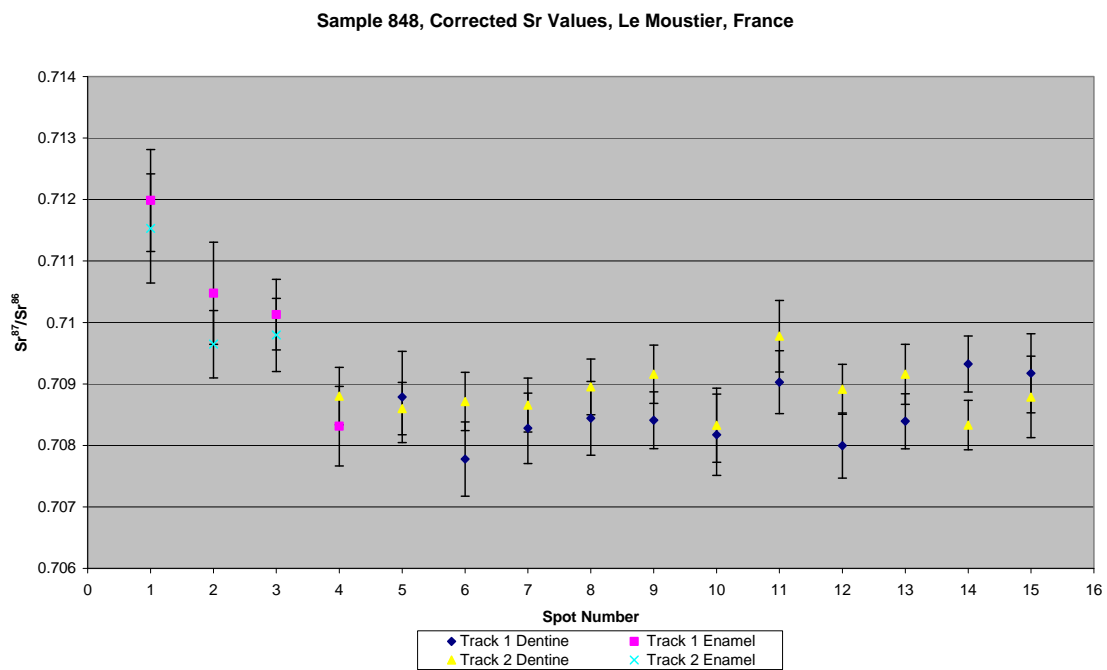


Figure A3.171 Detailed LA-MC-ICPMS Corrected Sr Isotope Results, Sample 848, Bovid, Layer G4, Le Moustier

Sample 849, a bovid from layer G5 of Le Moustier shown in Figure A2.57, was analysed in 2 tracks, with track 1 comprising 7 spots of enamel in 2 discontinuous sections and 14 spots of dentine and track 2 comprising 8 spots of enamel in 2 discontinuous sections and 9 spots of dentine, shown in Figure A3.172. The results from this sample are summarised in Table 5.32 and Figure 5.20. The enamel spots of track 1 have an average ^{88}Sr voltage of 0.526, a weighted average uncorrected $^{87}\text{Sr}/^{86}\text{Sr}$ value of 0.71302 ± 0.00046 , a weighted average corrected $^{87}\text{Sr}/^{86}\text{Sr}$ value of 0.71116 ± 0.00046 and a weighted average $^{84}\text{Sr}/^{86}\text{Sr}$ value of 0.05637 ± 0.00028 ($n=7$). The dentine spots of track 1 have an average ^{88}Sr voltage of 0.5462, a weighted average uncorrected $^{87}\text{Sr}/^{86}\text{Sr}$ value of 0.71191 ± 0.00034 , a weighted average corrected $^{87}\text{Sr}/^{86}\text{Sr}$ value of 0.70997 ± 0.00034 and a weighted average $^{84}\text{Sr}/^{86}\text{Sr}$ value of 0.05655 ± 0.00013 ($n=10$). The enamel spots of track 2 have an average ^{88}Sr voltage of 0.533, a weighted average uncorrected $^{87}\text{Sr}/^{86}\text{Sr}$ value of 0.71271 ± 0.00058 , a weighted average corrected $^{87}\text{Sr}/^{86}\text{Sr}$ value of 0.71085 ± 0.00058 and a weighted average $^{84}\text{Sr}/^{86}\text{Sr}$ value of 0.05639 ± 0.0002 ($n=8$). The dentine spots of track 2 have an average ^{88}Sr voltage of 0.537, a weighted average uncorrected $^{87}\text{Sr}/^{86}\text{Sr}$ value of 0.71160 ± 0.00033 , a weighted average corrected $^{87}\text{Sr}/^{86}\text{Sr}$ value of 0.70965 ± 0.00033 and a weighted average $^{84}\text{Sr}/^{86}\text{Sr}$ value of 0.05631 ± 0.00013 ($n=9$). Enamel values for track 1 are in the range of 0.712244 to 0.713641 (uncorrected), as well as 0.710384 to 0.711781 (corrected), and are just outside of 2σ error. The $^{87}\text{Sr}/^{86}\text{Sr}$ values decrease in value from spot 1 to spot 3 and then increase from spot 14 to spot 17. Dentine values for track 1 are in the range of 0.711145 to 0.712507 (uncorrected), as well as 0.709199 to 0.710562 (corrected), and are within 2σ error. Enamel values for track 2 are in the range of 0.712250 to 0.714140 (corrected), as well as 0.710390 to 0.712281 (uncorrected) and decrease in value from spot 1 to spot 4 and increase in value from spot 14 to spot 17. Dentine values for track 2 are in the range of 0.711038 to 0.712294 (uncorrected), as well as 0.709093 to 0.710349 (corrected), and are all homogeneous within 2σ error. Detailed values for enamel and dentine for sample 849 are shown in Table A3.93, Figure A3.173 and Figure A3.174.

Dentine and enamel strontium isotope values for this sample are heterogeneous overall. Enamel strontium isotope values vary systematically, decreasing from the outside of the enamel on both tracks. This heterogeneity suggests that the sample was mobile during amelogenesis. The correlation between the interior enamel and dentine values suggests that the vector of migration was towards the local area. The upper end-member of the uncorrected enamel range corresponds to samples from the Dordogne (FS031-S1) and another floodplain (FS046-S1). The corrected value of this domain correlates to values from the Vezere floodplain (FS029-S1) and alluvial valley fill (FS036-S1), both south of Le Moustier. The uncorrected lower end-member of this range corresponds to a number of mapping samples; however, the most likely source of this value is FS029-S1, which is a floodplain sample from the Vezere river that flows adjacent to Le Moustier. The corrected value of this end-member correlates with values from the Vezere floodplain in Les Eyzies. Dentine values are relatively homogeneous, suggesting homogeneous post-burial diagenesis.

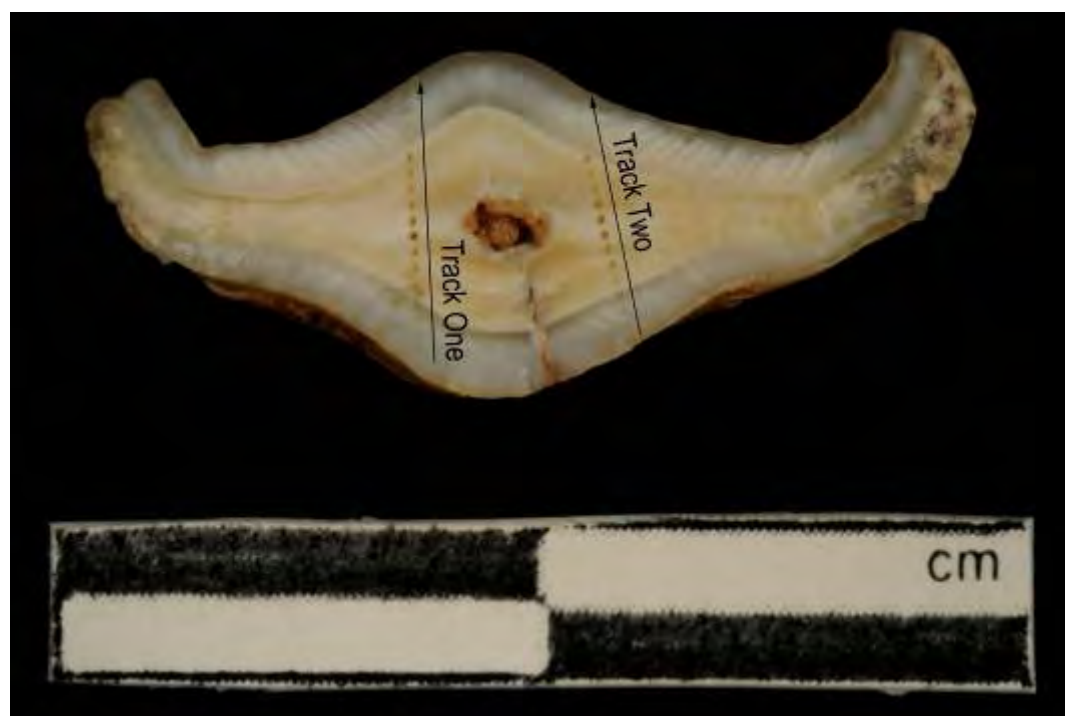


Figure A3.172 LA-MC-ICPMS Track for Sample 849, Bovid, Layer G5, Le Moustier

Sample	Material	Track	Point	^{88}Sr Volts	$^{84}\text{Sr}/^{86}\text{Sr}$	$^{84}\text{Sr}/^{86}\text{Sr} 2\sigma$ Error	Corrected $^{87}\text{Sr}/^{86}\text{Sr}$	$^{87}\text{Sr}/^{86}\text{Sr} 2\sigma$ Error	
849	Enamel	1	1	0.411	0.056660	0.000437	0.713641	0.711781	0.000511
849	Enamel	1	2	0.507	0.056590	0.000365	0.712967	0.711107	0.000444
849	Enamel	1	3	0.614	0.056220	0.000310	0.713086	0.711226	0.000463
849	Dentine	1	4	0.667	0.056764	0.000627	0.712103	0.710158	0.000463
849	Dentine	1	5	0.692	0.056541	0.000272	0.712075	0.710130	0.000403
849	Dentine	1	6	0.577	0.056580	0.000490	0.712225	0.710279	0.000395
849	Dentine	1	7	0.504	0.056295	0.000310	0.711350	0.709404	0.000460
849	Dentine	1	8	0.411	0.056851	0.000553	0.711348	0.709403	0.000518
849	Dentine	1	9	0.527	0.057019	0.000649	0.712189	0.710244	0.000416
849	Dentine	1	10	0.492	0.056683	0.000458	0.711999	0.710054	0.000444
849	Dentine	1	11	0.475	0.056340	0.000524	0.712351	0.710406	0.000562
849	Dentine	1	12	0.508	0.056666	0.000623	0.712507	0.710562	0.000508
849	Dentine	1	13	0.609	0.056527	0.000397	0.711145	0.709199	0.000394
849	Enamel	1	14	0.654	0.056653	0.000292	0.712244	F	0.000432
849	Enamel	1	15	0.591	0.056374	0.000332	0.712770	0.710910	0.000346
849	Enamel	1	16	0.477	0.056161	0.000404	0.713339	0.711479	0.000482
849	Enamel	1	17	0.428	0.055773	0.000402	0.713719	0.711859	0.000553
849	Enamel	2	1	0.400	0.056395	0.000469	0.714140	0.712281	0.000613
849	Enamel	2	2	0.515	0.056011	0.000394	0.713515	0.711655	0.000391
849	Enamel	2	3	0.631	0.056325	0.000278	0.712876	0.711016	0.000394
849	Enamel	2	4	0.720	0.056488	0.000351	0.712250	0.710390	0.000316
849	Dentine	2	5	0.614	0.056365	0.000295	0.711703	0.709758	0.000292
849	Dentine	2	6	0.510	0.056703	0.000451	0.712189	0.710244	0.000441
849	Dentine	2	7	0.486	0.056622	0.000685	0.712294	0.710349	0.000449
849	Dentine	2	8	0.441	0.056709	0.000700	0.711933	0.709988	0.000587
849	Dentine	2	9	0.473	0.056347	0.000409	0.711892	0.709947	0.000503
849	Dentine	2	10	0.481	0.056130	0.000444	0.711196	0.709251	0.000420
849	Dentine	2	11	0.487	0.056007	0.000421	0.711255	0.709310	0.000584
849	Dentine	2	12	0.663	0.056130	0.000339	0.711399	0.709454	0.000299
849	Dentine	2	13	0.681	0.056312	0.000319	0.711038	0.709093	0.000356
849	Enamel	2	14	0.617	0.056551	0.000452	0.712085	0.710226	0.000432
849	Enamel	2	15	0.560	0.056171	0.000391	0.712077	0.710218	0.000442
849	Enamel	2	16	0.447	0.056757	0.000430	0.712341	0.710481	0.000546
849	Enamel	2	17	0.375	0.056812	0.000639	0.713445	0.711585	0.000588

Table A3.93 Detailed LA-MC-ICPMS Sr Isotope Results for Dentine and Enamel, Sample 849, Bovid, Layer G5, Le Moustier

Sample 849, Le Moustier, France

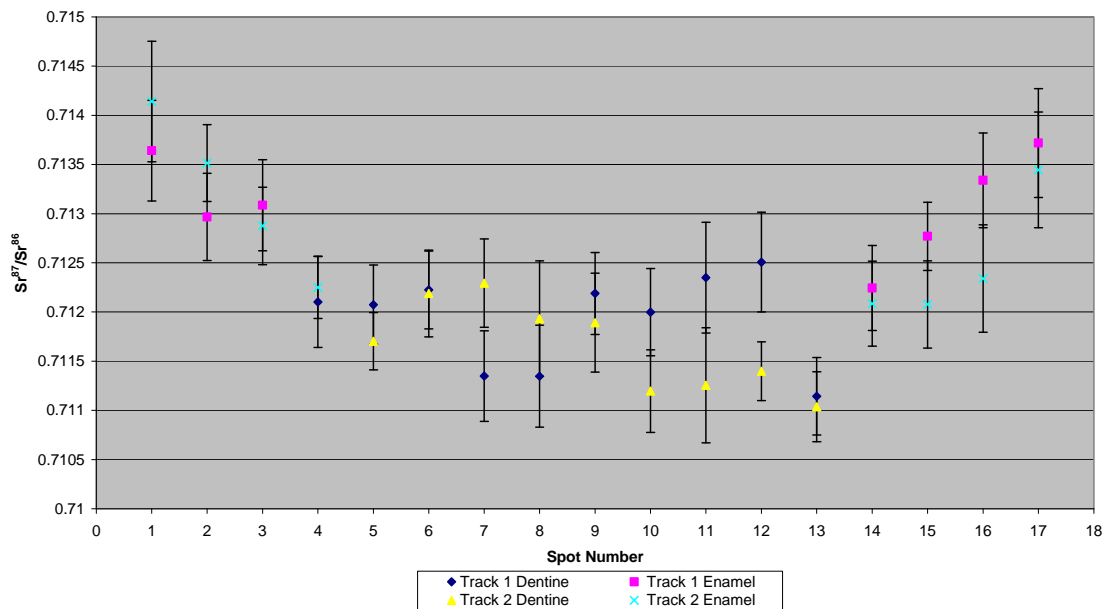


Figure A3.173 Detailed LA-MC-ICPMS Uncorrected Sr Isotope Results, Sample 849, Bovid, Layer G5, Le Moustier

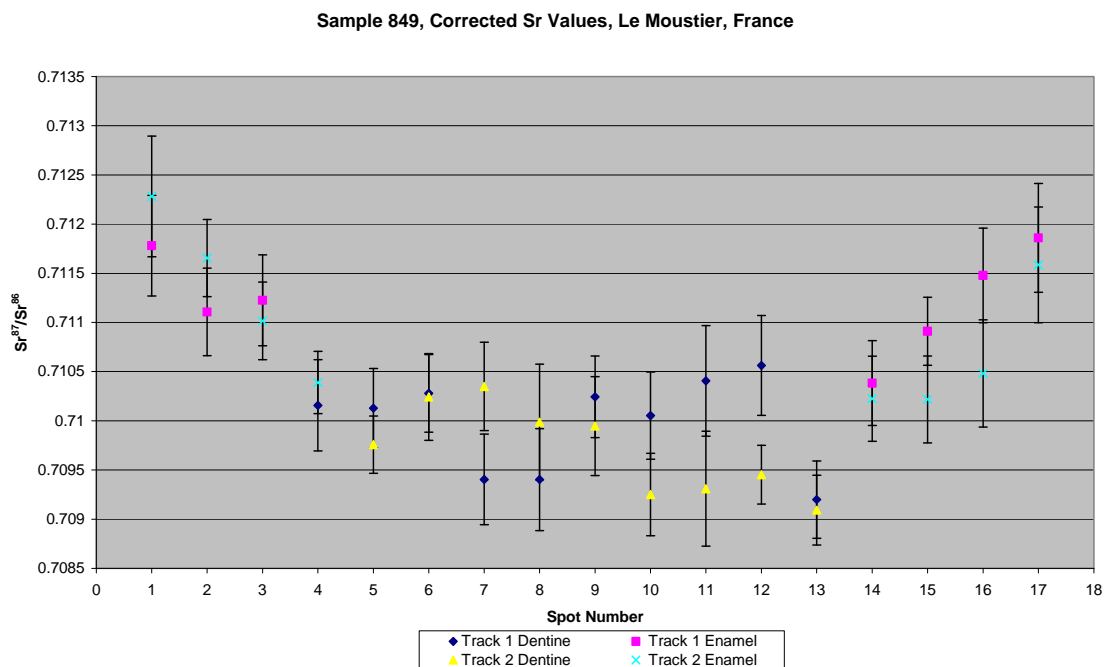


Figure A3.174 Detailed LA-MC-ICPMS Corrected Sr Isotope Results, Sample 849, Bovid, Layer G5, Le Moustier

Sample 850, a bovid from layer G6 of Les Moustier shown in Figure A2.58, was analysed in 2 tracks, with track 1 comprising 5 spots of enamel and 6 spots of dentine and track 2 comprising 11 spots of enamel in 2 discontinuous sections and 15 spots of dentine, shown in Figure A3.175. The results from this sample are summarised in Table 5.32 and Figure 5.20. The enamel spots of track 1 have an average ^{88}Sr voltage of 0.781, a weighted average uncorrected $^{87}\text{Sr}/^{86}\text{Sr}$ value of 0.71261 ± 0.00061 , a weighted average corrected $^{87}\text{Sr}/^{86}\text{Sr}$ value of 0.71150 ± 0.00061 and a weighted average $^{84}\text{Sr}/^{86}\text{Sr}$ value of 0.05662 ± 0.00029 ($n=5$). The dentine spots of track 1 have an average ^{88}Sr voltage of 0.609, a weighted average uncorrected $^{87}\text{Sr}/^{86}\text{Sr}$ value of 0.7122 ± 0.0014 , a weighted average corrected $^{87}\text{Sr}/^{86}\text{Sr}$ value of 0.71060 ± 0.0014 and a weighted average $^{84}\text{Sr}/^{86}\text{Sr}$ value of 0.05654 ± 0.00014 . The enamel spots of track 2 have an average ^{88}Sr voltage of 0.658, a weighted average uncorrected $^{87}\text{Sr}/^{86}\text{Sr}$ value of 0.71295 ± 0.00029 , a weighted average corrected $^{87}\text{Sr}/^{86}\text{Sr}$ value of 0.71171 ± 0.00029 and a weighted average $^{84}\text{Sr}/^{86}\text{Sr}$ value of 0.05655 ± 0.00016 ($n=11$). The dentine spots of track 2 have an average ^{88}Sr voltage of 0.613, a weighted average uncorrected $^{87}\text{Sr}/^{86}\text{Sr}$ value of 0.71164 ± 0.00036 , a weighted average corrected $^{87}\text{Sr}/^{86}\text{Sr}$ value of 0.71010 ± 0.00036 and a weighted average $^{84}\text{Sr}/^{86}\text{Sr}$ value of 0.05649 ± 0.0001 . Enamel values for track 1 are in the range of 0.712421 to 0.713530 (uncorrected), as well as 0.711176 to 0.712285 (corrected), and are slightly heterogeneous, being just outside of 2σ error. Dentine values for track 1 are in the range of 0.710855 to 0.714855 (uncorrected), as well as 0.709315 and 0.713315 (corrected), and are very heterogeneous. Enamel values for track 2 are in the range of 0.712319 to 0.714051 (uncorrected), as well as 0.711073 to 0.712805 (corrected), and are relatively heterogeneous, being just outside of 2σ error. Dentine values for track 2 are 0.710896 to 0.712692 (uncorrected), as well as 0.709357 to 0.711152 (corrected), and are relatively homogenous within 2σ error, with the exception of spots 11, 20 and 21. Detailed values for enamel and dentine for sample 850 are shown in Table A3.94, Figure A3.176 and Figure A3.177.

Enamel values for this sample are relatively homogenous at the start of tracks 1 and 2 (despite them being from different parts of the enamel); however, the enamel values from the end of track 2 have elevated values. The enamel values

can be divided into 4 domains; the first containing spot 26 from spot 2, the second containing spot 1 from track 1 and spots 1, 6, 22, 23 and 25 from track 2, the third containing spot 5 from track 1 and spot 3 from track 2 and the fourth containing spots 2, 3 and 4 from track 1 and spots 2, 4, 5 and 24 from track 2. Domain 1 has an uncorrected value of 0.714051 ± 0.000682 , which corresponds to a clay interbedded within a limestone unit from the location of FS031-S1 (0.714027 ± 0.000005), a floodplain sample from the location of FS046-S1 (0.714131 ± 0.000015) and a Dordogne river floodplain sample from FS058-S1 (0.713898 ± 0.000031). The corrected value of this domain is 0.712805 ± 0.000682 , which correlates to floodplain values from the Vezere and the Dordogne, as well as alluvial valley fill. Domain 2 has a weighted average corrected value of 0.71330 ± 0.00016 , which correlates to values from the Dordogne floodplain from location FS035-S1 (0.713096 ± 0.000014) and an uncorrected value of 0.71205 ± 0.00016 , which corresponds to Dordogne, Vezere floodplain and alluvial valley fill. Domain 3 has a weighted average uncorrected value of 0.71292 ± 0.00017 , which correlates to Dordogne floodplain sample FS035-S1 and a weighted average corrected value of 0.71167 ± 0.00017 , which correlates to F33R located in Permian monzogranite/granodiorite located approximately 100 km north-north-west of Le Moustier and outcropping within 55 km of the archaeological site. Domain 4 has an uncorrected weighted average of 0.71255 ± 0.00027 , which does not correlate to any mapping values; however, given the wide range of samples found within floodplains the Verezee river, sampled at FS029-S1 (0.712033 ± 0.000015), it might be expected to have values that correlate with domain 4. The corrected value of this domain is 0.71123 ± 0.00013 , which correlates with FS107-S1 sampled from a Lower Jurassic carbonate approximately 150 km to the south-west of Le Moustier which outcrops within 17.3 km of the site. Dentine values for this sample are relatively heterogeneous, suggesting a complex post-burial diagenesis regime.

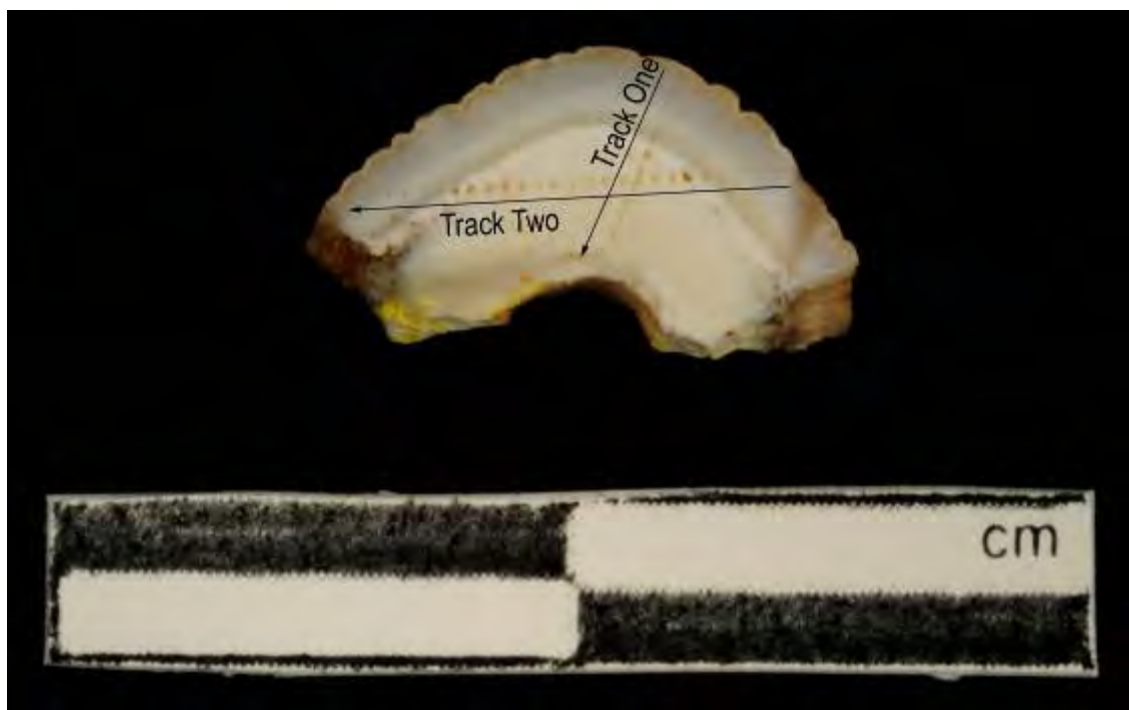


Figure A3.175 LA-MC-ICPMS Track for Sample 850, Bovid, Layer G6, Le Moustier

Sample	Material	Track	Point	^{88}Sr Volts	$^{84}\text{Sr}/^{86}\text{Sr}$	$^{84}\text{Sr}/^{86}\text{Sr}$ 2 σ Error	$^{87}\text{Sr}/^{86}\text{Sr}$	Corrected $^{87}\text{Sr}/^{86}\text{Sr}$	$^{87}\text{Sr}/^{86}\text{Sr}$ 2 σ Error
850	Enamel	1	1	0.583	0.056687	0.000286	0.713530	0.712285	0.000482
850	Enamel	1	2	0.609	0.057170	0.000518	0.712421	0.711176	0.000456
850	Enamel	1	3	0.666	0.056869	0.000280	0.712562	0.711317	0.000337
850	Enamel	1	4	0.771	0.056733	0.000280	0.712316	0.711071	0.000289
850	Enamel	1	5	1.277	0.056436	0.000153	0.712932	0.711686	0.000192
850	Dentine	1	6	0.610	0.056599	0.000284	0.711347	0.709807	0.000398
850	Dentine	1	7	0.598	0.056674	0.000392	0.710855	0.709315	0.000382
850	Dentine	1	8	0.569	0.056208	0.000394	0.712337	0.710797	0.000452
850	Dentine	1	9	0.570	0.056582	0.000351	0.711906	0.710367	0.000374
850	Dentine	1	10	0.657	0.056663	0.000351	0.714855	0.713315	0.000482
850	Dentine	1	11	0.648	0.056441	0.000320	0.713109	0.711570	0.000496
850	Enamel	2	1	0.567	0.056645	0.000297	0.713340	0.712095	0.000532
850	Enamel	2	2	0.494	0.056607	0.000452	0.712412	0.711167	0.000493
850	Enamel	2	3	0.591	0.056877	0.000349	0.712871	0.711626	0.000371
850	Enamel	2	4	0.742	0.056789	0.000439	0.712319	0.711073	0.000390
850	Enamel	2	5	0.738	0.056757	0.000275	0.712658	0.711413	0.000307
850	Enamel	2	6	0.992	0.056599	0.000193	0.713161	0.711916	0.000288
850	Dentine	2	7	0.447	0.056671	0.000529	0.711666	0.710126	0.000614
850	Dentine	2	8	0.623	0.056619	0.000293	0.711376	0.709836	0.000329

Sample	Material	Track	Point	^{88}Sr Volts	$^{84}\text{Sr}/^{86}\text{Sr}$	$^{84}\text{Sr}/^{86}\text{Sr} 2\sigma$ Error	$^{87}\text{Sr}/^{86}\text{Sr}$	Corrected $^{87}\text{Sr}/^{86}\text{Sr}$	$^{87}\text{Sr}/^{86}\text{Sr} 2\sigma$ Error
850	Dentine	2	9	0.644	0.056744	0.000491	0.711432	0.709893	0.000397
850	Dentine	2	10	0.766	0.056507	0.000265	0.711111	0.709571	0.000312
850	Dentine	2	11	0.546	0.056766	0.000304	0.712081	0.710541	0.000439
850	Dentine	2	12	0.565	0.056482	0.000439	0.710896	0.709357	0.000389
850	Dentine	2	13	0.527	0.056054	0.000272	0.711343	0.709803	0.000414
850	Dentine	2	14	0.499	0.056577	0.000238	0.711038	0.709498	0.000485
850	Dentine	2	15	0.537	0.056917	0.000546	0.711499	0.709959	0.000499
850	Dentine	2	16	0.454	0.056562	0.000464	0.711224	0.709685	0.000571
850	Dentine	2	17	0.550	0.056666	0.001208	0.711371	0.709831	0.000438
850	Dentine	2	18	0.621	0.056356	0.000338	0.711355	0.709815	0.000351
850	Dentine	2	19	0.758	0.056496	0.000195	0.711627	0.710087	0.000339
850	Dentine	2	20	0.776	0.056348	0.000244	0.712692	0.711152	0.000337
850	Dentine	2	21	0.880	0.056458	0.000240	0.712953	0.711413	0.000326
850	Enamel	2	22	0.747	0.056249	0.000235	0.713341	0.712096	0.000357
850	Enamel	2	23	0.669	0.056274	0.000339	0.713251	0.712006	0.000348
850	Enamel	2	24	0.679	0.056172	0.000348	0.712561	0.711316	0.000346
850	Enamel	2	25	0.556	0.056887	0.001219	0.713472	0.712227	0.000597
850	Enamel	2	26	0.465	0.056761	0.000348	0.714051	0.712805	0.000682

Table A3.94 Detailed LA-MC-ICPMS Sr Isotope Results for Dentine and Enamel, Sample 850, Bovid, Layer G6, Le Moustier

Sample 850, Le Moustier, France

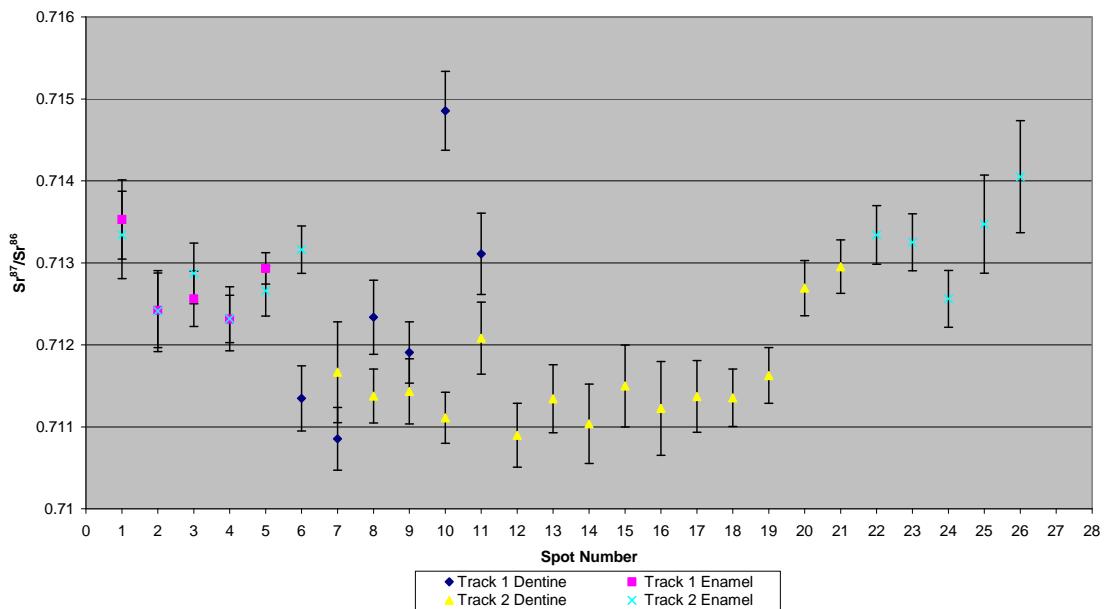


Figure A3.176 Detailed LA-MC-ICPMS Uncorrected Sr Isotope Results, Sample 850, Bovid, Layer G6, Le Moustier

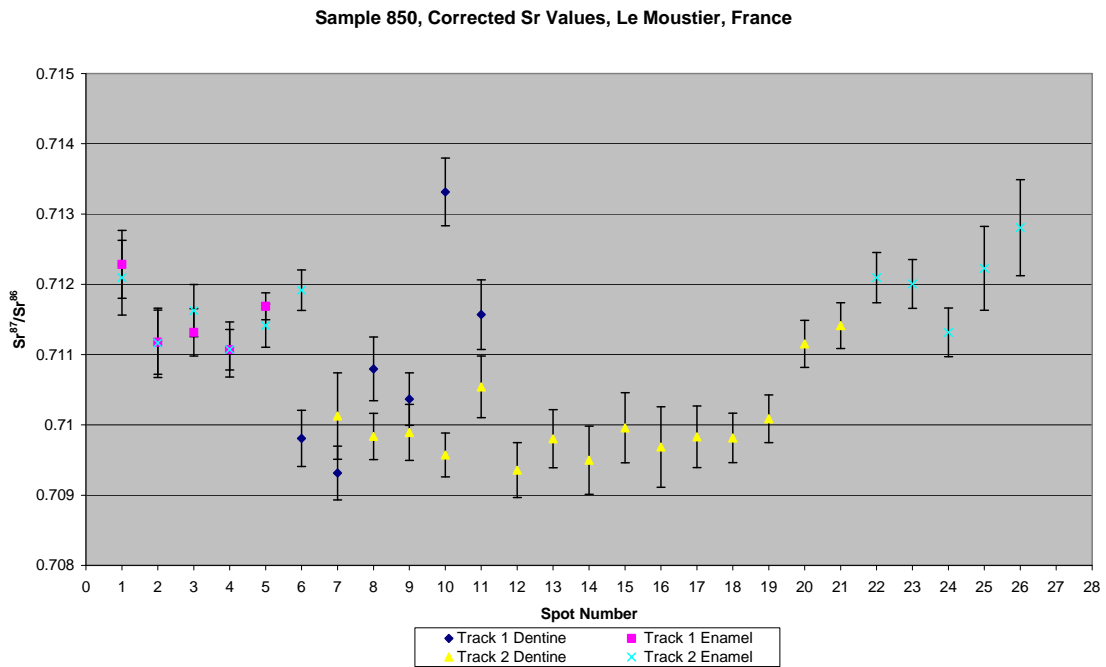


Figure A3.177 Detailed LA-MC-ICPMS Corrected Sr Isotope Results, Sample 850, Bovid, Layer G6, Le Moustier

A3.2.3.4. Pech de l'Azé II

Sample 614, a bovid from layer 9 of Pech de l'Azé II shown in Figure A2.59, was analysed in 2 tracks, with track 1 comprising 3 spots of enamel and 4 spots of dentine and track 2 comprising 4 spots of enamel and 5 spots of dentine, shown in Figure A3.178. The results from this sample are summarised in Table 5.34 and Figure 5.22. The enamel spots of track 1 have an average ^{88}Sr voltage of 0.404, a weighted average uncorrected $^{87}\text{Sr}/^{86}\text{Sr}$ value of 0.7130 ± 0.0056 , a weighted average corrected $^{87}\text{Sr}/^{86}\text{Sr}$ value of 0.71090 ± 0.0056 and a weighted average $^{84}\text{Sr}/^{86}\text{Sr}$ value of 0.05784 ± 0.00030 ($n=3$). The dentine spots of track 1 have an average ^{88}Sr voltage of 0.380, a weighted average uncorrected $^{87}\text{Sr}/^{86}\text{Sr}$ value of 0.7131 ± 0.0012 , a weighted average corrected $^{87}\text{Sr}/^{86}\text{Sr}$ value of 0.71150 ± 0.0012 and a weighted average $^{84}\text{Sr}/^{86}\text{Sr}$ value of 0.05767 ± 0.00046 ($n=4$). The enamel spots of track 2 have an average ^{88}Sr voltage of 0.271, a weighted average uncorrected $^{87}\text{Sr}/^{86}\text{Sr}$ value of 0.7120 ± 0.0059 , a weighted average corrected $^{87}\text{Sr}/^{86}\text{Sr}$ value of 0.70990 ± 0.0059 and a weighted average $^{84}\text{Sr}/^{86}\text{Sr}$ value of 0.05787 ± 0.00039 ($n=4$). The dentine spots of track 2 have an average ^{88}Sr voltage of 0.345, a weighted average uncorrected $^{87}\text{Sr}/^{86}\text{Sr}$ value of 0.71399 ± 0.00068 , a weighted average corrected $^{87}\text{Sr}/^{86}\text{Sr}$ value of 0.71239 ± 0.00068 and a weighted average $^{84}\text{Sr}/^{86}\text{Sr}$ value of 0.05742 ± 0.00028 ($n=5$). Enamel values for track 1 are in the range of 0.711662 to 0.716047 (uncorrected), as well as 0.709497 to 0.713882 (corrected), with spots 2 and 3 being heterogeneous within 2σ error, while spot 1 is elevated compared to the other samples. Dentine values for track 1 are in the range of 0.712402 to 0.714280 (uncorrected), as well as 0.710803 to 0.712681 (corrected), and are somewhat heterogeneous. Enamel values for track 2 are in the range of 0.710838 to 0.721293 (uncorrected), as well as 0.708674 to 0.719128 (corrected), with spots 7 to 9 homogeneous within 2σ error. Spot 6 is extremely elevated in $^{87}\text{Sr}/^{86}\text{Sr}$ value compared to all other spots on this track. Dentine values for track 2 are in the range of 0.713196 to 0.714376 (uncorrected), as well as 0.711597 to 0.712777 (corrected), and are

heterogeneous within 2σ error. Detailed values for enamel and dentine for sample 614 are shown in Table A3.95, Figure A3.179 and Figure A3.180.

The enamel results from this sample can be grouped into 4 domains: domain 1 contains spot 6 from track 2, domain 2 contains spot 1 from track 1, domain 3 contains spots 2 and 3 from track 1 and domain 4 contains spots 7, 8 and 9 from track 2. Domain 1 has an uncorrected value of 0.721293 ± 0.001481 and a corrected value of 0.719128 ± 0.001481 , both of which correlate with the mapping values from a Brioverian/Cambrian metamorphic package outcropping within 45 km of the site on the edge of the Massif Central, including locations FS060-S1, FS070-S1 and FS072-S1. Domain 2 has an uncorrected value of 0.716047 ± 0.000655 , which correlates to P8P with a value of 0.715615 ± 0.000026 on the eastern side of the Massif Central. This location is approximately 220 km to the east of Pech de l'Azé II; however, the Permian monzogranite/granodiorite (which has a heterogeneous strontium isotope composition) outcrops within 60 km of the site. This domain has a corrected value of 0.713882 ± 0.000655 , which correlates to Dordogne floodplain values such as FS031-S1 and FS058-S1 which outcrops within 1.4 km from the site. Domain 3 has a weighted average corrected value of 0.7119 ± 0.0030 and an uncorrected value of 0.7098 ± 0.0030 , which both have a very large error range, making it very difficult to determine the location of this sample during amelogenesis. Domain 4 has a weighted average uncorrected value of 0.71091 ± 0.00050 corresponding to the mapping value from FS089-S1 (0.710853 ± 0.000011), which is located within the Upper Cretaceous carbonate package that contains the site of Pech de l'Azé II. The corrected value of this domain is 0.70874 ± 0.00050 , which correlates with a large number of carbonate mapping values to the west, south and east of the archaeological site including from the Upper Cretaceous carbonate package (mapped at FS088-S1) that contains the site. Dentine values cover a wide range, suggesting a complicated post-diagenesis regime. This is supported by the high uranium results reported for this sample by Grün et al. (1991:46). $^{84}\text{Sr}/^{86}\text{Sr}$ values for all analysis spots from this sample have a weighted average of 0.05767 ± 0.00015 , which is significantly elevated compared to the ideal value of 0.0565.



Figure A3.178 LA-MC-ICPMS Track for Sample 614, Bovid, Layer 9, Pech de l'Azé II

Sample	Material	Track	Point	^{88}Sr Volts	$^{84}\text{Sr}/^{86}\text{Sr}$	$^{84}\text{Sr}/^{86}\text{Sr}$ 2σ Error	Corrected $^{87}\text{Sr}/^{86}\text{Sr}$	$^{87}\text{Sr}/^{86}\text{Sr}$ 2σ Error
614	Enamel	1	1	0.355	0.057911	0.000756	0.716047	0.713882
614	Enamel	1	2	0.398	0.057924	0.000461	0.712138	0.709974
614	Enamel	1	3	0.460	0.057713	0.000494	0.711662	0.709497
614	Dentine	1	4	0.362	0.058122	0.000594	0.712979	0.711380
614	Dentine	1	5	0.348	0.057848	0.000722	0.713038	0.711439
614	Dentine	1	6	0.420	0.057468	0.000418	0.712402	0.710803
614	Dentine	1	7	0.389	0.057568	0.000495	0.714031	0.712432
614	Dentine	2	1	0.367	0.057416	0.000792	0.714280	0.712681
614	Dentine	2	2	0.267	0.056995	0.000746	0.714048	0.712449
614	Dentine	2	3	0.310	0.057379	0.000601	0.714223	0.712624
614	Dentine	2	4	0.425	0.057400	0.000579	0.713196	0.711597
614	Enamel	2	5					
614	Enamel	2	6	0.235	0.057885	0.001148	0.721293	0.719128
614	Enamel	2	7	0.249	0.058353	0.000792	0.710918	0.708753
614	Enamel	2	8	0.269	0.057900	0.000870	0.711006	0.708841
614	Enamel	2	9	0.332	0.057564	0.000615	0.710838	0.708674
614	Dentine	2	10	0.356	0.057729	0.000565	0.714376	0.712777
								0.000485

Table A3.95 Detailed LA-MC-ICPMS Sr Isotope Results for Dentine and Enamel, Sample 614, Bovid, Layer 9, Pech de l'Azé II

Sample 614, Pech II, France

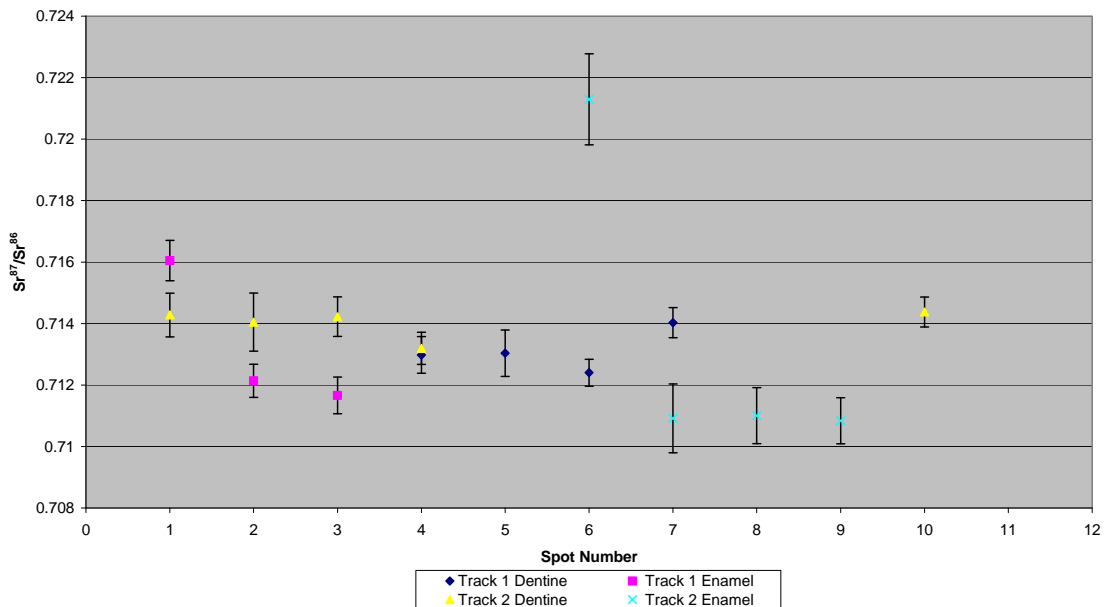


Figure A3.179 Detailed LA-MC-ICPMS Uncorrected Sr Isotope Results, Sample 614, Bovid, Layer 9, Pech de l'Azé II

Sample 614, Corrected Sr Values, Pech II, France

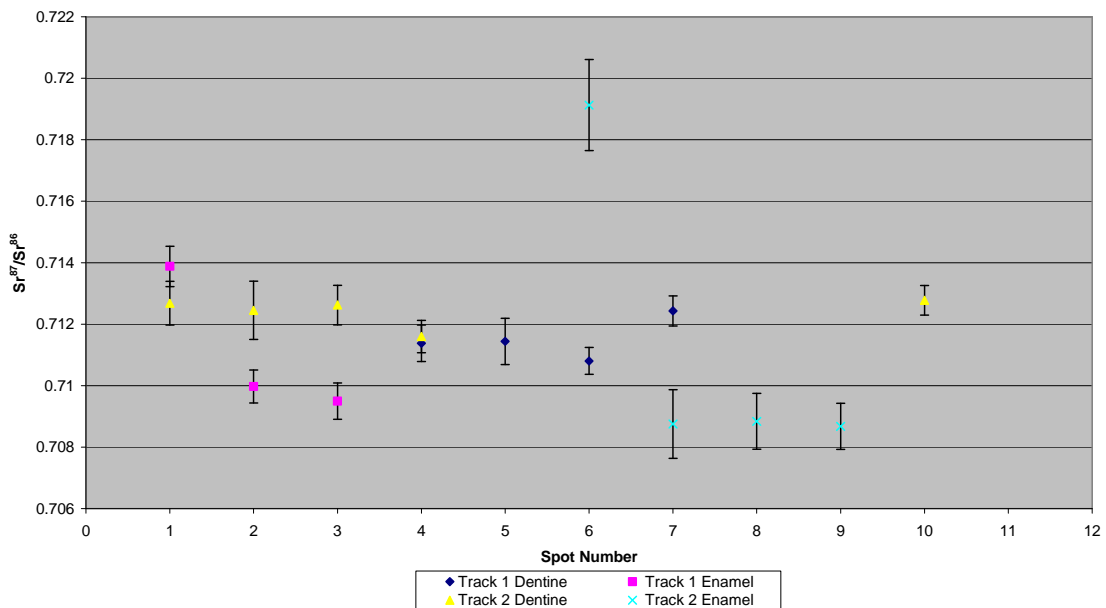


Figure A3.180 Detailed LA-MC-ICPMS Corrected Sr Isotope Results, Sample 614, Bovid, Layer 9, Pech de l'Azé II

Sample 615, a hippopotamus from layer 9 of Pech de l'Azé II shown in Figure A2.60, was analysed in 1 track comprising 8 spots of enamel and 24 spots of dentine, shown in Figure A3.181. The results from this sample are summarised in Table 5.34 and Figure 5.22. The enamel spots have an average ^{88}Sr voltage of 0.404, a weighted average uncorrected $^{87}\text{Sr}/^{86}\text{Sr}$ value of 0.7122 ± 0.0013 , a weighted average corrected $^{87}\text{Sr}/^{86}\text{Sr}$ value of 0.71090 ± 0.0013 and a weighted average $^{84}\text{Sr}/^{86}\text{Sr}$ value of 0.05754 ± 0.00037 ($n=8$). The dentine spots have an average ^{88}Sr voltage of 0.354, a weighted average uncorrected $^{87}\text{Sr}/^{86}\text{Sr}$ value of 0.71238 ± 0.00041 , a weighted average corrected $^{87}\text{Sr}/^{86}\text{Sr}$ value of 0.71105 ± 0.00041 and a weighted average $^{84}\text{Sr}/^{86}\text{Sr}$ value of 0.05744 ± 0.00015 ($n=24$). Enamel values are in the range of 0.710763 to 0.714737 (uncorrected), as well as 0.709466 to 0.713030 (corrected), and are very heterogeneous; they do not vary systematically along the sample track. Dentine values are in the range of 0.710902 to 0.714359 (uncorrected), as well as 0.709573 to 0.713030 (corrected), and are very heterogeneous. Detailed values for enamel and dentine for sample 615 are shown in Table A3.96 and Figure A3.182.

Enamel values for this sample vary without any systematic trend. The upper domain of these values, including spots 1 and 7, have a weighted average uncorrected value of 0.7144 ± 0.0051 and corrected value of 0.7131 ± 0.0051 , which, although it has a large error range, suggests residence in the more radiogenic Massif Central region to the east. The lower uncorrected domain corresponds to FS089-S1 located within the Upper Cretaceous carbonate material local to the site, and the lower corrected domain corresponds to Jurassic carbonates to the south and east of the site including the Upper Jurassic carbonate which outcrops within 8.2 km of this site. Overall, both the uncorrected and corrected values suggest a sample mobile between the area of the site and a region approximately 50 km to the east. Dentine values are very heterogeneous, suggesting a complex regime of post-burial diagenesis, which is supported by the high uranium concentration reported for this sample by Grün et al. (1991:46).

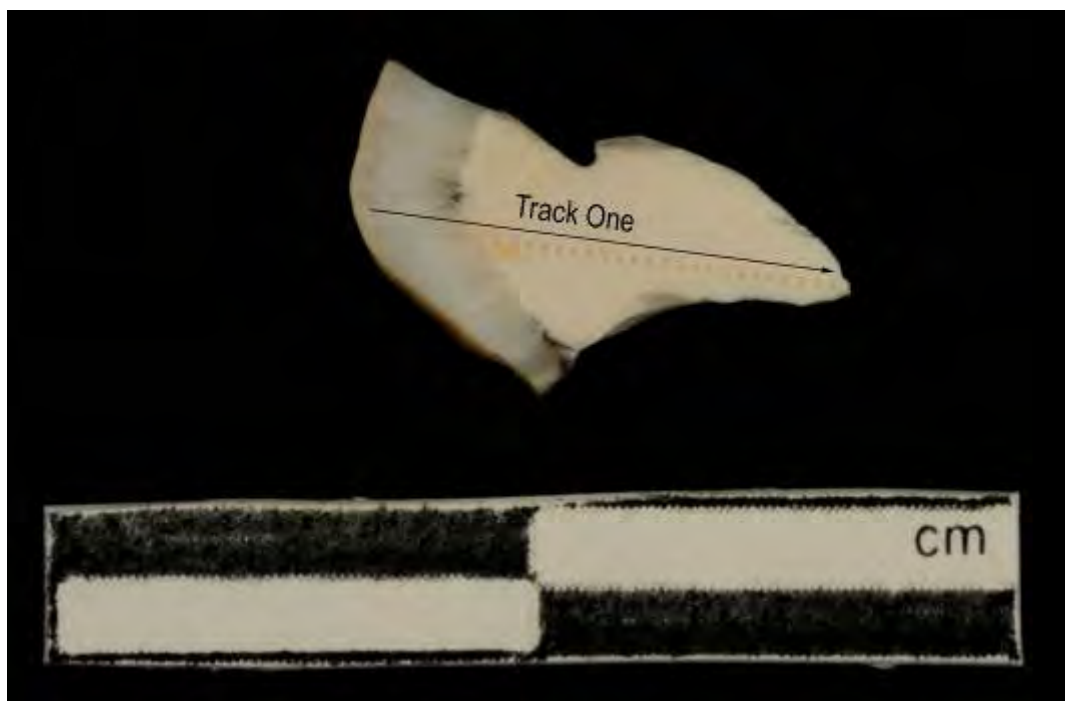


Figure A3.181 LA-MC-ICPMS Track for Sample 615, Hippotamus, Layer 9, Pech de l'Azé II

Sample	Material	Track	Point	^{88}Sr Volts	$^{84}\text{Sr}/^{86}\text{Sr}$	$^{84}\text{Sr}/^{86}\text{Sr} 2\sigma$	Corrected $^{87}\text{Sr}/^{86}\text{Sr}$	$^{87}\text{Sr}/^{86}\text{Sr} 2\sigma$
615	Enamel	1	1	0.396	0.057144	0.000527	0.714737	0.713440
615	Enamel	1	2	0.388	0.057995	0.000790	0.712530	0.711233
615	Enamel	1	3	0.340	0.058378	0.000897	0.711796	0.710499
615	Enamel	1	4	0.348	0.057515	0.000594	0.711098	0.709802
615	Enamel	1	5	0.388	0.057673	0.000575	0.711103	0.709806
615	Enamel	1	6	0.427	0.057300	0.000428	0.711766	0.710470
615	Enamel	1	7	0.465	0.058450	0.000682	0.713918	0.712621
615	Enamel	1	8	0.477	0.057289	0.000445	0.710763	0.709466
615	Dentine	1	9	0.396	0.057668	0.000499	0.710931	0.709602
615	Dentine	1	10	0.305	0.057191	0.000727	0.711504	0.710175
615	Dentine	1	11	0.305	0.056917	0.000801	0.713772	0.712443
615	Dentine	1	12	0.255	0.057913	0.000793	0.711292	0.709963
615	Dentine	1	13	0.263	0.057772	0.000891	0.711555	0.710226
615	Dentine	1	14	0.260	0.057661	0.000655	0.712067	0.710738
615	Dentine	1	15	0.307	0.058070	0.000825	0.713671	0.712342
615	Dentine	1	16	0.376	0.058112	0.000656	0.710902	0.709573
615	Dentine	1	17	0.317	0.058327	0.000748	0.712501	0.711172
615	Dentine	1	18	0.400	0.057611	0.000623	0.711760	0.710431
615	Dentine	1	19	0.463	0.057127	0.000407	0.713032	0.711703
615	Dentine	1	20	0.393	0.057558	0.000680	0.712611	0.711281

615	Dentine	1	21	0.363	0.057391	0.000574	0.713170	0.711841	0.000708
615	Dentine	1	22	0.422	0.057469	0.000496	0.713410	0.712081	0.000537
615	Dentine	1	23	0.351	0.057714	0.000740	0.713130	0.711801	0.000907
615	Dentine	1	24	0.304	0.057742	0.000894	0.713050	0.711721	0.000875
615	Dentine	1	25	0.300	0.057583	0.000783	0.714359	0.713030	0.000859
615	Dentine	1	26	0.353	0.057475	0.000622	0.711733	0.710404	0.000755
615	Dentine	1	27	0.462	0.057130	0.000468	0.711593	0.710264	0.000603
615	Dentine	1	28	0.367	0.057394	0.000484	0.711574	0.710245	0.000673
615	Dentine	1	29	0.398	0.056710	0.000464	0.712798	0.711469	0.000592
615	Dentine	1	30	0.396	0.057367	0.000549	0.712020	0.710691	0.000671
615	Dentine	1	31	0.384	0.057220	0.000633	0.712281	0.710952	0.000742
615	Dentine	1	32	0.362	0.057532	0.000564	0.713905	0.712576	0.000756

Table A3.96 Detailed LA-MC-ICPMS Sr Isotope Results for Dentine and Enamel, Sample 615, Hippotamus, Layer 9, Pech de l'Azé II

Sample 615, Pech II, France

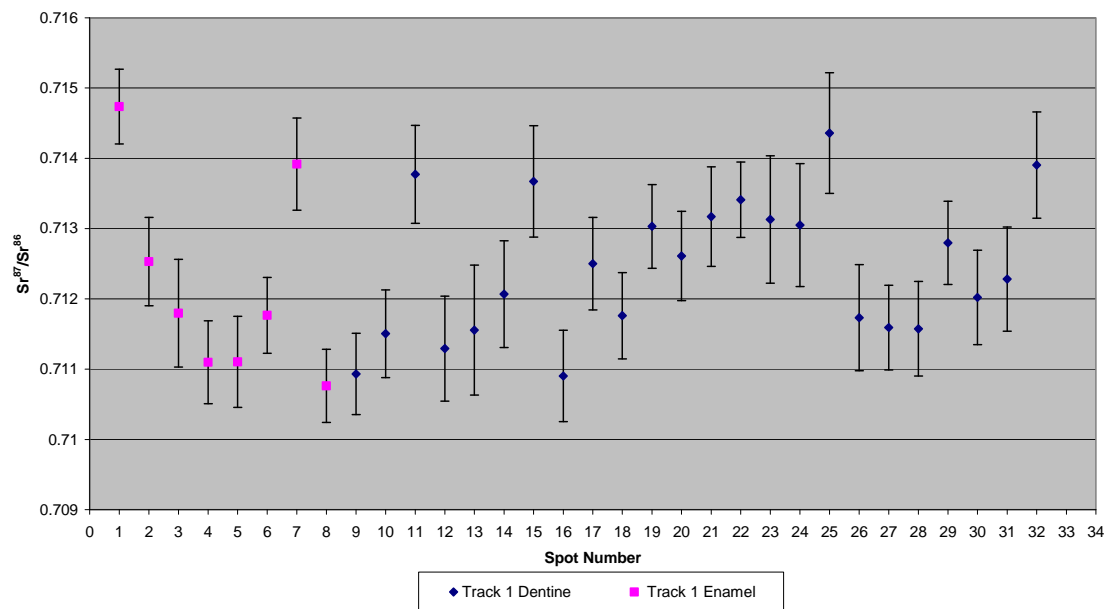


Figure A3.182 Detailed LA-MC-ICPMS Uncorrected Sr Isotope Results, Sample 615, Hippotamus, Layer 9, Pech de l'Azé II

Sample 615, Corrected Sr Values, Pech II, France

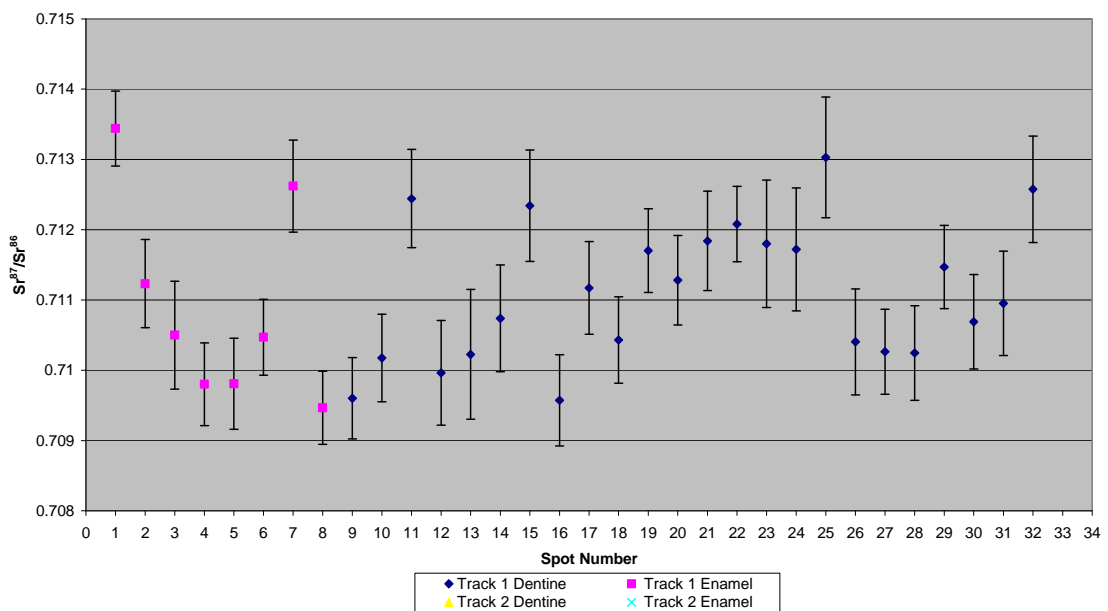


Figure A3.183 Detailed LA-MC-ICPMS Corrected Sr Isotope Results, Sample 615, Hippotamus, Layer 9, Pech de l'Azé II

Sample 617, a horse from layer 8 of Pech de l'Azé II shown in Figure A2.61, was analysed in 1 track comprising 2 spots of enamel and 21 spots of dentine, shown in Figure A3.184. The results from this sample are summarised in Table 5.34 and Figure 5.22. The enamel spots of track 1 have an average ^{88}Sr voltage of 0.286, a weighted average uncorrected $^{87}\text{Sr}/^{86}\text{Sr}$ value of 0.716 ± 0.030 , a weighted average corrected $^{87}\text{Sr}/^{86}\text{Sr}$ value of 0.71500 ± 0.030 and a weighted average $^{84}\text{Sr}/^{86}\text{Sr}$ value of 0.05744 ± 0.00045 ($n=2$). The dentine spots have an average ^{88}Sr voltage of 0.296, a weighted average uncorrected $^{87}\text{Sr}/^{86}\text{Sr}$ value of 0.71424 ± 0.00079 , a weighted average corrected $^{87}\text{Sr}/^{86}\text{Sr}$ value of 0.71285 ± 0.00079 and a weighted average $^{84}\text{Sr}/^{86}\text{Sr}$ value of 0.05733 ± 0.00014 . Enamel values are 0.714113 and 0.718846 (uncorrected), as well as 0.712689 and 0.717422 (corrected), and are very heterogeneous. Dentine values are 0.712480 to 0.721326 (uncorrected), as well as 0.711089 to 0.719935 (corrected), and heterogeneous. Detailed values for enamel and dentine for sample 617 are shown in Table A3.97, Figure A3.185 and Figure A3.186.

The 2 enamel spots from this sample vary by more than 0.0047, suggesting migration during amelogenesis between geological environments of dramatically different strontium composition, both of which are different to that of Pech de l'Azé II. The uncorrected value of spot 1 corresponds to FS053-S1 in Permian siliciclastic sediments (0.719269 ± 0.000027), FS092-S1 in Lower Jurassic in sandstone (0.718681 ± 0.000011), FS097-S1 (0.718429 ± 0.000013), which is regionally mapped as a Lower Jurassic carbonate but was recorded during sample collection as a meta-sediment, and FS105-S1 (0.718595 ± 0.000017), a Cambrian granite/orthogneiss. Regardless of which of these mapping areas correlates with this enamel domain, it clearly represents amelogenesis in the Massif Central region. The corrected value of this domain corresponds to FS067-S1 from a monzogranite/granodiorite (outcropping within 70 km) located in the Massif Central and FS037-S1 from a clay layer within the local Upper Cretaceous carbonate. This value from FS037-S1 (as discussed with reference to sample 854) is probably not representative of the regional value of this unit, and so this enamel value probably reflects movement from the Massif Central. The uncorrected value of spot 2 correlates to mapping sample

FS031-S1 (0.714027 ± 0.00005) collected adjacent to the Dordogne river, sample FS046-S1 collected from the overbank sediments of a small stream (0.714131 ± 0.000015) and sample FS058-S1 (0.713898 ± 0.000031) from the Dordogne floodplain. These mapping values suggest that this specimen was resident on a floodplain during amelogenesis. The corrected value of this enamel spot is 0.712689 ± 0.000831 , which also corresponds to values from the Dordogne (FS035-S1, FS059-S1) and Vezere (FS029-S1) floodplains, as well as alluvial valley fill (FS036-S1) which outcrop within 1.4 km of the site. Dentine values are extremely varied, particularly spots 20 to 24, suggesting a complicated regime of amelogenesis. The weighted average $^{84}\text{Sr}/^{86}\text{Sr}$ value for all spots in this analysis is 0.05734 ± 0.00014 , which is significantly elevated, suggesting that the $^{87}\text{Sr}/^{86}\text{Sr}$ values of this sample may not be robust.

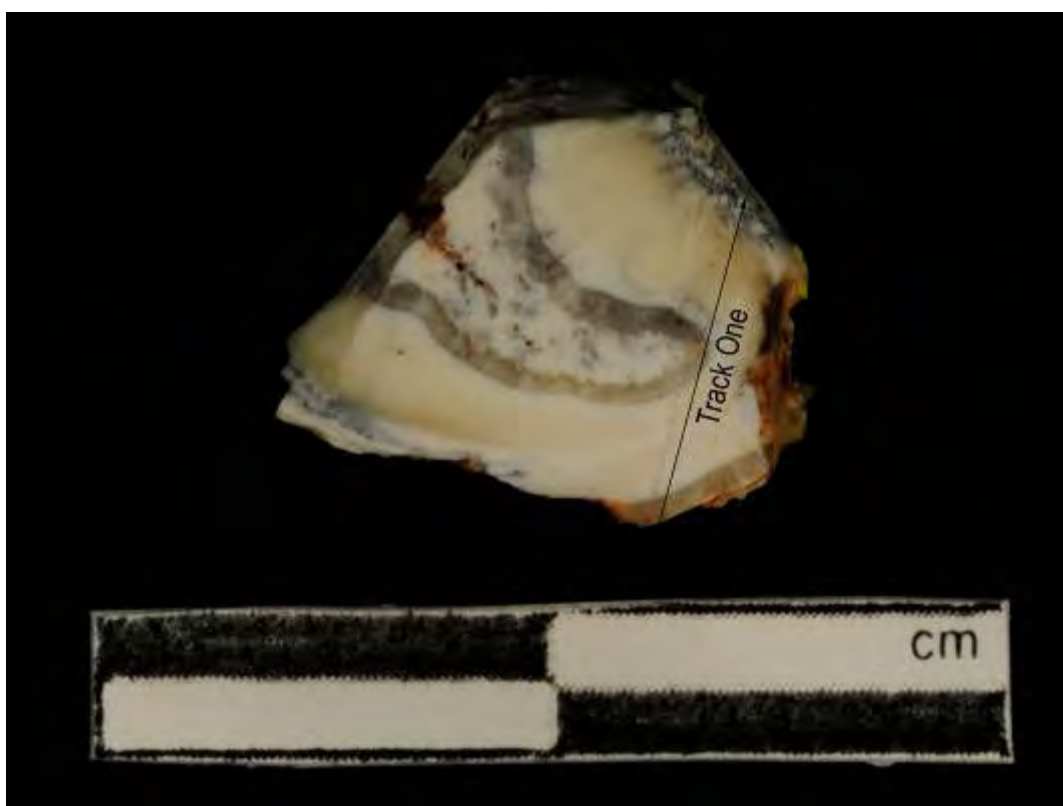


Figure A3.184 LA-MC-ICPMS Track for Sample 617, Horse, Layer 8, Pech de l'Azé II

Sample	Material	Track	Point	^{88}Sr Volts	$^{84}\text{Sr}/^{86}\text{Sr}$ 2 σ	Corrected $^{87}\text{Sr}/^{86}\text{Sr}$	$^{87}\text{Sr}/^{86}\text{Sr}$ 2 σ Error

617	Enamel	1	1	0.308	0.057454	0.000607	0.718846	0.717422	0.000952
617	Enamel	1	2	0.265	0.057414	0.000686	0.714113	0.712689	0.000831
617	Dentine	1	3	0.263	0.057804	0.000741	0.716292	0.714901	0.001064
617	Dentine	1	4	0.256	0.057260	0.000594	0.714226	0.712835	0.001117
617	Dentine	1	5	0.280	0.057369	0.000645	0.713241	0.711850	0.001018
617	Dentine	1	6	0.296	0.057479	0.000726	0.712729	0.711338	0.000890
617	Dentine	1	7	0.242	0.057378	0.000941	0.712747	0.711356	0.000968
617	Dentine	1	8	0.288	0.057217	0.000800	0.714256	0.712865	0.001401
617	Dentine	1	9	0.289	0.057374	0.000910	0.712617	0.711227	0.000853
617	Dentine	1	10	0.292	0.057179	0.000733	0.713720	0.712330	0.000823
617	Dentine	1	11	0.316	0.057594	0.000577	0.713461	0.712071	0.000738
617	Dentine	1	12	0.268	0.057537	0.000628	0.713182	0.711791	0.000776
617	Dentine	1	13						
617	Dentine	1	14	0.306	0.057881	0.000655	0.712903	0.711512	0.000924
617	Dentine	1	15	0.300	0.057500	0.000584	0.715728	0.714337	0.000572
617	Dentine	1	16	0.313	0.057111	0.000668	0.715503	0.714112	0.000655
617	Dentine	1	17	0.353	0.057101	0.000550	0.712480	0.711089	0.000632
617	Dentine	1	18	0.335	0.057018	0.000499	0.713180	0.711789	0.000766
617	Dentine	1	19	0.377	0.057339	0.000580	0.714843	0.713452	0.000808
617	Dentine	1	20	0.339	0.056913	0.000621	0.713711	0.712320	0.000653
617	Dentine	1	21	0.307	0.056945	0.000855	0.714349	0.712958	0.000669
617	Dentine	1	22	0.273	0.057420	0.000761	0.715449	0.714058	0.001094
617	Dentine	1	23	0.274	0.057426	0.000754	0.716965	0.715574	0.001128
617	Dentine	1	24	0.252	0.057370	0.000903	0.721326	0.719935	0.001087

Table A3.97 Detailed LA-MC-ICPMS Sr Isotope Results, Sample 617, Horse, Layer 8, Pech de l'Azé II

Sample 617, Pech II, France

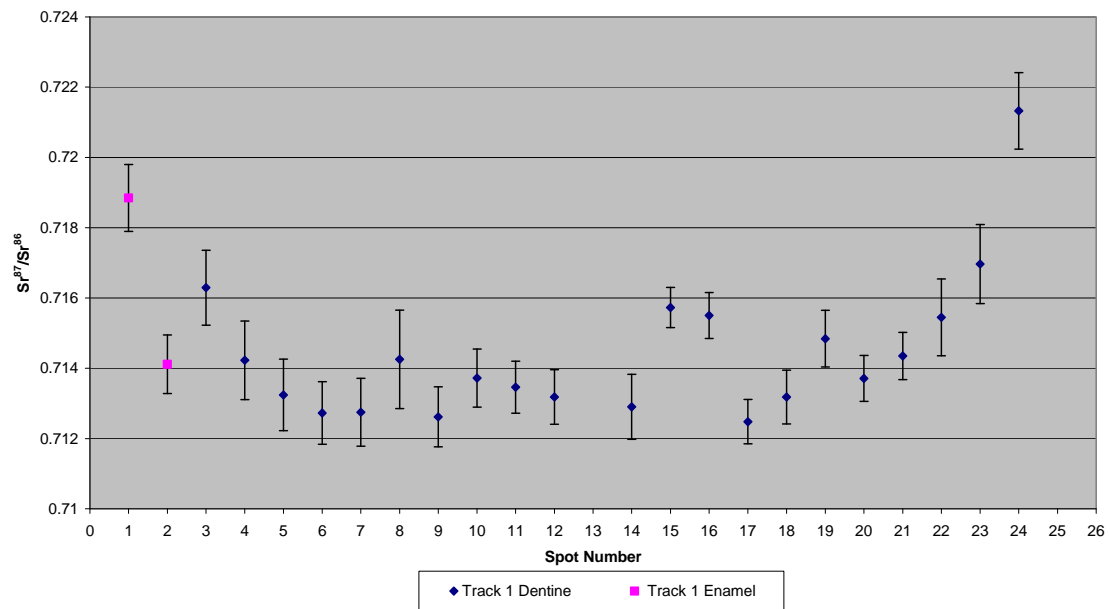


Figure A3.185 Detailed LA-MC-ICPMS Uncorrected Sr Isotope Results, Sample 617, Horse, Layer 8, Pech de l'Azé II

Sample 617, Corrected Sr Values, Pech II, France

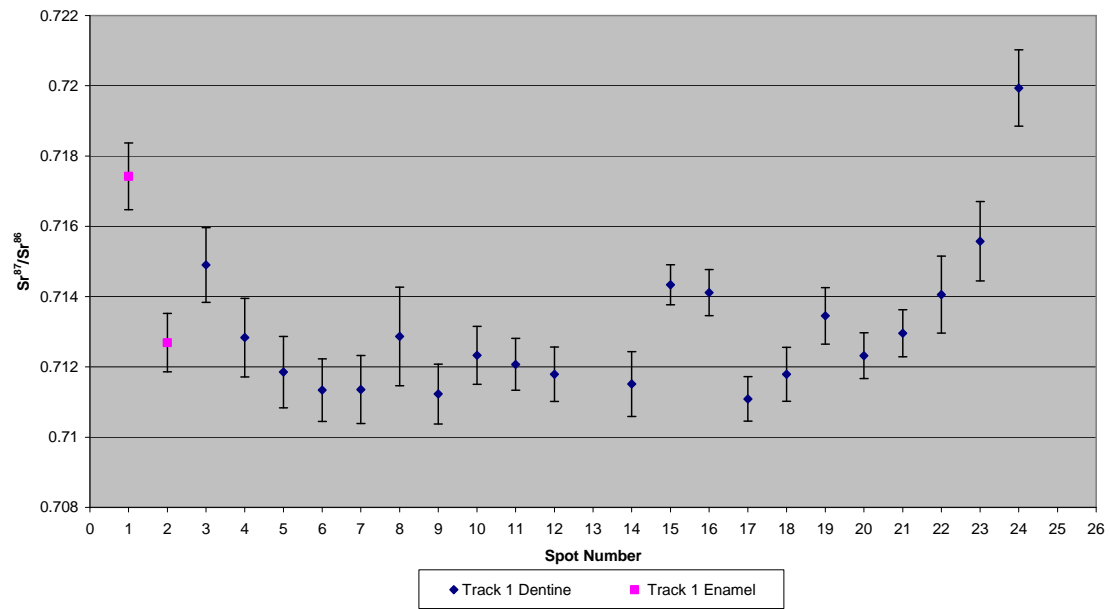


Figure A3.186 Detailed LA-MC-ICPMS Corrected Sr Isotope Results, Sample 617, Horse, Layer 8, Pech de l'Azé II

Sample 618, a deer from layer 8 of Pech de l'Azé II shown in Figure A2.62, was analysed in 2 tracks, with track 1 comprising 8 spots of enamel and 10 spots of dentine and track 2 comprising 7 spots of enamel and 7 spots of dentine, shown in Figure A3.187. The results from this sample are summarised in Table 5.34 and Figure 5.22. The enamel spots of track 1 have an average ^{88}Sr voltage of 0.488, a weighted average uncorrected $^{87}\text{Sr}/^{86}\text{Sr}$ value of 0.7186 ± 0.0012 , a weighted average corrected $^{87}\text{Sr}/^{86}\text{Sr}$ value of 0.71790 ± 0.0012 and a weighted average $^{84}\text{Sr}/^{86}\text{Sr}$ value of 0.05707 ± 0.00024 ($n=8$). The dentine spots of track 1 have an average ^{88}Sr voltage of 0.348, a weighted average uncorrected $^{87}\text{Sr}/^{86}\text{Sr}$ value of 0.7150 ± 0.0011 , a weighted average corrected $^{87}\text{Sr}/^{86}\text{Sr}$ value of 0.71380 ± 0.0011 and a weighted average $^{84}\text{Sr}/^{86}\text{Sr}$ value of 0.05735 ± 0.00018 ($n=10$). The enamel spots of track 2 have an average ^{88}Sr voltage of 0.440, a weighted average uncorrected $^{87}\text{Sr}/^{86}\text{Sr}$ value of 0.7200 ± 0.0026 , a weighted average corrected $^{87}\text{Sr}/^{86}\text{Sr}$ value of 0.71920 ± 0.0026 and a weighted average $^{84}\text{Sr}/^{86}\text{Sr}$ value of 0.05705 ± 0.00020 ($n=7$). The dentine spots of track 2 have an average ^{88}Sr voltage of 0.360, a weighted average uncorrected $^{87}\text{Sr}/^{86}\text{Sr}$ value of 0.7173 ± 0.0021 , a weighted average corrected $^{87}\text{Sr}/^{86}\text{Sr}$ value of 0.71610 ± 0.0021 and a weighted average $^{84}\text{Sr}/^{86}\text{Sr}$ value of 0.05727 ± 0.00022 ($n=7$). Enamel values for track 1 are in the range of 0.715787 to 0.720499 (uncorrected), as well as 0.715001 to 0.719713 (corrected), and are extremely heterogeneous, varying from elevated values on the exterior of the enamel to depressed values near the dentine. Dentine values for track 1 are in the range of 0.712930 to 0.716934 (uncorrected), as well as 0.711742 to 0.715746 (corrected), and are heterogeneous near the dentine-enamel junction and homogenous within 2σ error for spots 6 to 11. Enamel values for track 2 are in the range of 0.716380 to 0.725504 (uncorrected), as well as 0.715595 to 0.724718 (corrected), and are very heterogeneous, decreasing in value from the exterior of the enamel to the dentine-enamel junction. Dentine values for track 2 are in the range of 0.712896 to 0.720364 (uncorrected), as well as 0.711708 to 0.719176 (corrected), and are extremely heterogeneous. Detailed values for enamel and dentine for sample 618 are shown in Table A3.98, Figure A3.188 and Figure A3.189.

Enamel values from this sample are heterogeneous and decrease from the exterior of the enamel to the dentine-enamel junction, suggesting mobility during amelogenesis. The values of track 2 have a far more radiogenic end-member value compared to track 1. The enamel values are distributed regularly and not in discrete domains. The lower end-member of uncorrected and corrected enamel values corresponds to P8P (0.715615 ± 0.000026), a Permian monzogranite/granodiorite outcropping east of the site, as discussed with reference to sample 614. This unit outcrops within 70 km of the archaeological site. The upper end-member of uncorrected and corrected enamel values correspond to FS055-S2 (0.725528 ± 0.000017) from Cambrian/Ordovician anatectic orthogneiss to the north-east of Pech de l'Azé II which outcrop within 46.8 km from the site. Clearly, this sample spent the period of amelogenesis exclusively to the east of the site in a region of elevated $^{87}\text{Sr}/^{86}\text{Sr}$ values in the Massif Central. Dentine values are very heterogeneous in sample 2 and near the dentine-enamel junction in track 1. The interior of the dentine in track 1 (from spots 6 to 11) are relatively homogenous. The weighted average $^{84}\text{Sr}/^{86}\text{Sr}$ value for all spots is significantly elevated, with a value of 0.05716 ± 0.00010 .

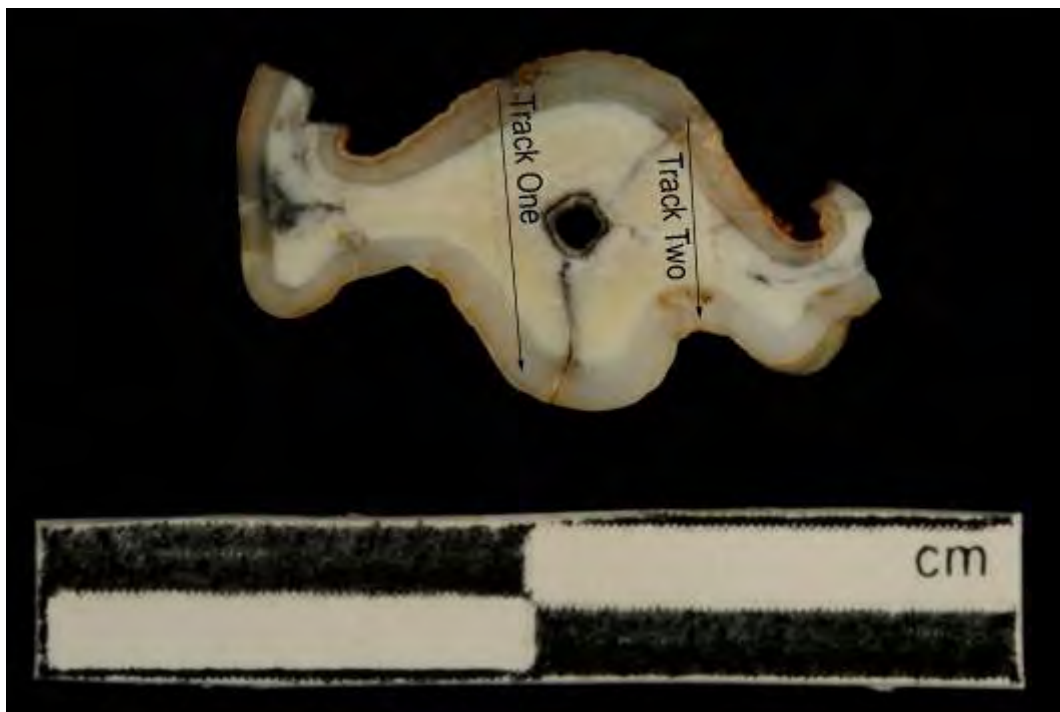


Figure A3.187 LA-MC-ICPMS Track for Sample 618, Deer, Layer 8, Pech de l'Azé II

Sample	Material	Track	Point	^{88}Sr Volts	$^{84}\text{Sr}/^{86}\text{Sr}$	$^{84}\text{Sr}/^{86}\text{Sr} 2\sigma$ Error	$^{87}\text{Sr}/^{86}\text{Sr}$	Corrected $^{87}\text{Sr}/^{86}\text{Sr}$	$^{87}\text{Sr}/^{86}\text{Sr} 2\sigma$ Error
618	Enamel	1	1	0.439	0.057350	0.000422	0.719302	0.718516	0.000554
618	Enamel	1	2	0.478	0.056609	0.000385	0.720003	0.719218	0.000631
618	Enamel	1	3	0.473	0.057102	0.000358	0.717729	0.716943	0.000494
618	Dentine	1	4	0.412	0.057303	0.000533	0.715827	0.714639	0.000675
618	Dentine	1	5	0.372	0.057033	0.000516	0.715547	0.714359	0.000668
618	Dentine	1	6	0.299	0.057584	0.000749	0.712930	0.711742	0.000878
618	Dentine	1	7	0.289	0.058079	0.000688	0.713114	0.711926	0.000755
618	Dentine	1	8	0.264	0.057664	0.001048	0.713318	0.712130	0.001087
618	Dentine	1	9	0.285	0.057430	0.000789	0.713580	0.712392	0.000838
618	Dentine	1	10	0.293	0.057373	0.000598	0.714171	0.712983	0.000911
618	Dentine	1	11	0.312	0.057207	0.000498	0.713866	0.712678	0.000766
618	Dentine	1	12	0.419	0.057258	0.000507	0.716373	0.715185	0.000707
618	Dentine	1	13	0.535	0.057333	0.000405	0.716934	0.715746	0.000530
618	Enamel	1	14	0.459	0.057076	0.000458	0.715787	0.715001	0.000609
618	Enamel	1	15	0.453	0.057451	0.000423	0.717578	0.716792	0.000572
618	Enamel	1	16	0.510	0.057448	0.000478	0.718925	0.718139	0.000454
618	Enamel	1	17	0.533	0.056937	0.000350	0.720499	0.719713	0.000669
618	Enamel	1	18	0.560	0.056887	0.000343	0.720226	0.719441	0.000657
618	Enamel	2	1	0.428	0.057159	0.000455	0.725504	0.724718	0.000847
618	Enamel	2	2	0.498	0.056801	0.000479	0.722784	0.721998	0.000590
618	Enamel	2	3	0.424	0.057612	0.001049	0.721538	0.720752	0.000860
618	Enamel	2	4	0.438	0.056918	0.000507	0.720642	0.719856	0.000493
618	Dentine	2	5	0.418	0.057008	0.000463	0.720364	0.719176	0.000609
618	Dentine	2	6	0.426	0.057689	0.000654	0.717712	0.716524	0.000741
618	Dentine	2	7	0.387	0.057234	0.000452	0.716897	0.715709	0.000570
618	Dentine	2	8	0.373	0.057927	0.000826	0.717950	0.716762	0.000577
618	Dentine	2	9	0.273	0.057003	0.000816	0.713094	0.711906	0.001143
618	Dentine	2	10	0.258	0.057333	0.000922	0.712896	0.711708	0.000914
618	Dentine	2	11	0.389	0.057224	0.000570	0.716927	0.715739	0.000605
618	Enamel	2	12	0.437	0.057028	0.000435	0.716380	0.715595	0.000488
618	Enamel	2	13	0.464	0.057218	0.000555	0.719351	0.718566	0.000642
618	Enamel	2	14	0.389	0.057100	0.000603	0.718464	0.717678	0.000582

Table A3.98 Detailed LA-MC-ICPMS Sr Isotope Results for Enamel and Dentine, Sample 618, Deer, Layer 8, Pech de l'Azé II

Sample 618, Pech II, France

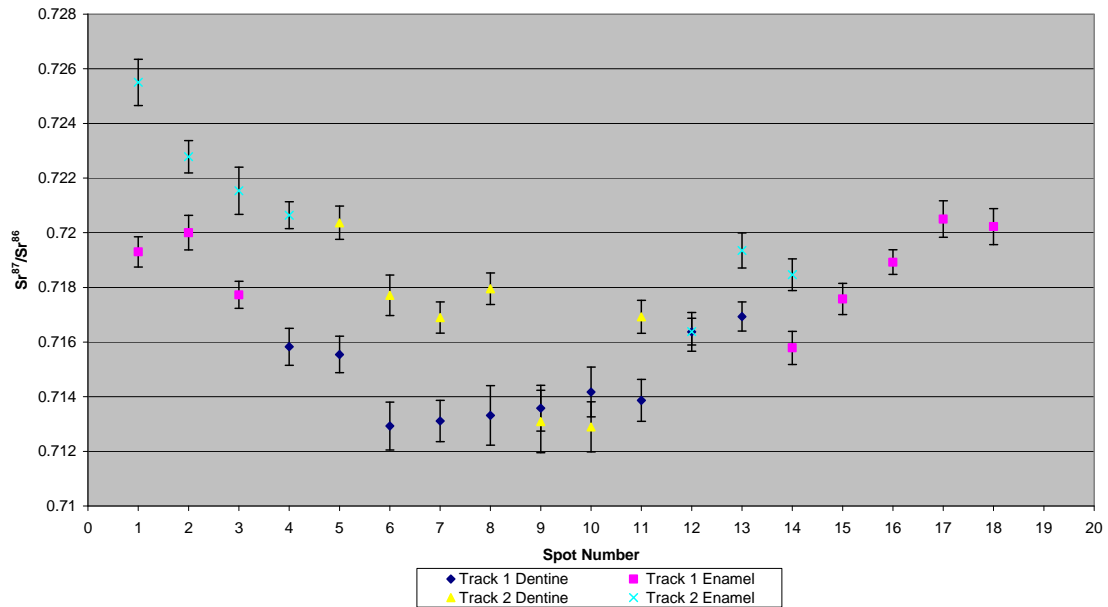


Figure A3.188 Detailed LA-MC-ICPMS Uncorrected Sr Isotope Results, Sample 618, Deer, Layer 8, Pech de l'Azé II

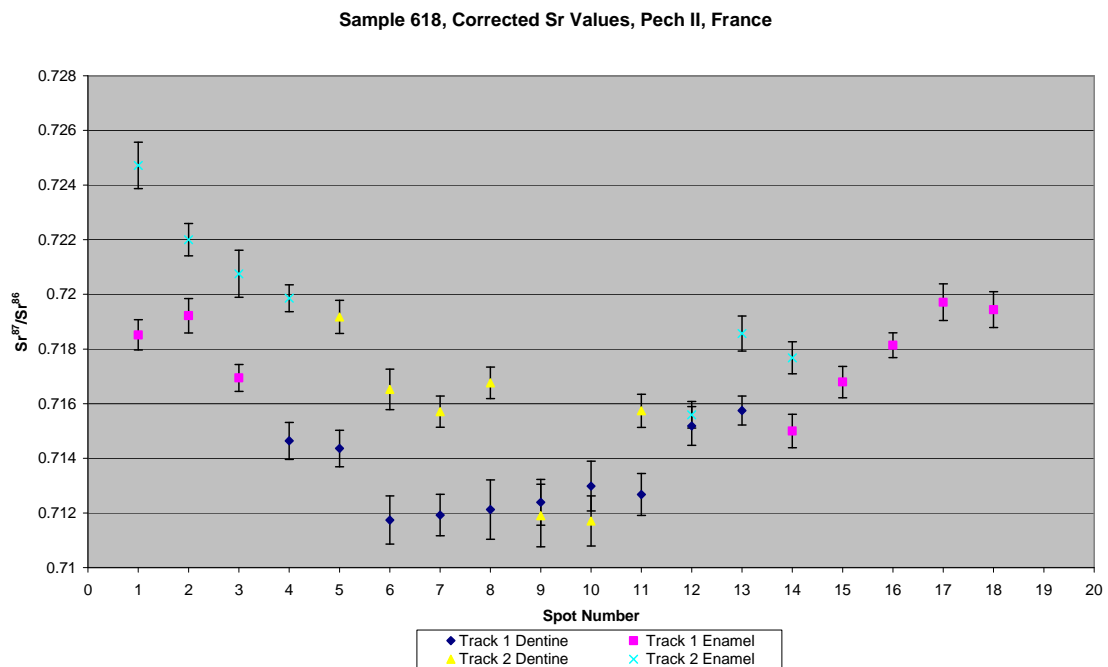


Figure A3.189 Detailed LA-MC-ICPMS Corrected Sr Isotope Results, Sample 618, Deer, Layer 8, Pech de l'Azé II

Sample 619, a horse from layer 8 of Pech de l'Azé II shown in Figure A2.63, was analysed in 1 track comprising 10 spots of enamel in 4 discontinuous sections and 13 spots of dentine in 4 discontinuous sections, shown in Figure A3.190. The results from this sample are summarised in Table 5.34 and Figure 5.22. The enamel spots of track 1 have an average ^{88}Sr voltage of 0.753, a weighted average uncorrected $^{87}\text{Sr}/^{86}\text{Sr}$ value of 0.71076 ± 0.00033 , a weighted average corrected $^{87}\text{Sr}/^{86}\text{Sr}$ value of 0.71039 ± 0.00033 and a weighted average $^{84}\text{Sr}/^{86}\text{Sr}$ value of 0.05679 ± 0.00014 ($n=10$). The dentine spots of track 1 have an average ^{88}Sr voltage of 0.705, a weighted average uncorrected $^{87}\text{Sr}/^{86}\text{Sr}$ value of 0.71062 ± 0.00022 , a weighted average corrected $^{87}\text{Sr}/^{86}\text{Sr}$ value of 0.71024 ± 0.00022 and a weighted average $^{84}\text{Sr}/^{86}\text{Sr}$ value of 0.056920 ± 0.000081 . Enamel values are in the range of 0.709866 to 0.711057 (uncorrected), as well as 0.709498 to 0.710689 (corrected), and most are homogeneous within 2σ error. Dentine values are in the range of 0.710092 to 0.711347 (uncorrected), as well as 0.709709 to 0.710964 (corrected), and are within 2σ error. Detailed values for enamel and dentine for sample 619 are shown in Table A3.99, Figure A3.191 and Figure A3.192.

This sample shows no statistical difference between enamel and dentine $^{87}\text{Sr}/^{86}\text{Sr}$ values, suggesting that the sample lived local to the site during amelogenesis. There is no systematic variation within enamel values, suggesting that the sample was not mobile between isotopically distinguishable geological units. Both the corrected and uncorrected enamel values correspond to a number of mapping samples, including from a fluvial terrace of the Vezere River in the village of Les Eyzies (FS027-S1: 0.710389 ± 0.000015) and from an Upper Cretaceous limestone at (FS089-S1 : 0.710853 ± 0.000011) which contains the archaeological site. The weighted average $^{84}\text{Sr}/^{86}\text{Sr}$ value for all enamel and dentine spots is 0.056856 ± 0.000078 , which is slightly elevated compared to the ideal value.



Figure A3.190 LA-MC-ICPMS Track for Sample 619, Horse, Layer 8, Pech de l'Azé II

Sample	Material	Track	Point	^{88}Sr Volts	$^{84}\text{Sr}/^{86}\text{Sr}$	Corrected $^{87}\text{Sr}/^{86}\text{Sr}$	$^{87}\text{Sr}/^{86}\text{Sr} 2\sigma$	Error	
619	Enamel	1	1	0.553	0.056795	0.000327	0.711660	0.711292	0.000523
619	Enamel	1	2	0.725	0.056927	0.000237	0.710649	0.710281	0.000330
619	Enamel	1	3	0.715	0.056972	0.000313	0.711057	0.710689	0.000378
619	Dentine	1	4	0.881	0.056926	0.000234	0.710892	0.710508	0.000598
619	Dentine	1	5	0.521	0.057185	0.000404	0.710460	0.710077	0.000423
619	Enamel	1	6	0.445	0.057330	0.000471	0.710348	0.709980	0.000637
619	Dentine	1	7	0.947	0.056728	0.000222	0.710756	0.710372	0.000617
619	Dentine	1	8	0.738	0.056848	0.000312	0.710689	0.710305	0.000422
619	Dentine	1	9	0.792	0.056843	0.000258	0.711052	0.710668	0.000607
619	Enamel	1	10	0.633	0.056485	0.000314	0.710716	0.710348	0.000616
619	Dentine	1	11	1.002	0.056848	0.000290	0.710855	0.710471	0.000832
619	Dentine	1	12	0.607	0.056917	0.000332	0.711108	0.710725	0.000551
619	Dentine	1	13	0.612	0.057029	0.000392	0.710692	0.710309	0.000443
619	Dentine	1	14	0.598	0.057100	0.000264	0.710226	0.709843	0.000430
619	Dentine	1	15	0.574	0.057193	0.000361	0.710092	0.709709	0.000563
619	Enamel	1	16	0.597	0.056292	0.000380	0.709866	0.709498	0.000469
619	Enamel	1	17	0.833	0.056817	0.000289	0.711013	0.710644	0.000426
619	Enamel	1	18	0.978	0.056785	0.000173	0.710644	0.710276	0.000604

619	Enamel	1	19	1.065	0.056824	0.000212	0.710639	0.710271	0.000635
619	Enamel	1	20	0.986	0.056737	0.000237	0.710741	0.710373	0.000591
619	Dentine	1	21	0.766	0.056761	0.000269	0.710380	0.709996	0.000349
619	Dentine	1	22	0.581	0.057047	0.000451	0.710336	0.709952	0.000632
619	Dentine	1	23	0.548	0.057061	0.000366	0.711347	0.710964	0.000528

Table A3.99 Detailed LA-MC-ICPMS Sr Isotope Results, Sample 619, Horse, Layer 8, Pech de l'Azé II

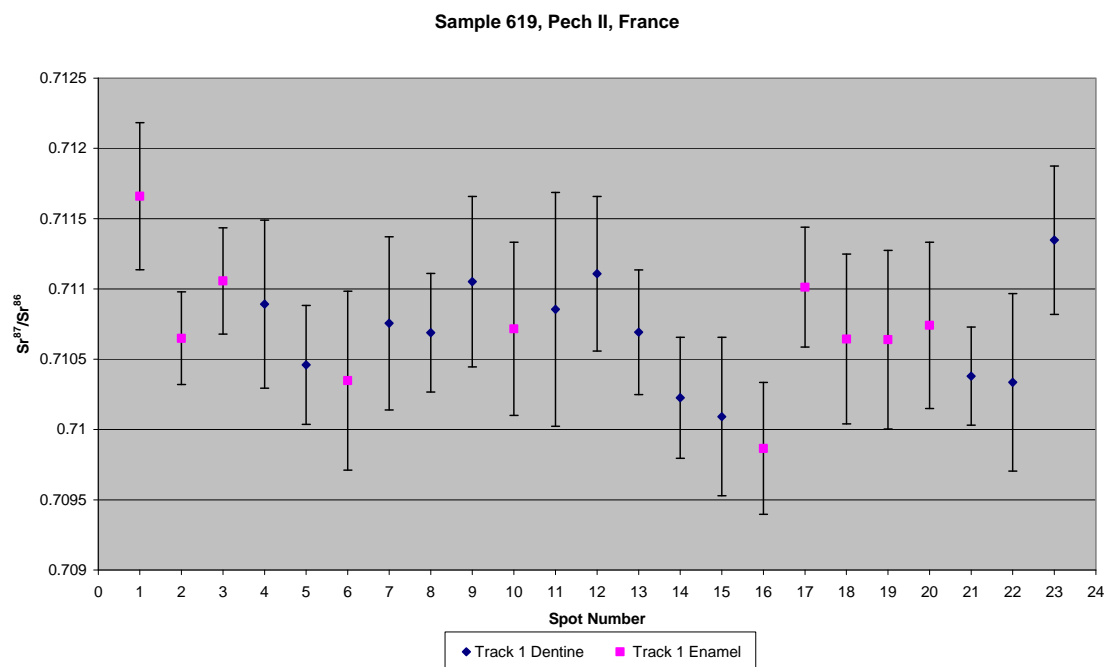


Figure A3.191 Detailed LA-MC-ICPMS Uncorrected Sr Isotope Results, Sample 619, Horse, Layer 8, Pech de l'Azé II

Sample 619, Corrected Sr Values, Pech II, France

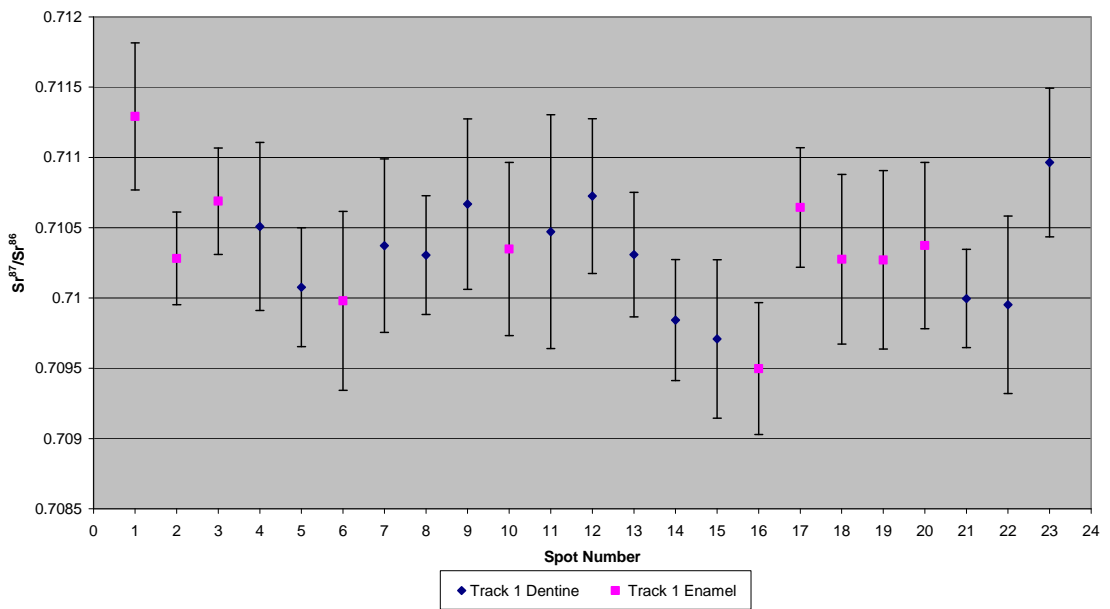


Figure A3.192 Detailed LA-MC-ICPMS Corrected Sr Isotope Results, Sample 619, Horse, Layer 8, Pech de l'Azé II

Sample 620, a bovid from layer 7 of Pech de l'Azé II shown in Figure A2.64, was analysed in 1 track comprising 10 spots of enamel in 4 discontinuous sections and 5 spots of dentine in 4 discontinuous sections, shown in Figure A3.193. The results from this sample are summarised in Table 5.34 and Figure 5.22. The enamel spots of track 1 have an average ^{88}Sr voltage of 0.319, a weighted average uncorrected $^{87}\text{Sr}/^{86}\text{Sr}$ value of 0.7146 ± 0.0010 , a weighted average corrected $^{87}\text{Sr}/^{86}\text{Sr}$ value of 0.71420 ± 0.0010 and a weighted average $^{84}\text{Sr}/^{86}\text{Sr}$ value of 0.05685 ± 0.00028 ($n=4$). The dentine spots of track 1 have an average ^{88}Sr voltage of 0.355, a weighted average uncorrected $^{87}\text{Sr}/^{86}\text{Sr}$ value of 0.71159 ± 0.00062 , a weighted average corrected $^{87}\text{Sr}/^{86}\text{Sr}$ value of 0.71120 ± 0.00062 and a weighted average $^{84}\text{Sr}/^{86}\text{Sr}$ value of 0.05684 ± 0.00027 ($n=5$). Enamel values are in the range of 0.713868 to 0.715581 (uncorrected), as well as 0.713500 to 0.715212 (corrected), and are all within 2σ error, although errors are large. Dentine values are in the range of 0.711105 to 0.712429 (uncorrected), as well as 0.710722 to 0.712045 (corrected), and are all within 2σ error. Detailed values for enamel and dentine for sample 620 are shown in Table A3.100, Figure A3.194 and Figure A3.195.

This sample has enamel and dentine $^{87}\text{Sr}/^{86}\text{Sr}$ values that are statistically indistinguishable. Within the enamel and dentine domains, the values are homogeneous within 2σ error, suggesting that the sample was not mobile during amelogenesis and that the regime of post-burial diagenesis was homogenous. Both the uncorrected and corrected enamel values correspond to mapping samples FS031-S1 (0.714027 ± 0.00005), FS058-S1 (0.713898 ± 0.000031) and FS046-S1 (0.714131 ± 0.000015), which are all located on floodplains and outcrop as close as 1.4 km from the site.

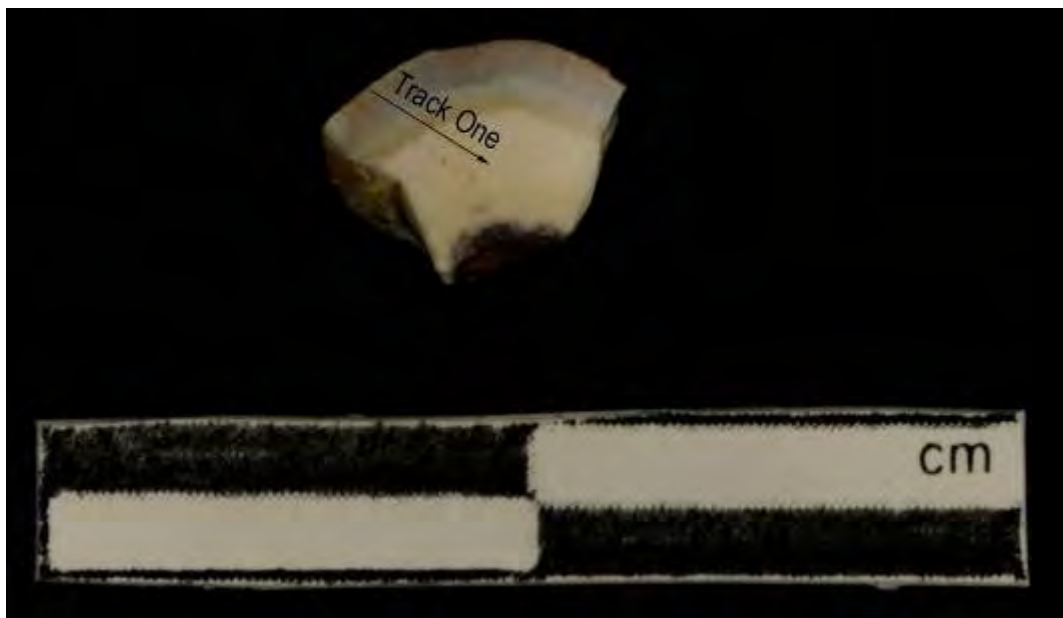


Figure A3.193 LA-MC-ICPMS Track for Sample 620, Bovid, Layer 7, Pech de l'Azé II

Sample	Material	Track	Point	^{88}Sr Volts	$^{84}\text{Sr}/^{86}\text{Sr}$	$^{84}\text{Sr}/^{86}\text{Sr} 2\sigma$ Error	Corrected $^{87}\text{Sr}/^{86}\text{Sr}$	$^{87}\text{Sr}/^{86}\text{Sr} 2\sigma$ Error
620	Enamel	1	1	0.266	0.056870	0.000481	0.715581	0.715212
620	Enamel	1	2	0.305	0.056833	0.000626	0.713868	0.713500
620	Enamel	1	3	0.334	0.056660	0.000604	0.714277	0.713909
620	Enamel	1	4	0.370	0.057042	0.000627	0.714754	0.714386
620	Dentine	1	5	0.364	0.056996	0.000535	0.712429	0.712045
620	Dentine	1	6	0.333	0.056914	0.000576	0.711604	0.711221
620	Dentine	1	7	0.364	0.056772	0.000657	0.711105	0.710722
620	Dentine	1	8	0.358	0.056519	0.000577	0.711600	0.711216
620	Dentine	1	9	0.357	0.057045	0.000743	0.711272	0.710889

Table A3.100 Detailed LA-MC-ICPMS Sr Isotope Results for Enamel and Dentine, Sample 620, Bovid, Layer 7, Pech de l'Azé II

Sample 620, Pech II, France

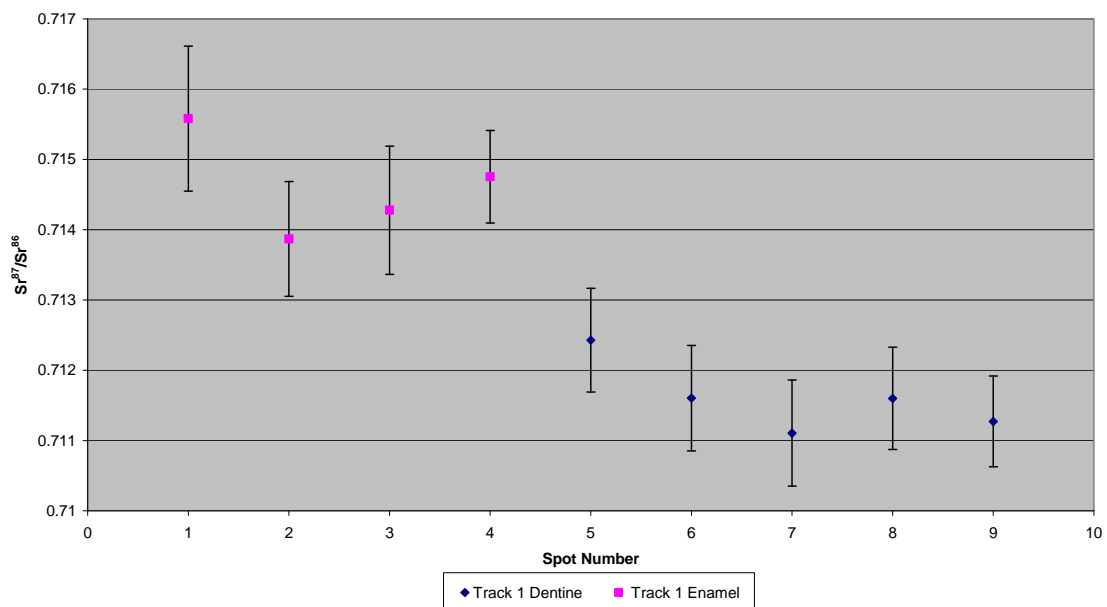


Figure A3.194 Detailed LA-MC-ICPMS Uncorrected Sr Isotope Results, Sample 620, Bovid, Layer 7, Pech de l'Azé II

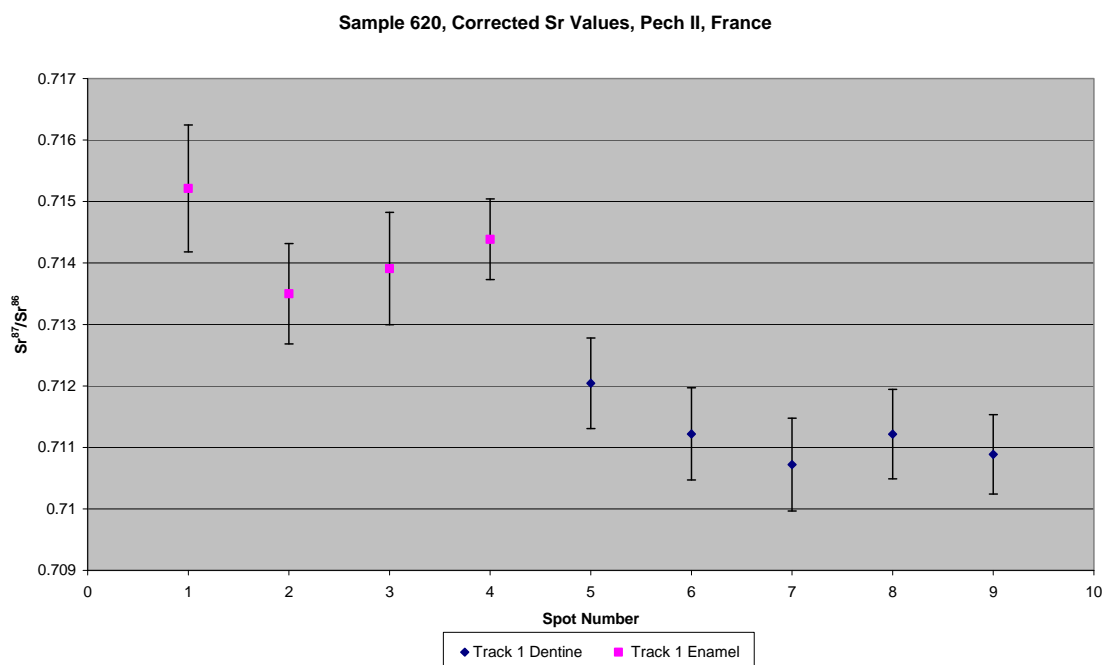


Figure A3.195 Detailed LA-MC-ICPMS Corrected Sr Isotope Results, Sample 620, Bovid, Layer 7, Pech de l'Azé II

Sample 622, a hippopotamus tooth from layer 7 of Pech de l'Azé II shown in Figure A2.65, was analysed in 2 tracks, with track 1 comprising 7 spots of

enamel and 11 spots of dentine and track 2 comprising 7 spots of enamel and 13 spots of dentine, shown in Figure A3.196. The results from this sample are summarised in Table 5.34 and Figure 5.22. The enamel spots of track 1 have an average ^{88}Sr voltage of 0.360, a weighted average uncorrected $^{87}\text{Sr}/^{86}\text{Sr}$ value of 0.7130 ± 0.0013 , a weighted average corrected $^{87}\text{Sr}/^{86}\text{Sr}$ value of 0.71040 ± 0.0013 and a weighted average $^{84}\text{Sr}/^{86}\text{Sr}$ value of 0.05749 ± 0.00034 ($n=7$). The dentine spots of track 1 have an average ^{88}Sr voltage of 0.406, a weighted average uncorrected $^{87}\text{Sr}/^{86}\text{Sr}$ value of 0.71196 ± 0.00041 , a weighted average corrected $^{87}\text{Sr}/^{86}\text{Sr}$ value of 0.70987 ± 0.00041 and a weighted average $^{84}\text{Sr}/^{86}\text{Sr}$ value of 0.05745 ± 0.00026 . The enamel spots of track 2 have an average ^{88}Sr voltage of 0.297, a weighted average uncorrected $^{87}\text{Sr}/^{86}\text{Sr}$ value of 0.7143 ± 0.0018 , a weighted average corrected $^{87}\text{Sr}/^{86}\text{Sr}$ value of 0.71160 ± 0.0018 and a weighted average $^{84}\text{Sr}/^{86}\text{Sr}$ value of 0.05810 ± 0.00047 . The dentine spots of track 2 have an average ^{88}Sr voltage of 0.358, a weighted average uncorrected $^{87}\text{Sr}/^{86}\text{Sr}$ value of 0.71165 ± 0.00037 , a weighted average corrected $^{87}\text{Sr}/^{86}\text{Sr}$ value of 0.70956 ± 0.00037 and a weighted average $^{84}\text{Sr}/^{86}\text{Sr}$ value of 0.05748 ± 0.00027 . Enamel values for track 1 are in the range of 0.711774 to 0.716660 (uncorrected), as well as 0.709108 to 0.713994 (corrected), and are heterogeneous, decreasing, with the exception of spot 2, from spot 1 to spot 7. Dentine values for track 1 are in the range of 0.711249 to 0.713303 (uncorrected), as well as 0.709155 to 0.711209 (corrected), and are homogeneous within 2σ error, with the exception of spot 18, which is elevated in value. Enamel values for track 2 are in the range of 0.712579 to 0.718057 (uncorrected), as well as 0.709914 to 0.715392 (corrected), and are relatively heterogeneous, decreasing in value from spot 1-spot 4 and increasing in values from spot 4 to spot 7. Dentine values for track 2 are in the range of 0.710783 to 0.712770 (uncorrected), as well as 0.708689 to 0.710676 (corrected), and are mostly within 2σ error. Detailed values for enamel and dentine for sample 622 are shown in Table A3.101, Figure A3.197 and Figure A3.198.

The enamel and dentine $^{87}\text{Sr}/^{86}\text{Sr}$ values of this sample are distinct, suggesting that this sample is a migrant to the area. Enamel values decrease in both tracks from the exterior of the enamel to the dentine-enamel junction (with the exception of spot 7 on track 2), suggesting that this individual migrated over

different geological environments during amelogenesis. The upper end-member of the uncorrected range represents a relatively radiogenic province, which corresponds to the value of FS041-S1 from floodplain sediments. The corrected value for this end-member corresponds to FS031-S1 from the floodplain of the Dordogne river which outcrops within 1.4 km. The lower end of the uncorrected range corresponds to Dordogne floodplain values from FS056-S1, located approximately 60 km north-east of the site, while the corrected range corresponds to Vezere (FS027-S1) and Dordogne (FS032-S1) floodplain samples, as well as upper Jurassic carbonate (FS087-S1). Dentine values are mostly within 2σ error, but errors are large and the values cover a large range. $^{84}\text{Sr}/^{86}\text{Sr}$ has a slightly elevated value of 0.05754 ± 0.00015 .



Figure A3.196 LA-MC-ICPMS Track for Sample 622, Hippopotamus, Layer 7, Pech de l'Azé II

Sample	Material	Track	Point	^{88}Sr Volts	$^{84}\text{Sr}/^{86}\text{Sr}$	$^{84}\text{Sr}/^{86}\text{Sr} 2\sigma$	Corrected $^{87}\text{Sr}/^{86}\text{Sr}$	$^{87}\text{Sr}/^{86}\text{Sr} 2\sigma$ Error
622	Enamel	1	1	0.295	0.057517	0.001067	0.716660	0.713994
622	Enamel	1	2	0.263	0.058075	0.000828	0.713837	0.711172

Sample	Material	Track	Point	^{88}Sr Volts	$^{84}\text{Sr}/^{86}\text{Sr}$	$^{84}\text{Sr}/^{86}\text{Sr} 2\sigma$ Error	$^{87}\text{Sr}/^{86}\text{Sr}$ Corrected	$^{87}\text{Sr}/^{86}\text{Sr} 2\sigma$ Error
622	Enamel	1	3	0.308	0.060415	0.002778	0.714969	0.712304
622	Enamel	1	4	0.324	0.057740	0.000683	0.714678	0.712012
622	Enamel	1	5	0.362	0.057474	0.000554	0.714161	0.711495
622	Enamel	1	6	0.403	0.057218	0.000505	0.712730	0.710065
622	Enamel	1	7	0.563	0.057396	0.000399	0.711774	0.709108
622	Dentine	1	8	0.324	0.058276	0.000705	0.711271	0.709177
622	Dentine	1	9	0.298	0.059104	0.001383	0.712297	0.710203
622	Dentine	1	10	0.307	0.057822	0.000860	0.711542	0.709448
622	Dentine	1	11	0.312	0.057722	0.000764	0.712096	0.710003
622	Dentine	1	12	0.393	0.058002	0.000476	0.712070	0.709976
622	Dentine	1	13	0.327	0.057271	0.000786	0.711474	0.709381
622	Dentine	1	14	0.356	0.057711	0.000728	0.712239	0.710146
622	Dentine	1	15	0.365	0.057664	0.000671	0.711249	0.709155
622	Dentine	1	16	0.575	0.057187	0.000261	0.712429	0.710335
622	Dentine	1	17	0.627	0.057258	0.000325	0.711493	0.709400
622	Dentine	1	18	0.580	0.057284	0.000414	0.713303	0.711209
622	Enamel	2	1	0.229	0.058230	0.001036	0.714821	0.712156
622	Enamel	2	2	0.234	0.059217	0.001429	0.714608	0.711943
622	Enamel	2	3	0.306	0.057380	0.000918	0.713544	0.710878
622	Enamel	2	4	0.332	0.058579	0.000572	0.712579	0.709914
622	Enamel	2	5	0.312	0.058198	0.000775	0.712765	0.710099
622	Enamel	2	6	0.306	0.058130	0.000713	0.714006	0.711341
622	Enamel	2	7	0.363	0.057604	0.000584	0.718057	0.715392
622	Dentine	2	8	0.293	0.058178	0.000708	0.711778	0.709684
622	Dentine	2	9	0.297	0.057964	0.000848	0.712091	0.709997
622	Dentine	2	10	0.358	0.057557	0.000616	0.711605	0.709512
622	Dentine	2	11	0.287	0.057557	0.000800	0.710904	0.708810
622	Dentine	2	12	0.271	0.057251	0.000880	0.711333	0.709240
622	Dentine	2	13	0.288	0.058639	0.000726	0.710783	0.708689
622	Dentine	2	14	0.327	0.057906	0.000716	0.710971	0.708878
622	Dentine	2	15	0.426	0.057260	0.000624	0.712770	0.710676
622	Dentine	2	16	0.506	0.057145	0.000449	0.711284	0.709190
622	Dentine	2	17	0.360	0.057721	0.000433	0.710974	0.708881
622	Dentine	2	18	0.339	0.057160	0.000623	0.712200	0.710107
622	Dentine	2	19	0.371	0.057172	0.000569	0.712456	0.710362
622	Dentine	2	20	0.529	0.057063	0.000401	0.711640	0.709547

Table A3.101 Detailed LA-MC-ICPMS Sr Isotope Results for Dentine and Enamel, Sample 622, Hippopotamus, Layer 7, Pech de l'Azé II

Sample 622, Pech II, France

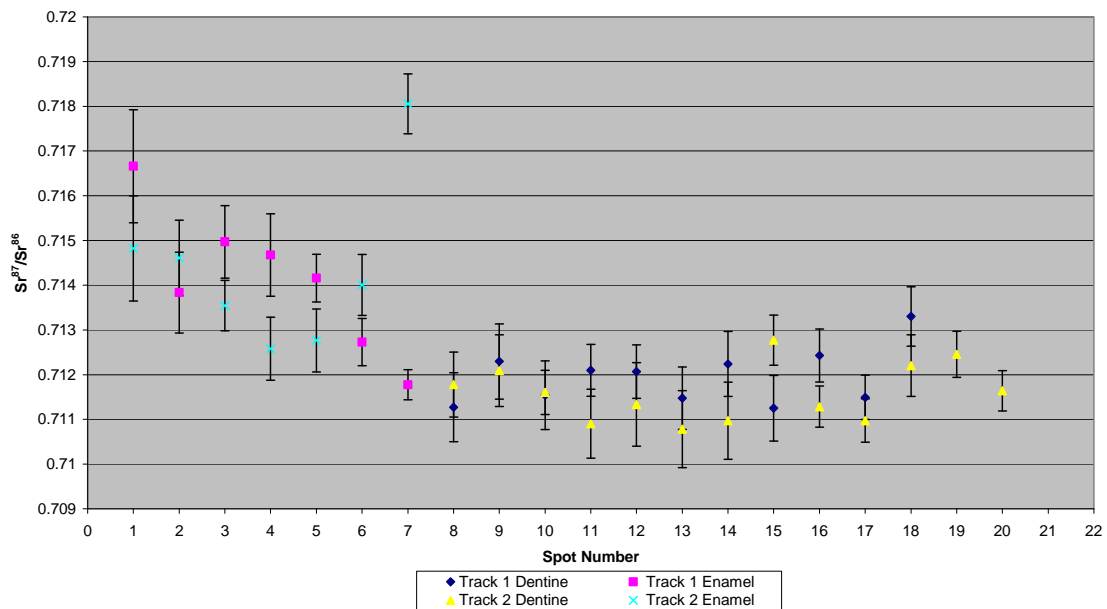


Figure A3.197 Detailed LA-MC-ICPMS Uncorrected Sr Isotope Results, Sample 622, Hippopotamus, Layer 7, Pech de l'Azé II

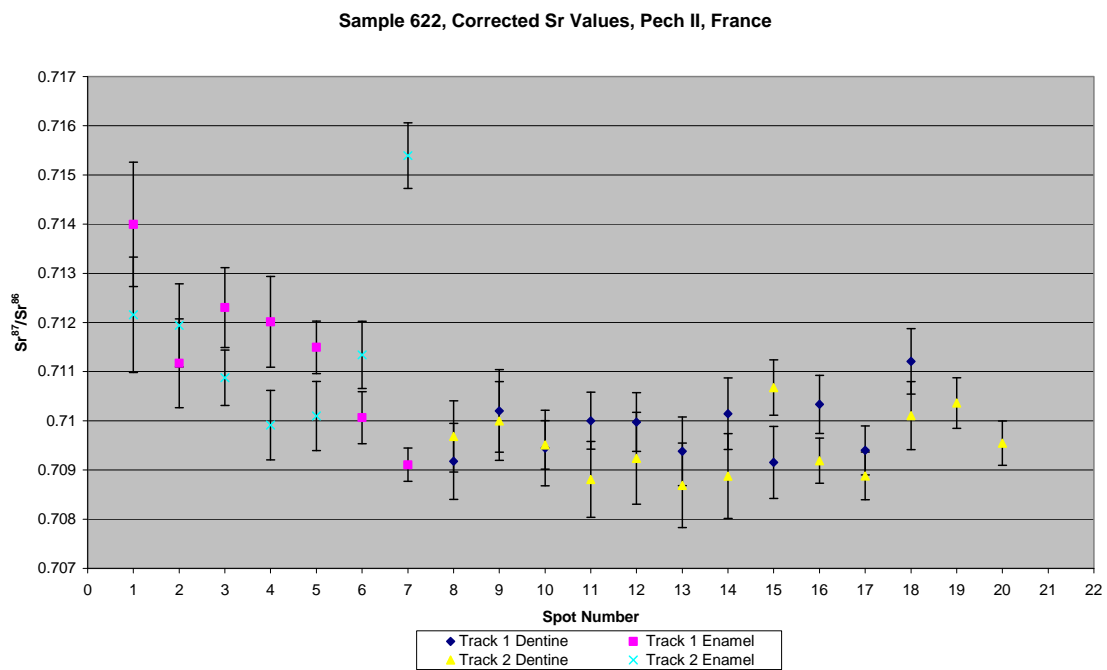


Figure A3.198 Detailed LA-MC-ICPMS Corrected Sr Isotope Results, Sample 622, Hippopotamus, Layer 7, Pech de l'Azé II

Sample 624, a deer from layer 6 of Pech de l'Azé II shown in Figure A2.66, was analysed in 1 track comprising 5 spots of enamel and 6 spots of dentine, shown

in Figure A3.200. The results from this sample are summarised in Table 5.34 and Figure 5.22. The enamel spots of track 1 have an average ^{88}Sr voltage of 0.355, a weighted average uncorrected $^{87}\text{Sr}/^{86}\text{Sr}$ value of 0.7174 ± 0.0071 , a weighted average corrected $^{87}\text{Sr}/^{86}\text{Sr}$ value of 0.71510 ± 0.0071 and a weighted average $^{84}\text{Sr}/^{86}\text{Sr}$ value of 0.05736 ± 0.00056 ($n=5$). The dentine spots of track 1 have an average ^{88}Sr voltage of 0.277, a weighted average uncorrected $^{87}\text{Sr}/^{86}\text{Sr}$ value of 0.7135 ± 0.0019 , a weighted average corrected $^{87}\text{Sr}/^{86}\text{Sr}$ value of 0.70970 ± 0.0019 and a weighted average $^{84}\text{Sr}/^{86}\text{Sr}$ value of 0.05772 ± 0.00054 ($n=6$). Enamel values are in the range of 0.714587 to 0.728461 (uncorrected), as well as 0.712323 to 0.726196 (corrected), and all enamel samples are homogeneous within 2σ error, with the exception of spot 1, which is elevated compared to all other samples in this track. Dentine values are in the range of 0.711319 to 0.715364 (uncorrected), as well as 0.707541 to 0.711586 (corrected), and are somewhat homogeneous in 2 domains, with spots 6 and 7 within 2σ error and spots 8 to 11 within 2σ error. Detailed values for enamel and dentine for sample 624 are shown in Table A3.102, Figure A3.200 and Figure A3.201.

Enamel values from this sample, excluding the elevated spot 1 (which is considered an erroneous value) are homogeneous within error. The uncorrected weighted average of these spots (0.71505 ± 0.00064) correspond to the mapping value of monzogranite/granodiorite samples P8P (0.715615 ± 0.000026) and P2P (0.715531 ± 0.000026), as well as floodplain sediments from P38P (0.715361 ± 0.000018). These samples are located between 220 to 350 km from the site; however, the same units outcrop within 80 km of the site, as discussed above with regards sample 848. This domain has a corrected weighted average value of 0.71279 ± 0.00064 , which correlates to Verezé and Dordogne floodplain and alluvial valley fill sediments. Enamel spot 1 has a value that is significantly higher than all other spots; however, this spot appears to be located partially off the edge of tooth and so may not be appropriately focused (as discussed above in more detail with reference to sample M008). Dentine spots 6 and 7 have $^{87}\text{Sr}/^{86}\text{Sr}$ values that are similar to those of the enamel and the dentine containing these spots has a dark staining, which may

reflect post-depositional alteration. $^{84}\text{Sr}/^{86}\text{Sr}$ values for this sample are 0.05747 \pm 0.00032, which is somewhat elevated.



Figure A3.199 LA-MC-ICPMS Track for Sample 624, Deer, Layer 6, Pech de l'Azé II

Sample	Material	Track	Point	^{88}Sr Volts	$^{84}\text{Sr}/^{86}\text{Sr}$	$^{84}\text{Sr}/^{86}\text{Sr} 2\sigma$	Corrected $^{87}\text{Sr}/^{86}\text{Sr}$	$^{87}\text{Sr}/^{86}\text{Sr} 2\sigma$	$^{87}\text{Sr}/^{86}\text{Sr}$ Error
624	Enamel	1	1	0.410	0.056742	0.000441	0.728461	0.726196	0.000668
624	Enamel	1	2	0.291	0.057557	0.000559	0.714951	0.712687	0.000697
624	Enamel	1	3	0.318	0.057766	0.000761	0.715185	0.712921	0.000695
624	Enamel	1	4	0.375	0.057703	0.000415	0.714587	0.712323	0.000573
624	Enamel	1	5	0.381	0.057287	0.000601	0.715455	0.713190	0.000544
624	Dentine	1	6	0.341	0.058354	0.001171	0.715285	0.711507	0.000744
624	Dentine	1	7	0.286	0.057585	0.000874	0.715364	0.711586	0.000875
624	Dentine	1	8	0.233	0.058247	0.000777	0.712369	0.708591	0.000859
624	Dentine	1	9	0.234	0.057736	0.000946	0.711319	0.707541	0.001022
624	Dentine	1	10	0.289	0.057050	0.000651	0.711383	0.707605	0.000994
624	Dentine	1	11	0.276	0.057966	0.000808	0.713580	0.709802	0.000779

Table A3.102 Detailed LA-MC-ICPMS Sr Isotope Results, Sample 624, Deer, Layer 6, Pech de l'Azé II

Sample 624, Pech II, France

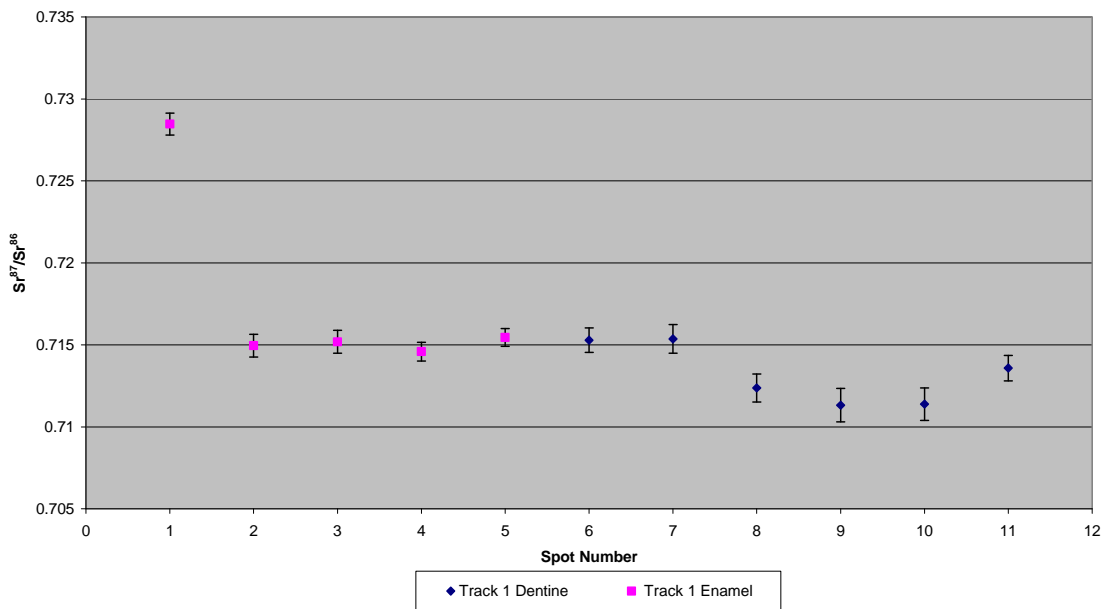


Figure A3.200 Detailed LA-MC-ICPMS Uncorrected Sr Isotope Results, Sample 624, Deer, Layer 6, Pech de l'Azé II

Sample 624, Corrected Sr Values, Pech II, France

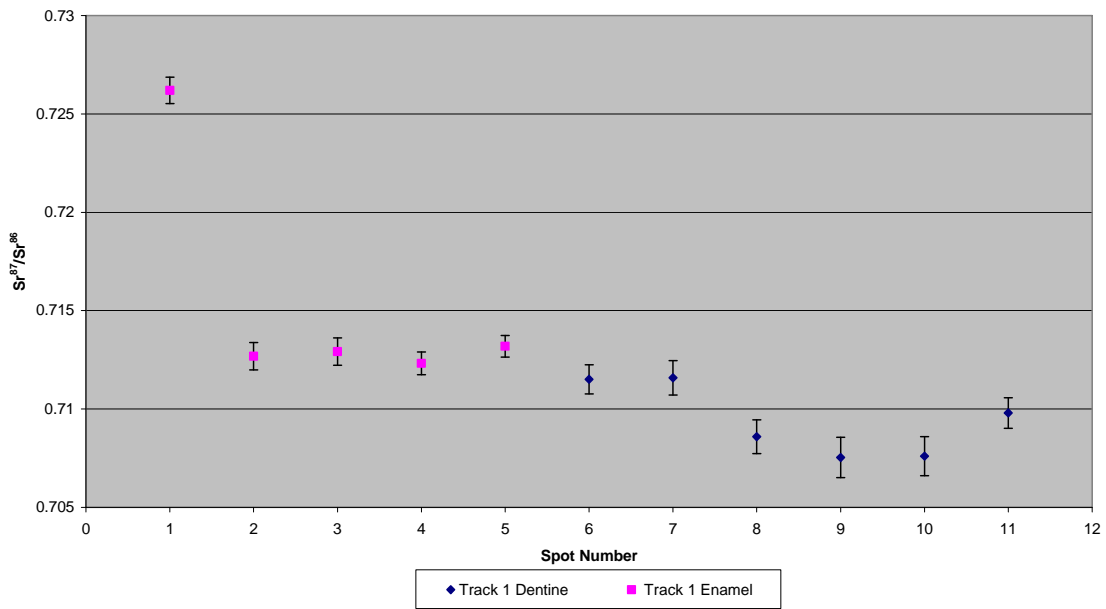


Figure A3.201 Detailed LA-MC-ICPMS Corrected Sr Isotope Results, Sample 624, Deer, Layer 6, Pech de l'Azé II

Sample 625, a horse from layer 6 of Pech de l'Azé II shown in Figure A2.67, was analysed in 2 tracks, with track 1 comprising 4 spots of enamel in 3 discontinuous sections and 15 spots of dentine in 4 discontinuous sections and track 2 comprising 5 spots of enamel in 2 discontinuous sections and 14 spots of dentine in 2 discontinuous sections, shown in Figure A3.202. The results from this sample are summarised in Table 5.34 and Figure 5.22. The enamel spots of track 1 have an average ^{88}Sr voltage of 0.347, a weighted average uncorrected $^{87}\text{Sr}/^{86}\text{Sr}$ value of 0.71380 ± 0.00082 , a weighted average corrected $^{87}\text{Sr}/^{86}\text{Sr}$ value of 0.70909 ± 0.00082 and a weighted average $^{84}\text{Sr}/^{86}\text{Sr}$ value of 0.05688 ± 0.00027 ($n=4$). The dentine spots of track 1 have an average ^{88}Sr voltage of 0.363, a weighted average uncorrected $^{87}\text{Sr}/^{86}\text{Sr}$ value of 0.71197 ± 0.00064 , a weighted average corrected $^{87}\text{Sr}/^{86}\text{Sr}$ value of 0.71090 ± 0.00064 and a weighted average $^{84}\text{Sr}/^{86}\text{Sr}$ value of 0.05673 ± 0.00024 ($n=15$). The enamel spots of track 2 have an average ^{88}Sr voltage of 0.376, a weighted average uncorrected $^{87}\text{Sr}/^{86}\text{Sr}$ value of 0.7120 ± 0.0014 , a weighted average corrected $^{87}\text{Sr}/^{86}\text{Sr}$ value of 0.70910 ± 0.0014 and a weighted average $^{84}\text{Sr}/^{86}\text{Sr}$ value of 0.05722 ± 0.00022 ($n=5$). The dentine spots of track 2 have an average ^{88}Sr voltage of 0.373, a weighted average uncorrected $^{87}\text{Sr}/^{86}\text{Sr}$ value of 0.7142 ± 0.0010 , a weighted average corrected $^{87}\text{Sr}/^{86}\text{Sr}$ value of 0.71130 ± 0.0010 and a weighted average $^{84}\text{Sr}/^{86}\text{Sr}$ value of 0.05715 ± 0.00024 ($n=14$). Enamel values for track 1 are in the range of 0.713087 to 0.714190 (uncorrected), as well as 0.710194 to 0.711297 (corrected), and are extremely homogenous, all being within 2σ error. Dentine values for track 1 are in the range of 0.710638 to 0.716227 (uncorrected), as well as 0.707760 to 0.713349 (corrected), and are extremely heterogeneous. Enamel values for track 2 are in the range of 0.710360 to 0.713374 (uncorrected), as well as 0.707467 to 0.709481 (corrected), and are somewhat heterogeneous. Dentine values for track 2 are 0.711363 to 0.717626 (uncorrected), as well as 0.708485 to 0.714748 (corrected), and extremely heterogeneous. Detailed values for enamel and dentine for sample 625 are shown in Table A3.103, Figure A3.203 and Figure A3.204.

This sample shows no statistical difference between enamel and dentine weighted average values. Enamel values are moderately homogenous, particularly in track 1, suggesting an individual that was not very mobile during amelogenesis. In contrast, the dentine is extremely heterogeneous in a similar fashion to other horse samples in this study, as discussed in section 7.2.4. The weighted average uncorrected enamel value corresponds to mapping samples F36R (0.712497 ± 0.000008), F37R (0.712145 ± 0.000025) and FS054-S1 (0.712245 ± 0.000026) located in metamorphics, and samples FS058-S1 (0.713898 ± 0.000031), FS035-S1 (0.713096 ± 0.000014) and FS029-S1 (0.712033 ± 0.000015) from floodplain sediments. The weighted average corrected enamel value (0.70989 ± 0.00098) corresponds to many floodplain and Jurassic carbonate values to the west, south and east of the site which outcrops within 1.4 km of the site. $^{84}\text{Sr}/^{86}\text{Sr}$ values for this sample are 0.05698 ± 0.00014 , which is somewhat elevated compared to the ideal value of 0.0565.



Figure A3.202 LA-MC-ICPMS Track for Sample 625, Horse, Layer 6, Pech de l'Azé II

Sample	Material	Track	Point	^{88}Sr Volts	$^{84}\text{Sr}/^{86}\text{Sr}$	$^{84}\text{Sr}/^{86}\text{Sr} 2\sigma$ Error	$^{87}\text{Sr}/^{86}\text{Sr}$	Corrected $^{87}\text{Sr}/^{86}\text{Sr}$	$^{87}\text{Sr}/^{86}\text{Sr} 2\sigma$ Error
625	Dentine	1	1	0.502	0.056202	0.000453	0.711766	0.708888	0.000453
625	Dentine	1	2	0.394	0.056037	0.000430	0.711618	0.708740	0.000439
625	Dentine	1	3	0.304	0.056148	0.000726	0.712549	0.709671	0.000669
625	Enamel	1	4	0.406	0.056781	0.000404	0.714190	0.711297	0.000587
625	Enamel	1	5	0.387	0.056762	0.000533	0.713087	0.710194	0.000640
625	Dentine	1	6	0.335	0.057028	0.000456	0.711753	0.708874	0.000564
625	Dentine	1	7	0.381	0.056805	0.000538	0.712739	0.709861	0.000552
625	Dentine	1	8	0.419	0.056886	0.000499	0.713508	0.710630	0.000697
625	Dentine	1	9	0.421	0.056715	0.000443	0.711011	0.708132	0.000559
625	Dentine	1	10	0.389	0.056838	0.000521	0.710638	0.707760	0.000610
625	Dentine	1	11	0.326	0.057245	0.000993	0.711800	0.708921	0.000893
625	Enamel	1	12	0.319	0.057128	0.000652	0.713666	0.710773	0.000847
625	Dentine	1	13	0.241	0.057252	0.000851	0.716227	0.713349	0.000992
625	Dentine	1	14	0.258	0.057444	0.000876	0.711618	0.708740	0.000812
625	Enamel	1	15	0.277	0.057243	0.000877	0.714065	0.711172	0.000585
625	Dentine	1	16	0.388	0.056600	0.000487	0.711013	0.708135	0.000538
625	Dentine	1	17	0.347	0.057004	0.000595	0.711219	0.708340	0.000640
625	Dentine	1	18	0.353	0.057207	0.000560	0.712605	0.709727	0.000758
625	Dentine	1	19	0.384	0.057842	0.001264	0.714472	0.711594	0.000820
625	Enamel	2	1	0.443	0.057158	0.000531	0.711654	0.708761	0.000570
625	Enamel	2	2	0.425	0.056963	0.000472	0.712374	0.709481	0.000565
625	Dentine	2	3	0.430	0.056947	0.000378	0.712788	0.709910	0.000531
625	Dentine	2	4	0.488	0.056990	0.000444	0.715069	0.712191	0.000572
625	Dentine	2	5	0.540	0.056869	0.000311	0.714187	0.711308	0.000390
625	Dentine	2	6	0.407	0.056886	0.000381	0.715530	0.712652	0.000506
625	Dentine	2	7	0.304	0.058109	0.000960	0.717626	0.714748	0.000699
625	Dentine	2	8	0.360	0.057924	0.001027	0.713428	0.710549	0.000543
625	Dentine	2	9	0.323	0.057027	0.000608	0.713130	0.710252	0.000660
625	Enamel	2	10	0.320	0.057444	0.000783	0.712825	0.709932	0.000747
625	Enamel	2	11	0.310	0.057445	0.000437	0.710360	0.707467	0.000623
625	Enamel	2	12	0.381	0.057200	0.000485	0.713374	0.710481	0.000742
625	Dentine	2	13	0.340	0.057372	0.000694	0.711363	0.708485	0.000690
625	Dentine	2	14	0.346	0.056930	0.000654	0.711406	0.708528	0.000592
625	Dentine	2	15					0.711561	
625	Dentine	2	16	0.390	0.057299	0.000508	0.717136	0.714258	0.000568
625	Dentine	2	17	0.341	0.058268	0.000678	0.713099	0.710221	0.001086

Sample	Material	Track	Point	^{88}Sr Volts	$^{84}\text{Sr}/^{86}\text{Sr}$	Corrected $^{87}\text{Sr}/^{86}\text{Sr}$	$^{87}\text{Sr}/^{86}\text{Sr}$	$^{87}\text{Sr}/^{86}\text{Sr} 2\sigma$	Error
625	Dentine	2	18	0.281	0.057994	0.000609	0.713913	0.711035	0.000810
625	Dentine	2	19	0.349	0.057202	0.000554	0.714822	0.711944	0.000917

Table A3.103 Detailed LA-MC-ICPMS Sr Isotope Results for Dentine and Enamel, Sample 625, Horse, Layer 6, Pech de l'Azé II

Sample 625, Pech II, France

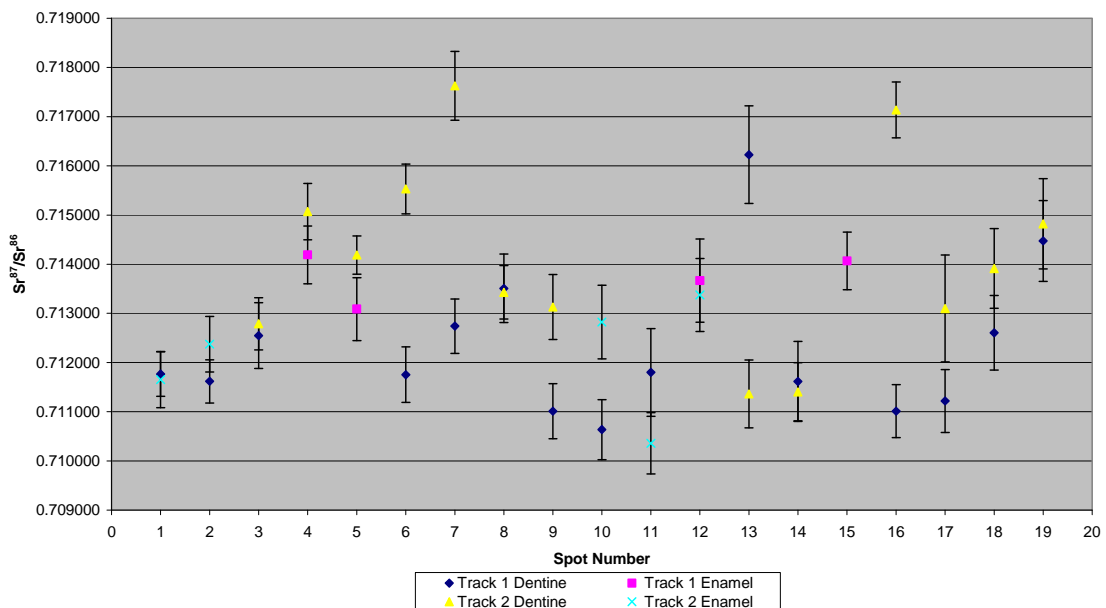


Figure A3.203 Detailed LA-MC-ICPMS Uncorrected Sr Isotope Results, Sample 625, Horse, Layer 6, Pech de l'Azé II

Sample 625, Corrected Sr Values, Pech II, France

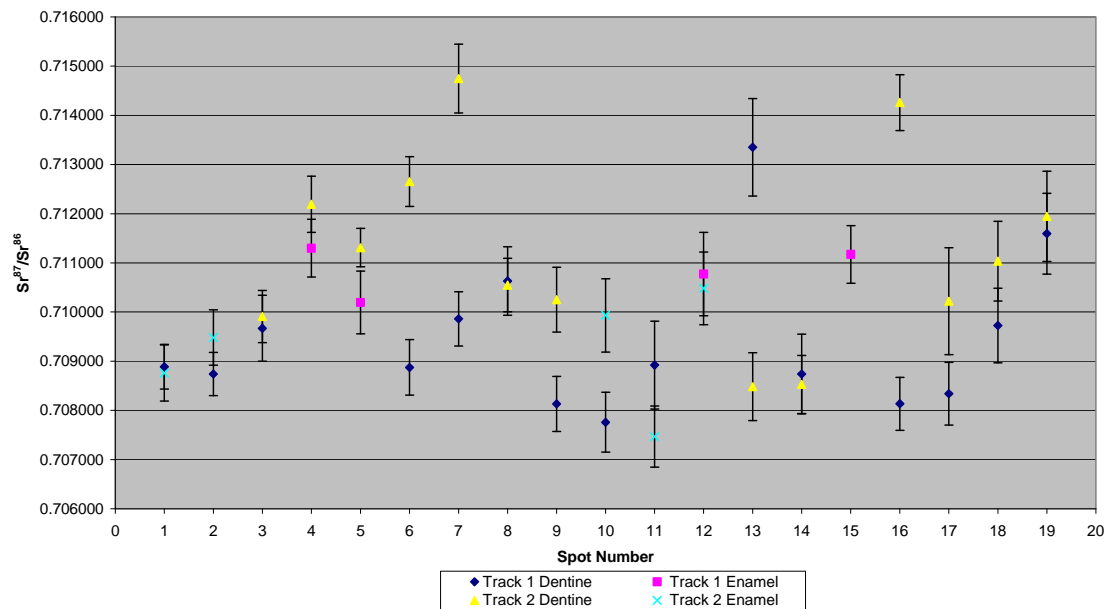


Figure A3.204 Detailed LA-MC-ICPMS Corrected Sr Isotope Results, Sample 625, Horse, Layer 6, Pech de l'Azé II

A3.2.3.5. Bois Roche

Sample 2417, a deciduous bovid upper premolar from layer 1C of Bois Roche shown in Figure A2.68, was analysed in 2 tracks, with track 1 comprising 2 spots of enamel and 5 spots of dentine and track 2 comprising 2 spots of enamel and 3 spots of dentine, shown in Figure A3.205. The results from this sample are summarised in Table 5.38 and Figure 5.24. The enamel spots of track 1 have an average ^{88}Sr voltage of 0.959, a weighted average uncorrected $^{87}\text{Sr}/^{86}\text{Sr}$ value of 0.712 ± 0.018 , a weighted average corrected $^{87}\text{Sr}/^{86}\text{Sr}$ value of 0.71200 ± 0.018 and a weighted average $^{84}\text{Sr}/^{86}\text{Sr}$ value of 0.05631 ± 0.00015 ($n=2$). The dentine spots of track 1 have an average ^{88}Sr voltage of 0.835, a weighted average uncorrected $^{87}\text{Sr}/^{86}\text{Sr}$ value of 0.70967 ± 0.00028 , a weighted average corrected $^{87}\text{Sr}/^{86}\text{Sr}$ value of 0.70896 ± 0.00028 and a weighted average $^{84}\text{Sr}/^{86}\text{Sr}$ value of 0.05641 ± 0.00010 ($n=5$). The enamel spots of track 2 have an average ^{88}Sr voltage of 0.902, a weighted average uncorrected $^{87}\text{Sr}/^{86}\text{Sr}$ value of 0.7109 ± 0.0051 , a weighted average corrected $^{87}\text{Sr}/^{86}\text{Sr}$ value of 0.71050 ± 0.0051 and a weighted average $^{84}\text{Sr}/^{86}\text{Sr}$ value of 0.05639 ± 0.00014 ($n=2$). The dentine spots of track 2 have an average ^{88}Sr voltage of 0.663, a weighted average uncorrected $^{87}\text{Sr}/^{86}\text{Sr}$ value of 0.70961 ± 0.00055 , a weighted average corrected $^{87}\text{Sr}/^{86}\text{Sr}$ value of 0.70890 ± 0.00055 and a weighted average $^{84}\text{Sr}/^{86}\text{Sr}$ value of 0.05617 ± 0.00055 . Enamel values for track 1 are 0.711382 and 0.714674 (uncorrected), as well as 0.710893 and 0.714185 (corrected), and are very heterogeneous. Dentine values for track 1 are in the range of 0.709408 to 0.709949 (uncorrected), as well as 0.708700 to 0.709241 (corrected), and are homogenous within 2σ error. Enamel values for track 2 are 0.710500 and 0.711307 (uncorrected), as well as 0.710011 and 0.710817 (corrected), and are somewhat heterogeneous. Dentine values for track 2 are in the range of 0.709455 to 0.709893 (uncorrected), as well as 0.708747 to 0.709185 (corrected). Detailed values for enamel and dentine for sample 2417 are shown in Table A3.104, Figure A3.206 and Figure A3.207.

There is a significant difference between the weighted average $^{87}\text{Sr}/^{86}\text{Sr}$ values for dentine and enamel from this sample, suggesting that this specimen is a

migrant. Spot 1 from track 1 is significantly elevated compared to other spots from this sample, suggesting that it may be inappropriately focused. Enamel values are heterogeneous, distributed in 2 domains, suggesting that this specimen was mobile during amelogenesis. The first domain, comprising spot 2 from track 1 and spot 1 from track 2, has a weighted average uncorrected value of 0.71135 ± 0.00018 , which corresponds to local mapping samples FS006 (0.711301 ± 0.00002) and FS010-S1 (0.711507 ± 0.000025). These samples are located in the floodplain of the Charente river (FS006) and on Upper Cretaceous carbonate bedrock (FS010-S1). It is more likely that value from FS006 is robust, as the value from FS010-S1 is significantly elevated compared to other samples from the same Upper Cretaceous units, such as FS011-S1 (0.708584 ± 0.000011), F6R (0.707582 ± 0.000035) and F8R (0.7075 ± 0.000031). This elevated value may suggest that FS010-S1 has been artificially elevated, perhaps by fertiliser use. The weighted average corrected value for this domain is 0.71086 ± 0.00018 , which corresponds to mapping samples approximately 150 km to the south-east of Bois Roche, including Upper Cretaceous limestone (FS089-S1) and Dordogne river floodplain (FS031-S1). The Upper Cretaceous limestone sampled in FS089-S1 is the same geological unit that contains Bois Roche, suggesting that there may be a nearby source for this value. The second domain of enamel values from sample 2417 has an uncorrected value of 0.710500 ± 0.000310 and a corrected value of 0.710011 ± 0.000310 , which corresponds to mapping sample FS021-S1 (0.710074 ± 0.000024), which was collected approximately 4 km north-west of the site of Bois Roche in the Upper Cretaceous carbonate that contains the archaeological site. This $^{87}\text{Sr}/^{86}\text{Sr}$ value of this mapping sample is elevated compared to others from the same unit (as discussed above); however, the rock associated with this sample has siliceous cobbles associated with it. The presence of these cobbles suggests that a local facies variation in the carbonate package may have led to this elevated value. The $^{84}\text{Sr}/^{86}\text{Sr}$ weighted average value for all enamel and dentine spots for this tooth is 0.056344 ± 0.000088 , which is slightly lower than the ideal value. Strontium concentration in this sample is relatively high and uranium is very low, suggesting that the $^{87}\text{Sr}/^{86}\text{Sr}$ results should be robust and that post-burial diagenesis is low.



Figure A3.205 LA-MC-ICPMS Track for Sample 2417, Bovid, Layer 1C, Bois Roche

Sample	Material	Track	Point	^{88}Sr Volts	$^{84}\text{Sr}/^{86}\text{Sr}$	$^{84}\text{Sr}/^{86}\text{Sr} 2\sigma$ Error	$^{87}\text{Sr}/^{86}\text{Sr}$	Corrected $^{87}\text{Sr}/^{86}\text{Sr}$	$^{87}\text{Sr}/^{86}\text{Sr} 2\sigma$ Error
2417	Enamel	1	1	0.963	0.056388	0.000237	0.714674	0.714185	0.000428
2417	Enamel	1	2	0.955	0.056253	0.000203	0.711382	0.710893	0.000244
2417	Dentine	1	3	0.857	0.056398	0.000208	0.709949	0.709241	0.000232
2417	Dentine	1	4	0.933	0.056442	0.000188	0.709408	0.708700	0.000254
2417	Dentine	1	5	0.849	0.056296	0.000265	0.709638	0.708930	0.000328
2417	Dentine	1	6	0.758	0.056419	0.000261	0.709599	0.708891	0.000335
2417	Dentine	1	7	0.778	0.056484	0.000250	0.709652	0.708944	0.000277
2417	Enamel	2	1	0.998	0.056334	0.000185	0.711307	0.710817	0.000283
2417	Enamel	2	2	0.805	0.056479	0.000237	0.710500	0.710011	0.000310
2417	Dentine	2	3	0.578	0.055839	0.000323	0.709893	0.709185	0.000357
2417	Dentine	2	4	0.786	0.056248	0.000223	0.709455	0.708747	0.000251
2417	Dentine	2	5	0.626	0.056302	0.000274	0.709647	0.708939	0.000360

Table A3.104 Detailed LA-MC-ICPMS Sr Isotope Results for Enamel and Dentine, Sample 2417, Bovid, Layer 1C, Bois Roche

Sample 2417, Bois Roche, France

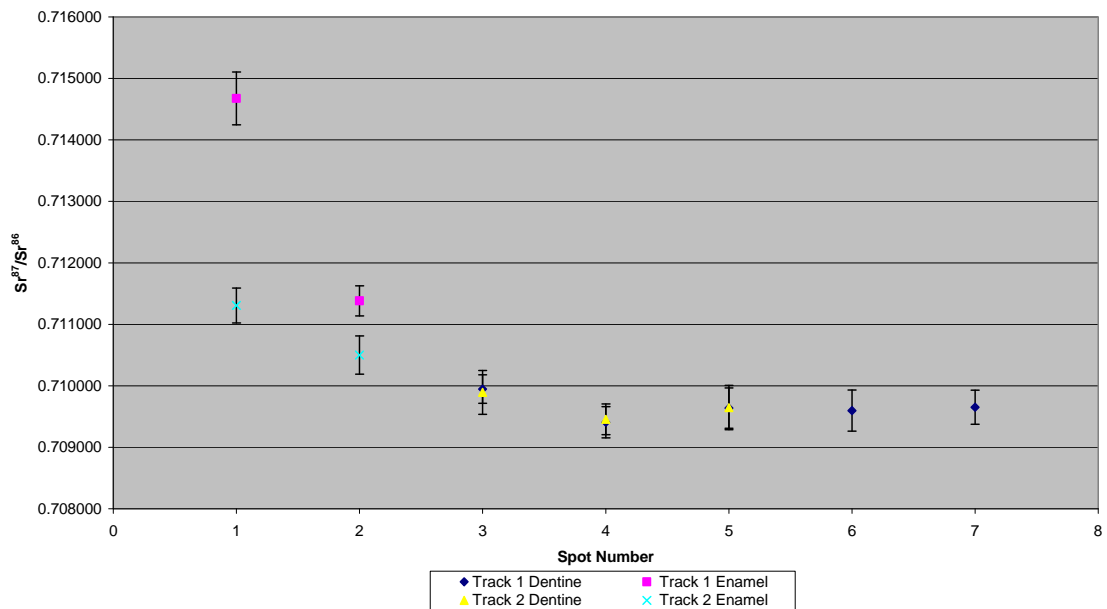


Figure A3.206 Detailed LA-MC-ICPMS Uncorrected Sr Isotope Results, Sample 2417, Bovid, Layer 1C, Bois Roche

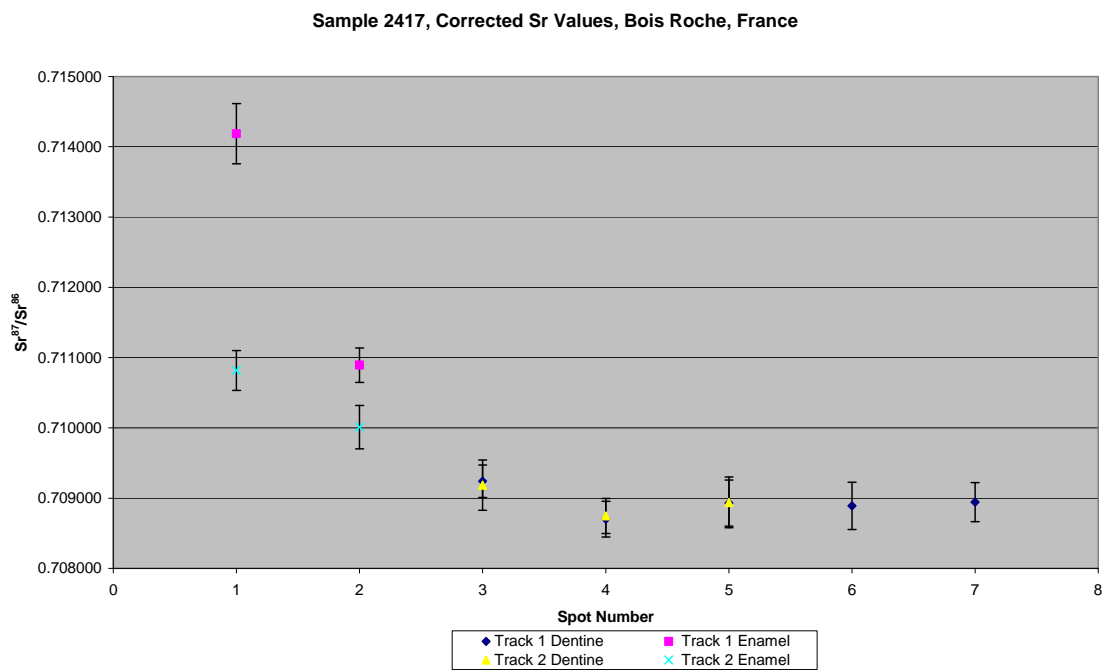


Figure A3.207 Detailed LA-MC-ICPMS Corrected Sr Isotope Results, Sample 2417, Bovid, Layer 1C, Bois Roche

Sample 2418, a bovid tooth from layer 1C of Bois Roche shown in Figure A2.69, was analysed in 2 tracks, with track 1 comprising 6 spots of enamel and track 2 comprising 5 spots of dentine, shown in Figure A3.208. The results from this sample are summarised in Table 5.38 and Figure 5.22. The enamel spots of track 1 have an average ^{88}Sr voltage of 0.572, a weighted average uncorrected $^{87}\text{Sr}/^{86}\text{Sr}$ value of 0.71292 ± 0.00042 , a weighted average corrected $^{87}\text{Sr}/^{86}\text{Sr}$ value of 0.71167 ± 0.00042 and a weighted average $^{84}\text{Sr}/^{86}\text{Sr}$ value of 0.05638 ± 0.00014 ($n=6$). The dentine spots of track 2 have an average ^{88}Sr voltage of 0.807, a weighted average uncorrected $^{87}\text{Sr}/^{86}\text{Sr}$ value of 0.71030 ± 0.00032 , a weighted average corrected $^{87}\text{Sr}/^{86}\text{Sr}$ value of 0.70966 ± 0.00032 and a weighted average $^{84}\text{Sr}/^{86}\text{Sr}$ value of 0.05651 ± 0.00022 ($n=5$). Enamel values for track 1 are in the range of 0.712552 to 0.713658 (uncorrected), as well as 0.711302 to 0.712408 (corrected), and are slightly heterogeneous, being just outside of 2σ error. Dentine values for track 2 are in the range of 0.709959 to 0.710531 (uncorrected), as well as 0.709318 to 0.709889 (corrected), and are homogenous within 2σ error. Detailed values for enamel and dentine for sample 2418 are shown in Table A3.105, Figure A3.209 and Figure A3.210.

Enamel and dentine $^{87}\text{Sr}/^{86}\text{Sr}$ values for this sample are distinct, suggesting that this sample is a migrant. Enamel values are slightly heterogeneous as spot 1 is outside of 2σ error from spots 5 and 6, suggesting some movement during amelogenesis. Despite this, it is difficult to define domains within the enamel values as each value overlaps in 2σ error with those adjacent to it. The overall weighted average uncorrected value for enamel (0.71248 ± 0.00014) corresponds to mapping values from F36R (0.712497 ± 0.000008) and F37R (0.712145 ± 0.000025), which are located in an area of Cambrian metamorphic bedrock within 70 km east of Bois Roche. The overall weighted average corrected value is 0.71167 ± 0.00042 , which corresponds to the Upper Cretaceous carbonate unit which contains the archaeological site, based on sample FS010-S1. This unit locally shows significant heterogeneity in strontium isotope values, which may reflect the fact that it is mapped as containing both carbonate and siliciclastic material. $^{84}\text{Sr}/^{86}\text{Sr}$ values for all spots is 0.056461 ± 0.000090 , suggesting that the $^{87}\text{Sr}/^{86}\text{Sr}$ values for this sample are robust. Strontium concentration in this sample is relatively low and uranium is very low,

suggesting that Ca+P+O interference may be significant; however, the degree of post-burial diagenesis is probably low.



Figure A3.208 LA-MC-ICPMS Track for Sample 2418, Bovid, Layer 1C, Bois Roche

Sample	Material	Track	Point	^{88}Sr Volts	$^{84}\text{Sr}/^{86}\text{Sr}$	$^{84}\text{Sr}/^{86}\text{Sr} 2\sigma$ Error	Corrected $^{87}\text{Sr}/^{86}\text{Sr}$	$^{87}\text{Sr}/^{86}\text{Sr} 2\sigma$ Error
2418	Enamel	1	1	0.551	0.056403	0.000471	0.713658	0.712408
2418	Enamel	1	2	0.571	0.056558	0.000340	0.712953	0.711703
2418	Enamel	1	3	0.594	0.056422	0.000334	0.713052	0.711802
2418	Enamel	1	4	0.550	0.056387	0.000366	0.712731	0.711481
2418	Enamel	1	5	0.580	0.056210	0.000401	0.712592	0.711342
2418	Enamel	1	6	0.584	0.056300	0.000303	0.712552	0.711302
2418	Dentine	2	1	0.805	0.056417	0.000251	0.710531	0.709889
2418	Dentine	2	2	0.833	0.056250	0.000293	0.709959	0.709318
2418	Dentine	2	3	0.728	0.056538	0.000301	0.710034	0.709392
2418	Dentine	2	4	0.816	0.056580	0.000227	0.710391	0.709749
2418	Dentine	2	5	0.852	0.056748	0.000280	0.710466	0.709825
2418	Dentine	2	6					0.000284

Table A3.105 Detailed LA-MC-ICPMS Sr Isotope Results for Enamel and Dentine, Sample 2418, Bovid, Layer 1C, Bois Roche

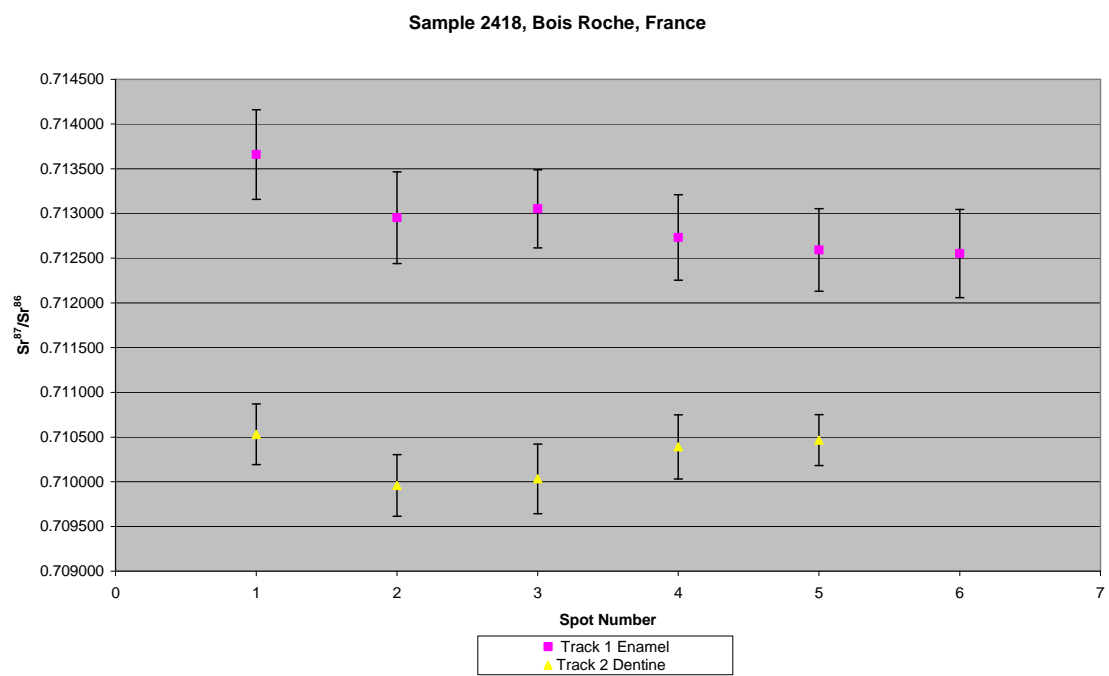


Figure A3.209 Detailed LA-MC-ICPMS Uncorrected Sr Isotope Results, Sample 2418, Bovid, Layer 1C, Bois Roche

Sample 2418, Corrected Sr Values, Bois Roche, France

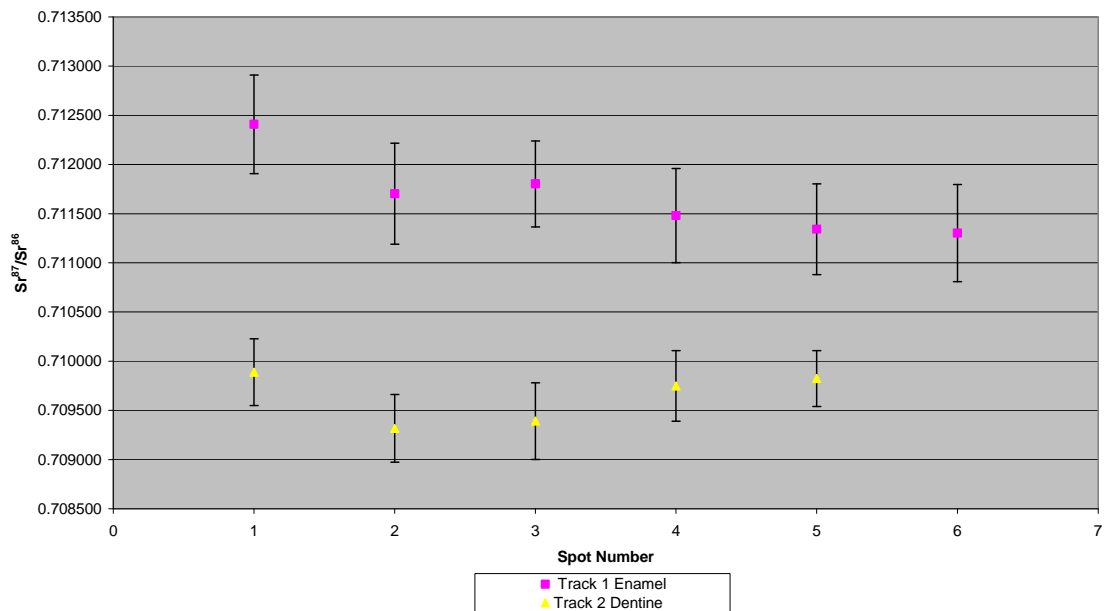


Figure A3.210 Detailed LA-MC-ICPMS Corrected Sr Isotope Results, Sample 2418, Bovid, Layer 1C, Bois Roche

Sample 2419, a bovid tooth from layer 1C of Bois Roche shown in Figure A2.70, was analysed in 1 track comprising 9 spots of enamel, shown in Figure A3.211. The results from this sample are summarised in Table 5.38 and Figure 5.22. The enamel spots of track 1 have an average ^{88}Sr voltage of 0.674, a weighted average uncorrected $^{87}\text{Sr}/^{86}\text{Sr}$ value of 0.71248 ± 0.00014 , a weighted average corrected $^{87}\text{Sr}/^{86}\text{Sr}$ value of 0.71095 ± 0.00014 and a weighted average $^{84}\text{Sr}/^{86}\text{Sr}$ value of 0.05607 ± 0.00015 ($n=9$). Enamel values for track 1 are in the range of 0.712214 to 0.712709 (uncorrected), as well as 0.710690 to 0.711185 (corrected), and are all very homogeneous within 2σ error. Detailed values for enamel and dentine for sample 2419 are shown in Table A3.106, Figure A3.212 and Figure A3.213.

This sample has very homogenous enamel values, suggesting that the specimen was not mobile between geological environments during amelogenesis. Enamel has a weighted average uncorrected value of 0.71248 ± 0.00014 , which corresponds to mapping values from F36R (0.712497 ± 0.000008) and F37R (0.712145 ± 0.000025) located in an area of Cambrian

metamorphic bedrock within 70 km east of Bois Roche. The corrected weighted average value of enamel is 0.71095 ± 0.00014 , which correlates with sample FS089-S1 located approximately 165 km south-east of Bois Roche within the Upper Cretaceous carbonate that contains the site. As discussed above with reference to sample 2418, this unit has an extremely heterogeneous strontium isotope composition. Sample 2419 has a weighted average $^{84}\text{Sr}/^{86}\text{Sr}$ value of 0.05607 ± 0.00015 , which is significantly lower than the expected value of 0.0565, suggesting that the $^{87}\text{Sr}/^{86}\text{Sr}$ values may not be robust.

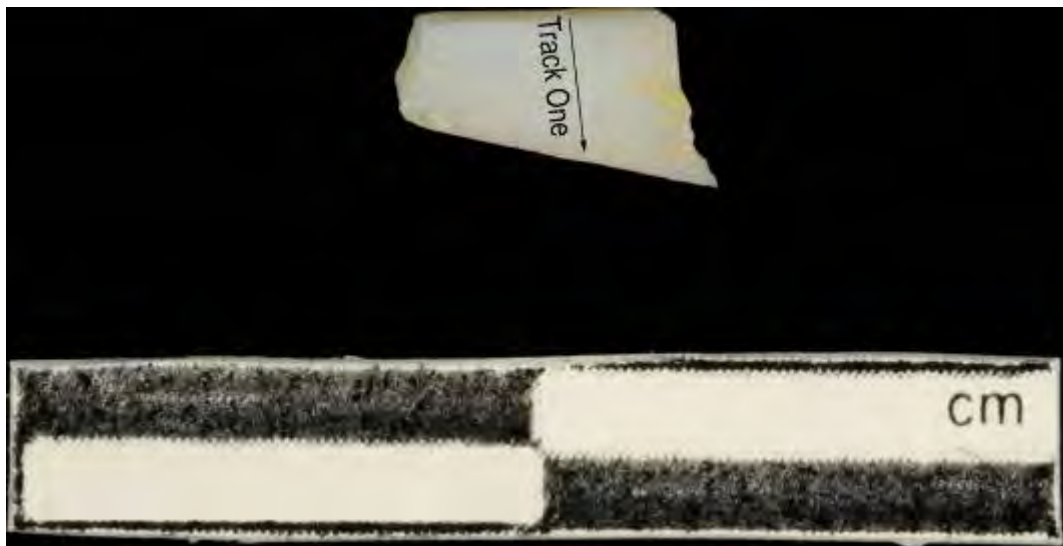


Figure A3.211 LA-MC-ICPMS Track for Sample 2419, Bovid, Layer 1C, Bois Roche

Sample	Material	Track	Point	^{88}Sr Volts	$^{84}\text{Sr}/^{86}\text{Sr}$	$^{84}\text{Sr}/^{86}\text{Sr} 2\sigma$	$^{87}\text{Sr}/^{86}\text{Sr}$	$^{87}\text{Sr}/^{86}\text{Sr} 2\sigma$	Error
2419	Enamel	1	1	0.819	0.056375	0.000279	0.712435	0.710911	0.000368
2419	Enamel	1	2	0.666	0.056066	0.000363	0.712630	0.711106	0.000470
2419	Enamel	1	3	0.668	0.056089	0.000259	0.712406	0.710882	0.000396
2419	Enamel	1	4	0.667	0.056277	0.000340	0.712496	0.710972	0.000417
2419	Enamel	1	5	0.644	0.055746	0.000308	0.712657	0.711133	0.000491
2419	Enamel	1	6	0.669	0.055874	0.000372	0.712509	0.710986	0.000452
2419	Enamel	1	7	0.648	0.056183	0.000298	0.712375	0.710851	0.000492
2419	Enamel	1	8	0.670	0.055929	0.000306	0.712214	0.710690	0.000440
2419	Enamel	1	9	0.612	0.056038	0.000256	0.712709	0.711185	0.000513

Table A3.106 Detailed LA-MC-ICPMS Sr Isotope Results for Enamel, Sample 2419, Bovid, Layer 1C, Bois Roche

Sample 2419, Bois Roche, France

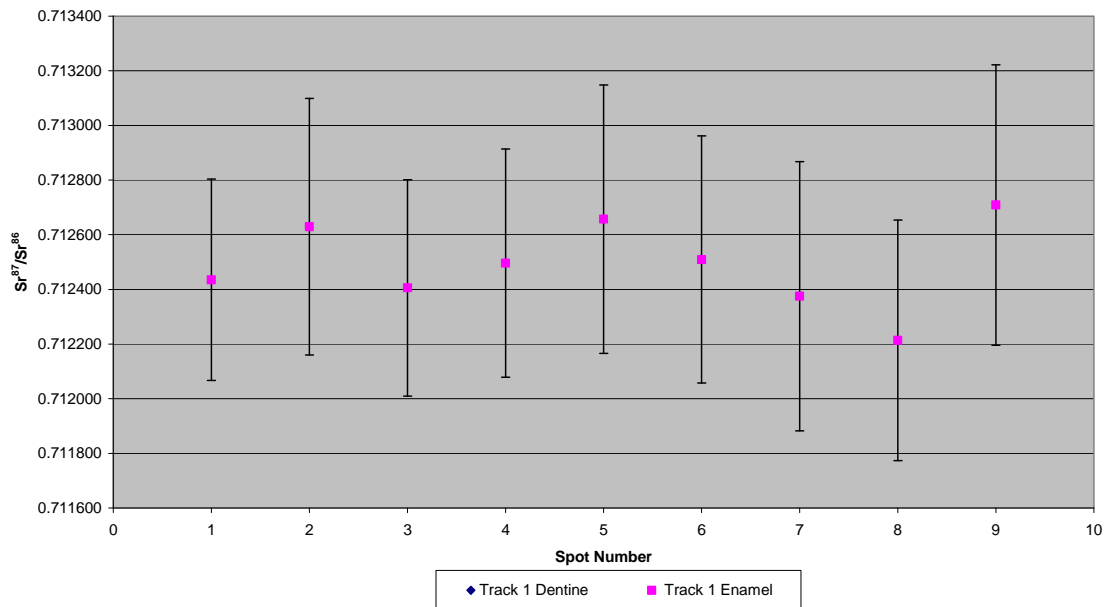


Figure A3.212 Detailed LA-MC-ICPMS Uncorrected Sr Isotope Results, Sample 2419, Bovid, Layer 1C, Bois Roche

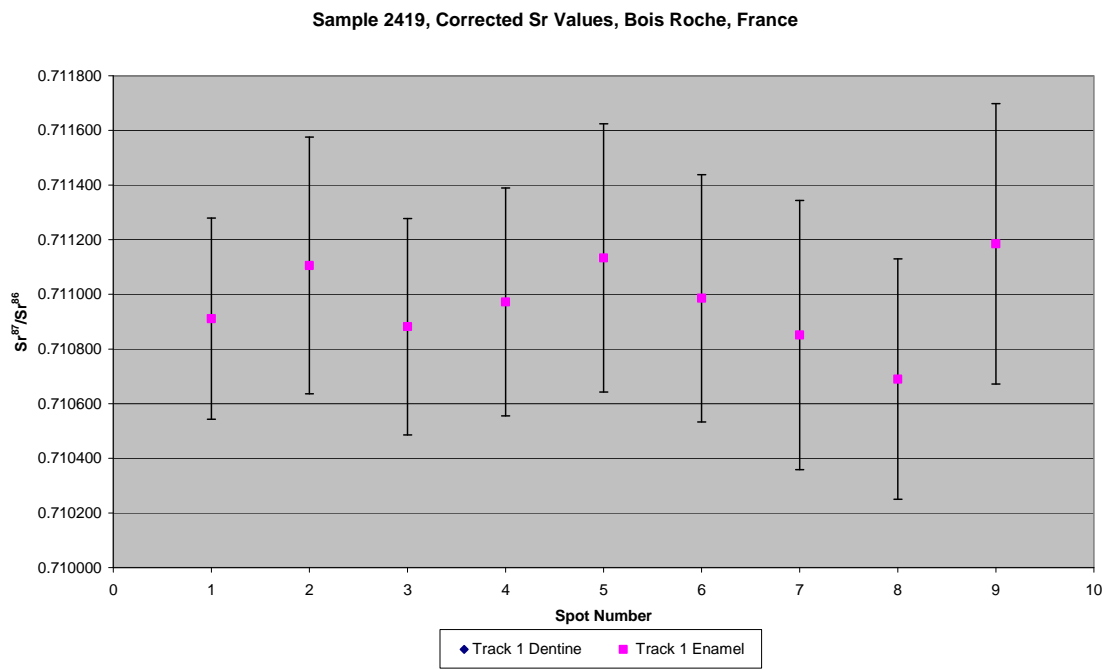


Figure A3.213 Detailed LA-MC-ICPMS Corrected Sr Isotope Results, Sample 2419, Bovid, Layer 1C, Bois Roche

Sample 2420, a bovid lower molar from layer 2 of Bois Roche shown in Figure A2.71, was analysed in 1 track comprising 15 spots of enamel, shown in Figure A3.214. The results from this sample are summarised in Table 5.38 and Figure 5.22. The enamel spots of track 1 have an average ^{88}Sr voltage of 1.039, a weighted average uncorrected $^{87}\text{Sr}/^{86}\text{Sr}$ value of 0.71184 ± 0.00027 , a weighted average corrected $^{87}\text{Sr}/^{86}\text{Sr}$ value of 0.71127 ± 0.00027 and a weighted average $^{84}\text{Sr}/^{86}\text{Sr}$ value of 0.056172 ± 0.000086 ($n=15$). Enamel values for track 1 are in the range of 0.711389 to 0.713021 (uncorrected), as well as 0.710816 to 0.712448 (corrected). Spots 1 to 13 are homogenous within 2σ error, although the mean value increases in spots 12 and 13. This trend continues with spots 14 and 15, which are outside of the 2σ error of other samples in this spot. Detailed values for enamel and dentine for sample 2420 are shown in Table A3.107, Figure A3.215 and Figure A3.216.

This sample has enamel values that are homogenous, particularly spots 1 to 11. The values increase significantly in $^{87}\text{Sr}/^{86}\text{Sr}$ value for spots 12 to 15. This suggests a sample that was sedentary during a period of amelogenesis and mobile at another period. The $^{87}\text{Sr}/^{86}\text{Sr}$ weighted average uncorrected value for spots 1 to 11 is 0.71160 ± 0.00013 and the corrected value is 0.71103 ± 0.00013 . The uncorrected value correlates to mapping sample FS010-S1 (0.711507 ± 0.000025) located in an Upper Cretaceous carbonate; however (as discussed in reference to sample 2417), this sample may have an artificially elevated value. Another correlation is sample F33R (0.711714 ± 0.000062), a Carboniferous monzogranite/granodiorite outcropping within 80 km east of Bois Roche. The corrected value for this domain is slightly depressed compared to FS006, the most parsimonious mapping sample for this domain; however, this was collected from the cutbank of the Charente river. Given the large range of values observed from the other floodplains investigated in this study, such as the Dordogne, it is likely that the Charente contains similar variability. The more elevated domain of $^{87}\text{Sr}/^{86}\text{Sr}$ enamel reaches a maximum uncorrected value of 0.713021 ± 0.000404 and a maximum corrected value of 0.712448 ± 0.000404 , which is more radiogenic than any local value; however, it is only slightly elevated or correlates to the value for F36R (0.712497 ± 0.000008), a Cambrian paragneiss/leptynite/amphibolite which outcrops within 72 km of the site.

$^{84}\text{Sr}/^{86}\text{Sr}$ values for this sample have a weighted average of 0.056172 ± 0.000085 , suggesting that the $^{87}\text{Sr}/^{86}\text{Sr}$ values may not be robust.



Figure A3.214 LA-MC-ICPMS Track for Sample 2420, Bovid, Layer 2, Bois Roche

Sample	Material	Track	Point	^{88}Sr Volts	$^{84}\text{Sr}/^{86}\text{Sr}$	$^{84}\text{Sr}/^{86}\text{Sr} 2\sigma$ Error	Corrected $^{87}\text{Sr}/^{86}\text{Sr}$	$^{87}\text{Sr}/^{86}\text{Sr} 2\sigma$ Error
2420	Enamel	1	1	1.135	0.056178	0.000238	0.711468	0.710894
2420	Enamel	1	2	1.083	0.056124	0.000210	0.711586	0.711013
2420	Enamel	1	3	1.157	0.056031	0.000183	0.711415	0.710842
2420	Enamel	1	4	1.055	0.056209	0.000204	0.711737	0.711164
2420	Enamel	1	5	0.943	0.056320	0.000229	0.711783	0.711210
2420	Enamel	1	6	0.951	0.056110	0.000201	0.711510	0.710936
2420	Enamel	1	7	0.949	0.056380	0.000208	0.711663	0.711090
2420	Enamel	1	8	1.092	0.056069	0.000188	0.711689	0.711116
2420	Enamel	1	9	1.190	0.056328	0.000130	0.711389	0.710816
2420	Enamel	1	10	1.274	0.056054	0.000169	0.711729	0.711156
2420	Enamel	1	11	1.236	0.056444	0.000250	0.711538	0.710965
2420	Enamel	1	12	1.101	0.056149	0.000171	0.711966	0.711393
2420	Enamel	1	13	0.920	0.056121	0.000280	0.712299	0.711726
2420	Enamel	1	14	0.737	0.056006	0.000339	0.712775	0.712202
2420	Enamel	1	15	0.767	0.055752	0.000277	0.713021	0.712448

Table A3.107 Detailed LA-MC-ICPMS Sr Isotope Results for Enamel, Sample 2420, Bovid, Layer 2, Bois Roche

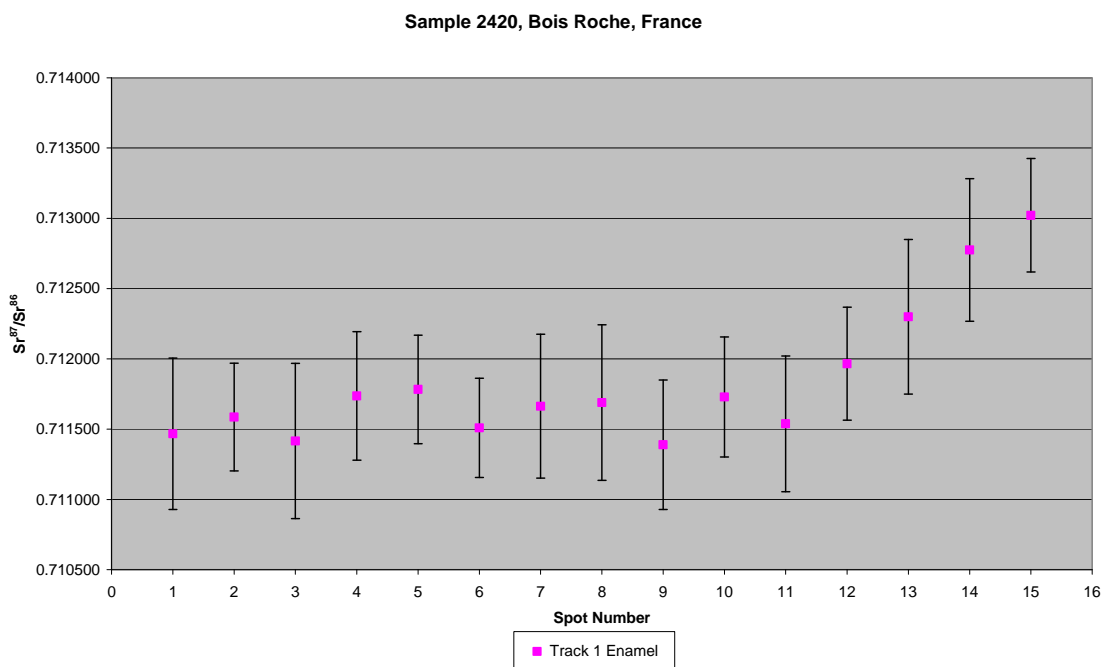


Figure A3.215 Detailed LA-MC-ICPMS Uncorrected Sr Isotope Results, Sample 2420, Bovid, Layer 2, Bois Roche

Sample 2420, Bois Roche, France

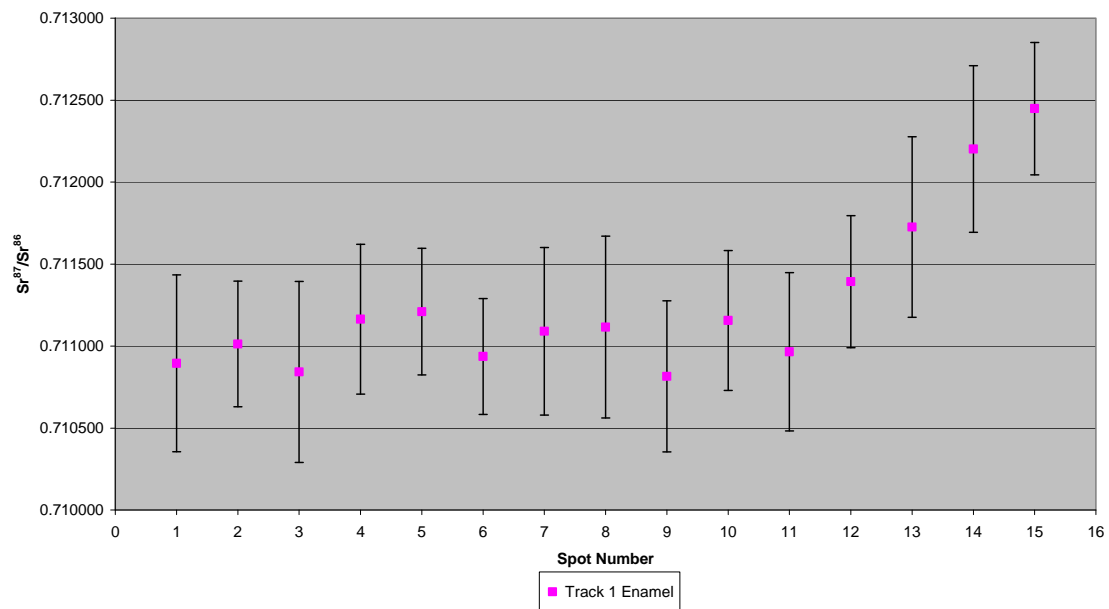


Figure A3.216 Detailed LA-MC-ICPMS Corrected Sr Isotope Results, Sample 2420, Bovid, Layer 2, Bois Roche

Sample 2421, a bovid tooth from a young adult from layer 2 of Bois Roche shown in Figure A2.72, was analysed in 3 tracks, with track 1 comprising 4 spots of enamel and 2 spots of dentine, track 2 comprising 4 spots of enamel and 3 spots of dentine and track 3 comprising 4 spots of enamel and 4 spots of dentine, shown in Figure A3.217. The results from this sample are summarised in Table 5.38 and Figure 5.22. The enamel spots of track 1 have an average ^{88}Sr voltage of 0.883, a weighted average uncorrected $^{87}\text{Sr}/^{86}\text{Sr}$ value of 0.71158 ± 0.00077 , a weighted average corrected $^{87}\text{Sr}/^{86}\text{Sr}$ value of 0.71090 ± 0.00077 and a weighted average $^{84}\text{Sr}/^{86}\text{Sr}$ value of 0.056479 ± 0.000097 ($n=4$). The dentine spots of track 1 have an average ^{88}Sr voltage of 0.732, a weighted average uncorrected $^{87}\text{Sr}/^{86}\text{Sr}$ value of 0.7110 ± 0.0024 , a weighted average corrected $^{87}\text{Sr}/^{86}\text{Sr}$ value of 0.70990 ± 0.0024 and a weighted average $^{84}\text{Sr}/^{86}\text{Sr}$ value of 0.05649 ± 0.00022 ($n=2$). The enamel spots of track 2 have an average ^{88}Sr voltage of 0.772, a weighted average uncorrected $^{87}\text{Sr}/^{86}\text{Sr}$ value of 0.71138 ± 0.00034 , a weighted average corrected $^{87}\text{Sr}/^{86}\text{Sr}$ value of 0.71071 ± 0.00034 and a weighted average $^{84}\text{Sr}/^{86}\text{Sr}$ value of 0.05640 ± 0.00029 ($n=4$). The dentine spots of track 2 have an average ^{88}Sr voltage of 0.487, a weighted average uncorrected $^{87}\text{Sr}/^{86}\text{Sr}$ value of 0.71080 ± 0.00028 , a weighted average corrected $^{87}\text{Sr}/^{86}\text{Sr}$ value of 0.70969 ± 0.00028 and a weighted average $^{84}\text{Sr}/^{86}\text{Sr}$ value of 0.05669 ± 0.00023 ($n=3$). The enamel spots of track 3 have an average ^{88}Sr voltage of 0.910, a weighted average uncorrected $^{87}\text{Sr}/^{86}\text{Sr}$ value of 0.71151 ± 0.00081 , a weighted average corrected $^{87}\text{Sr}/^{86}\text{Sr}$ value of 0.71084 ± 0.00081 and a weighted average $^{84}\text{Sr}/^{86}\text{Sr}$ value of 0.056523 ± 0.000091 ($n=4$). The dentine spots of track 3 have an average ^{88}Sr voltage of 0.672, a weighted average uncorrected $^{87}\text{Sr}/^{86}\text{Sr}$ value of 0.7109 ± 0.0013 , a weighted average corrected $^{87}\text{Sr}/^{86}\text{Sr}$ value of 0.70980 ± 0.0013 and a weighted average $^{84}\text{Sr}/^{86}\text{Sr}$ value of 0.05659 ± 0.00024 .

Enamel values for track 1 are in the range of 0.711072 to 0.712376 (uncorrected), as well as 0.710398 to 0.711702 (corrected), and are somewhat heterogeneous, decreasing in $^{87}\text{Sr}/^{86}\text{Sr}$ value from the exterior of the enamel to the dentine-enamel junction. Dentine values for track 1 are 0.710792 and 0.711175 (uncorrected), as well as 0.709688 and 0.710071 (corrected), and are relatively homogenous. Enamel values for track 2 are in the range of 0.711168

to 0.711609 (uncorrected), as well as 0.710493 to 0.710935 (corrected), and are very homogenous. Dentine values for track 2 are in the range of 0.710668 to 0.711068 (uncorrected) as well 0.709564 to 0.709964 (corrected), and are relatively homogenous. Enamel values for track 3 are in the range of 0.710899 to 0.711925 (uncorrected), as well as 0.710224 to 0.711251 (corrected), and are relatively homogenous with the exception of spot 4, which has a value much closer to the dentine values. Dentine values for track 3 are in the range of 0.710317 to 0.712368 (uncorrected), as well as 0.709213 to 0.711264 (corrected), and are moderately heterogeneous, particularly spot 5. Detailed values for enamel and dentine for sample 2421 are shown in Table A3.108, Figure A3.218 and Figure A3.219.

This sample has enamel and dentine values that are distinct, suggesting that this sample is a migrant. Enamel values are somewhat heterogeneous and are distributed in 2 domains. The first domain contains spots 1 to 3 on all tracks and has a weighted average uncorrected value of 0.71175 ± 0.00017 , which corresponds to mapping values of F33R (0.711714 ± 0.000062) from a Carboniferous monzogranite/granodiorite and F34R (0.711919 ± 0.000207) from a Cambrian paragneiss/leptynite/amphibolite. This domain has a corrected weighted average value of 0.71107 ± 0.00017 , which correlates best with sample FS006 from the Charente river cutbank. Spots 4 on all tracks have an overall weighted average uncorrected value of 0.71105 ± 0.00015 , which correlates to the mapping value of FS006 from the floodplain of the Charente River (0.711301 ± 0.00002). The corrected value for this domain is 0.71038 ± 0.00015 , which correlates best with the value of FS021-S1 collected approximately 4 km from Bois Roche in an Upper Cretaceous carbonate unit which contains the archaeological site. Enamel strontium concentrations for this sample are in the range of 232 to 240 ppm (as shown in Table 6.29) and the weighted average for $^{84}\text{Sr}/^{86}\text{Sr}$ enamel is 0.056484 ± 0.000060 , both of which suggest that the $^{87}\text{Sr}/^{86}\text{Sr}$ values for this sample are robust.



Figure A3.217 LA-MC-ICPMS Track for Sample 2421, Bovid, Layer 2, Bois Roche

Sample	Material	Track	Point	^{88}Sr Volts	$^{84}\text{Sr}/^{86}\text{Sr}$	$^{84}\text{Sr}/^{86}\text{Sr} 2\sigma$ Error	$^{87}\text{Sr}/^{86}\text{Sr}$	Corrected $^{87}\text{Sr}/^{86}\text{Sr}$	$^{87}\text{Sr}/^{86}\text{Sr} 2\sigma$ Error
2421	Enamel	1	1	0.809	0.056511	0.000185	0.712376	0.711702	0.000648
2421	Enamel	1	2	0.780	0.056543	0.000210	0.711897	0.711223	0.000246
2421	Enamel	1	3	0.855	0.056318	0.000294	0.711750	0.711076	0.000323
2421	Enamel	1	4	1.087	0.056465	0.000163	0.711072	0.710398	0.000238
2421	Dentine	1	5	0.777	0.056462	0.000363	0.710792	0.709688	0.000534
2421	Dentine	1	6	0.686	0.056512	0.000284	0.711175	0.710071	0.000443
2421	Enamel	2	1	0.898	0.056225	0.000245	0.711386	0.710712	0.000315
2421	Enamel	2	2	0.622	0.056726	0.000463	0.711571	0.710897	0.000384
2421	Enamel	2	3	0.778	0.056550	0.000291	0.711609	0.710935	0.000350
2421	Enamel	2	4	0.790	0.056382	0.000245	0.711168	0.710493	0.000261
2421	Dentine	2	5	0.525	0.056584	0.000365	0.710790	0.709686	0.000498
2421	Dentine	2	6	0.479	0.056802	0.000414	0.711068	0.709964	0.000592
2421	Dentine	2	7	0.458	0.056715	0.000421	0.710668	0.709564	0.000421
2421	Enamel	3	1	0.868	0.056407	0.000271	0.711925	0.711251	0.000329
2421	Enamel	3	2	0.734	0.056266	0.000382	0.711822	0.711147	0.000471
2421	Enamel	3	3	0.933	0.056588	0.000176	0.711741	0.711067	0.000299
2421	Enamel	3	4	1.103	0.056543	0.000125	0.710899	0.710224	0.000281
2421	Dentine	3	5	0.775	0.056319	0.000273	0.712368	0.711264	0.000498
2421	Dentine	3	6	0.659	0.056681	0.000167	0.711083	0.709980	0.000482
2421	Dentine	3	7	0.628	0.056608	0.000295	0.710839	0.709735	0.000433
2421	Dentine	3	8	0.627	0.056613	0.000273	0.710317	0.709213	0.000317

Table A3.108 LA-MC-ICPMS Sr Isotope Results for Enamel and Dentine, Sample 2421, Bovid, Layer 2, Bois Roche

Sample 2421, Bois Roche, France

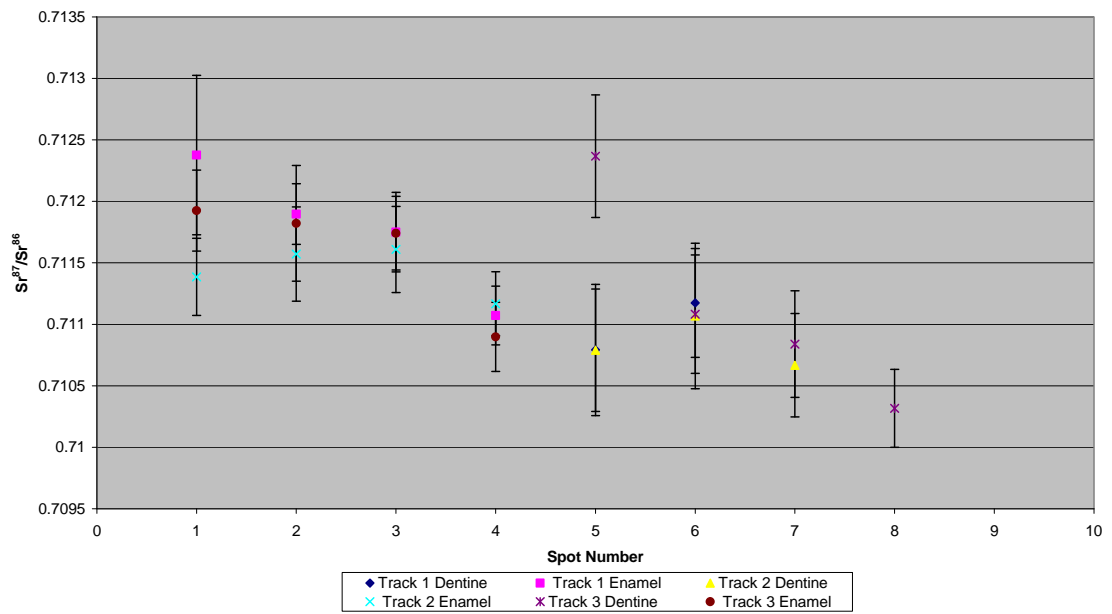


Figure A3.218 Detailed LA-MC-ICPMS Uncorrected Sr Isotope Results, Sample 2421, Bovid, Layer 2, Bois Roche

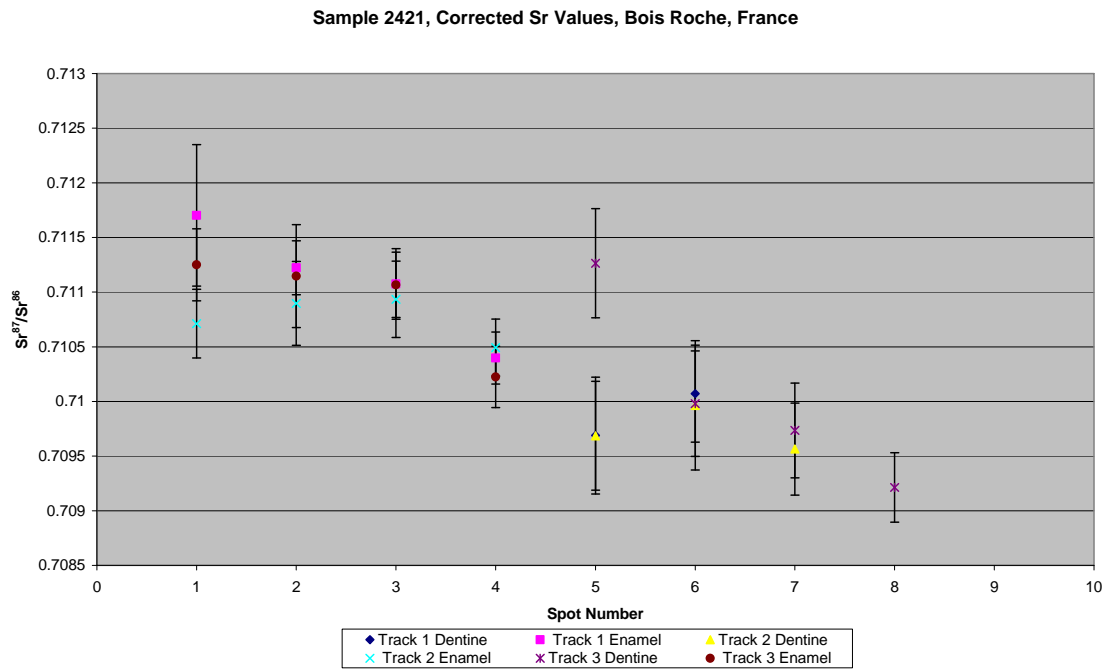


Figure A3.219 Detailed LA-MC-ICPMS Corrected Sr Isotope Results, Sample 2421, Bovid, Layer 2, Bois Roche

Sample 2422, an adult bovid upper molar from layer 1C of Bois Roche shown in Figure A2.73, was analysed in 1 track comprising 6 spots of enamel and 11 spots of dentine in 2 discontinuous sections, shown in Figure A3.220. The results from this sample are summarised in Table 5.38 and Figure 5.22. The enamel spots of track 1 have an average ^{88}Sr voltage of 0.594, a weighted average uncorrected $^{87}\text{Sr}/^{86}\text{Sr}$ value of 0.71088 ± 0.00050 , a weighted average corrected $^{87}\text{Sr}/^{86}\text{Sr}$ value of 0.70965 ± 0.00050 and a weighted average $^{84}\text{Sr}/^{86}\text{Sr}$ value of 0.05641 ± 0.00020 ($n=6$). The dentine spots of track 1 have an average ^{88}Sr voltage of 0.952, a weighted average uncorrected $^{87}\text{Sr}/^{86}\text{Sr}$ value of 0.70963 ± 0.00022 , a weighted average corrected $^{87}\text{Sr}/^{86}\text{Sr}$ value of 0.70915 ± 0.00022 and a weighted average $^{84}\text{Sr}/^{86}\text{Sr}$ value of 0.056476 ± 0.000061 ($n=11$). Enamel values are in the range of 0.710528 to 0.711930 (uncorrected), as well as 0.709299 to 0.710701 (corrected), and are somewhat homogenous, with spots 4, 7, 8 and 9 being homogenous and spots 5 and 6 being elevated in $^{87}\text{Sr}/^{86}\text{Sr}$ value. Dentine values for sample 2422 are in the range of 0.709303 to 0.710840 (uncorrected), as well as 0.708830 to 0.710368 (corrected), and are very homogenous with the exception of spot 1, which is elevated in $^{87}\text{Sr}/^{86}\text{Sr}$ value. Detailed values for enamel and dentine for sample 2422 are shown in Table A3.109, Figure A3.221 and Figure A3.222.

This sample has distinct enamel and dentine values, suggesting that this sample is a migrant. Enamel values are heterogeneous, suggesting that this specimen may have been mobile during amelogenesis. Uncorrected enamel values suggest a sample mobile from the metamorphic/igneous province to the east, including F33R (0.711714 ± 0.000062) from a Carboniferous monzogranite/granodiorite and F34R (0.711919 ± 0.000207) from a Cambrian paragneiss/leptynite/amphibolite to FS006 (0.711301 ± 0.00002) from the Charente river floodplain and then FS021-S1 (0.710074 ± 0.000024) of the Upper Cretaceous carbonate province. Corrected enamel values suggest a sample mobile within the Upper Cretaceous carbonate unit surrounding the site, such as from FS021-S1 to FS001. Dentine values are relatively homogenous, with the exception of spot 1, which has a significantly outlying value. Dentine of this sample has a relatively high concentration of strontium in the range of 239

to 262 ppm, while enamel has a concentration of approximately 150 ppm. $^{84}\text{Sr}/^{86}\text{Sr}$ values are 0.056464 ± 0.000056 , which suggests that the strontium isotope results for sample 2422 are robust.

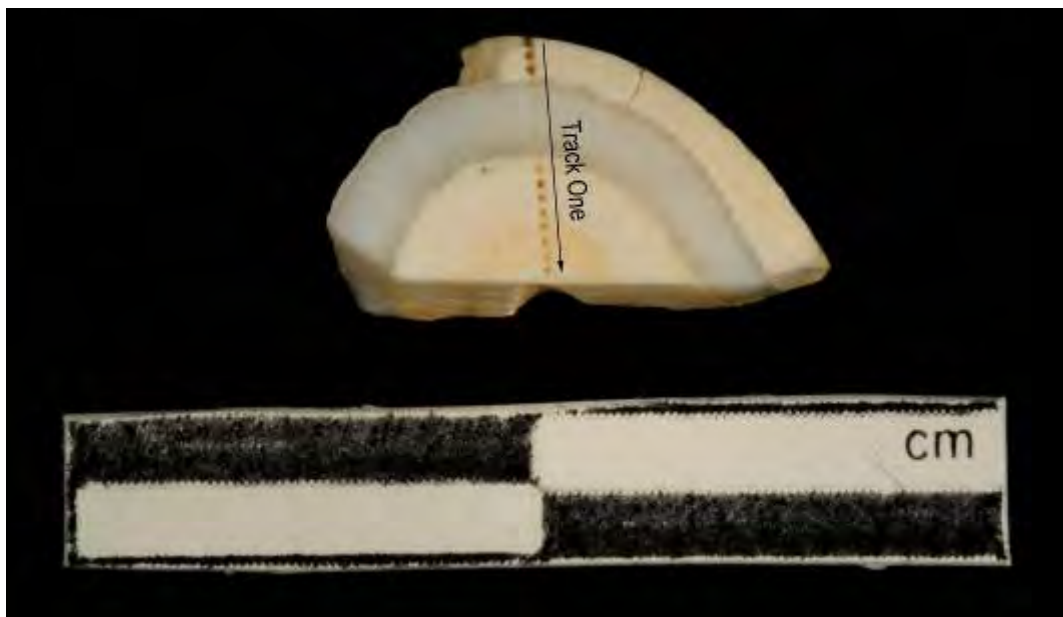


Figure A3.220 LA-MC-ICPMS Track for Sample 2422, Bovid, Layer 2, Bois Roche

Sample	Material	Track	Point	^{88}Sr Volts	$^{84}\text{Sr}/^{86}\text{Sr}$	$^{84}\text{Sr}/^{86}\text{Sr} 2\sigma$	Corrected $^{87}\text{Sr}/^{86}\text{Sr}$	$^{87}\text{Sr}/^{86}\text{Sr}$	$^{87}\text{Sr}/^{86}\text{Sr} 2\sigma$
2422	Dentine	1	1	1.487	0.056493	0.000194	0.710840	0.710368	0.000435
2422	Dentine	1	2	1.062	0.056544	0.000177	0.709394	0.708921	0.000285
2422	Dentine	1	3	0.796	0.056594	0.000212	0.709246	0.708773	0.000257
2422	Enamel	1	4	0.456	0.056097	0.000430	0.710771	0.709542	0.000543
2422	Enamel	1	5	0.485	0.056559	0.000396	0.711930	0.710701	0.000458
2422	Enamel	1	6	0.526	0.056758	0.000481	0.711339	0.710110	0.000523
2422	Enamel	1	7	0.631	0.056381	0.000323	0.710817	0.709588	0.000352
2422	Enamel	1	8	0.680	0.056252	0.000282	0.710938	0.709709	0.000396
2422	Enamel	1	9	0.785	0.056509	0.000271	0.710528	0.709299	0.000240
2422	Dentine	1	10	0.686	0.056343	0.000270	0.709577	0.709105	0.000413
2422	Dentine	1	11	0.733	0.056372	0.000298	0.709303	0.708830	0.000335
2422	Dentine	1	12	0.862	0.056412	0.000199	0.709563	0.709090	0.000319
2422	Dentine	1	13	0.805	0.056422	0.000247	0.709624	0.709151	0.000358
2422	Dentine	1	14	1.042	0.056567	0.000216	0.709670	0.709197	0.000207
2422	Dentine	1	15	0.954	0.056336	0.000219	0.709779	0.709307	0.000216
2422	Dentine	1	16	0.993	0.056567	0.000154	0.709604	0.709131	0.000296

2422	Dentine	1	17	1.055	0.056382	0.000189	0.709793	0.709320	0.000287
------	---------	---	----	-------	----------	----------	----------	----------	----------

Table A3.109 Detailed LA-MC-ICPMS Sr Isotope Results, Sample 2422, Bovid, Layer 2, Bois Roche

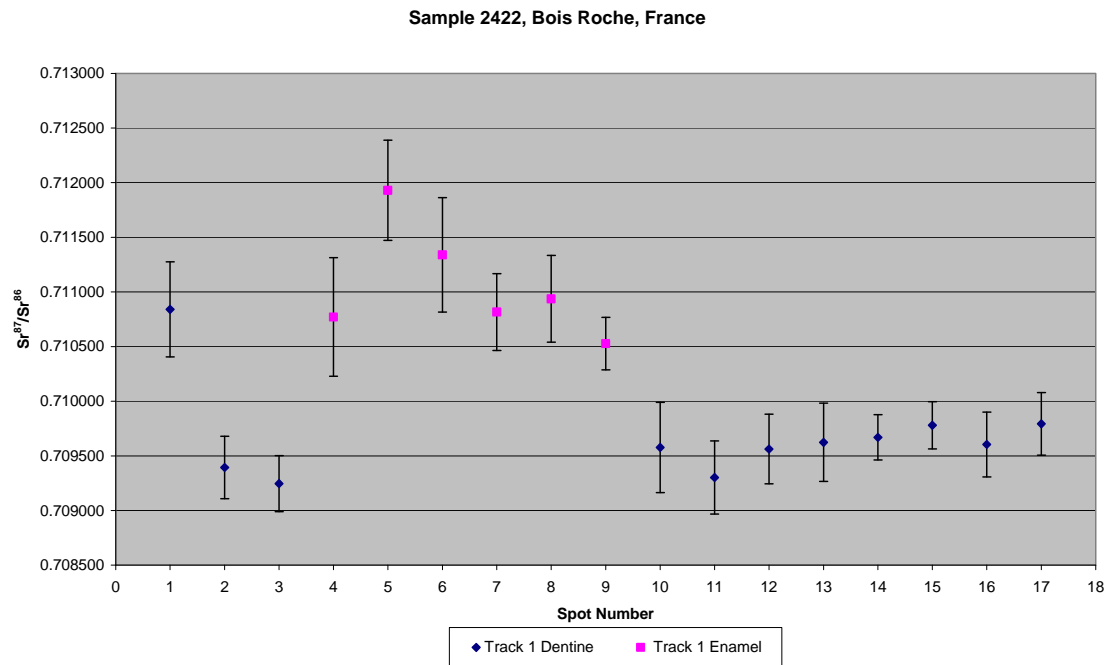


Figure A3.221 Detailed LA-MC-ICPMS Uncorrected Sr Isotope Results, Sample 2422, Bovid, Layer 2, Bois Roche

Sample 2422, Corrected Sr Values, Bois Roche, France

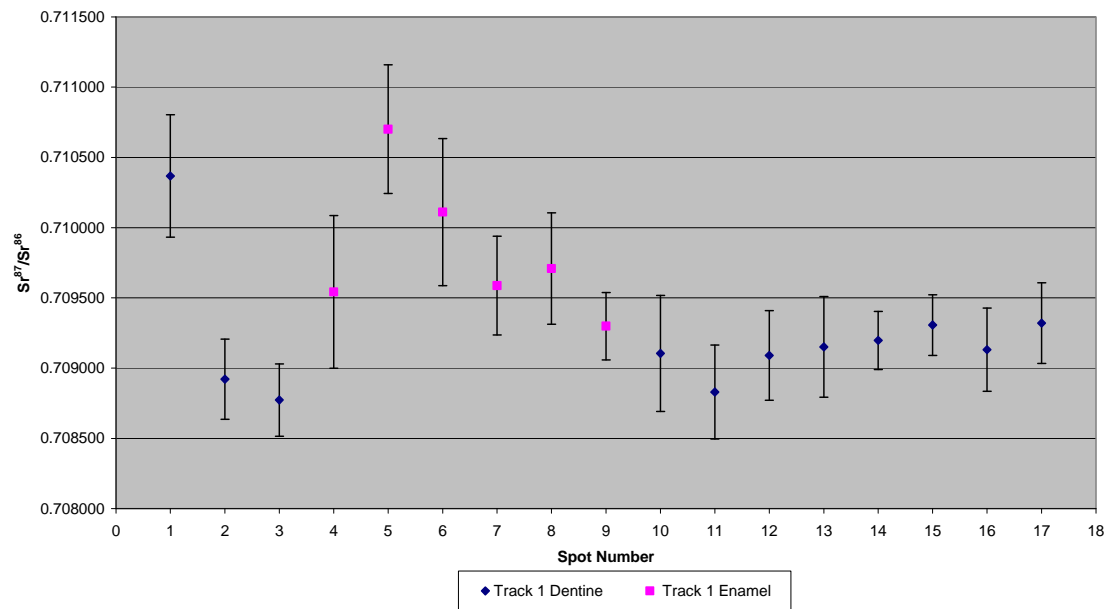


Figure A3.222 Detailed LA-MC-ICPMS Corrected Sr Isotope Results, Sample 2422, Bovid, Layer 2, Bois Roche

Sample 2423, an adult bovid upper premolar from layer 2 of Bois Roche shown in Figure A2.74, was analysed in 3 tracks, with track 1 comprising 3 spots of enamel and 8 spots of dentine, track 2 comprising 3 spots of enamel and 6 spots of dentine and track 3 comprising 3 spots of enamel and 8 spots of dentine, shown in Figure A3.223. The results from this sample are summarised in Table 5.38 and Figure 5.22. The enamel spots of track 1 have an average ^{88}Sr voltage of 0.842, a weighted average uncorrected $^{87}\text{Sr}/^{86}\text{Sr}$ value of 0.7136 ± 0.0017 , a weighted average corrected $^{87}\text{Sr}/^{86}\text{Sr}$ value of 0.71280 ± 0.0017 and a weighted average $^{84}\text{Sr}/^{86}\text{Sr}$ value of 0.05640 ± 0.00011 ($n=3$). The dentine spots of track 1 have an average ^{88}Sr voltage of 0.608, a weighted average uncorrected $^{87}\text{Sr}/^{86}\text{Sr}$ value of 0.71163 ± 0.00027 , a weighted average corrected $^{87}\text{Sr}/^{86}\text{Sr}$ value of 0.70982 ± 0.00027 and a weighted average $^{84}\text{Sr}/^{86}\text{Sr}$ value of 0.05640 ± 0.00012 ($n=8$). The enamel spots of track 2 have an average ^{88}Sr voltage of 1.004, a weighted average uncorrected $^{87}\text{Sr}/^{86}\text{Sr}$ value of 0.716 ± 0.016 , a weighted average corrected $^{87}\text{Sr}/^{86}\text{Sr}$ value of 0.71500 ± 0.016 and a weighted average $^{84}\text{Sr}/^{86}\text{Sr}$ value of 0.05628 ± 0.00011 ($n=3$). The dentine spots of track 2 have an average ^{88}Sr voltage of 0.723, a weighted average uncorrected $^{87}\text{Sr}/^{86}\text{Sr}$ value of 0.71158 ± 0.00040 , a weighted average corrected $^{87}\text{Sr}/^{86}\text{Sr}$ value of 0.70978 ± 0.00040 and a weighted average $^{84}\text{Sr}/^{86}\text{Sr}$ value of 0.05623 ± 0.00019 ($n=6$). The enamel spots of track 3 have an average ^{88}Sr voltage of 0.933, a weighted average uncorrected $^{87}\text{Sr}/^{86}\text{Sr}$ value of 0.718 ± 0.024 , a weighted average corrected $^{87}\text{Sr}/^{86}\text{Sr}$ value of 0.71700 ± 0.024 and a weighted average $^{84}\text{Sr}/^{86}\text{Sr}$ value of 0.05627 ± 0.00013 ($n=3$). The dentine spots of track 3 have an average ^{88}Sr voltage of 0.727, a weighted average uncorrected $^{87}\text{Sr}/^{86}\text{Sr}$ value of 0.71165 ± 0.00030 , a weighted average corrected $^{87}\text{Sr}/^{86}\text{Sr}$ value of 0.70985 ± 0.00030 and a weighted average $^{84}\text{Sr}/^{86}\text{Sr}$ value of 0.05617 ± 0.00016 ($n=8$).

Enamel values for track 1 are in the range of 0.712993 to 0.714455 (uncorrected), as well as 0.712176 to 0.713638 (corrected), and are somewhat heterogeneous. Dentine values for track 1 are in the range of 0.710972 to 0.712053 (uncorrected), as well as 0.709171 to 0.710252 (corrected), and are homogenous within 2σ error. Enamel values for track 2 are in the range of

0.712850 to 0.726719 (uncorrected), as well as 0.712033 to 0.725902 (corrected) with spot 1 being very elevated compared to other enamel values in this track. Dentine values for track 2 are in the range of 0.711132 to 0.712048 (uncorrected), as well as 0.709331 to 0.710248 (corrected), and are relatively homogenous. Enamel values for track 3 are in the range of 0.713356 to 0.732601 (uncorrected), as well as 0.712540 to 0.731785 (corrected), with spot 1 being extremely elevated compared to others in this track. Dentine values for track 3 are in the range of 0.711302 to 0.712317 (uncorrected), as well as 0.709501 to 0.710516 (corrected), and are relatively heterogeneous. Detailed values for enamel and dentine for sample 2423 are shown in Table A3.110, Figure A3.224 and Figure A3.225.

Spots 1 of tracks 2 and 3 from this sample have significantly elevated values that are probably erroneous values, perhaps related to inappropriate focusing of the laser (as discussed in more detail above with reference to sample M008) and so excluded from consideration. This sample has enamel and dentine values that are distinct, suggesting that this specimen was a migrant to the area of Bois Roche. Enamel values are moderately heterogeneous, suggesting that the sample was mobile during amelogenesis. The uncorrected weighted average (excluding the spots discussed above) is 0.71342 ± 0.00046 , which correlates to sample FS035-S1 located 165 km south-east of the site on the Dordogne floodplain. The corrected weighted average enamel value is 0.71260 ± 0.00047 , which corresponds to F36R, collected approximately 75 km to the east of Bois Roche in a Cambrian metamorphic unit.

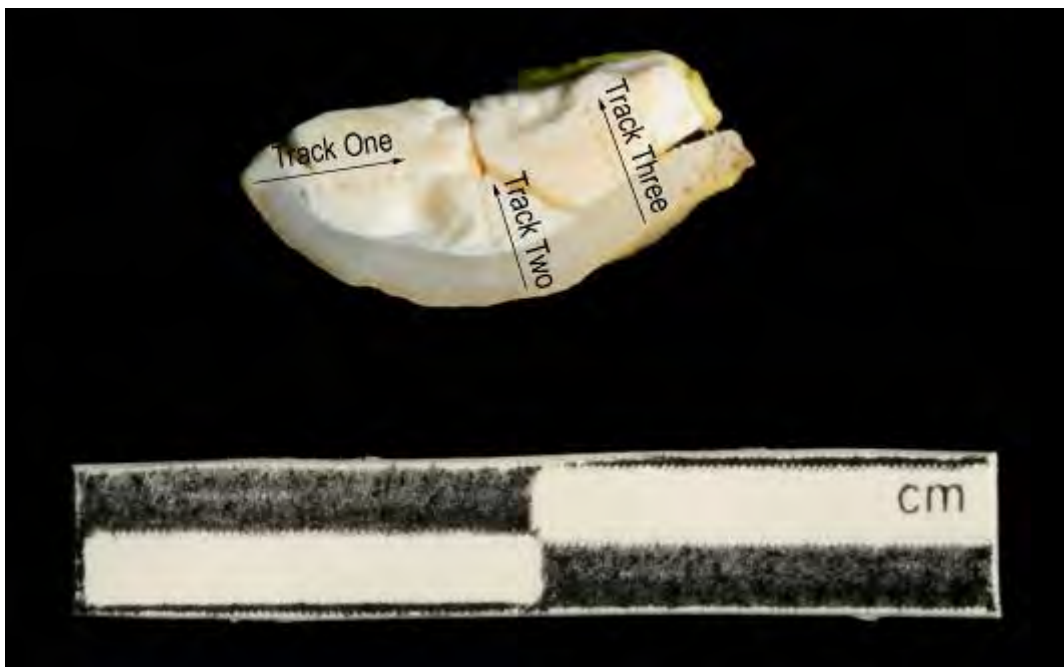


Figure A3.223 LA-MC-ICPMS Track for Sample 2423, Bovid, Layer 2, Bois Roche

Sample	Material	Track	Point	⁸⁸ Sr Volts	⁸⁴ Sr/ ⁸⁶ Sr	⁸⁴ Sr/ ⁸⁶ Sr 2 σ Error	⁸⁷ Sr/ ⁸⁶ Sr	Corrected ⁸⁷ Sr/ ⁸⁶ Sr	⁸⁷ Sr/ ⁸⁶ Sr 2 σ Error
2423	Enamel	1	1	0.773	0.056279	0.000245	0.714455	0.713638	0.000406
2423	Enamel	1	2	0.911	0.056399	0.000213	0.713635	0.712819	0.000335
2423	Enamel	1	3	1.063	0.056452	0.000171	0.712993	0.712176	0.000369
2423	Dentine	1	4	0.786	0.056368	0.000270	0.711781	0.709980	0.000606
2423	Dentine	1	5	0.738	0.056507	0.000216	0.711599	0.709798	0.000321
2423	Dentine	1	6	0.549	0.056336	0.000373	0.710972	0.709171	0.000423
2423	Dentine	1	7	0.593	0.056356	0.000371	0.711890	0.710089	0.000437
2423	Dentine	1	8	0.520	0.056276	0.000410	0.712053	0.710252	0.000495
2423	Dentine	1	9	0.535	0.056501	0.000412	0.711678	0.709877	0.000499
2423	Dentine	1	10	0.566	0.056414	0.000496	0.711584	0.709784	0.000463
2423	Dentine	1	11	0.576	0.056240	0.000392	0.711697	0.709896	0.000468
2423	Enamel	2	1	0.912	0.056188	0.000217	0.726719	0.725902	0.000429
2423	Enamel	2	2	0.998	0.056428	0.000238	0.713441	0.712624	0.000252
2423	Enamel	2	3	1.101	0.056255	0.000157	0.712850	0.712033	0.000424
2423	Dentine	2	4	1.150	0.056207	0.000162	0.712048	0.710248	0.000251
2423	Dentine	2	5	0.735	0.056137	0.000216	0.711393	0.709592	0.000415
2423	Dentine	2	6	0.785	0.056329	0.000181	0.711132	0.709331	0.000275
2423	Dentine	2	7	0.593	0.056237	0.000332	0.711571	0.709770	0.000306
2423	Dentine	2	8	0.527	0.055754	0.000382	0.711700	0.709899	0.000476
2423	Dentine	2	9	0.548	0.056594	0.000340	0.711399	0.709599	0.000462
2423	Enamel	3	1	1.033	0.056213	0.000224	0.732601	0.731785	0.000561
2423	Enamel	3	2	0.791	0.056329	0.000242	0.714410	0.713594	0.000469
2423	Enamel	3	3	0.976	0.056263	0.000220	0.713356	0.712540	0.000375
2423	Dentine	3	4	1.008	0.056216	0.000174	0.712317	0.710516	0.000380
2423	Dentine	3	5	0.899	0.056339	0.000195	0.711573	0.709773	0.000389
2423	Dentine	3	6	0.831	0.056213	0.000217	0.711996	0.710196	0.000387
2423	Dentine	3	7	0.692	0.055971	0.000277	0.711435	0.709634	0.000356
2423	Dentine	3	8	0.605	0.055690	0.000375	0.711373	0.709573	0.000474
2423	Dentine	3	9	0.665	0.056293	0.000306	0.711302	0.709501	0.000321
2423	Dentine	3	10	0.644	0.056103	0.000371	0.711503	0.709702	0.000421
2423	Dentine	3	11	0.473	0.055649	0.000586	0.711806	0.710006	0.000498

Table A3.110 Detailed LA-MC-ICPMS Sr Isotope Results for Enamel and Dentine, Sample 2423, Bovid, Layer 2, Bois Roche

Sample 2423, Bois Roche, France

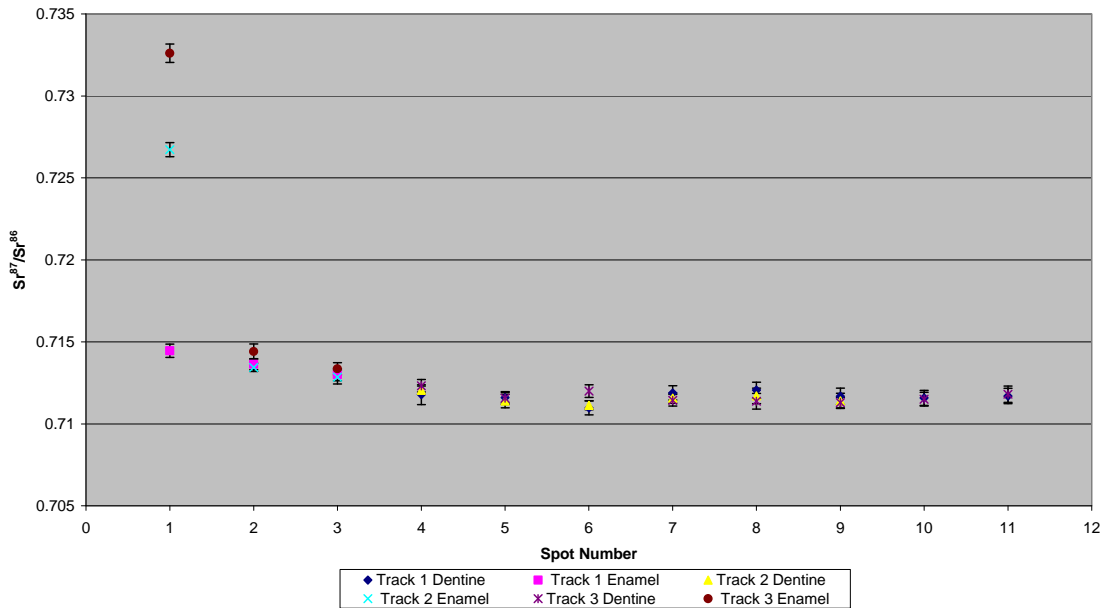


Figure A3.224 Detailed LA-MC-ICPMS Uncorrected Sr Isotope Results, Sample 2423, Bovid, Layer 2, Bois Roche

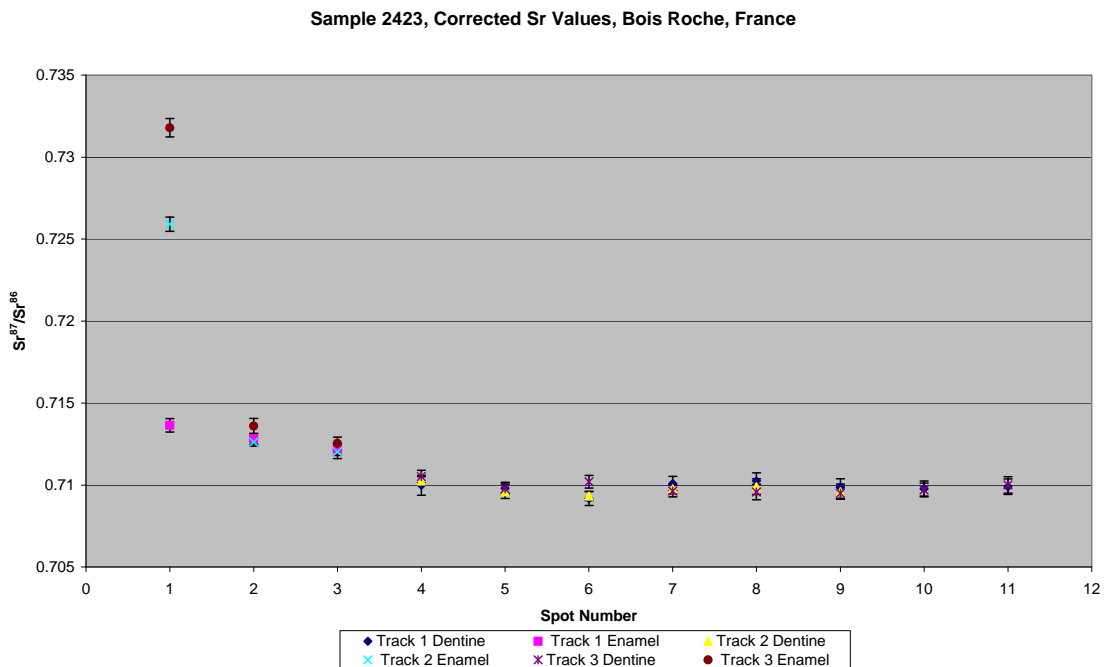


Figure A3.225 Detailed LA-MC-ICPMS Corrected Sr Isotope Results, Sample 2423, Bovid, Layer 2, Bois Roche

Sample 2424, a lower molar from a young adult bovid from layer 2 of Bois Roche shown in Figure A2.75, was analysed in 2 tracks, with track 1 comprising 5 spots of enamel and 7 spots of dentine and track 2 comprising 4 spots of enamel and 4 spots of dentine, shown in Figure A3.226. The results from this sample are summarised in Table 5.38 and Figure 5.22. The enamel spots of track 1 have an average ^{88}Sr voltage of 0.905, a weighted average uncorrected $^{87}\text{Sr}/^{86}\text{Sr}$ value of 0.7143 ± 0.0020 , a weighted average corrected $^{87}\text{Sr}/^{86}\text{Sr}$ value of 0.71270 ± 0.0020 and a weighted average $^{84}\text{Sr}/^{86}\text{Sr}$ value of 0.056601 ± 0.000087 ($n=5$). The dentine spots of track 1 have an average ^{88}Sr voltage of 1.084, a weighted average uncorrected $^{87}\text{Sr}/^{86}\text{Sr}$ value of 0.71128 ± 0.00029 , a weighted average corrected $^{87}\text{Sr}/^{86}\text{Sr}$ value of 0.71041 ± 0.00029 and a weighted average $^{84}\text{Sr}/^{86}\text{Sr}$ value of 0.05663 ± 0.00010 ($n=7$). The enamel spots of track 2 have an average ^{88}Sr voltage of 0.873, a weighted average uncorrected $^{87}\text{Sr}/^{86}\text{Sr}$ value of 0.7146 ± 0.0029 , a weighted average corrected $^{87}\text{Sr}/^{86}\text{Sr}$ value of 0.71300 ± 0.0029 and a weighted average $^{84}\text{Sr}/^{86}\text{Sr}$ value of 0.05669 ± 0.00031 ($n=4$). The dentine spots of track 2 have an average ^{88}Sr voltage of 1.076, a weighted average uncorrected $^{87}\text{Sr}/^{86}\text{Sr}$ value of 0.71111 ± 0.00052 , a weighted average corrected $^{87}\text{Sr}/^{86}\text{Sr}$ value of 0.71024 ± 0.00052 and a weighted average $^{84}\text{Sr}/^{86}\text{Sr}$ value of 0.056550 ± 0.000082 ($n=4$). Enamel values for track 1 of 2424 are in the range of 0.712785 to 0.716511 (uncorrected), as well as 0.711218 to 0.714944 (corrected), and decrease in value from spot 2 to spot 5. Dentine values for track 1 are in the range of 0.710675 to 0.711707 (uncorrected), as well as 0.709805 to 0.710837 (uncorrected) and relatively homogenous, with the exception of spot 6, which is reduced in value compared to the other dentine values. Enamel values for track 2 are in the range of 0.713286 to 0.717943 (uncorrected), as well as 0.711718 to 0.716376 (corrected), decreasing significantly from the exterior of the enamel to the enamel-dentine junction. Dentine values for track 2 are in the range of 0.710692 to 0.711367 (uncorrected), as well as 0.709821 to 0.710497 (corrected), and are very homogeneous, with the exception of spot 6, which has a lower $^{87}\text{Sr}/^{86}\text{Sr}$ value. Detailed values for enamel and dentine for sample 2424 are shown in Table A3.111, Figure A3.227 and Figure A3.228.

The weighted average enamel and dentine values from this sample are statistically distinguishable, suggesting that this specimen is a migrant. Enamel values are relatively heterogeneous and show a trend of decreasing $^{87}\text{Sr}/^{86}\text{Sr}$ values from a maximum at the exterior of the enamel to a minimum value at the dentine-enamel junction. The upper range of the uncorrected enamel values corresponds to mapping sample FS067-S1 from a Carboniferous monzogranite/granite. This sampling location is approximately 220 km to the south-east of Bois Roche; however, it outcrops within 150 km to the east of the site. The corrected enamel value for this upper range corresponds to sample FS041-S1 from a Lower Jurassic carbonate, which outcrops approximately 55 km north-east of the site. The lower range of the uncorrected enamel does not correlate to any sample from this study. The lower range of the corrected enamel correlates to FS006 from the Charente floodplain, which is located approximately 4.6 km south-west of the site. The heterogeneity in the enamel suggests that this sample was mobile during amelogenesis. $^{84}\text{Sr}/^{86}\text{Sr}$ values have an overall weighted average of 0.056613 ± 0.000053 , which is only slightly elevated compared to the ideal value.



Figure A3.226 LA-MC-ICPMS Track for Sample 2424, Bovid, Layer 2, Bois Roche

Sample	Material			^{88}Sr Volts	$^{84}\text{Sr}/^{86}\text{Sr}$	Error	$^{87}\text{Sr}/^{86}\text{Sr}$	Corrected $^{87}\text{Sr}/^{86}\text{Sr}$	$^{87}\text{Sr}/^{86}\text{Sr} 2\sigma$ Error
		Point	Track						
2424	Enamel	1	1	0.868	0.056511	0.000206	0.715298	0.713731	0.000380
2424	Enamel	1	2	0.733	0.056756	0.000233	0.716511	0.714944	0.000429
2424	Enamel	1	3	0.800	0.056664	0.000236	0.715331	0.713763	0.000521
2424	Enamel	1	4	1.031	0.056514	0.000189	0.713563	0.711996	0.000389
2424	Enamel	1	5	1.092	0.056615	0.000163	0.712785	0.711218	0.000285
2424	Dentine	1	6	0.792	0.056832	0.000205	0.710675	0.709805	0.000280
2424	Dentine	1	7	0.961	0.056707	0.000158	0.711344	0.710473	0.000268
2424	Dentine	1	8	1.114	0.056697	0.000175	0.711248	0.710378	0.000342
2424	Dentine	1	9	1.208	0.056554	0.000180	0.711707	0.710837	0.000242
2424	Dentine	1	10	1.210	0.056629	0.000127	0.711465	0.710595	0.000223
2424	Dentine	1	11	1.123	0.056625	0.000190	0.711212	0.710341	0.000224
2424	Dentine	1	12	1.178	0.056475	0.000135	0.711097	0.710227	0.000271
2424	Enamel	2	1	0.809	0.056440	0.000341	0.717943	0.716376	0.000543
2424	Enamel	2	2	0.742	0.057033	0.000266	0.715851	0.714284	0.000426
2424	Enamel	2	3	0.883	0.056579	0.000262	0.714324	0.712757	0.000373
2424	Enamel	2	4	1.058	0.056672	0.000142	0.713286	0.711718	0.000289
2424	Dentine	2	5	0.992	0.056661	0.000220	0.711367	0.710497	0.000316
2424	Dentine	2	6	1.043	0.056556	0.000186	0.710692	0.709821	0.000257
2424	Dentine	2	7	1.181	0.056529	0.000128	0.711351	0.710481	0.000204
2424	Dentine	2	8	1.088	0.056513	0.000177	0.710964	0.710094	0.000275

Table A3.111 Detailed LA-MC-ICPMS Sr Isotope Results for Enamel and Dentine, Sample 2424, Bovid, Layer 2, Bois Roche

Sample 2424, Bois Roche, France

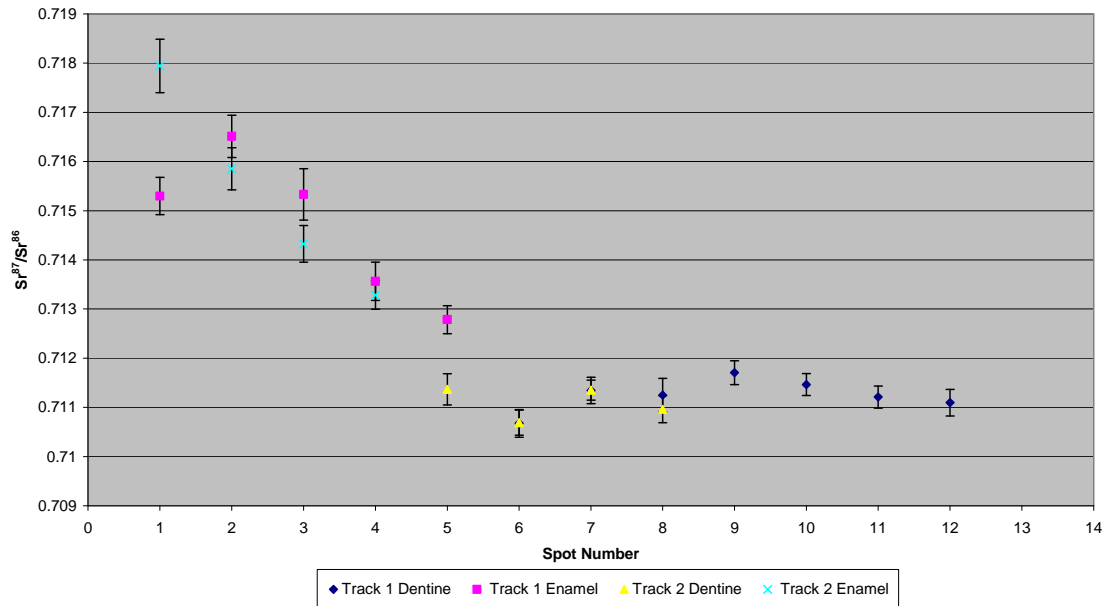


Figure A3.227 Detailed LA-MC-ICPMS Uncorrected Sr Isotope Results, Sample 2424, Bovid, Layer 2, Bois Roche

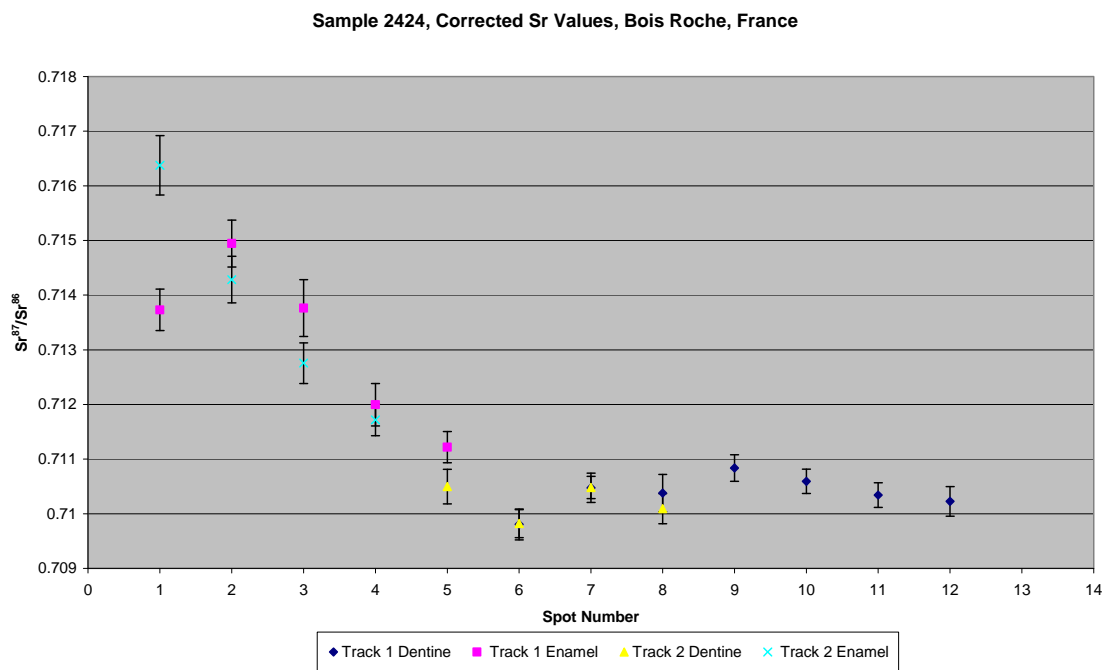


Figure A3.228 Detailed LA-MC-ICPMS Corrected Sr Isotope Results, Sample 2424, Bovid, Layer 2, Bois Roche

Sample 2425A, one of three subsamples from an adult bovid upper molar from layer 2 of Bois Roche shown in Figure A2.76, was analysed in 1 track comprising 10 spots of enamel in 2 discontinuous sections and 18 spots of dentine, shown in Figure A3.229. The results from this sample are summarised in Table 5.38 and Figure 5.22. The enamel spots of track 1 have an average ^{88}Sr voltage of 0.9361, a weighted average uncorrected $^{87}\text{Sr}/^{86}\text{Sr}$ value of 0.71232 ± 0.00026 , a weighted average corrected $^{87}\text{Sr}/^{86}\text{Sr}$ value of 0.71093 ± 0.00026 and a weighted average $^{84}\text{Sr}/^{86}\text{Sr}$ value of 0.05597 ± 0.00013 ($n=10$). The dentine spots of track 1 have an average ^{88}Sr voltage of 0.897, a weighted average uncorrected $^{87}\text{Sr}/^{86}\text{Sr}$ value of 0.71085 ± 0.00018 , a weighted average corrected $^{87}\text{Sr}/^{86}\text{Sr}$ value of 0.70969 ± 0.00018 and a weighted average $^{84}\text{Sr}/^{86}\text{Sr}$ value of 0.056011 ± 0.000049 ($n=18$). Enamel values for track 1 are in the range of 0.711782 to 0.712974 (uncorrected), as well as 0.709229 to 0.711804 (corrected), and are overall relatively homogenous, although spot 5 has a depressed $^{87}\text{Sr}/^{86}\text{Sr}$ value and spot 29 has an elevated $^{87}\text{Sr}/^{86}\text{Sr}$ value compared to the other enamel spots, which may suggest a contribution of dentine to this spot. Dentine values for track 1 are in the range of 0.710388 to 0.711893 (uncorrected), as well as 0.709229 to 0.710734 (corrected), and are relatively homogenous. Detailed values for enamel and dentine for sample 2425A are shown in Table A3.112, Figure A3.230 and Figure A3.231.

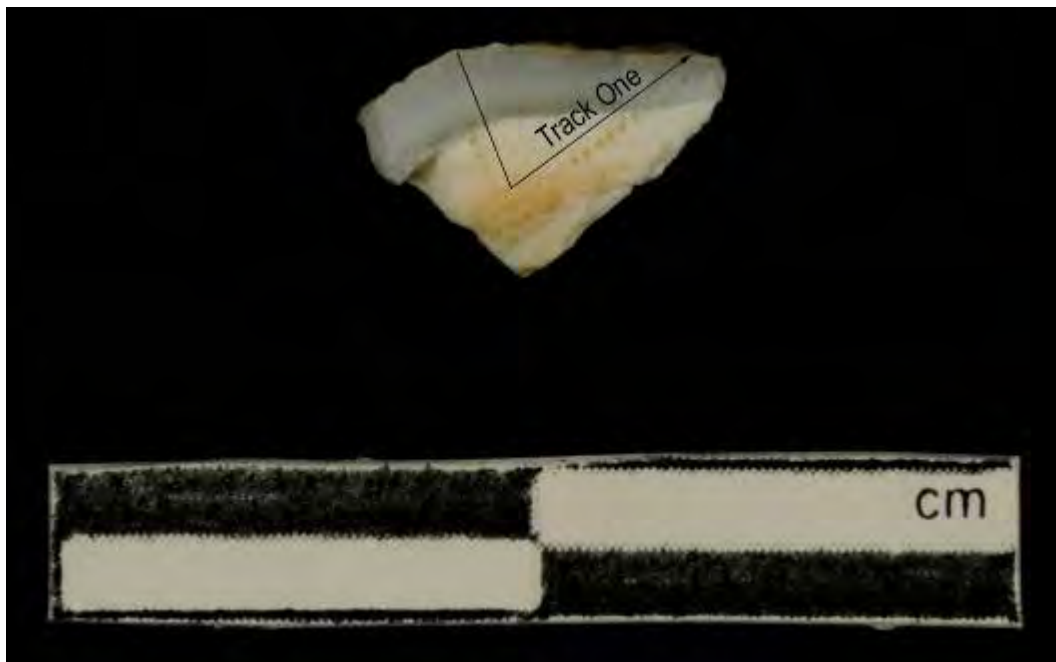


Figure A3.229 LA-MC-ICPMS Track for Sample 2425A, Bovid, Layer 2, Bois Roche

Sample	Material	Track	Point	^{88}Sr Volts	$^{84}\text{Sr}/^{86}\text{Sr}$	$^{84}\text{Sr}/^{86}\text{Sr} 2\sigma$ Error	$^{87}\text{Sr}/^{86}\text{Sr}$	Corrected $^{87}\text{Sr}/^{86}\text{Sr}$	$^{87}\text{Sr}/^{86}\text{Sr} 2\sigma$ Error
2425A	Enamel	1	1	0.858	0.056022	0.000224	0.712331	0.711161	0.000272
2425A	Enamel	1	2	0.961	0.056000	0.000192	0.712204	0.711034	0.000306
2425A	Enamel	1	3	1.050	0.056162	0.000168	0.712330	0.711160	0.000275
2425A	Enamel	1	4	0.967	0.056140	0.000218	0.712124	0.710954	0.000316
2425A	Enamel	1	5	1.289	0.056254	0.000203	0.711782	0.710612	0.000203
2425A	Dentine	1	6	0.802	0.056151	0.000277	0.710388	0.709229	0.000271
2425A	Dentine	1	7	0.773	0.055995	0.000265	0.710809	0.709650	0.000302
2425A	Dentine	1	8	0.953	0.056035	0.000201	0.710943	0.709784	0.000316
2425A	Dentine	1	9	1.102	0.056064	0.000184	0.710789	0.709629	0.000202
2425A	Dentine	1	10	0.975	0.056089	0.000212	0.710772	0.709613	0.000242
2425A	Dentine	1	11	0.896	0.055938	0.000241	0.710975	0.709816	0.000266
2425A	Dentine	1	12	0.907	0.055871	0.000219	0.711058	0.709899	0.000303
2425A	Dentine	1	13	0.894	0.056112	0.000206	0.710574	0.709415	0.000288
2425A	Dentine	1	14	0.896	0.055902	0.000251	0.711253	0.710093	0.000218
2425A	Dentine	1	15	0.997	0.056042	0.000174	0.710774	0.709615	0.000232
2425A	Dentine	1	16	0.950	0.056010	0.000149	0.710595	0.709436	0.000250
2425A	Dentine	1	17	0.770	0.056063	0.000261	0.710607	0.709448	0.000288
2425A	Dentine	1	18	0.868	0.056020	0.000237	0.710627	0.709468	0.000301
2425A	Dentine	1	19	0.831	0.055972	0.000305	0.710409	0.709250	0.000235
2425A	Dentine	1	20	0.717	0.055737	0.000231	0.710751	0.709592	0.000303
2425A	Dentine	1	21	0.750	0.055943	0.000202	0.711055	0.709896	0.000285
2425A	Dentine	1	22	0.976	0.056016	0.000204	0.710882	0.709723	0.000245
2425A	Dentine	1	23	1.092	0.056111	0.000179	0.711893	0.710734	0.000252
2425A	Enamel	1	24	0.908	0.055872	0.000193	0.712761	0.711591	0.000306
2425A	Enamel	1	25	0.853	0.055845	0.000225	0.712503	0.711332	0.000272
2425A	Enamel	1	26	0.793	0.055761	0.000189	0.712299	0.711129	0.000335
2425A	Enamel	1	27	0.837	0.055854	0.000251	0.712368	0.711197	0.000248
2425A	Enamel	1	28	0.845	0.055754	0.000182	0.712974	0.711804	0.000281

Table A3.112 Detailed LA-MC-ICPMS Sr Isotope Results for Enamel and Dentine, Sample 2425A, Bovid, Layer 2, Bois Roche

Sample 2425A, Bois Roche, France

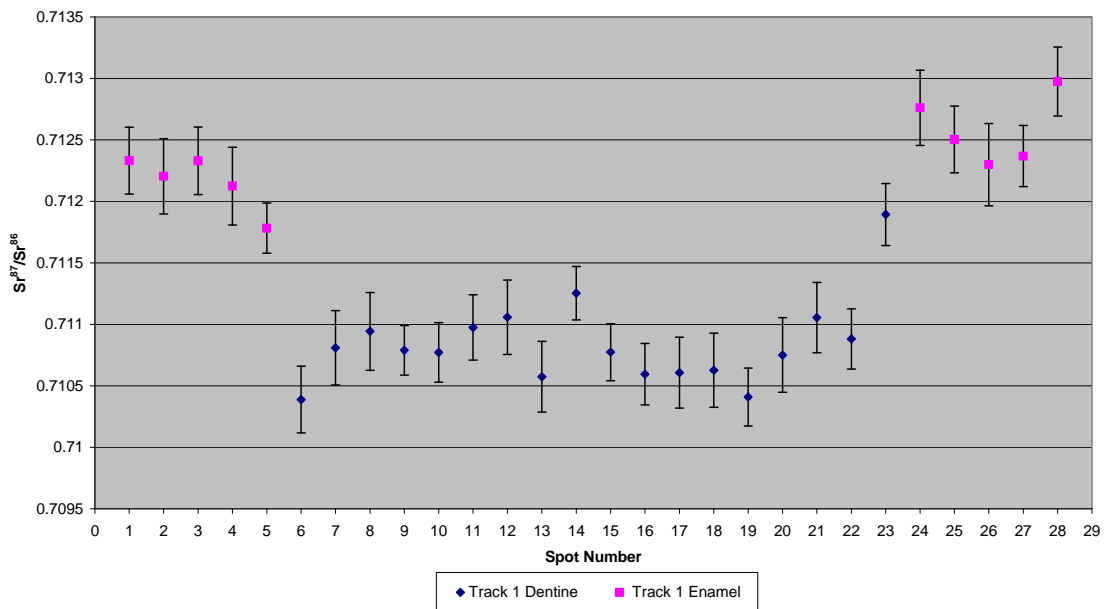


Figure A3.230 Detailed LA-MC-ICPMS Uncorrected Sr Isotope Results, Sample 2425A, Bovid, Layer 2, Bois Roche

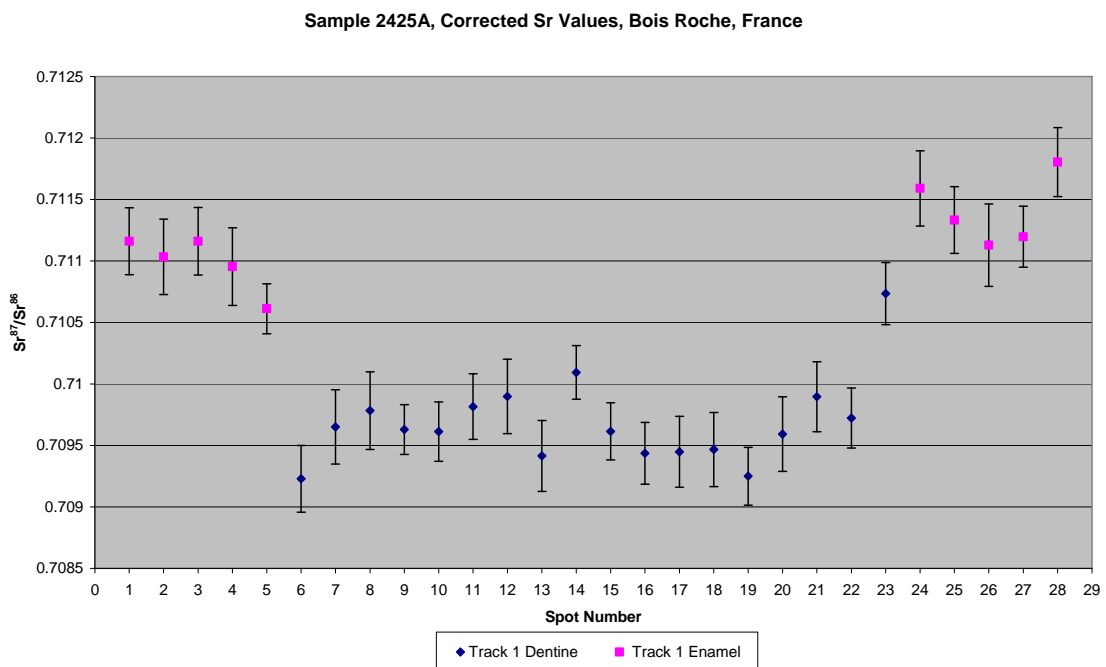


Figure A3.231 Detailed LA-MC-ICPMS Corrected Sr Isotope Results, Sample 2425A, Bovid, Layer 2, Bois Roche

Sample 2425B, one of three subsamples from an adult bovid upper molar from layer 2 of Bois Roche shown in Figure A2.77, was analysed in 2 tracks, with track 1 comprising 4 spots of enamel and 10 spots of dentine and track 2 comprising 27 spots of enamel, shown in Figure A3.232. The results from this sample are summarised in Table 5.38 and Figure 5.22. The enamel spots of track 1 have an average ^{88}Sr voltage of 1.129, a weighted average uncorrected $^{87}\text{Sr}/^{86}\text{Sr}$ value of 0.71153 ± 0.00052 , a weighted average corrected $^{87}\text{Sr}/^{86}\text{Sr}$ value of 0.71078 ± 0.00052 and a weighted average $^{84}\text{Sr}/^{86}\text{Sr}$ value of 0.056330 ± 0.000086 ($n=4$). The dentine spots of track 1 have an average ^{88}Sr voltage of 0.786, a weighted average uncorrected $^{87}\text{Sr}/^{86}\text{Sr}$ value of 0.71055 ± 0.00024 , a weighted average corrected $^{87}\text{Sr}/^{86}\text{Sr}$ value of 0.70897 ± 0.00024 and a weighted average $^{84}\text{Sr}/^{86}\text{Sr}$ value of 0.05622 ± 0.00015 ($n=10$). The enamel spots of track 2 have an average ^{88}Sr voltage of 1.238, a weighted average uncorrected $^{87}\text{Sr}/^{86}\text{Sr}$ value of 0.71167 ± 0.00011 , a weighted average corrected $^{87}\text{Sr}/^{86}\text{Sr}$ value of 0.71092 ± 0.00011 and a weighted average $^{84}\text{Sr}/^{86}\text{Sr}$ value of 0.056254 ± 0.000041 ($n=27$). Enamel values for track 1 are in the range of 0.711378 to 0.712471 (uncorrected), as well as 0.710632 to 0.711725 (corrected), and are very homogenous with the exception of spot 1. Dentine values for track 1 are in the range of 0.710131 to 0.711685 (uncorrected), as well as 0.708546 to 0.712020 (corrected), and are relatively heterogeneous. Enamel values for track 2 are in the range 0.711249 to 0.712765 (uncorrected), as well as 0.710503 to 0.712020 (corrected), and relatively heterogeneous. Detailed values for enamel and dentine for sample 2425B are shown in Table A3.113, Figure A3.233 and Figure A3.234.

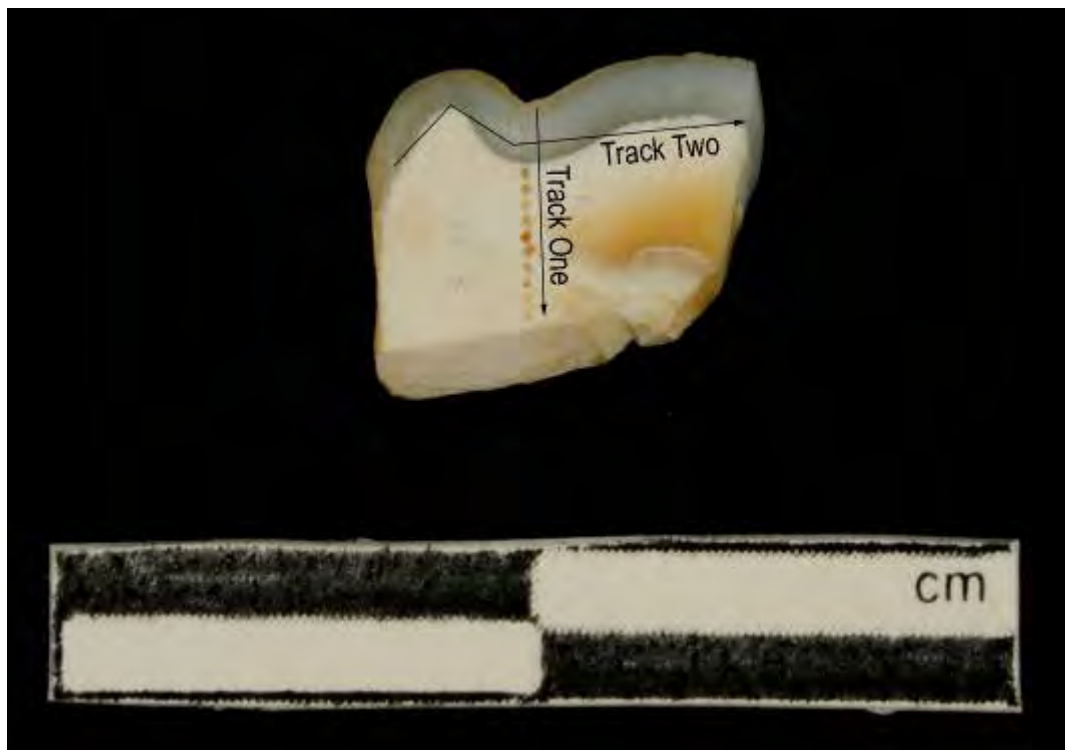


Figure A3.232 LA-MC-ICPMS Track for Sample 2425B, Bovid, Layer 2, Bois Roche

Sample	Material	Track	Point	$^{88}\text{Sr}/^{86}\text{Sr}$	$^{84}\text{Sr}/^{86}\text{Sr}$	$^{87}\text{Sr}/^{86}\text{Sr} 2\sigma$	Corrected $^{87}\text{Sr}/^{86}\text{Sr}$	Error	
2425B	Enamel	1	1	0.916	0.056424	0.000194	0.712471	0.711725	0.000432
2425B	Enamel	1	2	1.178	0.056296	0.000164	0.711549	0.710803	0.000262
2425B	Enamel	1	3	1.155	0.056365	0.000192	0.711433	0.710688	0.000183
2425B	Enamel	1	4	1.269	0.056271	0.000162	0.711378	0.710632	0.000242
2425B	Dentine	1	5	0.786	0.056430	0.000249	0.710268	0.708683	0.000272
2425B	Dentine	1	6	0.673	0.056082	0.000241	0.710131	0.708546	0.000317
2425B	Dentine	1	7	0.826	0.056159	0.000232	0.710522	0.708938	0.000334
2425B	Dentine	1	8	0.638	0.056254	0.000349	0.710255	0.708670	0.000417
2425B	Dentine	1	9	0.437	0.057935	0.000790	0.711685	0.710101	0.000809
2425B	Dentine	1	10	0.747	0.056443	0.000525	0.710374	0.708790	0.000445
2425B	Dentine	1	11	0.798	0.056062	0.000149	0.710283	0.708699	0.000325
2425B	Dentine	1	12	1.044	0.056263	0.000184	0.710439	0.708855	0.000264
2425B	Dentine	1	13	0.985	0.056248	0.000192	0.710748	0.709164	0.000232
2425B	Dentine	1	14	0.927	0.056270	0.000229	0.710946	0.709361	0.000202
2425B	Enamel	2	1	1.192	0.056238	0.000160	0.712765	0.712020	0.000288
2425B	Enamel	2	2	1.177	0.056264	0.000143	0.712257	0.711511	0.000203
2425B	Enamel	2	3	1.344	0.056347	0.000177	0.711836	0.711090	0.000211
2425B	Enamel	2	4	1.585	0.056362	0.000126	0.711482	0.710736	0.000140

Sample	Material	Track	Point	^{88}Sr Volts	$^{84}\text{Sr}/^{86}\text{Sr}$	$^{84}\text{Sr}/^{86}\text{Sr} 2\sigma$ Error	$^{87}\text{Sr}/^{86}\text{Sr}$	Corrected Sr^{86}Sr	$^{87}\text{Sr}/^{86}\text{Sr} 2\sigma$ Error
2425B	Enamel	2	5	1.662	0.056283	0.000123	0.711548	0.710802	0.000203
2425B	Enamel	2	6	1.760	0.056311	0.000102	0.711405	0.710659	0.000134
2425B	Enamel	2	7	1.649	0.056322	0.000094	0.711432	0.710687	0.000167
2425B	Enamel	2	8	1.386	0.056238	0.000138	0.711437	0.710691	0.000184
2425B	Enamel	2	9	1.354	0.056175	0.000159	0.711630	0.710884	0.000202
2425B	Enamel	2	10	1.219	0.056214	0.000159	0.711601	0.710855	0.000219
2425B	Enamel	2	11	1.157	0.056070	0.000154	0.711865	0.711119	0.000206
2425B	Enamel	2	12	1.104	0.056113	0.000191	0.711795	0.711049	0.000219
2425B	Enamel	2	13	1.208	0.056231	0.000148	0.711249	0.710503	0.000221
2425B	Enamel	2	14	1.223	0.056201	0.000162	0.711486	0.710741	0.000179
2425B	Enamel	2	15	1.156	0.056233	0.000157	0.711673	0.710927	0.000224
2425B	Enamel	2	16	1.246	0.056413	0.000129	0.711316	0.710570	0.000205
2425B	Enamel	2	17	1.070	0.056379	0.000145	0.711863	0.711117	0.000229
2425B	Enamel	2	18	1.014	0.056427	0.000236	0.711805	0.711059	0.000217
2425B	Enamel	2	19	1.089	0.056337	0.000207	0.711650	0.710904	0.000185
2425B	Enamel	2	20	1.113	0.056278	0.000184	0.711687	0.710941	0.000230
2425B	Enamel	2	21	1.091	0.056162	0.000201	0.711718	0.710972	0.000249
2425B	Enamel	2	22	1.163	0.056072	0.000173	0.711781	0.711035	0.000256
2425B	Enamel	2	23	1.059	0.056093	0.000175	0.711911	0.711165	0.000246
2425B	Enamel	2	24	1.134	0.056009	0.000218	0.711974	0.711228	0.000282
2425B	Enamel	2	25	1.074	0.056056	0.000193	0.711958	0.711212	0.000309
2425B	Enamel	2	26	1.149	0.056226	0.000183	0.711844	0.711099	0.000223
2425B	Enamel	2	27	1.055	0.056270	0.000182	0.712214	0.711468	0.000284

Table A3.113 Detailed LA-MC-ICPMS Sr Isotope Results for Dentine and Enamel, Sample 2425B, Bovid, Layer 2, Bois Roche

Sample 2425B, Bois Roche, France

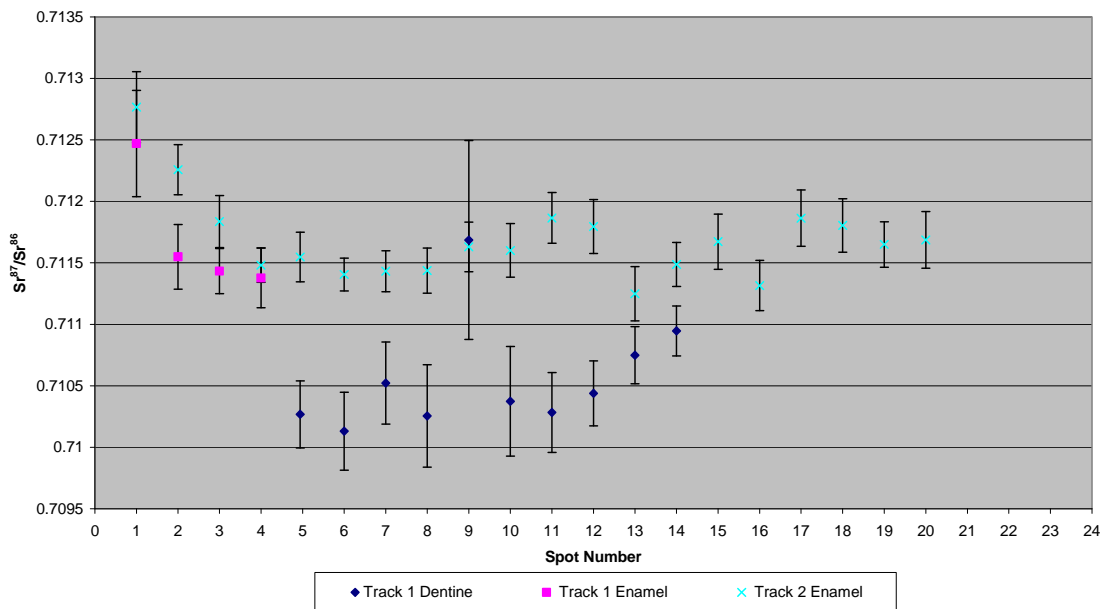


Figure A3.233 Detailed LA-MC-ICPMS Uncorrected Sr Isotope Results, Sample 2425B, Bovid, Layer 2, Bois Roche

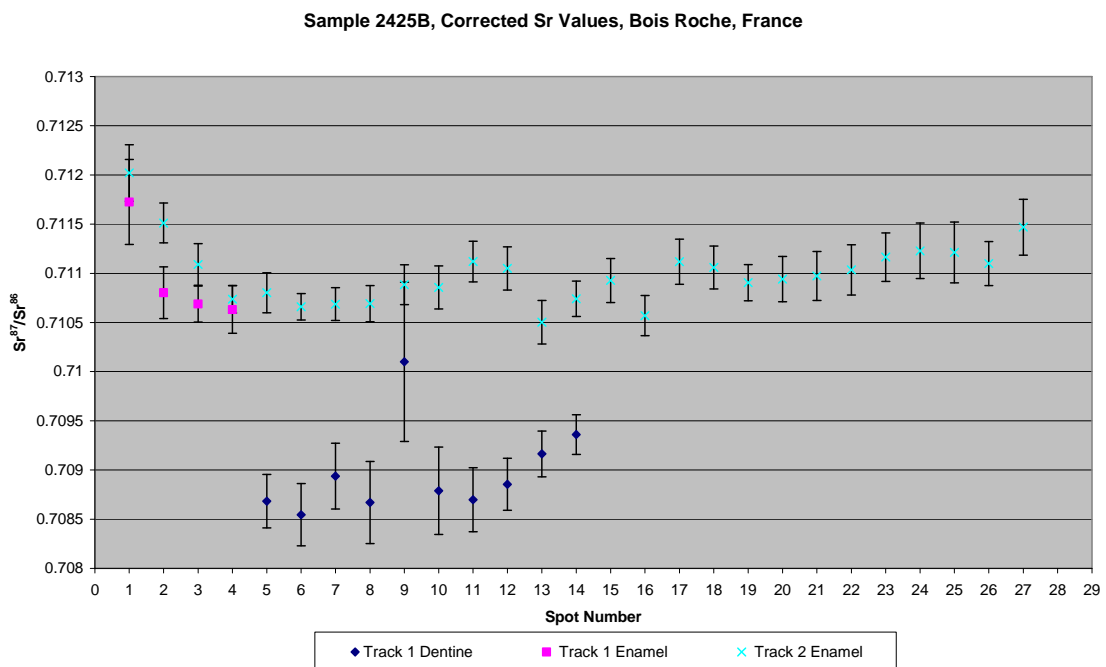


Figure A3.234 Detailed LA-MC-ICPMS Corrected Sr Isotope Results, Sample 2425B, Bovid, Layer 2, Bois Roche

Sample 2425C, one of three subsamples from an adult bovid upper molar from layer 2 of Bois Roche shown in Figure A2.78, was analysed in 2 tracks, with track 1 comprising 4 spots of enamel and 7 spots of dentine and track 2 comprising 4 spots of enamel and 9 spots of dentine, shown in Figure A3.235. The results from this sample are summarised in Table 5.38 and Figure 5.22. The enamel spots of track 1 have an average ^{88}Sr voltage of 1.340, a weighted average uncorrected $^{87}\text{Sr}/^{86}\text{Sr}$ value of 0.71164 ± 0.00053 , a weighted average corrected $^{87}\text{Sr}/^{86}\text{Sr}$ value of 0.71109 ± 0.00053 and a weighted average $^{84}\text{Sr}/^{86}\text{Sr}$ value of 0.056434 ± 0.000072 ($n=4$). The dentine spots of track 1 have an average ^{88}Sr voltage of 1.040, a weighted average uncorrected $^{87}\text{Sr}/^{86}\text{Sr}$ value of 0.71050 ± 0.00027 , a weighted average corrected $^{87}\text{Sr}/^{86}\text{Sr}$ value of 0.70975 ± 0.00027 and a weighted average $^{84}\text{Sr}/^{86}\text{Sr}$ value of 0.056448 ± 0.000066 ($n=7$). The enamel spots of track 2 have an average ^{88}Sr voltage of 1.292, a weighted average uncorrected $^{87}\text{Sr}/^{86}\text{Sr}$ value of 0.71164 ± 0.00055 , a weighted average corrected $^{87}\text{Sr}/^{86}\text{Sr}$ value of 0.71089 ± 0.00055 and a weighted average $^{84}\text{Sr}/^{86}\text{Sr}$ value of 0.05651 ± 0.00015 ($n=4$). The dentine spots of track 2 have an average ^{88}Sr voltage of 1.117, a weighted average uncorrected $^{87}\text{Sr}/^{86}\text{Sr}$ value of 0.71068 ± 0.00035 , a weighted average corrected $^{87}\text{Sr}/^{86}\text{Sr}$ value of 0.70993 ± 0.00035 and a weighted average $^{84}\text{Sr}/^{86}\text{Sr}$ value of 0.056438 ± 0.000056 ($n=9$). Enamel values for track 1 are in the range of 0.711503 to 0.712338 (uncorrected), as well as 0.710952 to 0.711787 (corrected), and are relatively heterogeneous, with the exception of spot 1, which is elevated compared to the rest of the enamel spots. Dentine values for track 1 are in the range of 0.709992 to 0.710854 (uncorrected), as well as 0.709241 to 0.710103 (corrected), and are relatively heterogeneous. Enamel values for track 2 are in the range of 0.711357 to 0.712119 (uncorrected), as well as 0.710606 to 0.711368 (corrected), and are somewhat homogeneous, particularly spots 3 and 4. Dentine values for track 2 are in the range of 0.710086 to 0.711433 (uncorrected), as well as 0.709335 to 0.710682 (corrected), and are relatively heterogeneous. Detailed values for enamel and dentine for sample 2425C are shown in Table A3.114, Figure A3.236 and Figure A3.237.

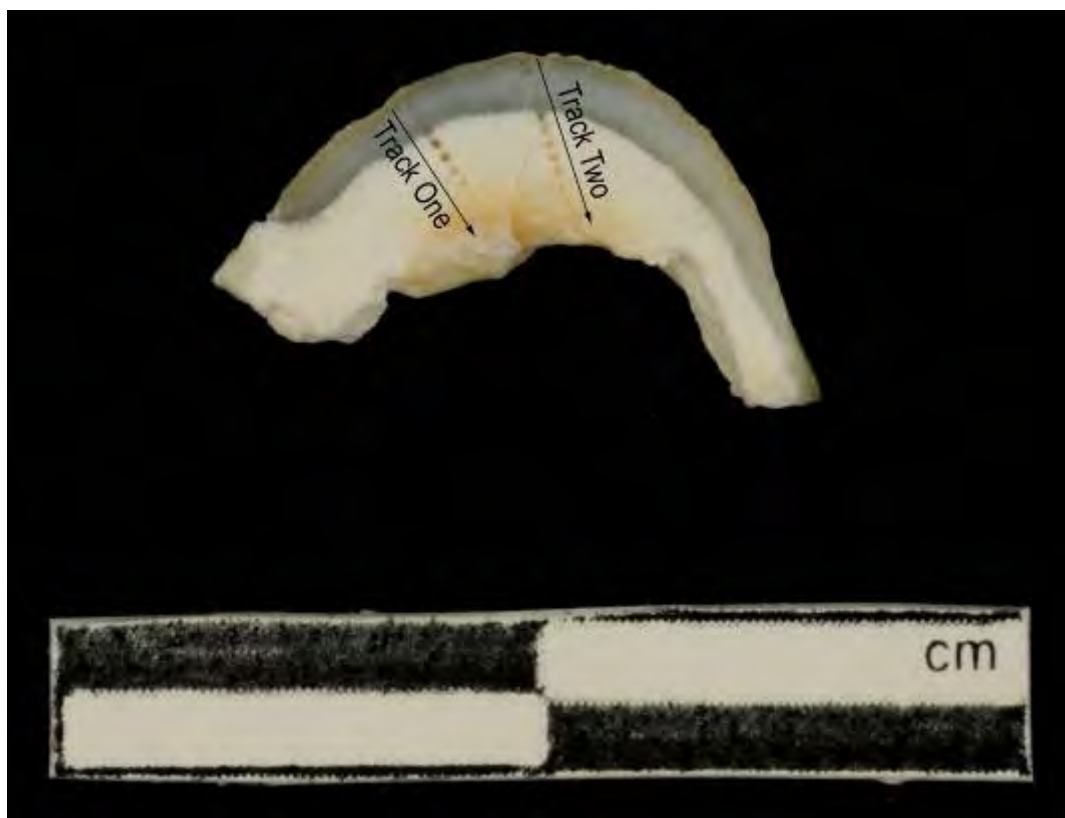


Figure A3.235 LA-MC-ICPMS Track for Sample 2425C, Bovid, Layer 2, Bois Roche

Sample	Material	Track	Point	^{88}Sr Volts	$^{84}\text{Sr}/^{86}\text{Sr}$	$^{84}\text{Sr}/^{86}\text{Sr} 2\sigma$ Error	$^{87}\text{Sr}/^{86}\text{Sr}$	Corrected $^{87}\text{Sr}/^{86}\text{Sr}$	$^{87}\text{Sr}/^{86}\text{Sr} 2\sigma$ Error
2425C	Enamel	1	1	1.123	0.056297	0.000191	0.712338	0.711787	0.000255
2425C	Enamel	1	2	1.362	0.056496	0.000125	0.711503	0.710952	0.000186
2425C	Enamel	1	3	1.415	0.056469	0.000155	0.711619	0.711068	0.000207
2425C	Enamel	1	4	1.459	0.056403	0.000136	0.711484	0.710933	0.000157
2425C	Dentine	1	5	0.775	0.056529	0.000281	0.710565	0.709814	0.000303
2425C	Dentine	1	6	0.703	0.056512	0.000303	0.709992	0.709241	0.000305
2425C	Dentine	1	7	1.188	0.056471	0.000166	0.710153	0.709402	0.000250
2425C	Dentine	1	8	0.973	0.056594	0.000214	0.710428	0.709678	0.000219
2425C	Dentine	1	9	1.190	0.056456	0.000138	0.710810	0.710060	0.000219
2425C	Dentine	1	10	1.227	0.056378	0.000135	0.710515	0.709764	0.000220
2425C	Dentine	1	11	1.223	0.056376	0.000177	0.710854	0.710103	0.000266
2425C	Enamel	2	1	1.092	0.056496	0.000209	0.711848	0.711097	0.000234
2425C	Enamel	2	2	1.370	0.056532	0.000142	0.712119	0.711368	0.000215
2425C	Enamel	2	3	1.314	0.056344	0.000180	0.711357	0.710606	0.000163
2425C	Enamel	2	4	1.390	0.056567	0.000123	0.711501	0.710750	0.000200
2425C	Dentine	2	5	1.268	0.056564	0.000154	0.711433	0.710682	0.000217
2425C	Dentine	2	6	0.972	0.056407	0.000176	0.710599	0.709848	0.000220
2425C	Dentine	2	7	0.911	0.056393	0.000219	0.710086	0.709335	0.000220
2425C	Dentine	2	8	1.180	0.056400	0.000147	0.710120	0.709369	0.000197
2425C	Dentine	2	9	1.165	0.056369	0.000171	0.710349	0.709598	0.000193
2425C	Dentine	2	10	1.016	0.056585	0.000170	0.710812	0.710061	0.000209
2425C	Dentine	2	11	1.105	0.056297	0.000203	0.711250	0.710499	0.000203
2425C	Dentine	2	12	1.216	0.056426	0.000153	0.710797	0.710046	0.000193
2425C	Dentine	2	13	1.223	0.056428	0.000176	0.710735	0.709984	0.000206

Table A3.114 Detailed LA-MC-ICPMS Sr Isotope Results for Dentine and Enamel, Sample 2425C, Bovid, Layer 2, Bois Roche

Sample 2425C, Bois Roche, France

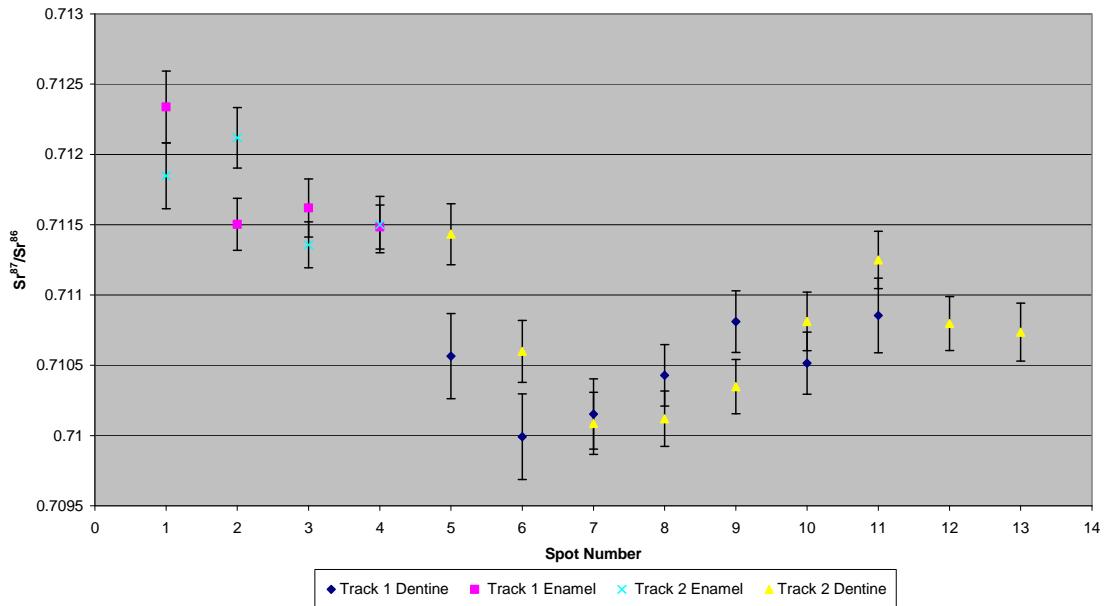


Figure A3.236 Detailed LA-MC-ICPMS Uncorrected Sr Isotope Results, Sample 2425C, Bovid, Layer 2, Bois Roche

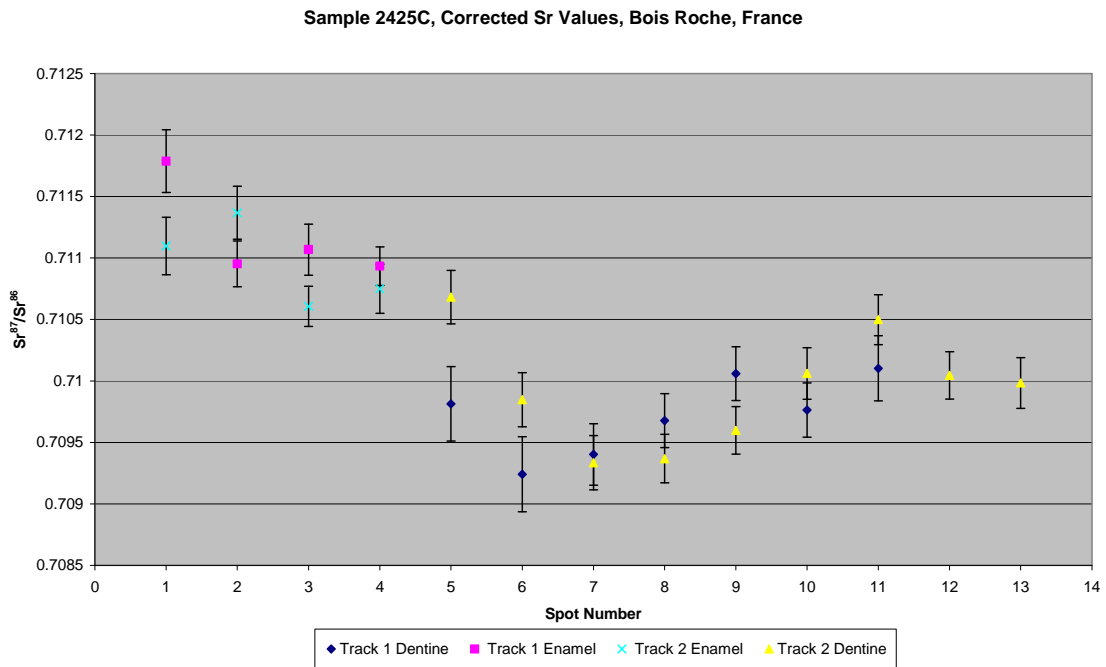


Figure A3.237 Detailed LA-MC-ICPMS Corrected Sr Isotope Results, Sample 2425C, Bovid, Layer 2, Bois Roche

There is a significant distinction between enamel and dentine $^{87}\text{Sr}/^{86}\text{Sr}$ values from the three subsamples of sample 2425, suggesting that this specimen was a migrant to the area of Bois Roche. Enamel values in all sub-samples are heterogeneous, suggesting mobility across different geological environments

during ameoleogenesis. Uncorrected enamel values suggest a sample mobile between the floodplain sediments of the Charente river floodplain (FS006: 0.711301 ± 0.00002) to Cambrian paragneiss/leptynites/amphibolites (FS069R: 0.712497 ± 0.000008). Corrected enamel values correlate with a number of mapping samples from carbonate and floodplain units approximately 160 km south-east of the site, as well as multiple mapping samples from the region of Cambrian metamorphics and Carboniferous igneous material approximately 75 km east of the site. The $^{87}\text{Sr}/^{86}\text{Sr}$ results from this sample may not be robust, based on the overall weighted average $^{84}\text{Sr}/^{86}\text{Sr}$ value of 0.056258 ± 0.000041 for all spots.

A3.2.3.6. Rescoundudou

Sample M033, a bovid M1 molar from layer C1 of Rescoundudou shown in Figure A2.79, was analysed in 1 track comprising 15 spots of enamel in 4 discontinuous sections and 26 spots of dentine in 3 discontinuous sections, shown in Figure A3.238. The results from this sample are summarised in Table 5.41 and Figure 5.26. The enamel spots of track 1 have an average ^{88}Sr voltage of 0.242, a weighted average uncorrected $^{87}\text{Sr}/^{86}\text{Sr}$ value of 0.7148 ± 0.0014 , a weighted average corrected $^{87}\text{Sr}/^{86}\text{Sr}$ value of 0.70360 ± 0.0014 and a weighted average $^{84}\text{Sr}/^{86}\text{Sr}$ value of 0.05708 ± 0.00021 ($n=15$). The dentine spots of track 1 have an average ^{88}Sr voltage of 0.258, a weighted average uncorrected $^{87}\text{Sr}/^{86}\text{Sr}$ value of 0.7149 ± 0.0020 , a weighted average corrected $^{87}\text{Sr}/^{86}\text{Sr}$ value of 0.70510 ± 0.0020 and a weighted average $^{84}\text{Sr}/^{86}\text{Sr}$ value of 0.05737 ± 0.00023 ($n=27$). Enamel values are in the range of 0.710957 to 0.719484 (uncorrected), as well as 0.699685 to 0.708212 (corrected), and are very heterogeneous. Dentine values are in the range of 0.711213 to 0.755005 (uncorrected), as well as 0.701341 to 0.745133 (corrected), and are very heterogeneous. Detailed values for enamel and dentine for sample M033 are shown in Table A3.115, Figure A3.239 and Figure A3.240.

This sample has highly variable values for enamel and dentine, suggesting a complex history of migration during amelogenesis and/or significant post-depositional alteration. The lower value of the corrected enamel results correspond to mapping values obtained from a Middle Jurassic carbonate. This unit is relatively homogenous with mapping values in the range of 0.708 ± 0.000011 (FS094-S1) to 0.714013 ± 0.000042 (FS114-S1). Examination of this package on the more detailed 1:50,000 geological map (Alabouvette 1988) shows a significant number of facies, including shales. This unit also contains features such as pyritised fossils and ferrigenous oolites. This significant variation in lithology could explain the variation observed in strontium isotope composition within this unit. The corrected value of this domain is significantly lower than any mapping value in this study. The higher end-member of the uncorrected enamel range corresponds to a number of mapping values

surrounding Rescoundudou, including FS105-S1 (0.718595 ± 0.000017), FS092-S1 (0.718681 ± 0.000011), FS096-S1 (0.72005 ± 0.000009), FS102-S1 (0.720363 ± 0.000023) and FS112-S1 (0.720635 ± 0.000032). This multiplicity of credible locations for amelogenesis, all located within 16 km of the site, makes it impossible to identify a single area of residence. The intermediate domain in corrected enamel values corresponds to the mapping value from FS118-S1, a Oligocene/Miocene basalt which outcrops within 12.2 km of the site. The higher domain of corrected value corresponds to FS094-S1 from the very heterogeneous (as discussed above) Middle Jurassic carbonate that contains the site. The $^{84}\text{Sr}/^{86}\text{Sr}$ weighted average value for all spots is 0.05727 ± 0.00016 , which is significantly elevated compared to the ideal value.

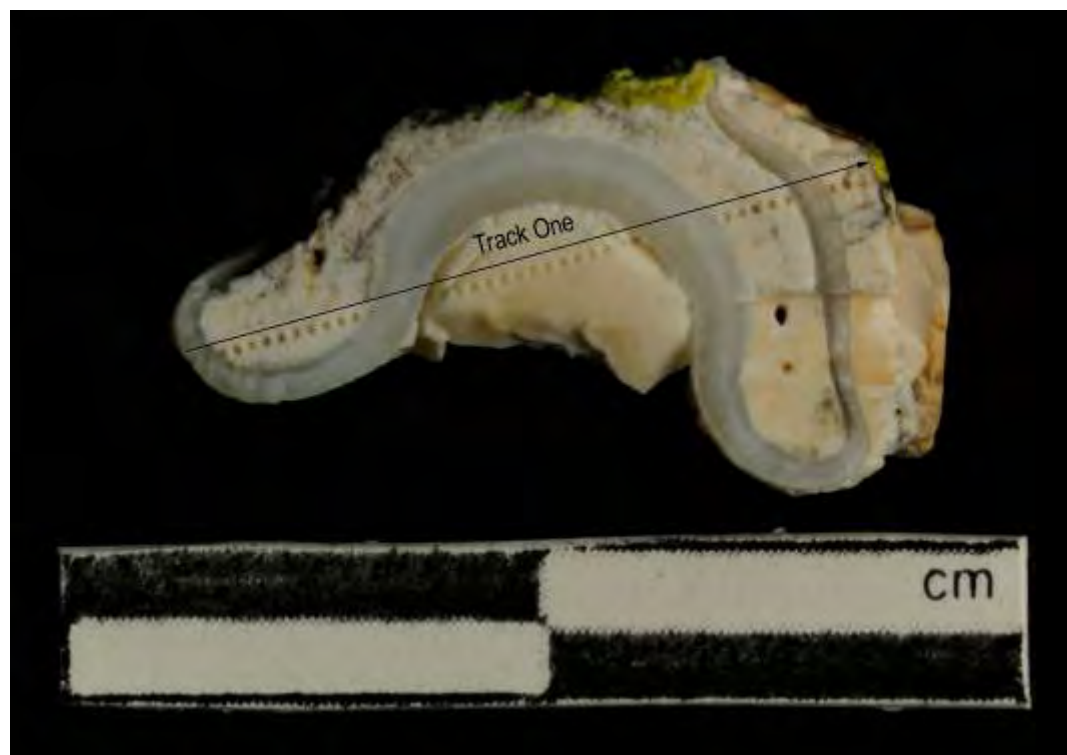


Figure A3.238 LA-MC-ICPMS Track for Sample M033, Bovid, Layer C1, Rescoundudou

Sample	Material	Track	Point	^{88}Sr Volts	$^{84}\text{Sr}/^{86}\text{Sr}$	$^{84}\text{Sr}/^{86}\text{Sr} 2\sigma$ Error	Corrected $^{87}\text{Sr}/^{86}\text{Sr}$	$^{87}\text{Sr}/^{86}\text{Sr} 2\sigma$ Error
M033	Enamel	1	1					
M033	Enamel	1	2	0.248	0.057872	0.000975	0.719484	0.708212
M033	Dentine	1	3	0.251	0.057540	0.000920	0.716656	0.706785
M033	Dentine	1	4	0.306	0.057556	0.000742	0.713717	0.703846
M033	Dentine	1	5					
M033	Dentine	1	6	0.210	0.058693	0.000960	0.755005	0.745133
M033	Dentine	1	7					
M033	Dentine	1	8					
M033	Dentine	1	9	0.274	0.057122	0.000850	0.716687	0.706815
M033	Dentine	1	10	0.258	0.057646	0.001107	0.712613	0.702741
M033	Dentine	1	11	0.284	0.057710	0.000771	0.713335	0.703463
M033	Dentine	1	12	0.253	0.057293	0.000930	0.719966	0.710095
M033	Dentine	1	13	0.159	0.057408	0.001437	0.716883	0.707012
M033	Enamel	1	14	0.163	0.057987	0.002314	0.717896	0.706624
M033	Enamel	1	15	0.188	0.056963	0.001255	0.715396	0.704124
M033	Enamel	1	16	0.231	0.056978	0.000770	0.715465	0.704193
M033	Enamel	1	17	0.311	0.057355	0.000719	0.710957	0.699685
M033	Dentine	1	18	0.343	0.056905	0.000616	0.711213	0.701341
M033	Dentine	1	19	0.258	0.056826	0.000721	0.713722	0.703851
M033	Dentine	1	20	0.292	0.057399	0.000706	0.716463	0.706592
M033	Dentine	1	21	0.282	0.057139	0.000627	0.713906	0.704035
M033	Dentine	1	22	0.264	0.058373	0.000697	0.715793	0.705921
M033	Dentine	1	23	0.259	0.057547	0.000805	0.715273	0.705401
M033	Dentine	1	24	0.258	0.057808	0.001020	0.714198	0.704327
M033	Dentine	1	25	0.256	0.058596	0.000999	0.713005	0.703134
M033	Dentine	1	26	0.247	0.057762	0.000860	0.713161	0.703289
M033	Dentine	1	27	0.254	0.056835	0.000847	0.714244	0.704372
M033	Dentine	1	28	0.262	0.056850	0.000627	0.713255	0.703383
M033	Dentine	1	29	0.274	0.057114	0.000720	0.712270	0.702398
M033	Dentine	1	30	0.260	0.057837	0.000790	0.712268	0.702396
M033	Dentine	1	31	0.227	0.056122	0.000923	0.711283	0.701412
M033	Enamel	1	32	0.253	0.057272	0.000810	0.713669	0.702397
M033	Enamel	1	33	0.262	0.057243	0.000582	0.714344	0.703072
M033	Enamel	1	34	0.196	0.057265	0.001066	0.717465	0.706193
M033	Enamel	1	35	0.189	0.057238	0.001024	0.717073	0.705801
M033	Enamel	1	36	0.160	0.058300	0.001534	0.718150	0.706879
M033	Dentine	1	37	0.247	0.057787	0.000870	0.728645	0.718774
M033	Dentine	1	38	0.217	0.056430	0.000892	0.737069	0.727198

Sample	Material	Track	Point	^{88}Sr Volts	$^{84}\text{Sr}/^{86}\text{Sr}$	Error	$^{87}\text{Sr}/^{86}\text{Sr}$	Corrected $^{87}\text{Sr}/^{86}\text{Sr}$	$^{87}\text{Sr}/^{86}\text{Sr} 2\sigma$ Error
M033	Dentine	1	39	0.262	0.057216	0.000929	0.713741	0.703870	0.000824
M033	Dentine	1	40	0.250	0.057430	0.001037	0.716277	0.706405	0.001098
M033	Dentine	1	41	0.254	0.057477	0.000728	0.712025	0.702153	0.000868
M033	Enamel	1	42	0.210	0.057278	0.000939	0.715622	0.704350	0.001044
M033	Enamel	1	43	0.234	0.056915	0.000829	0.715807	0.704535	0.000918
M033	Enamel	1	44	0.338	0.056755	0.000590	0.713084	0.701812	0.000657
M033	Enamel	1	45	0.303	0.056693	0.000744	0.712197	0.700925	0.000857
M033	Enamel	1	46	0.345	0.056528	0.000687	0.716170	0.704898	0.000740

Table A3.115 Detailed LA-MC-ICPMS Sr Isotope Results for Dentine and Enamel, Sample M033, Bovid, Layer C1, Rescoundudou

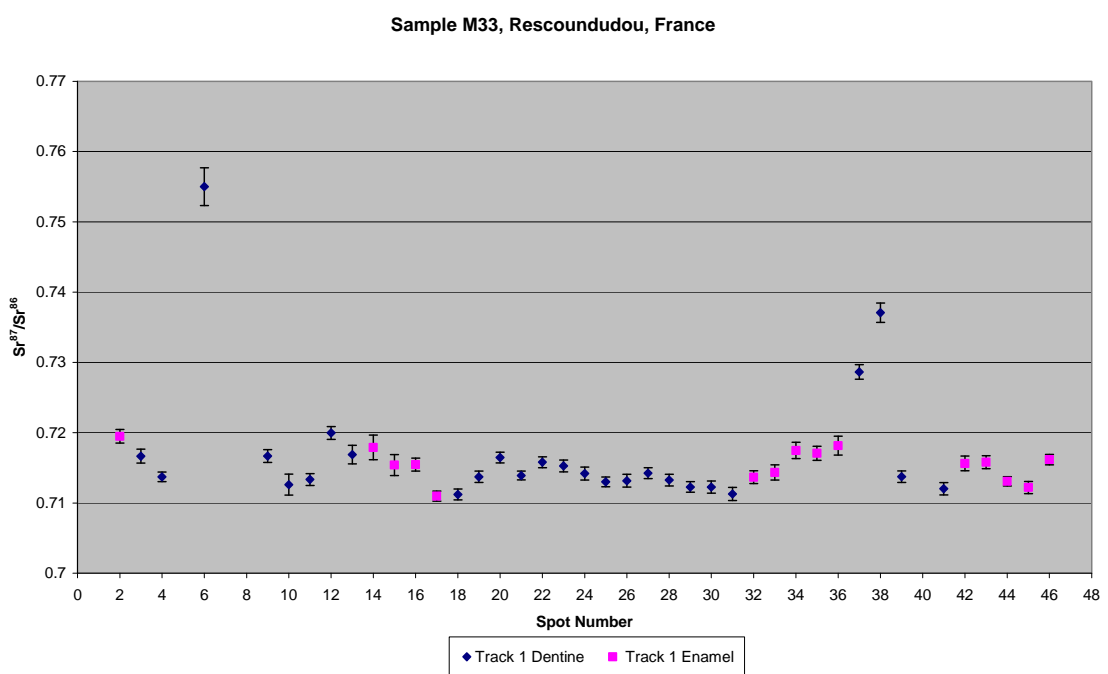


Figure A3.239 Detailed LA-MC-ICPMS Uncorrected Sr Isotope Results, Sample M033, Bovid, Layer C1, Rescoundudou

Sample M33, Corrected Sr Values, Rescoundudou, France

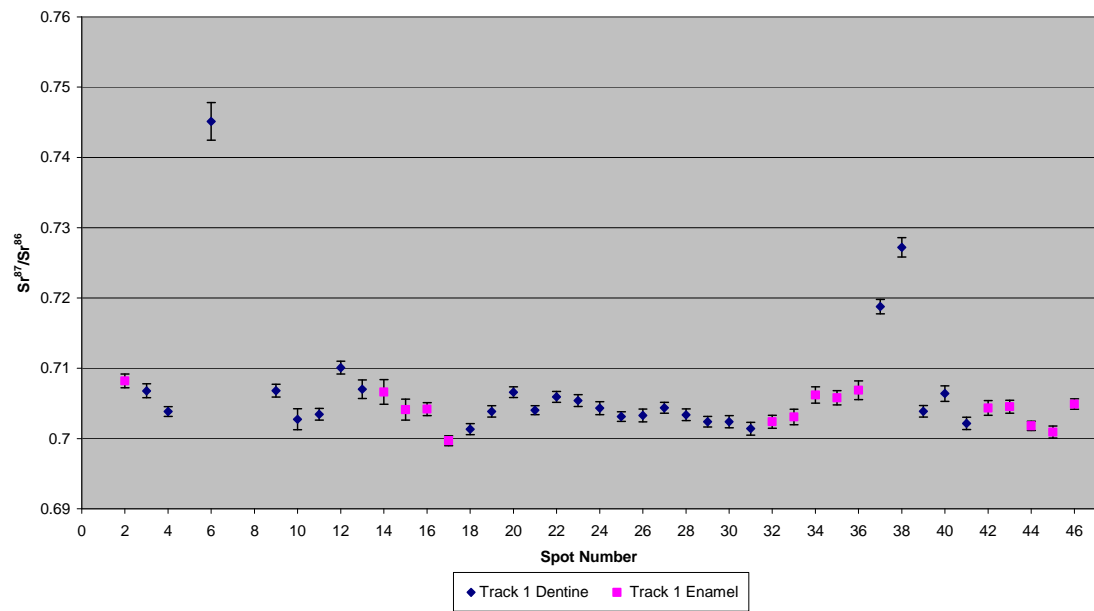


Figure A3.240 Detailed LA-MC-ICPMS Corrected Sr Isotope Results, Sample M033, Bovid, Layer C1, Rescoundudou

Sample M034, a bovid molar from layer C1 of Rescoundudou shown in Figure A2.80, was analysed in 1 track comprising 6 spots of enamel in 2 discontinuous sections and 13 spots of dentine, shown in Figure A3.241. The results from this sample are summarised in Table 5.41 and Figure 5.26. The enamel spots of track 1 have an average ^{88}Sr voltage of 0.231, a weighted average uncorrected $^{87}\text{Sr}/^{86}\text{Sr}$ value of 0.7157 ± 0.0013 , a weighted average corrected $^{87}\text{Sr}/^{86}\text{Sr}$ value of 0.70410 ± 0.0013 and a weighted average $^{84}\text{Sr}/^{86}\text{Sr}$ value of 0.05711 ± 0.00035 ($n=6$). The dentine spots of track 1 have an average ^{88}Sr voltage of 0.332, a weighted average uncorrected $^{87}\text{Sr}/^{86}\text{Sr}$ value of 0.71166 ± 0.00051 , a weighted average corrected $^{87}\text{Sr}/^{86}\text{Sr}$ value of 0.70572 ± 0.00051 and a weighted average $^{84}\text{Sr}/^{86}\text{Sr}$ value of 0.05675 ± 0.00025 ($n=13$). Enamel values are in the range of 0.714343 to 0.717516 (uncorrected), as well as 0.702742 to 0.705914 (corrected), and show significant variations between the 2 discontinuous sections. Spots 1 to 3 are homogenous within 2σ error and spots 17 to 19 are homogenous within 2σ error. Dentine values are in the range of 0.710550 to 0.713114 (uncorrected), as well as 0.704608 to 0.707172 (corrected), and are relatively heterogeneous. Detailed values for enamel and dentine for sample M034 are shown in Table A3.116, Figure A3.242 and Figure A3.243.

The enamel values from this sample are clustered in 2 domains. The weighted average uncorrected value of the lower domain (0.71459 ± 0.00056) corresponds to mapping sample FS114-S1 (0.714013 ± 0.000042) from the Middle Jurassic carbonate; however, the $^{87}\text{Sr}/^{86}\text{Sr}$ composition of this sample is significantly elevated compared to other values from this unit and the known oceanic strontium isotope composition during this period (~0.7075 (Elderfield 1986:77)). The weighted average corrected value of this domain (0.70299 ± 0.00056) is less radiogenic than any mapping sample in the study area. The higher weighted average domain of uncorrected enamel $^{87}\text{Sr}/^{86}\text{Sr}$ values for this sample (0.7166 ± 0.0024) corresponds to sample FS097-S1 (0.718429 ± 0.000013), described in the field as a meta-sediment, although it is mapped as a Lower Jurassic carbonate. This disparity may be explained by the sample being collected near the boundary of this unit on the geological map, suggesting this transition may be inaccurately mapped. The corrected weighted average of

this domain (0.7050 ± 0.0024) corresponds to FS118-S1, which is located approximately 40 km north-east of the site in a basalt unit. These enamel values are both very different from the dentine values for this sample, suggesting that this specimen is a migrant to the area of Rescoundudou. Dentine values are relatively heterogeneous, suggesting a complex post-burial diagenetic regime. The overall weighted average $^{84}\text{Sr}/^{86}\text{Sr}$ value of analysis spots from M034 is 0.05682 ± 0.00020 , which is slightly elevated compared to the ideal value.

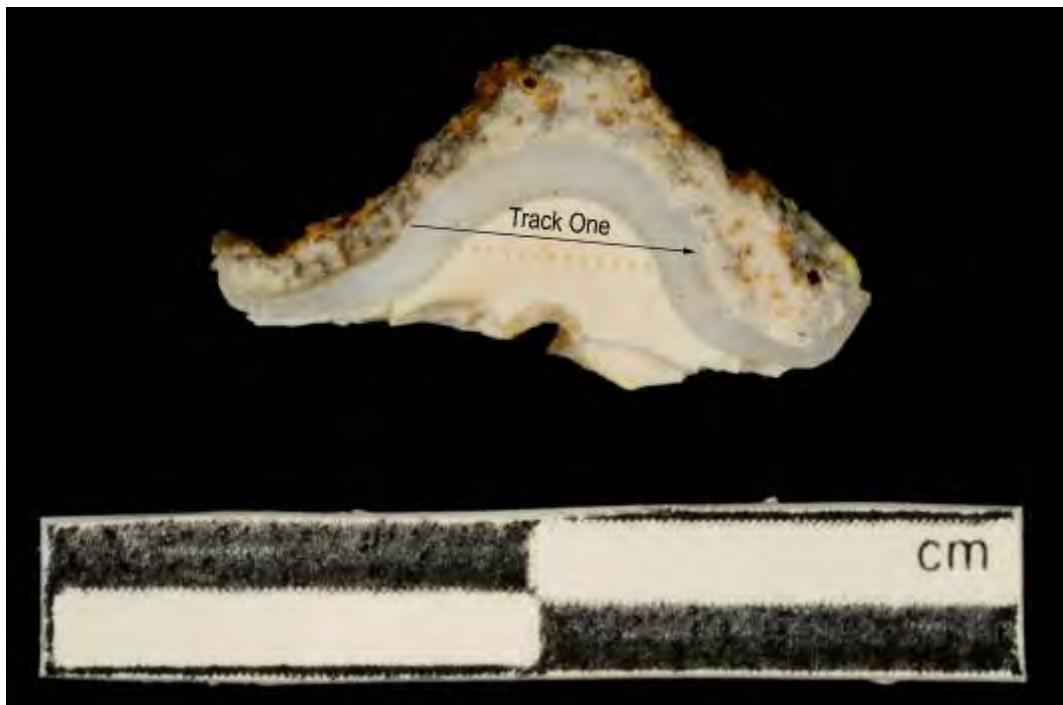


Figure A3.241 LA-MC-ICPMS Track for Sample M034, Bovid, Layer C1, Rescoundudou

Sample	Material	Track	Point	^{88}Sr Volts	$^{84}\text{Sr}/^{86}\text{Sr}$	$^{84}\text{Sr}/^{86}\text{Sr} 2\sigma$	Corrected $^{87}\text{Sr}/^{86}\text{Sr}$	$^{87}\text{Sr}/^{86}\text{Sr}$	$^{87}\text{Sr}/^{86}\text{Sr} 2\sigma$
M034	Enamel	1	1	0.231	0.057351	0.001012	0.714592	0.702990	0.000894
M034	Enamel	1	2	0.225	0.057094	0.000810	0.714894	0.703293	0.001108
M034	Enamel	1	3	0.237	0.057668	0.000941	0.714343	0.702742	0.000993
M034	Dentine	1	4	0.326	0.056849	0.000661	0.713114	0.707172	0.000761
M034	Dentine	1	5	0.277	0.057418	0.000793	0.711093	0.705151	0.000934
M034	Dentine	1	6	0.309	0.057102	0.000638	0.712428	0.706486	0.000748
M034	Dentine	1	7	0.358	0.057073	0.000547	0.710567	0.704625	0.000593
M034	Dentine	1	8	0.334	0.056590	0.000535	0.710550	0.704608	0.000607
M034	Dentine	1	9	0.349	0.057120	0.000738	0.711085	0.705143	0.000584

M034	Dentine	1	10	0.355	0.056374	0.000568	0.710910	0.704968	0.000632
M034	Dentine	1	11	0.356	0.056331	0.000555	0.712130	0.706188	0.000640
M034	Dentine	1	12	0.360	0.056783	0.000499	0.712022	0.706080	0.000578
M034	Dentine	1	13	0.362	0.056811	0.000548	0.711413	0.705471	0.000748
M034	Dentine	1	14	0.307	0.055977	0.000593	0.712662	0.706719	0.000685
M034	Dentine	1	15	0.304	0.056360	0.000831	0.711860	0.705917	0.000779
M034	Dentine	1	16	0.312	0.057415	0.000629	0.712475	0.706532	0.000620
M034	Enamel	1	17	0.272	0.056984	0.000744	0.715881	0.704279	0.000678
M034	Enamel	1	18	0.218	0.056746	0.000761	0.717377	0.705776	0.001132
M034	Enamel	1	19	0.201	0.057102	0.001146	0.717516	0.705914	0.000966

Table A3.116 Detailed LA-MC-ICPMS Sr Isotope Results for Dentine and Enamel, Sample M034, Bovid, Layer C1, Rescoundudou

Sample M34, Rescoundudou, France

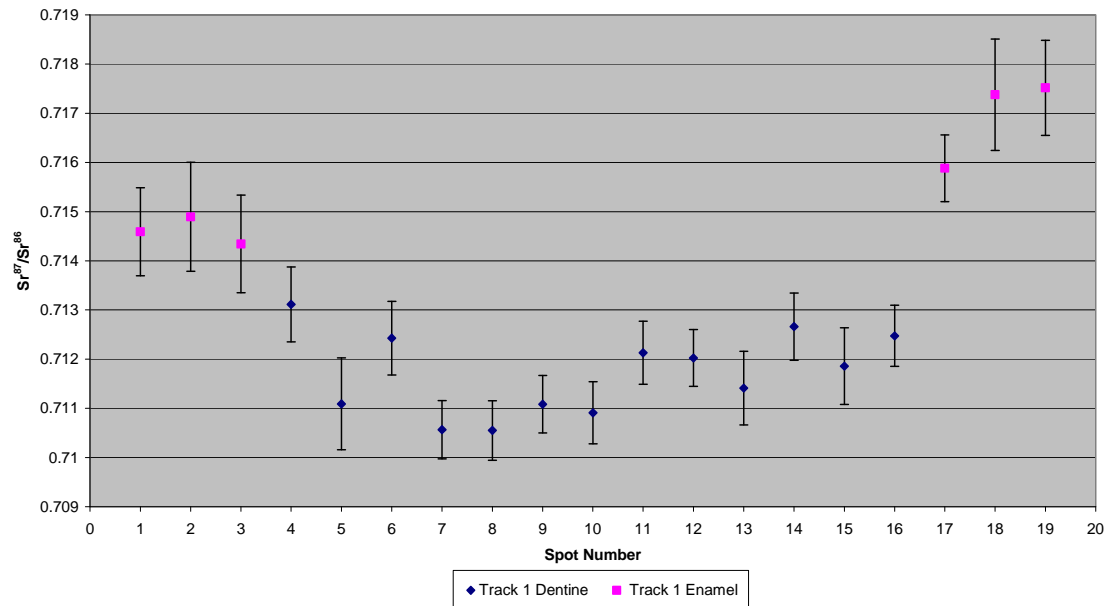


Figure A3.242 Detailed LA-MC-ICPMS Uncorrected Sr Isotope Results, Sample M034, Bovid, Layer C1, Rescoundudou

Sample M34, Corrected Sr Values, Rescoundudou, France

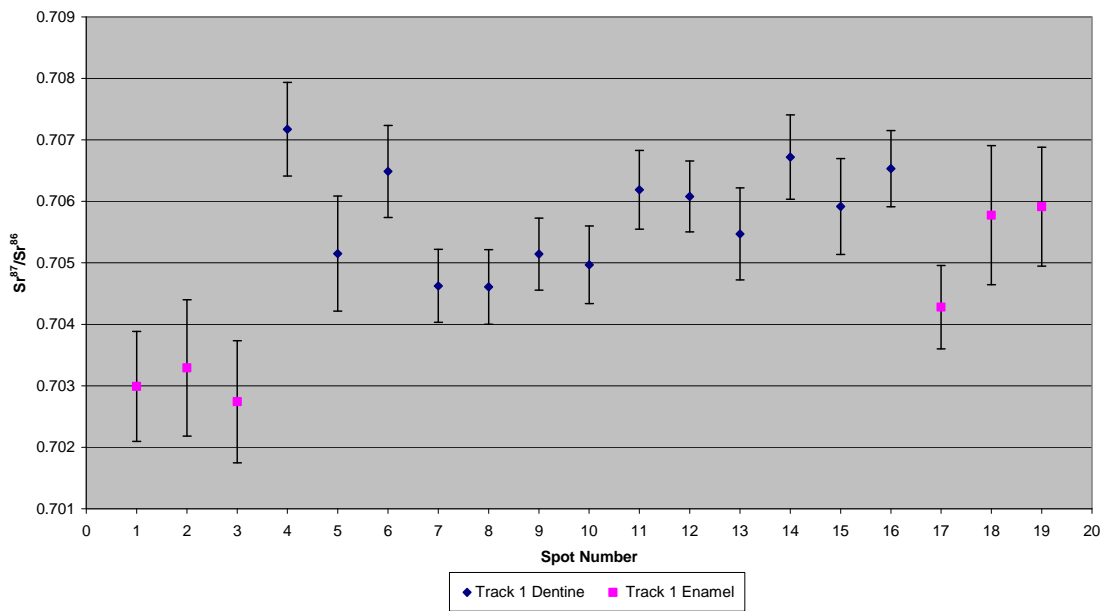


Figure A3.243 Detailed LA-MC-ICPMS Corrected Sr Isotope Results, Sample M034, Bovid, Layer C1, Rescoundudou

Sample M035, a P3-4 horse premolar from layer C1 of Rescoundudou shown in Figure A2.81, was analysed in 1 track comprising 9 spots of enamel in 3 discontinuous sections and 26 spots of dentine in 4 discontinuous sections, shown in Figure A3.244. The results from this sample are summarised in Table 5.41 and Figure 5.26. The enamel spots of track 1 have an average ^{88}Sr voltage of 0.347, a weighted average uncorrected $^{87}\text{Sr}/^{86}\text{Sr}$ value of 0.71324 ± 0.00032 , a weighted average corrected $^{87}\text{Sr}/^{86}\text{Sr}$ value of 0.70301 ± 0.00032 and a weighted average $^{84}\text{Sr}/^{86}\text{Sr}$ value of 0.05640 ± 0.00025 ($n=9$). The dentine spots of track 1 have an average ^{88}Sr voltage of 0.532, a weighted average uncorrected $^{87}\text{Sr}/^{86}\text{Sr}$ value of 0.71222 ± 0.00029 , a weighted average corrected $^{87}\text{Sr}/^{86}\text{Sr}$ value of 0.70769 ± 0.00029 and a weighted average $^{84}\text{Sr}/^{86}\text{Sr}$ value of 0.056467 ± 0.000095 ($n=26$). Enamel values are in the range of 0.712644 to 0.713763 (uncorrected), as well as 0.702417 to 0.703535 (corrected), and are homogenous within 2σ error. Dentine values are in the range of 0.711461 to 0.714078 (uncorrected), as well as 0.706929 to 0.709547 (corrected), and are extremely heterogeneous. Detailed values for enamel and dentine for sample M035 are shown in Table A3.117, Figure A3.245 and Figure A3.246.

The enamel of this sample is relatively homogenous, suggesting the sample was not mobile between different geological environments during amelogenesis. The uncorrected enamel weighted average value (0.71324 ± 0.00032) corresponds to the value from mapping sample FS108-S1 (0.713022 ± 0.000009), which is a Permian siliciclastic unit outcropping within 10 km of the site of Rescoundudou. The corrected weighted average value is 0.70301 ± 0.00032 , which does not correspond to any mapping sample in this study. Dentine spots for this sample have an overall weighted average value of 0.71222 ± 0.00029 . The heterogeneity of the dentine strontium isotope values suggests a complex regime of post-burial diagenesis. $^{84}\text{Sr}/^{86}\text{Sr}$ values have an overall value of 0.056456 ± 0.000085 , suggesting that the strontium isotope values from this sample are robust.

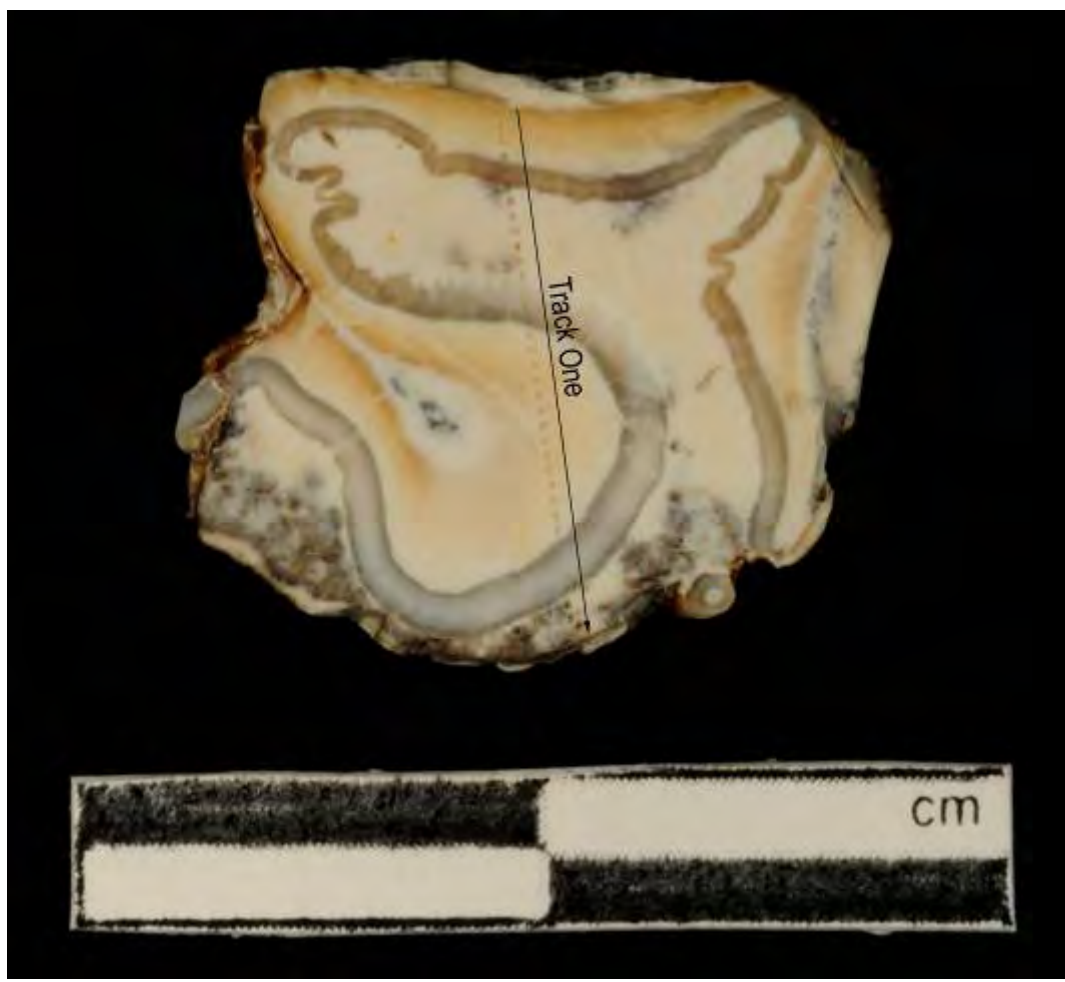


Figure A3.244 LA-MC-ICPMS Track for Sample M035, Horse, Layer C1, Rescoundudou

Sample	Material	Track	Point	^{88}Sr Volts	$^{84}\text{Sr}/^{86}\text{Sr}$	$^{84}\text{Sr}/^{86}\text{Sr} 2\sigma$	Corrected $^{87}\text{Sr}/^{86}\text{Sr}$	$^{87}\text{Sr}/^{86}\text{Sr} 2\sigma$
M035	Dentine	1	1	0.647	0.056866	0.000689	0.711986	0.707454
M035	Dentine	1	2	0.601	0.056484	0.000358	0.711461	0.706929
M035	Dentine	1	3	0.605	0.056335	0.000326	0.711913	0.707381
M035	Dentine	1	4	0.516	0.056654	0.000560	0.711732	0.707201
M035	Enamel	1	5	0.382	0.056911	0.000546	0.713013	0.702786
M035	Enamel	1	6	0.343	0.056414	0.000548	0.713341	0.703114
M035	Dentine	1	7	0.529	0.056899	0.000320	0.711662	0.707131
M035	Dentine	1	8	0.495	0.056372	0.000390	0.711640	0.707109
M035	Dentine	1	9	0.493	0.056714	0.000403	0.711766	0.707235
M035	Dentine	1	10	0.508	0.057251	0.000709	0.711613	0.707081
M035	Dentine	1	11	0.530	0.056557	0.000325	0.711526	0.706995
M035	Dentine	1	12	0.485	0.056541	0.000370	0.712912	0.708380
M035	Enamel	1	13	0.337	0.056577	0.000441	0.712644	0.702417

Sample	Material	Track	Point	^{88}Sr Volts	$^{84}\text{Sr}/^{86}\text{Sr}$	$^{84}\text{Sr}/^{86}\text{Sr} 2\sigma$ Error	Corrected $^{87}\text{Sr}/^{86}\text{Sr}$	$^{87}\text{Sr}/^{86}\text{Sr} 2\sigma$ Error	
M035	Enamel	1	14	0.360	0.055941	0.000519	0.712817	0.702589	0.000555
M035	Enamel	1	15	0.361	0.056144	0.000521	0.713439	0.703211	0.000581
M035	Dentine	1	16	0.488	0.056385	0.000501	0.713794	0.709263	0.000418
M035	Dentine	1	17	0.530	0.056758	0.000391	0.713761	0.709230	0.000432
M035	Dentine	1	18	0.584	0.056812	0.000445	0.712167	0.707635	0.000429
M035	Dentine	1	19	0.537	0.056126	0.000342	0.712601	0.708070	0.000478
M035	Dentine	1	20	0.524	0.056346	0.000462	0.711679	0.707147	0.000388
M035	Dentine	1	21	0.545	0.056302	0.000365	0.711874	0.707342	0.000399
M035	Dentine	1	22	0.501	0.056601	0.000486	0.712846	0.708315	0.000460
M035	Dentine	1	23	0.502	0.056311	0.000424	0.712073	0.707542	0.000500
M035	Dentine	1	24	0.520	0.056338	0.000422	0.711832	0.707301	0.000439
M035	Dentine	1	25	0.529	0.056590	0.000374	0.712249	0.707718	0.000459
M035	Dentine	1	26	0.548	0.056477	0.000474	0.712337	0.707805	0.000442
M035	Dentine	1	27	0.501	0.056266	0.000354	0.712019	0.707487	0.000433
M035	Dentine	1	28	0.482	0.056291	0.000372	0.712997	0.708466	0.000501
M035	Dentine	1	29	0.457	0.056188	0.000484	0.714078	0.709547	0.000500
M035	Enamel	1	30	0.394	0.056315	0.000519	0.713061	0.702834	0.000616
M035	Enamel	1	31	0.333	0.056394	0.000545	0.713763	0.703535	0.000655
M035	Enamel	1	32	0.300	0.055727	0.000945	0.712929	0.702702	0.000791
M035	Enamel	1	33	0.310	0.056678	0.000539	0.713952	0.703724	0.000661
M035	Dentine	1	34	0.578	0.056289	0.000385	0.711826	0.707295	0.000416
M035	Dentine	1	35	0.595	0.056248	0.000374	0.712321	0.707790	0.000422

Table A3.117 Detailed LA-MC-ICPMS Sr Isotope Results for Dentine and Enamel, Sample M035, Horse, Layer C1, Rescoundudou

Sample M35, Rescoundudou, France

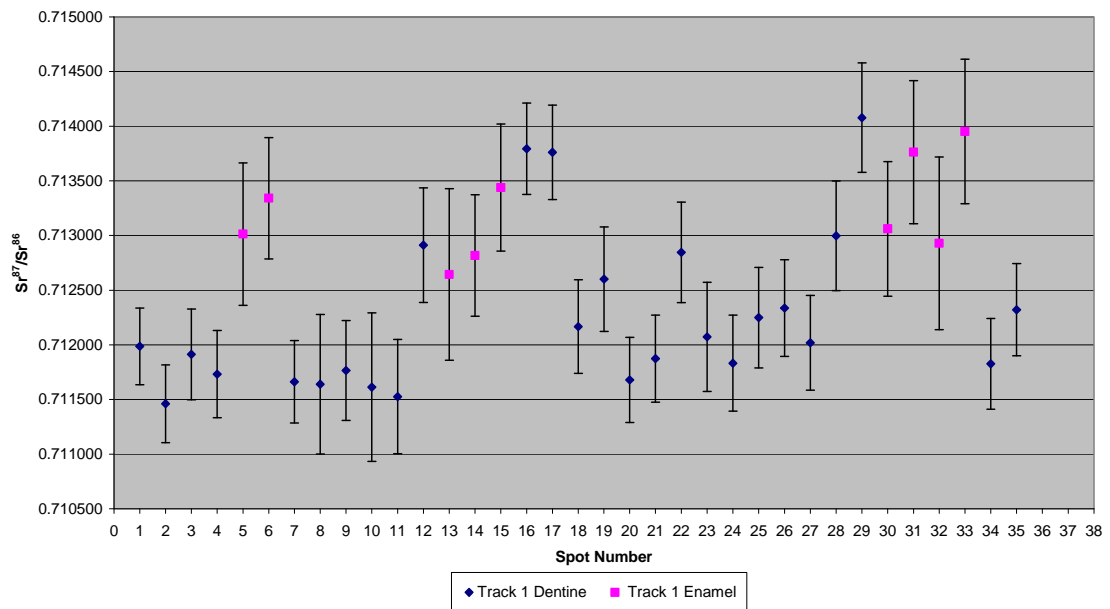


Figure A3.245 Detailed LA-MC-ICPMS Uncorrected Sr Isotope Results, Sample M035, Horse, Layer C1, Rescoundudou

Sample M35, Corrected Sr Values, Rescoundudou, France

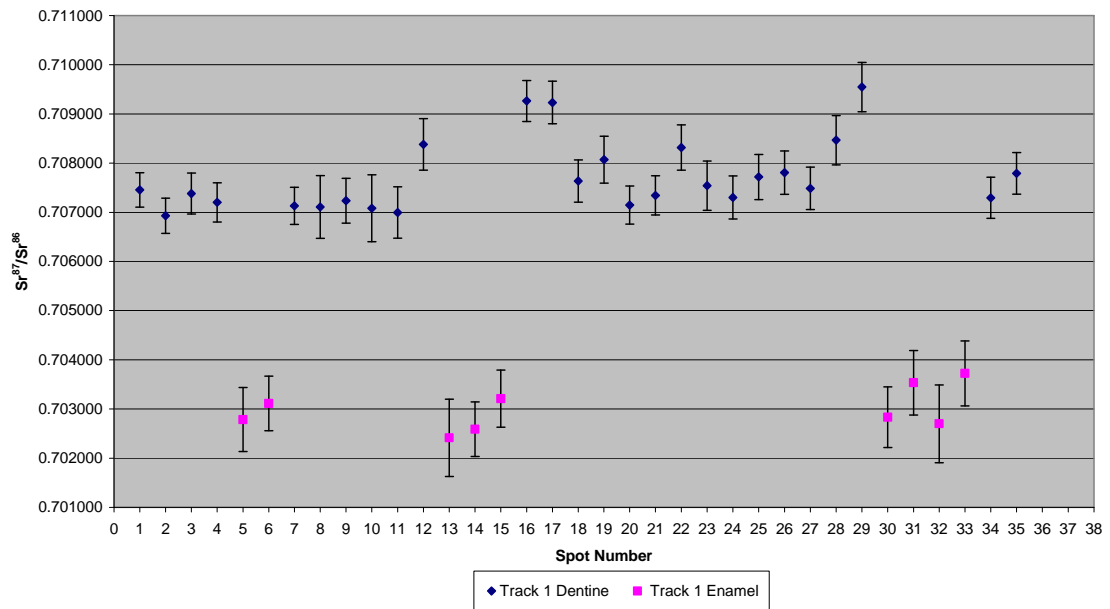


Figure A3.246 Detailed LA-MC-ICPMS Corrected Sr Isotope Results, Sample M035, Horse, Layer C1, Rescoundudou

Sample M036, a horse tooth from layer C1 of Rescoundudou shown in Figure A2.82, was analysed in 2 tracks with track 1 comprising 3 spots of enamel in 3 discontinuous sections and 16 spots of dentine in 4 discontinuous sections and track 2 comprising 7 spots of enamel in 2 discontinuous sections and 12 spots of dentine in 3 discontinuous sections, shown in Figure A3.247. The results from this sample are summarised in Table 5.41 and Figure 5.26. The enamel spots of track 1 have an average ^{88}Sr voltage of 0.718, a weighted average uncorrected $^{87}\text{Sr}/^{86}\text{Sr}$ value of 0.71259 ± 0.00050 , a weighted average corrected $^{87}\text{Sr}/^{86}\text{Sr}$ value of 0.70994 ± 0.00050 and a weighted average $^{84}\text{Sr}/^{86}\text{Sr}$ value of 0.05652 ± 0.00018 ($n=3$). The dentine spots of track 1 have an average ^{88}Sr voltage of 0.773, a weighted average uncorrected $^{87}\text{Sr}/^{86}\text{Sr}$ value of 0.71190 ± 0.00033 , a weighted average corrected $^{87}\text{Sr}/^{86}\text{Sr}$ value of 0.70919 ± 0.00033 and a weighted average $^{84}\text{Sr}/^{86}\text{Sr}$ value of 0.056578 ± 0.000097 ($n=16$). The enamel spots of track 2 have an average ^{88}Sr voltage of 0.690, a weighted average uncorrected $^{87}\text{Sr}/^{86}\text{Sr}$ value of 0.71226 ± 0.00062 , a weighted average corrected $^{87}\text{Sr}/^{86}\text{Sr}$ value of 0.70961 ± 0.00062 and a weighted average $^{84}\text{Sr}/^{86}\text{Sr}$ value of 0.05662 ± 0.00012 ($n=7$). The dentine spots of track 2 have an average ^{88}Sr voltage of 0.676, a weighted average uncorrected $^{87}\text{Sr}/^{86}\text{Sr}$ value of 0.71176 ± 0.00029 , a weighted average corrected $^{87}\text{Sr}/^{86}\text{Sr}$ value of 0.70906 ± 0.00029 and a weighted average $^{84}\text{Sr}/^{86}\text{Sr}$ value of 0.05662 ± 0.00014 ($n=12$). Enamel values of track 1 have a range of 0.712402 to 0.712784 (uncorrected), as well as 0.708503 and 0.710139 (corrected), and are relatively homogenous. Dentine values of track 1 have a range of 0.711213 to 0.714317 (uncorrected), as well as 0.708503 to 0.711608 (corrected), and are extremely heterogeneous. Enamel values of track 2 have a range of 0.711424 to 0.713034 (uncorrected), as well as 0.708779 to 0.710389 (corrected), and are relatively heterogeneous. Dentine values of track 2 have a range of 0.710635 to 0.712624 (uncorrected), as well as 0.707926 to 0.709915 (corrected), and are very heterogeneous. Detailed values for enamel and dentine for sample M036 are shown in Table A3.118, Figure A3.248 and Figure A3.249.

This sample has very heterogeneous dentine values, suggesting a complex regime of post-burial diagenesis. Enamel and dentine values for this sample are within 2σ error, suggesting that it is local to this site. Enamel values are distributed in 2 domains: the first containing spots 4, 8 and 15 from track 1 and spots 3, 4, 7, 12 and 13 from track 2, and the second containing spots 5 and 6 from track 2. Domain 1 has a weighted average uncorrected value of 0.71265 ± 0.00020 , which corresponds with mapping samples F36R from Cambrian paragneiss/leptynite/amphibolite. This sample location is approximately 215 km to the north-east; however, this geological unit outcrops within 25 km north of Rescoundudou. The weighted average corrected value of this domain (0.71001 ± 0.00020) corresponds to values from the Middle Jurassic carbonate unit that contains the site. Domain 2 has a weighted average uncorrected value of 0.71150 ± 0.00019 . This is slightly elevated compared to local sample FS107-S1 (0.711001 ± 0.00001), which is located approximately 15 km north-east of the site in a Lower Jurassic carbonate package. A better correlation is sample P54P, a Devonian amphibolite/micaschist/leptynite, which outcrops approximately 270 km to the north-east of Rescoundudou. This unit does not outcrop any closer to the site than the sample location of P54P, suggesting a very long distance mobility event. This is the same overall lithology, although different age, to that associated with domain 1 of this enamel, which may suggest the Cambrian paragneiss/leptynite/amphibolite contains sufficient heterogeneity to encompass this range of enamel values. The weighted average corrected value of the second domain is 0.70885 ± 0.00019 , which is within the range of the Middle Jurassic carbonate unit that contains the site.

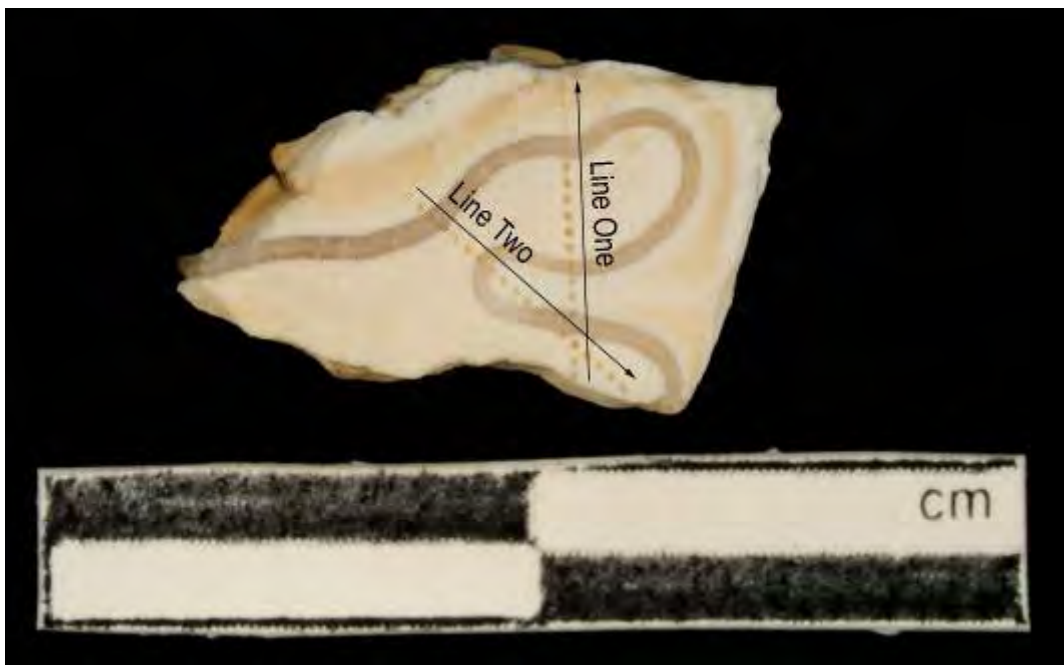


Figure A3.247 LA-MC-ICPMS Track for Sample M036, Horse, Layer C1, Rescoundudou

Sample	Material	Track	Point	88Sr Volts	84Sr/ ⁸⁶ Sr	84Sr/ ⁸⁶ Sr 2σ Error	Corrected 87Sr/ ⁸⁶ Sr	⁸⁷ Sr/ ⁸⁶ Sr 2σ Error
M036	Dentine	1	1	0.992	0.056608	0.000232	0.714317	0.711608
M036	Dentine	1	2	0.694	0.056792	0.000235	0.712543	0.709833
M036	Dentine	1	3	0.683	0.056633	0.000308	0.711563	0.708854
M036	Enamel	1	4	0.693	0.056568	0.000293	0.712402	0.709757
M036	Dentine	1	5	0.864	0.056568	0.000219	0.712746	0.710037
M036	Dentine	1	6	0.698	0.056854	0.000286	0.711496	0.708787
M036	Dentine	1	7	0.665	0.056589	0.000344	0.711809	0.709100
M036	Enamel	1	8	0.708	0.056633	0.000477	0.712784	0.710139
M036	Dentine	1	9	0.589	0.056383	0.000348	0.711493	0.708783
M036	Dentine	1	10	0.613	0.056287	0.000336	0.711213	0.708503
M036	Dentine	1	11	0.660	0.056898	0.000292	0.711306	0.708597
M036	Dentine	1	12	0.721	0.056819	0.000272	0.711393	0.708684
M036	Dentine	1	13	0.790	0.056726	0.000262	0.711746	0.709037
M036	Dentine	1	14	0.746	0.056505	0.000263	0.711369	0.708660
M036	Enamel	1	15	0.754	0.056436	0.000280	0.712482	0.709838
M036	Dentine	1	16	0.849	0.056576	0.000231	0.713092	0.710382
M036	Dentine	1	17	0.923	0.056463	0.000189	0.711939	0.709230
M036	Dentine	1	18	0.926	0.056297	0.000219	0.712442	0.709733

Sample	Material	Track	Point	^{88}Sr Volts	$^{84}\text{Sr}/^{86}\text{Sr}$	$^{84}\text{Sr}/^{86}\text{Sr} 2\sigma$ Error	$^{87}\text{Sr}/^{86}\text{Sr}$	Corrected $^{87}\text{Sr}/^{86}\text{Sr}$	$^{87}\text{Sr}/^{86}\text{Sr} 2\sigma$ Error
M036	Dentine	1	19	0.950	0.056426	0.000219	0.711677	0.708968	0.000301
M036	Dentine	2	1	0.828	0.056382	0.000210	0.712099	0.709390	0.000296
M036	Dentine	2	2	0.689	0.056385	0.000260	0.711533	0.708823	0.000303
M036	Enamel	2	3	0.811	0.056494	0.000401	0.713034	0.710389	0.000310
M036	Enamel	2	4	0.534	0.056792	0.000415	0.712422	0.709777	0.000379
M036	Enamel	2	5	0.705	0.056442	0.000257	0.711536	0.708891	0.000244
M036	Enamel	2	6	0.671	0.056755	0.000329	0.711424	0.708779	0.000331
M036	Enamel	2	7	0.645	0.056530	0.000359	0.712913	0.710268	0.000363
M036	Dentine	2	8	0.699	0.056827	0.000279	0.712160	0.709451	0.000435
M036	Dentine	2	9	0.672	0.056523	0.000301	0.711672	0.708963	0.000262
M036	Dentine	2	10	0.717	0.056892	0.000211	0.711509	0.708799	0.000373
M036	Dentine	2	11	0.613	0.057399	0.001360	0.712099	0.709389	0.000617
M036	Enamel	2	12	0.770	0.056730	0.000257	0.712453	0.709808	0.000280
M036	Enamel	2	13	0.696	0.056648	0.000338	0.712781	0.710136	0.000413
M036	Dentine	2	14	0.654	0.056658	0.000276	0.711600	0.708891	0.000348
M036	Dentine	2	15	0.570	0.056463	0.000253	0.710635	0.707926	0.000444
M036	Dentine	2	16	0.556	0.056905	0.000358	0.712276	0.709567	0.000416
M036	Dentine	2	17	0.673	0.056947	0.000317	0.711339	0.708630	0.000379
M036	Dentine	2	18	0.653	0.056454	0.000332	0.712624	0.709915	0.000378
M036	Dentine	2	19	0.789	0.056501	0.000253	0.711765	0.709056	0.000351

Table A3.118 Detailed LA-MC-ICPMS Sr Isotope Results for Dentine and Enamel, Sample M036, Horse, Layer C1, Rescoundudou

Sample M36, Rescoundudou, France

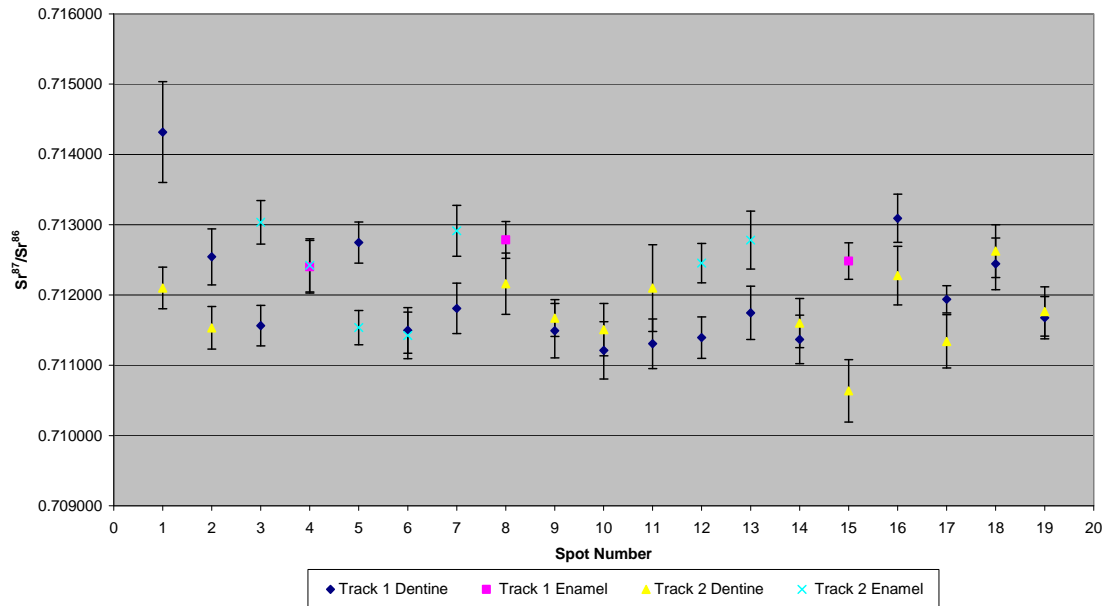


Figure A3.248 Detailed LA-MC-ICPMS Uncorrected Sr Isotope Results, Sample M036, Horse, Layer C1, Rescoundudou

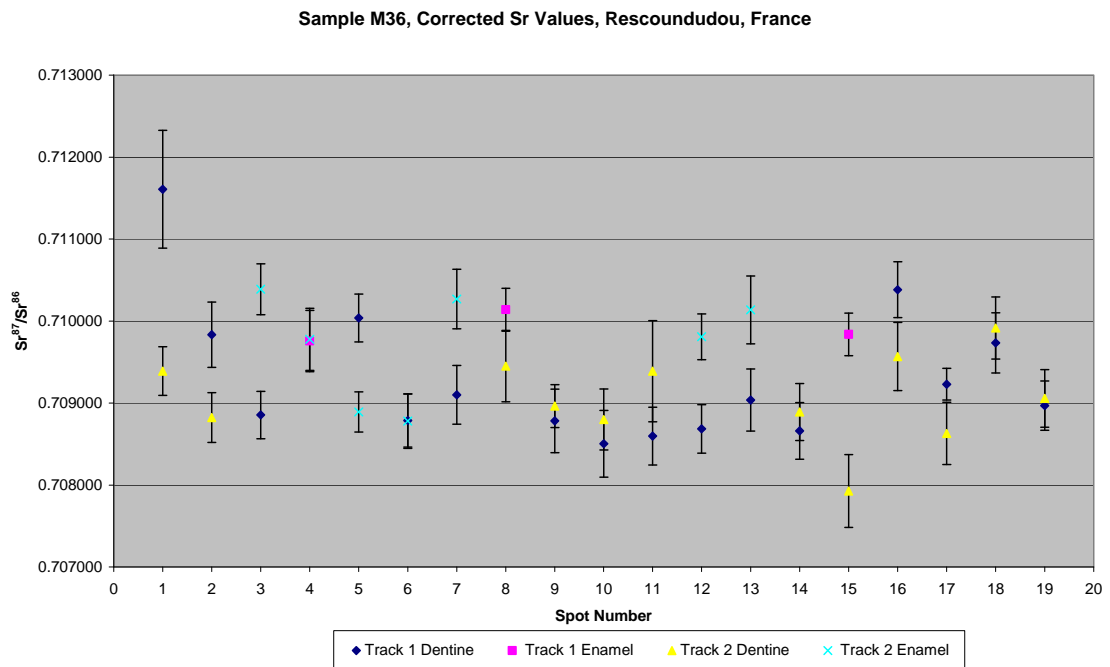


Figure A3.249 Detailed LA-MC-ICPMS Corrected Sr Isotope Results, Sample M036, Horse, Layer C1, Rescoundudou

Sample M037, a horse tooth from layer C1 of Rescoundudou shown in Figure A2.83, was analysed in 2 tracks with track 1 comprising 2 spots of enamel in 2 discontinuous sections and 19 spots of dentine in 3 discontinuous sections and track 2 comprising 5 spots of enamel in 2 discontinuous sections and 31 spots of dentine in 3 discontinuous sections, shown in Figure A3.250. The results from this sample are summarised in Table 5.41 and Figure 5.26. The enamel spots of track 1 have an average ^{88}Sr voltage of 0.686, a weighted average uncorrected $^{87}\text{Sr}/^{86}\text{Sr}$ value of 0.7119 ± 0.0022 , a weighted average corrected $^{87}\text{Sr}/^{86}\text{Sr}$ value of 0.70400 ± 0.0022 and a weighted average $^{84}\text{Sr}/^{86}\text{Sr}$ value of 0.0566 ± 0.0065 ($n=2$). The dentine spots of track 1 have an average ^{88}Sr voltage of 0.672, a weighted average uncorrected $^{87}\text{Sr}/^{86}\text{Sr}$ value of 0.71074 ± 0.00044 , a weighted average corrected $^{87}\text{Sr}/^{86}\text{Sr}$ value of 0.70302 ± 0.00044 and a weighted average $^{84}\text{Sr}/^{86}\text{Sr}$ value of 0.05680 ± 0.00031 ($n=19$). The enamel spots of track 2 have an average ^{88}Sr voltage of 0.496, a weighted average uncorrected $^{87}\text{Sr}/^{86}\text{Sr}$ value of 0.71260 ± 0.00060 , a weighted average corrected $^{87}\text{Sr}/^{86}\text{Sr}$ value of 0.70473 ± 0.00060 and a weighted average $^{84}\text{Sr}/^{86}\text{Sr}$ value of 0.0553 ± 0.0012 ($n=5$). The dentine spots of track 2 have an average ^{88}Sr voltage of 0.455, a weighted average uncorrected $^{87}\text{Sr}/^{86}\text{Sr}$ value of 0.71090 ± 0.00028 , a weighted average corrected $^{87}\text{Sr}/^{86}\text{Sr}$ value of 0.70318 ± 0.00028 and a weighted average $^{84}\text{Sr}/^{86}\text{Sr}$ value of 0.05500 ± 0.00024 ($n=31$). Enamel values for track 1 are 0.711768 to 0.712159 (uncorrected), as well as and homogenous within 2σ error. Dentine values for track 1 are in the range of 0.709352 to 0.712507 (uncorrected), as well as 0.701630 to 0.704785 (corrected). Enamel values for track 2 are in the range of 0.712069 to 0.713583 (uncorrected), as well as 0.704196 to 0.705710 (corrected), and are extremely homogenous. Dentine values for track 2 are in the range of 0.709881 to 0.713583 (uncorrected), as well as 0.702168 to 0.705710 (corrected), and are extremely heterogeneous. Detailed values for enamel and dentine for sample M037 are shown in Table A3.119, Figure A3.251 and Figure A3.252.

These samples have heterogeneous values for enamel and dentine, suggesting both a complex migratory and post-depositional diagenetic regime. The range of enamel values cannot be grouped into domains; however, the range of uncorrected values is similar to the heterogeneity found within the Middle

Jurassic carbonate package, which contains Rescoundudou. The only mapping sample that correlates with the range of corrected enamel is FS118-S1, located within a Oligocene/Miocene basalt unit which outcrops within 12.2 km of the site. Overall $^{84}\text{Sr}/^{86}\text{Sr}$ values for this sample are 0.05608 ± 0.00029 , which are lower than the expected value, suggesting that the strontium isotope values may not be robust.



Figure A3.250 LA-MC-ICPMS Track for Sample M037, Horse, Layer C1, Rescoundudou

Sample	Material	Track	Point	^{88}Sr Volts	$^{84}\text{Sr}/^{86}\text{Sr}$	$^{84}\text{Sr}/^{86}\text{Sr} 2\sigma$ Error	Corrected $^{87}\text{Sr}/^{86}\text{Sr}$	$^{87}\text{Sr}/^{86}\text{Sr} 2\sigma$ Error
M037	Dentine	1	1	0.669	0.058213	0.000279	0.711047	0.703325
M037	Dentine	1	2	0.666	0.057618	0.000238	0.710312	0.702590
M037	Dentine	1	3	0.963	0.057208	0.000233	0.710629	0.702907

Sample	Material	Track	Point	^{88}Sr Volts	$^{84}\text{Sr}/^{86}\text{Sr}$	$^{84}\text{Sr}/^{86}\text{Sr} 2\sigma$ Error	Corrected $^{87}\text{Sr}/^{86}\text{Sr}$	$^{87}\text{Sr}/^{86}\text{Sr} 2\sigma$ Error
M037	Enamel	1	4	0.746	0.057051	0.000246	0.711768	0.703895
M037	Dentine	1	5	0.553	0.057519	0.000337	0.712131	0.704409
M037	Dentine	1	6	0.575	0.057062	0.000360	0.710389	0.702666
M037	Dentine	1	7	0.609	0.057502	0.000593	0.710952	0.703230
M037	Dentine	1	8	0.701	0.057165	0.000257	0.709929	0.702206
M037	Dentine	1	9	0.605	0.057250	0.000310	0.710390	0.702667
M037	Dentine	1	10	0.742	0.056978	0.000240	0.710855	0.703132
M037	Dentine	1	11	0.625	0.056474	0.000316	0.711136	0.703414
M037	Dentine	1	12	0.598	0.056831	0.000268	0.709823	0.702100
M037	Dentine	1	13	0.623	0.056663	0.000377	0.709352	0.701630
M037	Dentine	1	14	0.599	0.056526	0.000363	0.712507	0.704785
M037	Dentine	1	15	0.702	0.056462	0.000340	0.712078	0.704355
M037	Dentine	1	16	0.634	0.056097	0.000199	0.710068	0.702345
M037	Dentine	1	17	0.693	0.056393	0.000288	0.710798	0.703075
M037	Dentine	1	18	0.682	0.055899	0.000394	0.710368	0.702646
M037	Dentine	1	19	0.843	0.056160	0.000217	0.709972	0.702249
M037	Enamel	1	20	0.626	0.055998	0.000302	0.712159	0.704286
M037	Dentine	1	21	0.685	0.056057	0.000247	0.712445	0.704722
M037	Enamel	2	1	0.795	0.056258	0.000305	0.712069	0.704196
M037	Enamel	2	2	0.493	0.055681	0.000443	0.712726	0.704853
M037	Dentine	2	3	0.437	0.055802	0.000524	0.711851	0.704129
M037	Dentine	2	4	0.507	0.055703	0.000387	0.709891	0.702168
M037	Dentine	2	5	0.443	0.055172	0.000435	0.711182	0.703460
M037	Dentine	2	6	0.554	0.055772	0.000417	0.711389	0.703666
M037	Dentine	2	7	0.521	0.055807	0.000295	0.710209	0.702487
M037	Dentine	2	8	0.471	0.055524	0.000370	0.710047	0.702325
M037	Dentine	2	9	0.508	0.055616	0.000383	0.709881	0.702159
M037	Dentine	2	10	0.566	0.055433	0.000361	0.711081	0.703358
M037	Dentine	2	11	0.450	0.055455	0.000785	0.711853	0.704130
M037	Dentine	2	12	0.482	0.055260	0.000665	0.711120	0.703397
M037	Dentine	2	13	0.405	0.054908	0.000592	0.711212	0.703490
M037	Dentine	2	14	0.407	0.054614	0.000576	0.710735	0.703013
M037	Dentine	2	15	0.439	0.055271	0.000314	0.710100	0.702377
M037	Enamel	2	16	0.321	0.054360	0.000658	0.713583	0.705710
M037	Enamel	2	17	0.413	0.054390	0.000365	0.713006	0.705133
M037	Enamel	2	18	0.455	0.054546	0.000559	0.712471	0.704598
M037	Dentine	2	19	0.455	0.054984	0.000442	0.710605	0.702882
M037	Dentine	2	20	0.403	0.054707	0.000585	0.710191	0.702469

Sample	Material	Track	Point	88Sr Volts	84Sr/ ⁸⁶ Sr	⁸⁴ Sr/ ⁸⁶ Sr 2 σ Error	Corrected ⁸⁷ Sr/ ⁸⁶ Sr	⁸⁷ Sr/ ⁸⁶ Sr 2 σ Error	
M037	Dentine	2	21	0.405	0.054495	0.000573	0.711350	0.703628	0.000481
M037	Dentine	2	22	0.428	0.054372	0.000581	0.710784	0.703061	0.000573
M037	Dentine	2	23	0.551	0.054888	0.000332	0.710722	0.703000	0.000505
M037	Dentine	2	24	0.641	0.055281	0.000292	0.710659	0.702936	0.000426
M037	Dentine	2	25	0.465	0.054810	0.000451	0.710456	0.702734	0.000427
M037	Dentine	2	26	0.281	0.052604	0.000800	0.710907	0.703185	0.000911
M037	Dentine	2	27	0.399	0.054198	0.000568	0.710676	0.702954	0.000615
M037	Dentine	2	28	0.413	0.054004	0.000525	0.711107	0.703384	0.000677
M037	Dentine	2	29	0.425	0.054234	0.000512	0.710368	0.702645	0.000515
M037	Dentine	2	30	0.552	0.054851	0.000416	0.710415	0.702692	0.000474
M037	Dentine	2	31	0.506	0.054766	0.000465	0.711580	0.703858	0.000491
M037	Dentine	2	32	0.421	0.053748	0.000411	0.711979	0.704256	0.000571
M037	Dentine	2	33	0.439	0.054326	0.000466	0.711695	0.703973	0.000495
M037	Dentine	2	34	0.395	0.053852	0.000516	0.710790	0.703067	0.000543
M037	Dentine	2	35	0.393	0.054011	0.000682	0.712595	0.704873	0.000612
M037	Dentine	2	36	0.349	0.054046	0.000680	0.714144	0.706421	0.000723

Table A3.119 Detailed LA-MC-ICPMS Sr Isotope Results for Dentine and Enamel, Sample M037, Horse, Layer C1, Rescoundudou

Sample M37, Rescoundudou, France

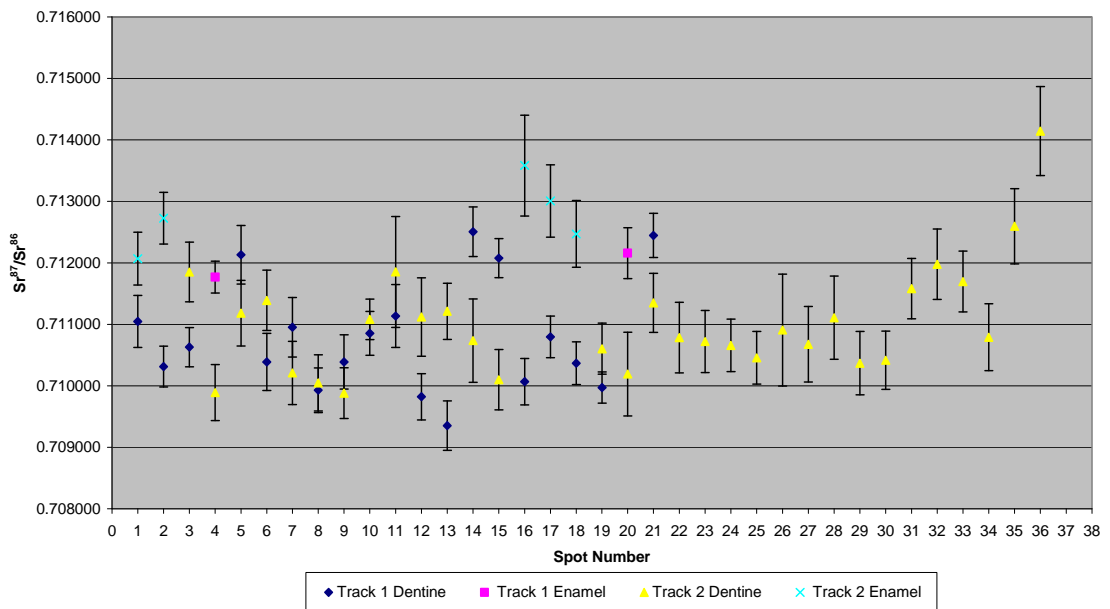


Figure A3.251 Detailed LA-MC-ICPMS Uncorrected Sr Isotope Results, Sample M037, Horse, Layer C1, Rescoundudou

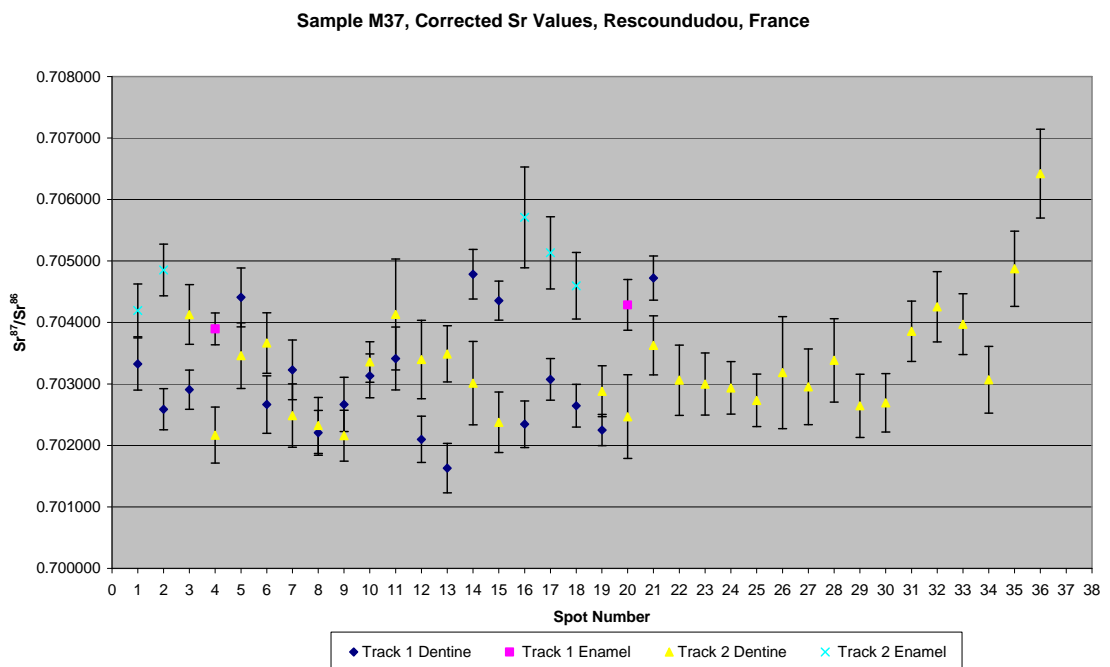


Figure A3.252 Detailed LA-MC-ICPMS Corrected Sr Isotope Results, Sample M037, Horse, Layer C1, Rescoundudou

Sample M038, a rhinoceros premolar from layer C1 of Rescoundudou shown in Figure A2.84, was analysed in 2 tracks with the first comprising 16 spots of enamel and the second comprising 14 spots of enamel, shown in Figure A3.253. The results from this sample are summarised in Table 5.41 and Figure 5.26. The enamel spots of track 1 have an average ^{88}Sr voltage of 0.297, a weighted average uncorrected $^{87}\text{Sr}/^{86}\text{Sr}$ value of 0.71608 ± 0.00021 , a weighted average corrected $^{87}\text{Sr}/^{86}\text{Sr}$ value of 0.71031 ± 0.00021 and a weighted average $^{84}\text{Sr}/^{86}\text{Sr}$ value of 0.05299 ± 0.00041 ($n=16$). The enamel spots of track 2 have an average ^{88}Sr voltage of 0.370, a weighted average uncorrected $^{87}\text{Sr}/^{86}\text{Sr}$ value of 0.71559 ± 0.00034 , a weighted average corrected $^{87}\text{Sr}/^{86}\text{Sr}$ value of 0.70982 ± 0.00034 and a weighted average $^{84}\text{Sr}/^{86}\text{Sr}$ value of 0.05304 ± 0.00023 ($n=14$). Enamel spots for track 1 are in the range of 0.715632 to 0.717037 (uncorrected), as well as 0.709859 to 0.711265 (corrected), and are homogenous within 2σ error. Enamel spots for track 2 are in the range of 0.714502 to 0.716576 (uncorrected), as well as 0.708729 to 0.710804 (corrected), and are homogenous within 2σ error. Detailed values for enamel and dentine for sample M038 are shown in Table A3.120, Figure A3.254 and Figure A3.255.

This sample has relatively homogenous values for enamel, suggesting that this sample did not migrate between different geological environments during amelogenesis. The uncorrected enamel $^{87}\text{Sr}/^{86}\text{Sr}$ value (weighted average 0.71579 ± 0.00021) corresponds to mapping sample P8P (0.715615 ± 0.000026) from a Permian monzogranite/granodiorite. This location is approximately 135 km to the north-east of Rescoundudou; however, this unit outcrops within 17 km of the site, although quite varied $^{87}\text{Sr}/^{86}\text{Sr}$ values were collected in this unit in this region (FS112-S1: 0.720635 ± 0.000032 and FS111-S1: 0.727959 ± 0.000011). Corrected enamel values for this sample have a weighted average of 0.71002 ± 0.00021 , which corresponds to values from the Middle Jurassic carbonate containing Rescoundudou. $^{84}\text{Sr}/^{86}\text{Sr}$ values for this sample have a weighted average of 0.05302 ± 0.00022 , which is significantly elevated compared to the ideal value.

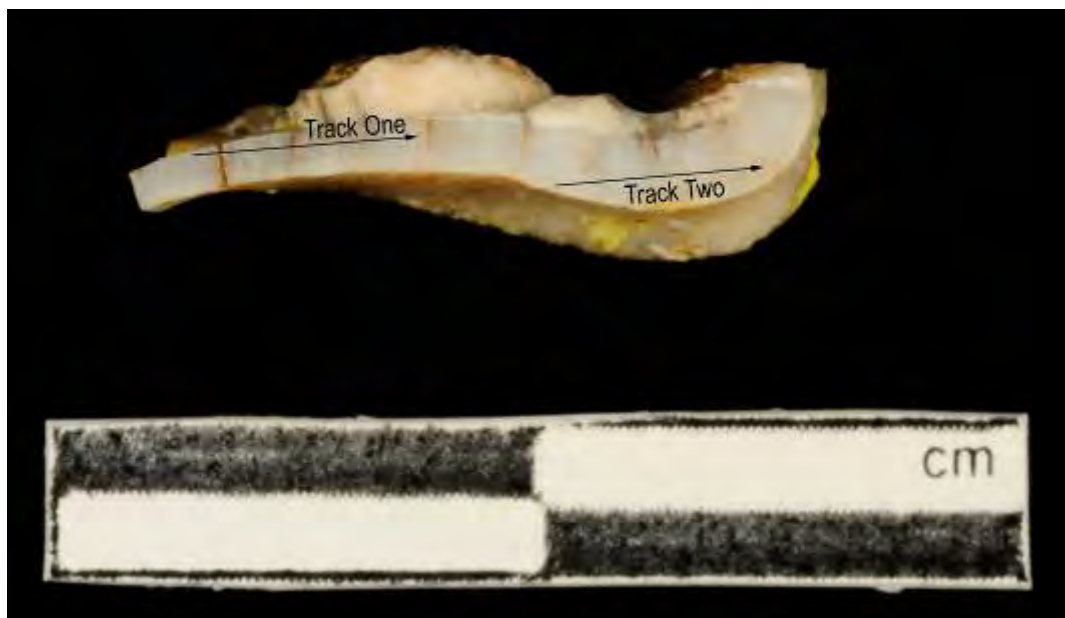


Figure A3.253 LA-MC-ICPMS Track for Sample M038, Rhinoceros, Layer C1, Rescoundudou

Sample	Material	Track	Point	^{88}Sr Volts	$^{84}\text{Sr}/^{86}\text{Sr}$	$^{84}\text{Sr}/^{86}\text{Sr} 2\sigma$	Corrected $^{87}\text{Sr}/^{86}\text{Sr}$	$^{87}\text{Sr}/^{86}\text{Sr} 2\sigma$	Error
M038	Enamel	1	1	0.473	0.054111	0.000414	0.715690	0.709917	0.000536
M038	Enamel	1	2	0.342	0.053388	0.000467	0.715725	0.709952	0.000740
M038	Enamel	1	3	0.341	0.053482	0.000610	0.716249	0.710477	0.000751
M038	Enamel	1	4	0.300	0.052825	0.000694	0.715699	0.709926	0.000952
M038	Enamel	1	5	0.294	0.053039	0.000743	0.716314	0.710542	0.000846
M038	Enamel	1	6	0.277	0.052302	0.000809	0.717037	0.711265	0.001057
M038	Enamel	1	7	0.271	0.052561	0.000816	0.716689	0.710917	0.001046
M038	Enamel	1	8	0.245	0.051494	0.000912	0.716920	0.711147	0.001135
M038	Enamel	1	9	0.266	0.052967	0.000763	0.715746	0.709974	0.000776
M038	Enamel	1	10	0.279	0.052814	0.000599	0.716184	0.710412	0.000782
M038	Enamel	1	11	0.273	0.053034	0.001188	0.716568	0.710796	0.001604
M038	Enamel	1	12	0.256	0.051649	0.001014	0.716046	0.710274	0.001135
M038	Enamel	1	13	0.258	0.051367	0.001016	0.716309	0.710537	0.000958
M038	Enamel	1	14	0.267	0.052157	0.000773	0.716289	0.710517	0.000993
M038	Enamel	1	15	0.281	0.052398	0.000793	0.716254	0.710482	0.000899
M038	Enamel	1	16	0.330	0.052861	0.000790	0.715632	0.709859	0.000849
M038	Enamel	2	1	0.406	0.053389	0.000387	0.715199	0.709426	0.000507
M038	Enamel	2	2	0.414	0.053387	0.000598	0.715314	0.709541	0.000623
M038	Enamel	2	3	0.397	0.053612	0.000638	0.716171	0.710399	0.000692

M038	Enamel	2	4	0.358	0.052743	0.000557	0.716199	0.710426	0.000622
M038	Enamel	2	5	0.356	0.053115	0.000451	0.715820	0.710048	0.000707
M038	Enamel	2	6	0.350	0.052709	0.000632	0.715296	0.709524	0.000769
M038	Enamel	2	7	0.356	0.052800	0.000543	0.716132	0.710359	0.000841
M038	Enamel	2	8	0.357	0.052501	0.000751	0.716170	0.710398	0.000634
M038	Enamel	2	9	0.341	0.052313	0.000576	0.716576	0.710804	0.000672
M038	Enamel	2	10	0.345	0.052865	0.000595	0.714777	0.709004	0.000760
M038	Enamel	2	11	0.380	0.053330	0.000484	0.715545	0.709773	0.000777
M038	Enamel	2	12	0.345	0.052402	0.000604	0.714502	0.708729	0.000764
M038	Enamel	2	13	0.394	0.053351	0.000564	0.715509	0.709736	0.000631
M038	Enamel	2	14	0.380	0.053336	0.000595	0.715059	0.709287	0.000650

Table A3.120 Detailed LA-MC-ICPMS Sr Isotope Results, Sample M038, Rhinoceros, Layer C1, Rescoundudou

Sample M38, Rescoundudou, France

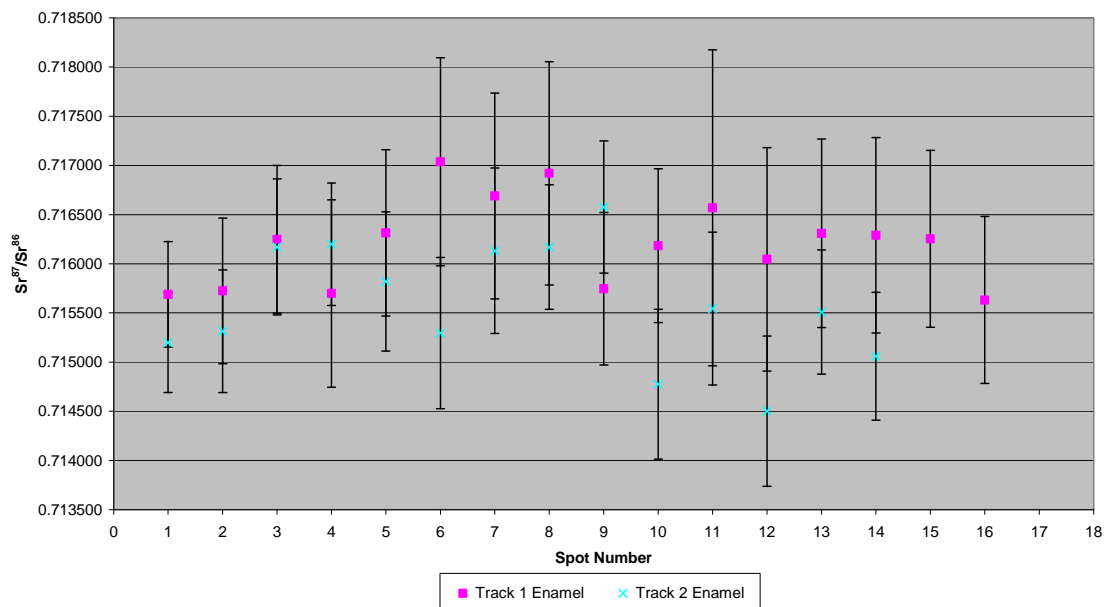


Figure A3.254 Detailed LA-MC-ICPMS Uncorrected Sr Isotope Results, Sample M038, Rhinoceros, Layer C1, Rescoundudou

Sample M38, Corrected Sr Values, Rescoundudou, France

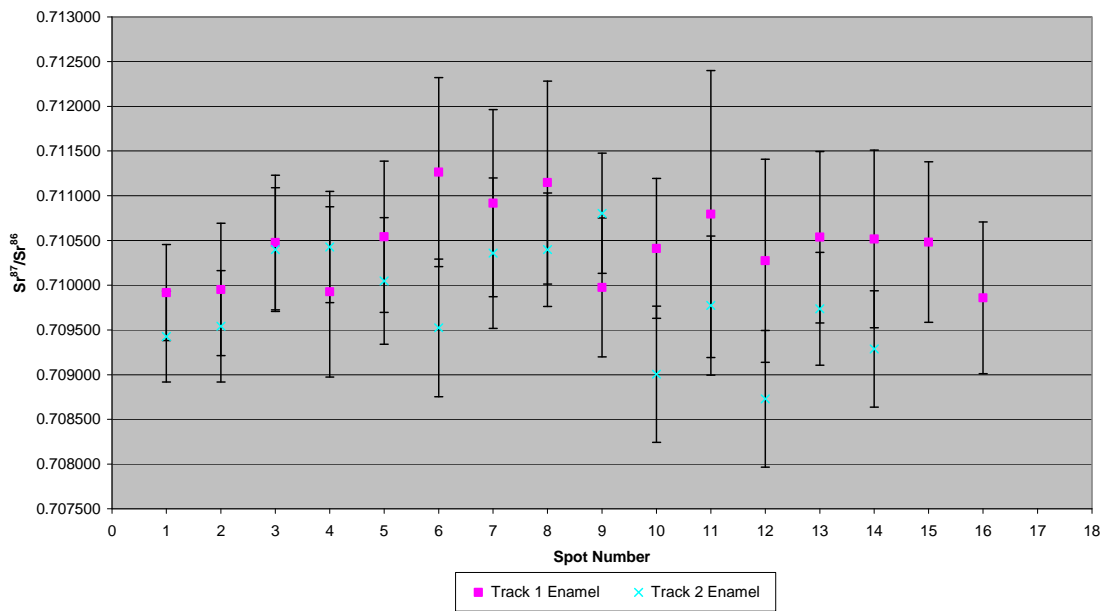


Figure A3.255 Detailed LA-MC-ICPMS Corrected Sr Isotope Results, Sample M038, Rhinoceros, Layer C1, Rescoundudou

Sample M039, a bovid molar from layer C1 of Rescoundudou shown in Figure A2.85, was analysed in 1 track comprising 7 spots of enamel in 2 discontinuous sections and 7 spots of dentine in 2 discontinuous sections, shown in Figure A3.256. The results from this sample are summarised in Table 5.41 and Figure 5.26. The enamel spots of track 1 have an average ^{88}Sr voltage of 0.535, a weighted average uncorrected $^{87}\text{Sr}/^{86}\text{Sr}$ value of 0.71364 ± 0.00038 , a weighted average corrected $^{87}\text{Sr}/^{86}\text{Sr}$ value of 0.71023 ± 0.00038 and a weighted average $^{84}\text{Sr}/^{86}\text{Sr}$ value of 0.05665 ± 0.00025 ($n=7$). The dentine spots of track 1 have an average ^{88}Sr voltage of 0.487, a weighted average uncorrected $^{87}\text{Sr}/^{86}\text{Sr}$ value of 0.71242 ± 0.00062 , a weighted average corrected $^{87}\text{Sr}/^{86}\text{Sr}$ value of 0.70792 ± 0.00062 and a weighted average $^{84}\text{Sr}/^{86}\text{Sr}$ value of 0.05654 ± 0.00027 ($n=7$). Enamel values are in the range of 0.711307 to 0.714237 (uncorrected), as well as 0.707898 to 0.710828 (corrected), and are somewhat heterogeneous. Dentine values are in the range of 0.712147 to 0.713783 (uncorrected), as well as 0.707506 to 0.709143 (corrected), and are heterogeneous. Detailed values for enamel and dentine for sample M039 are shown in Table A3.121, Figure A3.257 and Figure A3.258.

This sample has somewhat heterogeneous enamel values that are somewhat elevated compared to dentine. The range of uncorrected and corrected values is encompassed with the range of the very heterogeneous (as discussed with reference to sample M033) Middle Jurassic carbonate unit containing Rescoundudou. This sample has a weighted average $^{84}\text{Sr}/^{86}\text{Sr}$ value of 0.05661 ± 0.00016 , which is significantly elevated compared to the expected value, suggesting that the results of this analysis are robust.



Figure A3.256 LA-MC-ICPMS Track for Sample M039, Bovid, Layer C1, Rescoundudou

Sample	Material	Track	Point	^{88}Sr Volts	$^{84}\text{Sr}/^{86}\text{Sr}$	$^{84}\text{Sr}/^{86}\text{Sr} 2\sigma$	Corrected $^{87}\text{Sr}/^{86}\text{Sr}$	$^{87}\text{Sr}/^{86}\text{Sr}$	$^{87}\text{Sr}/^{86}\text{Sr} 2\sigma$	Error
M039	Enamel	1	1	0.564	0.056384	0.000370	0.713829	0.710420	0.000396	
M039	Enamel	1	2	0.540	0.056521	0.000400	0.713687	0.710278	0.000381	
M039	Dentine	1	3	0.450	0.056227	0.000558	0.712147	0.707506	0.000449	
M039	Dentine	1	4	0.506	0.056683	0.000363	0.712320	0.707680	0.000400	
M039	Dentine	1	5	0.520	0.056756	0.000464	0.712365	0.707725	0.000468	
M039	Dentine	1	6	0.477	0.056645	0.000558	0.712772	0.708132	0.000577	
M039	Enamel	1	7	0.520	0.056966	0.000387	0.713032	0.709623	0.000386	
M039	Enamel	1	8	0.549	0.056988	0.000287	0.714237	0.710828	0.000406	
M039	Enamel	1	9	0.551	0.056489	0.000326	0.713729	0.710320	0.000504	
M039	Enamel	1	10	0.494	0.056380	0.000435	0.713272	0.709862	0.000521	
M039	Enamel	1	11	0.529	0.056526	0.000426	0.713631	0.710222	0.000467	
M039	Dentine	1	12	0.437	0.056768	0.000511	0.713783	0.709143	0.000569	
M039	Dentine	1	13	0.374	0.056583	0.000523	0.712630	0.707990	0.000638	
M039	Dentine	1	14	0.644	0.055996	0.000462	0.711307	0.707898	0.000562	

Table A3.121 Detailed LA-MC-ICPMS Sr Isotope Results, Sample M039, Bovid, Layer C1, Rescoundudou

Sample M39, Rescoundudou, France

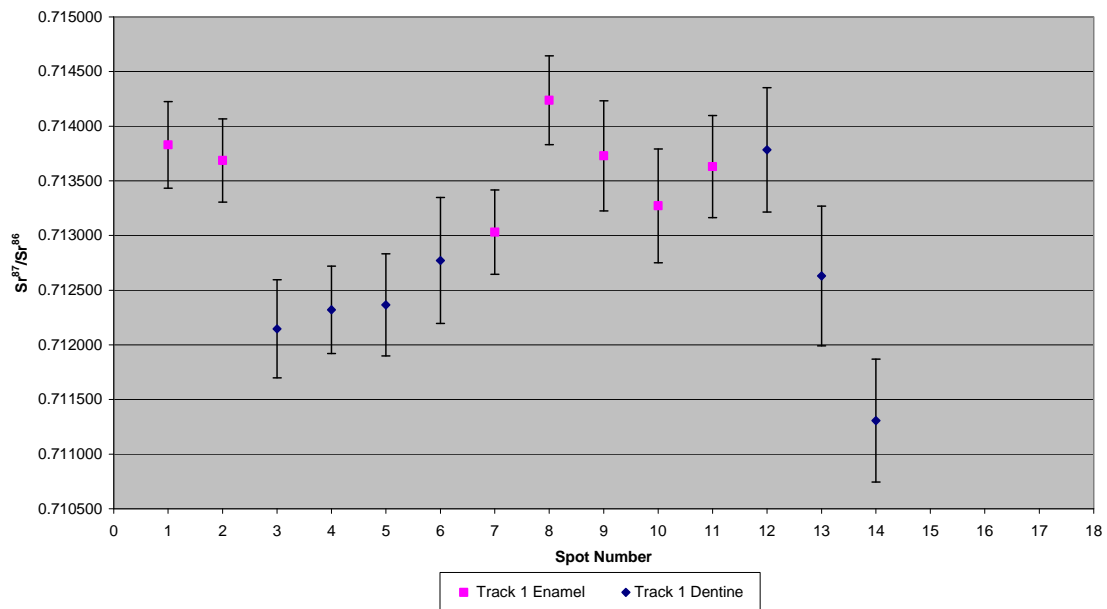


Figure A3.257 Detailed LA-MC-ICPMS Uncorrected Sr Isotope Results, Sample M039, Bovid, Layer C1, Rescoundudou

Sample M39, Corrected Sr Values, Rescoundudou, France

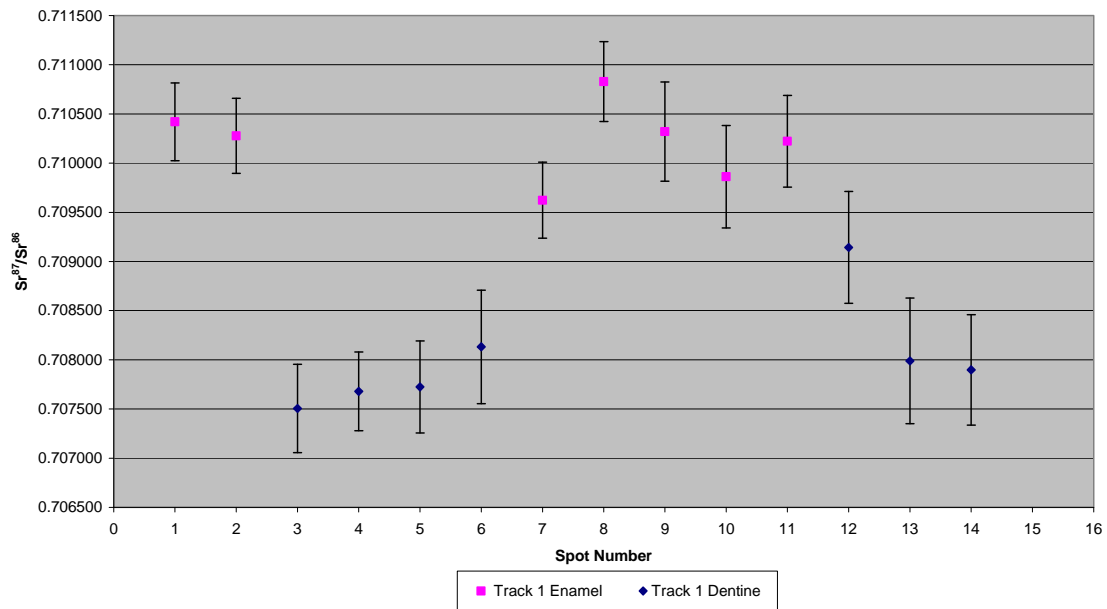


Figure A3.258 Detailed LA-MC-ICPMS Corrected Sr Isotope Results, Sample M039, Bovid, Layer C1, Rescoundudou

Sample M040, a M2 bovid molar from layer C1 of Rescoundudou shown in Figure A2.86, was analysed in 2 tracks with the first comprising 4 spots of

enamel and 4 spots of dentine and the second comprising 3 spots of enamel and 2 spots of dentine, shown in Figure A3.259. The results from this sample are summarised in Table 5.41 and Figure 5.26. The enamel spots of track 1 have an average ^{88}Sr voltage of 0.452, a weighted average uncorrected $^{87}\text{Sr}/^{86}\text{Sr}$ value of 0.71372 ± 0.00097 , a weighted average corrected $^{87}\text{Sr}/^{86}\text{Sr}$ value of 0.70769 ± 0.00097 and a weighted average $^{84}\text{Sr}/^{86}\text{Sr}$ value of 0.05661 ± 0.00024 ($n=4$). The dentine spots of track 1 have an average ^{88}Sr voltage of 0.433, a weighted average uncorrected $^{87}\text{Sr}/^{86}\text{Sr}$ value of 0.7132 ± 0.0011 , a weighted average corrected $^{87}\text{Sr}/^{86}\text{Sr}$ value of 0.70760 ± 0.0011 and a weighted average $^{84}\text{Sr}/^{86}\text{Sr}$ value of 0.05648 ± 0.00019 ($n=4$). The enamel spots of track 2 have an average ^{88}Sr voltage of 0.390, a weighted average uncorrected $^{87}\text{Sr}/^{86}\text{Sr}$ value of 0.7144 ± 0.0040 , a weighted average corrected $^{87}\text{Sr}/^{86}\text{Sr}$ value of 0.70840 ± 0.0040 and a weighted average $^{84}\text{Sr}/^{86}\text{Sr}$ value of 0.05634 ± 0.00028 ($n=3$). The dentine spots of track 2 have an average ^{88}Sr voltage of 0.392, a weighted average uncorrected $^{87}\text{Sr}/^{86}\text{Sr}$ value of 0.712 ± 0.013 , a weighted average corrected $^{87}\text{Sr}/^{86}\text{Sr}$ value of 0.70600 ± 0.013 and a weighted average $^{84}\text{Sr}/^{86}\text{Sr}$ value of 0.0568 ± 0.0024 ($n=2$). Enamel values for track 1 are in the range of 0.713105 to 0.714775 (uncorrected), as well as 0.707079 to 0.708750 (corrected), and decrease in value from the outside surface of the enamel to the dentine-enamel junction. Dentine values for track 1 are in the range of 0.712724 to 0.714244 (uncorrected), as well as 0.707097 to 0.708617 (corrected), with the first 3 spots being relatively homogeneous and the 4 being elevated in value. Enamel values for track 2 are in the range of 0.712962 to 0.715803 (uncorrected), as well as 0.706936 to 0.709778 (corrected), and decrease in value from the exterior of the enamel to the dentine-enamel junction. Dentine values for track 2 are 0.711279 and 0.713408 (uncorrected), as well as 0.705652 and 0.707782 (corrected), and are very heterogeneous. Detailed values for enamel and dentine for sample M040 are shown in Table A3.122, Figure A3.260 and Figure A3.261.

This sample has heterogeneous enamel, suggesting that this sample transitioned between different geological environments during amelogenesis. The lower end-member of the uncorrected enamel range is within 2σ error of the mapping sample FS090-S2 from the site of Rescoundudou. Corrected

values from the lower end-member correspond to a number of values from the Rhône Valley region (such as P25P and P26P), collected from a Lower Jurassic carbonate which outcrops within 75 km of the archaeological site. The higher end-member of the uncorrected enamel range does not correspond to any values in the study area; however, it is slightly elevated compared to the most elevated mapping sample (FS114-S1) from the Middle Jurassic carbonate unit that contains the site. The corrected values of the upper end-member are within the range of the Middle Jurassic carbonate unit that contains the site. Overall, the uncorrected values suggest that the sample was principally resident in the area surrounding Rescoundudou, with occasional incursions to the more radiogenic error further to the north. The enamel and dentine values are within 2σ error. Weighted average $^{84}\text{Sr}/^{86}\text{Sr}$ values of this sample are 0.05654 ± 0.00012 , suggesting that the strontium isotope results are robust.



Figure A3.259 LA-MC-ICPMS Track for Sample M040, Bovid, Layer C1, Rescoundudou

Sample	Material	Track	Point	^{88}Sr Volts	$^{84}\text{Sr}/^{86}\text{Sr}$	$^{84}\text{Sr}/^{86}\text{Sr} 2\sigma$ Error	Corrected $^{87}\text{Sr}/^{86}\text{Sr}$	$^{87}\text{Sr}/^{86}\text{Sr} 2\sigma$ Error
M040	Enamel	1	1	0.407	0.056495	0.000444	0.714775	0.708750
M040	Enamel	1	2	0.417	0.056515	0.000539	0.713807	0.707781
M040	Enamel	1	3	0.510	0.056636	0.000450	0.713565	0.707540
M040	Enamel	1	4	0.476	0.056874	0.000608	0.713105	0.707079
M040	Dentine	1	5	0.325	0.056606	0.000595	0.713221	0.707594
M040	Dentine	1	6	0.444	0.056278	0.000479	0.712956	0.707329
M040	Dentine	1	7	0.504	0.056510	0.000292	0.712724	0.707097
M040	Dentine	1	8	0.459	0.056516	0.000374	0.714244	0.708617
M040	Enamel	2	1	0.344	0.056460	0.000637	0.715803	0.709778
M040	Enamel	2	2	0.403	0.056469	0.000434	0.715482	0.709457
M040	Enamel	2	3	0.424	0.056118	0.000483	0.712962	0.706936
M040	Dentine	2	4	0.410	0.056967	0.000428	0.711279	0.705652
M040	Dentine	2	5	0.373	0.056583	0.000450	0.713408	0.707782

Table A3.122 Detailed LA-MC-ICPMS Sr Isotope Results, Sample M040, Bovid, Layer C1, Rescoundudou

Sample M40, Rescoundudou, France

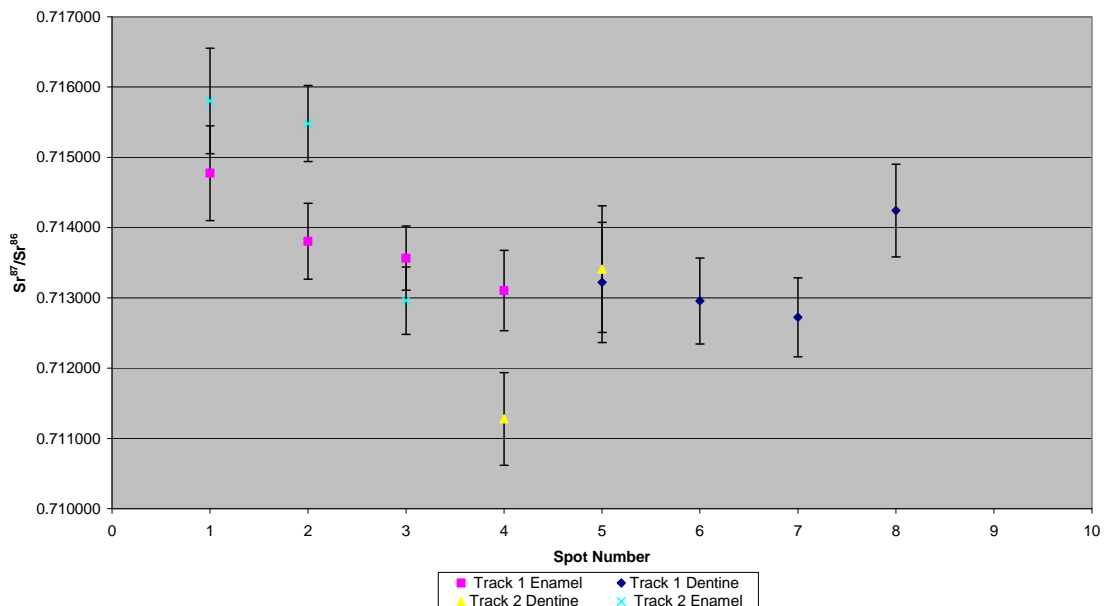


Figure A3.260 Detailed LA-MC-ICPMS Uncorrected Sr Isotope Results, Sample M040, Bovid, Layer C1, Rescoundudou

Sample M40, Corrected Sr Values, Rescoundudou, France

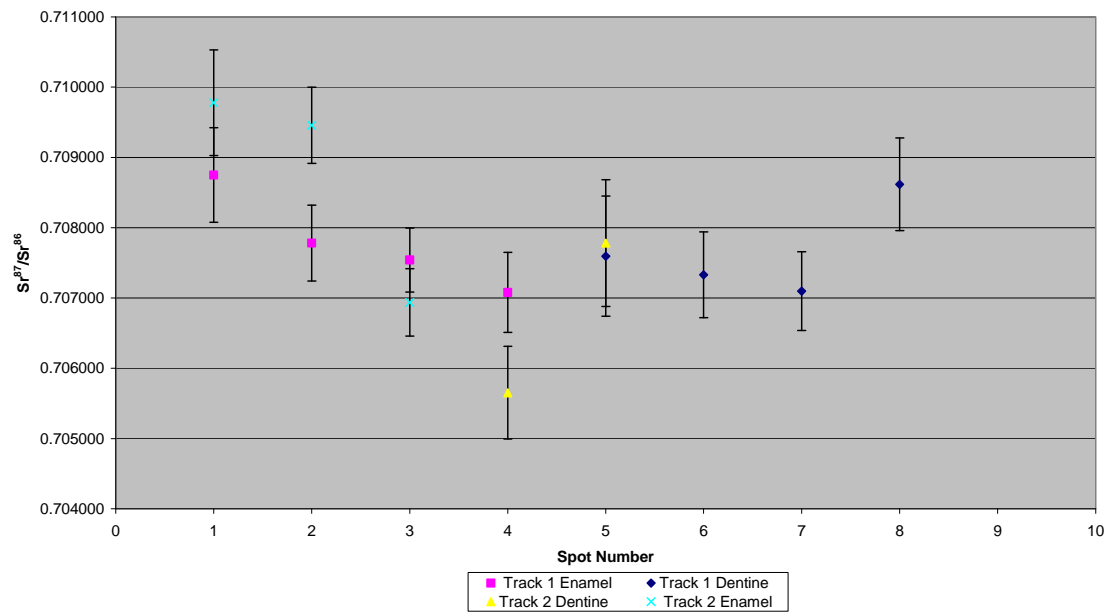


Figure A3.261 Detailed LA-MC-ICPMS Corrected Sr Isotope Results, Sample M040, Bovid, Layer C1, Rescoundudou

Sample M041, a bovid I1 incisor from layer C1 of Rescoundudou shown in Figure A2.87, was analysed in 3 tracks with the first comprising 5 spots of enamel and 7 spots of dentine, the second comprising 4 spots of enamel and 7 spots of dentine and the third comprising 13 spots of exterior enamel, shown in Figure A3.262 and Figure A3.263. The results from this sample are summarised in Table 5.41 and Figure 5.26. The enamel spots of track 1 have an average ^{88}Sr voltage of 2.421, a weighted average uncorrected $^{87}\text{Sr}/^{86}\text{Sr}$ value of 0.70788 ± 0.00074 , a weighted average corrected $^{87}\text{Sr}/^{86}\text{Sr}$ value of 0.70742 ± 0.00074 and a weighted average $^{84}\text{Sr}/^{86}\text{Sr}$ value of 0.056494 ± 0.000076 ($n=5$). The dentine spots of track 1 have an average ^{88}Sr voltage of 1.543, a weighted average uncorrected $^{87}\text{Sr}/^{86}\text{Sr}$ value of 0.70793 ± 0.00073 , a weighted average corrected $^{87}\text{Sr}/^{86}\text{Sr}$ value of 0.70689 ± 0.00073 and a weighted average $^{84}\text{Sr}/^{86}\text{Sr}$ value of 0.056543 ± 0.000040 ($n=7$). The enamel spots of track 2 have an average ^{88}Sr voltage of 2.415, a weighted average uncorrected $^{87}\text{Sr}/^{86}\text{Sr}$ value of 0.70740 ± 0.00034 , a weighted average corrected $^{87}\text{Sr}/^{86}\text{Sr}$ value of 0.70694 ± 0.00034 and a weighted average $^{84}\text{Sr}/^{86}\text{Sr}$ value of 0.056514 ± 0.000088 ($n=4$). The dentine spots of track 2 have an average ^{88}Sr voltage of 1.042, a weighted average uncorrected $^{87}\text{Sr}/^{86}\text{Sr}$ value of 0.70816 ± 0.00088 , a weighted average corrected $^{87}\text{Sr}/^{86}\text{Sr}$ value of 0.70713 ± 0.00088 and a weighted average $^{84}\text{Sr}/^{86}\text{Sr}$ value of 0.056705 ± 0.000074 ($n=5$). The enamel spots of track 3 have an average ^{88}Sr voltage of 1.612, a weighted average uncorrected $^{87}\text{Sr}/^{86}\text{Sr}$ value of 0.70768 ± 0.00018 , a weighted average corrected $^{87}\text{Sr}/^{86}\text{Sr}$ value of 0.70722 ± 0.00018 and a weighted average $^{84}\text{Sr}/^{86}\text{Sr}$ value of 0.056630 ± 0.000037 ($n=13$).

Enamel values for track 1 are in the range of 0.707219 to 0.708995 (uncorrected), as well as 0.706761 to 0.708537 (corrected), and decrease from the exterior of the enamel to the dentine-enamel junction. Dentine values for track 1 are in the range of 0.707141 to 0.709190 (uncorrected), as well as 0.706103 to 0.708152 (corrected), and are relatively heterogeneous. Enamel values of track 2 are in the range of 0.707290 to 0.707857 (uncorrected), as well as 0.706832 to 0.707399 (corrected), and decrease from the outer edge surface of the enamel to the dentine-enamel junction. Dentine values for track 2 are in the range of 0.707193 to 0.709109 (uncorrected), as well as 0.706155 to

0.708072 (corrected), and are very heterogeneous. Enamel values for track 3 are in the range of 0.707332 to 0.708229 (uncorrected), as well as 0.706873 to 0.707771 (corrected), and are vary regularly along the course of the track. Detailed values for enamel and dentine for sample M041 are shown in Table A3.123, Figure A3.264 and Figure A3.265.

This sample has heterogeneous enamel, which varies regularly along the course of the analysis tracks. Overall, dentine values are elevated in comparison to enamel, suggesting that this sample is a migrant to the area of Rescoundudou. It is difficult to define discrete domains within the enamel of this sample; however, the uncorrected values from the upper portion of the strontium isotope values correspond to carbonate bedrock areas to the east and west of the archaeological site. The corrected value of this domain is within error of the Middle Jurassic carbonate unit that contains the site. The lower end of the uncorrected range corresponds to the value of 0.707469 ± 0.000019 from P26P, a Lower Carboniferous carbonate and siliciclastic package approximately 150 km to the east of the site. The corrected value of this domain corresponds to mapping value F23 from the Upper Jurassic carbonate which outcrops within 36 km of the site. Dentine values are extremely heterogeneous, which indicates a complicated regime of post-burial diagnosis. $^{84}\text{Sr}/^{86}\text{Sr}$ values from this sample have a weighted average value of 0.056557 ± 0.000030 , suggesting that the strontium isotope results from this sample are robust.



Figure A3.262 LA-MC-ICPMS Track for Sample M041, Bovid, Layer C1, Rescoundudou



Figure A3.263 LA-MC-ICPMS Track for the External Enamel of Sample M041, Sample M041, Bovid, Layer C1, Rescoundudou

Sample	Material	Track	Point	^{88}Sr Volts	$^{84}\text{Sr}/^{86}\text{Sr}$	$^{87}\text{Sr}/^{86}\text{Sr} 2\sigma$	Corrected $^{87}\text{Sr}/^{86}\text{Sr}$	$^{87}\text{Sr}/^{86}\text{Sr} 2\sigma$
M041	Enamel	1	1	2.340	0.056561	0.000092	0.708995	0.708537
M041	Enamel	1	2	2.309	0.056487	0.000093	0.707991	0.707533
M041	Enamel	1	3	2.307	0.056512	0.000079	0.707930	0.707472

M041	Enamel	1	4	2.811	0.056517	0.000068	0.707466	0.707008	0.000149
M041	Enamel	1	5	2.338	0.056390	0.000084	0.707219	0.706761	0.000183
M041	Dentine	1	6	2.708	0.056558	0.000063	0.707141	0.706103	0.000115
M041	Dentine	1	7	2.307	0.056529	0.000086	0.707546	0.706509	0.000141
M041	Dentine	1	8	0.890	0.056551	0.000173	0.707659	0.706621	0.000261
M041	Dentine	1	9	1.411	0.056676	0.000143	0.708431	0.707393	0.000156
M041	Dentine	1	10	1.240	0.056516	0.000136	0.709190	0.708152	0.000170
M041	Dentine	1	11	1.146	0.056450	0.000185	0.708779	0.707741	0.000243
M041	Dentine	1	12	1.096	0.056454	0.000138	0.708171	0.707133	0.000224
M041	Enamel	2	1	1.959	0.056451	0.000099	0.707857	0.707399	0.000174
M041	Enamel	2	2	2.246	0.056520	0.000097	0.707404	0.706946	0.000149
M041	Enamel	2	3	2.588	0.056583	0.000081	0.707315	0.706856	0.000103
M041	Enamel	2	4	2.867	0.056488	0.000073	0.707290	0.706832	0.000115
M041	Dentine	2	5	0.777	0.056702	0.000274	0.708019	0.706981	0.000269
M041	Dentine	2	6	1.116	0.056745	0.000178	0.708445	0.707407	0.000225
M041	Dentine	2	7	1.148	0.056732	0.000154	0.709109	0.708072	0.000236
M041	Dentine	2	8	1.028	0.056800	0.000240	0.707983	0.706946	0.000232
M041	Dentine	2	9	1.144	0.056650	0.000118	0.707193	0.706155	0.000239
M041	Enamel	3	1	1.587	0.056600	0.000149	0.708162	0.707704	0.000204
M041	Enamel	3	2	1.585	0.056577	0.000176	0.708229	0.707771	0.000150
M041	Enamel	3	3	1.583	0.056636	0.000148	0.707953	0.707495	0.000187
M041	Enamel	3	4	1.607	0.056592	0.000114	0.707848	0.707390	0.000179
M041	Enamel	3	5	1.722	0.056604	0.000123	0.707600	0.707142	0.000171
M041	Enamel	3	6	1.669	0.056585	0.000130	0.707404	0.706946	0.000135
M041	Enamel	3	7	1.584	0.056581	0.000130	0.707624	0.707166	0.000151
M041	Enamel	3	8	1.619	0.056631	0.000124	0.707732	0.707274	0.000151
M041	Enamel	3	9	1.622	0.056742	0.000118	0.707487	0.707029	0.000162
M041	Enamel	3	10	1.622	0.056573	0.000136	0.707406	0.706948	0.000216
M041	Enamel	3	11	1.610	0.056690	0.000128	0.707332	0.706873	0.000189
M041	Enamel	3	12	1.574	0.056751	0.000186	0.707616	0.707158	0.000193
M041	Enamel	3	13	1.566	0.056656	0.000149	0.707421	0.706963	0.000188

Table A3.123 Detailed LA-MC-ICPMS Sr Isotope Results, Sample M041, Bovid, Layer C1, Rescoundudou

Sample M41, Rescoundudou, France

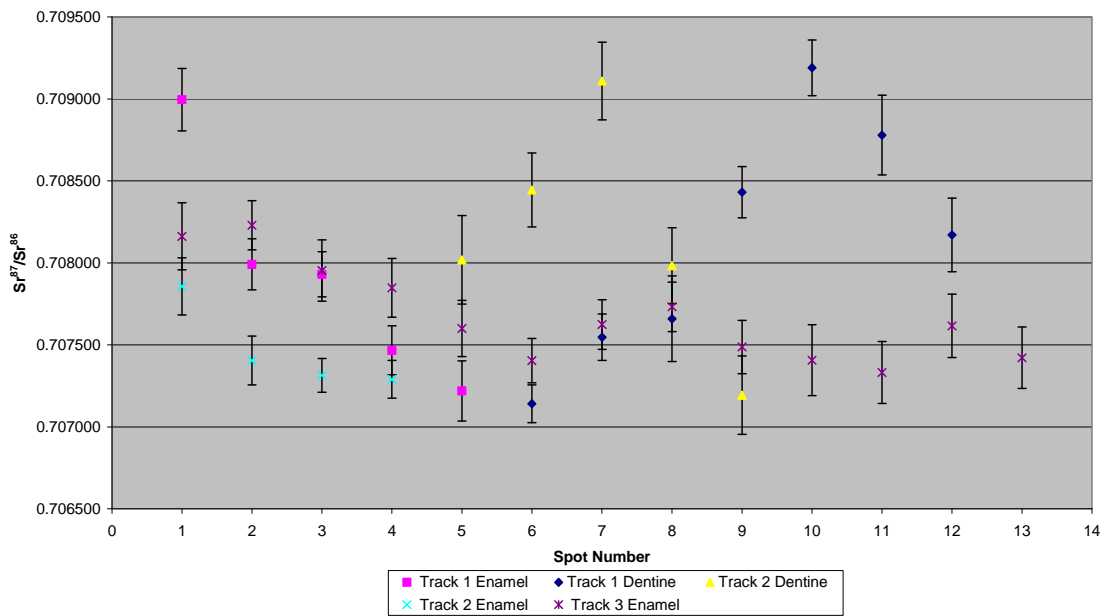


Figure A3.264 Detailed LA-MC-ICPMS Uncorrected Sr Isotope Results, Sample M041, Bovid, Layer C1, Rescoundudou

Sample M41, Corrected Sr Values, Rescoundudou, France

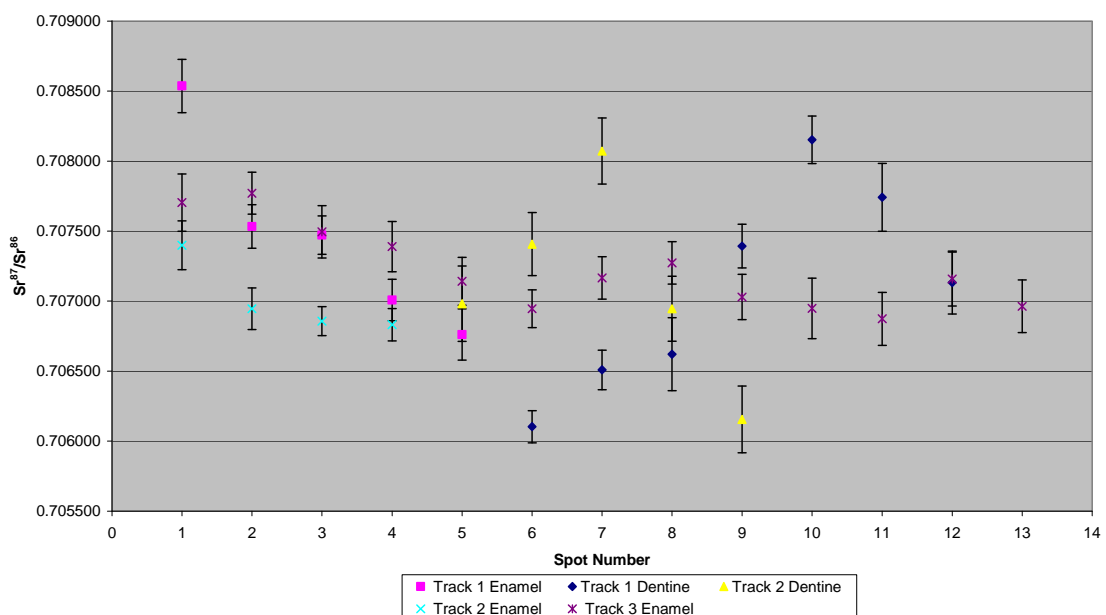


Figure A3.265 Detailed LA-MC-ICPMS Corrected Sr Isotope Results, Sample M041, Bovid, Layer C1, Rescoundudou

Sample M042, a horse M2 molar from layer C1 of Rescoundudou shown in Figure A2.88, was analysed in 3 tracks, with the first comprising 3 spots of enamel and 4 spots of dentine, the second comprising 6 spots of enamel and 4 spots of dentine and the third comprising 6 spots of enamel, shown in Figure A3.266. The results from this sample are summarised in Table 5.41 and Figure 5.26. The enamel spots of track 1 have an average ^{88}Sr voltage of 0.733, a weighted average uncorrected $^{87}\text{Sr}/^{86}\text{Sr}$ value of 0.71012 ± 0.00068 , a weighted average corrected $^{87}\text{Sr}/^{86}\text{Sr}$ value of 0.70793 ± 0.00068 and a weighted average $^{84}\text{Sr}/^{86}\text{Sr}$ value of 0.05666 ± 0.00015 ($n=3$). The dentine spots of track 1 have an average ^{88}Sr voltage of 0.675, a weighted average uncorrected $^{87}\text{Sr}/^{86}\text{Sr}$ value of 0.7088 ± 0.0020 , a weighted average corrected $^{87}\text{Sr}/^{86}\text{Sr}$ value of 0.70620 ± 0.0020 and a weighted average $^{84}\text{Sr}/^{86}\text{Sr}$ value of 0.05693 ± 0.00015 ($n=4$). The enamel spots of track 2 have an average ^{88}Sr voltage of 0.644, a weighted average uncorrected $^{87}\text{Sr}/^{86}\text{Sr}$ value of 0.7109 ± 0.0016 , a weighted average corrected $^{87}\text{Sr}/^{86}\text{Sr}$ value of 0.70870 ± 0.0016 and a weighted average $^{84}\text{Sr}/^{86}\text{Sr}$ value of 0.05685 ± 0.00014 ($n=6$). The dentine spots of track 2 have an average ^{88}Sr voltage of 0.608, a weighted average uncorrected $^{87}\text{Sr}/^{86}\text{Sr}$ value of 0.70964 ± 0.00095 , a weighted average corrected $^{87}\text{Sr}/^{86}\text{Sr}$ value of 0.70704 ± 0.00095 and a weighted average $^{84}\text{Sr}/^{86}\text{Sr}$ value of 0.05687 ± 0.00031 ($n=4$). The enamel spots of track 3 have an average ^{88}Sr voltage of 0.604, a weighted average uncorrected $^{87}\text{Sr}/^{86}\text{Sr}$ value of 0.71153 ± 0.00051 , a weighted average corrected $^{87}\text{Sr}/^{86}\text{Sr}$ value of 0.70934 ± 0.00051 and a weighted average $^{84}\text{Sr}/^{86}\text{Sr}$ value of 0.05707 ± 0.00021 ($n=6$). Enamel values for track 1 are in the range of 0.709896 to 0.710078 (uncorrected), as well as 0.707704 to 0.707886 (corrected), and are homogenous within 2σ error. Dentine values for track 1 are in the range of 0.707595 to 0.710338 (uncorrected), as well as 0.704998 to 0.707740 (corrected), and are heterogeneous. Enamel values for track 2 are in the range of 0.709972 to 0.714470 (uncorrected), as well as 0.707779 to 0.712277 (corrected), with all spots except 1 being homogenous within 2σ error. Dentine values for track 2 are in the range of 0.709083 to 0.710255 (uncorrected), as well as 0.706485 to 0.707657 (corrected), and are distributed in 2 homogenous groups. Enamel values for track 3 are in the range of 0.712201 to 0.710918 (uncorrected), as well as 0.710009 to 0.708726

(corrected), which, in general, decrease from the exterior of the enamel to the enamel-dentine junction. Detailed values for enamel and dentine for sample M042 are shown in Table A3.124, Figure A3.268 and Figure A3.269.

The enamel and dentine $^{87}\text{Sr}/^{86}\text{Sr}$ values of this sample are statistically indistinguishable. The wide range of enamel values suggests that the sample may have been mobile during amelogenesis; however, as discussed below, this was probably within the same geological unit. Both the corrected and uncorrected range is encompassed by the values found within the Middle Jurassic carbonate package that contains Rescoundudou, as discussed in detail with reference to sample M033. In common with other horse samples, the dentine has a wide range of $^{87}\text{Sr}/^{86}\text{Sr}$ values. The $^{87}\text{Sr}/^{86}\text{Sr}$ results from this analysis may not be robust, as the $^{84}\text{Sr}/^{86}\text{Sr}$ value (0.056882 ± 0.000084) is somewhat elevated compared to the ideal value.

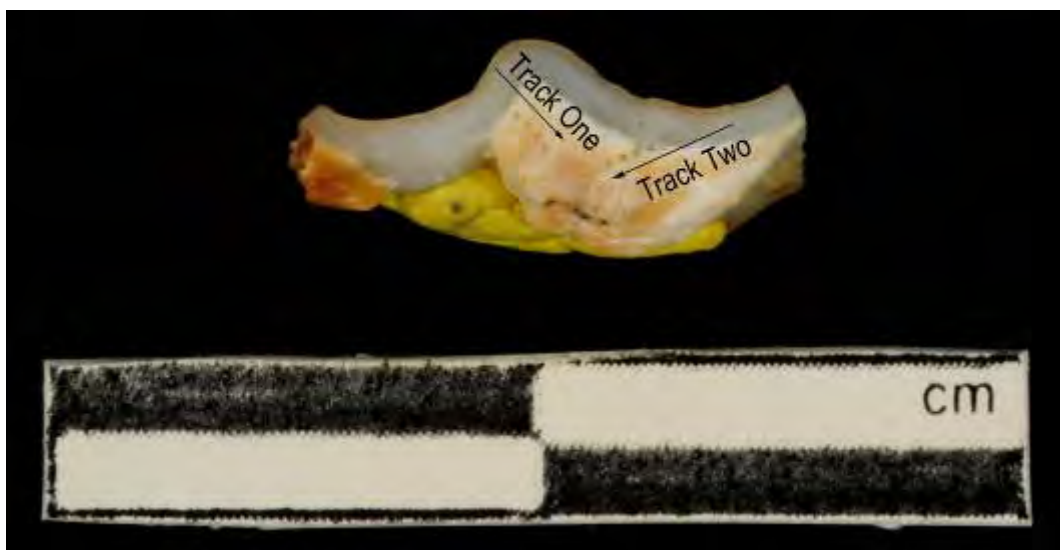


Figure A3.266 LA-MC-ICPMS Track for Sample M042, Deer, Layer C1, Rescoundudou

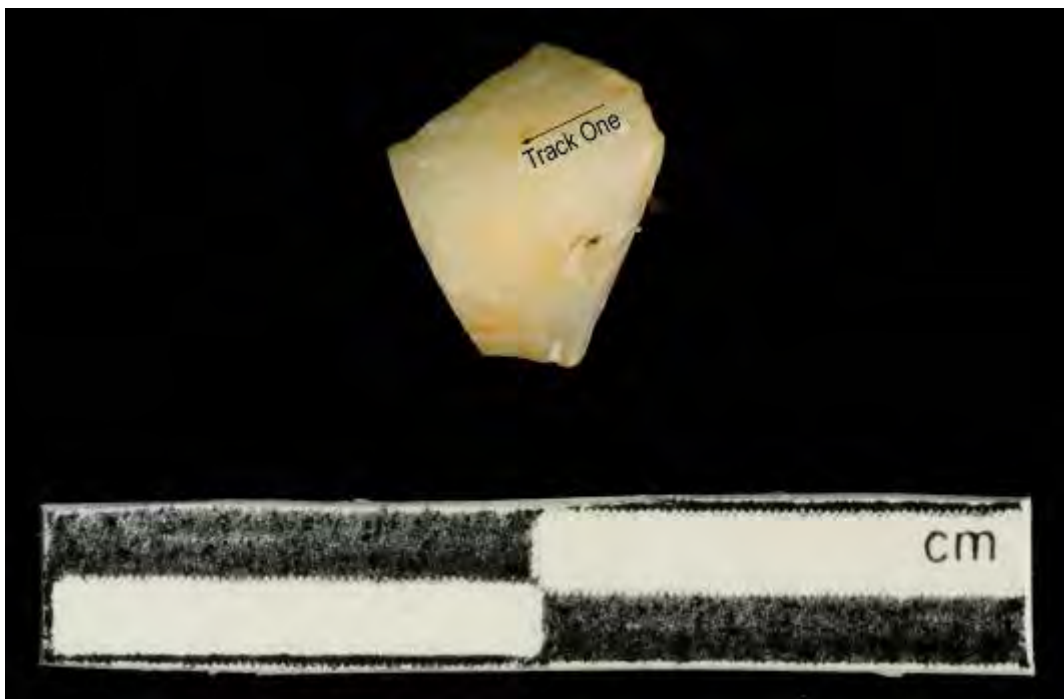


Figure A3.267 LA-MC-ICPMS Track for the External Enamel of Sample M042, Deer, Layer C1, Rescoundudou

Sample	Material	Track	Point	^{88}Sr Volts	$^{84}\text{Sr}/^{86}\text{Sr}$	$^{84}\text{Sr}/^{86}\text{Sr} 2\sigma$ Error	$^{87}\text{Sr}/^{86}\text{Sr}$	Corrected $^{87}\text{Sr}/^{86}\text{Sr}$	$^{87}\text{Sr}/^{86}\text{Sr} 2\sigma$ Error
M042	Enamel	1	1	0.723	0.056731	0.000247	0.709896	0.707704	0.000290
M042	Enamel	1	2	0.705	0.056618	0.000264	0.710414	0.708222	0.000315
M042	Enamel	1	3	0.771	0.056632	0.000261	0.710078	0.707886	0.000358
M042	Dentine	1	4	0.526	0.056914	0.000451	0.709197	0.706599	0.000450
M042	Dentine	1	5	0.593	0.057040	0.000328	0.709291	0.706693	0.000347
M042	Dentine	1	6	0.623	0.056900	0.000333	0.710338	0.707740	0.000402
M042	Dentine	1	7	0.957	0.056902	0.000240	0.707595	0.704998	0.000265
M042	Enamel	2	1	0.755	0.056709	0.000370	0.714470	0.712277	0.000442
M042	Enamel	2	2	0.620	0.056911	0.000382	0.710528	0.708335	0.000366
M042	Enamel	2	3	0.616	0.056948	0.000388	0.710401	0.708208	0.000367
M042	Enamel	2	4	0.588	0.057146	0.000488	0.710356	0.708164	0.000456
M042	Enamel	2	5	0.628	0.056785	0.000287	0.710681	0.708489	0.000351
M042	Enamel	2	6	0.660	0.056805	0.000308	0.709972	0.707779	0.000334
M042	Dentine	2	7	0.653	0.056892	0.000320	0.710255	0.707657	0.000383
M042	Dentine	2	8	0.626	0.056907	0.000321	0.709211	0.706613	0.000305
M042	Dentine	2	9	0.580	0.057063	0.000361	0.709083	0.706485	0.000426
M042	Dentine	2	10	0.572	0.056559	0.000377	0.710147	0.707549	0.000378

M042	Enamel	3	1	0.513	0.057150	0.000381	0.712166	0.709973	0.000403
M042	Enamel	3	2	0.557	0.057263	0.000338	0.712201	0.710009	0.000460
M042	Enamel	3	3	0.600	0.057120	0.000347	0.711667	0.709474	0.000325
M042	Enamel	3	4	0.627	0.057301	0.000369	0.711219	0.709026	0.000382
M042	Enamel	3	5	0.665	0.056793	0.000316	0.711332	0.709140	0.000338
M042	Enamel	3	6	0.663	0.056928	0.000303	0.710918	0.708726	0.000377

Table A3.124 Detailed LA-MC-ICPMS Sr Isotope Results for Dentine and Enamel, Sample M042, Deer, Layer C1, Rescoundudou

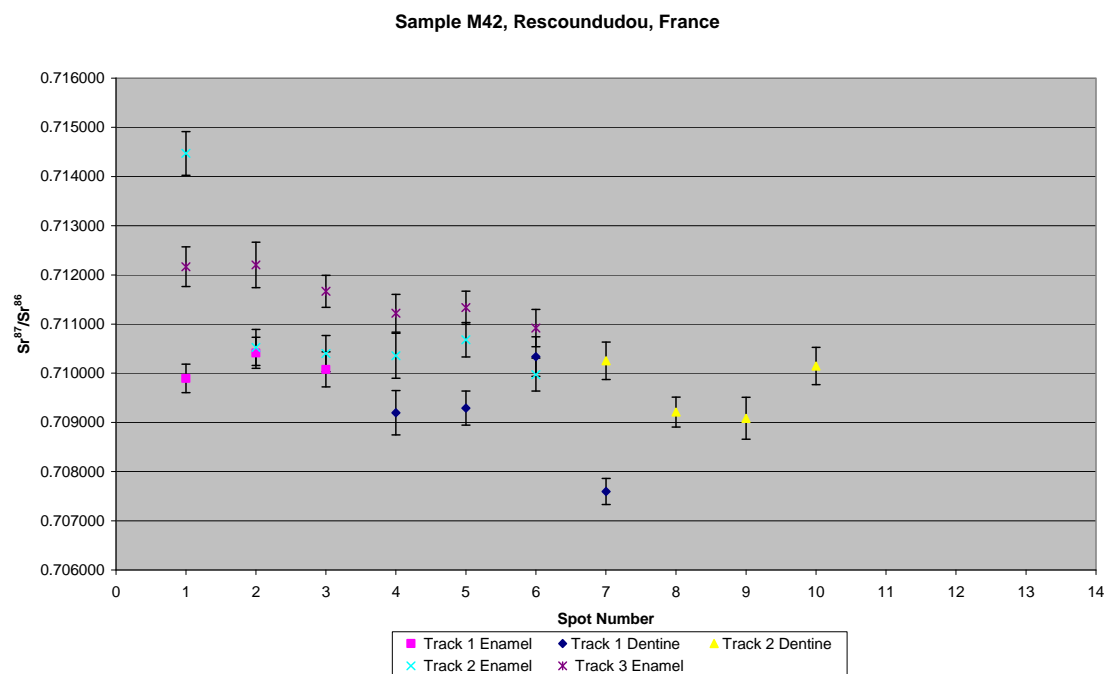


Figure A3.268 Detailed LA-MC-ICPMS Uncorrected Sr Isotope Results, Sample M042, Deer, Layer C1, Rescoundudou

Sample M42, Corrected Sr Values, Rescoundudou, France

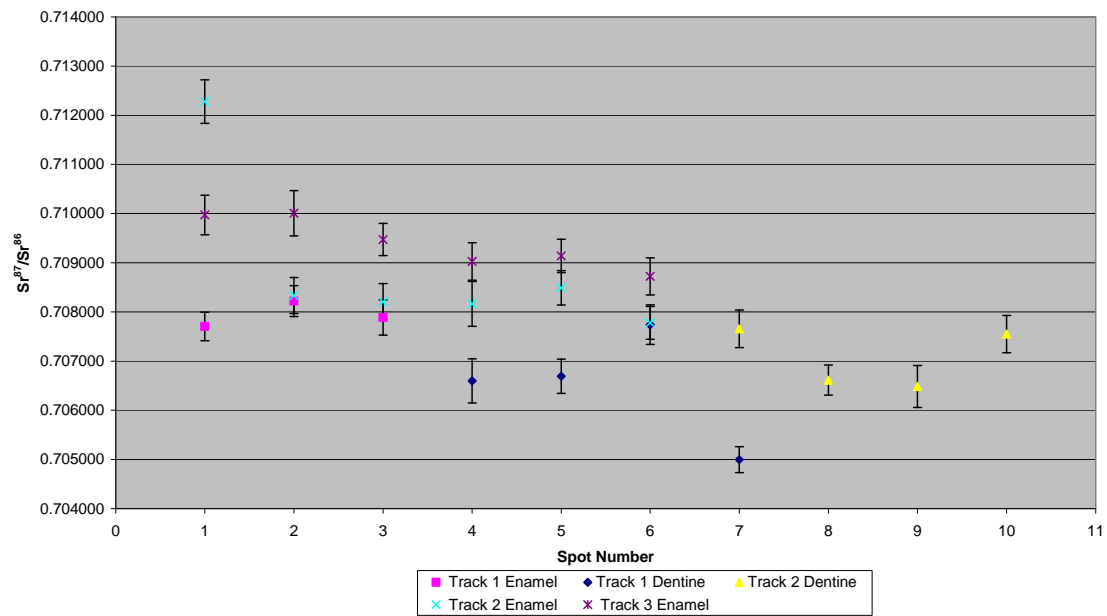


Figure A3.269 Detailed LA-MC-ICPMS Corrected Sr Isotope Results, Sample M042, Deer, Layer C1, Rescoundudou

Sample M043, a deer M3 molar from layer C1 of Rescoundudou shown in Figure A2.89, was analysed in 2 tracks with the first comprising 6 spots of enamel and 9 spots of dentine and the second comprising 3 spots of dentine and 2 spots of enamel, shown in Figure A3.270. The results from this sample are summarised in Table 5.41 and Figure 5.26. The enamel spots of track 1 have an average ^{88}Sr voltage of 0.150, a weighted average uncorrected $^{87}\text{Sr}/^{86}\text{Sr}$ value of 0.7229 ± 0.0049 , a weighted average corrected $^{87}\text{Sr}/^{86}\text{Sr}$ value of 0.68700 ± 0.0049 and a weighted average $^{84}\text{Sr}/^{86}\text{Sr}$ value of 0.05837 ± 0.00076 ($n=6$). The dentine spots of track 1 have an average ^{88}Sr voltage of 0.488, a weighted average uncorrected $^{87}\text{Sr}/^{86}\text{Sr}$ value of 0.71084 ± 0.00058 , a weighted average corrected $^{87}\text{Sr}/^{86}\text{Sr}$ value of 0.70754 ± 0.00058 and a weighted average $^{84}\text{Sr}/^{86}\text{Sr}$ value of 0.05698 ± 0.00020 ($n=3$). The enamel spots of track 2 have an average ^{88}Sr voltage of 0.111, a weighted average uncorrected $^{87}\text{Sr}/^{86}\text{Sr}$ value of 0.733 ± 0.026 , a weighted average corrected $^{87}\text{Sr}/^{86}\text{Sr}$ value of 0.69800 ± 0.026 and a weighted average $^{84}\text{Sr}/^{86}\text{Sr}$ value of 0.0576 ± 0.0014 ($n=3$). The dentine spots of track 2 have an average ^{88}Sr voltage of 0.470, a weighted average uncorrected $^{87}\text{Sr}/^{86}\text{Sr}$ value of 0.7116 ± 0.0014 , a weighted average uncorrected $^{87}\text{Sr}/^{86}\text{Sr}$ value of 0.70830 ± 0.0014 and a weighted average $^{84}\text{Sr}/^{86}\text{Sr}$ value of 0.05690 ± 0.00026 . Enamel values for track 1 are in the range of 0.718283 to 0.733291 (uncorrected), as well as 0.682372 to 0.697379 (corrected), and are very heterogeneous, decreasing overall from spot 1 to spot 4. Dentine values for track 1 are in the range of 0.710124 to 0.712810 (uncorrected), as well as 0.706821 to 0.709507 (corrected), and are generally homogenous within 2σ error, with the exception of spot 10, which has a slightly elevated $^{87}\text{Sr}/^{86}\text{Sr}$ value. Enamel values for track 2 are in the range of 0.729446 to 0.752929 (uncorrected), as well as 0.693535 to 0.717018 (corrected), and are very heterogeneous. Dentine values for track 2 are in the range of 0.711071 to 0.712279 (uncorrected), as well as 0.707768 to 0.708976 (corrected), and are slightly heterogeneous. Detailed values for enamel and dentine for sample M043 are shown in Table A3.125, Figure A3.271 and Figure A3.272.

This sample displays a significant difference between weighted average dentine and enamel values, which suggests this specimen is a migrant to the area of

this site. Dentine values are somewhat homogenous. The enamel $^{87}\text{Sr}/^{86}\text{Sr}$ values for this sample can be grouped within 4 domains: the first comprising spot 2 from track 2, the second containing spot 1 from track 1 and spots 6 and 7 from track 2, the third containing spots 2 and 3, 15 and 17 from track 1 and the fourth containing spot 4 from track 1. The uncorrected value of the first domain corresponds to mapping sample FS063-S1 from a Permian monzogranite/granodiorite that is located approximately 67 km north-west of the site. This corrected value from this domain corresponds to a number of mapping samples due to the large error, making it impossible to define the source location for this value. The uncorrected value of domain 2 corresponds to a number of mapping samples: FS111-S1 (0.727959 ± 0.000011) from a Permian monzogranite/granodiotire, FS113-S1 (0.732964 ± 0.000042) from a Permian sandstone, FS099-S1 (0.728262 ± 0.000011) from Cambrian/Ordovician granite/orthogneiss and FS103-S1 (0.728433 ± 0.000012) from a Cambrian anatetic orthogneiss. The uncorrected values from domain 3 corresponds to sample site P24P (0.72435 ± 0.000119), located approximately 156 km east of Rescoundudou in a Lower Cretaceous siliciclastic/carbonate package. The uncorrected values from domain 4 corresponds to FS097-S1 (0.718429 ± 0.000013 , probably meta-sediment, as discussed with reference to sample 617), FS104-S2 (0.751565 ± 0.000017 , Upper Cambrian granite/orthogneiss) and FS092-S1 (0.718681 ± 0.000011 , Lower Jurassic siliciclastic/carbonate). The corrected values from domains 2, 3 and 4 do not correspond to any mapping samples in the study area. The Sr^{88} voltages of this sample are very low and the $^{84}\text{Sr}/^{86}\text{Sr}$ value is elevated (0.05700 ± 0.00016), suggesting that these results are not reliable.

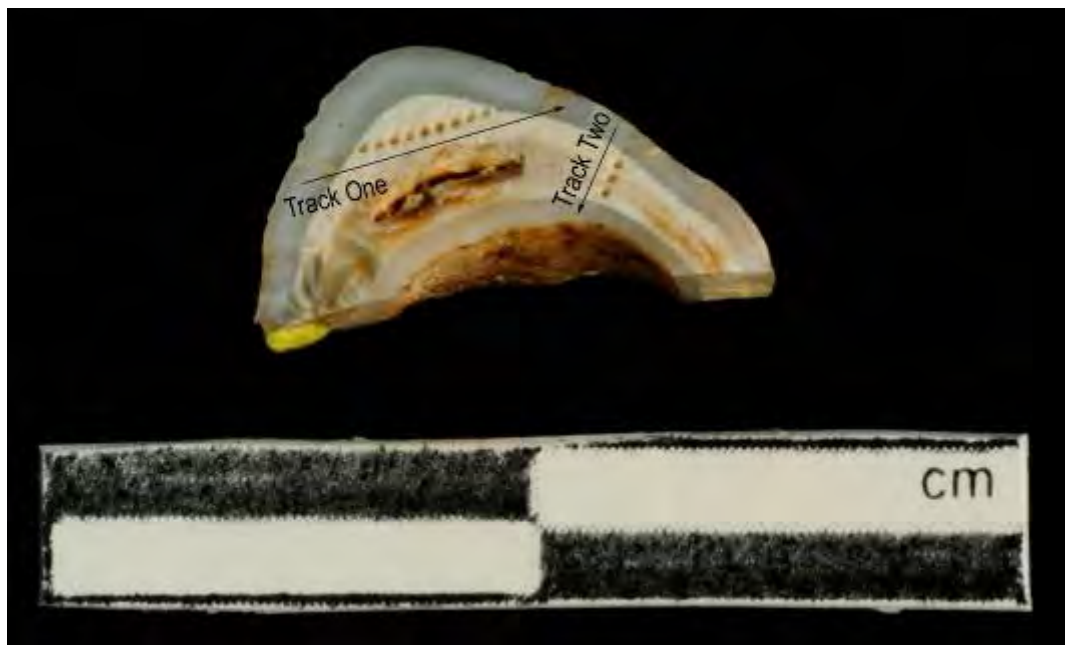


Figure A3.270 LA-MC-ICPMS Track for Sample M043, Deer, Layer C1, Rescoundudou

Sample	Material	Track	Point	^{88}Sr Volts	$^{84}\text{Sr}/^{86}\text{Sr}$	$^{84}\text{Sr}/^{86}\text{Sr} 2\sigma$ Error	$^{87}\text{Sr}/^{86}\text{Sr}$	Corrected $^{87}\text{Sr}/^{86}\text{Sr}$	$^{87}\text{Sr}/^{86}\text{Sr} 2\sigma$ Error
M043	Enamel	1	1	0.114	0.059567	0.002232	0.733291	0.697379	0.002447
M043	Enamel	1	2	0.136	0.056908	0.001842	0.725309	0.689398	0.001896
M043	Enamel	1	3	0.141	0.059030	0.002777	0.725071	0.689160	0.002006
M043	Enamel	1	4	0.214	0.058115	0.002303	0.718283	0.682372	0.001193
M043	Dentine	1	5	0.614	0.056728	0.000391	0.710726	0.707423	0.000325
M043	Dentine	1	6	0.561	0.056740	0.000334	0.710534	0.707231	0.000449
M043	Dentine	1	7	0.472	0.057088	0.000440	0.710492	0.707189	0.000484
M043	Dentine	1	8	0.445	0.056967	0.000508	0.710582	0.707279	0.000460
M043	Dentine	1	9	0.422	0.057519	0.000543	0.711112	0.707809	0.000637
M043	Dentine	1	10	0.512	0.056959	0.000354	0.712810	0.709507	0.000491
M043	Dentine	1	11	0.461	0.056911	0.000489	0.710616	0.707313	0.000570
M043	Dentine	1	12	0.485	0.056937	0.000479	0.710614	0.707311	0.000600
M043	Dentine	1	13	0.422	0.057405	0.000475	0.710124	0.706821	0.000561
M043	Enamel	1	14						
M043	Enamel	1	15	0.163	0.058876	0.001232	0.722886	0.686974	0.001726
M043	Enamel	1	16						
M043	Enamel	1	17	0.128	0.057519	0.002219	0.724484	0.688573	0.001991
M043	Enamel	2	1						
M043	Enamel	2	2	0.103	0.058070	0.002702	0.752929	0.717018	0.003630
M043	Dentine	2	3	0.455	0.056869	0.000400	0.712279	0.708976	0.000555
M043	Dentine	2	4	0.504	0.057018	0.000514	0.711507	0.708204	0.000480
M043	Dentine	2	5	0.449	0.056843	0.000482	0.711071	0.707768	0.000573
M043	Enamel	2	6	0.124	0.057181	0.002126	0.729446	0.693535	0.001978
M043	Enamel	2	7	0.106	0.057925	0.003104	0.730360	0.694448	0.002664

Table A3.125 Detailed LA-MC-ICPMS Sr Isotope Results for Dentine and Enamel, Sample M043, Deer, Layer C1, Rescoundudou

Sample M43, Rescoundudou, France

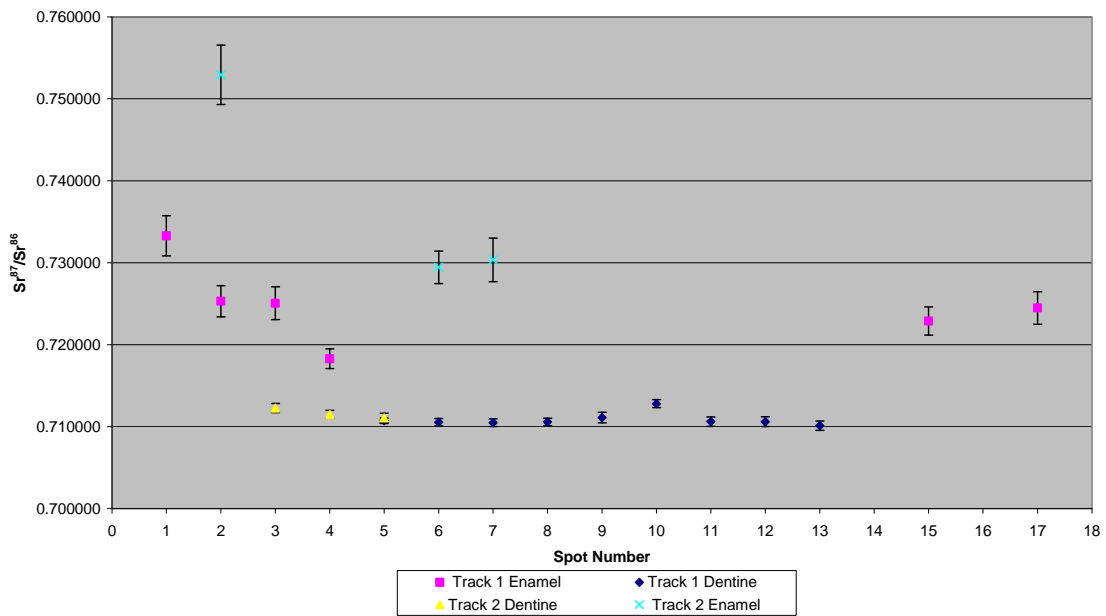


Figure A3.271 Detailed LA-MC-ICPMS Uncorrected Sr Isotope Results, Sample M043, Deer, Layer C1, Rescoundudou

Sample M43, Corrected Sr Values, Rescoundudou, France

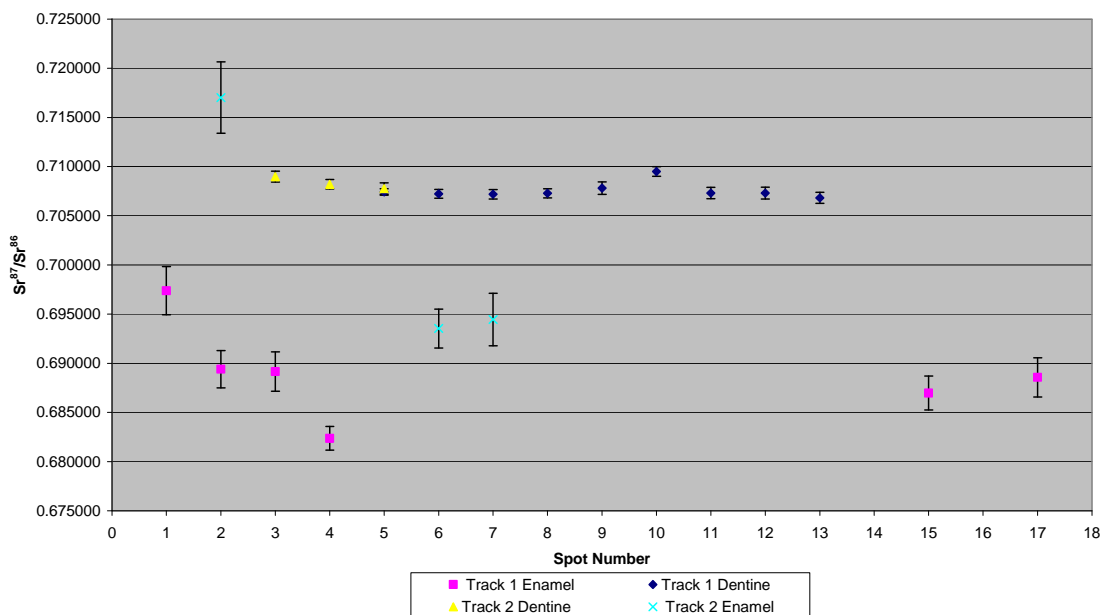


Figure A3.272 Detailed LA-MC-ICPMS Corrected Sr Isotope Results, Sample M043, Deer, Layer C1, Rescoundudou

Sample M044, a deer P3 premolar from layer C1 of Rescoundudou shown in Figure A2.90, was analysed in 1 track comprising 12 spots of enamel in 2 discontinuous sections and 17 spots of dentine, shown in Figure A3.273. The results from this sample are summarised in Table 5.41 and Figure 5.26. The enamel spots of track 1 have an average ^{88}Sr voltage of 0.456, a weighted average uncorrected $^{87}\text{Sr}/^{86}\text{Sr}$ value of 0.71630 ± 0.0015 and a weighted average $^{84}\text{Sr}/^{86}\text{Sr}$ value of 0.05705 ± 0.00013 ($n=12$). The dentine spots of track 1 have an average ^{88}Sr voltage of 0.425, a weighted average uncorrected $^{87}\text{Sr}/^{86}\text{Sr}$ value of 0.71432 ± 0.00082 , a weighted average corrected $^{87}\text{Sr}/^{86}\text{Sr}$ value of 0.71033 ± 0.00082 and a weighted average $^{84}\text{Sr}/^{86}\text{Sr}$ value of 0.05704 ± 0.00016 ($n=17$). Enamel values are in the range of 0.717994 to 0.726115 (uncorrected), as well as 0.715069 to 0.723190 (corrected), and are relatively homogenous, with the exception of spot 23, which has a significantly elevated $^{87}\text{Sr}/^{86}\text{Sr}$ value. Dentine values are in the range of 0.712621 to 0.718306 (uncorrected), as well as 0.708632 to 0.714316 (corrected), and are relatively heterogeneous, varying in a rhythmic fashion in the direction of the track. Detailed values for enamel and dentine for sample M044 are shown in Table A3.126, Figure A3.274 and Figure A3.275.

The strontium isotope values of this sample are summarised in Table 5.31 and Figure 5.26 and shown in detail in Table A3.126, Figure A3.274 and Figure A3.275. There is a significant difference in values for dentine and enamel, suggesting that this sample is a migrant. Enamel values are relatively homogenous (with the exception of the very elevated spot 23), suggesting that this specimen was not mobile across different geological environments during amelogenesis. The weighted average uncorrected enamel value corresponds to mapping sample FS053-S1 (0.719269 ± 0.000027), located approximately 101 km north-west of Rescoundudou in a Permian siliciclastic unit. This unit outcrops within approximately 500 m of the site. The weighted average corrected value (0.71562 ± 0.00022) correlates to P2P, located approximately 180 km north-west of Rescoundudou in a Carboniferous monzogranite/granodiorite unit which outcrops within 125 km of the site. The weighted average $^{84}\text{Sr}/^{86}\text{Sr}$ value for all analysis spots from this sample

(0.057043 ± 0.000097) is significantly elevated, suggesting that the strontium isotope values from this site may not be robust.

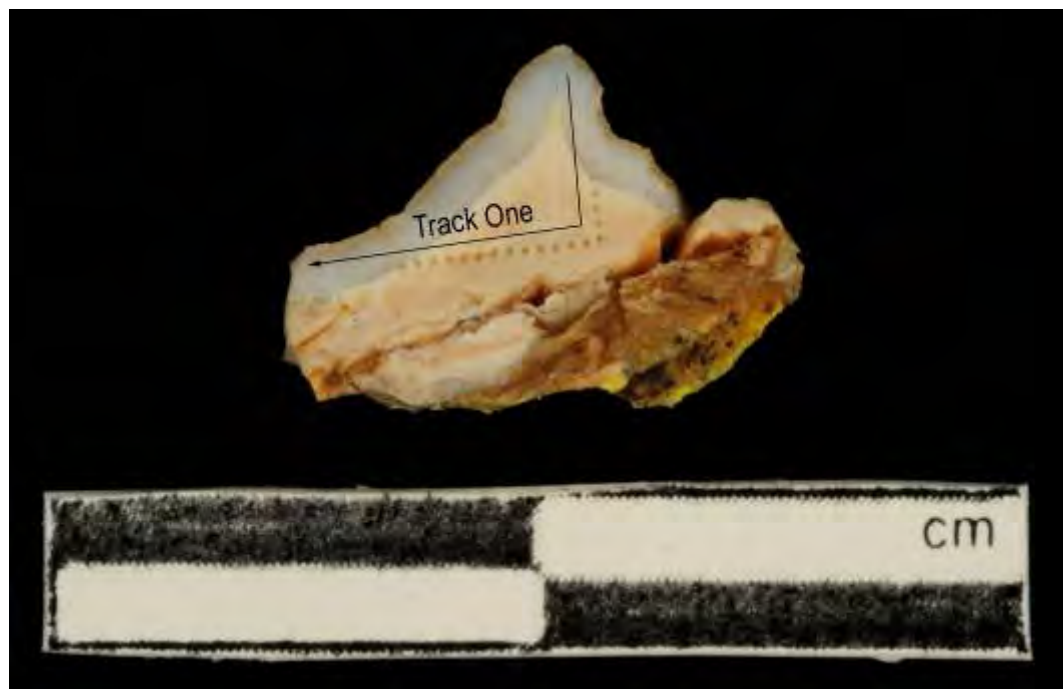


Figure A3.273 LA-MC-ICPMS Track for Sample M044, Deer, Layer C1, Rescoundudou

Sample	Material	Track	Point	⁸⁸ Sr Volts	⁸⁴ Sr/ ⁸⁶ Sr	⁸⁴ Sr/ ⁸⁶ Sr 2σ Error	⁸⁷ Sr/ ⁸⁶ Sr	Corrected ⁸⁷ Sr/ ⁸⁶ Sr	⁸⁷ Sr/ ⁸⁶ Sr 2σ Error
M044	Enamel	1	1	0.378	0.057221	0.000594	0.719059	0.716134	0.000684
M044	Enamel	1	2	0.384	0.057191	0.000558	0.718420	0.715495	0.000782
M044	Enamel	1	3	0.484	0.057178	0.000721	0.718954	0.716029	0.000661
M044	Enamel	1	4	0.449	0.057439	0.000611	0.718864	0.715939	0.000643
M044	Enamel	1	5	0.501	0.057149	0.000435	0.717994	0.715069	0.000545
M044	Dentine	1	6	0.602	0.057316	0.000510	0.718306	0.714316	0.000535
M044	Dentine	1	7	0.466	0.056891	0.000420	0.715183	0.711193	0.000555
M044	Dentine	1	8	0.356	0.057647	0.000572	0.712831	0.708842	0.000779
M044	Dentine	1	9	0.347	0.057924	0.000796	0.712621	0.708632	0.000780
M044	Dentine	1	10	0.398	0.056920	0.000546	0.713428	0.709438	0.000693
M044	Dentine	1	11	0.383	0.056809	0.000592	0.713065	0.709075	0.000749
M044	Dentine	1	12	0.395	0.057742	0.001357	0.714016	0.710027	0.000531
M044	Dentine	1	13	0.354	0.056710	0.000631	0.714065	0.710076	0.000664
M044	Dentine	1	14	0.375	0.057089	0.000561	0.713591	0.709602	0.000696
M044	Dentine	1	15	0.368	0.058606	0.001360	0.714339	0.710350	0.001257
M044	Dentine	1	16	0.393	0.056976	0.000577	0.713024	0.709035	0.000679
M044	Dentine	1	17	0.395	0.057113	0.000546	0.712924	0.708935	0.000675
M044	Dentine	1	18	0.393	0.057070	0.000534	0.713092	0.709103	0.000541
M044	Dentine	1	19	0.426	0.057290	0.000424	0.713194	0.709205	0.000662
M044	Dentine	1	20	0.504	0.056876	0.000325	0.713665	0.709676	0.000534
M044	Dentine	1	21	0.464	0.057250	0.000452	0.715055	0.711066	0.000611
M044	Dentine	1	22	0.601	0.056792	0.000238	0.715957	0.711968	0.000436
M044	Enamel	1	23	0.524	0.057009	0.000381	0.726115	0.723190	0.000563
M044	Enamel	1	24	0.544	0.056903	0.000372	0.718414	0.715489	0.000499
M044	Enamel	1	25	0.446	0.057110	0.000442	0.718522	0.715597	0.000712
M044	Enamel	1	26	0.407	0.056888	0.000386	0.718207	0.715282	0.000724
M044	Enamel	1	27	0.445	0.056831	0.000388	0.718431	0.715506	0.000538
M044	Enamel	1	28	0.454	0.057141	0.000426	0.718829	0.715904	0.000458
M044	Enamel	1	29	0.455	0.057269	0.000647	0.718414	0.715489	0.000522

Table A3.126 Detailed LA-MC-ICPMS Sr Isotope Results, Sample M044, Deer, Layer C1, Rescoundudou

Sample M44, Rescoundudou, France

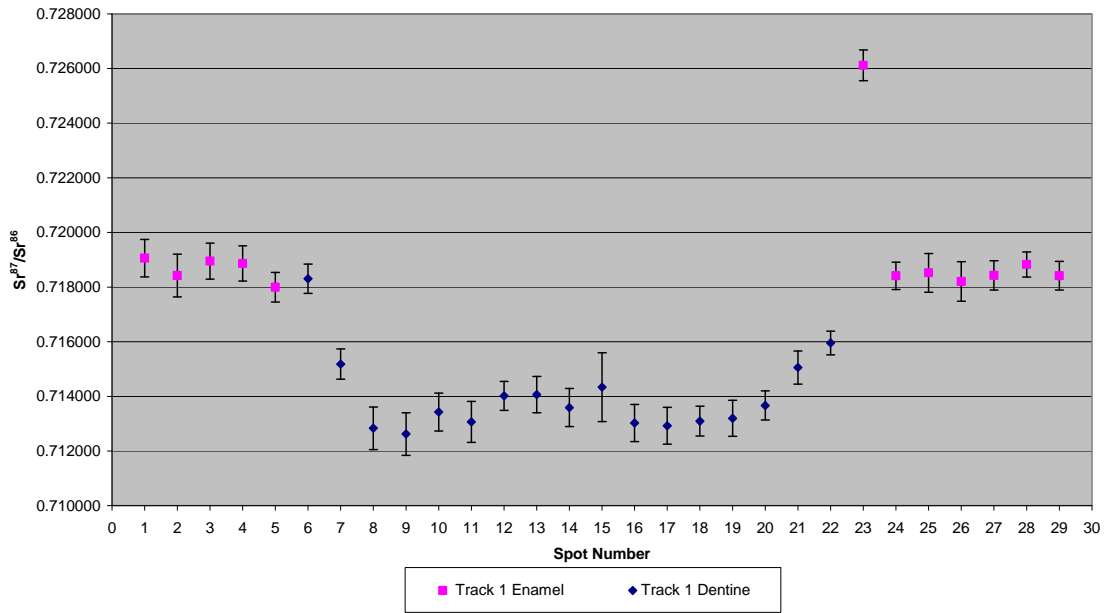


Figure A3.274 Detailed LA-MC-ICPMS Uncorrected Sr Isotope Results, Sample M044, Deer, Layer C1, Rescoundudou

Sample M44, Corrected Sr Values, Rescoundudou, France

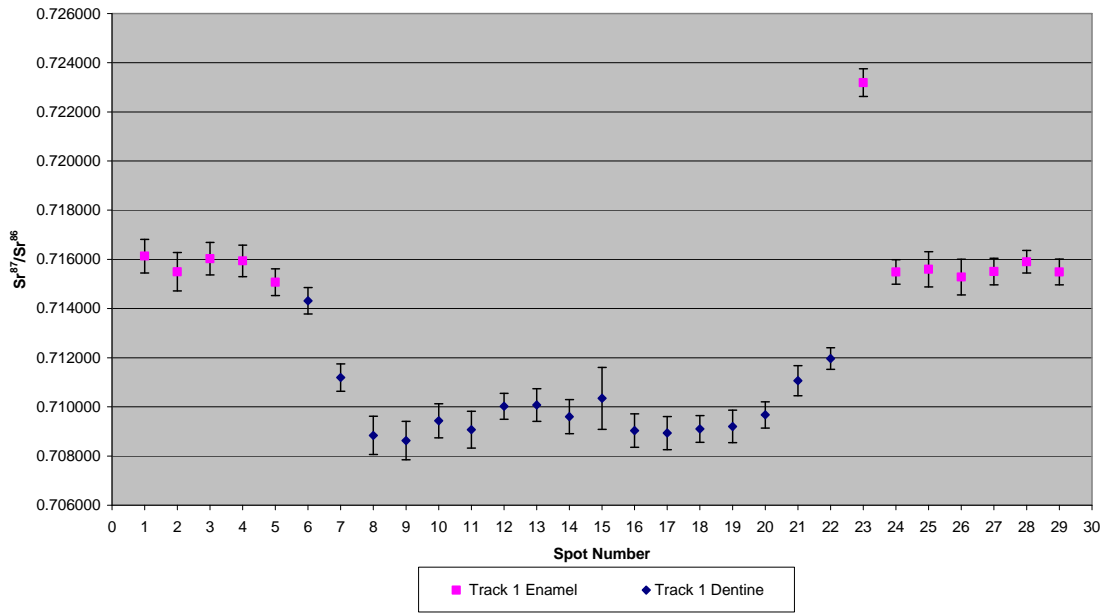


Figure A3.275 Detailed LA-MC-ICPMS Corrected Sr Isotope Results, Sample M044, Deer, Layer C1, Rescoundudou

Sample M045, a deer P4 premolar from layer C1 of Rescoundudou shown in Figure A2.91, was analysed in 2 tracks with the first comprising 3 spots of enamel and 6 spots of dentine and the second comprising 2 spots of dentine and 9 spots of enamel, shown in Figure A3.276. The results from this sample are summarised in Table 5.41 and Figure 5.26. The enamel spots of track 1 have an average ^{88}Sr voltage of 0.519, a weighted average uncorrected $^{87}\text{Sr}/^{86}\text{Sr}$ value of 0.71368 ± 0.00028 , a weighted average corrected $^{87}\text{Sr}/^{86}\text{Sr}$ value of 0.71131 ± 0.00028 and a weighted average $^{84}\text{Sr}/^{86}\text{Sr}$ value of 0.05707 ± 0.00022 ($n=3$). The dentine spots of track 1 have an average ^{88}Sr voltage of 0.591, a weighted average uncorrected $^{87}\text{Sr}/^{86}\text{Sr}$ value of 0.7106 ± 0.0023 , a weighted average corrected $^{87}\text{Sr}/^{86}\text{Sr}$ value of 0.70840 ± 0.0023 and a weighted average $^{84}\text{Sr}/^{86}\text{Sr}$ value of 0.05707 ± 0.00016 ($n=6$). The enamel spots of track 2 have an average ^{88}Sr voltage of 0.575, a weighted average uncorrected $^{87}\text{Sr}/^{86}\text{Sr}$ value of 0.714 ± 0.010 , a weighted average corrected $^{87}\text{Sr}/^{86}\text{Sr}$ value of 0.71100 ± 0.010 and a weighted average $^{84}\text{Sr}/^{86}\text{Sr}$ value of 0.05689 ± 0.00023 ($n=2$). The dentine spots of track 2 have an average ^{88}Sr voltage of 0.569, a weighted average uncorrected $^{87}\text{Sr}/^{86}\text{Sr}$ value of 0.7106 ± 0.0013 , a weighted average corrected $^{87}\text{Sr}/^{86}\text{Sr}$ value of 0.70840 ± 0.0013 and a weighted average $^{84}\text{Sr}/^{86}\text{Sr}$ value of 0.05698 ± 0.00012 ($n=9$). Enamel values for track 1 are in the range of 0.713503 to 0.714008 (uncorrected), as well as 0.711134 to 0.711639 (corrected), and are very homogenous. Dentine values for track 1 are in the range of 0.707905 to 0.714936 (uncorrected), as well as 0.705660 to 0.712692 (corrected), and are very heterogeneous. Enamel values for track 2 are 0.713178 and 0.714865 (uncorrected), as well as 0.710809 and 0.712496 (corrected), and are somewhat heterogeneous. Dentine values for track 2 are in the range of 0.707841 to 0.712914 (uncorrected), as well as 0.705596 to 0.710669 (corrected), and are very heterogeneous. Detailed values for enamel and dentine for sample M045 are shown in Table A3.127, Figure A3.277 and Figure A3.278.

This sample has extremely heterogeneous dentine values, suggesting a complex history of amelogenesis. Enamel and dentine are, overall, considerably different, suggesting that this sample is a migrant to the area of

Rescoundudou. The values of enamel are relatively homogenous and both the uncorrected and corrected values encompass the wide range of values for the Middle Jurassic carbonate that includes the site of Rescoundudou. This unit is extremely heterogeneous with respect to strontium isotope composition, as discussed above with reference to sample M033. $^{84}\text{Sr}/^{86}\text{Sr}$ values have a weighted average value of 0.057004 ± 0.000081 , which is elevated compared to the ideal value of 0.0565.



Figure A3.276 LA-MC-ICPMS Track for Sample M045, Deer, Layer C1, Rescoundudou

Sample	Material	Track	Point	^{88}Sr Volts	$^{84}\text{Sr}/^{86}\text{Sr}$	$^{84}\text{Sr}/^{86}\text{Sr} 2\sigma$ Error	$^{87}\text{Sr}/^{86}\text{Sr}$	Corrected $^{87}\text{Sr}/^{86}\text{Sr}$	$^{87}\text{Sr}/^{86}\text{Sr} 2\sigma$ Error
M045	Enamel	1	1	0.477	0.057430	0.000621	0.714008	0.711639	0.000589
M045	Enamel	1	2	0.551	0.056929	0.000466	0.713696	0.711327	0.000528
M045	Enamel	1	3	0.528	0.057044	0.000278	0.713503	0.711134	0.000422
M045	Dentine	1	4	0.459	0.057114	0.000469	0.712941	0.710697	0.000682
M045	Dentine	1	5	0.398	0.057267	0.000672	0.714936	0.712692	0.000713
M045	Dentine	1	6	0.711	0.057238	0.000363	0.711451	0.709207	0.000470
M045	Dentine	1	7	0.661	0.057189	0.000563	0.711210	0.708965	0.000481
M045	Dentine	1	8	0.662	0.057050	0.000455	0.707905	0.705660	0.000471
M045	Dentine	1	9	0.653	0.056947	0.000244	0.709520	0.707276	0.000397
M045	Enamel	2	1	0.473	0.056929	0.000476	0.714865	0.712496	0.000572
M045	Enamel	2	2	0.677	0.056877	0.000265	0.713178	0.710809	0.000454
M045	Dentine	2	3	0.552	0.056879	0.000301	0.712823	0.710578	0.000548

M045	Dentine	2	4	0.381	0.057164	0.000563	0.711743	0.709499	0.000748
M045	Dentine	2	5	0.674	0.057149	0.000539	0.710817	0.708572	0.000450
M045	Dentine	2	6	0.557	0.057480	0.000545	0.708214	0.705970	0.000545
M045	Dentine	2	7	0.573	0.056938	0.000392	0.707841	0.705596	0.000569
M045	Dentine	2	8	0.816	0.056955	0.000236	0.709675	0.707431	0.000520
M045	Dentine	2	9	0.501	0.056956	0.000381	0.710164	0.707920	0.000392
M045	Dentine	2	10	0.517	0.057012	0.000369	0.712914	0.710669	0.000446
M045	Dentine	2	11	0.550	0.056854	0.000315	0.711045	0.708800	0.000515

Table A3.127 Detailed LA-MC-ICPMS Sr Isotope Results, Sample M044, Deer, Layer C1, Rescoundudou

Sample M45, Rescoundudou, France

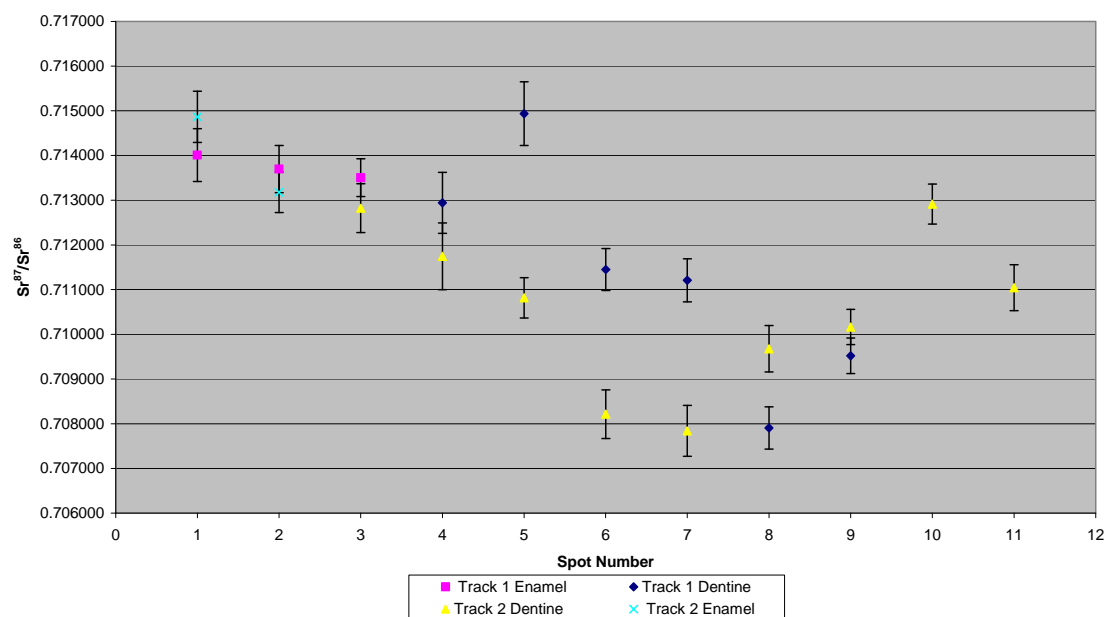


Figure A3.277 Detailed LA-MC-ICPMS Uncorrected Sr Isotope Results, Sample M044, Deer, Layer C1, Rescoundudou

Sample M45, Corrected Sr Values, Rescoundudou, France

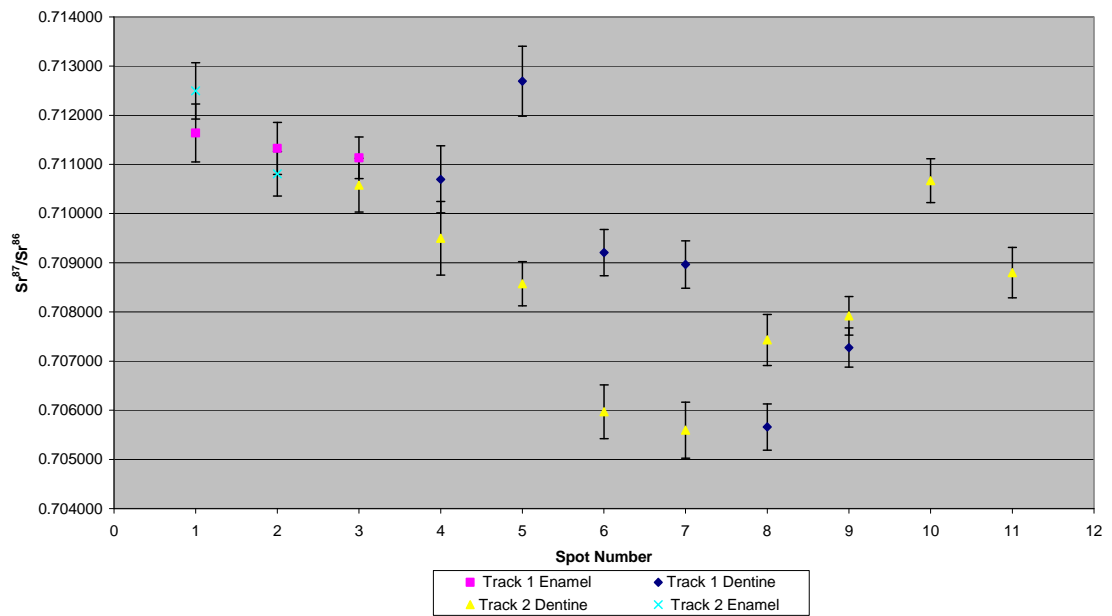


Figure A3.278 Detailed LA-MC-ICPMS Corrected Sr Isotope Results, Sample M044, Deer, Layer C1, Rescoundudou

Appendix Four: Tridacna Results

A4.2. Overview

As described in section 4.7.2, 631 Tridacna spots were collected during all LA-MC-ICPMS analysis to monitor any instrument inaccuracy. These values are summarised in Table 5.44 and Figure 5.27 and shown in detail in sections A4.3 through A4.19.

A4.3. Tridacna Spots Collected 29/11/2010

Start Time	Date	Pertains to Sample	^{88}Sr Volts	$^{84}\text{Sr}/^{86}\text{Sr}$	$^{84}\text{Sr}/^{86}\text{Sr} 2\sigma$ Error	$^{87}\text{Sr}/^{86}\text{Sr}$	$^{87}\text{Sr}/^{86}\text{Sr} 2\sigma$ Error
20:14:35:003	29/11/10	466	21.781	0.056416	0.000013	0.709173	0.000026
20:18:36:447	29/11/10	466	20.222	0.056419	0.000011	0.709185	0.000036
20:22:36:782	29/11/10	466	20.627	0.056431	0.000016	0.709178	0.000038
20:26:37:115	29/11/10	466	20.009	0.056448	0.000016	0.709164	0.000034
20:30:38:559	29/11/10	466	20.181	0.056419	0.000013	0.709153	0.000029
20:34:38:893	29/11/10	466	19.813	0.056416	0.000016	0.709149	0.000028
20:38:39:229	29/11/10	466	20.589	0.056407	0.000013	0.709167	0.000037
20:42:40:671	29/11/10	466	19.645	0.056404	0.000014	0.709187	0.000032
20:46:41:006	29/11/10	466	18.970	0.056410	0.000013	0.709161	0.000032
20:50:41:341	29/11/10	466	20.126	0.056442	0.000017	0.709116	0.000031
20:54:42:782	29/11/10	466	20.501	0.056430	0.000015	0.709158	0.000032
20:58:43:118	29/11/10	466	20.004	0.056412	0.000015	0.709154	0.000035
21:02:43:453	29/11/10	466	18.980	0.056397	0.000015	0.709171	0.000031
21:54:37:839	29/11/10	466	18.621	0.056418	0.000014	0.709178	0.000037
21:58:39:282	29/11/10	466	18.427	0.056437	0.000013	0.709172	0.000035
22:02:39:617	29/11/10	466	18.368	0.056436	0.000018	0.709156	0.000035
22:06:39:952	29/11/10	466	18.352	0.056423	0.000014	0.709146	0.000032
22:10:41:394	29/11/10	466	18.432	0.056404	0.000017	0.709132	0.000028

$^{87}\text{Sr}/^{86}\text{Sr}$ 2 σ Error	$^{87}\text{Sr}/^{86}\text{Sr}$	$^{84}\text{Sr}/^{86}\text{Sr}$ 2 σ Error	$^{84}\text{Sr}/^{86}\text{Sr}$ Error	Pertains to Sample	^{88}Sr Volts	Date	Start Time
0.000034	0.709181	0.000015	0.056381	466	18.079	29/11/10	22:14:41:730
0.000034	0.709152	0.000016	0.056394	466	19.108	29/11/10	22:18:42:064
0.000032	0.709162	0.000018	0.056402	466	18.306	29/11/10	22:22:43:506
0.000040	0.709161	0.000015	0.056414	466	18.797	29/11/10	22:26:43:842
0.000033	0.709158	0.000016	0.056404	466	20.760	29/11/10	22:30:44:177
0.000027	0.709127	0.000017	0.056389	466	21.364	29/11/10	22:34:44:512
0.000026	0.709157	0.000014	0.056375	466	21.199	29/11/10	22:38:45:954
0.000031	0.709166	0.000017	0.056403	263	20.923	29/11/10	22:59:39:529
0.000031	0.709176	0.000014	0.056361	263	19.420	29/11/10	23:03:39:864
0.000027	0.709185	0.000019	0.056386	263	17.798	29/11/10	23:07:41:306
0.000038	0.709154	0.000016	0.056384	263	17.556	29/11/10	23:11:41:641
0.000033	0.709169	0.000021	0.056402	263	18.653	29/11/10	23:15:41:976
0.000032	0.709163	0.000016	0.056381	263	19.264	29/11/10	23:19:43:420
0.000033	0.709169	0.000016	0.056368	263	19.480	29/11/10	23:23:43:753
0.000031	0.709177	0.000016	0.056359	263	19.615	29/11/10	23:27:44:088
0.000033	0.709167	0.000015	0.056363	263	19.704	29/11/10	23:31:44:424

Table A4.1 Detailed Tridacna Strontium Isotope Results Analysed 29/11/2010

A4.4. *Tridacna Spots Collected 30/11/2011*

$^{87}\text{Sr}/^{86}\text{Sr}$ 2 σ Error	$^{87}\text{Sr}/^{86}\text{Sr}$	$^{84}\text{Sr}/^{86}\text{Sr}$ 2 σ Error	$^{84}\text{Sr}/^{86}\text{Sr}$ Error	Pertains to Sample	^{88}Sr Volts	Date	Start Time
0.000034	0.709153	0.000018	0.056408	263	17.662	30/11/10	00:32:49:255
0.000031	0.709171	0.000019	0.056429	263	17.247	30/11/10	00:36:49:589
0.000039	0.709179	0.000018	0.056382	263	17.971	30/11/10	00:40:49:924
0.000039	0.709155	0.000015	0.056409	263	18.597	30/11/10	00:44:50:259
0.000033	0.709145	0.000017	0.056419	263	18.345	30/11/10	00:48:51:702
0.000031	0.709191	0.000017	0.056419	263	19.213	30/11/10	00:52:50:930
0.000035	0.709161	0.000017	0.056400	263	19.423	30/11/10	00:56:52:371
0.000037	0.709176	0.000016	0.056364	263	18.258	30/11/10	01:00:53:815
0.000030	0.709187	0.000020	0.056338	112	17.908	30/11/10	01:46:17:824
0.000037	0.709205	0.000016	0.056341	112	17.763	30/11/10	01:49:18:351
0.000034	0.709186	0.000014	0.056376	112	17.943	30/11/10	01:52:18:880
0.000033	0.709192	0.000020	0.056388	112	18.334	30/11/10	01:55:19:407
0.000033	0.709184	0.000015	0.056399	112	18.930	30/11/10	01:58:19:936

Start Time	Date	Pertains to Sample	^{88}Sr Volts	$^{84}\text{Sr}/^{86}\text{Sr}$	Error	$^{84}\text{Sr}/^{86}\text{Sr} 2\sigma$	$^{87}\text{Sr}/^{86}\text{Sr}$	Error	$^{87}\text{Sr}/^{86}\text{Sr} 2\sigma$
02:01:20:464	30/11/10	112	18.992	0.056374	0.000015	0.709184	0.000032		
02:04:20:993	30/11/10	112	19.069	0.056388	0.000015	0.709192	0.000038		
02:07:22:628	30/11/10	112	19.366	0.056348	0.000013	0.709161	0.000029		
02:10:23:156	30/11/10	112	18.259	0.056355	0.000017	0.709156	0.000030		
02:13:23:684	30/11/10	112	17.587	0.056337	0.000016	0.709180	0.000034		
02:16:24:213	30/11/10	112	19.041	0.056362	0.000016	0.709145	0.000027		
02:19:24:740	30/11/10	112	19.214	0.056379	0.000019	0.709157	0.000027		
02:22:25:269	30/11/10	112	18.806	0.056376	0.000013	0.709178	0.000036		
03:34:26:868	30/11/10	112	15.145	0.056403	0.000022	0.709162	0.000033		
03:37:27:397	30/11/10	112	16.314	0.056420	0.000023	0.709155	0.000032		
03:40:29:032	30/11/10	112	17.080	0.056371	0.000019	0.709180	0.000036		
03:43:29:559	30/11/10	112	16.995	0.056382	0.000016	0.709165	0.000037		
03:46:28:980	30/11/10	112	16.654	0.056370	0.000021	0.709161	0.000028		
03:49:30:617	30/11/10	112	16.879	0.056398	0.000019	0.709174	0.000027		
03:52:31:144	30/11/10	112	17.061	0.056375	0.000020	0.709163	0.000041		
03:55:31:673	30/11/10	112	17.483	0.056404	0.000019	0.709137	0.000034		
03:58:32:200	30/11/10	112	17.751	0.056385	0.000019	0.709191	0.000033		
04:01:33:837	30/11/10	112	18.357	0.056387	0.000017	0.709147	0.000034		
04:04:34:365	30/11/10	112	18.149	0.056354	0.000015	0.709158	0.000030		
04:07:34:893	30/11/10	112	17.665	0.056357	0.000016	0.709157	0.000038		
04:10:35:421	30/11/10	112	17.461	0.056353	0.000018	0.709147	0.000036		
05:10:44:923	30/11/10	861	15.093	0.056394	0.000022	0.709173	0.000038		
05:13:46:558	30/11/10	861	15.668	0.056364	0.000020	0.709166	0.000030		
05:16:47:085	30/11/10	861	16.347	0.056377	0.000016	0.709179	0.000039		
05:19:47:614	30/11/10	861	15.648	0.056335	0.000020	0.709185	0.000031		
05:22:48:141	30/11/10	861	15.450	0.056366	0.000019	0.709172	0.000035		
05:25:48:671	30/11/10	861	15.800	0.056361	0.000018	0.709183	0.000027		
05:28:49:199	30/11/10	861	15.558	0.056379	0.000032	0.709198	0.000032		
05:31:50:834	30/11/10	861	16.708	0.056364	0.000021	0.709177	0.000037		
05:34:51:362	30/11/10	861	16.948	0.056357	0.000018	0.709174	0.000030		
05:37:51:891	30/11/10	861	17.025	0.056369	0.000021	0.709179	0.000035		
05:40:52:418	30/11/10	861	17.629	0.056354	0.000015	0.709158	0.000031		
05:43:52:947	30/11/10	861	16.882	0.056354	0.000019	0.709158	0.000034		
05:46:53:475	30/11/10	861	16.721	0.056385	0.000020	0.709178	0.000035		
05:49:55:110	30/11/10	861	17.5771	0.056367	0.000016	0.709168	0.000035		
05:52:55:638	30/11/10	861	17.360	0.056377	0.000014	0.709174	0.000033		
05:55:56:167	30/11/10	861	16.683	0.056383	0.000019	0.709151	0.000037		
05:58:56:694	30/11/10	861	16.540	0.056362	0.000020	0.709163	0.000033		
06:01:58:331	30/11/10	861	16.283	0.056356	0.000018	0.709169	0.000035		

Start Time	Date	Pertains to Sample	⁸⁸ Sr Volts	⁸⁴ Sr/ ⁸⁶ Sr	⁸⁴ Sr/ ⁸⁶ Sr 2 σ	⁸⁷ Sr/ ⁸⁶ Sr	⁸⁷ Sr/ ⁸⁶ Sr 2 σ Error
06:04:58:858	30/11/10	861	16.296	0.056350	0.000017	0.709176	0.000032
06:07:59:387	30/11/10	861	15.701	0.056345	0.000019	0.709175	0.000035
07:16:53:812	30/11/10	861	13.827	0.056404	0.000022	0.709182	0.000041
07:19:54:342	30/11/10	861	15.168	0.056426	0.000020	0.709184	0.000037
07:22:54:870	30/11/10	861	15.409	0.056421	0.000019	0.709196	0.000034
07:25:55:398	30/11/10	861	15.248	0.056428	0.000021	0.709147	0.000034
07:28:55:926	30/11/10	861	15.440	0.056400	0.000025	0.709175	0.000033
07:31:56:454	30/11/10	861	15.790	0.056412	0.000017	0.709150	0.000038
07:34:58:088	30/11/10	861	15.579	0.056389	0.000022	0.709149	0.000037
07:37:58:618	30/11/10	861	16.108	0.056382	0.000018	0.709173	0.000032
07:40:59:145	30/11/10	861	15.330	0.056376	0.000021	0.709173	0.000035
07:43:59:674	30/11/10	861	16.002	0.056390	0.000019	0.709157	0.000031
07:47:00:202	30/11/10	861	15.840	0.056367	0.000019	0.709175	0.000036
07:50:01:838	30/11/10	861	15.801	0.056392	0.000019	0.709146	0.000037
07:53:02:365	30/11/10	861	15.449	0.056367	0.000018	0.709158	0.000035
07:56:02:894	30/11/10	861	15.830	0.056376	0.000020	0.709138	0.000027
07:59:03:421	30/11/10	861	15.775	0.056354	0.000016	0.709145	0.000037
08:02:03:950	30/11/10	861	14.987	0.056351	0.000021	0.709127	0.000041
08:05:04:477	30/11/10	861	15.113	0.056360	0.000028	0.709180	0.000040
08:08:05:006	30/11/10	861	15.003	0.056379	0.000020	0.709191	0.000039
08:11:06:641	30/11/10	861	14.292	0.056351	0.000020	0.709180	0.000033
08:14:07:170	30/11/10	861	13.731	0.056378	0.000019	0.709183	0.000034
08:17:07:699	30/11/10	861	13.121	0.056359	0.000024	0.709159	0.000046
08:20:08:226	30/11/10	861	12.898	0.056361	0.000026	0.709160	0.000046
08:23:08:753	30/11/10	861	12.916	0.056349	0.000026	0.709161	0.000037
13:21:06:989	30/11/10	861 E Traverse	15.015	0.056400	0.000018	0.709159	0.000045
13:24:07:516	30/11/10	861 E Traverse	14.299	0.056378	0.000020	0.709154	0.000029
13:27:08:046	30/11/10	861 E Traverse	14.027	0.056394	0.000019	0.709149	0.000042
13:30:08:574	30/11/10	861 E Traverse	13.179	0.056370	0.000020	0.709161	0.000043
13:33:10:209	30/11/10	861 E Traverse	13.223	0.056364	0.000026	0.709154	0.000038
13:36:10:736	30/11/10	861 E Traverse	13.482	0.056348	0.000023	0.709187	0.000063
13:39:10:157	30/11/10	861 E Traverse	13.219	0.056335	0.000020	0.709167	0.000035
13:42:11:793	30/11/10	861 E Traverse	13.406	0.056347	0.000021	0.709156	0.000039
13:45:12:322	30/11/10	861 E Traverse	13.356	0.056327	0.000021	0.709137	0.000031
13:48:11:742	30/11/10	861 E Traverse	12.675	0.056355	0.000030	0.709150	0.000043
13:51:13:378	30/11/10	861 E Traverse	12.232	0.056331	0.000028	0.709139	0.000039
13:54:13:906	30/11/10	861 E Traverse	12.215	0.056321	0.000021	0.709187	0.000048
16:57:37:259	30/11/10	861 E Traverse	13.310	0.056347	0.000024	0.709145	0.000038
17:00:37:786	30/11/10	861 E Traverse	11.950	0.056365	0.000024	0.709121	0.000035
17:03:38:315	30/11/10	861 E Traverse	11.600	0.056380	0.000031	0.709176	0.000037
17:06:38:842	30/11/10	861 E Traverse	11.702	0.056389	0.000025	0.709160	0.000040

						$^{87}\text{Sr}/^{86}\text{Sr} 2\sigma$	Error
						$^{87}\text{Sr}/^{86}\text{Sr}$	
						$^{84}\text{Sr}/^{86}\text{Sr} 2\sigma$	Error
17:09:39:371	30/11/10	861 E Traverse	11.305	0.056398	0.000030	0.709154	0.000050
17:12:39:900	30/11/10	861 E Traverse	10.900	0.056344	0.000023	0.709173	0.000041
17:15:41:535	30/11/10	861 E Traverse	10.628	0.056375	0.000026	0.709139	0.000047
17:18:42:062	30/11/10	861 E Traverse	10.920	0.056357	0.000035	0.709155	0.000046
17:21:42:592	30/11/10	861 E Traverse	10.407	0.056332	0.000028	0.709176	0.000042
17:24:43:120	30/11/10	861 E Traverse	10.572	0.056364	0.000030	0.709153	0.000039
17:27:43:648	30/11/10	861 E Traverse	10.700	0.056368	0.000030	0.709172	0.000051
17:30:45:282	30/11/10	861 E Traverse	11.016	0.056347	0.000031	0.709139	0.000044
17:33:45:812	30/11/10	861 E Traverse	10.958	0.056337	0.000024	0.709191	0.000055
17:36:46:338	30/11/10	861 E Traverse	11.028	0.056327	0.000025	0.709151	0.000042

Table A4.2 Detailed Tridacna Strontium Isotope Results Analysed 30/11/2010

A4.5. *Tridacna Spots Collected 10/02/2011*

						$^{87}\text{Sr}/^{86}\text{Sr} 2\sigma$	Error
						$^{87}\text{Sr}/^{86}\text{Sr}$	
						$^{84}\text{Sr}/^{86}\text{Sr} 2\sigma$	Error
14:08:56:746	10/02/11	373E	8.937	0.056671	0.000028	0.709169	0.000046
14:14:57:802	10/02/11	373E	8.782	0.056649	0.000025	0.709142	0.000040
14:20:57:750	10/02/11	373E	8.999	0.056690	0.000024	0.709186	0.000043
14:27:01:022	10/02/11	373E	8.683	0.056672	0.000025	0.709183	0.000050
14:32:58:756	10/02/11	373E	9.001	0.056676	0.000023	0.709177	0.000048
14:51:46:226	10/02/11	373E	6.211	0.055675	0.000052	0.709308	0.000058
14:57:47:283	10/02/11	373E	7.061	0.056013	0.000040	0.709229	0.000065
15:03:42:802	10/02/11	373E	7.189	0.056099	0.000034	0.709283	0.000043
15:09:43:858	10/02/11	373E	7.416	0.056184	0.000033	0.709246	0.000054
15:15:49:345	10/02/11	373E	7.397	0.056290	0.000026	0.709212	0.000078
15:42:18:332	10/02/11	1557	6.907	0.056575	0.000027	0.709155	0.000059
15:49:25:839	10/02/11	1557	6.159	0.056574	0.000034	0.709210	0.000070
15:56:25:595	10/02/11	1557	6.354	0.056519	0.000042	0.709228	0.000058
16:03:26:460	10/02/11	1557	6.638	0.056599	0.000027	0.709201	0.000051
16:10:27:322	10/02/11	1557	6.682	0.056610	0.000035	0.709167	0.000053
16:46:14:834	10/02/11	1557	5.179	0.055795	0.000054	0.709266	0.000069
16:53:10:158	10/02/11	1557	5.644	0.056032	0.000056	0.709247	0.000064
17:00:16:561	10/02/11	1557	5.520	0.056146	0.000051	0.709241	0.000072

$^{87}\text{Sr}/^{86}\text{Sr}$ 2 σ	$^{87}\text{Sr}/^{86}\text{Sr}$ Error
$^{87}\text{Sr}/^{86}\text{Sr}$	
$^{84}\text{Sr}/^{86}\text{Sr}$ 2 σ	$^{84}\text{Sr}/^{86}\text{Sr}$ Error
0.709263	0.000067
0.709161	0.000060
0.709315	0.000152
0.709238	0.000079
0.709158	0.000063
0.709215	0.000054
0.709172	0.000070
0.709224	0.000084
0.709199	0.000084
0.709205	0.000065
0.709134	0.000065
0.709152	0.000077
0.709203	0.000055
0.709169	0.000056
0.709201	0.000079
0.709214	0.000050
0.709169	0.000075
0.709181	0.000079
0.709194	0.000100
0.709150	0.000074
0.709135	0.000071
0.709115	0.000064

Table A4.3 Detailed Tridacna Strontium Isotope Results Analysed 10/02/2011

A4.6. *Tridacna* Spots Collected 11/02/2011

Start Time	Date	Pertains to Sample	^{88}Sr Volts	$^{84}\text{Sr}/^{86}\text{Sr}$	$^{84}\text{Sr}/^{86}\text{Sr} 2\sigma$ Error	$^{87}\text{Sr}/^{86}\text{Sr}$	$^{87}\text{Sr}/^{86}\text{Sr} 2\sigma$ Error
12:48:01:980	11/02/11	851E	13.391	0.056420	0.000018	0.709165	0.000038
12:54:57:306	11/02/11	851E	12.963	0.056394	0.000025	0.709166	0.000038
13:01:58:170	11/02/11	851E	12.406	0.056439	0.000017	0.709184	0.000041
13:08:59:032	11/02/11	851E	12.887	0.056494	0.000022	0.709151	0.000038
13:15:59:895	11/02/11	851E	12.786	0.056443	0.000018	0.709172	0.000040
16:33:29:408	11/02/11	851E	10.138	0.056257	0.000035	0.709185	0.000035
16:40:30:272	11/02/11	851E	9.863	0.056247	0.000034	0.709207	0.000039
16:47:36:673	11/02/11	851E	9.639	0.056232	0.000028	0.709210	0.000054
16:54:31:999	11/02/11	851E	11.877	0.056205	0.000030	0.709221	0.000105
17:01:32:861	11/02/11	851E	10.648	0.056181	0.000025	0.709183	0.000039
17:22:48:726	11/02/11	851D	9.482	0.056297	0.000028	0.709191	0.000048
17:29:44:052	11/02/11	851D	10.236	0.056311	0.000028	0.709175	0.000050
17:36:43:808	11/02/11	851D	11.426	0.056298	0.000023	0.709221	0.000050
17:43:46:885	11/02/11	851D	11.968	0.056297	0.000026	0.709148	0.000042
17:50:45:533	11/02/11	851D	11.426	0.056250	0.000027	0.709163	0.000041
21:08:16:153	11/02/11	851D	10.157	0.056282	0.000025	0.709209	0.000042
21:19:17:351	11/02/11	851D	10.468	0.056307	0.000022	0.709183	0.000043
21:30:17:441	11/02/11	851D	10.865	0.056293	0.000023	0.709161	0.000045
21:41:18:640	11/02/11	851D	11.115	0.056290	0.000023	0.709170	0.000040
21:52:24:268	11/02/11	851D	10.647	0.056242	0.000032	0.709197	0.000050
23:05:04:124	11/02/11	372D	11.638	0.056362	0.000021	0.709179	0.000041
23:12:04:986	11/02/11	372D	11.327	0.056321	0.000027	0.709229	0.000038
23:19:05:850	11/02/11	372D	11.580	0.056313	0.000022	0.709188	0.000043
23:26:06:713	11/02/11	372D	10.979	0.056285	0.000030	0.709155	0.000046
23:33:07:575	11/02/11	372D	11.868	0.056270	0.000024	0.709170	0.000039
00:22:53:489	11/02/11	372D	9.737	0.056294	0.000030	0.709185	0.000050

Table A4.4 Detailed Tridacna Strontium Isotope Results Analysed 11/02/2011

A4.7. *Tridacna* Spots Collected 12/02/2011

Start Time	Date	Pertains to Sample	^{88}Sr Volts	$^{84}\text{Sr}/^{86}\text{Sr}$	$^{84}\text{Sr}/^{86}\text{Sr} 2\sigma$ Error	$^{87}\text{Sr}/^{86}\text{Sr}$	$^{87}\text{Sr}/^{86}\text{Sr} 2\sigma$ Error
00:29:54:352	12/02/11	372D	10.217	0.056293	0.000033	0.709148	0.000048
00:36:55:216	12/02/11	372D	9.091	0.056276	0.000035	0.709167	0.000042
00:43:56:078	12/02/11	372D	9.578	0.056287	0.000028	0.709154	0.000046
00:50:56:941	12/02/11	372D	9.256	0.056254	0.000026	0.709158	0.000046
02:11:45:542	12/02/11	371E	11.882	0.056338	0.000027	0.709221	0.000039
02:18:39:759	12/02/11	371E	10.877	0.056351	0.000028	0.709207	0.000054
02:25:40:623	12/02/11	371E	10.488	0.056284	0.000034	0.709190	0.000045
02:32:41:486	12/02/11	371E	10.055	0.056247	0.000028	0.709195	0.000045
02:39:42:350	12/02/11	371E	10.558	0.056289	0.000033	0.709241	0.000042
04:04:35:901	12/02/11	371E	9.290	0.056430	0.000037	0.709202	0.000044
04:11:36:765	12/02/11	371E	8.988	0.056404	0.000035	0.709226	0.000048
04:18:37:628	12/02/11	371E	8.841	0.056381	0.000029	0.709199	0.000040
04:25:38:490	12/02/11	371E	8.838	0.056333	0.000036	0.709202	0.000053
04:32:39:354	12/02/11	371E	8.610	0.056273	0.000041	0.709203	0.000054
05:29:33:028	12/02/11	370E	10.062	0.056296	0.000031	0.709207	0.000042
05:36:33:891	12/02/11	370E	9.747	0.056327	0.000032	0.709175	0.000037
05:43:33:645	12/02/11	370E	9.469	0.056313	0.000033	0.709193	0.000046
05:50:34:509	12/02/11	370E	9.645	0.056322	0.000027	0.709197	0.000042
05:57:35:373	12/02/11	370E	8.921	0.056357	0.000030	0.709182	0.000045
07:08:21:661	12/02/11	370E	8.930	0.056471	0.000029	0.709146	0.000041
07:15:22:525	12/02/11	370E	8.870	0.056376	0.000030	0.709221	0.000048
07:22:23:388	12/02/11	370E	9.269	0.056326	0.000036	0.709295	0.000064
07:29:24:250	12/02/11	370E	8.955	0.056323	0.000035	0.709191	0.000052
07:36:25:112	12/02/11	370E	8.290	0.056323	0.000035	0.709229	0.000051

Table A4.5 Detailed Tridacna Strontium Isotope Results Analysed 12/02/2011

A4.8. *Tridacna* Spots Collected 7/04/2011

Start Time	Date	Pertains to Sample	⁸⁸ Sr Volts	⁸⁴ Sr/ ⁸⁶ Sr	⁸⁴ Sr/ ⁸⁶ Sr 2σ Error	⁸⁷ Sr/ ⁸⁶ Sr	⁸⁷ Sr/ ⁸⁶ Sr 2σ Error
17:26:30:325	7/04/11	852E	35.494	0.056517	0.000019	0.709256	0.000096
17:33:31:187	7/04/11	852E	33.116	0.056488	0.000018	0.709295	0.000138
17:40:37:588	7/04/11	852E	30.518	0.056478	0.000023	0.709305	0.000095
17:47:34:022	7/04/11	852E	30.134	0.056472	0.000020	0.709381	0.000127
17:54:34:884	7/04/11	852E	33.216	0.056456	0.000019	0.709422	0.000100
22:36:02:579	7/04/11	852E	19.443	0.056185	0.000016	0.710266	0.000256
22:43:12:304	7/04/11	852E	18.835	0.056167	0.000014	0.710338	0.000227
22:50:13:167	7/04/11	852E	18.842	0.056165	0.000014	0.710362	0.000252
22:57:08:492	7/04/11	852E	18.711	0.056181	0.000011	0.710217	0.000180
23:04:09:355	7/04/11	852E	19.419	0.056177	0.000014	0.710209	0.000238
23:06:18:937	7/04/11	852E	17.464	0.056167	0.000008	0.710258	0.000146

Table A4.6 Detailed Tridacna Strontium Isotope Results Analysed 07/04/2011

A4.9. *Tridacna* Spots Collected 8/04/2011

Start Time	Date	Pertains to Sample	^{88}Sr Volts	$^{84}\text{Sr}/^{86}\text{Sr}$	$^{84}\text{Sr}/^{86}\text{Sr}$ 2 σ Error	$^{87}\text{Sr}/^{86}\text{Sr}$	$^{87}\text{Sr}/^{86}\text{Sr}$ 2 σ Error
00:43:11:479	8/04/11	852D	19.485	0.056288	0.000012	0.710323	0.000319
00:50:12:342	8/04/11	852D	19.364	0.056299	0.000011	0.710303	0.000216
00:57:13:206	8/04/11	852D	18.818	0.056317	0.000011	0.710154	0.000210
01:04:11:855	8/04/11	852D	18.629	0.056318	0.000010	0.710193	0.000154
01:11:09:394	8/04/11	852D	18.880	0.056302	0.000014	0.710174	0.000197
06:13:52:970	8/04/11	852D	13.340	0.056264	0.000019	0.710574	0.000315
06:20:53:832	8/04/11	852D	13.205	0.056264	0.000016	0.710362	0.000228
06:27:54:696	8/04/11	852D	13.611	0.056255	0.000018	0.710331	0.000223
06:34:54:450	8/04/11	852D	13.235	0.056282	0.000022	0.710248	0.000266
06:41:55:315	8/04/11	852D	12.810	0.056259	0.000026	0.710369	0.000284
06:43:59:358	8/04/11	852D	12.913	0.056279	0.000007	0.710314	0.000167
11:44:33:016	8/04/11	853E	13.132	0.056469	0.000024	0.709015	0.000396
11:51:28:342	8/04/11	853E	13.555	0.056493	0.000016	0.709054	0.000354
11:58:29:206	8/04/11	853E	13.130	0.056467	0.000015	0.708967	0.000306
12:05:35:607	8/04/11	853E	11.643	0.056465	0.000021	0.709074	0.000405
12:12:40:900	8/04/11	853E	11.239	0.056462	0.000022	0.709103	0.000202
16:53:33:151	8/04/11	853E	10.666	0.056484	0.000020	0.709064	0.000350
17:00:34:013	8/04/11	853E	9.780	0.056453	0.000017	0.709040	0.000228
17:07:33:769	8/04/11	853E	10.332	0.056456	0.000018	0.709037	0.000227
17:14:32:417	8/04/11	853E	10.489	0.056461	0.000021	0.709044	0.000285
17:21:41:033	8/04/11	853E	9.815	0.056439	0.000020	0.709045	0.000312
18:21:03:417	8/04/11	853D	10.660	0.056491	0.000018	0.709105	0.000375
18:27:58:743	8/04/11	853D	10.070	0.056479	0.000022	0.709088	0.000273
18:34:59:605	8/04/11	853D	10.453	0.056478	0.000022	0.709104	0.000307
18:42:00:469	8/04/11	853D	10.649	0.056475	0.000016	0.709062	0.000262
18:49:01:332	8/04/11	853D	10.113	0.056462	0.000018	0.709046	0.000269
23:02:03:420	8/04/11	853D	8.739	0.056449	0.000026	0.709125	0.000245
23:09:08:713	8/04/11	853D	8.579	0.056428	0.000019	0.709105	0.000318
23:16:09:577	8/04/11	853D	8.909	0.056444	0.000025	0.709134	0.000211
23:23:04:901	8/04/11	853D	9.300	0.056460	0.000025	0.709072	0.000199
23:30:05:766	8/04/11	853D	9.152	0.056430	0.000018	0.709032	0.000175

Table A4.7 Detailed Tridacna Strontium Isotope Results Analysed 08/04/2011

A4.10. *Tridacna Spots Collected 9/04/2011*

Start Time	Date	Pertains to Sample	^{88}Sr Volts	$^{84}\text{Sr}/^{86}\text{Sr}$	$^{84}\text{Sr}/^{86}\text{Sr} 2\sigma$ Error	$^{87}\text{Sr}/^{86}\text{Sr}$	$^{87}\text{Sr}/^{86}\text{Sr} 2\sigma$ Error
14:55:19:390	9/04/11	M001-M004	8.452	0.056603	0.000037	0.709182	0.000141
15:02:21:361	9/04/11	M001-M004	7.083	0.056577	0.000039	0.709151	0.000126
16:08:14:153	9/04/11	M001-M004	6.622	0.056583	0.000037	0.709239	0.000096
16:15:13:908	9/04/11	M001-M004	7.589	0.056566	0.000032	0.709180	0.000110
17:00:03:003	9/04/11	M001-M004	6.226	0.056580	0.000042	0.709185	0.000120
17:18:40:506	9/04/11	M001-M004	6.230	0.056571	0.000041	0.709178	0.000093
18:17:33:543	9/04/11	M001-M004	5.466	0.056587	0.000046	0.709217	0.000083
18:24:34:407	9/04/11	M001-M004	5.640	0.056616	0.000046	0.709193	0.000092
19:23:21:906	9/04/11	M001-M004	5.431	0.056621	0.000041	0.709195	0.000085
19:45:55:056	9/04/11	557E, 558E, 564D, 565, 567	13.302	0.056488	0.000026	0.709118	0.000068
19:52:57:028	9/04/11	557E, 558E, 564D, 565, 567	14.245	0.056476	0.000024	0.709119	0.000066
20:37:56:089	9/04/11	557E, 558E, 564D, 565, 567	11.877	0.056483	0.000026	0.709077	0.000078
20:44:56:953	9/04/11	557E, 558E, 564D, 565, 567	13.132	0.056475	0.000026	0.709103	0.000081
21:55:48:779	9/04/11	557E, 558E, 564D, 565, 567	9.709	0.056502	0.000026	0.709090	0.000065
22:14:24:068	9/04/11	557E, 558E, 564D, 565, 567	10.351	0.056472	0.000030	0.709089	0.000062
23:11:11:952	9/04/11	557E, 558E, 564D, 565, 567	8.726	0.056461	0.000031	0.709119	0.000065
23:18:13:923	9/04/11	557E, 558E, 564D, 565, 567	8.807	0.056676	0.000307	0.710100	0.001454

Table A4.8 Detailed Tridacna Strontium Isotope Results Analysed 09/04/2011

A4.11. Tridacna Spots Collected 10/04/2011

Start Time	Date	Pertains to Sample	^{88}Sr Volts	$^{84}\text{Sr}/^{86}\text{Sr}$	$^{84}\text{Sr}/^{86}\text{Sr} 2\sigma$ Error	$^{87}\text{Sr}/^{86}\text{Sr}$	$^{87}\text{Sr}/^{86}\text{Sr} 2\sigma$ Error
00:14:00:893	10/04/11	557E, 558E, 564D, 565, 567	8.026	0.056451	0.000039	0.709100	0.000085
00:21:01:756	10/04/11	557E, 558E, 564D, 565, 567	9.358	0.056437	0.000033	0.709092	0.000103
01:06:08:572	10/04/11	557E, 558E, 564D, 565, 567	10.171	0.056451	0.000032	0.709143	0.000092
01:24:43:860	10/04/11	557E, 558E, 564D, 565, 567	9.705	0.056446	0.000026	0.709144	0.000083
03:11:57:841	10/04/11	554E, 556E, 557E, 561, 563	13.755	0.056444	0.000082	0.709189	0.000061
03:18:58:703	10/04/11	554E, 556E, 557E, 561, 563	13.440	0.056480	0.000020	0.709133	0.000063
04:25:32:476	10/04/11	554E, 556E, 557E, 561, 563	14.882	0.056481	0.000039	0.709012	0.000637
04:32:33:338	10/04/11	554E, 556E, 557E, 561, 563	13.489	0.056511	0.000043	0.709957	0.000656
05:18:03:411	10/04/11	554E, 556E, 557E, 561, 563	11.001	0.056500	0.000049	0.709354	0.000557
05:25:04:276	10/04/11	554E, 556E, 557E, 561, 563	11.179	0.056598	0.000047	0.709607	0.000557
06:10:38:779	10/04/11	554E, 556E, 557E, 561, 563	11.516	0.056502	0.000046	0.709273	0.000604
06:17:45:180	10/04/11	554E, 556E, 557E, 561, 563	11.597	0.056554	0.000052	0.708894	0.000705
07:03:13:039	10/04/11	554E, 556E, 557E, 561, 563	12.035	0.056496	0.000059	0.709003	0.000702
07:10:18:332	10/04/11	554E, 556E, 557E, 561, 563	11.882	0.056441	0.000042	0.709139	0.000490
08:42:32:684	10/04/11	554E, 556E, 557E, 561, 563	10.232	0.056368	0.000051	0.709189	0.000621
08:49:29:117	10/04/11	554E, 556E, 557E, 561, 563	12.238	0.056480	0.000051	0.709002	0.000675

Table A4.9 Detailed Tridacna Strontium Isotope Results Analysed 10/04/2011

A4.12. *Tridacna* Spots Collected 13/05/2011

Start Time	Date	Pertains to Sample	^{88}Sr Volts	$^{84}\text{Sr}/^{86}\text{Sr}$	$^{84}\text{Sr}/^{86}\text{Sr} 2\sigma$ Error	$^{87}\text{Sr}/^{86}\text{Sr}$	$^{87}\text{Sr}/^{86}\text{Sr} 2\sigma$ Error
04:21:12:176	13/05/11	M001-M004	15.051	0.056566	0.000014	0.709135	0.000055
04:23:12:898	13/05/11	M001-M004	16.409	0.056531	0.000023	0.709162	0.000137
04:25:13:618	13/05/11	M001-M004	13.205	0.056521	0.000023	0.709166	0.000072
05:27:10:506	13/05/11	M001-M004	7.101	0.056246	0.000044	0.709260	0.000118
05:29:11:227	13/05/11	M001-M004	7.269	0.056289	0.000038	0.709200	0.000108
05:31:13:055	13/05/11	M001-M004	7.421	0.056282	0.000041	0.709219	0.000147
06:06:16:975	13/05/11	M006-M010	6.558	0.056486	0.000035	0.709179	0.000115
06:08:17:696	13/05/11	M006-M010	6.502	0.056530	0.000032	0.709267	0.000105
06:10:18:417	13/05/11	M006-M010	6.698	0.056516	0.000028	0.709265	0.000143
09:03:59:213	13/05/11	M006-M010	4.927	0.056480	0.000040	0.709245	0.000167
09:05:59:934	13/05/11	M006-M010	4.746	0.056445	0.000036	0.709252	0.000155
09:08:00:656	13/05/11	M006-M010	4.613	0.056478	0.000038	0.709229	0.000150
09:51:02:253	13/05/11	2421, 2417, 2418, 2422	5.130	0.056528	0.000042	0.709226	0.000170
09:53:04:082	13/05/11	2421, 2417, 2418, 2422	4.784	0.056459	0.000061	0.709260	0.000147
09:55:04:804	13/05/11	2421, 2417, 2418, 2422	4.865	0.056454	0.000059	0.709220	0.000135
11:10:58:987	13/05/11	2421, 2417, 2418, 2422	4.658	0.056516	0.000046	0.709175	0.000165
11:12:59:709	13/05/11	2421, 2417, 2418, 2422	4.757	0.056591	0.000138	0.709459	0.000446
11:15:00:430	13/05/11	2421, 2417, 2418, 2422	4.701	0.056522	0.000044	0.709185	0.000141
12:21:04:299	13/05/11	2421, 2417, 2418, 2422	4.705	0.056510	0.000049	0.709299	0.000166
12:23:05:019	13/05/11	2421, 2417, 2418, 2422	4.576	0.056499	0.000051	0.709224	0.000130
12:25:05:742	13/05/11	2421, 2417, 2418, 2422	4.729	0.056547	0.000044	0.709189	0.000126
13:16:58:756	13/05/11	2425C, 2425B, 2425A	7.450	0.056468	0.000035	0.709100	0.000118
13:18:59:477	13/05/11	2425C, 2425B, 2425A	7.039	0.056494	0.000033	0.709120	0.000082
13:21:00:199	13/05/11	2425C, 2425B, 2425A	7.125	0.056443	0.000034	0.709092	0.000082
14:15:04:168	13/05/11	2425C, 2425B, 2425A	6.898	0.056469	0.000037	0.709162	0.000086
14:17:03:782	13/05/11	2425C, 2425B, 2425A	7.598	0.056443	0.000026	0.709126	0.000088

$^{87}\text{Sr}/^{86}\text{Sr}$ 2 σ	$^{87}\text{Sr}/^{86}\text{Sr}$ Error							
$^{84}\text{Sr}/^{86}\text{Sr}$ 2 σ	$^{84}\text{Sr}/^{86}\text{Sr}$ Error							
Start Time	Date	Pertains to Sample	88 Sr Volts	86 Sr	87 Sr	84 Sr	87 Sr/86 Sr 2 σ	87 Sr/86 Sr Error
14:19:04:503	13/05/11	2425C, 2425B, 2425A	7.609	0.056477	0.000033	0.709166	0.000157	
15:47:11:874	13/05/11	2425C, 2425B, 2425A	6.516	0.056426	0.000031	0.709085	0.000077	
15:49:12:595	13/05/11	2425C, 2425B, 2425A	7.295	0.056413	0.000033	0.709130	0.000102	
15:51:13:316	13/05/11	2425C, 2425B, 2425A	7.566	0.056432	0.000038	0.709091	0.000142	
16:53:14:633	13/05/11	2425C, 2425B, 2425A	7.389	0.056423	0.000029	0.709093	0.000061	
16:55:15:355	13/05/11	2425C, 2425B, 2425A	6.864	0.056416	0.000028	0.709082	0.000069	
16:57:14:967	13/05/11	2425C, 2425B, 2425A	6.456	0.056451	0.000034	0.709068	0.000082	

Table A4.10 Detailed Tridacna Strontium Isotope Results Analysed 13/05/2011

A4.13. *Tridacna* Spots Collected 14/05/2011

Start Time	Date	Pertains to Sample	^{88}Sr Volts	$^{84}\text{Sr}/^{86}\text{Sr}$	$^{84}\text{Sr}/^{86}\text{Sr} 2\sigma$ Error	$^{87}\text{Sr}/^{86}\text{Sr}$	$^{87}\text{Sr}/^{86}\text{Sr} 2\sigma$ Error
14:24:17:006	14/05/11	2424, 2423, 2419, 2420	7.768	0.056500	0.000025	0.709082	0.000277
14:26:15:512	14/05/11	2424, 2423, 2419, 2420	8.504	0.056495	0.000031	0.709043	0.000275
14:28:16:233	14/05/11	2424, 2423, 2419, 2420	8.723	0.056488	0.000027	0.708993	0.000216
15:14:16:210	14/05/11	2424, 2423, 2419, 2420	6.605	0.056468	0.000037	0.709027	0.000246
15:16:18:039	14/05/11	2424, 2423, 2419, 2420	6.828	0.056476	0.000028	0.709060	0.000232
15:18:18:760	14/05/11	2424, 2423, 2419, 2420	6.933	0.056472	0.000030	0.709067	0.000254
16:26:32:210	14/05/11	2424, 2423, 2419, 2420	6.042	0.056388	0.000037	0.709021	0.000227
16:28:32:930	14/05/11	2424, 2423, 2419, 2420	6.214	0.056434	0.000030	0.709021	0.000165
16:30:34:760	14/05/11	2424, 2423, 2419, 2420	5.998	0.056416	0.000035	0.709038	0.000242
17:28:06:947	14/05/11	2424, 2423, 2419, 2420	5.273	0.056350	0.000046	0.709004	0.000286
17:30:07:667	14/05/11	2424, 2423, 2419, 2420	5.536	0.056378	0.000033	0.708971	0.000360
17:32:08:390	14/05/11	2424, 2423, 2419, 2420	5.469	0.056359	0.000036	0.709054	0.000320

Table A4.11 Detailed Tridacna Strontium Isotope Results Analysed 14/05/2011

A4.14. Tridacna Spots Collected 15/05/2011

Start Time	Date	Pertains to Sample	88Sr Volts	$^{84}\text{Sr}/^{86}\text{Sr}$	$^{84}\text{Sr}/^{86}\text{Sr}$ 2 σ Error	$^{87}\text{Sr}/^{86}\text{Sr}$	$^{87}\text{Sr}/^{86}\text{Sr}$ 2 σ Error
00:16:33:358	15/05/11	592, 593, 595	3.309	0.056522	0.000172	0.709221	0.000250
00:18:34:079	15/05/11	592, 593, 595	3.997	0.056414	0.000063	0.709080	0.000279
00:20:40:338	15/05/11	592, 593, 595	3.948	0.056371	0.000062	0.709062	0.000392
02:31:10:608	15/05/11	592, 593, 595	4.113	0.056567	0.000044	0.709032	0.000260
02:33:11:328	15/05/11	592, 593, 595	4.174	0.056553	0.000076	0.709037	0.000320
02:35:12:051	15/05/11	592, 593, 595	4.225	0.056599	0.000048	0.709024	0.000343
03:59:29:051	15/05/11	592, 593, 595	4.534	0.056550	0.000048	0.709029	0.000281
04:01:29:772	15/05/11	592, 593, 595	4.917	0.056522	0.000044	0.708976	0.000393
04:03:30:493	15/05/11	592, 593, 595	4.980	0.056561	0.000039	0.708933	0.000481
05:01:35:903	15/05/11	592, 593, 595	4.487	0.056598	0.000108	0.709026	0.000328
05:03:36:624	15/05/11	592, 593, 595	4.331	0.056536	0.000044	0.709015	0.000281
05:05:37:345	15/05/11	592, 593, 595	4.528	0.056536	0.000047	0.708967	0.000344
05:54:22:342	15/05/11	592, 593, 595	4.205	0.056555	0.000047	0.708957	0.000300
05:56:23:062	15/05/11	592, 593, 595	4.235	0.056548	0.000051	0.709030	0.000279
05:58:23:783	15/05/11	592, 593, 595	4.588	0.056553	0.000038	0.708917	0.000307
06:42:46:296	15/05/11	592, 593, 595	4.366	0.056490	0.000044	0.709015	0.000387
06:44:47:016	15/05/11	592, 593, 595	4.554	0.056476	0.000045	0.708997	0.000380
06:46:47:737	15/05/11	592, 593, 595	4.716	0.056506	0.000042	0.708990	0.000359
07:12:34:962	15/05/11	592, 593, 595	4.566	0.056584	0.000061	0.709057	0.000362
07:14:35:684	15/05/11	592, 593, 595	4.666	0.056602	0.000046	0.709027	0.000310
07:16:36:404	15/05/11	592, 593, 595	4.617	0.056563	0.000034	0.708940	0.000302
07:26:14:536	15/05/11	592, 593, 595	4.5250	0.056511	0.000050	0.709052	0.000283
07:28:15:259	15/05/11	592, 593, 595	4.255	0.056523	0.000053	0.709038	0.000409
07:30:15:980	15/05/11	592, 593, 595	4.504	0.056492	0.000058	0.708973	0.000340
09:03:35:778	15/05/11	M011-M014	4.656	0.056514	0.000045	0.708985	0.000310
09:05:36:499	15/05/11	M011-M014	4.655	0.056550	0.000052	0.708955	0.000236
09:07:37:220	15/05/11	M011-M014	4.622	0.056506	0.000046	0.708916	0.000271
09:53:40:518	15/05/11	M011-M014	4.141	0.056428	0.000060	0.709071	0.000234
09:55:41:240	15/05/11	M011-M014	4.201	0.056496	0.000054	0.708967	0.000229
09:57:41:962	15/05/11	M011-M014	3.943	0.056471	0.000050	0.708988	0.000299
10:59:46:600	15/05/11	M011-M014	3.610	0.056442	0.000055	0.709110	0.000341
11:01:48:429	15/05/11	M011-M014	3.582	0.056470	0.000056	0.709070	0.000285
11:03:49:150	15/05/11	M011-M014	3.788	0.056477	0.000059	0.709019	0.000272
12:13:59:999	15/05/11	M011-M014	3.757	0.056473	0.000058	0.708994	0.000249
12:16:00:720	15/05/11	M011-M014	3.747	0.056459	0.000058	0.709057	0.000335
12:18:01:440	15/05/11	M011-M014	3.857	0.056426	0.000070	0.709027	0.000445
13:38:18:111	15/05/11	M011-M014	3.378	0.056447	0.000062	0.709095	0.000307

Start Time	Date	Pertains to Sample	^{88}Sr Volts	$^{84}\text{Sr}/^{86}\text{Sr}$	Error	$^{87}\text{Sr}/^{86}\text{Sr}$	Error	$^{87}\text{Sr}/^{86}\text{Sr} 2\sigma$
13:40:18:832	15/05/11	M011-M014	3.434	0.056374	0.000070	0.709032	0.000282	
13:42:20:661	15/05/11	M011-M014	3.288	0.056414	0.000058	0.708988	0.000296	
14:36:53:684	15/05/11	M015-M018	3.489	0.056544	0.000059	0.708944	0.000288	
14:38:59:943	15/05/11	M015-M018	3.218	0.056546	0.000063	0.708947	0.000294	
14:41:00:664	15/05/11	M015-M018	3.227	0.056546	0.000071	0.708956	0.000315	
15:23:14:704	15/05/11	M015-M018	3.000	0.056558	0.000176	0.709067	0.000562	
15:25:15:426	15/05/11	M015-M018	2.946	0.056477	0.000080	0.708832	0.000321	
15:27:16:147	15/05/11	M015-M018	3.240	0.056599	0.000074	0.708996	0.000269	
16:31:40:337	15/05/11	M015-M018	2.929	0.056431	0.000091	0.708850	0.000389	
16:33:41:058	15/05/11	M015-M018	2.936	0.056410	0.000077	0.708964	0.000366	
16:35:41:779	15/05/11	M015-M018	2.909	0.056509	0.000061	0.708952	0.000373	
17:37:22:055	15/05/11	M015-M018	2.825	0.056458	0.000071	0.708958	0.000307	
17:39:22:776	15/05/11	M015-M018	2.818	0.056491	0.000049	0.708872	0.000330	
17:41:23:496	15/05/11	M015-M018	2.925	0.056461	0.000063	0.708990	0.000271	
18:27:36:851	15/05/11	M019-M022	2.889	0.056544	0.000069	0.709057	0.000316	
18:29:37:572	15/05/11	M019-M022	3.029	0.056501	0.000053	0.709089	0.000294	
18:31:38:295	15/05/11	M019-M022	3.163	0.056548	0.000058	0.709107	0.000275	
19:25:22:329	15/05/11	M019-M022	2.805	0.056516	0.000073	0.709153	0.000224	
19:27:23:051	15/05/11	M019-M022	2.879	0.056493	0.000063	0.709005	0.000195	
19:29:18:235	15/05/11	M019-M022	3.019	0.056500	0.000061	0.709023	0.000229	
20:57:14:531	15/05/11	M019-M022	2.764	0.056421	0.000065	0.709002	0.000258	
20:59:15:250	15/05/11	M019-M022	2.689	0.056412	0.000064	0.709047	0.000262	
21:01:15:973	15/05/11	M019-M022	2.760	0.056483	0.000080	0.708969	0.000257	
23:21:31:002	15/05/11	1057, 1058, 568	3.105	0.056567	0.000052	0.708973	0.000348	
23:23:36:153	15/05/11	1057, 1058, 568	2.663	0.056563	0.000070	0.709067	0.000229	
23:25:31:337	15/05/11	1057, 1058, 568	3.013	0.056576	0.000055	0.709027	0.000161	

Table A4.12 Detailed Tridacna Strontium Isotope Results Analysed 15/05/2011

A4.15. Tridacna Spots Collected 16/05/2011

Start Time	Date	Pertains to Sample	^{88}Sr Volts	$^{84}\text{Sr}/^{86}\text{Sr}$	$^{84}\text{Sr}/^{86}\text{Sr} 2\sigma$ Error	$^{87}\text{Sr}/^{86}\text{Sr}$	$^{87}\text{Sr}/^{86}\text{Sr} 2\sigma$ Error
00:58:04:515	16/05/11	1057, 1058, 568	2.380	0.056551	0.000075	0.709074	0.000174
01:00:05:236	16/05/11	1057, 1058, 568	2.382	0.056522	0.000079	0.708931	0.000157
01:02:05:957	16/05/11	1057, 1058, 568	2.385	0.056551	0.000063	0.708963	0.000165
02:30:34:370	16/05/11	1057, 1058, 568	2.071	0.056523	0.000082	0.708928	0.000203
02:32:35:091	16/05/11	1057, 1058, 568	2.063	0.056436	0.000105	0.709128	0.000222
02:34:35:812	16/05/11	1057, 1058, 568	2.068	0.056482	0.000089	0.708980	0.000257
04:01:05:717	16/05/11	1057, 1058, 568	1.837	0.056567	0.000133	0.708987	0.000255
04:03:05:329	16/05/11	1057, 1058, 568	1.894	0.056439	0.000114	0.708847	0.000302
04:05:06:051	16/05/11	1057, 1058, 568	1.919	0.056439	0.000092	0.709078	0.000335
04:49:21:917	16/05/11	1057, 1058, 568	1.858	0.056547	0.000087	0.708876	0.000250
04:51:23:746	16/05/11	1057, 1058, 568	1.802	0.056518	0.000125	0.708788	0.000319
04:53:23:361	16/05/11	1057, 1058, 568	1.767	0.056414	0.000109	0.708886	0.000248
06:41:19:114	16/05/11	1057, 1058, 568	1.785	0.056773	0.000296	0.709122	0.000406
06:43:19:835	16/05/11	1057, 1058, 568	1.950	0.056866	0.000555	0.709380	0.000674
06:45:26:094	16/05/11	1057, 1058, 568	1.773	0.056512	0.000098	0.708975	0.000289

Table A4.13 Detailed Tridacna Strontium Isotope Results Analysed 16/05/2011

A4.16. Tridacna Spots Collected 20/06/2011

Start Time	Date	Pertains to Sample	^{88}Sr Volts	$^{84}\text{Sr}/^{86}\text{Sr}$	$^{84}\text{Sr}/^{86}\text{Sr} 2\sigma$ Error	$^{87}\text{Sr}/^{86}\text{Sr}$	$^{87}\text{Sr}/^{86}\text{Sr} 2\sigma$ Error
12:08:18:680	20/06/11	1024, 1025, 1026	21.705	0.056575	0.000010	0.708995	0.000061
12:10:20:509	20/06/11	1024, 1025, 1026	20.852	0.056570	0.000011	0.708977	0.000063
12:12:21:230	20/06/11	1024, 1025, 1026	22.216	0.056569	0.000012	0.708938	0.000075
12:56:26:022	20/06/11	1024, 1025, 1026	18.097	0.056494	0.000013	0.708994	0.000067
12:58:25:635	20/06/11	1024, 1025, 1026	18.298	0.056503	0.000013	0.708976	0.000061
13:00:27:464	20/06/11	1024, 1025, 1026	18.604	0.056490	0.000011	0.708998	0.000061
14:06:41:298	20/06/11	1024, 1025, 1026	14.298	0.056400	0.000015	0.708983	0.000068
14:08:42:019	20/06/11	1024, 1025, 1026	15.665	0.056415	0.000013	0.708961	0.000056
14:10:42:740	20/06/11	1024, 1025, 1026	15.697	0.056412	0.000012	0.708995	0.000061
15:08:58:118	20/06/11	1024, 1025, 1026	13.510	0.056372	0.000015	0.708943	0.000059

Start Time	Date	Pertains to Sample	⁸⁸ Sr Volts	⁸⁴ Sr/ ⁸⁶ Sr	⁸⁴ Sr/ ⁸⁶ Sr 2σ Error	⁸⁷ Sr/ ⁸⁶ Sr	⁸⁷ Sr/ ⁸⁶ Sr 2σ Error
15:10:58:841	20/06/11	1024, 1025, 1026	14.840	0.056385	0.000013	0.708945	0.000052
15:12:59:561	20/06/11	1024, 1025, 1026	14.518	0.056369	0.000017	0.708966	0.000069
16:11:06:219	20/06/11	M028, M029, M030	13.709	0.056515	0.000022	0.708987	0.000067
16:13:06:940	20/06/11	M028, M029, M030	13.788	0.056515	0.000015	0.709002	0.000067
16:15:07:661	20/06/11	M028, M029, M030	13.960	0.056502	0.000020	0.709004	0.000091
17:11:32:286	20/06/11	M028, M029, M030	12.949	0.056489	0.000019	0.709023	0.000073
17:13:34:115	20/06/11	M028, M029, M030	13.316	0.056509	0.000020	0.709000	0.000078
17:15:34:837	20/06/11	M028, M029, M030	12.681	0.056503	0.000018	0.709011	0.000081
18:41:49:236	20/06/11	M028, M029, M030	10.716	0.056446	0.000019	0.709013	0.000061
18:43:51:065	20/06/11	M028, M029, M030	11.552	0.056445	0.000020	0.708973	0.000067
18:45:51:786	20/06/11	M028, M029, M030	10.971	0.056454	0.000021	0.709007	0.000068
19:11:40:118	20/06/11	M028, M029, M030	11.529	0.056441	0.000019	0.709020	0.000066
19:13:40:841	20/06/11	M028, M029, M030	11.365	0.056453	0.000019	0.709045	0.000070
19:15:41:562	20/06/11	M028, M029, M030	9.811	0.056422	0.000022	0.709026	0.000060
19:39:55:855	20/06/11	M029 Uncut	10.057	0.056464	0.000018	0.708979	0.000082
19:41:56:577	20/06/11	M029 Uncut	10.008	0.056491	0.000019	0.709007	0.000087
19:43:57:298	20/06/11	M029 Uncut	9.956	0.056466	0.000021	0.708960	0.000081
20:02:19:295	20/06/11	M029 Uncut	10.178	0.056469	0.000022	0.709004	0.000086
20:04:20:016	20/06/11	M029 Uncut	9.427	0.056465	0.000013	0.709000	0.000073
20:06:21:845	20/06/11	M029 Uncut	10.119	0.056471	0.000019	0.709033	0.000081
20:47:38:174	20/06/11	M025, M027	10.587	0.056480	0.000019	0.709015	0.000074
20:49:38:894	20/06/11	M025, M027	10.667	0.056466	0.000022	0.709010	0.000061
20:51:39:615	20/06/11	M025, M027	10.602	0.056470	0.000020	0.709017	0.000089
21:45:50:229	20/06/11	M025, M027	10.026	0.056476	0.000016	0.709001	0.000067
21:47:50:950	20/06/11	M025, M027	10.554	0.056483	0.000017	0.709024	0.000082
21:49:51:671	20/06/11	M025, M027	10.947	0.056475	0.000021	0.709007	0.000078
22:40:04:164	20/06/11	M025, M027	9.540	0.056463	0.000019	0.708963	0.000083
22:42:04:885	20/06/11	M025, M027	9.765	0.056474	0.000027	0.708991	0.000067
22:44:05:607	20/06/11	M025, M027	9.998	0.056482	0.000022	0.708964	0.000071
23:29:55:582	20/06/11	M023, M024, M026	10.080	0.056505	0.000020	0.709012	0.000092
23:31:56:304	20/06/11	M023, M024, M026	9.734	0.056481	0.000017	0.708956	0.000100
23:33:57:026	20/06/11	M023, M024, M026	9.830	0.056484	0.000025	0.708996	0.000099

Table A4.14 Detailed Tridacna Strontium Isotope Results Analysed 20/06/2011

A4.17. Tridacna Spots Collected 21/06/2011

Start Time	Date	Pertains to Sample	88Sr Volts	84Sr/ ⁸⁶ Sr	84Sr/ ⁸⁶ Sr 2σ Error	87Sr/ ⁸⁶ Sr	⁸⁷ Sr/ ⁸⁶ Sr 2σ Error
01:24:25:618	21/06/11	M023, M024, M026	8.731	0.056472	0.000046	0.709062	0.000416
01:26:26:339	21/06/11	M023, M024, M026	8.590	0.056500	0.000048	0.709060	0.000483
01:28:27:061	21/06/11	M023, M024, M026	8.319	0.056478	0.000045	0.709111	0.000480
02:14:22:605	21/06/11	M023, M024, M026	8.785	0.056489	0.000047	0.708996	0.000419
02:16:22:220	21/06/11	M023, M024, M026	8.902	0.056539	0.000050	0.709178	0.000457
02:18:24:049	21/06/11	M023, M024, M026	8.231	0.056465	0.000039	0.708902	0.000437
03:32:38:551	21/06/11	M023, M024, M026	7.907	0.056502	0.000036	0.709242	0.000363
03:34:39:273	21/06/11	M023, M024, M026	7.843	0.056449	0.000038	0.709020	0.000361
03:36:39:993	21/06/11	M023, M024, M026	8.059	0.056405	0.000044	0.708966	0.000367
10:46:11:572	21/06/11	M031, M032	11.140	0.056550	0.000023	0.708987	0.000081
10:48:12:292	21/06/11	M031, M032	11.365	0.056552	0.000018	0.708993	0.000079
10:50:13:013	21/06/11	M031, M032	10.991	0.056549	0.000017	0.708983	0.000068
11:48:27:285	21/06/11	M031, M032	7.727	0.056474	0.000024	0.708977	0.000084
11:50:28:006	21/06/11	M031, M032	7.779	0.056454	0.000029	0.708974	0.000090
11:52:28:727	21/06/11	M031, M032	7.563	0.056455	0.000035	0.708976	0.000076
12:38:36:457	21/06/11	M031, M032	6.840	0.056418	0.000032	0.708988	0.000079
12:40:37:177	21/06/11	M031, M032	6.864	0.056415	0.000033	0.708950	0.000080
12:42:39:006	21/06/11	M031, M032	6.596	0.056415	0.000032	0.708988	0.000087
13:46:37:443	21/06/11	M037, M038E	15.017	0.056583	0.000015	0.708976	0.000097
13:48:38:164	21/06/11	M037, M038E	14.261	0.056589	0.000017	0.709012	0.000063
13:50:38:884	21/06/11	M037, M038E	14.054	0.056571	0.000017	0.709005	0.000065
15:51:05:546	21/06/11	M037, M038E	7.633	0.056391	0.000035	0.708950	0.000224
15:53:11:805	21/06/11	M037, M038E	7.383	0.056328	0.000020	0.708905	0.000150
15:55:18:065	21/06/11	M037, M038E	6.951	0.056322	0.000044	0.709046	0.000197
17:01:20:822	21/06/11	M037, M038E	5.633	0.056255	0.000045	0.709071	0.000242
17:03:21:543	21/06/11	M037, M038E	5.576	0.056278	0.000044	0.709044	0.000187
17:05:22:265	21/06/11	M037, M038E	5.106	0.056223	0.000048	0.708968	0.000193
18:02:51:421	21/06/11	M033, M034	6.095	0.056542	0.000027	0.709010	0.000103
18:04:47:713	21/06/11	M033, M034	7.148	0.056504	0.000024	0.709010	0.000077
18:06:48:434	21/06/11	M033, M034	6.330	0.056489	0.000024	0.709052	0.000076
19:45:09:377	21/06/11	M033, M034	6.041	0.056495	0.000035	0.709041	0.000091
19:47:11:206	21/06/11	M033, M034	5.908	0.056503	0.000035	0.709020	0.000072
19:49:11:927	21/06/11	M033, M034	5.953	0.056504	0.000031	0.709012	0.000086
20:33:15:612	21/06/11	M033, M034	6.659	0.056518	0.000025	0.709044	0.000064
20:35:17:440	21/06/11	M033, M034	6.372	0.056510	0.000037	0.709023	0.000072
20:37:18:163	21/06/11	M033, M034	6.777	0.056507	0.000029	0.709038	0.000071
21:21:07:792	21/06/11	M035, M036	8.745	0.056494	0.000024	0.708993	0.000094

						$^{87}\text{Sr}/^{86}\text{Sr} 2\sigma$	Error
						$^{87}\text{Sr}/^{86}\text{Sr}$	
21:23:08:513	21/06/11	M035, M036	8.143	0.056478	0.000028	0.708931	0.000087
21:25:09:235	21/06/11	M035, M036	8.758	0.056548	0.000045	0.708995	0.000085
22:47:18:870	21/06/11	M035, M036	8.382	0.056508	0.000036	0.709001	0.000092
22:49:19:591	21/06/11	M035, M036	8.259	0.056482	0.000023	0.708976	0.000075
22:51:20:312	21/06/11	M035, M036	8.435	0.056483	0.000023	0.709019	0.000088

Table A4.15 Detailed Tridacna Strontium Isotope Results Analysed 21/05/2011

A4.18. *Tridacna* Spots Collected 22/06/2011

						$^{87}\text{Sr}/^{86}\text{Sr} 2\sigma$	Error
						$^{87}\text{Sr}/^{86}\text{Sr}$	
00:07:25:569	22/06/11	M035, M036	7.752	0.056474	0.000025	0.708964	0.000090
00:09:26:289	22/06/11	M035, M036	8.399	0.056487	0.000021	0.708982	0.000086
00:11:25:904	22/06/11	M035, M036	8.108	0.056493	0.000023	0.709034	0.000082
00:40:18:713	22/06/11	M039, M040	8.163	0.056508	0.000023	0.708946	0.000107
00:42:20:542	22/06/11	M039, M040	7.406	0.056534	0.000043	0.709010	0.000084
00:44:21:263	22/06/11	M039, M040	7.920	0.056501	0.000025	0.709007	0.000101
01:48:00:042	22/06/11	M039, M040	7.491	0.056469	0.000022	0.708983	0.000089
01:50:00:763	22/06/11	M039, M040	7.455	0.056488	0.000034	0.708956	0.000093
01:52:01:483	22/06/11	M039, M040	7.133	0.056518	0.000028	0.708978	0.000092
03:44:20:710	22/06/11	595, M041-M045	9.437	0.056467	0.000016	0.709052	0.000059
03:46:21:430	22/06/11	595, M041-M045	8.533	0.056457	0.000025	0.709025	0.000102
03:48:22:153	22/06/11	595, M041-M045	9.600	0.056485	0.000017	0.709000	0.000088
05:02:44:408	22/06/11	595, M041-M045	7.443	0.056479	0.000023	0.708936	0.000083
05:04:45:130	22/06/11	595, M041-M045	7.750	0.056493	0.000028	0.708946	0.000096
05:06:46:959	22/06/11	595, M041-M045	7.579	0.056490	0.000029	0.708953	0.000077
05:58:54:635	22/06/11	595, M041-M045	6.567	0.056492	0.000025	0.708936	0.000094
06:00:55:357	22/06/11	595, M041-M045	6.474	0.056540	0.000039	0.708942	0.000079
06:02:56:078	22/06/11	595, M041-M045	7.146	0.056510	0.000022	0.708945	0.000089
06:57:11:121	22/06/11	595, M041-M045	6.270	0.056519	0.000035	0.709015	0.000205
06:59:11:842	22/06/11	595, M041-M045	6.077	0.056531	0.000039	0.708996	0.000173
07:01:13:671	22/06/11	595, M041-M045	5.669	0.056507	0.000050	0.708872	0.000236
07:47:14:753	22/06/11	595, M041-M045	6.086	0.056500	0.000041	0.708879	0.000184
07:49:15:475	22/06/11	595, M041-M045	6.315	0.056525	0.000035	0.708937	0.000170
07:51:16:197	22/06/11	595, M041-M045	6.436	0.056557	0.000030	0.709087	0.000196

Start Time	Date	Pertains to Sample	^{88}Sr Volts	$^{84}\text{Sr}/^{86}\text{Sr}$	$^{84}\text{Sr}/^{86}\text{Sr} 2\sigma$	$^{87}\text{Sr}/^{86}\text{Sr}$	$^{87}\text{Sr}/^{86}\text{Sr} 2\sigma$
				Sr	Error	Sr	Error
08:55:28:200	22/06/11	595, M041-M045	5.476	0.056501	0.000046	0.708926	0.000231
08:57:28:921	22/06/11	595, M041-M045	5.439	0.056484	0.000041	0.708947	0.000235
08:59:29:641	22/06/11	595, M041-M045	5.757	0.056507	0.000044	0.708886	0.000212
09:43:34:433	22/06/11	595, M041-M045	5.515	0.056498	0.000040	0.708781	0.000201
09:45:35:154	22/06/11	595, M041-M045	5.251	0.056495	0.000038	0.708917	0.000188
09:47:35:875	22/06/11	595, M041-M045	5.568	0.056547	0.000035	0.708934	0.000206
10:29:12:980	22/06/11	848, 849, 850	5.262	0.056560	0.000065	0.709089	0.000138
10:31:13:700	22/06/11	848, 849, 850	5.566	0.056475	0.000035	0.709011	0.000130
10:33:15:529	22/06/11	848, 849, 850	5.520	0.056554	0.000074	0.709050	0.000122
11:53:37:733	22/06/11	848, 849, 850	5.353	0.056485	0.000037	0.708934	0.000098
11:55:38:454	22/06/11	848, 849, 850	5.517	0.056466	0.000039	0.708883	0.000110
11:57:39:176	22/06/11	848, 849, 850	5.441	0.056467	0.000035	0.708980	0.000107
13:04:00:762	22/06/11	848, 849, 850	5.243	0.056465	0.000043	0.708996	0.000089
13:06:01:483	22/06/11	848, 849, 850	5.298	0.056462	0.000038	0.708942	0.000109
13:08:02:203	22/06/11	848, 849, 850	5.390	0.056474	0.000034	0.708926	0.000086
14:22:26:674	22/06/11	848, 849, 850	5.221	0.056455	0.000042	0.708946	0.000095
14:24:27:395	22/06/11	848, 849, 850	5.093	0.056487	0.000040	0.708928	0.000088
14:26:28:117	22/06/11	848, 849, 850	4.911	0.056467	0.000043	0.708909	0.000093
15:15:26:798	22/06/11	845, 846, 847	6.089	0.058007	0.000136	0.709134	0.000080
15:17:27:519	22/06/11	845, 846, 847	6.299	0.056899	0.000033	0.709081	0.000084
15:19:29:348	22/06/11	845, 846, 847	7.204	0.056557	0.000026	0.709050	0.000105
16:45:43:746	22/06/11	845, 846, 847	5.005	0.056475	0.000046	0.708860	0.000101
16:47:44:469	22/06/11	845, 846, 847	5.552	0.056509	0.000039	0.709007	0.000096
16:49:45:190	22/06/11	845, 846, 847	5.183	0.056497	0.000040	0.708981	0.000104
18:23:31:463	22/06/11	845, 846, 847	4.181	0.056472	0.000045	0.708925	0.000126
18:25:32:186	22/06/11	845, 846, 847	4.375	0.056483	0.000043	0.708997	0.000088
18:27:32:906	22/06/11	845, 846, 847	5.161	0.056454	0.000046	0.708969	0.000083
20:15:12:147	22/06/11	Durango, 622, 624, 625	5.562	0.056403	0.000031	0.709075	0.000104
20:17:12:868	22/06/11	Durango, 622, 624, 625	5.303	0.056407	0.000042	0.709081	0.000129
20:19:13:589	22/06/11	Durango, 622, 624, 625	5.112	0.056400	0.000048	0.709106	0.000090
22:15:50:990	22/06/11	Durango, 622, 624, 625	4.146	0.056503	0.000034	0.708939	0.000100
22:17:51:710	22/06/11	Durango, 622, 624, 625	4.334	0.056538	0.000041	0.708923	0.000080
22:19:52:433	22/06/11	Durango, 622, 624, 625	4.245	0.056558	0.000046	0.708845	0.000096

Table A4.16 Detailed Tridacna Strontium Isotope Results Analysed 22/06/2011

A4.19. *Tridacna* Spots Collected 23/06/2011

Start Time	Date	Pertains to Sample	^{88}Sr Volts	$^{84}\text{Sr}/^{86}\text{Sr}$	$^{84}\text{Sr}/^{86}\text{Sr} 2\sigma$ Error	$^{87}\text{Sr}/^{86}\text{Sr}$	$^{87}\text{Sr}/^{86}\text{Sr} 2\sigma$ Error
00:08:29:164	23/06/11	Durango, 622, 624, 625	3.475	0.056570	0.000053	0.708906	0.000111
00:10:29:884	23/06/11	Durango, 622, 624, 625	3.543	0.056604	0.000056	0.708931	0.000106
00:12:30:607	23/06/11	Durango, 622, 624, 625	3.478	0.056580	0.000046	0.708866	0.000117
01:55:01:197	23/06/11	614–620	3.416	0.056580	0.000060	0.708955	0.000102
01:57:01:917	23/06/11	614–620	3.546	0.056578	0.000047	0.708996	0.000097
01:59:02:638	23/06/11	614–620	3.448	0.056559	0.000062	0.708944	0.000107
03:46:46:209	23/06/11	614–620	3.134	0.056525	0.000073	0.708791	0.000391
03:48:46:929	23/06/11	614–620	2.832	0.056497	0.000066	0.709013	0.000373
03:50:47:651	23/06/11	614–620	2.937	0.056543	0.000084	0.708674	0.000449
05:01:00:710	23/06/11	614–620	3.304	0.056557	0.000094	0.709124	0.000333
05:03:01:431	23/06/11	614–620	2.632	0.056509	0.000082	0.709114	0.000496
05:05:02:153	23/06/11	614–620	2.751	0.056546	0.000096	0.708979	0.000485
06:18:47:858	23/06/11	614–620	2.498	0.056637	0.000102	0.708813	0.000437
06:20:49:687	23/06/11	614–620	2.605	0.056616	0.000122	0.708668	0.000524
06:22:50:408	23/06/11	614–620	2.410	0.056588	0.000081	0.708808	0.000410
07:17:08:775	23/06/11	614–620	2.500	0.056506	0.000094	0.708892	0.000392
07:19:09:496	23/06/11	614–620	2.532	0.056461	0.000084	0.708939	0.000420
07:21:10:217	23/06/11	614–620	2.555	0.056529	0.000072	0.709060	0.000488

Table A4.17 Detailed Tridacna Strontium Isotope Results Analysed 23/06/2011

A4.20. Summary

Appendix Four shows the detailed results from all of the 631 spots of Tridacna analysed during the course of this research. These results are summarised in Table 5.33 and Figure 5.27 and shown in detail above.